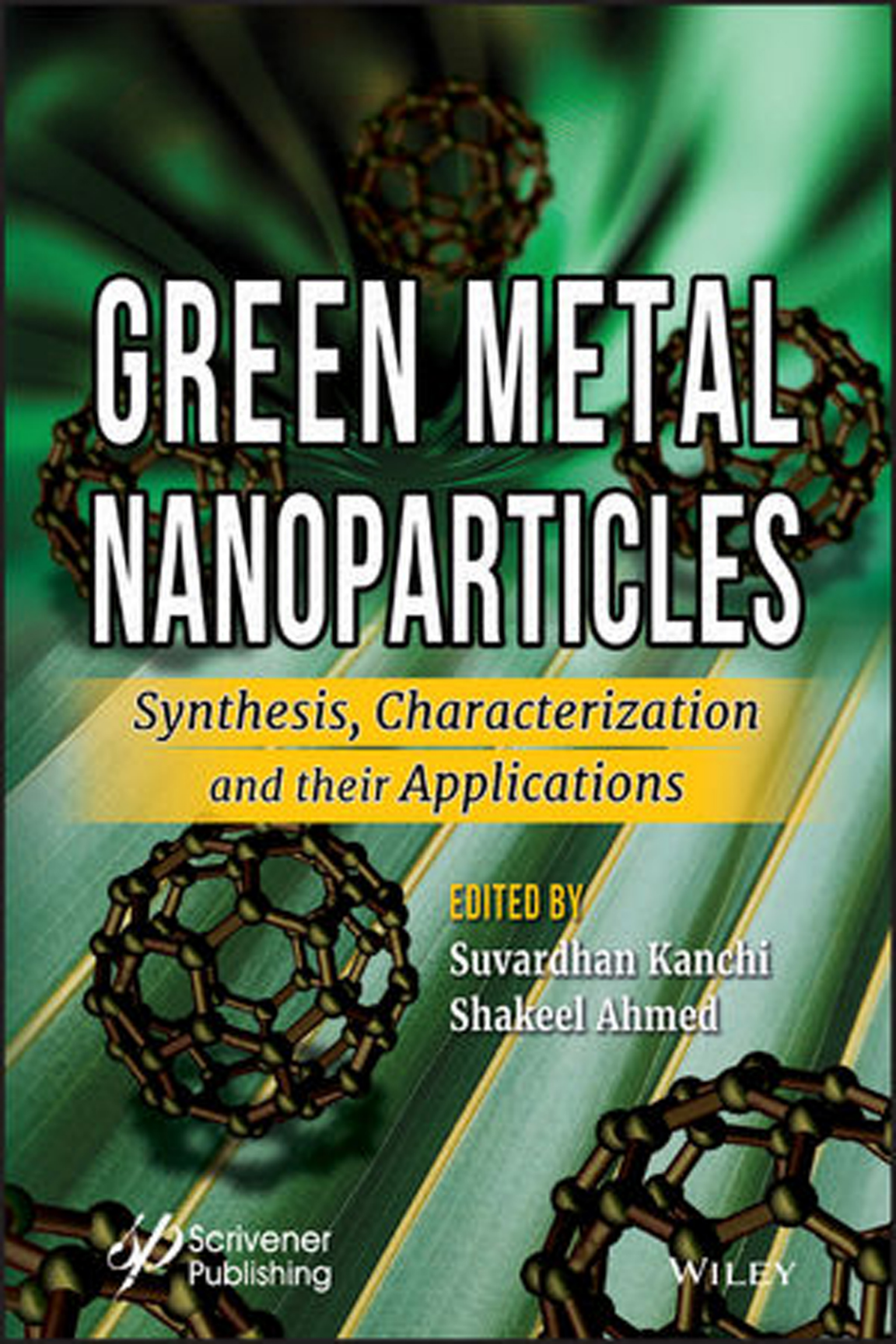

GREEN METAL NANOPARTICLES
Synthesis, Characterization and their Applications
EDITED BY
Suvardhan Kanchi
Shakeel Ahmed
Scrivener Publishing
WILEY

Green Metal Nanoparticles

Scrivener Publishing
100 Cummings Center, Suite 541J
Beverly, MA 01915-6106

Publishers at Scrivener
Martin Scrivener (martin@scrivenerpublishing.com)
Phillip Carmical (pcarmical@scrivenerpublishing.com)

Green Metal Nanoparticles

Synthesis, Characterization and Their Applications

Edited by
Suvardhan Kanchi and Shakeel Ahmed



WILEY

This edition first published 2018 by John Wiley & Sons, Inc., 111 River Street, Hoboken, NJ 07030, USA and Scrivener Publishing LLC, 100 Cummings Center, Suite 541J, Beverly, MA 01915, USA
© 2018 Scrivener Publishing LLC
For more information about Scrivener publications please visit www.scrivenerpublishing.com.

All rights reserved. No part of this publication may be reproduced, stored in a retrieval system, or transmitted, in any form or by any means, electronic, mechanical, photocopying, recording, or otherwise, except as permitted by law. Advice on how to obtain permission to reuse material from this title is available at http://www.wiley.com/go/permissions.

Wiley Global Headquarters
111 River Street, Hoboken, NJ 07030, USA

For details of our global editorial offices, customer services, and more information about Wiley products visit us at www.wiley.com.

Limit of Liability/Disclaimer of Warranty
While the publisher and authors have used their best efforts in preparing this work, they make no representations or warranties with respect to the accuracy or completeness of the contents of this work and specifically disclaim all warranties, including without limitation any implied warranties of merchantability or fitness for a particular purpose. No warranty may be created or extended by sales representatives, written sales materials, or promotional statements for this work. The fact that an organization, website, or product is referred to in this work as a citation and/or potential source of further information does not mean that the publisher and authors endorse the information or services the organization, website, or product may provide or recommendations it may make. This work is sold with the understanding that the publisher is not engaged in rendering professional services. The advice and strategies contained herein may not be suitable for your situation. You should consult with a specialist where appropriate. Neither the publisher nor authors shall be liable for any loss of profit or any other commercial damages, including but not limited to special, incidental, consequential, or other damages. Further, readers should be aware that websites listed in this work may have changed or disappeared between when this work was written and when it is read.

Library of Congress Cataloging-in-Publication Data
Names: Kanchi, Suvardhan, editor. | Ahmed, Shakeel, 1989- editor.
Title: Green metal nanoparticles : synthesis, characterization and their applications / edited by Suvardhan Kanchi and Shakeel Ahmed.
Description: Hoboken, NJ : Wiley-Scrivener, 2018. | Includes bibliographical references. |
Identifiers: LCCN 2018041174 (print) | LCCN 2018042491 (ebook) | ISBN 9781119418863 (ePub) | ISBN 9781119418870 (ePDF) | ISBN 9781119418238 (hardcover)
Subjects: LCSH: Nanoparticles. | Metal clusters. | Nanostructured materials--Synthesis. | Nanoparticles--Industrial applications.
Classification: LCC TA418.9.N35 (ebook) | LCC TA418.9.N35 G746 2018 (print) | DDC 620/.50286--dc23
LC record available at https://lccn.loc.gov/2018041174

Cover image: Pixabay.Com
Cover design by Russell Richardson

Set in size of 11pt and Minion Pro by Exeter Premedia Services Private Ltd., Chennai, India

Printed in the USA

10 9 8 7 6 5 4 3 2 1

Contents

Preface **xxi**

Part I Future Vision of Green Nanotechnology **1**

1 Recent Advances in Green Nanotechnology and the Vision for the Future **3**
Sukanchan Palit and Chaudhery Mustansar Hussain

1.1 Introduction 4
1.2 The Objective of this Study 4
1.3 The Rationale for this Study 5
1.4 What is Meant by Green Nanotechnology? 5
1.5 The Scientific Doctrine and Truth Behind Nanotechnology Applications 6
1.6 Recent Research Pursuit in the Field of Nanotechnology 7
1.7 Scientific Endeavors in the Field of Green Nanotechnology 8
1.8 Challenges and Opportunities in the Field of Green Nanotechnology 13
1.9 Environmental Sustainability, Humankind's Progress and Vision of Science 14
1.10 Scientific Cognizance, the Greatness of Research Pursuit and Green Nanotechnology 14
1.11 Global Water Crisis – The Vision and Challenge of Science 15
1.12 Heavy Metal and Arsenic Groundwater Contamination – The Vision for the Future 15
1.13 Groundwater Remediation and Water Purification Technologies 16
1.14 Application of Nanotechnology in Industrial Wastewater Treatment 17
1.15 The Vision of Renewable Energy Technologies 18
1.16 Future Research Trends and Flow of Thoughts 19
1.17 Conclusion and Future Perspectives 20
References 20

2 Green Synthesis of Metal-Based Nanoparticles and Their Applications 23
Shamaila Sajjad, Sajjad Ahmed Khan Leghari, Najam-Ul-Athar Ryma and Sidra Anis Farooqi
2.1 Introduction 24
2.2 Botanical Extract Mediated Green Synthesis 27
2.2.1 Green Metal NPs via Botanical Extract 30
2.2.2 Green Oxide NPs via Botanical Extract 40
2.3 Microbial Extract-Mediated Green Synthesis 47
2.3.1 Green Metal NPs via Microbes 49
2.3.1.1 Silver NPs 49
2.3.1.2 Gold NPs 51
2.3.1.3 Other Metallic NPs 52
2.3.2 Green Oxide NPs via Microbes 53
2.4 Conclusions 53
Acknowledgment 54
References 54

3 Plant and Tree Gums as Renewable Feedstocks for the Phytosynthesis of Nanoparticles: A Green Chemistry Approach 79
Aruna Jyothi Kora
3.1 Introduction 80
3.2 Different Varieties of Plant Gums 90
3.2.1 Gum Kondagogu 90
3.2.2 Gum Ghatti 91
3.2.3 Gum Olibanum 92
3.2.4 Gum Tragacanth 93
3.2.5 Gum Arabic 94
3.2.6 Gum Karaya 95
3.2.7 Gum Guar 96
3.3 Phytosynthesized Nanoparticles and Their Applications 96
3.3.1 Silver Nanoparticles 97
3.3.2 Gold Nanoparticles 98
3.3.3 Copper Nanoparticles 99
3.3.4 Platinum and Palladium Nanoparticles 99
3.3.5 Metal Oxide Nanoparticles 100
3.4 Conclusions and Future Prospects 101
Acknowledgment 102
References 102

4 Green Synthesis of Metal Nanoparticles and its Reaction Mechanisms 113
Rajasekhar Chokkareddy and Gan G. Redhi
4.1 Introduction 114
4.2 Green Synthesis Using Plant Extracts 117
4.3 Synthesis and Mechanism Action of Metal Nanoparticles 120
4.4 Conclusions 134
References 135

5 Toxicity of Metal/Metal Oxide Nanoparticles and Their Future Prospects 141
Subramanyam Deepika, Rajendran Harish Kumar, Chinnadurai Immanuel Selvaraj and Selvaraj Mohana Roopan
5.1 Introduction 142
5.1.1 Metals and Metal Oxide Nanoparticles 143
5.1.2 Parameters of Toxicity 144
5.1.3 Synthesis of Metal/Metal Oxide Nanoparticles 146
5.2 Applications of Metal/Metal Oxide Nanoparticles and Their Toxicity 149
5.2.1 Silver Nanoparticles (Ag Nanoparticles/AgNPs) 149
5.2.2 Zinc Oxide Nanoparticles (ZnO Nanoparticles or ZnNPs) 151
5.2.3 CuO Nanoparticles 153
5.2.4 Cadmium Nanoparticles (CdNPs) vs Silica Nanoparticles (SiNPs) 156
5.2.5 TiO_2 Nanoparticles 157
5.3 Future Perspectives 158
5.3.1 Curbing Menace Through Biodegradable Nanomaterials: An Alternative 159
5.4 Conclusion 159
Conflict of Interest 160
Acknowledgment 160
Abbreviations 160
References 161

Part II Biosynthesis of Metallic Nanoparticles 165

6 Current Advances in Biosynthesis of Silver Nanoparticles and Their Applications 167
Rajasekhar Chokkareddy, Niranjan Thondavada, Bakusele Kabane and Gan G. Redhi
6.1 Introduction 168
6.2 Synthesis of Nanoparticles 169
6.2.1 Green Synthesis of Nanoparticles and its Benefits 171
6.2.2 Synthesis of Silver Nanoparticles by Bacteria and Fungi 173
6.2.3 Synthesis of Silver Nanoparticles by Algae 176
6.2.4 Synthesis of Silver Nanoparticles by Plants 176
6.2.5 Need for Green Synthesis 177
6.3 Biomedical Applications of Silver Nanoparticles 180
6.3.1 Antibacterial Properties 180
6.3.2 Antimicrobial Activity 181
6.3.3 Anticancer Activity of Silver Nanoparticles 183
6.3.4 Antidiabetic Activity of Silver Nanoparticles 184
6.3.5 Wound Healing Activity of Silver Nanoparticles 184
6.3.6 Diagnosis and Imaging Activity of Silver Nanoparticles 188
6.3.7 Medicinal Textile and Device Activity of Silver Nanoparticles 188
6.3.8 Catalytic Activity of Silver Nanoparticles 189
6.3.9 Toxicity of Silver Nanoparticles 189
6.4 Conclusions 190
References 191

7 Green and Sustainable Synthesis of Metal Nanoparticles Using Orange Peel Pith 199
G. López-Téllez, A. R. Vílchis Néstor, E. Gutiérrez-Segura, J. E. Moreno-Marcelino, A. Alcántara-Cobos, J. M. Malvaez-Medina and A. Castrejón Mejía
7.1 Introduction 200
7.2 Biosynthesis of Nanoparticles by Plants 201
7.3 Bioreduction Mechanism 201
7.4 Suitable Characteristics of Nanoparticles for Remediation 202
7.5 Orange Peel Pith as a Support, Reducing and Capping Agent of Metallic Nanoparticles 203
7.5.1 FeOx Nanoparticles 203

7.5.2 ZnO Nanoparticles 204
7.5.3 Ag Nanoparticles 208
7.5.4 Cu and/or Cu_xO_x Nanoparticles 212
7.6 Conclusions 213
References 214

8 Biological and Biomedical Applications of Eco-Friendly Synthesized Gold Nanoparticles 217
G. Madhumitha, J. Fowsiya and Selvaraj Mohana Roopan
8.1 Introduction 217
8.2 Plant Extract as Bioreactors for Green Synthesis of AuNPs 218
8.2.1 Leaf Mediated Synthesis of AuNPs 219
8.2.2 Fruit Extract Mediated Synthesis of AuNPs 222
8.2.3 Flower Extract Mediated Synthesis of AuNPs 224
8.3 Role of Phytochemicals in AuNPs 225
8.4 Biological and Biomedical Applications of AuNPs 228
8.4.1 Bioimaging/Labeling 228
8.4.2 AuNPs in Anticancer Therapy 228
8.4.3 Targeted Drug Delivery Using AuNPs 230
8.4.4 Antimicrobial Activity of AuNPs 231
8.4.5 Inhibition of Free Radical and Determination of Antioxidant Capacity Using AuNPs 233
8.5 Conclusion and Future Prospective 235
Conflict of Interest 235
Acknowledgment 235
References 235

9 Green Tiny Magnets: An Economic and Eco-Friendly Remedy for Environmental Damage 245
Paramita Karfa and Rashmi Madhuri
9.1 Introduction 246
9.2 Classification of Magnetic Materials 247
9.2.1 Ferromagnetic Materials 248
9.2.2 Antiferromagnetic Materials 250
9.2.3 Ferrimagnetic Materials 251
9.2.4 Paramagnetic Materials 251
9.2.5 Diamagnetic Materials 252
9.2.6 Superparamagnetic Materials 252
9.3 Synthesis and Characterization of Magnetic Nanoparticles 253
9.3.1 Types of Magnetic Nanoparticles 260
9.4 Application of Magnetic Nanoparticles for Environmental Remediation 263

9.4.1 Dye Degradation 263
9.4.2 Removal of Heavy Metals 268
9.4.3 Removal of Toxic Anions 271
9.4.4 Treatment of Pesticides in Groundwater 273
9.4.5 Removal of Microbial Contamination 275
9.4.6 Elimination of other Hazardous Organic Pollutants 277
9.5 Toxicity of Nanoparticles 278
9.6 Future Aspects of Magnetic Nanoparticle 279
Acknowledgment 280
References 280

10 Green Synthesis of Metallic Nanoparticles Using Biopolymers and Plant Extracts 293
Ibrahim M. El-Sherbiny and Ehab Salih
10.1 Introduction 294
10.2 Types of Nanomaterials 295
10.2.1 Carbon-Based Nanomaterials 295
10.2.2 Polymer-Based Nanomaterials 295
10.2.3 Metal-Based Nanomaterials 296
10.2.3.1 Silver Nanoparticles (AgNPs) 296
10.2.3.2 Gold Nanoparticles (AuNPs) 297
10.2.3.3 Platinum Nanoparticles (PtNPs) 297
10.2.3.4 Palladium Nanoparticles (PdNPs) 297
10.3 Synthesis Approaches of Metal Nanoparticles 297
10.3.1 Top-Down Approaches 298
10.3.2 Bottom-Up Approaches 298
10.4 Green Synthesis of MNPs 300
10.4.1 Green Synthesis of MNPs Using Biopolymers 300
10.4.1.1 Using Biopolymers in the Ordinary Way 301
10.4.1.2 Using Biopolymers in the Form of NPs 303
10.4.2 Green Synthesis of MNPs Using Herbal Plant Extracts 304
10.4.2.1 Green Synthesis of AgNPs 305
10.4.2.2 Green Synthesis of AuNPs 306
10.4.2.3 Green Synthesis of Pt NPs 308
10.4.2.4 Green Synthesis of Pd NPs 308
10.5 Conclusion 310
References 310

11 Green Synthesis of Metallic Nanoparticles from Natural Resources and Food Waste and Their Environmental Application **321**
Hussein I. Abdel-Shafy and Mona S. M. Mansour
11.1 Introduction 322
11.2 Several Methods for Metallic Nanoparticle Synthesis 323
11.3 Biosynthesis of Different Metallic Nanoparticles from Plant Derivatives 324
11.3.1 Bioreduction Mechanism of Metal Ions 328
11.3.2 Secondary Metabolites Effect in the Bioreduction Reaction 330
11.3.3 Different Parts of Plants Used to Produce Metallic NPs 330
11.3.3.1 Zinc Oxide Nanoparticles (ZnO NPs) Using Different Parts of Plants 332
11.3.3.2 Palladium Nanoparticles (PdNPs) Using Different Parts of Plants 334
11.3.3.3 Platinum Nanoparticles (PtNPs) Using Different Parts of Plants 336
11.3.3.4 Copper Oxide Nanoparticles (CuO NPs) Using Different Parts of Plants 337
11.3.3.5 Titanium Dioxide Nanoparticles (TiO_2 NPs) Using Different Parts of Plants 339
11.3.3.6 Iron Oxide Nanoparticles (FeO NPs) Using Different Parts of Plants 341
11.3.3.7 Silver Nanoparticles (AgNPs) Using Different Parts of Plants 342
11.3.3.8 Gold Nanoparticles (AuNPs) Using Different Parts of Plants 344
11.3.3.9 Nickel Nanoparticles (NiNPs) Using Different Parts of Plants 347
11.3.4 Factors Influencing the Biosynthesis of Metallic Nanoparticles 348
11.4 Green Synthesis of Metallic Nanoparticles Using Food and Agro Wastes 349
11.4.1 Silver Nanoparticles (AgNps) Using Food and Agricultural Wastes 352
11.4.2 Gold Nanoparticles (AuNPs) Using Food and Agricultural Wastes 355

11.4.3 Zinc Oxide Nanoparticles (ZnO NPs) Using Food and Agricultural Wastes 357
11.4.4 Nickel Nanoparticles (NiNPs) Using Food and Agricultural Wastes 358
11.4.5 Palladium Nanoparticles (PdNPs) Using Food and Agricultural Wastes 358
11.4.6 Platinum Nanoparticles (PtNPs) Using Food and Agricultural Wastes 359
11.4.7 Titanium Dioxide Nanoparticles (TiO_2NPs) Using Food and Agricultural Wastes 360
11.4.8 Iron Oxide Nanoparticles (IONPs) Using Food and Agricultural Wastes 360
11.5 Nanotechnology in Environmental Applications 362
11.5.1 Wastewater Treatment 362
11.5.1.1 Iron Nanoparticles in Environmental Applications 363
11.5.1.2 Silver Nanoparticles in Environmental Applications 365
11.5.1.3 Zinc Nanoparticles in Environmental Applications 368
11.6 Conclusions 369
Acknowledgment 370
References 370

12 Green Synthesis of Silver Nanoparticles for Biomedical and Environmental Applications 387
Varadavenkatesan Thivaharan, Vinayagam Ramesh and Selvaraj Raja
12.1 Introduction 388
12.2 Mechanistic Aspects of Silver Nanoparticle Synthesis 390
12.3 Applications of Phytogenic Silver Nanoparticles 391
12.4 Biomedical Applications 391
12.4.1 Antibacterial Applications 391
12.4.2 Antifungal Applications 394
12.4.3 Antileishmanial (Antiparasitic) Applications 396
12.4.4 Antibiofilm Applications 398
12.4.5 Anticoagulant Applications 400
12.4.6 Antidiabetic Applications 402
12.4.7 Antioxidant Applications 404
12.4.8 Cytotoxicity Applications 406
12.4.8.1 Biocompatibility Applications 406
12.4.8.2 Anticancer Applications 408

12.4.9 Larvicidal, Pupicidal, Pediculocidal and Acaricidal Applications 410
12.5 Environmental Applications 412
12.5.1 Catalytic Activity 412
12.5.1.1 Degradation of Dyes 412
12.5.1.2 Degradation of other Pollutants 415
12.5.2 Metal Ion Detection 416
12.6 Conclusions and Future Directions 418
References 419

13 Green Synthesis of Silver, Copper and Iron Nanoparticles: Synthesis, Characterization and Their Applications in Wastewater Treatment 441
Th. Babita Devi and M. Ahmaruzzaman
13.1 Introduction 442
13.2 Plants Mediated Green Synthesis of Metal Nanoparticles 444
13.3 Synthesis, Mechanism and Characterization of Synthesized Metals Nanoparticles 444
13.3.1 Synthesis of Silver, Copper and Iron Nanoparticles Using Bio-Waste (*Coccinia Grandis*) Peel Extract 445
13.3.2 Characterization 445
13.3.2.1 Ultraviolet-Visible (UV-Vis) Spectroscopy 445
13.3.3 Morphology Studies (SEM and TEM) 447
13.3.3.1 Transmission Electron Microscopy (TEM) and Scanning Electron Microscopy (SEM) Analysis 447
13.3.3.2 X-Ray Diffraction (XRD) Analysis 448
13.3.3.3 Energy-Dispersive X-Ray Spectroscopy (EDX) Analysis 449
13.3.3.4 Fourier Transform Infrared (FTIR) Spectroscopy 449
13.4 Catalytic Activities of Silver, Copper and Iron Nanoparticles for the Reduction and Photodegradation Process (Waste Water Treatment) 450
13.4.1 Reduction of Para-Nitrophenol (PNP) using AgNPs, CuNPs and FeNPs as Catalysts 450
13.4.2 Photocatalytic Activities of AgNPs, CuNPs and FeNPs for the Degradation of Toxic Dye Victoria Blue B under Solar Irradiation 456

13.5 Toxicity and Future Prospect 457
13.5.1 Toxicity of Silver Nanoparticles 457
13.5.2 Toxicity of Iron Nanoparticles 460
13.5.3 Toxicity of Copper Nanoparticles 460
13.5.4 Future Prospect of Silver Copper and Iron Nanoparticles 461
13.6 Future of Green Route in Synthesis of Metal Nanoparticles 461
13.7 Concluding Summary 462
References 463

Part III Biosynthesis of Metal Oxide Nanoparticles 467

14 Current Scenario in Green Approaches for Metal/Metal Oxide Nanoparticles Synthesis 469
Selvaraj Mohana Roopan
14.1 Introduction 469
14.1.1 Synthesis of Nanoparticles 471
14.2 Overview of Biological Approach-Microbial Medium 473
14.2.1 Silver Nanoparticles (AgNPs) Synthesis Using Different Microbial Sources 473
14.2.1.1 Trichoderma Reesei 474
14.2.1.2 Bacillus Subtilis 475
14.2.1.3 Bacillus Licheniformis 475
14.2.1.4 Anogeissus Latifolia 476
14.2.1.5 Aspergillus Flavus, Trichoderma Gamsii, Talaromyces Flavus and Aspergillus Oryzae 476
14.2.1.6 Salmonella Typhirium 476
14.2.1.7 Aspergillus Terreus 477
14.2.1.8 Spirogyra Varians 477
14.2.1.9 Pestaloptiopsis Pauciseta 477
14.2.2 Gold Nanoparticles (AuNPs) Synthesis by Microbial Medium 478
14.2.2.1 Actinobacter spp. 478
14.2.2.2 Bacillus Marisflavi 478
14.2.2.3 Pseudomonas Veronii AS41G 479
14.2.2.4 Plectonema Boryanum 479
14.2.3 Zinc Oxide Nanoparticles (ZnO NPs) Synthesis Using Various Microbes 479
14.2.3.1 Aeromonas Hydrophila 479
14.2.3.2 Alternaria Alternata 479

14.2.3.3 Aspergillus Fumigatus 480
14.2.3.4 Rhodococcus Pyridinivorans 480
14.2.3.5 Lactobacillus Plantarum 480
14.2.3.6 Sargassum Muticum 480
14.2.3.7 Serratia Ureilytica 480
14.2.4 Copper Nanoparticles (CuNPs) Synthesis Using Microorganisms 481
14.2.4.1 Kocuria Flava 481
14.2.4.2 Pseudomonas Fluorescens 481
14.2.4.3 Morganella sp. 481
14.3 Biological Approach Using Plant Sources as Medium 481
14.3.1 Silver Nanoparticles (AgNPs) Synthesis by Plant Sources 481
14.3.1.1 Terminalia Chebula 481
14.3.1.2 Tinospora Cordifolia 482
14.3.1.3 Tamarix Gallica 482
14.3.1.4 Vitex Negundo 484
14.3.1.5 Tragia Involucrata, Cymbopogon Citronella, Solanum Verbascifolium and Tylophora Ovata 484
14.3.1.6 Myrmecodia Pendans 485
14.3.1.7 Pelargonium Graveolens (Geranium) 485
14.3.1.8 Phoenix Dactylifera 485
14.3.1.9 Cassia Tora 486
14.3.1.10 Allium Cepa (onion) 486
14.3.1.11 Phyllanthus Amarus 486
14.3.1.12 Terminalia Cuneata 487
14.3.1.13 Coleus Aromaticus 487
14.3.1.14 Argyreia Nervosa 487
14.3.1.15 Aloe Vera 487
14.3.1.16 Catuneregum Spinosa 488
14.3.2 Zinc Oxide Nanoparticles (ZnO NPs) Synthesis Using Green Sources 488
14.3.2.1 Jacaranda Mimosifolia 488
14.3.2.2 Plectranthus Amboinicus 488
14.3.2.3 Azadirachta Indica 489
14.3.2.4 Trifolium Pratense 489
14.3.2.5 Pongamia Pinnata 489
14.3.2.6 Laurus Nobilis 489
14.3.2.7 Vitex Trifolia 489

14.3.2.8 Euphorbia Jatropa 490
14.3.2.9 Moringa Oleifera 490
14.3.2.10 Carrisa Edulis 490
14.3.3 Gold Nanoparticles (AuNPs) Synthesis Using Plant Sources 490
14.3.3.1 Galaxaura Elongata 490
14.3.3.2 Capsicum Annuum 491
14.3.3.3 Cassia Auriculata 491
14.3.3.4 Euphorbia Hirta 492
14.3.3.5 Olea Europaea (Olive) 492
14.3.3.6 Solanum Tuberosum (Potato) 492
14.3.3.7 Camellia Sinensis 492
14.3.3.8 Amomum Subulatum 492
14.3.4 Copper Oxide Nanoparticles (CuO NPs) Synthesis Using Plant Sources 492
14.3.4.1 Punica Granatum 492
14.3.4.2 Thymus Vulgaris 493
14.3.4.3 Tecoma Castanifolia 493
14.3.4.4 Matricaria Chamomilla 493
14.3.5 Palladium Nanoparticles (PdNPs) Synthesis Using Plant Sources 493
14.3.5.1 Camellia Sinensis 493
14.3.5.2 Catharanthus Roseus 494
14.3.5.3 Euphorbia Thymifolia 494
14.3.5.4 Salvia Hydrangea 494
14.3.5.5 Cocos Nucifera 494
14.3.5.6 Phyllanthus Emblica 495
14.3.5.7 Annona Squamosa 495
14.3.6 Tin Oxide Nanoparticles (Sno_2 NPs) Synthesis Using Plant Sources 495
14.3.6.1 Cyphomandra Betacea 495
14.3.6.2 Persia Americana 495
14.3.6.3 Catunaregum Spinosa 495
14.3.6.4 Aspalathus Linearis 496
14.3.6.5 Piper Nigrum 496
14.3.7 Nickel And Nickel Oxide Nanoparticles (Ni and NiO NPs) Using Various Plant Sources 496
14.3.7.1 Cocos Nucifera 496
14.3.7.2 Ocimum Sanctum 496
14.3.7.3 Agathosma Betulina 496
14.3.7.4 Moringa Oleifera 497

14.4 Applications 497
14.4.1 Biomedical Application 497
14.4.2 Antibacterial Properties 500
14.4.3 Dye Degradation 501
14.4.4 Electrochemical Application 502
14.5 Conclusion 503
Conflict of Interest 503
Acknowledgment 503
Abbreviations 504
References 504

15 Advanced Tin-Oxide Nanostructures: Green Synthesis, Prospects and Challenges for Clean Energy and Environmental Sustainability 513
Dipyaman Mohanta and M. Ahmaruzzaman
15.1 Introduction 514
15.2 Green Strategies for the Fabrication of Tin-Oxide Nanostructures 515
15.3 Detection of Pollutants and Environmental Remediation 517
15.3.1 Advanced Tin-Oxide Nanostructured Materials as Sensors for Environmentally Hazardous Gases 517
15.3.1.1 Mechanism of Gas Sensing 518
15.3.1.2 Effect of Morphology on Gas-Sensing Properties of SnO_2 520
15.3.1.3 Effect of Heterojunction on Gas-Sensing Properties of SnO_2 522
15.3.1.4 Effect of Carbon Composites on Gas-Sensing Properties of SnO_2 525
15.3.2 Advanced Tin-Oxide Nanostructures as Efficient Photocatalysts and Adsorbents for Decontamination of Wastewater 526
15.4 Clean Energy Generation and Efficient Energy Storage 530
15.4.1 Clean Energy Generation 530
15.4.1.1 Advanced Tin-Oxide-Based Photo-Electro-Catalyst for Water Splitting 530
15.4.1.2 Advanced Tin-Oxide Nanostructures as Anode Materials for Dye-Sensitized Solar Cells 531
15.4.2 High-Performance Energy Storage Devices 533
15.4.2.1 Tin-Oxide-Based Nanomaterials for High-Energy Lithium Ion Batteries 533

15.4.2.2 Tin-Oxide Nanomaterials-Based Supercapacitors 536
15.5 Discussion and Future Prospects 537
15.6 Conclusion 538
References 539

Part IV Biosynthesis of Noble Metal Nanoparticles 553

16 Green Synthesis of Noble Metal Nanoparticles: A Step Forward to Economical and Sustainable Development 555
Santanu Patra and Rashmi Madhuri
16.1 Overview of Nanoparticles 556
16.1.1 What is Green Chemistry and Why is it Gaining Importance Nowadays? 558
16.1.2 Literature Survey on the Green Synthesis of Nanoparticles 560
16.2 Green Synthesis of Noble Metal Nanoparticles 561
16.2.1 Plant Mediated Synthesis 563
16.2.1.1 Synthesis of AuNPs 565
16.2.1.2 Synthesis of AgNPs 571
16.2.2 Microbes Mediated Synthesis of Nanoparticles 575
16.2.2.1 AuNPs by Microbe Mediated Synthesis 575
16.2.2.2 Microbe Mediated Synthesis of AgNPs 578
16.2.3 Algae Mediated Synthesis 579
16.2.3.1 AuNPs Synthesis 581
16.2.3.2 Algae and Fungi Mediated Synthesis of AgNPs 582
16.2.4 Other Environmental Friendly Synthesis Approaches for Ag/AuNPs 584
16.2.5 Green Synthesis of Platinum Nanoparticles 588
16.3 Synthesis of Different Shaped Noble Metal Nanoparticles by Green Synthesis Approach 590
16.4 Conclusion and Future Scope 592
Acknowledgment 593
References 593

17 Green Synthesis of Platinum Nanoparticles and Their Biomedical Applications 603
Niranjan Thondavada, Rajasekar Chokkareddy and Gan G. Redhi
17.1 Introduction 603
17.2 Synthesis of Platinum Nanoparticles 605

17.2.1 Chemical Processes 605
17.2.2 Physical Methods 607
17.2.3 Biological Processes 608
17.3 Toxicology of PtNPs 609
17.4 Biomedical Applications of PtNPs 610
17.4.1 PtNPs in Cancer Therapy 610
17.4.2 PtNPs in Photothermal Therapy and Radiotherapy 611
17.4.3 Antibacterial Applications of PtNPs 612
17.5 Enzymatic Properties of PtNPs and their Applications 613
17.5.1 PtNPs in Nanomedicine 613
17.5.2 PtNPs in Nanodiagnostics 614
17.6 Conclusion 616
References 616

18 Eco-Friendly Noble Metal Nanoparticles for Therapeutic Applications: Present and Future Scenario 629
Raksha Choudhary and Rashmi Madhuri
18.1 Introduction 630
18.2 Why Noble Metal Nanoparticles are Gaining in Popularity in the Biomedical Field 632
18.3 Biomedical Applications of Noble Metal Nanoparticles 632
18.3.1 As Anticancer Agent 633
18.3.2 Acaricidal Agent 636
18.3.3 Anti-Biofouling Agent 637
18.3.4 As an Anti-Inflammatory Agent and Anti-Cholinesterase 640
18.3.5 Antileishmanial Agent 641
18.3.6 Antimicrobial and Antifungal 642
18.3.6.1 Disc or Well Diffusion Method 644
18.3.6.2 Minimum Inhibitory Concentration (MIC) or Minimum Bactericidal Concentration (MBC) 645
18.3.7 As Antioxidant 646
18.3.8 Wound Healing 647
18.3.9 Drug Delivery and Hemolytic Activity 648
18.3.10 Antidiabetic and Cytotoxic 650
18.4 Conclusions and Future Directions 651
Acknowledgment 654
References 654

Part V Synthesis of Biopolymer Nanoparticles and Quantum Dots **667**

19 Role of Bioconjugated Quantum Dots in Detection and Reduction of Pathogenic Microbes **669**
Angappan Rameshkumar, Devanesan Arul Ananth, Sivagurunathan Periyasamy, Deviram Garlapati and Thilagar Sivasudha
19.1 Introduction 670
19.2 About QDs 671
19.3 General Applications of QDs 672
19.3.1 Applications of QDs as Analytical Fluorescent Probes 672
19.3.2 Application of QDs in Bioimaging 673
19.4 Mechanism of Action of QDs in Cell Lines 674
19.5 QDs as Antimicrobial Agents 674
19.6 Mechanism of QDs Exhibiting Antimicrobial Activity 675
19.6.1 Mechanism of Action of QDs Alone 675
19.6.2 Mechanism of Action of QDs with Complex Molecules 677
19.6.3 Mechanism of Action of QDs in Fluorescence Image Detection on Bacteria 679
19.7 Advantage and Disadvantages of QDs as Antimicrobial Agent 683
19.8 Conclusion and Future Prospects 684
References 684

Index **689**

Preface

Metal nanoparticles are the basic elements of nanotechnology as they are the primary source used in the design of nanostructured devices and materials. Nanomaterials can be manufactured either incidentally, with physical or chemical methods, or naturally; and the high demand for them has led to their large-scale production by various toxic solvents or high energy techniques. However, due to the growing awareness of environmental and safety issues, the use of clean, nontoxic and environment-friendly ways to synthesize metal nanoparticles has emerged out of necessity. The use of biological resources, such as microbes, plant parts, vegetable wastes, agricultural wastes, gums, etc., has grown to become an alternative way of synthesizing metal nanoparticles. This biogenic synthesis is green, environmentally friendly, cost-effective, and nontoxic.

The current multi-authored book includes recent information and builds a database of bioreducing agents for various metal nanoparticles using different precursor systems. This book also highlights different simple, cost-effective, environment-friendly and easily scalable strategies, and includes parameters for controlling the size and shape of the materials developed from the various greener methods. In order to exploit the utmost potential offered by the synthesis of metal nanoparticles from different sources, such as agricultural and food waste, flora and fauna, microbes and biopolymer systems, it is also crucial to recognize the biochemical and molecular mechanisms involved in the production of nanoparticles and their characterization. The contents of other books mainly include the fundamentals of nanoparticles, characterization, mechanisms and the methods thereof. However, this book more narrowly focuses on the exploration of the green synthesis of metal nanoparticles and their characterization and applications in a specific manner currently lacking in these other available books.

Suvardhan Kanchi, PhD
Shakeel Ahmed, PhD
August 2018

Part I

FUTURE VISION OF GREEN NANOTECHNOLOGY

Suvardhan Kanchi and Shakeel Ahmed (eds.) Green Metal Nanoparticles, (1–21)
© 2018 Scrivener Publishing LLC

1

Recent Advances in Green Nanotechnology and the Vision for the Future

Sukanchan Palit[1] and Chaudhery Mustansar Hussain[2]*

[1]Department of Chemical Engineering, University of Petroleum and Energy Studies, Energy Acres, Uttarakhand, India
[2]Department of Chemistry and Environmental Sciences, New Jersey Institute of Technology, University Heights, Newark, New Jersey, USA

Abstract

Nanotechnology today is moving from one visionary paradigm towards another. Green synthesis and green nanotechnology are a totally integral part of the domain of sustainable nanotechnology. According to the Brundtland Commission Report, sustainability can be defined as that development that meets the needs of the present without compromising the ability of future generations to meet their own needs. Humankind's immense scientific prowess, scientific advancements and futuristic vision will all lead to a long and visionary way towards the true realization of sustainable development. The challenges, vision and intricacies of scientific endeavors in green nanotechnology are opening new windows of innovation in nanoscience and nanotechnology as a whole. Nanotechnology for green innovation—green nanotechnology—aims for products and processes that are safe, energy efficient, reduce industrial wastes and lessen greenhouse gas emission. This chapter delves deep into the murky depths of scientific vision and scientific innovation in green synthesis and green nanotechnology. Green nanotechnology veritably and definitely addresses global water shortage and drinking water issues. The authors repeatedly address the issue of drinking water provision and heavy metals and arsenic groundwater contamination. Other areas of scientific endeavors are nanotechnology-based water treatment problems, better and more efficient renewable energy technologies, environmental and waste remediation and

**Corresponding author*: chaudhery.m.hussain@njit.edu

Suvardhan Kanchi and Shakeel Ahmed (eds.) Green Metal Nanoparticles, (3–21)
© 2018 Scrivener Publishing LLC

the application of nanotechnology in sustainable production. This chapter targets the wide and visionary domain of environmental sustainability and its vital and pivotal need in a nation's growth.

Keywords: Nanotechnology, green, synthesis, sustainability, process, advances

1.1 Introduction

Science and technology are moving at a rapid pace today. Environmental engineering science is witnessing drastic changes. In a similar manner, nanotechnology and green nanotechnology are moving from one visionary paradigm towards another. Environmental regulations, frequent environmental catastrophes and loss of ecological biodiversity have urged the scientific community to move forward towards a newer vision and newer innovations. Green nanotechnology is the frontier of science and engineering today. Human civilization's immense scientific prowess, wide futuristic vision and vast scientific and academic rigor all lead along a long and visionary path towards the true realization and emancipation of green nanotechnology. In this chapter, the authors focus deeply on recent scientific endeavors and scientific advances in the field of green nanotechnology with the sole objective of furthering science and engineering. Today the domain of nanotechnology needs to be re-envisioned and redefined with scientific rigor. The vision and challenge of environmental engineering science and nanotechnology are broadly combined in the evolution of a new branch of scientific endeavor known as green nanotechnology. This chapter also focuses on global water issues—mainly heavy metal groundwater contamination and subsequent remediation. Scientific research pursuit today is replete with vision and scientific profundity. The authors in this chapter have strived to open new windows into innovation in the field of green nanotechnology, which will continue to take place in decades to come.

1.2 The Objective of this Study

Today the scientific vision of nanotechnology, green nanotechnology and green synthesis are surpassing wide and visionary scientific frontiers. Technological vision and scientific validation are today's foundation stones of scientific endeavors in the field of nanotechnology and green nanotechnology. The endeavors in this chapter are replete with deep scientific contemplation and scientific introspection. Global nanotechnology applications

and their health risks are challenging the scientific landscape, hence the importance of green synthesis, green nanotechnology and green chemistry. This chapter pointedly focuses on the recent scientific research pursuits in green nanotechnology, especially on the vast domain of groundwater remediation and its vision for the future. Today global nanotechnology initiatives are targeted towards green chemistry, sustainable chemistry and green engineering. The vast scientific potential of green nanotechnology is delineated with scientific precision in this chapter. Deep scientific understanding, wide scientific contemplation and the vision of green science and technology are the basic foundations of this well-observed chapter [1, 2].

1.3 The Rationale for this Study

The rationale for this study surpasses vast scientific imagination and deep scientific discernment. Technology is moving at a rapid pace today. The global water shortage, frequent environmental disasters and stringent regulations have urged the scientific and engineering communities to be geared towards a newer visionary era of green technology. Today, humankind stands in the midst of a global water crisis. Heavy metal and arsenic groundwater contamination are the vexing issues of this century. Thus, the need for this well-observed study. Technological vision and scientific motivation are greatly needed as civilization wearily trudges a scientific path in this century. Scientific comprehension, the deep scientific avenues of this century and a futuristic vision are the forerunners of the recent emancipation of green nanotechnology today. Groundwater remediation and prevention of arsenic and heavy metal drinking water contamination are the futuristic vision of this chapter. Scientific success, scientific potential and wide scientific forbearance are of utmost importance as science and engineering moves into the second half of this visionary century. The rationale of this study goes beyond scientific imagination and scientific fortitude. Humankind and scientific endeavor today stands in the midst of deep vision and contemplation. Today green nanotechnology is a burgeoning area of science. This study pointedly focuses on the vast applications of green nanotechnology with the sole aim of furthering science and engineering.

1.4 What is Meant by Green Nanotechnology?

Today, nanotechnology can alleviate major sustainability issues. Sustainable development is the utmost need of the hour. The framework of green

nanotechnology involves the production and processes to make nanomaterials, green chemistry, green engineering, direct and indirect environmental applications; and also encompasses the production of nanomembranes, nanocatalysts and the greater emancipation of harnessed energy. Broadly speaking, green nanotechnology refers to the use of nanotechnology to enhance the environmental sustainability of processes, producing veritable negative externalities [1, 2]. It also encompasses the use of products of nanotechnology to enhance sustainability. It includes green nanoproducts and using nanoproducts in support of sustainability. Technological challenges, deep scientific vision and scientific insight are the pivotal elements of scientific rigor in green nanotechnology today. Green nanotechnology has been described as having a major pivotal role in the development of clean technologies.

1.5 The Scientific Doctrine and Truth Behind Nanotechnology Applications

Today, nanotechnology needs immense scientific vision and deep scientific forbearance. Green engineering and green science are the order of today's scientific research pursuits. Scientific doctrine, scientific truth and futuristic vision are all forerunners to a greater emancipation of green nanotechnology. The water shortage crisis is challenging the scientific fabric of today. Heavy metal and arsenic groundwater contamination are changing the face of civilization and the scientific endeavor of humans. The doctrine of the science of green nanotechnology and nanotechnology needs to be re-envisioned and redefined with every step of human life today. Technological vision and scientific validation are reframing the world of green nanotechnology and sustainable chemistry. The vision of environmental and energy sustainability and its immediate needs are forerunners to a greater realization of environmental engineering science today. Environmental engineering and green nanotechnology are the two opposite sides of the visionary coin.

Today scientific doctrine and scientific cognizance are the pathway to newer scientific regeneration and rejuvenation. Global water challenges and environmental engineering issues are veritably changing the face of scientific research pursuits today. Arsenic and heavy metal groundwater contamination are the vexing issues of scientific empowerment today. Technological validation and scientific vision are the definite rules of today's scientific research pursuit. Human civilization's immense scientific rigor, the academic rigor behind today's environmental engineering research and

the wide avenues of nanotechnology will all lead along a long and visionary path towards the true emancipation and realization of green nanotechnology and green chemistry. Scientific innovation and scientific advancements are on the pathway to immense rejuvenation and forbearance. This chapter emphasizes the success of application of green nanotechnology with the sole objective of furthering science and engineering [1, 2].

1.6 Recent Research Pursuit in the Field of Nanotechnology

Nanotechnology and nanoscience are the revolutionary avenues of scientific endeavor. The challenge and vision of science and engineering need to be redefined and re-envisioned in relation to scientific history and scientific vision with the passage of time. Today nanotechnology is the visionary domain of scientific research pursuit. The vision and challenge of this domain will be to open new windows of innovation in the field of nanotechnology in years to come.

The European Commission Report of 2011 [3] clearly discusses successful European nanotechnology research. According to the report, nanotechnology is an outstanding science and technology endeavor which matches the future needs of society. The fruits of nanotechnology are vast and versatile and cross visionary scientific frontiers. Nanotechnology is the new frontier of science and technology in Europe and around the world. Validation of nanoscience and nanotechnology are of utmost importance in the future of scientific and academic rigor. Setting up appropriate methodologies is a relevant and uphill task in the future of nanotechnology [3]. This report gives a sharp glimpse into the application of nanotechnology in energy and the environment, electronics and ICT, industrial applications, textiles, nanomaterials, nanomedicine and a wider approach towards ethical, legal and social aspects [3]. The avenues of nanotechnology are far-reaching and well-researched today. Technology barriers need to come down as nanoscience enters a newer era [3].

The United States Environmental Protection Agency White Paper of 2007 [4] provides a deep insight into mainly the environmental benefits of nanotechnology. Technology and engineering science are surpassing vast scientific boundaries. Humankind's immense scientific prowess is redefined as engineering and technology that ushers in a newer era in the field of nanotechnology. The authors touch upon the environmental benefits of nanotechnology, risk assessment of nanomaterials, EPA's research needs for nanomaterials and future recommendations [4]. The vision of

nanotechnology, the futuristic vision of science and the world of academic and scientific rigor will lead to the true realization of environmental protection and nanotechnology. The science of nanotechnology according to this report needs to be veritably re-envisioned and readdressed with the passage of scientific history and time.

1.7 Scientific Endeavors in the Field of Green Nanotechnology

Green technology and sustainability engineering are the path to immense scientific regeneration and scientific forbearance. Today, the avenues of scientific endeavor are ushering in a newer visionary era in green nanotechnology. Global water issues, global drinking water crisis and groundwater contamination by heavy metals are challenging the wide scientific frontier. This chapter pointedly focuses on the immense scientific vision and forbearance needed in the pursuit of green technology research.

Nanotechnology for green innovation was widely redefined by OECD Science, Technology and Industry Policy Paper No. 5 (2013) [5]. This paper brings together widespread and vital information collected through discussions and projects undertaken by the OECD Working Party on Nanotechnology (WPN), which is absolutely relevant to the development and use of nanotechnology for green sustainable development and vast innovation [5]. The aim and objective of this paper is to provide background information for future work by the WPN on the application of nanotechnology for green engineering and innovation. Green nanotechnology is today ushering in a new era in the furtherance of science and technology [5]. Technological vision, scientific motivation and vast academic rigor are forerunners to a greater emancipation of nanoscience and nanotechnology. Humankind today is in a state of immense scientific distress due to vast challenges. In their paper, the authors gleaned the tremendous challenges, deep scientific crisis and the success of nanoscience and nanotechnology today. The entire treatise is divided into three sections; 1) a thorough introduction to nanotechnology, 2) strategies for green innovation and green engineering through nanotechnology, and 3) the impact of green nanotechnology [5]. The immediate need for sustainable development of affordable and safe methods of addressing global challenges in areas, such as energy, the environment and health, has never been so pressing as in this century. Energy and environmental sustainability are the pillars and pivotal elements of today's scientific and engineering endeavors [5]. The global demand for energy is expected to

increase by more than 30% between 2010 and 2035 [5]. More than 800 million people throughout the world are currently without proper access to drinking water. Such challenges have changed the scientific mindset of scientists, engineers, policymakers and politicians in developed and developing economies. Scientific self-control and deep insight are the supports of a larger vision for a greater emancipation of green nanotechnology [5]. Green innovation targets the reduction of environmental impacts by increasing energy efficiency, reducing waste or greenhouse gas emissions and by minimizing the consumption of nonrenewable raw materials. Scientific research pursuits in green nanotechnology are today ushering in a new era of sustainable development and green engineering. The technology and science of green nanotechnology and engineering are highly advanced today. Scientific success, a visionary path and overcoming obstacles will all go a long way towards environmental sustainability and environmental engineering science today. Since it began its work in 2007, the OECD Working Party on Nanotechnology (WPN) developed a number of feasible projects addressing emerging and far-reaching policies of science, technology and innovation related to the cogent development of nanotechnology [5]. Nanotechnology of green innovation, or green nanotechnology, aims for wide-ranging scientific products and processes that are immensely safe, energy efficient, reduce waste and deeply lessen greenhouse gas emissions. Technological validation is of utmost importance in the progress of scientific and academic rigor. The WPN treatise widely researches the success of green nanotechnology and the authors pointedly focus on the immense scientific potential and deep scientific vision behind green engineering [5].

Karn and Bergeson [6] clearly present thoughtful insights into the immense promises and uncertainties in the vast world of green nanotechnology today. The technology and engineering science of nanoscience and nanotechnology are highly advanced today, ushering in a new technological era [6]. Green nanotechnology today is redefining the world of success in the field of application of nano-enabled products to human society. The article of Karn and Bergeson describes green nanotechnology and discusses the many feasible reasons why traditional chemical assessment and management approaches may not be enough in the pursuit of scientific research [6].

A project report by the Woodrow Wilson International Center for Scholars [7] describes green nanotechnology with immense clarity. Technological advancements, the vision to move forward and the targets of science will all lead towards the true realization of nanotechnology for green innovations [7]. In this report, clean and green nanotechnology,

nano-enhanced green technology and the global green nanopolicy are well observed. According to this report, the principles of green chemistry encompass prevention of waste, design of safer chemicals, design of less hazardous materials and less hazardous process syntheses. Also, this wide scientific frontier involves use of catalysts, avoids chemical reagents, maximizes atom economy and visualizes reuse of used products. Green chemistry also involves the minimization of the potential of accidents and the success of chemical process safety. This paper rigorously points out the scientific success and the deep scientific forbearance behind green nanotechnology [7]. Scientific vision is in a state of immense distress today as science and technology moves forward. The challenge of this research pursuit goes beyond scientific imagination and opens up new areas of endeavor and vision. This insightful report investigates the endeavors of research and educational institutions in North America [7].

Nath and Banerjee [8] provide clear insight into the success of green nanotechnology and its interfaces with medical biology. The development of eco-friendly technologies in material synthesis is of vital importance to extend their biological and biomedical applications. Today, technological splendor and depth are in a state of immense regeneration due to newer thoughts [8] Their review highlights the classification of nanoparticles, giving vital emphasis to the biosynthesis of metal nanoparticle by viable organisms [8]. The science of nanoparticles is always growing and crossing visionary boundaries. Biomedical engineering is also surpassing far-reaching scientific frontiers today. Technological validation and profundity are of utmost need as green nanotechnology ushers in a new era in the field of nanoscience and nanotechnology. This treatise also focuses on the applications of the biosynthesized nanoparticles in a wide spectrum of potential areas of medical biology, including catalysis, targeted drug delivery, cancer treatment, antibacterial agents and as biosensors [8]. Nanomaterials, with characteristic dimensions in the range of 1–100 nm, are at the leading edge of the scientific research pursuit in nanotechnology [8]. Nano vision and nanotechnology, especially metal nanoparticles, have received immense scientific interest in diverse fields of applied science, ranging from materials science to biotechnology. Because of the extremely small size and high surface volume ratio of nanoparticles, the physicochemical properties of nanoparticles-containing materials are quite different to those of the bulk materials. Scientific vision and scientific forbearance are the pillars of scientific research pursuit today. The authors touched upon classification of nanoparticles such as liposomes, superparamagnetic nanoparticles, fullerenes such as buckyballs and carbon nanotubes, dendrimers, quantum dots and liquid crystals [8]. The authors rigorously dealt with synthesis of metal

nanoparticles by traditional physical and chemical methods. The methods encompass laser ablation, inert gas condensation, sol-gel method, hydrothermal synthesis, and a wide range of colloidal methods. The authors also described bio-inspired green nanomaterial synthesis [8].

Virkutyte and Varma [9] intently discussed green synthesis of metal nanoparticles with more research forays into biodegradable polymers and enzymes in stabilization and surface functionalization. Engineering science and technology of green synthesis are ushering in a new era of scientific vision and scientific sagacity. Current scientific breakthroughs in green nanotechnology are intensely capable of transforming many of the existing processes and diverse products that enhance environmental quality, reduce pollution, and conserve natural resources. Science is moving through difficult terrains today. Scientific research avenues, the futuristic vision and the intense academic rigor of metal nanoparticles and biodegradable polymers are opening up new avenues of scientific and engineering research pursuit today [9].

Schwarz [10] presented a clear discussion of green nanotechnology with its tremendous vision and scientific forbearance. Nanotechnology has recently been identified along with principles of sustainability and with "green agenda" [10]. Schwarz's paper discusses and argues that deeper lying societal and cognitive structures are at work to target the true realization and true emancipation green nanotechnologies [10]. Green nanotechnology is today understood as a boundary concept in which wide and disparate discourses are dealt with immense scientific vision. This treatise also pointedly focuses on green nanotechnology and sustainability with the sole objective of furtherance of science and engineering. His paper gives a wider view of the relevance of green nanotechnology in the German-speaking countries in Europe. Green nanotechnology today is replete with scientific vision and encompasses technological validation and scientific fortitude [10].

Yehia *et al.* [11] dealt with immense lucidity the structural and magnetic properties of nanocrystalline spinel ferrite powders. These are synthesized by a novel green nanotechnology derivative of the sol-gel method. Nickel ferrite ($NiFe_2O_4$) has an inverse spinel structure. The science of nanotechnology and its wide scientific vision are documented with forbearance and deep scientific understanding in this treatise [11].

Shawkey *et al.* [12] presented an immensely insightful discussion of green nanotechnology and the anticancer activity of silver nanoparticles using *Citrullus colocynthis* aqueous extracts. Green nanotechnology and biotechnology are the two opposite sides of the visionary coin today. Green synthesis of metal nanoparticles is a growing research avenue because of

their potential applications in nanomedicines [12]. The science of nanomedicines is wide-ranging and far-reaching. The green synthesis of silver nanoparticles (SNPs) is a comparatively convenient, cheap and environmentally safe approach compared to chemical synthesis [12]. Technology is highly advanced today, crossing wide scientific frontiers. The engineering science of green nanotechnology today is replete with scientific vision and deep scientific cognizance. In their study, the authors synthesized SNPs from $AgNO_3$ using aqueous extracts (AEs) of fruits, leaves, roots and seeds of *C. colocynthis* as reducing and capping agents [12]. Nanoparticles of free metals have been extensively investigated because of their unique physical properties, chemical reactivity, biological labeling, biosensing, drug delivery, antibacterial activity, antiviral activity, detection of genetic disorders, gene therapy and DNA sequencing [12]. Green nanotechnology is opening new windows of scientific innovation today and deep scientific instinct in years to come. The present study explores the potential antitumor activity of greenly synthesized SNPs on cancer cells [12]. The wide world of green nanotechnology, the futuristic vision of cancer biology and the deep academic and scientific rigor will all lead to a long and visionary way towards the true emancipation of nanoscience today [12].

With immense foresight and clarity, Hutchison [13] discussed greener nanoscience as a proactive approach for advancing applications and reducing the implications of nanotechnology. Scientific cognizance, scientific sagacity and deep scientific understanding are the forerunners of research pursuit today [13]. A wide futuristic vision and overcoming the challenges of science and engineering will lead to the true realization and application of green nanotechnology. Nanotechnology continues to offer new materials and applications that will highly benefit human society, yet there is an ever-growing concern about the potential health and environmental impacts of the production and widespread use of nanoproducts [13]. The focus of this treatise is on the nanomaterial complexities through coordinated research on the applications and implications of new materials. Greener nanoscience is a revolutionary area of nanoscience today. Technological profundity and the scientific vision of the domain of green nanotechnology are veritably changing the face of scientific research pursuit today. Hutchison's treatise pointedly focuses on the research agenda in minimizing global nanomaterials and green technology issues [13].

Albrecht *et al.* [14] lucidly described green chemistry and the health implications of nanoparticles. Spectacular developments in nanotechnology have taken place in nanotechnology with disregard towards the veritable health issues involved in it. There are practically no specific regulations on nanoparticles except for existing regulations covering the same

material in bulk form [14]. Technology and engineering science are today faced with immense scientific obstacles and barriers. This review focuses on potential health effects of nanoparticles along with medical applications of nanoparticles, including imaging, drug delivery, disinfection and tissue repair. Validation of science and technology are slowly gearing up today towards a newer visionary scientific future in green chemistry and green nanotechnology [14].

Fagan *et al.* [15] discussed green nanotechnology with deep and cogent insight, along with the development of nanomaterials for environmental and energy applications. The technology and engineering science of green nanotechnology are highly advanced today and cross visionary boundaries. Fagan *et al.* discuss the synthesis of various nanomaterials for green nanotechnology applications in incisive detail. Special attention is focused on the development of emerging areas such as environmental and energy areas [15]. The challenge and vision of the technology and science of green nanotechnology are reaching immense scientific heights as human civilization enters into a newer scientific era. In this treatise, various approaches for preparing nanostructured photocatalysts, such as titanium dioxide, zinc oxide, iron oxide, and metal sulfides, and different conventional methods and novel methods, including sol-gel, hydrothermal, microwave-assisted and sonochemical methods, are discussed in deep detail [15]. The futuristic vision of nanotechnology, targets of scientific rigor and scientific passion and cognizance will all lead to a long and visionary way towards the true realization of nanotechnology science today [15].

1.8 Challenges and Opportunities in the Field of Green Nanotechnology

Today the challenges and opportunities in the field of green nanotechnology are surpassing vast and versatile scientific frontiers. The wide futuristic vision of nanotechnology, the technological challenges and the vision to move forward will all lead to a long and visionary way towards the true emancipation of nanoscience today. Human scientific endeavors in green nanotechnology and sustainable chemistry are transforming the visionary world of nanoscience and nanoengineering. In this chapter, the authors pinpoint the scientific success, immense scientific potential and future research trends in the field of green nanotechnology. Humankind's immense vision and scientific prowess and the girth of scientific endeavor are forerunners of newer scientific research pursuits and innovations. Today, science and engineering are colossal with a definite vision and willpower of their own.

Science, engineering and technology are transforming the scientific genre of nanotechnology today.

1.9 Environmental Sustainability, Humankind's Progress and Vision of Science

Environmental sustainability and humankind's progress are in a state of immense scientific contemplation and deep scientific introspection today. Today, the progress of human beings is stalled and re-envisioned as regards sustainable development and environmental sustainability. The vision of the science of nanotechnology needs to be reframed and restructured regarding application and scientific potential. Green nanotechnology is in a state of immense scientific restructuring and scientific revamping today. Environmental sustainability and human scientific research pursuit are two opposite sides of the visionary coin today. Dr. Gro Harlem Brundtland, the former Prime Minister of Norway, defined and envisioned the science of sustainability. While the modern concept of sustainable development is derived mostly from the 1987 Brundtland report, it is also rooted in earlier ideas about sustainable forest management and twentieth century environmental concerns. Technological vision, deep introspection and scientific candor will all lead to a long and visionary way towards the true emancipation of green nanotechnology and green engineering today. Environmental sustainability today stands amid immense scientific revamping and, in a similar vein, deep crisis due to frequent environmental disasters and wide environmental hiatus periods. The question of sustainability today stands widely challenged and is deeply entwined with past scientific history and vision and the passage of time.

1.10 Scientific Cognizance, the Greatness of Research Pursuit and Green Nanotechnology

Scientific awareness is highly challenged today, with green nanotechnology standing amid immense scientific comprehension and deep introspection. Environmental and energy sustainability are in a state of deep crisis today due to untold environmental catastrophes. The greatness of scientific research pursuits needs to be veritably overhauled as science and technology enters a new visionary age. Green nanotechnology and sustainable development are the two opposite sides of the visionary scientific coin today.

1.11 Global Water Crisis – The Vision and Challenge of Science

The global water crisis and the visionary world of water research and development initiatives today stand in the midst of deep scientific introspection and wide scientific girth. The vision and the challenge of science are the pillars of scientific endeavor today. Global water shortage, drinking water contamination and industrial wastewater treatment will all lead to a long and visionary way towards the true emancipation of global sustainability science and the true realization of environmental sustainability. The success and vision of science today are immense and groundbreaking. Technological validation and scientific candor are the pathway to scientific regeneration and scientific revamping. Many developing nations as well as developed nations are in the throes of a deep disaster regarding groundwater contamination and a drinking water crisis. Science and engineering has no answers to the immense questions and vexing issues of arsenic and heavy metal groundwater contamination. The success of scientific endeavors is in a state of deeply entrenched global water crisis. The immense scientific prowess of human beings and their civilization's scientific achievement along with the scientific girth and determination are the veritable forerunners of a newer scientific and technological age. Water scarcity and global water hiatus periods are reaching immense heights and taking on disastrous proportions today.

1.12 Heavy Metal and Arsenic Groundwater Contamination – The Vision for the Future

Heavy metal and arsenic groundwater contamination is a primordial issue, which has continued to pose a vexing problem over the course of scientific history and in the pursuit of scientific research in today's day-to-day civilization. Technological profundity today stands in the midst of deep catastrophe with the rising issues of global water shortage and contamination of drinking water. Developing and developed economies are in a veritable quagmire of arsenic groundwater contamination. Green nanotechnology and green chemistry are in the throes of a vicious scientific struggle to control their destiny. Yet environmental engineering science has a wide range of answers to this grave global water concern. The vision for the future needs to be reframed and redefined following the course of scientific history, scientific vision and time. Developing countries like India or

Bangladesh are in a veritable quagmire because of the scientific disaster brought about by the global water crisis. In this chapter the authors bring to the forefront the success of new technologies and innovations such as membrane science, advanced oxidation processes and the wide domain of nanoscience and nanotechnology. The crisis of drinking water contamination goes beyond scientific imagination and scientific adjudication. This chapter gives a veritable glimpse into the success of scientific endeavors in the field of green nanotechnology, green chemistry and sustainable chemistry.

Hashim *et al.* [16] discussed with immense lucidity remediation technologies for heavy metal contaminated groundwater. The contamination of groundwater by heavy metal is of grave concern for the progress of science and the vast progress of human civilization. Remediation of contaminated water is of highest priority since billions of people throughout the world use it for survival. Today, engineering science and technology are revamping the broad scientific panorama and vast scientific vision. Humankind's immense scientific prowess, scientific stature and futuristic vision are forerunners to the true realization of groundwater remediation technologies. In their paper, a large number of approaches for groundwater treatment have been reviewed, which are mainly classified under three large categories: chemical, biochemical/biological/biosorption, and physical-chemical absorption processes.

1.13 Groundwater Remediation and Water Purification Technologies

Groundwater remediation and removal of arsenic or heavy metal from drinking water stands as a major imperative to the furtherance of environmental engineering science today. Despite scientific progress, the questions concerning arsenic groundwater contamination have remained unanswered up till now. Technological profundity and scientific success are the pillars of environmental engineering science and nanotechnology today. Water purification technologies are in the throes of a deep crisis and an unimaginable scientific catastrophe. The scientific and academic rigor of groundwater remediation are being challenged today due to the intricacies of the pursuit of wide scientific research. Humankind today stands on the threshold of deep scientific vision and scientific introspection. Today, water technologies and environmental engineering science are replete with scientific forbearance and technological profundity. Drinking water contamination is in a state of immense scientific contemplation. Science and

the vision of humankind need to be readdressed and re-envisioned as scientific forbearance and profundity progresses.

1.14 Application of Nanotechnology in Industrial Wastewater Treatment

Nanotechnology applications are changing the face of human scientific endeavor. The crisis of environmental engineering science is highly inevitable, as the loss of ecological biodiversity and frequent environmental catastrophes are changing the face of human civilization. Industrial wastewater treatment, drinking water treatment and groundwater remediation are of utmost importance in today's world of scientific and academic rigor. Nanotechnology is a veritable answer to the numerous questions of industrial wastewater treatment. Environmental catastrophes and stringent environmental restrictions are challenging the scientific landscape and the deep technological vision. Scientific candor, scientific forbearance and deep scientific understanding are the forerunners to a newer scientific genre and scientific vision. Nanoscience and nanoengineering are changing the face of scientific endeavors today. The global water shortage and global water catastrophe are the primordial scientific issues of today.

Nanotechnology has been called the Second Industrial Revolution. Its seemingly limitless potential will continue to inspire innovations and discoveries in a wide array of beneficial applications and briskly transform human society. Despite the hope and definite promise nanotechnology brings, engineered nanomaterials, the tiny engines driving this new transformative technology, also generate a widely held apprehension due to their largely unknown implications on human health and the environment. Thus ushers in green nanotechnology, an approach to managing the potential environmental, health, and safety (EHS) risks associated with the manufacture and use of nano-enabled products while veritably fostering their responsible development and application.

Karn *et al.* [6] delineated with great lucidity the widely held promise and uncertainty in green nanotechnology. Their article describes green nanotechnology and discusses the reasons why traditional chemical-assessment and management approaches may not be adequate in all cases when applied to nanomaterials. Technological vision, the wonders of science and the futuristic vision of green nanotechnology will all lead to a long and visionary way towards the true transformation of nanovision today. Nanotechnology encompasses the science of nanomaterials, forms of matter in a particular size range, roughly between 1 and 100 nanometers (nm).

Nanomaterials are bigger than most molecules and smaller than bacteria cells. They can consist of groups of single elements such as metals, groups of compounds such as metal oxides, tubes or wires of elements, soccer ball structures, branching structures, and infinite combinations of these. Science and technology is highly advanced today as green nanotechnology surpasses visionary frontiers. This chapter widely researches the scientific success, the deep scientific potential, and the wide scientific vision in the field of application of green nanotechnology and green engineering. Sustainable chemistry, environmental sustainability and sustainability engineering are in the path of immense scientific regeneration and scientific rejuvenation today. Humankind today is on the path to deep scientific vision and rejuvenation as nanotechnology enters a new phase of scientific achievement and determination. While nanomaterials are intentionally designed to be unique, what is common to all is their super small size, which imparts properties that are surprising and special. The science and engineering of nanomaterials are entering a new phase of technological challenges and scientific profundity. This chapter widely observes the immense scientific potential, the scientific understanding and the scientific contemplation behind nanomaterials, engineered nanomaterials and the wide domain of nanotechnology. Electric properties also can change at the nanoscale. The rolled-up carbon chicken-wire structure of carbon nanotubes (CNTs) is a conductor when the chicken wire falls in a straight line.

According to Karn *et al.* [6], there are two aspects to green nanotechnology. The first involves nanoproducts that provide solutions to environmental challenges. These green nanoproducts are used to prevent harm from known pollutants and are incorporated into environmental technologies to remediate hazardous waste sites, clean up polluted streams, and desalinate water, among other applications. Technology needs to be revamped and restructured with the progress of scientific history, scientific vision and time.

1.15 The Vision of Renewable Energy Technologies

Renewable energy technologies are the visionary technologies of today and tomorrow. Energy sustainability and renewable energy technology are the two opposite sides of the visionary coin. Humankind today stands amid deep scientific hope and optimism. Technological challenges and scientific vision need to be re-envisioned with the passage of scientific history and time. Renewable energies are the next generation technologies. The path of science and the vision of scientific endeavor are immensely far-reaching today in the domain of renewable energy technologies. Today, green nanotechnology and sustainable engineering are linked with

renewable energy technologies in a visionary way. This chapter gives a wide vision and this section treads a visionary path in the direction of newer and futuristic trends in the field of renewable energy technologies such as solar energy, wind energy and wave energy. Technology is highly advanced today. The progress of humankind, the immense scientific and academic rigor and the future path of alternate energy sources will all lead to a long and visionary way towards the true emancipation of renewable energy technology today. Human civilization and scientific research pursuits are in a state of immense distress and unimaginable catastrophe, as environmental disasters, industrial pollution and loss of ecological biodiversity is destroying the deep scientific fabric [17]. Science and its pursuit and deep vision needs to be readdressed and re-envisioned with the passage of human history and time. Green nanotechnology and the wider domain of nanoscience and nanotechnology are rewriting scientific history today. This chapter explores the wider vision and vast challenges facing technology in order to have proper and true emancipation of nanotechnology today [18].

1.16 Future Research Trends and Flow of Thoughts

Future research trends are veritably opening new avenues of scientific thought and scientific vision. Nanoscience and nanotechnology are ushering in a new era in the field of scientific vision and forbearance. The scientific and technological truth needs to be re-envisioned as regards application of nanotechnology and green nanotechnology. The future of human civilization and human research pursuit lies in the hands of scientists and engineers. The science of green nanotechnology is witnessing a new beginning with the advent of sustainable chemistry and the wide domain of sustainable engineering. The question of energy and environmental sustainability is creating immense scientific obstacles and barriers. Future scientific endeavors lie in unfolding the unknown areas of the science and technology of green nanotechnology. Green engineering and green chemistry are ushering in a new era in the field of nanotechnology today. Global water research and development initiatives also encompass green chemistry and sustainable engineering. This chapter gives a wide glimpse of the scientific success and scientific potential of application of green nanotechnology. Today green nanotechnology is surpassing wide scientific frontiers. The immense visionary scientific and academic rigor of nanoscience and nanotechnology are the forerunners to a greater emancipation of green engineering and green nanotechnology today. Humankind's immense scientific prowess and the progress of science will be opening new windows of

scientific innovation and scientific instinct for decades to come. The future perspectives of science are immensely bright and far-reaching [19].

1.17 Conclusion and Future Perspectives

The science and engineering of green nanotechnology are moving towards newer knowledge dimensions and are crossing visionary boundaries. Environmental engineering science and environmental sustainability are veritably changing the scientific landscape [17–19]. The future progress of science and academic rigor lies in nanotechnology or green nanotechnology in particular. Technological vision, scientific splendor and futuristic vision are all forerunners to a newer visionary era in the field of sustainable development and green nanotechnology. Green chemistry, sustainable chemistry and green nanotechnology are challenging the wide scientific panorama today. This chapter gives a wider glimpse of the science of green nanotechnology with a greater emphasis on sustainable development and green engineering. Scientific success, scientific vision and scientific forbearance are changing the face of the pursuit of scientific research today. Chemical process engineering and environmental engineering science veritably need to be re-envisioned and re-envisioned with the progression of scientific history, scientific vision and time. Scientific fortitude and grandeur are on the path to scientific regeneration today, as this century moves towards a new era of space technology and nuclear science. Today science is a colossus with a wide and definite vision and stature of its own. Technological validation and scientific profundity needs to be restructured with the definite vision of nanotechnology, green engineering and environmental engineering science today. The scientific success and scientific splendor of nanotechnology will surely bear new and definite fruits with the progress of scientific and academic rigor. The challenge of green nanotechnology is just as immense and far-reaching. The targets of science and the immense success of nanotechnology applications will surely open windows of innovation for the furtherance of science in years to come.

References

1. Wikipedia, Green Nanotechnology, Wikipedia, the free encyclopedia, 2017.
2. Wikipedia, Green Chemistry, Wikipedia, the free encyclopedia, 2017.
3. European Commission Report, Successful European Nanotechnology Research, Outstanding science and technology to match the needs of the future society, 2011.

4. United States Environmental Protection Agency Report, Nanotechnology White Paper, 2007.
5. OECD, Nanotechnology for Green Innovation, OECD Science, Technology and Industry Policy Papers, No.5, OECD Publishing, 2013.
6. Karn, B.P., Bergeson, L.L., Green nanotechnology: Straddling promise and uncertainity, *Nat. Res. Environ.,* 24, 9–23, 2009.
7. Woodrow Wilson International Center for Scholars, Project for Emerging Technologies, Green Nanotechnology: Its easier than you think, April 2007.
8. Nath, D., Banerjee, P., Green nanotechnology: A new hope for medical biology, *Environ. Toxicol. Pharmacol.,* 36, 997–1014, 2013.
9. Virkutyte, J., Varma, R.S., Green synthesis of metal nanoparticles: Biodegradable polymers and enzymes in stabilization and surface functionalization, *Chem. Sci.,* 2, 837–846, 2011.
10. Schwarz, A., Green dreams of reason, Green nanotechnology between visions of excess and control, *Nanoethics.,* 3, 109–118, 2009.
11. Yehia, M., Labib, S., Ismail, S.M., Structural and magnetic properties of nano-$NiFe_2O_4$ prepared using green nanotechnology, *Phy. B.,* 446, 49–54, 2014.
12. Shawkey, A.M., Rabeh, M.A., Abdulall, A.K., Abdellatif, A.O., Green nanotechnology: Anticancer activity of silver nanoparticles using *Citrullus colocynthis* aqueous extracts, *Adv. Lif. Sci. Tech.,* 13, 60–70, 2013.
13. Hutchison, J.E., Greener nanoscience: A proactive approach to advancing applications and reducing implications of nanotechnology, *ACS Nano.,* 2, 395–402, 2008.
14. Albrecht, M.A., Evans, C.W., Raston, C.L., Green chemistry and the health implications of nanoparticles, *Green Chem.,* 8, 417–432, 2006.
15. Fagan, R., Han, C., Anderson, J., Pillai, S., Falaras, P., Byrne, A., Dunlop, P.S.M., Choi, H., Jiang, W., O'Shea, K., Dionysiou, D., Shamim, N., Green nanotechnology: Development of nanomaterials for environmental and energy applications, in: *Sustainable Nanotechnology and the Environment: Advances and Achievements*, pp. 201–209, Americal Chemical Society: Washington D.C., 2013.
16. Hashim, M.A., Mukhopadhayay, S., Sahu, J.N., Sengupta, B., Remediation technologies for heavy metal contaminated groundwater, *J. Environ. Man.,* 92, 2355–2388, 2011.
17. Palit, S., Nanofiltration and ultrafiltration—The next generation environmental engineering tool and a vision for the future, *Int. J. Chem. Tech. Res.,* 9, 848–856, 2016.
18. Palit, S., Filtration: Frontiers of the engineering and science of nanofiltration—a far-reaching review, *CRC Concise Encyclopedia of Nanotechnology*, pp. 205–214, Taylor and Francis, 2016.
19. Palit, S., Advanced oxidation processes, nanofiltration, and application of bubble column reactor, *Nanomaterials for Environmental Protection,* pp. 207–215, John Wiley & Sons, Inc., 2015.

2

Green Synthesis of Metal-Based Nanoparticles and Their Applications

Shamaila Sajjad[1]*, Sajjad Ahmed Khan Leghari[2], Najam-Ul-Athar Ryma[1] and Sidra Anis Farooqi[1]

[1]International Islamic University, Islamabad, Pakistan
[2]Pakistan Institute of Engineering and Applied Sciences, Islamabad, Pakistan

Abstract

Nature consists of rich sources of unrefined concentrates from hundreds of flora and fauna like earth and marine plants, aquatic living beings, microbes and so forth. These sources have diverse compositions of synthetic complexes which may be used instead of unsafe chemical compounds as harmless reducing and capping agents in synthesis procedures. Currently, the biosynthesis of nanoparticles is settled as a growing region of nanoscience examination and development. Due to the unique properties of nanoparticles, they have an acclaimed reputation compared to bulk materials. A lot of physical, chemical, biological and hybrid methods were applied successfully in the synthesis of numerous inorganic nanoparticles, yet they are expensive and require the use of harmful chemical reagents. Consequently, our surroundings are undergoing remarkable damage and a huge amount of undesirable substances is being emitted. Today, we need to find the enigmas which might be present in nature for alternative environmentally friendly and sustainable strategies involving less toxic reagents. These new clean technologies can drastically reduce environmental contamination and decrease the risk to human health as a consequence of using toxic chemicals and solvents. This chapter presents a brief but concise assessment and modern status of the latest methodologies evolved to this end and outlines the strategies enmeshed in the numerous procedures involved.

Keywords: Green synthesis, metal nanoparticles, botanical extract, green oxide nanoparticles, microbial extract, applications

**Corresponding author*: shamaila.sajjad@iiu.edu.pk, shalisajjad@yahoo.com

Suvardhan Kanchi and Shakeel Ahmed (eds.) Green Metal Nanoparticles, (23–77)
© 2018 Scrivener Publishing LLC

2.1 Introduction

The field of nanotechnology is one of the notable active analysis areas in modern materials science [1, 2]. Nanoparticles reveal new or amended properties that are supported with particular characteristics like size, distribution and morphology. There have been enormous advancements in the arena of nanotechnology within recent years related to the synthesis of nanoparticles with specific size and morphology that are reckoned for specific needs [3]. The extensive practical application of nanoparticles (NPs) (particles having single or more lengths less than 100 nm) is attributed to their numerous rare, exceptional and fascinating characteristics which are appreciated over their bulk correspondents [4–6]. The main task is to improve specific approaches to synthesize noble NPs of definite size, specific shape, desired composition, and well-ordered dispersity that influence their physical, chemical, catalytic, optical, magnetic, electronic, and electrical properties making them ideal candidates for environmental, biomedical and biotechnological applications [7–9]. The synthesis of biofunctional nanoparticles is extremely vital, and it has recently caught the attention of diverse analysis teams, creating a perpetually evolving space [10–13]. To address the growing demand for eco-friendly nanoparticles, researchers have utilized inexperienced strategies for the synthesis of varied metal oxide nanoparticles for pharmaceutical applications [14, 15]. There is an enormous number of physical, chemical, biological and hybrid procedures which are now usually used to fabricate different types of NPs with the preferred characteristics [14–18]. The synthetic procedures for NPs are listed in Figure 2.1. Usually the physical and chemical techniques are applied extensively but the physical techniques to synthesize NPs are highly expensive; however, the chemical techniques are detrimental to the environment and living organisms [19–21]. Development of these synthesis techniques for large-scale production is restricted due to the high production costs resulting from unexpected energy consumption, use of noxious organic solvents, fabrication of precarious intermediates and creation of harmful waste products, resulting in environmental contamination and numerous biological hazards. Mostly aqua chemical synthesis of nanoparticles is prevalent amongst several fabrication procedures. Agglomeration or aggregation generally come about during synthesis due to the occurrence of attractive forces among the nanoparticles.

Therefore, it is necessary to add some capping agent to avoid aggregation and to achieve the desired morphology of product. Figure 2.1 shows the classification of different NP synthesis techniques. Besides being contaminants of nature, various other problems also accompany these techniques;

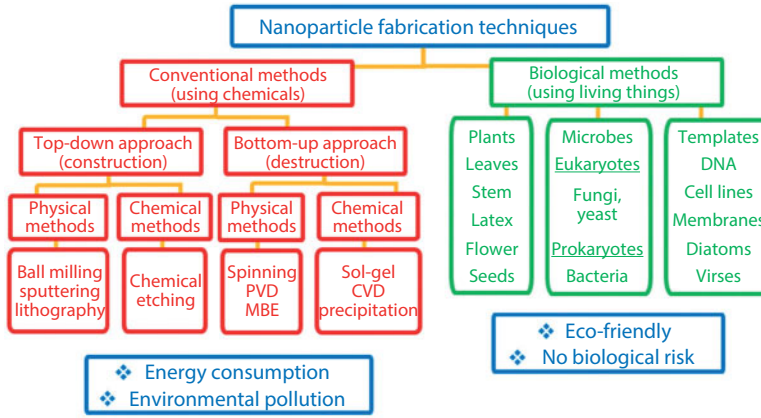


Figure 2.1 Classification of different NP synthesis methods.

for instance, slow production rate, inadequate growth and distorted structure of synthesized NPs. Size reduction may also lead to increased reactivity and toxicity of synthesized material. Hence, prior to the wide-scale implementation of these reactions, it is essential to predict the prospective hazards to the eco-system by making an allowance for the entire chemical process relating to all the species involved during the reaction mechanism.

The advancement, development and application of nanocolloids in medicine can present a whole new opportunity for the diagnosis and treatment of different diseases [22]. Furthermore, the utilization of poisonous, harmful chemicals, along with other biological consequences, has considerably restricted biomedical applications of nanomaterials, particularly in clinical fields [23]. These conditions have elevated an increasing ultimatum to inaugurate alternative reliable, nonhazardous and eco-friendly technologies for the production of NPs to expand their applications [24–26]. The restricted use of toxic precursors subsequently decreases the quantity of impurities and by-products, ensuing in cost effectiveness and the fabrication of desired products in high yields with no biological danger [7, 27].

There are several options to attain the goals presented in Figure 2.2. Previous reports cite the usage of microorganism, such as bacteria [28], algae [29], yeast [30] and fungi [31], for the biosynthesis of NPs. Lately, numerous plant extracts [7, 11, 32–48, 49–114], diatoms [115, 116] and human cells [117] have been shown to be innovative resources for their capability to produce safe and nontoxic nanoparticles, including iron, cobalt, gold, silver, platinum, iron oxide, zinc oxide alloys, sulfides, quantum dots, etc. During the green synthesis of NPs, products from nature or those imitative of natural products have been used as reducing and capping

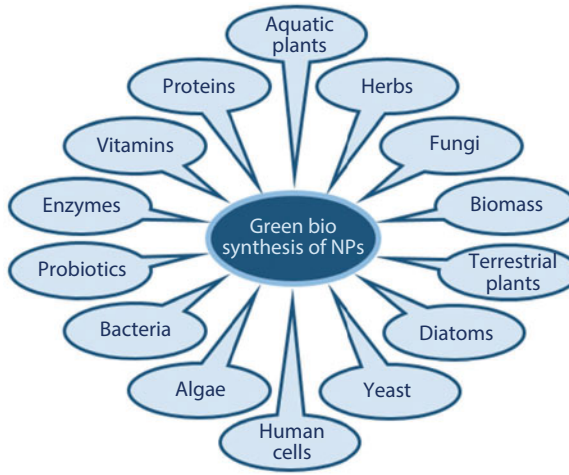


Figure 2.2 Various natural resources used to synthesize green NPs.

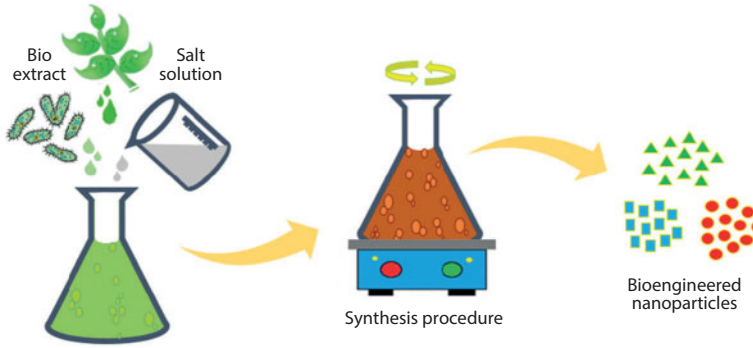


Figure 2.3 Green synthesis mechanism.

agents. The methods involved are typically simple, environmentally friendly and naturally compatible one-pot processes. It has been proved by various studies that the reductive abilities of the proteins and metabolites that are present in these biological systems can change inorganic metal ions into metal NPs [118–121]. Figure 2.3 shows a basic schematic diagram of the mechanism of green synthesis by using plant extracts.

This chapter highlights the recent research activities that focus on the green synthesis of inorganic NPs that have benefits over conventional methods containing chemical agents that are associated with poisoning the environment. In this chapter, we examine the conventional synthetic

techniques with an emphasis on recent advancements of greener routes in order to fabricate metal, metal oxides and other important NPs; followed by a discussion of formation mechanisms and the conditions used to control the surface morphology, dispersity and other properties of these biosynthesized NPs. These green synthesized NPs are employed in various areas of nanomedicine, chemistry and related fields for use in drug carriers for targeted delivery, antimicrobial agents, DNA investigations, biosensors, catalysts, separation science, cancer treatment, gene treatment and magnetic resonance imaging. This chapter concludes by focusing on the existing margins and future projections relating to nanoparticle fabrication through different green routes.

2.2 Botanical Extract Mediated Green Synthesis

Green plants have shown competency to soak up, hyperaccumulate and reduce inorganic metallic ions from their surroundings [122, 123]. It is now acknowledged that numerous organic entities existent in plant tissues are capable of performing as efficient biological factories to considerably lessen environmental contamination. Moreover, amalgamations of molecules found in plant extracts can behave as both reducing and stabilizing (capping) agents, all within nanoparticle synthesis [120, 121, 124]. Some of the essential and abundant phytochemicals of plants are listed in Figure 2.4.

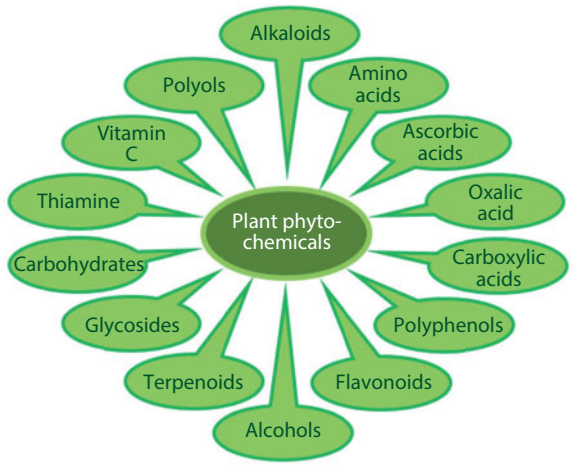


Figure 2.4 Important bioreductants found in plant extracts.

Nanoparticles attained from plant extracts are prepared from living plant extracts. Plant parts like leaf, root, latex, seed and stem are widely being used for metal- and metal oxide-based NP synthesis. Figure 2.4. shows important bioreductants found in plant extracts. Plant extracts are bioactive polyphenols, proteins, phenolic acids, alkaloids, sugars, terpenoids, etc., which are primarily composed to play a major role in relegating the metallic ions and then alleviating them [125, 126]. The discrepancy in concentration and conformation of these active biomolecules among different plants and their consequential association with aqueous metal ions are assumed to be the main supporting factor in the various sizes and shapes of fabricated nanoparticle [127].

The synthesis of NPs by metal salt reduction through plant extracts is a moderately facile ambient atmosphere action. The working process is incredibly simple. At room temperature, the plant extract and the solution of metal salt are mixed well [128]. The reaction is fulfilled within a few minutes. When the solutions of precursor combine, biochemical reduction of the salt instantly starts and the production of nanoparticles is typically shown by a transformation in color of the reaction solution. A flow chart showing the green synthesis procedure is shown in Figure 2.5.

The synthesis of plant-mediated green NPs can be divided into three stages: activation phase, growth phase and termination phase [129, 25, 130]. The activation phase is the primary stage in which the metal ions are recuperated from their salt precursors through the action of plant metabolites; biomolecules which have reduction abilities. The metal ions are

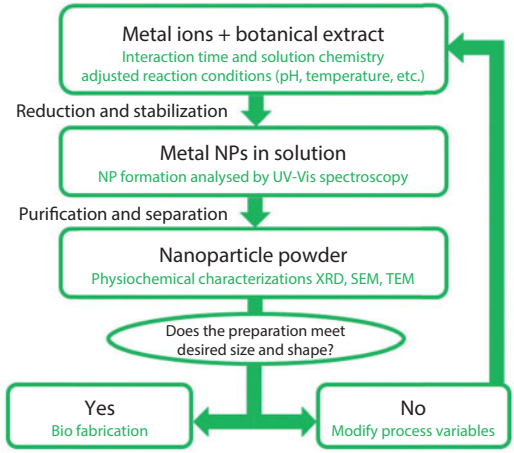


Figure 2.5 Flow chart of green biosynthesis.

altered from their mono- or divalent oxidation states to zero-valent states, then nucleation of the condensed metal atoms takes place [131]. This is followed by the growth period in which the seceded metal atoms coalesce to form metal NPs though more biological reduction of metal ions taking place. Laterally with the growth progression, nanoparticles collect to form a variety of morphologies like cubes, spheres, triangles, rods, hexagons, pentagons and wires [132]. The growth stage rises in enhanced thermodynamic stability of NPs whereas the extensive nucleation may result in aggregation of synthesized NPs, altering their morphologies. The last step in green NP synthesis is the termination phase. The NPs ultimately get their most keenly promising and stable morphology when capped by plant metabolites. The working mechanism of greener biosynthesis by plants is displayed in Figure 2.6.

Numerous properties of the solution mixture like metal salt concentration, concentration of plant extract, reaction solution pH, etc., and other reaction conditions like reaction time and temperature have extensive impacts on the size, morphology and quality of the synthesized nanoparticles [43, 133–136]. The pH approximation of reaction mixture has a great effect on the composition of NPs [137–139]. The pH amendment leads to the charge alteration in the plant metabolism and even affects its capacity to chelate and reduce metal ions during the process, which alters the dimensions, morphology and yield of synthesized NPs. Several plant metabolites vary in their nature and decrease capabilities from one another. This may also influence the NP synthesis process; for example, tryptophan and amino acids like tyrosine, arginine, and lysine are the most influential reducing agents amongst all the phytochemicals and therefore can decrease a huge amount of metal ions in less time. Temperature is also an essential parameter to influence properties of NP during synthesis [140, 42, 141–143]. High temperature improves certain crystallinity of synthesized NPs using improved rates of nucleation. The NP synthesis also

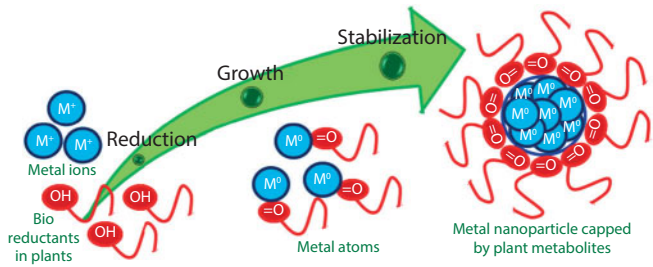


Figure 2.6 Green synthesis mechanism.

ensures metal ion potential. Metal ions which have higher electrochemical potentials are likely to be further condensed by plant phytochemicals [144]. For example, Ag^+ has better ionizing potential than Au^+ because of its lesser size and therefore will be condensed sooner.

Greener synthesis is economical, eco-friendly, sustainable, simple and relatively reproducible. Regarding these intriguing properties, plants have been ascertained to be a more eco-friendly alternative as biologically synthesizing metallic nanoparticles and also for detoxification applications [122, 145]. The biosynthetic method is uncertain and offers high-yield nano-sized materials having good crystalline conformation and appropriate properties. However, high calcination temperature is required to eradicate the precursor to form crystalline materials.

2.2.1 Green Metal NPs via Botanical Extract

Many scientists have synthesized metallic NPs by using broth of different parts of many plants, for instance the leaf extract of Aerva lanata [56], Hibiscus rosa sinensis [87], Chenopodium album leaf extract [43], *Jasminum sambac* Leaves [112], *Murraya koenigii* [89], Krishna tulsi [86], *Mentha piperita* [75], *Lansium domesticum* fruit peel [99], mushroom extract [85], seed aqueous extract of *Pistacia atlantica* [96], tea leaf extract [103], Sacha inchi (*Plukenetia volubilis*) leaf extracts [64], *Eucommia ulmoides* bark aqueous extract [48], Tephrosia purpurea leaf extract [32], *Ziziphus jujuba* leaf extract as a stabilizing and minimalizing agent at room temperature [45], seed extract of *Curcuma pseudomontana* [76], *Abelmoschus esculentus* [53], *Cinnamomum zeylanicum* leaf broth [100], *Geranium* [95], grape waste [61], fruit extract of *Hovenia dulcis* [40], maple leaf pine needle [60], *Magnolia kobus* [101], *Mangifera indica* [90], *Phoenix dactylifera* [114], *Pistacia integerrima* [50], *Pogostemon benghalensis* (B) O. Ktz. leaf [84], *Morinda citrifolia* [102], *Solanum nigrum* [79], *Stachys lavandulifolia* Vahl [38], *Terminalia arjuna* [46], *Zingiber officinale* extracts [66], *Vitex negundo* [172], ethanolic extract of petals of *Rosa indica* [173] and from *Prosopis juliflora* leaf extract [174]. Among these NPs, gold and silver NPs are cited extensively due to their potential applications in diverse fields. Other important green metallic NPs include iron, copper, palladium and lead. Green metal NPs prepared by various plant extracts are summarized in Table 2.1.

Pure crystalline and spherical green AgNPs fabricated by using seed aqueous extract of *Pistacia atlantica* confirmed high surface area with 27 nm average size. The growth of NPs stopped after 35 minutes and the reaction was accomplished [96].

Table 2.1 NPs green synthesized by plant extracts.

S. no.	Botanical extract	NPs	Morphology	Size (nm)	Ref.
1.	*Aerva lanata*	Ag	Mostly Spherical	18.62	[55]
2.	*Alternanthera sessilis*	Ag	Variable	0.1–10,000	[83]
3.	*Ananas comosus*	Ag	Spherical	12.4	[44]
4.	*Annona squamosa*	Ag	Spherical	20–100	[109]
5.	*Artemisia nilagirica*	Ag	Predominantly Square	70–90	[107]
6.	*Artocarpus heterophyllus* lam seed	Ag	Irregular	10.78	[52]
7.	Banana peel	Ag	Spherical	23.7	[49]
8.	Basil roots	Ag	Spherical	10	[11]
9.	Basil stem	Ag	Spherical	15	[11]
10.	Beetroot	Ag	Spherical	15	[41]
11.	*Biophytum sensitivum*	Ag	Almost Spherical	19.06	[55]
12.	*Boerhavia diffusa*	Ag	Spherical	25	[67]
13.	*Caesalpinia coriaria*	Ag	Triangular	40–52	[54]
14.	Callus	Ag	Spherical	5–20	[80]
15.	*Carica papaya*	Ag	Spherical	50–250	[39]
16.	*Catharanthus roseus*	Ag	Spherical	27–30	[59]
17.	*Ceropegia thwaitesii*	Ag	Spherical	100	[78]
18.	*Chenopodium album*	Ag	Spherical	Various	[43]
19.	*Cinnamon zeylanicum* bark	Ag	Variable	31–40	[97]
20.	Cocos nucifera	Ag	Spherical	22	[70]
21.	Coriandrum sativum	Ag	Spherical	13.09	[82]
22.	*Crataegus douglasii* fruit	Ag	Spherical	29.28	[73]
23.	*Croton sparsiflorus* morong	Ag	Spherical	22–52	[58]

(*Continued*)

Table 2.1 Cont.

S. no.	Botanical extract	NPs	Morphology	Size (nm)	Ref.
24.	*Dalbergia spinosa*	Ag	Spherical	18	[77]
25.	Delonix elata	Ag	Spherical	35–45	[98]
26.	*Emblica officinalis* fruit	Ag	Spherical	15	[93]
27.	Eucalyptus leaf	Ag	Spherical	4–60	[91]
28.	Eucalyptus leaf	Ag	Spherical	21	[91]
29.	Ficus carica	Ag	Spherical	13	[104]
30.	*Gloriosa superba*	Ag	Spherical	10–25	[36]
31.	*Gossypium hirsutum*	Ag	Spherical	30	[57]
32.	Hibiscus rosa sinensis	Ag	Variable	Various	[87]
33.	*Illicium verum*	Ag	Variable	< 10	[68]
34.	*A. indicum* leaf	Ag	Spherical	7–17	[37]
35.	J. sambac leaf	Ag	Spherical	20–50	[112]
36.	*Jatropha curcas* seed	Ag	Spherical	10–15	[146]
37.	Krishna tulsi	Ag	Spherical	10–20	[86]
38.	Lakshmi tulasi	Ag	Triangular	42	[94]
39.	Lansium domesticum fruit peel	Ag	Spherical	10–30	[99]
40.	*Lantana camara* leaf	Ag	Spherical	20–34	[34]
41.	Lippia citriodora	Ag	Spherical	15–30	[42]
42.	Malva parviflora	Ag	Spherical	19–25	[113]
43.	Mangifera indica	Ag	Spherical	20	[88]
44.	Mangosteen leaf	Ag	Spherical	35	[105]
45.	Maple leaf	Ag	Spherical	1–100	[110]
46.	Mentha p*iperita*	Ag	Spherical	90	[75]
47.	Murraya k*oenigii*	Ag	Spherical	10	[89]
48.	Mushroom extract	Ag	Spherical	15	[85]
49.	Neem gum	Ag	Spherical	< 30	[106]

(*Continued*)

Table 2.1 Cont.

S. no.	Botanical extract	NPs	Morphology	Size (nm)	Ref.
50.	*Papaver* somniferum	Ag	Spherical	3200–7600	[108]
51.	Piper l*ongum*	Ag	Spherical	17.6–41	[51]
52.	Piper n*igrum*	Ag	Spherical	32–1	[74]
53.	Pistacia a*tlantica*	Ag	Spherical	10–50	[96]
54.	*Plectranthus* a*mboinicus*	Ag	Spherical	18	[33]
55.	*Prosopis farcta*	Ag	Spherical	10.8	[71]
56.	Sacha inchi	Ag	Distorted Cube	60	[63]
57.	Sacha inchi	Ag	Spherical	7.2	[64]
58.	Sacha inchi leaf	Ag	Spherical	4–25	[64]
59.	Tea leaf	Ag	Spherical	20–90	[103]
60.	*Tephrosia purpurea*	Ag	Spherical	20	[32]
61.	*Tribulus terrestris*	Ag	Spherical	16–28	[47]
62.	Ziziphus *jujuba*	Ag	Variable	20–30	[45]
63.	*Abelmoschus esculentus*	Au	Spherical	45–75	[53]
64.	*Aerva lanata*	Au	Mostly Spherical	17.97	[55]
65.	*Chenopodium album*	Au	Spherical	Various	[43]
66.	*Cinnamomum zeylanicum*	Au	Nanoprisms & Spheres	25	[100]
67.	Curcuma pseudomontana	Au	Spherical	20	[76]
68.	*Eucommia ulmoides*	Au	Spherical	16.4	[48]
69.	Geranium	Au	Variable	8–20	[95]
70.	Grape waste	Au	Spherical	20–25	[61]
71.	*Hibiscus rosa sinensis*	Au	Variable	Various	[87]
72.	*Hovenia dulcis*	Au	Variable	15–20	[40]
73.	J. sambac leaves	Au	Spherical	20–50	[112]
74.	Krishna tulsi	Au	Spherical	30,	[86]

(*Continued*)

Table 2.1 Cont.

S. no.	Botanical extract	NPs	Morphology	Size (nm)	Ref.
75.	Lansium domesticum fruit peel	Au	Triangular, Hexagonal	20–40	[99]
76.	Magnolia kobus	Au	Variable	5–300	[101]
77.	Mangifera indica	Au	Spherical	17–20	[90]
78.	Maple leaf pine needle	Au	Spherical	< 100	[60]
79.	Mentha p*iperita*	Au	Spherical	150	[75]
80.	Morinda c*itrifolia*	Au	Spherical	12.17–38.26	[102]
81.	Murraya k*oenigii*	Au	Spherical	20	[89]
82.	Mushroom extract	Au	Spherical	20–150	[85]
83.	Phoenix d*actylifera*	Au	Spherical	35–45	[114]
84.	Pistacia i*ntegerrima*	Au	Spherical	20–200	[50]
85.	Pogostemon b*enghalensis* (B) O. Ktz. leaf	Au	Variable	10–50	[84]
86.	Solanum n*igrum*	Au	Spherical	50	[79]
87.	*Stachys lavandulifolia* vahl	Au	Variable	56.3	[38]
88.	Terminalia a*rjuna*	Au	Spherical	20–50	[46]
89.	Zingiber o*fficinale*	Au	Spherical	5–15	[66]
90.	*Euphorbia esula* leaf	Cu	Spherical	< 32	[81]
91.	*Eucalyptus* leaf	Fe	Spherical	20–80	[111]
92.	*Mentha spicata*	Fe	Spherical	20–45	[92]
93.	Terminalia *chebula*	Fe	Variable	< 80	[65]
94.	Various tree leaves	Fe	Spherical	10–20	[69]
95.	*Opuntia ficus-indica*	Li	Spherical	5	[35]
96.	Terminalia *chebula*	Pd	Variable	< 80	[65]
97.	Gum tragacanth	CeO_2	Spherical	20–40	[147]
98.	*Calotropis gigantea*	Co_3O_4	Spherical	60	[148]
99.	Aloe b*arbadensis* miller	CuO	Spherical	15–30	[149]
100.	*Calotropis gigantea*	CuO	Spherical	20–30	[150]

(*Continued*)

Table 2.1 Cont.

S. no.	Botanical extract	NPs	Morphology	Size (nm)	Ref.
101.	Gloriosa *superba*	CuO	Spherical	5–10	[150]
102.	Theobroma *cacao* L. seeds	CuO	Spherical	40	[151]
103.	Tinospora *cordifolia*	CuO	Spherical	6	[152]
104.	Punica *granatum* rind	Fe_3O_4	Nanorods	12.6	[153]
105.	Syzygium *cumini* seed	Fe_3O_4	Spherical	14	[153]
106.	Aqueous phytoextracts	GO_2	Sheets	5.3	[154]
107.	*Acacia* gum	MgO	Spherical	< 100	[155]
108.	Mushroom extract	RGO_2	Spherical	< 100	[156]
109.	Aloe b*arbadensis* miller	ZnO	Spherical	25–40	[157]
110.	*Artocarpus gomezianus*	ZnO	Spherical	11.53	[158]
111.	Borassus f*labellifer*	ZnO	Porous Disc-like	55	[159]
112.	*Cassia fistula*	ZnO	Spherical	5–15	[150]
113.	Citrus a*urantifolia*	ZnO	Spherical	50–200	[160]
114.	Gum tragacanth	ZnO	Spherical	< 50	[161]
115.	Maple leaf	ZnO	Spherical	5–20	[110]
116.	Moringa o*leifera*	ZnO	Spherical	24	[162]
117.	Parthenium h*ysterophorus*	ZnO	Spherical	27–84	[163]
118.	Plectranthus a*mboinicus*	ZnO	Spherical	20–50	[164]
119.	Plectranthus a*mboinicus*	ZnO	Spherical	88	[165]
120.	Solanum n*igrum*	ZnO	Quasi-spherical	29.79	[166]
121	Tamarindus i*ndica*	ZnO	Spherical	19–37	[167]
122.	*Cissus quadrangularis* linn	$AgCl_2$	Spherical	15–23	[168]

(*Continued*)

Table 2.1 Cont.

S. no.	Botanical extract	NPs	Morphology	Size (nm)	Ref.
123.	Lansium domesticum fruit peel	Au/Ag alloy	Branched, Spherical	150–300	[99]
124.	*E. tirucalli* plant latex	CeO_2:Eu^{3+}	Cubic	20–25	[169]
125.	*Vitis v*inifera stem	Core Shell Fe_3O_4	Spherical	50	[170]
126.	Theobroma *cacao* L. seeds	Pd/CuO	Spherical	40	[151]
127.	Calotropis p*rocera*	$ZnAl_2O_4$:Cr^{3+}	Irregular	15–26	[171]

The silver NPs with distorted cubic shape and a mean size of 60 nm, prepared using a Sacha inchi (SI) oil, showed high stability and crystalline morphology [63]. It is suggested that carbonyl groups present in SI oil were responsible for AgNPs production by reducing the $AgNO_3$ precursor. The synthesized AgNPs showed enhanced photodegradation capabilities for MB degradation in the absence of any other reducing agent.

Spherical AgNPs possessing diameter ranging between 4 to 25 nm synthesized by using Sacha inchi leaf extract, a nontoxic reducing agent, showed radical scavenging activity when DPPH was added into the reaction solution [64]. Carbonyl groups of SI played a significant reduction role during the synthesis process. Synthesized NPs showed significant antioxidant efficacy in comparison with SI leaf extracts against 1,1-diphenyl-2-picrylhydrazyl.

Spherical AgNPs with size ranging from 20 to 90 nm were prepared using leaf extract of tea [103]. The FTIR spectroscopy of tea extract confirmed the presence of poly phenols, amides, carboxyl and amino groups, which were surely responsible for $AgNO_3$ reduction and AgNPs stabilization through surface bonding. Silver ion released from the synthesized AgNPs showed a good stability in terms of time-dependent release of silver ions.

Tephrosia purpurea leaf extract is used to synthesize highly crystalline silver NPs with approximate size of 20 nm [32]. The biomolecules, flavonoids, proteins, amino acids, tannins, alkaloids and rotenoids present in the leaf extract were found to play a dual role of both reducing as well as capping agents for the formation of AgNPs. FTIR analysis showed asymmetric and symmetric stretching peaks of COO– (carboxylate group), indicating that AgNPs were bound to proteins through carboxylate groups.

It is suggested that flavonoids were responsible for the metal salt reduction while the carboxylate group acted as surfactant to stabilize the synthesized AgNPs. The obtained NPs were found to have good inhibitory activity towards *Pseudomonas* and *Penicillium* spp. compared to other test pathogens using standard Kirby-Bauer disc diffusion assay.

Biogenic crystalline AgNPs with face-centered cubic (fcc) structure were produced using *Ziziphus jujuba* leaf extract as a stabilizing and reducing agent at room temperature [45]. Nanoparticles obtained were of different shapes with diameter ranging between 20–30 nm. The hydrodynamic size of 28 nm is found from dynamic light scattering (DLS) data having high stability in a colloidal state. The FTIR analysis of *Z. jujuba* leaf extract confirmed the presence of bands corresponding to carboxyl groups, intermediate form of phenolic groups, proteins and carbohydrates, which were shifted after the completion of reaction, showing the involvement of bioreductants in AgNPs preparation. UV analysis of AgNPs showed that the intensity of absorption band in visible range (434 nm) increases with an increase in the quantity of extract, with the optimized quantity of extract being 1.5 mL for 100 mL of $AgNO_3$ (0.001 M). Moreover, the study of the effect of medium pH on synthesized particles indicated wider bands displaying red shift at acidic pH due to an increase in particle size, while at basic pH a decrease in particle size was demonstrated by band narrowing and blue shift. Ionization of phenolic groups in neutral and basic pH ensured rapid formation of AgNPs and the rather slow formation of aggregated particles in acidic medium is attributed to electrostatic repulsion of anions, concluding that optimum condition for synthesis of AgNPs is neutral pH because AgOH precipitation may occur at basic pH. Synthesized AgNPs showed high catalytic activity towards the reduction of anthropogenic pollutant 4-nitrophenol (4-NP) to 4-AP and MB within shorter reaction time and exhibited good antimicrobial activity against *Escherichia coli*.

Well-dispersed fcc-centered AgNPs having a diameter less than 20 nm were obtained through a biosynthetic route from aqueous silver nitrate using water extract of *Vitex negundo* leaves as a stabilizer and reducing agent [172]. FTIR peaks of *V. negundo* extract confirmed the presence of bioreductants, such as flavonoids, phenolic hydroxyl groups (friedelin, lupeol, and β-sitosterol groups) and C–H in the aromatic stretching, associated with the phenolic ring.

AgNPs synthesized with the use of ethanolic extract of rose (*Rosa indica*) petals exhibited effectual antibacterial activity against Gram-negative (*Klebsiella pneumoniae, Escherichia coli*) as compared to Gram-positive (*Enterococcus faecalis, Streptococcus mutans*) bacteria [175]. Analysis of nuclear morphology, MTT assay, protein expression of caspase 3 as well as

9, Bax and mRNA expression of Bcl-2 showed potential anticancer activity. These AgNPs also reduced nuclear morphology, cytotoxicity and free radical generation (NO and O^-_2) in rat peritoneal macrophages *in vitro*.

Synthesis of AgNPs with size range from 11 to 19 nm using an aqueous extract of fresh leaves of *Prosopis juliflora* was reported by Raja *et al.* [176]. The synthesized silver nanoparticles were triangular, tetragonal, pentagonal and hexagonal in structure. Phytochemical analysis of *P. juliflora* leaf broth showed the involvement of some proteins and metabolites, such as terpenoids or flavonoids, in the reduction and capping of AgNPs.

A simple microwave-assisted method reported for the green synthesis of gold NPs by the reduction of aqueous metal salt solutions using leaf extract of the medicinal plant *Aerva lanata* produced particles of crystalline nature, having different morphologies with an average diameter of 17.97 nm, with the majority of particles being in the 10–30 nm range [56]. Soon after the leaf extract addition, metal ions were reduced into atoms of nano-sized range. This reduction was believed to be carried out by various phytochemicals present in plant extract, which further capped them from agglomeration as well. The synthesized NPs were used as nanocatalysts in the reduction of 4-nitrophenol to 4-aminophenol by $NaBH_4$. The reported microwave-assisted process was found to be rapid and thus reduced the aggregation of synthesized NPs, eliminating the major problem in NPs synthesized by greener strategies.

Dwivedi and Gopal biosynthesized quasi-spherical AuNPs retaining a size range of 10–30 nm using the noxious weed *Chenopodium album* as a natural reagent [43]. The surface plasmon resonance (SPR) for gold NPs was found at 540 nm. Chemical constituents of *C. album* leaf extract include high concentrations of oxalic acid, $(COOH)_2$. Its dianion, i.e., oxalate, acted as biological reductant. The aldehyde group present in oxalate ion also makes it a good ligand, reducing the particle agglomeration. FTIR analysis confirmed the presence of carbonyl group, which surely performed as reducing agent, while carboxylate ions shielded the nanoparticles, imparting them with stability for several months.

The leaf extract of *Hibiscus rosa sinensis* produced crystalline AuNPs in the fcc structure [87]. It is observed that the AuNPs were bound to amine groups, which are responsible for bioreduction and stabilization.

Gold NPs, both individual and agglomerated, formed by seed aqueous extract of *Abelmoschus esculentus* showed crystalline nature having spherical morphology with a narrow size range of 45–75 nm [53]. The maximum zone of inhibition in the gold NPs was against *Puccinia graminis* (17 mm) and *Candida albicans* (18 mm), while synthesized gold NPs acted as an effective antifungal agent.

Cinnamomum zeylanicum leaf broth has been espoused as reducing agent for the fabrication of crystalline gold NPs with diameter of 25 nm [100]. As-synthesized AuNPs have mixed morphologies of spheres and nanoprisms with face-centered cubic crystal structure FCC (111) of gold. The prism-shaped gold nanoparticles were predominant at the lower concentration of the plant extract whereas spherical particles were more likely expected to be found at the higher concentrations. Chemical analysis of *C. zeylanicum* leaf broth showed the occurrence of several metabolites, such as sucrose, tannin and terpenoids comparable to eugenol and cinnamaldehyde, which are proficient at bioreduction. It has been demonstrated that terpenoids are responsible for metal ion reduction by oxidation of aldehyde group to carboxylic acid, although starch molecules preserved the alienated particles, imparting stability. The grown gold NPs were photoluminescent and the intensity of photoemission was set up to rise with the upsurge in leaf broth concentration.

Biologically active spherical AuNPs with an average diameter of 20 nm were formed by using *Curcuma pseudomontana* extracts [76].

Spherical AuNPs of 18.2 nm average size with FCC structure manufactured by using water extract of *Eucommia ulmoides* bark showed excellent photocatalytic activity for decolorization of model compounds of azo dyes, Congo Red and Reactive Yellow 179 [48]. The DLS measurements showed greater size due to the presence of the biomolecule envelope around the AuNPs' core.

Geranium extracts were used to produce AuNPs having different morphologies with an average homogeneous size of 12 ± 3 nm following Gaussian distribution between 6 and 35 nm [95]. The particles were mostly spherical, while a few were nanorods, pentagonal and triangular (in projection).

Gold NPs possessing 15–20 nm average size and having biomedical applications photosynthesized with the help of fruit extract of *Hovenia dulcis* have also been reported [40]. Molecules present in the fruit extracts reduced the gold metal ions into GNPs due to a change in the color of water extracts within 30 min.

An immobilization of copper NPs was studied on perlite [81]. The behavior of CuNPs/perlite were very encouraging in the catalytic reduction of 4-nitrophenol. It can also be recycled many times without any reduction in the catalytic activity. The pseudo-first-order reaction equation was used to find the reaction rate constant.

Green FeNPs were synthesized using *Eucalyptus* leaf extracts having some polyphenols, which are responsible for stabilizing and capping iron nanoparticles on the surfaces of *Eucalyptus* leaf (EL-FeNPs) [111]. The

reactivity of EL-FeNPs was calculated for the treatment of swine wastewater. As a result, removal of 84.5% of COD and 71.7% of total N were successfully obtained.

Lithium NPs fabricated via green route exhibited a size of nearly 5 nm [35]. The absorption bands were set up at 315 and 415 nm in samples after the formation of NPs. Distinguished Raman band attributed to the vibrational modes in small lithium NPs can be given specifically to RBM in small lithium metallic NPs.

A greener method for the synthesis of gelatin/pectin stabilized palladium nanoparticles as an efficient heterogeneous catalyst was carried out in the presence of aryl halide, alkene, n-Pr3N [177]. The products were obtained in highly short reaction times with excellent yields.

2.2.2 Green Oxide NPs via Botanical Extract

Many researchers have reported green synthesis routes for the preparation of metal oxide NPs using distinctive plant broth. The facts are concisely shown in Table 2.2.

Monodispersed ceria NPs having 20–40 nm size were synthesized by green method via Gum tragacanth [161]. The NPs displayed strong absorption peak appearing in the UV region and have direct band gap of 3.6 eV. *In-vitro* feasibility studies with CeNPs on neuro 2A cells exhibited a dose-dependent toxicity, with a nontoxic effect in concentrations lower than 30 m g/mL. The CeNPs synthesized by Gum tragacanth were discovered to be similar to those gotten by conventional reduction method using perilous polymers or surfactants.

Tinospora cordifolia was used to synthesizd cupric oxide NPs having phot-catalytic, antibacterial and antioxidant properties [152]. The particles possess a sponge-like structure and have a large surface area with the average crystallite sizes attained being 6–8 nm. CuO NPs are espoused as good catalyst intended for the efficient degradation of methylene blue (MB) in sunlight and UV. The degradation of MB was brought into pH-dependence. The NPs were found to efficiently impede the activity of 1,1-Diphenyl-2-picrylhydrazyl (DPPH) free radicaly. CuO NPs showed important bactericidal activity contrary to aerogenes, *Escherichia coli, Staphylococcus aureus* and *Pseudomonas aeruginosa.*

The magnesium oxide nano-flowers were fabricated by the green method using acacia gum which is further used for the exclusion of divalent metallic species from synthetic waste water [155]. The particle size of acacia gum treated MgO NPs was greater in comparison to untreated n-MgO particles which confirm crust of acacia gum on simple n-MgO.

Table 2.2 NPs green synthesized by microbes.

S. no.	Microbial culture	NP's	Morphology	Size (nm)	Ref.
1.	*Aspergillus flavus*	Ag	Spherical	8.92	[197]
2.	Aspergillus fumigatus	Ag	Spherical	5–25	[198]
3.	*Aspergillus terreus*	Ag	Spherical	1–20	[199]
4.	*Bacillus cereus*	Ag	Spherical	4–5	[200]
5.	*Bacillus licheniformis*	Ag	Irregular	50	[201]
6.	*Brevibacterium casei*	Ag	Spherical	10–50	[202]
7.	Cladosporium cladosporioides	Ag	Spherical	10–100	[203]
8.	*Coriolus versicolor*	Ag	Spherical	25–75	[204]
9.	*Corynebacterium glutamicum*	Ag	Irregular	5–50	[205]
10.	*Escherichia coli*	Ag	Irregular	50	[206]
11.	*Fusarium oxysporum*	Ag	Spherical	5–50	[207]
12.	*Fusarium oxysporum*	Ag	Irregular	5–15	[208]
13.	*Fusarium oxysporum*	Ag	Spherical	20–50	[209]
14.	Fusarium semitectum	Ag	Spherical	10–60	[210]
15.	*Macrophomina phaseolina*	Ag	Spherical	5–40	[211]
16.	*Penicillium fellutanum*	Ag	Spherical	5–25	[212]
17.	*Penicillium nalgiovense*	Ag	Spherical	25 ± 2.8	[213]
18.	*Pediococcus pentosaceus*	Ag	Irregular	< 100	[214]
19.	*Phaenerochaete chrysosporium*	Ag	Pyramidal	50–200	[215]
20.	*Phoma glomerata*	Ag	Spherical	60–80	[216]

(*Continued*)

Table 2.2 Cont.

S. no.	Microbial culture	NP's	Morphology	Size (nm)	Ref.
21.	*Pleurotus sajor-caju*	Ag	Spherical	30.5	[217]
22.	*Trichoderma reesei*	Ag	Spherical	5–50	[218]
23.	*Trichoderma viride*	Ag	Spherical	5–40	[219]
24.	*Trichoderma asperellum*	Ag	Spherical	13–18	[220]
25.	*Trichoderma viride*	Ag	Spherical	5–40	[219]
26.	*Trichoderma viride*	Ag	Irregular	2–4	[221]
27.	*Verticillium* sp.	Ag	Spherical	5–50	[207]
28.	Yeast	Ag	Irregular, Polygonal	9–25	[38]
29.	*Aspergillus oryzae* var. *viridis*	Au	Mostly Spherical	10–60	[222]
30.	*Aspergillus niger*	Au	Spherical	12.8 ± 5.6	[223]
31.	*Aspergillus niger*	Au	Polydispersed	10–20	[224]
32.	*Aspergillus sydowii*	Au	Spherical	8.7–15.6	[225]
33.	*Alternaria alternata*	Au	Spherical, Triangular	12 ± 5	[226]
34.	*Aspergillus clavatus*	Au	Triangular, Spherical	24.4 ± 11	[227]
35.	*Aureobasidium pullulans*	Au	Spherical	29 ± 6	[228]
36.	*Brevibacterium casei*	Au	Spherical	10–50	[202]
37.	*Candida albicans*	Au	Monodispersed, Spherical	5	[12]
38.	*Candida albicans*	Au	Spherical	20–40	[229]
39.	*Candida utilis*	Au	Irregular	< 100	[230]
40.	*Colletotrichum* sp.	Au	Spherical	8–40	[231]
41.	*Coriolus versicolor*	Au	Spherical	20–100	[232]
42.	*Cylindrocladium floridanum*	Au	Spherical	19.05	[233]
43.	*Cylindrocladium floridanum*	Au	Spherical	5–35	[234]
44.	*Epicoccum nigrum*	Au	–	5–50	[235]

(*Continued*)

Table 2.2 Cont.

S. no.	Microbial culture	NP's	Morphology	Size (nm)	Ref.
45.	*Escherichia coli*	Au	Triangular, Hexagons	20–30	[236]
46.	*Fusarium semitectum*	Au	Spherical	10–80	[237]
47.	*Fusarium oxysporum*	Au	Spherical	2–50	[13]
48.	*Fusarium oxysporum*	Au	Spherical, Triangular	8–40	[238]
49.	*Hansenula anomala*	Au	Irregular	14	[239]
50.	*Helminthosporium solani*	Au	Variable	2–70	[240]
51.	*Hormoconis resinae*	Au	Spherical	3–20	[241]
52.	*Neurospora crassa*	Au	Spherical	32	[242]
53.	*Penicillium rugulosum*	Au	Spherical	20–40	[243]
54.	*Pediococcus pentosaceus*	Au	Spherical	< 100	[244]
55.	*Penicillium brevicompactum*	Au	Various	10–60	[245]
56.	*Penicillium* sp.	Au	Spherical	30–50	[246]
57.	*Phanerochaete chrysosporium*	Au	Spherical	10–100	[247]
58.	*Plectonema boryanum*	Au	Octahedral	10–6000	[248]
59.	*Plectonema boryanum*	Au	Cubic	10–25	[249]
60.	*Pseudomonas aeruginosa*	Au	Irregular	15–30	[250]
61.	*Rhizopus oryzae*	Au	Spherical	16–25	[251]
62.	*Rhodococcus* sp.	Au	Spherical	5–15	[10]
63.	*Rhodopseudomonas capsulata*	Au	Spherical	10–20	[252]
64.	*Saccharomyces cerevisiae*	Au	Spherical	15–20	[253]

(*Continued*)

Table 2.2 Cont.

S. no.	Microbial culture	NP's	Morphology	Size (nm)	Ref.
65.	*Sargassum wightii*	Au	Planar	8–12	[254]
66.	*Sclerotium rolfsii*	Au	Spherical	25.2 ± 6.8	[255]
67.	*Shewanella algae*	Au	Irregular	10–20	[256]
68.	*Shewanella oneidensis*	Au	Spherical	< 100	[257]
69.	*Trichoderma koningii*	Au	Spherical	30–40	[258]
70.	*Trichoderma koningii*	Au	Spherical	10–14	[259]
71.	*Ureibacillus thermosphaericus*	Au	Irregular	50–70	[260]
72.	*Verticillum luteoalbum*	Au	Irregular	< 100	[230]
73.	*Volvariella volvacea*	Au	Triangular, Spherical	20–150	[261]
74.	*Verticillium* sp.	Au	Irregular	< 100	[262]
75.	*Verticillium* sp.	Au	Spherical	20 ± 8	[263]
76.	*Yarrowia lipolytica*	Au	Various	< 100	[264]
77.	*Yarrowia lipolytica*	Au	Triangles	15	[265]
78.	Yeast	Au	Irregular, Polygonal	9–25	[266]
79.	*Neurospora crassa*	Au,	Spherical	32	[242]
80.	*Escherichia coli*	Cd	Spherical	2.0–3.2	[267]
81.	*Escherichia coli*	Te	Spherical	2.0–3.2	[267]
82.	*Enterobacter* sp.	Hg	Spherical	2–5	[268]
83.	*Desulfovibrio desulfuricans*	Pd	Spherical	50	[269]
84.	*Fusarium oxysporum*	Pt	Variable	70–180	[270]
85.	*Shewanella algae*	Pt	Irregular	5	[271]
86.	*Shewanella* sp.	Se	Spherical	< 100	[272]
87.	*Pyrobaculum islandicum*	U, Tc, Cr, Co, Mn	Spherical	< 100	[273]

(*Continued*)

Table 2.2 Cont.

S. no.	Microbial culture	NP's	Morphology	Size (nm)	Ref.
88.	*Fusarium oxysporum*	$BaTiO_3$	Spherical	4–5	[274]
89.	*Lactobacillus* sp.	$BaTiO_3$	Tetragonal	20–80	[275]
90.	*Shewanella oneidensis* MR-1	Fe_2O_3	Irregular, Rhombohedral	30–43	[276]
91.	HSMV-1	Fe_3O_4	Bullet-shaped	< 100	[277]
92.	QH-2	Fe_3O_4	Rectangular	< 100	[278]
93.	Recombinant AMB-1	Fe_3O_4	Cubo-octahedral	20	[279]
94.	*Shewanella oneidensis*	Fe_3O_4	Rectangular, Rhombic, Hexagonal	40–50	[280]
95.	WM-1	Fe_3O_4	Cuboidal	< 100	[281]
96.	Yeast	Fe_3O_4	Wormhole-like	< 100	[282]
97.	Yeast	$FePO_4$	Nanopowder	< 100	[283]
98.	*Bacillus* sp.	MnO_2	Orthorhombic	4.62	[2]
99.	*Saccharomyces cerevisiae*	Sb_2O_3	Spherical	2–10	[270]
100.	*Fusarium oxysporum*	TiO_2	Spherical	6–13	[284]
101.	*Lactobacillus* sp.	TiO_2	Spherical	8–35	[285]
102.	Eukaryotes	Various	--	--	[286]
103.	*Aspergillus fumigatus*	ZnO	Spherical	1.2–6.8	[287]
104.	Aeromonas h*ydrophila*	ZnO	Spherical	57.72	[288]
105.	*Fusarium oxysporum*	ZrO_2	Spherical	3–11	[24]
106.	*Neurospora crassa*	Au/Ag Alloy	Spherical	20–50	[242]
107.	*Fusarium oxysporum*	Au/Ag Alloy	Spherical	8–14	[289]
108.	*Aspergillus tubingensis*	$Ca_3P_2O_8$	Spherical	28.2	[290]

(*Continued*)

Table 2.2 Cont.

S. no.	Microbial culture	NP's	Morphology	Size (nm)	Ref.
109.	*Fusarium oxysporum*	$CdCO_3$	Spherical	120–200	[291]
110.	*Candida glabrata*	CdS	Irregular	< 100	[292]
111.	*Coriolus versicolor*	CdS	Spherical	100–200	[293]
112.	*Escherichia coli*	CdS	Wurtzite	2–5	[294]
113.	*Fusarium oxysporum*	CdS	Spherical	5–20	[295]
114.	*Fusarium oxysporum*	CdS	Irregular	< 100	[296]
115.	*Lactobacillus*	CdS	Spherical	4.9	[297]
116.	*Rhodobacter sphaeroides*	CdS	Hexagonal	8	[298]
117.	*Rhodopseudomonas palustris*	CdS	Cubic	8	[299]
118.	*Schizosaccharomyces pombe*	CdS	Irregular	< 100	[292]
119.	*Schizosaccharomyces pombe*	CdS	Spherical	1.8–2.9	[300]
120.	*Schizosaccharomyces pombe, Candida glabrata*	CdS	Hexagonal	2	[300]
121	*Schizosaccharomyces pombe*	CdS	Hexagonal	1–1.5	[301]
122.	Yeast	CdS	Spherical	3.6	[297]
123.	*Fusarium oxysporum*	CdSe	Spherical	9–15	[208]
124.	*Aspergillus oryzae* TFR9	$FeCl_3$	Spherical	10–24.6	[302]
125.	Prokaryotes	Fe_3S_4	Irregular	< 100	[303]
126.	Bacteria	FeS	Spherical	2	[304]
127.	*Fusarium oxysporum*	$PbCO_3$,	Spherical	120–200	[291]
128.	Magnetotactic bacterium	Polyphosphate	Rectangular	< 100	[305]

(*Continued*)

Table 2.2 Cont.

S. no.	Microbial culture	NP's	Morphology	Size (nm)	Ref.
129.	*Rhodobacter sphaeroides*	PbS	Spherical	10	[306]
130.	*Fusarium oxysporum*	$SrCO_3$	Needlelike	10–50	[307]
131.	Desulfobacteraceae	ZnS	Biofilm	2–5	[308]

Adsorption studies showed that nanoflowers are accomplished at efficiently eliminating Co(II), Cd(II), Zn(II), Cu(II), Mn(II), Pb(II) and Ni(II) from synthetic wastewater.

Spherical magnetic Fe_3O_4 nanoparticles (SMNPs) having inverse spinel cubic structure were fabricated using *Syzygium cumini* seed extract, which is a safe and eco-friendly fruit waste material [170]. The hysteresis loop of Fe_3O_4 NPs showed an exceptional ferromagnetic behavior with a saturation magnetization value of 13.6 emu/g.

2.3 Microbial Extract-Mediated Green Synthesis

Microorganisms, both unicellular and multicellular, have been widely reported as remarkable candidates for biological synthesis [178]. Studies include formation of nanoparticles by using algae, viruses, bacteria, yeast and fungi, as presented in Table 2.2. In fact, the microbes reduce metal ions to form water-insoluble complexes in order to defend themselves from their toxicity. Hence, microorganisms possess the ability to produce organic/inorganic composites of varying size and shape with ordered structures through detoxification of target ions by using several biopolymers generated in them, due to various cell activities [179, 181].

Various reducing agents excreted by microbes are given in Figure 2.7. As different microbes follow different routes for nanoparticle formation, the definite reaction mechanism is not yet fully understood [182, 184]. Generally, the biopolymer, excreted by microbes, capture the metal ions from metal salts and convert them to their elemental form [24, 185, 186]. The microbial reduction can be attained either extracellularly or intracellularly through bioaccumulation, precipitation, biomineralization or biosorption [187, 190]. In extracellular synthesis reduction occurs on the surface of the microbial cell. The electrostatic interaction causes metal

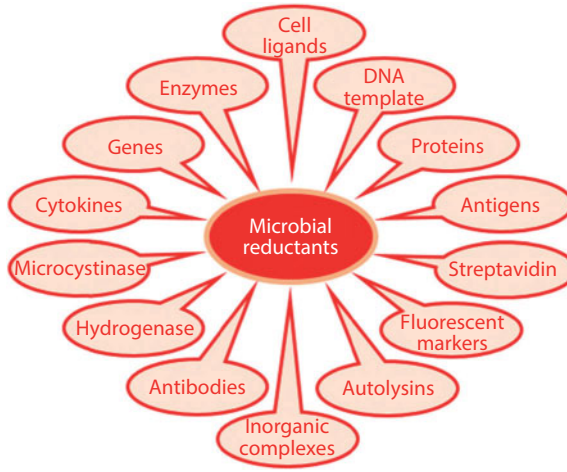


Figure 2.7 Reducing agents involved in microbial synthesis.

cations to attach with negatively charged enzymatic groups present at the cell wall where reduction takes place [191]. On the other hand, the intracellular mechanism involves the trapping of metal ion on the microbial cell and then reducing it in the presence of enzymes [192, 193].

The synthesis process consists of making microbial extract, mixing it with a metal salt solution of definite concentration, and providing the optimal temperature and pH to the reaction mixture; the completion of the reaction is indicated by a change in color of the reaction mixture. The microbial extract preparation involves development of the desired test strain in suitable media. Liquid or solid media may be chosen according to the microorganism. Typically, the test strain is taken from microbial suspension and poured into a sterilized test tube or Petri dish. Either the molten media is spread over the test strain or the test strain is spread over solidified media. It is then incubated in an orbital shaker at optimum temperature and centrifuged. In the case of a unicellular organism, supernatant is used as microbial source. But in the case of various multicellular organisms, supernatant is discarded and the developed biomass is washed thoroughly with distilled water several times and wet biomass is then treated as microbial culture. The prepared microbial culture is exposed to metal salt solution and incubated on an orbital shaker at required temperature until a visible color change is recorded, which ensures the formation of nanoparticles. The formation of silver, gold, manganese and zinc nanoparticles is specified by the generation of a brownish, pinkish and whitish yellow to yellow color in the solution mixture respectively.

Usually the nanoparticle synthesis is influenced by microbes in two distinctive ways. Firstly, the existence of microbes along with secreted enzymes alters the composition of the reaction mixture, making it more saturated. Secondly, the enzymes secreted by microbes either favor or inhibit nucleation of the initial particles formed [194, 195]. Both factors greatly affect the biosynthesis yield [196].

2.3.1 Green Metal NPs via Microbes

Up till now, various studies have been reported demonstrating the production of metal nanoparticles using fungi, algae bacteria and other microbes. However, studies focusing on the formation of silver and gold NPs are greater in number due to their vast applications in various fields.

2.3.1.1 Silver NPs

A fungus, *Aspergillus flavus,* was found to contain several peptides which have the ability to reduce Ag^{+} ions to Ag^{0} by extracellular process [197]. NPs were formed over the cell wall of fungal biomass. Fluorescence spectrum confirmed the presence of NADH-dependent reductase and similar peptides in the colloidal solution covering as-prepared AgNPs [309]. These proteins excreted by fungus acted as stabilizing and reducing agents for the Ag NP synthesis.

Aspergillus niger was found to follow an extracellular route to form highly stable silver NPs. Elemental spectroscopic analysis revealed that quinone and nitrate-dependent reductase excreted by *A. niger* played the role of capping and chelating agents to produce silver NPs [310].

Silver NPs were fabricated using the fungal proteins of *Coriolus versicolor*. FTIR analysis revealed that the AgNPs were entirely capped by amino groups during the synthesis, hence enhancing the stability of the product. Glucose also plays an important role in the synthesis process. By tailoring the synthesis parameters, growth time could be lowered to 1 h. Moreover, an intracellular synthesis route could also be developed for AgNP synthesis by altering the reaction mixture pH [311].

Fusarium oxysporum is found to have the ability to grow AgNPs by hydrolyzing $AgNO_3$ solution [284]. It is reported that *F. oxysporum* is capable of establishing highly stable hydrosol of AgNPs [208]. Kumar *et al.* prepared silver NPs having dimensions of 10–25 nm by incubating $AgNO_3$ with *F. oxysporum* [312]. *In-vitro* analysis confirmed that nitrate reductase along with phytochelatin was responsible for silver ions reduction and stabilization. In another study it is suggested that anthraquinones and nitrate

dependent reductase enzymes present in *F. oxysporum* reduced Ag ions to form silver NPs [209].

The UV-Vis spectrum of silver NPs synthesized extracellularly by *Fusarium semitectum* showed clear enhancement in the intensity of plasmon resonance peak (centered at 420 nm) with the passage of time [210]. The NPs in suspension were found to be capped by amino groups and other peptides, which are believed to be accountable for the accumulation of NPs.

Fusarium solani is reported to produce sphere-shaped AgNPs having average size of 16.23 nm. FTIR studies indicated the presence of peptides bound to the surface of NPs which surely acted as stabilizing and reducing agents to form poly-dispersed AgNPs [313].

Rhizopus stolonifera, upon exposure to $AgNO_3$, manufactured uniform AgNPs of 25–30 nm size [222]. Silver NPs were harvested intracellularly by incubation of *Verticillium* sp. with $AgNO_3$ solution [263].

Pseudomonas stutzeri AG259 bacteria is found to precipitate 35 to 46 nm sized AgNPs intracellularly [314]. By increasing the concentration of metal ion solution, particle size of AgNPs reaches 200 nm [25]. The increase in particle size is surely due to the change in growth mechanism.

Morganella sp. RP-42 bacterium, separated from an arthropod, extracellularly produced 20 nm sized Ag NP crystals when reacted with $AgNO_3$ solution [315]. A silver reductant protein was found responsible for the formation of AgNPs. The study enlightens the mechanism of AgNP synthesis, as the found protein displayed an almost exactly similar structure with formerly reported protein silE.

A rapid synthesis of AgNPs is reported using the microbial extract of Enterobacteriaceae (*Klebsiella pneumonia*, *Escherichia coli* and *Enterobacter cloacae*) [316]. The study demonstrated a decrease in reduction process when piperitone is added, indicating that nitroreductase protein is responsible for silver ion accumulation.

Dehydrated eatable blue green alga *Spirulina platensis* produced spherical AgNPs with size ranging from 6–10 nm [317]. The synthesis process followed extracellular route. The nucleotides secreted by alga capped and reduced Ag ions to AgNPs.

Sphere-shaped AgNPs with mean diameter of about 13 nm were reported by using an aquatic red alga *Porphyra vietnamensis* [318]. A carbohydrate secreted by alga was incubated with $AgNO_3$ solution to form AgNPs. FTIR analysis demonstrated the loss of sulphate groups present on carbohydrate, confirming that sulphate groups are responsible for the reduction and stabilization of AgNPs.

Chlorella vulgaris was used to synthesize nanosilver platelets [319]. The chemicals secreted by alga acted as capping and reducing agents for the

synthesis of Ag nanoplatelets. It is reported that a nucleotide Asp–Asp–Tyr–OMe was involved in the biological reduction of Ag ions.

2.3.1.2 Gold NPs

Uniform and spherical gold NPs were reported using extract of filamentous fungus *Rhizopus stolonifera* (KCCM 35486). AuNPs with 1–5 nm size were verified by transmission electron microscopy (TEM) and X-ray diffraction (XRD) spectra. Another study showed the synthesis of AuNPs by subjecting gold thiosulphate solution to sulphate-reducing bacteria [320].

Verticillium luteoalbum was found capable of forming AuNPs when subjected to Au cations. Gold NPs were formed as a purple black ppt, which is centrifuged to get purified NPs. The analysis confirmed the formation of AuNPs. AuNPs of desired size, shape and yield could be obtained by controlling the pH of reaction mixture [180].

AuNPs were successfully prepared by incubating *Fusarium oxysporum* extract with gold chloride solution. The *in-vitro* synthesis study showed the existence of reductase and peptides in the colloidal suspension as well as bound to the surface of AuNPs, which accounted for the formation and stabilization of gold NPs [238].

Intracellular gold NPs were formed when *Verticillium* sp. extract was incubated with gold ion solution. Purple ppt formed in the mycelium was thoroughly washed and characterized. The UV-Vis spectra displayed absorption peak at 550 nm, confirming the production of AuNPs [263].

Octahedral platelets of AuNPs were prepared by subjecting cyanobacteria (*Plectonema boryanum* UTEX 485) to gold chloride solution. The study showed that the reaction was completed in two steps. Gold sulfide NPs were first developed near the cell walls of bacteria, which were then converted to AuNPs. Chloride ions present in the reaction mixture seem to enhance the bioaccumulation of AuNPs [248].

Plectonema boryanum UTEX 485 produced intracellular AuNPs when challenged with gold thiosulphate complex. AuS NPs were also found along with AuNPs. Cubical AuNPs showed a size ranging between 10–25 nm in suspension and 10 nm inside bacterium. With the addition of gold chloride, octahedral platelets of AuNPs were obtained having size ranging from 1–10 μm [316].

Sargassum wightii Greville, an aquatic alga, transformed $AuCl_4$ anions into gold NPs [254]. The formation of AuNPs was possible due to the extracellular carbohydrate secreted by alga. The reaction almost completed in 12 h, which is much faster than other synthesis routes involving microbes. TEM images revealed monodispersed planar AuNPs having a diameter of about 8–12 nm.

A dehydrated green alga named *Chlorella vulgaris* is reported to form AuNPs [321]. Both intracellular and extracellular proteins created by single-celled alga performed as capping and reducing agents for the synthesis of AuNPs. The process showed high yield. TEM analysis indicated tetrahedral, decahedral and icosahedral morphologies of synthesized AuNPs. Another study demonstrated that 28-kDa protein secreted by *C. vulgaris* is responsible for various morphologies of gold NPs [224]. Triangular, hexagonal and platelike AuNPs were accumulated by varying the concentration of 28-kDa protein.

Micro-sized AuNPs were precipitated in the biomass of a brown alga called *Fucus vesiculosus* [322]. Reaction was accomplished at intense pH values. The hydroxyl groups contained by various carbohydrates and nucleotides secreted by *F. vesiculosus* were responsible for the whole reduction process. Brown alga shows promising results for NP formation in comparison with other algae [323, 324].

Extracellular proteins secreted by *Spirulina platensis,* blue green alga, are found capable of reducing gold ions present in solution. Dehydrated *S. platensis* formed stable sphere-shaped AuNPs with size ranging from 7–16 nm [317].

2.3.1.3 Other Metallic NPs

A fungus, *Aspergillus terreus,* is reported to extracellularly harvest spherical Se NPs having average diameter of about 47 nm in about 1 h [325]. It is considered to be a relatively fast process as compared to other biological synthesis protocols.

Spherical crystalline Pt NPs, having size ranging from 3–4 nm, were obtained by consuming the extract and biomass of a fungus, *Neurospora crassa* [326]. The comparative study demonstrated that Pt NPs formed extracellularly, i.e., obtained from *N. crassa* biomass, showed more agglomeration than intracellularly produced Pt NPs. Also, the product yield of both the routes varies intensely.

Fusarium oxysporum has been reported to produce Vanadium (V) [327]. *Fusarium moniliforme* has the ability to transform ferric ion Fe(III) to ferrous ion Fe(II) [328].

An alga, *Chlorella* sp., was explored for its ability to reduce and stabilize numerous metals like copper, cadmium, nickel and uranium [329, 330].

An aquatic alga, *Sargassum wightii,* was reported to form palladium and platinum NPs when incubated with their corresponding metal chlorides [254].

2.3.2 Green Oxide NPs via Microbes

Silica, titania, zinc oxide, manganese dioxide, magnetite and other metal oxides have been synthesized using various microbes, including fungi, bacteria, algae, viruses, etc. Some of those reported are discussed below.

Barium titanate NPs having tetragonal morphology and average size of 10 nm were reported by using *Fusarium oxysporum* extracts [274].

Another similar approach displayed the formation of nanocrystalline silica and titania NPs upon subjecting *Fusarium oxysporum* to corresponding ions in aqueous solutions. *F. oxysporum* is found to excrete various cationic proteins which have the ability to hydrolyze ZrF^{4-} ions [331]. Zirconia NPs were formed extracellularly at ambient temperature in aqueous medium. Excreted proteins having a molar mass of 21–24 kDa were capable of hydrolyzing precursor halides in acidic medium [284]. *F. oxysporum* and *Verticillium* sp. are used to produce magnetite Fe_3O_4 NPs [332].

Magnetite NPs were fabricated by incubation of *Verticillium* sp. extract with iron cyanide complex solution. An extracellular cationic protein secreted by fungus capped and reduced iron cyanide ions into iron oxide NPs. The reducing protein was found to have a molar mass of 55 kDa [332].

A bacterium, *Saccharomyces cerevisiae,* was used to form Sb_2O_3 NPs at ambient temperature [333]. TEM micrographs demonstrated agglomerated sphere-like Sb_2O_3 NPs with 2–10 nm diameter.

Manganese dioxide NPs were reported by using *Bacillus* sp. [2]. TEM micrographs revealed monodispersed NPs with 4.62 nm diameter and orthorhombic morphology. The metal-resistant bacterium possesses several proteins capable of reducing and stabilizing the synthesized product.

2.4 Conclusions

The advent and execution of innovative technologies and development of scientific cognizance has cleared the way towards a newly revolutionized nano-age. In this nano-age, biological entities are employed for the synthesis of stable NPs, with significant consideration explicitly being given to economically integrated, effortlessly scaled-up and ecologically considerate biocompatible NPs. Rapid biological reducing agents present in *bio*-resources, such as global and marine microbes and plants, possess huge potential for biogenic synthesis of NPs. Among the above-mentioned entities, plants have emerged as the best candidates, due to their being abundant and easy to handle character. Green strategies utilize inexpensive harmless chemicals, eco-friendly solvents and renewable materials and occur at

neutral pH close to ambient temperature and pressures. Green principles provide cleaner, safer, simpler and controllable alternatives for the synthesis of NPs with desired characteristics, imparting greater importance to them for more effective utilization in diverse fields. Accelerating the investigations of green routes using living beings, natural resources or conditions will oust ordinary traditional methods by overcoming their limitations. Hence, the present chapter envisions the importance of green metals, and metal oxide, NP fabrication schemes by referring to several reports stated so far. With the enormous variety of natural resources available, many additional species are in line to be explored for prospective use.

Acknowledgments

The authors acknowledge the International Islamic University Pakistan, Higher Education Commission of Pakistan and Pakistan Institute of Engineering and Applied Sciences, Islamabad, Pakistan for their support.

References

1. Chaudhury, K., Kumar, V., Kandasamy, J., Choudhury, S.R., Regenerative nanomedicine: Current perspectives and future directions. *Int. J. Nanomedicine*, 9, 4153, 2014.
2. Sinha, A., Singh, V.N., Mehta, B.R., Khare, S.K., Synthesis and characterization of monodispersed orthorhombic manganese oxide nanoparticles produced by *Bacillus* sp. cells simultaneous to its bioremediation. *J. Hazard. Mater.*, 192, 620–627, 2011.
3. Mirzaei, H., Darroudi, M., Zinc oxide nanoparticles: biological synthesis and biomedical applications. *Ceram. Int.*, 43, 907–914, 2017.
4. Agency, E.P., Nanotechnology White Paper, USEPA 100/B-07/001, 2007.
5. Kato, H., *In vitro* assays: Tracking nanoparticles inside cells. *Nat. Nanotechnol.*, 6, 139–40, 2011.
6. Daniel, M.C., Astruc, D., Gold nanoparticles: Assembly, supramolecular chemistry, quantum-size-related properties, and applications toward biology, catalysis, and nanotechnology. *Chem. Rev.*, 104, 293–346, 2004.
7. Bar, H., Bhui, D.K., Sahoo, G.P., Sarkar, P., Pyne, S., Misra, A., Green synthesis of silver nanoparticles using seed extract of *Jatropha curcas*. *Colloids Surf. A*, 348, 212–216, 2009.
8. Kim, J.Y., Kim, M., Kim, H., Joo, J., Choi, J.H., Electrical and optical studies of organic light emitting devices using SWCNTs-polymer nanocomposites. *Opt. Mater.*, 21, 147–151, 2003.

9. Wei, G., Zhou, H., Liu, Z., Li, Z., A simple method for the preparation of ultrahigh sensitivity surface enhanced Raman scattering (SERS) active substrate. *Appl. Surf. Sci.* 240, 260–267, 2005.
10. Ahmad, A., Senapati, S., Khan, M.I., Intracellular synthesis of gold nanoparticles by a novel alkalotolerant actinomycete, *Rhodococcus* species. *Nanotechnology*, 14, 824–828, 2003.
11. Ahmad, N., Sharma, S., Alam, M.K., Singh, V.N., Shamsi, S.F., Mehta, B.R., Fatma, A., Rapid synthesis of silver nanoparticles using dried medicinal plant of basil. *Colloids Surf. B*, 81, 81–86, 2010.
12. Ahmad, T., Wani, I.A., Manzoor, N., Ahmed, J., Asiri, A.M., Biosynthesis, structural characterization and antimicrobial activity of gold and silver nanoparticles. *Colloids Surf. B*, 107, 227–234, 2013.
13. Ahmed, A., Senapati, S., Khan, M.I., Kumar, R., Sastry, M., Extracellular biosynthesis of monodisperse gold nanoparticles by a novel extremophilic actinomycete, *Thermomonospora* sp. *Langmuir*, 19, 3550–3553, 2003.
14. Liu, J., Qiao, S.Z., Hu, Q.H., Lu, G.Q., Magnetic nanocomposites with mesoporous structures: Synthesis and applications. *Small*, 7, 425–443, 2011.
15. Lee, Y.-R., Jang, M.-S., Cho, H.-Y., Kwon, H.-J., Kim, S., Ahn, W.-S., ZIF-8: A comparison of synthesis methods. *Chem. Eng. J.*, 271, 276–280, 2015.
16. Luechinger, N.A., Grass, R.N., Athanassiou, E.K., Stark, W.J., Bottom-up fabrication of metal/metal nanocomposites from nanoparticles of immiscible metals. *Chem. Mater.*, 22, 155–160, 2010.
17. Mohanpuria, P., Rana, N.K., Yadav, S.K., Biosynthesis of nanoparticles: technological concepts and future applications. *J. Nanopart. Res.*, 10, 507–517, 2008.
18. Tiwari, D.K., Behari, J., Sen, P., Time and dose-dependent antimicrobial potential of Ag nanoparticles synthesized by top-down approach *Curr. Sci.*, 95, 647–655, 2008.
19. Narayanan, K.B., Sakthivel, N., Biological synthesis of metal nanoparticles by microbes. *Adv. Colloid Interface Sci.*, 156, 1–13, 2010.
20. Panigrahi, S., Kundu, S., Ghosh, S.K., Nath, S., Pal, T., General method of synthesis for metal nanoparticles. *J. Nanopart. Res.*, 6, 411–414, 2004.
21. Thakkar, K.N., Mhatre, S.S., Parikh, R.Y., Biological synthesis of metallic nanoparticles. *Nanomedicine*, 6, 257–262, 2010.
22. Bhumkar, D.R., Joshi, H.M., Sastry, M., Pokharkar, V.B., Chitosan reduced gold nanoparticles as novel carriers for transmucosal delivery of insulin. *Pharm. Res.*, 24, 1415–1426, 2007.
23. Gan, P.P., Ng, S.H., Huang, Y., Li, S.F., Green synthesis of gold nanoparticles using palm oil mill effluent (POME): A low-cost and eco-friendly viable approach. *Bioresour. Technol.*, 113, 132–135, 2012.
24. Bansal, V., Rautaray, D., Ahmad, A., Sastry, M., Biosynthesis of zirconia nanoparticles using the fungus *Fusarium oxysporum*. *J. Mater. Chem.*, 14, 3303–3305, 2004.

25. Klaus, T., Joerger, R., Olsson, E., Granqvist, C.G., Silver-based crystalline nanoparticles, microbially fabricated. *Proc. Natl. Acad. Sci. U. S. A.*, 96, 13611–13614, 1999.
26. Senapati, S., Ahmad, A., Khan, M.I., Sastry, M., Kumar, R., Extracellular biosynthesis of bimetallic Au-Ag alloy nanoparticles. *Small*, 1, 517–20, 2005.
27. Poliakoff, M., Fitzpatrick, J.M., Farren, T.R., Anastas, P.T., Green chemistry: science and politics of change. *Science*, 297, 807–810, 2002.
28. Lengke, M.F., Fleet, M.E., Southam, G., Biosynthesis of silver nanoparticles by filamentous cyanobacteria from a silver (I) nitrate complex. *Langmuir*, 23, 2694–2699, 2007.
29. Govindaraju, K., Shan, J., Levesque, K., Hussain, S.N., Powell, W.S., Eidelman, D.H., Nitration of respiratory epithelial cells by myeloperoxidase depends on extracellular nitrite. *Nitric Oxide*, 18, 184–94, 2008.
30. Kowshik, M., Deshmukh, N., Vogel, W., Urban, J., Kulkarni, S.K., Paknikar, K.M., Microbial synthesis of semiconductor CdS nanoparticles, their characterization, and their use in the fabrication of an ideal diode. *Biotechnol. Bioeng.*, 78, 583–588, 2002.
31. Rautaray, D., Ahmad, A., Sastry, M., Biosynthesis of CaCO3 crystals of complex morphology using a fungus and an actinomycete. *J. Am. Chem. Soc.*, 125, 14656–7, 2003.
32. Ajitha, B., Reddy, Y.A.K., Reddy, P.S., Biogenic nano-scale silver particles by *Tephrosia purpurea* leaf extract and their inborn antimicrobial activity. *Spectrochim. Acta A*, 121, 164–172, 2014.
33. Ajitha, B., Reddy, Y.A.K., Reddy, P.S., Biosynthesis of silver nanoparticles using *Plectranthus amboinicus* leaf extract and its antimicrobial activity. *Spectrochim. Acta A*, 128, 257–262, 2014.
34. Ajitha, B., Reddy, Y.A.K., Reddy, P.S., Green synthesis and characterization of silver nanoparticles using *Lantana camara* leaf extract. *Mater. Sci. Eng. C*, 49, 373–381, 2015.
35. Álvarez, R.A.B., Valadez, M.C., Hurtado, R.B., Bueno, L.O.N., Lopez, N.S.F., Martínez, A.R.H., Corrales, R.G., Ortiz, R.V., Chacon, J.-G.B., Chavez, H.A., Acosta, M.F., Raman scattering and optical properties of lithium nanoparticles obtained by green synthesis. Vib. Spectrosc., 77, 5–9, 2015.
36. Ashokkumar, S., Ravi, S., Velmurugan, S., Green synthesis of silver nanoparticles from *Gloriosa superba* L. leaf extract and their catalytic activity. *Spectrochim. Acta A*, 115, 388–392, 2013.
37. Ashokkumar, S., Ravi, S., Kathiravan, V., Velmurugan, S., Synthesis of silver nanoparticles using *A. indicum* leaf extract and their antibacterial activity. *Spectrochim. Acta A*, 134, 34–39, 2015.
38. Azandehi, P.K., Moghaddam, J., Green synthesis, characterization and physiological stability of gold nanoparticles from *Stachys lavandulifolia* Vahl extract. *Particuology*, 19, 22–26, 2015.

39. Banala, R.R., Nagati, V.B., Karnati, P.R., Green synthesis and characterization of *Carica papaya* leaf extract coated silver nanoparticles through X-ray diffraction, electron microscopy and evaluation of bactericidal properties. *Saudi J. Biol. Sci.*, 22, 637–644, 2015.
40. Basavegowda, N., Idhayadhulla, A., Lee, Y.R., Phyto-synthesis of gold nanoparticles using fruit extract of *Hovenia dulcis* and their biological activities. *Ind. Crops Prod.*, 52, 745–751, 2014.
41. Bindhu, M.R., Umadevi, M., Antibacterial and catalytic activities of green synthesized silver nanoparticles. *Spectrochim. Acta A*, 135, 373–378, 2015.
42. Cruz, D., Falé, P.L., Mourato, A., Vaz, P.D., Serralheiro, M.L., Lino, A.R.L., Preparation and physicochemical characterization of Ag nanoparticles biosynthesized by *Lippia citriodora* (Lemon Verbena). *Colloids Surf. B*, 81, 67–73, 2010.
43. Dwivedi, A.D., Gopal, K., Biosynthesis of silver and gold nanoparticles using *Chenopodium album* leaf extract. *Colloids Surf. A*, 369, 27–33, 2010.
44. Emeka, E.E., Ojiefoh, O.C., Aleruchi, C., Hassan, L.A., Christiana, O.M., Rebecca, M., Dare, E.O., Temitope, A.E., Evaluation of antibacterial activities of silver nanoparticles green-synthesized using pineapple leaf (*Ananas comosus*). *Micron*, 57, 1–5, 2014.
45. Gavade, N.L., Kadam, A.N., Suwarnkar, M.B., Ghodake, V.P., Garadkar, K.M., Biogenic synthesis of multi-applicative silver nanoparticles by using *Ziziphus Jujuba* leaf extract. *Spectrochim. Acta A*, 136, 953–960, 2015.
46. Gopinath, K., Venkatesh, K.S., Ilangovan, R., Sankaranarayanan, K., Arumugam, A., Green synthesis of gold nanoparticles from leaf extract of *Terminalia arjuna*, for the enhanced mitotic cell division and pollen germination activity. *Ind. Crops Prod.*, 50, 737–742, 2013.
47. Gopinath, V., MubarakAli, D., Priyadarshini, S., Priyadharsshini, N.M., Thajuddin, N., Velusamy, P., Biosynthesis of silver nanoparticles from *Tribulus terrestris* and its antimicrobial activity: A novel biological approach. *Colloids Surf. B*, 96, 69–74, 2012.
48. Guo, M., Li, W., Yang, F., Liu, H., Controllable biosynthesis of gold nanoparticles from a *Eucommia ulmoides* bark aqueous extract. *Spectrochim. Acta A*, 142, 73–79, 2015.
49. Ibrahim, H.M.M., Green synthesis and characterization of silver nanoparticles using banana peel extract and their intimicrobial activity against representative microorganisms. *J. Radiat. Res. Appl. Sci.*, 8, 265–275, 2015.
50. Islam, N.U., Jalil, K., Shahid, M., Muhammad, N., Rauf, A., *Pistacia integerrima* gall extract mediated green synthesis of gold nanoparticles and their biological activities. *Arab. J. Chem.*, 2015.
51. Jacob, S.J.P., Finub, J.S., Narayanan, A., Synthesis of silver nanoparticles using *Piper longum* leaf extracts and its cytotoxic activity against Hep-2 cell line. *Colloids Surf. B*, 91, 212–214, 2012.

52. Jagtap, U.B., Bapat, V.A., Green synthesis of silver nanoparticles using *Artocarpus heterophyllus* Lam. seed extract and its antibacterial activity. *Ind. Crops Prod.*, 46, 132–137, 2013.
53. Jayaseelan, C., Ramkumar, R., Rahuman, A.A., Perumal, P., Green synthesis of gold nanoparticles using seed aqueous extract of *Abelmoschus esculentus* and its antifungal activity. *Ind. Crops Prod.*, 45, 423–429, 2013.
54. Jeeva, K., Thiyagarajan, M., Elangovan, V., Geetha, N., Venkatachalam, P., *Caesalpinia coriaria* leaf extracts mediated biosynthesis of metallic silver nanoparticles and their antibacterial activity against clinically isolated pathogens. *Ind. Crops Prod.*, 52, 714–720, 2014.
55. Joseph, S., Mathew, B., Microwave-assisted green synthesis of silver nanoparticles and the study on catalytic activity in the degradation of dyes. *J. Mol. Liq.*, 204, 184–191, 2015.
56. Joseph, S., Mathew, B., Microwave assisted facile green synthesis of silver and gold nanocatalysts using the leaf extract of *Aerva lanata*. *Spectrochim. Acta A*, 136 1371–1379, 2015.
57. Kanipandian, N., Thirumurugan, R., A feasible approach to phyto-mediated synthesis of silver nanoparticles using industrial crop *Gossypium hirsutum* (cotton) extract as stabilizing agent and assessment of its *in vitro* biomedical potential. *Ind. Crops Prod.*, 55, 1–10, 2014.
58. Kathiravan, V., Ravi, S., Ashokkumar, S., Velmurugan, S., Elumalai, K., Khatiwada, C.P., Green synthesis of silver nanoparticles using C*roton sparsiflorus morong* leaf extract and their antibacterial and antifungal activities. *Spectrochim. Acta A*, 139, 200–205, 2015.
59. Kotakadi, V.S., Rao, Y.S., Gaddam, S.A., Prasad, T.N., Reddy, A.V., Gopal, D.V., Simple and rapid biosynthesis of stable silver nanoparticles using dried leaves of *Catharanthus roseus.* Linn. G. Donn and its anti microbial activity. *Colloids Surf. B*, 105, 194–198, 2013.
60. Krishnaswamy, K., Orsat, V., Insight into the nanodielectric properties of gold nanoparticles synthesized from maple leaf and pine needle extracts. *Ind. Crops Prod.*, 66, 131–136, 2015.
61. Krishnaswamy, K., Vali, H., Orsat, V., Value-adding to grape waste: Green synthesis of gold nanoparticles. *J. Food Eng.*, 142, 210–220, 2014.
62. Kumar, B., Smita, K., Cumbal, L., Debut, A., Sacha inchi (*Plukenetia volubilis* L.) oil for one pot synthesis of silver nanocatalyst: An ecofriendly approach. *Ind. Crops Prod.*, 58, 238–243, 2014.
63. Kumar, B., Smita, K., Cumbal, L., Debut, A., Sacha inchi (*Plukenetia volubilis* L.) shell biomass for synthesis of silver nanocatalyst. *J. Saudi Chem. Soc.*, 21, S293-S298, 2017.
64. Kumar, B., Smita, K., Cumbal, L., Debut, A., Synthesis of silver nanoparticles using Sacha inchi (*Plukenetia volubilis* L.) leaf extracts. *Saudi J. Biol. Sci.*, 21, 605–609, 2014.
65. Kumar, K.M., Mandal, B.K., Kumar, K.S., Reddy, P.S., Sreedhar, B., Biobased green method to synthesise palladium and iron nanoparticles using

Terminalia chebula aqueous extract. *Spectrochim. Acta A*, 102, 128–133, 2013.

66. Kumar, K.P., Paul, W., Sharma, C.P., Green synthesis of gold nanoparticles with *Zingiber officinale* extract: Characterization and blood compatibility. *Process Biochem.*, 46, 2007–2013, 2011.
67. Kumar, P.P.N.V., Pammi, S.V.N., Kollu, P., Satyanarayana, K.V.V., Shameem, U., Green synthesis and characterization of silver nanoparticles using *Boerhaavia diffusa* plant extract and their anti bacterial activity. *Ind. Crops Prod.*, 52, 562–566, 2014.
68. Luna, C., Chávez, V.H.G., Castro, E.D.B., Núñez, N.O., Reséndez, R.M., Biosynthesis of silver fine particles and particles decorated with nanoparticles using the extract of *Illicium verum* (star anise) seeds. *Spectrochim. Acta A*, 141, 43–50, 2015.
69. Machado, S., Pinto, S.L., Grosso, J.P., Nouws, H.P.A., Albergaria, J.T., Delerue-Matos, C., Green production of zero-valent iron nanoparticles using tree leaf extracts. *Sci. Total Environ.*, 445–446, 1–8, 2013.
70. Mariselvam, R., Ranjitsingh, A.J.A., Nanthini, A.U.R., Kalirajan, K., Padmalatha, C., Selvakumar, P.M., Green synthesis of silver nanoparticles from the extract of the inflorescence of *Cocos nucifera* (Family: *Arecaceae*) for enhanced antibacterial activity. *Spectrochim. Acta A*, 129, 537–541, 2014.
71. Miri, A., Sarani, M., Bazaz, M.R., Darroudi, M., Plant-mediated biosynthesis of silver nanoparticles using *Prosopis farcta* extract and its antibacterial properties. *Spectrochim. Acta A*, 141, 287–291, 2015.
72. Mo, Y.Y., Tang, Y.K., Wang, S.Y., Lin, J.M., Zhang, H.B., Luo, D.Y., Green synthesis of silver nanoparticles using eucalyptus leaf extract. *Mater. Lett.*, 144, 165–167, 2015.
73. Moghaddam, M.G., Dabanlou, R.H., Plant mediated green synthesis and antibacterial activity of silver nanoparticles using *Crataegus douglasii* fruit extract. *J. Ind. Eng. Chem.*, 20, 739–744, 2014.
74. Mohapatra, B., Kuriakose, S., Mohapatra, S., Rapid green synthesis of silver nanoparticles and nanorods using *Piper nigrum* extract. *J. Alloys Compd.*, 637, 119–126, 2015.
75. MubarakAli, D., Thajuddin, N., Jeganathan, K., Gunasekaran, M., Plant extract mediated synthesis of silver and gold nanoparticles and its antibacterial activity against clinically isolated pathogens. *Colloids Surf. B*, 85, 360–365, 2011.
76. Muniyappan, N., Nagarajan, N.S., Green synthesis of gold nanoparticles using *Curcuma pseudomontana* essential oil, its biological activity and cytotoxicity against human ductal breast carcinoma cells T47D. *J. Environ. Chem. Eng.*, 2, 2037–2044, 2014.
77. Muniyappan, N., Nagarajan, N.S., Green synthesis of silver nanoparticles with *Dalbergia spinosa* leaves and their applications in biological and catalytic activities. *Process Biochem.*, 49, 1054–1061, 2014.

78. Muthukrishnan, S., Bhakya, S., Kumar, T.S., Rao, M.V., Biosynthesis, characterization and antibacterial effect of plant-mediated silver nanoparticles using *Ceropegia thwaitesii* – An endemic species. *Ind. Crops Prod.*, 63, 119–124, 2015.
79. Muthuvel, A., Adavallan, K., Balamurugan, K., Krishnakumar, N., Biosynthesis of gold nanoparticles using *Solanum nigrum* leaf extract and screening their free radical scavenging and antibacterial properties. *Biomed. Prev. Nutr.*, 4, 325–332, 2014.
80. Nabikhan, A., Kandasamy, K., Raj, A., Alikunhi, N.M., Synthesis of antimicrobial silver nanoparticles by callus and leaf extracts from saltmarsh plant, *Sesuvium portulacastrum* L. *Colloids Surf. B*, 79, 488–493, 2010.
81. Nasrollahzadeh, M., Sajadi, S.M., Rostami-Vartooni, A., Bagherzadeh, M., Safari, R., Immobilization of copper nanoparticles on perlite: Green synthesis, characterization and catalytic activity on aqueous reduction of 4-nitrophenol. *J. Mol. Catal. A Chem.*, 400, 22–30, 2015.
82. Nazeruddin, G.M., Prasad, N.R., Prasad, S.R., Shaikh, Y.I., Waghmare, S.R., Adhyapak, P., *Coriandrum sativum* seed extract assisted *in situ* green synthesis of silver nanoparticle and its anti-microbial activity. *Ind. Crops Prod.*, 60, 212–216, 2014.
83. Niraimathi, K.L., Sudha, V., Lavanya, R., Brindha, P., Biosynthesis of silver nanoparticles using *Alternanthera sessilis* (Linn.) extract and their antimicrobial, antioxidant activities. *Colloids Surf. B*, 102, 288–291, 2013.
84. Paul, B., Bhuyan, B., Purkayastha, D.D., Dey, M., Dhar, S.S., Green synthesis of gold nanoparticles using *Pogestemon benghalensis* (B) O. Ktz. leaf extract and studies of their photocatalytic activity in degradation of methylene blue. *Mater. Lett.*, 148, 37–40, 2015.
85. Philip, D., Biosynthesis of Au, Ag and Au–Ag nanoparticles using edible mushroom extract. *Spectrochim. Acta A*, 73, 374–381, 2009.
86. Philip, D., Unni, C., Extracellular biosynthesis of gold and silver nanoparticles using Krishna tulsi (*Ocimum sanctum*) leaf. *Physica E*, 43, 1318–1322, 2011.
87. Philip, D., Green synthesis of gold and silver nanoparticles using *Hibiscus rosa sinensis*. *Physica E*, 42, 1417–1424, 2010.
88. Philip, D., *Mangifera Indica* leaf-assisted biosynthesis of well-dispersed silver nanoparticles. *Spectrochim. Acta A*, 78, 327–31, 2011.
89. Philip, D., Unni, C., Aromal, S.A., Vidhu, V.K., *Murraya koenigii* leaf-assisted rapid green synthesis of silver and gold nanoparticles. *Spectrochim. Acta A*, 78, 899–904, 2011.
90. Philip, D., Rapid green synthesis of spherical gold nanoparticles using *Mangifera indica* leaf. *Spectrochim. Acta A*, 77, 807–810, 2010.
91. Pourmortazavi, S.M., Taghdiri, M., Makari, V., Nasrabadi, M.R., Procedure optimization for green synthesis of silver nanoparticles by aqueous extract of *Eucalyptus oleosa*. *Spectrochim. Acta A*, 136, 1249–1254, 2015.

92. Prasad, K.S., Gandhi, P., Selvaraj, K., Synthesis of green nano iron particles (GnIP) and their application in adsorptive removal of As(III) and As(V) from aqueous solution. *Appl. Surf. Sci.*, 317, 1052–1059, 2014.
93. Ramesh, P.S., Kokil, T., Geetha, D., Plant mediated green synthesis and antibacterial activity of silver nanoparticles using E*mblica officinalis* fruit extract. *Spectrochim. Acta A*, 142, 339–343, 2015.
94. Rao, Y.S., Kotakadi, V.S., Prasad, T.N.V.K.V., Reddy, A.V., Gopal, D.V.R.S., Green synthesis and spectral characterization of silver nanoparticles from Lakshmi tulasi (*Ocimum sanctum*) leaf extract. *Spectrochim. Acta A*, 103, 156–159, 2013.
95. Romano, M.F., Gil, M.L.A., Santander, J.M.P., Jaén, J.J.D., Rodríguez, I.N., Cisneros, J.L.H.d., Aguilera, L.M.C., Sonosynthesis of gold nanoparticles from a geranium leaf extract. *Ultrason. Sonochem.*, 21, 1570–1577, 2014.
96. Sadeghi, B., Rostami, A., Momeni, S.S., Facile green synthesis of silver nanoparticles using seed aqueous extract of *Pistacia atlantica* and its antibacterial activity. *Spectrochim. Acta A*, 134, 326–332, 2015.
97. Sathishkumar, M., Sneha, K., Won, S.W., Cho, C.W., Kim, S., Yun, Y.S., *Cinnamon zeylanicum* bark extract and powder mediated green synthesis of nano-crystalline silver particles and its bactericidal activity. *Colloids Surf. B*, 73, 332–338, 2009.
98. Sathiya, C.K., Akilandeswari, S., Fabrication and characterization of silver nanoparticles using *Delonix elata* leaf broth. *Spectrochim. Acta A*, 128, 337–341, 2014.
99. Shankar, S., Jaiswal, L., Aparna, R.S.L., Prasad, R.G.S.V., Synthesis, characterization, *in vitro* biocompatibility, and antimicrobial activity of gold, silver and gold silver alloy nanoparticles prepared from *Lansium domesticum* fruit peel extract. *Mater. Lett.*, 137, 75–78, 2014.
100. Smitha, S.L., Philip, D., Gopchandran, K.G., Green synthesis of gold nanoparticles using *Cinnamomum zeylanicum* leaf broth. *Spectrochim. Acta A*, 74, 735–739, 2009.
101. Song, J.Y., Jang, H.K., Kim, B.S., Biological synthesis of gold nanoparticles using Magnolia kobus and Diopyros kaki leaf extracts. *Process Biochem.*, 44, 1133–1138, 2009.
102. Suman, T.Y., Rajasree, S.R.R., Ramkumar, R., Rajthilak, C., Perumal, P., The green synthesis of gold nanoparticles using an aqueous root extract of *Morinda citrifolia* L. *Spectrochim. Acta A*, 118, 11–16, 2014.
103. Sun, Q., Cai, X., Li, J., Zheng, M., Chen, Z., Yu, C.-P., Green synthesis of silver nanoparticles using tea leaf extract and evaluation of their stability and antibacterial activity. *Colloids Surf. A*, 444, 226–231, 2014.
104. Ulug, B., Turkdemir, M.H., Cicek, A., Mete, A., Role of irradiation in the green synthesis of silver nanoparticles mediated by fig (*Ficus carica*) leaf extract. *Spectrochim. Acta A*, 135, 153–161, 2015.
105. Veerasamy, R., Xin, T.Z., Gunasagaran, S., Xiang, T.F.W., Yang, E.F.C., Jeyakumar, N., Dhanaraj, S.A., Biosynthesis of silver nanoparticles using

mangosteen leaf extract and evaluation of their antimicrobial activities. *J. Saudi Chem. Soc.*, 15, 113–120, 2011.
106. Velusamy, P., Das, J., Pachaiappan, R., Vaseeharan, B., Pandian, K., Greener approach for synthesis of antibacterial silver nanoparticles using aqueous solution of neem gum (*Azadirachta indica* L.). *Ind. Crops Prod.*, 66, 103–109, 2015.
107. Vijayakumar, M., Priya, K., Nancy, F.T., Noorlidah, A., Ahmed, A.B.A., Biosynthesis, characterisation and anti-bacterial effect of plant-mediated silver nanoparticles using *Artemisia nilagirica*. *Ind. Crops Prod.*, 41, 235–240, 2013.
108. Vijayaraghavan, K., Nalini, S.P.K., Prakash, N.U., Madhankumar, D., One step green synthesis of silver nano/microparticles using extracts of *Trachyspermum ammi* and *Papaver somniferum*. *Colloids Surf. B*, 94, 114–117, 2012.
109. Vivek, R., Thangam, R., Muthuchelian, K., Gunasekaran, P., Kaveri, K., Kannan, S., Green biosynthesis of silver nanoparticles from *Annona squamosa* leaf extract and its *in vitro* cytotoxic effect on MCF-7 cells. *Process Biochem.*, 47, 2405–2410, 2012.
110. Vivekanandhan, S., Schreiber, M., Mason, C., Mohanty, A.K., Misra, M., Maple leaf (*Acer* sp.) extract mediated green process for the functionalization of ZnO powders with silver nanoparticles. *Colloids Surf. B*, 113, 169–175, 2014.
111. Wang, T., Jin, X., Chen, Z., Megharaj, M., Naidu, R., Green synthesis of Fe nanoparticles using eucalyptus leaf extracts for treatment of eutrophic wastewater. *Sci. Total Environ.* 466–467, 210–213, 2014.
112. Yallappa, S., Manjanna, J., Dhananjaya, B.L., Phytosynthesis of stable Au, Ag and Au–Ag alloy nanoparticles using *J. Sambac* leaves extract, and their enhanced antimicrobial activity in presence of organic antimicrobials. *Spectrochim. Acta A*, 137, 236–243, 2015.
113. Zayed, M.F., Eisa, W.H., Shabaka, A.A., *Malva parviflora* extract assisted green synthesis of silver nanoparticles. *Spectrochim. Acta A*, 98, 423–428, 2012.
114. Zayed, M.F., Eisa, W.H., *Phoenix dactylifera* L. leaf extract phytosynthesized gold nanoparticles; controlled synthesis and catalytic activity. *Spectrochim. Acta A*, 121, 238–244, 2014.
115. Scarano, G., Morelli, E., Characterization of cadmium- and lead-phytochelatin complexes formed in a marine microalga in response to metal exposure. *Biometals*, 15, 145–151, 2002.
116. Scarano, G., Morelli, M., Properties of phytochelatin-coated CdS nanochrystallites formed in a marine phytoplanktonic alga (*Phaeodactylum tricornutum*, Bohlin) in response to Cd. *Plant Sci.*, 165, 803–810, 2003.
117. Anshup, A., Venkataraman, J.S., Subramaniam, C., Kumar, R.R., Priya, S., Kumar, T.R.S., Omkumar, R.V., John, A., Pradeep, T., Growth of gold nanoparticles in human cells. *Langmuir*, 21, 11562–7, 2005.

118. Shankar, S.S., Rai, A., Ahmad, A., Sastry, M., Rapid synthesis of Au, Ag, and bimetallic Au core–Ag shell nanoparticles using Neem (*Azadirachta indica*) leaf broth. *J. Colloid Interface Sci.*, 275, 496–502, 2004.
119. Shiv Shankar, S., Ahmad, A., Pasricha, R., Sastry, M., Bioreduction of chloroaurate ions by geranium leaves and its endophytic fungus yields gold nanoparticles of different shapes. *J. Mater. Chem.*, 13, 1822–1846, 2003.
120. Song, J.Y., Kim, B.S., Rapid biological synthesis of silver nanoparticles using plant leaf extracts. *Bioprocess. Biosyst. Eng.*, 32, 79–84, 2009.
121. Song, J.Y., Kwon, E.Y., Kim, B.S., Biological synthesis of platinum nanoparticles using *Diopyros kaki* leaf extract. *Bioprocess. Biosyst. Eng.*, 33, 159–164, 2010.
122. Kale, A., Bao, Y., Zhou, Z., Prevelige, P.E., Gupta, A., Directed self-assembly of CdS quantum dots on bacteriophage P22 coat protein templates. *Nanotechnology*, 24, 045603, 2013.
123. Shah, M., Fawcett, D., Sharma, S., Tripathy, S.K., Poinern, G.E.J., Green synthesis of metallic nanoparticles via biological entities. *Materials*, 8, 7278–7308, 2015.
124. Vilchis-Nestor, A.R., Sánchez-Mendieta, V., Camacho-López, M.A., Gómez-Espinosa, R.M., Camacho-López, M.A., Arenas-Alatorre, J.A., Solventless synthesis and optical properties of Au and Ag nanoparticles using *Camellia sinensis* extract. *Mater. Lett.*, 62, 3103–3105, 2008.
125. Castro, L., Blázquez, M.L., Muñoz, J.A., González, F., García-Balboa, C., Ballester, A., Biosynthesis of gold nanowires using sugar beet pulp. *Process Biochem.*, 46, 1076–1082, 2011.
126. Marshall, A.T., Haverkamp, R.G., Davies, C.E., Parsons, J.G., Gardea-Torresdey, J.L., van Agterveld, D., Accumulation of gold nanoparticles in *Brassic juncea*. *Int. J. Phytoremediation*, 9, 197–206, 2007.
127. Njagi, E.C., Huang, H., Stafford, L., Genuino, H., Galindo, H.M., Collins, J.B., Hoag, G.E., Suib, S.L., Biosynthesis of iron and silver nanoparticles at room temperature using aqueous sorghum bran extracts. *Langmuir*, 27, 264–271, 2010.
128. Park, Y., Hong, Y,N., Weyers, A., Kim, Y.S., Linhardt, R.J., Polysaccharides and phytochemicals: A natural reservoir for the green synthesis of gold and silver nanoparticles. *IET nanobiotechnol.*, 5, 69–78, 2011.
129. Kim, J., Rheem, Y., Yoo, B., Chong, Y., Bozhilov, K.N., Kim, D., Sadowsky, M.J., Hur, H.G., Myung, N.V., Peptide-mediated shape-and size-tunable synthesis of gold nanostructures. *Acta Biomater.*, 6, 2681–2689, 2010.
130. Si, S., Mandal, T.K., Tryptophan-based peptides to synthesize gold and silver nanoparticles: A mechanistic and kinetic study. *Chemistry*, 13, 3160–3168, 2007.
131. Malik, P., Shankar, R., Malik, V., Sharma, N., Mukherjee, T.K., Green chemistry based benign routes for nanoparticle synthesis. *J. Nanopart.*, 2014, 302429, 2014.
132. Akhtar, M.S., Jitendra Panwar, Yun, Y.S., Biogenic synthesis of metallic nanoparticles by plant extracts. *ACS Sustain. Chem. Eng.*, 1, 591–602, 2013.

133. Mittal, A.K., Chisti, Y., Banerjee, U.C., Synthesis of metallic nanoparticles using plant extracts. *Biotechnol. Adv.*, 31, 346–356, 2013.
134. Raveendran, P., Fu, J., Wallen, S.L., Completely "green" synthesis and stabilization of metal nanoparticles. *J. Am. Chem. Soc.*, 125, 13940–13941, 2003.
135. Selvakannan, P.R., Mandal, S., Phadtare, S., Gole, A., Pasricha, R., Adyanthaya, S.D., Sastry, M., Water-dispersible tryptophan-protected gold nanoparticles prepared by the spontaneous reduction of aqueous chloroaurate ions by the amino acid. *J. Colloid Interface Sci.*, 269, 97–102, 2004.
136. Willett, R.L., Baldwin, K.W., West, K.W., Pfeiffer, L.N., Differential adhesion of amino acids to inorganic surfaces. *Proc. Natl. Acad. Sci.*, 102, 7817–7822, 2005.
137. Gan, P.P., Li, S.F.Y., Potential of plant as a biological factory to synthesize gold and silver nanoparticles and their applications. *Rev. Environ. Sci. Bio.*, 11, 169–206, 2012.
138. Ghodake, G.S., Deshpande, N.G., Lee, Y.P., Jin, E.S., Pear fruit extract-assisted room-temperature biosynthesis of gold nanoplates. *Colloids Surf. B*, 75, 584–589, 2010.
139. Sathishkumar, M., Sneha, K., Yun, Y.S., Immobilization of silver nanoparticles synthesized using *Curcuma longa* tuber powder and extract on cotton cloth for bactericidal activity. *Bioresour. Technol.*, 101, 7958–7965, 2010.
140. Bankar, A., Joshi, B., Kumar, A.R., Zinjarde, S., Banana peel extract mediated synthesis of gold nanoparticles. *Colloids Surf. B*, 80, 45–50, 2010.
141. Das, R.K., Gogoi, N., Bora, U., Green synthesis of gold nanoparticles using *Nyctanthes arbortristis* flower extract. *Bioprocess Biosyst. Eng.*, 34, 615–619, 2011.
142. Lin, L., Wang, W., Huang, J., Li, Q., Sun, D., Yang, X., Wang, H., He, N., Wang, Y., Nature factory of silver nanowires: Plant-mediated synthesis using broth of *Cassia fistula* leaf. *Chem. Eng. J.*, 162, 852–858, 2010.
143. Lukman, A.I., Gong, B., Marjo, C.E., Roessner, U., Harris, A.T., Facile synthesis, stabilization, and anti-bacterial performance of discrete Ag nanoparticles using *Medicago sativa* seed exudates. *J. Colloid Interface Sci.*, 353, 433–444, 2011.
144. Haverkamp, R.G., Marshall, A.T., The mechanism of metal nanoparticle formation in plants: Limits on accumulation. *J. Nanopart. Res.*, 11, 1453–1463, 2009.
145. Khan, A.A., Fox, E.K., Górzny, M.Ł., Nikulina, E., Brougham, D.F., Wege, C., Bittner, A.M., pH control of the electrostatic binding of gold and iron oxide nanoparticles to tobacco mosaic virus. *Langmuir*, 29, 2094–2098, 2013.
146. Bar, H., Bhui, D.K., Sahoo, G.P., Sarkar, P., Pyne, S., Misra, A., Green synthesis of silver nanoparticles using seed extract of *Jatropha curcas*. *Colloids Surf. A*, 348, 212–216, 2009.
147. Darroudi, M., Sarani, M., Oskuee, R.K., Zak, A.K., Amiri, M.S., Nanoceria: Gum mediated synthesis and *in vitro* viability assay. *Ceram. Int.*, 40, 2863–2868, 2014.

148. Sharma, J.K., Srivastava, P., Singh, G., Akhtar, M.S., Ameen, S., Green synthesis of Co_3O_4 nanoparticles and their applications in thermal decomposition of ammonium perchlorate and dye-sensitized solar cells. *Mater. Sci. Eng. B*, 193, 181–188, 2015.
149. Gunalan, S., Sivaraj, R., Venckatesh, R., *Aloe barbadensis* Miller mediated green synthesis of mono-disperse copper oxide nanoparticles: Optical properties. *Spectrochim. Acta A*, 97, 1140–1144, 2012.
150. Suresh, D., Nethravathi, P.C., Gowda, U.C., Rajanaika, H., Nagabhushana, H., Sharma, S.C., Green synthesis of multifunctional zinc oxide (ZnO) nanoparticles using *Cassia fistula* plant extract and their photodegradative, antioxidant and antibacterial activities. *Mater. Sci. Semicond. Process.*, 31, 446–454, 2015.
151. Nasrollahzadeh, M., Sajadi, S.M., Vartooni, A.R., Bagherzadeh, M., Green synthesis of Pd/CuO nanoparticles by *Theobroma cacao* L. seeds extract and their catalytic performance for the reduction of 4-nitrophenol and phosphine-free Heck coupling reaction under aerobic conditions. *J. Colloid Interface Sci.*, 448, 106–113, 2015.
152. Udayabhanu, Nethravathi, P.C., Kumar, M.A.P., Suresh, D., Lingaraju, K., Rajanaika, H., Nagabhushana, H., Sharma, S.C., *Tinospora cordifolia* mediated facile green synthesis of cupric oxide nanoparticles and their photocatalytic, antioxidant and antibacterial properties. *Mater. Sci. Semicond. Process.*, 33, 81–88, 2015.
153. Venkateswarlu, S., Kumar, B.N., Prasad, C.H., Venkateswarlu, P., Jyothi, N.V.V., Bio-inspired green synthesis of Fe_3O_4 spherical magnetic nanoparticles using *Syzygium cumini* seed extract. *Physica B*, 449, 67–71, 2014.
154. Thakur, S., Karak, N., Green reduction of graphene oxide by aqueous phytoextracts. *Carbon*, 50, 5331–5339, 2012.
155. Srivastava, V., Sharma, Y.C., Sillanpää, M., Green synthesis of magnesium oxide nanoflower and its application for the removal of divalent metallic species from synthetic waste water. *Ceram. Int.*, 41, 6702–6709, 2015.
156. Chen, R., Zhang, Q., Gu, Y., Tang, L., Li, C., Zhang, Z., One-pot green synthesis of Prussian blue nanocubes decorated reduced graphene oxide using mushroom extract for efficient 4-nitrophenol reduction. *Anal. Chim. Acta*, 853, 579–587, 2015.
157. Sangeetha, G., Rajeshwari, S., Venckatesh, R., Green synthesis of zinc oxide nanoparticles by aloe barbadensis miller leaf extract: Structure and optical properties. *Mater. Res. Bull.*, 46, 2560–2566, 2011.
158. Suresh, D., Shobharani, R.M., Nethravathi, P.C., Pavan Kumar, M.A., Nagabhushana, H., Sharma, S.C., *Artocarpus gomezianus* aided green synthesis of ZnO nanoparticles: Luminescence, photocatalytic and antioxidant properties. *Spectrochim. Acta A*, 141, 128–134, 2015.
159. Vimala, K., Sundarraj, S., Paulpandi, M., Vengatesan, S., Kannan, S., Green synthesized doxorubicin loaded zinc oxide nanoparticles regulates the Bax and Bcl-2 expression in breast and colon carcinoma. *Process Biochem.*, 49, 160–172, 2014.

160. Samata, N.A., Nor, R.M., Sol–gel synthesis of zinc oxide nanoparticles using *Citrus aurantifolia* extracts. *Ceram. Int.*, 39, S545-S548, 2013.
161. Darroudi, M., Sabouri, Z., Oskuee, R.K., Zak, A.K., Kargar, H., Hamid, M.H.N.A., Sol-gel synthesis, characterization, and neurotoxicity effect of zinc oxide nanoparticles using gum tragacanth. *Ceram. Int.*, 39, 9195–9199, 2013.
162. Elumalai, K., Velmurugan, S., Ravi, S., Kathiravan, V., Ashokkumar, S., Green synthesis of zinc oxide nanoparticles using *Moringa oleifera* leaf extract and evaluation of its antimicrobial activity. *Spectrochim. Acta A*, 143, 158–164, 2015.
163. Rajiv, P., Rajeshwari, S., Venckatesh, R., Bio-fabrication of zinc oxide nanoparticles using leaf extract of *Parthenium hysterophorus* L. and its size-dependent antifungal activity against plant fungal pathogens. S*pectrochim. Acta A*, 112, 384–387, 2013.
164. Vijayakumar, S., Vinoj, G., Malaikozhundan, B., Shanthi, S., Vaseeharan, B., *Plectranthus amboinicus* leaf extract mediated synthesis of zinc oxide nanoparticles and its control of methicillin resistant *Staphylococcus aureus* biofilm and blood sucking mosquito larvae. *Spectrochim. Acta A*, 137, 886–891, 2015.
165. Fu, L., Fu, Z., Plectranthus amboinicus leaf extract–assisted biosynthesis of ZnO nanoparticles and their photocatalytic activity. *Ceram. Int.*, 41, 2492–2496, 2015.
166. Ramesh, M., Anbuvannan, M., Viruthagiri, G., Green synthesis of ZnO nanoparticles using *Solanum nigrum* leaf extract and their antibacterial activity. *Spectrochim. Acta A*, 136, 864–870, 2015.
167. Elumalai, K., Velmurugan, S., Ravi, S., Kathiravan, V., Ashokkumar, S., Facile, eco-friendly and template free photosynthesis of cauliflower like ZnO nanoparticles using leaf extract of *Tamarindus indica* (L.) and its biological evolution of antibacterial and antifungal activities. *Spectrochim. Acta A*, 136, 1052–1057, 2015.
168. Gopinath, V., Priyadarshini, S., Priyadharsshini, N.M., Pandian, K., Velusamy, P., Biogenic synthesis of antibacterial silver chloride nanoparticles using leaf extracts of *Cissus quadrangularis* Linn. *Mater. Lett.*, 91, 224–227, 2013.
169. Malleshappa, J., Nagabhushana, H., Prashantha, S.C., Sharma, S.C., Dhananjaya, N., Nagabhushana, B.M., Shivakumara, C., Abreu, F., Eco-friendly green synthesis, structural and photoluminescent studies of CeO_2:Eu^{3+} nanophosphors using *E. tirucalli* plant latex. *J. Alloys Compd.*, 612, 425–434, 2014.
170. Venkateswarlu, S., Kumar, B.N., Prathima, B., Anitha, K., Jyothi, N.V.V., A novel green synthesis of Fe_3O_4-Ag core shell recyclable nanoparticles using *Vitis vinifera* stem extract and its enhanced antibacterial performance. *Physica B*, 457, 30–35, 2015.
171. Ravikumar, B.S., Nagabhushana, H., Sharma, S.C., Vidya, Y.S., Anantharaju, K.S., *Calotropis procera* mediated combustion synthesis of $ZnAl_2O_4$:Cr^{3+}

nanophosphors: Structural and luminescence studies. *Spectrochim. Acta A*, 136, 1027–1037, 2015.
172. Zargar, M., Kamyar, S., Najafi, R., Farahani, F., Plant mediated green biosynthesis of silver nanoparticles using *Vitex negundo* L. extract. *J. Ind. Eng. Chem.*, 20, 4169–4175, 2014.
173. Ramar, M., Manikandan, B., Raman, T., Arunagirinathan, K., Prabhu, N.M., Basu, M.J., Perumal, M., Biosynthesis of silver nanoparticles using ethanolic petals extract of *Rosa indica* and characterization of its antibacterial, anticancer and anti-inflammatory activities. *Spectrochim. Acta A*, 138, 120–129, 2015.
174. Raja, K., Saravanakumar, A., Vijayakumar, R., Efficient synthesis of silver nanoparticles from *Prosopis juliflora* leaf extract and its antimicrobial activity using sewage. *Spectrochim. Acta A*, 97, 490–494, 2012.
175. Manikandan, R., Manikandan, B., Raman, T., Arunagirinathan, K., Prabhu, N.M., Jothi Basu, M., Perumal, M., Palanisamy, S., Munusamy, A., Biosynthesis of silver nanoparticles using ethanolic petals extract of *Rosa indica* and characterization of its antibacterial, anticancer and anti-inflammatory activities. *Spectrochim. Acta A*, 138, 120–129, 2015.
176. Raja, K., Saravanakumar, A., Vijayakumar R., Efficient synthesis of silver nanoparticles from *Prosopis juliflora* leaf extract and its antimicrobial activity using sewage. *Spectrochim. Acta A*, 97, 490–494, 2012.
177. Khazaei, A., Khazaei, M., Rahmati, S., A green method for the synthesis of gelatin/pectin stabilized palladium nano-particles as efficient heterogeneous catalyst for solvent-free Mizoroki–Heck reaction. *J. Mol. Catal. A Chem.*, 398, 241–247, 2015.
178. Dhillon, G.S., Brar, S.K., Kaur, S., Verma, M., Green approach for nanoparticle biosynthesis by fungi: Current trends and applications. *Crit. Rev. Biotechnol.*, 32, 49–73, 2012.
179. Durán, N., Marcato, P.D., Durán, M., Yadav, A., Gade, A., Rai, M., Mechanistic aspects in the biogenic synthesis of extracellular metal nanoparticles by peptide, bacteria, fungi, and plants. *Appl. Microbiol. Biotechnol.*, 90, 1609–1624, 2011.
180. Gericke, M., Pinches, A., Microbial production of gold nanoparticles. *Gold Bull.*, 39, 22–28, 2006.
181. Li, X., Xu, H., Chen, Z.S., Biosynthesis of nanoparticles by microorganisms and their applications. *J. Nanomater.*, 2011, 270974, 2011.
182. Correa-Llantén, D.N., Muñoz-Ibacache, S.A., Castro, M.E., Muñoz, P.A., Blamey, J.M., Gold nanoparticles synthesized by *Geobacillus* sp. strain ID17 a thermophilic bacterium isolated from Deception Island, Antarctica. *Microb. Cell Fact.*, 12, 75, 2013.
183. Pantidos, N., Horsfall, L.E., Biological synthesis of metallic nanoparticles by bacteria, fungi and plants. *J. Nanomed. Nanotechnol.*, 5, 5, 2014.
184. Taherzadeh, M.J., Fox, M., Hjorth, H., Edebo, L., Production of mycelium biomass and ethanol from paper pulp sulfite liquor by *Rhizopus oryzae*. *Bioresour. Technol.*, 88, 167–177, 2003.

185. Moghaddam, K.M., An Introduction to microbial metal nanoparticle preparation method. *JYI*, 19, 2010.
186. Narayanan, K.B., Sakthivel, N., Biological synthesis of metal nanoparticles by microbes. *Adv. Colloid Interface Sci.*, 156, 1–13, 2010.
187. Husen, A., Siddiqi, K.S., Plants and microbes assisted selenium nanoparticles: characterization and application. *J. Nanobiotechnol.*, 12, 2014.
188. Iravani, S., Bacteria in nanoparticle synthesis: Current status and future prospects. *Int. Sch. Res. Notices*, 18, 359–316, 2014.
189. Prabhu, S., Poulose, E.K., Silver nanoparticles: Mechanism of antimicrobial action, synthesis, medical applications, and toxicity effects. *Int. Nano Lett.*, 2, 32, 2012.
190. Singh, R., Shedbalkar, U.U., Wadhwani, S.A., Chopade, B.A., Bacteriagenic silver nanoparticles: Synthesis, mechanism, and applications. *Appl. Microbiol. Biotechnol.*, 99, 4579–4593, 2015.
191. Zhang, X., Yan, S., Tyagi, R.D., Surampalli, R.Y., Synthesis of nanoparticles by microorganisms and their application in enhancing microbiological reaction rates. *Chemosphere*, 82, 489–494, 2011.
192. Mann, S., *Biomineralization:* Principles and Concepts in Bioinorganic Materials Chemistry, Oxford University Press: Oxford, UK, 2001.
193. Simkiss, K., Wilbur, K.M., *Biomineralization*, 1st ed., Academic Press, 1989.
194. Sastry, M., Ahmad, A., Islam, N.I., Kumar, R., Biosynthesis of metal nanoparticles using fungi and actinomycetes. *Curr. Sci.*, 85, 162–170, 2003.
195. Sastry, M., Ahmad, A., Khan, M.I., Kumar, R., Microbial nanoparticle production in nanobiotechnology. *Current Sc.*, 85, 163–169, 2003.
196. Benzerara, K., Miot, J., Morin, G., Nguema, G.O., Panet, F.S., Férard, C., Significance, mechanisms and environmental implications of microbial biomineralization. *C. R. Geosci.*, 343, 160–167, 2010.
197. Vigneshwaran, N., Ashtaputre, N.M., Varadarajan, P.V., Nachane, R.P., Paralikar, K.M., Balasubramanya, R.H., Biological synthesis of silver nanoparticles using the fungus *Aspergillus flavus*. *Mater. Lett.*, 61, 1413–1418, 2007.
198. Bhainsa, K.C., D'Souza, S.F., Extracellular biosynthesis of silver nanoparticles using the fungus *Aspergillus fumigatus*. *Colloids Surf. B*, 47, 160–164, 2006.
199. Li, G., He, D., Qian, Y., Guan, B., Gao, S., Cui, Y., Yokoyama, K., Wang, L., Fungus-mediated green synthesis of silver nanoparticles using *Aspergillus terreus*. *Int. J. Mol. Sci.*, 13, 466–476, 2012.
200. Babu, M.M.G., Gunasekaran, P., Production and structural characterization of crystalline silver nanoparticles from *Bacillus cereus* isolate. *Colloids Surf. B*, 74, 191–195, 2009.
201. Kalimuthu, K., Babu, R.S., Venkataraman, D., Bilal, M., Gurunathan, S., Biosynthesis of silver nanocrystals by *Bacillus licheniformis*. *Colloids Surf. B*, 65, 150–153, 2008.
202. Kalishwaralal, K., Deepak, V., Pandian, S.R.K., Biosynthesis of silver and gold nanoparticles using *Brevibacterium casei*. *Colloids Surf. B*, 77, 257–262, 2010.

203. Balaji, D.S., Basavaraja, S., Deshpande, R., Mahesh, D.B., Prabhakar, B.K., Venkataraman, A., Extracellular biosynthesis of functionalized silver nanoparticles by strains of *Cladosporium cladosporioides* fungus. *Colloids Surf. B*, 68, 88–92, 2009.
204. Sanghi, R., Verma, P., Biomimetic synthesis and characterisation of protein capped silver nanoparticles. *Bioresour. Technol.*, 100, 501–504, 2009.
205. Sneha, K., Sathishkumar, M., Mao, J., Kwak, I.S., Yun, Y.S., *Corynebacterium glutamicum*-mediated crystallization of silver ions through sorption and reduction processes. *Chem. Eng. J.*, 162, 989–996, 2010.
206. Gurunathan, S., Kalishwaralal, K., Vaidyanathan, R., Biosynthesis, purification and characterization of silver nanoparticles using *Escherichia coli*. *Colloids Surf. B*, 74, 328–335, 2009.
207. Senapati, S., Mandal, D., Ahmad, A., Fungus mediated synthesis of silver nanoparticles: A novel biological approach. *Indian J. Phys. A*, 789, 101–105, 2004.
208. Shiv Shankar, S., Ahmad, A., Pasricha, R., Sastry, M., Bioreduction of chloroaurate ions by geranium leaves and its endophytic fungus yields gold nanoparticles of different shapes. *J. Mater. Chem.*, 13, 1822–1846, 2003.
209. Durán, N., Marcato, P.D., Alves, O.L., De Souza, G., Esposito, E., Mechanistic aspects of biosynthesis of silver nanoparticles by several *Fusarium oxysporum* strains. *J. Nanobiotechnol.*, 3, 1–8, 2005.
210. Basavaraja, S., Balaji, S.D., Lagashetty, A., Rajasab, A.H., Venkataraman, A., Extracellular biosynthesis of silver nanoparticles using the fungus *Fusarium semitectum*. *Mater. Res. Bull.*, 43, 1164–1170, 2008.
211. Chowdhury, S., Basu, A., Kundu, S., Green synthesis of protein capped silver nanoparticles from phytopathogenic fungus *Macrophomina phaseolina* (Tassi) Goid with antimicrobial properties against multidrugresistant bacteria. *Nano Res. Lett.*, 9, 365, 2014.
212. Kathiresan, K., Manivannan, S., Nabeel, M., Dhivya, B., Studies on silver nanoparticles synthesized by a marine fungus, *Penicillium fellutanum* isolated from coastal mangrove sediment. *Colloids Surf. B*, 71, 133–137, 2009.
213. Maliszewska, I., Juraszek, A., Bielska, K., Green synthesis and characterization of silver nanoparticles using ascomycota fungi *Penicillium nalgiovense* AJ12. *J. Clust. Sci.*, 25, 989–1004, 2014.
214. Shahverdi, A.R., Minaeian, S., Shahverdi, H.R., Jamalifar, H., Nohi, A.A., Rapid synthesis of silver nanoparticles using culture supernatants of enterobacteria: A novel biological approach. *Process Biochem.*, 42, 919–923, 2007.
215. Vigneshwaran, N., Kathe, A.A., Varadarajan, P.V., Nachane, R.P., Balasubramanya, R.H., Biomimetics of silver nanoparticles by white rot fungus, *Phaenerochaete chrysosporium*. *Colloids Surf. B*, 53, 55–59, 2006.
216. Birla, S.S., Tiwari, V.V., Gade, A.K., Ingle, A.P., Yadav, A.P., Rai, M.K., Fabrication of silver nanoparticles by *Phoma glomerata* and its combined

effect against *Escherichia coli, Pseudomonas aeruginosa* and *Staphylococcus aureus*. *Lett. Appl. Microbiol. Biotechnol.*, 48, 173–179, 2009.
217. Vigneshwaran, N., Kathe, A., Silver-protein (core-shell) nanoparticle production using spent mushroom substrate. *Langmuir*, 23, 7113–7117, 2007.
218. Vahabi, K., Mansoori, G.A., Karimi, S., Biosynthesis of silver nanoparticles by fungus *Trichoderma reesei* (a route for large-scale production of AgNPs). *Insciences J.*, 1, 65–79, 2011.
219. Fayaz, A.M., Balaji, K., Girilal, M., Yadav, R., Kalaichelvan, P.T., Venketesan, R., Biogenic synthesis of silver nanoparticles and their synergistic effect with antibiotics: A study against gram-positive and gram-negative bacteria. *Nanomedicine*, 6, 103–109, 2010.
220. Mukherjee, P., Roy, M., Mandal, B.P., Dey, G.K., Mukherjee, P.K., Ghatak, J., Tyagi, A.K., Kale, S.P., Green synthesis of highly stabilized nanocrystalline silver particles by a non-pathogenic and agriculturally important fungus *T. asperellum*. *Nanotechnology*, 19, 1–7, 2008.
221. Fayaz, A.M., Balaji, K., Kalaichelvan, P.T., Venkatesan, R., Fungal based synthesis of silver nanoparticles—An effect of temperature on the size of particles. *Colloids Surf. B*, 74, 123–126, 2009.
222. Binupriya, A.R., Sathishkumar, M., Vijayaraghavan, K., Yun, S.I., Bioreduction of trivalent aurum to nano-crystalline gold particles by active and inactive cells and cell-free extract of *Aspergillus oryzae* var. *viridis*. *J. Hazard. Mater.*, 177, 539–545, 2010.
223. Bhambure, R., Bule, M., Shaligram, N., Kamat, M., Singhal, R., Extracellular biosynthesis of gold nanoparticles using *Aspergillus niger*—its characterisation and stability. *Chem. Eng. Technol.*, 32, 1036–1041, 2009.
224. Xie, J., Lee, J.Y., Wang, D.I.C., Ting, Y.P., High-yield synthesis of complex gold nanostructures in a fungal system. *J. Phys. Chem. C*, 111, 16858–16865, 2007.
225. Vala, A.K., Exploration on green synthesis of gold nanoparticles by a marine-derived fungus *Aspergillus sydowii*. *Environ. Prog. Sustain. Energy*, 34, 194–197, 2015.
226. Sarkar, J., Ray, S., Chattopadhyay, D., Laskar, A., Acharya, K., Mycogenesis of gold nanoparticles using a phytopathogen *Alternaria alternata*. *Bioprocess Biosyst. Eng.*, 35, 637–643, 2012.
227. Verma, V.C., Singh, S.K., Solanki, R., Prakash, S., Biofabrication of anisotropic gold nanotriangles using extract of endophytic *Aspergillus clavatus* as a dual functional reductant and stabilizer. *Nanoscale Res. Lett.*, 6, 16–22, 2011.
228. Zhang, X., He, X., Wang, K., Yang, X., Different active biomolecules involved in biosynthesis of gold nanoparticles by three fungus species. *J. Biomed. Nanotechnol.*, 7, 245–254, 2011.
229. Chauhan, A., Zubair, S., Tufail, S., Sherwani, A., Sajid, M., Raman, S.C., Azam, A., Owais, M., Fungus-mediated biological synthesis of gold nanoparticles: Potential in detection of liver cancer. *Int. J. Nanomedicine*, 6, 2305–2319, 2011.

230. Gericke, M., Pinches, A., Biological synthesis of metal nanoparticles. *Hydrometallurgy*, 83, 132–140, 2006.
231. Shankar, S.S., Ahmad, A., Pasricha, R., Sastry, M., Bioreduction of chloroaurate ions by geranium leaves and its endophytic fungus yields gold nanoparticles of different shapes. *J. Mater. Chem.*, 13, 1822–1826, 2003.
232. Sanghi, R., Verma, P., pH dependant fungal proteins in the "green" synthesis of gold nanoparticles. *Adv. Mater. Lett.*, 1, 193–199, 2010.
233. Narayanan, K.B., Sakthivel, N., Mycocrystallization of gold ions by the fungus *Cylindrocladium floridanum*. *World J. Microbiol. Biotechnol.*, 29, 2207–2211, 2013.
234. Narayanan, K.B., Sakthivel, N., Synthesis and characterization of nanogold composite using *Cylindrocladium floridanum* and its heterogeneous catalysis in the degradation of 4-nitrophenol. *J. Hazard. Mater.*, 189, 519–525, 2011.
235. Sheikhloo, Z., Salouti, M., Katiraee, F., Biological synthesis of gold nanoparticles by fungus *Epicoccum nigrum*. *J. Clust. Sci.* 22, 661–665, 2011.
236. Du, L., Jiang, H., Liu, X., Wang, E., Biosynthesis of gold nanoparticles assisted by *Escherichia coli* DH5α and its application on direct electrochemistry of hemoglobin. *Electrochem. Commun.*, 9, 1165–1170, 2007.
237. Sawle, B.D., Salimath, B., Deshpande, R., Bedre, M.D., Prabhakar, B.K., Venkataraman, A., Biosynthesis and stabilization of Au and Au-Ag alloy nanoparticles by fungus, *Fusarium semitectum*. *Sci. Tech. Adv. Mater.*, 9, 1–6, 2008.
238. Mukherjee, P., Senapati, S., Mandal, D., Ahmad, A., Khan, M.I., Kumar, R., Sastry, M., Extracellular synthesis of gold nanoparticles by the fungus *Fusarium oxysporum*. *ChemBioChem*, 3, 461–463, 2002.
239. Sathish Kumar, K., Amutha, R., Arumugam, P., Berchmans, S., Synthesis of gold nanoparticles: an ecofriendly approach using *Hansenula anomala*. *ACS Appl. Mater. Interfaces*, 3, 1418–1425, 2011.
240. Kumar, S.K., Peter, Y.A., Nadeau, J.L., Facile biosynthesis, separation and conjugation of gold nanoparticles to doxorubicin. *Nanotechnology*, 19, 495101, 2008.
241. Mishra, A.N., Bhadaurla, S., Singh Gaur, M., Pasricha, R., Extracellular microbial synthesis of gold nanoparticles using fungus *Hormoconis resinae*. *JOM*, 62, 45–48, 2010.
242. Castro-Longoria, E., Vilchis-Nestor, A.R., Avalos-Borja, M., Biosynthesis of silver, gold and bimetallic nanoparticles using the filamentous fungus *Neurospora crassa*. *Colloids Surf. B*, 83, 42–48, 2011.
243. Mishra, A., Tripathy, S.K., Yuna, S.I., Fungus mediated synthesis of gold nanoparticles and their conjugation with genomic DNA isolated from *Escherichia coli* and *Staphylococcus aureus*. *Process Biochem.*, 47, 701–711, 2012.
244. Ma, Y., Li, N., Yang, C., Yang, X., One-step synthesis of amino-dextran protected gold and silver nanoparticles and its application in biosensors. *Anal. Bioanal. Chem.*, 382, 1044–1048, 2005.

245. Mishra, A., Tripathy, S.K., Wahab, R., Jeong, S.H., Hwang, I., Yang, Y.B., Kim, Y.S., Shin, H.S., Yun, S.I.I., Microbial synthesis of gold nanoparticles using the fungus *Penicillium brevicompactum* and their cytotoxic effects against mouse mayo blast cancer C2C cells. *Appl. Microbiol. Biotechnol.*, 92, 617–630, 2011.
246. Du, L., Xian, L., Feng, J.X., Rapid extra-/intracellular biosynthesis of gold nanoparticles by the fungus *Penicillium* sp. *J. Nanopart. Res.*, 13, 921–930, 2011.
247. Sanghi, R., Verma, P., Puri, S., Enzymatic formation of gold nanoparticles using *Phanerochaete chrysosporium*. *Adv. Chem. Eng. Sci.*, 1, 154–162, 2011.
248. Lengke, M.F., Ravel, B., Fleet, M.E., Wanger, G., Gordon, R.A., Southam, G., Mechanisms of gold bioaccumulation by filamentous cyanobacteria from gold(III)-chloride complex. *Environ. Sci. Technol.*, 40, 6304–6309, 2006.
249. Lengke, M.F., Fleet, M.E., Southam, G., Morphology of gold nanoparticles synthesized by filamentous cyanobacteria from gold(I)-thiosulfate and gold(III)-chloride complexes. *Langmuir*, 22, 2780–2787, 2006.
250. Husseiny, M.I., El-Aziz, M.A., Badr, Y., Mahmoud, M.A., Biosynthesis of gold nanoparticles using *Pseudomonas aeruginosa*. *Spectrochim. Acta A*, 67, 1003–1006, 2007.
251. Das, S.K., Dickinson, C., Laffir, F., Brougham, D.F., Marsili, E., Synthesis, characterization and catalytic activity of gold nanoparticles biosynthesized with *Rhizopus oryzae* protein extract. *Green Chem.*, 14, 1322–1344, 2012.
252. He, S., Guo, Z., Zhang, Y., Zhang, S., Wang, J., Gu, N., Biosynthesis of gold nanoparticles using the bacteria *Rhodopseudomonas capsulata*. *Mater. Lett.*, 61, 3984–3987, 2007.
253. Sen, K., Sinha, P., Lahiri, S., Time dependent formation of gold nanoparticles in yeast cells: A comparative study. *Biochem. Eng. J.*, 55, 1–6, 2011.
254. Singaravelu, G., Arockiamary, J.S., Kumar, V.G., Govindaraju, K., A novel extracellular synthesis of monodisperse gold nanoparticles using marine alga, *Sargassum wightii* Greville. *Colloids Surf. B*, 57, 97–101, 2007.
255. Narayanan, K.B., Sakthivel, N., Facile green synthesis of gold nanostructures by NADPH-dependent enzyme from the extract of *Sclerotium rolfsii*. *Colloids Surf. A*, 380, 156–161, 2011.
256. Konishi, Y., Tsukiyama, T., Tachimi, T., Saitoh, N., Nomura, T., Nagamine, S., Microbial deposition of gold nanoparticles by the metal-reducing bacterium *Shewanella algae*. *Electrochim. Acta*, 53, 186–192, 2007.
257. Suresh, A.K., Pelletier, D.A., Wang, W., Biofabrication of discrete spherical gold nanoparticles using the metal-reducing bacterium *Shewanella oneidensis*. *Acta Biomater.*, 7, 2148–2152, 2011.
258. Maliszewska, I., Aniszkiewicz, L., Sadowski, Z., Biological synthesis of gold nanostructures using the extract of *Trichoderma koningii*. *Acta Phys. Pol. A*, 116, 163–165, 2009.

259. Maliszewska, I., Microbial mediated synthesis of gold nanoparticles: Preparation, characterization and cytotoxicity studies. *Dig. J. Nanomater. Bios.*, 8, 1123–1131, 2013.
260. Juibari, M.M., Abbasalizadeh, S., Jouzani, G.S., Noruzi, M., Intensified biosynthesis of silver nanoparticles using a native extremophilic *Ureibacillus thermosphaericus* strain. *Mater. Lett.*, 65, 1014–1017, 2011.
261. Philip, D., Biosynthesis of Au, Ag and Au-Ag nanoparticles using edible mushroom extract. *Spectrochim. Acta A*, 73, 374–381, 2009.
262. Ramanathan, R., Field, M.R., O'Mullane, A.P., Smooker, P.M., Bhargava, S.K., Bansal, V., Aqueous phase synthesis of copper nanoparticles: A link between heavy metal resistance and nanoparticle synthesis ability in bacterial systems. *Nanoscale Res. Lett.*, 5, 2300–2306, 2013.
263. Mukherjee, P., Ahmad, A., Mandal, D., Senapati, S., Sainkar, S.R., Khan, M.I., Ramani, R., Parischa, R., Ajaykumar, P.V., Alam, M., Sastry, M., Kumar, R., Bioreduction of $AuCl^-$ ions by the fungus, *Verticillium* sp. and surface trapping of the gold nanoparticles formed. *Angew. Chem. Int. Ed.*, 40, 3585–3588, 2001.
264. Pimprikar, P.S., Joshi, S.S., Kumar, A.R., Zinjarde, S.S., Kulkarni, S.K., Influence of biomass and gold salt concentration on nanoparticle synthesis by the tropical marine yeast *Yarrowia lipolytica* NCIM. *Colloids Surf. B*, 74, 309–316, 2009.
265. Agnihotri, M., Joshi, S., Kumar, A.R., Zinjarde, S., Kulkarni, S., Biosynthesis of gold nanoparticles by the tropical marine yeast *Yarrowia lipolytica* NCIM 3589. *Mater. Lett.*, 63, 1231–1234, 2009.
266. Zheng, D., Hu, C., Gan, T., Dang, X., Hu, S., Preparation and application of a novel vanillin sensor based on biosynthesis of Au-Ag alloy nanoparticles. *Sens. Actuators B Chem.*, 148, 247–252, 2010.
267. Bao, H., Lu, Z., Cui, X., Extracellular microbial synthesis of biocompatible CdTe quantum dots. *Acta Biomater.*, 6, 3534–3541, 2010.
268. Sinha, A., Khare, S.K., Mercury bioaccumulation and simultaneous nanoparticle synthesis by *Enterobacter* sp. cells. *Bioresour. Technol.*, 102, 4281–4284, 2011.
269. Lloyd, J.R., Yong, P., Macaskie, L.E., Enzymatic recovery of elemental palladium by using sulfate-reducing bacteria. *Appl. Environ. Microbiol.*, 64, 4607–4609, 1998.
270. Govender, Y., Riddin, T., Gericke, M., Whiteley, C.G., Bioreduction of platinum salts into nanoparticles: A mechanistic perspective. *Biotechnol. Lett.*, 31, 95–100, 2009.
271. Konishi, Y., Ohno, K., Saitoh, N., Bioreductive deposition of platinum nanoparticles on the bacterium *Shewanella algae*. *J. Biotechnol.*, 128, 648–653, 2007.
272. Lee, J.H., Han, J., Choi, H., Hur, H.G., Effects of temperature and dissolved oxygen on Se(IV) removal and Se(0) precipitation by *Shewanella* sp. HN-41. *Chemosphere*, 68, 1898–1905, 2007.

273. Kashefi, K., Lovley, D.R., Reduction of Fe(III), Mn(IV), and toxic metals at 100°C by *Pyrobaculum islandicum*. *Appl. Environ. Microbiol.*, 66, 1050–1056, 2000.
274. Bansal, V., Poddar, P., Ahmad, A., Sastry, M., Room-temperature biosynthesis of ferroelectric barium titanate nanoparticles. *J. Am. Chem. Soc.*, 128, 11958–11963, 2006.
275. Jha, A.K., Prasad, K., Ferroelectric $BaTiO_3$ nanoparticles: Biosynthesis and characterization. *Colloids Surf. B*, 75, 330–334, 2010.
276. Bose, S., Hochella, M.F., Gorby, Y.A., Bioreduction of hematite nanoparticles by the dissimilatory iron reducing bacterium *Shewanella oneidensis* MR-1. *Geochim. Cosmochim. Acta*, 73, 962–976, 2009.
277. Lefèvre, C.T., Abreu, F., Schmidt, M.L., Moderately thermophilic magnetotactic bacteria from hot springs in Nevada. *Appl. Environ. Microbiol.*, 76, 3740–3743, 2010.
278. Zhu, K., Pan, H., Li, J., Isolation and characterization of a marine magnetotactic spirillum axenic culture QH-2 from an intertidal zone of the China Sea. *Res. Microbiol.*, 161, 276–283, 2010.
279. Amemiya, Y., Arakaki, A., Staniland, S.S., Tanaka, T., Matsunaga, T., Controlled formation of magnetite crystal by partial oxidation of ferrous hydroxide in the presence of recombinant magnetotactic bacterial protein Mms6. *Biomaterials*, 28, 5381–5389, 2007.
280. Perez-Gonzalez, T., Jimenez-Lopez, C., Neal, A.L., Magnetite biomineralization induced by *Shewanella oneidensis*. *Geochim. Cosmochim. Acta*, 74, 967–979, 2010.
281. Li, W., Yu, L., Zhou, P., Zhu, M., A *Magnetospirillum* strain WM-1 from a freshwater sediment with intracellular magnetosomes. *World J. Microbiol. Biotechnol.*, 23, 1489–1492, 2007.
282. Zhou, W., He, W., Zhong, S., Biosynthesis and magnetic properties of mesoporous Fe_3O_4 composites. *J. Magn. Magn. Mater.*, 321, 1025–1028, 2009.
283. Zhou, W., He, W., Zhang, X., Biosynthesis of iron phosphate nanopowders. *Powder Technol.*, 194, 106–108, 2009.
284. Bansal, V., Rautaray, D., Bharde, A., Ahire, K., Sanyal, A., Ahmad, A., Sastry, M., Fungus-mediated biosynthesis of silica and titania particles. *J. Mater. Chem.*, 15, 2583–2589, 2005.
285. Jha, A.K., Prasad, K., Kulkarni, A.R., Synthesis of TiO_2 nanoparticles using microorganisms. *Colloids Surf. B*, 71, 226–229, 2009.
286. Narayanan, K.B., Sakthivel, N., Green synthesis of biogenic metal nanoparticles by terrestrial and aquatic phototrophic and heterotrophic eukaryotes and biocompatible agents. *Adv. Colloid Interface Sci.*, 169, 59–79, 2011.
287. Raliya, R., Tarafdar, J.C., ZnO nanoparticle biosynthesis and its effect on phosphorous-mobilizing enzyme secretion and gum contents in cluster bean (*Cyamopsis tetragonoloba* L.). *Agric. Res.*, 2, 48–57, 2013.
288. Jayaseelan, C., Abdul Rahuman, A., Vishnu Kirthi, A., Marimuthu, S., Santhoshkumar, T., Bagavan, A., Gaurav, K., Karthik, L., Bhaskara Rao, K.V.,

Novel microbial route to synthesize ZnO nanoparticles using *Aeromonas hydrophila* and their activity against pathogenic bacteria and fungi. *Spectrochim. Acta A*, 90, 78–84, 2012.
289. Senapati, S., Ahmad, A., Khan, M.I., Sastry, M., Kumar, R., Extracellular biosynthesis of bimetallic Au-Ag alloy nanoparticles. *Small*, 1, 517–520, 2005.
290. Tarafdar, J.C., Raliya, R., Rathore, I., Microbial synthesis of phosphorous nanoparticle from tri-calcium phosphate using *Aspergillus tubingensis* TFR-5. *J. Bionanosci.*, 6, 84–89, 2012.
291. Sanyal, A., Rautaray, D., Bansal, V., Ahmad, A., Sastry, M., Heavy-metal remediation by a fungus as a means of production of lead and cadmium carbonate crystals. *Langmuir*, 21, 7220–7224, 2005.
292. Krumov, N., Oder, S., Perner-Nochta, I., Angelov, A., Posten, C., Accumulation of CdS nanoparticles by yeasts in a fed-batch bioprocess. *J. Biotechnol.*, 132, 481–486, 2007.
293. Sanghi, R., Verma, P., A facile green extracellular biosynthesis of CdS nanoparticles by immobilized fungus. *Chem. Eng. J.*, 155, 886–891, 2009.
294. Sweeney, R.Y., Mao, C., Gao, X., Bacterial biosynthesis of cadmium sulfide nanocrystals. *Chem. Biol.*, 11, 1553–1559, 2004.
295. Ahmad, A., Mukherjee, P., Mandal, D., Enzyme mediated extracellular synthesis of CdS nanoparticles by the fungus, *Fusarium oxysporum*. *J. Am. Chem. Soc.*, 124, 12108–12109, 2002.
296. Rai, M., Yadav, A., Gade, A., Silver nanoparticles as a new generation of antimicrobials. *Biotechnol. Adv.*, 27, 76–83, 2009.
297. Prasad, K., Jha, A.K., Biosynthesis of CdS nanoparticles: An improved green and rapid procedure. *J. Colloid Interface Sci.*, 342, 68–72, 2010.
298. Bai, H.J., Zhang, Z.M., Gong, J., Biological synthesis of semiconductor zinc sulfide nanoparticles by immobilized *Rhodobacter sphaeroides*. *Biotechnol. Lett.*, 28, 1135–1139, 2006.
299. Bai, H.J., Zhang, Z.M., Guo, Y., Yang, G.E., Biosynthesis of cadmium sulfide nanoparticles by photosynthetic bacteria *Rhodopseudomonas palustris*. *Colloids Surf. B*, 70, 142–146, 2009.
300. Dameron, C.T., Reese, R.N., Mehra, R.K., Kortan, A.R., Carroll, P.J., Steigerwald, M.L., Brus, L.E., Winge, D.R., Biosynthesis of cadmium sulphide quantum semiconductor crystallites. *Nature*, 338, 596–597, 1989.
301. Kowshik, M., Deshmuke, N., Vogal, W., Microbial synthesis of semiconductor CdS nanoparticles, their characterization, and their use in the fabrication of an ideal diode. *Biotechnol. Bioeng.,* 78, 583–588, 2002.
302. Raliya, R., Rapid, low-cost, and ecofriendly approach her for iron nanoparticle synthesis using *Aspergillus oryzae* TFR9. *J. Nanopart. Res.*, 4, 141274, 2013.
303. Lefèvre, C.T., Abreu, F., Lins, U., Bazylinski, D.A., Nonmagnetotactic multicellular prokaryotes from low-saline, nonmarine aquatic environments and their unusual negative phototactic behavior. *Appl. Environ. Microbiol.*, 76, 3220–3227, 2010.

304. Watson, J.H.P., Ellwood, D.C., Soper, A.K., Charnock, J., Nanosized strongly-magnetic bacterially-produced iron sulfide materials. *J. Magn. Magn. Mater.*, 203, 69–72, 1999.
305. Arakaki, A., Shibusawa, M., Hosokawa, M., Matsunaga, T., Preparation of genomic DNA from a single species of uncultured magnetotactic bacterium by multiple-displacement amplification. *Appl. Environ. Microbiol.*, 76, 1480–1485, 2010.
306. Bai, H.J., Zhang, Z.M., Microbial synthesis of semiconductor lead sulfide nanoparticles using immobilized *Rhodobacter sphaeroides*. *Mater. Lett.*, 63, 764–766, 2009.
307. Rautaray, D., Sanyal, A., Adyanthaya, S.D., Ahmad, A., Sastry, M., Biological synthesis of strontium carbonate crystals using the fungus *Fusarium oxysporum*. *Langmuir*, 20, 6827–6833, 2004.
308. Labrenz, M., Druschel, G.K., Thomsen-Ebert, T., Formation of sphalerite (ZnS) deposits in natural biofilms of sulfate-reducing bacteria. *Science*, 290, 1744–1747, 2000.
309. Macdonald, I.D.G., Smith, W.E., Orientation of cytochromec adsorbed on a citrate-reduced silver colloid. *Langmuir*, 12, 706–713, 1996.
310. Gade, A.K., Bonde, P., Ingle, A.P., Marcato, P.D., Duran, N., Rai, M.K., Exploitation of *Aspergillus niger* for synthesis of silver nanoparticles. *J. Biobased Mater. Bio.*, 2, 243–247, 2008.
311. Sanghi, R., Verma, P., Biomimetic synthesis and characterisation of protein capped silver nanoparticles. *Bioresour. Technol.*, 100, 501–504, 2009.
312. Kumar, S.A., Abyaneh, M.K., Gosavi, S.W., Kulkarni, S.K., Pasricha, R., Ahmad, A., Khan, M.I., Nitrate reductase-mediated synthesis of silver nanoparticles from $AgNO_3$. *Biotechnol. Lett.*, 29, 439–45, 2007.
313. Ingle, A., Gade, A., Pierrat, S., Sonnichsen, C., Rai, M., Mycosynthesis of silver nanoparticles using the fungus *Fusarium acuminatum* and its activity against some human pathogenic bacteria. *Curr. Nanosci.*, 4, 141–144, 2008.
314. Slawson, R.M., Van Dyke, M.I., Lee, H., Trevor, J.T., Germanium and silver resistance, accumulation and toxicity in microorganisms. *Plasmid*, 27, 73–79, 1992.
315. Parikh, R.P., Singh, S., Prasad, B.L.V., Patole, M.S., Sastry, M., Shouche, Y.S., Extracellular synthesis of crystalline silver nanoparticles and molecular evidence of silver resistance from *Morganella* sp.: Towards understanding biochemical synthesis mechanism. *ChemBioChem*, 9, 1415–1422, 2008.
316. Narayanan, K.B., Sakthivel, N., Biological synthesis of metal nanoparticles by microbes. *Adv. Colloid Interface Sci.*, 156, 1–13, 2010.
317. Govindaraju, K., Basha, S.K., Kumar, V.G., Singaravelu, G., Silver, gold and bimetallic nanoparticles production using single-cell protein (*Spirulina platensis*) Geitler. *J. Mater. Sci.*, 43, 5115–5122, 2008.
318. Venkatpurwar, V., Pokharkar, V., Green synthesis of silver nanoparticles using marine polysaccharide: Study of *in vitro* antibacterial activity. *Mater Lett*, 65, 999–1002, 2011.

319. Xie, J., Lee, J.Y., Wang, D.I.C., Ting, Y.P., Silver nanoplates: From biological to biomimetic synthesis. *ACS Nano*, 1, 429–439, 2007.
320. Lengke, M., Southam, G., Bioaccumulation of gold by sulfate-reducing bacteria cultured in the presence of gold(I)-thiosulfate complex. *Geochim. Cosmochim. Acta*, 70, 3646–3661, 2006.
321. Hosea, M., Greene, B., Mcpherson, R., Henzl, M., Alexander, M.D., Darnall, D.W., *Inorg. Chim. Acta*, 123, 161, 1986.
322. Mata, Y.N., Torres, E., Blázquez, M.L., Ballester, A., González, F., Muñoz, J.A., Gold(III) biosorption and bioreduction with the brown alga *Fucus vesiculosus*. *J. Hazard. Mater.*, 166, 612–618, 2009.
323. Mata, Y.N., Blázquez, M., Ballester, A., González, F., Muñoz, J.A., Characterization of the biosorption of cadmium, lead and copper with the brown alga *Fucus vesiculosus*. *J. Hazard. Mater.*, 158, 316–323, 2008.
324. Romera, E., Gonzalez, F., Ballester, A., Blazquez, M.L., Munoz, J.A., Comparative study of biosorption of heavy metals using different types of algae. *Bioresour. Technol.*, 98, 3344, 2007.
325. Zare, B., Babaie, S., Setayesh, N., Shahverdi, A.R., Isolation and characterization of a fungus for extracellular synthesis of small selenium nanoparticles. *Nanomed. J.*, 1, 13–19, 2013.
326. Castro-Longoria, E., Moreno-Velázquez, S.D., Vilchis-Nestor, A.R., Arenas-Berumen, E., Avalos-Borja, M., Production of platinum nanoparticles and nanoaggregates using *Neurospora crassa*. *J. Microbiol. Biotechnol.*, 22, 1000–1004, 2012.
327. Lloyd, J.R., Microbial reduction of metals and radionuclides. *FEMS Microbiol. Rev.*, 27, 411–425, 2003.
328. Klittich, C., Leslie, J., Nitrate reduction mutants of *Fusarium moniliforme* (*Gibberella fujikuroi*). *Genetics*, 118, 417–23, 1988.
329. Awadalla, F., Pesic, B., Biosorption of cobalt with the AMTTM metal removing agent. *Hydrometallurgy*, 28, 65–80, 1992.
330. Wilde, E., Benemann, J., Bioremoval of heavy metals by the use of microalgae. *Biotech. Adv.*, 11, 781–812, 1993.
331. Kumar, C.V., McLendon, G.L., Nanoencapsulation of cytochrome c and horseradish peroxidase at the galleries of a-zirconium phosphate. *Chem. Mater.*, 9, 863–870, 1997.
332. Bharde, A., Rautaray, D., Bansal, V., Ahmad, A., Sarkar, I., Yusuf, S.M., Sanyal, M., Sastry, M., Extracellular biosynthesis of magnetite using fungi. *Small*, 2, 135–141, 2006.
333. Jha, A.K., Prasad, K., Prasad, K., A green low-cost biosynthesis of Sb_2O_3 nanoparticles. *Biochem. Eng. J.*, 43, 303–306, 2009.

3

Plant and Tree Gums as Renewable Feedstocks for the Phytosynthesis of Nanoparticles: A Green Chemistry Approach

Aruna Jyothi Kora

National Centre for Compositional Characterisation of Materials (NCCCM), Bhabha Atomic Research Centre (BARC), Hyderabad, India

Abstract

The green synthesis of nanoparticles has gained importance as a simple possible alternative to chemical and physical methods,. Particularly, the biosynthetic protocols utilizing plant gums are of considerable interest due to the implementation of the basic requirements of green chemistry; the solvent medium, the benign reducing agent and the nonhazardous stabilizing agent. A review of the literature suggests that various plant and trees gums are most widely used for the fabrication of metal and metal oxide nanoparticles. Among the gum-based methods, the exudate gums, such as kondagogu, ghatti, olibanum, tragacanth, arabic, karaya, etc., are extensively utilized for the synthesis of inorganic nanoparticles. The appealing features of plant gums for the synthesis and stabilization of nanoparticles are their natural availability and low cost, nontoxic, nonmutagenic and biodegradable nature; abundance of various functional groups, greater stability to pH change, electrolyte addition and high-pressure treatment; medicinal values and metal biosorption properties. The gums serve as renewable, biodegradable, nontoxic, natural biobased feedstocks for the reduction and stabilization of metal ions, thus meeting the requirements of green chemistry. Most of the synthesis is carried out in environmentally, biologically benign aqueous medium under ambient conditions, while a few require either chemical additives or energy in the form of heat or

Corresponding author: koramaganti@gmail.com

Suvardhan Kanchi and Shakeel Ahmed (eds.) Green Metal Nanoparticles, (79–111)
© 2018 Scrivener Publishing LLC

microwave to progress the reaction. The phytosynthesis of nanoparticles utilizing plant gums bestows virtues such as particle mean diameter and size distribution control; atom economy, superior stability towards higher temperatures, pH change and storage conditions; biocompatibility, surface functionalization, etc. Thus, the biogenic, surface-functionalized nanoparticles could be easily integrated for various biological, pharmaceutical and medical applications.

Keywords: Biogenic, exudate tree gums, green synthesis, feedstocks, nanoparticles, reductant, stabilizer, phytosynthesis

3.1 Introduction

The manufacturing techniques used for nanoparticle production are broadly classified as top-down and bottom-up. In the top-down approach, the larger starting materials are broken or milled down using specific tools and physically reduced into nanosized particles and used in many industrial processes. The bottom-up approach is involved in the building up of nanostructured materials from the bottom, i.e., atoms, molecules or clusters as building blocks [1]. For the generation of inorganic nanoparticles, a wide variety of physical, chemical and biological routes are employed in current times. The physical methods include pyrolysis and mechanical attrition. In pyrolysis, the organic precursors decompose into solid powders with a wide particle size distribution. Whereas in attrition, the nanoparticles are recovered by grinding the macro- or microscale particles using a ball or planetary mill or other size-reducing mechanisms. Among the chemical methods, two familiar and extensively used wet chemical techniques are chemical reduction and photoreduction. A diverse range of chemical reductants, such as sodium borohydride, citrate, glucose, hydrazine, ascorbic acid, dimethyl formamide, poly(ethylene glycol), hydroquinone, etc., have been reported for nanoparticle synthesis, using a combination of different capping and stabilizing agents, such as sodium dodecyl sulfate, citrate, cetyltrimethylammonium chloride, cetyltrimethylammonium bromide, polyvinylpyrrolidone, polyvinyl alcohol, polyoxyethylenesorbitan monooleate, oleate, etc., have been successfully employed. Various methodologies have been reported for nanoparticle synthesis, using different radiation sources, such as laser, microwave, ultraviolet light and gamma rays, and a combination of different capping and stabilizing agents such as sodium dodecyl sulfate, citrate, polyacrylic acid, polyvinylpyrrolidone and hyperbranched polyester [2]. The nanoparticle suspensions produced by wet chemical methods are usually referred to as colloids, in which small particles are dispersed evenly through a fluid.

The nanoparticles synthesized by chemical methods are very popular and most of these protocols depend on the use of organic solvents and toxic reducing agents. It is significant to note that the chemicals employed for production are highly reactive, generate unwanted by-products and cause potential environmental and biological risks [3, 4]. However, the physical methods necessitate sophisticated equipment and stringent conditions. They are limited by low production rates, high energy consumption and high costs. On the other hand, microbial synthetic methods have certain disadvantages, including microorganism cultivation, growth parameter optimization such as nutrient medium, salt concentration, temperature, pH, incubation time, inoculum quantity, etc. All the steps involved in these processes are time consuming and need expertise [5]. A combination of different physical factors, such as light, ultrasonic waves, microwaves, heating, etc., is required for nanoparticle production [1]. All these factors lead to a search for new synthetic routes that follow the rules of green chemistry.

When compared to physical and chemical synthetic protocols for nanoparticle production, the biosynthetic methods utilizing plant gums have received immense attention. The thrust is shifted to greener methods that exploit renewable, cost-effective and biodegradable sources as feedstocks. This is mainly to alleviate the environmental hazards caused by chemical methods. It is significant to note that feedstocks based on fossil fuels are going to be depleted with an increase in demand for energy, which leads to an impact on human health and the environment, while the plant gum-based methods implement the basic requirements of green chemistry; the solvent medium, the benign reducing agent and the nonhazardous stabilizing agent [6]. This is because of the innate abundance of reductant and stabilizer biomolecules in the plant gums from a variety of plants. A survey of the earlier literature suggests that exudate gums, such as kondagogu, ghatti, olibanum, tragacanth, arabic, karaya, etc., are extensively utilized for the synthesis of inorganic nanoparticles. The interesting features of plant gums, which are utilized as biotemplates for the synthesis and stabilization of nanoparticles, are their (i) natural availability and low cost, (ii) nontoxic, nonmutagenic and biodegradable nature, (iii) abundance of various functionalities, including hydroxyl, acetyl, carbonyl and carboxylic groups, (iv) greater stability to pH acidification, electrolyte addition and high-pressure treatment, (vi) medicinal values and (vii) metal biosorption properties [7–15]. The synthesis is carried out in environmentally benign aqueous-solvent medium without the requirement of any added external chemicals. As the plant gums are soluble in water, the use of organic solvents could be avoided. In comparison with conventional solvents, water is preferred for reactions because it exhibits unequaled and unique physical properties. Besides, it is nontoxic,

cost-effective and nonhazardous while handling. Being natural polymers, the gums are also amenable for biodegradation. By virtue of being biogenic and encapsulated with proteins, these surface-functionalized nanoparticles could be easily integrated for various biological, pharmaceutical and medical applications. The use of environmentally benign, inexpensive and renewable materials and benign solvent medium offers several benefits, including one-pot synthesis, catalyst free, simple yet clean reaction conditions, no waste generation and environmental safety.

One of the most important criterion for nanoparticle production is the prevention of particle aggregation. The nanoparticles could be stabilized with capping agents either by electrostatic or steric forces. It is pertinent to note that in chemosynthetic methods, the capping agent has to be present to prevent aggregation of nanoparticles during synthesis. But, the plant gums perform as dual functional reductant and stabilizers during the nanoparticle synthesis. Thus, we could achieve atom economy by incorporating all materials used in the process into the product to maximize the efficiency of synthesis. Hence, by adopting the sustainable processes, we can follow the twelve fundamental principles of green chemistry. In addition, the biogenic nanoparticles produced from plant gums show excellent tolerance/stability towards higher temperatures, pH change and storage conditions, expanding their applicability under various conditions [11]. Thus, a comparison of biogenic versus chemogenic synthesis suggests that plant gum-based nanoparticle synthesis is advantageous. The nanoparticles stabilized by natural polymers make them nontoxic to cells and render them as a suitable candidate of choice for safe delivery of drugs, molecular imaging, biomedical diagnostics and coating materials for biomedical devices and food packaging [16]. Besides, the preparation of nanoparticles with hydroxylated water-soluble polymers facilitates the control of mean diameter and size distribution of the nanoparticles [8, 14, 17].

In view of these observations, the present chapter focuses on selected plant and tree gums which are employed for the development of facile, cost-effective and eco-friendly green methods of nanoparticle synthesis and is restricted to the applications of gum reduced/stabilized nanoparticles (Table 3.1). The biogenic nanoparticles produced by plant gums are usually characterized by wide varieties of analytical techniques such as UV-visible absorption spectroscopy (UV-Vis) for surface plasmon resonance, transmission electron microscopy (TEM) for size and shape, X-ray diffraction (XRD) for crystal structure, Fourier transform infrared spectroscopy (FTIR) for functional groups of the biomolecules, thermogravimetric analysis (TGA) for thermal stability, zeta potential for surface charge, Raman spectroscopy for surface capping, etc.

Table 3.1 Plant- and tree gum-mediated phytosynthesis of nanoparticles and their applications.

S No	Plant gum	Gum's role	Synthesized NP	Nanoparticle size/ size range (nm)	Studied application/activity	Ref.
1	Kondagogu	Reductant, stabilizer	Ag	4.5	Antibacterial, antibiofilm, cytotoxic	[12, 14, 18, 19]
		Reductant, stabilizer	Ag	5	Colorimetric Hg sensor	[20]
		Reductant, stabilizer	Ag	5.5	-	[21]
		Reductant, stabilizer	Ag	10.5	-	[22]
		Reductant, stabilizer	Au	7.8	-	[21]
		Reductant, stabilizer	Au	6.9	Catalytic	[23]
		Reductant, stabilizer	Au	12	Antibacterial, catalytic	[24]
		Reductant, stabilizer	Au	4–12.7	Anti-proliferative	[25]
		Stabilizer	Cu	15	Antibiofilm	[26]
		Reductant, stabilizer	Pd	6.5	Catalytic	[27]
		Reductant, stabilizer	Pd	6.7	Colorimetric glucose sensor	[28]
		Reductant, stabilizer	Pt	2.4	-	[21]
		Surface modifier	Fe_3O_4	8–15	Nano-adsorbent	[29]
		Precursor	Carbon nanofibre	250	Heavy metal adsorbent	[30]

(*Continued*)

Table 3.1 Cont.

S No	Plant gum	Gum's role	Synthesized NP	Nanoparticle size/ size range (nm)	Studied application/activity	Ref.
2	Ghatti	Reductant, stabilizer	Ag	5.7	Antibacterial, antibiofilm, cytotoxic	[8, 13, 31]
		Reductant, stabilizer	Au	112.5	-	[32]
		Reductant, stabilizer	Pd	4.8	Catalyst, antioxidant	[9, 31]
		Polymer matrix	Fe_3O_4	80	Nanocomposite adsorbent	[33]
		Polymer matrix	Fe_3O_4	70	Nanocomposite adsorbent	[34]
		Polymer matrix	TiO_2	30	Nanocomposite adsorbent	[35]
3	Olibanum	Reductant, stabilizer	Ag	7.5	Antibacterial, antibiofilm, biocompatibility	[13, 15]
		Reductant, stabilizer	Pd	6.5	Catalyst, antioxidant	[10]
		Reductant, stabilizer	Pt	4.4	Colorimetric Hg sensor	[11]
4	Tragacanth	Reductant, stabilizer	Ag	13.1	Antibacterial	[7]
		Polymer backbone	Ag	13	Antibacterial	[36]
		Reductant	Ag	77.5	Antibacterial	[37]
		Reductant, stabilizer	Au	54	Drug carrier	[37]
		Reductant, stabilizer	ZnO	33	Neurotoxic	[38]
		Reductant, stabilizer	ZnO	62	Photocatalytic, antimicrobial	[39]
		Viscosifier	SiO_2	50	Fracturing fluid	[40]
		Polymer backbone	Graphene oxide	1.1	Heavy metal adsorbent	[36]

5	Arabic	Reductant, stabilizer	Ag	5	-	[17]
		Stabilizer	Ag	3	-	[41]
		Stabilizer	Ag	2–5	Antibacterial	[42]
		Reductant, stabilizer	Ag	35	Antibacterial	[43]
		Reductant, stabilizer	Ag	2–20	-	[44]
		Stabilizer	Ag	40.2	-	[45]
		Reductant, stabilizer	Ag	18	Catalytic	[46]
		Reductant, stabilizer	Ag	15–25	-	[47]
		Stabilizer	Au	15–20	Tissue specific distribution	[48]
		Stabilizer	Au	15–18	Cytotoxicity, apoptotic, anti-inflammatory, lipid peroxidation, anti-neovascular	[49]
		Reductant, stabilizer	Au	6.5	Antioxidant	[50]
		Stabilizer	Au	4	Antioxidant	[50]
		Reductant, stabilizer	Au	5.5	Photothermal	[51]
		Stabilizer	Au	15–20	Biocompatibility	[52]
		Reductant, stabilizer	Au	21.1	-	[53]
		Stabilizer	Au	21	Phototoxicity, cytotoxicity, anti-neoplastic, anti-inflammatory,	[54]

(*Continued*)

Table 3.1 Cont.

S No	Plant gum	Gum's role	Synthesized NP	Nanoparticle size/ size range (nm)	Studied application/activity	Ref.
		Stabilizer	Ag	33–35	Aggregation kinetics	[55]
		Stabilizer	Cu	3–9, 5	-	[56]
		Reductant, stabilizer	Pd	9.1	-	[57]
		Reductant	Pd	5	Catalytic	[58]
		Stabilizer	Se	34.9	Antioxidant	[59]
		Stabilizer	Hydroxyapatite	20–150	Surface modification	[60]
		Scaffold material	Hydroxyapatite		Bone tissue regeneration	[61]
		Stabilizer	Fe_3O_4	6–10	Surface modification	[60]
		Surface modifier	Fe_3O_4	11	Biocompatibility	[62]
		Surface modifier	Fe_3O_4	34.1	Nano adsorbent	[63]
		Surface modifier	Fe_3O_4	20	Bacterial isolation	[64]
		Surface modifier	Fe_3O_4	1000	Cytotoxic	[65]
		Surface coating	Fe_3O_4	< 50	Hyperthermia	[66]
		Polymer matrix	Fe_3O_4	15–20	Electrical conductivity	[67]
		Encapsulator	SiO_2	6–22	Electrical conductivity	[68]
		Carrier	ZnO	15–20	Cytotoxic, antibacterial	[69]
		Hydrogel matrix	ZnO	40–60	Antibacterial	[70]
		Hydrogel matrix	ZnO	90.3	Antibacterial, cytotoxic, anti-inflammatory	[71]

		Hydrogel matrix	ZnO	58.9	Hemolytic, oxidative stress	[72]
6	Karaya	Reductant, stabilizer	Ag	2–4	Antibacterial, catalytic	[73]
		Reductant, stabilizer	Ag	7–10	Antibacterial	[74]
		Reductant, stabilizer	Ag	12.5	-	[75]
		Reductant, stabilizer	Ag	16	Catalytic	[76]
		Reductant, stabilizer	Au	7.8	-	[75]
		Reductant, stabilizer	Au	20–25	Drug delivery carrier	[77]
		Reductant, stabilizer	Au	14	Colorimetric copper sensor	[78]
		Reductant, stabilizer	Pt	5	-	[75]
		Reductant, stabilizer	CuO	10.5	-	[75]
		Reductant, stabilizer	CuO	4.8	Antibacterial	[79]
		Reductant, stabilizer	Fe_3O_4	18.5	-	[75]
		Stabilizer	Fe_3O_4	10–15	Nanocomposite adsorbent	[80]
		Stabilizer	Zerovalent Fe	20–100	Cr reduction, VOC degradation	[81]
		Polymer matrix	SiC	60.7	Nanocomposite adsorbent	[82]
7	Guar	Reductant, stabilizer	Ag	8	Optical ammonia sensor	[83]
		Reductant, stabilizer	Ag	10–50	SERS substrate, catalytic	[84]
		Film former	Ag-Cu	< 100	Antibacterial	[85]
		Reductant, stabilizer	Au	6.5	Optical ammonia sensor	[86]

(*Continued*)

Table 3.1 Cont.

S No	Plant gum	Gum's role	Synthesized NP	Nanoparticle size/ size range (nm)	Studied application/activity	Ref.
		Reductant, stabilizer	Pt	6	Catalytic	[87]
		Polymer matrix	Pd	2–6	Nitrobenzene detection	[88]
		Stabilizer	Zerovalent Fe	200	-	[89]
		Polymer matrix	Ni	60–80	Catalytic, superparamagnetism	[90]
		Reductant, stabilizer	Fe_3O_4	48	Catalytic	[91]
		Polymer matrix	Fe_3O_4	25	Sustained drug release	[92]
		Stabilizer	SiO_2	135	Colon specific drug delivery	[93]
		Template	SiO_2	4–6	Nanocomposite adsorbent	[94]
		Template	SiO_2	3–6	Nanocomposite adsorbent	[95]
		Encapsulator	SnO_2	11	Hydrazine determination	[96]
		Stabilizer	ZnO	6–12	Photocatalytic dye degradation	[97]
8	Neem	Reductant, stabilizer	Ag	23.4	Antibacterial	[98]
9	Sour cherry	Reductant, stabilizer	Pd	5	Catalytic	[99]
10	Prunus	Reductant, stabilizer	Pt	10–50	Antifungal	[100]

11	Apricot	Reductant, stabilizer	Ag	10–40	Antibacterial, antinociceptive, anti-inflammatory	[101]
		Reductant, stabilizer	Au	5–30	Antibacterial, antinociceptive, anti-inflammatory	[101]
12	Cashew	Reductant, stabilizer	Ag	4.3	Antibacterial, cytotoxic	[102]
13	Locust bean	Reductant, stabilizer	Ag	22	Fiber optic hydrogen peroxide sensor	[103]
14	Almond	Grafting backbone	Ag	75	Antibacterial	[104]

3.2 Different Varieties of Plant Gums

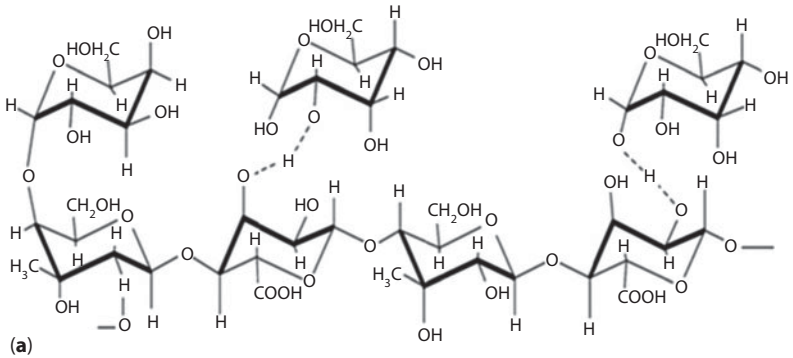
Plant and tree gums are produced by a process known as gummosis, as a result of decomposition of cellulose. Most of the plant and tree gums are water soluble, complex polysaccharides derived as exudates from the bark or roots; produced either from natural wounds or artificial incisions. While guar and locust bean gums are seed gums derived from endosperm. In the area of nanobiotechnology, the plant gums are used as reductant, stabilizer, template, precursor, surface modifier, surface coating, film former, polymer matrix, hydrogel matrix, polymer backbone, grafting backbone, scaffold material, viscosifier, encapsulator, carrier, etc., during the synthesis and post-synthesis modifications of nanoparticles and nanocomposites (Table 3.1).

3.2.1 Gum Kondagogu

Gum kondagogu is a nontoxic, natural polysaccharide produced as an exudate from the bark of *Cochlospermum gossypium* (Bixaceae family), a native Indian tree (Figure 3.1a). The gum is collected from the forests of Andhra Pradesh state by the tribals and marketed through Girijan Co-operative Corporation Ltd, Visakhapatnam, India. It is one of the important non-timber forest products in Andhra Pradesh state and is exported from India. The gum is classified as rhamnogalacturonan type and the primary structure is composed of sugars, including arabinose, galactose, glucose, mannose, rhamnose, glucuronic acid and galacturonic acid with sugar linkage of (1→2) β-D-Gal p, (1→6) β-D-Gal p, (1→4) β-D-Glc p A, 4-O-Me-α -D-Glc p A, (1→2) α-L-Rha. Its molecular weight is 7.2×10^6 g/mol (Figure 3.2a). The amino and fatty acid profiles of gum kondagogu could be used as molecular markers to differentiate it from the rest of rhamnogalacturonan gums [105–109].



Figure 3.1 Photographs of tears of gum (a) kondagogu, (b) ghatti, (c) olibanum and (d) karaya [8, 10, 14].



(**a**)

• main chain structures

β-Gal*p*-(1→6)-[β-Gal*p*-(1→6)]$_{0-3}$-Ara*p*

β-Gal*p*-[(1→6)-β-Gal*p*]$_{0-4}$-(1→6)-Gal*p*

• others

R-(1→3)-Gal*p*-(1→6)-Gal*p*-(1→6)-Gal*p*-(1→3)-Ara*p*-

→4)-Glc*p*A-(1→6)-Gal*p*-(1→

(**b**)

Figure 3.2 The assigned structure of gum (a) kondagogu and (b) ghatti [20, 31].

The studies carried out on gum kondagogu have ascertained that it is nontoxic, nonimmunogenic and has potential applications as an additive in the food and pharma industries [110, 111]. The gum is widely utilized in Ayurvedic and Unani medicine for treatment of various ailments. It is used in calico printing, marbling paper, leather dressing, cigar paste, ice creams and tussar silk polishing. It is employed as a drug delivery matrix for diclofenac, metformin and metoprolol [112]. It is extensively studied as a biosorbent for remediation of toxic metals, including cadmium, lead, copper, iron, selenium, chromium, nickel, zinc, cobalt, arsenic and uranium [18, 109].

3.2.2 Gum Ghatti

Gum ghatti is a natural, water-soluble, complex polysaccharide derived as an exudate from the bark of *Anogeissus latifolia* (Combretaceae family), a native tree of the Indian subcontinent (Figure 3.1b). The name gum ghatti

originates from its transportation route through mountain passes or *ghats*. It is a high-arabinose, protein-rich, acidic heteropolysaccharide, mixed salt of calcium, magnesium, potassium and sodium; and categorized under the arabinogalactan class. The primary structure is composed of sugars, such as L-arabinose, D-galactose, D-mannose, D-xylose and D-glucuronic acid, in a molar ratio of 48:29:10:5:10 and <1% of rhamnose, which is present as non-reducing end-groups. The gum has alternating 4-*O*-substituted and 2-*O*-substituted α-D-mannopyranose units and chains of 1 → 6 linked β-D-galactopyranose units with side chains of L-arabinofuranose residues; 6% of the rhamnose in the polysaccharide is linked to the galactose backbone as α -Rhap-(1 → 4) β-galactopyranose side chain. It has a molecular weight of 8.94×10^7 g/mol (Figure 3.2b) [8].

The gum is entitled with CAS number 9000-28-6 and recognized as "generally recognized as safe" (GRAS). It is an approved food ingredient (Code 184.1333) by the U.S. Food and Drug Administration (FDA) under the function of emulsifier and emulsifier salt. Its use in food is also approved in various countries such as Japan, China, South Korea, Singapore, Russia, Australia, South Africa, Iran, Saudi Arabia and Latin America. It is considered as a food grade additive by the Bureau of Indian Standards, India, under Indian Standard IS 7239:1974. In India, this hydrocolloid application in traditional medicine and food preparations has been well-known for centuries. The gum is composed of around 80% soluble dietary fiber and acts as a prebiotic, thereby aiding in bifidus fermentation. The gum has hypolipidemic activity and is used as a release modifier for controlled drug delivery. It has long been used in non-food applications [8, 31].

3.2.3 Gum Olibanum

Gum olibanum is a naturally occurring gum oleoresin derived as an exudate from the bark of *Boswellia serrata* (Burseraceae family) (Figure 3.1c). This native Indian gum, commonly known as *Salai guggul*, is produced in the states of Madhya Pradesh, Andhra Pradesh, Rajasthan, Gujarat, Maharashtra, Bihar, Odisha and Assam and collected and exported from Mumbai. Besides its use as an incense, fumigant and multipurpose aromatic, it is also exploited in a wide variety of industries. It has a broad spectrum of properties, including anti-inflammatory, anti-arthritic, analgesic, diaphoretic, astringent, stimulant, expectorant and diuretic activities, and has long been used in the traditional Ayurvedic and Unani medicines.

Typically, the gum olibanum consists of 10% volatile essential oil, 15–20% water-soluble polysaccharides, 70% resin and 4–5% insoluble matter. Among the pentacyclic triterpenes, boswellic acid is the main

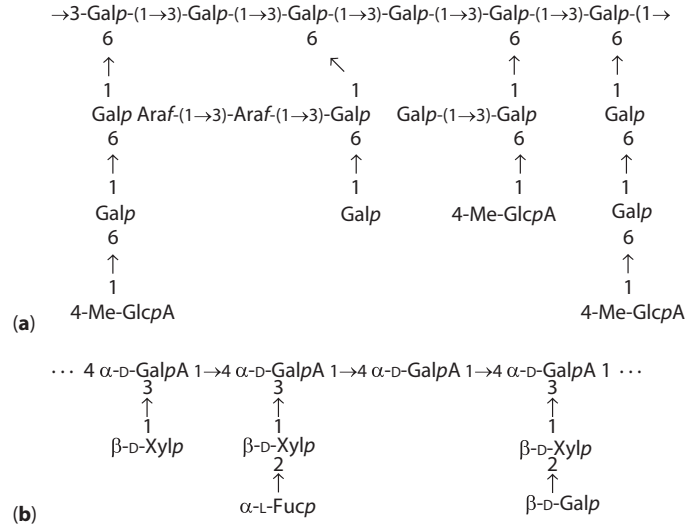


Figure 3.3 The assigned structure of gum (a) olibanum and (b) tragacanth [10, 37].

pharmacological constituent in the lipophilic fraction. The 4-*O*-methyl-glucuronoarabino-galactan is identified as one of the polysaccharides and has a molecular weight of 5.1–5.6 × 10^5 g/mol (Figure 3.3a). The primary structure of the polysaccharide is abundant in neutral sugars and mainly composed of galactose, arabinose, xylose and D-glucuronic acid. The water-soluble polysaccharide fraction is employed as potent vaccine adjuvant, matrix for controlled release of diclofenac, hypolipidemic, hepato-protective and reno-protective agents; and is a candidate agent for vascular smooth muscle cell migration inhibition and proliferation. Acute, sub-acute and chronic toxicity and safety studies carried out in mice, rats and monkeys have established that gum olibanum is nontoxic and safe for use in different animals [15].

3.2.4 Gum Tragacanth

Gum tragacanth is a naturally occurring complex, acidic polysaccharide derived as an exudate from the roots of *Astragalus gummifer* (Fabaceae family), a native shrub of western Asia. Mostly, it is commercially produced in Iran and Turkey. The name tragacanth originates from the Greek words *tragos* (goat) and *akantha* (thorn), indicating the curved shape of the gum. This biopolymer is an arabinogalactan type of natural gum and its structural, physicochemical, compositional, solution, thermal, rheological and

emulsifying properties have been well characterized and studied. This biopolymer is a high-arabinose, protein-containing, acidic heteropolysaccharide, which occurs in nature as mixed calcium, magnesium, and sodium salts. It has a molecular weight of ~ 8.4×10^5 g/mol. This natural polymer consists of a mixture of water-soluble (tragacanthin) and water-swellable (bassorin) polysaccharide fractions. The water-soluble tragacanthin constitutes around 30–40% of the gum and it is a neutral, highly branched, type II arabinogalactan comprising (1→6)- and (1→3)- linked core chain containing galactose and arabinose and side groups of (1→2)-, (1→3)- and (1→5)-linked arabinose units occurring as monosaccharides or oligosaccharides. The primary structure of tragacanthin is composed of sugars, such as L-fucose, L-arabinose, D-xylose, D-mannose, D-galactose and D-glucose, in a molar ratio of 3:52:29:6:5:5 (Figure 3.3b).

The gum tragacanth with a CAS number 9000–65–1 is considered as "generally recognized as safe" (GRAS) and approved as a food ingredient (21CFR184.1351) by the FDA under the function of emulsifier, stabilizer and thickener. It is also approved as a food additive within the class of thickeners, stabilizers, emulsifiers and gelling agents in the European Union and is accorded with food safety E number E413. It is considered as a food grade additive by the Bureau of Indian Standards, India, under Indian Standard IS 7238:1997. Several studies have established that gum tragacanth is nontoxic, nonmutagenic, nonteratogenic, noncarcinogenic and has potential application as a food additive, dressing bandage for burn healing, immobilizing agent in viral plaque assay, superabsorbent hydrogel and carrier for controlled release of drugs. This hydrocolloid is resistant to gastrointestinal enzymes and enzymatically degraded only by the specific microflora of the colon, thereby aiding in bifidus fermentation. Thus, it functions as a soluble dietary fiber and acts as a laxative [7].

3.2.5 Gum Arabic

Gum arabic or acacia is a branched, neutral or slightly acidic, complex mixture of polysaccharides and glycoproteins derived as an exudate from the bark of *Acacia senegal* and *Acacia seyal* trees (Fabaceae family). The gum exists as a mixed salt of calcium, magnesium, and potassium and has a backbone of 1,3-linked β-galactopyranose units and side chains of 1,6-linked galactopyranose units terminating in glucuronic acid or 4-O-methylglucuronic acid residues. The gum is made up of 44% galactose, 13% rhamnose, 27% arabinose and 16% glucuronic acid and 4-O-methyl glucuronic acid. It contains 2–3% of peptide moieties as part of the structure. The three major fractions in the gum are arabinogalactan protein

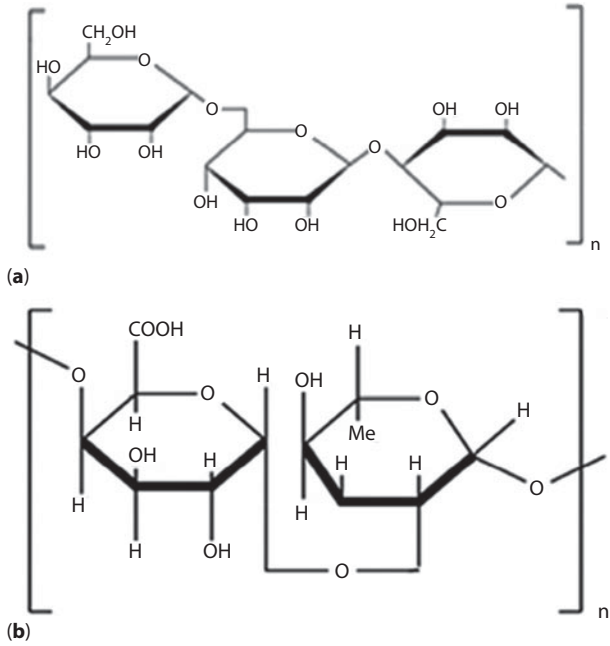


Figure 3.4 The assigned structure of gum (a) arabic and (b) karaya [113].

complex (1.4×10^6 g/mol), arabinogalactan (2.8×10^5 g/mol) and glycoprotein (Figure 3.4a). It is a biocompatible, biodegradable, nontoxic food additive with an E number of E414 with wide acceptance as an ingredient in the food and pharmaceutical industries, due to its remarkable structural, physical, chemical, surface active, rheological and electrical properties. It is declared as ADI (acceptable daily intake) non-specified additive for human consumption by the FDA [41, 48, 59, 62, 66, 67, 70, 113].

3.2.6 Gum Karaya

Gum karaya is a naturally available, highly branched, partially acetylated, anionic polysaccharide derived as an exudate from the bark of *Sterculia urens* and other species of *Sterculia* (Sterculiaceae family), a traditional gum of India (Figure 3.1d). It has a molecular weight of 1.6×10^{10} g/mol and protein content of about 1%, a value lower that of other exudate gums. This biopolymer is categorized under substituted rhamnogalacturonoglycan tree gum and its structural, physicochemical properties, food and non-food applications have been well characterized and studied. The gum is composed of 60% neutral sugars (rhamnose, galactose, and arabinose) and

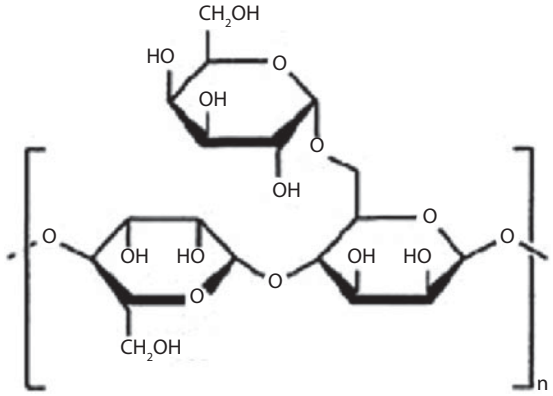


Figure 3.5 The assigned structure of gum guar [97].

40% acidic sugars (glucuronic and galacturonic acids). The backbone of the gum consists of α-D-galacturonic acid and α-l-rhamnose residues. The side chains are attached by 1,2-linkage of β-D-galactose or by 1,3-linkage of β-D glucuronic acid to the galacturonic acid of the main chain. Also, half of the rhamnose residues of the main chain is 1,4-linked to β-D-galactose units (Figure 3.4b). The gum is nontoxic and applied as a food additive under emulsifier, stabilizer, thickener, binder and drug release modifier in pharmaceutical; and metal biosorbent, bulk laxative, denture powder, textile sizer in non-food industries [74, 80, 81, 106, 113].

3.2.7 Gum Guar

Gum guar is a naturally abundant, high-molecular-weight, nonionic polysaccharide endosperm gum isolated from the seeds of *Cyamopsis tetragonoloba* (Fabaceae family). The structure is composed of a backbone of β-D-(1→4)-mannopyranosyl units with α-D-galactopyranosyl units as side chains. It is nontoxic, biocompatible, biodegradable and has a molecular weight of about × 10^6 g/mol (Figure 3.5). The gum functions as thickener, stabilizer, gel former, stabilizer, flocculent, etc. [86, 87, 91, 97, 114].

3.3 Phytosynthesized Nanoparticles and Their Applications

There are different types of nanoparticles consisting of metal, metal oxide, organic, inorganic, polymeric nanoparticles; quantum dots, carbon

nanotubes, graphene, etc. The metal/metal oxide nanoparticles are detailed here with due emphasis on their spectrum of activities.

3.3.1 Silver Nanoparticles

Silver nanoparticles are of great interest due to the ease of their synthesis at desired sizes and shapes and their size- and shape-dependent antimicrobial activities [2]. Plant gums are extensively utilized as reductant and stabilizers for the synthesis of silver nanoparticles (Figure 3.6). They are applied as antimicrobial, antibacterial, antibiofilm, cytotoxic, anti-inflammatory, antinociceptive, biocompatible, photocatalytic, catalytic agents; SERS substrate, colorimetric sensor for mercury and hydrogen peroxide; fiber optic sensor for hydrogen peroxide, optical sensor for ammonia, aggregation kinetic studies, etc. (Table 3.1). Most of the chemogenic silver nanoparticles are cytotoxic and nonbiocompatible due to the chemical precursor contamination, used solvent toxicity and hazardous by-product generation, etc. [115]. Hence, they can't be considered as ideal candidates for biomedical and pharmaceutical applications. In view of this, in our laboratory we have studied and compared the antibacterial activity of natural plant gum synthesized silver nanoparticles using various susceptibility assays. Also, we have demonstrated the superior antibacterial action of the biogenic silver nanoparticles on Gram-positive and Gram-negative bacteria in both planktonic and biofilm modes of growth (Figure 3.7). The efficient antibacterial and antiproliferation activities are attributed to its smaller particle size, monodispersity and higher zeta potential value. The possible

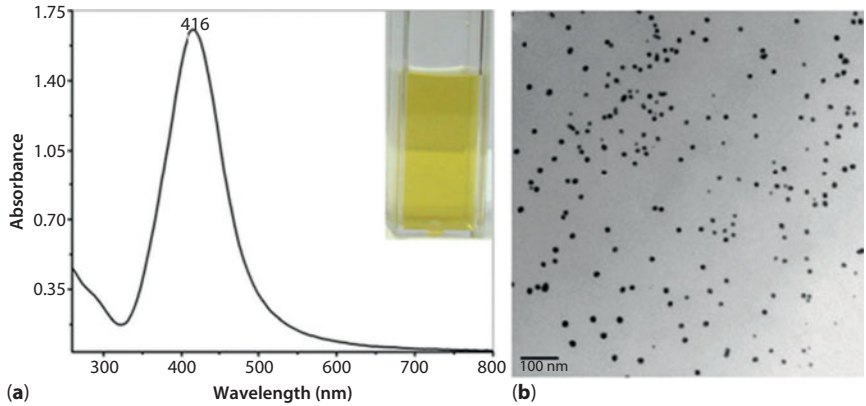


Figure 3.6 Characterization of gum kondagogu synthesized silver nanoparticles: (a) UV-visible spectrum, Inset: Solution color; (b) TEM image.

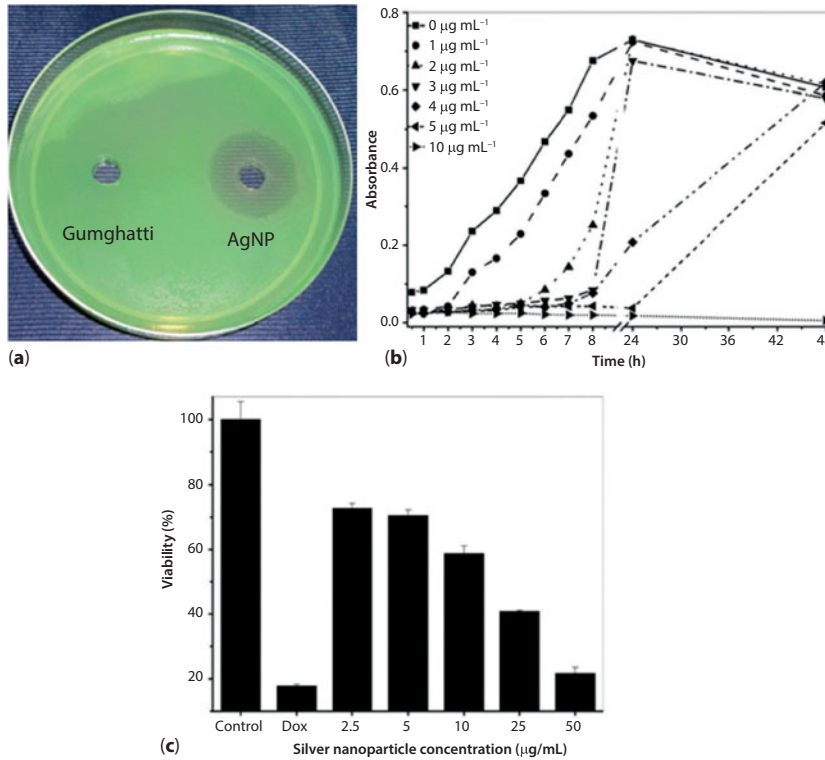


Figure 3.7 Antibacterial and cytotoxic activities of gum ghatti-based silver nanoparticles. (a) Well diffusion assay showing the inhibition zone around the silver nanoparticle loaded well in *Pseudomonas aeruginosa* culture plate, (b) Growth curve inhibition of *P. aeruginosa* in liquid medium supplemented with different concentrations (1–10 μg/mL) of silver nanoparticles and (c) Effect of silver nanoparticles on the cell viability of HeLa cell line at various concentrations.

mode of action involved in the bactericidal activity of nanoparticles is elucidated [12, 13].

3.3.2 Gold Nanoparticles

The gold nanoparticles are well-suited for a range of biological applications due to their nontoxic and biologically inert nature, convenient synthesis in different sizes with great control; effectual attachment of pharmaceutical compounds through electrostatic, covalent or noncovalent interactions; and stabilizing agent tailorability for specific cell targeting, controlled release of the drug, etc. (Figure 3.8) [116]. The gum-based gold

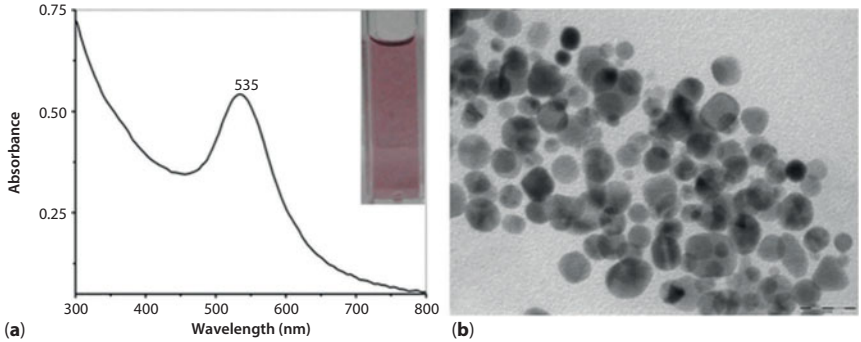


Figure 3.8 Characterization of gum ghatti synthesized gold nanoparticles: (a) UV-visible spectrum, Inset: Solution color; (b) TEM image.

nanoparticles are employed as antibacterial, antiproliferative, cytotoxic, apoptotic, anti-inflammatory, anti-neovascular, antineoplastic, antinociceptive, lipid peroxidation, tissue specific distribution, biocompatible, antioxidant, photothermal, phototoxic, catalytic agents; drug delivery carrier, colorimetric sensor for copper, optical sensor for ammonia, etc. (Table 3.1).

3.3.3 Copper Nanoparticles

The application of copper as an effective antibacterial agent with low toxicity has been known for years. The copper nanoparticles are commonly synthesized using liquid-based chemical reduction, sonochemical reduction, laser ablation, microemulsion, reverse micelle and radiation. However, for most of these methods inert atmosphere is a prerequisite and limited by agglomerate formation [117]. The antibacterial, antibiofilm, and antifungal activities of copper and copper oxide nanoparticles are demonstrated against various bacteria and fungi [79, 117].

3.3.4 Platinum and Palladium Nanoparticles

Plant gum-derived platinum and palladium nanoparticles (Figures 3.9 and 3.10) are applied as antifungal, catalytic, antioxidant agents; colorimetric sensor for glucose, mercury; detector for nitrobenzene, etc. (Figure 3.11). Other gum stabilized selenium, iron, nickel nanoparticles are used as antioxidant, chromium reducing and VOC degrading; catalytic and superparamagnetic agents, respectively (Table 3.1).

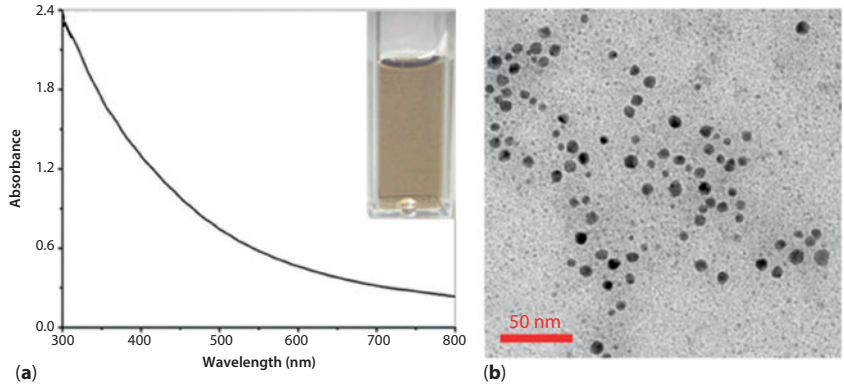


Figure 3.9 Characterization of gum olibanum synthesized palladium nanoparticles: (a) UV-visible spectrum, Inset: Solution color; (b) TEM image.

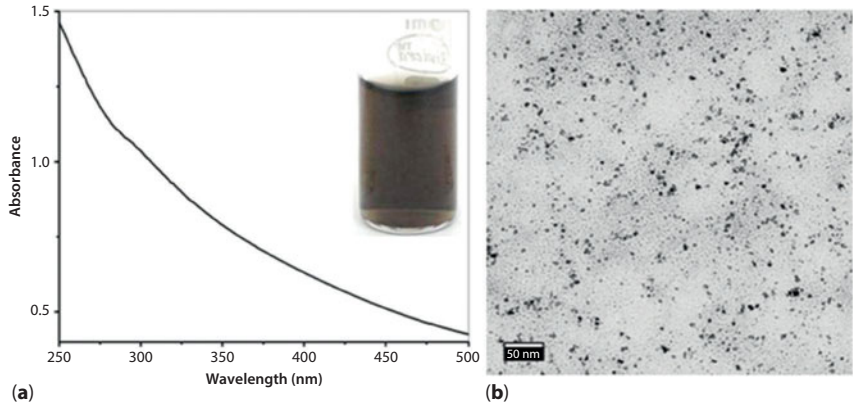


Figure 3.10 Characterization of gum ghatti synthesized platinum nanoparticles: (a) UV-visible spectrum, Inset: Solution color; (b) TEM image.

3.3.5 Metal Oxide Nanoparticles

Widely synthesized, gum-coated/modified iron oxide nanoparticles are implemented as nanocomposite adsorbent, catalytic, cytotoxic, biocompatible agents; and studied for surface modification, electrical conductivity, hyperthermia, bacterial isolation, sustained drug release, etc. Zinc oxide nanoparticles embedded in hydrogel gum matrix are exploited as antimicrobial, antibacterial, cytotoxic, anti-inflammatory, hemolytic, photocatalytic, dye degradative, neurotoxic, oxidative stress agents, etc. Gum templated silicon dioxide nanoparticles are used for fracturing

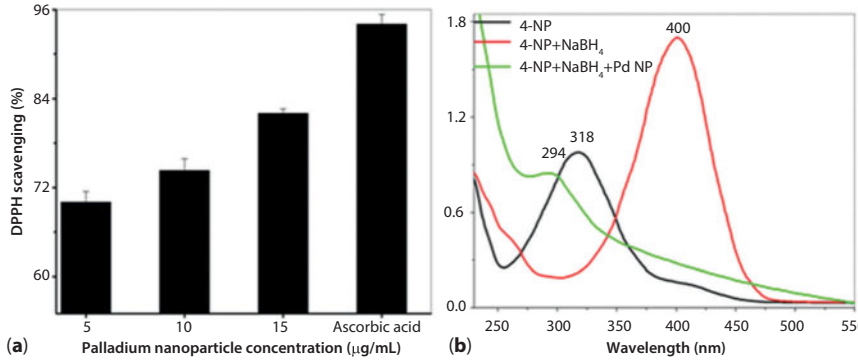


Figure 3.11 (a) DPPH radical scavenging activity of (a) gum ghatti produced palladium nanoparticles, in comparison with ascorbic acid and (b) UV-Vis spectra of 4-nitrophenol reduction by $NaBH_4$ using gum olibanum reduced palladium nanoparticles as catalyst.

fluid, electrical conductivity, colon-specific drug delivery, nanocomposite adsorbent, etc.; while the titanium dioxide nanoparticles are applied as nanocomposite adsorbents. The other metal oxide nanoparticles, such as hydroxyapatite, are applied for surface modification and bone tissue regeneration (Table 3.1).

3.4 Conclusions and Future Prospects

The plant and tree gum-based metal nanoparticles are simple to synthesize, yet cost-effective, eco-friendly and easily scalable. By acting as renewable feedstocks, the gums meet the principle of green chemistry. The size- and shape-controlled nanoparticles could be produced in large scale for industrial/commercial applications. The molecular mechanisms involved during the metal ion reduction and subsequent nanoparticle capping/stabilization by the gum molecules require in-depth study. Furthermore, the applications of biogenic nanoparticles should be explored in the areas of water purification, antimicrobial textiles, food packaging, agriculture, tissue engineering, pharmacy, etc.

The ever-increasing antimicrobial activity of the silver nanoparticles applied in various industrial sectors raise apprehensions about their biological impacts either by direct or indirect exposure and risk posed to the environment and health [118]. Due to their smaller size and large surface area, the nanoparticles exhibit higher toxicity as compared to bulk metal. The area of nanoparticle-mediated cytotoxicity and genotoxicity in diverse organisms is relatively new and the effects of various

nanoparticles of different sizes, shapes and methods of synthesis have to be evaluated. Studies carried out with cellular models, rats, *Allium cepa,* etc., are reported in the literature. As the nanoparticles have the capacity to cross cellular membranes and contact the nucleus, more studies on the mechanisms of genotoxicity and impact on health and the environment are very much essential. Also, a comparison of the existing data on genotoxicity studies carried out with various cell cultures and animals is difficult at different exposed doses of nanoparticles [119]. Thus, standard methodologies for *in-vitro* and *in-vivo* assessment of nanoparticle-induced genotoxicity and cytotoxicity have to be established to better understand and utilize them in a safer way. Also, its impact on the global economy necessitates a special regulation for nanotechnology [120].

Acknowledgment

The author would like to thank Dr. A. C. Sahayam, Head, Bulk Analysis Section, and Dr. Sunil Jai Kumar, Head, NCCCM/BARC, for their constant support and encouragement throughout the work.

References

1. Faramarzi, M.A., Sadighi, A., Insights into biogenic and chemical production of inorganic nanomaterials and nanostructures. *Adv. Colloid Interf. Sci*., 189–190, 1–20, 2013.
2. Kora, A.J., Manjusha, R., Arunachalam, J., Superior bactericidal activity of SDS capped silver nanoparticles: Synthesis and characterization. *Mater. Sci. Eng. C*, 29, 2104–2109, 2009.
3. Raveendran, P., Fu, J., Wallen, S.L., Completely 'green' synthesis and stabilization of metal nanoparticles. *J. Am. Chem. Soci.,* 125, 13940–13941, 2003.
4. Vigneshwaran, N., Nachane, R.P., Balasubramanya, R.H., Varadarajan, P.V., A novel one-pot 'green' synthesis of stable silver nanoparticles using soluble starch. *Carbohydr. Res*., 341, 2012–2018, 2006.
5. Gericke, M., Pinches, A., Microbial production of gold nanoparticles. *Gold Bull.,* 39, 22–28, 2006.
6. Anastas, P.T., Warner, J.C., *Green Chemistry: Theory and Practice*, pp. 30, Oxford University Press: New York, 1998.
7. Kora, A.J., Arunachalam, J., Green fabrication of silver nanoparticles by gum tragacanth (*Astragalus gummifer*): A dual functional reductant and stabilizer. *J. Nanomater.,* 2012, 8, 2012.

8. Kora, A.J., Beedu, S.R., Jayaraman, A., Size-controlled green synthesis of silver nanoparticles mediated by gum ghatti (*Anogeissus latifolia*) and its biological activity. *Org. Med. Chem. Lett.,*.2, 17, 2012.
9. Kora, A.J., Rastogi, L., Green synthesis of palladium nanoparticles using gum ghatti (*Anogeissus latifolia*) and its application as an antioxidant and catalyst. *Arab. J. Chem.,* 1–9, 2015.
10. Kora, A.J., Rastogi, L., Catalytic degradation of anthropogenic dye pollutants using palladium nanoparticles synthesized by gum olibanum, a glucurono-arabinogalactan biopolymer. *Ind. Crops Products,* 81, 1–10, 2016.
11. Kora, A.J., Rastogi, L., Peroxidase activity of biogenic platinum nanoparticles: A colorimetric probe towards selective detection of mercuric ions in water samples. *Sens. Act. B: Chem.,* 254, 690–700, 2018.
12. Kora, A.J., Sashidhar, R.B., Biogenic silver nanoparticles synthesized with rhamnogalacturonan gum: Antibacterial activity, cytotoxicity and its mode of action. *Arab. J. Chem.,* 43(3) 2014.
13. Kora, A.J., Sashidhar, R.B., Antibacterial activity of biogenic silver nanoparticles synthesized with gum ghatti and gum olibanum: A comparative study. *J. Antibiotics*., 68, 88–97, 2015.
14. Kora, A.J., Sashidhar, R.B., Arunachalam, J., Gum kondagogu (*Cochlospermum gossypium*): A template for the green synthesis and stabilization of silver nanoparticles with antibacterial application. *Carbohydr. Polym.,* 82, 670–679, 2010.
15. Kora, A.J., Sashidhar, R.B., Arunachalam, J., Aqueous extract of gum olibanum (*Boswellia serrata*): A reductant and stabilizer for the biosynthesis of antibacterial silver nanoparticles. *Process Biochem.,* 47, 1516–1520, 2012.
16. Cao, X., Cheng, C., Ma, Y., Zhao, C., Preparation of silver nanoparticles with antimicrobial activities and the researches of their biocompatibilities. *J. Mater. Sci. Mater. Med.,* 21, 2861–2868, 2010.
17. Mohan, Y.M., Raju, K.M., Sambasivudu, K., Singh, S., Sreedhar, B., Preparation of acacia-stabilized silver nanoparticles: A green approach. *J. Appl. Polym. Sci.,* 106, 3375–3381, 2007.
18. Sashidhar, R.B., Raju, D., Karuna, R., Tree gum: Gum kondagogu, in: *Polysaccharides Bioactivity and Biotechnology*, pp. 185–217, Springer, 2015.
19. Rastogi, L., Kora, A.J., Sashidhar, R.B., Antibacterial effects of gum kondagogu reduced/stabilized silver nanoparticles in combination with various antibiotics: A mechanistic approach. *Appl. Nanosci.,* 5, 535–543, 2015.
20. Rastogi, L., Sashidhar, R.B., Karunasagar, D., Arunachalam, J., Gum kondagogu reduced/stabilized silver nanoparticles as direct colorimetric sensor for the sensitive detection of Hg^{2+} in aqueous system. *Talanta,* 118, 111–117, 2014.
21. Vinod, V.T.P., Saravanan, P., Sreedhar, B., Devi, D.K., Sashidhar, R.B., A facile synthesis and characterization of Ag, Au and Pt nanoparticles using a natural hydrocolloid gum kondagogu (*Cochlospermum gossypium*). *Colloid. Surf. B: Biointerf.,* 83, 291–298, 2011.

22. Padil, V.V.T., Stuchlík, M., Černík, M., Plasma modified nanofibres based on gum kondagogu and their use for collection of nanoparticulate silver, gold and platinum. *Carbohydr. Polym.,* 121, 468–476, 2015.
23. Maity, S., Kumar Sen, I., Sirajul Islam, S., Green synthesis of gold nanoparticles using gum polysaccharide of *Cochlospermum religiosum* (katira gum) and study of catalytic activity. *Physica E,* 45, 130–134, 2012.
24. Reddy, G.B., Madhusudhan, A., Ramakrishna, D., Ayodhya, D., Venkatesham, M., Veerabhadram, G., Green chemistry approach for the synthesis of gold nanoparticles with gum kondagogu: Characterization, catalytic and antibacterial activity. *J. Nanostr. Chem.,* 5, 185–193, 2015.
25. Kalaignana Selvi, S., Mahesh Kumar, J., Sashidhar, R.B., Anti-proliferative activity of Gum kondagogu (*Cochlospermum gossypium*)-gold nanoparticle constructs on B16F10 melanoma cells: An *in vitro* model. *Bioactive Carbohydr. Diet. Fibre,* 11, 38–47, 2017.
26. Suresh, Y., Annapurna, S., Singh, A.K., Chetana, A., Pasha, C., Bhikshamaiah, G., Characterization and evaluation of anti-biofilm effect of green synthesized copper nanoparticles. *Mater. Today: Proceed.,* 3, 1678–1685, 2016.
27. Rastogi, L., Beedu, S.R., Kora, A.J., Facile synthesis of palladium nanocatalyst using gum kondagogu *Cochlospermum gossypium*: A natural biopolymer. *IET Nanobiotechnol.,* 9, 362–367, 2015.
28. Rastogi, L., Karunasagar, D., Sashidhar, R.B., Giri, A., Peroxidase-like activity of gum kondagogu reduced/stabilized palladium nanoparticles and its analytical application for colorimetric detection of glucose in biological samples. *Sens. Act. B: Chem.,* 240, 1182–1188, 2017.
29. Saravanan, P., Vinod, V.T.P., Sreedhar, B., Sashidhar, R.B., Gum kondagogu modified magnetic nano-adsorbent: An efficient protocol for removal of various toxic metal ions. *Mater. Sci. Eng. C*, 32, 581–586, 2012.
30. Padil, V., Wacławek, S., Cernik, M., Activated carbon nanofibres from gum kondagogu for remediation of toxic metals, NANOCON 2015, Oct 14th–16th, Brono, Czech Republic, 2015.
31. Kora, A.J., Gum ghatti (*Anogeissus latifolia*), a proteinaceous edible biopolymer and its multifaceted biological applications, in: *Biopolymers: Structure, Performance and Applications*, Mishra, A.K., Hussain, C.M., Mishra, S.B. (Eds.), pp. 155–172, Nova Science Publishers, Inc.: New York, USA, 2017.
32. Alam, M.S., Garg, A., Pottoo, F.H., Saifullah, M.K., Tareq, A.I., Manzoor, O., Mohsin, M., Javed, M.N., Gum ghatti mediated, one pot green synthesis of optimized gold nanoparticles: Investigation of process-variables impact using Box-Behnken based statistical design. *Int. J. Biol. Macromol.,* 104, 758–767, 2017.
33. Mittal, H., Ballav, N., Mishra, S.B., Gum ghatti and Fe_3O_4 magnetic nanoparticles based nanocomposites for the effective adsorption of methylene blue from aqueous solution. *J. Ind. Eng. Chem.,* 20, 2184–2192, 2014.
34. Mittal, H., Mishra, S.B., Gum ghatti and Fe_3O_4 magnetic nanoparticles based nanocomposites for the effective adsorption of rhodamine B. *Carbohydr. Polym.,* 101, 1255–1264, 2014.

35. Mittal, H., Ray, S.S., A study on the adsorption of methylene blue onto gum ghatti/TiO_2 nanoparticles-based hydrogel nanocomposite. *Int. J. Biol. Macromol.,* 88, 66–80, 2016.
36. Sahraei, R., Ghaemy, M., Synthesis of modified gum tragacanth/graphene oxide composite hydrogel for heavy metal ions removal and preparation of silver nanocomposite for antibacterial activity. *Carbohydr. Polym.,* 157, 823–833, 2017.
37. Rao, K., Imran, M., Jabri, T., Ali, I., Perveen, S., Shafiullah, Ahmed, S., Shah, M.R., Gum tragacanth stabilized green gold nanoparticles as cargos for Naringin loading: A morphological investigation through AFM. *Carbohydr. Polym.,* 174, 243–252, 2017.
38. Darroudi, M., Sabouri, Z., Kazemi Oskuee, R., Khorsand Zak, A., Kargar, H., Hamid, M.H.N.A., Sol–gel synthesis, characterization, and neurotoxicity effect of zinc oxide nanoparticles using gum tragacanth. *Ceram. Int.,* 39, 9195–9199, 2013.
39. Ghayempour, S., Montazer, M., Ultrasound irradiation based *in-situ* synthesis of star-like Tragacanth gum/zinc oxide nanoparticles on cotton fabric. *Ultrason. Sonochem.,* 34, 458–465, 2017.
40. Chauhan, G., Verma, A., Hazarika, A., Ojha, K., Rheological, structural and morphological studies of Gum Tragacanth and its inorganic SiO_2 nanocomposite for fracturing fluid application. *J. Taiwan Inst. Chem. Eng.,* 000, 1–11, 2017.
41. Rao, Y.N., Banerjee, D., Datta, A., Das, S.K., Guin, R., Saha, A., Gamma irradiation route to synthesis of highly re-dispersible natural polymer capped silver nanoparticles. *Rad. Phy. Chem.,* 79, 1240–1246, 2010.
42. Vimala, K., Samba Sivudu, K., Murali Mohan, Y., Sreedhar, B., Mohana Raju, K., Controlled silver nanoparticles synthesis in semi-hydrogel networks of poly(acrylamide) and carbohydrates: A rational methodology for antibacterial application. *Carbohydr. Polym.,* 75, 463–471, 2009.
43. Thakur, M., Pandey, S., Mewada, A., Shah, R., Oza, G., Sharon, M., Understanding the stability of silver nanoparticles bio-fabricated using *Acacia arabica* (Babool gum) and its hostile effect on microorganisms. *Spectrochim. Acta A,* 109, 344–347, 2013.
44. Dong, C., Zhang, X., Cai, H., Cao, C., Facile and one-step synthesis of monodisperse silver nanoparticles using gum acacia in aqueous solution. *J. Mol. Liquids,* 196, 135–141, 2014.
45. Medina-Ramirez, I., Bashir, S., Luo, Z., Liu, J.L., Green synthesis and characterization of polymer-stabilized silver nanoparticles. *Colloid. Surf. B,* 73, 185–191, 2009.
46. Mane Gavade, S.J., Nikam, G.H., Sabale, S.R., Tamhankar, B.V., Green synthesis of fluorescent silver nanoparticles using *Acacia nilotica* gum extract for kinetic studies of 4-nitrophenol reduction. *Mater. Today Proceed.,* 3, 4109–4114, 2016.
47. Li, Y.-f., Gan, W.-p., Zhou, J., Lu, Z.-q., Yang, C., Ge, T.-t., Hydrothermal synthesis of silver nanoparticles in Arabic gum aqueous solutions. *Transact. Nonferrous Metals Soc. China,* 25, 2081–2086, 2015.

48. Fent, G.M., Casteel, S.W., Kim, D.Y., Kannan, R., Katti, K., Chanda, N., Katti, K., Biodistribution of maltose and gum arabic hybrid gold nanoparticles after intravenous injection in juvenile swine. *Nanomed.: Nanotechnol. Biol. Med.,* 5, 128–135, 2009.
49. Gamal-Eldeen, A.M., Moustafa, D., El-Daly, S.M., Abo-Zeid, M.A.M., Saleh, S., Khoobchandani, M., Katti, K., Shukla, R., Katti, K.V., Gum Arabic-encapsulated gold nanoparticles for a non-invasive photothermal ablation of lung tumor in mice. *Biomed. Pharmacother.,* 89, 1045–1054, 2017.
50. Joshita, D., Cholimi, S., Pujiyanto, A., Antioxidant activity of gold nanoparticles using gum arabic as a stabilizing agent. *Inter. J. Pharm. Pharmaceut. Sci.,* 6, 462–465, 2014.
51. Shalaby, T., Green synthesis ofgold nanoparticles using cumin seeds and gum arabic: Studying their photothermal efficiency. *Nanosci. Nanotechnol.,* 5, 89–96, 2015.
52. Kattumuri, V., Katti, K., Bhaskaran, S., Boote, E.J., Casteel, S.W., Fent, G.M., Robertson, D.J., Chandrasekhar, M., Kannan, R., Katti, K.V., Gum arabic as a phytochemical construct for the stabilization of gold nanoparticles: *In vivo* pharmacokinetics and X-ray-contrast-imaging studies. *Small*, 3, 333–41, 2007.
53. Wu, C.-C., Chen, D.-H., Facile green synthesis of gold nanoparticles with gum arabic as a stabilizing agent and reducing agent. *Gold Bull.,* 43, 234–240, 2010.
54. Gamal-Eldeen, A.M., Moustafa, D., El-Daly, S.M., El-Hussieny, E.A., Saleh, S., Khoobchandani, M., Bacon, K.L., Gupta, S., Katti, K., Shukla, R., Katti, K.V., Photothermal therapy mediated by gum Arabic-conjugated gold nanoparticles suppresses liver preneoplastic lesions in mice. *J. Photochem. Photobiol. B: Biol.,* 163, 47–56, 2016.
55. Lodeiro, P., Achterberg, E.P., Pampín, J., Affatati, A., El-Shahawi, M.S., Silver nanoparticles coated with natural polysaccharides as models to study AgNP aggregation kinetics using UV-Visible spectrophotometry upon discharge in complex environments. *Sci. Total Environ.,* 539, 7–16, 2016.
56. Dong, C., Cai, H., Zhang, X., Cao, C., Synthesis and characterization of monodisperse copper nanoparticles using gum acacia. *Physica E,* 57, 12–20, 2014.
57. Devi, D.K., Pratap, S.V., Haritha, R., Sivudu, K.S., Radhika, P., Sreedhar, B., Gum acacia as a facile reducing, stabilizing, and templating agent for palladium nanoparticles. *J. Appl. Polym. Sci.,* 121, 1765–1773, 2011.
58. Vilian, A.T.E., Choe, S.R., Giribabu, K., Jang, S.-C., Roh, C., Huh, Y.S., Han, Y.-K., Pd nanospheres decorated reduced graphene oxide with multifunctions: Highly efficient catalytic reduction and ultrasensitive sensing of hazardous 4-nitrophenol pollutant. *J. Hazard. Mater.,* 333, 54–62, 2017.
59. Kong, H., Yang, J., Zhang, Y., Fang, Y., Nishinari, K., Phillips, G.O., Synthesis and antioxidant properties of gum arabic-stabilized selenium nanoparticles. *Int. J. Biol. Macromol.,* 65, 155–162, 2014.

60. Roque, A.C.A., Wilson, O.C., Adsorption of gum Arabic on bioceramic nanoparticles. *Mater. Sci. Eng. C*, 28, 443–447, 2008.
61. Hadavi, M., Hasannia, S., Faghihi, S., Mashayekhi, F., Zadeh, H.H., Mostofi, S.B., Novel calcified gum Arabic porous nano-composite scaffold for bone tissue regeneration. *Biochem. Biophy. Res. Comm., J. Biotechnol.,* 488, 671–678, 2017.
62. Roque, A.C.A., Bicho, A., Batalha, I.L., Cardoso, A.S., Hussain, A., Biocompatible and bioactive gum Arabic coated iron oxide magnetic nanoparticles. *J. Biotechnol.,* 144, 313–320, 2009.
63. Banerjee, S.S., Chen, D.-H., Fast removal of copper ions by gum arabic modified magnetic nano-adsorbent. *J. Hazard. Mater.,* 147, 792–799, 2007.
64. Chockalingam, A.M., Babu, H.K.R.R., Chittor, R., Tiwari, J.P., Gum arabic modified Fe_3O_4 nanoparticles cross linked with collagen for isolation of bacteria. *J. Nanotechnol.,* 8, 30–30, 2010.
65. Wilson, O.C., Blair, E., Kennedy, S., Rivera, G., Mehl, P., Surface modification of magnetic nanoparticles with oleylamine and gum Arabic. *Mater. Sci. Eng. C*, 28, 438–442, 2008.
66. Horst, M.F., Coral, D.F., Fernández van Raap, M.B., Alvarez, M., Lassalle, V., Hybrid nanomaterials based on gum Arabic and magnetite for hyperthermia treatments. *Mater. Sci. Eng. C*, 74, 443–450, 2017.
67. Bhakat, D., Barik, P., Bhattacharjee, A., Electrical conductivity behavior of Gum Arabic biopolymer-Fe_3O_4 nanocomposites. *J. Phy. Chem. Solids,* 112, 73–79, 2018.
68. Tiwari, A., Mishra, A.P., Dhakate, S.R., Khan, R., Shukla, S.K., Synthesis of electrically active biopolymer–SiO_2 nanocomposite aerogel. *Mater. Lett.,* 61, 4587–4590, 2007.
69. Chopra, M., Bernela, M., Kaur, P., Manuja, A., Kumar, B., Thakur, R., Alginate/gum acacia bipolymeric nanohydrogels—Promising carrier for Zinc oxide nanoparticles. *Int. J. Biol. Macromol.,* 72, 827–833, 2015.
70. Bajpai, S.K., Jadaun, M., Tiwari, S., Synthesis, characterization and antimicrobial applications of zinc oxide nanoparticles loaded gum acacia/poly(SA) hydrogels. *Carbohydr. Polym.,* 153, 60–65, 2016.
71. Raguvaran, R., Manuja, B.K., Chopra, M., Thakur, R., Anand, T., Kalia, A., Manuja, A., Sodium alginate and gum acacia hydrogels of ZnO nanoparticles show wound healing effect on fibroblast cells. *Int. J. Biol. Macromol.,* 96, 185–191, 2017.
72. Raguvaran, R., Manuja, A., Manuja, B.K., Riyesh, T., Singh, S., Kesavan, M., Dimri, U., Sodium alginate and gum acacia hydrogels of zinc oxide nanoparticles reduce hemolytic and oxidative stress inflicted by zinc oxide nanoparticles on mammalian cells. *Int. J. Biol. Macromol.,* 101, 967–972, 2017.
73. Venkatesham, M., Ayodhya, D., Madhusudhan, A., Santoshi Kumari, A., Veerabhadram, G., Girija Mangatayaru, K., A novel green synthesis of silver nanoparticles using gum karaya: Characterization, antimicrobial and catalytic activity studies. *J. Cluster Sci.,* 25, 409–422, 2014.

74. Padil, V.V.T., Nguyen, N.H.A., Ševců, A., Cerník, M., Fabrication, characterization, and antibacterial properties of electrospun membrane composed of gum karaya, polyvinyl alcohol, and silver nanoparticles. *J. Nanomater.,* 2015, 10, 2015.
75. Padil, V.V.T., Černík, M., Poly (vinyl alcohol)/gum karaya electrospun plasma treated membrane for the removal of nanoparticles (Au, Ag, Pt, CuO and Fe_3O_4) from aqueous solutions. *J. Hazard. Mater.,* 287, 102–110, 2015.
76. Akele, M.L., Assefa, A., Madhusudhan, A., Microwave-assisted green synthesis of silver nanoparticles by using gum acacia: Synthesis, characterization and catalytic activity studies. *Inter. J. Green Chem. Bioprocess,* 5, 21–27, 2015.
77. Pooja, D., Panyaram, S., Kulhari, H., Reddy, B., Rachamalla, S.S., Sistla, R., Natural polysaccharide functionalized gold nanoparticles as biocompatible drug delivery carrier. *Int. J. Biol. Macromol.,* 80, 48–56, 2015.
78. Gangapuram, B.R., Bandi, R., Dadigala, R., Kotu, G.M., Guttena, V., Facile green synthesis of gold nanoparticles with carboxymethyl gum karaya, selective and sensitive colorimetric detection of Copper (II) ions. *J. Cluster Sci.,* 28, 2873–2890, 2017.
79. Padil, V.V.T., Černík, M., Green synthesis of copper oxide nanoparticles using gum karaya as a biotemplate and their antibacterial application. *Inter. J. Nanomed.,* 8, 889–898, 2013.
80. Padil, V.V.T., Rouha, M., Cernik, M., Hydrocolloid-stabilized magnetite for efficient removal of radioactive phosphates. *BioMed Res. Inter.,* 2014, 10, 2014.
81. Padil, V.V.T., Waclawek, S., Senan, C., Kupcik, J., Peskova, K., Cernik, M., Somashekarappa, H.M., Gum karaya (*Sterculia urens*) stabilized zero-valent iron nanoparticles: characterization and applications for the removal of chromium and volatile organic pollutants from water. *RSC Adv.,* 7, 13997–14009, 2017.
82. Mittal, H., Maity, A., Ray, S.S., Gum karaya based hydrogel nanocomposites for the effective removal of cationic dyes from aqueous solutions. *Appl. Surf. Sci.,* 364, 917–930, 2016.
83. Pandey, S., Goswami, G.K., Nanda, K.K., Green synthesis of biopolymer–silver nanoparticle nanocomposite: An optical sensor for ammonia detection. *Int. J. Biol. Macromol.*, 51, 583–589, 2012.
84. Vanamudan, A., Sudhakar, P.P., Biopolymer capped silver nanoparticles with potential for multifaceted applications. *Int. J. Biol. Macromol.,* 86, 262–268, 2016.
85. Arfat, Y.A., Ejaz, M., Jacob, H., Ahmed, J., Deciphering the potential of guar gum/Ag-Cu nanocomposite films as an active food packaging material. *Carbohydr. Polym.,* 157, 65–71, 2017.
86. Pandey, S., Goswami, G.K., Nanda, K.K., Green synthesis of polysaccharide/gold nanoparticle nanocomposite: An efficient ammonia sensor. *Carbohydr. Polym.,* 94, 229–234, 2013.

87. Pandey, S., Mishra, S.B., Catalytic reduction of p-nitrophenol by using platinum nanoparticles stabilised by guar gum. *Carbohydr. Polym.,* 113, 525–531, 2014.
88. Rastogi, P.K., Ganesan, V., Krishnamoorthi, S., Palladium nanoparticles incorporated polymer-silica nanocomposite based electrochemical sensing platform for nitrobenzene detection. *Electrochim. Acta,* 47, 442–450, 2014.
89. Tiraferri, A., Chen, K.L., Sethi, R., Elimelech, M., Reduced aggregation and sedimentation of zero-valent iron nanoparticles in the presence of guar gum. *J. Colloid Interf. Sci.,* 324, 71–79, 2008.
90. Sardar, D., Sengupta, M., Bordoloi, A., Ahmed, M.A., Neogi, S.K., Bandyopadhyay, S., Jain, R., Gopinath, C.S., Bala, T., Multiple functionalities of Ni nanoparticles embedded in carboxymethyl guar gum polymer: catalytic activity and superparamagnetism. *Appl. Surf. Sci.,* 405, 231–239, 2017.
91. Balachandramohan, J., Anandan, S., Sivasankar, T., A simple approach for the sonochemical synthesis of Fe_3O_4-guar gum nanocomposite and its catalytic reduction of p-nitroaniline. *Ultrason. Sonochem.,* 40, 1–10, 2018.
92. Murali, R., Vidhya, P., Thanikaivelan, P., Thermoresponsive magnetic nanoparticle – Aminated guar gum hydrogel system for sustained release of doxorubicin hydrochloride. *Carbohydr. Polym.,* 110, 440–445, 2014.
93. Kumar, B., Kulanthaivel, S., Mondal, A., Mishra, S., Banerjee, B., Bhaumik, A., Banerjee, I., Giri, S., Mesoporous silica nanoparticle based enzyme responsive system for colon specific drug delivery through guar gum capping. *Colloid. Surf. B,* 150, 352–361, 2017.
94. Patra, A.S., Ghorai, S., Sarkar, D., Das, R., Sarkar, S., Pal, S., Anionically functionalized guar gum embedded with silica nanoparticles: An efficient nanocomposite adsorbent for rapid adsorptive removal of toxic cationic dyes and metal ions. *Bioresour. Technol.,* 225, 367–376, 2017.
95. Patra, A.S., Ghorai, S., Ghosh, S., Mandal, B., Pal, S., Selective removal of toxic anionic dyes using a novel nanocomposite derived from cationically modified guar gum and silica nanoparticles. *J. Hazard. Mater.,* 301, 127–136, 2016.
96. Malik, P., Srivastava, M., Verma, R., Kumar, M., Kumar, D., Singh, J., Nanostructured SnO_2 encapsulated guar-gum hybrid nanocomposites for electrocatalytic determination of hydrazine. *Mater. Sci. Eng. C*, 58, 432–441, 2016.
97. Dhiman, N., Markandeya, Singh, A., Verma, N.K., Ajaria, N., Patnaik, S., Statistical optimization and artificial neural network modeling for acridine orange dye degradation using *in-situ* synthesized polymer capped ZnO nanoparticles. *J. Colloid Interf. Sci.,* 493, 295–306, 2017.
98. Velusamy, P., Das, J., Pachaiappan, R., Vaseeharan, B., Pandian, K., Greener approach for synthesis of antibacterial silver nanoparticles using aqueous solution of neem gum (*Azadirachta indica* L.). *Ind. Crops Prod.,* 66, 103–109, 2015.

99. Khazaei, M., Khazaei, A., Nasrollahzadeh, M., Tahsili, M.R., Highly efficient reusable Pd nanoparticles based on eggshell: Green synthesis, characterization and their application in catalytic reduction of variety of organic dyes and ligand-free oxidative hydroxylation of phenylboronic acid at room temperature. *Tetrahedron,* 73, 5613–5623, 2017.
100. Velmurugan, P., Shim, J., Kim, K., Oh, B.-T., *Prunus* × *yedoensis* tree gum mediated synthesis of platinum nanoparticles with antifungal activity against phytopathogens. *Mater. Lett.,* 174, 61–65, 2016.
101. Islam, N.U., Amin, R., Shahid, M., Amin, M., Gummy gold and silver nanoparticles of apricot (*Prunus armeniaca*) confer high stability and biological activity. *Arab. J. Chem.,* https://doi.org/10.1016/j.arabjc.2016.02.017.
102. Quelemes, P.V., Araruna, F.B., de Faria, B.E., Kuckelhaus, S.A., da Silva, D.A., Mendonça, R.Z., Eiras, C., Dos S Soares, M.J., Leite, J.R., Development and antibacterial activity of cashew gum-based silver nanoparticles. *Int. J. Biol. Macromol.,* 14, 4969–81, 2013.
103. Tagad, C.K., Dugasani, S.R., Aiyer, R., Park, S., Kulkarni, A., Sabharwal, S., Green synthesis of silver nanoparticles and their application for the development of optical fiber based hydrogen peroxide sensor. *Sens. Act. B: Chem.,* 183, 144–149, 2013.
104. Syed Ahamed Hussain, I., Jaisankar, V., An eco-friendly synthesis, characterization and antibacterial applications of novel almond gum– poly(acrylamide) based hydrogel silver nanocomposite. *Polym. Test.,* 62, 154–161, 2017.
105. Vinod, V.T.P., Sashidhar, R.B., Solution and conformational properties of gum kondagogu (*Cochlospermum gossypium*) – A natural product with immense potential as a food additive. *Food Chem.,* 116, 686–692, 2009.
106. Vinod, V.T.P., Sashidhar, R.B., Sarma, V.U.M., Raju, S.S., Comparative amino acid and fatty acid compositions of edible gums kondagogu (*Cochlospermum gossypium*) and karaya (*Sterculia urens*). *Food Chem.,* 123, 57–62, 2010.
107. Vinod, V.T.P., Sashidhar, R.B., Sarma, V.U.M., Vijaya Saradhi, U.V.R., Compositional analysis and rheological properties of gum kondagogu (*Cochlospermum gossypium*): A tree gum from India. *J. Agric. Food Chem.,* 56 2199–2207, 2008.
108. Vinod, V.T.P., Sashidhar, R.B., Suresh, K.I., Rama Rao, B., Vijaya Saradhi, U.V.R., Prabhakar Rao, T., Morphological, physico-chemical and structural characterization of gum kondagogu (*Cochlospermum gossypium*): A tree gum from India. *Food Hydrocolloids,* 22, 899–915, 2008.
109. Sashidhar, R.B., Selvi, S.K., Vinod, V.T.P., Kosuri, T., Raju, D., Karuna, R., Bioprospecting of gum kondagogu (*Cochlospermum gossypium*) for bioremediation of uranium (VI) from aqueous solution and synthetic nuclear power reactor effluents. *J. Environ. Radioactiv.,* 48, 33–41, 2015.
110. Janaki, B., Sashidhar, R.B., Subchronic (90-day) toxicity study in rats fed gum kondagogu (*Cochlospermum gossypium*). *Food Chem. Toxicol.,* 38, 523–534, 2000.

111. Puskuri, J., Katukam, V., Sashidhar, R.B., Immunological evaluation of Gum kondagogu (*Cochlospermum gossypium*): A tree gum with potential applications in food and pharma industry. *Bioactive Carbohydr. Diet. Fibre,* 11, 48–52, 2017.
112. Naidu, V.G.M., Madhusudhana, K., Sashidhar, R.B., Ramakrishna, S., Khar, R.K., Ahmed, F.J., Diwan, P.V., Polyelectrolyte complexes of gum kondagogu and chitosan, as diclofenac carriers. *Carbohydr. Polym.,* 76, 464–471, 2009.
113. Padil, V.V.T., Wacławek, S., Černík, M., Green synthesis: Nanoparticles and nanofibres based on tree gums for environmental applications. *Ecol. Chem. Eng. S.,* 23, 533–557, 2016.
114. Singhal, V., Ansari, M.F., Mohanasundaram, A., Kumar, A., *Physico-chemical properties of some Indian plant gums of commercial importance*. Bulletin (Technical) No: 01/2012, lndian Institute of Natural Resins & Gums, Ranchi, 2012.
115. Thakkar, K.N., Mhatre, S.S., Parikh, R.Y., Biological synthesis of metallic nanoparticles. *Nanomed.: Nanotechnol. Biol. Med.,* 6, 257–262, 2010.
116. Rastogi, L., Arunachalam, J., Synthesis and characterization of bovine serum albumin–copper nanocomposites for antibacterial applications. *Colloid. Surf. B: Biointerf.,* 108, 134–141, 2013.
117. Kim, Y.H., Lee, D.K., Cha, H.G., Kim, C.W., Kang, Y.C., Kang, Y.S., Preparation and characterization of the antibacterial Cu nanoparticle formed on the surface of SiO_2 nanoparticles. *J. Phy. Chem. B,* 110, 24923–24928, 2006.
118. Panda, K.K., Achary, V.M.M., Krishnaveni, R., Padhi, B.K., Sarangi, S.N., Sahu, S.N., Panda, B.B., *In vitro* biosynthesis and genotoxicity bioassay of silver nanoparticles using plants. *Toxicol. in Vitro,* 25, 1097–1105, 2011.
119. de Lima, R., Seabra, A.B., Durán, N., Silver nanoparticles: A brief review of cytotoxicity and genotoxicity of chemically and biogenically synthesized nanoparticles. *J. Appl. Toxicol.,* 32, 867–879, 2012.
120. Thomas, J.W., Michael, C.W., Janice, L.M., Rachel, L.P., Jeremiah, U.E., Nanobiotechnology: Carbon nanofibres as improved neural and orthopaedic implants. *Nanotechnol.,* 15, 48–54, 2004.

4

Green Synthesis of Metal Nanoparticles and its Reaction Mechanisms

Rajasekhar Chokkareddy and Gan G. Redhi*

Electroanalytical Laboratories, Department of Chemistry, Durban University of Technology, Durban, South Africa

Abstract

In recent years, the development of efficient green chemistry procedures for synthesis of metal nanoparticles has attracted the attention of many researchers. Sustained work is being done in order to find eco-friendly methods for the manufacture of well-characterized nanoparticles. In addition, the limitation to the use of these nanoparticles is being addressed by a novel effective technique of production that will produce identical size and shape nanoparticles, as well as particles with partial or no toxicity to human health and the atmosphere. Unlike chemically synthesized nanoparticles, biosynthesized metal nanoparticles based on green chemistry propose to enforce limited exposure to the environment and are comparatively biocompatible. Green synthesis involves many promising methodologies for the synthesis of metal nanoparticles with desired properties. Plants represent the maximum explored group of living organisms for the green synthesis of metal nanoparticles and, to date, hundreds of types have been used. The nanotechnology advances have short- to long-term uses like eco-friendly pollution cleanup, effective and nontoxic drug delivery mechanisms with fewer side effects, self-cleaning window glass, expansions in information technology.

Keywords: Green synthesis, metal nanoparticles, plant extract, bioreductants, reduction, stabilization, reaction mechanisms

**Corresponding author*: redhigg@dut.ac.za; chokkareddys@gmail.com

Suvardhan Kanchi and Shakeel Ahmed (eds.) Green Metal Nanoparticles, (113–139)
© 2018 Scrivener Publishing LLC

4.1 Introduction

In recent years, the subject of nanoparticles has garnered specific attention in an extensive variety of fields. The term "*nano*" originates from the Greek word "*nano*s," meaning dwarf, and signifies a dimension on the scale of one-billionth (10^{-9}) of a meter in size [1]. In addition, an aspect of DNA is 2.5 nm in diameter; a usual virus is around 100 nm wide and a typical bacterium is around 1–3 μm wide [2, 3]. Metal nanoparticles are defined as particulate diffusions of solid units with at least one measurement at a size range of 10–1000 nm. The maximum significant feature of metal nanoparticles is their surface area to volume aspect ratio, allowing them to interact easily with other particles [4]. There have been huge advances in the field of nanotechnology in recent years, with many established methodologies to synthesize nanoparticles with specific form and size, which have been calculated for specific needs. Moreover, new applications for nanoparticles and nanomaterials are increasing dramatically; while the acceptance of effective nanomaterials has led to a much better appreciation of biology [5]. As a consequence, there is the possibility of focusing on providing new ways of acting on diseases that were antecedently strong, due to size limitations. For example, in the medical field, the production of biofunctional nanoparticles is very energetic, and has recently been the focus of consideration of different analysis teams [6]. Many physical and chemical procedures are presently used to manufacture metal nanoparticles, which allow one to attain particles with the preferred characteristics [7]. But, these synthetic procedures are generally expensive, labor-intensive, and are potentially dangerous to the environment and living organisms [8]. Therefore, there is an obvious essential need for an alternative, cost-effective, safe and environmentally sound technique for nanoparticle production [9, 10]. Through the previous studies, it has been established that many biological systems with plants and algae [11], bacteria [12], fungi [13], diatoms [14], yeast [15], and human cells [16] can convert inorganic metal ions into metal nanoparticles through the reductive abilities of the proteins and metabolites existing in these organisms. Properties of nanomaterials vary significantly from macro- and micro-size materials, which play an active role in human health and medicine, as illustrated in Table 4.1. Moreover, nanoparticles are usually classified based on their dimensionality, morphology, alignment, regularity and accumulation (Figure 4.1). The shape and morphology of nanoparticles play a significant role in their functionality and toxic effect on the environment and human beings [17]. Based on dimensionality, nanoparticles can be classified as one-, two- and three-dimensional nanoparticles. One-dimensional nanoparticles contain thin

Table 4.1 Current applications of nanotechnology in biomedicine.

Application	Role of nanotechnology	Ref.
Antimicrobial activity	Bactericidal activity Bacteriostatic activity	[19]
Cancer treatment	Detection of precancerous and malignant lesions Clinical testing for patients with solid tumours Delivery of therapeutic agents to specific molecular targets	[20]
Respiratory medicine	Aid in treatment of lung cancer, tuberculosis, and pulmonary fibrosis Vectors for gene therapy in cystic fibrosis Lung diagnostics with magnetic resonance imaging and computer tomography (CT)	[21]
Gastroenterology	Treatment of gastric and colorectal cancer Treatment of inflammatory bowel disease Diagnosis of different gastric diseases Organogenesis and transplant surgery	[22]
Reproductive medicine	For treatment of Endometriosis, Uterine fibroids, Ectopic pregnancy, Genital infections Sperm-mediated transfer of genes and biological compounds Selection of gametes and embryos Gene therapy of reproductive diseases	[23]
Dermatology	Skin cancer imaging and targeted therapeutics Immunomodulation and vaccine delivery via skin Antimicrobials and wound healing	[24]

films used in electronics and sensor devices. Two-dimensional nanoparticles comprise carbon nanotubes which have high adsorption ability and stability. Three-dimensional nanoparticles contain dendrimers, quantum dots, etc. [18]. Hence, on the basis of morphology, nanoparticles may be flat, spherical and crystalline in structure. Similarly, they can be present in single form or in the form of nanocomposites. Engineered nanomaterials are considered for a specific determination or for a specific procedure. The applications of metal nanoparticles are numerous and contain, but are not limited to, the following areas: biomedical, catalysis, biosensing, pest control, environmental remediation/reclamation, and water treatment. In general, the synthesis of metallic metal nanoparticles is attained through the reduction of the parent ion in many methods. The synthesis of metal nanoparticles differs and is reliant on the preferred product, and there are

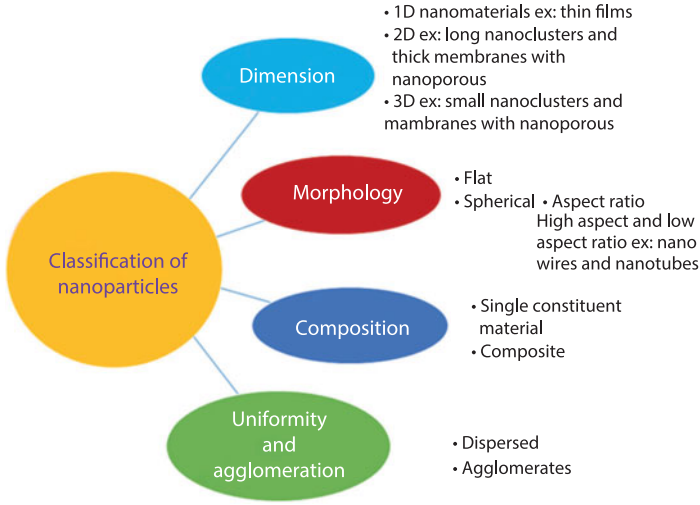

Classification of nanoparticles
Dimension
• 1D nanomaterials ex: thin films
• 2D ex: long nanoclusters and thick membranes with nanoporous
• 3D ex: small nanoclusters and mambranes with nanoporous
Morphology
• Flat
• Spherical • Aspect ratio
High aspect and low aspect ratio ex: nano wires and nanotubes
Composition
• Single constituent material
• Composite
Uniformity and agglomeration
• Dispersed
• Agglomerates

Figure 4.1 Classification of nanoparticles.

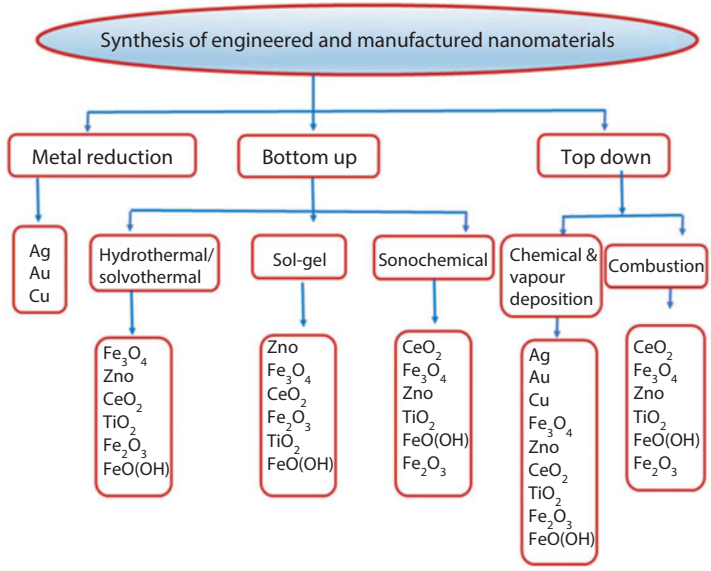


Figure 4.2 Traditional techniques for the synthesis of engineered and manufactured metal-based nanomaterials.

many procedures for their manufacture. Figure 4.2 displays a summary of techniques used for the synthesis of metal nanoparticles.

This chapter contains descriptions of traditional methods as well as green methods using plants/plant-derived ingredients for the synthesis of

metal nanoparticles from plants/plant-derived materials. We evaluate features of the most highly produced and used nanoparticles containing Ag, Au, CeO_2, Cu, ZnO, TiO_2, and Fe NPs. In addition, some of the reasons why the green synthesis methods have not been used for mass production of extensively useful metal nanoparticles will be discussed.

4.2 Green Synthesis Using Plant Extracts

For a long time, plants have shown the capability to absorb, hyperaccumulate and reduce inorganic metallic ions from the surrounding environment [25]. It is now well established that various organic components present in plant tissues are capable of acting as effective biological factories to significantly reduce eco-friendly infection, and can retrieve metals from industrialized waste. Moreover, mixtures of molecules identified in plant extracts can act as both stabilizing (capping) and reducing agents all through nanoparticle synthesis [26]. In this regard, plants (especially those which have very strong metal ion hyperaccumulating and reductive capacity) have been used for removing valuable metals from land which would be economically untenable to mine; a method known as *phytomining*. The metals composed by the plants can be improved after collecting via sintering and melting procedures. Some of the vital and abundant plant phytochemicals are shown in Figure 4.3. Plant-mediated green nanoparticle preparation can be classified into three levels: activation phase, growth phase and termination phase. The

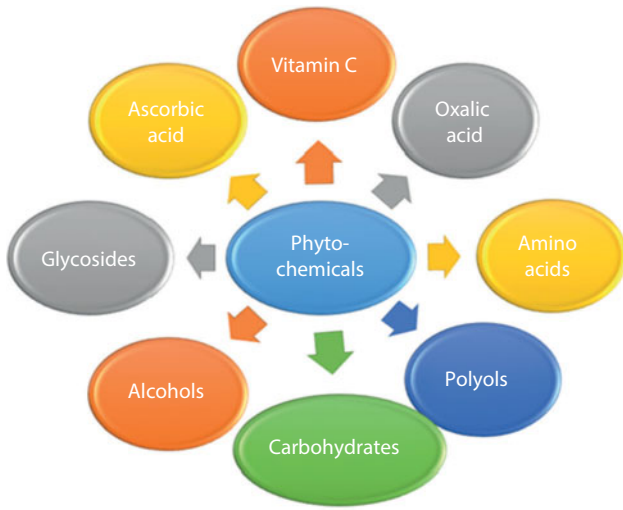


Figure 4.3 Important bioreductants found in plant extracts.

primary stage is the activation phase in which the metal ions are recovered from their salt precursors by the action of plant metabolites; biomolecules having reduction capabilities. Moreover, the metal ions are changed from their mono- or divalent oxidation states to zero-valent states and nucleation of the reduced metal atoms takes place [27].

This is monitored by the development period through which the divided metal atoms associate to form metal nanoparticles while further biological reduction of metal ions takes place. Then along with the growth development, nanoparticles join to form an assortment of morphologies such as cubes, spheres, triangles, hexagons, pentagons, rods, and wires. The growth stage results in enhanced thermodynamic permanence of nanoparticles while the stretched nucleation could result in accumulation of synthesized metal nanoparticles, altering their morphologies. The final step in green nanoparticles synthesis is the termination phase in which the nanoparticles eventually achieve their maximum activity possible and constant morphology is covered by plant metabolites. The main mechanism of green biosynthesis through plants is illustrated in Figure 4.4.

Metal nanoparticles attained from plant extracts are prepared from living plant extracts. Plant parts, such as root, leaf, latex, seed and stem, are widely being used for metal-based nanoparticle synthesis. In addition, plant extracts constitute bioactive polyphenols, alkaloids, proteins, sugars, phenolic acids, terpenoids, etc., which are made-up to have an important role in primarily reducing the metallic ions and then stabilizing them [28]. The difference in conformation and concentration of these energetic biomolecules among many plants and their resulting collaboration with

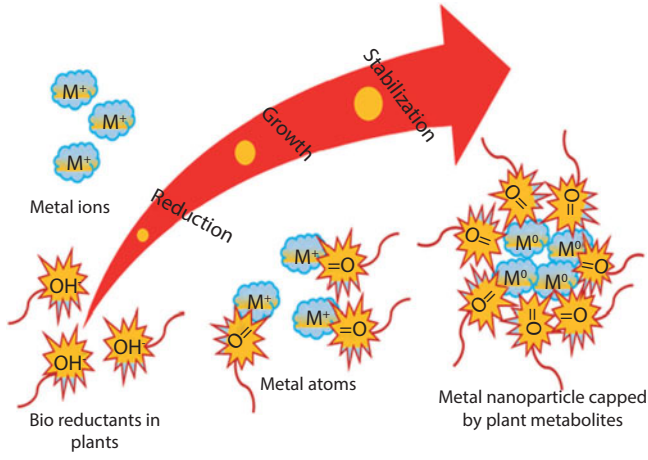


Figure 4.4 Green synthesis mechanism.

aqueous metal ions are thought to be one of the key factors associated with the variety of nanoparticle sizes and shapes fabricated [29].

Many plants vary in the concentration and composition of these biologically active components. This might partially explain the morphological range of the designated nanoparticle shapes: hexagons, triangles, pentagons, spheres, cubes, ellipsoids, nanowires, and nanorods. Furthermore, the diversity in the morphology and size of nanoparticles produced from a variety of metal ions in extracts of several plants has been defined in detail in the many papers [30, 31]. For example, Figure 4.5 displays images of the zinc, iron, silver, copper, titanium and gold nanoparticles produced

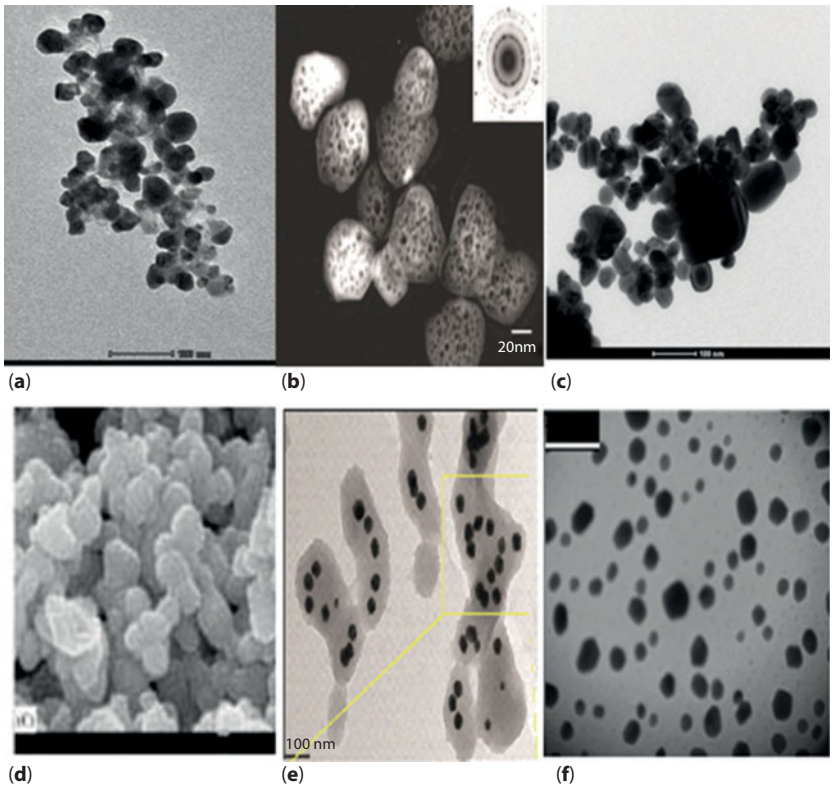


Figure 4.5 (a) TEM image of zinc oxide nanoparticles synthesized from *Lantana aculeata L.* leaf extract; (b) TEM image of iron nanoparticles synthesized by green tea leaves; (c) TEM image of silver nanoparticles synthesized using an aloe vera plant-extract solution; (d) TEM image of titanium oxide nanoparticles synthesized using *Psidium guajava* extract; (e) TEM image of the gold nanoparticles forms using *Garcinia mangostana* peel extract; and (f) TEM image of the copper nanoparticles forms using *Plantago asiatica* leaf extract.

in various plant extracts. Furthermore, many properties of the solution mixtures, such as the concentration of plant extract, metal salt concentration, reaction solution pH, etc., and other reaction conditions, like reaction time and temperature, have extensive influence on the size, quality and morphology of the synthesized nanoparticles [30]. The pH assessment of reaction mixture has a very specific influence on the preparation of metal nanoparticles. The pH modification leads to the charge conversion even in the plant metabolite, prompting its ability to chelate and degrade metal ions through the procedure, thus altering the morphology, dimensions, and yield of synthesized nanoparticles. Finally, green synthesis is cost-effective, eco-friendly, simple and relatively reproducible. Because of these attractive properties, plants have been proven to be more environmentally friendly as biologically synthesizing metallic nanoparticles, and also for decontamination applications [25]. The biosynthetic process is uncertain and offers high-yield, nano-sized materials having good crystalline configuration and appropriate properties. Therefore, a high calcination temperature is essential to remove the precursor to form crystalline materials.

4.3 Synthesis and Mechanism Action of Metal Nanoparticles

In recent years, many microbes and plant extracts have been used in the biosynthesis of metal and metal oxide nanoparticles, i.e., AgNPs, AuNPs, FeONPs, ZnONPs, CuNPs, etc. The phytosynthesis of nanoparticles and its mechanism is dependent on phytochemicals such as phenols, alkaloids, flavonoids, saponins, tannins, terpenoids, carbohydrates, etc. These phytoconstituents play an important role in their production using plant extracts. In addition, microbes-mediated synthesis is classified into extracellular and intracellular synthesis according to the location where metal nanoparticles are formed. In intracellular synthesis, metal ions are transported into the microbial cell, and the nanoparticle easily forms there in the presence of enzymes inside the cell. Furthermore, in extracellular biosynthesis, metal ions are trapped on the surface of microbial cells and reduced to nanoparticles in the presence of the many enzymes available at the surface. Karnan and Selvakumar [32] synthesized ZnONPs by using *Nephelium lappaceum* peel extract. They demonstrated from their studies that the phenolic components (ellagitannins, ellagic acid, geranin and corilagin) existing in the extract act as ligation agents, and at pH 5–7, the aromatic hydroxyl groups of ellagic acid react readily with zinc ions, which leads to the formation of a stable complex of zinc and ellagate displacement (Figure 4.6).

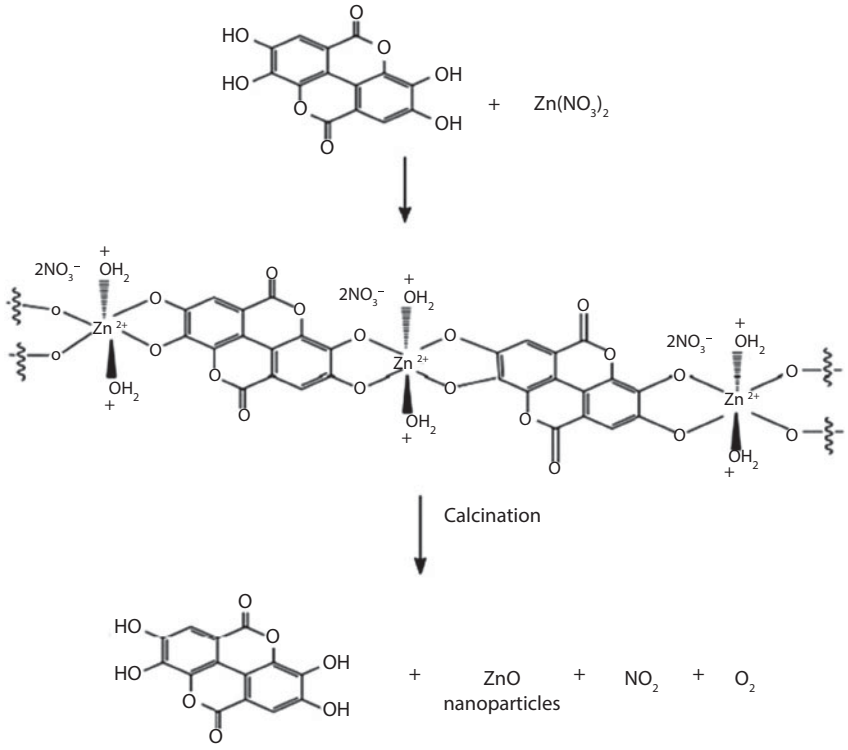


Figure 4.6 Possible mechanism of formation for ZnONPs by using peel extract of *Nephelium lappaceum*. The plant extract of *N. lappaceum* acts as ligation, and the aromatic hydroxyl group present in polyphenolic ellagic acid ligate with zinc ions to form zinc-ellagate complex (pH 5–7). Calcification of this complex at 450 °C in static air leads to the formation of ZnONPs [32].

At 450 °C, under static air atmosphere, this complex decomposed, which gave rise to ZnONPs [32]. Sharma synthesized the ZnONPs by using *Carica papaya* milk. The ZnONPs formed via this method consist of some major steps, including: (a) complex reaction, (b) aggregation of NPs and (c) oxidation of compounds existing in the extract. Essentially, bridges have been recognized among two hydroxyl groups when interaction occurred amid extract components and Zn^{2+} ions and these Zn^{2+} ions kept the molecules in proximity, and therefore formed many morphologies of ZnONPs [33]. In the ZnONPs synthesized using *Vitex negundo* leaves extract, functional active ingredients and polyphenolic compounds, such as isoorientin and luteolin, are responsible for their bioreduction. Furthermore, aromatic hydroxyl groups existing in *V. negundo* extracts isoorientin with zinc ions form the zinc-isoorientin complex with acid

medium [34]. Azizi *et al.* developed the flower extract of *Anchusa italica* for biosynthesis of ZnONPs [35]. The extract consists of essential oil rich in diisobutyl phthalate, dibutyl phthalate and hexahydrofarnesyl acetone. They described the mechanism of the formation of ZnONPs as follows: (i) complexation of biomolecules with Zn^{2+}, which, due to the presence of carbonyl group, stabilized the ZnONPs and prevented crystal growth; (ii) O-atom of the carbonyl group of the ligand donates its π electrons to Zn^{2+} with hydrolysis; (iii) thermal decomposition of source precursor $Zn(OH)_2$ (Figure 4.7).

According to Matinise *et al.* [36], various databases are included, and there is appreciable conversion of $Zn(NO_3)_2$ $6H_2O$ salt to ZnO nanoparticles by the action of different biological compounds which act as both chelating and capping agents; the proposed mechanism of biosynthesis of nano-scaled ZnO is displayed in Figure 4.8. Moreover, three chemical reactions of the solvated Zn^{2+} ions are measured with the phytochemicals of the *Moringa oleifera*; for example, with a phenolic acid, a flavonoid and vitamin-based compounds. There is improved chemical behavior of l-ascorbic acid and zinc nitrate, probable oxidation of biological compound, i.e., l-ascorbic acid to l-dehydroascorbic acid, via free radicals, followed by electrostatic attraction between free radical and cation of the precursors.

Kumar *et al.* suggest a tentative mechanism based on other works for the formation of ZnONPs induced by *Chrysopelea paradisi* peel extracts, as displayed in Figure 4.9 [37]. The flavonoids/limonoids/carotenoid molecules have free OH/COOH, which can react with $ZnSO_4$ to form zinc flavonoids/limonoids/carotenoid complex. In addition, after completion

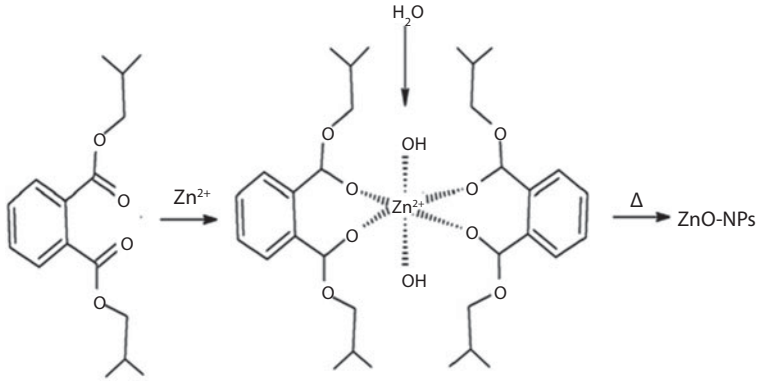


Figure 4.7 Schematic illustration showing the synthesis of ZnONPs through diisobutyl phthalate [35].

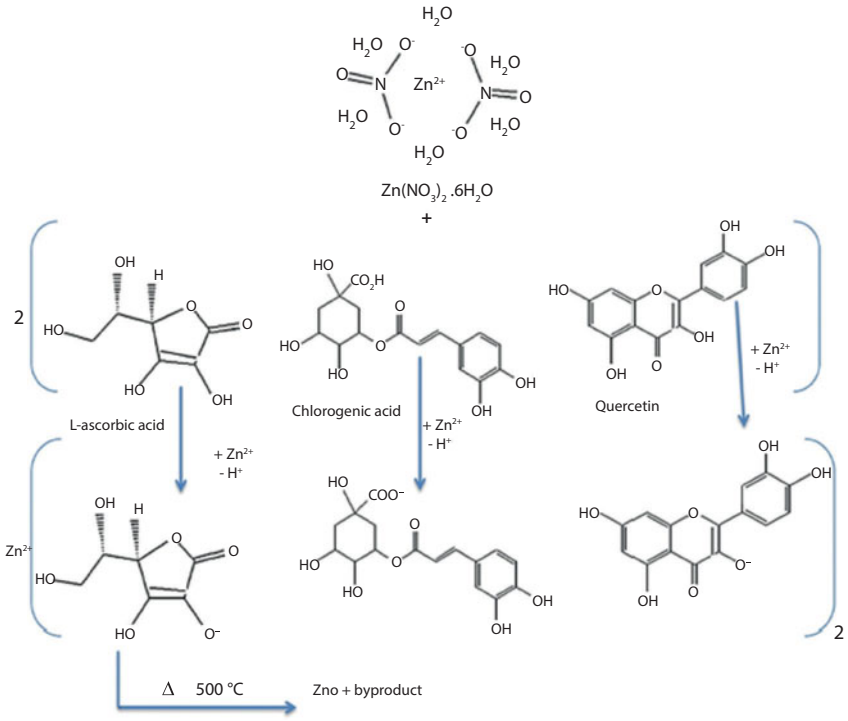


Figure 4.8 Proposed mechanism for synthesized ZnO nanoparticles through different biological compounds [36].

of the reaction, the solution was centrifuged and dried in a hot air oven. During drying, conversion of zinc flavonoids/limonoids/carotenoid complex into ZnO nanoparticles takes place.

Sutradhar and Saha reported a synthesis and mechanism of ZnONPs, and in this process zinc nitrate was used as precursor for the synthesis of ZnONPs [38]. A 1:3 ratio of zinc nitrate and tomato extract were mixed, and the solution was subjected to heating at 80 °C for 5 min. Furthermore, the same ratio of solutions was also subjected to microwave treatment at different power outputs of 180, 360 and 540 W, which formed brown to brownish-black precipitates after 5 min in the case of 360 and 540 W. The precipitates were filtered and dried in a hot air oven for 4 to 5 h. The possible mechanism of the formation of ZnONPs from tomato extract is displayed in Figure 4.10.

Gaya and Abdullah reported a photocatalytic oxidation mechanism for ZnONPs. The photocatalytic oxidation reaction originated when a photogenerated excited electron moved from the filled valence band of the

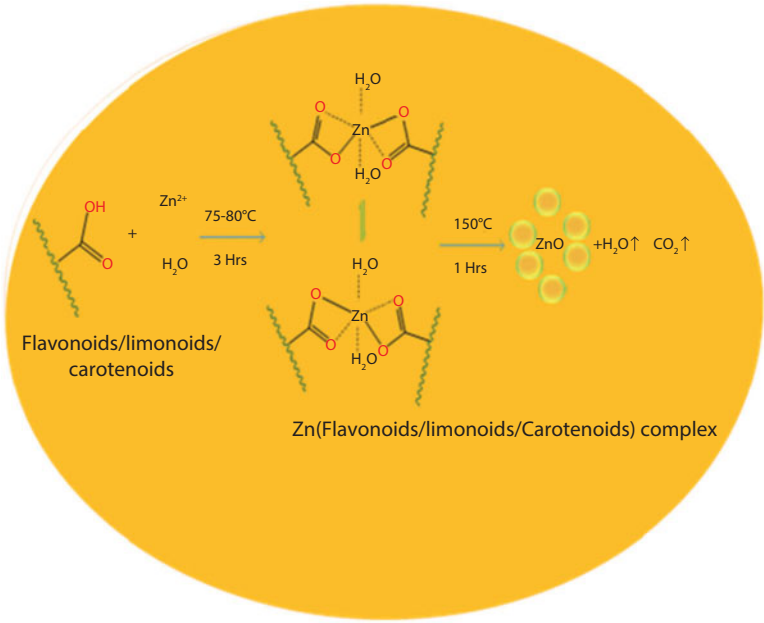


Figure 4.9 A tentative mechanism for the formation of ZnONPs [37].

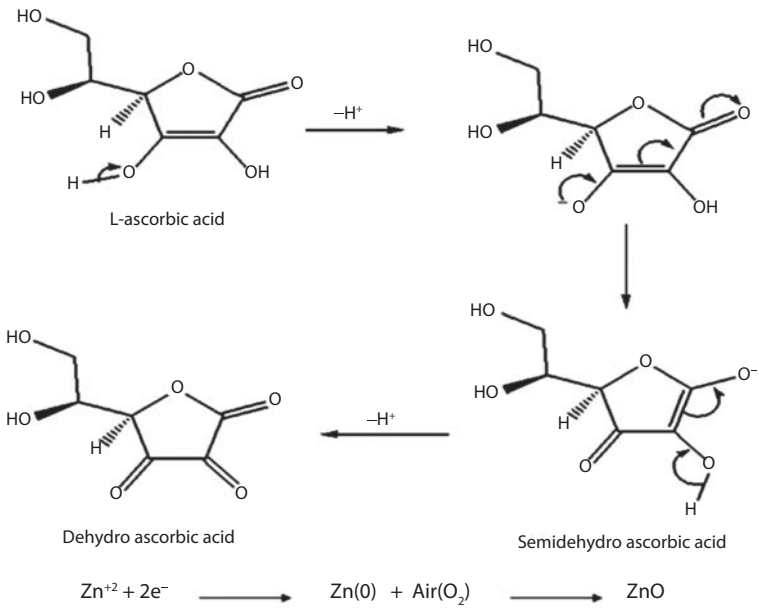


Figure 4.10 Reaction of formation of ZnONPs [38].

photocatalyst to the empty transmission band as the absorbed photon energy, hν, and equals or exceeds the band gap of the photocatalyst. In addition, the photogenerated electrons and holes have been initiated to degrade several types of organic and inorganic pollutants [39]. Moreover, it is possible to suggest that the electron-hole pair ($e^- - h^+$) is generated at the surface of ZnONPs photocatalyst through possible reactions, leading to the formation of reactive oxidative hydroxide radicals through catalytic photo-oxidation using ZnONPs as follows:

$$\text{photoexcitation: } ZnO + h\nu \rightarrow e^- + h^+ \tag{4.1}$$

$$\text{oxygen absorption: } (O_2)\ \text{ads} + e^- \rightarrow O_2^{-*} \tag{4.2}$$

$$\text{ionization of water: } H_2O \rightarrow OH^- + H^+ \tag{4.3}$$

$$\text{protonation of super oxides: } O_2^{-*} + H^+ \rightarrow HOO^* \tag{4.4}$$

$$HOO^* + e^- \rightarrow HO_2^- \tag{4.5}$$

$$HOO^- + H^+ \rightarrow H_2O_2 \tag{4.6}$$

$$H_2O_2 + e^- \rightarrow OH^- + {}^*OH \tag{4.7}$$

$$H_2O + h^+ \rightarrow H^+ + {}^*OH \tag{4.8}$$

It has been reported that the hydroxyl radical (•OH) is a great oxidant for the degradation of many organic compounds [40]. Figures 4.11 and 4.12 show the possible degradation pathway for anthracene by-products via the hydroxyl radical (•OH) [41].

Ali *et al.* reported a method for the synthesis of ZnONPs from *Bacillus subtilis* through a green approach [43]. The produced nanoparticles were used as catalyst in the synthesis of steroidal thiophenes. While the typical reaction started without a catalyst, even with a long reaction time, no improvement was observed; but, in the presence of ZnONPs, the reaction was significantly enhanced. Furthermore, the reaction yield was improved from 38% to 70% when the concentration of catalyst increased from 0.5 to 2.5 mol%. In addition, in concentrations above 2.5%, no increase in the reaction rate, and so in the reaction yield, was observed; this was possibly due to a decrease in the surface area of catalyst as a result of coagulation of ZnONPs. One-pot three-component production of steroidal thiophene

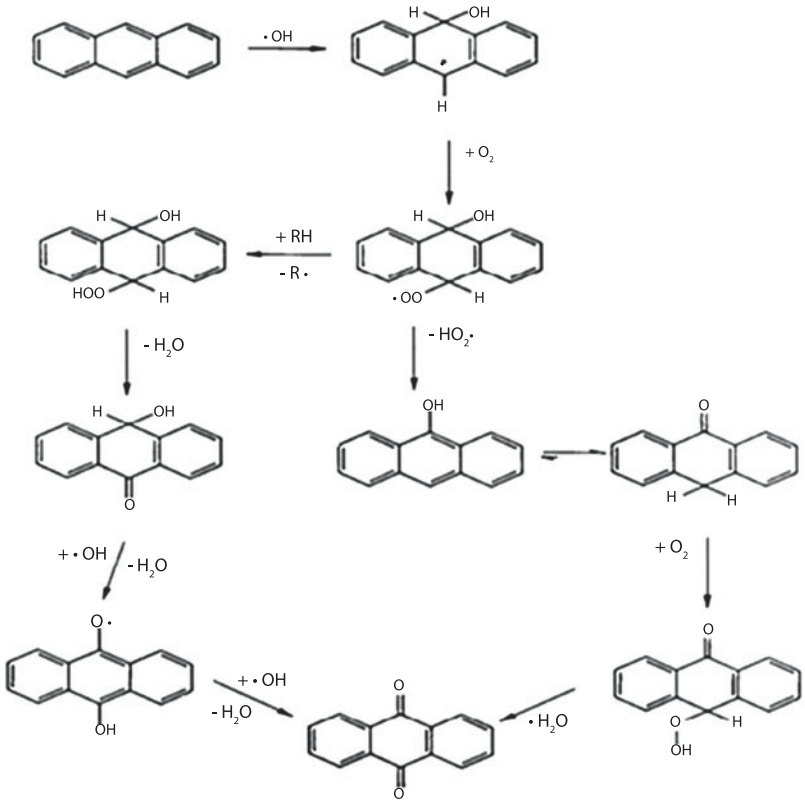


Figure 4.11 Pathway of the degradation process of anthracene to 9,10 anthraquinone [42].

products is shown in Figure 4.13. Many steroidal compounds are combined in the reaction so as to examine the scope of the reaction [43].

Khalil *et al.* [44] reported a green synthesis of ZnONPs and their antibacterial activity, the antibacterial effect of ZnO NPs against two Gram-positive bacterial strains, *Bacillus subtilis* (ATCC: 6633) and *Staphylococcus epidermidis* (ATCC: 14990), and three Gram-negative bacterial strains, *Klebsiella pneumonia* (ATCC: 4617), *Escherichia coli* (ATCC: 15224) and *Pseudomonas aeruginosa* (ATCC: 9721), using disc diffusion technique carried out at many concentrations from 2000 to 62.5 µg/ml. It was found that ZnONPs were most active against *K. pneumonia* while somewhat least effective against *P. aeruginosa*. In addition, the bactericidal effects of the ZnONPs has been well known in earlier reports; however, the improvement of the antibacterial effect with and without UV exposure to the nanoparticles has been debatable [45]. Overall, there is an increase in the

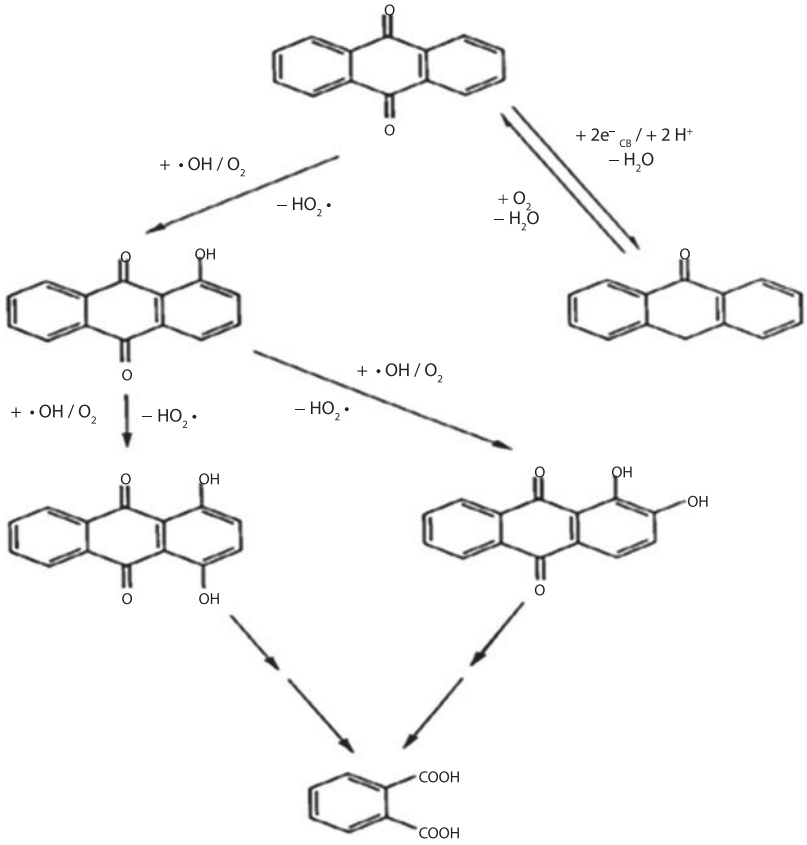


Figure 4.12 Pathway of the degradation process of 9,10 anthraquinone to phthalic acid [42].

antibacterial effect after UV exposure; however, the enrichment is not significantly high. For instance, the MIC calculated for *K. pneumonia* was found to be 7.81 μg/ml while with UV exposure the MIC was reduced to 3.90 μg/ml. Moreover, the enhanced bactericidal effect due to UV light can be attributed to the raised production of reactive oxygen species (ROS) due to UV exposure. High production of negative oxygen species due to UV has been established earlier [46]. The ROS, such as H_2O_2, can selectively penetrate the organism to initiate the genotoxic effects. Other researchers have shown the formation of novel complexes due to UV irradiation that donates to the increase in antibacterial activity [47]. In general, the antibacterial and cytotoxic effects can be displayed through various other mechanisms shown in Figure 4.14.

Figure 4.15 displays the mechanism of photocatalysis, where a series of reactions occur on the surface of ZnONPs. Photocatalysis is primarily

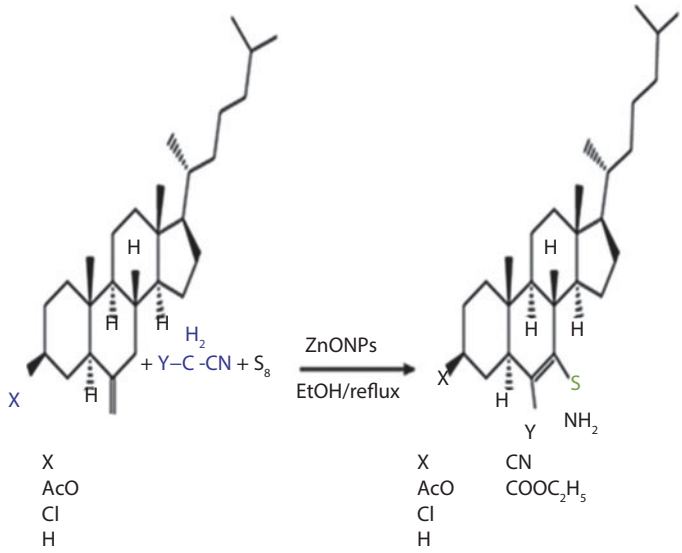


Figure 4.13 Synthesis of steroidal thiophene derivatives using biosynthesized ZnONPs [43].

introduced by placing ZnONPs suspension under natural sunlight; an electron (e-) will be stimulated from the valence band (VB) to the conduction band (CB) of the semiconductor, over-absorbing energy from UV light and producing an excited electron and a hole (see Equation 4.9).

$$ZnO + h\nu \rightarrow ZnO\ (h^+ + e^-) \tag{4.9}$$

This electron and hole pair can also be recombined with each other or initiate a sequence of photooxidation and photoreduction reactions with oxygen on the surface of the ZnO NPs semiconductor, as shown in Equations 4.10 to 4.17.

$$O_2 + e^- \rightarrow O_2^- \tag{4.10}$$

$$O_2^- + H^+ \rightarrow HO_2^{\cdot} \tag{4.11}$$

$$HO_2^{\cdot} + HO_2^{\cdot} \rightarrow H_2O_2 + O_2 \tag{4.12}$$

$$O_2^{\cdot -} + HO_2^{\cdot} \rightarrow O_2 + HO_2^{\cdot} \tag{4.13}$$

$$HO_2^{\cdot} + H^+ \rightarrow H_2O_2 \tag{4.14}$$

$$H_2O_2 + h\nu \rightarrow 2HO^{\cdot} \tag{4.15}$$

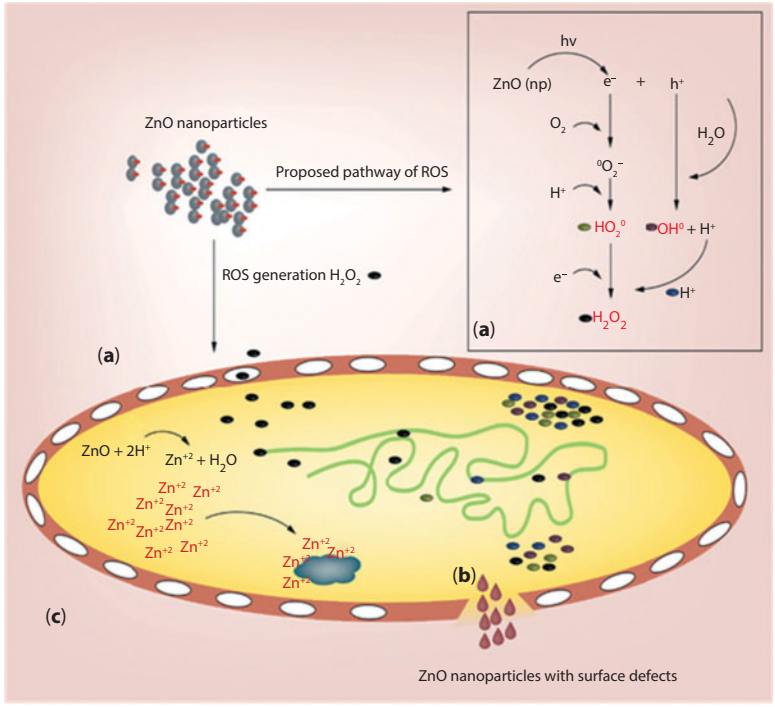


Figure 4.14 Proposed mechanisms demonstrating cytotoxicity as indicated by numerous earlier studies. (a) ROS: Proposed pathway of generation; ROS generation is considered as a primary cause of cytotoxicity to cells. Negatively charged ionic species do not have the tendency to enter inside the cell; however, when they are converted to hydrogen peroxide they can easily penetrate inside the cell, subsequently interfering with the cellular machinery, leading to cidal effects. (b) Surface defects: Surface defects in ZnO nanoparticles have the ability to rupture the living cell membranes and get inside the organism, where they interact with the cellular machinery as well as facilitate the release of additional ionic species that produce genotoxic and oxidative stress. (c) Zn^{+2} dissolution: Following the internalization of the ZnONP, cytosolic dissolution in Zn^{+2} occurs. In eukaryotes the process of internalization and dissolution occurs in endosomes. After the release of Zn^{+2}, these ions can interact with the mitochondrial membrane, leading to mitochondrial dysfunction. Note: For further details on the cytotoxicity mechanism, we recommend the work presented in [44, 47].

$$H_2O_2 + O_2^{\cdot -} \rightarrow OH^{\cdot} + OH^{-} + O_2 \tag{4.16}$$

$$H_2O_2 + e^{-} \rightarrow HO^{\cdot} + OH^{-} \tag{4.17}$$

In the solution, the produced hole oxidizes the hydroxide ion (-OH) and water (H_2O), developing the hydroxyl radical, as shown in Equations 4.18

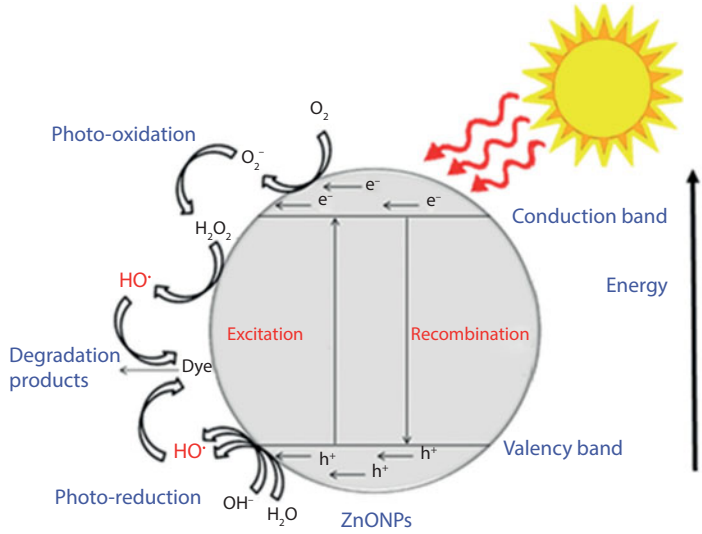


Figure 4.15 Schematic illustration of photocatalysis degradation mechanism in the presence of ZnONPs [48].

and 4.19. In addition, these reactions resulted in the formation of an identical powerful oxidizing agent, hydroxyl radical (HO), which are the types responsible for the complete mineralization of dye molecules (OM) into end products carbon dioxide (CO_2) and water (H_2O), if time permitted (Eq. 4.20).

$$H^+ + OH^- \rightarrow HO \cdot \quad (4.18)$$

$$H^+ + H_2O \rightarrow HO \cdot + H^+ \quad (4.19)$$

$$HO \cdot + OM \rightarrow \text{Degradation intermediates} \rightarrow CO_2 + H_2O + \text{Salt} \quad (4.20)$$

A highly effective microorganism, *Stenotrophomonas maltophilia,* has been described for synthesis of gold nanoparticles of desired size and shape. The results confirmed that a specific NADPH-dependent enzyme existing in the isolated strain reduces Au^{3+} to Au^0 through an electron traveling mechanism. A schematic representation of the potential mechanism of gold nanoparticles synthesis by *Stenotrophomonas maltophilia* through the enzymatic reduction proposed is displayed in Figure 4.16, where a specific reductase enzyme present in microorganisms could be induced by the definite ions and reduced metal ions to metallic nanoparticles. In addition, biosynthesis of 10 nm size gold nanoparticles using leaf extract of *Zingiber officinale* was also reported in the literature [50]. Furthermore,

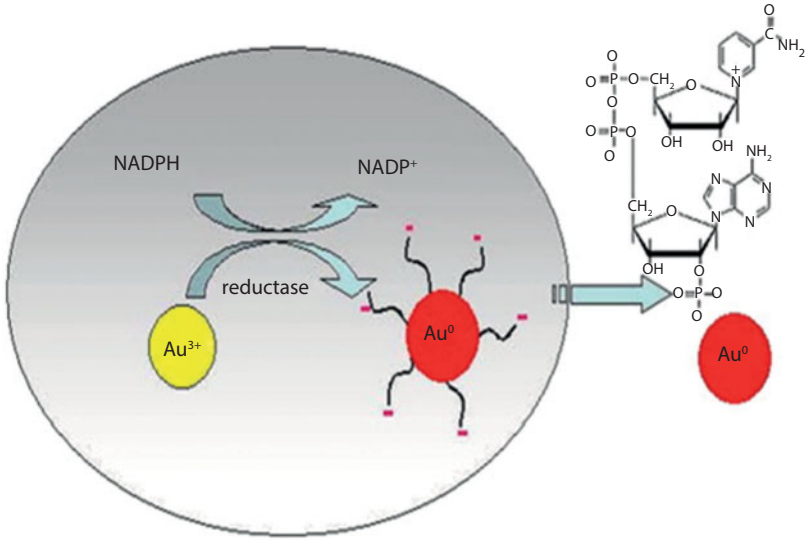


Figure 4.16 Proposed synthesis mechanism of gold nanoparticles by *Stenotrophomonas maltophilia* through enzymatic reduction [51].

the triangular and spherically shaped metal nanoparticle with an average size of 50 nm and 100 nm are produced by using leaf extract of *Nepenthes khasiana*. At ambient temperature and pressure, the rate of reduction of metal ions using plant agents is initiated at a much faster rate. The biosynthesis of gold nanoparticles assisted by *Escherichia coli* DH5a for application on the direct electrochemistry of hemoglobin (Hb) is reported. The nanoparticles bound to the surface of the bacteria and this complex might be used for application in realizing the direct electrochemistry of Hb [51].

The flavanone and terpenoid components of the leaf broth of neem extract are thought to be the surface active molecules stabilizing the nanoparticles. The formation of pure metallic and bimetallic nanoparticles by reduction of the metal ions may be enabled by reducing sugars and/or terpenoids present in Neem leaf broth [53]. Alfalfa plants were used for synthesis of gold particles with an estimated size of 4 nm and icosahedral structure. In addition, the gold particles have a face-centered cubic twinned structure where the particle size ranges between 6 and 10 nm. Anisotropy gold and quasi-spherical silver nanoparticles were produced by biogenic synthesis in which apiin was used as a steadying as well as reducing agent. As shown in Figure 4.17, the hydroxyl group present in apiin reduced the Au^{3+}/Ag^{+} ions where hydroxyl groups are oxidized to carbonyl groups.

Shiying *et al.*[55] reported an electron shuttling mechanism [56] related to NADH-dependent reductase. The first step includes the reduction of

Au^{3+} from $AuCl_4^-$ ionic system to Au^+, and it is reduced again to gold nanoparticles, as shown in Equations 4.21 and 4.22.

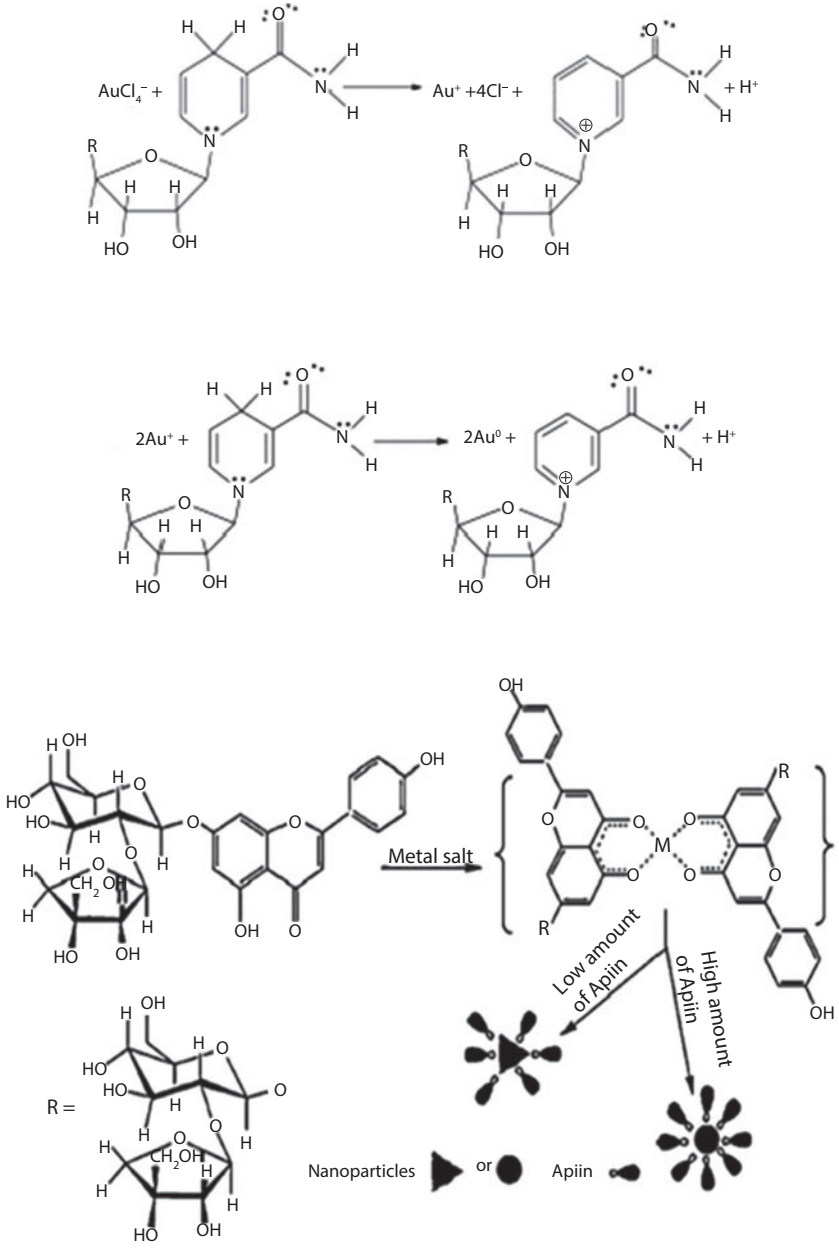


Figure 4.17 Schematic illustration of the formation of apiin-stabilized gold nanoparticles [53].

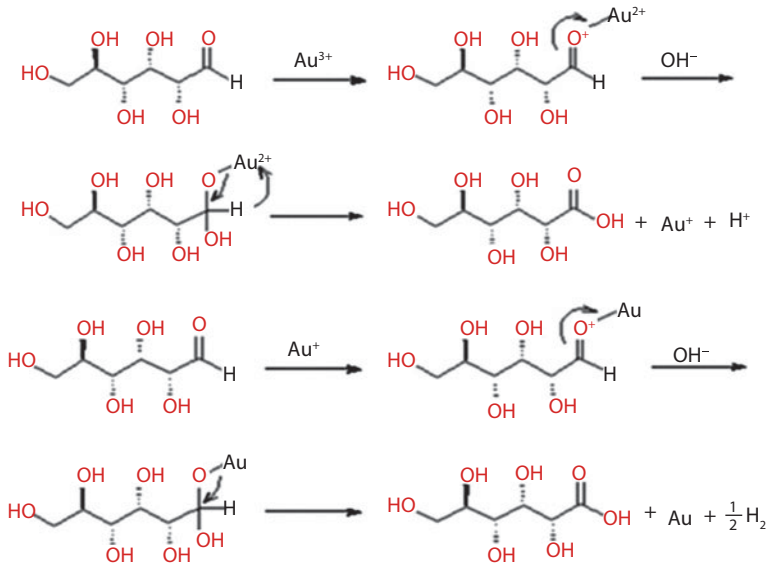


Figure 4.18 Schematic illustration of the proposed Au ion reduction reactions via potato extract [55].

In Figure 4.18 different steps of the redox reactions of gold ions with d-glucose are schematically shown. Moreover, upon addition of Au solution in the reaction mixture, first the Au^{3+} ions get close to the oxygen of the aldehyde groups because of their free electrons, and then get reduced to Au^{2+} ions. The process is followed by nucleophilic substitution, where a hydroxyl radical (OH^-) gets attached to the sixth carbon of the glucose chain. In addition, due to the instability of this carbon in the presence of OH^- ion, the hydrogen atom gets unlinked from the carbon, and transfers its electron to Au^{2+} ion, reducing it to Au^{1+}. The oxygen of the carbonyl group recovers its double bond.

Thus, D-glucose is converted to gluconic acid, as illustrated in Equation 4.23. Furthermore, reduction of Au^{1+} to atomic gold (Au^0) is also carried out through a similar reaction (illustrated in Equation 4.24). Castillo-López and Pal reported the use of potato extract as a stabilizing agent for gold nanoparticles. In their method, the potato extract solution used for the reduction of gold ions containing d-glucose units also limited short-chained amylose and amylopectin. Amylose and amylopectin chains have a mutual d-glucose unit in one of their ends where no anomeric carbon is involved to form glycosidic bond, and this end is known as the reducing end.

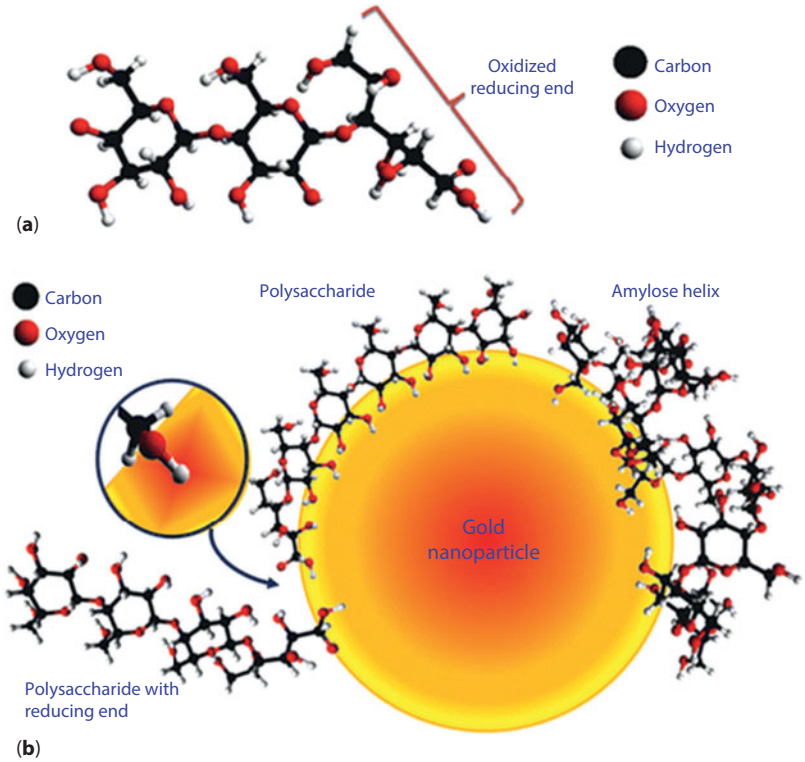


Figure 4.19 (a) A polysaccharide chain with oxidized reducing end, and (b) a schematic illustration of polysaccharide adsorption process at the surface of gold nanoparticle bonded through (OH^-) groups [55].

Furthermore, the reducing end gets oxidized in the presence of Au ions, transforming the terminal D-glucose unit to gluconic acid, as shown in Figure 4.18 (Eq. 4.23) and Figure 4.19a. The negative charge on the oxygen of the hydroxyl group of gluconic acid interacts with the surface positive charge of AuNPs via electrostatic interaction, producing their bonding. On the other hand, hydroxyl groups of the amylopectin chains, especially the external hydroxyl groups of amylose helical chains, get bonded with the surface of Au nanoparticles through electrostatic interaction. Based on the capping mechanisms, these are responsible for the stabilization of AuNPs, as shown in Figure 4.19.

4.4 Conclusions

Green synthesis of metal nanoparticles using plant by-products has been intensively studied over the last two decades. Moreover, the plant

metabolites have given rise to inventions for the production of metallic nanoparticles in an eco-friendly manner. The outlook for the future is the eco-friendly preparation of metal nanoparticles using plant crude extracts and disinfected metabolites as novel substrates for large-scale production. However, to compete cost-effectively with metal nanoparticles attained through physical and chemical methods, it is essential to scale these approaches of nanoparticle production. In addition, metal nanoparticles of controlled morphology and size are also produced in massive amounts. Their stability and reduction potential are qualified by bioactive molecules existing in these biological resources. Among these bioreductants, plant extracts are more useful than other biological resources. Hence, from this prospectve, using plant sources for metal nanoparticles synthesis can open new horizons in the future. Then, a complete study is needed to explore the exact mechanism and metabolites involved in the reduction process. Once explored, it will transform the synthesis of metal nanoparticles at both the laboratory and commercial scale.

References

1. Narayanan, K.B., Sakthivel, N., Biological synthesis of metal nanoparticles by microbes. *Adv. Colloid Interface Sci.*, 156, 1–13, 2010.
2. Wagner, E., Plank, C., Zatloukal, K., Cotten, M., Birnstiel, M.L., Influenza virus hemagglutinin HA-2 N-terminal fusogenic peptides augment gene transfer by transferrin-polylysine-DNA complexes: Toward a synthetic virus-like gene-transfer vehicle. *Proc.National Acad. Sci.*, 89, 7934–7938, 1992.
3. Katz, A., Alimova, A., Xu, M., Rudolph, E., Shah, M.K., Savage, H.E., Rosen, R.B., McCormick, S.A., Alfano, R.R., Bacteria size determination by elastic light scattering. *IEEE J. Sel. Top. Quantum Electron.*, 9, 277–287, 2003.
4. Thakkar, K.N., Mhatre, S.S., Parikh, R.Y., Biological synthesis of metallic nanoparticles. *Nanomed: NBM*, 6, 257–262, 2010.
5. Taylor, E., Webster, T.J., Reducing infections through nanotechnology and nanoparticles. *Int. J. Nanomed.*, 6, 1463, 2011.
6. Darroudi, M., Hakimi, M., Goodarzi, E., Oskuee, R.K., Superparamagnetic iron oxide nanoparticles (SPIONs): Green preparation, characterization and their cytotoxicity effects. *Ceram. Int.*, 40, 14641–14645, 2014.
7. Tsuji, M., Miyamae, N., Lim, S., Kimura, K., Zhang, X., Hikino, S., Nishio, M., Crystal structures and growth mechanisms of Au@ Ag core–shell nanoparticles prepared by the microwave–polyol method. *Cryst. Growth Des.*, 6, 1801–1807, 2006.
8. Gan, P.P., Li, S.F.Y., Potential of plant as a biological factory to synthesize gold and silver nanoparticles and their applications. *Rev. Environ. Sci. Bio.*, 11, 169–206, 2012.

9. Sharma, H.S., Ali, S.F., Hussain, S.M., Schlager, J.J., Sharma, A., Influence of engineered nanoparticles from metals on the blood-brain barrier permeability, cerebral blood flow, brain edema and neurotoxicity. An experimental study in the rat and mice using biochemical and morphological approaches. *J. Nano Sci. Nanotech.* 9, 5055–5072, 2009.
10. Porel, S., Singh, S., Harsha, S.S., Rao, D.N., Radhakrishnan, T., Nanoparticle-embedded polymer: *In situ* synthesis, free-standing films with highly monodisperse silver nanoparticles and optical limiting. *Chem. Mater.* 17, 9–12, 2005.
11. Govindaraju, K., Basha, S.K., Kumar, V.G., Singaravelu, G., Silver, gold and bimetallic nanoparticles production using single-cell protein (*Spirulina platensis*) Geitler. *J. Mater. Sci.* 43, 5115–5122, 2008.
12. Lengke, M.F., Fleet, M.E., Southam, G., Biosynthesis of silver nanoparticles by filamentous cyanobacteria from a silver (I) nitrate complex. *Langmuir.* 23, 2694–2699, 2007.
13. Rautaray, D., Ahmad, A., Sastry, M., Biosynthesis of $CaCO_3$ crystals of complex morphology using a fungus and an actinomycete. *J. Amer. Chem. Soc.* 125, 14656–14657, 2003.
14. Scarano, G., Morelli, E., Characterization of cadmium- and lead-phytochelatin complexes formed in a marine microalga in response to metal exposure. *Biometals*, 15, 145–151, 2002.
15. Kowshik, M., Deshmukh, N., Vogel, W., Urban, J., Kulkarni, S.K., Paknikar, K., Microbial synthesis of semiconductor CdS nanoparticles, their characterization, and their use in the fabrication of an ideal diode. *Biotechnol. Bioeng.* 78, 583–588, 2002.
16. Anshup, Venkataraman, J.S., Subramaniam, C., Kumar, R.R., Priya, S., Kumar, T.S., Omkumar, R., John, A., Pradeep, T., Growth of gold nanoparticles in human cells. *Langmuir*, 21, 11562–11567, 2005.
17. Buzea, C., Pacheco, I.I., Robbie, K., Nanomaterials and nanoparticles: Sources and toxicity. *Biointerphases*, 2, 17–71, 2007.
18. Pal, S.L., Jana, U., Manna, P.K., Mohanta, G.P., Manavalan, R., Nanoparticle: An overview of preparation and characterization. *J. Appl. Pharm. Sci.*, 01, 228–234, 2011.
19. Seil, J.T., Webster, T.J., Antimicrobial applications of nanotechnology: Methods and literature. *Int. J. Nanomedicine*, 7, 2767, 2012.
20. Sanna, V., Pala, N., Sechi, M., Targeted therapy using nanotechnology: focus on cancer. *Int. J. Nanomedicine*, 9, 467, 2014.
21. Omlor, A.J., Nguyen, J., Bals, R., Dinh, Q.T., Nanotechnology in respiratory medicine. *Resp. Res.*, 16, 64, 2015.
22. Brakmane, G., Winslet, M., Seifalian, A., Systematic review: The applications of nanotechnology in gastroenterology. *Aliment. Pharmacol. Ther.*, 36, 213–221, 2012.
23. Barkalina, N., Charalambous, C., Jones, C., Coward, K., Nanotechnology in reproductive medicine: Emerging applications of nanomaterials. *Nanomedicine: NBM*, 10, e921-e938, 2014.

24. DeLouise, L.A., Applications of nanotechnology in dermatology. *J. Invest. Dermatol.*, 132, 964–975, 2012.
25. Kale, A., Bao, Y., Zhou, Z., Prevelige, P.E., Gupta, A., Directed self-assembly of CdS quantum dots on bacteriophage P22 coat protein templates. *Nanotechnology*, 24, 045603, 2013.
26. Song, J.Y., Kim, B.S., Rapid biological synthesis of silver nanoparticles using plant leaf extracts. *Bioprocess Biosyst. Eng.*, 32, 79, 2009.
27. Malik, P., Shankar, R., Malik, V., Sharma, N., Mukherjee, T.K., Green chemistry based benign routes for nanoparticle synthesis. *J. Nano.,* 302429, 2014.
28. Marshall, A.T., Haverkamp, R.G., Davies, C.E., Parsons, J.G., Gardea-Torresdey, J.L., van Agterveld, D., Accumulation of gold nanoparticles in *Brassic juncea*. *Int. J. Phyt.*, 9, 197–206, 2007.
29. Njagi, E.C., Huang, H., Stafford, L., Genuino, H., Galindo, H.M., Collins, J.B., Hoag, G.E., Suib, S.L., Biosynthesis of iron and silver nanoparticles at room temperature using aqueous sorghum bran extracts. *Langmuir*, 27, 264–271, 2010.
30. Raveendran, P., Fu, J., Wallen, S.L., Completely "green" synthesis and stabilization of metal nanoparticles. *J. Amer. Chem. Soc.*, 125, 13940–13941, 2003.
31. Dimkpa, C.O., McLean, J.E., Martineau, N., Britt, D.W., Haverkamp, R., Anderson, A.J., Silver nanoparticles disrupt wheat (*Triticum aestivum* L.) growth in a sand matrix. *Environ. Sci. Tech.*, 47, 1082–1090, 2013.
32. Karnan, T., Selvakumar, S.A.S., Biosynthesis of ZnO nanoparticles using rambutan (*Nephelium lappaceum* L.) peel extract and their photocatalytic activity on methyl orange dye. *J. Mol. Struct.*, 1125, 358–365, 2016.
33. Sharma, S., ZnO nano-flowers from *Carica papaya* milk: Degradation of Alizarin Red-S dye and antibacterial activity against *Pseudomonas aeruginosa* and *Staphylococcus aureus*. *Optik*, 127, 6498–6512, 2016.
34. Ambika, S., Sundrarajan, M., Antibacterial behaviour of *Vitex negundo* extract assisted ZnO nanoparticles against pathogenic bacteria. *J. Photochem. Photobiol.*, 146, 52–57, 2015.
35. Azizi, S., Mohamad, R., Bahadoran, A., Bayat, S., Rahim, R.A., Ariff, A., Saad, W.Z., Effect of annealing temperature on antimicrobial and structural properties of bio-synthesized zinc oxide nanoparticles using flower extract of *Anchusa italica*. *J. Photochem. Photobiol.*, 161, 441–449, 2016.
36. Matinise, N., Fuku, X., Kaviyarasu, K., Mayedwa, N., Maaza, M., ZnO nanoparticles via *Moringa oleifera* green synthesis: Physical properties and mechanism of formation. *Appl. Surf. Sci.* 406, 339–347, 2017.
37. Kumar, B., Smita, K., Cumbal, L., Debut, A., Green approach for fabrication and applications of zinc oxide nanoparticles. *Bioinorg. Chem. Appl.*, 2014, 523869, 2014.
38. Sutradhar, P., Saha, M., Green synthesis of zinc oxide nanoparticles using tomato (*Lycopersicon esculentum*) extract and its photovoltaic application. *J. Exp. Nanosci.*, 11, 314–327, 2016.

39. Gaya, U.I., Abdullah, A.H., Heterogeneous photocatalytic degradation of organic contaminants over titanium dioxide: A review of fundamentals, progress and problems. *J. Photochem. Photobiol. C*, 9, 1–12, 2008.
40. Peiró, A.M., Ayllón, J.A., Peral, J., Doménech, X., TiO_2-photocatalyzed degradation of phenol and ortho-substituted phenolic compounds. *Appl. Catal. B*, 30, 359–373, 2001.
41. Theurich, J., Bahnemann, D., Vogel, R., Ehamed, F., Alhakimi, G., Rajab, I., Photocatalytic degradation of naphthalene and anthracene: GC-MS analysis of the degradation pathway. *Res. Chem. Intermed.*, 23, 247–274, 1997.
42. Hassan, S.S., El Azab, W.I., Ali, H.R., Mansour, M.S., Green synthesis and characterization of ZnO nanoparticles for photocatalytic degradation of anthracene. *Nanosci. Nanotech.*, 6, 045012, 2015.
43. Ali, A.A., Asif, M.A., Mashrai, A.M., Khanam, H.K., Green synthesis of ZnO nanoparticles using *Bacillus subtilis* and their catalytic performance in the one-pot synthesis of steroidal thiophenes. *Eur. Chem. Bull.*, 3, 939–945, 2014.
44. Khalil, A.T., Ovais, M., Ullah, I., Ali, M., Shinwari, Z.K., Khamlich S., Maaza, M., Sageretia thea (Osbeck.) mediated synthesis of zinc oxide nanoparticles and its biological applications. *Nanomedicine* (Lond.), 1–23, 2017.
45. Sirelkhatim, A., Mahmud, S., Seeni, A., Kaus, N.H.M., Ann, L.C., Bakhori, S.K.M., Hasan, H., Mohamad, D., Review on zinc oxide nanoparticles: Antibacterial activity and toxicity mechanism. *Nano-Micro Lett.*, 7, 219–242, 2015.
46. Zhang, H., Chen, B., Jiang, H., Wang, C., Wang, H., Wang, X., A strategy for ZnO nanorod mediated multi-mode cancer treatment. *Biomaterials*, 32, 1906–1914, 2011.
47. Zhou, G., Li, Y., Xiao, W., Zhang, L., Zuo, Y., Xue, J., Jansen, J.A., Synthesis, characterization, and antibacterial activities of a novel nanohydroxyapatite/zinc oxide complex. *J. Biomed. Mater. Res. A*, 85, 929–937, 2008.
48. Kao, Y.-Y., Chen, Y.-C., Cheng, T.-J., Chiung, Y.-M., Liu, P.-S., Zinc oxide nanoparticles interfere with zinc ion homeostasis to cause cytotoxicity. *Toxicol. Sci.*, 125, 462–472, 2011.
49. Giwa, A., Nkeonye, P.O., Bello, K.A., Kolawole, K.A., Photocatalytic decolourization and degradation of CI Basic Blue 41 using TiO_2 nanoparticles. *J. Environ. Protec.*, 3, 1063, 2012.
50. Singh, C., Sharma, V., Naik, P.K., Khandelwal, V., Singh, H., A green biogenic approach for synthesis of gold and silver nanoparticles using *Zingiber officinale*. *Dig. J. Nanomater. Biostruct.*, 6, 535–542, 2011.
51. Sharma, N., Pinnaka, A.K., Raje, M., Ashish, F., Bhattacharyya, M.S., Choudhury, A.R., Exploitation of marine bacteria for production of gold nanoparticles. *Microb. Cell Fact.*, 11, 86, 2012.
52. Nangia, Y., Wangoo, N., Goyal, N., Shekhawat, G., Suri, C.R., A novel bacterial isolate *Stenotrophomonas maltophilia* as living factory for synthesis of gold nanoparticles. *Microb. Cell Fact.*, 8, 39, 2009.

53. Shankar, S.S., Rai, A., Ahmad, A., Sastry, M., Rapid synthesis of Au, Ag, and bimetallic Au core–Ag shell nanoparticles using Neem (*Azadirachta indica*) leaf broth. *J. Colloid Iinterface Sci.*, 275, 496–502, 2004.
54. Kasthuri, J., Veerapandian, S., Rajendiran, N., Biological synthesis of silver and gold nanoparticles using apiin as reducing agent. *Colloids Surf. B*, 68, 55–60, 2009.
55. Shiying, H., Guo, Z., Zhang, Y., Zhang, S., Wang, J., Gu. N., Biosynthesis of gold nanoparticles using the bacteria Rhodopseudomonas capsulate, *Mater. Lett*. 61, 3984-3987, 2007.
56. Gardea-Torresdey, J.L., Becker-Hapak, M.K., Hosea, J.M., Darnall, D.W., Effect of chemical modification of algal carboxyl groups on metal ion binding. *Environ. Sci. Technol.*, 24, 1372–1378, 1990.
57. Castillo-López, D.N., Pal, U., Green synthesis of Au nanoparticles using potato extract: stability and growth mechanism. *J. Nano. Res.*, 16, 2571, 2014.

5

Toxicity of Metal/Metal Oxide Nanoparticles and Their Future Prospects

Subramanyam Deepika[1], Rajendran Harish Kumar[1], Chinnadurai Immanuel Selvaraj[1] and Selvaraj Mohana Roopan[2]*

[1]Department of Biotechnology, School of Biosciences and Technology, Vellore Institute of Technology, Tamil Nadu, India
[2]Chemistry of Heterocycles & Natural Product Research Laboratory, Department of Chemistry, School of Advanced Sciences, Vellore Institute of Technology, Tamil Nadu, India

Abstract

Usage of nanoparticles holds great potential in many technical as well as medical applications. Metal and metal oxide nanoparticles are often used as catalysts in industries for improving the functional properties of the product. Various fields, like medical imaging and biology, environmental remediation, sensors and biomedicine, are benefitting from the recent advanced nanotechnology. Conversely, these developments are connected with unwanted risks and uncertainties. The same properties which can be beneficial from a technical point of view can be harmful in another aspect. Controversies still remain with respect to the toxic effects and mechanisms of these nanoparticles. In order to avoid such unnecessary risks and to facilitate the use of nanoparticles effectively, there is a need for ample toxicological research as well as risk assessment of the nanoparticles. The relation between the properties of material and its toxicity seems to be complex and difficult to understand, which can be partly due to the incomplete characterization of the nanomaterial and experimental artifacts in the nanomaterial's characterization and its interaction with living organisms. Nanotoxicology, which studies nanoparticle interaction with the biological system and measures the level of toxicity related to human health, is the focus of many researchers. In this chapter, we focus on the hazards or toxicity of the nanoparticles and more specifically the

**Corresponding author*: mohanaroopan.s@gmail.com; mohanaroopan.s@vit.ac.in

Suvardhan Kanchi and Shakeel Ahmed (eds.) Green Metal Nanoparticles, (141–164)
© 2018 Scrivener Publishing LLC

metal- and metal oxide-containing nanoparticles. The mechanism underlying the toxicity of the nanomaterials is discussed herein. This includes the generation of relative oxygen species resulting in the subsequent formation of oxidative stress, leading to DNA damage, apoptosis and initiation of cancer. In addition, critical factors, like size, shape, particle dissolution, UV light activation, aggregation, etc., and future prospects of nanoparticles are also discussed.

Keywords: Nanoparticles, nanotoxicology, toxicity, metal and metal oxide nanoparticles

5.1 Introduction

At present, the nano industry is considered one of the rapidly developing industries and it might be the future industrial revolution. The manufactured nanoparticles are sometimes in unbound or in aggregate or agglomerate state. Most particles in these states are in the number size distribution, but in a few cases the external dimensions of particles are within 1–100 nm size range, which is considered safe for the environment and human health and competitive with nanoparticles. Apart from that, it is well known that being nano size is advantageous for higher reactivity with enhanced and efficient properties, due to the increase in relative surface area [1]. Nanotechnology is the construction of novel devices, materials and diverse technological systems with several prospective applications at the molecular and atomic level. Because of their captivating physicochemical properties, they are applied in chemical, biological and other industrial fields. Nanomaterials and nanodevices are being created purposely or deliberately, engineered by various methods and exposed to the environment without any safety assessment. Now nanotoxicity is more of a focus in nanoscience and nanotechnology, due to the increasing toxic effects of nanoparticles on living organisms. They also get distributed freely compared to the large-sized materials/bulky particles; as a result, they are more toxic. These nanoparticles indirectly help humans by destroying the single-cell pathogens, like viruses, fungi and bacteria, to utilize their enzymes for oxygen intake instead of human enzymes, which are protected. The metal nanoparticles are synthesized by microorganisms, algae and fungi from any kind of metal salt, which involves either their intracellular or extracellular pathways, and by using biochemicals/enzymes available within them. However, the reducing substances and enzymes are known to play a major role.

In many places, copper oxide (CuO), zinc oxide (ZnO) and silver (Ag) nanoparticles (NPs) are intentionally used to control or to act against undesirable bacterial, fungus and algal growth. Discharge of these NPs

from user and household products, i.e., for which these nanoparticles were designed, to the non-target environment which may cause risk to nonpathogenic natural microbes and other living organisms, especially aquatic organisms. Consequently, proper disposal of nanoparticles from consumer products after their usage is very essential to avoid or prevent the accidental exposure to untargeted species. In the year 2010, the socio-economic rate of nanotechnologies increased globally after receiving funds of about 17.8 billion dollars from several public and private sector companies operating worldwide [2]. Previously it was reported that there are 313 consumer products associated with AgNPs from over 1,300 nanotechnological products existing in the market in 2011 [3], while for ZnONPs the annual production was between 550 to 33,400 tons; for SiO_2 it was 5,500 tons and for TiO_2 NPs it was 3,000 tons [4]. Because of their higher production and massive applications, these nanoparticles have created an awareness focusing on their causes of toxicity and various levels of harm. In some of the literature, it was claimed that released metal particles react according to the behavior of test material (pH, presence of proteins and humic acids), so even toxicity is dependent on or reflected in that [5].

5.1.1 Metals and Metal Oxide Nanoparticles

The concept of nanomedicine has become advantageous due to its efficient transformation inside the cell and role in cell recovery from intracellular damage. Metals and metal oxides are widely used to make nanomaterials but have lately been unappreciated due to their severe effect on the environment and other biological systems. Nanoparticles are prepared and their size (range: 1–100 nm) measured by a nano-analyzer; stability was assessed by zeta potential. The corresponding metals are zinc (Zn), copper (Cu), silver (Ag), gold (Au), cerium (Ce), palladium (Pd), aluminium (Al) and titanium (Ti), and their oxide forms were used for making nanoparticles. There are very many novel approaches to the synthesis of these nanoparticles. They are:

- Chemical methods
- Thermal methods
- Deposition and precipitation
- Photodeposition
- Sputtering
- Pulsed electrodeposition
- Physical vapor deposition

By utilizing these methods, various noble metal or metal oxide nanostructures were recently observed. For example, core-shell nanostructures, yolk-shell nanostructures, NM-decorated metal oxide nanoarrays and Janus noble metal-metal oxide nanostructures. Their applications are highly involved in reduction of toxic chemical 4-nitrophenol, CO oxidation, photodegradation of dyes and formic acid oxidation [6]. Though they have some useful applications in industries, they are reported to be highly toxic, may accumulate intracellularly and are unable to be eliminated from living systems. Various toxic models reveal that they are totally affecting the biological sources of the ecosystem (Figure 5.1). However, their significant noxious effect on the environment should be highly considered. The toxic effect of these metal-based nanoparticles and their involvement in cellular damage are discussed below.

5.1.2 Parameters of Toxicity

Nanoparticles have a heterogeneous nature. The good or bad impact of nanoparticles to living organisms depends on their shape and size more than the nature of the particular metal ion used. Metals with a high rate of dissolution, like ZnO and CuO, are considered as highly toxic. Other

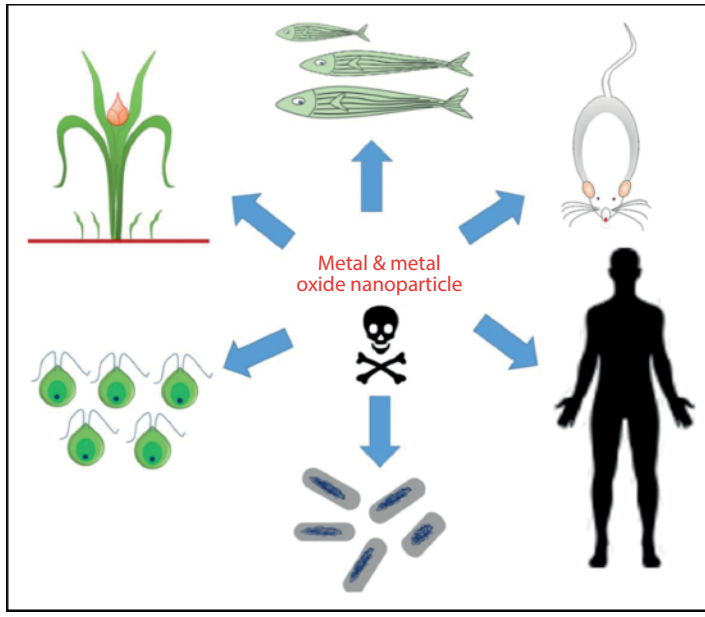


Figure 5.1 Overall toxicity of metal and metal oxide nanoparticles in living system.

parameters like composition, morphology, concentration, particle size, chemical reactivity, aggregation and dispersion directly influence the behavior and interactions of nanoparticles with the environment. The release of ionic species from synthesized nanoparticles is one of the major contributors to toxicity.

i) Size and shape of nanoparticles

Synthesis of nanoparticles results in different forms with different properties which can be studied by TEM and SEM. They use electrons with 100,000 times shorter wavelength and hence give better resolution and magnification than a light microscope, which uses photons.

ii) Zeta potential of nanoparticles

It is considered as charge of the synthesized nanoparticle. It is sensitive to the constituents in the solution and is affected by adsorption. In addition to determining the factor responsible for the agglomeration and stability of nanoparticles, it also impacts the interaction of nanoparticles with cellular components.

iii) Agglomeration of nanoparticles

Agglomerates are the assembly of particles combined by weak forces respectively. They are mostly dependent on the charge, particle concentration and the constituents of the surrounding medium. It affects the biodistribution and interaction of the nanoparticles when exposed to cells. It can be analyzed using laser diffraction/DLS techniques. It can be investigated and calculated by the Brownian motion in the suspension using Stokes-Einstein equation.

iii) Surface area and surface chemical composition of nanoparticles

It can be measured with BET analysis by studying the adsorption of nitrogen atoms on the surface of nanoparticles. When the size of particles decreases, the relative surface area per unit mass increases and as a result more atoms are found on the surface than the interior of the particle. This results in an increased surface area, which can drive toxic reactions. Surface chemical composition can be analyzed by XRD, FTIR and XPS. CRM can be used to analyze the surface composition of silver and copper nanoparticles after exposure to the cells.

iv) Metal release and dissolution of nanoparticles

Stable particles can accumulate and remain active in the body for a long time but the degradable ones cause severe effects by releasing reactive oxygen species. During sample analysis by AAS, a known quantity of energy is passed through an atomized sample and its concentration will be determined by measuring the amount of light lasting after absorption by the element.

5.1.3 Synthesis of Metal/Metal Oxide Nanoparticles

The core objective of biology-oriented technologies, green chemistry and nanotechnology is to create innovative materials and manufacturing processes that decrease or eliminate the usage of hazardous substances. Many fresh water and marine algae, such as *Stoechospermum marginatum, Bifurcaria bifurcate, Ecklonia cava, Chlamydomonas reinhardtii, Fucus vesiculosus, Pithophora oedogonia, Oscillatoria willei, Sargassum muticum, Sophora wightii, Chlorella vulgaris* and *Spirulina platensis,* are part of the developing nano-based industries and technology; they also prevent the causes of pollution to the atmosphere. Based on their composition, nanomaterials can be classified into organic and inorganic, in which carbon-based materials alone belong to the organic category and the remaining gold, platinum, silver, iron oxide, Fe_3O_4, titanium dioxide (semiconductors) and zinc oxide come under the inorganic nanomaterial category.

To synthesize properly defined shape and size metal/metal oxide nanoparticles, the concentration of extract/biomass and metal salt, pH (reaction mixture), incubation time and temperature are key ingredients. The synthesized nanoparticles can be characterized by UV-visible spectrophotometry, Fourier-transform infrared spectroscopy (FTIR), Transmission electron microscopy (TEM), scanning electron microscopy (SEM), energy-dispersive X-ray spectroscopy (EDX), X-ray diffraction (XRD) and dynamic light scattering (DLS).

The silver nanoparticles were synthesized from *Cystophora moniliformis* extract in aqueous medium at 65 °C. The SPR peak was stable between the optimized temperatures of 65 °C and 75 °C. The peak formed between 450 and 452 nm corresponds to polydispersed spherical nanoparticles [7]. The marine algae, namely *Pterocladia capillacea*, *Jania rubens*, *Ulva fasciata* and *Colpomenia peregrina,* were used. Their polysaccharide extracts were found to synthesize silver nanoparticles of spherical shape with size 7–20 nm diameter [8]. After a 1 h period, the yellow colored reaction mixture having $AgNO_3$ and aqueous extract of algae turned to

brown color with pH 8.4 and the incubation process was completed in 32 h. The synthesized nanoparticles were analyzed for antifungal activity against *Aspergillus fumigatus*, *Candida albicans* and *Fusarium* sp. [9]. The fresh water green algae, *Pithophora oedogonia,* was reported to have primary (carbohydrates and proteins) and secondary metabolites (saponins and steroids), which were used to synthesize NPs of 25–44 nm diameter. The marine alga, *Caulerpa racemosa,* formed NPs of 5–25 nm crystalline structure along with face-centered cubic geometric structure. It was also reported to have antibacterial activity against *Staphylococcus aureus* and *Proteus mirabilis* (human pathogens) in 5 to 15 µL concentration. Cyanobacteria such as *Phormidium valderianum, Phormidium tenue* and *Microcoleus chthonoplastes;* and green algae, like *Rhizoclonium fontinale, Ulva intestinalis, Chara zeylanica* and *Pithophora oedogoniana,* were used in synthesizing gold nanoparticles by maintaining a temperature of 20 °C. As a result, spherical shape formation was observed at pH 7, hexagonal and triangular at pH 9, and at pH 5 both spherical (15 nm) and nanorods (411 × 32 nm and 17 nm), as described in Figure 5.2. At a concentration of 10^{-3}M, $AuCl_3$ was found to be toxic to *Euglena gracilis.*

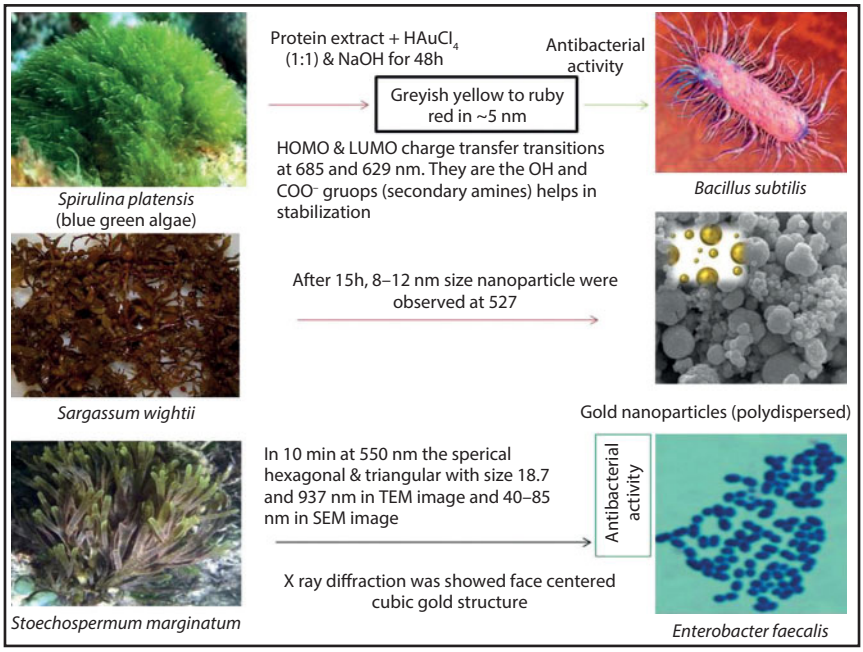

Protein extract + HAuCl4 (1:1) & NaOH for 48h
Antibacterial activity
Greyish yellow to ruby red in ~5 nm
HOMO & LUMO charge transfer transitions at 685 and 629 nm. They are the OH and COO⁻ gruops (secondary amines) helps in stabilization
Spirulina platensis (blue green algae)
Bacillus subtilis
After 15h, 8–12 nm size nanoparticle were observed at 527
Sargassum wightii
Gold nanoparticles (polydispersed)
In 10 min at 550 nm the sperical hexagonal & triangular with size 18.7 and 937 nm in TEM image and 40–85 nm in SEM image
Antibacterial activity
X ray diffraction was showed face centered cubic gold structure
Stoechospermum marginatum
Enterobacter faecalis

Figure 5.2 Synthesis of gold nanoparticle by using algae as source and its antibacterial activity.

In transition metals, silver and gold are most commonly used to synthesize nanoparticles, as mentioned above. It is due to their application in tumor imaging, drug delivery, and determination of heavy metals content and identification of microbial pathogens. Apart from that, the synthesized silver nanoparticles can control bacterial biofilm formation whereas gold nanoparticles are capable of efficiently acting against bacterial cultures. This is possible because of their size, as they are smaller than the thickness of the bacterial cell wall and can penetrate the cell easily and inhibit its growth. Generally, synthesizing nanoparticles have two approaches, i.e., size reduction, which occurs through physical or chemical processes. The achieved size, shape and surface structure of the particles are related to the techniques incorporated. They tend to bring surface imperfection and thus also impact the physicochemical properties of synthesized nanoparticles. In another approach, the nanoparticles are manufactured by the assembly of atoms, molecules and smaller particles or monomers. This approach has major drawbacks like less material conversion rates, technical complexity , high energy supplies needed, is expensive and employs hazardous chemicals (as reducing agents, organic solvents and non-biodegradable stabilizing agents). The processes like chemical precipitation and pyrolysis take place during this conventional approach and, as mentioned above, deposit toxic chemical species on the surface of formed nanoparticles.

Aqueous extract of *Sargassum muticum* (marine brown macroalgae) was used to synthesize zinc oxide nanoparticles. It changed its appearance from dark brown to pale white color, which confirmed the conversion and its ability to act as a reducing agent. Formation of agglomerated nanoparticles along with hexagonal structure of 30–57 nm were observed [10]. Synthesis of copper oxide nanoparticles carried out with *Bifurcaria bifurcata* extract and $CuSO_4$ solution (1 mM) resulted in 5–45 nm dimension NPs. They result from a mixture of cuprous and cupric oxides (blood red color) and are crystalline and important semiconductors in nature. As they are partly filled with 'd' orbitals they are applied in electronics, magnetic storage media and energy transformation. The presence of diterpenoids and formation of Cu (I and II) oxide nanoparticles were confirmed by their UV-vis spectrum at 260 and 650 nm respectively. Potential antibacterial activity was exhibited against *Enterobacter aerogenes* and *Staphylococcus aureus*. The polysaccharides, consisting of aqueous extract of *Sargassum muticum* and $FeCl_3$ salt, were used to synthesize iron oxide (Fe_3O_4) nanoparticles. Throughout the experiment, the temperature was maintained at 25 °C and thus leads to the production of 18 ± 4 nm size and cubic-shaped nanoparticles.

5.2 Applications of Metal/Metal Oxide Nanoparticles and Their Toxicity

Metal/metal oxide nanoparticles have a wide range of applications like environmental remediation, labeling for immunoassay and in hyperthermia treatment of tumors, as shown in Figure 5.3. Beyond studying the toxicity of nanomaterials, physicochemical analysis must also be carried out. In recent years, researchers have particularly been performing studies that elucidate the properties of NPs that result in toxicity. Consequently, with this information, the NPs can ideally be designed/prepared with only desired material properties that do not include any toxicity.

5.2.1 Silver Nanoparticles (Ag Nanoparticles/AgNPs)

The significant antimicrobial property of Ag nanoparticles was shown by the interaction of Ag nanoparticles with microbial cellular membranes, which causes membrane damage and biosorption due to the generation of free radicals. The increased cellular uptake of nanoparticles leads to toxicological damage to cellular DNA. The mechanism involved in DNA damage

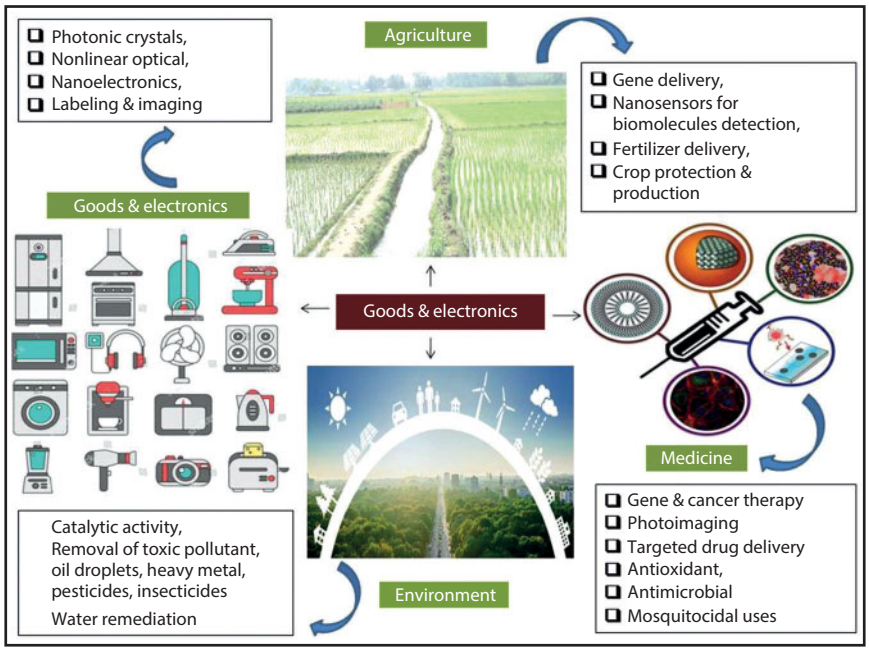


Figure 5.3 Applications of nanoparticles in various fields.

initiated by nanoparticles is their passage into cell nuclei either during mitosis or through the nuclear pores and contact with DNA to cause damage. The nanoparticles may directly interact with damage or induce the target cells to generate ROS by disturbing the electron transport taking place in mitochondria, and by stimulating cytochrome P450-enzymes/NADPH-oxidase. The nanoparticles may activate the inflammatory system by means of ROS derived from neutrophils and macrophages (phagocytes) and thus causes DNA damage [11].

Silver nanoparticles are a commonly used nanomaterial in many products and several industries. AgNps are known for their potent antibacterial activity by efficient diffusion around the plasma membrane and equal distribution inside the cell. Nevertheless, their major toxicity evaluation is highly notable before usage of AgNPs [12]. As mentioned below, it is based on their administration and different types of model organisms. Intranasal (IN) administration of AgNPs can induce oxidative stress at the cellular level, which was studied by decreasing the concentration of glutathione:glutathione disulfide (GSH:GSSG) ratio; and behavioral changes were observed with the intranasal (IN) administration of 50 mg/kg body weight of AgNPs. There was an upregulation of oxidative stress marker (HMOX1) from hippocampal sample of AgNPs treated mice. It is evident that AgNPs are neurotoxic and may induce memory loss by increasing oxidative cellular damage in the brain. A immunosuppressive response was observed and showed decreased NK-cell and T-cell population [13].

Oral administration of AgNPs (60 nm) has been reported to cause an upturn in genotoxicity in both genders of Sprague-Dawley rats after a 28 day period of administration (30, 300 and 1000 mg/kg). The blood biochemical parameters and histopathological study exhibited a harmful effect on rats at a dosage of 300 and 1000 mg/kg. Remarkable damage was observed in the liver tissue and blood parameters alkaline phosphatase and total cholesterol level [14]. Another report clearly explains that in the oral administration of (3 to 20 nm) AgNPs to Swiss albino male mice with different concentrations (5, 10, 15 and 20 mg/kg), a dose above 10 mg/kg showed maximum weight loss and microscopic images obtained by light emission microscopy (LEM) and transmission electron microscopy (TEM) showed the entrapment of AgNPs on epithelial microvilli. It was understood that weight loss due to blockage of microvilli causes non-absorption of nutrients by intestine [15].

Silver nanoparticles capped with bovine serum albumin (Ag-BSA) were investigated against zebrafish (*Danio rerio*) to evaluate toxicity. Different concentrations of BSA bound AgNPs (5, 10, 25, 50 and 100 μg/ml) along

with Ag^+ ions-control (2.5, 5, 10, 15 and 20 nM) and BSA and starch-control (500 and 1000 µg/ml respectively) were chosen and evaluated for embryo toxicity. Each well of a 24-well plate having 10 embryos was incubated along with their respective drugs for 24, 48 and 72 h. The mortality was determined by the transformation of opaque embryos into pale white; deformity and heart rates were also measured. This study confirmed that the BSA bound AgNPs showed a gradual death rate, while in other controls much less mortality and deformity were observed in both treatments. Heart rate gradually decreased with increased hatching rate in BSA-AgNPs compared to Ag-starch control, which might be due to BSA-AgNPs increased oxidative stress on the embryos that results in lipid peroxidation [16]. The intraperitoneal (IP) administration of AgNPs (about 8.7 nm sized) with different concentrations (1, 2 and 4 mg/kg) to Swiss albino rats for 28 days revealed that there was hepatotoxicity due to generation of reactive oxygen species, which was evidenced by identifying the oxidative markers; reduced glutathione and malondialdehyde (MDA). Histopathological images showed hyperplasia, cholangiofibrosis and hepatocellular necrosis in liver tissue. Genotoxicity was assessed by bone marrow metaphase preparation. Investigation showed chromosomal aberrations due to the formation of chromatid gaps in 4 mg/kg AgNPs treated groups [17].

Silver nanoparticles were not only tested as toxic on the above-stated models but were also harmful on unicellular flagellated green algae, *Chlamydomonas reinhardtii.* The acute toxicity of AgNPs and Ag^+ ions was studied for their toxic effect. Both Ag^+ and AgNPs showed higher toxicity on algae and inhibited their photosynthetic functions [18].

5.2.2 Zinc Oxide Nanoparticles (ZnO Nanoparticles or ZnNPs)

Zinc is an essential trace element for all living cells. Zinc oxide is mostly added to cosmetics, such as sunscreens, for scattering UV light or because of its ability to reflect sunlight; and in toothpastes. In spite of its use as an anti-fouler in paints, it also has wide applications in other industries like rubber manufacture, production of chemical fibers, chemical sensors, solar cells, transparent UV protection films, LCDs, electronics, pigments (for whitening) and textiles [19]. In medical application, it is applied to selectively kill proliferative cells and in antimicrobial drugs. But there are drawbacks to using it as nanoparticle, since it interferes with the hatching system of zebrafish embryo, reduces biomass, biodiversity of soil bacteria, metabolic activities and causes an inflammatory response in mice. Beyond these problems, the major and primary cause of toxicity is generation of reactive oxygen species (ROS), which often leads to cellular oxidative

stress. It was proven that nanoparticle-treated human and bacterial cells were found to have elevated intracellular ROS and oxidative damage [20]. Other than that, accumulation of mitochondrial membrane depolarization/leakage and perturbed intracellular calcium flux were also found.

Zinc oxide nanoparticles are reported to be an antibacterial against *Escherichia coli* (*E. coli*) and *Staphylococcus aureus* (*S. aureus*), which according to the study were inhibited due to ZnNPs [21]. Though they suppressed bacterial growth, they were also studied for their toxicity in other higher models like zebrafish and rats. ZnNPs of 30 nm size had a harmful effect on zebrafish (*Danio rerio*). Different concentrations of dissolved Zn^{+} ions (0.598, 2.152, 3.629, 4.066, 5.311 and 6.305 mg/L) and ZnNPs (1, 5, 10, 25, 50 and 100 mg/L) in the E3 medium were tested against zebrafish embryos. The embryos were monitored and mortality was observed at each checkpoint (8, 24, 32, 48 and 96 hpf). This study indicated that the hatching rate and length of the organism were observed to be influenced above the concentration of 10 mg/L in ZnNPs whereas it was observed at 5.311/mg/L in Zn^{+} ion solution [22].

The topical application of the ZnNP-embedded drugs or ointments also had a direct toxic effect on the epidermal cells. This was confirmed by *in-vitro* analysis using epidermal cells and was proven in a study. Human epidermal cells (A431) were treated with different concentrations of ZnNPs (0.008, 0.08, 0.8, 5, 8 and 20 μg/ml) dissolved in DMEM (Dulbecco's modified Eagle medium). The reduced cell viability was observed in all the doses of ZnNPs with respect to their exposure time. ZnNPs created an oxidative stress inside the cells where the ROS gradually increased as the exposure time increased. Lipid peroxidation increment and reduced superoxide dismutase (SOD), catalase (CAT) and glutathione (GSH) levels showed that cells were losing these antioxidant defense mechanisms due to the higher progression of oxidative damage by ZnNPs. Genotoxicity of ZnNPs was proven based on the single-cell gel electrophoresis (comet assay), where the comet formation was observed in the treatment groups 0.8 and 5 μg/ml after 6 h of exposure. Damage in plasma membrane integrity was not only recorded by natural red uptake (NRU) assay but also by assessing intracellular enzyme lactate dehydrogenase (LDH) from the extracellular medium [23].

A comparative study between two metal oxide nanoparticles, such as cerium oxide (CeO_2), zinc oxide (ZnO_2) and titanium dioxide (TiO_2), was conducted and the research outcomes are discussed below. The cytotoxicity assessment revealed that the ZnNPs reduced the cell population in both murine macrophage (RAW 264.7) and human bronchial epithelial (BEAS-2B). ZnNPs caused cell death via oxidative stress by generating

reactive oxygen species (ROS), oxidative cellular damage and inflammatory responses. This is in contrast to the other nanoparticles, where the fluorescently labeled CeO_2 nanoparticles suppressed ROS generation and provided resistance to cells whereas fluorescently labeled TiO_2 nanoparticles showed no effect on both cells [24]. However, ZnNPs are reported to have anticancer activity against hepatocarcinoma (Hep G2), human adenocarcinoma alveolar basal epithelium (A549) by inducing apoptosis through ROS [25]. Nevertheless, it also affected the normal cells, as mentioned above. A sub-acute toxicity study using 300 mg/kg body weight of ZnNPs for 14 consecutive days showed pathological injuries to the liver with notable necrotic lesions along with kidney cystic dilation of tubules with hypertrophy [26].

5.2.3 CuO Nanoparticles

A redox element rarely applied as nanoparticle consists of negative surface charge obtained from oxygen atom [27]. It is commonly observed in fields including semiconductors, heat transfer nanofluids electronic chips, lithium batteries and sensors in gas. Finally, because of its antimicrobial and antiviral characteristics, it is used as an antiseptic in wound dressings, face masks and socks [28]. It replaces fine metal catalysts for carbon monoxide and as a nanofluid (CuO nanoparticle suspension) it has excellent thermal conductivity for use as a heat transfer fluid in machine tools. Copper oxide was found to be a more active against *S. aureus* and *E. coli* while other oxide nanoparticles inhibited their growth only at higher concentration of 100 mgL^{-1}. ZnO and CuO are toxic to protozoa *Tetrahymena thermophila* at 6 mg L^{-1} and they also inhibit *Pseudokirchneriella subcapitata* at 100 and 430 μg L^{-1}.

Oral toxicity of copper nanoparticles, micro-sized particles and $CuCl_2$ (soluble salt) were conducted. The copper dose was higher in the kidney of the animals when exposed to nanoparticles, due to its increased transportation capacity to peripheral target organs. LD_{50} values for nanoparticles were exhibited at 413 mg/kg, but the micro-sized particles showed >5000 mg/kg. Later, when the animals were exposed to nanoparticles, serious pathological changes were seen in major digestive and excretory organs (kidney, liver and spleen). However, the ionic species (Cu) from $CuCl_2$ salt showed still lesser LD_{50} value as 110 mg/kg, which was correlated to the higher dose of copper in their kidneys.

Exposure of copper oxide nanoparticles could induce mortality, growth inhibition and metamorphic inhibition at concentrations lower than those used in acute studies [29]. Copper oxide nanoparticle exposure could

induce mortality in subchronic and chronic exposures but acute 4 days exposure produces less to no mortality. The maximum mortality expressed with acute exposure was 3.33% at 100 μg to 1000 μg L^{-1} concentration. Subchronic exposure to 1250 μg L^{-1} induces 85% mortality. The sub chronic exposure of 1250 μgL^{-1} for 14 days produces 1/3rd more mortality. The increase in mortality after day 4 could be attributed to the fact that *Xenopus laevis* tadpoles feed from their yolk for the first 3 to 4 days post hatch. From day 5 to day 47, i.e., end of the study, 94.7% of total mortality occurred. LC_{50} for subchronic exposure was decreased with increasing exposure time. *Bufo arenarum* embryos exposed to Cu^{2+} solutions had increased mortality in 7 days. The mortality percent in both subchronic (0.313 mgL^{-1}) and chronic (0.3 mgL^{-1}) exposures were related (11.1 ± 8% and 15.6 ± 2.6% correspondingly) and symptoms were observed to have slower stage progression, lesser body measurements and physiological stresses. It is reversed in a positive manner at a lower dose of 0.125 mgL^{-1}. Thus, within two weeks of exposure to 0.3 mgL^{-1} CuO nanoparticles, *X. laevis* tadpoles adapt to nanoparticle suspensions, which involves modifications in uptake and removal rates, binding capability and decreased enzyme sensitivity. Rapid completion of metamorphosis in larger body size is beneficial, as smaller body size can enhance the possibility of predation, lack of ability to compete for food and reduced survival rates.

Tadpole development was affected by copper by increasing the time to complete metamorphosis and by dropping the size and weight of metamorphs. The exposure can affect aquatic organisms even at low concentrations of 0.00258 mgL^{-1}, which is less than in fresh water criteria (0.009 mg L^{-1}). The lower concentrations of dissolved copper were found to affect an environmentally significant sub-lethal reaction such as anti-predator and sensory behavior in amphibians [30].

Pseudokirchneriella subcapitata was found to be the most sensitive organism among the used bacterial species and protozoan. It showed EC_{50} values of < 100 mg/l and sensitivity for 10 nanoparticles out of 12 NPs (Al_2O_3, CO_3O_4, CuO, Fe_3O_4, MgO, Mn_3O_4, Sb_2O_3, SiO_2, ZnO, TiO_2, WO_3 and Pd) tested. In the case of *T. thermophila,* the EC_{50} values could be calculated for ZnO (1.8 mg/L), CuO (2mg/L), Fe_3O_4 (26mg/L) and TiO_2 (53mg/L) NPs. NPs in concentrations below 100 mg/L did not affect the viability of protozoa but the remarkable accumulation of NPs in food vacuoles of protozoan might ultimately affect the food web transfer and bioaccumulation, which is an indication of potential harm. The bacterium *Vibrio fischeri* was tested against CuO, ZnO and Pd nanoparticles for 30 min with EC_{50} values of 1.8, 11.5 and 55 mg/L respectively, while for Sb_2O_3 and WO_3, the toxicity effects were seen at < 100 mg/L. Regardless of the association with primary

particle size, the nanoparticles with diverse elemental composition will result in suspensions that have various levels of agglomeration/solubility, thus creating additional complexity. The cells in the toxicity assays will be subjected to agglomerates of NPs of different sizes and surface charges, as well as varying concentrations of soluble ions, which further complicates the interpretations of results. To understand the mechanisms of NPs in aquatic toxicity, several approaches were developed for toxicity prediction from quantitative assessment to mechanisms. They must be suitable for all types of test species belonging to different tropic levels, including minimum and primary producers, i.e., algae, consumers (protozoa) and decomposers (bacteria) [31].

In human alveolar epithelial cell lines (A549) treated with copper oxide nanoparticles, the microscopical evidence showed that efficient nanoparticle internalization occurs through endocytosis and enters the mitochondrial level early on in exposure time. This led to deterioration of mitochondrial morphological functions, including compromising oxidative chain and common ultrastructural damages that help to determine cell death occurring due to necrosis. It exhibits cell cycle progression arrested at G_2/M phase; thus, no further duplication was observed by intracellular LDH content. It also disturbs spindle machinery assembly, blockage of cell proliferation, disorganization of microtubules and deregulation of intracellular calcium homeostasis [32]. In a study that examined mice with pulmonary edema, it caused death within 24 h. Cytotoxicity of CuO NPs was also investigated against $HEPG_2$, melanoma cells and neuronal toxicity. CuO NPs coated with folic acid were shown to be efficient against triple negative breast cancer cells (MDAMB-231 cells) by mediating cytosolic retardation of NF-κB, inactivation of miR-425; finally, activation of PTEN induces apoptosis [33].

Among the 11 metal oxide nanoparticles (CuO, Al_2O_3, Fe_3O_4, Co_3O_4, MgO, Sb_2O_3, Mn_3O_4, SiO_2, ZnO, WO_3 and TiO_2) used against mammalian epithelial cell lines ($Caco_2$ and A549) and murine fibroblast cell line BALB/c 3T3 in neutral red uptake cytotoxicity assay, NPs like Sb_2O_3, CuO, Co_3O_4, ZnO and Mn_3O_4 were toxic at concentrations > 100 μg/mL for 24 h exposure. IC_{50} values ranged from 10–100 μg/mL, i.e., 2.3–6.4 (ZnO), 2.3–6.1 (CuO), 2.1–14.2 (Sb_2O_3), 10.9–22.1 (Mn_3O_4) and 33.4–64.4 (Co_3O_4).

More than the size (smaller) of particles and their agglomeration, metal ions released from the particles are probably the main driving force of the toxic effects and contributed to cytotoxicity. Dissolution of CuO NPs observed in sterile water was < 2.4% while in DMEM medium containing serum, it was time-dependent and reaches 44% in 24 h. The highest dissolution was observed for copper oxide (41–50%), followed by Sb_2O_3

(10–15%) and ZnO (11–14%). Mn_3O_4 and especially Co_3O_4 has low solubility (> 4 and 1%). Release of metal ions into cells may also take place after the uptake of nanoparticles by the cells, as studied in BEAS-2B (human bronchial epithelial cells). Due to the polar nature (charge) of metal ions, they are not able to cross the cellular lipid bilayer and need special transporters/membrane channels. So far, the internalized NPs enter the cells freely and release metal ions intracellularly. For ZnO and CuO, the LD_{50} value was calculated as > 50 mg/kg to < 300 mg/kg; and Sb_2O_3, Mn_3O_4, Co_3O_4 nanoparticles include LD_{50} values > 300 mg/kg to < 2000 mg/kg [34].

5.2.4 Cadmium Nanoparticles (CdNPs) vs Silica Nanoparticles (SiNPs)

Cadmium is one of the toxic elements in the environment. However, although it was reported as a toxic metal and can invade biological systems, more outcomes have arisen from research with various models. Cadmium is a transition metal holding eight stable isotopes; it is available in different forms such as cadmium sulfide, chloride, carbonate and oxide. It has been highly reviewed for its harmful effect on pregnancy. It may be absorbed through inhalation. At the time of necropsy, it was identified in different organs of the body, such as liver, kidney, placenta, uterus and fetus, and is also secreted in milk. At the cellular level, it interferes with other elemental uptake which is involved in their metabolism such as Ca and Zinc. This leads to the homeostasis imbalance of their membrane transport mechanism [35]. On the other hand, albumin-conjugated CdNPs were reported to be toxic for human breast cancer cells. In this study, 0.2 mg/ml of CdNPs were treated on the adhered KB cells on different consecutive days (1, 2, 3 and 4). After the exposure, the MTT assay resulted in the formation of significantly less formazan crystals compared to the control. This study indicates that CdNPs also have anticancer property [36].

Cadmium quantum dots are responsible for causing oxidative stress, which impairs their behavior. This was assessed by using *Scrobicularia plana,* a peppery furrow shell and bivalve mollusc belonging to the Semelidae family. Oxidative markers CAT and glutathione-S-transferase (GST) were increased in the treatment of Cd quantum dots nanoparticles. The physical impairments in foot movements were observed only in Cd treated clams. This study highly supports the toxicity level of Cd in estuarine ecosystem [37]. Some other interesting facts were also noted, i.e., Cd^{2+} can become trapped within the rice plant via accumulation of silica (Si) where Cd-mediated toxicity has been alleviated when conjugated with Si. It enhanced the growth of live cells in rice suspension culture and

prevented uptake of Cd^{2+} in the cells. It was monitored by the expression of two important transporters and is responsible for accumulation of Cd^{2+} in the cells. Such proteins also had low-affinity cation transporter protein (OsLCT1) and natural resistance-associated macrophage protein (Nramp) family. These genes (OsLCT1, OsNramp5) were highly expressed inside the cells when exposed to medium containing Cd^{2+} without SiNPs as control, but dose-dependent suppression was observed in various concentrations (10, 20 and 40 μM) of Cd^{2+}. Cellular morphological abnormalities were observed in the Cd^{2+} treated cells; no abnormalities were observed in SiNPs and SiNPs with Cd^{2+} [38].

The inverse of the above statement was reported in the case of human pulmonary epithelial cells/lung cancer cells (A549), when treated with cadmium-coated silica nanoparticles (Cd^2 and SiNPs). It was mentioned that the Cd and SiNPs (1 μg/ml) showed 50% mortality, whereas in $CdCl_2$ it was higher (25 μg/ml). This effect was further confirmed as cytotoxicity to cells was due to the induction and progression of oxidative stress [39].

Silica occurs in different forms like amorphous, α-quartz, ß-quartz, trydimite and cristobalite. It is known for its application in batteries, paints and adhesives. The hydroxyl groups on the silica surface are silanols, which affect the hemolytic capacity and cytotoxic activity. It can be protected by shielding the reactive surface with protein or lipid corona [40]. The pro-inflammatory effect of quartz was also reduced by treating the particles surface with aluminium lactate. There was only less sensitivity observed in growth and reproduction in nematodes exposed to 5l g/L of SiO_2 nanoparticles and even prolonged exposure to 30 nm SiO_2 nanoparticles at 16 or 24.5l g/L, 76 l g/L and 0.0007 l g/L concentrations was considered as safe.

5.2.5 TiO_2 Nanoparticles

Titanium dioxide (TiO_2) disrupts the membrane integrity and loss of energy, generating potential of bacterial cells. Lack of toxicity in TiO_2 is due to the conduction of band energy, which is closer to the higher edge of cellular redox potential, thus it may not provide enough driving force for electron transfer. In green algae, *Desmodesmus subspicatus,* the smaller size particles (25 nm) were found to be more toxic with EC_{50} value of 44 mg/L after exposing for 72 h, while 100 nm particles showed EC_{50} value of >50 mg/l. TiO_2 nanoparticles are found to be toxic to *P. subcapitata* in all three sizes formed (10, 30 and 300 nm). ZnO and TiO_2 (anatase) inhibited the growth of *Chlorella* sps. in both 20 and 30 mg L^{-1} concentration and were analyzed as more toxic than its rutin form since the anatase type of ZnO and TiO_2

induces cell death by necrosis instead of apoptosis. Cytotoxicity of ZnO nanoparticles against *Bacillus subtilis, V. fischeri* and *E. coli* was higher than the TiO_2 nanoparticles [41]. The abundancy of nematodes in the soil ecosystem, its convenient handling and sensitivity to stresses or toxicants were what made researchers carry out toxicity experiments on it. Size of 30 nm was selected, as NPs > 30 nm did not show any positive activity and they would need regulatory examination more than that required for bulk particles. In addition, the adverse effects of nanoparticles preferably resulted from smaller size nanoparticles. Nematodes exposed to TiO_2 nanoparticles and ZnO nanoparticles at the concentration of 0.05 to 0.05l g/L were found to cause adverse effects like alterations in locomotion behavior and ROS production. When *Caenorhabditis elegans* was given acute exposure to TiO_2 nanoparticles, it did not influence the lifespan of nematodes but induced the reduction of progeny production to some degree [42]. And treatment with ascorbate or N-acetyl-L-cysteine (antioxidants) inhibited the toxicity in nematodes exposed to TiO_2, ZnO and SiO_2 at concentration of 50 l g/L [43]. When TiO_2 nanoparticles were internalized in $Caco_2$ cells (colorectal adenocarcinoma), no cytotoxicity was induced, which showed that not every internalized metal oxide nanoparticle causes evident loss of cell metabolic activity during similar exposure for 24 h [44].

5.3 Future Perspectives

A distinctive size and shape are relevant to physicochemical surface properties for formulation of nanoparticles which are more interactive and reactive to certain chemical species compared to their bulk form. Au nanoparticles have been applied in a variety of biomedical areas such as biosensors, carriers of anticancer drugs and targeting tumors for thermal treatment therapy. Magnetite (Fe_3O_4) nanoparticles are nanometer-scale material with paramagnetic properties. They are applied in magnetic resonance imaging (MRI) and in targeted drug delivery. By accumulating in treated human cancer cell lines, they could enhance cell apoptosis and thereby act against leukemia, breast, cervical and liver cancer [45]. Suppression of cell growth and proliferation in WEHI-3 (murine) cell lines by ZnO proved that they are a future alternative chemotherapeutic drug. During reactive milling, $Zn(NO_3)_2$ as precursor was transformed into a crystalline hexagonal wurtzite structure of 18–50 nm size. The produced porous ZnO nanoparticles could effectively degrade phenol aqueous solution after undergoing calcination process at temperature of 600 °C.

5.3.1 Curbing Menace Through Biodegradable Nanomaterials: An Alternative

Over the past few decades, novel and biodegradable nanomaterials are expected to be synthesized more due to their high efficiency in drug delivery system and eco-friendliness. Naturally derived biopolymers are highly selected for production along with precise drug combinations. Those polymers are selected based on their bioavailability, efficient degradation, pharmacokinetic and pharmacodynamic properties in drug discovery. Such biopolymers are biodegradable polyesters, polylactic acid (PLA), poly ε-caprolactone (PCL), nanostructured lipid carriers (NLC) or liposomes and nanocellulose [46]. A study supports this drug delivery system, where the four nano-based carriers used are polymeric nanospheres (PNS), poly-ε-caprolactone (PCL), caprylic/capric triglycerides-based nanocapsules (NC) and nanostructured lipid carriers (NLC) in a size of about 130 and 200 nm resulted in no cytotoxicity to human lymphocytes and were non-hemolytic [47].

Another *in-vivo* study was conducted on anti-hyperglycemic activity of insulin-loaded alginate/dextran sulfate-based nanoparticles that are double bound with chitosan and technetium-99m-albumin (99mTc-BSA) after oral administration. The oral administration of insulin-loaded (50 IU/kg) nanoparticles for type 1 diabetic rats resulted in prolonged anti-hyperglycemic effects up to 12 h and relative pharmacological availability of 5.04%. The effect was also compared between type 1 and type 2 diabetic rats by an intraperitoneal glucose tolerance test, which showed longer anti-hyperglycemic effect in type 1 when compared to type 2 diabetes (Figure 5.4). Thus, the biodegradable polymer-based nanoparticles-mediated delivery system is a promising tool for any diseases in the future [48].

5.4 Conclusion

This is a critical review on emerging nanoparticles, their potential and their hazardous effects on society. Here, we discussed the synthesis, application and causes of toxicity by metal and metal oxide nanoparticles. Toxicity studies were presented, which held up in amphibian, nematode and rat models. Thus, instead of incorporating toxin-inducing metals/metal oxides in various applications exposed to the environment, the biodegradable and biologically nontoxic nanomaterials having similar or more active biological, chemical and other properties required can be replaced.

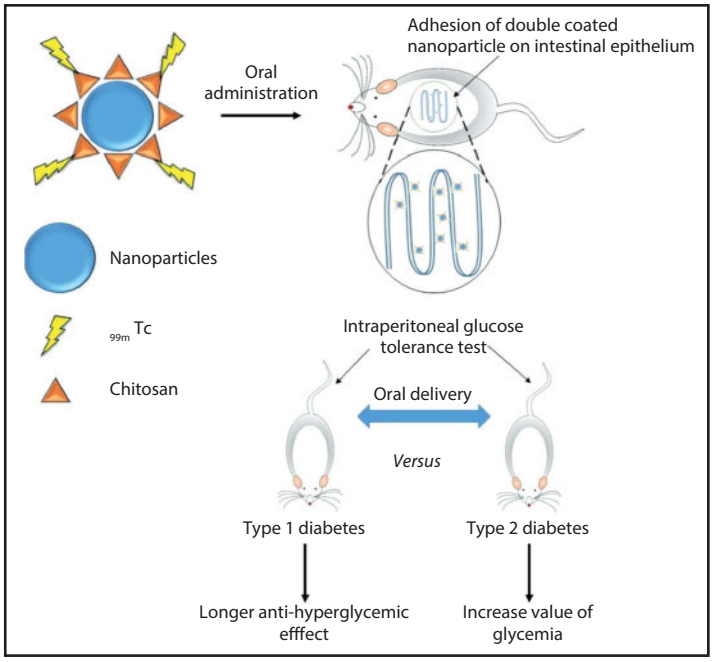


Figure 5.4 Alleviation of hyperglycemia using double-coated insulin bound nanoparticles.

Conflict of Interest

The authors declare that there is no conflict of interest.

Acknowledgment

We thank the management of VIT University, Vellore, for providing facilities and support to carry out our work.

Abbreviations

AAS Atomic absorption spectroscopy
AFM Atomic force microscope
BET Brauner-Emmett-Teller
BSA Bovine serum albumin

CLSM Confocal laser scanning microscope
DLS Dynamic light scattering
EDX Energy dispersive X-ray spectroscopy
FTIR Fourier transform-infrared spectroscopy
MBC Minimum bactericidal concentration
MIC Minimum inhibitory concentration
SEM Scanning electron microscope
SPR Surface plasmon resonance
TEM Transmission electron microscope
XPS X-ray photoelectron spectroscopy
XRD X-ray diffraction

References

1. Bondarenko, O., Juganson, K., Ivask, A., Kasemets, K., Mortimer, M., Kahru, A., Toxicity of Ag, CuO and ZnO nanoparticles to selected environmentally relevant test organisms and mammalian cells *in vitro:* A critical review. *Arch. Toxicol.*, 87, 1181–1200, 2013.
2. Sargent, J.F., Nanotechnology: A Policy Primer. http://www.fas.org/sgp/crs/misc/RL34511.pdf, 2012.
3. Wilson, W., Consumer products inventory, Project on Emerging Nanotechnologies, a project of the Woodrow Wilson International Center for Scholars. http://www.nanotechproject.org, 2012.
4. Piccinno, F., Gottschalk, F., Seeger, S., Nowack, B., Industrial production quantities and uses of ten engineered nanomaterials for Europe and the world. *J. Nanopart. Res.*, 14,1109–1120, 2012.
5. Casals, E., Gonzalez, E., Puntes, V.F., Reactivity of inorganic nanoparticles in biological environments: Insights into nanotoxicity mechanisms. *J. Phys. D Appl. Phys.*, 45, 443001–443015, 2012.
6. Ray, C., Pal, T., Recent advances of metal–metal oxide nanocomposites and their tailored nanostructures in numerous catalytic applications. *J. Mat. Chem. A*, 5, 9465–9487, 2017.
7. Prasad, T.N., Kambala, V.S.R., Naidu, R., Phyconanotechnology: Synthesis of silver nanoparticles using brown marine algae *Cystophora moniliformis* and their characterisation. *J. Appl. Phycol.*, 25, 177–182, 2013.
8. El-Rafie, H.M., El-Rafie, M.H., Zahran, M.K., Green synthesis of silver nanoparticles using polysaccharides extracted from marine macro algae. *Carb. Poly.*, 96,403–410, 2013.
9. Rajeshkumar, S., Malarkodi, C., Paulkumar, K., Vanaja, M., Gnanajobitha, G., Annadurai, G., Algae mediated green fabrication of silver nanoparticles and examination of its antifungal activity against clinical pathogens. *Int. J. Met.*, 2014, 1–9, 2014.

10. Azizi, S., Ahmad, M.B., Namvar, F., Mohamad, R., Green biosynthesis and characterization of zinc oxide nanoparticles using brown marine macroalga *Sargassum muticum* aqueous extract. *Mater Lett.*, 116, 275–277, 2014.
11. Karlsson, H.L., The comet assay in nanotoxicology research. *Anal. Bioanal. Chem.,* 398, 651–66, 2010.
12. Ema, M., Okuda, H., Gamo, M., Honda, K., A review of reproductive and developmental toxicity of silver nanoparticles in laboratory animals. *Rep. Toxicol.*, 67, 1–16, 2017.
13. Davenport, L.L., Hsieh, H., Eppert, B.L., Carreira, V.S., Krishan, M., Ingle, T., Howard, P.C., Williams, M.T., Vorhees, C.V., Genter, M.B., Systemic and behavioral effects of intranasal administration of silver nanoparticles. *Neurotoxicol. Teratol.*, 51, 68–76, 2015.
14. Kim, Y.S., Kim, J.S., Cho, H.S., Rha, D.S., Kim, J.M., Park, J.D., Choi, B.S., Lim, R., Chang, H.K., Chung, Y.H., Kwon, I.H., Twenty-eight-day oral toxicity, genotoxicity, and gender-related tissue distribution of silver nanoparticles in Sprague-Dawley rats. *Inhal. Toxicol.*, 20, 575–583, 2008.
15. Shahare, B., Yashpal, M., Toxic effects of repeated oral exposure of silver nanoparticles on small intestine mucosa of mice. *Toxicol. Mech. Meth.*, 23, 161–167. 2013.
16. Asharani, P.V., Wu, Y.L., Gong, Z., Valiyaveettil, S., Toxicity of silver nanoparticles in zebra fish models. *Nanotech.*, 19, 25–31, 2008.
17. El Mahdy, M.M., Eldin, T.A.S., Aly, H.S., Mohammed, F.F., Shaalan, M.I., Evaluation of hepatotoxic and genotoxic potential of silver nanoparticles in albino rats. *Exp. Toxicol. Pathol.*, 67, 21–29, 2015.
18. Navarro, E., Piccapietra, F., Wagner, B., Marconi, F., Kaegi, R., Odzak, N., Sigg, L., Behra, R., Toxicity of silver nanoparticles to *Chlamydomonas reinhardtii*. *Environ. Sci. Tech.,* 42, 8959–8964, 2008.
19. Song, W., Zhang, J., Guo, J., Zhang, J., Ding, F., Li, L., Sun, Z., Role of the dissolved zinc ion and reactive oxygen species in cytotoxicity of ZnO nanoparticles. *Toxicol. Lett.,* 199(3), 389–397, 2010.
20. Pujalté, I., Passagne, I., Brouillaud, B., Tréguer, M., Durand, E., Ohayon-Courtès, C., L'Azou, B., Cytotoxicity and oxidative stress induced by different metallic nanoparticles on human kidney cells. *Part. Fibr. Toxicol.*, 8, 1–16, 2011.
21. Reddy, K.M., Feris, K., Bell, J., Wingett, D.G., Hanley, C., Punnoose, A., Selective toxicity of zinc oxide nanoparticles to prokaryotic and eukaryotic systems. *Appl. Phy. Lett.*, 90, 213902–213907, 2007.
22. Bai, W., Zhang, Z., Tian, W., He, X., Ma, Y., Zhao, Y., Chai, Z., Toxicity of zinc oxide nanoparticles to zebrafish embryo: A physicochemical study of toxicity mechanism. *J. Nano. Res.*, 12(5), 1645–1654, 2010.
23. Sharma, V., Shukla, R.K., Saxena, N., Parmar, D., Das, M., Dhawan, A., DNA damaging potential of zinc oxide nanoparticles in human epidermal cells. *Toxicol Lett.*, 185, 211–218, 2009.
24. Xia, T., Kovochich, M., Liong, M., Mädler, L., Gilbert, B., Shi, H., Yeh, J.I., Zink, J.I., Nel, A.E., Comparison of the mechanism of toxicity of zinc oxide

and cerium oxide nanoparticles based on dissolution and oxidative stress properties. *ACS Nano.*, 2, 2121–2134, 2008.
25. Akhtar, M.J., Ahamed, M., Kumar, S., Khan, M.M., Ahmad, J., Alrokayan, S.A., Zinc oxide nanoparticles selectively induce apoptosis in human cancer cells through reactive oxygen species. *Int. J. Nano.*, 7, 845–851, 2012.
26. Sharma, V., Singh, P., Pandey, A.K., Dhawan, A., Induction of oxidative stress, DNA damage and apoptosis in mouse liver after sub-acute oral exposure to zinc oxide nanoparticles. *Mutat. Res. Genet. Toxicol. Environ. Mutagen.*, 745, 84–91, 2012.
27. Levard, C, Hotze, E.M., Lowry, G.V., Brown, G.E., Environmental transformations of silver nanoparticles: Impact on stability and toxicity. *Environ. Sci. Tech.*, 46, 6900–6914, 2012.
28. Borkow, G., Zhou, S.S., Page, T., Gabbay, J., A novel anti influenza copper oxide containing respiratory face mask. *PLoS One*, 5(6), 11295–11300, 2010.
29. Nations, S., Wages, M., Long, M., Theodorakis, C., Cobb, G.P., Acute effects of ZnO and CuO nanoparticles on *Xenopus laevis*. *Chemosphere*, 83, 1053–1061, 2011.
30. Nations, S., Long, M., Wages, M., Maul, J.D., Theodorakis, C.W., Cobb, G.P., Subchronic and chronic developmental effects of copper oxide (CuO) nanoparticles on *Xenopus laevis*. *Chemosphere.,* 135, 166–174, 2015.
31. Aruoja, V., Pokhrel, S., Sihtmäe, M., Mortimer, M., Mädler, L., Kahru, A., Toxicity of 12 metal-based nanoparticles to algae, bacteria and protozoa. *Environ. Sci. Nano.,* 2, 630–644, 2015.
32. Chibber, S., Ansari, S.A., Satar, R., New vision to CuO, ZnO, and TiO_2 nanoparticles: Their outcome and effects. *J. Nanopart Res.,* 15, 1492–1498, 2013.
33. Ahir, M., Bhattacharya, S., Karmakar, S., Mukhopadhyay, A., Mukherjee, S., Ghosh, S., Chattopadhyay, S., Patra, P., Adhikary, A., Tailored-CuO-nanowire decorated with folic acid mediated coupling of the mitochondrial-ROS generation and miR425-PTEN axis in furnishing potent anti-cancer activity in human triple negative breast carcinoma cells. *Biomaterials*, 76, 115–132, 2016.
34. Ivask, A., Titma, T., Visnapuu, M., Vija, H., Kakinen, A., Sihtmae, M., Shimmo, R., Toxicity of 11 metal oxide nanoparticles to three mammalian cell types *in vitro*. *Curr. Med. Chem.*, 15, 1914–1929, 2015.
35. Jacobo-Estrada, T., Santoyo-Sánchez, M., Thévenod, F., Barbier, O., Cadmium handling, toxicity and molecular targets involved during pregnancy: Lessons from experimental models. *Int. J. Mol. Sci.*, 18, 1590–1596, 2017.
36. Selim, K.K., Kang, I.K., Guo, H., Albumin-conjugated cadmium sulfide nanoparticles and their interaction with KB cells. *Macromol. Res.*, 17, 403–410, 2009.
37. Buffet, P.E., Zalouk-Vergnoux, A., Poirier, L., Lopes, C., Risso-de-Faverney, C., Guibbolini, M., Gilliland, D., Perrein-Ettajani, H., Valsami-Jones, E., Mouneyrac, C., Cadmium sulfide quantum dots induce oxidative stress and behavioral impairments in the marine clam *Scrobicularia plana*. *Environ Toxicol. Chem.*, 34, 1659–1664. 2015.

38. Cui, J., Liu, T., Li, F., Yi, J., Liu, C., Yu, H., Silica nanoparticles alleviate cadmium toxicity in rice cells: Mechanisms and size effects. *Environ. Pollut.,* 228, 363–369, 2017.
39. De Simone, U., Manzo, L., Profumo, A., Coccini, T., *In vitro* toxicity evaluation of engineered cadmium-coated silica nanoparticles on human pulmonary cells. *J. Toxicol.*, 1–11, 2013.
40. Shi, J., Hedberg, Y., Lundin, M., Odnevall Wallinder, I., Karlsson, H.L., Moller, L., Hemolytic properties of synthetic nano- and porous silica particles: The effect of surface properties and the protection by the plasma corona. *Acta Biomater.*, 8, 3478–3490, 2012.
41. Heinlaan, M., Ivask, A., Bilnova, I., Dubourguier, H.C., Kahru, A., Toxicity of nanosized and bulk ZnO, CuO and TiO_2 to bacteria *Vibrio fischeri* and crustaceans *Daphina magna* and *Thamnocephalus platyurus*. *Chemosphere*, 71, 1308–1316, 2008.
42. Pluskota, A., Horzowski, E., Bossinger, O., von Mikecz, A., In *Caenorhabditis elegans* nanoparticle-bio-interactions become transparent: Silica-nanoparticles induce reproductive senescence. *PLoS One*, 4, 6622–6628, 2009.
43. Wu, Q., Nouara, A., Li, Y., Zhang, M., Wang, W., Tang, M., Wang, D., Comparison of toxicities from three metal oxide nanoparticles at environmental relevant concentrations in nematode *Caenorhabditis elegans*. *Chemosphere*, 90, 1123–1131, 2013.
44. Slowing, I.I., Vivero Escoto, J.L., Wu, C.W., Lin, V.S.Y., Mesoporous silica nanoparticles as controlled release drug delivery and gene transfection carriers. *Adv. Drug. Deliv, Rev.*, 60, 1278–1288, 2008.
45. Namvar, F., Rahman, H.S.., Mohamad R., Cytotoxic effect of magnetic iron oxide nanoparticles synthesized via seaweed aqueous extract. *Int. J. Nanomed.*, 9, 2479–2488. 2014.
46. Fukushima, K., Tabuani, D., Abbate, C., Biopolymer-based nanocomposites, in: *A Handbook of Applied Biopolymer Technology: Synthesis, Degradation and Applications*, Sharma, S.K., Mudhoo, A. (Eds.), pp. 129–148, Royal Society of Chemistry, 2011.
47. Mendes, L.P., Delgado, J.M.F., Costa, A.D.A., Vieira, M.S., Benfica, P.L., Lima, E.M. Valadares, M.C., Biodegradable nanoparticles designed for drug delivery: the number of nanoparticles impacts on cytotoxicity. *Toxicol. In Vitro*, 29, 1268–1274, 2015.
48. Lopes, M., Aniceto, D., Abrantes, M., Simões, S., Branco, F., Vitória, I., Botelho, M.F., Seiça, R., Veiga, F., Ribeiro, A., *In vivo* biodistribution of antihyperglycemic biopolymer-based nanoparticles for the treatment of type 1 and type 2 diabetes. *Eur. J. Phar. Biopharm.*, 113, 88–96, 2017.

Part II

BIOSYNTHESIS OF METALLIC NANOPARTICLES

Suvardhan Kanchi and Shakeel Ahmed (eds.) Green Metal Nanoparticles, (165–198)
© 2018 Scrivener Publishing LLC

6

Current Advances in Biosynthesis of Silver Nanoparticles and Their Applications

Rajasekhar Chokkareddy, Niranjan Thondavada, Bakusele Kabane and Gan G. Redhi*

Electroanalytical Laboratories, Department of Chemistry, Durban University of Technology, Durban, South Africa

Abstract

Recent advances in nanotechnology and nanoscience have resulted in more enhanced techniques on the way we analyze, treat, and inhibit numerous diseases in all facets of human life. Silver nanoparticles (AgNPs) are one of the most vital and interesting nanomaterials amongst some of the metallic nanoparticles that are elaborated in many biomedical applications. For the development of silver nanoparticles, the biomolecules from various plant constituents and microbial species have been utilized as potential agents. These AgNPs are greatly used due to their orientation, physical properties, and small size, which are reported to have influence in conversion of the performance of any other material which is in contact with these tiny particles. In addition, AgNPs can be prepared by simple chemical, physical, and biological approaches. Furthermore, biosynthesis of AgNPs has been increased substantially in many of the established countries due to their improved response of environmentally friendly technology for measurable synthesis. However, the biological method is the most emerging approach in preparation, as this technique is easier when compared to other methods used, viz., less time consuming, eco-friendly, nontoxic and cheap. Furthermore, the significance of AgNPs are broadly discussed based on their multifunctional bioapplications; i.e., as antifungal, anti-inflammatory, antibacterial, antiviral, antiangiogenic and anticancer agents, and the anticancer activity mechanism of AgNPs.

Keywords: Biosynthesis, silver nanoparticles, bacteria and algae, antimicrobial and anticancer properties, catalytic activity and toxicity, anti-biomedical applications

**Corresponding author*: redhigg@dut.ac.za; chokkareddys@gmail.com

Suvardhan Kanchi and Shakeel Ahmed (eds.) Green Metal Nanoparticles, (167–198)
© 2018 Scrivener Publishing LLC

6.1 Introduction

Due to recent economic developments and industrialization the environment has suffered immensely, with huge amounts of dangerous and unessential chemicals, gases or materials being released into the air. The onus is now upon us in the scientific community to learn more about the mysteries of nature and its crops, which leads to increased innovation in the synthesis methods of nanoparticles [1]. Nanotechnology applications are extremely suitable for biological molecules because of their high-class properties. The biological particles undergo greatly controlled association processes to prepare them for suitable metal nanoparticle production, which was found to be reliable and environmentally friendly [2]. A number of chemical and physical procedures have been used for the synthesis of metal nanoparticles; however, some of these existing techniques have disadvantages, i.e., use of toxic solvents, formation of hazardous products and high-energy consumption, etc. As a result, there is a crucial requirement to improve eco-friendly processes for the preparation of metal nanoparticles. The expansion of eco-friendly technologies in physical synthesis is of great importance so as to expand their application to biological systems [3, 4]. In recent years, many synthesis methods of green nanoparticles with well-defined sizes, chemical composition, and morphology have been introduced, and their applications in several innovative technological areas have been explored. Hence, green synthesis methods using different biological organisms, such as mold, yeast, bacteria, algae and plant extracts, have been established for the synthesis of nanoparticles [5]. Moreover, AgNPs have been used commercially for a wide range of coating areas with energy contact actions, electronics, and medicines. AgNPs play a key role in the commercial applications of these nanoparticles in the field of pharmaceutical and other medical sciences (Figure 6.1). In addition, AgNPs, owing to their great bioactivity against bacteria, protozoa, fungi and viruses, are measured to be the most promising of any antimicrobial agent [6–8]. A large number of microorganisms, such as fungus, bacteria, yeasts, and plants, either intra- or extracellular, which are of higher crop yields and lower costs have been revealed to be capable of synthesizing nanoparticles [9]. The high efficiency of AgNPs is essentially due to the accessibility of larger surface area to volume ratio for interactions, easing the penetration and disruption of nanoparticles into the bacterial cells, as compared to micro-sized silver ions [10]. The purpose of our study is to open new views and probe future applications of nanomaterial biosynthesis as potential antimicrobial agents.

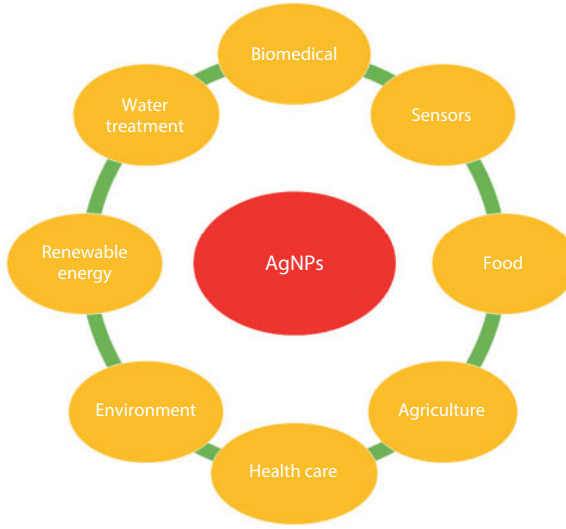


Figure 6.1 Various applications of silver nanoparticles.

6.2 Synthesis of Nanoparticles

The preparation of metallic nanoparticles mainly consists of two approches, i.e., top-down or bottom-up, by physical, chemical, and biological methods. Biogenic syntheses of silver nanoparticles are classified under bottom-up approach. The top-down method essentially works with the solid in its bulk form, and the size reduction to the nanoscale is then attained by specific ablations, i.e., thermal decomposition, mechanical milling, etching, lithography, laser ablation, and sputtering [11]. Furthermore, the "bottom-up" method is superior for the synthesis of nanoparticles, containing an identical system in which catalysts (e.g., reducing agent and enzymes) manufacture nanostructures that are organized by catalyst assets, reaction media, and conditions (e.g., solvents, stabilizers and temperature). For example, chemical reduction process is the most common artificial pathway for metal nanoparticles prepartion [12]. The top-down and bottom-up preparations are shown in Figure 6.2.

Morover, wide-ranging chemical, biological, physical and hybrid techniques (Figure 6.3) are employed to prepare the various nanoparticles [6]. Hence, the synthesis of nanoparticles is usally dependant on two methods, i.e., chemical and physical. These methods contain solvothermal synthesis, ion sputtering, sol-gel techniques and reduction. Furthermore, in

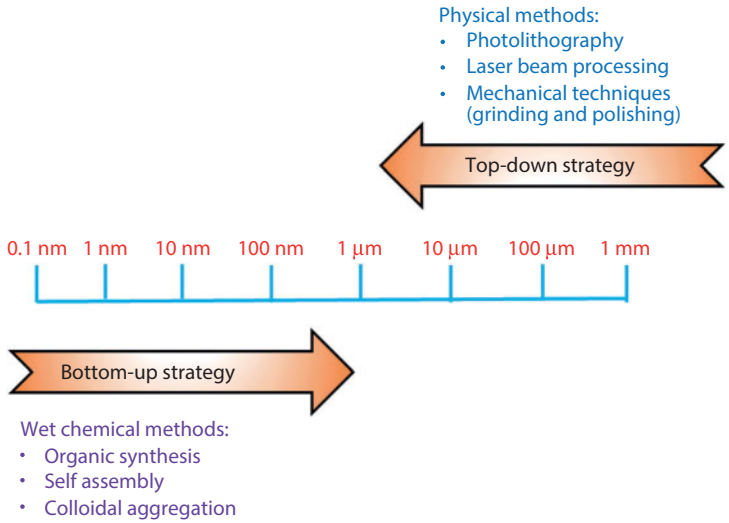


Figure 6.2 Top-down and Bottom-up synthesis approaches [13].

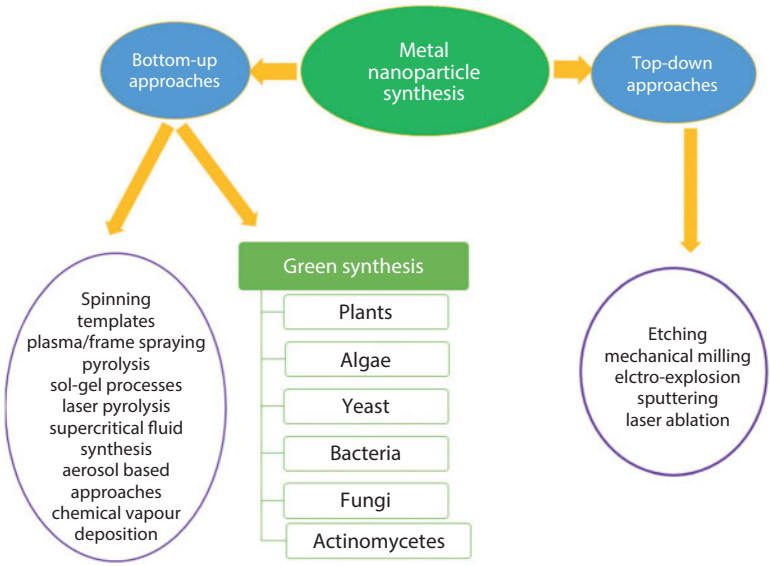


Figure 6.3 Different approaches for synthesis of silver nanoparticles.

biological procedures where the microbes and plants are used as reducing agents or protective agents these procedures can be used to synthesize the nanoparticels [14]. A lot of biological organisms that are mutually unicellular and multicultural, are known to produce inorganic materials either

intra- or extracellularly, regularly of nanoscale dimensions and of attractive morphology and classified assembly. In addition, the biosynthesis of nanoparticles employs usage of biological agents like fungi, bacteria, yeast, actinomycetes, algae and plants [15, 16]. The rate of reduction of metal ions using biological agents is found to be much faster and also occurs under ambient temperature and pressure conditions. Here, we summarize some of the organisms used in the biosynthesis of nanomaterials and describe the properties that should be inherent for the production of nanoparticles with desired characteristics.

6.2.1 Green Synthesis of Nanoparticles and its Benefits

Green synthesis of silver nanoparticles includes choosing properties and materials which are cost effective and include bulk preparations. These techniques are associated with atmospheric pressure, less energy consumption, low temperature and are free of toxic chemicals [17]. Green synthesis of nanoparticles are mainly classfied into five methods: Tollens' technique, irradiation method, polysaccharide method, polyoxometalates method and biological method. Tollens' process is involved in a one-step process. In this method, the reduction of Ag^+ ions is done by introducing saccharides in the existence of ammonia, yielding silver nanoparticles with various sizes and shapes of 50–200 nm [18]. In the irradiation method, the metal nanoparticles can be synthesized by using many irradiation procedures at room temperature without the use of a dipping agent. Therefore, temperature-dependent covering agents can also be used in the irradiation process. In addition, silver nanoparticles with a distinct shape and size distribution, for example, can be found from laser irradiation of an aqueous solution of silver salt and surfactant [19]. By using the polysaccharide process, metal nanoparticles are produced by using water and polysaccharide substitutes as a stabilizing agent, a reducing agent, or both reducing and stabilizing agents. For example, the fabrication of silver nanoparticles can be achieved by using starch as a defensive agent and β-d-glucose as a reductant in a mild-heating system. Furthermore, in this way the magnetism among starch and silver nanoparticles is weak and flexible at higher temperatures, enabling the separation of the produced silver nanoparticles [20]. Polyoxometalates have the potential of manufacturing silver nanoparticles since they are soluble in water and have the ability of experiencing a stepwise, multi-electron redox process without distressing their structure [21]. Extracts from bioorganisms might perform both as reducing and capping agents in silver nanoparticles preparation. In addition, the reduction of Ag^+ ions by amalgamation of biomolecules found in these extracts, such as enzymes/proteins, polysaccharides, amino acids, and vitamins, is

environmentally benign, yet chemically complex. A large volume of the literature reports include effective synthesis of silver nanoparticles using bio-organic compounds. The rate of reduction of silver ions using biological agents is said to be much faster and also occurs at ambient temperature and pressure situations. Figure 6.4 shows some of the TEM images of silver nanoparticles by various methods. Green chemistry unites a few novel approches for the synthesis, processing and uses of chemical substaences in such a way as to decrease threats to health and environment. The novel approaches are:

- Clean chemistry
- Atom economy
- Environmentally caring chemistry
- Benign-by-design chemistry

The main aim of green chemistry is to protect the envionment from pollutants. Green chemistry is the methodology to design, manufacture and use chemical products to intentionally decrease or remove chemical hazards.

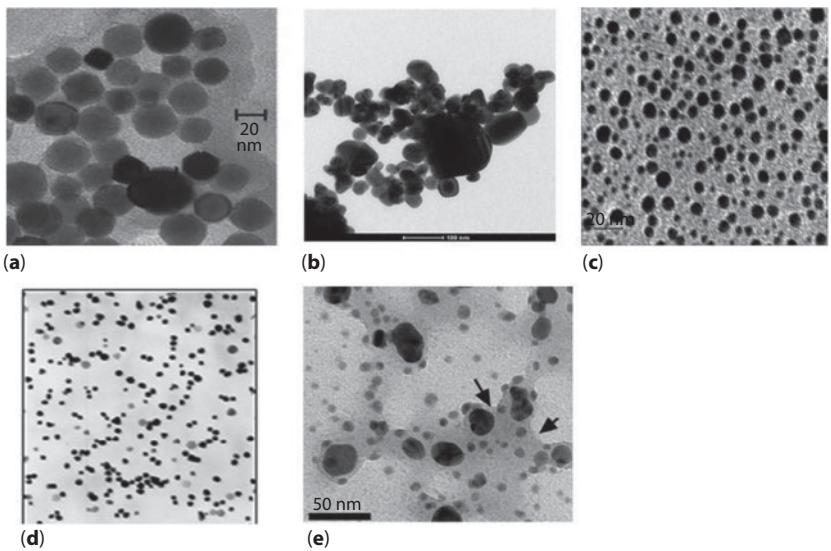


Figure 6.4 (a) TEM image of silver nanoparticles by Tollens' method [22]. (b) TEM image of silver nanoparticles by irradiation method [23]. (c) TEM image of starch silver nanoparticles by polysaccaride method [24]. (d) TEM image of silver nanoparticles by polyoxometalate method [25]. (e) TEM image of silver nanoparticles by biological method [26].

Advantages of green syntheses include:

- Energy efficiency
- Economical
- Less waste
- Fewer accidents
- Lower cost of production and regulation
- Competitive
- Safer products
- Healthier work places and communities
- Protects human health and the environment
- Compatible for pharmaceutical and other biomedical applications
- Can be used for large-scale production of nanoparticles and external experimental conditions like high energy and high pressure are not required, leading to substantial energy saving processes.

6.2.2 Synthesis of Silver Nanoparticles by Bacteria and Fungi

The first silver nanoparticle synthesizing bacteria were prepared using the *Pseudomonas stutzeri* AG259 strain that was isolated from the soil of silver mines. In this synthesis, some microorganisms that can survive high metal ion concentrations, can also develop under those environments, and this occurrence is due to their resistance to that metal. These elaborating mechanisms in the resistance are efflux organisms, which modify solubility and toxicity through oxidation or reduction, bioaccumulation, biosorption, extracellular composite development or precipitation of metals, and absence of definite metal transportation systems. After that, many syntheses procedures were established, i.e., green synthesis of silver naoparticles using 30 cyanobacteria was examined [27]. Cyanobacterial aqueous sources were then subjected to silver nanoparticles synthesis at 30 °C. The results are primarily confirmed by UV, in this case scanning of these aqueous extracts with silver nanoparticles in UV-visible range exhibited a single peak. SEM micrographs of silver nanoparticles from cyanobacterial extracts showed that though preparation of nanoparticles followed in all strains, their reaction time (30 to 360 h), shape, and size (38 to 88 nm) varied (Table 6.1). Moreover, extracellular green synthesis of silver nanoparticles using *Pseudomonas aeruginosa* [28] and *Escherichia coli* [29] were described. Fungi and other microorganisms are superior candidates

Table 6.1 Fungal and bacterial green synthesis of silver nanoparticles of different sizes.

Producer organism	Size (nm)	Ref.
Candida albicans	50–100	[31]
Fusarium sp.	12–20	[34]
Trichoderma harzianum	19–63	[35]
Fusarium solani	5–30	[36]
Cunninghamella phaeospora	12.2	[27]
Aspergillus versicolor	15.5	[37]
Colletotrichum sp.	20–50	[38]
Aspergillus clavatus	25–145	[39]
Aspergillus niger	25–175	[39]
Aspergillus flavus	45–185	[39]
Aspergillus fumigatus	5–95	[39]
Trichoderma viride	15.5	[40]
Penicillium expansum	14–25	[41]
Aspergillus terreus	10–18	[41]
Cyanobacteria aqueous	38–88	[27]
Nocardiopsis valliformis	5–50	[42]
Bacillus pumilus, B. persicus	77–92	[43]
Pilimelia columellifera	12.7	[44]
Bacillus safensis	5–30	[45]
Corynebacterium glutamicum	15	[46]
Pseudomonas mandelii	1.9–10	[47]

in the preparation of metal nanoparticles (Figure 6.5) with dissimilar sizes (Table 6.1), due to their capability to discharge a large amount of enzymes. Many reducing agents are emitted by microbes (Figure 6.6). For example, Salvadori *et al.* [30] described a biological method that used dead biomass of the fungus *Hypocrea lixii,* as a new, effective and eco-friendly bioprocess for the synthesis of nanomaterials. Biological synthesis of silver nanoparticles was initiated to be between 123–195 nm size [9], 50–100 nm using the fungus *Pestaloptiopsis pauciseta* [31] and 20–80 nm using *Candida albicans* [32]. While in comparison with bacteria, fungi can produce superior amounts of nanoparticles, as they can secrete larger amounts of proteins which simply translate to higher production of nanoparticles [6]. In

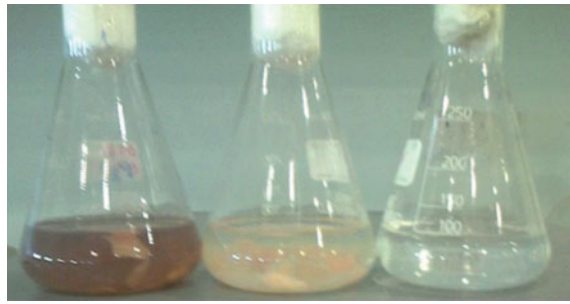


Figure 6.5 Conversion of silver nitrate to silver nanoparticles: (a) silver nitrate solution inoculated with biomass of *Fusarium moniliforme*, (b) distilled water immunized with biomass of *F. moniliforme*, (c) silver nitrate solution without biomass of *F. moniliforme* [33].

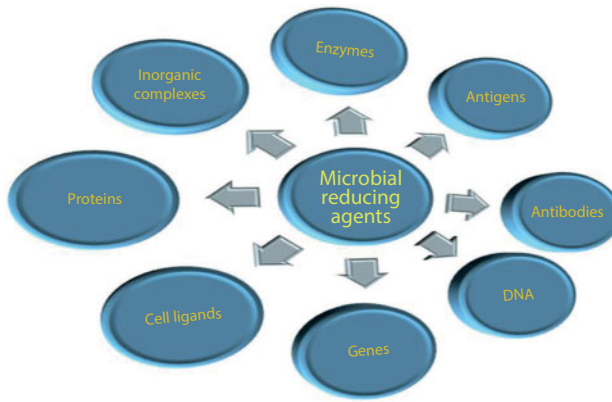


Figure 6.6 Reducing agents within microbial synthesis of silver nanoparticles.

addition, the mechanism of silver nanoparticle manufacture by fungi is known to follow the following steps: trapping of Ag^+ ions at the surface of the fungal cells and the subsequent reduction of the silver ions by the enzymes present in the fungal system. However, although the exact mechanism for elaborating silver nanoparticle construction by fungi is not fully understood, it is thought that the above-stated occurrence is responsible for the procedure. The main disadvantage of using microbes to synthesize silver nanoparticles is that it is a very sluggish procedure in comparison to plant extracts. Therefore, the use of plant extracts to synthesize silver nanoparticles represents a choice that is more plausible.

6.2.3 Synthesis of Silver Nanoparticles by Algae

Sinha *et al.* [48] described a method in which silver nanoparticles (size of 34.03 nm) were produced within a few minutes of silver ions coming in contact with the algal extract of *Pithophora oedogonium*. Patel *et al.* [49] describe silver nanoparticles manufactured by various strains of microalgae, including *Botryococcus braunii, Coelastrum* sp., *Spirulina* sp. and *Limnothrix* sp. exhibited diameters of 15.67, 19.28, 13.85 and 25.65 nm, respectively, silver nanoparticles of sizes between 15 and 47 nm were biosynthesized using aqueous extract of *Chlorella vulgaris* as reducing agent [50]. Later, Abdelghany *et al.* [27] estimated the antitumor efficiency of several concentrations of silver nanoparticles biosynthesized by the blue green algae *Anabaena oryzae, Nostoc muscorum* and *Calothrix marchic* on Ehrlich-Lettre ascites carcinoma *in vitro*. These procedures provide appropriate evidence for cellular internalization and biotransformation of silver nanoparticles in *Chlamydomonas reinhardtii*, which are very functional for accepting the performance and fate of silver nanoparticles in an aquatic environment. AgNPs were synthesized using *Spirulina platensis* (average size of most particles was 11.5 nm) and *Nostoc* sp. (average size of most particles was 20.3 nm) at room temperature and were calculated by Abdelghany *et al.* [27].

6.2.4 Synthesis of Silver Nanoparticles by Plants

In recent years, nanoparticle preparation has been one the most attractive scientific areas of interest, and attention has been evolving to producing nanoparticles using plant extracts. The main benefit of using plant extracts for silver nanoparticle preparation is that they are easily available, safe and nontoxic in extreme cases, have a wide-ranging variety of metabolites that can aid in the reduction of silver ions, are faster than microbes in synthesis and have significant phytochemicals that can be used as reducing agents for silver nanoparticles synthesis (Figure 6.7). Table 6.2 shows the names of the plant extracts used to prepare silver nanoparticles, as well as the shape and size of the nanoparticles. The main mechanism measured for the procedure is plant-assisted reduction, due to phytochemicals. Green synthesis of silver nanoparticles was attained using extracts from sixteen usually accessible plants by sonication method [51]; and an antibacterial evaluation of the effects of biosynthesized silver nanoparticles against bacteria (*E. coli, Salmonella paratyphi, S. aureus* and *B. subtilis*) was carried out, which revealed outstanding antibacterial activity. Moreover, synthesis of silver naoparticles has been established using extracts of *Chrysophyllum*

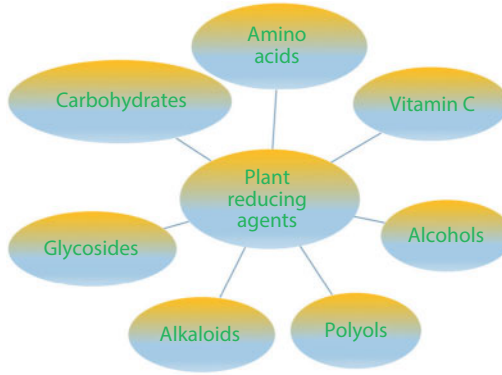


Figure 6.7 Bioreductant phytochemicals.

oliviforme, reducing aqueous silver nitrate [52]. In addition, the silver nanoparticles were prepared over a green route with the use of *Momordica charantia* leaf extracts equally with reductant and stabilizer [53].

6.2.5 Need for Green Synthesis

Nature has invented numerous processes for the preparation of nano- and micro-length scaled inorganic materials, which have contributed to the enhancement of this moderately new and largely unexplored area of research based on the biosynthesis of nanomaterials. Moreover, synthesis using bio-organisms is compatible with the green chemistry principles. "Green synthesis" of nanoparticles makes use of eco-friendly, nontoxic and safe reagents. Nanoparticles synthesized using biological methods or green technology have diverse natures, with greater stability and suitable sizes, since they are manufactured using a one-step procedure. Furthermore, green synthesis of nanoparticles is a careful bottom-up approach where the key reaction arising is reduction/oxidation. The biosynthesis of designed nanoparticles is costly in terms of the physical and chemical methods needed. A lot of chemical synthesis processes lead to the existence of some of the toxic chemicals engaged on the surface, which may have adverse effects in medical applications [74]. This is, however, not an issue when it comes to biosynthesized nanoparticles via the green synthesis route [75]. Therefore, in the examination of cheaper pathways for nanoparticle synthesis, scientists have used microbial enzymes and plant extracts (phytochemicals). Their antioxidant or reducing properties are regularly responsible for the reduction of metal compounds into their individual nanoparticles. Green synthesis offers innovation over chemical and physical techniques,

Table 6.2 Bionanoparticles synthesized using botanicals with their size, shape and references.

Plant	Parts used	Metal/ alloy	Size/shape	Ref.
Pelargonium graveolens	Leaves	Ag^+	16–40 nm/ quasilinear superstructures	[54]
Aloe vera	Pulp	Ag^+	25 nm/ spherical	[55]
Eclipta	Leaves	$AgNO_3$	-	[56]
Cycas	Leaves	Ag^+	3.29	[56]
Jatropha curcas	Latex	Ag^+	-	[1]
Cinnamomum zeylanicum	Bark	Ag^+	-	[57]
Black tea	Leaves	Au^{3+} Ag^+	-	[58]
Desmodium triflorum		Ag^+	5–20 nm/ spherical	[59]
Murraya koenigii	Leaves	Ag^+	20 nm/ hexagonal and nearly spherical	[60]
Citrus limon		Ag^+	-	[61]
Coriandrum sativum	Leaves	Ag^+	26 nm/ spherical	[62]
Gliricidia sepium	Leaves	Ag^+	27 nm/ spherical	[63]
Hibiscus rosa sinensis	Leaves	Ag^+		[64]
Jatropha curcas	seeds	Ag^+	15–50 nm	[1]
Capsicum annuum	Leaves	Ag^+	10–12 nm	[65]
Medicago sativa	Leaves	Ag^+	2–20 nm/ spherical	[66]
Quercetin	Leaves	Ag^+	Radius 1–1.5 mm	[67]
Rice paper plant stem	-	Ag^+	Below 100 nm	[54]

Aloe vera	Leaves	Silver, gold	Triangular, spherical	[68]
Emblica officinalis	Leaves	Silver, gold	10–20 nm, 15–25 nm	[69]
Azadirachta indica	Leaves	Ag^{+} gold	Ag core–Au shell Polydisperse, flat, plate-like, spherical, peculiar core–shell structure 5–35 nm diameter, 50–100 nm	[70]
Cinnamomum camphora	Leaves	Silver, gold	Triangular, spherical 55–80 nm	[71]
Capsicum annuum	Leaves	Silver	-	[72]
Pelargonium graveolens	Leaves	Silver	16–40 nm	[73]
Brassica juncea	Leaves	Silver, gold, copper	-	

as it is cost-effective, eco-friendly, easily scaled up for large-scale synthesis, and in this process there is no need to use high energy, pressure, temperature and toxic chemicals.

6.3 Biomedical Applications of Silver Nanoparticles

Green synthesis nanoparticles having numerous medical applications, i.e., antifungal, antibacterial, chemotherapy, drug carrier and antiviral. The main mechanism of action is silver nanoparticles entering the human body via the respiratory tract, gastrointestinal tract, skin and female genital tract through direct exchange of materials with the environment, creating an eco-friendly environment [76]. In addition, green synthesized silver nanoparticles act as reducing agents and stabilizers; silver nanoparticles are stabilized with proteins, bacteria, fungi, carbohydrates, plants and algae. For example, Naik *et al.* prepared silver nanoparticles from peptides with average size of 60–150 nm, these silver nanoparticles are combined with peptides to form a combinatorial phage-display peptide library [77]. The combinatorial peptide phase interacts with aerobic and anaerobic bacteria to produce the bacterial cellular proteins and these block the microbial respiratory chain system. Furthermore, the respiratory system forms a thin layer with peptidoglycan within the cytoplasmic membrane and outer membrane [78]. These layers interact with silver nanoparticles and enhance the cytoplasm, and bacterial activity. Silver nanoparticles have larger surface area, and due to the larger surface area easily interact with bacteria and fungi, which may create free radicals and induce oxidative stress, thus further enhancing their bactericidal activity [79]. In addition, silver nanoparticles are used for treatment of wounds and burns or as a contraceptive and marketed as a water disinfectant and room spray. The use of silver nanoparticles is becoming more and more popular in medicine and associated applications.

6.3.1 Antibacterial Properties

Silver nanoparticles have a wide range of antibacterial impact on a range of Gram-positive and Gram-negative bacteria as well as antibiotic-resistant bacteria strains. The antibacterial efficiency of silver nanoparticles mainly depends on their size, concentration and shape. Moreover, the silver nanoparticles have greater antimicrobial properties, and therefore are regularly used in coating of bone prostheses, surgical devices, distillation methods and dental composites [80]. Silver nanoparticles are known to possess

oligodynamic properties and can destroy antibiotic-resistant microbes while applying partial cytotoxicity against mammalian cells. Gram-negative bacteria easily retain the color of the stain even after washing with any alcohols or acetone and include genera such as *Escherichia, Acinetobacter, Salmonella, Pseudomonas* and *Vibrio*. *Acinetobacter* types are related to nosocomial contagions, i.e., infections that are the result of treatment in hospitals or at healthcare service units, but secondary to the patient's original condition [81]. Gram-positive bacteria are those which lose the color of the stain after washing with alcohol or acetone, and include many well-known genera such as *Listeria, Enterococcus, Clostridium, Bacillus, Staphylococcus* and *Streptococcus*. The mechanisms of silver nanoparticles which caused cell death were observed in *E. coli* through the leakage of reducing sugars and proteins. In addition, silver nanoparticles are capable of terminating the permeability of the bacterial membranes via the bacterial membranes through the generation of several depths and gaps, signifying that silver nanoparticles might damage the structure of the bacterial cell membrane [82]. The activity of silver nanoparticles can thus be changed by numerous factors, and also by the characteristics of the nanoparticles (size, shape, coating); or attributable to the medium (presence of light, oxidative species, presence of other potential ligands for silver, ionic strength). Hence, these limitations will have an influence on many phenomena that can easily increase or decrease the antibacterial activity via complex pathways, as shown in Figure 6.8. Due to their large surface area to volume ratios, truncated triangular silver nanoplates show the strongest antibacterial activity.

6.3.2 Antimicrobial Activity

The risk posed by the potential outbreak of antibiotic-resistant microbes is increasing universally and demands a production outline of unique progressive stages for the study and expansion of additional effective antimicrobial agents against multidrug-resistant strains. Moreover, silver nanoparticles prepared by using *Abutilon indicum* leaf extract have revealed extremely powerful antibacterial activity on *Bacillus subtilis* (18.3 mm), *Staphylococcus aureus* (16.8 mm), *Salmonella typhi* (14.5 mm), and *Escherichia coli* (17.2 mm) [84]. In addition, the impregnation of *Ipomea carnea* silver nanoparticles with a cellulose acetate membrane to form a designed antimycobacterial membrane exhibited a 14 mm zone of inhibition on *Mycobacterium smegmatis* [85]. In many cases, the exact mechanisms behind these activities cannot be assumed. The mechanisms of antimicrobial effects of silver nanoparticles are still not completely

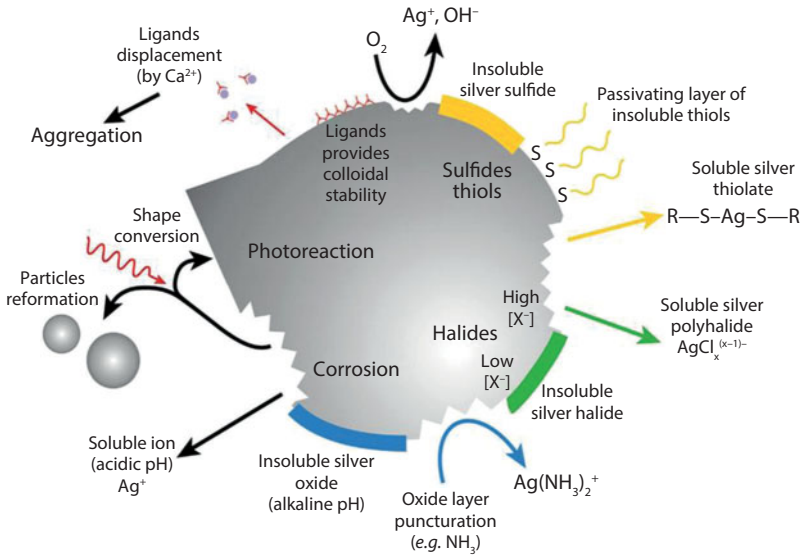


Figure 6.8 Graphical illustration of several phenomena affecting silver nanopartcles dissolution [83].

understood, but some studies have exposed that silver nanoparticles may be attributed to the adversely charged bacterial cell wall and separation, which leads to denaturation of protein and finally cell death, as shown in Table 6.3. Several studies propose that:

1. silver nanoparticles can be assigned to the surface of the cell membrane, disturbing penetrability and inhalation functions of the cell. Bactericidal action depends upon the surface area of the nanoparticles. For example, smaller silver nanoparticles having a large surface area accessible for interaction would give more bactericidal effect than the larger silver nanoparticles.
2. It is also possible that silver nanoparticles not only interact with the surface of membrane, but can also penetrate inside the cell wall of the bacteria.
3. silver nanoparticles synthesized with disaccharides, maltose and lactose, have a higher antibacterial activity than those synthesized using monosaccharides, glucose and galactose
4. Sodium dodecyl sulfate (SDS) and Tween 80 has the ability to modify antibacterial activity. Hence, they can easily

Table 6.3 Applications of silver nanoparticles in pharmaceutics, medicine and dentistry.

Pharmaceutics & Medicines	Treatment of dermatitis; inhibition of HIV-1 replication
	Treatment of ulcerative colitis & acne
	Antimicrobial effects against infectious organisms
	Remote laser light-induced opening of microcapsules
	Silver/dendrimer nanocomposite for cell labeling
	Molecular imaging of cancer cells
	Enhanced Raman scattering (SERS) spectroscopy
	Detection of viral structures (SERS & Silver nanorods)
	Coating of hospital textile (surgical gowns, face mask)
	Additive in bone cement
	Implantable material using clay layers with starch-stabilized silver nanoparticles
	Orthopedic stocking
	Hydrogel for wound dressing
Dentistry	Additive in polymerizable dental materials Patent
	Silver-loaded SiO_2 nanocomposite resin filler (dental resin composite)
	Polyethylene tubes filled with fibrin sponge embedded with AgNPs dispersion

bind to constituents of the bacterial cell and disturb the usual functions of the cell. Additional possible mechanisms involve the release of Ag cations, which are antibacterial, from silver nanoparticles [86].

6.3.3 Anticancer Activity of Silver Nanoparticles

Conventional plans for combating cancer interference include surgery, radiation therapy and chemotherapy. While several chemotherapeutic agents are now being used on various types of cancers, the side effects are huge, and administrations of chemotherapeutic agents by intravenous infusion is often a deadly process [87]. Hence, it is essential to develop technologies to avoid systemic side effects. Silver nanoparticles perform well as cancer therapeutics as they can interrupt the mitochondrial respirational chain, which makes the generation of reactive oxygen species

(ROS), and ATP synthesis, which can induce DNA damage [88], useful. Moreover, at this stage, numerous researchers are interested in developing nanomaterials as a substitute tool to create preparations that can target tumor cells directly. Some research laboratories have used many cell lines to address the chances of discovering a new molecule to fight cancer. For example, Gopinath *et al.* [89] examined the molecular mechanism of silver naoparticles and found that automatic cell death was concentration-dependent. Furthermore, they detected a synergistic effect on apoptosis using uracil phosphoribosyltransferase (UPRT)-expressing cells and non-UPRT-expressing cells in the presence of fluorouracil (5-FU). Under these investigational conditions, they identified that silver nanoparticles not only induce apoptosis but also alert cancer cells. Furtehrmore, the usage of nanoparticles as a carrier is extremely developed. However, a different feature of nanoparticles that needs close attention is their impressive property of acting as a drug by themselves. The major demand that arises when such features are put into focus is the mechanism by which the nanoparticles avoid the cancer cells. This response is yet to be revealed. Numerous attempts have been made to use silver nanoparticles as an anticancer agent and they have all turned up positive. In addition, the next milestone will be the detection of the mechanism of action. Figure 6.9 displays the possible mechanism by which silver nanoparticles target cancer cells.

6.3.4 Antidiabetic Activity of Silver Nanoparticles

Diabetes is one of the most common and interesting diseases whose prevalence is increasing globally. Type-I diabetes, which is the total deficiency of insulin secretion and related autoimmune damage of pancreatic β-cells, is expected to be widespread among relatives of those with the disease. However, Type-II diabetes, which accounts for 90% of cases, is initiated by the combination of resistance to insulin action and decreased insulin secretion [90]. The aptitude of silver nanoparticles produced using stem extract of *Tephrosia tinctoria* to regulate blood sugar levels was calculated. Silver nanoparticles searched out free radicals, lowered levels of enzymes that catalyze the hydrolysis of composite carbohydrates (α-glucosidase and α-amylase), and improved the consumption rate of glucose [91].

6.3.5 Wound Healing Activity of Silver Nanoparticles

Silver nanoparticles find remarkable use in topical ointments as well as creams used to inhibit wounds, burns and infections. Silver nanoparticles

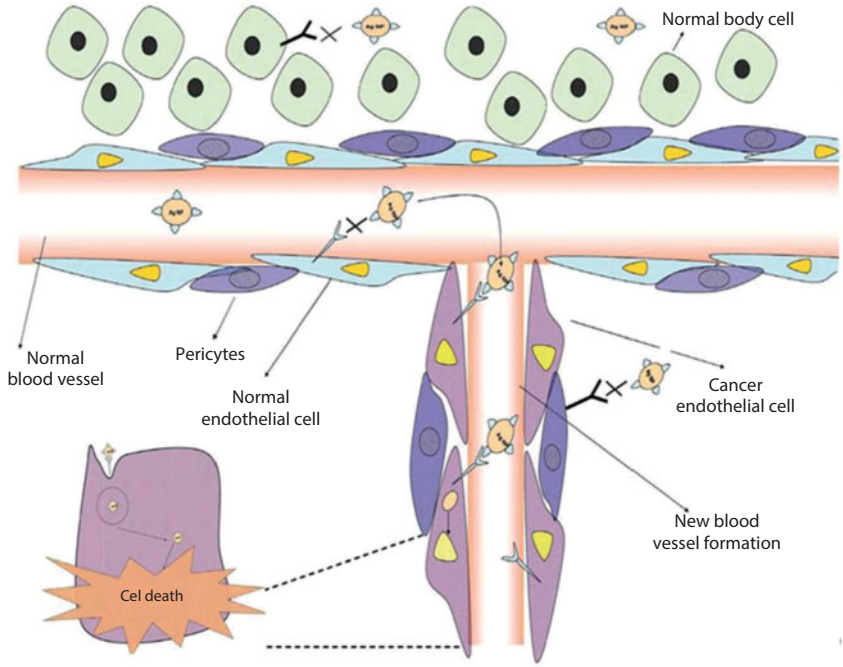


Figure 6.9 Possible mechanism for targeted delivery of silver nanoparticles in cancer therapy.

are extensively used in medical devices and implants. Furthermore, they are also added to consumer products, such as colloidal silver gel and silver-embedded materials, which are now available in generous amounts [92]. Silver nanoparticles manufactured *in situ* within the system of peptide fibers using UV radiation inhibited bacterial growth of *Pseudomonas aeruginosa, Escherichia coli* and *Staphylococcus aureus*. Silver nanoparticles-based hydrogels on HDFa cells did not display any important effect on cell viability. Silver-coated implants, biomedical devices [93] and textile fibers are being actively used for the treatment of wounds or burns, in addition to glass windows and other exterior parts, to preserve cleansing and hygienic conditions. In addition, metallic silver nanoparticles are active microbicides; therefore, they have garnered important attention in many products extending from paints to textiles. Silver nanoparticles synthesized extracellularly using the fungus *Aspergillus niger* are useful in controlling and elaborating cytokines in wound healing, as shown in a rat model [94]. An important reduction in cytokines was detected in wound healing in an average time of 3.35 days

for the silver nanoparticles fused onto the cotton fabric and bandages; bacterial clearance was also increased from diseased wounds with no adverse effects [95]. Silver nanoparticles utilize antimicrobial properties, producing reduction in wound irritation and modulation of fibrogenic cytokines. For example, some of the excised tissues were marked for histological analysis and wound area measurement using an H&E stain, which is shown in Figure 6.10. The epithelial tissue, which can be seen at the wound edge, signifies the migration of keratinocytes from the surrounding tissue to the wound bed. Epithelial and dermal tissues were redeveloped from under the wound bed, and cell movement from both sides of the wound margin to the central area of the wound was

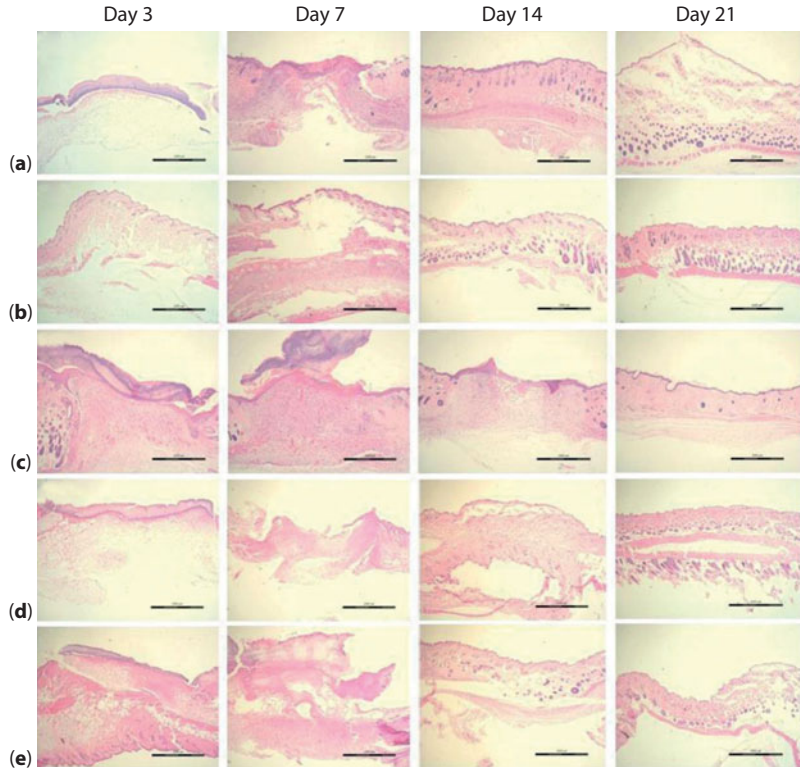


Figure 6.10 CS-AgNPs and AS-AgNPs ointment-stimulated wound closure under histological examination. Wounds were treated as follows: (a) not treated; (b) Silmazin® 1% cream; (c) Vaseline®; (d) CS-AgNPs ointment; and (e) AS-AgNPs ointment. The photomicrographs are representative of sections taken from wounds, which were stained using H&E. CKX41 microscopy (Olympus, Japan) was used at a 40× magnification. Scale bars represent 2000 μm [96].

identified. After 21 days, the skin morphology was somewhat normal, displaying an adequate thickness of the epidermal layer and the dermal layer in the Silmazin® 1% cream, chondroitin sulphate silver nanoparticles ointment (CS-AgNPs), and acharan sulphate silver nanoparticles ointment-treated groups (AS-AgNPs).

Figure 6.11 shows that the high collagen installation was observed along the granulation area in the CS-AgNPs and AS-AgNPs ointment-treated mice. After three days, no newly formed collagen deposition was observed in any group of mice due to the start of the inflammation phase.

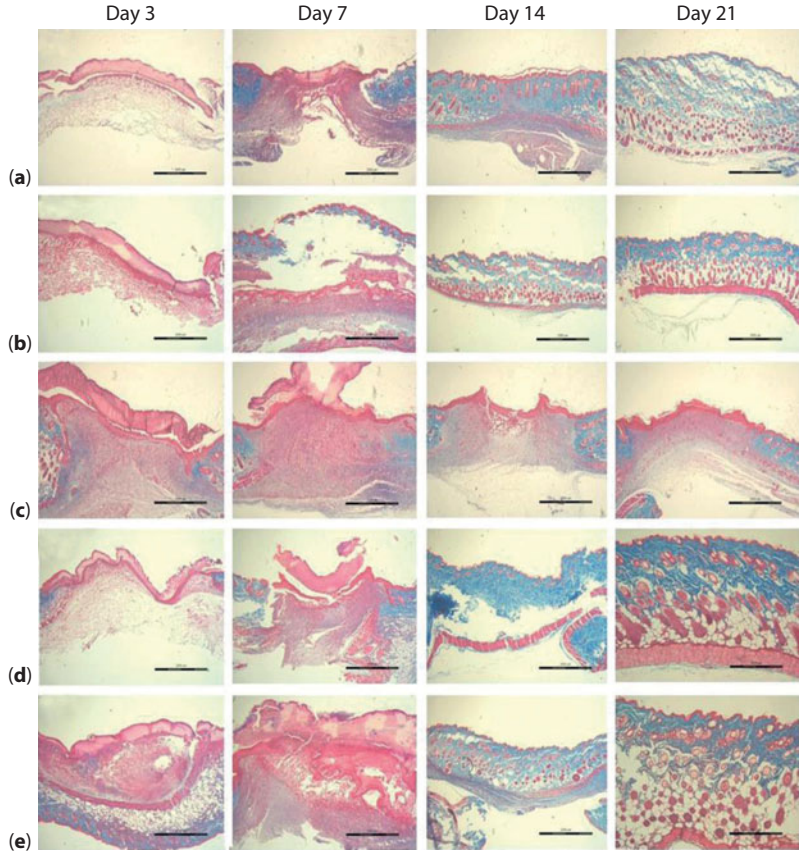


Figure 6.11 The CS-AgNPs and AS-AgNPs ointments accelerate granulation tissue and collagen deposition in the wound area. Wounds were treated as follows: (a) not treated; (b) Silmazin® 1% cream; (c) Vaseline®; (d) CS-AgNPs ointment; and (e) AS-AgNPs ointment. The photomicrographs are representative of sections taken from wounds, which were stained using Masson-Trichrome. CKX41 microscopy (Olympus, Japan) was used at 40× magnification. Scale bars represent 2000 μm [96].

6.3.6 Diagnosis and Imaging Activity of Silver Nanoparticles

Green synthesis was stimulated by scientists to develop new and advanced nanomaterials to offer improved biomolecular diagnosis, imaging and therapy. Silver nanoparticles are prominent for their exclusive and remarkable visual properties (intense color and high scattering of light), which are initiated due to localized surface plasmon resonance (SPR); for example, the mutual oscillations of free electrons at a metal dielectric interface when the frequency of instance light intersects with the frequency of electron oscillation. Moreover, these optical assets of silver nanoparticles are based on many limitations, such as their size, shape, composition and surroundings, along with the three-dimensional (3D) arrangement of elements. The size-reliant absorbance of silver nanoparticles was calculated to expose how the size and composition of nanoparticles can be active in changing the optoelectronic properties [97]. Based on these properties (excitation wavelength), Nie and Emory explained how the size and shape of silver nanoparticles and these nanoparticles are easily enhanced by signals in the region of 1014 to 1015 [98]. These enhancement signal properties were standardized and the results strongly recommend the idea of size-dependent localized SPR subsidizing surface-enhanced Raman signals, which are strong and sufficient to observe single molecules. The plasmonic properties of silver nanoparticles contribute to the large forces which were observed in the surface-enhanced Raman spectroscopy (SERS). Moreover, by using SERS, the Raman signal of a biomolecular analyte can be significantly increased by its being adsorbed onto hot-spot areas of the silver nanoparticles, such as gaps and intersections, primarily due to an increase in signal, which is strong and sufficient to allow even single biomolecule detection. In addition, conjugation of silver nanoparticles to proteins has more applications in imaging, catalysis, biosensing, drug delivery, therapy and control of protein assembly and activity. Walkey *et al.* calculated the interaction of serum albumins with silver nanoparticles, representing a two-fold increase in hysteresis results due to exposure of aggregated silver nanoparticles and the conformational change of serum albumins, signifying that this hysteresis system might be suitable in the bio-detection and bio-analysis applications of silver nanoparticles [99].

6.3.7 Medicinal Textile and Device Activity of Silver Nanoparticles

Green synthesized silver nanoparticles using *A. indica* and *A. dubius* leaf extract were fabricated on cotton cloth and moisture pad samples, which

displayed high resistance towards *Corynebacterium,* a sweat bacterium. Moreover, the antibacterial action of gauze cloth discs combined with silver nanoparticles manufactured by green mature thalli of *Anthoceros* exhibited antimicrobial activity against *Pseudomonas aeruginosa*. Based on these antibacterial activities, silver nanoparticles are widely used in medical and functional textiles, such as antibacterial fabrics which claim to prevent infection or deodorize [100]. Furthermore, the use of nanosilver in similar textiles, like home-cleaning textiles, gloves, sportswear, socks, and anti-odor clothes, have been reported.

6.3.8 Catalytic Activity of Silver Nanoparticles

Generally, high surface area and large surface energy evident from metal nanoparticles are necessary for the existence of effective catalytic medium. Developing small particles of silver nanoparticles have been perceived to be more active catalysts than constant colloidal nanoparticles. Silver nanoparticles are of specific interest in the present research of nanotechnology due to their exclusive properties, which can be combined in a broad range of applications such as catalysis, antiseptic agents in the medical industry, cosmetics, food packaging, bioengineering, electrochemistry, and environmental uses. In addition, when compared to their bulk materials, these noble nanoparticles have shown many catalytic activities. Nanocatalysis has generated much attention, giving rise to many new methods. For example, gold, silver, platinum and metal ions are well-known catalysts in the process of decomposition of H_2O_2 to oxygen [101]. Guo *et al.* explain the catalytic potential of silver nanoparticles compared to the gold and platinum nanoparticles in the emission system of chemiluminescence from luminol–H_2O_2 [102]. In this comparison, silver nanoparticles showed higher catalytic response than gold and platinum nanoparticles. Moreover, catalysis of the reduction of dyes by sodium borohydride ($NaBH_4$) can be enhanced by using silver nanoparticles immobilized on silica spheres. In the absence of silver nanoparticles as catalysts, the rate of reaction was almost stationary and it was shown that very little or even no reduction of the dyes occurred. Figure 6.12 shows more catalytic applications.

6.3.9 Toxicity of Silver Nanoparticles

Usually, silver nanoparticles can be regarded as an ideal candidate for numerous applications in many fields. This is particularly true for the biomedical industry, where they are used for diagnosis, cell imaging, drug delivery and implantation, even though some studies have reported that

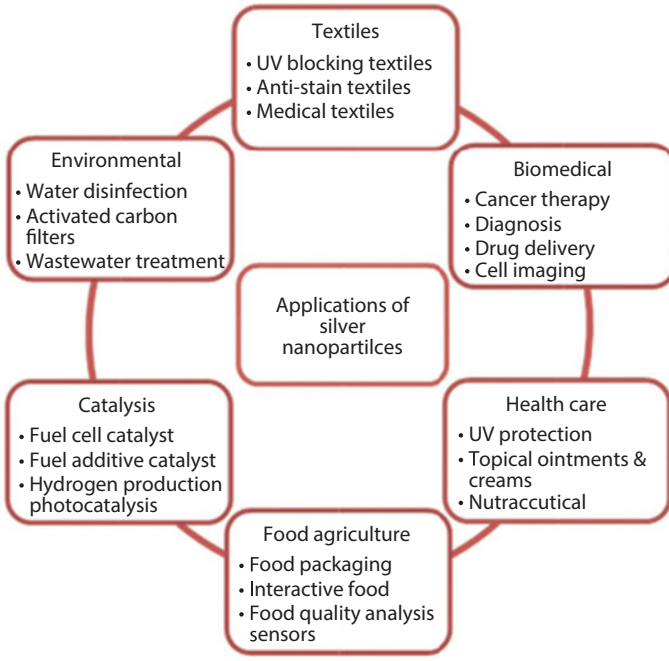


Figure 6.12 Applications of silver nanoparticles.

silver nanoparticles have an adverse effect on humans as well as the environment. One toxicological study on silver nanoparticles showed an *in-vitro* toxicity assay in rat liver cells, which confirmed that silver nanoparticles caused oxidative stress and cessation of mitochondrial function even at low level of exposure to silver nanoparticles (10–50 μg mL^{-1}). Yet, at higher doses (> 1.0 mg L^{-1}), silver nanoparticles revealed an important cytotoxicity and produced abnormal cellular shrinkage, cellular morphology, and attainment of an irregular shape. However, the above-mentioned studies tend to suggest that silver nanoparticles can adversely affect living beings, whilst comparatively less in *in-vivo* toxicology studies. Therefore, further study is essential to assess the toxicity effect of silver nanoparticles in *in-vivo* conditions for estimating their exact toxicity to humans and animals.

6.4 Conclusions

The main advantage of green methodology in the synthesis of nanoparticles over microbes, algae and plants is that the procedure can overcome

the time-consuming system of culturing microbes and putting in appropriate safeguards against losing the potentiality of synthesis of nanoparticles. These green synthesized silver nanoparticles are cost efficient, easy to synthesize, and focus on greener methodologies. Therefore, increasing awareness of green chemistry and use of the green route for preparation of silver nanopartcles leads to a desire to improve eco-friendly methods. Moreover, in spite of the fact that many biological substrates have been used for the manufacture of silver nanoparticles, the use of plants, algae and yeasts for the facile robust synthesis of silver nanoparticles is largely due to their ready availability, nonhazardous nature, variety of choices available, and the advantage of quicker synthesis over other techniques. Essentially, the green synthesis of metal nanoparticles using plant extracts have different uses, such as in therapeutics, pharmaceuticals, ecological and renewable energy as well as other commercial products; and have an estimated effect on diagnosis and action of numerous diseases with precise side effects. In addition, silver nanoparticles have a widerange of bioactivities which make them favorable agents not only in aggressive infections but also in attacking malignant tumors and, particularly, multidrug-resistant cancer cells. Silver nanoparticles are also used in cancer diagnosis and treatment monitoring. Numerous anticancer studies are underway in *in-vitro* analysis and a few *in-vivo* studies. Hence, this is an exposed area for several novel studies in cancer treatment with silver nanoparticles. Currently, the application of silver nanoparticles has been growing in many areas such as molecular diagnosis and imaging, drug delivery, cancer therapy, cure of vascular diseases and wound curing; and extended to include novel medical devices such as catheters with antimicrobial properties. Similarly, these silver nanoparticles would offer a potential solution to the present energy crisis by discovering their use as energy-driven devices.

References

1. Bar, H., Bhui, D.K., Sahoo, G.P., Sarkar, P., De, S.P., Misra, A., Green synthesis of silver nanoparticles using latex of *Jatropha curcas*. *Colloids Surf. A*, 339(1), 134–139, 2009.
2. Bar, H., Bhui, D.K., Sahoo, G.P., Sarkar, P., Pyne, S., Misra, A., Green synthesis of silver nanoparticles using seed extract of *Jatropha curcas*. *Colloids Surf. A*, 348(1), 212–216, 2009.
3. Nath, D., Banerjee, P., Green nanotechnology–A new hope for medical biology. *Environ. Toxicol. Pharmacol.*, 36(3), 997–1014, 2013.

4. Khademi-Azandehi, P., Moghaddam, J., Green synthesis, characterization and physiological stability of gold nanoparticles from *Stachys lavandulifolia* Vahl extract. *Particuology*, 19, 22–26, 2015.
5. Kaviya, S., Santhanalakshmi, J., Viswanathan, B., Muthumary, J., Srinivasan, K., Biosynthesis of silver nanoparticles using *Citrus sinensis* peel extract and its antibacterial activity. *Spectrochim. Acta A*, 79(3), 594–598, 2011.
6. Mohanpuria, P., Rana, N.K., Yadav, S.K., Biosynthesis of nanoparticles: Technological concepts and future applications. *J. Nano. Res.*, 10(3), 507–517, 2008.
7. Govindappa, M., Farheen, H., Chandrappa, C., Rai, V.R., Vinay, B., Mycosynthesis of silver nanoparticles using extract of endophytic fungi, *Penicillium* species of *Glycosmis mauritiana*, and its antioxidant, antimicrobial, anti-inflammatory and tyrokinase inhibitory activity. *Adv. Nat. Sci.: Nanosci. Nanotech.*, 7(3), 1–9, 2016.
8. Sharma, V.K., Yngard, R.A., Lin, Y., Silver nanoparticles: Green synthesis and their antimicrobial activities. *Adv. Colloid Interface Sci.*, 145(1), 83–96, 2009.
9. Vardhana, J., Kathiravan, G., Biosynthesis of silver nanoparticles by endophytic fungi *Pestaloptiopsis pauciseta* isolated from the leaves of *Psidium guajava* Linn. *Int. J. Pharm. Sci. Rev. Res.*, 31(1), 29–31, 2015.
10. Tennant, D.A., Durán, R.V., Gottlieb, E., Targeting metabolic transformation for cancer therapy. *Nat. Rev. Cancer*, 10(4), 267, 2010.
11. El-Nour, K.M.A., Eftaiha, A.A., Al-Warthan, A., Ammar, R.A., Synthesis and applications of silver nanoparticles. *Arab. J. Chem.*, 3(3), 135–140, 2010.
12. Wykes, T., Huddy, V., Cellard, C., McGurk, S.R., Czobor, P., A meta-analysis of cognitive remediation for schizophrenia: Methodology and effect sizes. *Am. J. Psychiatry*, 168(5), 472–485, 2011.
13. Ju-Nam, Y., Lead, J.R., Manufactured nanoparticles: An overview of their chemistry, interactions and potential environmental implications. *Sci. Total Environ.*, 400(1), 396–414, 2008.
14. Leutenegger, S., Chli, M., Siegwart, R.Y., BRISK: Binary robust invariant scalable keypoints, in: *Computer Vision (ICCV), 2011 IEEE International Conference*, pp. 2548–2555, IEEE, 2011.
15. Rai, P.K., Jaiswal, R.K. Singh, R.K. Gupta, Watal, G., Glycemic properties of *Trichosanthes dioica* leaves. *Pharm. Biol.*, 46(12) 894–899, 2008.
16. Thakkar, K.N., Mhatre, S.S., Parikh, R.Y., Biological synthesis of metallic nanoparticles. *Nanomedicine: NBM*, 6(2), 257–262, 2010.
17. Sasidharan, S., Chen, Y., Saravanan, D., Sundram, K., Latha, L.Y., Extraction, isolation and characterization of bioactive compounds from plants' extracts. *Afri. J. Tradit. Complement. Altern. Med.*, 8(1), 1–10, 2011.
18. Korbekandi, H., Iravani, S., Silver nanoparticles: The delivery of nanoparticles. *InTech Open*, 2012.
19. Van Phu, D., Duy, N.N., Lan, N.T.K., Du, B.D., Hien, N.Q., Study on antibacterial activity of silver nanoparticles synthesized by gamma irradiation method using different stabilizers. *Nanoscale Res. Lett.*, 9(1), 162, 2014.

20. Mochochoko, T., Oluwafemi, O.S., Jumbam, D.N., Songca, S.P., Green synthesis of silver nanoparticles using cellulose extracted from an aquatic weed; Water hyacinth. *Carbohydr. Polym.*, 98(1), 290–294, 2013.
21. Cauerhff, A., Castro, G.R., Bionanoparticles, a green nanochemistry approach. *Electron. J. Biotechnol.*, 16(3), 11, 2013.
22. Kvítek, L., Prucek, R., Panáček, A., Novotný, R., Hrbáč, J., Zbořil, R., The influence of complexing agent concentration on particle size in the process of SERS active silver colloid synthesis. *J. Mater. Chem.* 15(10), 1099–1105, 2005.
23. Van Phu, D., Quoc, L.A., Duy, N.N., Lan, N.T.K., Du, B.D., Luan, L.Q., Hien, N.Q., Study on antibacterial activity of silver nanoparticles synthesized by gamma irradiation method using different stabilizers. *Nanoscale Res. Lett.*, 9(1), 162, 2014.
24. Raveendran, P., Fu, J., Wallen, S.L., Completely "green" synthesis and stabilization of metal nanoparticles. *J. Am. Chem. Soc.*, 125(46), 13940–13941, 2003.
25. Tippayawat, P., Phromviyo, N., Boueroy, P., Chompoosor, A., Green synthesis of silver nanoparticles in aloe vera plant extract prepared by a hydrothermal method and their synergistic antibacterial activity. *PeerJ*, 4, e2589, 2016.
26. Ali, M., Kim, B., Belfield, K.D., Norman, D., Brennan, M., Ali, G.S., Green synthesis and characterization of silver nanoparticles using *Artemisia absinthium* aqueous extract—A comprehensive study. *Mater. Sci. Eng. C*, 58, 359–365, 2016.
27. Abdelghany, T., Al-Rajhi, A.M., Al Abboud, M.A., Alawlaqi, M., Magdah, A.G., Helmy, E.A., Mabrouk, A.S., Recent advances in green synthesis of silver nanoparticles and their applications: About future directions. A review. *BioNanoSci.*, 8, 5–16, 2018.
28. Quinteros, M.A., Aiassa I.M., Martínez, A., Dalmasso, P.R., Páez, P.L., Silver nanoparticles: Biosynthesis using an ATCC reference strain of *Pseudomonas aeruginosa* and activity as broad spectrum clinical antibacterial agents. *Int. J. Biomater.* 2016, 5971047, 2016.
29. Divya, K., Kurian, L.C., Vijayan, S., Manakulam Shaikmoideen, J., Green synthesis of silver nanoparticles by *Escherichia coli*: Analysis of antibacterial activity. *J. Water Environ. Nanotechnol.*, 1(1), 63–74, 2016.
30. Salvadori, M.R., Ando, R.A., Nascimento, C.A.O., Corrêa, B., Extra and intracellular synthesis of nickel oxide nanoparticles mediated by dead fungal biomass. *PloS One*, 10(6), e0129799, 2015.
31. Saminathan, K., Biosynthesis of silver nanoparticles from dental caries causing fungi *Candida albicans*. *Int. J. Curr. Microbiol. Appl. Sci.*, 4, 1084–1091, 2015.
32. Rahimi, G., Alizadeh, F., Khodavandi, A., Mycosynthesis of silver nanoparticles from *Candida albicans* and its antibacterial activity against *Escherichia coli* and *Staphylococcus aureus*. *Trop. J. Pharm. Res.*, 15(2), 371–375, 2016.

33. Al Abboud, M., Alawlaqi, M., Silver nanoparticles biosynthesis by *Fusarium moniliforme* and their antimicrobial activity against some food-borne bacteria. *Mycopath*, 11(1), 1–7, 2013.
34. Singh, A.K., Rathod, V., Singh, D., Ninganagouda, S., Kulkarni, P., Mathew, J., Haq, M.U., Bioactive silver nanoparticles from endophytic fungus *Fusarium* sp. isolated from an ethanomedicinal plant *Withania somnifera* (Ashwagandha) and its antibacterial activity. *Int. J. Nanomater. Biostruct.*, 5(1), 15–19, 2015.
35. Shelar, G.B., Chavan, A.M., Myco-synthesis of silver nanoparticles from *Trichoderma harzianum* and its impact on germination status of oil seed. *Biolife*, 3(1), 109–113, 2015.
36. EL-Aziz, A., Al-Othman, M., Mahmoud, M., Metwaly, H., Biosynthesis of silver nanoparticles using *Fusarium solani* and its impact on grain borne fungi. *Dig. J. Nanomater. Biostruct.*, 10(2), 655–662, 2015.
37. Netala, V.R., Kotakadi, V.S., Bobbu, P., Gaddam, S.A., Tartte, V., Endophytic fungal isolate mediated biosynthesis of silver nanoparticles and their free radical scavenging activity and anti microbial studies. *Biotech*, 6(2), 1–9, 2016.
38. Azmath, P., Baker, S., Rakshith, D., Satish, S., Mycosynthesis of silver nanoparticles bearing antibacterial activity. *Saudi Pharm. J.*, 24(2), 140–146, 2016.
39. Zomorodian, K., Pourshahid, S., Sadatsharifi, A., Mehryar, P., Pakshir, K., Rahimi, M.J., Arabi Monfared, A., Biosynthesis and characterization of silver nanoparticles by *Aspergillus* species. *BioMed Res. Int.*, 2016, 5435397, 2016.
40. Elgorban, A.M., Al-Rahmah, A.N., Sayed, S.R., Hirad, A., Mostafa, A.A.-F., Bahkali, A.H., Antimicrobial activity and green synthesis of silver nanoparticles using *Trichoderma viride*. *Biotechnol. Biotechnol. Equip.*, 30(2), 299–304, 2016.
41. Ammar, H., El-Desouky, T., Green synthesis of nanosilver particles by *Aspergillus terreus* HA1N and *Penicillium expansum* HA2N and its antifungal activity against mycotoxigenic fungi. *J. Appl. Microbio.*, 121(1), 89–100, 2016.
42. Rathod, D., Golinska, P., Wypij, M., Dahm, H., Rai, M., A new report of *Nocardiopsis valliformis* strain OT1 from alkaline Lonar crater of India and its use in synthesis of silver nanoparticles with special reference to evaluation of antibacterial activity and cytotoxicity. *Med. Microbiol. Immunol.*, 205(5), 435–447, 2016.
43. Elbeshehy, E.K., Elazzazy, A.M., Aggelis, G., Silver nanoparticles synthesis mediated by new isolates of *Bacillus* spp., nanoparticle characterization and their activity against Bean Yellow Mosaic Virus and human pathogens. *Front. Microbiol.*, 6, 453, 2015.
44. Golińska, P., Wypij, M., Rathod, D., Tikar, S., Dahm, H., Rai, M., Synthesis of silver nanoparticles from two acidophilic strains of *Pilimelia columellifera*

subsp. *pallida* and their antibacterial activities. *J. Basic Microbiol*., 56(5), 541–556, 2016.
45. Lateef, A., Adelere, I., Gueguim-Kana, E., Asafa, T., Beukes, L., Green synthesis of silver nanoparticles using keratinase obtained from a strain of *Bacillus safensis* LAU 13. *Int. Nano Lett*., 5(1), 29–35, 2015.
46. Gowramma, B., Keerthi, U., Rafi, M., Rao, D.M., Biogenic silver nanoparticles production and characterization from native stain of *Corynebacterium* species and its antimicrobial activity. *Biotech*, 5(2), 195–201, 2015.
47. Mageswari, A., Subramanian, P., Ravindran, V., Yesodharan, S., Bagavan, A., Rahuman, A.A., Karthikeyan, S., Gothandam, K.M., Synthesis and larvicidal activity of low-temperature stable silver nanoparticles from psychrotolerant *Pseudomonas mandelii*. *Environ*. *Sci. Pollut. Res*., 22(7), 5383–5394, 2015.
48. Sinha, S.N., Paul, D., Halder, N., Sengupta, D., Patra, S.K., Green synthesis of silver nanoparticles using fresh water green alga P*ithophora oedogonia* (Mont.) Wittrock and evaluation of their antibacterial activity. *Appl. Nanosci.*, 5(6), 703–709, 2015.
49. Patel, V., Berthold, D., Puranik, P., Gantar, M., Screening of cyanobacteria and microalgae for their ability to synthesize silver nanoparticles with antibacterial activity. *Biotechnol. Rep.*, 5, 112–119, 2015.
50. Annamalai, J., Nallamuthu, T., Green synthesis of silver nanoparticles: Characterization and determination of antibacterial potency. *Appl. Nanosci.*, 6(2), 259–265, 2016.
51. Firdhouse, M.J., Lalitha, P., Biogenic silver nanoparticles–Synthesis, characterization and its potential against cancer inducing bacteria. *J. Mol. Liq*., 222, 1041–1050, 2016.
52. Anju Varghesee, R., Anandhi, P., Arunadevi, R., Satin leaf (*Chrysophyllum oliviforme*) extract mediated green synthesis of silver nanoparticles: Antioxidant and anticancer activities. *J. Pharm. Sci. Res.*, 7(6), 266–273, 2015.
53. Ajitha, B., Reddy, Y.A.K., Reddy, P.S., Biosynthesis of silver nanoparticles using *Momordica charantia* leaf broth: Evaluation of their innate antimicrobial and catalytic activities. *J. Photochem. Photobiol. B*, 146, 1–9, 2015.
54. Shankar, S.S., Ahmad, A., Sastry, M., Geranium leaf assisted biosynthesis of silver nanoparticles. *Biotechnol. Prog*., 19(6), 1627–1631, 2003.
55. Zhang, Y., Yang, D., Kong, Y., Wang, X., Pandoli, O., Gao, G., Synergetic antibacterial effects of silver nanoparticles@aloe vera prepared via a green method. *Nano Biomed. Eng*., 2(4), 252–257, 2010.
56. Jha, A.K., Prasad, K., Kumar, V., Prasad, K., Biosynthesis of silver nanoparticles using *Eclipta* leaf. *Biotechnol. Prog*., 25(5), 1476–1479, 2009.
57. Sathishkumar, M., Sneha, K., Won, S., Cho, C.-W., Kim, S., Yun, Y.-S., *Cinnamon zeylanicum* bark extract and powder mediated green synthesis of nano-crystalline silver particles and its bactericidal activity. *Colloids Surf. B*, 73(2), 332–338, 2009.

58. Begum, N.A., Mondal, S., Basu, S., Laskar, R.A., Mandal, D., Biogenic synthesis of Au and Ag nanoparticles using aqueous solutions of Black Tea leaf extracts. *Colloids Surf. B.*, 71(1), 113–118, 2009.
59. Ahmad, N., Sharma, S., Singh, V., Shamsi, S., Fatma, A., Mehta, B., Biosynthesis of silver nanoparticles from *Desmodium triflorum*: A novel approach towards weed utilization. *Biotechnol. Res. Int.* 2011, 454090, 2011.
60. Philip, D., Unni, C., Aromal, S.A., Vidhu, V., Murraya Koenigii leaf-assisted rapid green synthesis of silver and gold nanoparticles. *Spectrochim. Acta A*, 78(2), 899–904, 2011.
61. Prathna, T., Chandrasekaran, N., Raichur, A.M., Mukherjee, A., Biomimetic synthesis of silver nanoparticles by *Citrus limon* (lemon) aqueous extract and theoretical prediction of particle size. *Colloids Surf. B.*, 82(1), 152–159, 2011.
62. Sathyavathi, R., Krishna, M.B., Rao, S.V., Saritha, R., Rao, D.N., Biosynthesis of silver nanoparticles using *Coriandrum sativum* leaf extract and their application in nonlinear optics. *Adv. Sci. Lett.*, 3(2), 138–143, 2010.
63. Raut Rajesh, W., Lakkakula Jaya, R., Kolekar Niranjan, S., Mendhulkar Vijay, D., Kashid Sahebrao, B., Phytosynthesis of silver nanoparticle using *Gliricidia sepium* (Jacq.). *Curr. Nanosci.*, 5(1), 117–122, 2009.
64. Philip, D., Green synthesis of gold and silver nanoparticles using *Hibiscus rosa sinensis*. *Physica E: Low Dimens. Syst. Nanostruct.*, 42(5), 1417–1424, 2010.
65. Li, S., Shen, Y., Xie, A., Yu, X., Qiu, L., Zhang, L., Zhang, Q., Green synthesis of silver nanoparticles using *Capsicum annuum* L. extract. *Green Chem.*, 9(8), 852–858, 2007.
66. Gardea-Torresdey, J.L., Gomez, E., Peralta-Videa, J.R., Parsons, J.G., Troiani, H., Jose-Yacaman, M., Alfalfa sprouts: A natural source for the synthesis of silver nanoparticles. *Langmuir*, 19(4), 1357–1361, 2003.
67. Egorova, E., Revina, A., Synthesis of metallic nanoparticles in reverse micelles in the presence of quercetin. *Colloids Surf. Physicochem. Eng. Asp.*, 168(1), 87–96, 2000.
68. Chandran, S.P., Chaudhary, M., Pasricha, R., Ahmad, A., Sastry, M., Synthesis of gold nanotriangles and silver nanoparticles using *Aloevera* plant extract. *Biotechnol. Prog.*, 22(2), 577–583, 2006.
69. Ankamwar, B., Chaudhary, M., Sastry, M., Gold nanotriangles biologically synthesized using tamarind leaf extract and potential application in vapor sensing. *Synth. React. Inorg. M.*, 35(1), 19–26, 2005.
70. Shankar, S.S., Rai, A., Ahmad, A., Sastry, M., Rapid synthesis of Au, Ag, and bimetallic Au core–Ag shell nanoparticles using Neem (*Azadirachta indica*) leaf broth. *J. Colloid Interface Sci.*, 275(2), 496–502, 2004.
71. Huang, J., Li, Q., Sun, D., Lu, Y., Su, Y., Yang, X., Wang, H., Wang, Y., Shao, W., He, N., Biosynthesis of silver and gold nanoparticles by novel sundried *Cinnamomum camphora* leaf. *Nanotechnology*, 18(10), 105104, 2007.
72. Singh, A., Chaudhari, M., Sastry, M., Construction of conductive multilayer films of biogenic triangular gold nanoparticles and their application in chemical vapour sensing. *Nanotechnology*, 17(9), 2399, 2006.

73. Haverkamp, R.G., Marshall, A.T., van Agterveld, D., Pick your carats: Nanoparticles of gold–silver–copper alloy produced *in vivo*. *J. Nanopart. Res.*, 9(4), 697–700, 2007.
74. Panigrahi, T., Synthesis and characterization of silver nanoparticles using leaf extract of *Azadirachta indica*. MSc thesis, National Institute of Technology, 2013.
75. Saif, S., Tahir, A., Chen, Y., Green synthesis of iron nanoparticles and their environmental applications and implications. *Nanomater.*, 6(11), 1–26, 2016.
76. Ge, L., Li, Q., Wang, M., Ouyang, J., Li, X., Xing, M.M., Nanosilver particles in medical applications: Synthesis, performance, and toxicity. *Int. J. Nanomedicine*, 9 2399, 2014.
77. Naik, R.R., Stringer, S.J., Agarwal, G., Jones, S.E., Stone, M.O., Biomimetic synthesis and patterning of silver nanoparticles. *Nat. Mater.*, 1(3), 169, 2002.
78. Saifuddin, N., Wong, C., Yasumira, A., Rapid biosynthesis of silver nanoparticles using culture supernatant of bacteria with microwave irradiation, *J. Chem.*, 6(1), 61–70, 2009.
79. Chen, X., Schluesener, H., Nanosilver: A nanoproduct in medical application. *Toxicol. Lett.*, 176(1), 1–12, 2008.
80. Percival, S.L., Bowler, P.G., Dolman, J., Antimicrobial activity of silver-containing dressings on wound microorganisms using an *in vitro* biofilm model. *Int. Wound J.*, 4(2), 186–191, 2007.
81. Sanpui, P., Murugadoss, A., Prasad, P.D., Ghosh, S.S., Chattopadhyay, A., The antibacterial properties of a novel chitosan–Ag-nanoparticle composite. *Int. J. Food Microbiol.*, 124(2), 142–146, 2008.
82. Li, W.-R., Xie, X.-B., Shi, Q.-S., Zeng, H.-Y., You-Sheng, O.-Y., Chen, Y.-B., Antibacterial activity and mechanism of silver nanoparticles on *Escherichia coli*. *Appl. Microbiol. Biotechnol.*, 85(4), 1115–1122, 2010.
83. Liu, J., Sonshine, D.A., Shervani, S., Hurt, R.H., Controlled release of biologically active silver from nanosilver surfaces. *ACS Nano*, 4(11), 6903–6913, 2010.
84. Kathiravan, V., Ravi, S., Ashokkumar, S., Velmurugan, S., Elumalai, K., Khatiwada, C.P., Green synthesis of silver nanoparticles using *Croton sparsiflorus morong* leaf extract and their antibacterial and antifungal activities. *Spectrochim. Acta A*, 139, 200–205, 2015.
85. Kumar, P.V., Pammi, S., Kollu, P., Satyanarayana, K., Shameem, U., Green synthesis and characterization of silver nanoparticles using *Boerhaavia diffusa* plant extract and their anti bacterial activity. *Ind. Crops Prod.*, 52, 562–566, 2014.
86. Chung, I.-M., Park, I., Seung-Hyun, K., Thiruvengadam, M., Rajakumar, G., Plant-mediated synthesis of silver nanoparticles: Their characteristic properties and therapeutic applications. *Nanoscale Res. Lett.*, 11(1), 40, 2016.
87. Thorley, A.J., Tetley, T.D., New perspectives in nanomedicine. *Pharmacol. Therapeut.*, 140(2), 176–185, 2013.
88. Morones, J.R., Elechiguerra, J.L., Camacho, A., Holt, K., Kouri, J.B., Ramírez, J.T., Yacaman, M.J., The bactericidal effect of silver nanoparticles. *Nanotechnol.*, 16(10), 2346, 2005.

89. Gopinath, P., Gogoi, S.K., Chattopadhyay, A., Ghosh, S.S., Implications of silver nanoparticle induced cell apoptosis for *in vitro* gene therapy. *Nanotechnol.*, 19(7), 075104, 2008.
90. Tabish, S.A., Is diabetes becoming the biggest epidemic of the twenty-first century? *Int. J. Health Sci. (Qassim)*, 1(2), V-VIII, 2007.
91. Rajaram, K., Aiswarya, D., Sureshkumar, P., Green synthesis of silver nanoparticle using *Tephrosia tinctoria* and its antidiabetic activity. *Mater. Lett.*, 138, 251–254, 2015.
92. Becker, R.O., Silver ions in the treatment of local infections. *Metal-Based Drugs*, 6(4–5), 311–314, 1999.
93. Rupp, M.E., Fitzgerald, T., Marion, N., Helget, V., Puumala, S., Anderson, J.R., Fey, P.D., Effect of silver-coated urinary catheters: efficacy, cost-effectiveness, and antimicrobial resistance. *Am. J. Infect. Control*, 32(8), 445–450, 2004.
94. Kalaiselvan, V., Rajasekaran, A., Biosynthesis of silver nanoparticles from *Aspergillus niger* and evaluation of its wound healing activity in experimental rat model. *Int. J. Pharm. Tech. Res.*, 4, 1523–1529, 2009.
95. Pal, S., Tak, Y.K., Song, J.M., Does the antibacterial activity of silver nanoparticles depend on the shape of the nanoparticle? A study of the gram-negative bacterium *Escherichia coli*. *Appl. Environ. Microbiol.*, 73(6), 1712–1720, 2007.
96. Im, A.-R., Kim, J.Y., Kim, H.-S., Cho, S., Park, Y., Kim, Y.S., Wound healing and antibacterial activities of chondroitin sulfate-and acharan sulfate-reduced silver nanoparticles. *Nanotechnol.*, 24(39), 395102, 2013.
97. Krutyakov, Y.A., Kudrinskiy, A.A., Olenin, A.Y., Lisichkin, G.V., Synthesis and properties of silver nanoparticles: Advances and prospects. *Russ. Chem. Rev.*, 77(3), 233–257, 2008.
98. Nie, S., Emory, S.R., Probing single molecules and single nanoparticles by surface-enhanced Raman scattering. *Science*, 275(5303), 1102–1106, 1997.
99. Walkey, C.D., Olsen, J.B., Guo, H., Emili, A., Chan. W.C., Nanoparticle size and surface chemistry determine serum protein adsorption and macrophage uptake. *J. Am. Chem. Soc.*, 134, 2139–2147, 2011
100. Mantovani, E., Zappelli, P., ObservatoryNano Report on Textiles N°1, EU 7th Framework Program, 2009.
101. Merga, G., Wilson, R., Lynn, G., Milosavljevic, B.H., Meisel, D., Redox catalysis on "naked" silver nanoparticles. *J. Phys. Chem. C*, 111(33), 12220–12226, 2007.
102. Guo, J.Z., Cui, H., Lucigenin chemiluminescence induced by noble metal nanoparticles in the presence of adsorbates. *J. Phy. Chem.*, 111(33), 12254–12259, 2007.

7

Green and Sustainable Synthesis of Metal Nanoparticles Using Orange Peel Pith

G. López-Téllez, A. R. Vílchis Néstor, E. Gutiérrez-Segura*, J. E. Moreno-Marcelino, A. Alcántara-Cobos, J. M. Malvaez-Medina and A. Castrejón Mejía

Faculty of Chemistry, Autonomous University of Mexico State, Toluca, México

Abstract

Current trends in nanoparticle synthesis involve the implementation of green and sustainable methods, that avoid the use of hazardous and often toxic chemicals and solvents, and that can be done without high temperatures or pressures. This has led to bioreduction methods such as using a variety of plant and fruit extracts; there are many successful syntheses of metal nanoparticles in the literature that use extracts as mild and nontoxic reductive agents. The final products of such synthesis are metal nanoparticles in aqueous solution and capped with the same biomolecules that helped in the reduction of the metal ions. The use of a biomaterial, such as orange peel pith, that can function as both support and mild reducing agent is proposed as a green, sustainable and cheap alternative to obtain metal nanoparticles stabilized and supported in a biomaterial, which can be easily obtained since it's considered a waste material. There is also the added benefit of having both a cellulosic material, which has been studied extensively as an adsorbent for treatment of waters contaminated with heavy metals, and metal nanoparticles that can further contribute to the remediation.

Keywords: Green and sustainable synthesis, metal nanoparticles, bioreduction mechanism, orange peel pith, remediation, reducing and capping agent

**Corresponding author*: eegutierrezs@uaemex.mx

Suvardhan Kanchi and Shakeel Ahmed (eds.) Green Metal Nanoparticles, (199–215)
© 2018 Scrivener Publishing LLC

7.1 Introduction

Nanomaterials are composed of particles with at least one dimension measuring between 1.0–100 nm [1]. Nanoparticles are classified into major types, viz., organic and inorganic nanoparticles. Carbon nanoparticles are called the organic nanoparticles. Magnetic nanoparticles, noble metal nanoparticles (platinum, gold and silver) and semiconductor nanoparticles (titanium dioxide and zinc oxide) are grouped as inorganic nanoparticles [2].

Nanoparticle has multifunctional properties and very interesting applications in various fields such as medicine, nutrition, catalysis, energy, agriculture and technology; however, nanoparticles can return to the environment either accidentally or deliberately. Uncontrolled release of nanoparticles into the environment will deteriorate the quality of abiotic and biotic components such as microorganisms, algae, animals or plants [3]. Due to high surface area to volume ratio of these nanoparticles compared to their respective bulk material, nanoparticles are highly reactive and effective in their action [4].

Several methods are used for synthesis of nanoparticles such as physical, chemical, and biological (green synthesis). Physical methods include plasma arcing, thermal evaporation, spray pyrolysis, ultrathin films, lithographic techniques, sputter deposition, etc., and the chemical methods include electrodeposition, sol-gel process, chemical solution deposition, hydrolysis, co-precipitation, wet chemical method and others [5]. In the physical method, physical forces are involved in the attraction of nanoscale particles and formation of large, stable, well-defined nanostructures, while the chemical method involves the use of toxic chemicals, which can prove to be hazardous for the environment and the person handling them. Physical and chemical methods use high radiation and highly concentrated reductants and stabilizing agents that are harmful to environmental and human health [6].

Biosynthesis of nanoparticles is an approach of synthesizing nanoparticles using eco-friendly resources such as plant extracts, bacteria, fungi and microalgae such as cyanobacteria, diatom, seaweed (macroalgae) and enzymes [5, 6].

Biosynthesis of nanoparticles offers different applications such as biomedical, drug delivery and cancer treatment, medical diagnostics, sensors, imaging applications, energy-related industrial applications such as electrodes and sensors, environmental remediation applications, coupling biosorption with catalytic contaminant degradation, and catalytic degradation of organic and inorganic pollutants [7]. This approach is an

environment-friendly, cost-effective, nontoxic, biocompatible, clear, safe, green approach. Hence, biological synthesis of nanoparticles is a single-step bioreduction method and less energy is used to synthesize eco-friendly nanoparticles. Among the key advantages the biological approach has over traditional chemical and physical NP synthesis methods is the biological capacity to catalyze reactions in aqueous media at standard temperature and pressure. Biosynthesis can be implemented in nearly any setting and at any scale [2, 8]. The natural growth of living organisms is a common bottom-up approach to nanoparticles formation [9].

7.2 Biosynthesis of Nanoparticles by Plants

Introduction of nanoparticles into terrestrial ecosystems may change the profile of soil-plant systems. Plants are the predominant photosynthetic autotrophs at the first level and producers in the food chain with high biomass production in terrestrial environment. They capture almost 75% of light energy from the sun and convert it into chemical energy of glucose.

The entry of nanoparticles or nanomaterials into the tissues of terrestrial plants can generate multiple implications such as adverse or beneficial effects on seed germination, seedling elongation, photosynthesis, antioxidative stress response, agronomic and yield characteristics [10]. Nanoparticles are able to enter plant tissues through the root system and affect cells either directly or indirectly depending on particle size [11]. Some authors have recently shown that nanoparticles can be absorbed by plants during the germination process or during their growth by supplying them with nutrient solutions or soils supplemented with nanomaterials, which, once they have entered, can produce changes in the cellular metabolism of plant [10]. By contrast, plant parts like roots, leaves, stems, seeds and fruits have also been utilized for the synthesis of nanoparticles, as their extract is rich in phytochemicals, which act as both reducing and stabilizing agent [6].

7.3 Bioreduction Mechanism

Plant-mediated synthesis of metal nanoparticles has become very popular due to ease and availability of plant material which contain reducing compounds such as amino acids, enzymes, flavonoids, sugars, aldehydes, ketones, amines, carboxylic acids, phenols, proteins, alkaloids, terpenoids, pigments and other reducing agents present in the plant extracts and microbial cells [2, 3, 12].

Synthesis of nanoparticles of well-defined shape and size depends on the concentration of plant extract/biomass, metal salt, pH of the reaction mixture, temperature, incubation time [12], reducing capacity, precursor concentration, solvent polarity, and stabilizer [9]. The exact mechanism of nanoparticles synthesis by biological extracts is yet to be understood. This is because different biological agents react differently with metal ions, leading to the formation of nanoparticles [13].

Reduction and stabilization of nanoparticles are attributed to the phenolic and/or hydroxyl-substituted functional groups and various metabolites of terpenoids and reduced sugar in the plants. They can act as both reducing and stabilizing ligands in the development of nanoparticles. Redox ability is primarily due to a complex system of phenolic compounds, which act as hydrogen donors, singlet oxygen quenchers and metal chelating agents in nanoparticles formation [9]. Different parts of plants are used to produce nanoparticles. For instance, bio-capping is done by carboxylic and phenolic acids present in fruit extract [6]. A considerable amount of effort has been devoted to tea extracts, which, owing to a number of polyphenols present, can act as both chelating/reducing and capping agents for the nanoparticles. Therefore, the resulting particles are protected from further reactions and aggregation, which increases their stability and longevity [14].

7.4 Suitable Characteristics of Nanoparticles for Remediation

Nanoparticles have superior properties over their bulk counterparts in the field of remediation technology. They exhibit much greater specific surface area to volume ratio, greater reactivity and mobility, and are subject to quantum confinement due to their ultrafine size, enhanced magnetic and special catalytic properties, etc. [1, 4]. So, a larger surface area and surface reactivity of nanomaterials than their respective bulk material enables them to remediate the contamination at a fast rate with a reduced amount of hazardous by-products [4].

The application of nanoparticles in the remediation of the environment not only reduces the concentration of potential noxious substances, but also reduces the cost of large-scale remediation and the duration of the process [8].

This chapter concentrates on some recent advances in biological synthesis to produce nanoparticles using orange fruit waste.

7.5 Orange Peel Pith as a Support, Reducing and Capping Agent of Metallic Nanoparticles

7.5.1 FeOx Nanoparticles

In a previous work [15], successfully obtained iron oxide (FeOx) nanoparticles were supported and stabilized on orange peel pith by using $NaBH_4$ as a chemical reductor agent. It was reported that an octahedral morphology was obtained (approximately 10 nm in size); however, some rod-shaped morphologies were also observed (approx.. 20 nm in diameter). X-ray photoelectron spectroscopy (XPS) analysis confirmed the presence of both metallic iron and iron oxides forming the nanoparticles. The mechanism for the synthesis of nanoparticles was proposed in three steps:

First, Fe^{+2} ions from a 1×10^{-2} M iron acetate solution are electrostatically bonded to the oxygen atoms that conform with the alcohol groups present on the structure of cellulose. In the second step, these ions are reduced via the chemical reduction with a $NaBH_4$ solution. Finally, in the third step, the metallic atoms coalesce and start growing into octahedral nanoparticles, which remain supported in the cellulose fibers. It should be noted, however, that XPS analysis shows the presence of metallic and oxidized iron, since the entire process occurs in the presence of oxygen from the surrounding air, which quickly starts oxidizing the nanoparticles.

In another work, the same authors [16] reported that orange peel pith also has reducing capabilities on its own. In a typical experiment, orange peel powder was put in contact with an iron acetate solution and after 6 hours iron oxide nanoparticles formed. These nanoparticles, however, exhibit a tubular growth (Figure 7.1), and though there are little octahedral structures as well, the majority are wire-shaped particles of about 20 nm in diameter and about 60 to 80 nm in length (Figure 7.2).

The mechanism proposed occurs in a similar way as the one explained using $NaBH_4$, but in this case the reduction takes place when the alcohol groups of cellulose and hemicellulose oxidize, eventually reacting to form carbonyl groups, hence reducing iron ions to Fe^0. Although these atoms begin to coalesce, the fibrous structure of cellulose blocks some of the planes in which these atoms can adhere, resulting in only one plane available for the growth of nanoparticles, and this results in the formation of wire-like structures.

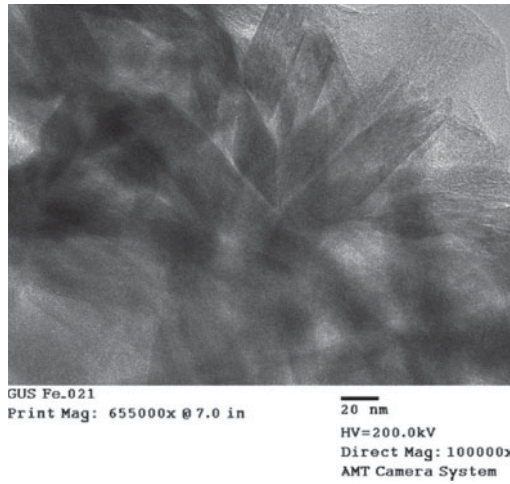


Figure 7.1 FeOx nanoparticles supported on orange peel pith, growing in a rod-like structure.

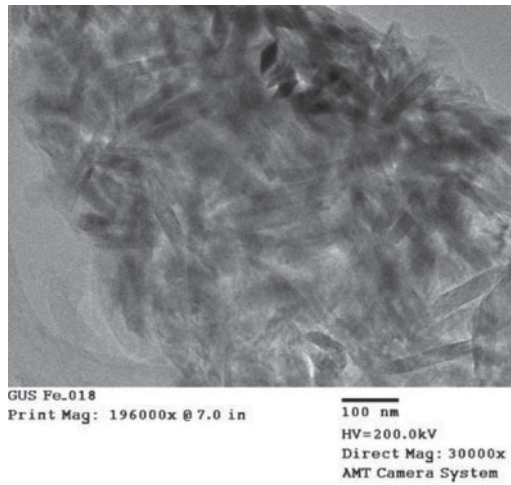


Figure 7.2 FeOx structures found supported on orange peel pith, growing in wire and octahedral structures.

7.5.2 ZnO Nanoparticles

Following the success of using orange peel pith to obtain FeOx nanoparticles, other metals were tested to see if the same procedure could be applied to obtain nanoparticles of zinc oxide (ZnO), silver (Ag) and copper (Cu). The following discussion refers to ZnO nanoparticles.

The methodology was similar to the one reported for FeOx nanoparticles. First, orange peel was dried for 12 hours and then cut into small 5 × 5 mm squares, followed by several rinses in ethanol and one final rinse with deionized water; then it was dried again for 24 hours. Afterwards, the dry squares of orange peel were pulverized in a mill and sieved to obtain a uniform powder.

The powder obtained was used without further treatment, 0.6 g of said powder was put in contact with aqueous solutions of Zinc acetate or Zinc chloride, varying its concentrations from 1×10^{-3}, 1×10^{-2}, and 1×10^{-1} M. The contact time was evaluated from 30 minutes, 1, 3, 6, 12 and 24 hours and finally a week. After the proper time lapse, filtering took place; the solid consisted of orange peel powder, presumably with ZnO nanoparticles supported on it. In order to test the presence of Zn, a sample of the biocomposite was analyzed in a scanning electron microscope (SEM), with an energy dispersive spectrometer (EDS) attached to the microscope. The SEM used for the study was a JEOL JSM 6510 LV and the EDS was an Oxford PentaFetx5.

Figures 7.3 and 7.4 show a typical image of the biocomposite, in which the microstructure of orange peel is readily identified as consisting of fiber structures and pores; and although no nanoparticles can be seen, due to the resolution limits of the equipment used, the EDS spectra in Figure 7.5 shows the presence of Zn.

In order to evaluate the shape and size distribution of the ZnO nanoparticles, it was necessary to isolate them from the support, so a typical extraction procedure consisted of putting 0.1 g of biocomposite in a vial with 3 mL of ethanol, and then leaving it in an ultrasonic bath for 15 minutes;

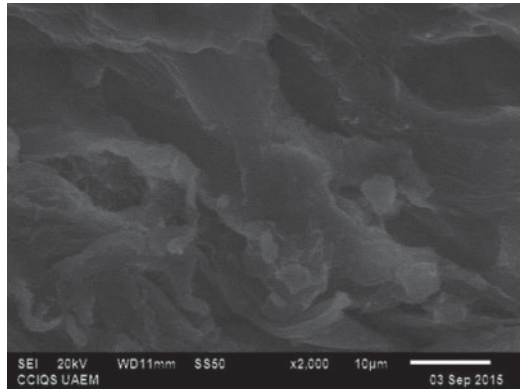


Figure 7.3 Low magnification image of orange peel pith composite.

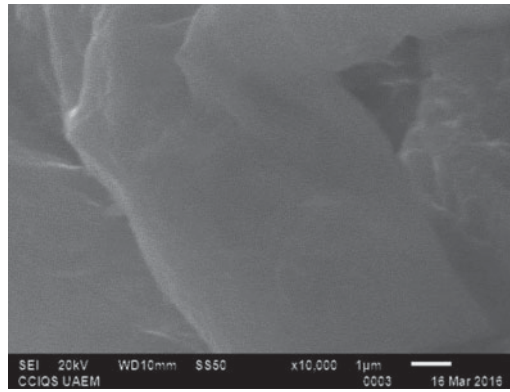


Figure 7.4 Higher magnification image of orange peel pith composite.

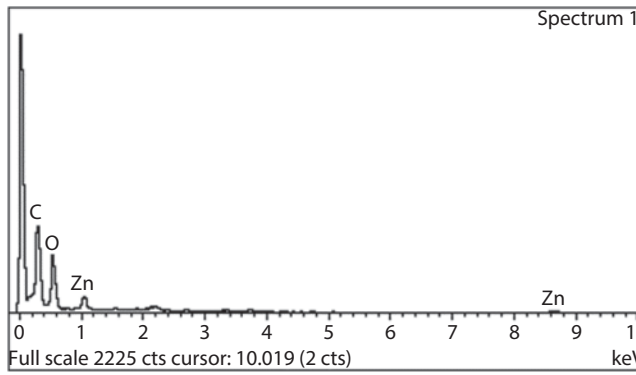


Figure 7.5 EDS spectra of composite showing the presence of Zn.

afterwards, the solid material was separated by filtration and the remaining solution was used to put a drop onto a transmission electron microscope (TEM) copper grid. It can be seen from Figures 7.6 and 7.7 that there are indeed nanoparticles with a spherical shape. A size distribution was calculated and is shown in Figure 7.8; there is a narrow distribution from 6 nm to 26 nm, but it is the size of 12–14 nm that is found more frequently. It's worth noting that the narrow distribution obtained and size of nanoparticles is very good for a bioreduction method.

Another characteristic observed was the contact time between orange peel powder and the precursor salt solution; at times between 1 h up to 6 h the size would not vary considerably, but beyond 6 h the size of the particles increased, due to more aggregation between the smallest nanoparticles

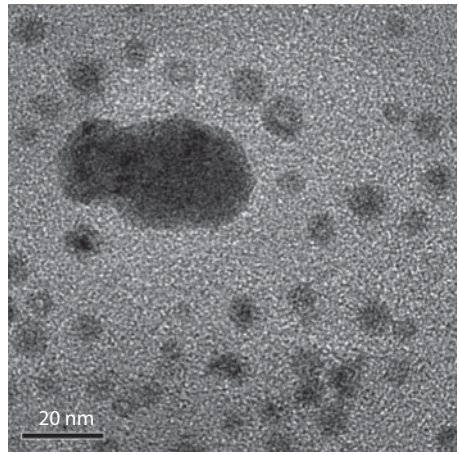


Figure 7.6 TEM image of ZnO nanoparticles extracted from orange peel pith.

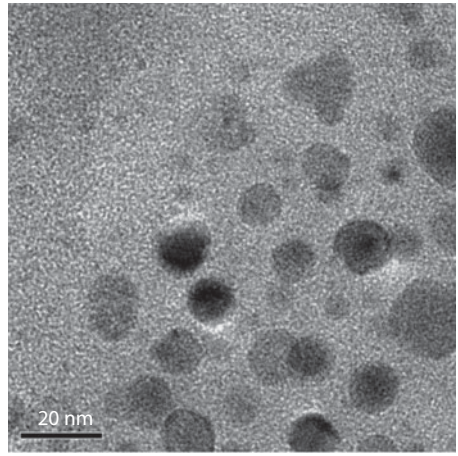


Figure 7.7 TEM image of ZnO nanoparticles extracted from orange peel pith.

formed, hence resulting in bigger particles; at lower contact times it is hypothesized that several nucleation sites form and there is not enough time for them to begin agglomerating, hence the lower sizes observed.

To verify that the zinc present in the biocomposite consists of ZnO, an XPS study was performed. Figure 7.9 shows the Zn 2p 3/2 region; the peak was curve fit and 3 peaks appeared, one which can be related to ZnO located at 1021.73 eV, another one to residual metallic Zn located at 1020.06 eV, and the third one to residual $ZnCl_2$ located at 1023.70 eV. This last one

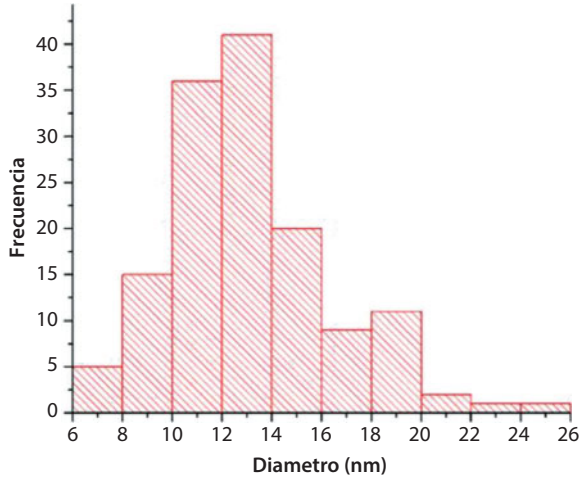


Figure 7.8 Size distribution of ZnO nanoparticles.

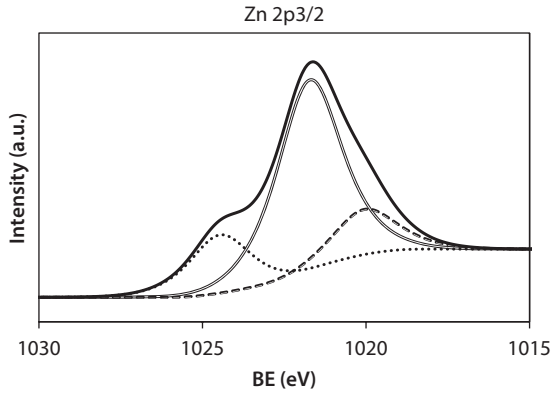


Figure 7.9 XPS of the Zn 2p3/2 region.

is less intense and indicates that residual reactive from the precursor salt solution is still present and unreacted; the presence of Zn^0 indicates that the oxidation is not complete. Further studies are being made to evaluate if longer contact times eliminate the presence of Zn^0 and $ZnCl_2$ on the spectra.

7.5.3 Ag Nanoparticles

A similar procedure to the one used for the synthesis of ZnO nanoparticles was applied to evaluate if silver (Ag) nanoparticles could be made on the

surface of orange peel. Unlike the previous results for Zinc and Fe, silver needed only 1 hour for the formation of nanoparticles; at times of 3 and 6 hours or more, the particles agglomerated considerably. As with the previous characterizations, the composite was characterized using SEM and EDS. Figure 7.10, shows an image of orange peel in which silver cannot be seen due to the resolution limit of the equipment used; however, Figure 7.11 shows the presence of silver in the analysis, indicating that there must be nanoparticles below 60 nm; there are no alterations to the orange peel morphology.

Based on SEM and EDS results, Ag nanoparticles were extracted from the orange peel support in an identical way as the one described for ZnO. Figure 7.12 is a TEM image of Ag nanoparticles obtained with 1 h of contact time of the precursor salt solution ($AgNO_3$) with orange peel pith, and

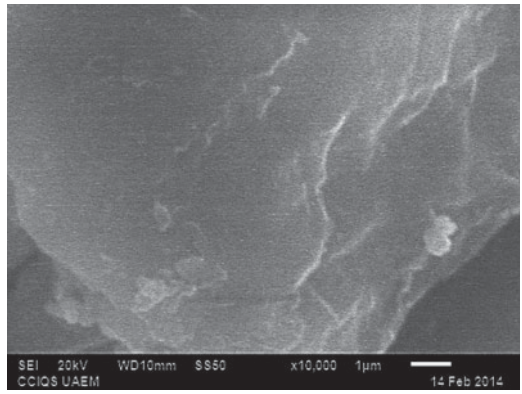


Figure 7.10 SEM image of orange peel pith composite with Ag.

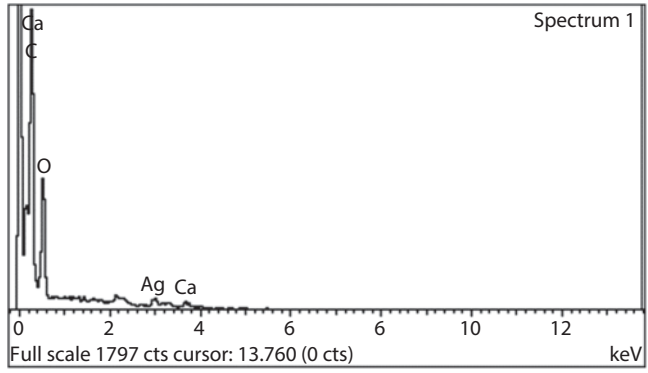


Figure 7.11 EDS spectra of composite showing the presence of Ag.

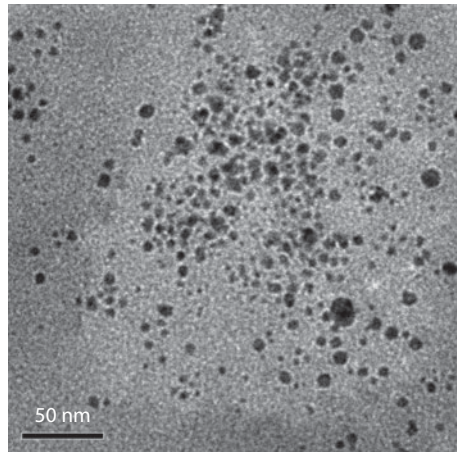


Figure 7.12 Silver nanoparticles formed with 1 h of contact time with orange peel.

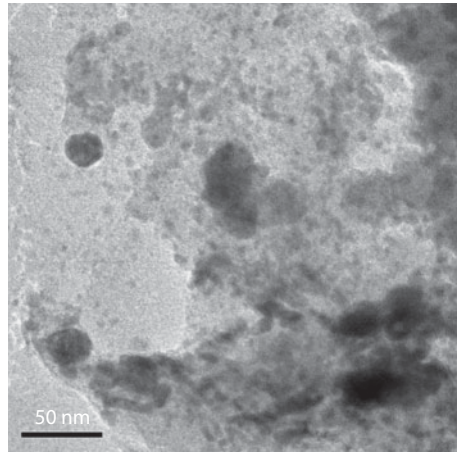


Figure 7.13 Silver nanoparticles formed with 3 h of contact time with orange peel.

Figure 7.13 is an image of the particles obtained with 3 h of contact time. At times greater than 3 h, several agglomerates of silver were observed even in SEM analysis, with sizes ranging from 500 nm and up; hence, the optimal time to obtain nanoparticles of less than 100 nm was 1 h.

Size distribution of silver nanoparticles with 1 h of contact time is depicted in Figure 7.14, where it can be seen that the predominant size is about 5 nm; also, there is a really narrow size distribution which is remarkable for a bioreduction method, usually similar synthesis using plant or

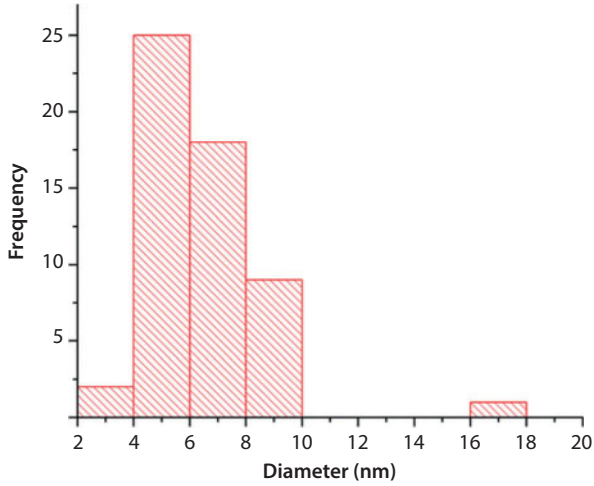


Figure 7.14 Size distribution of Ag nanoparticles.

fruit extracts produce a larger size distribution. As previously mentioned, longer contact times between orange peel and precursor salt solution (>3 h) form agglomerates and even though there are still nanoparticles below 100 nm, the majority of them are above that size, hence increasing the polydispersity.

It is hypothesized that the cellulose and hemi cellulose present in orange peel pith, and even the lignin molecules, limit the growth of nanoparticles due to the interactions between silver atoms and functional groups. At contact times higher than 3 h, the stirring and consequently the diffusion is greater and the nanoparticles start coalescing with one another, forming agglomerates and bulkier particles, which overrun the steric limitations that occur at times less than 3 h.

Finally, XPS analyses were made to evaluate the presence of Ag^0 or ionic Ag. Figure 7.15 shows the 3d5/2 region for silver; based on the HWFM (half width at half maximum) reported for silver there is only one signal and no curve fit was necessary. This signal corresponds to metallic silver at 368.2 eV, hence suggesting that orange peel molecules can also cap Ag nanoparticles, preventing them from suffering further chemical modifications. However, it must be noted that these analyses were made on samples with up to 3 h of contact time with orange peel, there is a possibility that at longer times these particles will grow in size, as seen in ZnO nanoparticles, and even could suffer oxidation from the media surrounding them. Further analysis is needed to explore these possibilities.

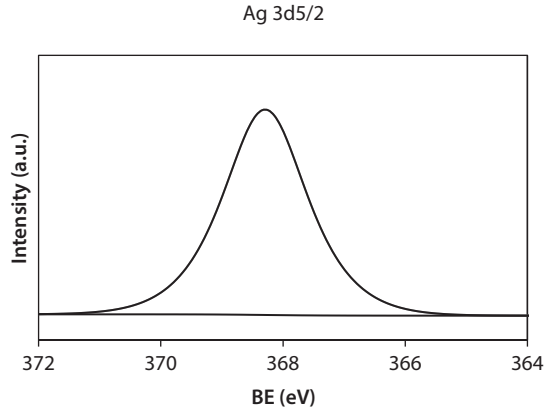


Figure 7.15 XPS of silver 3d5/2 region.

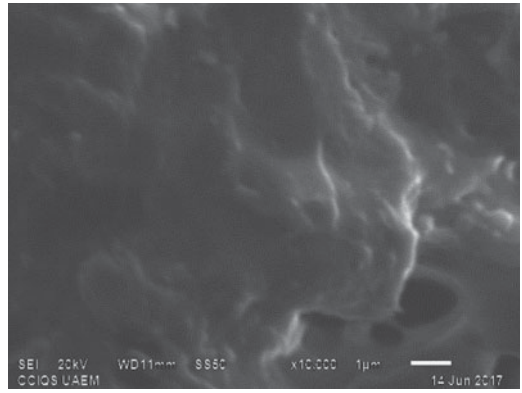


Figure 7.16 SEM image of orange peel pith composite with Cu.

7.5.4 Cu and/or Cu_xO_x Nanoparticles

There is a work in progress to evaluate the feasibility of orange peel pith to also form Copper (Cu) and/or Cu_xO_x nanoparticles. At the time of this writing the same procedure used for ZnO and silver is being tested for copper; so far the results seem promising, with SEM and EDS analysis similar to the ones obtained for the other composites. Even though no nanoparticles can be seen in the SEM images (Figure 7.16), the EDS analysis shows the presence of copper from the samples (Figure 7.17), indicating that there must be particles below 60 nm in size, which is the limit that can be observed with the equipment used.

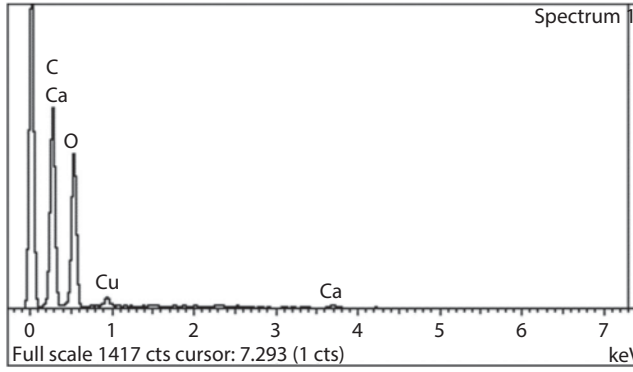


Figure 7.17 EDS spectra of composite showing the presence of Cu.

Samples are being prepared for TEM analysis in order to verify the presence of copper nanoparticles, and to evaluate their size distribution and morphology, and also for XPS analysis to evaluate the chemical characteristics of copper.

7.6 Conclusions

This chapter has summarized the recent research work in the field of biological and green synthesis of nanoparticles by using plants, specifically orange fruit waste.

Orange peel pith is a suitable support and reducing agent for the green synthesis of silver, iron oxide, and zinc oxide nanoparticles. Since almost all the literature uses extracts obtained from the peel, to the best of our knowledge, there are no studies specifically related to the use of orange peel pith as a support, reducing, and capping agent, in which a novel method for the recycling of a waste material is proposed.

Nanoparticles can be easily removed from the support if need be, by simply leaving the composite in an ultrasonic bath for 5 to 15 min in ethanol. These nanoparticles have a good size distribution for a bioreduction method; furthermore, there are some specific morphologies obtained; spherical in the case of ZnO and Ag, and rod-like for FeO_x.

Being an abundant and low-cost material, orange peel, which is based in cellulose, could be chemically modified in order to favor more specific morphologies and sizes. The mechanism proposed consists of the electrostatic attraction of metal ions towards the negative density of oxygen groups present in cellulose and hemicellulose, followed by the redox

reaction between metal ions and alcohol groups. Later, the stabilization of formed nanoparticles occurs via the structural steric limits of all the cellulose and hemicellulose molecules present in orange peel. Finally, there is a work in progress for the synthesis of Cu_xO_x and/or Cu^0 nanoparticles using the same method, and also the synthesis of bimetallic systems.

References

1. Sweet, M.J., Chessher, A., Singleton, I., Metal-based nanoparticles; Size, function, and areas for advancement in applied microbiology. *Adv. Appl. Microbiol.,* 80, 113–142, 2012.
2. Asmathunisha, N., Kathiresan, K., A review on biosynthesis of nanoparticles by marine organisms. *Colloids Surf. B,* 103, 283–287, 2013.
3. Hatami, M., Kariman, K., Ghorbanpour, M., Engineered nanomaterial-mediated changes in the metabolism of terrestrial plants. *Sci. Environ.,* 571, 275–291, 2016.
4. Kumari, B., Singh, D.P., A review on multifaceted application of nanoparticles in the field of bioremediation of petroleum hydrocarbons. *Ecol. Eng.,* 97, 98–105, 2016.
5. Kuppusamy, P., Yusoff, M.M., Maniam, G.P., Govindan, N., Biosynthesis of metallic nanoparticles using plant derivatives and their new avenues in pharmacological applications – An updated report. *Saud. Pharm. J.,* 24, 473–484, 2016.
6. Agarwal, H., Kumar, S.V., Rajeshkumar, S., A review on green synthesis of zinc oxide nanoparticles – An eco-friendly approach. *Resource-Efficient Technol.*, 3, 406–413, 2017.
7. Schröfel, A., Kratošová, G., Šafařík, I., Šafařiková, M., Raška, I., Shor, L.M., Review applications of biosynthesized metallic nanoparticles – A review. *Acta Biomater.*, 10, 4023–4042, 2014.
8. Stefaniuk, M., Oleszczuk, P., Ok, Y.S., Review on nano zerovalent iron (nZVI): From synthesis to environmental applications. *Chem. Eng. J.,* 287, 618–632, 2016.
9. Dwivedi, A.D., Dubey, S.P., Sillanpää, M., Kwon, Y-N., Lee C., Varma, R.S., Fate of engineered nanoparticles: Implications in the environment. *Coord. Chem. Rev.,* 287, 64–78, 2015.
10. Du, W., Tan, W., Peralta-Videa, J.R., Gardea-Torresdey, J.L., Ji, R., Yin, Y., Guo, H., Interaction of metal oxide nanoparticles with higher terrestrial plants: Physiological and biochemical aspects. *Plant Physiol. Biochem.,* 110, 210–225, 2017.
11. Mustafa, G., Komatsu, S., Toxicity of heavy metals and metal-containing nanoparticles on plants. *Biochim. Biophy. Acta,* 1864, 932–944, 2016.

12. Siddiqi, K.S., Husen, A., Recent advances in plant-mediated engineered gold nanoparticles and their application in biological system. *J. Trace Elem. Med. Biol.,* 40, 10–23, 2017.
13. Hulkoti, N.I., Taranath, T.C., Biosynthesis of nanoparticles using microbes – A review. *Colloids Surf. B,* 121, 474–483, 2014.
14. Kharissova, O.V., Dias, H.V.R., Kharisov, B.I., Olvera Pérez, B., Jiménez Pérez, V.M., The greener synthesis of nanoparticles. *Trends Biotechnol.,* 31(4), 240–248, 2013.
15. López-Téllez, G., Barrera-Díaz, C.E., Balderas-Hernández, P., Roa-Morales, G., Bilyeu, B., Removal of hexavalent chromium in aquatic solutions by iron nanoparticles embedded in orange peel pith. *Chem. Eng. J.,* 173, 480–485, 2011.
16. López-Téllez, G., Balderas-Hernández, P., Barrera-Díaz, C.E., Vilchis-Néstor, A.R., Roa-Morales, G., Bilyeu, B., Green method to form iron oxide nanorods in orange peels for chromium (VI) reduction. *J. Nanosci. Nanotechnol.,* 13(3), 2354–2361, 2013.

8

Biological and Biomedical Applications of Eco-Friendly Synthesized Gold Nanoparticles

G. Madhumitha, J. Fowsiya and Selvaraj Mohana Roopan*

Chemistry of Heterocycles & Natural Product Research Laboratory, Department of Chemistry, School of Advanced Sciences, Vellore Institute of Technology, Tamil Nadu, India

Abstract

Eco-friendly nanoparticles research is one of the fascinating branches of nanotechnology science. Among various metal nanoparticles, gold nanoparticles (AuNPs) have attracted huge scientific and technology attention due to their nontoxicity, stability, nano-size structure, etc. AuNPs are inert in many biological environments and carry several physical properties which play an important role in biomedical applications. To date, AuNPs have been successfully employed in tumor radiotherapy, drug carriers, biomedical imaging, biosensors, antimicrobial agent, photocatalyst, antidiabetics, etc. Distinct from other reviews, in this chapter we present the green chemical approach for the preparation and remarkable biological activity of AuNPs.

Keywords: Gold nanoparticles, plant extracts, biological activity, nanomedicine, nanotoxicity, biomedical applications

8.1 Introduction

Growing numbers of researchers and engineers are discovering and changing ultra-small material properties to produce various materials that eventually might enhance the effectiveness of current energy sources or

**Corresponding author*: mohanaroopan.s@gmail.com; mohanaroopan.s@vit.ac.in

Suvardhan Kanchi and Shakeel Ahmed (eds.) Green Metal Nanoparticles, (217–244)
© 2018 Scrivener Publishing LLC

make new energy sources practical on an industrial scale [1]. At the nano-size, fundamental mechanical, electrical, optical, biomedical and biological applications can vary from their bulk materials [2–8]. On the other hand, the nano-size materials or nano-structure materials revolution was directly affected by nanotechnology, which has taken a big step forward towards upcoming technological developments [9–13]. During the last few decades, metal nanoparticles (NPs) have been of great interest due to their distinct physical, chemical and biological applications. Owing to the attention and significance of NPs, researchers have focused on the production of nanoparticles [14–20]. The synthesis of NPs towards sustainable practice is a promising challenge for future nanotechnology. The synthesis of NPs provides enhanced characteristics such as nano size, morphology, distribution, etc. [21, 22]. There are more developments in the synthesis of NPs with definite size and form, which account for certain applications [23–25].

With the development of nanotechnology, various methods have been adapted to synthesize NPs like ion sputtering, chemical reduction, hydrothermal process, sol-gel, etc. [26–30]. But unfortunately, these methods are high cost, cause side effects and are toxic to the environment. Therefore, scientists are merging eco-friendly or green process to synthesis NPs, called "green nano." The green synthesis methods are easy, nontoxic, one-pot synthesis, environmentally safe, etc. [31–35]. Green methods include plant extracts, bacteria, sugars, fungi and naturally available polymers as alternatives for NPs [36–40]. During the last few years, gold nanoparticles (AuNPs) have been found to have unique properties towards biological and biomedical applications compared to other NPs (Figure 8.1). According to recent reports, biomedical applications for AuNPs found in Chinese civilization in 2500 BC were used to cure smallpox, skin ulcers and syphilis [41]. The present area of nanoscience and technology involves the use of AuNPs to cure diseases like rheumatoid arthritis and also in antimicrobial, anticancer and biomedical applications. The AuNPs are being applied in biomedical applications due to their being chemically stable, less toxic, easy to synthesis, biocompatible and non-interfering with other biomarkers [42, 43]. Therefore, the aim of this chapter is to summarize the green synthesis of AuNPs and its biological and biomedical applications.

8.2 Plant Extract as Bioreactors for Green Synthesis of AuNPs

It has long been known that plant extract acts as a reducing as well as stabilizing agent in synthesis of AuNPs. Furthermore, AuNPs surrounded by plant extract can be recovered by calcinations or sintering and smelting

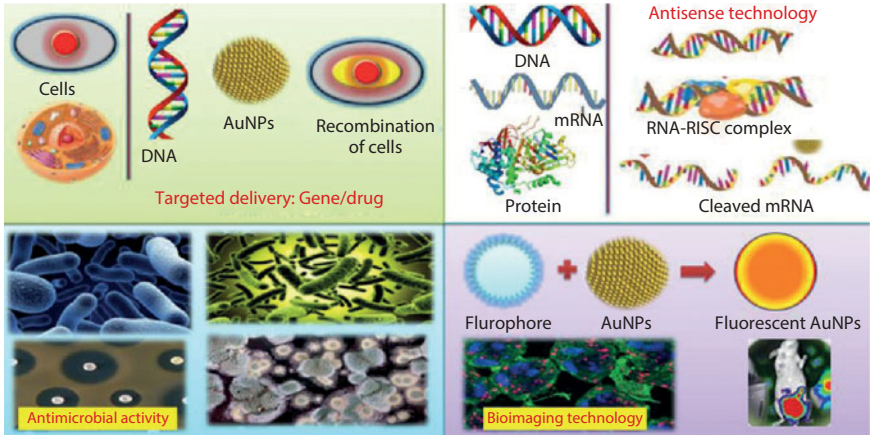


Figure 8.1 Various applications of AuNPs.

methods. From the synthesis of AuNPs it was found that the bioaccumulation process displayed metals in the form of NPs. The size and shape of AuNPs can be controlled using the flexible green synthesis method by changing the pH, temperature and time [44]. These processes are much faster than chemical reduction and sol-gel methods because the reduction of gold is almost instantaneous, without any delay for uptake and localization of metal throughout the plant extract (Figure 8.2).

8.2.1 Leaf Mediated Synthesis of AuNPs

Traditionally used plants, namely *Cucurbita pepo* and *Malva crispa,* were reported for AuNPs synthesis with good antimicrobial property against food pathogens [45]. About 20–30 nm size AuNPs were synthesized using *Acalypha indica* leaf extract as a reductant and used as potential anticancer agent in cancer therapy against human cancer cells [46]. The aerial parts of *Cymbopogon citrates* were used as a capping and stabilizing agent for preparation of AuNPs. The synthesized AuNPs were evaluated for their larvicidal and ovicidal activity against blood-feeding and dengue-causing vectors such as *Anopheles stephensi* and *Aedes aegypti* [47].

Traditionally, *Zingiber officinale* has been used for the biogenic production of AuNPs, which found to have a nano size of between 10–12 nm [48]. *Pelargonium graveolens* phytochemicals mediated AuNPs were synthesized with different shapes and about 50–100 nm size; AuNPs were also formed with triangular and spherical shapes using leaves of *Nepenthes khasiana* [49, 50]. The reduction of auric chloride in AuNPs was studied

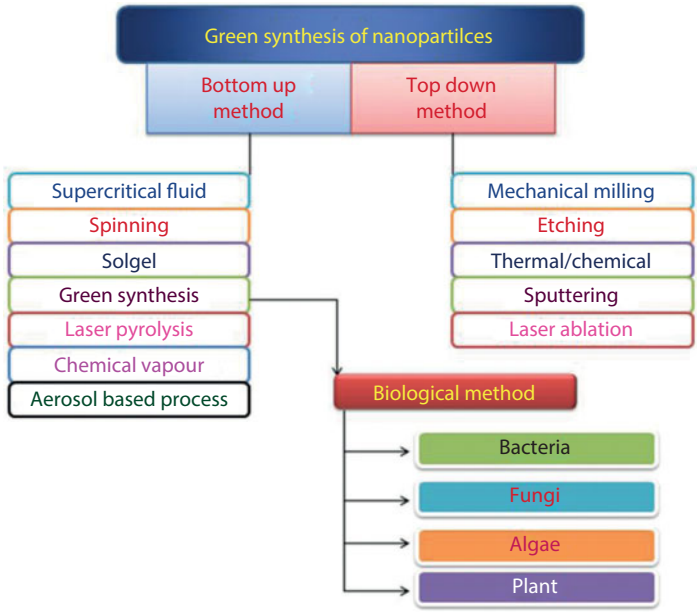


Figure 8.2 Green synthesis of nanoparticles by different methods.

using *Cassia auriculata* leaf extract and the formation of NPs was confirmed by the absorbance at 536 nm at 10 min intervals [51]. The aqueous extract of coriander leaves was utilized to synthesis AuNPs and a nano size between 6–57 nm was confirmed. Moreover, green synthesized AuNPs used for drug delivery were synthesized using *Punica granutum*. Different sizes and shapes of AuNPs were achieved using hibiscus leaf extract and also reported using *Stevia rebaudiana* [52–56].

The rapid reduction of chloroaurate ions was observed using a treatment of tamarind leaf extract with aqueous chloroauric acid solution, leading to the formation of gold nanoparticles. Flat and thin single crystalline gold nanoparticles with size of 20–40 nm were formed in this biogenic synthesis [57]. The flavonoids of *Syzygium aromaticum* were involved in AuNPs synthesis, resulting in 5–50 nm size AuNPS. An antimicrobial investigation was carried out on AuNPS synthesized using *Mentha piperita, Madhuca longifolia* and *Suaeda monoica*. The results showed good inhibition against *Staphylococcus aureus* and *Escherichia coli* [58–61] (Table 8.1).

The leaf extract of *Dracocephalum kotschyi* was prepared at different temperatures. UV-Vis analysis was carried out. The color change from yellow to pink violet indicated the presence of redox reaction. Moreover, it indicated the conversion of Au^{3+} ions excited state to ground state of Au^{0}

Table 8.1 Leaf mediated synthesis of AuNPs.

S. no.	Plant name	Size (nm)	Shape
1.	*Terminalia catappa*	10–35	Spherical
2.	*Dracocephalum kotschyi*	11	Spherical
3.	*Olea europaea*	50–100	Triangular, hexagonal and spherical
4.	*Cacumen platycladi*	2–70	Spherical and triangular
5.	*Nelumbo nucifera*	20–80	Spherical
6.	*Cinnamomum zeylanicum*	25	Spherical
7.	*Argemone mexicana*	22–26	Spherical
8.	*Bauhinia tomentosa*	31–32	Crystalline
9.	*Bauhinia tomentosa*	20–50	Cubical
10.	*Gymnema sylvestre*	72.8	Spherical
11.	*Azadirachta indica*	1.25–17.5	Spherical
12.	*Magnolia kobus*	100–300	Plate and spherical
13.	*Ficus benghalensis*	2–100	Spherical
14.	*Ficus benghalensis*	10–300	Disk
15.	*Ficus benghalensis*	10.74	Spherical

by plant compounds. The bioactive compounds in the leaf extract were engaged in the AuNPs, which was further identified by FTIR analysis. The synthesis of AuNPs was confirmed by surface plasmon resonance (SPR) band obtained at 536 nm in a UV-Vis spectrophotometer [62].

The leaf extract of *Olea europaea* was utilized to synthesis AuNPs by observing color change from pink to dark pink. The FTIR results showed C–C stretching modes and –C–O–H bond obtained at 799.92 cm^{-1} and 1261.17 for AuNPs, which confirmed that the presence of phytochemicals of the extract acted as a reducing and stabilizing agent. A sharp strong band observed at 1077 cm^{-1} was assigned to the C-OH bond of the protein in *O. europaea* [63].

The leaves of *Ipomoea carnea* were utilized for the AuNPs synthesis. The synthesis process was confirmed by the characteristic change in color from yellow to wine red color. X-ray diffractometer analysis was carried out to find the crystalline nature of the AuNPs and the result showed it had a face-centered cubic (fcc) structure. The FTIR analysis of AuNPs displaced a band which corresponded to the C-N bond of extract. The C-N band of amine was reduced and acted as a reducing agent in AuNPs synthesis [64].

One of the studies using *Nerium oleander* leaves confirmed synthesis of AuNPs by green and one-pot synthesis. The authors reported that at different time intervals the SPR peaks were observed. The formation of gold NPs was confirmed by a strong peak, which was observed after 70 min incubation at 560 nm. The stabilizing ability and the reducing ability of the leaf extract were observed by FTIR spectra. The active groups responsible for gold NPs synthesis were observed by the FTIR absorption bands at 3433, 2923, 1626, 1385, 1054 and 535 cm^{-1} [65].

8.2.2 Fruit Extract Mediated Synthesis of AuNPs

The fruit and seed extract of *Syzygium cumini* and *Abelmoschus esculentus* was studied for AuNPs and evaluated for antifungal studies against *Puccinia graminis tritci, Aspergillus flavus, Aspergillus niger* and *Candida albicans*. The antifungal studies showed good potential inhibition of fungus and are of interest for the synthesis of drugs which are used against fungal diseases [66, 67]. Waste management is one of the challenges of the era in agriculture and food industries and there is high demand for recycling of wastes such as peel and seed (Table 8.2). The waste seed and peel of grapes were used in a study to synthesis 20–25 nm of AuNPs for use as an effective antibacterial [68]. Unlike the spherical shape of AuNPs, a few other morphologies, like hexagonal shapes, were found using *Hovenia dulcis* in 20 nm. The well-dispersed AuNPs were also found using *Scutellaria barbata* as reducing and stabilizing agent. The size of AuNPs

Table 8.2 Fruit mediated synthesis of AuNPs.

S. no.	Plant name	Size (nm)	Shape
1.	*Citrus maxima*	25.7–35	Rod, spherical
2.	*Citrus limon*	15–80	Spherical
3.	*Genipa americana*	15–40	Spherical
4.	*Averrhoa bilimbi*	75–150	Rhomboidal
5.	*Lansium domesticum*	20–40	Triangular, Hexagonal
6.	*Punica granatum*	70	Spherical
7.	*Garcinia cambogia*	17	Spherical
8.	*Couroupita guianensis* Aubl.	25–31	Spherical
9.	*Terminalia arjuna*	20	Pentagonal
10.	*Nitraria schoberi*	30–40	Circular

was 5–30 nm due to the phytochemicals of alkaloids, flavonoids and phenolic compounds [69].

The extract of *Citrus maxima* fruit underwent green synthesis to obtain AuNPs. The UV-Vis spectrum showed a peak at 535 nm and FTIR results showed a peak of 1658 cm^{-1}, which corresponded to vibration modes of C=C double bonds of biomolecules (Figure 8.3). Flavonoids, terpenes and vitamins are some of the reducing agents among which chloroauric acid showed a peak of 1376 cm^{-1}, which is thought to be due to the axial vibrations of C-N bonds in the acid [70]. Low-cost and one-pot synthesis of citrus fruit (*Citrus limon*, *Citrus sinensis*, *Citrus reticulate*) mediated AuNPs were obtained with different concentrations of precursors. The concentration quantity of aqueous medium was varied, which resulted in the formation of AuNPs, which were identified by UV-Vis spectroscopy. The peaks obtained were fairly sharp for the values. The SPR band observed for the colloid was found to be 530 nm, from which spherical shape of NPs can be inferred [71].

Fruit extracts from *Genipa americana* L., considered a photosynthetic plant, were also used for synthesis of AuNPs. The color of extract changed from pink to ruby red and showed a maximum absorbance at 590 nm, which confirmed the AuNPs formation. FTIR spectra showed different peaks for different biomolecule compounds, but the synthesis process was hindered by secondary -OH group interaction with Au^{3+} via hydrogen bonding [72]. *Punica granatum* fruit peels facilitated ultra-fast synthesis of AuNPs, which showed a change of color to wine red, indicating the formation of the extract. The AuNPs showed SPR of 530 nm and spherical shape according to SEM results. Pomegranate extract showed peaks at 1346 cm^{-1} to 1384 cm^{-1} in FTIR analysis, indicating that AuNPs attached through adjacent phenolic hydroxyls formed quinines [73]. Shape-tailored AuNPs were synthesized using *Garcinia cambogia* fruit

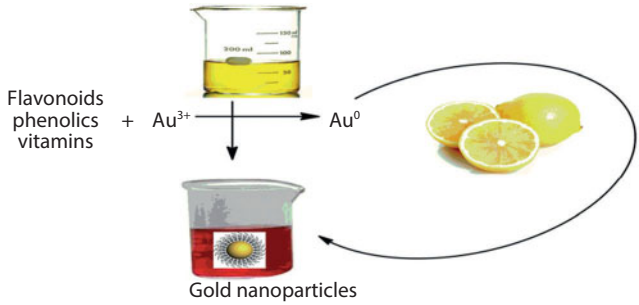


Figure 8.3 Fruit extract mediated synthesis of AuNPs.

extract. The SPR band occurred at 531 nm and extract mediated AuNPs displayed band at 1631 cm^{-1}, which corresponded to the C=O stretch of carboxyl group [74]. The size control analysis of AuNPs was done using aqueous extract of *Terminalia arjuna* fruit pericarp. In the typical synthesis process, different concentrations of extract were mixed with chloroauric acid. The AuNPs synthesis was monitored for color change from yellow to ruby red. The FTIR result revealed the reduction of gold ions due to the presence of –OH and C=O in the extract. The phenolic compounds in the extract possess reducing and stabilizing property in AuNPs synthesis [75].

8.2.3 Flower Extract Mediated Synthesis of AuNPs

At present, green synthesis processes have achieved an importance in biological and biomedical applications. Lately, leaves, fruits and roots were utilized for synthesis of AuNPs due to their ability to reduce gold ions. Synthesis of flower extract mediated AuNPs were also used for various applications. The phytochemicals, such as phenolic compounds, essential oils, flavonoids and terpenes, can develop AuNPs. The *Ixora coccinea* flower was used to synthesize AuNPs with antimicrobial activity. The formation of nanoparticles was observed with change in color from yellow to deep brownish within 30 min. The formed nanoparticles were examined by UV-visible spectra, which indicated a wavelength of 550 nm [76]. In the biogenic production of AuNPs using flower extract of *Cassia auriculata* a color change from light yellow brown to ruby red color in 3 min intervals was observed (Table 8.3). The reduction process of Au^{3+} ions to Au^{0} was obtained in the presence of –OH group, which was displaced in FTIR band around 3366 cm^{-1} [77].

The color change from yellow to brown was observed in the case of *Tagetes erecta* flower mediated AuNPs synthesis. The AuNPs were formed at 30 min intervals and UV-Vis monitoring recorded a broad peak at 550 nm [78]. The identification of reducing agent in the synthesis of *Couroupita guianensi* flower mediated AuNPs has been achieved by several techniques. Lately, a cyclic voltammetry method was used to identify the reducing agent present in the extract which was responsible for formation of AuNPs. The obtained result revealed the presence of electron-donating methoxy and –OH groups in the extract and confirmed formation of AuNPs [79]. Moreover, *Bauhinia purpurea, Plumeria alba* and *Gnidia glauca* flowers were also reported for the synthesis of AuNPs, where FTIR results showed that reduced intensity of C-H bond bending was obtained at 763 and C-H stretches at 3000 cm^{-1}.

Table 8.3 Flower extract stabilized AuNPs.

S. no.	Plant name	Size (nm)	Shape
1.	*Ixora coccinea*	5–10	Rod, spherical
2.	*Ixora coccinea*	1240	Spherical
3.	*Tagetes erecta*	30–50	Spherical
4.	*Moringa oleifera*	3–5	Spherical
5.	*Nyctanthes arbor-tristis*	19.8	Spherical
6.	*Nyctanthes arbor-tristis*	10–20	Spherical
7.	*Couroupita guianensis*	25–45	Spherical
8.	*Bauhinia purpurea*	20–50	Cubical
9.	*Plumeria alba* Linn.	20–30	Spherical
10.	*Gnidia glauca*	5–20	Spherical

8.3 Role of Phytochemicals in AuNPs

As discussed earlier, extracts present in AuNPs synthesis and various secondary metabolites present in the extract play an important role in reducing gold ions. The phytochemicals or secondary metabolites, such as terpenoids, polyphenols, flavonoid, glycosides, alkaloids and proteins, are responsible for the bioreduction of gold ions producing AuNPs (Figure 8.4). The identification of phytochemicals involved in bioreduction can be confirmed by FTIR spectroscopy, which is used to determine the functional group of extract [80].

Terpenes are one of the naturally occurring five-carbon isoprene units also reported for AuNPs synthesis. At first, terpenoids play a key role in silver ion reduction and later are also responsible for gold ions. One of the terpenoids from *Cinnamomum zeylanisum,* namely eugenol, has been reported for gold ion reduction. Based on FTIR results, it is found that hydrogen from eugenol (-OH group) acts as capping and reducing agent in AuNPs [81]. Flavonoids, another bioactive compound, are a large class of polyphenols that comprises various subclasses, including isoflavonoids, flavanones, flavones, etc. The flavonoids generally have the efficiency to undergo chelation and have reducing properties due to the presence of various –OH functional group that are capable of forming AuNPs. It is proposed that the tautomeric conversion (enol to keto group) of flavonoids donates hydrogen to reduce the gold ions in AuNPs. Furthermore, the internal transformation of keto to acid in flavonoids occurred in the case

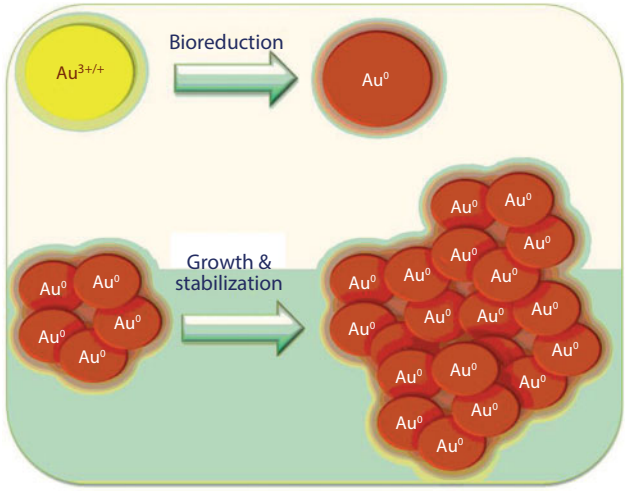


Figure 8.4 Mechanism of formation of AuNPs by green synthesis.

of Au^{3+} reduction. Few other flavonoids have the capacity to chelate gold ion with carbonyl group π-electrons in the process of AuNPs formation. Quercetin and catechin are two of the flavonoids that have efficient chelating property with gold ions due to the three carbonyl and –OH groups (Figure 8.5). The chelating property can also be engaged with other metal ions, such as iron, copper, zinc, aluminum, lead and cobalt, in NPs formation. The presence of such functional groups in flavonoids has the ability to act as capping agents on particle surface of gold ions, yielding AuNPs. The mechanism of formation of AuNPS involves initiation (nucleation) and aggregation processes with bioreduction of gold ion [82].

For example, luteolin, rosmarinic and apigenin glycosides from *Ocimum basilicum* and *Lawsonia inermis* were reported for AuNPs. The transformation of enol to keto group plays an important role in bioreduction of gold with average size of 21–30 nm [83]. From the FTIR analysis of AuNPs, it was confirmed that carbonyl group of apiin was attached to AuNPs and sugars from plant extracts were also capable of reducing gold ions into AuNPs. The aldehyde group of sugars, such as glucose, acts as reducing and stabilizing agent. The transformation of keto group to an aldehyde occurs in fructose and reducing property depends on the open chain of oligomer that is attached to the metal ion through aldehyde bond. Disaccharides, such as maltose and lactose, also were reported for AuNPs due to open chain form, while sucrose has no bioreduction property due to there being no access to open chain form. It was found that glucose mediated AuNPs

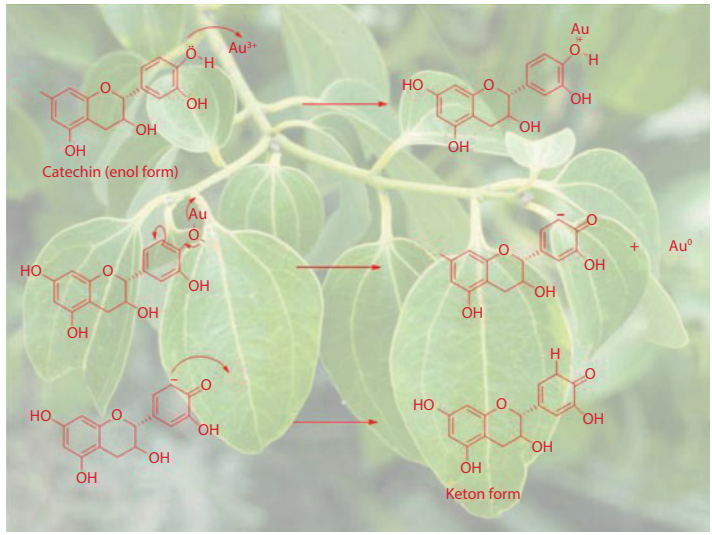


Figure 8.5 Phytochemical mediated synthesis of AuNPs.

showed different morphological studies whereas fructose can form well-dispersed AuNPs. It was also noticed that glucose has a greater reducing property than fructose due to a kinetic study in the transformation of tautomerism. In recent years, the conversion of aldehyde to acid group through oxidation and nucleophilic addition of –OH was achieved through AuNPs synthesis [84].

The FTIR analysis of AuNPs also revealed that protein in extracts plays an important role in bioreduction of gold ions. Amino acids, such as cysteine, arginine and methionine, were reported for AuNPs formation whereas valine and lysine do not obey this mechanism. During the last few years, about 20 amino acids were reported for formation of AuNPs. The mechanism involves binding of amino and acid groups with gold ions, while glutanic acid has the capacity to attach to gold ion through nitrogen bonding [85, 86]. Therefore, the mechanism involved three steps, namely activation of metal ions, growth of nanoparticles via heterogeneous nucleation and termination with final shape. Different shapes were observed while the duration process increases and were displayed as nanotubes, nanoprisms, nanospheres, etc. In the case of triangular shape, AuNPs have high surface energy and less stability. If the stability of nanoparticles is not supported in given extracts, then the nanotriangles will acquire a more stable morphology, such as a truncated triangle, in order to minimize the Gibbs free energy [87].

8.4 Biological and Biomedical Applications of AuNPs

8.4.1 Bioimaging/Labeling

Due to the unique characteristic properties of AuNPs, researchers have focused on their biological and biomedical applications. In recent years, AuNPs have been used for bioimaging and labeling applications using several techniques such as microscopy, photometry and flow cytometry. High electron intensity, absorption, scattering in visible region of electromagnetic spectrum are some of the characteristics which permit detection or identification and imaging of AuNPs [88]. Due to the facile properties of AuNPs, they can be used in diagnostics, biosensing and bioimaging. The optical properties exhibited by AuNPs include absorption, scattering, fluorescence, etc., which can be used for development of many sensor applications [89]. In the past few years, AuNPs have been utilized as distinct material in bioimaging, which allow measuring and describing the bioprocess of cells or molecules. These distinct AuNPs, which target specific organs and accumulate in them, provide signals depending on cells and subcellular organelles via colorimetric detection. Due to its bioimaging property, AuNPs have been used to visualize quantum dots, lanthanides, fluorophores and magnetic materials. The AuNPs have a strong imaging capability in delocalized lanthanide chelates and cytotoxic materials [90–93].

It also observed that AuNPs are perfect material in bioimaging applications due to their stability and binding capacity towards objects without affecting surroundings. Materials of more than 150 nm size will not be able to enter cells via endocytosis and 30–150 nm size materials are more suitable for bioimaging. Therefore, scattered light from AuNPs is very intense and allows localizing every material in optical microscopy [94]. Even so, the AuNPs were more attracted to other bioimaging techniques such as photothermal, two-photon photoluminescence, X-ray, magnetic resonance imaging and X-ray imaging [95–100].

8.4.2 AuNPs in Anticancer Therapy

Cancer is a term for disease in which irregular growth of abnormal cells attacks other normal cells in the human body. The cancer cells spread to other body parts through the bloodstream or lymphatic system.

Chemotherapy, radiation and surgery are techniques used for the treatment of cancer usually associated with side effects. In the last few years, anticancer drugs have been available commercially, but some serious

limitations are found to be side effects, resistance, nondirected to organ and toxicity [101, 102]. To overcome all these limitations, there is an urgent need for an alternate material for more specific and nontoxic purposes. Hence, AuNP-loaded drugs have been invented for anticancer therapy which are nontoxic and more directed towards cancer cells even in high concentrations. Several approaches have been applied to enhance the efficiency of drug loaded with AuNPs towards a targeted area. To address these limitations, AuNPs are widely used in cancer treatment as potential anticancer agent by enhancing drug potential or by heat-activated destruction of cancer cells. Table 8.4 lists a few examples of AuNPs as anticancer agent.

Interestingly, AuNPs with absorption between 650–900 nm are applied in cancer therapy where cells and water absorb radiation at the same wavelength. AuNPs exhibited some anticancer agents to allow more specific diagnosis and targeted delivery. In addition to cancer therapy, AuNPs were also used in tumor diagnostic tests. Photothermal therapy is one of the widely used methods in cancer therapy, which involves AuNPs followed by radiation. As a result of this, a cancer cell undergoes heating and

Table 8.4 Green synthesized AuNPs used as anticancer agent.

S. no.	Plant name	AuNPs size (nm)	AuNPs shape	Cancer cell used
1.	*Achyranthes aspera* Linn.	20–30	Spherical, hexagonal	Cervical cancer cell
2.	*Dendropanax morbifera*	10–20	Hexagonal	Lung cancer cell
3.	*Couroupita guianensis*	7–48	Spherical	HL-60
4.	*Diospyros ferrea*	70–90	Rod	HeLa cell
5.	*Taxus baccata*	20	Spherical	MCF-7, Caov-4, HeLa cells
6.	*Taxus baccata*	20	Spherical	MCF-7, Hep-2
7.	*Gymnema sylvestre*	75	Spherical	HT-29
8.	*Sargassum glaucescens*	3.65–5.34	Spherical	HeLa cell
9.	*Camellia sinensis*	30	Spherical	MCF-7
10.	*Zataria multiflora*	10–42	Pentagonal, triangular	HeLa

destruction of tumor. On the other hand, AuNPs have targeted delivery of drug and high sensitivity to distinguish between tumor cells and normal cells. Therefore, AuNPs are allowed to circulate in the bloodstream for long periods of time to enhance their permeability and retention time [103–105].

8.4.3 Targeted Drug Delivery Using AuNPs

Due to their high surface area, biocompatibility and easy synthesis process, AuNPs are an attractive option for enhancing drug delivery and potential capacity of drugs in targeted drug delivery system. The AuNPs were attached to the drug through covalent or noncovalent bond for controlled release of drug at the directed organ site for various applications. Most of the techniques release drug by photothermal, triggered or ultrasonic method [106]. The AuNPs can release drug by stimuli or triggered method depending on the pH and temperature or biomolecule levels. Targeted drug delivery using AuNPs has gained more attention particularly in cancer or tumor tissue treatment, which was observed in a comparison of normal cells with affected cells [107, 108]. For example, glutathione-AuNPs were achieved which delivered DNA fragment for transcription recovery and doxorubicin release that depended on a pH-responsive method using AuNPs. On the other hand, a photothermal technique using AuNPs was involved in heating of AuNPs using radiation, which results in melting of AuNPs with controlled drug release. Generally, the tumor cells are more highly sensitive to temperature than normal cells. Therefore, drug capped on AuNPs can be desorbed on the targeted spot during the heating process and lose the bonding between drug and AuNPs. This is the basic principle behind drug release of glutathione-AuNPs in tumor cells [109].

Ultrasound radiation is another approach which involves formation of layers of AuNPs deposition on drugs. During ultrasound radiation, these layered AuNP drugs undergo a breakdown of the bond that lies between AuNPs and drug. Finally, the drug will be released on the surface of AuNPs. Drug delivery using AuNPs was also achieved for various drugs such as antibiotics, antivirals and heart medications. One of the studies showed bacterial activity against multidrug-resistant bacteria using AuNPs coated antibiotics. As a result of this application, AuNPs showed potent antibacterial activity against Gram-positive (*Staphylococcus aureus*) and Gram-negative (*Escherichia coli)* using ampicillin-AuNPs. All the studies using drug-coated AuNPs have increased drug delivery significantly for many diseases with improved efficiency [110, 111].

8.4.4 Antimicrobial Activity of AuNPs

Over the last few decades, various diseases have been cured with treatment by AuNPs. Apart from biomedical applications, AuNPs have been utilized for antimicrobial activity against human, food and agricultural pathogens, as shown in Table 8.5 [112]. AuNPs mostly hinder the ionic interaction change in cell membrane, which results in damaged membrane by pathogens. Furthermore, AuNPs increase expression of genes in the redox process and cause the death of bacteria and fungi. The antimicrobial activity was directly influenced by the nano size, surface area and photothermic nature of AuNPs. Still, the mechanism behind antimicrobial activity has not yet been explained. But a few studies have reported the possible mechanism in which AuNPs attack the sulfur or phosphorous base in cells. If the

Table 8.5 List of plants used for AuNPs formation and its antimicrobial activity.

S. no.	Plant name	Microbes tested	Method used
1.	*Acorus calamus*	*Escherichia coli, Staphylococcus aureus*	Agar well diffusion
2.	*Dracocephalum kotschyi*	*E. coli, Pseudomonas aeruginosa* and *Proteus vulgaris*	Agar cup-plate
3.	*Mentha piperita*	*S. aureus* and *E. coli*	Müller-Hinton agar
4.	*Nepenthes khasiana*	*E. coli, Bacillus, Candida albicans* and *Aspergillus niger*	Well diffusion
5.	*Salicornia brachiate*	*Salmonella typhi, E. coli, P. aeruginosa* and *S. aureus*	Disc diffusion
6.	*Gloriosa superba*	*S. aureus, Streptococcus pneumoniae, Klebsiella pneumoniae* and *E. coli*	Disc diffusion
7.	*Solanum nigrum*	*Staphylococcus saprophyticus, Bacillus subtilis* and *E. coli*	Disc diffusion
8.	*Zizyphus mauritiana*	*S. aureus*	Luria medium
9.	*Solanum lycopersicum*	*S. aureus* and *P. aeruginosa*	Well diffusion
10.	*Trianthema decandra* L.	*S. aureus, Enterococcus faecalis, Streptococcus faecalis, E. coli, P. vulgaris, P. aeruginosa, B. subtilis, Yersinia enterocolitica, Klebsiella pneumoniae* and *C. albicans*	Disc diffusion

AuNPs are attached to a thiol group of enzymes, the respiratory chain is suddenly disturbed by generation of a large quantity of free radicals, leading to death. On the other hand, AuNPs decrease ATP activities wherein they reduce the tRNA and ribosomal interaction [113].

There was another mechanism proposed for AuNPS antimicrobial activity in which AuNPs hinder the transmembrane hydrogen efflux (Figure 8.6). However, a lesser concentration of AuNPs can inhibit bacterial growth about 250-fold when the size of NPs is much smaller than bacterial cell so that AuNPs stick on the cell wall of pathogen and delay cell process, causing death. A few other reports showed diverse mechanism when compared to other NPs. AuNPs have the capacity to attract DNA of bacteria by means of the electrostatic force of attraction on the cell wall. When the surface area is high and nano size is small, the possibility of cell death will increase. Apart from the electrostatic force of attraction, AuNPs show diverse activity on Gram-positive and Gram-negative bacteria, which are classified based on the thick layer called peptidoglycan. Peptidoglycan generally consists of small peptides in a long chain, forming an inflexible structure to diffuse the AuNPs. Therefore, the peptidoglycan is very strong in gram positive bacteria that penetrate AuNPs across cell wall whereas Gram-negative bacteria contains a thin layer which easily undergoes cell death [114–116].

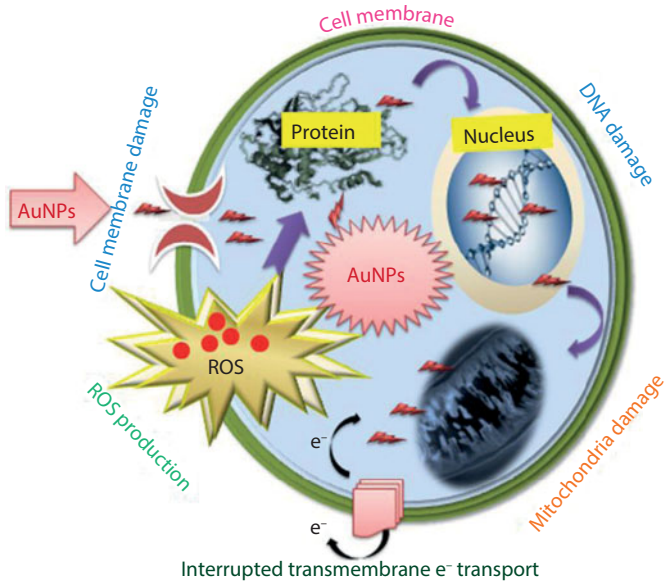


Figure 8.6 Antibacterial mechanism using AuNPs.

Apart from the size of AuNPs and thickness of peptidoglycan layer, a few other factors affect antimicrobial activity, including capping agents, concentration and purification methods. In such cases, AuNPs coated on cotton showed good inhibition and antibiotic-coated AuNPs increased the inhibition of individual antibiotics. It was also observed that plant extract used for the synthesis of AuNPs showed greater inhibition than AuNPs prepared by chemical method. The antimicrobial activities of green synthesized AuNPs may be due to the synergistic effect of AuNPs with plant extract [117–120].

8.4.5 Inhibition of Free Radical and Determination of Antioxidant Capacity Using AuNPs

Free radicals carry one or more unpaired electrons with highly unstable and reactive properties, which cause many diseases in the human body. To stabilize the free radical, it needs to gain an electron from antioxidants. Many reactive oxygen species, including hydrogen peroxide, superoxide and hydroxyl radicals, lead to oxidative damage in living organisms. The free radicals are reported as causing many diseases such as cancer, hypertension and arthritis. AuNPs are one of the constituents that prevent oxidative stress in cell membrane. The AuNPs have displayed scavenging of free radicals and reduce the concentration of reactive oxygen species, thus acting as antioxidant.

The seeds of *Elettaria cardamomum* were used to synthesize AuNPs and for free radical scavenging of DPPH (2,2-diphenyl-1-picrylhydrazyl) and NO (nitric oxide) scavenging activity. DPPH is one of the nitrogen-centered free radicals which can be stabilized by donation of electron or hydrogen from antioxidant. The AuNPs acted as an adsorbent to reduce the concentration of DPPH and NO radicals. The higher quenching capacity of AuNPs was observed for antioxidant capacity of the obtained AuNPs. The NO production generates harmful effects and is inhibited by AuNPs [121]. In another report, AuNPs were synthesized using *Nerium oleander* leaf extract employed for DPPH radical inhibition. The green synthesized AuNPs inhibited DPPH radical and showed effective inhibition compared with standard vitamin C [122]. Fruits are considered as a phenolic acid-rich source with great antioxidant property. The fruit of *Couroupita guianensis* was used in AuNPs synthesis as reducing and stabilizing agent. The AuNPs quenched with DPPH and hydroxyl free radical showed significant inhibition. All the concentrations used in inhibition showed a dose-dependent manner and the IC_{50} value was found to be 37 μg/mL [123]. The quenching capacity of AuNPs depends on the surface area, size and morphology of

AuNPs. Therefore, the AuNPs are still a challenging material in biological applications.

Apart from the inhibition of free radicals, AuNPs were also utilized for determination of antioxidant capacity. The antioxidant capacity can be determined by three different methods: One method is based on scavenging efficiency against reactive oxygen species, another method uses complete standard assays, and a third method is based on hydrogen transformation or single electron transfer methods. However, nanotechnology is a great platform, which has opened up applications in a wide range [124]. One of the most recent applications of AuNPs was their utilization in determination of antioxidant capacity. The antioxidant capacity was measured based on synthesis of AuNPs with different extracts and phytochemicals. Scampicchio *et al.* were the first to develop this method to determine antioxidant capacity. The citric acid was used as a precursor to synthesize AuNPs and the capacity was determined from UV-Vis spectrophotometry (Table 8.6). The phenolic-rich honey, soy extract and tea were used to synthesize AuNPs and the antioxidant capacity determined from sigmoidal curves [125].

Table 8.6 AuNPs-based assay for antioxidant capacity determination.

S. no.	Mechanism	Standard	Reducing agent	Application
1.	Reduction of gold ions	Phenolic acid	Tea	Total optical antioxidant capacity assessment
		Phenolic acid	Fruits	Adulteration of oils
		Polyphenols	Honey, soy extract	Antioxidant capacity
2.	Color change based on varying sizes of AuNPs in gold nanoshell by antioxidant action	Tartaric acid, citric acid	–	Screening analysis based on H_2O_2 scavenging activity
		Phenolic acids	Tea, herbs	Optical nanoprobes Comparison with DPPH
3.	Color change from dispersed (red) to aggregated (blue)	Polyphenols	Tea, juice	Antioxidant capacity

8.5 Conclusion and Future Prospective

The enormous growth in the developing field of nanotechnology is due to its wide range of applications in various fields. The synthesis of AuNPs has been reported by several methods, particularly green synthesis using plant extracts, which deals with nontoxic and eco-friendly approaches. Obviously, AuNPs have great biological and biomedical applications that directly depend on the synthesis process, size, shape and stability. As AuNPs stand now, many commercially available drugs with AuNPs are reported for biomedical applications. Specifically, AuNPs in cancer therapy, targeted drug delivery and bioimaging are being widely studied and may create many applications in the future, which will require clinical trials. Considering the exclusive properties of AuNPs, efforts have been made towards their potential use in biological activities over the past few years. There are a few hidden applications that have to be developed using AuNPs. Plant extracts have enormous potential in the synthesis of AuNPs of desired size and shape. Great effort should be taken to explain the mechanisms of green synthesis using extracts and phytochemicals, which will be important in obtaining better properties of AuNPs.

Conflict of Interest

The authors declare no conflict of interest.

Acknowledgment

Financial support from DST-SERB (FTYS-SB/FT/CS-113/2013) and kind support from Vellore Institute of Technology, are gratefully acknowledged.

References

1. Naghdi, M., Taheran, M., Satinder, K.B., Verma, M., Surampalli, R.Y., Valero, J.R., Green and energy-efficient methods for the production of metallic nanoparticles. *Beilstein J. Nanotechnol.*, 6, 2354–2376, 2015.
2. Epa, V.C., Burden, F.R., Tassa, C., Weissleder, R., Shaw, S., Winkler, D.A., Modeling biological activities of nanoparticles. *Nano. Lett.,* 12, 5808–5812, 2012.

3. Mostafa, A.A., Sayed, S.R.M., Solkamy, E.N., Khan, M., Shaik, M.R., Al-Warthan, A., Adil, S.F., Evaluation of biological activities of chemically synthesized silver nanoparticles. *J. Nanomater.,* 38–47, 2015.
4. Salata, O.V., Applications of nanoparticles in biology and medicine. *J. Nanobiotechnol.,* 2, 1–6, 2004.
5. Yurkov, G.Y., Fionov, A.S., Koksharovc, Y.A., Kolesovb, V.V., Gubin, S.P., Electrical and magnetic properties of nanomaterials containing iron or cobalt nanoparticles. *Inorg. Mater.,* 43, 834–844, 2007.
6. Su, H., Li, Y., Li, X.Y., Wong, K.S., Optical and electrical properties of Au nanoparticles in two-dimensional networks: An effective cluster model. *Optic. Exp.,* 17, 22223–22234, 2009.
7. Kittler, S., Greulich, C., Koller, M., Epple, M., Synthesis of PVP-coated silver nanoparticles and their biological activity towards human mesenchymal stem cells. *Mater. Sci. Eng. Technol.,* 40, 258–264, 2009.
8. Yadav, L.S.R., Archana, B., Lingaraju, K., Kavitha, C., Suresh, D., Nagabhushana, H., Nagaraju, G., Electrochemical sensing, photocatalytic and biological activities of ZnO nanoparticles: Synthesis via green chemistry route. *Int. J. Nanosci.,* 15, 1–11, 2016.
9. Sajja, H.K., East, M.P., Mao, H., Wang, Y.A., Nie, S., Yang, L., Development of multifunctional nanoparticles for targeted drug delivery and non-invasive imaging of therapeutic effect. *Curr. Drug. Discov. Technol.,* 6, 43–51, 2009.
10. Calderón-Jiménez, B., Johnson, M.E., Montoro Bustos, A.R., Murphy, K.E., Winchester, M.R., Vega Baudrit, J.R., Silver nanoparticles: Technological advances, societal impacts and metrological challenges. *Front. Chem.,* 5, 1–26, 2017.
11. Govan, J., Gun'ko, Y.K., Recent advances in the application of magnetic nanoparticles as a support for homogeneous catalysts. *Nanomater.,* 4, 222–241, 2014.
12. Desai, N., Challenges in development of nanoparticle-based therapeutics. *AAPS J.,* 14, 282–295, 2012.
13. Shin, T.H., Choi, Y., Kim, S., Cheon, J., Recent advances in magnetic nanoparticle-based multi-modal imaging. Chem. Soc. Rev., 44, 4501–4516, 2015.
14. De, M., Ghosh, P.S., Rotello, V.M., Applications of nanoparticles in biology. *Adv. Mater.,* 20, 4225–4271, 2008.
15. Chen, M., Cai, Y., Yan, Z., Goodman, D.W., On the origin of the unique properties of supported Au nanoparticles. *J. Am. Chem. Soc.,* 128, 6341–6346, 2006.
16. Senanayake, S.D., Stacchiola, D., Rodriguez, J.A., Unique properties of ceria nanoparticles supported on metals: Novel inverse ceria/copper catalysts for CO oxidation and the water-gas shift reaction. *Acct. Chem. Res.,* 46, 1702–1711, 2013.
17. Kwizera, E.A., Chaffin, E., Shen, X., Chen, J., Zou, Q., Wu, Z., Gai, Z., Bhana, S., O'Connor, R., Wang, L., Adhikari, H., Mishra, S.R., Wang, Y., Huang, X.,

Size and shape controlled synthesis and properties of magnetic plasmonic core–shell nanoparticles. *J. Phys. Chem.,* 120, 10530–10546, 2016.
18. Hu, G., Jiao, B., Shi, X., Valle, R.P., Fan, Q., Zuo, Y,Y., Physicochemical properties of nanoparticles regulate translocation across pulmonary surfactant monolayer and formation of lipoprotein corona. *ACS Nano.,* 7, 10525–10533, 2013.
19. Shin, S.W., Song, I.H., Soong, H.U., Role of physicochemical properties in nanoparticle toxicity. *Nanomater*., 5, 1351–1365, 2015.
20. Gatoo, M.A., Naseem, S., Arfat, M.Y., Dar, A.M., Qasim, K., Zubair, S., Physicochemical properties of nanomaterials: Implication in associated toxic manifestations. *Biomed. Res. Int.,* 1–9, 2014.
21. Helmlinger, J., Sengstock, C., Groß-Heitfeld, C., Mayer, C., Schildhauer, T.A., Köller, M., Epple, M., Silver nanoparticles with different size and shape: equal cytotoxicity, but different antibacterial effects. *RSC Adv.,* 6, 18490–18501, 2016.
22. Mosselhy, D.A., El-Aziz, M.A., Hanna, M., Ahmed, M.A., Husien, M.M., Feng, Q., Comparative synthesis and antimicrobial action of silver nanoparticles and silver nitrate. *J. Nanopart. Res.,* 17, 473–483, 2015.
23. Fleming, D.A., Williams, M.E., Size-controlled synthesis of gold nanoparticles via high-temperature reduction. *Langmuir,* 20, 3021–3023, 2004.
24. Piella, J., Neus, G.B., Puntes., V., Size-controlled synthesis of sub-10-nanometer citrate-stabilized gold nanoparticles and related optical properties. *Chem. Mater.,* 28, 1066–1075, 2016.
25. Koushik, P., Braja, G.B., Samanta, K., Green coconut (*Cocos nucifera* Linn) shell extract mediated size controlled green synthesis of polyshaped gold nanoparticles and its application in catalysis. *Appl. Nanosci.,* 4, 769–775, 2014.
26. Hayashi, H., Hakuta, Y., Hydrothermal synthesis of metal oxide nanoparticles in supercritical Water. *Materials,* 3, 3794–3817, 2010.
27. Rahman, I.A., Padavettan, V., Synthesis of silica nanoparticles by sol-gel: Size-dependent properties, surface modification, and applications in silica-polymer nanocomposites–A review. *J. Nanomater.,* 2012, 132424, 2012.
28. Duan, H., Wang, D., Li, Y., Green chemistry for nanoparticle synthesis. *Chem. Soc. Rev.,* 44, 5778–5792, 2015.
29. Dhand, C., Dwivedi, N., Loh, X.J., Ying A.N.J., Verma, N.K., Beuerman, R.W., Rajamani Lakshminarayanan, R., Seeram Ramakrishna, S., Methods and strategies for the synthesis of diverse nanoparticles and their applications: a comprehensive overview. *RSC Adv.,* 5, 105003–105037, 2015.
30. Bang, J.H., Suslick, K.S., Applications of ultrasound to the synthesis of nanostructured materials. *Adv. Mater.,* 22, 1039–1059, 2010.
31. Singh, P., Kim, Y.J., Zhang, D., Yang, D.C., Biological synthesis of nanoparticles from plants and microorganisms. *Trend. Biotechnol.,* 34, 588–599, 2016.
32. Rajakumar, G., Rahuman, A.A., Roopan, S.M., Chung, I.M., Anbarasan, K., Karthikeyan, V., Efficacy of larvicidal activity of green synthesized titanium

dioxide nanoparticles using *Mangifera indica* extract against blood-feeding parasites. *Parasitol. Res.,* 114, 571–581, 2014.
33. Surendra, T.V., Roopan, S.M., Photocatalytic and antibacterial properties of phytosynthesized CeO_2 NPs using *Moringa oleifera* peel extract. *J. PhotoChem. Photobiol. B,* 161, 122–128, 2016.
34. Roopan, S.M., An Overview of phytoconstituents, biotechnological applications, and nutritive aspects of Coconut (*Cocos nucifera*). *Appl. Biochem. Biotechnol.,* 179, 1309–1324, 2016.
35. Fowsiya, J., Madhumtiha, G., Al-Dhabi, N.A., Arasu, M.V., Photocatalytic degradation of Congo red using *Carissa edulis* extract capped zinc oxide nanoparticles. *J. Photochem. Photobiol. B,* 162, 395–401, 2016.
36. Bhosale, R.R., Kulkarni, A.S., Gilda, S.S., Aloorkar, N.H., Osmani, R.A., Harkare, B.R., Innovative eco-friendly approaches for green synthesis of silver nanoparticles. *Int. J. Pharm. Sci. Nanotechnol.,* 7, 2328–2337, 2014.
37. Banerjee, P., Satapathy, M., Mukhopahayay, A., Das, P., Leaf extract mediated green synthesis of silver nanoparticles from widely available Indian plants: synthesis, characterization, antimicrobial property and toxicity analysis. *Bioresour. Bioprocess.,* 1, 1–10, 2014.
38. Srikar, S.K., Giri, D.D., Pal, D.B., Mishra, P.K., Upadhyay, S.N., Green synthesis of silver nanoparticles: A review. *Green. Sustain. Chem.,* 6, 34–56, 2016.
39. Amini, N., Amin, G., Azar, Z.J., Green synthesis of silver nanoparticles using *Avena sativa* extract. *Nanomed. Res.,* 2, 57–63, 2017.
40. Roy, S., Das, T.K., Plant mediated green synthesis of silver nanoparticles-A review. *Int. J. Plant. Biol. Res.,* 3, 1044–1055, 2015.
41. Daniel, M.C., Astruc. D., Gold Nanoparticles: Assembly, supramolecular chemistry, quantum-size-related properties, and applications toward biology, catalysis, and nanotechnology. *Chem. Rev.*, 104, 293–346, 2004.
42. Wang, Y.Z., Huang, B., Lv, J., Liang, X.J., Current status of nanotechnology applied in biomedicine. *Acta Biophys. Sinica*, 25, 168–174, 2009.
43. Ho, J.A.A., Chang, H.C., Shih, N.Y., *et al.,* Diagnostic detection of human lung cancer-associated antigen using a gold nanoparticle-based electrochemical immune sensor. *Anal. Chem.*, 82, 5944–5950, 2010.
44. Chandran, K., Song, S., Yun, S., Effect of size and shape controlled biogenic synthesis of gold nanoparticles and their mode of interactions against food borne bacterial pathogens. *Arab. J. Chem.,* 1–14, 2014.
45. Krishnaraj, C., Muthukumaran, P., Ramachandran, R., Balakumaran, M.D., Kalaichelvan P.T., *Acalypha indica* Linn: Biogenic synthesis of silver and gold nanoparticles and their cytotoxic effects against MDA-MB-231, human breast cancer cells. *Biotechnol. Rep.,* 4, 42–49, 2014.
46. Rai, A., Chaudhary, M., Ahmad, A., Bhargava, S., Sastry, M., Synthesis of triangular Au core-Ag shell nanoparticles. *Mater. Res. Bull.,* 42, 1212- 1220, 2007.
47. Murugan, K., Benelli, G., Panneerselvam, C., Subramaniam, J., Jeyalalitha, T., *et al., Cymbopogon citratus*-synthesized gold nanoparticles boost the

predation efficiency of copepod *Mesocyclops aspericornis* against malaria and dengue mosquitoes. *Exp. Parasitol.,* 153, 129–38, 2015.
48. Singh, C., Sharma, V., Naik, P.K.R., Khandelwal, V., Singh, H., A Green biogenic approach for synthesis of gold and silver. *Dig. J. Nanomater. Biostruct.,* 6, 535–542, 2011.
49. Shankar, S.S., Ahmad, A., Pasricha, R., Sastry, M., Bioreduction of chloroaurate ions by geranium leaves and its endophytic fungus yields gold nanoparticles of different shapes. *J Mater. Chem.,* 13, 1822, 2003.
50. Bhau, B.S., Ghosh, S., Puri, S., Borah, B., Sarmah, D.K., Khan, R., Green synthesis of gold nanoparticles from the leaf extract of *Nepenthes khasiana* and antimicrobial assay. *Adv. Mater. Lett*., 6, 55–58, 2015.
51. Kumar, V.G., Gokavarapu, S.D., Rajeswari, A., Dhas, T.S., Karthick, V., Kapadia, Z., Shrestha, T., Barathy, I.A., Roy, A, Sinha, S., Facile green synthesis of gold nanoparticles using leaf extract of antidiabetic potent *Cassia auriculata*. *Colloids Surf. B*, 87, 159–163, 2011.
52. Narayanan, K.B., Sakthivel, N., Coriander leaf mediated biosynthesis of gold nanoparticles. *Mater. Lett*., 62, 4588–4590, 2008.
53. Ganeshkumar, M., Sathishkumar, M., Ponrasu, T., Dinesh, M.G., Suguna, L., Spontaneous ultra fast synthesis of gold nanoparticles using *Punica granatum* for cancer targeted drug delivery. *Colloids Surf. B*, 106, 208–216, 2013.
54. Philip, D., Green synthesis of gold and silver nanoparticles using *Hibiscus rosasinensis*. *Physica E*., 42, 1417–1424, 2010.
55. Yilmaz, M., Turkdemir, H., Kilic, M.A., Bayram, E., Cicek, A., Mete, A., Ulug, B., Biosynthesis of silver nanoparticles using leaves of *Stevia rebaudiana*. *Mater. Chem. Phys.,*130, 1195–1202, 2011.
56. Rao, K.J., Paria, S., Green synthesis of gold nanoparticles using aqueous *Aegle marmelos* leaf extract and their application for thiamine detection. *RSC Adv.,* 4, 28645–28652, 2014.
57. Huang, J., Li, Q., Sun, D., Lu, Y., Su, Y., Yang, X., Wang, H., Wang, Y., Shao, W., He, N., Biosynthesis of silver and gold nanoparticles by novel sundried *Cinnamomum camphora* leaf. *Nanotechnol.,* 18, 105104–105115, 2007.
58. Wang, Y., He, X., Wang, K., Zhang, X., Tan, W., *Barbated skullcup* herb extract-mediated biosynthesis of gold nanoparticles and its primary application in electrochemistry. *Colloids Surf. B,* 73, 75–79, 2009.
59. Gardea-Torresdey, J.L., Parsons, J.G., Gomez, E., Peralta-Videa, J., Troiani, H.E., Santiago, P., Yacaman, Jose, M.J., Formation and growth of Au nanoparticles in live side live alfalfa plants. *Nano. Lett.,* 2, 397–401, 2002.
60. Khaleel, B.S., Govindaraju, K., Manikandan, R., Ahn, J.S., Bae, E.Y., Singaravelu, G., Phytochemical mediated gold nanoparticles and their PTP 1B inhibitory activity. *Colloids Surf. B,* 75, 405–409, 2010.
61. Ankamwar, B., Chaudhary, M., Sastry, M., Gold nanotriangles biologically synthesized using tamarind leaf extract and potential application in vapor sensing. *Syn. React. Inorg. Metal. Nano. Metal. Chem.,* 35, 19–26, 2005.

62. Dorosti, N., Jamshidi, F., Plant-mediated gold nanoparticles by *Dracocephalum kotschyi* as anticholinesterase agent: Synthesis, characterization, and evaluation of anticancer and antibacterial activity. *J. Econ. Financ. Adm. Sci.,* 14, 235–245, 2016.
63. Khalil, M.M.H., Ismail, E.H., El-Magdoub, F., Biosynthesis of Au nanoparticles using olive leaf extract. *Arab. J. Chem.,* 5, 431–437, 2012.
64. Anuradha, J., Abbasi, T., Abbasi, S.A., An eco-friendly method of synthesizing gold nanoparticles using an otherwise worthless weed pistia (*Pistia stratiotes* L.). *J. Adv. Res.,* 6, 711–720, 2015.
65. Tahir, K., Nazir, S., Li, B., Khan, A.U., Khan, Z.U.H., Gong, P.Y., Khan, S.U., Ahmad, A., *Nerium oleander* leaves extract mediated synthesis of gold nanoparticles and its antioxidant activity. *Mater. Lett.,* 156, 198–201, 2015.
66. Mittal, A.K., Bhaumik, J., Kumar, S., Banerjee, U.C., Biosynthesis of silver nanoparticles: Elucidation of prospective mechanism and therapeutic potential. *J. Colloid Interface Sci.,* 415, 39–47, 2014.
67. Jayaseelan, C., Ramkumar, R., Rahuman, A.A., Perumal, P., Green synthesis of gold nanoparticles using seed aqueous extract of *Abelmoschus esculentus* and its antifungal activity. *Ind. Crop. Prod.,* 45, 423–429, 2013.
68. Krishnaswamy, K., Vali, H., Orsat, V., Value-adding to grape waste: Green synthesis of gold nanoparticles. *J. Food. Eng.,* 142, 210–220, 2014.
69. Basavegowda, N., Idhayadhulla, A., Lee, Y.R., Phyto-synthesis of gold nanoparticles using fruit extract of *Hovenia dulcis* and their biological activities. *Ind. Crop. Prod.,* 52, 745–751, 2014.
70. Yu, J., Xu, D., Guan, H.N., Wang, C., Huang, L.K., Chi, D.F., Facile one-step green synthesis of gold nanoparticles using *Citrus maxima* aqueous extracts and its catalytic activity. *Mater. Lett.,* 166, 110–112, 2016.
71. Sujitha, M.V., Kannan, S., Green synthesis of gold nanoparticles using Citrus fruits (*Citrus limon, Citrus reticulata* and *Citrus sinensis*) aqueous extract and its characterization. *Spectrochim. Acta A,* 102, 15–23, 2013.
72. Kumar, B., Smita, K., Cumbal, L., Camacho, J., Hernández-Gallegos, E., Chávez-López, M.G., Grijalva, M., Andrade, K., One pot phytosynthesis of gold nanoparticles using *Genipa americana* fruit extract and its biological applications. *Mater. Sci. Eng. C,* 62, 725–731, 2016.
73. Ganeshkumar, M., Sathishkumar, M., Ponrasu, T., Dinesh, M.G., Suguna, L., Spontaneous ultra fast synthesis of gold nanoparticles using *Punica granatum* for cancer targeted drug delivery. *Colloids Surf. B,* 106, 208–216, 2013.
74. Rajan, A., Meenakumari, M., Philip, D., Shape tailored green synthesis and catalytic properties of gold nanocrystals. *Spectrochim. Acta. A*, 118, 793–799, 2014.
75. Kumar, K.M., Mandal, B.K., Kumar, H.A.K., Maddinedi, S.B., Green synthesis of size controllable gold nanoparticles. *Spectrochim. Acta A,* 116, 539–545, 2013.
76. Nagaraj, B., Malakar, B., Divya, T.K., Krishnamurthy, N.B., Liny, P., Dinesh, R., Environmental benign synthesis of gold nanoparticles from the flower

extracts of *Plumeria alba* Linn. (Frangipani) and evaluation of their biological activities. *Int. J. Drug Dev. Res.,* 4, 144–150, 2012.
77. Venkatachalam, M., Govindaraju, K., Sadiq, A.M., Tamilselvan, S., Kumar, V.G., Singaravelu, G., Functionalization of gold nanoparticles as antidiabetic nanomaterial, *Spectrochim. Acta A,* 116, 331–338, 2013.
78. Krishnamoorthy, G., Shabi, M.M., Ravindhran, D., Uthrapathy, S., Rajamanickam, G.V., Dubey, G.P., *Nardostachys jatamansi*: Cardioprotective and hypolipidemic herb. *J. Pharm. Res.,* 2, 574–578, 2009.
79. Radha, R., Murugalakshmi, M., Kokila, S., Eco friendly synthesis and characterization of gold nanoparticles from *Bauhinia purpurea* flower extract. *Imp. J. Interdisp. Res.,* 2, 306–310, 2016.
80. Shiv, S.S., Ahmad A., Pasricha R., Sastry M.J., Bioreduction of chloroaurate ions by germanium leaves and its endophytic fungus yields gold nanoparticles of different shapes. *Mater. Chem*., 13, 1822–1846, 2013.
81. Singh, A.K., Talat M., Singh, D.P., Srivastava, O.N., Biosynthesis of gold and silver nanoparticles by natural precursor clove and their functionalization with amine group. *J. Nanopart. Res.,* 12, 1667–1675, 2010.
82. Ahmad, N., Sharma S., Alam, M.K., Singh, V.N., Shamsi S.F., Mehta, B.R., Fatma, A., Rapid synthesis of silver nanoparticles using dried medicinal plant of basil. *Colloids Surf. B,* 81, 81–86, 2010.
83. Kasthuri, J., Veerapandian, S., Rajendiran, N., Biological synthesis of silver and gold nanoparticles using apiin as reducing agent. *Colloids Surf. B*, 68, 55–60, 2009.
84. Panigrahi, S., Kundu, S., Ghosh, S., Nath, S., Pal, T.J., General method of synthesis for metal nanoparticles. *Nanopart. Res.,* 6, 411–414, 2004.
85. Saikat, M., Selvakannan, P.R., Phadtare S., Renu P., Sastry M., Synthesis of a stable gold hydrosol by the reduction of chloroaurate ions by the amino acid, aspartic acid. *J. Chem. Sci.,* 114, 513–520, 2002.
86. Tan, Y.N., Lee, J.Y., Wang, D.I., Uncovering the design rules for peptide synthesis of metal nanoparticles. *J. Am. Chem. Soc.,* 132, 5677–5686, 2010.
87. Si, S., Bhattacharjee, R.R., Banerjee, A., Mandal, T.K., A mechanistic and kinetic study of the formation of metal nanoparticles by using synthetic tyrosine-based oligopeptides. *Chem*., 12, 1256–1265, 2006.
88. Pan, D., Lanza, G.M., Wickline, S.A., Caruthers, S.D., Nanomedicine: Perspective and promises with ligand directed molecular imaging. *Eur. J. Radiol.,* 70, 274–285, 2009.
89. Hainfeld, J.F., Powell, R.D. New frontiers in gold labeling. *J. Histochem. Cytochem.,* 48, 471–480, 2000.
90. Loo, C., Lowery, A., Halas, N., West, J., Drezek, R., Immunotargeted nanoshells for integrated cancer imaging and therapy. *Nano. Lett.,* 5, 709–711, 2005.
91. Huang, X., El-Sayed, I.H., Qian, W., El-Sayed, M.A., Cancer cell imaging and photothermal therapy in the near infrared region by using gold nanorods. *J. Am. Chem. Soc.,* 128, 2115–2120, 2006.

92. Ipe, B.I., Yoosaf, K., Thomas, K.G., Functionalized gold nanoparticles as phosphorescent nanomaterials and sensors. *J. Am. Chem. Soc.,* 128, 1907–1913, 2006.
93. Comby, S., C., Gunnlaugsson, T., Luminescent lanthanide functionalized golf nanoparticles: Exploiting the interaction with bovine serum albumin for potential sensing applicaitions. *ACS Nano,* 5, 7184–7197, 2011.
94. Park, J., Estrada, A., Sharp, K., Sang, K., Schwartz, J.A., Smith, D.K., Coleman, C., Payne, J.D., Korgel, B.A., Dunn, A.K., Tunnell, J.W., Two photon induced photoluminescence imaging of tumors using near infrared excited gold nanoshells. *Opt. Exp.,* 16, 1590–1599, 2008.
95. Okamoto, H., Imura, K., Near field imaging of optical field and plasmon wavefunctions in metal nanoparticles. *J. Mater. Chem.,* 16, 3920–3928, 2006.
96. Durr, N.J., Larson, T., Smith, D.K., Korgel, B.A., Sokolov, K., Ben-Yakar, A., Two-photon luminescence imaging of cancer cells using molecularly targeted gold nanorods. *Nano Lett.,* 7, 941–945, 2007.
97. Tong, L., Zhao, Y., Huff, T.B., Hansen, M.N., Wei, A., Cheng, J.X., Gold nanorods mediate tumor cell death by compromising membrane integrity. *Adv. Mater.,* 19, 3136–3141, 2007.
98. Huff, T.B., Hansen, M.N., Zhao, Y., Cheng, J., Wei, A., Controlling the cellular uptake of gold nanorods. *Langmuir,* 23, 1596–1599, 2007.
99. Debouttiere, P.J., Roux, S., Vocanson, F., Billotey, C., Beuf, O., Favre-Réguillon, A., Lin, Y., Pellet-Rostaing, S., Lamartine, R., Perriat, P., Tillement, O., Design of gold nanoparticles for magnetic resonance imaging. *Adv. Funct. Mater.,* 16, 2330–2339, 2006.
100. Hainfeld, J.F., Slatkin, D.N., Focella, T.M., Smilowitz, H.M., Gold nanoparticles: A new X-ray contrast agent. *Br. J. Radiol.,* 79, 248–253, 2006.
101. Pender, D.S., Vangala, L.M., Badwaik, V.D., Willis, C.B., Aguilar, Z.P., Sangoi, T.N., Paripelly, R., Dakshinamurthy, R., Bactericidal activity of starch encapsulated gold nanoparticles. *Front. Biosci.,* 18, 993–1002, 2013.
102. Chanda, N., Kattumuri, V., Shukla, R., Zambre, A., Katti, K., Upendran, A., *et al.,* Bombesin functionalized gold nanoparticles show *in vitro* and *in vivo* cancer receptor specificity. *Proc. Natl. Acad. Sci.,* 107, 8760–8765, 2011.
103. Jana, N.R., Gearheart, L., Murphy, C.J., Wet chemical synthesis of high aspect ratio cylindrical gold nanorods. *J. Phys. Chem. B,* 105, 4065–4067, 2001.
104. Medley, C.D., Smith, J.E., Tang, Z., Wu, Y., Bamrungsap, S., Tan, W., Gold nanoparticle based colorimetric assay for the direct detection of cancerous cells. *Anal. Chem.,* 80, 1067–1072, 2008.
105. Lu, W., Singh, A.K., Khan, S.A., Senapati, D., Yu, H., Ray, P.C., Gold nano-popcorn-based targeted diagnosis, nanotherapy treatment, and *in situ* monitoring of photothermal therapy response of prostate cancer cells using surface enhanced Raman spectroscopy. *J. Am. Chem. Soc.,* 132, 18103–18114, 2010.
106. Moon, G.D., Choi, S.W., Cai, X., Li, W., Cho, E.C., Jeong, U., Wang, L.V., Xia, Y., A new theranostic system based on gold nanocages and phase-change

materials with unique features for photoacoustic imaging and controlled release. *J. Am. Chem. Soc.,* 133, 4762–4765, 2011.
107. Nakanishi, J., Nakayama, H., Shimizu, T., Ishida, H., Kikuchi, Y., Yamaguchi, K., Horiike, Y., Light-regulated activation of cellular signaling by gold nanoparticles that capture and release amines. *J. Am. Chem. Soc.,* 131, 3822–3823, 2009.
108. Thiel, J., Pakstis, L., Buzby, S., Raffi, M., Ni, C., Pochan, D.J., Shah, S.I., Antibacterial properties of silver doped titania. *Small*, 3, 799–803, 2007.
109. Saha, B., Bhattacharya, J., Mukherjee, A., Ghosh, A.K., Santra, C.R., Dasgupta, A.K., Karmakar, P., *In vitro* structural and functional evaluation of gold nanoparticles conjugated antibiotics. *Nanoscale Res. Lett.,* 2, 614–622, 2007.
110. Pissuwan, D., Valenzuela, S.M., Miller, C.M., Cortie, M.B., A golden bullet? Selective targeting of Toxoplasma gondii tachyzoites using antibody-functionalized gold nanorods. *Nano Lett.,* 7, 3808–3812, 2007.
111. El-Batal, A.I., Hashem, A.A.M., Abdelbaky, N.M., Gamma radiation mediated green synthesis of gold nanoparticles using fermented soybean-garlic aqueous extract and their antimicrobial activity. *SpringerPlus,* 2, 129–139, 2013.
112. Glišić B.Đ., Djuran, M.I., Gold complexes as antimicrobial agents: An overview of different biological activities in relation to the oxidation state of the gold ion and the ligand structure. *Dalton Trans*., 43, 5950–5969, 2014.
113. Gopinath, K., Gowri, S., Arumugam, A., Phytosynthesis of silver nanoparticles using *Pterocarpus santalinus* leaf extract and their antibacterial properties. *J. Nanostruct. Chem.,* 3, 68–75, 2013.
114. Cui, Y., Zhao, Y., Tian, Y., Zhang, W., Lü, X., Jiang, X., The molecular mechanism of action of bactericidal gold nanoparticles on *Escherichia coli*. *Biomater.,* 33, 2327–2333, 2012.
115. Ahmad, T., Wani, I.A., Lone, I.H., Ganguly, A., Manzoor, N., Ahmad, A., Ahmed, J., Al-Shihri, A.S., Antifungal activity of gold nanoparticles prepared by solvothermal method. *Mater. Res. Bull.*, 48, 12–20, 2013.
116. Herdt, A.R., Drawz, S.M., Kang, Y., Taton, T.A., DNA dissociation and degradation at gold nanoparticle surfaces. *Colloids Surf. B,* 51, 130–139, 2006.
117. Kaviya, S., Santhanalakshmi, J., Viswanathan, B., Muthumary, J., Srinivasan, K., Biosynthesis of silver nanoparticles using *Citrus sinensis* peel extract and its antibacterial activity. *Spectrochim. Acta. A,* 79, 594–598, 2011.
118. Bindhu, M.R., Umadevi, M., Antibacterial activities of green synthesized gold nanoparticles. *Mater. Lett.,* 120, 122–125, 2014.
119. Ramesh, V., Armash, A., Green synthesis of gold nanoparticles against pathogens and cancer cells. *Int. J. Pharmacol. Res.,* 5, 250–256, 2015.
120. Bhau, B.S., Ghosh, S., Puri, S., Borah, B., Sarmah, D.K., Khan, R., Green synthesis of gold nanoparticles from the leaf extract of *Nepenthes khasiana* and antimicrobial assay. *Adv. Mater. Lett.*, 26, 55–58, 2015.
121. Rajan, A., Rajan, A.R., Philip, D., *Elettaria cardamomum* seed mediated rapid synthesis of gold nanoparticles and its biological activities. *OpenNano,* 2, 1–8, 2017.

122. Tahir, K., Nazir, S., Li, B., Khan, A.U., Khan, Z.U.H., Gong, P.Y., Khan, S.U., Ahmad, A., *Nerium oleander* leaves extract mediated synthesis of gold nanoparticles and its antioxidant activity. *Mater. Lett.,* 156, 198–201, 2015.
123. Sathishkumar, G., Pradeep, K.J., Vignesh, V., Rajkuberan, C., Jeyaraj M., Selvakumar, M., Jha, R., Sivaramakrishnan, S., Cannonball fruit (*Couroupita guianensis*, Aubl.) extract mediated synthesis of gold nanoparticles and evaluation of its antioxidant activity. *J. Molecul. Liquid.,* 215, 229–236, 2016.
124. Tsao, R., Deng, Z., Separation procedures for naturally occurring antioxidant phytochemicals. *J. Chromatogr. B*, 812, 85–99, 2009.
125. Scampicchio, M., Wang, J., Blasco, A.J., Arribas, A.S., Mannino, S., Escarpa, A., Nanoparticle-based assays of antioxidant activity. *Anal. Chem.,* 78, 2060–2063, 2006.

9

Green Tiny Magnets: An Economic and Eco-friendly Remedy for Environmental Damage

Paramita Karfa and Rashmi Madhuri*

Department of Applied Chemistry, Indian Institute of Technology (Indian School of Mines), Dhanbad, Jharkhand, India

Abstract

In the current era, we enjoy a lavish lifestyle due to the use of nanomaterials. They are an integral part of our life and now we are totally dependent on them. For example, nanomaterials are a part of medicines for different serious diseases, abundant energy production, food safety and homeland security, electronic gadgets, cosmetics, etc. But like the two faces of a coin, they are also the real culprit behind the generation of environmental pollution. To overcome these drawbacks, nowadays researchers are focused on the development of green techniques or reactions which are beneficial to the environment and fruitful in terms of cost. Among the various nanoparticles, the class of magnetic nanoparticles is most popular in terms of environmental applications. Magnetic nanoparticles have the best adsorptive property, quick recovery ability, extraordinary stability and an adsorptive surface on which specific ligands of contaminants are attached. In this chapter, we will summarize the applications of magnetic nanoparticles which do not have any role in environment contamination, i.e., nanoparticles prepared through green chemistry routes only. We will also focus on the applications of magnetic nanoparticles for curing environmental damage like purification of contaminated water or soil, industrial waste removal, and fabrication of sensors to detect heavy metals or organic contaminants present in air or water. In addition, the future of magnetic nanoparticles in combination with other nanomaterials applicable to making a green and healthy environment is also discussed in the concluding part of this chapter.

**Corresponding author*: paramitakarfa@gmail.com

Suvardhan Kanchi and Shakeel Ahmed (eds.) Green Metal Nanoparticles, (245–292)
© 2018 Scrivener Publishing LLC

Keywords: Green synthesis, magnets, environmental remediation, environmental applications

9.1 Introduction

In past decades, evolution of nanoscience was proven to be a boon for the research and industrial communities to expand their idea of nanotechnology in various fields of modern science. Now we are dealing with nanotechnology in every step of our lives, with inventions that improve our quality of life, starting with electronic devices [1], water purification [2], wastewater treatment, disease rehabilitation [3], disease diagnosis [4], cell labeling and imaging [5], tissue engineering [6], sensors, catalysis, and detection of agro-waste [7].

Nanotechnology is a technology consisting of materials/particles having size in the range of 1–100 nm, termed nanomaterials or nanoparticles. Their reduced dimensionality results in different but outstanding physical and chemical, optical, electrical, thermal, catalytic and magnetic properties [8–10]. Nanoparticles play a major role in substituting and reformulating existing production equipment with new nano-dimensional equipment. This can lead to user-friendly equipment with much higher efficacy and low energy consumption, which is also benign to the environment and can be used in a sustainable manner for various purposes. Nanoparticles can be categorized into various classes like metallic, inorganic, magnetic, polymeric, etc. [11, 12]. But, among the different class of nanoparticles, magnetic nanomaterials or magnetic nanoparticles are the highlights of nanotechnology [13]. Although magnetic properties or magnetism has been studied for a long time, a lot of study is still required about the properties of magnetic nanoparticles (MNPs). In a very small span of time, MNPs have shown great potential in environmental, biomedical and clinical applications [14, 15]. They have been frequently used in magnetic resonance imaging, data storage, defect sensor, catalysis, biomedicine and tissue-specific targeting [16–18]. Among the various applications of magnetic nanoparticles, their very important and popular role is in environmental remediation [19, 20].

In recent times, the environment has become contaminated at every level, i.e., air, water and land, due to excess use of pesticides/fertilizers, global industrialization, and dumping of chemicals and pollutants from industries. An attempt to solve this perennial problem is now being sorted out by the use of nanotechnology. Extensive research work is going on to explore different aspects of environment remediation using MNPs

in a fast, user-friendly, economic, and commercially viable technique Environmental remediation includes cleaning of various components of the environment, including atmosphere, soil, sediment, groundwater and surface water [21, 22]. Both ground water and surface water come under the water remediation process whereas soil remediation process incorporates topsoil, subsoil and sediment [23]. However, air remediation includes removal of toxic gases from the environment, which is emitted by various automobile engines or industrial chimneys [24]. Surface water (i.e., lake or river water) is generally polluted by release of pollutant materials directly into the water or by runoff from the ground. While groundwater is mainly polluted by leaching of hazardous contaminants from the soil and sediment above it or from certain industrial work such as mining or drilling for oil and natural gas. To revitalize the soil by purifying it from contaminants, like hazardous chemical spills into clear water, certain fertilizers/pesticides added during industrial activity is the main plan of soil remediation [25].

To solve the above problem, magnetic nanoparticles have proved to be the main champion. MNPs are able to detoxify environmental components owing to their large surface area, high surface area to volume ratio, and because of quantum confinement effects [26]. The larger exposed surface area of MNPs helps them to act as a "superabsorbent" for many compounds, chemically transforming contaminants to their nontoxic form. In addition, the nanoparticle-based sensors have also become very popular for playing a promising and vital role in the trace level detection of pollutants [27]. The general mechanism of magnetic nanoparticles for the purification or treatment of water is shown in Figure 9.1.

Magnetic nanoparticles are the class of nanoparticles that can be manipulated using magnetic fields which are commonly derived from iron, nickel, cobalt or their oxides like cobalt ferrite (Fe_2COO_4), magnetite (Fe_3O_4), maghemite (Fe_2O_3), chromium dioxide (CrO_2), etc. [28, 29, 30]. These types of particles have two components; a magnetic material, often iron, nickel and cobalt, and a chemical component that has functionality. Magnetic properties of the nanoparticle depend on various factors like shape and size, chemical composition, crystal lattice, magnetic moment, magneto-crystalline anisotropy, etc. [31, 32].

9.2 Classification of Magnetic Materials

On the basis of their reaction to an externally applied magnetic field, magnetic nanoparticles can be classified into five different types, i.e.,

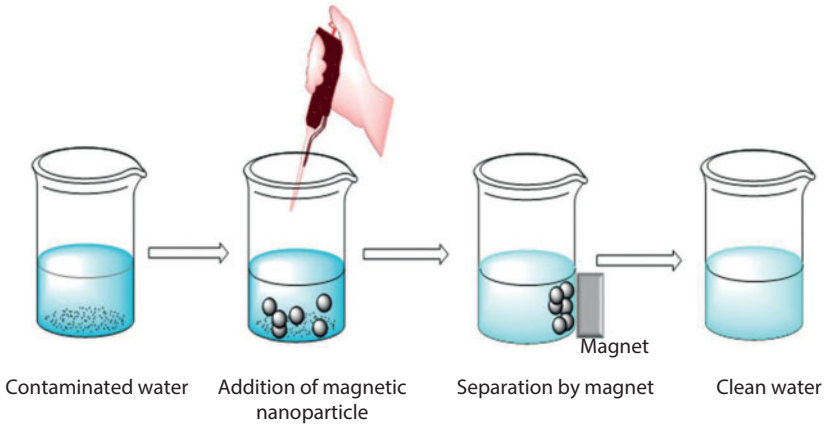


Figure 9.1 General mechanism of magnetic nanoparticles for the purification or treatment of water.

paramagnetic, diamagnetic, ferromagnetic, ferrimagnetic and antiferromagnetic [33]. Magnetic nanoparticles are classified by their "weak" (diamagnetic and paramagnetic) and "strong" (ferromagnetic, ferrimagnetic, antiferromagnetic) magnetic properties. The alignment of the magnetic moment of individual atoms with an external magnetic field in different magnetic materials is shown in Figure 9.2.

9.2.1 Ferromagnetic Materials

Ferromagnetic materials fall under the group of highly magnetic material. These materials are strongly attracted by a magnetic field or magnets, e.g., iron, nickel, cobalt. In this material the magnetic moments align parallel to the magnetic field and coupling interactions between the electrons of the material results in equally oriented magnetic states. The susceptibilities of these materials depend upon temperature, external magnetic field and atomic orientation. At small size they maintain a single magnetic domain and therefore maintain a large magnetic moment. Iron in zero-valent state is the strongest ferromagnetic material with a high magnetic moment density along with additional strong reducing properties; it is very popular for the degradation of a wide range of environmental pollutants. The synthesis of pure zero-valent iron is difficult to achieve because it contains oxides, carbides and other impurities. However, several chemical methods

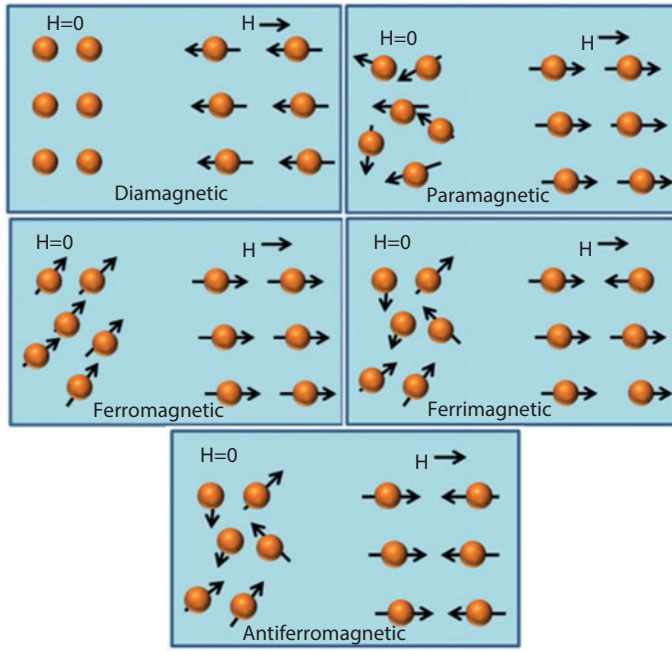


Figure 9.2 Different magnetic materials characterized according to alignment of the magnetic moment of individual atoms in applied external magnetic field.

are reported in the literature for synthesis of zero-valent iron by reducing metal salts by means of different reducing agents, like $NaBH_4$, in organic solvents [34].

Some iron derivatives are also ferromagnetic in nature, such as iron(III) oxide or Fe_2O_3, otherwise known as hematite, and γ-Fe_2O_3 (maghemite) having cubic structure. In addition, cobalt nanoparticles (CoNPs) have also attracted the particular attention of researchers because of their excellent electrical, magnetic and catalytic properties [35]. Small-sized cobalt nanoparticle possesses quantum size effects, superparamagnetism and large magnetic anisotropies. Cobalt nanoparticles (CoNPs) can be synthesized by various approaches, like ultrasonic spray pyrolysis, DC magnetron sputtering [36], thermal decomposition [37], electrochemical synthesis [38], liquid-phase reduction [39] and biological methods [40]. Nickle nanoparticles (NiNPs) also come under this category of magnetic nanomaterials and are widely studied in magnetic storage, ferrofluids, medical diagnosis, multilayer capacitors and catalysis [41].

After 1930, the magnetic property of rare earth elements was also studied. The first invented magnetic behavior was found in gadolinium (Gd), which has a Curie point of 292 K [42]. After that, neodymium magnets were discovered in the 1980s and were found to be the most affordable rare earth magnets. Among the nine rare earth elements (i.e., scandium, yttrium, lanthanum, gadolinium, terbium, dysprosium, holmium, erbium, and thulium), six rare earth elements are ferromagnetic in nature, namely gadolinium, neodymium, dysprosium, holmium, erbium, thulium. The presence of unfilled electron in the 4f orbital gives rise to magnetic properties in the rare earth elements. Dysprosium, holmium, erbium and thulium exist in transition phase, where lowering of the temperature results in ordered magnetic state. EuO and EuS are interesting insulating ferromagnets, with $4f_7$, S = 7/2 ions and a Curie temperature of 69 K [43, 44]. Rare earth elements-based ferromagnets are still under research, due to their high chemical activity. Recently, Zhang *et al.* have synthesized 10-nm gadolinium-based nanoparticles with dextran as the reducing agent by green synthesis approach for high potential magnetic resonance study [45].

9.2.2 Antiferromagnetic Materials

In antiferromagnetic material, magnetic moments or atoms are aligned in a regular pattern with neighboring spins posting in opposite direction to each other. Antiferromagnetism exists at sufficiently low temperatures, losing magnetic property at and above a certain temperature, called the Néel temperature. Above Néel temperature (T_N) they are mainly paramagnetic in nature. Without a magnetic field the total magnetization of antiferromagnetic nanoparticles vanishes [46]. Common examples of antiferromagnetic nanoparticles are FeO (Wustite), chromium, iron manganese alloy, nickel oxide (NiO), etc. Among the known oxide hydroxides antiferromagnetic in the bulk state $Fe_2O_3.H_2O$, the orthorhombic α-FeOOH (goethite) has Curie temperature (T_c) = 393 K [47]. It exhibits magnetization at very low temperature, which vanishes above Néel temperature and behaves like paramagnetic material. Cubic NaCl structure with a tiny rhombohedral distortion is mainly observed in nickel oxide (NiO) NPs. It is an antiferromagnetic charge-transfer insulator with a Néel temperature of 525 K. The Ni^{2+} ions have a $3d_8$ configuration with S=1. Cubic cobalt oxide is also a popular antiferromagnetic material having T_N = 291 K. In addition, some of the rare earths, like cerium, neodymium and samarium, show antiferromagnetic properties at about 10 K [48].

9.2.3 Ferrimagnetic Materials

These materials have a weak form of ferromagnetism but, unlike antiferromagnetic materials, the net magnetic moment does not cancel out in the absence of magnetic field. Magnetic materials whose atoms or ions are oriented in an ordered manner but in a nonparallel arrangement in a zero magnetic field below a certain characteristic temperature, known as the Néel temperature, are the ferrimagnetic elements like Fe_3O_4 and Fe_3S_4. The main reason for ferrimagnetism is the composition of the material. Here, the material consists of different oxidation state ions of the same element or different elements like a mixture of Fe^{2+}& Fe^{3+}. Known and popular ferrimagnetic materials include yttrium iron garnets and ferrites. Ferrites can be classified into two categories, i.e., soft ferrites and hard ferrites [49]. Soft ferrites are mainly iron oxide, Fe_2O_3, with one or more divalent oxide such as NiO, MnO or ZnO. These magnetic materials have a square hysteresis loop, high resistance and quick demagnetization property. Just like non-magnetic oxide nanoparticles, the face of ferrite nanoparticles is often modified by surfactants, silica, silicones or phosphoric acid derivatives to increase their stability in solution. Hard ferrites have the basic composition of MO. Fe_2O_3, where M stands for barium (Ba) ion or strontium (Sr) ion [50]. They are mainly used in generators, relays and motors.

The oldest of the ferrimagnetic materials is magnetite, i.e., Fe_3O_4 or iron(II, III) oxide. Magnetite nanomaterial holds ferromagnetic property at room temperature with Curie temperature of 850 K. In magnetite there are two types of sites; the octahedral sites occupied by an equiatomic blend of ferric and ferrous iron with rapid Fe^{2+}-Fe^{3+} electron hopping, and the tetrahedral sites, which are occupied by ferric cations. The formula can be written as $[Fe^{3+}]\{Fe^{2+}Fe^{3+}\}O_4$. Their various applications are magnetic optical devices, electromagnetic devices, recording media, catalysts, pigments and gas sensors [51].

9.2.4 Paramagnetic Materials

Paramagnetic materials are not very attracted by magnetic fields and therefore fall in the group of weak magnetic material. Examples of paramagnetic materials are aluminium, lithium, tin, magnesium, copper, gold, platinum, molybdenum, tungsten, etc. Some of the oxides like aluminium oxide (Al_2O_3) and nitric oxide (NO) are also paramagnetic in nature. In the absence of magnetic field these materials do not retain their magnetic properties. They are magnetized only when placed in super high magnetic field and then act in the direction of the magnetic field. The atoms of these

substances contain electrons, most of which spin in the same direction, which provides some polarity to the atoms. These materials have individual atomic dipoles oriented in random fashion with resultant zero magnetic force. Some of the synthetic goethite nanoparticles, like β-FeOOH (akagenite) and γ-FeOOH (lipidocrokite), are paramagnetic at 300 K [52].

9.2.5 Diamagnetic Materials

Diamagnetic materials also come under the category of weak magnetic materials. Metals with many core but paired electrons, which are repelled by magnets such as zinc, mercury, lead, silver, bismuth, etc., are called diamagnetic materials. They are magnetized very little when placed in a strong magnetic field and act in the direction opposite that of the applied magnetic field. They are not magnetized in the absence of magnetic field at any temperature. In these materials, due to the pairing of all the electrons there is no permanent net magnetic moment per atom. Due to the orbital revolution and axial rotation of electrons around the nucleus, which are in opposite direction to each other, the magnetic moments are canceled out [53].

9.2.6 Superparamagnetic Materials

These are a special class of magnetic material which forms inside the small ferromagnetic or ferrimagnetic nanoparticles. They have a different kind of magnetic behavior in between ferromagnetic and ferrimagnetic materials. The superparamagnetic behavior is achieved when they are placed in an external magnetic field, and they develop a strong internal magnetization from exchange coupling of electrons within the domain [54]. They have single domain magnetization and due to the presence of single domain, the susceptibility of superparamagnetic material is not as great as ferromagnetic material. Unlike the ferromagnetic materials, this material does not retain the magnetization after the magnetic field is removed. According to the literature, this property is dependent on the size of the nanoparticles and it is assumed that every magnetic material with size less than 20 nm possesses superparamagnetic property. Most of the transition elements oxides having size in the range of 3–50 nm demonstrate superparamagnetic behavior. However, magnetic alloy nanoparticles of size 12–80 nm are superparamagnetic over a broad temperature range. A very popular and well-known example of this category is superparamagnetic iron oxide nanoparticles, also known as SPIONs [55]. They consist of an inner core made of iron oxides, which can be targeted to the required area through

external magnets. This type of material holds high saturation field, field irreversibility, extra anisotropy contributions or shifted loops after field cooling. Typically, SPIONs have a core–shell-like structure in which the magnetic particle core (usually magnetite, Fe_3O_4, or maghemite, γ- Fe_2O_3) was coated with a biocompatible polymer. Or in the pores of biocompatible polymer, SPIONs are precipitated to make a core–shell-like structure. This coating of the biocompatible materials helps to protect the magnetic nanoparticle from the environment. SPIONs are comparatively more stable in water and different pH solutions, therefore more popular in the field of biology, medical diagnosis and clinical therapies [56, 57].

9.3 Synthesis and Characterization of Magnetic Nanoparticles

For the fabrication of magnetic nanoparticles, such as metal oxide, pure metal, metal alloys and core-shell structures, different approaches has been investigated which result in different shape- and size-controlled nanoparticles. Top-down and bottom-up approaches are the two procedures broadly categorized for the synthesis of nanoparticle. The top-down approach is the phenomenon in which magnetic nanoparticles are prepared by reducing suitable bulk material to nano-dimensional material using various chemical or physical processes [58]. In the top-down approach different techniques, like milling, cutting, and shaping, are known to convert the bulk material into the preferred order, size and shape [59]. The top-down approach includes certain physical methods like atomization [60], laser ablation [61], lithography [62], pyrolysis [63], thermolysis [64], radiation-induced methods [65] and electrospinning. The top-down approach has major drawbacks, like generation of defects on the surface of metallic nanoparticles, which has a significant effect on their properties [66]. During the synthesis procedure, in order to maintain the high-pressure and high-temperature condition the top-down process includes massive consumption of energy.

In the bottom-up approach, different from the top-down approach, nanoparticles are synthesized through assemblage of atoms, molecules or clusters [67]. The bottom-up approach excludes certain drawbacks of the top-down approach and provides a friendly way to obtain metallic nanoparticles with less surface defects and more homogeneous chemical composition at a much less-expensive cost. The bottom-up approach is commonly done by wet synthesis procedures, such as chemical [68], electrochemical [69] sonochemical [70], polyol reduction [71], templated

synthesis [72] and sol-gel process [73]. In this approach, wet synthesis technique is more popular and taken as the best option for synthesis of magnetic nanoparticles. However, the drawback related to the wet chemical synthesis method is use of excess hazardous chemicals. Due to the use of hazardous chemicals and solvents, toxic reducing agents are mixing with our environment, resulting in severe damage to plant and animal life [74].

Researchers are trying their best to synthesize environmentally friendly magnetic nanoparticle with benign and sustainable sources. Now they have confined their focus on the "Green synthesis" approach. Here, plant and plant products are used as renewable resources for the fabrication of nanoparticles. In recent days, the green-synthesis approach is in great demand, owing to its economical and bulk production rate of nanoparticles. The phytochemicals extract contains certain reducing agents or redox chemicals, like amino acids, enzymes, vitamins, proteins, polysaccharides, and organic acids such as citrates, which allow efficient reduction of metal precursors into their corresponding metallic nanoparticles [75]. Plant-mediated synthesis has various advantages [76]:

1. Requires aqueous solvents like water for the reaction;
2. Phytoelements extracted from plants work as both reducing as well as stabilizing agent;
3. Procedure is simple and quick;
4. Results in large-scale synthesis of nanoparticles at comparatively less cost.

In addition to the plant components, various microorganisms like bacteria, actinomycetes, fungi, yeast and viruses, are also used in green synthesis of nanoparticles as eco-friendly and sustainable precursors [77]. However, the exact mechanism of microorganism-mediated synthesis has yet to be explored. It is assumed that microbial synthesis of magnetic nanoparticles results from the metal reductase enzyme produced by the microorganism to covert the metal salt in their nanoparticles. For example, iron reductase enzyme is able to extracellularly reduce Fe^{3+} into Fe^{2+} leads in the formation of iron oxide magnetic nanoparticles [78]. Similarly, fungi secrete cationic proteins, which cause an extracellular hydrolysis of the anionic iron complexes. The magnetic material synthesized by algae cells is due to the presence of carbonyl and amine functional groups derived from polysaccharides and glycoproteins like biomolecules [79].

It was found that iron nanoparticles synthesized from the green synthesis approach are able to impart steric stabilization of iron nanoparticles against aggregation and help to overcome the concerns related to the use

of certain hazardous reducing agents, like sodium borohydride, in routine synthesis procedures. Sodium borohydride is a very popular and strong reducing agent but is defamed for its corrosiveness and flammability. In the literature, a large number of articles have been reported for synthesis of magnetic nanoparticles via green synthesis approach, some of the recent ones are also included in this chapter. Ahmed *et al.* have used methanol extract of *Conocarpus erectus* and *Nerium indicum* leaves and Koyyati *et al.* have used *Raphanus sativus* var. Longipinnatus leaf extract for synthesis of CoNPs. In both cases, leaf extracts were used as reducing agent for Co-salts [40, 80]. Devatha *et al.* have synthesized iron nanoparticle from various leaf extract like *Mangifera indica, Murraya koenigii, Azadiracta indica* and *Magnolia champaca* [81]. Fazlzadeh *et al.* synthesized zero-valent iron nanoparticle from various plant extracts, including *Rosa damascena* (RD), *Thymus vulgaris* (TV) and *Urtica dioica* (UD) [82]. Weng *et al.* have synthesized iron nanoparticle from *Eucalyptus* leaf extract [83]. Hoag *et al.* have synthesized zero-valent iron from *Camellia sinensis* leaf extract having spherical morphology and size of 5–15 nm [84]. Shahwan *et al.* have synthesized iron nanoparticles of amorphous nature from green tea leaf extract [85]. Luo *et al.* synthesized iron-based nanoparticles from grape leaf having size of 15–100 nm with quasi-spherical shape and amorphous nature [86]. Pattanayak and his group have synthesized iron nanoparticle from *Azadirachta indica* leaf with size 50–100 nm [87]. Periyathambi and his coworkers synthesized iron oxide nanoparticle from river sand containing magnetite and explored its application in MRI sensitivity [88]. Mukherjee *et al.* synthesized α-Fe_2O_3 nanoparticle using *Aloe vera* leaf extract as a reducing agent for metal oxide synthesis [89]. Martínez-Cabanas *et al.* synthesized iron oxide nanoparticle from Chestnut tree (*Castanea sativa*), eucalyptus (*Eucalyptus globulus*), gorse (*Ulex europaeus*) and pine (*Pinus pinaster*) [90]. Makarov *et al.* biosynthesized stable iron oxide nanoparticles in aqueous extracts of *Hordeum vulgare* and *Rumex acetosa* plants [91]. Different green synthesis approaches and applications for various Fe and Fe compounds are presented in Table 9.1.

Other than Fe and Co, nickel nanoparticles (NiNPs) were also fabricated via green synthesis approach. Here, Pandian *et al.* have synthesized nickel nanoparticle from *Osimum sanctum* leaf extract. In aqueous solution the nickel precursor gets dissociated and the hydrated electron from aqueous *O. sanctum* leaf extract reduces Ni^{2+} into zero-valent nickel [123]. Thema *et al.* have synthesized single phase Bunsenite NiO nanoparticles using *Agathosma betulina* as a reducing/oxidizing agent [124]. Chekin *et al.* have synthesized cobalt oxide nanoparticles (CoO NPs) in aqueous medium using gelatin [125]. Bibi *et al.* have synthesized CoO nanoparticle

Table 9.1 Green synthesis approaches for the preparation of various magnetic iron nanoparticles and their applications.

S. N.	Green source	Synthesized magnetic iron nanoparticle	Shape	Size (in nm)	Applications	Ref.
1.	*Mangifera indica, Murraya koenigii, Azadiracta indica, Magnolia champaca*	Zero-valent iron nanoparticles (NZVI)	Spherical	96–100 99–129	Treatment of domestic wastewater	[81]
2.	*Rosa damascene* (RD), *Thymus vulgaris* (TV), *Urtica dioica* (UD)	Zero-valent iron nanoparticles (nZVI)	Irregular	100	Removal of Cr(VI) from aqueous solutions	[82]
3.	*Eucalyptus* leaf extracts	Zero-valent iron nanoparticles (nZVI)	–	20–80	Removal of Cr(VI) and Cu(II)	[83]
4.	Tea (*Camellia sinensis*) polyphenols	Nano-scale zero-valent iron (nZVI)	Spherical	5–15	Degradation of bromothymol blue	[84]
5.	Green tea leaves	Zero-valent iron nanoparticles (nZVI)	Irregular	40–60	Degradation of aqueous cationic and anionic dyes	[85]
6.	Methanolic extract of grape leaves	Zero-valent iron nanoparticles (nZVI)	–	60	Degradation of Acid Orange II	[86]
7.	*Azadirachta indica* leaf	Zero-valent iron nanoparticles (nZVI)	Spherical	–100	–	[87]
8.	River sand	Iron oxide	Spherical	15–35	Enhanced MRI sensitivity and drug delivery	[88]
9.	*Aloe vera* leaf extract	α-Fe_2O_3	Rod	100	Arsenic(V) remediation	[89]
10.	Chestnut tree (*Castanea sativa*), eucalyptus (*Eucalyptus globulus*), gorse (Ulex europaeus) and pine (Pinus pinaster)	Iron-oxide	Irregular	–	As(V) removal	[90]

11.	*Hordeum vulgare* and *Rumex acetosa* plants	Iron-oxide	Spherical	30	–	[91]
12.	*Moringa oleifera*	Ni/Fe_3O_4	Spherical	16–20	Organic dye degradation	[92]
13.	*Ceiba pentandra* (RKF), oil palm empty fruit bunches (EFB) and celluloses (CEL) extracted from EFB	Magnetic biosorbent	Hexagonal	5–50	Heavy metal ions removal	[93]
14.	*Eucalyptus* leaf extract	Fe_3O_4	Spherical	80–90	Phosphate removal	[94]
15.	*Euphorbiaceae cochinchinensis* leaf extracts	Zero-valent iron nanoparticles (nZVI)	Spherical	100	Removal of 2,4-dichlorophenol	[95]
16.	Extracts of leaves and blueberry shoots (*Vaccinium corymbosum*)	iron (oxide, oxyhydroxides and zero-valent)	Heterogeneity in shape	61.1– 100.6	Removal of arsenate	[96]
17.	Ridge gourd peels (RG)	Fe_3O_4	Spherical	20–35	Degradation of methylene blue in aqueous solution	[97]
18.	Pomegranate leaves (PG).	Fe_3O_4	Rod	45–60	Congo red dye degradation studies for water treatment	[98]
19.	*Camellia sinensis* tea extract	Fe(II)/Fe(III) oxides/ oxohydroxides	Irregular chain	20–100	Dye degradation	[99]
20.	Rich polyphenols in Omani mango tree leaves	Fe_2O_3	Rod	(15 ± 2) average length and (3.0 ± 0.2) nm average diameter	Heavy oil viscosity treatment	[100]

(*Continued*)

Table 9.1 Cont.

S. N.	Green source	Synthesized magnetic iron nanoparticle	Shape	Size (in nm)	Applications	Ref.
21.	Green tea polyphenols (GTP)	Fe_3O_4@GTP	Spherical	10 ± 3	Removal of dye pollutant from aqueous solution	[101]
22.	*Murraya koenigii* leaves extract	Fe_3O_4	Spherical	12	Removal of Pb(II)	[102]
23.	*Sapindus mukorossi*	Iron hexacyanoferrate	Hexagonal nanorods, spheres and rhombus shaped nanoparticles	10–60	Degradation of toxic PAHs	[103]
24.	*Sapindus mukorossi* (raw reetha)	(α-FeOOH, β-FeOOH and α-Fe_2O_3)	Rod	< 50	Interaction of 2, 3 and 4-Aminopyridines	[104]
25.	*Eucalyptus* leaf extracts	Zero-valent iron nanoparticles (nZVI)	Spherical	20–70	Degradation of herbicide Ametryn in water	[105]
26.	Tea polyphenol (TP)	Zero-valent iron nanoparticles (nZVI)	Irregular	20–80	Decolorization of cationic dyes	[106]
27.	Pinewood sawdust	Zero-valent iron nanoparticles (nZVI)	Spherical	4–5	Catalytic decomposition of phenol	[107]
28.	Oak, mulberry and cherry leaf extracts	Zero-valent iron nanoparticles (nZVI)	Spherical	10–30	As(III) and Cr(VI) removal	[108]
29.	Green tea	Zero-valent iron nanoparticles (nZVI)	Spherical	40–60	Removal of phosphorus	[109]
30.	Green tea (GT-Fe) and *Eucalyptus* leaves (EL-Fe) extracts	Zero-valent iron nanoparticles (nZVI) and Fe_3O_4 nanoparticles	Quasi-spherical	20–80	Removal of nitrate	[110]

31.	Green tea extracts	Zero-valent iron nanoparticles (nZVI)	Spherical	40–50	Degradation of malachite green (MG)	[111]
32.	Oolong tea extracts	Zero-valent iron nanoparticles (nZVI)	Spherical	40–50	Degradation of malachite green	[112]
33.	*Cynometra ramiflora*	Iron oxide	Spherical	200–800	Antibacterial drug development	[113]
34.	*Withania coagulans*	Pd/RGO/ Fe_3O_4	Spherical	< 15	Reduction of 4-nitrophenol	[114]
35.	*Eucalyptus* leaf extract	Zero-valent iron nanoparticles (NZVI)	Spherical	20–80	Treatment of eutrophic wastewater	[115]
36.	*Eucalyptus* leaf extract	Fe/Ni	Irregular	20–50	Identification of biomolecules	[116]
37	Grape leaf aqueous extract	Bimettalic Fe/Pd	Quasi-spherical	10–100	Degradation of Orange II	[117]
38.	Green tea extract	Bimettalic Fe/Pd	Spherical	30	Degradation of methyl orange	[118]
39.	*Micrococcus luteus, Staphylococcus aureus, Aspergillus niger*	Iron oxide	Spherical	20–90	Ultrasound-assisted phytosynthesis	[119]
40.	*Lantana camera*	Iron oxide	Rod	10–20	Biological activities	[120]
41.	Coffee, green tea, and Virginia creeper (*Parthenocissus tricuspidata*) leaf extracts	Nano-scale zero-valent iron (nZVI)	Triangular	124.2 ± 31.8	Remediation applications	[121]
42.	*Amaranthus spinosus* leaf extract	Iron oxide	Spherical	54–270	Physicochemical traits, photocatalytic and antioxidant activity	[122]

using *Punica granatum* peel extract as reducing agent and cobalt nitrate hexahydrate as precursor [126]. Vasudeo and Pramod have synthesized nickel nanoparticle from Coriander leaf extract, which also acts as reducing agent during synthesis [127].

Some microorganism-assisted green synthesis techniques were also reported in the literature for successful synthesis of MNPs. For example, Pavani *et al.* have synthesized iron nanoparticle from *Aspergillus* which have size of 50 nm [128]. Mohamed *et al.* experimented on the mycosynthesis of iron nanoparticles by *Alternaria alternata,* which is a fungus [129].

For the characterization of MNPs, some of the very popular techniques used are listed below:

- Gauss/Tesla meter for the magnetic density study;
- Vibrating sample magnetometer (VSM) for the measurement of magnetic properties;
- Field emission scanning electron microscope (FE-SEM) and Transmission electron microscope (TEM) for morphological study;
- Hysteresis loop, field-cooled and zero-field-cooled curves are investigated by superconducting quantum interference magnetometer;
- Particle size distribution is measured by dynamic laser scattering analyzer (DLS);
- Magnetite content is studied by Thermogravimetric analysis (TGA) and Inductively coupled plasma atomic emission spectrometer (ICP-AES);
- X-ray diffraction (XRD) is commonly used for determination of chemical composition, which is able to estimate the crystalline size of particle by Scherrer equation;
- X-ray photoelectron spectroscopy (XPS) is used to determine oxidation state of prepared nanoparticle.

9.3.1 Types of Magnetic Nanoparticles

There are different types of magnetic nanoparticles presented in the literature, which are differentiated according to their surface modification or functionalization, shape and composition, resulting in their characteristic features such as inertness to redox reactions, very little cytotoxicity and high stability under acidic conditions. In this chapter, we have compiled information regarding the role of magnetic nanoparticles towards the control or prevention of environmental damage. Therefore, we have classified

the MNPs on the basis of their various applications and modifications [130]. The classification is as follows:

- Silane modified magnetic nanoparticle
- Polymer modified magnetic nanoparticle
- Bimetallic magnetic nanoparticle
- Miscellaneous nanoparticle
- Zero-valent iron (ZVI)

As discussed above, the MNPs are synthesized based on their role in various applications. But here, we have emphasized only on their environmental applications. For example, being a strong reductant, iron-based magnetic nanoparticles (e.g., zero valent iron [nZVI], Fe_3O_4 and α-Fe_2O_3) are very popular for environmental research related to the removal of contaminants from groundwater, soil and sediments. A schematic of the adsorption and desorption mechanism of different magnetic iron materials for environmental remediation is shown in Figure 9.3.

The inexpensive and nontoxic zero-valent iron is popular for its multifunctional applications like degradation of dye, dehalogenation and reduction of aromatic nitro compound, and removal of toxic elements [131]. Polycyclic aromatic hydrocarbon (PAH), like stable and harmful pesticides,

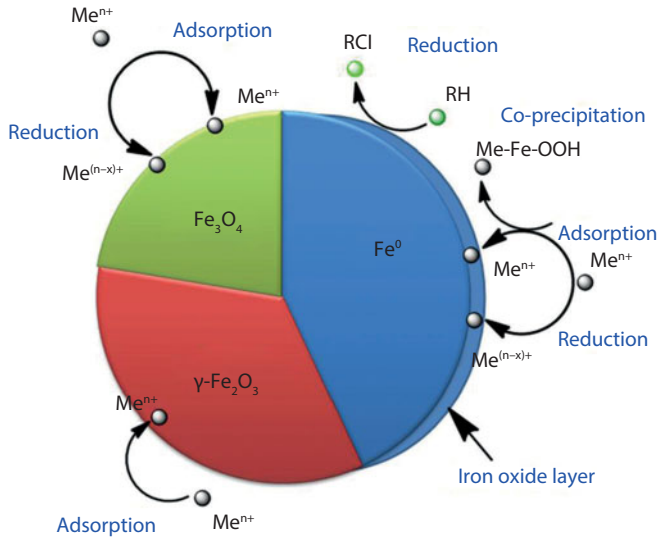


Figure 9.3 Schematic showing the adsorption and desorption mechanism of different magnetic iron materials for environmental remediation.

can be readily decomposed by reactive ZVI. Pollutants, like sulfates (SO_4^{2-}) and nitrates (NO_3^-), etc., are easi–ly reduced by ZVI particles due to the high reducing potential and maximally reduces all the pollutants present in water. Some of the chemical reactions responsible for removal of environmental pollutants using zero-valent iron are discussed below [132, 133]:

$$4Fe^0 + NO_3^- + 10H^+ \longleftrightarrow 4Fe^{2+} + NH_4^+ + 3H_2O \quad (9.1)$$

$$3Fe^0 + 2Cr^{6+} \longleftrightarrow 3Fe^{2+} + 2Cr^{3+} \quad (9.2)$$

$$4Fe^0 + C_2HCl_3C_2H_6 \longleftrightarrow 4Fe^{2+} + 3Cl^- \quad (9.3)$$

$$5Fe^0 + C_2Cl_4 + 6H^+ \longleftrightarrow C_2H_6 + 5Fe^{2+} + 4Cl^- \quad (9.4)$$

Similarly, heavy metals, like Cr, Tc, As, Mo, etc., are easily adsorbed and co-precipitated by nano-iron. Ferrous and ferrous ammonium sulphates along with hydrogen peroxide (H_2O_2) are also popular in the treatment of contaminated water, known as Fenton's treatment. It is used for removal of pesticides, inorganic contaminants, explosives, organic contaminants, etc., from water samples. In this technique, both Fe^0 and Fe^{2+} are utilized for the reduction of peroxide, resulting in formation of highly reactive hydroxy radical (HO) [134]. The reaction for Fenton's reagents for water treatment is as follows: First, $Fe^0 + H_2O_2 \longrightarrow Fe^{2+} + 2OH^-$, after that the resultant and compositional Fe^{2+} further reacts with H_2O_2 to produce (HO): $Fe^{2+} + H_2O_2 \longrightarrow Fe^{3+} + HO + OH^-$. The generated peroxide radicals have very high activity and are capable of reducing pollutants.

Although this zero-valent iron has so many excellent applications, its high reactivity makes it susceptible to rapid oxidation in the presence of dissolved air in water, resulting in its low durability. When oxygen or acidic environment is present, ZVI can be easily oxidized to Fe^{2+} or Fe^{3+} ions. The reduction process is highly influenced by the presence of stabilizers, contact time, humic acids and pH influence. Therefore, research is going on towards the surface coatings of zero-valent iron with different metallic or organic layers to alleviate this problem by reducing their contact with oxygen, thereby retaining the reactivity of ZVI. Stabilizer like carboxymethyl cellulose prevents the aggregation of ZVIs and prevents them from oxidizing. The influence of starch stabilizer is seen in chromium remediation from groundwater to prevent aggregation for better stabilization [135]. Stabilization of nanoparticle by modifying it with lactate is also popular for remediation of pentachlorophenol and dinitrotoluene from various types of soil and

groundwater samples. Different catalytic metals are also responsible for stabilizing Fe^0 (e.g., Pd, Pt, Ni). According to the literature, the MNPs synthesized from the green synthesis approach are comparatively more stable and have a high affinity towards water/contaminant interface, which make them the darling of researchers in the field of environmental remediation [134]. The MNPs synthesized via green synthesis approach used in environmental remediation are discussed in the next sections of this chapter.

9.4 Application of Magnetic Nanoparticles for Environmental Remediation

9.4.1 Dye Degradation

Dyes are the colored, ionizing organic compounds, which have high affinity towards substrate, owing to the presence of enormous functional groups. They can absorb light with particular wavelength more than others, which results in their bright colors, owing to the presence of chromophore and conjugated system [136]. According to the chemical composition, use and their origin, dyes can be classified into various kinds like natural and synthetic; mordant or direct; acidic or basic; sulfur or azo group-containing, reactive, vat, disperse medium. Acidic dyes are water-soluble anionic dyes used in coloring of silk, wool, and nylon fibers. Basic dyes are also water soluble but cationic in nature and used for coloring of paper, wool and acrylic fibers. The most studied dyes which are responsible for environmental pollution are methylene blue, acid red 1, rhodamine B, methyl orange and crystal violet. Many industries consume dyes in order to color their different materials, from textile, paper and carpet to leather. Based on their use, several industries, like distillery and printing industries, are using dyes at a larger scale and discard the colored waste materials into rivers and natural streams. These dyes prevent the penetration of sunlight and re-oxygenation of water by cutting off the photosynthetic process, resulting in the death of algae, which further hampers the food chain. They also increase the biological oxygen demand (BOD) and cause lack of dissolved oxygen, which is required to sustain aquatic life. In addition to this, colorful dyes themselves are harmful to microorganism and aquatic life. They also cause dermatological problems in human beings. Some dyes are also carcinogenic and mutagenic in nature, which cause respiratory tract problems in workers. Dyes can be retained in the environment for several months due to their high photo-thermal stability, which resists their biodegradation [137].

Over the past few decades, advanced oxidation technologies (AOTs) have been used for degradation of organic dyes. Homogeneous Fenton oxidation (Fe^{2+}/H_2O_2) is the most popular process for treating organic pollutants present in aqueous solution. As we have discussed previously, during the Fenton reaction, hydroxyl radical results in degradation of organic material. However, the consumed Fe^{2+} can be further regenerated by the reaction of ferric ion with hydrogen peroxide [136].

$$Fe^{3+} + H_2O_2 \longrightarrow Fe^{2+} + H^+ + HO_2^{\bullet} \tag{9.5}$$

$$Fe^{3+} + HO_2^{\bullet} \longrightarrow Fe^{2+} + O_2 + H^+ \tag{9.6}$$

But, instead of these advantages, Fenton's reagent also has certain drawbacks:

a. For the use of Fenton process, an optimal pH value of 3 is required but in general it is known that wastewater has either neutral or alkaline pH. Therefore, it is necessary to bring the solution pH to 3 for effective Fenton reactions.
b. As the by-product of the reaction is ferric ion, with reaction time the amount of ferric ions increases, which may lead to the formation of insoluble complex and a lot of iron sludge.

To overcome the above disadvantages of Fenton processes, extensive research has been focused on heterogeneous Fenton processes. In the heterogeneous processes, a solid catalyst is used as a source of iron, so that the rate of sludge production can be regulated [138].

In recent years, iron-nanoparticle supported heterogeneous catalyst has become very popular in this field. In 2017, Wang *et al.* synthesized nanoscale zero-valent iron nanoparticle using high-purity tea polyphenol (TP); here, the epicatechin present in the TP was used as the reducing agent [106]. The prepared nanoparticle shows enhanced activity, anti-oxidizing properties and high stability. The advantage of this method is high content of Fe in the nanoparticle and use of cost-effective and environmentally friendly reducing agent. The synthesized TP-Fe was used to degrade methylene blue (MB) and malachite green (MG) with the assistance of ultrasound radiation (US). The ultrasound helps to increase the reaction mass transfer, improves the dispersion of TP-Fe nanoparticle, and causes activation of the TP-Fe NPs. It also expels the pollutants deposited on the surface of iron NPs and the undesired corrosion products. This study is a great help for the treatment of cationic dyes present in wastewater in a greener way.

Belachew *et al.*,[139] have synthesized functionalized magnetite nanoparticles (Fe_3O_4 NPs) by the one-pot co-precipitation method using L-methionine (L-Met) as a capping agent [139]. The prepared MNPs were well characterized by UV, FTIR, XRD, FE-SEM, EDS and TEM analysis. Furthermore, magnetic properties were tested by vibrating sample magnetometer (VSM) and, finally, the synthesized nanoparticle was applied for degradation of Rhodamine B (RhB). The dye was degraded within the first 40 min following pseudo-second order kinetic model. Shahwan *et al.* have tried green tea extract for synthesis of iron nanoparticle and used it as heterogeneous Fenton catalyst for degradation of aqueous cationic and anionic dyes (i.e., methylene blue and methyl orange) [85]. The major constituent of green tea is polyphenol, which shows its dual behavior in this reaction, i.e., reducing as well as capping agent. This study also compares the catalytic behavior of the iron nanoparticle prepared from sodium borohydride with respect to the green MNPs. The synthesized nanoparticle was characterized by TEM, SEM/EDX, XPS, XRD, and FTIR analysis. The experiment shows the potential of iron nanoparticle for complete removal of both dyes over a wide concentration range of 10–200 mg L^{-1}. Wu and his group also tried for the synthesis of iron nanoparticle by tea extract [111]. The prepared MNPs show Fenton-like oxidation of malachite green (MG). The nanoparticle shows 85% degradation of dye present in the wastewater. The main mechanisms of adsorption and degradation of dye in this paper are as follows:

$$\text{Adsorption: MG + Fe-NPs} \longrightarrow \text{MG-Fe-NPs} \tag{9.7}$$

$$\text{MG} + Fe_3O_4/\gamma\text{-}Fe_2O_3 \longrightarrow \text{MG-}Fe_3O_4/\gamma\text{-}Fe_2O_3 \tag{9.8}$$

Hydroxyl radical was generated by the Fenton-like reaction, which is further used for the degradation of dyes.

Degradation:

$$\text{MG/Fe-NPs} + {}^{\bullet}OH \longrightarrow \text{Reaction intermediates/Fe-NPs} \tag{9.9}$$

$$\text{Reaction intermediates/Fe-NPs} + {}^{\bullet}OH \longrightarrow CO_2 + H_2O \tag{9.10}$$

Huang *et al.* have synthesized iron nanoparticle using oolong tea extract, which was used for complete degradation of malachite green (MG) [112]. The nanoparticle is characterized by EDS, XRD, UV–Vis and FTIR techniques. The oolong tea-derived MNPs show pseudo-first-order reaction

kinetics for MG adsorption and successfully remove 75.5% of MG from the sample having concentration 50 mg L^{-1}. Weng *et al.* have also synthesized green tea-derived MNPs. The NPs were used for degradation of malachite green dye (MG). It was found that 96% of the dye is degraded with prepared nanoparticle [140]. Hoag *et al.* have synthesized iron nanoparticle from *Camellia sinensis* tea [84]. The NPs were used to catalyze the degradation of an organic contaminant, i.e., bromothymol blue, in the presence of H_2O_2. It is seen that the iron nanoparticle prepared from green tea shows more catalytic activity than Fe-ethylenediamine tetraacetate complex Fe-EDTA and Fe-(S,S)-ethylenediamine-N,N'-disuccinic acid (Fe-EDDS). It was also found that with an increase in the concentration of green tea the catalytic property of the hydrogen peroxide also increases. Carvalho *et al.* have synthesized iron(II)/(III) oxides and oxohydroxides composites from *Camellia sinensis* tea extract [99]. Afterwards, their application in heterogeneous Fenton degradation of methyl orange (MO) was also studied. From the TEM images, it is seen that the morphology of iron nanoparticles is irregular and chain-like, having size in the range of 20–100 nm. Prasad *et al.* synthesized nanorod-shaped Fe_3O_4 magnetic nanoparticles (MNRs) using pomegranate leaves [98]. The synthesized pomegranate-Fe_3O_4 (PG-Fe_3O_4) was characterized by Raman scattering and X-ray photoelectron spectroscopy. The synthesized PG-Fe_3O_4 MNRs show fcc structure and particle size of 45 to 60 nm. The group applied this nanoparticle for the degradation of Congo red dye. Singh *et al.* have synthesized superparamagnetic Fe_3O_4@GTPs nanoparticles coated with green tea polyphenols (GTP) in an environmentally benign approach [101]. The coated NPs were characterized by TEM, XRD, FTIR, Raman spectroscopy, FE-SEM and EDS. The prepared nanoparticle shows high adsorption capacity of 7.25 mg/g for removal of methylene blue (MB) dye. Prasad *et al.* synthesized nickel-supported iron oxide magnetic nanoparticles (Ni/Fe_3O_4 MNPs) using *Moringa oleifera* (MO) leaf extract as a reducing and capping agent [92]. The prepared nanoparticle was characterized by FTIR, powder XRD, XPS, TEM and Brunauer–Emmett–Teller (BET) adsorption methods. It has spherical shape and size of 16–20 nm. The prepared nanoparticle shows catalytic degradation of malachite green by UV-visible spectroscopy. Pandian *et al.* have biosynthesized magnetic nickel nanoparticle using *Ocimum sanctum* leaf extract and explored its application in dye adsorption [123]. The nanoparticle was characterized by UV-Vis spectroscopy, FTIR, XRD and TEM studies. The nanoparticle was used as adsorbent for the removal of dyes, such as orange II (OR), eosin Y (EY) and crystal violet (CV); and some of the anionic pollutants, like sulfate (SO_4^{2-}) and nitrate (NO_3^-), from wastewater. Adsorption kinetics data was better

fitted to pseudo-second-order kinetics for all dyes. Bibi *et al.* have synthesized cobalt-oxide nanoparticles using *Punica granatum* peel extract and cobalt nitrate hexahydrate [126]. The nanoparticle was characterized by XRD, SEM, EDX, and atomic force microscopy (AFM) studies. The synthesized nanoparticles show photocatalytic activity towards degradation of Remazol Brilliant Orange 3R dye and 78.45% degradation was achieved with dye concentration of 150 mg L^{-1}. Cheera *et al.* have synthesized spherical Fe_3O_4 magnetic nanoparticles using Ridge gourd peel (RG) extract as reducing and capping agent [97]. The resulting nanoparticle was characterized by XRD, FTIR, Raman, BET, FE-SEM, VSM and TEM methods. Synthesized nanoparticle has a size of 20–35 nm and is used for degradation of methylene blue. The high surface area of the nanoparticle shows high adsorption capacity, i.e., 96% for the dye. Njagi *et al.* biosynthesized iron nanoparticles from aqueous *Sorghum* bran extracts and showed its application in degradation of bromothymol blue dye [141]. The degradation was done in the presence of 2% H_2O_2 and iron nanoparticles, leading to a 90% decrease in the concentration of bromothymol blue (BTB) within 30 min. Muthukumar and Matheswaran synthesized magnetic iron oxide nanoparticle (FeO) multifunctional magnet material from ferric chloride using *Amaranthus spinosus* leaf aqueous extracts [122]. The synthesized nanoparticle shows 75% and 69% degradation of methyl orange and methylene blue, respectively, in the presence of sunlight. A schematic diagram of the multifunctional behavior of the prepared magnetic nanoparticle is shown in Figure 9.4.

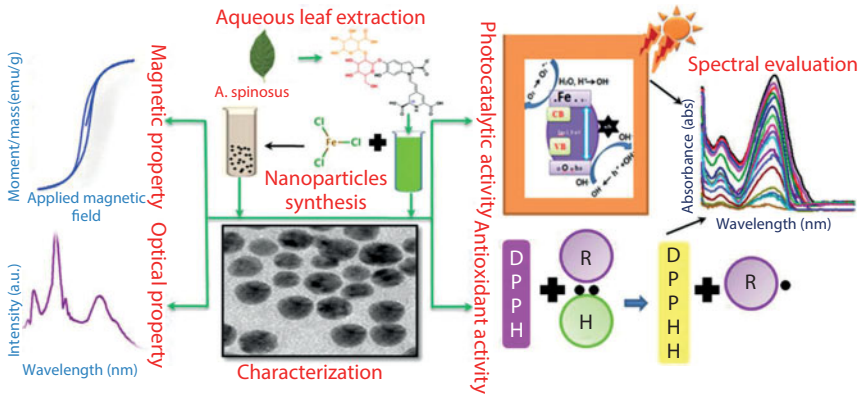


Figure 9.4 Schematic diagram showing the multifunctional behavior of *Amaranthus spinosus* leaf extract mediated FeO nanoparticles synthesized for their physicochemical traits, photocatalytic activity in methyl orange and methylene blue, and antioxidant activity. (Reproduced with permission from [122])

9.4.2 Removal of Heavy Metals

Heavy metals are elements having atomic weight in the range of 50 to 200.6 and specific gravity greater than 5.0 [142]. Water pollution caused by heavy metals is a consequence of industrial activities, which has now become a global concern because it is growing day by day at a very high rate. Metallurgical, fertilizer, battery, mining and mineral industries produce heavy metal effluents which are directly discharged into the water. The heavy metal effluents are easily soluble in aquatic environment and are not biodegradable. After that, they are absorbed by aquatic life, enter the food chain and are consumed by human beings. If they are consumed by human beings above the permissible level, they can result in life-threatening diseases. So, the treatment of water or removal of heavy metals from the environment is very important to avoid chronic toxicity, which can cause certain disabilities and also cancer. The toxic heavy metals which are mainly responsible for water contamination include copper, zinc, mercury, nickel, cadmium, arsenic, lead and chromium [143]. Each and every element has a specific toxic effect on the human body. For example, zinc causes health problems like vomiting, nausea, anemia, stomach cramps and skin irritations; while excess copper causes vomiting, cramps, convulsions or even death. Nickel has imminent toxicological effects, resulting in lung/skin/nasopharynx diseases, malignant tumors and gastrointestinal distress. Mercury directly affects the central nervous system and high consumption leads to impairment of pulmonary as well as kidney function, chest pain and dyspnea. Cadmium is considered one of the carcinogenic elements and chronic exposure to it can cause allergies or kidney disease. The aquatic environment contains two oxidation states of chromium, i.e., Cr(III) and Cr(VI), in which Cr(VI) is more toxic. It has a wider range of effects, from simple skin allergies to carcinogenic effects. It is clear from the above stated problems, that it is very important to remove these toxic elements from the environment to maintain healthy living beings [144]. There are various methods used by environmental researchers to sort out this problem, like ion-exchange, chemical precipitation, adsorption, electrochemical treatment, membrane filtration, etc. Among them, adsorption of these toxic metals is the most eco-friendly and cost-effective technique. In this method, we can reuse the water after it is treated by certain adsorbents and the used adsorbents can be recycled by the appropriate desorption process.

Adsorption is defined as the phenomenon in which a substance is transferred from the liquid phase to the surface of a solid and gets enclosed by a chemical and/or physical interaction by mass transfer process. The adsorption is mainly due to the interaction between the attractive forces of a surface

and the metal to be absorbed. Depending upon the intermolecular attractive forces, adsorption is called physical or chemical adsorption. The adsorption process has several advantages over other techniques; it is economical, does not produce waste product or sludge and can also be reused [145].

Environmental remediation by magnetic nanoparticles involves chemical adsorption process involving the chemical reaction between adsorbent and adsorbate. A very strong interaction is created between NPs and metal ions, called an electronic bond. Magnetic nanoparticles have high affinity towards heavy metals having large specific surface area, extremely high reactivity and reducing capacity. In this regard, several researchers have tried to use MNPs for metal ion removal synthesized through a green synthesis approach. Fazlzadeh *et al.* synthesized zero-valent iron nanoparticles (nZVI) using three plant extracts, *Rosa damascene* (RD), *Thymus vulgaris* (TV) and *Urtica dioica* (UD), and studied their role in removal of Cr(VI) [82]. The polyphenols, proteins and organic acids serve a dual functionality, i.e., reducing and stabilizing agent. The characterization of nZVI was done by SEM and FTIR studies. The removal mechanism of Cr(VI) is due to the small size of iron, which results in monolayer adsorption of Cr(VI) ions. Due to small pore size and high agglomeration capacity of iron nanoparticle, Cr(VI) ions get easily absorbed and show highest removal efficiency. By applying the dose of 0.2 g L^{-1} and contact time of 10 min the nanoparticle showed a removal efficiency of ~ 90%. The highest efficiency is seen in nanoparticles synthesized with *Rosa damascene,* i.e., 94.87%. Es'haghi *et al.* have synthesized functionalized magnetic iron nanoparticles using olive oil. By applying a dose of 0.5 g L^{-1}, the NPs show the high removal efficiency of 82% for nickel ion [146]. Weng *et al.* have synthesized iron nanoparticle from *Eucalyptus* leaf and showed its efficiency in removal of mixed contaminants, i.e., Cr(VI) and Cu(II) [83]. The *Eucalyptus* leaf extract contains aldehydes, phenols, amines and alkenes, which serve as a reducing and capping agent. The synthesized nanoparticle was characterized by SEM, XPS, XRD, and FTIR techniques. The plausible reactions between the iron nanoparticle and the Cr(VI) and Cu(II) contaminants are also described in this work and shown as follows:

$$\text{Metal ion} + \text{FeNPs} \longrightarrow \text{metal ions-FeNPs} \tag{9.11}$$

$$CrO_4^{2-} + Fe^0 + 8H^+ \longrightarrow Fe^{3+} + Cr^{3+} + 4H_2O \tag{9.12}$$

$$(1-x)Fe^{3+} + xCr^{3+} + 2H_2O \longrightarrow Fe_{(1-x)}Cr_xOOH + 3H^+ \tag{9.13}$$

$$Fe^0 + Cu^{2+} \longrightarrow Fe^{2+} + Cu^0 \tag{9.14}$$

The prepared nanoparticle showed 58.9% and 33.0% removal efficiency for Cr(VI) and Cu(II), respectively. Manquián-Cerda *et al.* synthesized nanoscale iron (oxide, oxyhydroxides and zero-valent) from blueberry shoots (*Vaccinium corymbosum*), which acts as a reducing agent for $FeCl_3 \cdot 6H_2O$ solution [96]. The nanoparticle was characterized by TEM, SEM, electrophoretic migration, BET and XRD techniques. The prepared nanoparticle is used for the removal of As(V). The nanoparticle was prepared by two green techniques; blueberry shoots-Fe (BB-Fe NPs) and "chemical" (nZVI). From the adsorption experiment, it was found that adsorption of metal ion followed Langmuir-Freundlich model and adsorption capacity of ZVI and BB-FeNPs was found to be 52.23 ± 6.06 and 50.40 ± 5.90 $mg \cdot g^{-1}$. A schematic diagram of the mechanisms of As(V) removal is shown in Figure 9.5.

Safinejad *et al.* have synthesized magnetic bio-adsorbent from walnut shell (LMWS) as an efficient lead remover [147]. A novel approach was taken to grow magnetic domain on top of the LMWS surface via co-precipitation of minimum amounts of Fe^{2+} and Fe^{3+} ions. The adsorption of Pb(II) ions by LMWS showed a slightly better fit with the Langmuir model compared to the Freundlich one. Wen *et al.* have synthesized magnetic nanoparticles decorated tea waste (Fe_3O_4-tea) and explored its application in Cu(II) and Zn(II) removal [148]. From different characterizations, it was found that tea powder was attached to the surface of iron nanoparticle. It is seen that maximum sorption capacities of Fe_3O_4-tea calculated from Langmuir isotherm model were 95.44 mg g^{-1} for Cu(II) and 68.78 mg g^{-1}

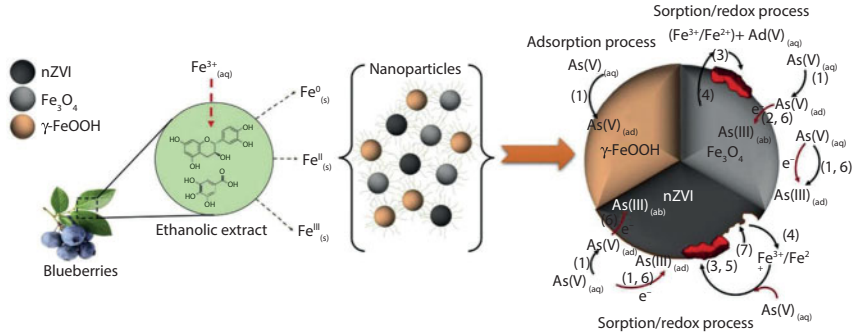


Figure 9.5 Schematic illustration of the probable mechanisms of As(V) removal and structural changes in lepidocrocite (γ-FeOOH), magnetite (Fe3O4), and nZVI. As(V) can be removed by different procedures: adsorption (1), absorption (2), precipitation (3), dissolution (4), co-precipitation (5) and reduction (6). The structure of nZVI is determined by dissolution or passivation (4 and 7). (Reproduced with permission from [96])

for Zn(II) at pH 6.0. Prasad *et al.* have synthesized reduced graphene oxide and iron oxide (RGO/Fe_3O_4) nanocomposite using *Murraya koenigii* leaf extract for the removal of Pb(II) from aqueous solution [102]. The nanoparticle was characterized by FTIR, FE-SEM, XRD, Raman spectroscopy measurements, TEM, nitrogen adsorption-desorption (BET) and VSM studies. A batch binding adsorption experiment was done to study the removal of Pb(II). Both Langmuir model and Freundlich model were fitted in the adsorption isotherm study and the adsorption capacity was found to be 48 mg g^{-1}.

Mystrioti *et al.* have synthesized ZVI coated with polyphenol of green tea, having the appearance of colloidal suspensions, and studied their chromium removal efficiency [149]. Xiao *et al.* synthesized iron nanoparticles from different plant extracts like *Syzygium jambos* (L.) Alston (SJA), Oolong tea (OT) and *Aleurites moluccana* (L.) Willd (AMW) and used it for the removal of chromium(VI) [150]. Madhavi *et al.* synthesized photogenic iron nanoparticle from *Eucalyptus globules* leaf extract, which was used in the adsorption of Cr(VI) metal [151].

9.4.3 Removal of Toxic Anions

There are number of inorganic anions, like nitrates, nitrites, phosphates, fluorides and perchlorate, which are potentially very harmful and are found in considerable amounts in drinking as well as ground water [152]. When the concentration of these anions increases to a threshold value, they can be a serious threat to human beings, as well as aquatic ecosystems, and lead to eutrophication. For example, contamination by nitrates is caused by widespread use of artificial fertilizers and poorly treated or untreated human waste, and radioactive waste used in radioactive industries in the form of nitric acid for processing extremely toxic radioactive elements. Nitrate can also enter into the system as a by-product of many industrial processes and also the production of nitro-organic and pharmaceutical compounds, including paper and explosives manufacturing. There are serious health hazards caused by nitrates, like blue baby syndrome, and it is also a major precursor to carcinogenic nitrosamines [153]. Similarly, fluoride is also very important in terms of environmental pollutants and is even found in drinking water in some areas of the world, like the Bengal and Jharkhand states of India, through dental aids or naturally occurring processes. Fluoride is also used in various industries as a glass and silica etchant. However, its higher use in geological and various anthropogenic activities is also responsible for groundwater fluoride contamination. The harmful effects of free fluoride ion on bone structure results in fluorosis,

cancer, etc. In the bloodstream it readily ties up the free calcium electrolytes, which may cause heart failure [154]. Phosphates are an essential element which act as nutrients for the aquatic environment, but an excessive amount of anything is dangerous. Excess of phosphates causes eutrophication and algal blooms, thereby causing harm to aquatic life. Phosphates are introduced into the environment by several exogenous sources like fertilizers, cracker industries, household detergents, etc. [152].

Various techniques are used for the removal of these anions, involving ion exchange or reverse osmosis, electrocatalysis, biological denitrification and chemical reduction. Out of these conventional techniques, the use of magnetic nanoparticles in treating groundwater has engendered a significant breakthrough. In this chapter, we have compiled some of the greener approaches for the synthesis of magnetic nanoparticle in treatment of inorganic anions. Wang *et al.* have synthesized zero valent iron nanoparticle from the extracts of green tea (GT-Fe) and *Eucalyptus* leaves (EL-FeNPs) for the removal of nitrate [110]. The prepared nanoparticle was characterized by SEM, EDS, XRD and FTIR techniques. The polyphenols from green tea were used as a capping agent. The probable mechanism for synthesis of iron nanoparticle from polyphenols is: $nFe^{2+} + 2Ar(OH)_n \rightarrow nFe^0 + 2nAr = O + 2nH^+$, where Ar is the phenyl group and n is the number of hydroxyl groups oxidized by Fe^{2+}. From the batch binding study, it is noticed that 59.7% and 41.4% of nitrate was removed by GT-Fe and EL-Fe NPs, respectively. Prabhakar and his group synthesized iron nanoparticles from aquatic and terrestrial weeds such as *Eichhornia crassipes, Lantana camara* and *Mimosa pudica* [155]. The nanoparticle was characterized by UV, dynamic light scattering (DLS), FE-SEM, EDS, TEM, XRD and FTIR techniques. From the experiment it is found that *E. crassipes, L. camara* and *M. pudica* mediated iron nanoparticles showed 74.52%, 71.12% and 65.23% of nitrate removal, respectively.-

Ali *et al.* have synthesized nanomagnetic iron incorporated adsorbent for wastewater treatment for fluoride ion. The experimental data fitted to Langmuir, Freundlich and Temkin models. Maximum fluoride removal was seen to about 90%, with sample concentration of 4.0 mg/L, contact time of 25.0 min and pH = 7.0 pH at 293 K temperature [156]. Gan *et al.* have synthesized iron oxide nanoparticles from *Eucalyptus* leaf extract with assistance from a surfactant as well as capping agent cetyltrimethyl ammonium bromide (CTAB) and used them for the removal of phosphate from groundwater [94]. The particle size was controlled with the help of CTAB and therefore phosphate removal was estimated with respect to CTAB concentration. The 95.13% to 89.5% removal was found with an increase in concentration of CTAB from 0.4 to 10 mM.

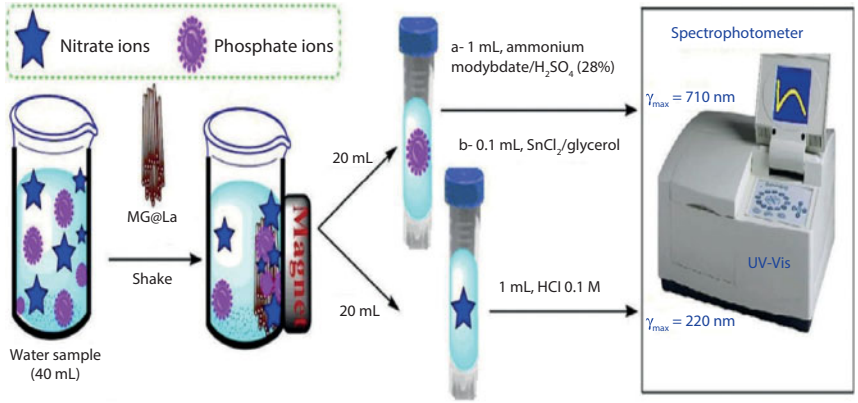


Figure 9.6 Graphical representation of the adsorption of phosphate and nitrate ions using lanthanum hydroxide doped onto magnetic reduced graphene oxide (MG@La). (Reproduced with permission from [157])

A miscellaneous nanocomposite named lanthanum hydroxide doped onto magnetic reduced graphene oxide (MG@La) was prepared by Nodeh *et al.* for the removal of phosphate and nitrate ions [157]. A graphical representation of the adsorption of phosphate and nitrate ions using lanthanum hydroxide doped onto MG@La is shown in Figure 9.6. The author studied both adsorption isotherm and adsorption kinetics and found that it follows Langmuir isotherm and pseudo-second-order kinetic models. The developed adsorbent showed high adsorption capacities of 116.28 mg g^{-1} and 138.88 mg g^{-1} for phosphate and nitrate ions, respectively. The nanoparticle shows 74%–90% removal of anions, phosphate and nitrate. Soliemanzadeh and Fekri synthesized clay-supported nanoscale zero-valent iron using green tea extract in the presence of natural bentonite (B-nZVI). The nanoparticle prepared is used for the removal of phosphorus compounds from aqueous solution [109]. Adsorption experiment was found to be pH-dependent and the results show that the maximum sorption capacities of natural bentonite and B-nZVI were 4.61 and 27.63 mg·g^{-1}. The study confirms the role of nZVI to improve the adsorption capacity of material.

9.4.4 Treatment of Pesticides in Groundwater

Sewage, which is mainly the wastewater released by different industries, fields, business communities and residential areas, contains disease-causing pathogens and microorganisms. The cloudiness of the wastewater is caused

by the suspended particles having concertation in the range of 100 to 350 mg L^{-1} and is termed untreated sewage. In addition to the pathogens and microorganisms, sewage also contains different organic pollutants like pesticides. Pesticides are the class of chemicals used all over the world under the names of herbicides, insecticides, fungicides, rodenticides, molluscicides and nematicides [158]. The constructive approach of pesticides is to help in crop/food productivity by drastically reducing the vector-borne diseases. In spite of their good uses, they are unregulated and surplus doses are causing serious health hazards in the living world. Some organochlorine and organophosphorus compounds are the least biodegradable pesticides, which is why they are banned in many countries but are still used in excessive amounts to increase crop productivity. Pesticides can cause severe health hazards, which could be monitored at molecular or behavioral levels and biochemical levels. In general, a majority of pesticides that remain unused get mixed with air, water and soil, having harmful effects on human beings, pets and the environment. The adverse effects of pesticides on the human body are oncological, pulmonary and hematological problems. They can also lead to large immune system deficiencies and inborn deformities, reproductive failure, disruption of endocrine (hormonal) system, and DNA damage of the immune system. Consumption of fish and shell fish, which are contaminated with pesticides, runoff soils from the field to small ponds and water bodies, are the main source of pesticides in our system. Some of the famous organochlorine pesticides are gamma-hexachloro-cyclohexane (lindane), dichlorodiphenyltrichloroethane (DDT) and hexachlorocyclohexane (HCH), which cover ~70% of the pesticides used in agro fields. Among the organophosphorus pesticides, malathion and chlorpyrifos are the most common. The weedicides used to control broad leaf weeds are atrazine, prometryn, simazine, simeton and ametryn [159]. Nanoscale zero-valent iron (nZVI) and other magnetic material, have proved to be the most promising environmental remediation material for all types of halogenated pesticides. The magnetically separable adsorbent does not require a time-consuming filtration or separation process, they are cost effective and easily available too. Guo *et al.* have synthesized iron-based nanoparticle from *Euphorbiaceae cochinchinensis leaf* extracts and used it for the degradation of 2,4-dichlorophenol [95]. It is a pesticide with potential carcinogenic and mutagenic activity. The prepared nanoparticle has a size of 100 nm and from XPS study it is confirmed that nanoparticles have Fe(III) and Fe(II) in the form of oxide and hydroxides. It is observed from the adsorption study that the nanoparticle having Fenton-like oxidation reaction can remove up to 64% of 2,4-dichlorophenol. Ali *et al.* have synthesized functionalized iron nanoparticles using black tea and used it

for the removal of ametryn from water with the help of molecular liquid phase adsorption method [160]. One of the second generation herbicides for controlling the growth of weeds in maize, pineapple and sugarcane fields is Ametryn [2-(ethylamino)-4-isopropylamino-6-methyl-thio-s-triazine]. The adsorption study follows Langmuir, Freundlich, Temkin and Dubinin-Radushkevich models. The nanoparticle shows 88% removal of ametryn pesticides. Lian *et al.* synthesized magnetic pillared bentonite material (Fe_3O_4@Al-B) by green solvothermal technique, having size of 200 nm. Microcystins are the cyanobacterial toxins distributed widely in aquatic systems. From the adsorption study it can be seen that the adsorption data follows Langmuir and Freundlich models and the adsorption capacity of Fe_3O_4@Al-B is 161.29 mg/g [161]. Sangami and Manu prepared iron nanoparticles using raw laterite as the iron source and *Eucalyptus* leaf extract as the reducing agent for the removal of ametryn herbicide from water. The prepared nanoparticle acts like heterogeneous Fenton catalyst and exhibited 100% removal of ametryn [105].

9.4.5 Removal of Microbial Contamination

Microbial contamination of drinking water, particularly in growing urban areas, is a serious problem. It mainly comes from the excreted feces of living beings and the growth of microbes in the rotten sewage of slaughterhouses [162]. These microbes consist of bacterial pathogens, including enteric viruses, enteric and aquatic bacteria and enteric protozoa; some examples of these are *Giardia* and *Cryptosporidium, Shigella* spp., *Salmonella* spp. and *Escherichia coli, Legionella* spp., *Aeromonas* spp., *Pseudomonas aeruginosa* and *Mycobacterium avium.* Drinking water storage is the secondary water supply facility in both rural and urban areas. Due to the lack of cleaning and maintenance in the water supply process, the explosive growth of microbes in water storage tanks results in severe contamination of supplied water. To prevent diseases spreading via drinking water, China promulgates their own Standards for Drinking Water Quality. It is declared that the total number of *E. coli* colonies should not be more than 100 CFU mL^{-1} in terminal drinking water [163]. Waterborne diseases are transmitted through drinking of contaminated water and the infected water is the passive carrier of these pathogens. So, it is necessary to purify the drinking water through a cost-effective and easy process before it reaches the consumption level. Patra and Baek have synthesized magnetic iron oxide (Fe_3O_4) nanoparticles through green synthesis approach using extract of food processing waste, i.e., silky hairs of corn (*Zea mays* L.) and outer leaves of Chinese cabbage (*Brassica rapa* L. subsp. *pekinensis*), and

the resultant nanoparticles were named accordingly as MH-FeNPs and CCP-FeNPs [164]. When the nanoparticle is mixed with kanamycin and rifampicin, it shows great antibacterial activity against pathogenic bacteria. When the nanoparticle is mixed with amphotericin b, it exhibits anticandidal activity against five different pathogenic *Candida* species. Irshad *et al.* have synthesized iron oxide using *Punica granatum* peel extract [165]. The synthesis of the nanoparticle was optimized by controlling the concentration of *P. granatum* peel extract. The nanoparticle prepared with 40 mL extract concentrations shows the strongest antibacterial activity against *Pseudomonas aeruginosa*. Credit for the greater antibacterial activity of the prepared nanoparticle is given to their small size and high surface area. The antibacterial activity of the magnetic nanoparticle is shown in the schematic in Figure 9.7.

Groiss *et al.* have synthesized iron oxide nanoparticle from the leaf extract of *Cynometra ramiflora* [113]. This is a fast and simple technique for the synthesis of iron oxide nanoparticle. The phytochemicals from *C. ramiflora* leaves are responsible for the synthesis and stabilization of the nanoparticle. The resultant iron oxide nanoparticle showed antibacterial efficiency against *E. coli* and *S. epidermidis*. Helen and Rani synthesized magnetic nickel nanoparticle using aqueous tuber extract of *Dioscorea* (elephant yam) [166]. The plant extract acts as a reducing, stabilizing and capping agent. The nanoparticle was characterized by UV-Vis, XRD and SEM with EDAX analysis technique**.** The nanoparticle was synthesized by an eco-friendly process and was found to be very toxic towards *E. coli,*

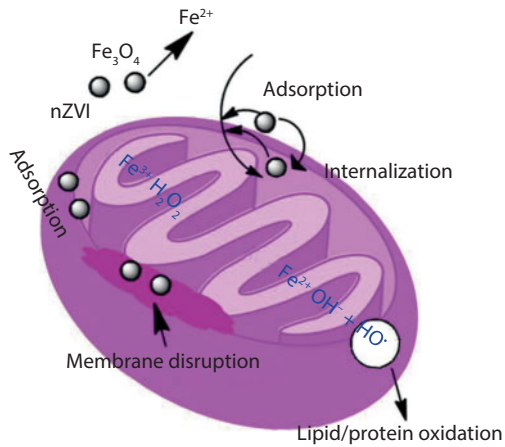


Figure 9.7 Schematic for the potential cell damage of the pathogenic bacteria or virus after exposure to magnetic nanoparticle.

Klebsiella pneumoniae (Gram-negative), *Bacillus cereus* and *Staphylococcus aureus* (Gram-positive) bacterial strains. Elango and his group synthesized nickel from the methanolic extract of *Cocos nucifera* using a Soxhlet apparatus [167]. The nanoparticle shows lethal pesticidal activity against agricultural pest *Callosobruchus maculatus* and the nanoparticle also shows larvicidal property against Aedes aegypti larvae. Koyyati *et al.* synthesized magnetic cobalt nanoparticle from the leaf extract of *Raphanus sativus* var. *longipinnatus* [80]. The antibacterial activity of the prepared nanoparticle is studied through disc diffusion test against human pathogenic strains like *Pseudomonas putida* and *Klebsiella pneumoniae*.

9.4.6 Elimination of other Hazardous Organic Pollutants

In addition to the above-mentioned contaminants, there are several other organic pollutants also present in the environment which are known to be potential hazards to living beings. These types of organic pollutants enter the environment through natural (volcanic eruptions, forest fires, etc.) and/or anthropogenic activities (oil spills, incomplete combustion of fuel, coal, etc.). It is reported that when the molecular weight of the organic molecules is increased, their toxic property increases. Chiou *et al.* have synthesized silver-iron oxide composite for the reduction of 4-nitrophenol [168]. The nanoparticle was synthesized by one-pot synthesis using L-arginine, which acts as reducing agent for both iron and silver. The nanoparticle has good catalytic activity for the conversion of 4-nitrophenol to 4-aminophenol. Stan *et al.* have performed green synthesis of magnetic nanoparticle (Fe_3O_4 NPs) from the aqueous peel of lemon (*Citrus limon*), black grapes (*Vitis vinifera*) and cucumber (*Cucumis sativus*), which they referred to as Fe_3O_4 (lem), Fe_3O_4 (grp) and Fe_3O_4 (cum) [169]. These nanoparticles were used for the removal of seven antibiotics, i.e., piperacillin (PIP), tazobactam (TAZ), sulfamethoxazole (SUL), tetracycline (TET), trimethoprim (TRI), ampicillin (AMP) and erythromycin (ERY), from aqueous media. Langmuir, Freundlich and Temkin adsorption isotherm models were used to study the adsorption kinetics. The nanoparticle shows a high removal efficiency of about 90%.

Shanker *et al.* synthesized iron hexacyanoferrate nanoparticles for the degradation of toxic polycyclic aromatic hydrocarbons (PAHs) [103]. In this synthesis, *Sapindus mukorossi* was used as natural surfactant. The prepared nanoparticle shows photocatalytic degradation of hazardous PAHs like anthracene, phenanthrene, chrysene, fluorene and benzopyrene. Jassal *et al.* have synthesized various forms of iron oxide nanoparticles (i.e., α-FeOOH, β-FeOOH and α-Fe_2O_3) using *Sapindus mukorossi* (raw

reetha) as a natural surfactant for the adsorption of 2-Amino, 3-Amino, and 4-Aminopyridines [104]. Gai *et al.* have synthesized iron-based nanocatalysts by green synthesis approach with one-pot hydrothermal carbonization process. Iron salt was heated together with the lignocellulosic matrix (i.e., pinewood sawdust) at 200 °C for an hour in an autoclave. The resultant nanoparticle shows high catalytic activities towards phenol degradation [107].

9.5 Toxicity of Nanoparticles

Since MNPs are considered a nontoxic class of nanoparticles, a very limited number of studies have been done on their toxicity. As previously mentioned, magnetic nanoparticles are toxic to microorganisms such as *Escherichia coli, Pseudomonas stutzeri* and *Bacillus cereus*. This means that the properties harmful to environmental components are advantageous for us to implement for treatment and remediation processes [170]. The catalytic and magnetic properties can also have a toxic response when taken up by the various organisms and cells, including other organisms like earthworms, invertebrates and plants. It is also possible that living beings may be affected by the toxic effect of magnetic nanoparticle, which falls under the remediation area. Investigative studies have shown that magnetic nanoparticles have a lethal effect on some terrestrial organisms and can even lead to their death. Therefore, a thorough study is needed prior to considering the use of magnetic nanoparticle for environmental remediation. During some of the studies, it was found that Fe-based nanoparticles have a toxic effect on aquatic organisms in terms of acute lethality and oxidative stress [171]. If the concentration of magnetic nanoparticle exceeds 100 mg L^{-1}, it causes a disruption in the oxidative defense system of larvae and embryos as well as acute lethality in embryos. Moreover, it was also found that toxicity of the magnetic nanoparticle mainly depends on their size, structural properties, dosage, and the intended use. Magnetic nanoparticle may interfere with the biological components of cell when directly attached to the cell membrane. Aggregation and coagulation properties are decided according to the shape and size of the nanoparticles, which may result in their toxic responses. Some other problems occur when the by-products of the nanoparticle have a harmful effect on the tissues and organs of living beings [172]. When the nanoparticles and their by-products enter the body, there is an interaction between biological macromolecules, such as lipids, proteins, and enzymes, found within biological fluids. The magnetic nanoparticles interact with the biological components to form a complex

called corona. Similarly, different types of cells bind in different ways to MNPs. As a result, the binding of exogenous objects to MNPs may cause different responses and affect uptake and metabolism depending on cell type. Furthermore, another problem is posed by the sedimentation of MNPs, as this phenomenon effectively occurs when there is an apparent increase in MNP concentration at cell surfaces and therefore must be taken into account when performing MNP-related toxicity assays [173].

9.6 Future Aspects of Magnetic Nanoparticle

Even though there has been exceptional progress in the use of magnetic nanoparticle for remediation of soil and water contaminated sites, certain drawbacks have also been reported:

1. Costly synthesis procedure for modifying magnetic nanoparticles for special sites;
2. Insufficient knowledge of the interaction mechanism of nanoparticle on contaminant sites;
3. Final fate of the nanoparticle after interaction with the contaminants.

It is important to note that magnetic nanoparticles lack research in real field work. The development of magnetic nanoparticle-based technology is due to its being low cost, nontoxic and less toxic to the environment. But, we are still not very sure about these facts; therefore, with modification by current technologies the unique properties of magnetic nanoparticle can be transformed into new assets. In the future, we can expect the use of magnetic nanoparticle in real field work because many governmental agencies are encouraging this ongoing research work on magnetic nanoparticles in remediation of contaminated soils and groundwater. In addition, further research on MNPs should be encouraged for the treatment of organic complex pollutants, halogenated aromatic compounds, PCBs, pesticides, dioxins, and others, which has not been very popular till now. In addition to these studies and exploration of the role of MNPs in various new fields, the degradation kinetics (e.g., competing contaminants, pH as well as ionic strength) must be explored to understand the reaction mechanism of nanoparticle-water interface. However, to realize their full potential it is necessary to describe the relationship between the structure of the catalyst, including its catalytic performance, which can subsidize the expansion of novel MNPs with low metal leaching rate

and high fouling resistance. From the overall studies, it is suggested that further research is necessary at all scales (i.e., nanoscale to field scale) to improve the understanding of potential magnetic nanoparticles used for site remediation. We think that an improved understanding at the nanoscale to regulate chemical reactions and physical mechanisms will definitely transform the MNPs from lab-scale development to real field-scale applications.

Acknowledgment

Ms. Karfa is gratefully acknowledged for the major contribution in writing this book chapter along with drawing the Figures and Tables, taking the copy right permission etc.

References

1. Mazzola, L., Commercializing nanotechnology. *Nat. Biotechnol*., 21, 1137–1143, 2003.
2. Cheng, S.F., Wu, S.C., The enhancement methods for the degradation of TCE by zero-valent metals. *Chemosphere*, 41, 1263–1270, 2000.
3. Paull, R., Wolfe, J., Hebert, P., Sinkula, M., Investing in nanotechnology. *Nat. Biotechnol.,* 21, 1134–1147, 2003.
4. Weissleder, R., Elizondo, G., Wittenburg, J., Rabito, C.A, Bengele, H.H., Josephson, L., Ultrasmall superparamagnetic iron oxide: Characterization of a new class of contrast agents for MR imaging. *Radiology,* 175, 489–493,1990.
5. Wang, S., Mamedova, N., Kotov, N.A., Chen, W., Studer, J., Antigen/antibody immunocomplex from CdTe nanoparticle bioconjugates. *Nano Lett.,* 2, 817–822. 2002.
6. Ma, J., Wong, H., Kong, L.B., Peng, K.W., Biomimetic processing of nanocrystallite bioactive apatite coating on titanium. *Nanotechnology*, 14, 619–623,2003.
7. Baruah, S., Dutta, J., Nanotechnology applications in pollution sensing and degradation in agriculture: A review, *Environ. Chem. Lett.*, 7, 191–204, 2009.
8. Crozals, G.D., Nanoparticles with multiple properties for biomedical applications: A strategic guide. *Nano Today*, 11, 435–463, 2016.
9. Farre, M., Sanchis, J., Barcelo, D., Anaysis and assessement of the occurrence, the fate and the behavior of nanomaterials in the environment. *Trend. Anal. Chem.*, 30, 515–527, 2011.

10. Liu, W.T., Nanoparticles and their biological and environmental applications. *J. Biosci. Bioeng.*, 102, 1–7, 2006.
11. Murphy, C.J., Sau, T.K., Gole, A.M., Orendorff, C.J., Gao, J., Gou, L., Hunyadi, S.E., Li, T., Anisotropic metal nanoparticles: Synthesis, assembly, and optical applications. *J. Phys. Chem. B*, 109, 13857–13870, 2005.
12. Zhang, L., Gu, F.X., Chan, J.M., Wang, A.Z., Langer, R.S., Farokhzad, O.C., Nanoparticles in medicine: Therapeutic applications and developments. *Clin. Pharmacol. Ther.*, 83,761–780, 2008.
13. Akbarzadeh, A., Samiei, M., Daravan, S., Magnetic nanoparticles: Preparation, physical properties, and applications in biomedicine. *Nanoscale Res. Lett.*, 7, 1–13, 2012.
14. Tang, S.C.N., Lo, I.M.C., Magnetic nanoparticles: Essential factors for sustainable environmental applications. *Water Res.* 47, 2613–2632, 2013.
15. Oh, J.K., Park, J.M., Iron oxide-based superparamagnetic polymeric nanomaterials: Design, preparation, and biomedical application. *Prog. Polym. Sci.,* 36, 168–189, 2011.
16. Colombo, M., Carregal-Romero, S., Casula, M.F., Gutierrez, L., Morales, M.P., Bohm, I.B., Biological applications of magnetic nanoparticles. *Chem. Soc. Rev.*, 12, 4306–4334, 2012.
17. Huang, S.-H., Juang, R.-S., Biochemical and biomedical applications of multifunctional magnetic nanoparticles: A review. *J. Nanopart. Res.,* 13, 4411–4430, 2011.
18. Chen, L., Wang, T., Tong, J., Application of derivatized magnetic materials to the separation and the preconcentration of pollutants in water samples. *Trend, Anal. Chem.*, 30, 1095–1108, 2011.
19. Tang, S.C.N., Lo, I.M.C., Magnetic nanoparticles: Essential factors for sustainable environmental applications. *Water Res.* 47, 2613–2632, 2013.
20. Santhosh, C., Role of nanomaterials in water treatment applications: A review. *Chem. Eng. J.,* 306, 1116–1137, 2016.
21. Wang, L.Y., Luo, J., Fan, Q., Suzuki, M., Suzuki, I.S., Monodispersed core-shell Fe_3O_4@Au nanoparticles. *J. Phys. Chem. B*, 109, 21593–21601, 2005.
22. Watlington, K., *Emerging Nanotechnologies for Site Remediation and Wastewater Treatment*, 1st ed., pp. 1–55, National Service Center for Environmental Publications, 2005.
23. Zhang, W., Elliott, D.W., Applications of iron nanoparticles for groundwater remediation. *Remediation*, 16, 7–21, 2006.
24. Anon., How safe is our bottle water?. *Down Earth* 11, 27–32, 2003.
25. Li, X., Elliot, D.W., Zhang, W., Zero-valent iron nanoparticles for abatement of environmental pollutions: materials and engineering aspects. *Crit. Rev. Solid State*, 31, 111–122, 2006.
26. Haes, A.J., Van, P., Duyne, R.P., A nanoscale optical biosensor: Sensitivity and selectivity of an approach based on the localized surface plasmon resonance spectroscopy of triangular silver nanoparticles. *J. Am. Chem. Soc.,* 124, 10596–10604, 2002.

27. Rocha-Santos, T.A.P., Sensors and biosensors based on magnetic nanoparticles. *Trends Anal. Chem.,* 62, 28–36, 2014.
28. Jhung, J.Y., Kim, S., Synthesis and thermoelectric properties of n-Type Mg_2Si. *Electron. Mater. Lett.,* 6, 187–191, 2007.
29. Singamaneni, S., Bliznyuk, V.N., Binek, C., Tsymbal. E.Y., Magnetic nanoparticles: Recent advances in synthesis, self-assembly and applications. *J. Mater. Chem.,* 21, 16819–16845, 2011.
30. Leslie-Pelecky, D.L., Rieke, R.D., Magnetic properties of nanostructured materials. *Chem. Mater.*, 8, 1770–1783, 1996.
31. Akbarzadeh, A., Samiei, M., Davaran, S., Magnetic nanoparticles: Preparation, physical properties, and applications in biomedicine. *Nanoscale Res. Lett.* 7, 1–13. 2012.
32. Faraji, M., Yamini, Y., Rezaee, M., Magnetic nanoparticles: Synthesis, stabilization, functionalization, characterization and applications. *J. Iran. Chem Soc.*, 7, 1–37, 2010.
33. Mohammed, L., Gomaa, H.G., Ragab, D., Zhu, J., Magnetic nanoparticles for environmental and biomedical applications: A review. *Particuology* 30, 1–14, 2017.
34. Ponder, S.M., Darab, J.G., Bucher, J., Caulder, D., Craig, I., Davis, L., Edelstein, N., Lukens, W., Nitsche, H., Rao, L., Shuh, D.K., Mallouk, T.E., Surface chemistry and electrochemistry of supported zerovalent iron nanoparticles in the remediation of aqueous metal contaminants. *Chem. Mater.*, 13, 479–486, 2001.
35. Lu, A.H., Salabas, E.L., Schuth, F., Magnetic nanoparticles: Synthesis, protection, functionalization, and application. *Angew. Chem. Int. Ed.*, 46, 1222–1244, 2007.
36. Chung, B.X., Liu, C.P., Synthesis of cobalt nanoparticles by DC magnetron sputtering and the effects of electron bombardment. *Mater. Lett.,* 58, 1437–1440. 2004.
37. Sowka, E., Leonowicz, M., Andrzejewski B., Pomogailo, A.D., Dzhardimalieva, G.I., Cobalt nanoparticles processed by thermal decomposition of metal-containing monomers. *Mater. Sci.,* 24, 312–317 2006.
38. Ledo-Suárez, A., Rodríguez-Sánchez, L., Blanco, M.C., López-Quintela, M.A., Electrochemical synthesis and stabilization of cobalt nanoparticles. *Phys. Stat. Sol.,* 203, 1234–1240, 2006.
39. Farhadi, S., Safabakhsh, J., Zaringhadam, P., Synthesis, characterization, and investigation of optical and magnetic properties of cobalt oxide (Co_3O_4) nanoparticles. *J. Nanostruct. Chem*., 3(69), 1–9, 2013
40. Ahmed, K., Tariq, I., Siddiqui, S.U., Mudassir, M., Green synthesis of cobalt nanoparticles by using methanol extract of plant leaf as reducing agent. *Pure Appl. Biol*., 5, 453–457, 2016.
41. Chandra, S., Kumar, A., Tomar, P.K., Synthesis of Ni nanoparticles and their characterizations, *J. Saudi Chem. Soc.*, 18, 437–442, 2014.

42. Tishin, A.M., Spichkin, Y.I., *The Magnetocaloric Effect and Its Applications*, Institute of Physics: Bristol, Philadelphia, 2016.
43. Thongchant, S., Hasegawa, Y., Wada, Y., Yanagia, S., Spindle type EuO nanocrystals and the magnetic property. *Chem. Lett.*, 30, 1274–1275, 2001.
44. Thongchant, S., Hasegawa, Y., Wada, Y., Yanagia, S., Size selective synthesis of surface modified Eus nanocrystals and their physical properties. *Chem. Lett.*, 32, 706–707, 2003.
45. Zhang, B., Yang, W., Yu, J., Guo, W., Wang, J., Liu, S., Xiao, Y., Shi, D., Green synthesis of sub-10 nm gadolinium-based nanoparticles for sparkling kidneys, tumor, and angiogenesis of tumor-bearing mice in magnetic resonance imaging. *Adv. Healthc. Mater.,* 6, 1600865–1600867, 2017.
46. Biju,V., Khadar, A.M., Dielectric properties of consolidated nanoparticles of NiO. *J. Mater. Sci.*, 38, 40–45, 2003.
47. Jun, Y., Choi, J., Cheon, J., Hetero-structured magnetic nanoparticles: Their versatility and high performance capabilities. *Chem. Commun.*, 12, 1203–2014, 2007.
48. Häfeli, U., Schütt, W., Teller, J., Zborowski, M. (Eds.), *Scientific and Clinical Applications of Magnetic Carriers*, Plenum, New York, 1997.
49. Abu-Dief, A.M., Abdel-Fatah, S.M., Development and functionalization of magnetic nanoparticles as powerful and green catalysts for organic synthesis. *Beni-Seuf Univ. J. Appl. Sci.,* 1–13, 2017.
50. Kim, D.K., Mikhaylova, M., Anchoring of phosphonate and phosphinate coupling molecules on titania particles. *Chem. Mater.* 15, 1617–1627, 2003.
51. Gupta, A.K., Gupta, M., Synthesis and surface engineering of iron oxide nanoparticles for biomedical applications. *Biomaterials.,* 26, 3995–4021, 2005.
52. Mørup, S., Meaz, T.M., Koch, C.B., Hansen, H.C.B., Nanocrystallinity induced by heating. *Z. Phys. D,* 40, 167–172, 1997.
53. Cullity, B.D, *Introduction to Magnetic Materials*, Addison-Wesley: Reading, 1972.
54. Mørup, S., Tronc, E., Superparamagnetic relaxation of weakly interacting particles. *Phys. Rev. Lett*., 72, 3278–3281, 1994.
55. Gossuin, Y., Gillis, P., Hocq, A., Vuong, Q.L., Roch, A., Magnetic resonance relaxation properties of superparamagnetic particles. *Wiley Interdiscip. Rev. Nanomed. Nanobiotechnol.,* 1, 299–310, 2009.
56. Chen, D., Tang, X., Wu, J., Zhang, W., Liu, Q., Jiang, Y., Effect of grain size on the magnetic properties of superparamagnetic $Ni_{0.5}Zn_{0.5}Fe_2O_4$ nanoparticles by co-precipitation process. *J. Magn. Magn. Mater.,* 323, 1717–1721, 2011.
57. Roth, H.C., Schwaminger, S.P., Schindler, M., Wagner, F.E., Berensmeier, S., Influencing factors in the c-precipitation process of superparamagnetic iron oxide nano particles: A model based study. *J. Magn. Magn. Mater.*, 377, 81–89, 2015.

58. Mittal, A.K., Chisti, Y., Banerjee, U.C., Synthesis of metallic nanoparticles using plant extracts. *Biotechnol. Adv.* 31, 346–356, 2013.
59. Dauthal, P., Mukhopadhyay, M., Noble metal nanoparticles: Plant-mediated synthesis, mechanistic aspects of synthesis, and applications. *Ind. Eng. Chem. Res.*, 55, 9557–9577, 2016.
60. Lafont, U., Simonin, L., Tabrizi, N.S., Schmidt-Ott, A., Kelder, E.M., Synthesis of nanoparticles of Cu, Sb, Sn, SnSb and Cu_2Sb by densification and atomization process. *J. Nanosci. Nanotechnol.*, 9, 2546–2552, 2009.
61. Ganjali, M., Ganjali, M., Vahdatkhah, P., Marashi, S.M.B., Synthesis of Ni nanoparticles by pulsed laser ablation method in liquid phase. *Procedia Mater. Sci.,* 11, 359–363, 2015.
62. Li, Y., Duan, X., Qian, Y., Yang, L., Liao, H., Nanocrystalline silver particles: Synthesis, agglomeration, and sputtering induced by electron beam. *J. Colloid Interface Sci.*, 347–349, 209. 1999.
63. Tsai, S.C., Song, Y.L., Tsai, C.S., Yang, C.C., Chiu, W.Y., Lin, H.M., Ultrasonic spray pyrolysis for nanoparticles synthesis. *J. Mater. Sci.,* 39, 3647–3657, 2004.
64. Shubin, Y., Plyusnin, P., Sharafutdinov, M., *In situ* synchrotron study of Au-Pd nanoporous alloy formation by single-source precursor thermolysis. *Nanotechnology,* 23, 405302–405307, 2012.
65. Treguer, M., de Cointet, C., Remita, H., Khatouri, J., Mostafavi, M., Amblard, J., Belloni, J., de Keyzer, R., Dose rate effects on radiolytic synthesis of gold-silver bimetallic clusters in solution. *J. Phys. Chem. B*, 102, 4310–4321, 1998.
66. Rotello, V.M., *Nanoparticles: Building Blocks for Nanotechnology*, Springer Science & Business Media: New York, NY, USA, 2004.
67. Thakkar, K.N., Mhatre, S.S., Parikh, R.Y., Biological synthesis of metallic nanoparticles. *Nanomedicine*, 6, 257–262, 2010.
68. Jegan, A., Ramasubbu, A., Saravanan, S., Vasanthkumar, S., One-pot synthesis and characterization of biopolymer – Iron oxide nanocomposite. *Int. J. Nano Dimens.,* 2, 105–110, 2011.
69. Yang, F., Cheng, K., Wu, T., Zhang, Y., Yin, J., Wang, G., Cao, D., Au-Pd nanoparticles supported on carbon fiber cloth as the electrocatalyst for H_2O_2 electroreduction in acid medium. *J. Power Sources*, 233, 252–258, 2013.
70. Nemamcha, A., Rehspringer, J.L., Khatmi, D., Synthesis of palladium nanoparticles by sonochemical reduction of palladium(II) nitrate in aqueous solution. *J. Phys. Chem. B*, 110, 383–387, 2006.
71. Xiong, Y., Chen, J., Wiley, B., Xia, Y., Aloni, S., Yin, Y., Understanding the role of oxidative etching in the polyol synthesis of Pd nanoparticles with uniform shape and size. *J. Am. Chem. Soc.*, 127, 7332–7333, 2005.
72. Yan, Y., Pillai, P.P., Timonen, J.V.I., Emami, F.S., Vahid, A., Grzybowski, B.A., Synthesis of toroidal gold nanoparticles assisted by soft templates. *Langmuir,* 30, 9886–9890, 2014.
73. Pritchard, J., Kesavan, L., Piccinini, M., He, Q., Tiruvalam, R., Dimitratos, N., Lopez-Sanchez, J.A., Carley, A.F., Edwards, J.K., Kiely, C.J., Hutchings,

G.J., Direct synthesis of hydrogen peroxide and benzyl alcohol oxidation using Au-Pd catalysts prepared by sol immobilization. *Langmuir*, 26, 16568–16577, 2010.
74. Virkutyte, J., Varma, R.S., Environmentally friendly preparation of metal nanoparticles, in: Sustainable Preparation of Metal Nanoparticles: Methods and Applications, Luque, R., Varma, R.S. (Eds.), chap. 2, pp. 7–33, *The Royal Society of Chemistry*: London, UK, 2013.
75. Narayanan, K.B., Sakthivel, N., Green synthesis of biogenic metal nanoparticles by terrestrial and aquatic phototrophic and heterotrophic eukaryotes and biocompatible agents. *Adv. Colloid Interface Sci*., 169, 59–79, 2011.
76. Parsons, J.G., Peralta-Videa, J.R., Gardea-Torresdey, J.L., Use of plants in biotechnology: synthesis of metal nanoparticles by inactivated plant tissues, plant extracts, and living plants. *Dev. Environ. Sci.*, 5, 463–485, 2007.
77. Durán, N., Marcato, P.D., Durán, M., Yadav, A., Gade, A., Rai, M., Mechanistic aspects in the biogenic synthesis of extracellular metal nanoparticles by peptides, bacteria, fungi, and plants. *Appl. Microbiol. Biotechnol.,* 90, 1609–1624, 2011.
78. Bharde, A., Wani, A., Shouche, Y., Joy, P.A., Prasad, B.L.V., Sastry, M., Bacterial aerobic synthesis of nanocrystalline magnetite. *J. Am. Chem. Soc.,* 127, 9326–9327,2005.
79. Subramaniyam, V., Subashchandrabose, S.R., Thavamani, P., Megharaj, M., Chen, Z., Naidu, R., *Chlorococcum* sp. MM11 – A novel phyco-nanofactory for the synthesis of iron nanoparticles. *J. Appl. Phycol.,* 27, 1861–1869, 2015.
80. Koyyati, R., Kudle, K.R., Padigya, P.R.M., Evaluation of antibacterial and cytotoxic activity of green synthesized cobalt nanoparticles using *Raphanus sativus* var. longipinnatus leaf extract. *Int. J. PharmTech Res.,* 9, 466–472, 2016.
81. Devatha, C.P., Thalla, A.K., Katte, S.Y., Green synthesis of iron nanoparticles using different leaf extracts for treatment of domestic waste water. *J. Clean Prod.,* 139, 1425–1435, 2016.
82. Fazlzadeh, M., Rahmani, K., Zarei, A., Abdoallahzadeh, H., Nasiri, F., Khosravi, R., A novel green synthesis of zero valent iron nanoparticles (NZVI) using three plant extracts and their efficient application for removal of Cr(VI) from aqueous solutions. *Adv. Powder Technol.,* 28, 122–130, 2017.
83. Weng, X., Jin, X., Lin, J., Naidu, R., Chen., Z., Removal of mixed contaminants Cr(VI) and Cu(II) by green synthesized iron based nanoparticles. *Ecol. Eng.,* 97, 32–39, 2016.
84. Hoag, G.E., Collins, J.B., Holcomb, J.L., Hoag, J.R., Nadagoudab, M.N., Varma, R.S., Degradation of bromothymol blue by 'greener' nano-scale zero-valent iron synthesized using tea polyphenols. *J. Mater. Chem.,* 19, 8671–8677, 2009.
85. Shahwan, T., Sirriah S.A., Nairat, M., Boyac, E., Eroğlu, A.E, Scott, T.B., Hallam, K.R., Green synthesis of iron nanoparticles and their application as

a Fenton-like catalyst for the degradation of aqueous cationic and anionic dyes. *Chem. Eng. J.,* 172 258–266, 2011.
86. Luo, F., Chen, Z., Megharaj, M., Naidu, R., Biomolecules in grape leaf extract involved in one-step synthesis of iron-based nanoparticles. *RSC Adv.* 4, 53467–53474. 2014.
87. Pattanayak, M., Nayak, P.L., Ecofriendly green synthesis of iron nanoparticles from various plants and spices extract. *Int. J. Plant Anim. Environ. Sci.*, 3, 68–76, 2013.
88. Periyathambi, P., Vedakumari, W.S., Bojja, S., Kumar, S.B., Sastry, T.P., Green biosynthesis and characterization of fibrin functionalized iron oxide nanoparticles with MRI sensitivity and increased cellular internalization. *Mater. Chem. Phys.*, 148, 1212–1220, 2014.
89. Mukherjee, D., Ghosh, S., Majumdar, S., Annapurna K., Green synthesis of a-Fe_2O_3 nanoparticles for arsenic(V) remediation with a novel aspect for sludge management. *J. Environ. Chem. Eng.*, 4, 639–650, 2016.
90. Martínez-Cabanas, M., López-García, M., Barriada, J.L., Herrero, R., de Vicente., M.E.S., Green synthesis of iron oxide nanoparticles. Development of magnetic hybrid materials for efficient As(V) removal. *Chem. Eng. J.*, 301, 83–91, 2016.
91. Makarov, V.V., Makarova, S.S., Love, A.J., Sinitsyna, O.V., Dudnik, A.O., Yaminsky, I.V., Taliansky, M.E., Kalinina, N.O., Biosynthesis of stable iron oxide nanoparticles in aqueous extracts of *Hordeum vulgare* and *Rumex acetosa* plants. *Langmuir*, 30, 5982–5988, 2014.
92. Prasad, C., Sreenivasulu, K., Gangadhara, S., Venkateswarlu, P., Bio inspired green synthesis of Ni/Fe3O4 magnetic nanoparticles using Moringa oleifera leaves extract: A magnetically recoverable catalyst for organic dye degradation in aqueous solution. *J. Alloys Compd.,* 700, 252–258, 2017.
93. Daneshfozoun, S., Abdullah, M.A., Abdullah. B., Preparation and characterization of magnetic biosorbent based on oil palm empty fruit bunch fibers, cellulose and *Ceiba pentandra* for heavy metal ion removal. *Ind. Crops Prod.,* 105, 93–103, 2017.
94. Gan, L., Lu, Z., Cao, D., Chen, Z., Effects of cetyltrimethylammonium bromide on the morphology of green synthesized Fe_3O_4 nanoparticles used to remove phosphate. *Mater. Sci. Eng. C,* 82, 41–45, 2018.
95. Guo, M., Weng, X., Wang, T., Chen, Z., Biosynthesized iron-based nanoparticles used as a heterogeneous catalyst for the removal of 2,4-dichlorophenol. *Sep. Purif. Technol.,* 175, 222–228, 2017.
96. Manquián-Cerda, K., Cruces, E., Rubio, M.A., Reyes, C., Arancibia-Miranda, N., Preparation of nanoscale iron (oxide, oxyhydroxides and zero-valent) particles derived from blueberries: Reactivity, characterization and removal mechanism of arsenate. *Ecotoxicol. Environ. Safe.,* 145, 69–77, 2017.
97. Cheera, P., Karlapudi, S., Sellola, G., Ponneri, V., A facile green synthesis of spherical Fe_3O_4 magnetic nanoparticles and their effect on degradation of methylene blue in aqueous solution. *J. Mol. Liq.,* 221, 993–998, 2016.

98. Prasad, C., Karlapudi, S., Venkateswarlu, P., Bahadur, I., Kumar, S., Green arbitrated synthesis of Fe_3O_4 magnetic nanoparticles with nanorod structure from pomegranate leaves and Congo red dye degradation studies for water treatment. *J. Mol. Liq.,* 240, 322–328, 2017.
99. Carvalho, S.S.F., Carvalho, N.M.F., Dye degradation by green heterogeneous Fenton catalysts prepared in presence of *Camellia sinensis*. *J. Environ. Manage.,* 187, 82–88, 2017.
100. Al-Ruqeishi, M.S., Mohiuddin, T., Al-Saadi, L.K., Green synthesis of iron oxide nanorods from deciduous Omani mango tree leaves for heavy oil viscosity treatment. *Arab J. Chem.,* 1–15, 2016.
101. Singh, K.K., Senapati, K.K., Sarma, K.C., Synthesis of superparamagnetic Fe_3O_4 nanoparticles coated with green tea polyphenols and their use for removal of dye pollutant from aqueous solution. *J. Environ. Chem. Eng.,* 5, 2214–2221, 2017.
102. Prasad, C., Krishna Murthy, P., Hari Krishna, R., Rao, R.S., Suneetha, V., Venkateswarlu, P., Bio-inspired green synthesis of RGO/Fe_3O_4 magnetic nanoparticles using *Murrayakoenigii* leaves extract and its application for removal of Pb(II) from aqueous solution. *J. Environ. Chem. Eng.,* 1–32, 2017.
103. Shanker, U., Jassal, V., Rani, M., Green synthesis of iron hexacyanoferrate nanoparticles: Potential candidate for the degradation of toxic PAHs. *J. Environ. Chem. Eng.,* 5, 4108–4120, 2017.
104. Jassal, V., Shanker, U., Gahlot, S., Green synthesis of some iron oxide nanoparticles and their interaction with 2-Amino, 3-Amino and 4-Aminopyridines. *Mater. Today: Proceedings*, 3, 1874–1882, 2016.
105. Sangami, S., Manu, B., Synthesis of green iron nanoparticles using laterite and their application as a Fenton-like catalyst for the degradation of herbicide Ametryn in water. *Environ. Tech. Innov*, 8, 150–163, 2017.
106. Wang, X., Wang, A., Ma, J., Fu, M., Facile green synthesis of functional nanoscale zero-valent iron and studies of its activity toward ultrasound-enhanced decolorization of cationic dyes. *Chemosphere*, 166, 80–88. 2017.
107. Gai, C., Zhang, F, Lang, Q., Liu, T., Peng, N., Liu, Z., Facile one-pot synthesis of iron nanoparticles immobilized into the porous hydrochar for catalytic decomposition of phenol. *Appl. Catal. B: Environ*, 204, 566–576, 2017.
108. Poguberović, S.S., Krčmar, D.M., Maletić, S.P., Kónya, Z., Pilipović, D.D.T., Kerkez, D.V., Rončević, S.D., Removal of As(III) and Cr(VI) from aqueous solutions using "green" zero-valent iron nanoparticles produced by oak, mulberry and cherry leaf extracts. *Ecol. Eng.,* 90, 42–49, 2016.
109. Soliemanzadeh, A., Fekri, M., Synthesis of clay-supported nanoscale zero-valent iron using green tea extract for the removal of phosphorus from aqueous solutions. *Chin. J. Chem. Eng.,* 25, 924–930, 2017.
110. Wang, T., Lin, J., Chen, Z., Megharaj, M., Naidu, R., Green synthesized iron nanoparticles by green tea and eucalyptus leaves extracts used for removal of nitrate in aqueous solution. *J. Clean Prod.,* 83, 413–419, 2014.

111. Wu, Y., Zeng, S., Wang, F., Megharaj, M., Naidu, R., Chen, Z., Heterogeneous Fenton-like oxidation of malachite green by iron-based nanoparticles synthesized by tea extract as a catalyst. *Sep. Purif. Technol.,* 154, 161–167, 2015.
112. Huang, L., Weng, X., Chen, Z., Megharaj, M., Naidu, R., Synthesis of iron-based nanoparticles using oolong tea extract for the degradation of malachite green. *Spectrochim. Acta A,* 117, 801–804, 2014.
113. Groiss, S., Selvaraj, R., Varadavenkatesan, T., Vinayagam. R., Structural characterization, antibacterial and catalytic effect of iron oxide nanoparticles synthesised using the leaf extract of *Cynometra ramiflora*. *J. Mol. Struct.,* 1128, 572–578, 2017.
114. Atarod, M., Nasrollahzadeh, M., Sajadi, S.M., Green synthesis of Pd/RGO/Fe3O4 nanocomposite using *Withania coagulans* leaf extract and its application as magnetically separable and reusable catalyst for the reduction of 4-nitrophenol. *J. Colloid Interface Sci.,* 465, 249–258, 2016.
115. Wang, T., Jin, X., Chen, Z., Megharaj, M., Naidu, R., Green synthesis of Fe nanoparticles using eucalyptus leaf extracts for treatment of eutrophic wastewater. *Sci. Total Environ.,* 466, 210–213, 2014.
116. Luo, F., Yang, D., Chen, Z., Megharaj, M., Naidu, R., Characterization of bimetallic Fe/Pd nanoparticles by grape leaf aqueous extract and identification of active biomolecules involved in the synthesis. *Sci. Total Environ.,* 562, 526–532, 2016.
117. Luo, F., Yang, D., Chen, Z., Megharaj, M., Naidu, R., One-step green synthesis of bimetallic Fe/Pd nanoparticles used to degrade Orange II. *J. Hazard Mater.,* 303, 145–153, 2016.
118. Weng, X., Guo, M., Luo, F., Chen, Z. One-step green synthesis of bimetallic Fe/Ni nanoparticles by eucalyptus leaf extract: Biomolecules identification, characterization and catalytic activity. *Chem. Eng. J.,* 308, 904–911, 2017.
119. Sathyaa, K., Saravanathamizhan, R., Baskar, G., Ultrasound assisted phytosynthesis of iron oxide nanoparticle. *Ultrason. Sonochem.,* 39, 446–451, 2017.
120. Rajiv, P., Bavadharani, B., Naveen Kumar, M., Vanathi. P., Synthesis and characterization of biogenic iron oxide nanoparticles using green chemistry approach and evaluating their biological activities. *Biocatal. Agric. Biotechnol.* 12, 45–49, 2017.
121. Kozma., G, Rónavári, A., Kónya, Z., Kukovecz, A., Environmentally benign synthesis methods of zero-valent iron nanoparticles. *ACS Sustain. Chem. Eng.,* 4, 291–297, 2016.
122. Muthukumar, H., Matheswaran, M., *Amaranthus spinosus* leaf extract mediated Feo nanoparticles. Physicochemical traits, photocatalytic and antioxidant activity. *ACS Sustain. Chem. Eng.,* 3, 3149–3156, 2015.
123. Pandian, C.J., Palanivel, R., Dhananasekaran, S., Green synthesis of nickel nanoparticles using Ocimum sanctum and their application in dye and pollutant adsorption. *Chin. J. Chem, Eng.,* 23, 1307–1315, 2015.

124. Thema, F.T., Manikandan, E., Gurib-Fakim, A., Maaza, M., Single phase Bunsenite NiO nanoparticles green synthesis by *Agathosma betulina* natural extract. *J. Alloys Compds*., 657, 655–661, 2016.
125. Chekin, F., Vahdat, S.M., Asadi, M.J., Green synthesis and characterization of cobalt oxide nanoparticles and its electrocatalytic behavior. *Russ. J. Appl. Chem.,* 89, 816–822, 2016.
126. Bibi, I., Nazar, N., Iqbal, M., Kamal, S., Nawaz, H., Nouren, S., Safa, Y., Jilani, K., Sultan, M., Ata, S., Rehman, F., Abbas, M., Green and eco-friendly synthesis of cobalt-oxide nanoparticle: Characterization and photo-catalytic activity. *Adv. Powder Technol.,* 28, 2035–2043, 2017.
127. Vasudeo, K., Pramod K., Biosynthesis of nickel nanoparticles using leaf extract of coriander. *Biotechnol. Ind. J.*, 12, 106, 2016.
128. Pavani, K.V., Kumar, N.S., Adsorption of iron and synthesis of iron nanoparticles by *Aspergillus* species kvp 12. *Am. J. Nanomater.*, 1, 24–26, 2013.
129. Mohamed, Y.M., Azzam, A.M., Amin, B.H., Safwat, N.A., Mycosynthesis of iron nanoparticles by *Alternaria alternata* and its antibacterial activity. *Afr. J. Biotechnol.,* 14, 1234–1241, 2015.
130. Sadeghia, S., Azhdaria, H., Arabib, H., Moghaddam, A.Z., Surface modified magnetic Fe_3O_4 nanoparticles as a selective sorbent for solid phase extraction of uranyl ions from water samples. *J. Hazard Mater.,* 216, 208–216, 2012.
131. Crane, R.A., Scott, T.B., Nanoscale zero-valent iron: Future prospects for an emerging water treatment technology. *J. Hazard. Mater.*, 212, 112–125, 2012.
132. Grieger, K.D., Annika, F., Hartmann, N.B., Eriksson, E., Poul, L.B., Anders, B., Environmental benefits and risks of zero-valent iron nanoparticles (nZVI) for *in situ* remediation: Risk mitigation or trade-off?. *J. Contam. Hydrol.*, 118, 165–183. 2010.
133. Reddy, A.V.B., Yusop, Z., Jaafar, J., Reddy, Y.V.M., Aris, A.B., Majid, Z.A., Talib, J., Madhavi, G., Recent progress on Fe-based nanoparticles: Synthesis, properties, characterization and environmental applications. *J. Environ. Chem. Eng.,* 4, 3537–3553, 2016.
134. Wang, Y., Zhao, H., Zhao, G., Iron-copper bimetallic nanoparticles embedded within ordered mesoporous carbon as effective and stable heterogeneous Fenton catalyst for the degradation of organic contaminants. *Appl. Catal. B*, 164, 396–406, 2015.
135. Singh, R., Misra, V., Singh, R.P., Synthesis, characterization and role of zerovalent iron nanoparticle in removal of hexavalent chromium from chromium-spiked soil. *J. Nanopart. Res.*, 13, 4063–4073, 2011.
136. Bergendahl, J.A., Thies, T.P., Fenton's oxidation of MTBE with zero-valent iron. *Water Res.*, 38, 327–334, 2004.
137. Diao, Z., Li, M., Zeng, F., Song, L., Qiu, R., Degradation pathway of malachite green in a novel dual-tank photoelectrochemical catalytic reactor. *J. Hazard. Mater.,* 260, 585–592, 2013.

138. Nidheesh, P.V., Heterogeneous Fenton catalysts for the abatement of organic pollutants from aqueous solution: A review. *RSC Adv.,* 5, 40552–40577, 2015.
139. Belachew, N., Devi, D.R., Basavaiah, K., Facile green synthesis of l-methionine capped magnetite nanoparticles for adsorption of pollutant Rhodamine B. *J. Mol. Liq*. 224, 713–720, 2016.
140. Weng, X., Huang, L., Chen, Z., Megharaj, M., Naidu, R., Synthesis of iron-based nanoparticles by green tea extract and their degradation of malachite. *Inds. Crops Prod.,* 51, 342–347, 2013.
141. Njagi, E.C., Huang, H., Stafford, L., Genuino, H., Galindo, H.M., Collins, J.B., Hoag, G.E., Suib, S.L., Biosynthesis of iron and silver nanoparticles at room temperature using aqueous sorghum bran extracts. *Langmuir,* 27, 264–271, 2011.
142. Dave, P.N., Chopda, L.V., Application of iron oxide nanomaterials for the removal of heavy metals, *J. Nanotechnol.,* 2014, 398569, 2014.
143. Liu, J.F., Zhao, Z.S., Jiang, G.B., Coating Fe_3O_4 magnetic nanoparticles with humic acid for high efficient removal of heavy metals in water. *Environ. Sci. Technol.,* 42, 6949–6954, 2008.
144. Ray, P.Z., Shipley, H.J., Inorganic nano-adsorbents for the removal of heavy metals and arsenic: A review, *RSC Adv.,* 5, 29885–29907, 2015.
145. Fu, F., Wang, Q., Removal of heavy metal ions from wastewaters: A review. *J. Environ. Manag.,* 92, 407–418, 2011.
146. Es'haghi, Z., Vafaeinezhad, F., Hooshmand, S., Green synthesis of magnetic iron nanoparticles coated by olive oil and verifying its efficiency in extraction of nickel from environmental samples via UV–vis spectrophotometry. *Process Safe. Environ. Protection,* 102, 403–409, 2016.
147. Safinejad, A., Chamjangali, M.A., Goudarzi, N., Bagherian. G., Synthesis and characterization of a new magnetic bio-adsorbent using walnut shell powder and its application in ultrasonic assisted removal of lead. *J. Environ. Chem. Eng.,* 5, 1429–1437, 2017.
148. Wen, T., Wang, J., Li, X., Huang, S., Chen, Z., Wang, S., Hayat, T., Alsaedi, A., Wang, X., Production of a generic magnetic Fe_3O_4 nanoparticles decorated tea waste composites for highly efficient sorption of Cu(II) and Zn(II). *J. Environ. Chem. Eng.,* 5, 3656–3666, 2017.
149. Mystrioti, C., Xenidis, A., Papassiopi, N., Reduction of hexavalent chromium with polyphenol-coated nano zero-valent iron: Column studies. *Desalination Water Treat.*, 56, 1162–1170, 2014.
150. Xiao, Z., Yuan, M., Yang, B., Liu, Z., Huang, J., Sun, D., Plant-mediated synthesis of highly active iron nanoparticles for Cr(VI) removal: Investigation of the leading biomolecules. *Chemosphere,* 150 ,357–364, 2016.
151. Madhavi, V., Prasad, T.N., Reddy, A.V., Ravindra Reddy, B., Madhavi, G., Application of phytogenic zerovalent iron nanoparticles in the adsorption of hexavalent chromium. *Spectrochim. Acta A,* 116, 17–25, 2013.
152. Das, J., Patra, B.S., Baliarsingh, N., Parida, K.M., Adsorption of phosphate by layered double hydroxides in aqueous solutions. *Appl. Clay Sci.,* 32, 252–260, 2006.

153. Eneji, A.E., Islam, R., An, P., Amalu, U.C., Nitrate retention and physiological adjustment of maize to soil amendment with superabsorbent polymers. *J. Clean. Prod.*, 52, 474–480, 2013.
154. Habuda-Stanic, M., Ravancic, M.E., Flanagan, A. Review on adsorption of fluoride from aqueous solution. *Materials,* 7, 6317–6366, 2014.
155. Prabhakar, R., Samadder, S.R., Jyotsana, Aquatic and terrestrial weed mediated synthesis of iron nanoparticles for possible application in wastewater remediation. *J. Clean. Prod.,* 168, 1201–1210, 2017.
156. Ali, I., Alothman, Z.A., Sanagi, M.M., Green synthesis of iron nano-impregnated adsorbent for fast removal of fluoride from water. *J. Mol. Liq.,* 211, 457–465, 2015.
157. Nodeh, H.R., Sereshti, H., Afsharian, E.Z., Nouri, N., Enhanced removal of phosphate and nitrate ions from aqueous media using nanosized lanthanum hydrous doped on magnetic graphene nanocomposite. *J. Environ. Manag.*, 197 265–274, 2017.
158. Aragay, G., Pino, F., Merkoçi, A., Nanomaterials for sensing and destroying pesticides. *Chem. Rev.,* 112, 5317–533, 2012.
159. Meister, R.T. (Ed.), *Farm Chemicals Handbook*, Meister Publishing Company: Willoughby, OH, 1992.
160. Ali, I., AL-Othman, Z.A., Alwarthan A., Green synthesis of functionalized iron nano particles and molecular liquid phase adsorption of ametryn from water. *J. Mol. Liq.,* 221, 1168–1174, 2016.
161. Lian, L., Cao, X., Wu, Y., Sun, D., Lou, D., A green synthesis of magnetic bentonite material and its application for removal of microcystin-LR in water. *Appl. Surf. Sci.,* 289, 245–251, 2014.
162. Senthil, M., Ramesh, C., Biogenic synthesis of Fe_3O_4 nanoparticles using *Tridax procumbens* leaf extract and its antibacterial activity on *Pseudomonas aeruginosa*. *Dig. J. Nanomater. Biostruct.*, 7, 1655–1660, 2012.
163. Gleick, P.H., Cohen, M.J., *The World's Water 2008–2009: The Biennial Report on Freshwater Resources*, pp. 79–100, Island Press, 2009.
164. Patra, J.K., Baek., K-H., Green biosynthesis of magnetic iron oxide (Fe_3O_4) nanoparticles using the aqueous extracts of food processing wastes under photo-catalyzed condition and investigation of their antimicrobial and antioxidant activity. *J. Photochem. Photobiol. B,* 173, 291–300, 2017.
165. Irshad, R., Tahir, K., Li, B., Ahmad, Siddiqui, A.R., Nazir, S., Antibacterial activity of biochemically capped iron oxide nanoparticles: A view towards green chemistry. *J. Photochem. Photobiol. B,* 170, 241–246, 2017.
166. Helen, S.M., Rani, M.H.E., Characterization and antimicrobial study of nickel nanoparticles synthesized from *Dioscorea* (elephant yam) by green route. *Int. J. Sci. Res.*, 4, 216–219, 2015.
167. Elango, G., Roopan, S.M., Dhamodaran, K.I., Elumalai, K., Al-Dhabi, N.A., Arasu, M.V., Spectroscopic investigation of biosynthesized nickel nanoparticles and its larvicidal, pesticidal activities. *J. Photochem. Photobiol. B,* 162, 162–167, 2016.

168. Chiou, J.R., Lai, B.H., Hsu, K.C., Chen, DH., One-pot green synthesis of silver/iron oxide composite nanoparticles for 4-nitrophenol reduction. *J. Hazard. Mater.,* 248–249, 394–400, 2013.
169. Stan, M., Lung, I., Soran, M.-L., Leostean, C., Popa, A., Stefan, M., Lazar, M.D., Opris, O., Silipas, T.-D, Porav, M.A.S., Removal of antibiotics from aqueous solutions by green synthesized magnetite nanoparticles with selected agro-waste extracts. *Process Saf. Environ. Prot.,* 107, 357–372, 2017.
170. Markides, H., Rotherham, M., El Haj, A.J., Biocompatibility and toxicity of magnetic nanoparticles in regenerative medicine. *J. Nanomat*., 1, 1–13, 2012.
171. Sharifi, S., Behzadi, S., Laurent, S., Forrest, M.L., Stroeve, P., Mahmoudi, M., Toxicity of nanomaterials. *Chem. Soc. Rev*., 41, 2323–2343, 2012.
172. Yang, W.J., Lee, J.H., Hong, S.C., Lee, J., Lee, J., Han, D.-W., Difference between toxicities of iron oxide magnetic nanoparticles with various surface-functional groups against human normal fibroblasts and fibrosarcoma cells. *Materials,* 6, 4689–4706. 2013.
173. Brar, S.K., Verma, M., Tyagi, R.D., Surampalli, R.Y., Engineered nanoparticles in wastewater and wastewater sludge – Evidence and impacts. *Waste Manag.,* 30, 504–520, 2010.

10

Green Synthesis of Metallic Nanoparticles Using Biopolymers and Plant Extracts

Ibrahim M. El-Sherbiny[1]* and Ehab Salih[2]

[1]*Center for Materials Science, Zewail City of Science and Technology, 6th of October City, Giza, Egypt*
[2]*Department of Math, Statistics and Physics, College of Arts and Sciences, Qatar University, Doha, Qatar*

Abstract

Over the last few decades, the metal nanoparticles (MNPs) have been extensively studied because of their attractive optical and electronic properties related to the quantum size effect in addition to their promising applications in a wide range of fields such as optics, catalysis, nanostructures fabrication, chemical/biochemical sensing, and medicine. Therefore, the synthesis of MNPs is an expanding research area. There are two main approaches for the preparation of MNPs, top-down and bottom-up techniques. The top-down methods depend mainly on the production of isolated atoms from the bulk materials using a variety of distribution techniques. Milling or attrition, repeated quenching and photolithography are some of the approaches that are usually involved in the top-down strategies. On the other hand, the bottom-up techniques start with metal salt precursor (dissolved in a solvent) that is reduced in a chemical reaction, followed by formation of the MNPs through nucleation and growth. With the bottom-up approaches, the use of capping agents is of great importance to control the particle size, shape, and stability for the resulting NPs. Depending on the type of capping agent, the bottom-up approach could be classified into either green or non-green. Green approaches use environmentally friendly agents such as sugars and plant extracts to form and stabilize MNPs. This chapter summarizes the various green approaches for synthesis

**Corresponding author*: ielsherbiny@zewailcity.edu.eg

Suvardhan Kanchi and Shakeel Ahmed (eds.) Green Metal Nanoparticles, (293–319)
© 2018 Scrivener Publishing LLC

of MNPs using biopolymers, and plant extracts which qualify as a green chemistry concept and also retain their biological properties.

Keywords: Biopolymers, green synthesis, top-down and bottom-up approach, plant extracts, metal, nanoparticle

10.1 Introduction

The American physicist Richard Feynman (1918–1988) was the first to hint about what we now know as "Nanoscience" [1]. Nanoscience is the field of science which focuses particularly on studying the characteristics and synthesis of nanomaterials (any object with at least one dimension in the range from 1 to 100 nm) of variable sizes, shapes and chemical compositions.

Nanoscience is an extremely interesting research field for several reasons. For instance, quantum mechanics must be applied upon studying nanoscience since many of the classical laws are not valid anymore at the nanometric regime [2]. Besides, some of the metastable phases can only be observed in materials with very small sizes [3]. Finally, in the last few decades, scientists in a wide spectrum of technology areas have directed their attention towards fabricating smaller components at the nano level for many application such as electronics, smart materials-related applications, health-related application as well as in the field of renewable energy [1].

The importance of nano-objects comes from attaining a very high surface area to volume ratio. For example, when a solid material becomes very small, its specific surface area increases while maintaining its volume constant, which leads to a significant increase in the reactivity of the surface and quantum-related effects. Consequently, both chemical and physical characteristics of a material in the nanoscale range are totally different from those of the same material in its larger bulk form. It is also worth mentioning that the material particles in the nanoscale range can be classified based on their size, and may or may not exhibit size-related characteristics that differ remarkably from those observed in bulk materials [4].

If we are dealing, for example, with a spherical particle, the surface area to volume ratio can be given by the following formula [5]:

$$\frac{s}{v} = \frac{4\pi r^2}{4/3\,\pi r^3} = \frac{3}{r} \tag{10.1}$$

So, in a simple form, the surface area to volume ratio is given by $\left(\frac{s}{v} \alpha \frac{1}{r}\right)$, where S is the surface area and V is the volume. As indicated in the

relationship, decreasing the particle radius increases the surface area to volume ratio. Upon moving down to the nanometer scale, a highly remarkable increase in the surface area will be observed. For instance, 1 cm^3 of 1 nm particles would have an active surface area around 100 m^2 [6]. Consequently, in the applications where the surface area plays a pivotal role, such as catalysis, thermal conducting, and controlled drug delivery, the nanomaterials can offer several benefits as compared with the current technologies.

10.2 Types of Nanomaterials

There are various categories of nanomaterials depending on the ingredients used in their production and the synthesis approach. These include, carbon-based, polymer-based, lipid-based, metal-based, metal oxide-based, and magnetic nanomaterials. The following section will refer to some of these categories with an emphasis on the metal-based nanomaterials.

10.2.1 Carbon-Based Nanomaterials

Carbon-based nanomaterials (CNMs), the nanomaterials made mainly of carbon, are one of the most broadly studied nanomaterials in the last couple of decades [7–13]. The importance of CNMs comes from their remarkable electronic, magnetic and optical properties, as well as their chemical versatility, biocompatibility and their desirable performance as a chemically robust platform [14]. These materials can be classified according to the number of their dimensions into; (i) zero-dimensional (0-D) in the form of nanoparticles such as fullerenes, (ii) one-dimensional (1-D) in the form of nanowires or nanotubes such as carbon nanotubes, (iii) two-dimensional (2-D) in the form of flakes or layers such as graphene and graphene oxide, and (iv) three-dimensional (3-D) such as nanocomposites [14, 15].

10.2.2 Polymer-Based Nanomaterials

The development of polymeric-based nanomaterials (PNMs), nanomaterials made of mainly polymers, has gained considerable interest over the past few decades. This may be due to their increased surface area to volume ratio, leading to the attainment of various unique properties that makes them desirable in different applications such as electronics, photonics, conducting materials, sensors, medicine, biotechnology, pollution control and environmental technology [16–24]. The PNMs can be fabricated via two main approaches; the first one through using monomers as initials (chemical polymerization methods), and the second

approach involves the use of preformed polymers as initials (physical methods) [25]. Conventional emulsion polymerization [26], surfactant-free emulsion polymerization [27], mini-emulsion polymerization [28], micro-emulsion polymerization [29], interfacial polymerization [30], and free radical polymerization [29] are the most common examples of the chemical polymerization methods. While, spray drying [31], dialysis [32], solvent evaporation [33], emulsion solvent diffusion [34], nanoprecipitation [35], fast evaporation [36], salting out [37], freeze-drying [38], freeze-extraction [39], spreading evaporation [40], and supercritical fluid technology [41] are the common examples of the physical synthesis approach.

10.2.3 Metal-Based Nanomaterials

For many years, the metal-based nanomaterials (MNMs), nanomaterials made of mainly metals, have been extensively studied because of their attractive optical and electronic properties related to the quantum size effect, in addition to their promising applications in a wide-spectrum of fields ranging from optics and catalysis to chemical/biochemical sensing [42]. Among the MNMs, noble nanoparticles (NPs), such as silver nanoparticles (AgNPs), gold nanoparticles (AuNPs), platinum nanoparticles (PtNPs), and palladium nanoparticles (PdNPs), are well known to have important applications in the fields of electronics, magnetics, optoelectronics, and information storage [43, 44]. The remarkable characteristics of these noble MNPs can be attributed to their size, shape, composition, crystallinity, and structure [45]. In the following sections, a summary of the various green approaches used for synthesis of MNPs will be provided. These green synthesis approaches include the use of biopolymers and plant extracts, which qualify as a green chemistry concept and also retain the biological properties of the developed MNPs.

10.2.3.1 Silver Nanoparticles (AgNPs)

Of the noble MNPs, the AgNPs are the most widely recognized for their applications in different areas such as photonics [46], micro-electronics [47], photocatalysis [48], medicine, and lithography [49]. For instance, the common use of AgNPs in medicine can be credited to their powerful antimicrobial activity against a wide range of pathogenic microorganisms [50]. Various physical and chemical techniques, including laser ablation [51], lithography [52], and photochemical reduction [53], are used efficiently for the production of significant amounts of AgNPs. Nevertheless,

these techniques remain comparatively expensive and sometimes involve the use of some hazardous moieties [54]. Consequently, the development of a green and effective method to develop AgNPs is of great importance.

10.2.3.2 Gold Nanoparticles (AuNPs)

Because of their potential applications in various fields, such as catalysis, non-linear optics, nanoelectronics, gene expression and disease diagnosis, the AuNPs are considered to be the most attractive member of noble MNPs [55]. The widespread use of AuNPs in many biomedical applications has drawn considerable interest towards the urgent necessity for a synthesis technique of AuNPs without using any hazardous chemicals.

10.2.3.3 Platinum Nanoparticles (PtNPs)

Recently, the PtNPs have been widely used for the oxidation and hydrogenation processes in the petrochemical industry [56]. This is owing to their high surface area and many other characteristics, making synthesis of PtNPs for catalytic applications, for instance, of great interest [56]. Consequently, there is a growing need to develop processes for fabricating PtNPs that do not use toxic chemicals and use other eco-friendly materials.

10.2.3.4 Palladium Nanoparticles (PdNPs)

The catalytic properties and affinity for hydrogen of PdNPs are attracting remarkable interest. PdNPs are used in different unique applications, particularly sensors and catalyst active membranes [57]. PdNPs have been synthesized by different wet chemical approaches, including chemical reduction, electrochemical, and polyol methods [58, 59].

10.3 Synthesis Approaches of Metal Nanoparticles

In general, the applied approaches for MNPs synthesis can be classified into two main approaches; top-down and bottom-up. The top-down approaches depend particularly on the production of isolated atoms from the bulk materials using a variety of distribution techniques. Milling or attrition, repeated quenching and photolithography are some of the basic approaches that usually are involved in the top-down fabrication strategies [60]. On the other hand, the bottom-up approaches start with metal salt precursor (dissolved in a solvent) that is reduced in a chemical reaction

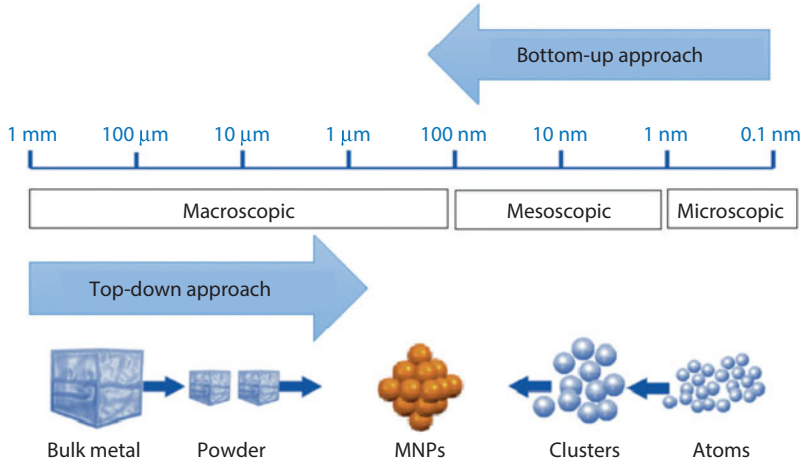


Figure 10.1 A schematic illustration of both top-down and bottom-up approaches for fabrication/synthesis of MNPs.

and the NPs are formed through nucleation process followed by a growth of the formed clusters [61]. In the bottom-up approaches, the use of appropriate capping agent(s) is of great importance to control the particle size, shape and stability of the resulting MNPs [62]. Figure 10.1 presents a schematic illustration for the top-down versus bottom-up techniques.

10.3.1 Top-Down Approaches

Cutting, grinding and etching of a bulk piece of material are some of the top-down approaches for the production of MNPs (Figure 10.2). Of note, the top-down approaches are the methods of choice for the synthesis of highly complex structures and for the mass production of MNPs. The main disadvantage of these top-down approaches is the imperfection of the surface structure, which can remarkably affect the properties of the resulting MNPs [63]. A good strategy to resolve this issue is via bottom-up approaches.

10.3.2 Bottom-Up Approaches

The bottom-up approaches have been utilized particularly to evade the disadvantages of the top-down approaches via producing homogeneous and stable MNP suspensions with the ability to control the particle size, shape and functionalization of MNPs with capping agents that make it convenient for various applications. Many techniques are involved in bottom-up

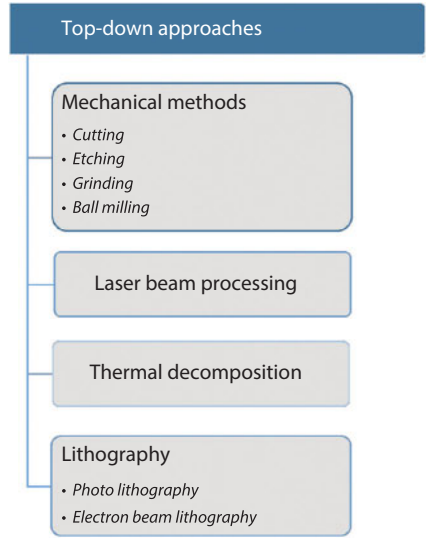


Figure 10.2 A classification of some of the common top-down approaches used for MNPs synthesis.

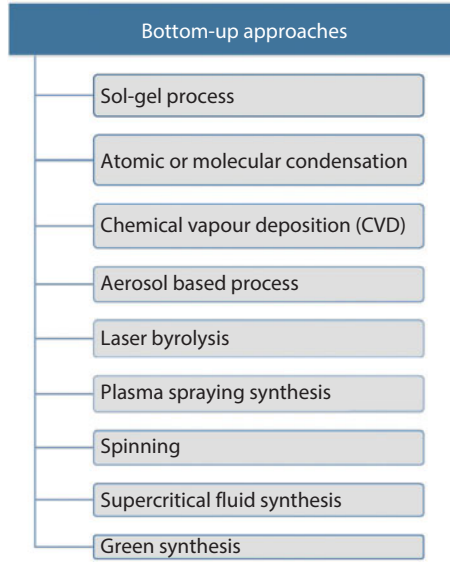


Figure 10.3 Some of the bottom-up approaches used for MNPs synthesis.

approaches (Figure 10.3). For instance, to synthesize MNPs by using, for example, the wet chemistry techniques, the reaction mixture must contain three important reactants, metal salt precursor, a reducing agent, and capping agent(s) [64]. The chemical nature of the capping agent, the molar

ratio of that agent to the metal salt, and the redox potential of the reducing agent are some of the reaction parameters that control the morphology and surface chemistry of the resulting MNPs [64]. However, the concentration of the capping agent perhaps has the highest influence, particularly on the size. Sometimes, the capping agents can also be used as reducing agent for the metal salt precursor [61]. The mass production of MNPs is a problem in the bottom-up approaches because not all methods can be used for the massive production of enough quantities of MNPs for industrial use [61]. Another problem with the wet chemical methods is the presence of residual chemicals in the MNPs suspension at the end of the processes. These residual chemicals may affect their use in many applications such as in medicine, catalysis, microelectronics and sensing devices. The residual chemicals mainly include metallic ions since the reduction efficiency doesn't reach 100% [65]. This problem also has been resolved via green approaches, in which eco-friendly materials were used instead of toxic chemicals as reducing and capping agents to synthesis the MNPs, as will be described in the next section.

10.4 Green Synthesis of MNPs

Synthesis methods of MNPs can also be classified into eco-friendly (green) and non-green methods depending on the nature of reactants. The green methods overcome the disadvantages of the wet chemical methods by using environmentally friendly agents, such as biopolymers and plant extracts, to form and stabilize MNPs [66]. Any green synthesis method should involve the minimum use of unsafe products and maximize the use of environmentally benign, nontoxic chemicals [66]. Many methods can be used in the green synthesis of MNPs, as indicated in Figure 10.4. The next section highlights the various green approaches applied for synthesis of MNPs using biopolymers and plant extracts, which qualify as a green chemistry concept and also retain their biological properties.

10.4.1 Green Synthesis of MNPs Using Biopolymers

Nowadays, a wide range of naturally occurring polymers derived from renewable resources, such as cellulose and starch, are available for various applications. There are many benefits from using naturally occurring polymers in applications such as the enhancement of the environmental compatibility and the biodegradability. Besides, the use of polymers derived from renewable resources provides the means to extend nonrenewable

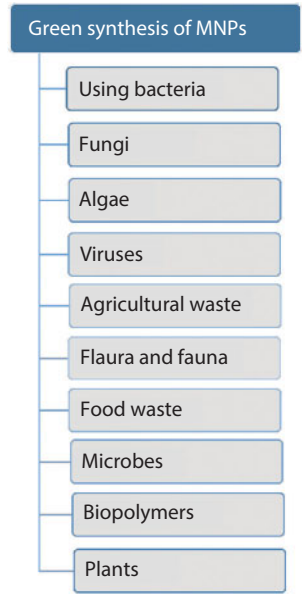


Figure 10.4 Some of the eco-friendly (green) methods used in the preparation of MNPs.

petrochemical supplies [67]. Figure 10.5 reveals some of the known naturally occurring biopolymers. Some of these biopolymers have been reported for use in the green synthesis of MNPs. These biopolymers can be used either as a stabilizer for the MNPs or as a reducing agent, while some of them can be used for both functions. Besides, these biopolymers can be used either in the ordinary way (dissolved) or in the form of polymeric nanostructures or NPs as a template for the efficient synthesis of MNPs.

10.4.1.1 Using Biopolymers in the Ordinary Way

In the past decades, a significant body of research has focused on the preparation and characterization of MNPs using biopolymers due to their remarkable characteristics such as nontoxicity, biodegradability and biocompatibility. Chitosan, for example, was used for the preparation of AgNPs [68]. In this study, the chitosan was dissolved in a very low concentration of acetic acid and used in the ordinary way to synthesis AgNPs. The chitosan was used in this study as both reducing and capping agent. The prepared AgNPs reflected a significant enhancement in their antibacterial activity against *Bacillus thuringiensis* and *Pseudomonas aeruginosa* bacteria as compared to the control, and the antibacterial activity was found to increase with increasing the concentration of the

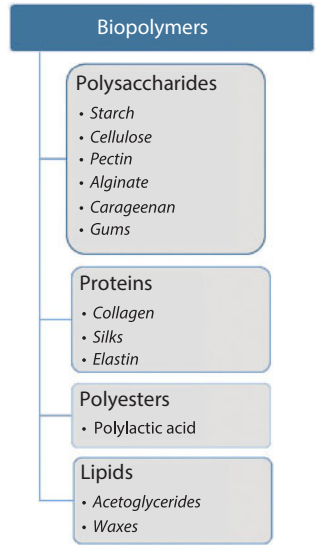


Figure 10.5 Classifications of some types of biopolymers [67].

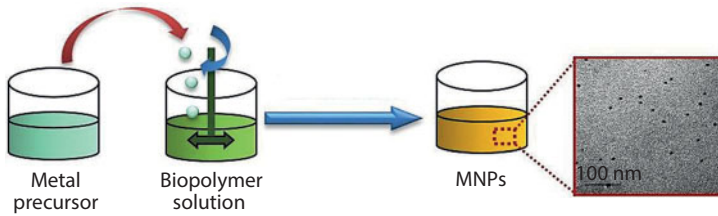


Figure 10.6 Schematic illustration of the green synthesis of MNPs using biopolymers [71].

NPs [68]. In another study, carboxymethylated-curdlan and fucoidan were used in a green approach to fabricate AgNPs [69]. The carboxymethylated-curdlan and fucoidan were used as both reducing and stabilizing agents. The results demonstrated that the size of prepared NPs can be controlled by using different concentrations of biopolymers or metal precursor [69]. *Gum kondagogu* has also been used in a facile and eco-friendly method to synthesize AgNPs from silver nitrate, as a reducing and stabilizing agent [70]. The developed NPs used in this way showed significant antibacterial action on various bacteria. The general schematic shown in Figure 10.6 demonstrates the green synthesis of MNPs using biopolymers.

10.4.1.2 Using Biopolymers in the Form of NPs

A new era has begun in the preparation of MNPs using biopolymers. Instead of using biopolymers in the ordinary way, researchers first develop these biopolymers as nanostructures or NPs, followed by their use as a template for the preparation of hybrid MNPs. Figure 10.7 shows a schematic illustration of this process. For instance, cellulose nanocrystals (CNC) were used as a novel template for the synthesis of MNPs using a green method [72]. To increase the NPs stability, a cationic surfactant, cetyl trimethyl ammonium bromide (CTAB), was used. Ag, Au, and Pt NPs were successfully fabricated on CNCs. The results demonstrated that the NPs concentration and size were controlled by varying the concentration of CTAB, the pH of the salt solution, and the reduction time [72]. In another study, Ag and Au NPs have been synthesized using calcium alginate gel beads using a green photochemical approach [73]. The gel was used as a reducing agent as well as a stabilizing agent. The results illustrated that the developed NPs were very efficient, stable, easy to prepare, eco-friendly, cost-effective, and have the potential for industrial applications [73]. In this regard, in one of our recent studies chitosan (Cs) was used as a nano-core for the fabrication of new core-shell amino-terminated hyperbranched Cs NPs (HBCs-NH_2 NPs) [74]. The developed HBCs-NH_2 NPs were then characterized and used as a platform for the

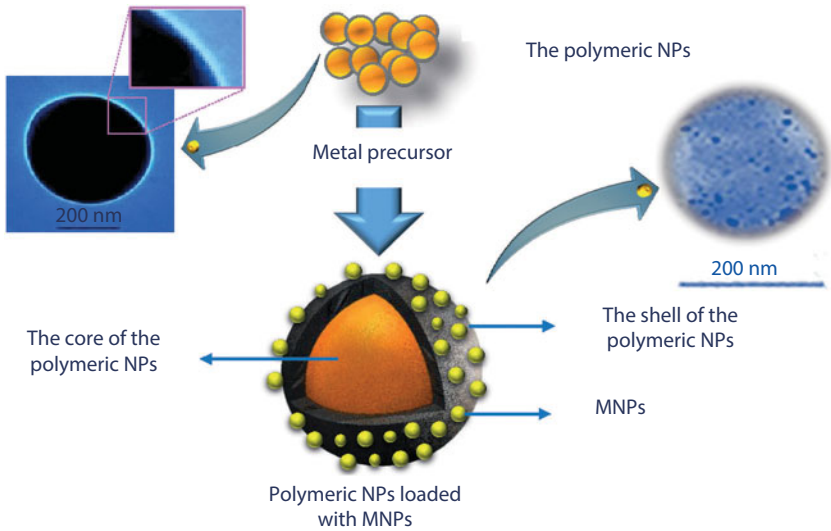


Figure 10.7 A schematic diagram of the green synthesis of MNPs using polymeric NPs [75].

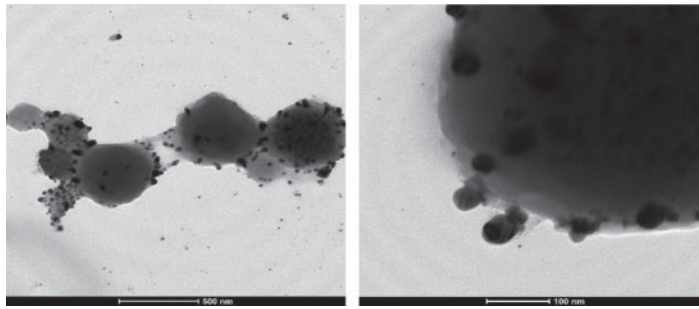


Figure 10.8 TEM images of the developed HBCs NPs-AgNPs [74].

controlled synthesis of AgNPs on their surfaces due to their uniform spherical morphology and the large number of terminal amino groups. The resulting (HBCs-NH_2) NPs-AgNPs were then used as an optical sensor for the detection of ammonia content in solutions based on the change in the SPR band intensity and peak position. The results illustrated that the AgNPs were formed mainly on the surface of the (HBCs-NH_2 NPs), as indicated in Figure 10.8. The results also showed that the developed NPs had great potential as optical sensor for efficient detection of the ammonia concentration in solutions [74].

10.4.2 Green Synthesis of MNPs Using Herbal Plant Extracts

Since ancient times, plants and their derivatives have been used in a variety of medical applications. A huge number of potential plant species have been used in recent years in nanotechnology to create the next generation of nanopharmaceuticals. The biological molecules, such as phytochemicals, present in these plants are well known to prevent diseases by inhibiting microorganisms [76]. These biological molecules are the reason for minimizing the use of toxic chemicals. The widespread use of plant products in a wide spectrum of areas, especially in medical applications, increases the demand for "green" synthesis methods in nanotechnology. The green synthesis of MNPs by using plant extracts as reducing and capping agents has been extensively studied in the last few years. The plant extracts are known to be rich in biological molecules such as enzymes, proteins, amino acids, polysaccharides, flavonoids, and vitamins, which are environmentally benign [76]. These molecules play the main role in reducing and stabilizing the MNPs. Figure 10.9 shows a schematic illustration of the green synthesis of MNPs using plant extracts. In the process of fabricating MNPs using plant extracts, the extract is simply mixed with

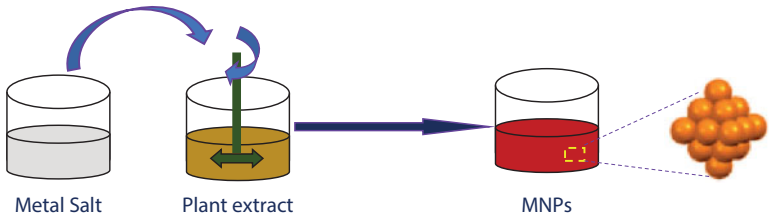


Figure 10.9 Schematic illustration of the green synthesis of MNPs using plant extracts.

the metal salt precursor at room temperature and sometimes at high temperature for a few minutes.

10.4.2.1 Green Synthesis of AgNPs

In the past decade, numerous plants have been used for the green synthesis of AgNPs. The extracts were used in these studies as both reducing and capping agents with the aid of the biological molecules present in them. These phytomolecules are responsible for the reduction of the Ag ions to form Ag atoms which then produce AgNPs. For instance, *Curcuma longa* tuber powder and extract have been used in the synthesis of AgNPs through a facile and green method. The plant was used as a reducing and capping agent based on its water-soluble organics. The results showed that the prepared AgNPs were quasi-spherical, triangular and small rod-shaped. The results also demonstrated that the developed AgNPs reflected good antibacterial activity [77]. In another study, the sulfated polysaccharides isolated from marine red algae (*Porphyra vietnamensis*) were used in a one-pot green route to synthesize AgNPs. The results showed that the AgNPs were successfully formed with an average size of 13 ± 3 nm. The results also demonstrated that the developed AgNPs showed good antibacterial activity against both Gram-positive and Gram-negative bacteria. However, the synthesized AgNPs revealed stronger antibacterial activity against Gram-negative bacteria than Gram-positive bacteria [78]. In this regard, in one of our recent studies the green synthesis of densely dispersed and stable AgNPs using myrrh extract as green reducing and stabilizing agent was investigated. The AgNPs were formed successfully with diameters in the range of 5–100 nm. The results revealed that the developed NPs showed significant antibacterial activity against *Bacillus thuringiensis* and *Pseudomonas aeruginosa* bacteria as compared to that of myrrh extract. The antibacterial activity increased with increasing the AgNP concentration [79]. Table 10.1 lists some of the plants that have been used to synthesize AgNPs by different researchers along with the shape and size of the developed NPs.

Table 10.1 Green synthesis of AgNPs using plant extracts studied by different researchers [99].

Plants	Shape of AgNPs	Size (nm)	Ref.
Cocos nucifera	Spherical	22	[80]
Pistacia atlantica	Spherical	10–50	[81]
Boerhaavia diffusa	Spherical	25	[82]
Tribulus terrestris	Spherical	16–28	[83]
Eclipta prostrata	Triangular, pentagonal, hexagonal	35–60	[84]
Aloe vera	Spherical, triangular	50–350	[85]
Alternanthera dentata	Spherical	50–100	[86]
Myrrh	Spherical	10–100	[79]
Premna herbacea	Spherical	10–30	[87]
Vitex negundo	Spherical & fcc	5–30	[88]
Centella asiatica	Spherical	30–50	[89]
Rumex dentatus	Spherical	5–30	[90]
Ziziphora tenuior	Spherical	8–40	[91]
Calotropis procera	Spherical	19–45	[92]
Datura metel	Quasilinear superstructures	16–40	[93]
Acalypha indica	Spherical	20–30	[94]
Allium sativum	Spherical	4–22	[95]
Memecylon edule	Triangular, circular, hexagonal	20–50	[96]
Tea leaf extract	Spherical	20–90	[97]
Nelumbo nucifera	Spherical, triangular	25–80	[98]

10.4.2.2 Green Synthesis of AuNPs

In this approach, the synthesis of AuNPs using plant extracts can be done within minutes. The extract is simply mixed with a solution of the metal salt, such as $HAuCl_4$, at room temperature. The role of the extract is to reduce the Au ions into atoms and then produce AuNPs. The plants in this approach were used to stabilize the AuNPs as well. In one of the studies in this regard, AuNPs have been prepared using the aqueous extract of rose petals in a rapid and green route. The rate of the reaction was relatively high and was completed within 5 minutes. The results demonstrated that the AuNPs were successfully formed with different shapes such as spherical, triangular and hexagonal. The average particle size was found to be 10 nm. The results also revealed that the AuNPs were functionalized with

biomolecules that have primary amine group (–NH_2), carbonyl group, –OH groups and other stabilizing functional groups present in the aqueous extract of rose petals [100]. In another study, the synthesis of AuNPs using seed aqueous extract of *Abelmoschus esculentus* was described. The results demonstrated that OH functional group present in the extracts played a vital role in the AuNPs synthesis. The prepared NPs in this article were found to be spherical with a narrow size range of 45–75 nm. The antifungal activity of AuNPs was tested against different types of fungi using standard well diffusion method. The end results suggested that the synthesized AuNPs act as an effective antifungal agent [101]. Table 10.2 lists some of the other plants used for the synthesis of AuNPs by different researchers along with the shape and size of the developed NPs.

Table 10.2 Green synthesis of AuNPs using plants extracts.

Plants	Shape of AuNPs	Size (nm)	Ref.
Cymbopogon sp.	Spherical, triangular	200–500	[102]
Dioscorea bulbifer	Spherical	11–30	[103]
Emblica officinalis	Polyhedral	15–25	[104]
Tamarindus indica	Triangular	20–40	[105]
Cinnamomum camphora	Spherical, triangular	55–80	[106]
Cymbopogon flexuosus	Triangular	–	[107]
Cinnamomum zeylanicum	Spherical	25	[108]
Sesbania	Spherical	6–20	[109]
Aloe vera	Triangular, spherical	–	[85]
Pelargonium graveolens	Spherical rods, flat, sheets and triangular	21–70	[110]
Salvia officinalis	Spherical, triangular, truncated triangles, pentagons and hexagons.	4–72	[111]
Lippia citriodora	Spherical, triangular, truncated triangles, pentagons and hexagons	2.6–50	[111]
Pelargonium graveolens	Spherical, triangular, truncated triangles, pentagons and hexagons.	6–78	[111]
Punica granatum	Spherical, triangular, truncated triangles, pentagons and hexagons.	34–312	[111]

10.4.2.3 Green Synthesis of Pt NPs

To synthesize the PtNPs using plant extracts, the extract is simply mixed with a solution of the metal salt such as Na_2PtCl_4, and $H_2PtCl_6.6H_2O$. The plants in this route are used as reducing and capping agents. For instance, the PtNPs were prepared using the leaf extract of *Diospyros kaki* as a reducing agent in an eco-friendly extracellular synthesis route from an aqueous $H_2PtCl_6.6H_2O$ solution. The results demonstrated that greater than 90% of Pt ions were successfully converted to PtNPs with a reaction temperature of 95 °C and a leaf broth concentration of > 10%. The average particle size was found to be between 2 and 12 nm, depending on the reaction temperature, concentrations of the leaf broth and $PtCl_6^{2-}$. The end results suggested that the synthesis process of the developed PtNPs using *Diopyros kaki* is not an enzyme-mediated process [112]. In another example, the PtNPs were synthesized by reducing the Pt ions in the aqueous Na_2PtCl_4 with *Cacumen Platycladi* extract in a biological route. The results showed that the PtNPs were successfully prepared with average diameters of 2.4 ± 0.8 nm. The results also demonstrated that the bioreduction of Pt ions was attributed to the reducing sugars and flavonoids present in the plant extract. In conclusion, the bioreduction mechanism of Pt ions was described by studying the changes in concentration of the reducing sugars, flavonoids and proteins in the plant extract, leading to a good insight into the formation mechanism of such biosynthesized PtNPs [113]. Table 10.3 summarizes some other plants used for the synthesis of PtNPs by different researchers along with the resulting shape and size of the developed NPs.

10.4.2.4 Green Synthesis of Pd NPs

In the preparation technique of PdNPs using plant extracts, the extract has to be mixed with a solution of metal salt such as $PdCl_2$ or $Pd(OAc)_2$.

Table 10.3 Green synthesis of PtNPs using plant extracts as studied by different researchers.

Plants	Shape of PtNPs	Size (nm)	Ref.
Ocimum sanctum	Spherical	23	[114]
Azadirachta indica	Spherical	5–50	[115]
Fumariae herba	Hexagonal, pentagonal	10–30	[116]
Anacardium occidentale	Irregular rod-shaped	–	[117]
Taraxacum laevigatum	Spherical	2–7	[118]
Water hyacinth	Spherical	3.74	[119]
Punica granatum peel	Spherical	16–23	[120]

The phytochemicals in the plant extracts are responsible for reducing the Pd ions into atoms and then producing PdNPs. The plants also have a role in the stabilization of the prepared NPs. The aqueous extract of *Eclipta prostrata* leaf is one of the plant extracts that have been used in recent years to synthesize PdNPs in a green route. The PdNPs were prepared in that study by mixing the aqueous solution of palladium acetate [$Pd(OAc)_2$] with the aqueous extract. The results reflected that the PdNPs were successfully prepared with an average size of 63 ± 1.4 nm. The cytotoxicity of the aqueous leaf extract of *Eclipta prostrata*, palladium acetate, and PdNPs was evaluated against Hep-G2 cell lines [121]. In another study, *Curcuma longa* tuber extract was used to prepare PdNPs in the presence of $PdCl_2$. Some parameters such as the effect of extract dosage, pH and temperature on the preparation of PdNPs were investigated, which did not remarkably change the size and shape of the developed PdNPs. The results showed that the PdNPs were well formed with an average size ranging between 10–15 nm. The results also demonstrated the important role of the *Curcuma longa* in the reduction process of more than 60% of Pd ions into zero-valent form and then to PdNPs. In the end, they came to the conclusion that the polyphenols present in the extract play an important role in the PdNPs synthesis through the reduction of Pd ions [122]. Table 10.4

Table 10.4 Green synthesis of PdNPs using plant extracts as studied by different researchers.

Plants	Shape of PdNPs	Size (nm)	Ref.
Terminalia chebula	Triangular, pentagonal	100	[123]
Delonix regia	–	2–4	[124]
Cinnamomum zeylanicum	Spherical	15–20	[125]
Stachys lavandulifolia	Spherical	5–7	[126]
Euphorbia thymifolia	Spherical	20–30	[127]
Banana peel	Dendrites composed of microcubes arranged in a specific array	50	[128]
Piper betle	Spherical	4±1	[129]
Euphorbia granulate	Spherical	25–35	[130]
Annona squamosa	Spherical	80±5	[131]
Soybean	Spherical	15	[132]
Cinnamomum camphora	Spherical	3.2–6	[133]
Hippophae rhamnoides Linn	Spherical	2.5–14	[134]
Catharanthus roseus	Spherical	38	[135]
Solanum trilobatum	Spherical	60–70	[136]

lists some other plants used to synthesize PdNPs by different researchers along with the shape and size of the developed NPs.

10.5 Conclusion

Different techniques have been widely used in recent decades for the synthesis of MNPs. Some of these techniques involve the use of hazardous chemical moieties in the synthesis process. The resulting MNPs showed great importance in a variety of applications ranging from electronics, chemical sensing, photocatalysis, and lithography. The MNPs also showed outstanding properties in medical applications, and for this reason the application of an eco-friendly (green) route for the preparation of MNPs is of great importance to researchers in this field. In this chapter, we summarized the various approaches used for the synthesis of MNPs along with discussing the advantages and disadvantages of each method. Finally, we explicitly dealt with the green synthesis of MNPs, especially the noble metals by using, in particular, biopolymers and plant extracts.

References

1. Hornyak, G.L., Dutta, J., Tibbals, H.F., Rao, A., *Introduction to Nanoscience*, CRC press 2008.
2. Trave, A., Buda, F., Fasolino, A., Band-gap engineering by iii-v infill in sodalite. *Phys. Rev. Lett.*, 77, 5405–5408, 1996.
3. Ricolleau, C., Audinet, L., Gandais, M., Gacoin, T., Structural transformations in ii-vi semiconductor nanocrystals. *Eur. Phys. J. D*, 9, 565–570, 1999.
4. Buzea, C., Pacheco, I.I., Robbie, K., Nanomaterials and nanoparticles: Sources and toxicity. *Biointerphases*, 2, 17–71, 2007.
5. Dadgostar, N., Investigations on colloidal synthesis of copper nanoparticles in a two-phase liquid-liquid system, MS Thesis, University of Waterloo, 2008.
6. Ichinose, N., Ozaki, Y., Kashu, S., *Superfine Particle Technology*. Springer Science & Business Media, 2012.
7. Dresselhaus, M.S., Terrones, M., Carbon-based nanomaterials from a historical perspective. *Proc. IEEE*, 101, 1522–1535, 2013.
8. Kroto, H.W., Heath, J.R., O'Brien, S.C., Curl, R.F., Smalley, R.E., C60: Buckminsterfullerene, *Nature*, 318, 162–167, 1985.
9. Ajayan, P., Ebbesen, T., Ichihashi, T., Iijima, S., Tanigaki, K., Hiura, H., Opening carbon nanotubes with oxygen and implications for filling, *Nature*, 362, 522–527, 1993.
10. Iijima, S., Ichihashi, T., Single-shell carbon nanotubes of 1-nm diameter. *Nature*, 363, 603–608, 1993.

11. Kuznetsov, V.L., Chuvilin, A.L., Butenko, Y.V., Mal'kov, I.Y., Titov, V.M., Onion-like carbon from ultra-disperse diamond. *Chem. Phys. Lett.*, 222, 343–348, 1994.
12. Iijima, S., Yudasaka, M., Yamada, R., Bandow, S., Suenaga, K., Kokai, F., Takahashi, K., Nano-aggregates of single-walled graphitic carbon nanohorns. *Chem. Phys. Lett.*, 309, 165–170, 1999.
13. Danilenko, V., On the history of the discovery of nanodiamond synthesis. *Phys. Solid State*, 46, 595–599, 2004.
14. Baptista, F.R., Belhout, S., Giordani, S., Quinn, S., Recent developments in carbon nanomaterial sensors. *Chem. Soci. Rev.*, 44, 4433–4453, 2015.
15. Jariwala, D., Sangwan, V.K., Lauhon, L.J., Marks, T.J., Hersam, M.C., Carbon nanomaterials for electronics, optoelectronics, photovoltaics, and sensing. *Chem. Soc. Rev.*, 42, 2824–2860, 2013.
16. Schmid, G. (Ed.), *Nanoparticles: From Theory to Application*, John Wiley & Sons, 2011.
17. Li, J., Zhang, J.Z., Optical properties and applications of hybrid semiconductor nanomaterials. *Coord. Chem. Rev.*, 253, 3015–3041, 2009.
18. Wang, X., Summers, C.J., Wang, Z.L., Large-scale hexagonal-patterned growth of aligned zno nanorods for nano-optoelectronics and nanosensor arrays. *Nano Lett.*, 4, 423–426, 2004.
19. Jang, J., Oh, J.H., Novel crystalline supramolecular assemblies of amorphous polypyrrole nanoparticles through surfactant templating. *Chem. Comm.*, 19, 2200–2201, 2002.
20. Fudouzi, H., Xia, Y., Photonic papers and inks: Color writing with colorless materials. *Adv. Mater.*, 15, 892–896, 2003.
21. Brahim, S., Narinesingh, D., Guiseppi-Elie, A., Amperometric determination of cholesterol in serum using a biosensor of cholesterol oxidase contained within a polypyrrole–hydrogel membrane. *Anal. Chim. Acta*, 448, 27–36, 2001.
22. Zhang, Q., Chuang, K.T., Adsorption of organic pollutants from effluents of a kraft pulp mill on activated carbon and polymer resin. *Adv. Environ. Res.*, 5, 251–258, 2001.
23. Nagavarma, B., Yadav, H.K., Ayaz, A., Vasudha, L., Shivakumar, H., Different techniques for preparation of polymeric nanoparticles - A review. *Asian J. Pharm. Clin. Res*, 5, 16–23, 2012.
24. Fu, R., Fu, G.-D., Polymeric nanomaterials from combined click chemistry and controlled radical polymerization. *Polym. Chem.*, 2, 465–475, 2011.
25. Nasir, A., Kausar, A., Younus, A., A review on preparation, properties and applications of polymeric nanoparticle-based materials. *Polym. Plast. Technol. Eng.*, 54, 325–341, 2015.
26. Cismaru, L., Popa, M., Polymeric nanoparticles with biomedical applications. *Rev. Roum Chim.*, 55, 433–442, 2010.
27. Shouldice, G.T., Vandezande, G.A., Rudin, A., Practical aspects of the emulsifier-free emulsion polymerization of styrene. *Eur. Polym. J.*, 30, 179–183, 1994.

28. Yildiz, U., Landfester, K., Miniemulsion polymerization of styrene in the presence of macromonomeric initiators. *Polymer*, 49, 4930–4934, 2008.
29. Rao, J.P., Geckeler, K.E., Polymer nanoparticles: Preparation techniques and size-control parameters. *Prog. Polym. Sci.*, 36, 887–913, 2011.
30. Gaudin, F., Sintes-Zydowicz, N., Core–shell biocompatible polyurethane nanocapsules obtained by interfacial step polymerisation in miniemulsion. *Colloids. Surf. A*, 331, 133–142, 2008.
31. Lee, S.H., Heng, D., Ng, W.K., Chan, H.-K., Tan, R.B., Nano spray drying: A novel method for preparing protein nanoparticles for protein therapy. *Int. J. Pharm.*, 403, 192–200, 2011.
32. Jeong, Y.I., Cho, C.S., Kim, S.H., Ko, K.S., Kim, S.I., Shim, Y.H., Nah, J.W., Preparation of poly (dl-lactide-co-glycolide) nanoparticles without surfactant. *J. Appl. Polym. Sci.*, 80, 2228–2236, 2001.
33. Tansık, G., Yakar, A., Gündüz, U., Tailoring magnetic plga nanoparticles suitable for doxorubicin delivery. *J. Nanopart. Res.*, 16, 2171–1276, 2014.
34. Quintanar-Guerrero, D., Zambrano-Zaragoza, Mde. L., Gutiérrez-Cortez, E., Mendoza-Muñoz, N., Impact of the emulsification-diffusion method on the development of pharmaceutical nanoparticles, *Recent Pat. Drug Deliv. Formul.*, 6, 184–194, 2012.
35. Mehrotra, A., Pandit, J., Critical process parameters evaluation of modified nanoprecipitation method on lomustine nanoparticles and cytostatic activity study on l132 human cancer cell line. *J. Nanomed. Nanotech.*, 3, 8–13, 2012.
36. Huang, D., Yang, Y., Zhuang, G., Li, B., Influence of intermolecular entanglements on the glass transition and structural relaxation behaviors of macromolecules. 2. Polystyrene and phenolphthalein poly (ether sulfone), *Macromol.*, 33, 461–464, 2000.
37. Galindo-Rodriguez, S., Allémann, E., Fessi, H., Doelker, E., Physicochemical parameters associated with nanoparticle formation in the salting-out, emulsification-diffusion, and nanoprecipitation methods. *Pharm. Res.*, 21, 1428–1439, 2004.
38. Liu, C.Y., Morawetz, H., Kinetics of the unfolding of collapsed polystyrene chains above the glass transition temperature. *Macromol.*, 21, 515–518, 1988.
39. Zhou, D., Li, L., Li, Y., Zhang, J., Xue, G., Metastable isotactic polystyrene prepared by freeze-extracting concentrated solutions in solvents of middle molecular size. *Macromol.*, 36, 4609–4613, 2003.
40. Kumaki, J., Polystyrene monomolecular particles obtained by spreading dilute solutions on the water surface. *Macromol.*, 19, 2258–2263, 1986.
41. Sekhon, B.S., Supercritical fluid technology: An overview of pharmaceutical applications. *Int. J. Pharm. Tech. Res.*, 2, 810–826, 2010.
42. Qi, Z.-m., Zhou, H.-s., Matsuda, N., Honma, I., Shimada, K., Takatsu, A., Kato, K., Characterization of gold nanoparticles synthesized using sucrose by seeding formation in the solid phase and seeding growth in aqueous solution. *J. Phys. Chem. B*, 108, 7006–7011, 2004.

43. O'regan, B., Grätzel, M., A low-cost, high-efficiency solar cell based on dye-sensitized colloidal tio 2 films. *Nature*, 353, 737–747, 1991.
44. Okuda, M., Kobayashi, Y., Suzuki, K., Sonoda, K., Kondoh, T., Wagawa, A., Kondo, A., Yoshimura, H., Self-organized inorganic nanoparticle arrays on protein lattices. *Nano Lett.*, 5, 991–993, 2005.
45. Ahmad, N., Sharma, S., Alam, M.K., Singh, V., Shamsi, S., Mehta, B., Fatma, A., Rapid synthesis of silver nanoparticles using dried medicinal plant of basil. *Colloids Surf. B*, 81, 81–86, 2010.
46. Gould, I.R., Lenhard, J.R., Muenter, A.A., Godleski, S.A., Farid, S., Two-electron sensitization: A new concept for silver halide photography. *J. Am. Chem. Soc.*, 122, 11934–11943, 2000.
47. De Heer, W.A., The physics of simple metal clusters: Experimental aspects and simple models. *Rev. Mod. Phys.*, 65, 611, 1993.
48. Bawendi, M.G., Steigerwald, M.L., Brus, L.E., The quantum mechanics of larger semiconductor clusters ("quantum dots"). *Annu. Rev. Phys. Chem.*, 41, 477–496, 1990.
49. Shipway, A.N., Lahav, M., Willner, I., Nanostructured gold colloid electrodes. *Adv. Mater.*, 12, 993–998, 2000.
50. Klaine, S.J., Alvarez, P.J., Batley, G.E., Fernandes, T.F., Handy, R.D., Lyon, D.Y., Mahendra, S., McLaughlin, M.J., Lead, J.R., Nanomaterials in the environment: Behavior, fate, bioavailability, and effects, *Environ. Toxicol. Chem.*, 27, 1825–1851, 2008.
51. Tsuji, T., Kakita, T., Tsuji, M., Preparation of nano-size particles of silver with femtosecond laser ablation in water. *Appl. Surf. Sci.*, 206, 314–320, 2003.
52. Jensen, T.R., Malinsky, M.D., Haynes, C.L., Van Duyne, R.P., Nanosphere lithography: Tunable localized surface plasmon resonance spectra of silver nanoparticles. *J. Phys. Chem. B*, 104, 10549–10556, 2000.
53. Lu, H., Liu, S., Wang, X., Qian, X., Yin, J., Zhu, Z., Silver nanocrystals by hyperbranched polyurethane-assisted photochemical reduction of Ag+, *Mater. Chem. Phys.*, 81, 104–107, 2003.
54. Lukman, A.I., Gong, B., Marjo, C.E., Roessner, U., Harris, A.T., Facile synthesis, stabilization, and anti-bacterial performance of discrete ag nanoparticles using *Medicago sativa* seed exudates. *J. Colloid Interface Sci.*, 353, 433–444, 2011.
55. Aromal, S.A., Philip, D., Green synthesis of gold nanoparticles using trigonella foenum-graecum and its size-dependent catalytic activity. *Spectrochim. Acta A*, 97, 1–5, 2012.
56. Chen, A., Holt-Hindle, P., Platinum-based nanostructured materials: Synthesis, properties, and applications. *Chem. Rev*, 110, 3767–3804, 2010.
57. Fritsch, D., Kuhr, K., Mackenzie, K., Kopinke, F.-D., Hydrodechlorination of chloroorganic compounds in ground water by palladium catalysts: Part 1. Development of polymer-based catalysts and membrane reactor tests. *Catal. Today*, 82, 105–118, 2003.

58. Chen, W., Cai, W., Lei, Y., Zhang, L., A sonochemical approach to the confined synthesis of palladium nanoparticles in mesoporous silica. *Mater. Lett.*, 50, 53–56, 2001.
59. Korovchenko, P., Renken, A., Kiwi-Minsker, L., Microwave plasma assisted preparation of Pd-nanoparticles with controlled dispersion on woven activated carbon fibres. *Catal. Today*, 102, 133–141, 2005.
60. Cao, G., Wang, Y., *Nanostructures and Nanomaterials: Synthesis, Properties and Applications*, World Scientific, 2004.
61. Tolaymat, T.M., El Badawy, A.M., Genaidy, A., Scheckel, K.G., Luxton, T.P., Suidan, M., An evidence-based environmental perspective of manufactured silver nanoparticle in syntheses and applications: A systematic review and critical appraisal of peer-reviewed scientific papers. *Sci. Total Environ.*, 408, 999–1006, 2010.
62. Balan, L., Malval, J.-P., Schneider, R., Burget, D., Silver nanoparticles: New synthesis, characterization and photophysical properties. *Mater. Chem. Phys.*, 104, 417–421, 2007.
63. Yan, W., Wang, R., Xu, Z., Xu, J., Lin, L., Shen, Z., Zhou, Y., A novel, practical and green synthesis of Ag nanoparticles catalyst and its application in three-component coupling of aldehyde, alkyne, and amine. *J. Mol. Catal.*, 255, 81–85, 2006.
64. Gulrajani, M., Gupta, D., Periyasamy, S., Muthu, S., Preparation and application of silver nanoparticles on silk for imparting antimicrobial properties. *J. Appl. Poly Sci.*, 108, 614–623, 2008.
65. Badawy, A.M.E., Luxton, T.P., Silva, R.G., Scheckel, K.G., Suidan, M.T., Tolaymat, T.M., Impact of environmental conditions (pH, ionic strength, and electrolyte type) on the surface charge and aggregation of silver nanoparticles suspensions. *Environ. Sci. Technol.*, 44, 1260–1266, 2010.
66. Sharma, V.K., Yngard, R.A., Lin, Y., Silver nanoparticles: Green synthesis and their antimicrobial activities. *Adv. Colloid Interface Sci.*, 145, 83–96, 2009.
67. Kaplan, D.L., Biopolymers from renewable resources, in: *Introduction to Biopolymers from Renewable Resources*, pp. 1–7, Springer, 1998.
68. Reicha, F.M., Sarhan, A., Abdel-Hamid, M.I., El-Sherbiny, I.M., Preparation of silver nanoparticles in the presence of chitosan by electrochemical method. *Carbohydr. Polym.*, 89, 236–244, 2012.
69. Leung, T.C.-Y., Wong, C.K., Xie, Y., Green synthesis of silver nanoparticles using biopolymers, carboxymethylated-curdlan and fucoidan. *Mater. Chem. Phys.*, 121, 402–405, 2010.
70. Kora, A.J., Sashidhar, R., Arunachalam, J., Gum kondagogu (*Cochlospermum gossypium*): A template for the green synthesis and stabilization of silver nanoparticles with antibacterial application. *Carbohydr. Polym.*, 82, 670–679, 2010.
71. El-Sherbiny, I.M., Salih, E., Yassin, A.M., Hafez, E.E., Newly developed chitosan-silver hybrid nanoparticles: Biosafety and apoptosis induction in HepG2 cells. *J. Nanopart. Res.*, 18, 1–17, 2016.

72. Padalkar, S., Capadona, J.R., Rowan, S.J., Weder, C., Won, Y.-H., Stanciu, L.A., Moon, R.J., Natural biopolymers: Novel templates for the synthesis of nanostructures. *Langmuir*, 26, 8497–8502, 2010.
73. Saha, S., Pal, A., Kundu, S., Basu, S., Pal, T., Photochemical green synthesis of calcium-alginate-stabilized Ag and Au nanoparticles and their catalytic application to 4-nitrophenol reduction. *Langmuir*, 26, 2885–2893, 2009.
74. El-Sherbiny, I.M., Hefnawy, A., Salih, E., New core–shell hyperbranched chitosan-based nanoparticles as optical sensor for ammonia detection. *Int. J. Biol. Macromol.*, 86, 782–788, 2016.
75. El-Sherbiny, I.M., El-Shibiny, A., Salih, E., Photo-induced green synthesis and antimicrobial efficacy of poly (ε-caprolactone)/curcumin/grape leaf extract-silver hybrid nanoparticles. *J. Photochem. Photobiol.*, 160, 355–363, 2016.
76. Jagadeesh, B.H., Prabha, T.N., Srinivasan, K., Activities of β-hexosaminidase and α-mannosidase during development and ripening of bell capsicum (*Capsicum annuum* var. *variata*). *Plant Sci.*, 167, 1263–1271, 2004.
77. Sathishkumar, M., Sneha, K., Yun, Y.-S., Immobilization of silver nanoparticles synthesized using *Curcuma longa* tuber powder and extract on cotton cloth for bactericidal activity. *Biosour. Technol.*, 101, 7958–7963, 2010.
78. Venkatpurwar, V., Pokharkar, V., Green synthesis of silver nanoparticles using marine polysaccharide: Study of *in-vitro* antibacterial activity. *Mater. Lett.*, 65, 999–1002, 2011.
79. El-Sherbiny, I.M., Salih, E., Reicha, F.M., Green synthesis of densely dispersed and stable silver nanoparticles using myrrh extract and evaluation of their antibacterial activity. *J. Nanostruct. Chem.*, 3, 8–14, 2013.
80. Mariselvam, R., Ranjitsingh, A., Nanthini, A.U.R., Kalirajan, K., Padmalatha, C., Selvakumar, P.M., Green synthesis of silver nanoparticles from the extract of the inflorescence of *Cocos nucifera* (family: *Arecaceae*) for enhanced antibacterial activity. *Spectrochim. Acta A*, 129, 537–541, 2014.
81. Sadeghi, B., Rostami, A., Momeni, S., Facile green synthesis of silver nanoparticles using seed aqueous extract of *Pistacia atlantica* and its antibacterial activity. *Spectrochim. Acta A*, 134, 326–332, 2015.
82. Kumar, P.V., Pammi, S., Kollu, P., Satyanarayana, K., Shameem, U., Green synthesis and characterization of silver nanoparticles using *Boerhaavia diffusa* plant extract and their anti bacterial activity. *Ind. Crops. Prod.*, 52, 562–566, 2014.
83. Gopinath, V., MubarakAli, D., Priyadarshini, S., Priyadharsshini, N.M., Thajuddin, N., Velusamy, P., Biosynthesis of silver nanoparticles from *Tribulus terrestris* and its antimicrobial activity: A novel biological approach. *Colloids Surf. B*, 96, 69–74, 2012.
84. Rajakumar, G., Rahuman, A.A., Larvicidal activity of synthesized silver nanoparticles using *Eclipta prostrata* leaf extract against filariasis and malaria vectors. *Acta Trop.*, 118, 196–203, 2011.

85. Chandran, S.P., Chaudhary, M., Pasricha, R., Ahmad, A., Sastry, M., Synthesis of gold nanotriangles and silver nanoparticles using *Aloevera* plant extract. *Biotechnol. Prog.*, 22, 577–583, 2006.
86. Kumar, D.A., Palanichamy, V., Roopan, S.M., Green synthesis of silver nanoparticles using *Alternanthera dentata* leaf extract at room temperature and their antimicrobial activity. *Spectrochim. Acta A*, 127, 168–171, 2014.
87. Kumar, S., Daimary, R.M., Swargiary, M., Brahma, A., Kumar, S., Singh, M., Biosynthesis of silver nanoparticles using *Premna herbacea* leaf extract and evaluation of its antimicrobial activity against bacteria causing dysentery. *Int. J. Pharm. Biol. Sci.*, 4, 378–384, 2013.
88. Zargar, M., Hamid, A.A., Bakar, F.A., Shamsudin, M.N., Shameli, K., Jahanshiri, F., Farahani, F., Green synthesis and antibacterial effect of silver nanoparticles using *Vitex negundo* L. *Molecules*, 16, 6667–6676, 2011.
89. Rout, A., Jena, P.K., Parida, U.K., Bindhani, B.K., Green synthesis of silver nanoparticles using leaves extract of *Centella asiatica* L. for studies against human pathogens. *Int. J. Pharm. Biol. Sci.*, 4, 661–674, 2013.
90. El-Sherbiny, I., Salih, E., Reicha, F., New trimethyl chitosan-based composite nanoparticles as promising antibacterial agents. *Drug Develop. Ind. Pharm.*, 42, 720–729, 2016.
91. Sedaghat, S., Afshar, P., Green bio-synthesis of silver nanoparticles using *Ziziphora tenuior* L. water extract, *J. Appl. Chem. Res.*, 10, 103–109, 2016.
92. Gondwal, M., Pant, G., Biological evaluation and green synthesis of silver nanoparticles using aqueous extract of *Calotropis procera*. *Int. J. Pharm. Biol. Sci.*, 4, 635–643, 2013.
93. Kesharwani, J., Yoon, K.Y., Hwang, J., Rai, M., Phytofabrication of silver nanoparticles by leaf extract of *Datura metel*: Hypothetical mechanism involved in synthesis. *J. Bionanosci.,* 3, 39–44, 2009.
94. Krishnaraj, C., Jagan, E., Rajasekar, S., Selvakumar, P., Kalaichelvan, P., Mohan, N., Synthesis of silver nanoparticles using *Acalypha indica* leaf extracts and its antibacterial activity against water borne pathogens. *Colloids Surf. B*, 76, 50–56, 2010.
95. Ahamed, M., Khan, M.M., Siddiqui, M., AlSalhi, M.S., Alrokayan, S.A., Green synthesis, characterization and evaluation of biocompatibility of silver nanoparticles. *Phys. E.,* 43, 1266–1271, 2011.
96. Elavazhagan, T., Arunachalam, K.D., *Memecylon edule* leaf extract mediated green synthesis of silver and gold nanoparticles. *Int. J. Nanomed.*, 6, 1265–1271, 2011.
97. Sun, Q., Cai, X., Li, J., Zheng, M., Chen, Z., Yu, C.-P., Green synthesis of silver nanoparticles using tea leaf extract and evaluation of their stability and antibacterial activity. *Colloids Surf. A*, 444, 226–231, 2014.
98. Santhoshkumar, T., Rahuman, A.A., Rajakumar, G., Marimuthu, S., Bagavan, A., Jayaseelan, C., Zahir, A.A., Elango, G., Kamaraj, C., Synthesis of silver nanoparticles using *Nelumbo nucifera* leaf extract and its larvicidal activity against malaria and filariasis vectors. *Parasitol. Res.*, 108, 693–702, 2011.

99. Ahmed, S., Ahmad, M., Swami, B.L., Ikram, S., A review on plants extract mediated synthesis of silver nanoparticles for antimicrobial applications: A green expertise. *J. Adv. Res.*, 7, 17–28, 2016.
100. Noruzi, M., Zare, D., Khoshnevisan, K., Davoodi, D., Rapid green synthesis of gold nanoparticles using *Rosa hybrida* petal extract at room temperature. *Spectrochim. Acta A*, 79, 1461–1465, 2011.
101. Jayaseelan, C., Ramkumar, R., Rahuman, A.A., Perumal, P., Green synthesis of gold nanoparticles using seed aqueous extract of *Abelmoschus esculentus* and its antifungal activity. *Ind. Crop. Prod.,* 45, 423–429, 2013.
102. Shankar, S.S., Rai, A., Ahmad, A., Sastry, M., Controlling the optical properties of lemongrass extract synthesized gold nanotriangles and potential application in infrared-absorbing optical coatings. *Chem. Mat.*, 17, 566–572, 2005.
103. Ghosh, S., Patil, S., Ahire, M., Kitture, R., Jabgunde, A., Kale, S., Pardesi, K., Bellare, J., Dhavale, D.D., Chopade, B.A., Synthesis of gold nanoanisotrops using *Dioscorea bulbifera* tuber extract. *J. Nanomater.*, 2011, 45–51, 2011.
104. Ankamwar, B., Damle, C., Ahmad, A., Sastry, M., Biosynthesis of gold and silver nanoparticles using *Emblica officinalis* fruit extract, their phase transfer and transmetallation in an organic solution. *J. Nanosci. Nanotechnol.*, 5, 1665–1671, 2005.
105. Ankamwar, B., Chaudhary, M., Sastry, M., Gold nanotriangles biologically synthesized using tamarind leaf extract and potential application in vapor sensing. *Synth. React. Inorg. Met. Org. Chem.*, 35, 19–26, 2005.
106. Huang, J., Li, Q., Sun, D., Lu, Y., Su, Y., Yang, X., Wang, H., Wang, Y., Shao, W., He, N., Biosynthesis of silver and gold nanoparticles by novel sundried cinnamomum camphora leaf. *Nanotechnol.*, 18, 105104–105110, 2007.
107. Shankar, S.S., Rai, A., Ankamwar, B., Singh, A., Ahmad, A., Sastry, M., Biological synthesis of triangular gold nanoprisms. *Nature.,* 3, 482–488, 2004.
108. Smitha, S., Philip, D., Gopchandran, K., Green synthesis of gold nanoparticles using *Cinnamomum zeylanicum* leaf broth. *Spectrochim. Acta A*, 74, 735–739, 2009.
109. Sharma, N.C., Sahi, S.V., Nath, S., Parsons, J.G., Gardea-Torresde, J.L., Pal, T., Synthesis of plant-mediated gold nanoparticles and catalytic role of biomatrix-embedded nanomaterials. *Environ. Sci. Technol.*, 41, 5137–5142, 2007.
110. Shankar, S.S., Ahmad, A., Pasricha, R., Sastry, M., Bioreduction of chloroaurate ions by geranium leaves and its endophytic fungus yields gold nanoparticles of different shapes. *J. Mater. Chem.*, 13, 1822–1826, 2003.
111. Elia, P., Zach, R., Hazan, S., Kolusheva, S., Porat, Z., Zeiri, Y., Green synthesis of gold nanoparticles using plant extracts as reducing agents. *Int. J. Nanomed.*, 9, 4007–4012, 2014.
112. Song, J.Y., Kwon, E.-Y., Kim, B.S., Biological synthesis of platinum nanoparticles using *Diopyros kaki* leaf extract. *Bioprocess Biosyst. Eng.*, 33, 159–164, 2010.
113. Zheng, B., Kong, T., Jing, X., Odoom-Wubah, T., Li, X., Sun, D., Lu, F., Zheng, Y., Huang, J., Li, Q., Plant-mediated synthesis of platinum nanoparticles and its bioreductive mechanism. *J. Colloid Interface Sci.*, 396, 138–145, 2013.

114. Soundarrajan, C., Sankari, A., Dhandapani, P., Maruthamuthu, S., Ravichandran, S., Sozhan, G., Palaniswamy, N., Rapid biological synthesis of platinum nanoparticles using *Ocimum sanctum* for water electrolysis applications. *Bioprocess Biosyst. Eng.*, 35, 827–833, 2012.
115. Thirumurugan, A., Aswitha, P., Kiruthika, C., Nagarajan, S., Christy, A.N., Green synthesis of platinum nanoparticles using azadirachta indica – An eco-friendly approach. *Mater. Lett.*, 170, 175–178, 2016.
116. Dobrucka, R., Biofabrication of platinum nanoparticles using *Fumariae herba* extract and their catalytic properties. *Saudi J. Biol. Sci.*, 2016.
117. Sheny, D.S., Philip, D., Mathew, J., Synthesis of platinum nanoparticles using dried *Anacardium occidentale* leaf and its catalytic and thermal applications. *Spectrochim. Acta A*, 114, 267–271, 2013.
118. Tahir, K., Nazir, S., Ahmad, A., Li, B., Khan, A.U., Khan, Z.U.H., Khan, F.U., Khan, Q.U., Khan, A., Rahman, A.U., Facile and green synthesis of phytochemicals capped platinum nanoparticles and *in vitro* their superior antibacterial activity. *J. Photochem. Photobiol. B*, 166, 246–251, 2017.
119. John Leo, A., Oluwafemi, O.S., Plant-mediated synthesis of platinum nanoparticles using water hyacinth as an efficient biomatrix source – An eco-friendly development. *Mater. Lett.*, 196, 141–144, 2017.
120. Dauthal, P., Mukhopadhyay, M., Biofabrication, characterization, and possible bio-reduction mechanism of platinum nanoparticles mediated by agro-industrial waste and their catalytic activity. *J. Ind. Eng. Chem.*, 22, 185–191, 2015.
121. Rajakumar, G., Rahuman, A.A., Chung, I.-M., Kirthi, A.V., Marimuthu, S., Anbarasan, K., Antiplasmodial activity of eco-friendly synthesized palladium nanoparticles using *Eclipta prostrata* extract against *Plasmodium berghei* in Swiss albino mice. *Parasitol. Res.*, 114, 1397–1406, 2015.
122. Sathishkumar, M., Sneha, K., Yun, Y., Palladium nanocrystal synthesis using *Curcuma longa* tuber extract. *Int. J. Mater. Sci.*, 4, 11–17, 2009.
123. Mohan Kumar, K., Mandal, B.K., Siva Kumar, K., Sreedhara Reddy, P., Sreedhar, B., Biobased green method to synthesise palladium and iron nanoparticles using Terminalia chebula aqueous extract. *Spectrochim. Acta A*, 102, 128–133, 2013.
124. Dauthal, P., Mukhopadhyay, M., Biosynthesis of palladium nanoparticles using *Delonix regia* leaf extract and its catalytic activity for nitro-aromatics hydrogenation. *Ind. Eng. Chem. Res.*, 52, 18131–18139, 2013.
125. Sathishkumar, M., Sneha, K., Kwak, I.S., Mao, J., Tripathy, S.J., Yun, Y.S., Phyto-crystallization of palladium through reduction process using *Cinnamom zeylanicum* bark extract. *J. Hazard. Mater.*, 171, 400–404, 2009.
126. Veisi, H., Ghorbani-Vaghei, R., Hemmati, S., Aliani, M.H., Ozturk, T., Green and effective route for the synthesis of monodispersed palladium nanoparticles using herbal tea extract (*Stachys lavandulifolia*) as reductant, stabilizer and capping agent, and their application as homogeneous and reusable

catalyst in Suzuki coupling reactions in water. *Appl. Organomet. Chem.*, 29, 26–32, 2015.
127. Nasrollahzadeh, M., Sajadi, S.M., Honarmand, E., Maham, M., Preparation of palladium nanoparticles using *Euphorbia thymifolia* L. leaf extract and evaluation of catalytic activity in the ligand-free Stille and Hiyama cross-coupling reactions in water. *New J. Chem.*, 39, 4745–4752, 2015.
128. Bankar, A., Joshi, B., Kumar, A.R., Zinjarde, S., Banana peel extract mediated novel route for the synthesis of palladium nanoparticles. *Mater. Lett.*, 64, 1951–1953, 2010.
129. Mallikarjuna, K., Sushma, N.J., Subba Reddy, B.V., Narasimha, G., Deva Prasad Raju, B., Palladium nanoparticles: Single-step plant-mediated green chemical procedure using *Piper betle* leaves broth and their anti-fungal studies. *Int. J. Chem. Anal. Sci.*, 4, 14–18, 2013.
130. Nasrollahzadeh, M., Mohammad Sajadi, S., Pd nanoparticles synthesized *in situ* with the use of *Euphorbia granulate* leaf extract: Catalytic properties of the resulting particles. *J. Colloid Interface Sci.*, 462, 243–251, 2016.
131. Roopan, S.M., Bharathi, A., Kumar, R., Khanna, V.G., Prabhakarn, A., Acaricidal, insecticidal, and larvicidal efficacy of aqueous extract of *Annona squamosa* L peel as biomaterial for the reduction of palladium salts into nanoparticles. *Colloids Surf. B.*, 92, 209–212, 2012.
132. Petla, R.K., Vivekanandhan, S., Misra, M., Mohanty, A.K., Satyanarayana, N., Soybean (*Glycine max*) leaf extract based green synthesis of palladium nanoparticles. *J. Biomater. Nanobiotechnol.*, 3, 14–19, 2012.
133. Yang, X., Li, Q., Wang, H., Huang, J., Lin, L., Wang, W., Sun, D., Su, Y., Opiyo, J.B., Hong, L., Green synthesis of palladium nanoparticles using broth of *Cinnamomum camphora* leaf. *J. Nanopart. Res.*, 12, 1589–1598, 2010.
134. Nasrollahzadeh, M., Sajadi, S.M., Maham, M., Green synthesis of palladium nanoparticles using *Hippophae rhamnoides* Linn leaf extract and their catalytic activity for the Suzuki–Miyaura coupling in water. *J. Mol. Catal. A*, 396, 297–303, 2015.
135. Kalaiselvi, A., Roopan, S.M., Madhumitha, G., Ramalingam, C., Elango, G., Synthesis and characterization of palladium nanoparticles using *Catharanthus roseus* leaf extract and its application in the photo-catalytic degradation. *Spectrochim. Acta A,* 135, 116–119, 2015.
136. Kanchana, A., Devarajan, S., Ayyappan, S.R., Green synthesis and characterization of palladium nanoparticles and its conjugates from *Solanum trilobatum* leaf extract. *Nano-Micro Lett.*, 2, 169–175, 2010.

11

Green Synthesis of Metallic Nanoparticles from Natural Resources and Food Waste and Their Environmental Application

Hussein I. Abdel-Shafy[1]* and Mona S. M. Mansour[2]

[1]Water Research & Polluted Control Department, National Research Centre, Dokki, Cairo, Egypt
[2]Analyses & Evaluation Department, Egyptian Petroleum Research Institute, Nasr City, Cairo, Egypt

Abstract

Nanoparticles and nanobiotechnology are new fields that focus on the creation and use of nanometer materials. In green chemistry, nanoscience opens new opportunities in chemical, physical, biochemical and biophysical transformations. The nanoparticles have made the fields of catalysis, synthesis, enzyme immobilizations and molecular interactions easier, rapid and controllable.

Noble metallic nanoparticles are currently being widely used in several areas of application, including cosmetics, medicine and biomedical sciences, disease diagnostics, separation techniques and antibacterial and anti-inflammatory drugs that promote faster wound healing. Moreover, they have recently been integrated into commercial wound dressings, medical implant coatings and pharmaceutical preparations.

Metallic nanoparticles are also widely used in biomedical applications in a pure form or as alloys in catalysis and electrocatalysis, electronics, chemical sensors, and antibacterials. The promising applications of nanotechnology are their efficiency in water, wastewater treatment and remediation, including removal of chemical and biological substances.

The present chapter throws light on the most recent and important alternative green synthesis routes for metallic nanoparticles from different sources, plants,

**Corresponding author*: hshafywater@yahoo.com; waterbiotech@yahoo.com

Suvardhan Kanchi and Shakeel Ahmed (eds.) Green Metal Nanoparticles, (321–385)
© 2018 Scrivener Publishing LLC

microbes and chemical routes via microwaving, sonication, and/or many others. The review also outlines the recent approaches in nanotechnology for environmental applications.

Keywords: Green synthesis, metallic nanoparticles, metal oxide nanoparticles, natural resources, food waste, water treatment, wastewater treatment

11.1 Introduction

Green chemistry has been one of the most interesting sciences of the past few years as an alternative to traditional chemistry. This is mainly due to the energy crisis and its constraints, particularly in developing countries. Therefore, serious consideration given to the development of green chemistry has resulted in significant efforts in the multidisciplinary and interdisciplinary scientific fields [1]. Meanwhile, the convergence of nanometer-size-scale technologies has created the new field of nanoscience, including nanotechnology and nanobiotechnology. This relatively new field focuses on the creation and use of materials at the nanometer scale for advanced biotechnology. Thus, nanoscience in green chemistry has opened the door to multiple opportunities by enabling variable numbers of chemical, physical, biochemical, and biophysical transformations in a reliable manner. In this respect, the use of nanoparticles has made the fields of catalysis, synthesis, and enzyme immobilizations as well as molecular interactions, much easier, rapid and controllable [2].

During the last four decades, nanoparticles and nanofibers demonstrated superior performance in numerous applications such as medicine, energy, the environment, water, wastewater, health care, etc. [1]. There have been extensive studies on the potential environmental and health impacts of nanoparticles which are reported in the literature [2, 3]. However, several materials and processes that are currently used for the synthesis of nanoparticles generate hazardous wastes and depend on nonrenewable resources. Green nanotechnology is the combination of nanotechnology as well as the practices and principles of green chemistry. In the near future, green nanotechnology may hold the key to build an environmentally sustainable society. Besides which, nanomaterials offer applications to reduce and prevent pollution by utilizing certain catalytic processes to create less waste production, destroy harmful bacteria and viruses, sense pollutants in water, create clean water, and clean up the environment [4]. Thus, green chemistry is a set of practices or principles that encourage the design of products and processes that eliminate or reduce the use of hazardous substances [5–7]. Often the current practices of green nanotechnology involve

the use of natural sources, biodegradable and biocompatible materials, energy-efficient processes, and non-hazardous solvents in the preparation of nanoparticles [8, 9].

For the future of humanity and the environment, nanoparticles are important for developing sustainable technologies. In green chemistry, synthesis of nanoparticles from plants is the interconnection of nanotechnology and plant biotechnology. Plant extracts are usually used for the bioreduction of metal ions to form nanoparticles. It has recently been proved that plant metabolites like proteins, sugars, polyphenols, terpenoids, phenolic acids, and alkaloids play an important role in the reduction of metal ions into nanoparticles, as well as supporting their subsequent stability [8].

Properties of nonmetric material's atoms are greatly different from the bulk materials. Scientists are concerned about conventionally synthesizing nanoparticles by chemical method because of their toxicity; thus, they prefer to develop environmentally friendly processes [10]. Many recent studies have proved that plant extracts act as a potential precursor for the eco-friendly synthesis of nanomaterials in non-hazardous ways [8, 10]. Plants are successfully used in the synthesis of several greener nanoparticles, including platinum, gold, cobalt, silver, copper, palladium, magnetite, and zinc oxide. It has been demonstrated in the last decade that many biological systems, including diatoms, plants and algae [11, 12], yeast and bacteria [13, 14], fungi [15], and human cells [16], are capable of transforming inorganic metal ions into metal nanoparticles through the reductive capacities of the proteins and metabolites present in these organisms. In addition, synthesis of metallic nanoparticles by biological entities is of great interest because of their unusual optical [17] and chemical properties [18].

11.2 Several Methods for Metallic Nanoparticle Synthesis

Different methods are used for synthesis of nanoparticles (NPs), including physical, chemical, enzymatic, and biological. Physical methods include ball milling, thermal evaporation, plasma arcing, spray pyrolysis, ultrathin films, sputter deposition, layer-by-layer growth, pulsed laser desorption, molecular beam epistaxis, lithographic techniques, and diffusion flame synthesis of nanoparticles [19]. In addition, the chemical methods used to synthesize NPs are sol-gel process, electro deposition, chemical vapor deposition and chemical solution deposition, [20], hydrolysis, soft chemical method, catalytic route; Langmuir-Blodgett method [21], wet chemical method and co-precipitation method [22]. In this respect, physical and

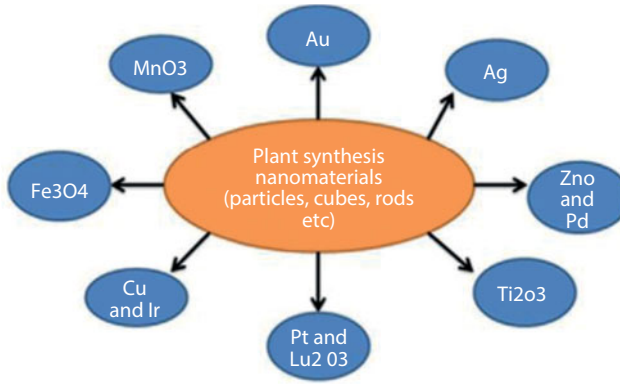


Figure 11.1 Variable types of nanoparticle synthesized from plant resources. (Reproduced from [25]).

chemical methods include high radiation and highly concentrated reductants and stabilizing agents that are considered harmful to environmental and human health. Thus, biological synthesis of nanoparticles is a single-step bioreduction method that uses less energy to synthesize eco-friendly NPs [23]. The biological methods also employ eco-friendly resources such as plant extracts, bacteria, fungi, and microalgae (i.e., cyanobacteria, diatom, seaweed, macroalgae, and enzymes) [24]. Figure 11.1 exhibits different types of metallic nanoparticles that are synthesized from plant resources [25].

11.3 Biosynthesis of Different Metallic Nanoparticles from Plant Derivatives

The biogenic syntheses of monodispersed nanoparticles with specific shapes and sizes have been an important challenge in biomaterial science. Besides which, it has created significant advantages in the field of pharmacology to cure various bacterial and viral diseases [26]. These biosynthesis methods have more advantages over many other classical synthesis procedures. This is mainly due to the availability of more biological entities and eco-friendly procedures. In addition, the rich biodiversity and easy availability of plant entities have been greatly explored for the synthesis of nanomaterials [27]. Successful biosynthesis of nano-sized particles, tubes, wires, and flowers has been reported [25, 27]. Such biologically synthesized nanomaterials have important potential applications in different areas,

including treatment, development of surgical nanodevices, diagnosis, and manufacturing of commercial products [28]. Also, nanomedicine makes a huge improvement in the healthcare sector in treating different chronic diseases. Thus, eco-friendly synthesis of nanoparticles is considered a building block to control different diseases in coming generations [29].

Furthermore, plant crude extract contains novel secondary metabolites, including phenolic acid, flavonoids, alkaloids, and terpenoids. Thus, these natural compounds are mainly responsible for the reduction of ionic into bulk metallic nanoparticles formation [30]. Such primary and secondary metabolites are constantly involved in the redox reaction to synthesize the eco-friendly nano-sized particles. As a result, the green synthesis of nanoparticles by plants is gaining tremendous importance nowadays because of its single-step biosynthesis process, occurrence of natural capping agents and absence of toxicants. The advantages of using plants for synthesizing nanoparticles are that they are easily available, safe to handle and possess a broad variety of metabolites that can aid in reduction [31]. On one hand, fungi and bacteria require a comparatively long incubation period for the reduction of metal ions. On the other hand, water-soluble phytochemicals do this in a much shorter time. Thus, compared to bacteria and fungi, plants are much better candidates for synthesizing nanoparticles. By considering the use of plant tissue culture techniques and downstream processing procedures, it is thus possible to synthesize metallic as well as oxide nanoparticles on an industrial scale once issues, such as the metabolic status of the plant, are properly addressed. It is clear from the compiled information that the effect of nanoparticles varies greatly from plant to plant, depending on their mode of application, concentrations and size [32]. Figure 11.2 illustrates some of the herbs, shrubs and trees that are used for nanoparticle synthesis [33].

Vilchis-Nestor *et al.* [34] stated that a one-step green methodology was achieved for the synthesis of AgNPs using an aqueous extract of *Camellia sinensis* (green tea) supported by a carbonaceous material (Ag-CM) originated from the pyrolysis of sewage sludge. Meanwhile, the synthesized Ag-CM exhibited very good catalytic activity in the degradation of methylene blue dye in aqueous solution without the effect of UV radiation or sunlight. The Ag-CM could remove 91% of 30 mg/l methylene blue in a 9-h period. The carbonaceous material alone, on the other hand, could only remove 60% of the dye in a 30-h period.

In addition, AgNPs were successfully synthesized using aqueous callus extract of *Gymnema sylvestre*. This aqueous callus extract of *G. sylvestre* was treated with 1 nM silver nitrate solution, which resulted in the formation of AgNPs. In the UV-visible (UV-Vis) spectrum, the surface plasmon

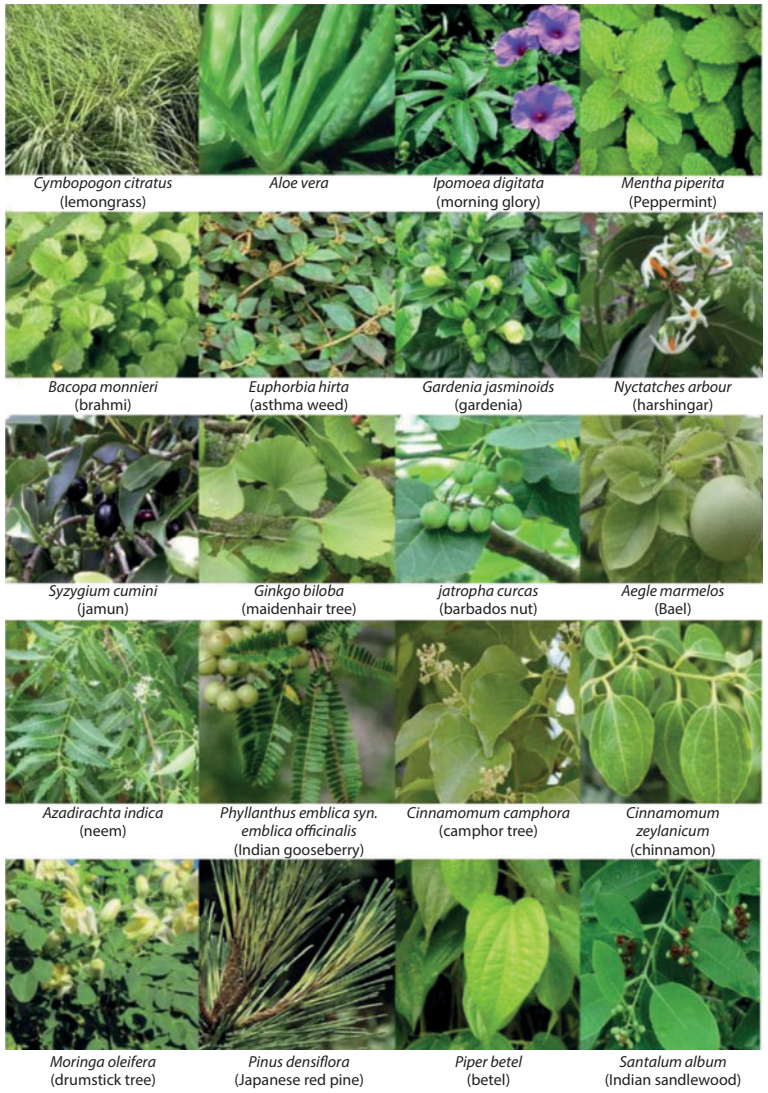


Figure 11.2 Some herbs, shrubs and trees that are used for nanoparticle fabrication. (Reproduced from [33])

resonance (SPR) of the formed AgNPs showed a peak at 437 nm. Using a TEM micrograph for the detection of AgNPs size clearly revealed that they are in the range of 3–30 nm, with a spherical shape. The synthesized AgNPs exhibited effective antifungal activity against non-*albicans Candida, Candida albicans* and *Candida tropicalis* [35].

Moreover, an investigation was carried out by Begum *et al.* [36] on the performances of three different aqueous extracts of black tea in the formation of Ag and Au NPs from $HAuCl_4$ and $AgNO_3$. In this study, they used the extracts of compounds that were soluble in either water, dichloromethane (CH_2Cl_2), ethyl acetate ($C_4H_8O_2$), or for the reduction of the precursors and stabilization of the NPs. They found that the first two extracts could efficiently lead to a rapid formation of stable NPs with variable shapes, including rods, spheres, prisms and trapezoids. In the case of the third extract, the investigators found that no NP generation was detected under similar reaction conditions. Thus, they concluded that polyphenols, including flavonoids that are soluble in water and ethyl acetate, but insoluble in dichloromethane, are responsible for the metallic ion reduction [36].

Meanwhile, gold nanoparticles were synthesized by using onion (*Allium cepa*) extract as a reducing agent. The obtained nanoparticles were characterized by UV-Vis, XRD, SEM, and TEM methods. The characterization showed that the absorption peak at 540 nm was found to be broadening with increase in time, indicating the polydisperse nature of these nanoparticles [37].

Furthermore, Markova *et al.* [38] investigated the preparation of iron(II,III)-polyphenol complex nanoparticles with a diameter of 70 nm size by the addition of $Fe(NO_3)_3{\cdot}9H_2O$ to the green tea extract. In this study, Fe-based nanoparticles were prepared by introducing 0.5 M $Fe(NO_3)_3{\cdot}9H_2O$ into the green tea extract at a ratio of 1:5 by volume under nitrogen atmosphere. In addition, Makarov *et al.* [39] reported the synthesis of iron oxide NPs using aqueous extracts of monocotyledonous plant *Hordeum vulgare* (< 30 nm, unstable) and dicotyledonous plant *Rumex acetosa* (10–40 nm, highly stable). Moreover, magnetite (Fe_3O_4) nanoparticles have been successfully prepared by a novel hydrothermal method by using ferric acetylacetonate ($Fe(C_5H_8O_2)_3$) and *Aloe vera* plant extracted solution. The synthesized nanoparticles are crystalline and have particle sizes of ~6–30 nm [40].

Meanwhile, iron hexacyanoferrate (FeHCF) nanoparticles were synthesized using *Sapindus mukorossi* as natural surfactant and water as solvent. Characterization by TEM revealed the formation of FeHCF nanoparticles in a size range of 10–60 nm, with rod, hexagonal, and spherical shape. In addition, the potential of the synthesized FeHCF nanoparticles was studied for the photocatalytic degradation of hazardous PAHs (chrysene, benzo(a) pyrene, anthracene, phenanthrene, and fluorene) in both water and soil. Almost all treated PAH compounds were transformed into smaller nontoxic by-products. Anthracene compound and its isomer named phenanthrene, were degraded to the maximum extent of 80 to 90% in water

and in soil. But the degradation of chrysene, benzo(a)pyrene, and fluorene was between ~70–80%. Finally, FeHCF nanoparticles were found to be an excellent adsorbent and photocatalyst for the degradation of persistent organic pollutants. The advantage of the present work, after all, lies in its quick approach to green synthesis of low-cost and efficient catalyst, along with the ability to fabricate almost uniformly distributed nanoparticles and their eco-friendly application, which makes our environment green [41].

Further investigation was carried out by Kuang *et al.* [42], in which they used three different tea extracts, namely, Black tea (BT), Green tea (GT), and Oolong tea (OT), to synthesize iron nanoparticles. The obtained nanoparticles were tested for their capacity to act as a catalyst for Fenton-like oxidation of monochlorobenzene (MCB). The study showed that the GT-FeNPs could remove 69% of MCB followed by 53% by OT-FeNPs and 39% by BT-FeNPs during a 180 minute period. Under their optimum experimental conditions, the GT-FeNPs could degrade 81% of the MCB as well as a 31% reduction in chemical oxygen demand (COD).

On the other hand, Elango and Roopan [43] synthesized Pb nanoparticles, at the particle size of 47 nm, using *Cocos nucifera* plant extract with $Pb(COOH)_2$ at 37 °C. The synthesized nanoparticles showed great ability for absorption of carcinogenic dye.

In similar studies, biosynthesis of TiO_2 NPs was achieved by using *Curcuma longa* aqueous extract via two methods. With the first method, TiO_2 was found in both colloidal solutions (CS) and nanopowder, while it was found in just nanopowder in the second method. All biosynthesized nanoparticles were in nano-size range between 91.37 nm and 76.36 nm as CS and nanopowder for the first methods respectively. But, the nanopowder size was 92.6 nm in the second method. All the biosynthesis nanoparticles have good optical properties. The crystal shapes of nanopowder were in three different forms, namely, anatase, rutile and brookite. The anatase was in colloidal solution in the first method while it was pure anatase in nanopowder in the second method. The average crystallite sizes, as calculated by Scherrer's equation, were 43.088 nm and 22.881 nm for nanopowder and colloidal solution, respectively, in the first method, and was 45.808 nm for nanopowder in the second method [44].

11.3.1 Bioreduction Mechanism of Metal Ions

Bioreduction of metal precursors takes place for the synthesis of nanomaterials. Nevertheless, sugars, proteins, enzymes and phytochemicals, like phenolics, flavonoids, terpenoids, cofactors, etc., mainly act as stabilizing and reducing agents [45]. The reaction takes place spontaneously at

room temperature [46]. Sometimes, additional heating and stirring may be needed [47]. Among the biological entities, plants or their extracts seem to be the best agents because they are easily available, suitable for mass production of NPs and their waste products are eco-friendly, unlike most microbial extracts [48]. The proposed mechanism of nanoparticles synthesis by biological method [49] is illustrated in Figure 11.3.

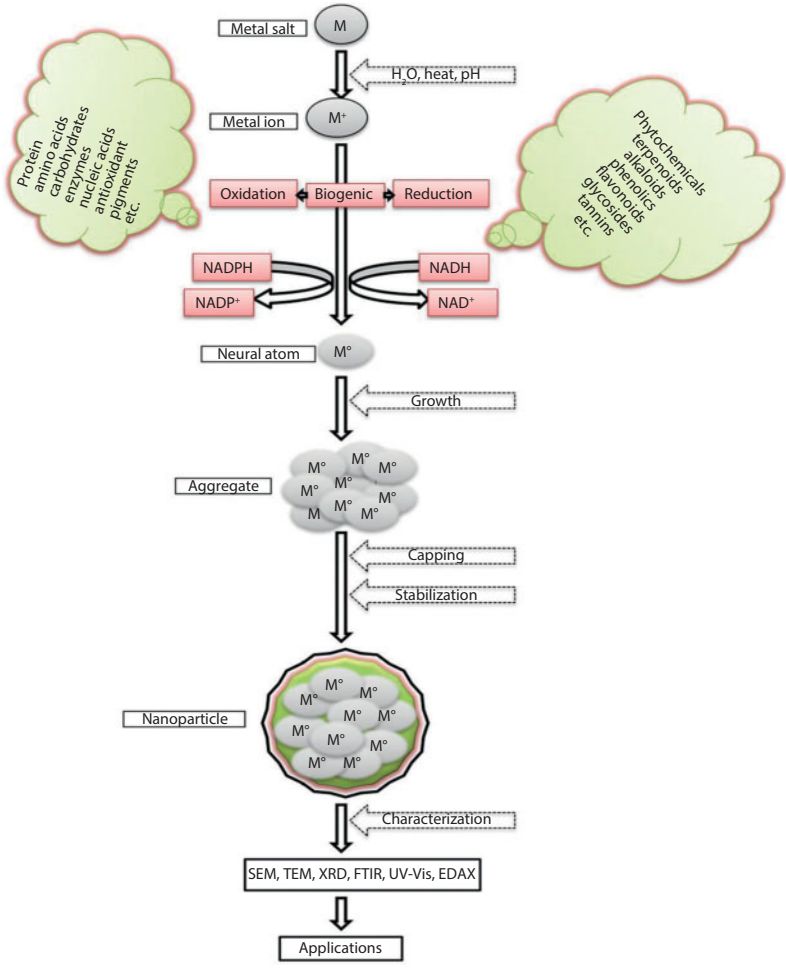


Figure 11.3 Diagram illustrating the possible mechanism of biologically mediated synthesis of nanoparticles. M, M^+ and M^o are metal salt, metal ion, and neutral atom respectively. Note: NAD, NADH, NADP, and NADPH are the abbreviations for nicotinamide adenine dinucleotide (phosphate) in the oxidized and reduced forms (non-hazardous by-products). (Reproduced from [49])

11.3.2 Secondary Metabolites Effect in the Bioreduction Reaction

Variable secondary metabolites and enzymes have relatively promoted the formation of metallic nanoparticles from the corresponding ionic compounds. The reduction reaction mechanism mainly involves plant biomolecules (secondary metabolites) such as organic compounds, sugars (polysaccharides), pigments, proteins, and plant resins. The plants' natural products are simply involved in the reduction reaction to synthesize green nanoparticles. In this respect, plants are particularly participating in defense mechanisms to produce various chemical compounds, including terpenoids, polyphenols, antioxidant enzymes, saponins, and alkaloids. Such secondary metabolites are well known as key sources for controlling the various acute diseases [50]. Thus, this proposed reduction reaction proved that secondary metabolites are essential factors for the biosynthesis of metallic nanoparticles. The plant extracts contain several functional groups, including C–H, C=C (Alkenyl), C=N (amide), O=H (phenolic and alcohol), N–H (amine), and COO– (carboxylic group). They are mainly symbolized as plant secondary metabolites and might be micro- or macrobiomolecules or both [51]. Such chemical substances and compounds fully participate in the nanoparticle production. For example, *Rumex hymenosepalus* plant extract promotes the nanoparticle syntheses at room temperature with fast reaction kinetics. Here, the solvent extract of *R. hymenosepalus* is very rich in polyphenols (i.e., stilbene and catechin molecules). These molecules act as reducing and stabilizing agents for silver nanoparticles production [52]. The plant-derived secondary metabolites, including phenolics [53], proteins [54], tannins, flavonoids, and polysaccharides [55, 56], were used to synthesize all nanoparticles in an eco-friendly method. Figure 11.4(a–c) shows the different chemical compounds of the secondary metabolites synthesize metallic nanoparticles [25]. Some of these chemical compounds are used as antioxidants and others are used in medicine.

11.3.3 Different Parts of Plants Used to Produce Metallic NPs

Recently, scientists have focused more attention on the plant-mediated nanomaterials because of their vast application in various fields due to their physical-chemical properties. The different metallic nanoparticles were synthesized from natural resources and were studied extensively, including platinum, gold, silver, copper, zinc, magnetite, titanium oxide, and nickel. The different parts of the plant, such as root, stem, leaves, fruit,

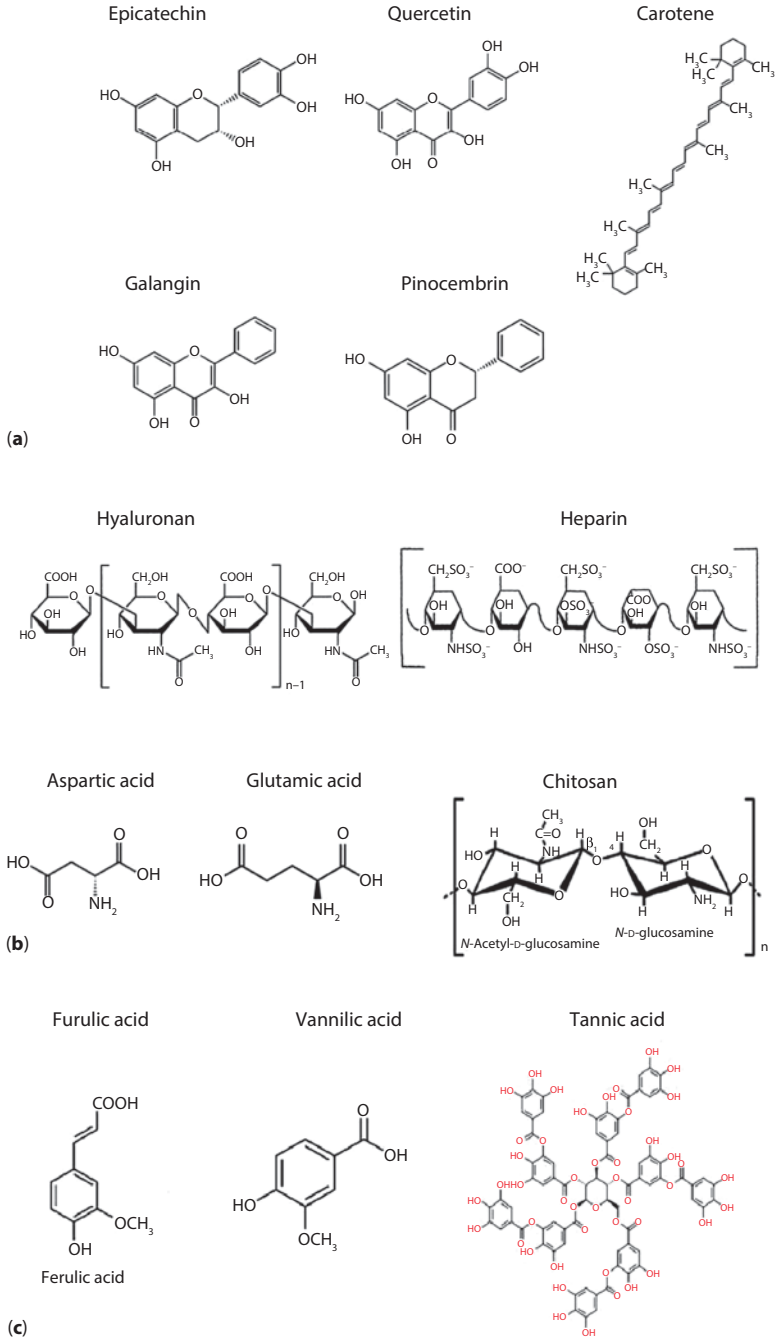


Figure 11.4 (a–c) Different chemical compounds of the secondary metabolites synthesized metallic nanoparticles. (Reproduced from [25]).

peel, callus, seed, and flower, are used to synthesize metallic nanoparticles in various shapes and sizes by eco-friendly biological approaches. Nevertheless, the reaction of the biosynthesis can be altered by a wide range of metal concentrations and by the amount of plant extract in the reaction medium. Thus, the shapes and sizes of the synthesized nanoparticles may be transformed [50].

11.3.3.1 Zinc Oxide Nanoparticles (ZnO NPs) Using Different Parts of Plants

Zinc oxide nanoparticles (ZnO NPs) were synthesized from the aqueous extracts of plant roots, stems, flowers, leaves, and fruits of *Melia azedarach* L. by Manokari *et al.* [57]. The plant is enriched with phenolic compounds, alkaloids, sterols, tannins, glycosides, saponins, flavonoids, and other biologically active phytocompounds. Zinc nitrate hexahydrate [$Zn(NO_3)_2.6H_2O$] was used as a precursor to synthesize ZnO nanoparticles. UV-visible spectral studies were employed for the characterization and confirmation of these synthesized ZnO nanoparticles. The test solutions showed a strong absorbance in the range of 290–330 nm. Thus, the biogenic synthesis of ZnO nanoparticles from the aqueous extract using *M. azedarach* could be explored in various fields.

Moreover, Ramesh *et al.* [58] synthesized ZnO using *Cassia auriculata* flower with $ZnNO_3$ at 60–80 °C. Furthermore, renewable leaf extract of the test plant can be used as an effective stabilizing and reducing agent for the synthesis of NPs.

Also, Zn acetate was used by Hassan *et al.* as a precursor with *Coriandrum sativum* leaf extract to synthesize ZnO nanoparticles [59]. The particle size of the green synthesized nanoparticles ranged from 9 nm to 18 nm. The synthesized ZnO nanoparticles showed high photocatalytic activity for the degradation of anthracene [59].

In addition, *Aloe barbadensis* plant gel and $Zn(NO_3)_2$ were successfully employed for the synthesis of ZnO nanoparticles at 150 °C. The size ranging from 25–40 nm, was controlled by varying the concentrations of leaf broth solution [60].

In a further study, zinc oxide nanoparticles were similarly prepared using Madar (*Calotropis procera*) latex [61]. The characterization of the synthesized zinc nanoparticles by TEM and SEM revealed that the particle size is 40 nm and the shape is spherical [61].

When zinc nitrate and *Aloe vera* leaf extract were used, highly stable and spherical zinc oxide nanoparticles were produced [62]. In this investigation, greater than 95% conversion to nanoparticles has been achieved with

aloe leaf broth concentration greater than 25%. The obtained ZnO NPs were polydisperse while the average size ranged from 25 to 40 nm. The characterization showed that the particles were found to be predominantly spherical and the particle size could be controlled by varying the concentrations of leaf broth solution [62].

Furthermore, ZnO NPs were synthesized from *Lagerstroemia speciosa* leaf extract [63]. Highly stable and hexagonal phase ZnO NPs with average particle size of 40 nm was obtained. The photocatalytic properties of the synthesized ZnO NPs were studied using UV–Vis spectroscopy by exposing methyl orange to sunlight. It was found to degrade by up to 93.5% within 2 h. The chemical oxygen demand (COD) was significantly reduced from 5600 mg/L to 374 mg/L after 100 min of solar radiation, with a removal rate at 93.3%. Meanwhile, the hemolytic activity of synthesized ZnO NPs was performed on human erythrocyte cells. The study concluded that synthesis with *L. speciosa* leaf extract provides a simple and eco-friendly method for the preparation of multifunctional properties of ZnO NPs [63].

An additional study was carried out in which zinc oxide nanoparticles were synthesized by employing aqueous flower extract of *Nyctanthes arbortristis* [64]. The flower extract was used as a biological reducing agent for synthesizing ZnO NPs from zinc acetate dihydrate. Upon synthesis under optimum conditions, the study showed that the size of these nanoparticles ranged from 12 to 32 nm. Moreover, the nanoparticles were tested for their antifungal potential and were found to be active against all five tested phytopathogens, with the lowest minimum inhibitory concentration (MIC) MIC value recorded as 16 lg/mL [64].

In a further investigation, ZnO NPs were efficiently synthesized from the leaf extract of *Ipomoea pes-caprae* [65]. The particle size of the synthesized ZnO NPs ranged from 2–20 nm. The UV–Vis spectrum absorbed peak was at 322 nm. It was found that the ZnO NPs exhibited concentration-dependent cytotoxic reactivity to Vero cells after 24 h contact. In the presence of sunlight, ZnO NPs exhibited efficient dye degradation of methylene blue. Due to the versatile properties and applications of ZnO NPs, these were widely studied by eco-friendly approaches as being green, simple and economical [65].

In an important study, green synthesis of ZnO NPs using an aqueous extract of *Tectona grandis* L. leaves was also reported [66]. In this study, zinc nitrate acts as the precursor while the leaf extract acts as the reducing agent. These synthesized ZnO NPs were characterized by using powder X-ray diffraction (PXRD) analysis. The crystalline size was calculated by the Scherrer formula. FTIR analysis proved the presence of various

functional groups in the *T. grandis* L. leaf extract as well as in the synthesized NPs. The UV–Vis absorption peak was observed at 360 nm. The calculated energy band gap was found to be 3.4 eV and dynamic light scattering (DLS) analysis proved the stability and particle size of the ZnO NPs. Meanwhile, the crystalline size, shape and surface morphology of the synthesized ZnO NPs were determined using field emission scanning electron microscopy (FE-SEM). The synthesized ZnO NPs exhibited very interesting antibacterial activity against both Gram-positive and Gram-negative bacteria and they exerted an excellent DPPH [di(phenyl)-(2,4,6-trinitrophenyl)iminoazanium] free radical scavenging activity. In addition, they showed maximum inhibition of protein denaturation (90.46 ± 0.02) and proteinase inhibitory activity (87.68 ± 0.03) at a dose of 200 μg ml^{-1} respectively. It is important to mention that the anticancer activity of ZnO NPs was tested against normal and cancer osteoblast MC3t3-E1 cell lines, with the results showing a reduction in the size of cancer cells [66].

11.3.3.2 Palladium Nanoparticles (PdNPs) Using Different Parts of Plants

For the first time, nanocrystalline palladium particles were produced using *Cinnamom zeylanicum* bark extract (CBE) as a biomaterial [67]. The characterization by transmission electron microscopy (TEM) observations confirmed the synthesis of nano-sized palladium particles. The particle size of the synthesized palladium nanoparticles ranged from 15 to 20 nm [67].

Furthermore, palladium nanoparticles were synthesized from *Solanum trilobatum* leaf extracts [68]. The *S. trilobatum* was greatly enriched with phytochemicals to reduce the palladium chloride ions. Poly-MVA, a dietary supplement based on the nontoxic chemotherapeutic lipoic acid-palladium complex (LA-Pd), has been hypothesized to be the new paradigm for cancer therapy. Lipoic acid (S-Pd Np-LA) and vitamins (S-Pd Np-Vitamin-LA) conjugated to palladium nanoparticles were synthesized from *S. trilobatum* leaf extract. These synthesized nanoparticles (S-Pd NPs, S-Pd NPs-LA, S-Pd NPs-Vitamin-LA) were characterized by UV-Vis spectroscopy, SEM and FTIR analysis. The characterization revealed that the S-Pd Np are polydisperse at different morphologies, ranging in size from 60 ~ 70 nm (S-Pd NPs), 65 ~ 80 nm (S-Pd NPs-LA) and 75 ~ 100 nm (S-Pd NPs-Vitamin-LA) [68].

Moreover, palladium nanoparticles were synthesized using a protein-rich soybean (*Glycine max*) leaf extract-based biological process [69]. Reduction of palladium ions by soybean leaf extract was examined by UV-Vis spectroscopic technique. In TEM images of palladium nanoparticles a particle size of ~ 15 nm was recorded [69].

A further study was conducted on the synthesis of Pd/Fe_3O_4, with average particle size equal to 39 nm, by using *Euphorbia condylocarpa* root and $PdCl_2$ and $FeCl_3.6H_2O$ at 60 °C [70]. The synthesized nanoparticles were magnetically recoverable and recyclable catalyst [70].

Moreover, Kalaiselvi *et al*. [71] synthesized Pd nanoparticles with spherical particle size of 38 nm using *Catharanthus* plant leaves and Pd(OAc) at 60 °C. These synthesized nanoparticles were effective in the remediation of textile wastewater effluent.

In addition, a facile and green route for the synthesis of palladium nanoparticles was carried out from palladium chloride [72]. The investigators used the nontoxic, renewable plant polymer, gum ghatti exuded from the *Anogeissus latifolia* tree as both a reducing and stabilizing agent. The synthesized nanoparticles were characterized using UV-Vis spectroscopy, transmission electron microscopy (TEM), dynamic light scattering (DLS), and X-ray diffraction (XRD) techniques. The synthesized nanoparticles exhibited excellent catalytic activity in dye degradation. The results of this study demonstrated the possible application of biogenic PdNPs as nanocatalyst in environmental remediation [72].

Ultrasonication and Andean blackberry leaf extract were also employed for the fabrication of palladium nanoparticles, and were further evaluated for their photocatalytic activity against methylene blue (MB). The synthesized nanoparticles were characterized by using UV-Vis spectroscopy, DLS, TEM, and XRD. The TEM analysis showed the formation of decahedron shape palladium nanoparticles with a diameter of 55–60 nm. In addition, the XRD confirmed their crystalline nature. It demonstrated photocatalytic decomposition of MB (> 72%, $k = 0.002164\ min^{-1}$, 10 mg/L) in an aqueous solution under solar light irradiation. From these results it was concluded that ultrasound agitated aqueous leaf extract is a simple, rapid, inexpensive method. It was thus suggested that this method should be utilized in the future as a green technology for the fabrication of PdNPs [73].

Another facile and eco-friendly synthesis of palladium nanoparticles by using an aqueous extract of aerial parts of *Origanum vulgare* L. (OV) as a bioreductant was reported by other investigators [74]. The OV plant is well known as a rich source of phenolic components. Moreover, the OV extract phytomolecules are not only accountable for the reduction and progression of nanoparticles, but also act as stabilizing agents. This was confirmed by several characterization methods that were achieved by using UV-Vis spectroscopy, XRD, EDX (X-ray spectroscopy), FTIR (Fourier-transform infrared spectroscopy), TEM, and TGA (thermal gravimetric analysis). Further, FTIR study on the PdNPs has proven that the OV does not merely represent a bioreductant but also functionalizes the Pd nanoparticles. In

addition, the green synthesized metallic palladium nanoparticles were successfully applied as catalysts for selective oxidation of alcohols [74].

An additional facile and green route method was conducted for synthesizing palladium nanoparticles using nontoxic and renewable natural black tea (*Camellia sinensis*) leaves extract as the reducing and stabilizing agent [75]. The prepared Pd@B.tea NPs catalyst was characterized by UV-Vis spectroscopy, FTIR, XRD, TEM, FE-SEM (field emission scanning electron microscopy) and EDS (energy dispersive X-ray spectroscopy). The study stated that Pd@B.tea NPs catalyst could be used as an efficient and heterogeneous catalyst for Suzuki coupling reactions between phenylboronic acid and a range of aryl halides (X=I, Br, Cl), in addition to the reduction of 4-nitrophenol (4-NP) using sodium borohydride in an eco-friendly medium. This investigation reported that excellent yields of products were obtained with a wide range of substrates. The catalyst was recycled 7 times without any significant loss of its catalytic activity [75].

11.3.3.3 Platinum Nanoparticles (PtNPs) Using Different Parts of Plants

An investigation was carried out on the leaf extract of *Diopyros kaki* as a reducing agent in the eco-friendly extracellular synthesis of platinum nanoparticles from an aqueous $H_2PtCl_6.6H_2O$ solution [76]. In this study a greater than 90% conversion of platinum ions to nanoparticles was successfully achieved. The reaction temperature was at 95 °C and a leaf broth concentration was > 10%. For the characterization of the platinum nanoparticles, a variety of methods were used, namely, inductively coupled plasma spectrometry, X-ray photoelectron spectroscopy, energy dispersive X-ray spectroscopy, transmission electron microscopy (TEM), and Fourier-transform infrared spectroscopy (FTIR). The average particle size of the synthesized nanoparticles ranged from 2 to 12 nm depending on the concentrations of the leaf broth, reaction temperature and the aqueous $PtCl_6^{2-}$. The FTIR analysis suggested that platinum nanoparticle synthesis using *D. kaki* is not an enzyme-mediated process. This was the first report of platinum nanoparticle synthesis employing a plant extract [76].

An additional successful study was carried out that synthesized platinum nanoparticles using an aqueous solution of gum kondagogu (*Cochlospermum gossypium*), which was also accomplished by other investigators [77]. In this study, both the synthesis and stabilization of colloidal Pt nanoparticles have been achieved in an aqueous medium containing gum kondagogu. The obtained colloidal suspensions were highly stable

for prolonged periods, without undergoing any oxidation. UV-Vis spectroscopy, FTIR, XRD, TEM and SEM-EDXA (scanning electron microscopy–energy dispersive X-ray analysis) techniques were employed to characterize the Pt nanoparticles. The synthesized Pt nanoparticles were in the size range of 2.4 ± 0.7 nm [77].

Furthermore, the leaf extract of *Ocimum sanctum* (Tulsi) was employed as a reducing agent for the synthesis of platinum nanoparticles using an aqueous chloroplatinic acid ($H_2PtCl_6.6H_2O$) [78]. The platinum ions were successfully converted to nanoparticles by using a Tulsi leaf broth at a reaction temperature of 100 °C. The average nanoparticle size of the platinum was 23 nm [78].

An environmentally friendly approach for the synthesis of Pt nanoparticles (NPs) was conducted by Sheny *et al.* [79] in which they used dried leaf powder of *Anacardium occidentale*. They monitored the formation of PtNPs using a UV-Vis spectrophotometer. The spectra of FTIR revealed that proteins are bound to PtNPs. Furthermore, the TEM images indicated that the particles have a crystalline, irregular rod shape. They concluded that the quantity of leaf powder plays a vital role in determining the size of the synthesized nanoparticles. These NPs exhibited good catalytic activity in the reduction of aromatic nitro-compound. The effective thermal conductivity of synthesized Pt/water nanofluid was measured and was found to be enhanced [79].

In addition, Thirumurugan *et al.* [80] investigated the biological synthesis of platinum NPs and their characterization using neem (*Azadirachta indica*) leaf extracts. The synthesized nanoparticle dispersions were characterized by UV-Vis spectrophotometry. The particle size was determined by TEM and was found to range from 5–50 nm with polydisperse small sphere to larger spheres. The spectra of FTIR measurement indicated that protein is the biomolecule which is possibly responsible for the reduction of chloroplatinic ion into PtNPs. The authors [80] proved that medicinally valuable neem (*Azadirachta indica*) extracts have the capability to synthesize PtNPs. They also mentioned that this green synthesis is an eco-friendly and cost-effective method [80].

11.3.3.4 Copper Oxide Nanoparticles (CuO NPs) Using Different Parts of Plants

Copper oxide nanoparticles (CuO NPs) were synthesized by Awwad *et al.* [81] using *Malva sylvestris* leaves with $CuCl_2.2H_2O$ at 80 °C. The synthesized nanoparticles were 5–30 nm and spherical in shape. The CuO NPs were effective against both Gram-positive and Gram-negative bacteria.

Moreover, Jayalakshmi and Yogamoorthi [82] synthesized CuO NPs using *Cassia alata* flower with $CuSO_4$ at 80 °C. The size and shape of the nanoparticles were 110–280 nm and spherical, respectively.

Vellora *et al*. [83], moreover, synthesized copper oxide nanoparticles using karaya gum and $CuCl_2.2H_2O$ at 75 °C. The average particle size was 4.8 nm. The synthesized CuO NPs exhibited antimicrobial activity against *E. coli* (MTCC443).

Furthermore, plant extract of *Terminalia arjuna* bark has been used by Yallappa *et al*. [84] for the synthesis of CuO NPs. The size of the synthesized nanoparticles was within 23 nm [84].

Naikaa *et al*. [85] synthesized copper oxide nanoparticles using *Gloriosa superba* L. leaf extract. They used 1 mL of *G. superba* L. leaves extract added to cupric nitrate and a small amount of distilled water. The prepared mixture was stirred constantly and heated in a furnace at 400 °C. The copper oxide nanoparticles were formed within 3–4 minutes.

For the same purpose, Sankar *et al*. [86] synthesized copper oxide nanoparticles by treating 5 mM cupric sulfate with Carica papaya leaf extract. The kinetics of the reaction were investigated using UV-Vis spectrophotometry. Between 250–300 nm in the UV-Vis spectrum, an intense surface plasmon resonance clearly reveals the formation of CuO NPs. The results of dynamic light scattering (DLS) and scanning electron microscopy (SEM) indicated that the mean particle size of the green synthesized CuO NPs was 140 nm and was rod-shaped. Furthermore, negative zeta potential discloses its stability at –28.9 mV. The results of Fourier-transform infrared (FTIR) spectroscopy exhibited the occurrence of bioactive functional groups that are required for the reduction of copper ions. The spectra of the X-ray diffraction (XRD) confirmed the copper oxide nanoparticles crystalline nature. Moreover, colloidal CuO NPs were found to be effective in degrading the Coomassie Brilliant Blue R-250 dye beneath the sunlight [86].

An interesting attempt was made to synthesize CuO NPs through a green and eco-friendly route using juice extract as a bioreductant. The synthesized nanoparticles were characterized through UV-Vis spectroscopy, FE-SEM (field-emission scanning electron microscopy), XRD, FTIR, and TEM (transmission electron microscopy). This synthesized CuO NPs were employed for Cr(VI) removal from water and wastewater through an adsorption process in batch mode [87].

Additional investigation was conducted to synthesize copper oxide nanoparticles using *Centella asiatica* L. leaf extracts at room temperature. The absolutely green method is free from harmful or toxic solvent. The prepared copper oxide particles were in nanoscale. Their morphology and size

were characterized by using UV-Vis spectroscopy, infrared (IR) spectroscopy, SEM, and X-ray spectroscopy (EDX). The investigators confirmed that the CuO NPs synthesized by this method can be effectively used for the photocatalytic degradation of methyl orange [88]. In the abscence of reducing agents, these NPs can reduce methyl orange to its leuco form in the aqueous medium [88].

11.3.3.5 Titanium Dioxide Nanoparticles (TiO_2 NPs) Using Different Parts of Plants

Sundrarajan and Gowri [89] synthesized titanium dioxide nanoparticles (TiO_2 NPs) via the interreaction between titanium tetra isopropoxide and ethanolic *Nyctanthes arbor-tristis* leaf extract under stirring at 50 °C for a period of 4 h. The mixer was calcined at 500 °C. TiO_2 NPS were characterized by particle size analyzer, SEM and XRD. The later revealed that the average grain size was around 100 nm. The SEM study showed that the average size of synthesized TiO_2 NPS ranged between 100–150 nm and the morphological shape was spherical.

Moreover, Hudlikar *et al*. [90] reported that TiO_2 NPS were synthesized by the reaction between latex of *Jatropha curcas* L and $TiO(OH)_2$. The characterization by TEM and XRD revealed that the size of synthesized TiO_2 NPs was 100–200 nm. The FTIR spectra of latex-capped TiO_2 NPs indicated the presence of capping/stabilizing agent, like protein/peptide material, that also prevents the TiO_2 NPs from agglomerating [90].

In addition, Marimuthu *et al*. [91] synthesized titanium dioxide nanoparticles using an aqueous extract of *Calotropis gigantea* flower with $TiO(OH)_2$ as precursor. The synthesized TiO_2 NPs were achieved with aqueous plant extract that was added with precursor and constantly magnetically stirred for 6 h. The mixture was then subjected to ultrasonication for 30 min to separate out the formed agglomerates. Characterization with SEM micrographs showed that the aggregate particles were spherical in shape with average particle size between 160 and 220 nm.

Furthermore, Santhoshkumar *et al.* [92] used the aqueous leaf extract of *Psidium guajava* mediated for the biosynthesis of TiO_2 NPs. Characterization of synthesized TiO_2 NPs by FTIR spectra exhibited prominent peaks at 3 410 cm^{-1} (alkynes), 1 578 cm^{-1}, 1 451 cm^{-1} (alkanes), and 1 123 cm^{-1} (C-O absorption). Further characterization was done by field emission scanning electron microscopy (FESEM) to determine the morphology of TiO_2 NPs, which showed nanoparticles of spherical shape and clusters with an average size of 32.58 nm. The maximum inhibition zone was observed in synthesized TiO_2 NPs (20 μg/mL) against *Staphylococcus aureus* (25 mm) as

well as *Escherichia coli* (23 mm). The synthesized nanoparticles confirmed more antibacterial activity than the standard antibiotic disk, tetracycline, which drastically reduces the chances for the development of antibiotic resistance of bacterial species. Moreover, the plant aqueous extract and synthesized TiO_2 NPs were found to exhibit maximum antioxidant activity as compared with ascorbic acid. In addition, the content of phenolic compounds (mg/g) in leaf aqueous extract and synthesized TiO_2 NPs were 85.4 and 18.3 mg TA/g, respectively [92].

In a further study, Sankar *et al*. [47] studied the possibility of amide, carboxyl and nitro groups from *Azadirachta indica* leaf extract in the synthesis of titanium dioxide nanoparticles. The average size is 124 nm with a spherical shape. They also examined the role of TiO_2 NPs as an effective photocatalyst to remediate pollutants [47].

Also, Valli [93] synthesized titanium dioxide nanoparticles by using an ethanolic extract of *Cassia auriculata* leaf. They used titanium(IV) isopropoxide for the synthesis of TiO_2 NPs. They added 50 ml ethanolic leaf extract and 4 ml titanium tetra isopropoxide under stirring at 50 °C. Characterization with FESEM indicated that the average particle size of obtaining nanoparticles was from 38–44.2 nm.

Moreover, biosynthesized TiO_2 NPs were achieved by using an aqueous solution of *Echinacea purpurea* herb extract as an interesting novel bioreduction method [94]. The biosynthesized TiO_2 NPs were characterized using UV-Vis spectroscopy, total reflection X-Ray fluorescence analysis (TXRF), Fourier transform infrared spectroscopy (FTIR), and transmission electron microscopy (TEM). The nanoparticles size was within the range of 120 nm. Furthermore, the alkaline reaction of the solution at pH 8 resulted in an increase in the absorbance at 280 nm that facilitates the growth of the number of nanoparticles in the given solution. Meanwhile, biosynthesis of TiO_2 NPs using the *E. purpurea* herb as a green resource, is pollution-free and eco-friendly [94].

Another green method was carried out to synthesize titanium nanoparticles using leaf extract of *Murraya koenigii*. FESEM and FTIR spectroscopy were used to characterize the synthesized TiO_2 NPs. Electron microscopy analysis revealed that these nanoparticles were spherical in shape. The antibacterial activity of the TiO_2 NPs was investigated against *Pseudomonas aeruginosa* and *Escherichia coli*. This investigation reveals that low concentrations of TiO_2 NPs inhibited the growth of both *P. aeruginosa* and *E. coli*, as these nanoparticles were effective against clinical pathogens, such as microorganisms, due to the presence of their hydroxyl bonds. It was concluded that the synthesized TiO_2 NPs can be used in antibiotic drugs [95].

11.3.3.6 Iron Oxide Nanoparticles (FeO NPs) Using Different Parts of Plants

Iron oxide nanoparticles (FeO NPs) were synthesized by Kumar *et al.* [96] using aqueous extracts of *Terminalia chebula* dry fruit pericarp. The synthesized FeO NPs were pure iron oxide that was stable up to 21 days, as confirmed by energy dispersive X-ray spectroscopy (EDS).

On the other hand, Wang *et al.* [97] explored the efficiency of the leaves of three Australian native plants for synthesizing FeO NPs. The three plants are *Eucalyptus tereticornis* (A), *Melaleuca nesophila* (B) and *Rosmarinus officinalis* (C). They are used as heterogeneous Fenton-like catalyst for decolorization of azo dye (Acid Black 194) and total organic carbon (TOC). The study showed that Fe-PNPs (A) exhibited a maximum removal capacity of dye followed by Fe-P NPs (B) and Fe-P NPs (C). The efficiency of removal depends on the size of the synthesized nanoparticles. Without any pH adjustment, a complete decolorization was achieved in 200 min at an initial concentration of 50 ppm of FeO NPs. These synthesized nanoparticles proved to remove more than 87% of TOC within four days [97].

In a successful attempt, highly pure hematite (α-Fe_2O_3) nanoparticles were synthesized by Ahmmad *et al.* [98]. They used green tea (*Camellia sinensis*) leaf extract. The surface area of the synthesized hematite (α-Fe_2O_3) nanoparticles, namely 22.5 m^2/g, was four times higher. Whereas the photocatalytic activities (known as the capacity to generate OH radical when irradiated with visible light) were found to be about two times higher than common available hematite nanoparticles in the commercial form. Besides which, the performance of photoelectrochemical cells was enhanced when these hematite (α-Fe_2O_3) nanoparticles were applied in a wet-type solar cell [98].

For synthesizing iron oxide nanoparticles, seed extract of *Syzygium cumini* was used as a reducing agent and sodium acetate as an electrostatic stabilizing agent by Venkateswarlu *et al.* [99]. X-ray diffraction (XRD) investigation reveals that spherical magnetic nanoparticles (SMNPs) were synthesized. Transmission electron microscopy (TEM) showed that the cubic structure was 9–20 nm in diameter. Fourier transform infrared (FTIR) spectroscopy technique confirmed the presence of polyphenols, flavonoids, and other biomolecules in the *S. cumini* seed. Brunauer–Emmett–Teller (BET) analysis found that the surface area of the synthesized iron oxide nanoparticles was 3.517 m^2/g. Also, the particles were classified as mesoporous. The average pore size of these nanoparticles was detected according to the single-point adsorption total volume at a relative pressure P/PO = 0.9905 cm^3/g. From this study it was concluded that these

synthesized nanoparticles can be employed in the field of water and wastewater remediation for the removal of toxic dyes [99].

11.3.3.7 Silver Nanoparticles (AgNPs) Using Different Parts of Plants

Silver nanoparticles (AgNPs) were synthesized by Suman *et al.* [100] using the root of *Morinda citrifolia*. The synthesized nanoparticles were characterized by UV-Vis spectroscopy at 413 nm. The formation of silver nanoparticles was, thus, clearly confirmed. The TEM analysis indicated that these silver nanoparticles are spherical in nature with a size of 30–55 nm.

In addition, Patil *et al.* [101] synthesized AgNPs using the latex-producing plant *Pergularia daemia*. Characterization and analysis of particle size showed a range from 44 to 255 nm, with average size of 123.50 nm.

Furthermore, AgNPs were synthesized by using leaf extract of *Mimusops elengi* L. at room temperature. The synthesized AgNPs were stable at 1 mM concentration of silver nitrate ($AgNO_3$) and were spherical in shape. Particle size diameter ranged from 55 to 83 nm. These AgNPs were found to possess higher antimicrobial efficacy against multidrug-resistant clinical isolates [102].

In a further successful study, reduction of silver nitrate to nanosilver particles was accomplished by using leaves and stems of Tetradenia riparia (Iboza). These leaves and stems contain various terpenoids and pyrones which can reduce the silver nitrates. UV-Vis spectra were employed for the characterization of $AgNO_3$. Characterization and analysis of particle size showed synthesized nanosilver particles at 410 nm. Scanning electron microscopy (SEM) analysis revealed aggregated spherically shaped silver nanoparticles with a size range of 20–50 nm and an average diameter of 26 nm [103].

Logaranjan *et al.* [104] synthesized silver nanoparticles using *Ficus carica* fruit extract at room temperature. The *F. carica* fruit extract was used as reducing and capping agent without adding any external reducing agents. The rate of $AgNO_3$ formation was monitored by using UV- Vis spectroscopy by measuring the absorbance at 420 nm. The particle size ranged between 20–25 nm with face-centered cubic crystal structure of AgNPs. Better antimicrobial activity was observed with AgNPs synthesized from the fruit extract method as compared with AgNPs synthesized by EDTA (ethylenediaminetetraacetic acid) [104].

Moreover, biosynthesis of AgNPs using *Cissus quadrangularis* leaf extracts within 20–30 min was reported by Valli and Vaseeharan [105]. An investigation by ultraviolet spectrum gave surface plasmon resonance

(SPR) of AgNPs at 450 nm. Characterization of the synthesized nanoparticles was accomplished by employing FTIR spectra and XRD pattern. Scanning electron microscopy (SEM) and atomic force microscopy (AFM) determined well-dispersed and spherically shaped (50–100 nm) AgNPs. Meanwhile, the antibacterial activity of AgNPs by using *C. quadrangularis* significantly controls the growth of Gram-positive and Gram-negative bacteria at a lower (10 μg/mL) minimal inhibitory concentration. In addition, the results highlighted the ambient, fast, and convenient synthesis of AgNPs by using *C. quadrangularis* extract for the possibility of controlling aquatic bacteria [105].

In the meantime, the synthesis of silver nanoparticles by using hot water olive leaf extracts (OLE) as stabilizing and reducing agent was investigated and evaluated for antibacterial activity against drug-resistant bacterial isolates [106]. The results revealed that the rate of AgNPs formation increased significantly in the basic medium by increasing the temperature. The nature of silver nanoparticles was characterized by UV-Vis spectroscopy, thermal gravimetric analysis (TGA), X-ray diffraction (XRD), and scanning electron microscopy (SEM). The AgNPs average particle size was 20–25 nm and was mostly spherical [106].

Furthermore, silver nanoparticles were synthesized by aqueous extract of *Rosa damascena* petals [107]. The study of these green synthesized nanoparticles was found to be biocompatible and possess anticancer activity against human lung adenocarcinoma [107].

Another study was conducted for preparing silver nanoparticles using aqueous extract of Neem (*Azadirachta indica*) leaves and silver salt. FTIR, XRD, optical absorption and photoluminescence (PL) and SEM were measured and analyzed. The synthesized silver nanoparticles exhibit the lowest energy absorption band at 400 nm. The effects of different parameters, including extract concentration, reactant ratio, pH, interaction time, and temperature, on the synthesis of silver nanoparticles were studied. It was found that the formation of these silver nanoparticles was greatly enhanced with time at higher temperatures and alkaline pH. In addition, the investigators [108] found that the antimicrobial properties were also enhanced. Moreover, the AgNPs showed an inhibition zone against isolated bacteria (*Escherichia coli*) from garden soil sample. Based on these results, it was concluded that the resources obtained from plants can be efficiently used in the production of silver nanoparticles and could be utilized in different fields, including nanotechnology, biomedical, etc. [108].

Furthermore, synthesized silver nanoparticles (AgNPs) were achieved by using an aqueous extract of *Cocos nucifera* (CN) mesocarp. The AgNPs photocatalytic activity was evaluated under solar irradiation. A green

method of harnessing bioactive phyto-components from the mesocarp of *C. nucifera* was employed to synthesize the AgNPs. Large-scale application of this method necessitates the maneuvering of the process parameters for increasing the conversion of silver ions to nanoparticles. These process parameters that influence the morphological characteristics of silver nanoparticles were studied, including pH of the synthesis mixture and precursor salt concentration. The nanoparticles were characterized by UV-Vis spectroscopy, EDX (energy-dispersive X-ray), FTIR, XRD, and SEM analysis. The optimum condition for synthesizing AgNPs was found to be CN extract and silver nitrate solution at a ratio of 1:4 (v/v) in the synthesis mixture. The alkaline initial pH value of the synthesis mixture was found to favor the synthesis of smaller sized monodispersed AgNPs. It is worth mentioning that solar energy was harnessed for the photocatalytic degradation of malachite green dye using silver nanoparticles obtained through this green synthesis method. The overall process aims at the eco-friendly utilization of naturally available resources for the synthesis of AgNPs and the degradation of dyes by using such nanoparticles, making it efficient in the treatment of wastewater [109].

In a further investigation, AgNPs were synthesized by using an aqueous leaf extract of *Solanum nigrum*. The formation of dark brown color of these particles confirmed the synthesis of silver nanoparticles. The synthesis of AgNPs was at the optimum by using aqueous extract and silver nitrate ($AgNO_3$) ratio of 5:95 at pH 7, 4 h reaction time, and 70 °C. The AgNPs were characterized using transmission electron microscopy that confirmed the nanoparticles are almost spherical in shape and have the mean particle size of 17.54 nm. It was concluded from this investigation that good modification of the bioprocess parameters improves the potential of the desired silver nanoparticles for particular applications [110].

11.3.3.8 Gold Nanoparticles (AuNPs) Using Different Parts of Plants

Gold nanoparticles (AuNPs) were successfully produced from auric chloride by using an aqueous extract of *Mirabilis jalapa* flowers. This flower extract acts as a reducing agent in the preparation process and encapsulating cage for the AuNPs. The production of these nanoparticles was done by the controlled reduction of Au^{3+} ion to Au^0. The gold nanoparticles were characterized by UV-Vis spectroscopy, Fourier-transform infrared spectroscopy (FTIR), X-ray diffraction (XRD), transmission electron microscopy (TEM), atomic force microscopy (AFM), and energy-dispersive X-ray

analysis (EDXA). It was concluded from this study that *M. jalapa* flowers can be a cheap source of reductant for the production of AuNPs [111].

In addition, the synthesis of AuNPs by using *Cinnamomum zeylanicum* leaf broth as a reducing agent was reported. The morphology of the nanoparticles formed was a mixture of gold nanoprisms and gold spherical structures [112].

Furthermore, stable gold nanoparticles were synthesized by Ganapuram *et al.* [113]. They used Salmalia malabarica gum as both reducing and capping agent. The successful formation of gold nanoparticles was confirmed by FTIR, UV-Vis spectroscopy, TEM, and X-ray powder diffraction (XRD). In the UV–Vis spectrum, the synthesized gold nanoparticles were characterized by a peak at 520–535 nm. The X-ray diffraction studies showed that the obtained gold nanoparticles were highly crystalline with face-centered cubic geometry. TEM results exhibited the average particle size of the synthesized gold nanoparticles at 12 ± 2 nm. FTIR analysis showed that –OH groups present in the gum matrix might be responsible for the reduction of Au^{+3} to gold nanoparticles. The synthesized gold nanoparticles also exhibited good catalytic properties in the reduction of methylene blue and Congo red [113].

Moreover, a facile synthesis of AuNPs was reported using leaf and stem extract of *Hibiscus sabdariffa*. The stability of the gold nanoparticles was studied in varying concentrations of glucose that suggested their possible application under hyperglycemic conditions [114]. The synthesized AuNPs exhibited selective toxicity towards U87 glioblastoma multiform cell line under normal and hyperglycemic conditions. This indicated the potential of using AuNPs in the development of value-added products in the biochemical industries. The possible mode of activity to synthesize nanoparticles was also studied by *in-vitro* molecular techniques [114].

Another green method was reported by Nakkala *et al.* [115] for the synthesis of gold nanoparticles (AuNPs) using *Piper longum* fruit extract (PLFE) along with data on their *in-vitro* antioxidant and catalytic activities. The catalytic activity of PL gold nanoparticles (PL AuNPs) against four organic dyes, namely methyl blue, methyl red, crystal violet, and acridine orange, was examined. The test resulted in respective degradation of 65, 28, 39, and 34% after 28 h of mixing. The authors concluded that these green nanoparticles with potent catalytic properties are useful in clearing the toxic dyes in industrial effluents [115].

In another study, gold nanoparticles were synthesized by the reduction of chloroaurate ions with the fresh leaf extract of *Justicia glauca*. The formation of gold nanoparticles was confirmed by using UV-Vis spectroscopy with surface plasmon resonance. The average size of the synthesized

gold nanoparticles was in the range of 32.5 ± 0.25. Meanwhile, a good cathodic response current was observed at the gold nanoparticles modified electrode (AuNPs-ME). Nevertheless, the unmodified electrode did not show any response in the presence of Pb^{2+}. With optimum condition, this AuNPs-ME exhibited a good response towards Pb^{2+} with a linear response range from 0.005 to 800 μM L^{-1} and the lowest detection limit of 0.07 nM L^{-1}. The fabricated sensor showed a high selectivity towards Pb^{2+} in the presence of 100-fold concentrations of other metal ions. Also, the proposed sensor showed a good practicality towards Pb^{2+} in river water samples [116].

Furthermore, a green method was employed to synthesize gold nanoparticles using aqueous *Plumeria alba* flower extract (PAFE). The study examined the use of 1% and 5% concentrations of PAFE that resulted in two different sizes of *P. alba* gold nanoparticles (PAGNPs), namely PAGNPs1 and PAGNPs2, with surface plasmon resonance (SPR) peaks at 552 and 536 nm, respectively. Size-controlled formation of gold nanoparticles was indicated by the SPR shift observed with increasing extract concentration of PAFE. The accurate size and morphology of PAGNPs1 and PAGNPs2 were detected by TEM. The results showed that the particles are spherical in shape at the size between 28 ± 5.6 and 15.6 ± 3.4 nm, respectively. In addition, the antibacterial activity of PAGNPs1 and PAGNPs2 was examined against *Escherichia coli*. The results showed that the small-sized PAGNPs2 exhibited better antibacterial activity with a 16-mm inhibition zone at a concentration of 400 μg/mL. In the meantime, the catalytic activity of PAGNPs1 and PAGNPs2 was analyzed using six hazardous dyes. The PAGNPs2 exhibited more pronounced catalytic activity than PAGNPs1. Among all of the dyes, 4-nitrophenol was quickly degraded to 4-aminophenol by PAGNPs2 within 5 min. The mechanism of catalysis in the presence of PAGNPs1 and PAGNPs2 was described as an electron transfer process from donor $NaBH_4$ to an acceptor. The investigator mentioned that this eco-friendly and facile green synthesis of nanoparticles in bulk suggested this method for potential industrial applications [117].

It is interesting to note that the bark extract of *Mimusops elengi* is rich in different types of plant secondary metabolites such as tannins, flavonoids, saponins, and triterpenoids. The bark extract of *M. elengi* was used for the green synthesis of AuNPs under very mild conditions in water at room temperature. The synthesis of the AuNPs was completed within a few minutes without any extra stabilizing or capping agents. The polyphenols present in the bark extract acted as both reducing as well as stabilizing agents. The synthesized colloidal AuNPs were characterized by X-ray diffraction, surface plasmon resonance spectroscopy, and high-resolution transmission

electron microscopy (HRTEM). The synthesized Au NPs were used as an efficient catalyst for the reduction of 3-nitrophenol and 4-nitrophenol to their corresponding aminophenol in water at room temperature [118].

Moreover, plant mediated synthesis of AuNPs by using an aqueous extract of *Momordica cochinchinensis* rhizome at room temperature as a reducing and stabilizing agent was reported. The AuNPs synthesized by this green chemical approach were characterized by energy dispersive X-ray (EDX), UV-Vis spectroscopy, TEM, FTIR, and XRD. The formation of gold NPs was observed by color changes from yellow to ruby red and was confirmed by UV-Vis spectroscopy that showed the surface plasma resonance band at 535 nm. The crystalline nature of the gold nanoparticles formed as face-centered cubic structure was evident from the XRD pattern and selected area electron diffraction (SAED). The FTIR spectrum showed the presence of different biomolecules in the *M. cochinchinensis* rhizomes aqueous extract responsible for the reduction and stabilization of the gold NPs. The phytosynthesized AuNPs were proven to have better antioxidant activity than the aqueous extract when analyzed by DPPH, NO, H_2O_2 and reducing power assay methods. In addition, the biosynthesized gold NPs showed significant inhibition of the growth of medically important pathogenic Gram-positive bacteria and Gram-negative bacteria [119].

11.3.3.9 Nickel Nanoparticles (NiNPs) Using Different Parts of Plants

An investigation into the synthesis of face-centered cubic nickel nanoparticles (NiNPs) by reducing aqueous solution of $Ni(NO_3)_2$ with aqueous leaf extract of *Medicago sativa* (alfalfa), was reported by Chen *et al.* [120]. The typical synthetic process of NiNPs involved 4 h of vigorous stirring of the precursor solution with alfalfa solution at 60 °C. The reaction was conducted at 60 °C because at room temperature it was difficult to complete the reduction of Ni(II) to Ni(0). The nanoparticles solution was then freeze-dried for 24 h in order to obtain nickel nanoparticles powder.

In another study, Pandian *et al.* [121] synthesized NiNPs by using an aqueous solution of $Ni(NO_3)_2{\cdot}6H_2O$ as precursor and leaf extract of *Ocimum sanctum* as reducing agent and stabilizing agent. The Ni(II) ions were also reduced to Ni(0) by hydrated electrons of *O. sanctum* aqueous leaf extract, thus forming Ni(0) nuclei. Such Ni(0) atoms then aggregate and nickel nanoparticles were formed. A UV-Vis spectrum of the sample was then recorded. The peak centered at 395 nm corresponding to nickel nanoparticles confirmed the formation of NiNPs. Meanwhile, an examination of XRD patterns of these nanoparticles confirmed that NiNPs have

face-centered cubic structure and the average particle size was 30 nm as calculated by the Debye-Scherrer equation. Such particle size exhibited good agreement with that calculated by TEM (particle size was 12 and 36 nm) and by SEM (particle size was 15 and 36 nm) [121].

Furthermore, Kar and Ray [122] developed a new green method for fabrication of metallic nickel nanoparticles by using the petals of *Hibiscus rosa-sinensis* as bio-template and reducing agent. The petals of *H. rosa-sinensis* flowers are porous and beneath these pores tunnels are present that supply nutrients and moisture to all parts of the petal. These pores adsorbed $NiCl_2 \cdot 6H_2O$ that subsequently was reduced to nickel nanoparticles by C_2H_4, which is one of the products obtained during pyrolysis of petals. The formation of nickel nanoparticles was confirmed by the attraction of the end product of the reaction towards the magnet. The size of the obtained nanoparticles ranged from 10 nm to 200 nm. They were coated with mesoporous carbon that prevents them from agglomerating. The synthesized nickel nanoparticles were stable even after a period of 20 days.

11.3.4 Factors Influencing the Biosynthesis of Metallic Nanoparticles

There are several factors that greatly affect the synthesis, characterization, and/or application of nanoparticles. Many investigators have reported a change in the nature of the synthesized nanoparticles according to the type of the adsorbate and the activity of the catalysts used in the synthesis process [123]. Some of these researchers have reported the dynamic nature of the synthesized nanoparticles and their types of symptoms and implications by changing the time, biosynthesis, environment, and many other factors [124]. Other important factors that affect the synthesis of the nanoparticles include temperature, pH of the solution, the concentration of the raw materials used, the concentration of the extracts used, etc. [125].

It was reported by Shankar *et al.* [126] that different concentrations of hydrogen ion responds to the different sizes and shapes of nanoparticles formation. They also mentioned that aloe vera extract produced Au-Ag core nanoparticles in various sizes and shapes by fluctuating the pH of the solvent medium [126]. Also, the size of the nanoparticles biosynthesized by alfalfa plant extract is affected by the pH [126].

Meanwhile, temperature is also an important stimulating factor for the biosynthesis of nanoparticles that affects their size and shape. As reported by Raju *et al.* [127], the formation of gold nanoparticles using leaf extract of *Cymbopogon flexuosus* revealed that high temperatures will lead to the

formation of higher spherical NPs and nanotriangles. Thus, lower reaction temperature mostly increases the nanotriangle formation [127].

It was confirmed by Sarathy *et al.* [128] that the environment plays an important role in determining the formation and nature of the synthesized nanoparticles. In many environments, each single particle quickly becomes the core-shell nanoparticles by absorbing the surrounding materials or reacting with other materials from the environment via the process of oxidation or corrosion [128]. In a biological system, the synthesized nanoparticles form a coating that makes such particles thicker and larger-sized [129]. Meanwhile, the environment can greatly affect the physical structure and chemistry of the synthesized nanoparticles. In this respect, there are a few examples that show the greatest effect that the environment has on the nature of the synthesized particles. For example, there is a fast and immediate change in the crystalline nature of zinc sulfide (ZnS) nanoparticles if the environment changes from wet to dry. In the meantime, the chemical nature of cerium nitrate nanoparticles varies in the presence of peroxide in the surrounding solution in which they are suspended [130].

Moreover, the reduction reaction time (minutes or hours) is one of the important factors in reducing ions into bulk metal at variable shapes. The optimum time period produces highest absorbance peak to identify the higher NPs concentration in the selected medium. It determines the growth conditions and formation of different NP sizes (i.e., spherical, triangular, hexagonal and rectangular) [131].

Pressure is another important factor in synthesizing the nanoparticles. It affects the shape and size of the synthesized nanoparticles when applied to the reaction medium [132]. Using biological agents, the rate of reduction of metal ions is much faster at ambient pressure conditions [133].

11.4 Green Synthesis of Metallic Nanoparticles Using Food and Agro Wastes

Utilization of food waste resources is a sustainable, effective and important eco-friendly method for managing plant wastes and biomass [134]. Nanoparticles have been successfully synthesized by using a variety of food wastes, including corn cob, *Cocos nucifera* coir, fruit seeds and peels, rice bran, wheat bran, and palm oil mill effluent [135–139]. Such food wastes are rich in biomolecules such as phenolics, flavonoids, and proteins. In the green synthesis of diverse metallic nanoparticles, food wastes can serve as bioreducing agents. In a laboratory study, food wastes used in the synthesis of silver nanoparticles include the extracts of kola

seed shell [140], kola pod [141], and cocoa pod husk [142]. Figure 11.5 exhibits some food wastes that are used for the biogenic synthesis of nanoparticles [143].

Different types of metallic nanoparticles have been successfully synthesized from food and agro-industrial wastes. Extracts from these wastes were usually used as reducing and stabilizing agents for nanoparticle synthesis with a widely diverse activities ranging from larvicidal, antioxidant, antimicrobial, and catalytic to cytotoxicity against cancer cells. Such food

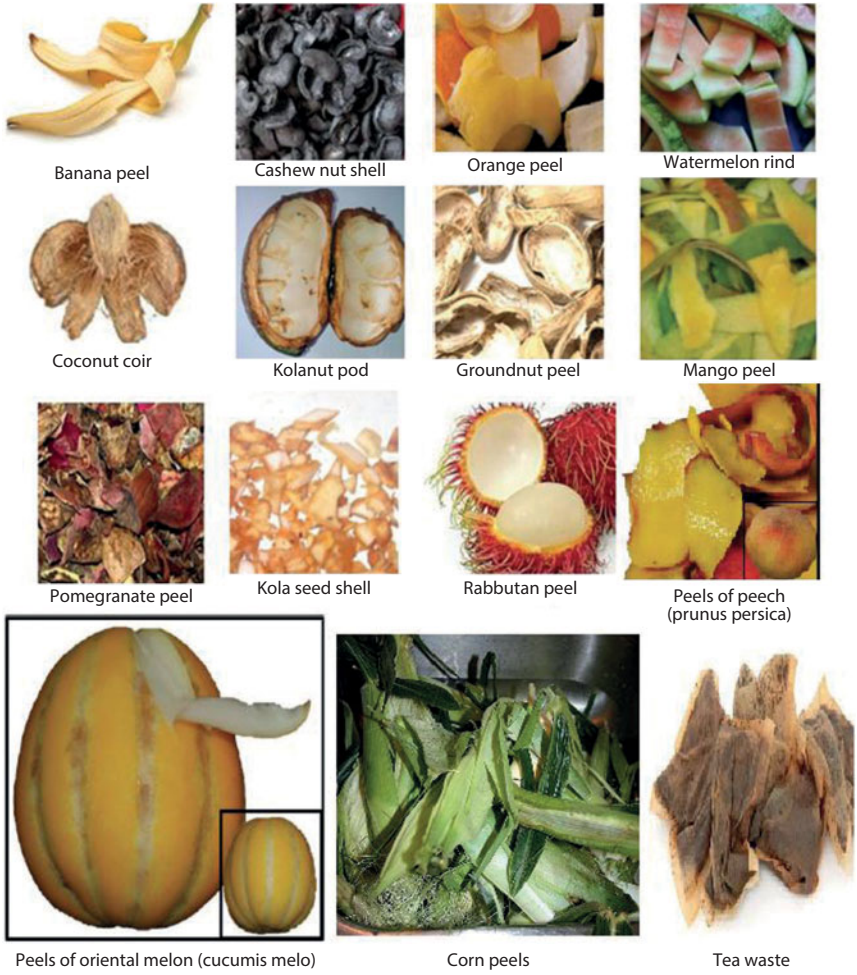


Figure 11.5 Some food wastes that are used for the biogenic synthesis of nanoparticles. (Reproduced from [143])

and agricultural wastes are abundantly produced during the processing of agricultural wastes. They are often discharged into the environment as solid waste. Mostly, they are of poor nutritional value and may even contain antinutritional factors. This limits their value or applications as animal feeds [144]. Several biotechnological processes have been developed to utilize these agro-wastes to improve their nutritional values by solid-state fermentation [144], as renewable materials for the production of biogas [145], organic acids [146], and production of enzymes [147]. Further studies were conducted for the utilization of agro-wastes as sources of biomolecules in green nanotechnology. As a result, several agro-wastes have been documented for their relevance in nanobiotechnology. Mostly, the formation of nanoparticles in these studies was obtained using extracts containing active biomolecules through the simple procedure of hot water extraction of dried and ground agro-waste materials. It is clearly evident that agro-wastes have been used extensively for the synthesis of different nanoparticles. In this respect, the abundance of agro-wastes can be successfully employed on a large scale for the biogenic synthesis of nanoparticles. The process is cost effective and can create useful products and wealth through nanotechnology. Figure 11.6 represents the mechanism of the nanoparticles formation from food and agricultural wastes extract [148].

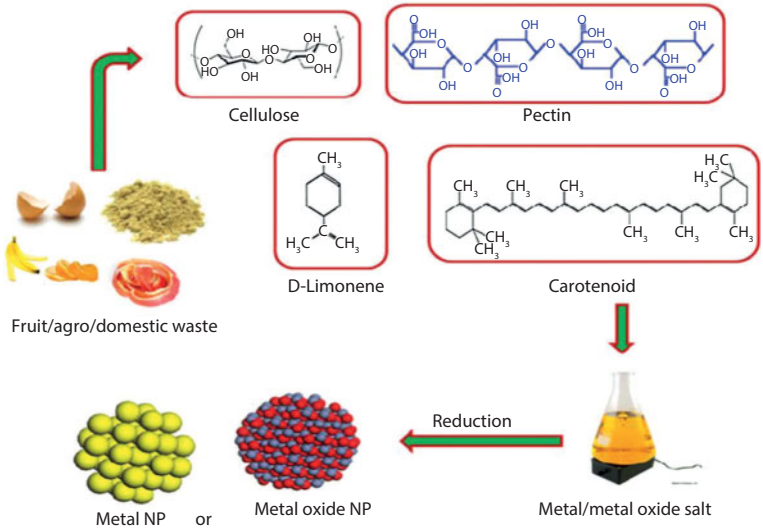


Figure 11.6 Mechanism of nanoparticles formation in the presence of food and agro waste materials. (Reproduced from [148])

11.4.1 Silver Nanoparticles (AgNps) Using Food and Agricultural Wastes

The extract of pomegranate fruit peel is an important solid waste used to reduce silver ion to form silver nanoparticles (AgNPs). The maximum absorption AgNPs was at 427 nm and they were polydisperse and spherical in shape. The ellagic acid is a naturally occurring phenolic compound abundantly present in fruit peel. The authors [149] proposed that ellagic acid was responsible for the formation of nanoparticles via its electron loss capacity. X-ray diffraction (XRD) analysis confirmed that the particles are face-centered cubic in symmetry with an average size of 5–10 nm [149].

In a similar study, Edison and Sethuraman [150] used *Punica granatum* peel extract to synthesize silver nanoparticles. The formation of these nanoparticles was confirmed by the appearance of brownish yellow color as well as the surface plasmon resonance (SPR) peak obtained at 432 nm. The particle had a distorted spherical shape of around 30 nm size, with high negative zeta potential values that revealed the high stability of the formed AgNPs. In the presence of solid sodium borohydride, the synthesized AgNPs effectively catalyzed the instantaneous reduction of anthropogenic pollutant, 4-nitrophenol (4-NP) [150].

Moreover, Kumar *et al.* [151] confirmed the synthesis of silver nanoparticles (AgNPs) by using the peel extract of *Nephelium lappaceum* L. (Rambutan). On the UV-Vis spectra, the particles showed two peaks at 370 and 495 nm, respectively. The transmission electron microscopy (TEM) confirmed the formation of triangular, truncated triangular, and hexagonal shapes with an average size of 132.6 ± 42 nm. According to selected area electron diffraction (SAED) and XRD analyses, the nanoparticles were crystalline in nature with face-centered cubic symmetry. It is worth mentioning that the free radical scavenging activity of 80% displayed by the particles against 2,2-diphenyl-1-picrylhydrazyl (DPPH) was remarkable, indicating their relevance and importance in biomedicine [151].

For silver nanoparticles formation, a biosynthetic approach by using oak fruit hull extract has also been developed [152]. The optimum reaction condition was determined as follows: $AgNO_3$ concentration, 1 mm; extract concentration, 40 g/l (4% w/v); temperature, 45 °C and pH 9. Both dynamic light scattering (DLS) and TEM showed that the synthesized AgNPs were spherical in shape with an average size of 40 nm. The zeta potential analysis indicated a long-term stability of the nanoparticles. These nanoparticles displayed mild cytotoxic activity against human breast cancer cell (MCF-7) with IC50 of 50 and 0.04 μg/ml for the isolated and dispersed silver nanoparticles in the extract, respectively.

On the other hand, Velmurugan *et al.* [153] employed defatted cashew nut shell (CNS) starch to reduce silver ion for the formation of silver nanoparticles. The synthesized nanoparticles were compared with the commercially available AgNPs. It was observed that both were structurally identical according to energy dispersive X-ray spectroscopy (EDS), FTIR and SEM analyses. However, silver was found to be predominantly responsible. Meanwhile, they both have parallel functional groups, and the particle size ranged from 10 to 50 nm. Therefore, the investigators concluded that the use of renewable, cost-effective, and eco-friendly materials is a good alternative to toxic, laborious, and expensive physical and chemical methods for the synthesis of nanoparticles.

Moreover, the synthesis of AgNPs was investigated by Kahrilas *et al.* [154] using an aqueous extract of citrus peels such as grapefruit, orange, lemon, tangelo, and lime. The synthesis of silver nanoparticles was achieved with orange peel extract within 15 min in a microwave at 90 °C and 15 psi pressure. These synthesized nanoparticles showed maximum absorbance within 402–428 nm. The transmission electron microscopy (TEM) analysis confirmed the particle size as 7.36 ± 8.06 nm. The GC-MS indicated that aldehydes present in the extract were mainly responsible for the reduction and capping of the synthesized silver nanoparticles.

In a related study, Ibrahim [155] reported the use of banana peel extract to synthesize silver nanoparticles as spherical and monodispersed AgNPs. These particles had maximum absorbance at 433 nm. The average particle size was 23.7 nm. As indicated from FTIR data, the formed AgNPs were due to the activities of pectin, proteins, hemicelluloses, and cellulose present in the extract. The AgNPs exhibited growth inhibitions of 12–20 mm against strains of *Escherichia coli, Staphylococcus aureus, Bacillus subtilis* and *Pseudomonas aeruginosa*. It was also found that AgNPs enhanced the activity of the antibiotic levofloxacin in a synergistic manner, producing a 1.16–1.32-fold improvement in antibacterial activity against the tested bacteria.

In addition, synthesis of AgNPs was carried out by Velu *et al.* [156] by reacting $AgNO_3$ solution with groundnut (*Arachis hypogaea*) peel aqueous extracts at 28 °C for 1 h. The particle size of the biosynthesized nanoparticles ranged from 20 to 50 nm. The particles are crystalline with face-centered cubic structure. The data of FTIR spectrum showed that carboxyl groups, polyphenolics, and amino acid residues and amino groups present in the extract were responsible for the formation of silver nanoparticles. The nanoparticles displayed good larvicidal activity against the fourth instar larvae of dengue (*Aedes aegypti*) and malaria (*Anopheles stephensi*) vectors with LC50 of 1.85 and 3.13 ppm, respectively, in the 24 h study.

Agro-wastes from the processing of certain tropical economic trees were utilized to synthesize nanoparticles. The aqueous extract of seed shell of *Cola nitida* was used to form spherical silver nanoparticles of 5–40 nm size [141]. The synthesized AgNPs were absorbed maximally at 454.5 nm. These nanoparticles were formed due to the catalytic roles of proteins and alkaloids in the aqueous extract. The MIC of 50 μg/ml was obtained against multidrug-resistant isolates of *Klebsiella granulomatis, P. aeruginosa* and *E. coli*.

In the meantime, the aqueous pod extract of *Cola nitida* was used to synthesize spherical silver nanoparticles from $AgNO_3$ [142]. The silver nanoparticles were absorbed maximally at 431.5 nm. The particle size ranged from 12 to 80 nm. The data of FTIR spectrum established the roles of proteins and alkaloids in the green synthesis of silver nanoparticles. At concentrations of 50–150 μg/ml, the AgNPs extract inhibited growth of *K. granulomatis, E. coli* and *P. aeruginosa* to the tune of 12–30 mm. At 5 μg/ml, complete inhibition of growth of *E. coli, S. aureus, P. aeruginosa, Aspergillus flavus, Aspergillus fumigatus* and *Aspergillus niger* were achieved in AgNPs-paint admixture, showing the potential protective role in the suppression of microbial deterioration of emulsion paint. Moreover, the silver nanoparticles showed potent antioxidant activity with IC50 of 43.98 μg/ml against DPPH, and ferric ion reduction that ranged from 13.62%–49.96%.

Recently, cocoa pod husk extract was used to synthesize spherical silver nanoparticles. The silver nanoparticles were absorbed maximally at 428.5 nm [143]. The FTIR spectrum showed that phenolics and proteins were responsible for the formation of these nanoparticles with size ranging from 4–32 nm. The synthesized nanoparticles inhibited the growth of *E. coli* and *K. pneumoniae* with zones of 10–44 mm. The improved antibacterial activities of 42.9–100% were achieved when the particles were used in synergistic studies in combination with cefuroxime and ampicillin. Also, the particles showed good DPPH scavenging (IC50 of 49.70 μg/ml), ferric ion reduction (14.44–83.94%) and *Anopheles* mosquito larvicidal (LC50 of 43.52 μg/ml) activities. In addition, it completely inhibited the growth of *E. coli, K. pneumoniae, S. aureus, Streptococcus pyogenes, P. aeruginosa, A. flavus, A. niger* and *A. fumigatus* as additives in emulsion paint.

The novel use of animal wastes, particularly hen's egg shell and membrane, have been successfully used for the green synthesis of silver nanoparticles. Apalangya *et al.* [157] reported the mechanochemical synthesis of silver nanoparticles using boiled egg shell as a source of calcium carbonate to reduce the silver ions to metallic particles. The shape of the formed particles was spherical, and the particle size ranged from 5–20 nm in dimension. The maximum absorption of AgNPs was at 461 nm, which existed as

a hybrid composite with the calcite from the egg shell. The nanocomposite exhibited good antibacterial activity against *E. coli* [157].

In a similar study, Liang *et al.* [158] used an egg membrane to synthesize silver nanoparticles through the involvement of functional groups present in the membrane. The nanocomposite AgNPs/ESM confirmed the presence of uniform distribution of small-sized AgNPs, which catalytically reduced 4NP to 4-aminophenol in the presence of borohydride [158].

11.4.2 Gold Nanoparticles (AuNPs) Using Food and Agricultural Wastes

AuNPs were synthesized by Yang and coworkers [159] using mango peel extract, with size ranging from 6.03 ± 2.77 to 18.01 ± 3.67 nm. The synthesized nanoparticles showed biocompatibility with African green monkey kidney normal cells (CV-1) and normal human fetal lung fibroblast cells (wI-38) at a high concentration of 160 μg/ml.

In another study, synthesis of gold nanoparticles using rice bran extract was reported by Malhotra and coworkers [138]. The characterization of rice bran extract by liquid chromatography-mass spectrometry (LC-MS) and high-performance liquid chromatography (HPLC) showed that ferulic acid in the extract was responsible for the reduction of Au^{3+} to Au^{0}.

Grape wastes obtained after processing have been successfully used in another remarkable study to synthesize 20–25 nm size gold nanoparticles in a single-step method at room temperature. Stable nanoparticles with maximal absorbance at 536–538 nm were synthesized within 5 min. The nanoparticles were characterized by energy-dispersive X-ray spectroscopy (EDX), high-resolution transmission electron microscopy (HRTEM), and UV-Vis spectroscopy. The investigation concluded that polyphenolic compounds, including catechin, anthocyanidin, epicatechin, condensed tannins, and proanthocyanidins, abundantly present in grape wastes could be responsible for the formation of the gold nanoparticles [160].

Moreover, the aqueous extract of watermelon rind was employed by Patra and Baek [161] for synthesis of the gold nanoparticles. They were spherical in shape, 20–140 nm in size and were absorbed maximally at 560 nm. The synthesized nanoparticles facilitated by the catalytic action of citrulline, phenolic compounds, lycopene, and flavonoids exhibited potential antibacterial activity against certain foodborne pathogens; *E. coli* ATCC 43890, *Bacillus cereus* ATCC 13061 and *Salmonella typhimurium* ATCC 43174, in the range of 9.23–11.58 mm. The combination of the nanoparticles with low concentrations of rifampicin and knamycin (5 μg/ml) led to great improvement in antibacterial activity through synergy between

the gold nanoparticles and the antibiotics. The nanoparticles also demonstrated remarkable antioxidant and anti-proteasome inhibitory potential, exhibiting potential as an anticancer agent.

A similar study by Kanchi and coworkers [162] reported a single-step green synthesis of gold nanoparticles from an aqueous extract of de-oiled *Jatropha* waste. The synthesis parameters, including the concentration of the reacting molecules as affected by temperature and pH, were optimized to favor the particle morphology. Gold nanoparticles (approximately 14 nm) of different shapes, including triangular, spherical, and hexagonal shapes, were obtained through the catalytic action of proteins present in the de-oiled *Jatropha* waste. The peak SPR of the gold nanoparticles was obtained at 520 nm.

In another study, Mohamed and coworkers [163] investigated the potential of seed shell and detoxified-defatted seed meal aqueous extracts of *Jatropha curcas* to synthesize gold nanoparticles. The synthesized nanoparticles were found to be of uniform shape and size in the range of 5–20 nm as obtained in the optimized ratio of 1:1 (seed meal/shell:chloroauric acid) under constant shaking in a water bath at 60 °C. Nevertheless, isotropic particles of pentagons, triangles, rhombi, pyramids, rods, plates, wires, needles, diamonds, spheres, truncated flakes, and gold dots were obtained upon increasing the concentration, temperature, reducing agents, and pressure. Biosynthesized gold nanoparticles were characterized by HRTEM, UV-Vis spectroscopy, atomic force microscopy (AFM), thermogravimetric analysis (TGA), and Fourier-transform infrared spectroscopy (FTIR). The nanoparticles that were absorbed maximally at 540 nm confirmed the involvement of protein molecules in the biosynthesis. The gold nanoparticles displayed a high level of biocompatibility (more than 90% cell viability of brain cancer glioma GI-1 and neuronal HCN-1A cell lines), efficient bioimaging, and photoluminescent properties. The laser exposure of cancer cells treated with gold nanoparticles led to the killing of cancer cells, thus establishing the cancer therapeutic potential of gold nanoparticles through photothermal ablation.

Furthermore, Gan and coworkers [135] successfully used palm oil mill effluent as an agro-waste for the green synthesis of gold nanoparticles. The produced nanoparticles had an average size of 18.75 ± 5.95 nm. The nanoparticles were mainly spherical, with the presence of some hexagonal, and triangular shapes [136].

In addition, Bankar and coworkers [164] studied novel banana peel mediated synthesis of gold nanoparticles with chloroauric acid as a metal precursor. The extract obtained from crushed, boiled, acetone-precipitated banana peels was used to reduce chloroauric acid to form the gold

nanoparticles. The reaction conditions, including temperature, pH, BPE contents, and concentration of chloroauric acid, were varied to favor the formation of the gold nanoparticles. The synthesized nanoparticles were confirmed by a change of color, X-ray diffraction (XRD), UV-Vis spectroscopy, FTIR, and scanning electron microscopy SEM analyses. The obtained nanoparticles possessed appreciable antimicrobial activities against the examined bacterial and fungal isolates.

Another successful attempt has been reported by Zheng *et al.* [165] by using egg shell membrane for facile green synthesis of AuNPs. The synthesized AuNPs with core size of 25 ± 7 nm were achieved by immersing the membrane in chloroauric acid under ambient conditions through the activities of aldehyde moieties present in the membrane. The synthesized gold nanoparticles were formed on the immobilized membrane and used successfully to further immobilize glucose oxidase for the sensing of glucose. The study proved that egg shell membrane can be used as an efficient agro-waste for the green synthesis of gold nanoparticles that are applicable in biosensing through complexation with glucose oxidase [165].

An additional remarkable study by Devi *et al.* [166] used egg shell membrane as a natural bio-template to synthesize fluorescent gold nanoparticles of varying triangular, truncated triangular, spherical, and hexagonal shapes. The synthesis of colloidal gold nanoparticles was successfully achieved *in situ*. The resultant nanoparticles were formed with size <20 nm. The study revealed that aldehyde and amino functional groups in the membrane were responsible mainly for the synthesis of gold nanoparticles with blue (437 ± 5 nm) and red (630 ± 5 nm) emissions, which may be suitable for application as bioimaging and biolabeling agent.

11.4.3 Zinc Oxide Nanoparticles (ZnO NPs) Using Food and Agricultural Wastes

Biogenic zinc oxide nanocrystals were synthesized by Yuvakkumar *et al.* [167] from rambutan peels. The process was as follows: zinc-ellagate complex was formed by reacting Zn $(NO_3)_2 \cdot 6H_2O$ with rambutan peel extract for 2 h at 80 °C. The zinc-ellagate complex was then oven dried at 40 °C for 8 h followed by calcination in a muffle furnace at 450 °C for the purpose of obtaining zinc oxide nanocrystals. The synthesis of zinc oxide nanocrystals was facilitated by polyphenols through the p-track conjugation effect was confirmed by employing the standard characterization studies, including scanning electron microscopy with energy dispersive X-ray spectroscopy (SEM-EDX), X-ray diffraction (XRD), Fourier-transform infrared spectroscopy (FTIR) and X-ray photoelectron spectroscopy (XPS). This

study showed that the cotton fabric coated with zinc oxide nanocrystals exhibited remarkable antibacterial activity against *E. coli* (18.5 mm) and *S. aureus* (23 mm), due to the increasing ZnO nanocrystals adsorption on the cotton surface.

Another study was carried out by Hassan *et al.* [168] in which they synthesized ZnO NPs by using tea solid waste extract mixed with Zn acetate at 80 °C. The obtained precipitates were dried at 70 °C overnight to obtain ZnO nanoparticles. The green synthesized ZnO nanoparticles was confirmed by energy-dispersive X-ray analysis (EDXA), XRD, high-resolution transmission electron microscopy (HRTEM), scanning electron microscopy (SEM), and dynamic light scattering (DLS). The average nanoparticle size was 19.5 nm. The determined zeta potential of the green synthesized ZnO nanoparticles was (–41.3) mV, which indicates good stability.

Moreover, ZnO nanoparticles were also synthesized by Karnan and Selvakumar [169] from rambutan (*Nephelium lappaceum* L.) peel extract. During this synthesis, fruit peel extract acted as a natural ligation agent. The successfully prepared nanoparticles were characterized by UV-Vis absorption spectroscopy, UV-Vis diffuse reflectance spectra (UV-Vis DRS), HRTEM, XRD, field emission scanning electron microscopy (FESEM), and N_2 adsorption-desorption isotherm. The photocatalytic activity of ZnO nanoparticles was further evaluated by photodegradation of methyl orange (MO) dye under UV light. The result depicts around 83.99% decolorization efficiency at 120 min of illumination. Besides the photo-decolorization, mineralization was also achieved. This mineralization has been confirmed by detecting the chemical oxygen demand (COD).

11.4.4 Nickel Nanoparticles (NiNPs) Using Food and Agricultural Wastes

For the first time, a successful synthesis of nickel oxide (NiO) nanocrystals was achieved via nickel ellagate complex formation by using rambutan peels [170]. In this method, the polyphenols in the extract facilitated the formation of nickel oxide nanocrystals from $Ni(NO_3)_2{\cdot}6H_2O$. The cotton fabric coated with the synthesized NiO nanocrystals exhibited strong antibacterial activity of 35 and 25 mm against *S. aureus* and *E. coli,* respectively.

11.4.5 Palladium Nanoparticles (PdNPs) Using Food and Agricultural Wastes

Palladium nanoparticles (PdNPs) were synthesized using *Annona squamosa* aqueous peel extract [171]. In this investigation, 80 ml of 1 mm palladium

acetate $Pd(OAc)_2$ was reacted with 10 ml of aqueous extract at 60 °C for 4 h. The synthesized nanoparticles were characterized by X-ray diffraction (XRD), UV-Vis spectroscopy, and transmission electron microscopy (TEM). Spherical-shaped palladium nanoparticles were confirmed. The average particle size was 100 nm. The obtained results clearly indicated that these compounds containing OH as a functional group played a critical role in capping the synthesized nanoparticles. The results also highlighted the possibility of green pathways to produce Pd nanoparticles [171].

Meanwhile, the aqueous extract from watermelon rind was used as capping and reducing agents for Pd nanoparticles by Lakshmipathy *et al.* [172]. The involvement of polyhydroxyl groups was established in the extract for the synthesis of palladium nanoparticles. The PdNPs were found to have an average size of 96.4 nm. The polydispersity index of 0.243 exhibited potential catalytic industrial applications by the Suzuki coupling reaction of aryl halide with phenyl boronic acid at room temperature [172].

In a similar study, bioinspired Pd nanoparticles were synthesized using banana peel extract (BPE) as a nontoxic eco-friendly solid waste. In this study, the boiled, crushed, acetone precipitated, air-dried peel powder was employed to reduce Pd chloride. The PdNPs were characterized by using scanning electron microscopy-energy dispersive spectra (SEM-EDS), XRD, and UV-Vis spectroscopy. Studies of dynamic light scattering (DLS) revealed that the average nanoparticle size was 50 nm. In addition, Fourier transform infrared spectroscopy (FTIR) implicated the role of carboxyl, amine and hydroxyl groups in the synthetic process [173].

11.4.6 Platinum Nanoparticles (PtNPs) Using Food and Agricultural Wastes

Recently, synthesis of platinum nanoparticles (PtNPs) was studied by Dauthal and Mukhopadhyay [174] using *Punica granatum* peel extract. The synthesized PtNPs were crystalline and spherical with a particle size range of 16–23 nm. The negative zeta potential of the platinum nanoparticles indicated high stability. Characterization using Fourier transform infrared spectroscopy (FTIR) analysis indicated that the hydroxyl and carbonyl functional groups present in polyphenolic compounds and the quinones of the peel extract were responsible for the capping and stabilization of the synthesized nanoparticles. These PtNPs displayed good catalytic activity by reducing the anthropogenic pollutant, 3-nitrophenol, by $NaBH_4$. The presence of a hydroxyl group containing compounds was found to be responsible for the catalytic action of the rambutan peel extract in the formation of Pd and Ni metallic nanoparticles.

11.4.7 Titanium Dioxide Nanoparticles (TiO_2NPs) Using Food and Agricultural Wastes

Rice straw has been employed as a lignocellulosic solid waste material for the production of titanium dioxide nanoparticles. The investigators used a sol-gel method and further modification of the pore volume and size. The study showed that the decreased particle size enhanced the surface area that made TiO_2NPs highly potential photocatalyst [175].

In a similar study, the extract of *Annona squamosa* L. peel was successfully used for the formation of polydisperse, spherically shaped and 23 ± 2 nm sized titanium dioxide nanoparticles [176].

11.4.8 Iron Oxide Nanoparticles (IONPs) Using Food and Agricultural Wastes

The synthesis of magnetic iron oxide nanoparticles IONPs (Fe_3O_4) has been achieved by using the extract of watermelon rind [177]. The synthesis reaction is as follows: $FeCl_3 \cdot 6H_2O$ was mixed with sodium acetate under continuous stirring for 3 h at 80 °C. The nanoparticles are spherically shaped as biogenic particles of 2–20 nm in size with tremendous magnetic response behavior. These nanoparticles were characterized by X-ray diffraction (XRD), UV-Vis spectroscopy, Fourier transform infrared spectroscopy (FTIR), atomic force microscopy (AFM), transmission electron microscopy (TEM), and dynamic light scattering (DLS). The particles were formed through the activities of polyphenols in the extract. They displayed remarkable catalytic activities in the organic synthesis of 2-oxo-1,2,3,4-tetra-hydro-pyrimidine derivatives with excellent yields of 94%.

In a similar study, Venkateswarlu *et al.* [178] investigated the synthesis of Fe_3O_4 magnetic nanoparticles (MNPs) through plantain peel extract. The biogenic nanoparticles were characterized by the standard analytical techniques. The particles were found to be spherical in shape and well dispersed. The TEM indicated that their size was below 50 nm. The biosynthesized iron oxide Fe_3O_4 magnetic nanoparticles displayed very good magnetic property with saturation magnetization of 15.8 emu/g.

Furthermore, synthesized Fe_2O_3 was achieved by Hassan *et al.* [179] by using pomegranate peel extract mixed with ferrous sulfate. The average particle size determined by TEM revealed that it is 2.7 nm. The green synthesized Fe_2O_3 proved to be efficient for the removal of benzo(a)pyrene and pyrene from contaminated water.

In another remarkable study, α-Fe_2O_3 nanoparticles (NPs) were prepared by using the hot water extract of mandarin (*Citrus reticulum*) peels

as an eco-friendly way to recycle domestic solid waste into a valuable product. The synthesized hematite was characterized by TGA (thermal gravimetric analysis), UV-Vis spectroscopy, XRD, TEM, SEM (scanning electron microscopy) and FTIR. The results revealed that the synthesized hematite was a porous irregular sphere-shaped NP with an average size of 20–63 nm, and that it possesses weak ferromagnetic properties and band gap (Eg) of 2.38 eV. Thus, the prepared α-Fe_2O_3 NPs expressed good photocatalytic degradation activity. Meanwhile, they exhibited a good capacity for the decontamination of polluted water from anionic and cationic dyes and dicholorophenols under visible light irradiation [180].

In a further study, Ramasahayam *et al.* [181] developed a new protocol for microwave-assisted synthesis of magnetic nanocomposite by using pine wood shavings and a spacer (saturated NaCl). In their study, tannin was the renewable resource and the microwaving process played a very important role in the production of reduced iron oxide. This reduced iron oxide nanocomposite was employed to remove phosphorus from water.

Moreover, ethanol treated orange peel powder was employed by López-Téllez *et al.* [182] to synthesize iron oxide nanorods. Cellulose content of orange peel reduced the divalent iron Fe(II) metal ions and the nanoparticles formed were stabilized on the surface of the orange peel by means of electrostatic and weak van der Waals interactions between the reduced form of metal and functional groups of cellulose and hemicellulose components.

In addition, the synthesis of superparamagnetic Fe_3O_4 nanoparticles at room temperature and atmospheric pressure was first reported by Cai *et al.* [183] by using soya bean sprouts as bio-template. This was the first time a plant template was used for magnetite nanoparticle synthesis at room temperature. It served as the nucleation site during the synthesis of nanoparticle and to control the size and morphology of nanoparticles. These nanoparticles were then simultaneously formed on the epidermal surface as well as in the interior stem wall. The synthesized nanoparticles were recovered from the template by the processes of milling, magnetic separation, washing, and drying. Characterization by FTIR analysis confirmed the role of soya bean sprout proteins and other biomolecules in nanoparticle synthesis. As synthesized nanoparticles, they possess a saturation magnetization value of 37.1 emu/g.

Another study was conducted by Njagi *et al.* [184] in which they explored the diverse phenolic compounds of sorghum bran for the synthesis of metallic iron nanoparticles. During this investigation a reaction was carried out at room temperature for 1 h by adding 0.1 M ferric chloride solution to the sorghum bran extract at the ratio 2:1 by volume. High resolution transmission electron microscopy (HRTEM) analysis indicated that

sorghum bran mediated iron nanoparticles were amorphous in nature, with a diameter of 40–50 nm. Also, the results of HRTEM revealed that the obtained nanoparticles were spherical iron, well dispersed and capped with water-soluble heterocyclic components present in the sorghum extracts. Moreover, sorghum bran mediated iron nanoparticles can be used as catalyst for the degradation of bromothymol blue.

In a further investigation, green banana peel (*Musa acuminata*) extract was used as a reducing agent to synthesize iron nanoparticles. The synthesized nanoparticles were characterized by UV-Vis spectroscopy, FTIR, and AFM. The obtained results confirmed that iron nanoparticles were produced within 2 minutes and absorption reached maximum at 207 nm. The reduction of Fe^{3+} to Fe ions was proved by FTIR spectra. Furthermore, the spectrum of FeNPs showed peaks at 3390.0, 2852.8, 1608.7, 1508.1, and 1376.7cm^{-1}. It is the characteristics of N-H amine, C-H alkanes and C=C alkenes that induce the reduction of ions. Results of AFM also showed that the structural shape of FeNPs was spherical, with different sizes. The particle size ranged from 100–200 nm [185].

11.5 Nanotechnology in Environmental Applications

Discharged industrial effluent, agricultural drainage water and sewage water are the main sources of the environmental contamination of air, water, soil, and plants at all levels. Contaminants such as pesticides, fertilizers, oil spills, and heavy metals are among the major threats to the environment [186]. Environmental pollution is one of the important issues that the world is confronting today. These pollution problems are expanding with each passing year, leading to hazardous and harmful effects on water resources, groundwater, man and the environment [187, 188].

11.5.1 Wastewater Treatment

Wastewater collection, treatment, and disposal are a big challenge to the environment. Meanwhile, wastewater and sludge treatment [189] and reuse [190] are important issues to environmental security [190]. This is mainly due to the fact that there are many factors controlling the solution of these problems. Water and soil are subjected to contamination with both organic and inorganic pollutants. The constituents of concern in domestic and municipal wastewater are: pathogens, parasites, nutrients, oxygen-demanding compounds, and suspended solids. Meanwhile, health problems, including waterborne diseases and skin irritations, may

infect people coming into direct contact with raw or inadequately treated wastewater.

Thus, reuse of inadequately treated wastewater can result in chronic health problems. Removal of heavy metals from the wastewater contributes to environmental safety [191]. Wastewater treatment and recycling for safe reuse has become an essential and valuable part of water sources in both urban and rural communities. Wastewater treatment systems include physical, chemical and biological technologies. A combination of two or more of these technologies can also be employed to achieve adequate treatment. Several traditional technologies have already been employed to remediate all types of organic, inorganic, and hazardous wastes, including sedimentation, chemical coagulation, and physical adsorption, as well as anaerobic and aerobic treatment [190, 192].

On the other hand, rapid growth of nanotechnology has gained a great deal of interest in the application of nanomaterials as a promising solution for environmental cleanup. Nanomaterials are excellent adsorbents, catalysts, and sensors due to their large specific surface areas and high reactivity. Some nanotechnology applications are nearly commercialized, including nanosensors and nanoscale coatings to replace other conventional materials, due to their great efficiency to remove pollutants from water and wastewater [193]. Besides which, nanoparticles are able to break down hazardous organics at room temperature through smart particles and a novel photocatalyst for environmental purification and cleanup.

11.5.1.1 Iron Nanoparticles in Environmental Applications

Biosynthesized iron nanoparticles were employed by Wang *et al.* [194] for treatment of eutrophic wastewater. In this study, the iron nanoparticles were biosynthesized through a one-step process at room temperature using *Eucalyptus* leaf extracts. The authors reported that this is the first study to report on utilizing nanomaterial synthesized from green tea for the remediation of eutrophic wastewater. The extract was obtained from *Eucalyptus* leaf litter. Because of the presence of different phytochemicals, each one with varied reducing power in the extract form, the synthesized nanoparticles were polydisperse. This preparation is unlike the more common practice where nanoparticles are synthesized using a chemical reducing agent. Biologically synthesized nanoparticles were used for the first time in the treatment of eutrophic wastewater. After 21 days, the rate of removal of COD, total phosphates, and total nitrogen, was 84.5%, 30.4%, and 71.7%, respectively. The reason for the very low phosphate removal

was assigned mainly to the absence of precipitating agents such as magnesium, calcium, or aluminum.

A further study was conducted by Wang *et al.* [195] in which they utilized the leaf extracts of green tea and *Eucalyptus* separately to form iron nanoparticles (FeNPs). The synthesized nanoparticles were employed efficiently for the removal of nitrate from wastewater. The different characterization techniques were used to confirm the synthesis of the spheroidal FeNPs. An interesting comparison study was carried out to investigate the efficiency of the plant-synthesized and chemically synthesized FeNPs. The comparison between green tea and *Eucalyptus* mediated FeNPs proved that the removal of nitrates from wastewater was 59.7% and 41.4%, respectively, compared to 87.6% and 11.7% by nZVI (nano zero-valent iron) and Fe_3O_4 nanoparticles, successively. Despite the highest removal efficiency by using nZVI, it was confirmed that the green synthesized FeNPs were more stable in nature. In a further interesting investigation [195], the reactivity of aged nZVI, green tea and *Eucalyptus* synthesized FeNPs was compared after being completely exposed to air for a period of two months. It was found that green tea and *Eucalyptus* synthesized FeNPs retained the same efficiency at 51.7% and 40.7%, respectively, whereas the efficiency of nZVI significantly dropped about 2.1-fold at 45.4%.

In a remarkable study, synthesis of iron nanoparticles (FeNPs) was carried out by using various leaf extracts, viz., *Mangifera indica, Murraya koenigii, Azadiracta indica, Magnolia champaca,* for domestic wastewater treatment. The characterization of the synthesized nanoparticles was conducted by UV-Vis spectrophotometry, Fourier transform infrared spectroscopy (FTIR), and scanning electron microscopy coupled with X-ray energy-dispersive spectroscopy (SEM-EDX). The characterization results confirmed the formation and presence of iron nanoparticles and biomolecules that could help in capping the FeNPs. The obtained nanoparticles were evaluated for the removal of chemical oxygen demand (COD), total phosphates, and ammonia nitrogen. Among the different plant mediated syntheses, the *A. indica* synthesized FeNPs showed removal of 82.35% chemical oxygen demand, 84.32% ammonia nitrogen, and 98.08% phosphate. Overall efficiency of *A. indica* synthesized FeNPs showed better results compared to other leaf extracts for treating the examined domestic wastewater [196].

Moreover, iron oxide (magnetite) nanoparticles were synthesized by using two abundant agro-wastes common in India [197]. These agro-wastes are turmeric (*Curcuma longa* L.) leaves and sweet lime/mosambi (*Citrus limetta*) peel. For characterization, SEM-EDX and UV-Vis spectroscopy were used to confirm the formation of iron oxide nanoparticles.

The synthesized nanoparticles using turmeric leaves (TL-FeNPs) and mosambi peel (MP-FeNPs) were examined for the removal of chemical oxygen demand (COD), ortho phosphate (PO_4), and *Escherichia coli* from domestic wastewater. TL-FeNPs exhibited better removal of organic matter (82%) and complete inhibition of *E. coli*. On the other hand, MP-FeNPs showed better removal of PO4 (65%) within 24 hours. The feasibility of this study proved that agro-wastes can be efficiently used for biosynthesis of FeNPs, which can provide a novel option for the treatment of municipal wastewater [197].

In another successful attempt, *Averrhoa carambola* extract (ACE) was exploited as a green and novel stabilizer in the synthesis of stabilized magnetite nanoparticles (SMNPs). The latter was used efficiently for the removal of Chlorazol Black E from wastewater. Meanwhile, bare magnetite nanoparticles (BMNPs) were synthesized as a reference material. The synthesized nanoparticles were characterized with X-ray diffraction (XRD), FTIR, transmission electron microscopy (TEM), energy dispersive X-ray (EDX), selected area electron diffraction (SAED), and value stream mapping (VSM) techniques. The obtained bands at 580–790 cm^{-1} and 3367 cm^{-1} correspond to Fe-O vibrations and H-bonded OH groups. Meanwhile, the obtained diffraction planes at (2 2 0), (3 1 1), (4 0 0), (4 2 2), (5 1 1) and (4 4 0) correspond to face-centered cubic Fe_3O_4. The determined average particle sizes of the BMNPs and ACE-SMNPs were 10.39 nm and 2.38 nm, respectively. From EDX spectra, the presence of both Fe and O in the nanoparticles was also confirmed. The SMNPs exhibited high saturation magnetization and low remanent magnetization, and demonstrated co-reactivity, which facilitated easy magnetic separation and reuse. The efficiency of dye removal by the ACE-SMNPs was around 98.67%, with a sequestration capacity of 38.64 mg g^{-1}. Pseudo-second-order kinetics and a Langmuir isotherm best represented the nanoparticles equilibrium data. The dye removal process was endothermic and spontaneous. This process is governed by electrostatic and H-bonding interactions. In addition, the CBE-loaded nanoparticles were effectively regenerated. The renewed material demonstrated a removal efficiency similar to the fresh nanoparticles [198].

11.5.1.2 Silver Nanoparticles in Environmental Applications

It is well known that silver nanoparticles (AgNPs) can be used for purification in water filtering apparatus. This may be due to its enhanced antimicrobial nature in contaminated water. An overview of the treatment of wastewater using AgNPs is schematically represented in Figure 11.7 [199].

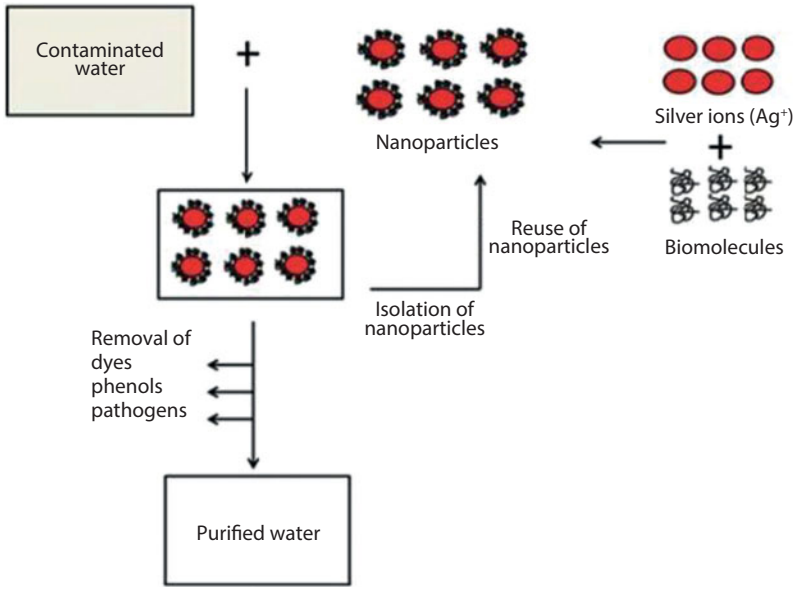


Figure 11.7 Schematic representation of plant-assisted silver nanoparticles in removing water contaminants. (Reproduced from [199])

The World Health Organization (WHO) approved the use of silver nanotechnology in water purification systems for the purpose of preventing the growth of harmful microorganisms by coating or modifying surfaces with antimicrobial agents. This advantage of AgNPs has received much consideration for application in biomedical devices and health-related fields, as well as in the food and hygiene industries. Silver and silver-containing surfaces have been widely employed as antimicrobial coatings. Such antimicrobial coatings should possess antibacterial efficacy, ease of fabrication, along with low toxicity. However, continuous exposure of these agents might lead to an increased occurrence of microbial resistance to treatment [199].

In another remarkable study, the biological synthesis of silver nanoparticles (AgNPs) using ethanoic extracts of two medicinal plants was reported [200]. This biosynthesis was carried out using *Ocimum sanctum* and *Artemesia annua* leaf extracts. The silver nitrate solution was exposed to leaf extracts, after which there was a rapid reduction of silver ions, thus leading to the formation of silver nanoparticles in the solution. The biosynthesized AgNPs were characterized by transmission electron microscopy (TEM), UV-Vis spectroscopy, high-resolution transmission electron

microscopy (HRTEM), Fourier-transform infrared spectroscopy (FTIR), X-ray diffraction (XRD), energy dispersive X-ray (EDX), and selected area electron diffraction (SAED). The *Ocimum sanctum* and *Artemesia annua* leaf extracts-assisted silver nanoparticles were investigated for their potential in removing phenols, textile dyes, and microbial contaminants from water. The silver nanoparticles from *Ocimum sanctum* were found to catalyze the reduction of 4NP within 20 min in the presence of $NaBH_4$. The biosynthesized nanoparticles can efficiently adsorb toxic textile dyes (namely: Reactive Blue 4, Reactive Orange 4, and Reactive Red 120) from aqueous solutions. Moreover, fresh water sample collected from the Yamuna River was tested and treated with the biosynthesized AgNPs. After treatment, a sharp reduction was observed in all the physical and chemical parameters, including odor, color, pH, dissolved oxygen (DO) and biochemical oxygen demand (BOD), etc., in the sample throughout the investigations. Furthermore, the antimicrobial activity of the biosynthesized AgNPs was also exploited for the removal of microbial contaminants from the water samples of the Yamuna River. The nanoparticles demonstrated excellent antimicrobial properties and could be reused repeatedly. These biosynthesized AgNPs can also remove phenols, dyes, and pathogenic bacteria from contaminated water without adding any chemicals [200].

In addition, leaf extract mediated green synthesis of silver nanoparticles (AgNPs) using *Ocimum tenuiflorum* (Black Tulsi) was carried out [201]. The silver nanoparticles were characterized using TEM and SEM (scanning electron microscopy) analysis. These silver nanoparticles were further utilized for preparing Ag nanocomposites with soil. The latter was applied as a novel nanocomposite for adsorption of reactive dye. Nevertheless, these nanocomposites were determined to possess higher efficiency in comparison to soil as adsorbent to remove reactive turquoise blue dye under the same experimental conditions. Furthermore, using these silver nanocomposites as adsorbent helped in achieving about 96.8% removal of reactive turquoise blue dye from wastewater effluent [201].

In a similar investigation, silver nanoparticles were prepared using green and wet chemical method by employing plant extract of garlic (*Allium sativum*). This extract is well known to reduce metal during synthesis and it acts as stabilizing ligand. Both synthesized silver nanoparticles (Ag_p) and (Ag_w) were applied as adsorbents in the treatment of synthetic batch mode experiments at varying parameters of temperature and pH. A concentration of 0.01 mg/L of pyrene, anthracene, and phenanthrene were induced at a fixed dosage of 1 mg/Kg of adsorbent. The residual concentration of each PAH was detected using UV-Vis spectrophotometry. The obtained results revealed that both adsorbents follow the sequence of

phenanthrene > pyrene > anthracene with optimal removal of more than 85% in each case. A distinguishing advantage was attained by Ag_p adsorbent, exhibiting 11, 3, and 3 orders of magnitude higher efficiency than Ag_w. This may be attributed to the presence of more functional groups in the plant extract participating in the binding of PAH to the surface. Each of the synthesized adsorbents were characterized by EDX, SEM and FTIR. The average particle size was determined, which was 13–26 nm. The present study concluded the use of alternate economical and green adsorbents for controlling the polyaromatic hydrocarbons (PAHs) pollutants [202].

11.5.1.3 Zinc Nanoparticles in Environmental Applications

Studies were carried out on the green synthesis of zinc nanoparticles (ZnNPs) and zinc nanobeads using an aqueous extract of the dry fruit of *Cuminum cyminum* (Jeera) [203]. The synthesized Zn nanoparticles were characterized by color change, pH change, UV-Vis spectroscopy, and particle size analysis. The synthesized nanoparticles were uniform in size and spherical, with an average diameter of about 56.8 nm, as determined by dynamic light scattering method. On the other hand, the synthesized nanobeads were efficiently employed for Alizarin Red degradation. In preliminary investigations, the nanobeads were applied for the removal of Alizarin Red dye from wastewater [203].

Similarly, ZnO nanoparticles (ZnO NPs) were synthesized in zerumbone solution by a green approach and appraised for their ability to absorb Pb(II) ions from aqueous solution. Zerumbone is a sesquiterpene found in subtropical ginger. The formation of synthesized ZnO NPs was established by UV-Vis studies, transmission electron microscopy (TEM), and X-ray diffraction (XRD). The TEM and XRD analyses proved high purity and wurtzite hexagonal structure of ZnO nanoparticles with a mean size of 10.01 ± 2.6 nm. Batch experiments were carried out to investigate the impact of process parameters, viz., Pb(II) concentration, adsorbent mass, and the variations of pH, temperature, and contact times on the removal efficiency of Pb(II). The obtained adsorption isotherm data showed that the adsorption process was mainly monolayer on ZnO nanoparticles. The adsorption process follows the kinetic model of pseudo-second-order reaction. The optimum removal efficiencies were 93% at pH 5. The thermodynamic parameters, including free energy change (ΔG^0), enthalpy change (ΔH^0), and entropy change (ΔS^0), were calculated. The adsorption processes were spontaneous and endothermic. Thus, the high efficiency of the synthesized nanoparticles makes them attractive for applications in water and wastewater treatment, for the removal of heavy metals [204].

Green chemistry was also employed in another investigation for synthesizing ZnO nanoparticles (ZnO NPs) using the extract of black tea solid waste and Zn acetate dihydrate. Human urine samples from donors under medication with propranolol, ephedrine, and ibuprofen were separated and collected using a diversion toilet. A batch experiment was carried out to determine the optimum dose of green synthesized ZnO NPs for the removal of the pharmaceutical compounds from the collected urine. The determined optimum dose of the ZnO NPs was 1.5 g/l. This study revealed that ZnO NPs possess the ability to adsorb pharmaceutical active compounds (PACs) on the nanoparticles surface. Besides which, it binds such adsorbed particles as well as facilitating their precipitation. This study was extended to a semi-pilot plant that consisted of a mixing tank for chemical coagulation using the predetermined ZnO NPs followed by a microfiltration unit. The system operated continuously for the treatment of the separated urine. The overall results of this continuous system showed that the concentration of propranolol, ephedrine and ibuprofen decreased from 15.2, 10.15, and 5.0 mg/l to 0.03, 0.10, and 0.01 mg/l respectively [168].

11.6 Conclusions

Nanoparticles can exhibit totally novel characteristics due to their high surface/volume ratio. This makes them much more reactive than bulk forms of the same materials. When in nano-sized forms, materials (e.g., metals) can exhibit properties that are completely different from those of the same material in the non-nano form. The unique characteristics of these nano-sized materials have great advantages for several applications in different fields, including pharmaceuticals, biomedicine, cosmetics, environmental, and many others. For example, certain plastics at the nanometric range possess the strength of steel.

Studies have proved that a variety of factors have a strong influence on the synthesis process. Characteristics have great influence are the size, shape, stability, and physicochemical properties of the prepared nanoparticles. The important factors that influence these characteristics include process kinetics involving the interplay between the metal ion precursors and the reducing agent, process parameters (temperature, concentrations, etc.), and adsorption kinetics involving the stabilizing agent and the nanoparticles.

Metallic nanoparticles of gold, silver, platinum, and palladium noble metals have been widely used in several applications, from cosmetics to pharmaceutical and medical products. Nanoparticles of gold have

been widely used in biomedical applications, disease diagnostics, separation, and pharmaceutical sciences. Meanwhile, the properties of silver nanoparticles are being used in biomedical applications, including antibacterial and anti-inflammatory properties to promote faster wound healing. Due to such advantageous properties, silver nanoparticles have recently been integrated into commercial wound dressings, medical implant coatings, and pharmaceutical preparations, which are all available on the market. In addition, platinum nanoparticles are also widely used in biomedical applications in a pure form or alloyed with other nanoparticles. Moreover, palladium nanoparticles have been extensively used in catalysis and electrocatalysis applications, optoelectronics, chemical sensors, and antibacterial applications. On the other hand, non-noble metallic nanoparticles, including iron, copper, zinc oxide, and selenium, are also used in medical treatments, antibacterial applications, and cosmetic formulations.

One of the most promising applications of nanotechnology is their efficiency in water, wastewater treatment and remediation. This includes different mechanisms such as adsorption of pollutants, heavy metals, removal and inactivation of pathogens, as well as diversion of toxic materials into less toxic compounds. Presently, various nanotechnologies (i.e., nanoparticles, nanopowder and nanomembrane) are being employed for the removal of chemical and biological substances such as heavy metals, nutrients (e.g., phosphate, nitrate, nitrite, and ammonia), algae (e.g., cyanobacterial toxins), viruses, bacteria, and parasites.

Acknowledgment

The authors are greatly indebted to the facilities provided by the project titled "Sustainable Development for Wastewater Treatment and Reuse via Constructed Wetlands in Sinai (SWWTR)" that is funded by the Egyptian STDF.

References

1. Matlack, A.S. (Ed.), *Introduction to Green Chemistry*, CRC Press: New York/London, 2010.
2. Dwivedi, A.D., Dubey, S.P., Sillanpää, M., Kwon, Y.N., Lee, C., Varma, R.S., Fate of engineered nanoparticles: Implications in the environment. *Coord. Chem. Rev.*, 287, 64–78, 2015.

3. Sharma, V.K., Filip, J., Zboril, R., Varma, R.S., Rizzello, L., Pompa, P.P., *et al*., Natural inorganic nanoparticles – Formation, fate, and toxicity in the environment. *Chem. Soc. Rev.,* 44, 8410–8423, 2015.
4. Varma, R.S., Greener and sustainable trends in synthesis of organics and nanomaterials. *ACS Sustain. Chem. Eng*., 4, 5866–5878, 2016.
5. Shamim, N., Sharma, V.K. (Eds.), *Sustainable Nanotechnology and the Environment: Advances and Achievements*, American Chemical Society: Washington, DC, 2013.
6. Luque, R., Varma, R.S. (Eds.), *Sustainable Preparation of Metal Nanoparticles*, Royal Society of Chemistry, Cambridge, 2012.
7. Virkutyte, J., Varma, R.S., Kumar, V., Yadav, S.K., Dahl, J.A., Maddux, B.L.S., *et al.,* Green synthesis of metal nanoparticles: Biodegradable polymers and enzymes in stabilization and surface functionalization. *Chem. Sci.*, 2, 837–846, 2011.
8. Iravani, S., Klefenz, H., Chan, W.C.W., Nie, S., Tian, Z., Ren, B., *et al.,* Green synthesis of metal nanoparticles using plants. *Green Chem.*, 13, 2638–2650, 2011.
9. Hebbalalu, D., Lalley, J., Nadagouda, M.N., Varma, R.S., Greener techniques for the synthesis of silver nanoparticles using plant extracts, enzymes, bacteria, biodegradable polymers, and microwaves. *ACS Sustain. Chem Eng.*, 1, 703–712, 2013.
10. Parveen, K., Banse, V., Ledwani, L., Green synthesis of nanoparticles: Their advantages and disadvantages. 2nd International Conference on Emerging Technologies: Micro to Nano 2015. *AIP Conf. Proc.* 1724, 020048-1–020048-7, 2015.
11. Govindaraju, K., Khaleel, B.S., Ganesh, K.V., Singaravelu, G., Silver, gold and bimetallic nanoparticles production using single-cell protein (Spirulina platensis) Geitler. *J. Mater. Sci.*, 43, 5115–5122, 2008.
12. Lengke, M.F., Fleet, M.E., Southam, G., Biosynthesis of silver nanoparticles by filamentous cyanobacteria from a silver(i) nitrate complex. *Langmuir*, 23(5), 2694–2699, 2007.
13. Kowshik, M., Deshmukh, N., Vogel, W., Urban J., Kulkarni, S.K., Paknikar, K.M., Microbial synthesis of semiconductor CdS nanoparticles, their characterization, and their use in the fabrication of an ideal diode. *Biotechnol. Bioeng*, 78(5), 583–588, 2002.
14. Rautaray, D., Ahmad, A., Sastry, M., Biosynthesis of $CaCO_3$ crystals of complex morphology using a fungus and an actinomycete. *J. Am. Chem. Soc.* 125(48), 14656–14657, 2003.
15. Anshup, A., Venkataraman, J.S, Subramaniam, C., Kumar, R.R., Priya, S., Kumar, T.R., Omkumar R.V., John, A., Pradeep T., Growth of gold nanoparticles in human cells. *Langmuir*, 21(25), 11562–11567, 2005.
16. Sastry, M., Ahmad, A., Khan, M.I., Kumar, R., Niemeyer, C.M, Mirkin, C. (Eds.), Microbial Nanoparticle Production in Nano-biotechnology, Wiley-VCH: Weinheim, 2004.

17. Krolikowska, A., Kudelski, A., Michota, A., Bukowska, J., SERS studies on the structure of thioglycolic acid monolayers on silver and gold. *Surf. Sci.*, 532, 227–232, 2003.
18. Kumar, A., Mandal, S., Selvakannan, P.R., Parischa, R., Mandale, A.B., Sastry, M., Investigation into the interaction between surface-bound alkylamines and gold nanoparticles. *Langmuir*, 19, 6277–6282, 2003.
19. Joerger, R., Klaus, T., Granqvist, C.G., Biologically produced silver–carbon composite materials for optically functional thin-film coatings. *Adv. Mater.*, 12, 407–409, 2000.
20. Oliveira, M.M., Ugarte, D., Zanchet, D., Zarbin, A.J.G., Influence of synthetic parameters on the size, structure, and stability of dodecanethiol-stabilized silver nanoparticles. *J. Colloid Interface Sci.*, 292, 429–435, 2005.
21. Pileni, M.P., Nanosized particles made in colloidal assemblies. *Langmuir*, 13, 3266–3276, 1997.
22. Gan, P.P., Ng, S.H., Huang, Y., Li, S.F.Y., Green synthesis of gold nanoparticles using palm oil mill effluent (POME): A low-cost and eco-friendly viable approach. *Bioresour. Technol.*, 113, 132–135, 2012.
23. Sathishkumar, M., Sneha, K., Won, S.W., Cho, C.W., Kim, S., Yun, Y.S., *Cinnamon zeylanicum* bark extract and powder mediated green synthesis of nano-crystalline silver particles and its bactericidal activity. *Colloids Surf. B*, 73, 332–338, 2009.
24. Iravani, S., Critical review – Green synthesis of metal nanoparticles using plants. *Green Chem.*, 13, 2638–2650, 2011.
25. Kuppusamy, P., Yusoff, M.M., Maniam, G.P., Govindan, N., Biosynthesis of metallic nanoparticles using plant derivatives and their new avenues in pharmacological applications – An updated report. *Saudi Pharm. J.*, 24, 473–484, 2016.
26. Song, J.Y., Kim, B.S., Biological synthesis of bimetallic Au/Ag nanoparticles using Persimmon (*Diospyros kaki*) leaf extract. *Korean J. Chem. Eng.,* 25, 808–811, 2009.
27. Monda, S., Roy, N., Laskar, R.A., Sk, I., Basu, S., Mandal, D., Begum, N.A., Biogenic synthesis of Ag, Au and bimetallic Au/Ag alloy nanoparticles using aqueous extract of mahogany (*Swietenia mahogani* JACQ.) leaves. *Colloids Surf. B,* 82, 497–504, 2011.
28. Bar, H., Bhui, D.K., Sahoo, G.P., Sarkar, P., De, S.P., Misra, A., Green synthesis of silver nanoparticles using latex of *Jatropha curcas*. *Colloids Surf. A,* 339, 134–139, 2009.
29. Cruz, D., Faléa, P.L., Mourato, A., Vaz, P.D., Serralheiro, M.L., Lino, A.R.L., Preparation and physicochemical characterization of Ag nanoparticles biosynthesized by *Lippia citriodora* (Lemon Verbena). *Colloids Surf. B,* 81, 67–73, 2010.
30. Aromal, S.A., Philip, D., Green synthesis of gold nanoparticles using *Trigonella foenum-graecum* and its size dependent catalytic activity. *Spectrochim. Acta A,* 97, 1–5, 2012.

31. Gurunathan, S., Kalishwaralal, K., Vaidyanathan, R., Venkataraman, D., Pandian, S.R., Muniyandi, J., Hariharan, N., Eom, S.H., Biosynthesis, purification and characterization of silver nanoparticles using *Escherichia coli*. *Colloids Surf. B,* 74, 328–335, 2009.
32. Manzer, H., Mohamed, H.S., Whaibi, A., Firoz, M., Mutahhar, Y., Khaishany, A., Siddiqui, M.H. (Eds.), *Nanoparticles and Their Impact on Plants*, Springer International Publishing, Switzerland, 2015.
33. Husen, A., Siddiqi, K.S., Phytosynthesis of nanoparticles: Concept, controversy and application. *Nanoscale Res. Lett.*, 9, 229–235, 2014.
34. Vilchis-Nestor, A.R., Trujillo-Reyes, J., Colín-Molina, J.A., SánchezMendieta, V., Avalos-Borja, M., Biogenic silver nanoparticles on carbonaceous material from sewage sludge for degradation of methylene blue in aqueous solution. *Int. J. Environ. Sci. Technol.*, 11, 977–986, 2013.
35. Netala1, V.R., Kotakadi, V.S., Domdi, L., Gaddam, S.A., Bobbu, P., Venkata, S.K., Ghosh, S.B., Tartte, V., Biogenic silver nanoparticles: Efficient and effective antifungal agents. *Appl. Nanosci.*, 6, 475–484, 2016.
36. Begum, N.A., Mondal, S., Basu, S., Laskar, R.A., Mandal, D., Biogenic synthesis of Au and Ag nanoparticles using aqueous solutions of black tea leaf extracts. *Colloids Surf. B*, 71, 113–118, 2009.
37. Parida, U.K., Bindhani, B.K., Nayak, P., Green synthesis and characterization of gold nanoparticles using onion (*Allium cepa*) extract. *World J. Nano Sci. Eng.*, 1, 93–99, 2011.
38. Markova, Z., Novak, P., Kaslik, J., Plachtova, P., Brazdova, M., Jancula, D., Siskova, K.M., Machala, L., Marsalek, B., Zboril, R., Varma, R., Iron(II,III)–polyphenol complex nanoparticles derived from green tea with remarkable eco-toxicological impact. *ACS Sustain. Chem. Eng.*, 2(7), 1674–1680, 2014.
39. Makarov, V.V., Makarova, S.S., Love, A.J., Sinitsyna, O.V., Dudnik, A.O., Yaminsky, I.V., *et al.,* Biosynthesis of stable iron oxide nanoparticles in aqueous extracts of *Hordeum vulgare* and *Rumex acetosa* plants. *Langmuir*, 30, 5982–5988, 2014.
40. Phumying, S., Labuayai, S., Thomas, C., Amornkitbamrung, V., Swatsitang, E., Maensiri, S., Aloe vera plant-extracted solution hydrothermal synthesis and magnetic properties of magnetite (Fe_3O_4) nanoparticles. *Appl Phys. A*, 111, 1187–1193, 2013.
41. Shanker, U., Jassal, V., Rani, M., Green synthesis of iron hexacyanoferrate nanoparticles: Potential candidate for the degradation of toxic PAHs. *J. Environ. Chem. Eng.,* 5(4), 4108–4120, 2017.
42. Kuang, Y., Wang, Q., Chen, Z., Megharaj, M., Naidu, R., Heterogeneous Fenton-like oxidation of monochlorobenzene using green synthesis of iron nanoparticles. *J. Colloid Interface Sci.*, 410, 67–73, 2013.
43. Elango, G., Roopan, S.M., Green synthesis, spectroscopic investigation and photocatalytic activity of lead nanoparticles. *Spectrochim. Acta A*, 139, 367–373, 2015.

44. Abdul Jalill, R.D.H., Nuaman, R.S., Abd, A.N., Biological synthesis of Titanium Dioxide nanoparticles by *Curcuma longa* plant extract and study its biological properties. *WSN*, 49(2), 204–222, 2016.
45. Kharissova, O.V., Dias, H.V.R., Kharisov, B.I., Perez, B.O., Victor, M., Perez, J., The greener synthesis of nanoparticles. *Trends Biotechnol*., 31, 240–248, 2013.
46. Rajakumara, G., Rahumana, A.A., Roopan, S.M., Khannac, V.G., Elangoa, G., Kamaraja, C., *et al.,* Fungus-mediated biosynthesis and characterization of TiO_2 nanoparticles and their activity against pathogenic bacteria. *Spectrochim. Acta A*, 91, 23–29, 2012.
47. Sankar, R., Rizwana, K., Shivashangari, K.S., Ravikumar, V., Ultra-rapid photocatalytic activity of *Azadirachta indica* engineered colloidal titanium dioxide nanoparticles. *Appl. Nanosci*., 5, 731–736, 2014.
48. Lee, H.J., Lee, G., Jang, N.R., Yun, J.M., Song, J.Y., Kim, B.S., Biological synthesis of copper nanoparticles using plant extract. *Nanotechnology*, 1, 371–376, 2011.
49. Hussain, I., Singh, N.B., Singh, A., Singh, H., Singh, S.C., Green synthesis of nanoparticles and its potential application. *Biotechnol. Lett*., 38, 545–560, 2016.
50. Dubey, S.P., Lahtinen, M., Sarkka, H., Sillanpaa, M., Bioprospective of *Sorbus aucuparia* leaf extract in development of silver and gold nanocolloids. *Colloids Surf. B*, 80, 26–33, 2010.
51. Jha, A.K., Prasad, K., Kumar, V., Prasad, K., Biosynthesis of silver nanoparticles using *Eclipta* leaf. *Biotechnol. Prog*., 25, 1475–1479, 2009.
52. Awwad, A.M., Salem, N.M., Abdeen, A.O., Green synthesis of silver nanoparticles using carob leaf extract and its antibacterial activity. *Int. J. Ind. Chem*., 4, 29–36, 2013.
53. Moulton, M.C., Braydich-Stolle, L.K., Nadagouda, M.N., Kunzelman, S., Hussaina, S.M., Varma, R.S., Synthesis, characterization and biocompatibility of "green" synthesized silver nanoparticles using tea polyphenols. *Nanoscale*, 2, 763–770, 2010.
54. Sanghi, R., Verma, P., Biomimetic synthesis and characterization of protein capped silver nanoparticles. *Bioresource Technol*., 100, 501–504, 2009.
55. Wei, D., Qian, W., Facile synthesis of Ag and Au nanoparticles utilizing chitosan as a mediator agent. *Colloids Surf. B*, 62, 136–142, 2008.
56. Nam, K.T., Lee, Y.J., Krauland, E.M., Kottmann, S.T., Belcher, A.M., Peptide mediated reduction of silver ions on engineered biological scaffolds. *ACS Nano*, 2, 1480–1486, 2008.
57. Manokari, M, Ravindran, C.P, Shekhawat, M.S., Biosynthesis of zinc oxide nanoparticles using *Melia azedarach* L. extracts and their characterization. *Int. J. Pharm. Sci. Res.*, 1(1), 31–36, 2016.
58. Ramesh, P., Rajendran, A., Shisundaram, M.M., Green synthesis of zinc oxide nanoparticles using flower extract cassia. *J. Nanosci. Nanotechnol*., 2, 41–45, 2014.

59. Hassan, S.S.M., El Azab, W.I.M., Ali, H.R., Mansour, M.S.M., Green synthesis and characterization of ZnO nanoparticles for photocatalytic degradation of anthracene. *Adv. Nat. Sci.: Nanosci. Nanotechnol*., 6, 045012 11pp., 2015.
60. Gunalan, S., Sivaraj, R., Venckatesh, R., Green synthesis of zinc oxide nanoparticles by *Aloe barbadensis* Miller leaf extract: Structure and optical properties. *Mater. Res. Bull*., 46, 2560–2566, 2011.
61. Singh, R.P., Shukla, V.K., Yadav, R.S., Sharma, P.K., Singh, P.K., Pandey, A.C., Biological approach of zinc oxide nanoparticles formation and its characterization. *Adv. Mater. Lett*., 2(4), 313–317, 2011.
62. Sangeetha, G., Rajeshwari, S., Venckatesh, R., Green synthesis of zinc oxide nanoparticles by *Aloe barbadensis* Miller leaf extract: structure and optical properties. *Mater. Res. Bull*., 46, 2560–2566, 2011.
63. Saraswathi, V.S., Tatsugi, J., Shin, P.K., Santhakumar, K., Facile biosynthesis, characterization, and solar assisted photocatalytic effect of ZnO nanoparticles mediated by leaves of *L. speciosa*. *J. Photochem. Photobiol. B*, 167, 89–98, 2017.
64. Jamdagni, P., Khatri, P., Rana, J.S., Green synthesis of zinc oxide nanoparticles using flower extract of *Nyctanthes arbor-tristis* and their antifungal activity. *J. King Saud University – Science*, 1–8, 2016.
65. Venkateasan, A., Prabakaran, R., Sujatha, V., Phyto-extract-mediated synthesis of zinc oxide nanoparticles using aqueous leaves extract of *Ipomoea pes-caprae (L).R.br* revealing its biological properties and photocatalytic activity. *Nanotechnol. Environ. Eng*., 2, 8, 2017.
66. Senthilkumar, N., Nandhakumar, E., Priya, P., Soni, D., Vimalan, M., Potheher, I.V., Synthesis of ZnO nanoparticles using leaf extract of *Tectona grandis* (L.) and their anti-bacterial, anti-arthritic, anti-oxidant and *in vitro* cytotoxicity activities. *New J. Chem.*, 41, 10347–10356, 2017.
67. Sathishkumar, M., Sneha, K., Kwak, I.S., Mao, J., Tripathy, S.J., Yun, Y.S., Phyto-crystallization of palladium through reduction process using *Cinnamom zeylanicum* bark extract. *J. Hazard. Mater*., 171(1–3), 400–404, 2009.
68. Kanchana, A., Devarajan, S., Ayyappan, S.R., Green synthesis and characterization of palladium nanoparticles and its conjugates from *Solanum trilobatum* leaf extract. *NanoMicro Lett*., 2, 169–176, 2010.
69. Petla, R.K., Vivekanandhan, S., Misra, M., Mohanty, A.K., Satyanarayana, N., Soybean (*Glycine max*) leaf extract based green synthesis of palladium nanoparticles. *J. Biomater. Nanobiotechnol.*, 3, 14–19, 2012.
70. Nasrollahzadeha, M., Sajadib, S.M., Vartoonia, A.R., Khalajc, M., Green synthesis of Pd/Fe_3O_4 nanoparticles using *Euphorbia condylocarpa* M. Bieb root extract and their catalytic applications as magnetically recoverable and stable recyclable catalysts for the phosphine-free Sonogashira and Suzuki coupling reactions. *J. Mol. Catal. A*, 396, 31–39, 2015.
71. Kalaiselvi, A., Roopan, S.M., Madhumitha, G., Ramalingam, C., Elango, G., Synthesis and characterization of palladium nanoparticles using

Catharanthus roseus leaf extract and its application in the photo-catalytic degradation. *Spectrochim. Acta A*, 135, 116–119, 2015.
72. Kora, A.J., Rastogi, L., Green synthesis of palladium nanoparticles using gum ghatti (*Anogeissus latifolia*) and its application as an antioxidant and catalyst. *Arab. J. Chem.*, 2015.
73. Kumar, B., Smita, K., Cumbal, L., Debut, A., Ultrasound agitated phytofabrication of palladium nanoparticles using Andean blackberry leaf and its photocatalytic activity. *J. Saudi Chem. Soc.*, 19, 574–580, 2015.
74. Shaik, M.R., Ali, Z.J.Q., Khan, M., Kuniyil, M., Assal, M.E., Alkhathlan, H.Z., Al-Warthan, A., Siddiqui, M.R.H., Khan, M., Adil, S.F., Green synthesis and characterization of palladium nanoparticles using *Origanum vulgare* L. extract and their catalytic activity. *Molecules*, 22, 165–172, 2017.
75. Lebaschi, S., Hekmati, M., Veisi, H., Green synthesis of palladium nanoparticles mediated by black tea leaves (*Camellia sinensis*) extract: Catalytic activity in the reduction of 4 nitrophenol and Suzuki-Miyaura coupling reaction under ligand free conditions. *J Colloid Interface Sci.*, 485, 223–231, 2017.
76. Song, J.Y., Kwon, E.Y., Kim, B.S., Biological synthesis of platinum nanoparticles using *Diopyros kaki* leaf extract. *Bioprocess Biosyst. Eng.*, 33, 159–165, 2010.
77. Vinod, V.T., Saravanan, P., Sreedhar, B., Devi, D.K., Sashidhar, R.B., A facile synthesis and characterization of Ag, Au and Pt nanoparticles using a natural hydrocolloid gum kondagogu (*Cochlospermum gossypium*). *Colloids Surf. B*, 83(2), 291–298, 2011.
78. Soundarrajan, C., Sankari, A., Dhandapani, P., Maruthamuthu, S., Ravichandran, S., Sozhan, G., Palaniswamy, N., Rapid biological synthesis of platinum nanoparticles *Ocimum sanctum* for water electrolysis applications. *Bioprocess Biosyst. Eng.*, 35, 827–833, 2012.
79. Sheny, D.S., Philip, D., Mathew, J., Synthesis of platinum nanoparticles using dried *Anacardium occidentale* leaf and its catalytic and thermal applications. *Spectroscopy*, 114, 267–271, 2013.
80. Thirumurugan, A., Aswitha, P., Kiruthika, C., Nagarajan, S., Christy, A.N., Green synthesis of platinum nanoparticles using *Azadirachta indica* – An eco-friendly approach. *Materials Letters*, 170, 175–178, 2016.
81. Awwad, A.M., Albiss, B.A., Salem, N.M., Antibacterial activity of synthesized copper oxide nanoparticles using *Malva sylvestris* leaf extract. *SMU Med. J.*, 2, 91–101, 2015.
82. Jayalakshmi, and Yogamoorthi, A., Green synthesis of copper oxide nanoparticles using aqueous extract of flowers of *Cassia alata* and particles characterisation. *Int. J. Nanomater. Biostruct.*, 4, 66–71, 2014.
83. Vellora, V., Padil, T., Černík, M., Green synthesis of copper oxide nanoparticles using Gum karaya as a biotemplate and their antibacterial application. *Int. J. Nanomed.*, 8, 889–895, 2013.
84. Yallappa, S., Manjanna, J., Sindhe, M.A., Satyanarayan, N.D., Pramod, S.N., Nagaraja, K., Microwave assisted rapid synthesis and biological evaluation of

stable copper nanoparticles using *T. arjuna* bark extract. *Spectrochim. Acta A*, 110, 108–115, 2013.
85. Naikaa, H.R., Lingarajua, K., Manjunathb, K., Kumar, D., Nagarajuc, G., Sureshd, D., Nagabhushanae, H., Green synthesis of CuO nanoparticles using *Gloriosa superba* L. extract and their antibacterial activity. *J. Taibah Univ. Sci*., 9, 7–12, 2015.
86. Sankar, R., Manikandan, P., Malarvizhi, V., Fathima, T., Shivashangari, K.S., Ravikumar, Green synthesis of colloidal copper oxide nanoparticles using *Carica papaya* and its application in photocatalytic dye degradation. *Spectrochim. Acta A*, 121, 746–750, 2014.
87. Mohan, V.S., Singh, Y., Verma, D.K., Hasan, S.H., Synthesis of CuO nanoparticles through green route using *Citrus limon* juice and its application as nano-sorbent for Cr(VI) remediation: Process optimization with RSM and ANN-GA based model. *Process Saf. Environ*., 96, 156–166, 2015.
88. Devi, H.S., and Singh, T.D., Synthesis of copper oxide nanoparticles by a novel method and its application in the degradation of methyl orange. *Adv. Electr. Electron. Eng.*, 4 (1), 83–88, 2014.
89. Sundrarajan, M., Gowri, S., Green synthesis of titanium dioxide nanoparticles by *Nyctanthes arbor-tristis* leaves extract. *Chalcogenide Lett*., 8(8), 447–451, 2011.
90. Hudlikar, M., Joglekar, S., Dhaygude, M., Kodam, K., Green synthesis of TiO_2 nanoparticles by using aqueous extract of *Jatropha curcas* L. latex. *Mater. Lett*., 75, 196–199, 2012.
91. Marimuthu, S., Rahuman, A.A., Jayaseelan, C., Kirthi, V.A., Santoshkumar, T., Velayutham, K., Bagavan, A., Kamraj, C., Elango, G., Iyappan, M., Siva, C., Karthik, L., Rao, B.V.K., Acaricidal activity of synthesized titanium dioxide nanoparticles using *Calotropis gigantea* against *Rhipicephalus microplus* and *Haemaphysalis bispinosa*. *Asian Pac. J. Trop. Med*., 6, 682–688, 2013.
92. Santhoshkumar, T., Rahuman, A.A., Jayaseelan, C., Rajakumar, G., Marimuthu, S., Kirthi, A.V., Velayutham, K., Thomas, J., Venkatesan, J., Kim, S.K., Green synthesis of titanium dioxide nanoparticles using *Psidium guajava* extract and its antibacterial and antioxidant properties. *Asian Pac. J. Trop. Med.*, 7(12), 968–976, 2014.
93. Valli, G.G.S., A green method for the synthesis of titanium dioxide nanoparticles using *Cassia auriculata* leaves extract. *Eur. J. Biomed. Pharm. Sci*., 2(3), 490–497, 2015.
94. Dobrucka, R., Synthesis of titanium dioxide nanoparticles using *Echinacea purpurea* herba. *Iran. J. Pharm. Res.*, 16 (2), 753–756, 2017.
95. Farook, M.A., Mohamed, H.S.M., Sathiyaseelan, K., Venkatesan, R., Kaviyarasu, R., *Murraya koenigii* leaf extract mediated synthesis of titanium dioxide nanoparticles. *Life Science Archives*, 3(2), 953–958, 2017.
96. Kumar, K.M., Mandal, B.K., Kumar, K.S., Reddy, P.S., Sreedhar, B., Biobased green method to synthesize palladium and iron nanoparticles using *Terminalia chebula* aqueous extract. *Spectrochim. Acta A*, 102, 128–133, 2013.

97. Wang, Z., Fang, C., Megharaj, M., Characterization of iron polyphenol nanoparticles synthesized by three plant extracts and their Fenton oxidation of azo dye. *ACS Sustain. Chem. Eng.*, 2(4), 1022–1025, 2014.
98. Ahmmad, B., Leonard, K., Islam, M.S., *et al.,* Green synthesis of mesoporous hematite (α-Fe_2O_3) nanoparticles and their photocatalytic activity. *Adv. Powder Technol.*, 24(1), 160–167, 2013.
99. Venkateswarlu, S., Natesh Kumar, B., Prasad, C.H., Venkateswarlu, P., Jyothi, N.V.V., Bio-inspired green synthesis of Fe_3O_4 spherical magnetic nanoparticles using *Syzygium cumini* seed extract. *Phys. B*, 449, 67–71, 2014.
100. Suman, T.Y., Rajasree, S.R., Kanchana, A., Elizabeth, S.B., Biosynthesis, characterization and cytotoxic effect of plant mediated silver nanoparticles using *Morinda citrifolia* root extract. *Colloids Surf. B*, 106, 74–78, 2013.
101. Patil, C.D., Patil, S.V., Borase, H.P., Salunke, B.K., Salunkhe, R.B., Larvicidal activity of silver nanoparticles synthesized using *Plumeria rubra* plant latex against *Aedes aegypti* and *Anopheles stephensi*. *J. Parasitol. Res.*, 110(5), 1815–1822, 2012.
102. Prakash, P., Gnanaprakasam, P., Emmanuel, R., Arokiyaraj, S., Saravanan, M., Green synthesis of silver nanoparticles from leaf extract of *Mimusops elengi*, Linn. for enhanced antibacterial activity against multi drug resistant clinical isolates. *Colloids Surf. B,* 108, 255–259, 2013.
103. Shaika, S., Mkizea, L., Khumaloa, M., and Singh, N., Green synthesis of nanosilver particles from leaf and stem extracts of iboza (*Tetradenia riparia*). *Afr. J. Tradit. Complement Altern. Med.*, 12(6), 33–38, 2015.
104. Logaranjan, K., Devi, S., Pandian, K., Biogenic synthesis of silver nanoparticles using fruit extract of *Ficus carica* and study its antimicrobial activity. *Nano Biomed. Eng.*, 4(4), 177–182, 2012.
105. Valli, J.S., Vaseeharan, B., Biosynthesis of silver nanoparticles by *Cissus quadrangularis* extracts. *Mater. Lett.*, 82, 171–173, 2012.
106. Khalil, M.M.H., Ismail, E.H., El-Baghdady, K.Z., Mohamed, D., Green synthesis of silver nanoparticles using olive leaf extract and its antibacterial activity. *Arab. J. Chem.*, 7, 1131–1139, 2014.
107. Tripathy, A., Raichur, A.M., Chandrasekaran, N., Prathna, T.C., Mukherjee, A., Process variables in biomimetic synthesis of silver nanoparticles by aqueous extract of *Azadirachta indica* (Neem) leaves. *J. Nanopart. Res.*, 12, 237–246, 2010.
108. Verma, A., Mehata, M.S., Controllable synthesis of silver nanoparticles using Neem leaves and their antimicrobial activity. *J. Radiat. Res. Appl. Sci.*, 9, 109–115, 2016.
109. Sumi, M.B., Devadiga, A., Vidya, S.K., Saidutta, M.B., Solar photocatalytically active, engineered silver nanoparticle synthesis using aqueous extract of mesocarp of *Cocos nucifera* (Red Spicata Dwarf). *J. Exp. Nanosci.*, 12(1), 14–32, 2017.
110. Verma, A., Tyagi, S., Verma, A., Singh, J., Joshi, P., Optimization of different reaction conditions for the bio-inspired synthesis of silver nanoparticles using

aqueous extract of *Solanum nigrum* leaves. *J. Nanomater. Mol. Nanotechnol*., 6, 2–8, 2017.
111. Vankar, P.S., Bajpai, D., Preparation of gold nanoparticles from *Mirabilis jalapa* flowers. *Indian J. Biochem. Biophys*., 47, 157–161, 2010.
112. Smitha, S.L., Philip, D., Gopchandran, K.G., Green synthesis of gold nanoparticles using *Cinnamomum zeylanicum* leaf broth. *Spectrochim. Acta A*., 74(3), 735–739, 2009.
113. Ganapuram, B.R., Alle, M., Dadigala, R., Dasari, A., Maragoni, V., Guttena, V., Catalytic reduction of methylene blue and Congo red dyes using green synthesized gold nanoparticles capped by *Salmalia malabarica* gum. *Int. Nano. Lett*., 5, 215–222, 2015.
114. Mishra, P., Ray, S., Sinha, S., Das, B., Khan, I., Behera, S.K., Yun, S., Tripathy, S.K., Mishra, A., Facile bio-synthesis of gold nanoparticles by using extract of *Hibiscus sabdariffa* and evaluation of its cytotoxicity against U87 glioblastoma cells under hyperglycemic condition. *Biochem. Eng. J.*, 105, 264–272, 2016.
115. Nakkala, J.R., Mata, R., Sadras, S.R., The antioxidant and catalytic activities of green synthesized gold nanoparticles from *Piper longum* fruit extract. *Process Saf. Environ.*, 100, 288–294, 2016.
116. Karuppiah, C., Palanisamy, S., Chen, S.M., Emmanuel, R., Muthupandib, K., Prakash, P., Green synthesis of gold nanoparticles and its application for the trace level determination of painter's colic. *RSC Adv*., 5, 16284–16290, 2015.
117. Mata, R., Bhaskaran, A., Sadras, S.R., Green-synthesized gold nanoparticles from *Plumeria alba* flower extract to augment catalytic degradation of organic dyes and inhibit bacterial growth. *Particuology*, 24, 78–86, 2016.
118. Majumdar, R., Bag, B.G., Ghosh, P., *Mimusops elengi* bark extract mediated green synthesis of gold nanoparticles and study of its catalytic activity. *Appl. Nanosci*., 6, 521–528, 2016.
119. Lakshmanan, A., Umamaheswari, C., Nagarajan, N.S., A facile phyto-mediated synthesis of gold nanoparticles using aqueous extract of *Momordica cochinchinensis* rhizome and their biological activities. *J. Nanosci. Technol.*, 2(2), 76–80, 2016.
120. Chen, H., Wang, J., Huang, D., *et al.,* Plant-mediated synthesis of size-controllable Ni nanoparticles with alfalfa extract. *Mater. Lett.*, 122, 166–169, 2014.
121. Pandian, C.J., Palanivel, R., Dhananasekaran, S., Green synthesis of nickel nanoparticles using *Ocimum sanctum* and their application in dye and pollutant adsorption. *Chin. J. Chem. Eng.*, 23(8), 1307–1315, 2015.
122. Kar, A., Ray, A.K., Synthesis of nano-spherical nickel by templating hibiscus flower petals. *J. Nanosci. Nanotechnol.*, 2(2), 17–20, 2014.
123. Somorjai, G.A., Park, J.Y., Colloid science of metal nanoparticle catalysts in 2D and 3D structures. Challenges of nucleation, growth, composition, particle shape, size control and their influence on activity and selectivity. *Top. Catal.*, 49(3–4), 126–135, 2008.

124. Pennycook, T.J., McBride, J.R., Rosenthal, S.J., Pennycook, S.J., Pantelides, S.T., Dynamic fluctuations in ultra-small nanocrystals induce white light emission. *Nano Lett.*, 12(6), 3038–3042, 2012.
125. Baker, S., Rakshith, D., Kavitha, K.S., *et al.,* Plants: Emerging as nanofactories towards facile route in synthesis of nanoparticles. *BioImpacts*, 3(3), 111–115, 2013.
126. Shankar, S.S., Ahmad, A., Sastry, M., Geranium leaf assisted biosynthesis of silver nanoparticles. *Biotechnol. Prog.*, 19, 1627–1631, 2003.
127. Raju, D., Mehta, U.J., Hazra, S., Synthesis of gold nanoparticles by various leaf fractions of *Semecarpus anacardium* L. *Trees*, 25, 145–151, 2011.
128. Sarathy, V., Tratnyek, P.G., Nurmi, J.T., *et al.,* Aging of iron nanoparticles in aqueous solution: Effects on structure and reactivity. *J. Phys. Chem.*, 112(7), 2286–2293, 2008.
129. Lynch, I., Cedervall, T., Lundqvist, M., Cabaleiro-Lago, C., Linse, S., Dawson, K.A., The nanoparticle-protein complex as a biological entity; A complex fluids and surface science challenge for the 21st century. *Adv. Colloid Interface Sci.*, 167,134–135, 2007.
130. Kuchibhatla, S.V.N.T., Karakoti, A.S., Baer, D.R., *et al.,* Influence of aging and environment on nanoparticle chemistry: Implication to confnement effects in nanoceria. *J. Phys. Chem.*, 116(26), 14108–14112, 2012.
131. Rai, A.A., Singh, A., Ahmed, A., Sastry, M., Role of halide ions and temperature on the morphology of biologically synthesized gold nano-triangles. *Langmuir*, 22, 736–741, 2006.
132. Abhilash, B.D.P., Synthesis of zinc-based nanomaterials: A biological perspective. *IET Nanobiotechnol.*, 6(4), 144–148, 2012.
133. Tran, Q.H., Nguyen, V.Q., Le, A.T., Silver nanoparticles: Synthesis, properties, toxicology, applications and perspectives. *Adv. Nat. Sci.: Nanosci. Nanotech.*, 4, 033001–033009, 2013.
134. Devadiga, A., Shetty, K.V., Saidutta, M.B., Timber industry waste teak (*Tectona grandis* Linn.) leaf extract mediated synthesis of antibacterial silver nanoparticles. *Int. Nano Lett.*, 5, 205–214, 2015.
135. Gan, P.P., Ng, S.H., Huang, Y., Li, S.F.Y., Green synthesis of gold nanoparticles using palm oil mill effluent (POME): A low-cost and eco-friendly viable approach. *Bioresour. Technol.*, 113, 132–135, 2012.
136. Basavegowda, N., Lee, Y.R., Synthesis of silver nanoparticles using Satsuma mandarin (*Citrus unshiu*) peel extract: A novel approach towards waste utilization. *Mater. Lett.*, 109, 31–33, 2013.
137. Roopan, R.G., Madhumitha, G., Rahuman, A.A., Kamaraj, C., Bharathi, A., Surendra, T.V., Low-cost and eco-friendly phyto-synthesis of silver nanoparticles using *Cocos nucifera* coir extract and its larvicidal activity. *Ind. Crops Prod.*, 43, 631–635, 2013.
138. Malhotra, A., Sharma, N., Kumar, N., Dolma, K., Sharma, D., Nandanwar, H.S., Choudhury, A.R., Multi-analytical approach to understand biomineralization of gold using rice bran: A novel and economical route. *RSC Adv.*, 4, 39484–39490, 2014.

139. Harish, B.S., Uppuluri, K.B., Anbazhagan, V., Synthesis of fibrinolytic active silver nanoparticle using wheat bran xylan as a reducing and stabilizing agent. *Carbohydr. Polym.*, 132, 104–110, 2015.
140. Lateef, A., Azeez, M.A., Asafa, T.B., Yekeen, T.A., Akinboro, A., Oladipo, I.C., Ajetomobi, F.E., Gueguim-Kana, E.B., Beukes, L.S., Cola nitidamediated biogenic synthesis of silver nanoparticles using seed and seed shell extracts and evaluation of antibacterial activities. *BioNanoScience*, 5, 196–205, 2015.
141. Lateef, A., Azeez, M.A., Asafa, T.B., Yekeen, T.A., Akinboro, A., Oladipo, I.C., Azeez, L., Ajibade, S.E., Ojo, S.A., Gueguim-Kana, E.B., Beukes, L.S., Biogenic synthesis of silver nanoparticles using pod extract of *Cola nitida*: Antibacterial, antioxidant activities and application as paint additive. *J. Taibah Univ. Sci*., 10 (4), 551–562, 2016.
142. Lateef, A., Azeez, M.A., Asafa, T.B., Yekeen, T.A., Akinboro, A., Oladipo, I.C., Azeez, L, Ojo, S.A., Gueguim-Kana, E.B., Beukes, L.S., Cocoa pod extract-mediated biosynthesis of silver nanoparticles: Its antimicrobial, antioxidant and larvicidal activities. *J. Nanostruct. Chem*., 6, 159–169, 2016.
143. Adelere, I.A., Lateef, A., A novel approach to the green synthesis of metallic nanoparticles: The use of agro-wastes, enzymes, and pigments. *Nanotechnol. Rev.*, 5(6), 567–587, 2016.
144. Lateef, A., Oloke, J.K., Gueguim-Kana, E.B., Oyeniyi, S.O., Onifade, O.R., Oyeleye, A.O., Oladosu, O.C., Oyelami, A.O., Improving the quality of agro-wastes by solid state fermentation: Enhanced antioxidant activities and nutritional qualities. *World J. Microbiol. Biotechnol*., 24, 2369–2374, 2008.
145. Abdel-Shafy, H.I., Mansour, M.S.M., Biogas production as affected by heavy metals in the anaerobic digestion of sludge. *Egypt. J. Petrol.*, 23(4), 409–417, 2014.
146. Adeoye, A.O., Lateef, A., Gueguim-Kana, E.B., Optimization of citric acid production using a mutant strain of *Aspergillus niger* on cassava peel substrate. *Biocatal. Agric. Biotechnol*., 4, 568–574, 2015.
147. Lateef, A., Gueguim-Kana, E.B., Utilization of cassava wastes in the production of fructosyl transferase by *Rhizopus stolonifera* LAU 07. *Rom. Biotechnol. Lett*., 17, 7309–7316, 2012.
148. Sharma, D., Kanchi, S., Bisetty, K., Biogenic synthesis of nanoparticles: A review. *Arab. J. Chem*., 2015.
149. Ahmad, N., Sharma, S., Rai, R., Rapid green synthesis of silver and gold nanoparticles using peels of *Punica granatum*. *Adv. Mater. Lett*., 3, 376–380, 2012.
150. Edison, T.J.I., Sethuraman, M.G., Biogenic robust synthesis of silver nanoparticles using *Punica granatum* peel and its application as a green catalyst for the reduction of an anthropogenic pollutant 4-nitrophenol. *Spectrochim. Acta A*, 104, 262–264, 2013.
151. Kumar, B., Smita, K., Cumbal, L., Angulo, Y., Fabrication of silver nanoplates using *Nephelium lappaceum* (Rambutan) peel: A sustainable approach. *J. Mol. Liq.*, 211, 476–480, 2015.

152. Heydari, R., Rashidipour, M., Green synthesis of silver nanoparticles using extract of Oak fruit hull (Jaft): Synthesis and *in vitro* cytotoxic effect on MCF-7 cells. *Int. J. Breast Cancer*, 2015, 1–7, 2015.
153. Velmurugan, P., Park, J., Lee, S., Jang, J., Yi, Y., Han, S., Lee, S., Cho, K., Cho, M., Oh, B., Reduction of silver (I) using defatted cashew nut shell starch and its structural comparison with commercial product. *Carbohydr. Polym*., 133, 39–45, 2015.
154. Kahrilas, G.A., Wally, L.M., Fredrick, S.J., Hiskey, M., Prieto, A.L., Owens, J.E., Microwave-assisted green synthesis of silver nanoparticles using orange peel extract. *ACS Sustain. Chem. Eng.*, 2, 367–376, 2013.
155. Ibrahim, H.M.M., Green synthesis and characterization of silver nanoparticles using banana peel extract and their antimicrobial activity against representative microorganisms. *J. Radiat. Res. Appl. Sci*., 8, 265–275, 2015.
156. Velu, K., Elumalai, D., Hemalatha, P., Janaki, A., Babu, M., Hemavathi, M., Kaleena, P.K., Evaluation of silver nanoparticles toxicity of *Arachis hypogaea* peel extracts and its larvicidal activity against malaria and dengue vectors. *Environ. Sci. Poll. Res. Int. Res*., 22, 17769–17779, 2015.
157. Apalangya, V., Rangari, V., Tiimob, B., Jeelani, S., Samuel, T., Development of antimicrobial water filtration hybrid material from bio source calcium carbonate and silver nanoparticles. *Appl. Surf. Sci*., 295, 108–114, 2014.
158. Liang, M., Su, R., Qi, W., Yu, Y., Wang, L., He, Z., Synthesis of well dispersed Ag nanoparticles on eggshell membrane for catalytic reduction of 4-nitrophenol. *J. Mater. Sci.*, 49, 1639–1647, 2014.
159. Yang, N., Weihong, L., Hao, L., Biosynthesis of Au nanoparticles using agricultural waste mango peel extract and its *in vitro* cytotoxic effect on two normal cells. *Mater. Lett*., 134, 67–70, 2014.
160. Krishnaswamy, K., Vali, H., Orsat, V., Value-adding to grape waste: Green synthesis of gold nanoparticles. *J. Food Eng*., 142, 210–220, 2014.
161. Patra, J.K., Baek, K., Novel green synthesis of gold nanoparticles using *Citrullus lanatus* rind and investigation of proteasome inhibitory activity, antibacterial, and antioxidant potential. *Int. J. Nanomed*., 10, 7253–7260, 2015.
162. Kanchi, S., Kumar, G., Lo, A., Tseng, C., Chen, S., Lin, C., Chin, T.T., Exploitation of de-oiled Jatropha waste for gold nanoparticles synthesis: A green approach. *Arab. J. Chem*. 2014.
163. Mohamed, M.S., Baliyan, A., Veeranarayanan, S., Poulose, A.C., Nagaoka, Y., Non-destructive harvesting of biogenic gold nanoparticles from *Jatropha curcas* seed meal and shell extracts and their application as bio-diagnostic photothermal ablaters lending shine to the biodiesel byproducts. *Nanomater. Environ*., 1, 3–17, 2013.
164. Bankar, A., Joshi, B., Kumar, A.R., Ziniarde, S., Banana peel extract mediated synthesis of gold nanoparticles. *Colloids Surf. B*, 80, 45–50, 2010.
165. Zheng, B., Qian, L., Yuan, H., Xiao, D., Yang, X., Paau, M.C., Choi, M.M., Preparation of gold nanoparticles on eggshell membrane and their biosensing application. *Talanta*, 82, 177–183, 2010.

166. Devi, P.S., Banerjee, S., Chowdhury, S.R., Kumar, G.S., Eggshell membrane: A natural biotemplate to synthesize fluorescent gold nanoparticles. *RSC Adv.*, 2, 11578–11585, 2012.
167. Yuvakkumar, R., Suresh, J., Nathanael, A.J., Sundrarajan, M., Hong, S.I., Rambutan (nephelium lappaceum L.) peel extract assisted biomimetic synthesis of nickel oxide nanocrystals. *Mater. Lett.*, 128, 170–174, 2014.
168. Hassan, S.S.M., Abdel-Shafy, H.I., Mansour, M.S.M., Removal of pharmaceutical compounds from urine via chemical coagulation by green synthesized ZnO nanoparticles followed by microfiltration for safe reuse. *Arab. J. Chem.*, 2016.
169. Karnan, T., Selvakumar, S.A.S., Biosynthesis of ZnO nanoparticles using rambutan (*Nephelium lappaceum* L.) peel extract and their photocatalytic activity on methyl orange dye. *J. Mol. Struct.*, 1125(5), 358–365, 2016.
170. Yuvakkumar, R., Suresh, J., Nathanael, A.J., Sundrarajan, M., Hong, S.I., Novel green synthetic strategy to prepare ZnO nanocrystals using rambutan (*Nephelium lappaceum* L.) peel extract and its antibacterial applications. *Mater. Sci. Eng. C*, 41, 17–27, 2014.
171. Roopan, S.M., Bharathi, A., Kumar, R., Khanna, V.G., Prabhakarn, A., Acaricidal, insecticidal, and larvicidal efficacy of aqueous extract *Annona squamosa* L peel as biomaterial for the reduction of palladium salts into nanoparticles. *Colloids Surf. B*, 92, 209–212, 2012.
172. Lakshmipathy, R., Reddy, B.P., Sarada, N.C., Chidambaram, K., Pasha, S.K., Watermelon rind-mediated green synthesis of noble palladium nanoparticles: Catalytic application. *Appl. Nanosci.*, 5, 223–228, 2015.
173. Bankar, A., Joshi, B., Kumar, A.R., Zinjarde, S., Banana peel extract mediated novel route for the synthesis of palladium nanoparticles. *Mater. Lett.*, 64, 1951–1953, 2010.
174. Dauthal, P., Mukhopadhyay, M., Biofabrication, characterization, and possible bio-reduction mechanism of platinum nanoparticles mediated by agro-industrial waste and their catalytic activity. *J. Ind. Eng. Chem.*, 22, 185–191, 2015.
175. Ramimoghadam, D., Bagheri, S., Abd Hamid, S.B., Biotemplated synthesis of anatase titanium dioxide nanoparticles via lignocellulosic waste material. *BioMed Res. Int.*, 2014, 205636, 2014.
176. Roopan, S.M., Bharathi, A., Prabhakarn, A., Abdul Rahuman, A., Velayutham, K., Rajakumar, G., Padmaja, R.D., Lekshmi, M., Madhumitha, G., Efficient phyto-synthesis and structural characterization of rutile TiO_2 nanoparticles using *Annona squamosa* peel extract. *Mol. Biomol. Spectrosc.*, 98, 86–90, 2012.
177. Prasad, C., Gangadhara, S., Venkateswarlu, P., Bio-inspired green synthesis of Fe_3O_4 magnetic nanoparticles using watermelon rinds and their catalytic activity. *Appl Nanosci.*, 6, 797–802, 2016.
178. Venkateswarlu, S., Rao, Y.S., Balaji, T., Prathima, B., Jyothi, N.V.V., Biogenic synthesis of Fe_3O_4 magnetic nanoparticles using plantain peel extract. *Mater. Lett.*, 100, 241–244, 2013.

179. Hassan, S.S.M., Abdel Shafy, H.I., Mona Mansour, S.M., Removal of polycyclic aromatic hydrocarbons micropollutant from water via adsorption by green synthesized iron oxide nanoparticles. *Adv. Nat. Sci.: Nanosci. Nanotechnol.,* 9, 015006 14pp, 2018.
180. Ali, H.R., Nassar, H.N., El-Gendy, N.S., Green synthesis of α-Fe_2O_3 using *Citrus reticulum* peels extract and water decontamination from different organic pollutants. *Energ. Source. Part A*, 39(13), 1425–1434, 2017.
181. Ramasahayam, S.K., Gunawan, G., Finlay, C., Viswanathan, T., Renewable resource-based magnetic nanocomposites for removal and recovery of phosphorous from contaminated waters. *Water Air Soil Pollut.*, 223(8), 4853–4863, 2012.
182. López-Téllez, G., Balderas-Hernández, P., Barrera-Díaz, C.E., Vilchis-Nestor, A.R., Roa-Morales, G., Bilyeu, B., Green method to form iron oxide nanorods in orange peels for chromium(VI) reduction. *J. Nanosci. Nanotechnol.*, 13(3), 2354–2360, 2013.
183. Cai, Y., Shen, Y., Xie, A., Li, S., Wang, X., Green synthesis of soya bean sprouts-mediated superparamagnetic Fe_3O_4 nanoparticles. *J. Magn. Magn. Mater.*, 322(19), 2938–2943, 2010.
184. Njagi, E.C., Huang, H., Stafford, L., Genuino, H., Galindo, H.M., Collins, J.B., Hoag, G.E., Suib, S.L., Biosynthesis of iron and silver nanoparticles at room temperature using aqueous Sorghum bran extracts. *Langmuir*, 27, 264–271, 2011.
185. Sudha, K., Anitta, S., Devi, P.M., Thejomayah, G., Biosynthesis of iron nanoparticle from green banana peel extract. *Int. J. Social Sci. Interdiscipl. Res.*, 4(6), 165–171, 2015.
186. Abdel-Shafy, H.I., Aly, R.O., Wastewater management in Egypt, in: *Wastewater Reuse – Risk Assessment, Decision-Making and Environmental Security*, Zaidi, M.K. (Ed.), Springer: Netherlands, 2007.
187. Abdel-Shafy, H.I., Abdel-Sabour, M.F., Wastewater reuse for irrigation on the desert sandy soil of egypt: Long-term effect, in: *Integrated Urban Water Resources Management*, Hlavinek, P., *et al.* (Eds.), Springer: Netherlands, 2006.
188. Abdel-Shafy, H.I., Guindi, K.A., Tawfik, N.S., Groundwater Contamination as Affected by Long-Term Sewage Irrigation in Egypt, in: *Efficient Management of Wastewater and Reuse in Water Scarce Countries*, Al Baz, I., Otterpohl, R., Wendland, C. (Eds.), Springer: Netherlands, 2008.
189. Nasr, F.A., Abdel-Shafy, H.I., Biodegradation of sewage sludge: Toxic effects of heavy metals. *Environ. Manag. Health*, 3(4), 18–25, 1992.
190. Abdel-Shafy, H.I., Mansour, M.S.M., Treatment of pharmaceutical industrial wastewater via anaerobic/aerobic system for unrestricted reuse. *J. Sci. Ind. Res.,* 76, 119–127, 2017.
191. Abdel-Shafy, H.I., Chemical treatment for removal of heavy metals from industrial wastewater. *Egypt. J. Chem.*, 58(1), 1–6, 2015.

192. Abdel-Shafy, H.I., El-Khateeb, M.A., Mansour, M.S.M., Treatment of leather industrial wastewater via combined advanced oxidation and membrane filtration. *Water Sci. Tech.*, 74.3, 586–594, 2016.
193. Abdel-Shafy, H.I., Sayour, H.A., Mansour, M.S. M., Molecular imprinted membrane based on molecular imprinted nanoparticle polymers for separation of polycyclic aromatic hydrocarbons. *Polym. Adv. Technol.*, 27, 724–732, 2016.
194. Wang, T., Jin, X., Chen, Z., Megharaj, M., Naidu, R., Green synthesis of Fe nanoparticles using eucalyptus leaf extracts for treatment of eutrophic wastewater. *Sci. Total Environ.*, 466–467, 210–213, 2014.
195. Wang, T., Lin, J., Chen, Z., Megharaj, M., Naidu, R., Green synthesized iron nanoparticles by green tea and eucalyptus leaves extracts used for removal of nitrate in aqueous solution. *J. Clean. Prod.*, 83, 413–419, 2014.
196. Devatha, C.P., Thalla, A.K., Katte, S.Y., Green synthesis of iron nanoparticles using different leaf extracts for treatment of domestic waste water. *J. Clean. Prod.*, 139, 1425–1435, 2016.
197. Ahmed, J.K., Ahmaruzzaman, M., Bordoloi, M.H., Novel *Averrhoa carambola* extract stabilized magnetite nanoparticles: A green synthesis route for the removal of chlorazol black E from wastewater. *RSC Adv*., 5, 74645–74655, 2015.
198. Herlekar, M., Barve, S., Kumar, R., Biological synthesis of iron oxide nanoparticles using agro-wastes and feasibility for municipal wastewater treatment. 47th Indian Water Works Annual Convention in Kolkata, 2015.
199. Khatoon, N., Mazumder, J.A., Sardar, M., Biotechnological applications of green synthesized silver nanoparticles. *J. Nanosci. Curr. Res*., 2, 1–6, 2017.
200. Sardar, M., Khatoon, N., Green and sustainable silver nanoparticles for waste water treatment. 5th Annual Congress on Microbiology (WATTECH), Chicago, USA, 2016.
201. Abbasi, M., Saeed, F., Rafique, U., Preparation of silver nanoparticles from synthetic and natural sources: Remediation model for PAHs. *Mater. Sci. Eng.*, 60, 1–10, 2014.
202. Banerjee, P., Sau, S., Das, P., Mukhopadhyay, A., Green synthesis of silver – Nanocomposite for treatment of textile dye. *Nanosci. Technol.*, 1(2), 1–18, 2014.
203. Sirisha, S.A.D., Mary, A., Green synthesis of nanoparticle of zinc and treatment of nanobeads for waste water of alizarin red dye. *Int. J. Environ. Res. Develop.*, 6(1), 11–17, 2016.
204. Azizi, S., Shahri, M.M., Mohamad, R., Green synthesis of zinc oxide nanoparticles for enhanced adsorption of lead ions from aqueous solutions: Equilibrium, kinetic and thermodynamic studies. *Molecules*, 22(831), 1–14, 2017.

12

Green Synthesis of Silver Nanoparticles for Biomedical and Environmental Applications

Varadavenkatesan Thivaharan[1], Vinayagam Ramesh[2] and Selvaraj Raja[2]*

[1]Department of Biotechnology, Manipal Institute of Technology, Manipal Academy of Higher Education, Manipal, Karnataka, India
[2]Department of Chemical Engineering, Manipal Institute of Technology, Manipal Academy of Higher Education, Manipal, Karnataka, India

Abstract

Nanobiotechnology has been making rapid strides in diverse fields. The green techniques are straight forward in their approach, involve usage of low-cost procedures, present better reducing potential and result in near-zero contamination. Of the noble metals, silver takes the lion's share, in terms of ongoing research and published literature. Plant-mediated synthesis offers numerous advantages over chemical, thermal, sonic and microbial methods. It is possible to optimize the overall yield, size and shape of the silver nanoparticles by altering the reaction parameters. The usage of plant parts like leaves, fruits, pods, seeds, flowers and roots paves the way for an eco-friendly utilization of easily accessible raw materials. The phytochemicals in the plant extracts serve two important roles. First, they act as reducing agents for the conversion of silver in its monovalent form to zerovalent form. Second, they stabilize the nanoparticles, preventing their agglomeration and precipitation. The potential pharmaceutical applications include their antimicrobial, antibiofilm, anticoagulant, antidiabetic, antioxidant, anticancer, larvicidal, pupicidal, pediculocidal and acaricidal activities. The environmental applications include their catalytic activity against dyes and ability to detect heavy metal ions. The current chapter presents an overview of the published literature with regard to the phytosynthesis and applications of silver nanoparticles.

**Corresponding author*: rajaselvaraj@gmail.com

Suvardhan Kanchi and Shakeel Ahmed (eds.) Green Metal Nanoparticles, (387–439)
© 2018 Scrivener Publishing LLC

Keywords: Green synthesis, silver nanoparticles, antimicrobial, anticancer, antioxidant, dye degradation

12.1 Introduction

The earliest seeds of nanotechnology were sown by the American physicist Richard Feynman. With his trendsetting statement, "There's plenty of room at the bottom," that he uttered at the American Physical Society meeting on December 29, 1959, he transformed into one of most iconic scientists to carve a niche for the subject and himself. From then on, the body of scientific literature surrounding nanotechnology grew in leaps and bounds, revolutionizing many practices in its wake. The influence of nanotechnology was all-encompassing and left no field untouched.

The foremost characteristic of the nanoparticles, their size range (defined in the 1–100 nm range), led to the widespread exploitation of a plethora of nanoparticles being synthesized. When compared to the source material, the surface area of the nanoparticles was extremely high; nanoparticles were the preferred choice for a multitude of applications [1]. The initiation of this technique begins at the stage involving the synthesis of nanoparticles, which could be physical, chemical or biological.

Most of the physical methods are difficult to carry out owing to the maintenance of a considerable number of parameters, like temperature and pressure [2]. Likewise, the chemical means of deriving nanoparticles involves the use of toxic solvents to sustain the chemical reactions [3–5]. Overuse of the chemicals could be a potential source of environmental contamination and ecological imbalance. At large-scale, both the physical and chemical conditions become unviable. The chance formation of chemical intermediates may interfere with the biology of the living systems. The parallel development of biological approaches to synthesizing nanoparticles also witnessed a huge surge in terms of the starting material used. In the biological route, the protocols for the synthesis of nanoparticles necessitate the use of sources derived from the living world, viz., bacteria, fungi, algae and plant parts [6–9]. The microbe-mediated protocols suffer from the inherent setbacks of culturing and maintaining a specimen [10, 11]. The chances of contamination cannot be ruled out during the sub-culturing steps, in which case, the synthesis takes a longer time. Plants and the parts thereof have proven to be a stable source for the synthesis of nanoparticles. This approach, termed

"green synthesis," accelerated the search for novel sources of plant-based materials to direct the synthesis of nanoparticles. The nanoparticles synthesized through this route are found to be more stable and biocompatible, with a far lesser degree of toxicity. This is mainly attributed to the fact that the nanoparticles are coated with the phytochemicals that serve as the capping agents [12].

A copious amount of literature exists that prove the versatile use of plant parts to synthesize a range of metal nanoparticles. The noble metals—gold, silver and palladium—have been synthesized in the nano form and exploited in a number of applications. The leaf extract (LE) of *Lippia citriodora* has been used for the synthesis of silver nanoparticles (SINAPs) [13]. The synthesis of SINAPs has also been extensively reported by researchers using the LE of *Cassia roxburghii* [14], cocoa bean extract [15], LE of black tea [3], root extract (RE) of *Potentilla fulgens* [16], bark extract (BE) of *Butea monosperma* [17], flower extract (FE) of *Saraca indica* [18] and the RE of *Parthenium hysterophorus* [19]. Gold nanoparticles have been fabricated using the LE and BE of *Syzygium jambos* [20], LE of *Sphaeranthus indicus* [21], LE of *Momordica cochinchinensis* [22] , FE of *Citrus maxima* [23], peel extract (PE) of *Stachys lavandulifolia* [24], LE of *Hibiscus rosa sinensis* [25] and LE of *Saraca asoca* and *Azadirachta indica* [26]. Although palladium nanoparticles have been reported to a relatively lesser extent, they also find many catalytic applications. Some of the works include the use of LEs of *Solanum trilobatum* [27], *Catharanthus roseus* [28] and *Euphorbia condylocarpa* M. Bieb [29]. Zinc oxide nanoparticles have been synthesized using coffee powder extract [30], LE of *Hibiscus subdariffa* [31] and the FE of *Nyctanthes arbor-tristis* [32]. With regard to iron, nanoparticles have been synthesized in two forms: iron as well as iron oxide (Fe_3O_4). The aqueous PE of *C. maxima* [33] and the plant extract of *S. jambos* [34] have been exploited for the synthesis of iron nanoparticles. Reports of iron oxide nanoparticles are recorded in the experiments using the LE of *Ocimum sanctum* [35] and the aqueous plant extracts of *Hordeum vulgare* and *Rumex acetosa* [36]. The green synthesis of iron hexacyanoferrate nanoparticles using *Sapindus mukorossi* has been reported [37]. Among the lesser reported nanoparticle syntheses, sulphur nanoparticles using the PE of *Punica granatum* peel [38] and titanium dioxide nanoparticles using the FE of *Calotropis gigantean* [39] and LE of *Psidium guajava* [40] find many applications. Cerium oxide nanoparticles have been designed using the LE of the common *Azadirachta indica* [41]. Among the others, nanoparticles have also been reported regarding ruthenium [42, 43], copper [44, 45], copper oxide [46, 47], cadmium sulphide [48, 49] and lead [50].

12.2 Mechanistic Aspects of Silver Nanoparticle Synthesis

The synthesis of SINAPs is primarily arbitrated by the phytochemicals derived from the plant-based sources. However, owing to the great diversity of the constituent phytochemicals resident in any plant system, it becomes a daunting task to zero-in on the specific role(s) played by the component(s). It thus becomes difficult to postulate a mechanism for the synthesis of nanoparticles in general. Apart from the Ag^{+}-to-Ag^{0} reduction, the method by which the phytochemicals protect (cap) the as-synthesized SINAPs largely remains unknown. However, the results of the characterization techniques (such as UV-visible spectroscopy, FTIR, AFM, etc.) before and after the biogenic synthesis, have helped in part to formulate the most feasible strategy in the formation of SINAPs. Prior screening of the secondary metabolites in the extract proves the presence of a variable mixture of terpenoids, flavonoids [51–54], polyphenols [55–66] essential oils [67], saponins [51, 68], amines [69], starch [70], alkaloids [67], proteins [71–81] and carbohydrates (arabinose, galactose [82]) in the plant extract. These plant metabolites are further composed of carbonyl, hydroxyl and amine groups [83]. The protein-based amino bonds and carbonyl moieties are strongly implicated in binding the metal atoms [84].

To start with, any general scheme for the green synthesis of SINAPs begins with obtaining the extract of a specific plant part. Nearly all parts of the plants—leaves, flowers, fruits, peels, seeds/pods and callus—form the source of materials to initiate nanoparticle synthesis. The extract in most cases is aqueous, while some workers have also reported considering extraction using organic solvents. Silver is introduced into the reaction sequence in the form of silver nitrate or silver sulphate that dissociates into the monovalent Ag^{+} and other ions, as the case may be. When the plant-based extract is then added, the phytochemical-rich solution supports the reduction of monovalent silver ion to zero-valent silver in the nano range. A change of color in the admixture is considered a touchstone for the realization of SINAPs. This is then followed by a horde of characterization techniques—spectroscopy (ultraviolet-visible, Fourier-transform infrared, energy-dispersive X-ray), X-ray diffraction, dynamic light scattering, BET surface area analysis, zeta potential analysis and microscopy (scanning electron, transmission electron, scanning tunneling electron, atomic force). Owing to the simplicity and rapidity of the ultraviolet-visible spectroscopic procedure, most of the researchers perform the same for first-hand validation of nanoparticle formation, before proceeding to verify specific features of the nanoparticles using the other techniques.

Due to the capacity to bind to metals and reduce their salts, the hydroxyl as well as ketone groups may be responsible for providing stability to the SINAPs and prevent them from getting clustered up [84]. The proteins in the plant extract assist in capping, hence stabilizing the SINAPs [85]. So, there is no further constraint to incorporate an externally sourced capping/stabilizing agent and this becomes one of the fundamental reasons as to why the entire nanoparticle synthesis is termed "green." Biocompatibility of the so-derived nanoparticles is thus achieved in the ecologically benign green approach [83].

12.3 Applications of Phytogenic Silver Nanoparticles

As early as 4000 BC, the Chaldeans already had enough knowledge about metallic silver and its applications. Over the decades, silver has remained the most sought-after metal for myriad antimicrobial applications. It was probably used even before the notion of the nexus between microbes and diseases was put forward [86]. The use of silver is not just limited to the microbicidal applications against bacteria, fungi, larvae, parasites, arachnids, lice and tumour cells. The SINAPs have also been exploited for environmental remediation owing to their catalytic activity and sensing ability. They also show an inhibitory effect against restriction endonucleases, showing promise in phage therapy. Because the specific surface area of the diminutive nanoparticles is humongous, it opens up many opportunities for their use in diverse fields. Added to this, the synthesis of nanoparticles can be controlled in terms of their size and shape, as deemed fit for a specific application. These physical parameters supplement and amplify the effectiveness of the biological properties of the SINAPs. As can be witnessed from the following applications in diverse domains, the influence of green-synthesized SINAPs is here to stay and will continue to grow for a long time to come.

12.4 Biomedical Applications

12.4.1 Antibacterial Applications

Over the years of pharmaceutical development, the indiscriminate use of antibiotics paved the way for the evolution of clinically resistant bacterial strains. The problem is only getting worse by the day, with the emergence of newer and deadlier strains that would have otherwise remained harmless. It is at this juncture that the steady development of nanoparticle-based antibacterial activity was harnessed. Nearly two decades of research in this field has resulted in an enormous body of work, waiting to be actively exploited and released through the pharmaceutical pipeline.

Gram-positive bacteria have cell walls that are largely composed of murein (peptidoglycan) layers. They are polymers of linear polysaccharides, which are further crosslinked by oligopeptides, yielding a tough structural barrier. This makes it difficult for the SINAPs to penetrate, in the case of Gram-positive bacteria. The comparatively thinner layer of peptidoglycan in the cell walls of Gram-negative pathogens has the opposite effect in this context [87]. The antibacterial effect is due to the escalation of cell membrane permeability once the silver ions interact with the bacterial membrane structure [88]. The SINAPs lead to destabilization of the outer membrane of Gram-negative bacteria [89]. Since the SINAPs have the ability to form free radicals, they could be the potential agents that kill the microbial cells. Studies based on electron spin resonance spectroscopy have corroborated the fact that when free radicals come in contact with microbial cells, the radicals puncture and thus mutilate the cell, leading to its death [90, 91]. The binding of SINAPs to the plasmalemma leads to the arrest of respiratory tasks of the cell. It could also arise from the interference of the nanoparticles with the electron transport chain of the microbial cell, ultimately leading to ATP shutdown. Incorporation of either Ag^{+} or Ag^{0} nanoparticles into the microbial cell wall leads to the accretion of envelope protein precursors that leads to dissipation of the proton motive force. In a different mechanism proposed, silver was reasoned to have higher affinity to biological moieties that contain sulphur or phosphorus [92, 93]. Sulphur is largely present in amino acids of proteins, either embedded in the membrane or internally. Likewise, phosphorus is richly present in the nucleotides. This leads to the possible notion that the SINAPs favor binding with these sites, thus initiating antibacterial activity.

The SINAPs synthesized through the plant-mediated approach have been investigated for their antibacterial activity against a range of Gram-positive and Gram-negative organisms. Both aqueous and solvent-based extracts have been used to source the phytochemicals. *A. indica,* or the common neem, is usually seen as the quintessential example for antimicrobial activity. The SINAPs synthesized using its aqueous LE showed decent antibacterial activity against *E. coli* and *S. aureus*, representative of Gram-negative and Gram-positive microbes [94]. Surprisingly, the study noted that they did not obtain any zone of inhibition against the same pathogens when the aqueous extract was used as such. The group concluded that this observation may be due to very low activity in the extraction medium and lower concentration in the experiment. The SINAPs were synthesized using the aqueous LE of *Tephrosia purpurea* against Gram-negative (*Pseudomonas* spp. & *Escherichia coli*) and Gram-positive (*Bacillus* spp. & *Staphylococcus* spp.) [95]. Using the aqueous LE of *Andrographis echioides* [96], SINAPs

were shown to have antibacterial activity against *E. coli*, *Staphylococcus aureus*, *Salmonella typhi*, *Micrococcus luteus* and *Pseudomonas aeruginosa*. Both *E. coli* and *P. aeruginosa* were more susceptible to the SINAPs synthesized using aqueous *Artocarpus altilis* LE, while, *S. aureus* showed nominal resistance [94].

Alternatively, the crude methanolic LE of *Trichosanthes tricuspidata* was used for the synthesis and then tested against *Shigella boydii*, *Proteus vulgaris* and *Enterococcus faecalis* [97]. The results showed excellent activity against the microbes in terms of the zones of inhibition, which were 12 mm, 10 mm and 10 mm respectively. Interestingly, the assay was also performed using petroleum ether, chloroform and aqueous extract of the same plant source. A moderate-level activity was noted against *S. boydii*, *Klebsiella aerogenes*, *E. coli* and *E. faecalis*—11 mm for the first and 9 mm for the rest. No activity was registered against *P. vulgaris*, *Vibrio cholorae* and *S. aureus*. An agro-waste from the timber industry, LE of waste teak leaves, was used in another study [98]. They obtained significant zones of inhibition for both *E. coli* and *S. aureus*. They also determined the minimum inhibitory concentration (MIC) of the SINAPs upon *E. coli* and *S. aureus* to be 25.6 µg/mL. Aqueous pepper extract was used as the source of phytochemical for the reduction of monovalent silver [99]. The study demonstrated the antibacterial activity against the Gram-negative organisms *E. coli* and *Salmonella* spp. Similarly, SINAPs were fabricated using the aqueous LE and BE of *Sonneratia apetala* and *Heritiera fomes*, respectively, against *S. aureus* and *V. cholorae* [100]. The results turned out exceedingly well in the case of *S. aureus*. Triplicate studies were performed with nanoparticles synthesized using the aqueous LE of *Heterotheca inuloides* as a reductant against *E. coli* and *S. aureus* [101]. Likewise, the leaves of *Sesbania grandiflora* were used to make SINAPs and investigated for antibacterial activity against *E. coli*, *Pseudomonas* spp., *Bacillus* spp. and *Staphylococcus* spp. using Kirby-Bauer disc diffusion method [102]. The aqueous LE of *Xanthium strumarium* was tested towards the synthesis of SINAPs [103]. *S. aureus* and *E. coli* exhibited a maximum inhibitory effect of 1.68 mg/mL and 2.55 mg/mL respectively. It was noted that the nanoparticles showed greater antibacterial effect for *E. coli* and *S. aureus*, even when compared to the antibiotic, penicillin [104].

Among sources other than the leaf, the rhizome extract of a fern species, *Dryopteris crassirhizoma,* was used in conjugation with sunlight or light from a LED source (red, green, blue or white) to synthesize SINAPs [105]. Considerable antimicrobial activity was noted against *Bacillus cereus* and *P. aeruginosa*. The BE of *Pongamia pinnata* was used as the source of phytoreductants for SINAP synthesis [106]. The highest zone of inhibition was

noted against the Gram-negative *Klebsiella planticola* and it was minimum against the Gram-positive *S. aureus*. As was the case in most studies, the antimicrobial activity was considerably higher than when compared to the BE and the silver salt ($AgNO_3$).

12.4.2 Antifungal Applications

Candidiasis and candidemia are two highly recurring fungal-based infections which lead to substantial rates of mortality and morbidity [107]. Among the most common fungal infections in human beings are the ones caused by *Candida* spp. A pathogenic yeast, many resistant forms have developed because of which the treatment options are restricted in terms of availability and associated costs [108]. The advent of SINAPs synthesized through the use of plant parts is beginning to show new promise in resolving the problems posed by fungal pathogens.

The aqueous LE of *Tephrosia purpurea* was used to synthesize SINAPs [95]. The efficacy of the spherical nanoparticles was tested against the fungal species *Penicillium* and *Rhizopus*, using Kirby-Bauer disc diffusion method. The nanoparticles exhibited good activity against *Penicillium* spp. The water-soluble phytochemical extract derived from *Jatropha glauca* leaves was used to fabricate SINAPs [109]. Aimed at organisms responsible for dental caries and periodontal disease, *Candida albicans* was chosen for the antifungal study that measured the zone of inhibition. The antifungal efficacy was very significant, as it showed a 26-mm zone and a minimum inhibitory concentration (MIC) range of 25 μg nanoparticle/mL for *C. albicans*. Likewise, SINAPs were engineered employing the aqueous LE of *Rosmarinus officinalis* [110]. In this study, *Aspergillus oryzae* and *C. albicans* were utilized to define the antifungal efficacy of SINAPs. A dose-dependent (20–80 mg per disk) study was carried out and the zone of inhibition was observed to be slightly higher for *C. albicans* at 32.4 mm at 80 mg/disk. At a concentration of 0.03 mg/disk, the antibiotic, amphotericin, registered a lower value of 28.1 mm. Fungal pathogens of agricultural relevance were the subject of a study where the aqueous extract of peanut shells was used for the green synthesis of SINAPs [111]. The fungal organisms, *Phytophthora infestans* and *Phytophthora capsici,* were chosen for the study, the results of which proved that the green-synthesized nanoparticles were as good as commercially available SINAPs in showing fungicidal action. *Aspergillus* spp. and *Pneumocystis* spp. were subjected to antifungal tests [112]. In this work, the organic (ethanolic) fraction of the phytochemicals derived from *Brassica oleracea* L. was used to synthesize SINAPs. The fungal organisms showed zones of inhibition which were on

par with the antifungal medication, fluconazole, that served as the control. It was interesting to note that at similar concentrations of 50 μg/mL, fluconazole and the eco-friendly SINAPs shared a similar zone of inhibition of 6 mm in the case of *Aspergillus*. It was a hairline better with respect to *Pneumocystis*; it was 7 mm using the nanoparticles and 6 mm using fluconazole, implying good potential of the nanoparticle to be used as an effective antifungal agent. The aqueous BE of *Syzygium alternifolium* (Wt.) Walp. was used in proving the antifungal efficacy of SINAPs synthesized using this extract [113]. A total of five fungal specimens were picked for the study— *Alternaria solani, Aspergillus niger, Aspergillus flavus, Penicillium chrysogenum* and *Trichoderma harzianum*. The zone of inhibition recorded was the highest in the case of *A. flavus*. In their study, which also included antibacterial assays, the bacterial strains showed higher susceptibility when compared to the fungal test strains. The reason for this was attributed to the rigid nature of fungal cell walls that had chitin with glucosamine strands which were further criss-crossed with hydrogen bonds. In another study, the aqueous LE of *Rauvolfia serpentina* Benth was used to formulate SINAPs and used against *A. niger* and *C. albicans* to determine the antifungal activity [114]. The antifungal activity was most effective against *A. niger*; even at a low concentration of 25 μg/mL, the organism displayed a significant zone of inhibition of 12.67 mm. Aqueous extract obtained using the fruit pulp of *Adansonia digitata* served as the source of reductants to mediate the production of SINAPs [115]. Antifungal assays were conducted against five fungal pathogens that included *A. solani*, *A. flavus*, *A. niger*, *P. chrysogenum* and *T. harzianum*. The tests remained positive in all of the cases, with higher zones of inhibition than those obtained with just the pulp extracts. Likewise, SINAPs synthesized using the pre-hydrolyzed liquor of *Eucalyptus* wood showed inhibitory property against the fungi *C. oxysporum, P. chrysogenum, C. albicans* and *A. niger* [116]. When SINAPs synthesized using the aqueous plant extract of *Luffa acutangula* were tested against *Saccharomyces cerevisiae*, a zone of inhibition of 11 mm was evidenced, proving the antifungal efficacy [117]. The fungal specimen, *Aspergillus vesicolor,* showed minimal susceptibility towards SINAPs synthesized using the aqueous LE of *Atrocarpus altilis* [118]. A similar antifungal action was observed against *Penicillium* spp. when SINAPs were fabricated using the LE of *Sesbania grandiflora* [102].

Studies involving SINAPs fabricated using the aqueous LE of *Lippia citriodora* showed moderate activity against *C. albicans*, with an MIC of 100 μg/mL. In a recent study, the aqueous LE of *Paederia foetida* Linn. was used for nanoparticle synthesis [119]. The same was then used to study the growth inhibition rates of microbes. *A. niger* showed a growth inhibition

rate of 13.4%. Even an aquatic plant source has been used for similar studies. The aqueous extract of seaweed, *Eschweilera compressa,* was used to check whether the component phytochemicals could act as reductants for SINAP synthesis [120]. It proved beneficial and further proved the antifungal action against pathogenic fungi like *Fusarium moniliforme*, *Aspergillus terreus*, *A. flavus*, *A. niger* and *Aspergillus ochraceus*.

A waste by-product sourced from the corn industry was used to synthesize SINAPs [121]. A water-based extract was obtained using the leaves of *Zea mays*. The group worked on determining the synergistic effect of the nanoparticles and amphotericin on fungal specimens. Of the five types of pathogenic *Candida* spp. tested, *C. albicans* KACC 30003 exhibited the highest mean zone of inhibition of 12.88 mm.

The variation in the zones of inhibition obtained by different research groups could be because of the nature (primarily, size and shape) of the SINAPs attained in their respective synthetic conditions. It was proposed that the antifungal property is because of the inactivation of the critical sulfhydryl (–SH) group, present as a component of the fungal cell wall [122]. This might lead to the creation of insoluble complexes. Alteration of crucial enzyme and lipid bound to the cell membrane may also occur, which would ultimately lead to cell lysis.

12.4.3 Antileishmanial (Antiparasitic) Applications

Noble metal nanoparticles have the ability to yield reactive oxygen species (ROS), which through a process called "respiratory burst mechanism" kills the pathogenic microbes. Microbes, in general, and especially *Leishmania* spp., are highly reactive to ROS, and so those agents that can produce ROS could be potential candidates for antileishmanial drugs. Under *in-vivo* conditions, it is the macrophages that possess the ability to generate high concentrations of ROS, thereby disinfecting the microbes in the process [123]. In a protective mechanism evolved by *Leishmania* spp., the pathogens circumvent the oxidative impairment (caused by ROS) by inactivating the ROS-producing enzymes [124]. Under these circumstances, the SINAPs synthesized and incorporated in the experiments serve as a huge buffer, supplying the necessary silver moieties on a non-enzymatic basis to kill the pathogenic leishmanial parasites.

An exhaustive study was conducted by employing the aqueous LE of *Euphorbia prostrata,* to verify their potential as antileishmanial agents [125]. The promastigotes of *Leishmania donovani* were put to test using alamarBlue® (as an indicator of cell viability) and propidium iodide uptake assays (as an indicator of apoptotic activity). Giemsa stain was used to

verify the antileishmanial activity of the SINAPs on intracellular amastigotes. Finally, DNA fragmentation assay and transmission electron microscopy techniques were employed to assess the antileishmanial effect of the nanoparticles. The nanoparticles worked against the parasites within 24 hours of exposure. They showed IC50 values of 3.89 g/mL and 14.94 g/mL in intracellular amastigotes and promastigotes, respectively. With regard to the events in the cell cycle, the G0/G1 phase had notably risen with a corresponding dip in S and G2/M phases. The growth-inhibitory effect of SINAPs could be due to an amplified S-phase. Necrotic cell death was implied from the fragmentation of high-molecular-weight DNA. The phytocomponents in the aqueous fraction of the bulk plant material of *Sargentodoxa cuneata* were used as reducing-cum-stabilizing agents to aid the synthesis of SINAPs [126]. The study proved excellent activity against *Leishmania* spp., yielding an IC50 value of 4.37 mg/L. The leishmanial count saw a major dip in the initial 24 hours of incubation with SINAPs. During this time period, 90% inhibition was observed, which then experienced an even higher inhibition of 95.45% after 48 hours of incubation. The antileishmanial activity of SINAPs was tested against *Leishmania tropica* in another study [127]. The nanoparticles were synthesized using the dried and powdered plant material of an acclaimed Chinese herb, *Isatis tinctoria*. Conducted in a dose-dependent manner in the concentration range of 5–80 μg/mL, a notable reduction in the viable count was seen after exposure to the green-synthesized SINAPs. A maximum value of 73% growth inhibition was evidenced in the dark in a time frame of 48 hours. When the same study was conducted with samples irradiated with visible light, the percentage of growth inhibition rose significantly to 83%. In order to study the accelerated action of the common antileishmanial drug, it was tested along with SINAPs synthesized using the aqueous LE of *Anethum graveolens* [128]. The study showed that the nanoparticles did not inhibit the promastigote phase of *Leishmania* on their own. However, when complemented with miltefosine, the nanoparticles clearly augmented the efficacy of miltefosine by nearly two times, thus nearly halving the IC50 of miltefosine. The aqueous LE of *Xanthium strumarium* was employed to synthesize SINAPs to test against the promastigotes of *Leishmania donovani* [103], and exhibited positive antileishmanial activity. In a novel application of SINAPs for investigating potential antileishmanial activity, the tuber extract of *Dioscorea bulbifera* was employed [129]. In the study, bimetallic Au_{core}-Ag_{shell} nanoparticles were engineered and were shown to exhibit antileishmanial activity with an MIC of 32 μg/mL using MTT assay. When subjected to treatment with the core-shell assembly, a marked deformation was observed in terms of

the parasite's morphology; the spindle shape turned spherical at the end of the treatment period. The antileishmanial activity was also confirmed by the DNA fragmentation assay.

12.4.4 Antibiofilm Applications

Biofilms are natural three-dimensional formations of microorganisms (especially pathogens) bound to surfaces, wherein the cells are impregnated onto the self-synthesized gel-like polymeric substances that chemically contain proteins, polysaccharides and nucleic acids. Distinct water channels separate the matrix-encompassed microbial colonies and hence afford an unobstructed pathway for circulation of nutrients in the biofilm [130–132]. These resin-like hydrated matrices help in reducing the penetrability of antibiotics into microbial biofilms by hampering antibiotic diffusion or nullifying such agents chemically, aided by the biofilm constituents. Nonetheless, SINAPs, owing to the scale of their size, possess the ability to breach the protective biofilms of pathogens [133]. A major chunk of bacteria colonize in the form of biofilms in their natural environments. When compared to bacteria that exist in a planktonic form, those that form biofilms are more resistant to antibacterial agents [134]. Biofilms are relatively more resistant to the host's defense mechanisms, and also against antibiotics. This feature of biofilms is responsible for a higher mortality among infections. On a related note, the body of research work involving disruption of biofilm-forming species is less than antibiotics developed against the non-biofilm bacteria.

The dried powder of gum derived from *Styrax benzoin* was water-extracted to aid the synthesis of SINAPs [131]. The influence of SINAPs on the formation of *E. coli* biofilm was studied over a range of nanoparticle concentrations between 1 and 10 μg/mL, which resulted in a corresponding impedance of biofilm formation between 11% and 66%, over an exposure duration of 24 hours. The reduction of monovalent silver to zerovalent silver was mediated by phytochemicals present in the decoction of tea leaves [135]. The group aimed to study bacterial biofilm formation ability on the surface of polystyrene. Representing Gram-negative and positive bacteria respectively, *E. coli* and *S. aureus* were chosen to check if the nanoparticles were effective in arresting the formation of biofilm. Safranin was used for staining the bacterial biofilm sticking onto test surfaces. A flatbed scanner coupled with light microscopy helped in detection of the biofilm. At a SINAP concentration of 15 μg/mL, the biofilm inhibition was maximum at 75% and 89% for *E. coli* and *S. aureus*, respectively. The aqueous LE of *Allophylus cobbe* was used to synthesize SINAPs, which was followed by a

dose-dependent assay to determine how effectively the particles impede the formation of biofilms [136]. Colorimetry-based quantitation of the incorporation of crystal violet by sessile forms of pathogenic microbes was carried out *in vitro.* Upwards of 90% reduction in biofilm formation was observed with 0.5 μg/mL of SINAPs in the case of *Shigella flexneri* and *Pseudomonas aeruginosa*. It was 0.7 μg/mL for *Streptococcus pneumoniae* and *Staphylococcus aureus* for a similar reduction. The methanolic LE of *Syzygium cumini* was used as the source for the reducing agents in the fabrication of SINAPs [137]. In the study, a modified version of the tissue culture plate (TCP) method was performed for the *in-vitro* biofilm inhibition assay. The yeast, *C. albicans,* and the bacteria, *P. aeruginosa* and *S. aureus,* were tested by checking how effectively the crystal violet bound the adherent cells, thereby giving a direct indication of the degree of biofilm formation. At SINAP concentrations of 125 μg/mL and 250 μg/mL, the pathogenic biofilm was inhibited to the tune of 85% and 90% respectively. A low MIC value of 62.5 μg/mL was supportive of the idea of the nanoparticles to be used as inhibitors of biofilms. A microtiter plate-based technique was used to study the inhibition of biofilms by SINAPs synthesized using the aqueous LE of *Euphorbia rothiana* [138]. A total of four microbes were picked up for the study—two Gram-positive bacteria (*Enterococcus faecalis* and *Lactobacillus* spp.) and two Gram-negative bacteria (*Shigella sonnei* and *Vibrio parahaemolyticus*). Light as well as confocal laser scanning microscopy helped to examine the discontinuity in the biofilms and their further disintegration at a SINAP concentration of 75 μg/mL.

The leaves of *Lagerstroemia speciosa* were used to produce an aqueous extract of the resident phytochemicals in the sample and were then used to fabricate SINAPs [139]. The efficacy of the nanoparticles in warding off microbial biofilm (*P. aeruginosa*) was put to the test by preliminary screening using SINAPs in the concentration range of 50–250 μg/mL. The highest inhibition of nearly 87% was observed at a SINAP concentration of 50 μg/mL. In a similar study, starch-stabilized SINAPs were synthesized to investigate their efficacy in disruption of biofilms formed by pathogenic microbes [140]. The study considered pathogens usually linked to food-, water- and air-borne infections. When compared against human-derived LL-37 antimicrobial peptide, the biogenic SINAPs unsettled the biofilms. The inhibition of biofilms formed by clinical isolates was studied by synthesizing SINAPs using the broth of *Azadiracta indica* leaves [141]. The particles were later conjugated with the organic extract of *Vitex negundo* and *Allium sativum*. *E. coli* and *P. aeruginosa* recorded a maximum of 84% and 81% inhibition of biofilm when treated with SINAPs coupled to *V. negundo*. The leaves of *Convolvulus arvensis* were sourced to get an extract

for the phytoreduction of silver and the nanoparticles so obtained were tested against microbes for biofilm formation [142]. Minimum biofilm eradication concentration (MBEC) is a method that gives an estimate of the minimum antibiotic concentration required for bacterial biofilm treatment. The MBEC of the SINAPs against *S. aureus* and *P. aeruginosa* measured using atomic absorption spectrophotometry was established at 20 and 50 μg/mL, respectively. Fluorescence-based staining (SYTO-9 and propidium iodide) was coupled to confocal laser scanning microscopy to differentiate between viable and dead cells. When the cells were subjected to a SINAP concentration of 20 μg/mL, nearly all of the cells in the biofilm were inhibited.

12.4.5 Anticoagulant Applications

The realization of blood clots in the event of bleeding is one of the greatest instantaneous blessings under normal conditions. The process, however, is a double-edged sword; the development of blood clots must be carefully prevented, as the uncontrolled progress of this process may damage stable blood flow processes. When the free flow of blood is impaired, this could lead to ischemic stroke, wherein the organ systems of a living organism are depleted of oxygen and vital nutrients. The essence of disorders concerning blood coagulation lies in the imbalance between prevention of unwarranted bleeding and blood coagulation. A host of reasons could be attributed to blood coagulation disorders, from simple injuries to allergy, autoimmune responses and impaired cardiovascular conditions [143, 144].

Noble metal nanoparticles synthesized through the green route are by far the best alternatives to develop, as they are fully compatible with biological systems. The mechanism by which the SINAPs mediate anticoagulation is attributed to the inactivation of platelet response (mediated by integrin) to restrain fibrinogen [145]. The anticoagulant activity of SINAPs serves a prime purpose in the field of nanomedicine to disallow blood coagulation in subjects afflicted with serious malfunctions in the blood coagulation mechanism. However, when encouraging the use of SINAPs as an anticoagulant, one must tread with caution. This is because of the same property that they have *in vivo*; when SINAPs are used as drug delivery agents, the contact attained with blood will not initiate blood coagulation process [146]. It is probable that the SINAPs may have the ability to inhibit the activity of fibrinogen, thus arresting fibrin formation and blood coagulation. The combined effects of fibrinolytic, antiplatelet,

and fibrinogen-inactivating mechanisms lead to the anticoagulant property of SINAPs.

With a view to verify the anticoagulant nature of SINAPs, the same were synthesized using the aqueous extract of *Peltophorum pterocarpum* pods [147]. When human blood was mixed with the SINAPs at 0.5% (v/v) concentration, the clot formation was completely avoided. Similar results were obtained by the same research group with the aqueous fruit extract of *Bridelia retusa* [148] and the aqueous seed hull extract of *Vigna mungo* [149]. The aqueous extract prepared using cocoa beans was employed to fabricate SINAPs and test their anticoagulant capability [15]. Human blood and the as-synthesized SINAPs (170 μg/mL) were mixed in equal volumes, along with separate control samples. After about an hour of incubation, the SINAPs resisted the *in-vitro* coagulation process. Microscopic observation of the sample proved that the core morphology of the erythrocytes was maintained intact. In contrast, incubation of blood with just the extract and silver nitrate saw the formation of blood clots. When gallic acid-reduced SINAPs were used, the influence of SINAPs on coagulation of blood was studied using plasma-based assays under *in-vitro* conditions. The nanoparticles are also deemed to portray cytotoxic qualities against macrophages, probably leading to an inflammatory reaction [150]. The dried biomass of an edible fern, *Diplazium esculentum* (Retz.) Sw., was used to mediate the formation of SINAPs, which show intense anticoagulant action towards human blood [151]. Multiple parts of *Cola nitida* (viz., seed, seed shell and nut) were used to biosynthesize SINAPs [152]. An mL of 100 μg/mL nanoparticle solution was mixed with human blood in similar proportion. Even after 4 hours of observation, the anticoagulant activity of the SINAPs was strong enough and showed comparable activity to ethylenediaminetetraacetic acid, which served as the positive control. The tender leaves of *Convolvulus arvensis* were used to mediate the synthesis of SINAPs, which were then tested for anticoagulant activity [142]. Fresh human blood sourced from volunteers was combined with the as-synthesized SINAPs at 1% (v/v) concentration. On a visual basis, it was observed that the SINAPs inhibited the coagulation process and prevented blood clot formation. The aqueous extract of dried green husk of *Juglans regia* acted as the source of phytochemicals for the conversion of monovalent silver to the zero-valent form [145]. Upon treating the blood obtained from volunteering students, the anticoagulant effect was observed for a long duration of 72 hours. The phytosynthesis of SINAPs was facilitated by the aqueous extracts of leaves and seeds obtained from *Synsepalum dulcificum* [153]. The SINAPs demonstrated their anticoagulant and thrombolytic abilities.

12.4.6 Antidiabetic Applications

Interest in searching for traditional herbs has seen a gradual surge over the years. Pharmaceutical companies have been convinced by the low-level toxicity and financial viability associated with plant-based options. The digestive enzymes α-amylase and α-glucosidase help in the metabolism of carbohydrates by breaking them down into easily assimilated monosaccharides [154, 155]. Hence, naturally derived compounds that impede the two digestive enzymes could prove useful for treating cases of non-insulin diabetes. In one of the mechanisms affected by blood glucose-controlling herbs, there could be a change in the activity of certain enzymes involved in glucose breakdown. Inhibitors of α-amylase may act by blocking digestion and further absorption of carbohydrates [156]. An example of such a synthetic inhibitor of α-amylase is acarbose; it is a complex oligosaccharide that lengthens the duration of carbohydrate digestion. It works by inhibiting the action of pancreatic amylase. However, artificial inhibitor molecules would cause side-effects such as diarrhea, abdominal pain and soft feces [157].

Leaves of *Argyreia nervosa* were boiled to a broth and the extract served to synthesize SINAPs [158]. The ability of the nanoparticles to possess an antidiabetic effect was verified by investigating if the particles showed inhibition against the digestive enzymes α-amylase and α-glucosidase. As the concentration of SINAPs rose, the inhibition percentage also escalated significantly. The IC50 parameter for α-amylase was 55.5 μg/mL while it was 51.7 μg/mL for α-glucosidase, thus signifying the antidiabetic potential of the green-synthesized SINAPs. The LE of *Cinnamomum tsoi* was exploited to fabricate SINAPs to check their antidiabetic activity [159]. The nanocolloid registered an increase in percent inhibition from 45% to 93% against α-amylase when the concentration of SINAPs rose from 10 to 75 μg/mL. Likewise, for a similar rise in SINAP concentration, the percent inhibition against α-glucosidase went up from 57% to 80%. In both cases, the inhibition was more enhanced as compared to the extract alone. With prior knowledge of the medicinal plant, *Tephrosia tinctoria,* possessing rich phenolic and flavonoid composition, its aqueous extract was used to mediate the synthesis of SINAPs [160]. Enzyme assays using α-glucosidase and α-amylase attested to their inhibition, with an augmentation in uptake rate of glucose. The SINAPs synthesized using the aqueous extract derived from the whole *Sphaeranthus amaranthoides* plant were evaluated to verify the possible hypoglycemic activity [157]. Upon using the α-amylase inhibition *in-vitro* model, it was determined that the SINAPs, inhibiting α-amylase, presented an IC50 value of

0.28 μg/mL while that of acarbose (an oral synthetic α-glucosidase inhibitor) was higher at 0.75μg/mL. The finding obviously suggested that the SINAPs were more efficient than acarbose. Inhibition by the SINAPs was determined to be of the competitive-type, which may possibly point out that a few enzyme-inhibitory constituents in *S. amaranthoides* could be structurally analogous to the substrate of α-amylase. Another study concentrated on the phytosynthesis of SINAPs using aqueous LE of *Pouteria sapota* and their evaluation of antidiabetic activity [161]. Under *in-vitro* conditions, the antidiabetic property was established by glycosylation of hemoglobin, inhibition of α-amylase and uptake of glucose by yeasts cells (upon prior exposure to known concentration of glucose). For *in-vivo* testing, streptozotocin-induced rats were used. The SINAPs were administered to the rats at 10 mg/kg for a duration of 28 days after which they were sacrificed for histopathological studies. Both sets of results showed the antidiabetic potential of the SINAPs. Aqueous extract derived from the leaves of *Lonicera japonica* was used in the production of SINAPs, which were subsequently used for the testing of antidiabetic potential [162]. A dose-dependent assay for α-amylase and α-glucosidase proved that they were increasingly inhibited with rise in nanoparticle dosage. The analysis resulted in IC50 value of nearly 55 μg/mL for α-amylase and approximately 38 μg/mL for α-glucosidase. As in any phytosynthetic protocol, the LE of *Punica granatum* was used to facilitate the synthesis of SINAPs and investigate their antidiabetic property [163]. The enzyme inhibition assays involving α-amylase and α-glucosidase yielded IC50 values of 65.2 μg/mL and 53.8 μg/mL, respectively. Ethanol was used as the solvent in the soxhlet extraction of phytocomponents from the leaves of *Solanum nigrum* to produce SINAPs [164]. Alloxan was intraperitoneally administered in Wistar albino rats at 200 mg/kg body weight, thus inducing diabetes. After a period of 3 weeks, oral glucose tolerance testing was carried out. The rats into which SINAPs were injected showed marked reduction in glucose level in the blood and the value was higher than with the LE alone. Also, the study did not present drug-induced signs of toxicity, physically or otherwise, in the course of the experimentation and there was no observed mortality. As determined by acute toxicity studies, a nanoparticle level of 10 mg/kg body weight was agreed upon as the ideal concentration for treating the diabetic rats. The chloroform extract of the leaves of *Andrographis paniculata* helped in the mediation of SINAP synthesis [165]. Herein, the antidiabetic potential was determined by glucose oxidase method [166, 167] with colorimetric quantitation. The SINAPs exhibited remarkable antidiabetic property even when incorporated at lesser concentrations.

12.4.7 Antioxidant Applications

Oxidative stress is frequently acknowledged to be a vital reason for a multitude of chronic diseases [95]. When cells undergo oxidative stress, undue formation of free radicals is experienced. This also happens during ordinary metabolic and respiratory processes, where these radicals are linked to cardiac arrest, cancer and aging [168]. Antioxidant activity, otherwise known as free radical scavenging, encompasses all those mechanisms that work to inhibit the subcellular oxidation processes by inactivation of the initial step in the cascade of oxidative reactions. The stable radicals thus formed are nonreactive in nature. Antioxidants, like the phytochemicals in plants, possess the chemical moieties that aid the transfer of an electron to the (destructive) free radicals, thus hindering the induction of stress by creating more stable paired electrons.

The aqueous PE of orange (*Citrus* × *clementina*) was used for arbitrating the formation of SINAPs to check their scavenging potential against free radicals under *in-vitro* conditions [169]. Assays were performed using 2,2-diphenyl-1-picrylhydrazyl (DPPH) and 2,2′-azino-bis(3-ethylbenzothiazoline-6-sulfonate (ABTS) as the sources of free radicals. Using the DPPH assay, the scavenging activity of SINAPs was dose-based, registering 68.2% inhibition at 100 μg/mL and up to 82% via the ABTS assay. The IC50 value in this assay was 63.4 μg/mL, while it showed 49.6 μg/mL with the ABTS assay. The robust scavenging potential of the SINAPs could be because they are of extremely fine size and are able to donate electrons or H^+ ions along with the phytochemicals (capping agents) on the nanoparticle surface [100, 162, 170]. The natural extract of *Viburnum opulus* L. fruits was the phytomediator for the synthesis of SINAPs, whose anti-inflammatory activity was evaluated [171]. On an *in-vitro* basis, the discharge of the two cytokines, IL-1α and IL-6 (both being pro-inflammatory) from HaCaT cell line was monitored. The nanoparticles initially increased the secretion of IL-1α and boosted the pro-inflammatory influence. With time, the process reversed. With respect to IL-6, its secretion showed a decreasing trend throughout. Thus, if the incubation was longer, the SINAPs displayed anti-inflammatory mechanism by impeding the release of IL-6 and IL-1α. As part of the *in-vivo* assay, the concentration of the interleukins 1α, 1β, 6, 10 and TNF-α were determined in the tissue homogenate of Wistar rat hind paw. The level of cytokines witnessed a reduction soon after the initiation of inflammation. The paw volume also decreased as the inflammatory mechanisms were impaired. Thus, the studies clearly proved the treatability of inflammatory conditions using phytosynthesized SINAPs. The Amazonian fruit, *Eugenia stipitata* McVaugh, was extracted under

aqueous conditions and the resulting extract was utilized for the synthesis of SINAPs [172]. Using DPPH as a free radical source, studies indicated that the radical scavenging activity was found to increase as the concentration of the nanoparticles rose higher. There was a maximum of 77% scavenging activity with the SINAPs and it was just 35% with the fruit extract. The huge surge in antioxidant action could be because of two reasons; one, the extremely high specific surface area of the SINAPs, and two, the dynamic interactions of silver moieties with the functional groups in the phytochemicals of the fruit extract [168, 173, 174].

The aqueous LE of *Alternanthera sessilis* (Linn.) was similarly used for the synthesis of SINAPs and evaluation of their antioxidant efficacy [175]. DPPH assay showed a radical scavenging activity of 62% at 500 μg/mL SINAP concentration with an IC50 value of 300.6 μg/mL. An extract of ripened berries was obtained from *Lantana camara* to facilitate the synthesis of SINAPs [176]. DPPH analysis of their scavenging potential determined a maximum efficacy of 10.5%. Using the aqueous PE of *Nephelium lappaceum* L., silver nanoplates were fabricated with a view to estimating their antioxidant activity by the DPPH assay [173]. Application of 0.05 mM SINAPs resulted in a maximum scavenging activity of 80%. It was pointed out that the flavonoid and polyphenolic constituents in the peel held significant antioxidant activity [177]. This was deemed to have defended the cells from free radical activity and protect them against oxidative damage. The RE of *Nelumbo nucifera* presented the required phytochemicals for enabling the synthesis of SINAPs [168]. As the dose of the nanoparticles increased from 0.125 mM to 1 mM, the DPPH radical scavenging potential went up from nearly 26% to 46%. The aqueous LE of *Elephantopus scaber* Linn. was used to produce SINAPs [178].With ascorbic acid as the standard, the assessment of free radical scavenging was performed with SINAP concentration ranging from 50 to 250 μg/mL. The corresponding values of scavenging capacity ranged from 15% to 86%. At a similar concentration level of the LE, the study showed a corresponding surge of antioxidant activity from 13% to 73%, with an IC50 value of 113.06 μg/mL. Two different assays—DPPH scavenging and β-carotene bleaching—were employed to gauge the antioxidant potential of SINAPs produced using the aqueous LE of *Chenopodium murale* [179]. Over a nanoparticle concentration range of 5 to 10 mg/L, the DPPH radical scavenging capacity rose from approximately 13% to 65%. The values were comparatively higher than when the plant extract was used to check the antioxidant activity. The results obtained from the other assay were also asserted by the same finding. A host of antioxidant assays were employed to check the efficiency of SINAPs engineered with the aqueous LE of *Morinda pubescens* [180]. The

DPPH-based assay yielded an IC50 value of 84 μg/mL, proving the strong radical scavenging capacity of the SINAPs. The results were consistently echoed by other assays used in the work; superoxide radical scavenging activity at 34%, hydroxyl radical scavenging activity at 37%, metal chelation activity at 56%, phosphomolybdenum complex reduction at 57% and inhibition of lipid peroxidation at 44% and 46% using two approaches. The mediation of free radical scavenging by the SINAPs was thus clearly proved beyond doubt.

12.4.8 Cytotoxicity Applications

12.4.8.1 Biocompatibility Applications

The biocompatibility of SINAPs, whatever the mode of synthesis, must be evaluated in the utmost detail. The incorporation of nanoparticles in biomedicine and food supplements warrants such a detailed examination for all possible cellular damage. Normal cell lines are thus chosen to test for any such side effects before they are deemed safe. It was pointed out that the biocompatible property of the SINAPs could be due to: (i) non-conjugation of the active principles in the plant extract with the biosynthesized SINAPs, leading to near-zero cytotoxicity and (ii) non-release of the nanoparticles after the active conjugation of phytochemicals [181]. As regards the mechanism of action, the SINAPs have a strong ability to reduce adenosine triphosphate in the cell that ultimately causes damage to the mitochondria and elevates the formation of ROS [182]. Hence, it becomes imperative for the comprehensive study of metal nanoparticles involving product safety and biocompatibility.

The biocompatibility of SINAPs synthesized using the aqueous LE of *Protium serratum* was examined by treating the human fibroblast cell line, L-929, with the nanoparticles in the concentration range of 100 to 700 μg/Ml [183]. Cell viability was evaluated using 3-(4,5-dimethylthiazol-2-yl)-2,5-diphenyltetrazolium bromide (MTT) assay followed by spectrophotometric quantitation of formazan. At lower SINAP levels, no signs of cell inhibition were noted. With rise in nanoparticle concentration, the cell viability saw a decline and an IC50 value of 600.28 μg/mL against the cell line was obtained. The aqueous extract of dried *Ficus carica* fruits was used for the production of SINAPs, which were then used to conduct an acute toxicity study on Swiss albino female rats [184]. Administered with a 2 g/kg sole dose, the rats were periodically monitored for 14 days for varied physiological changes. Histopathological studies on the brain,

heart, liver and kidney showed normal fiber integrity, hepatic veins and intact neurons. No symptoms of necropsy, infarcts, inflammation, edema and hemorrhage were observed, thus proving the compatibility of the green-synthesized SINAPs. The leaves of the plant *Spinacia oleracea* were water-extracted and the resident phytochemicals helped in the formation of SINAPs [185]. In this study, a zebrafish embryo toxicity test was performed to judge how compatible the nanoparticles are towards normal cells. After a duration of 96 hours of nanoparticle treatment, the mortality rate was determined and possible malformations on embryos were tested with stereomicroscopy. The SINAPs exhibited complete mortality at 3 μg/mL and tail malformation with yolk sac edema was noted at 2 μg/mL. The aqueous LE of *Azadirachta indica* proved successful in mediating the synthesis of SINAPs [186]. To assess any probable damage on the erythrocytes by the nanoparticles, erythrocyte aggregation assay was carried out and it was revealed that there was no toxic effect on the red blood cells. In a parallel study, the nauplii of *Artemia salina* Leach (brine shrimps) were chosen to check if there is any toxicity pertaining to the nanoparticles. Substantial toxicity was observed at 240 ppm and it was observed that with an increase in nanoparticle levels, the lethality also surged. When compared against chemically derived nanoparticles, the toxic effects against erythrocytes and shrimps were lesser. Human umbilical vein endothelial cells (HUVEC) and their transformed version cell lines (ECV-304) were used to study any impending damage inflicted by the SINAPs synthesized using the aqueous LE of *Butea monosperma* [181]. Cell viability using MTT assay proved that the green-synthesized SINAPs were fully biocompatible. The aqueous LE of *Nigella sativa* was helpful in creating SINAPs, which were consequently tested for cytotoxicity against mesenchymal stem cells sourced from bone marrow of a mouse [187]. After an exposure period of 1, 3 and 4 days to SINAPs, it was observed through MTT assay that the stem cell viability was higher when the phytosynthesized nanoparticles were used than when chemically derived nanoparticles were used. At an equal concentration of 0.2 mg/mL, the vital cell count in the extract-derived and chemically derived nanoparticles was 415×10^3 and 35.5×10^3, respectively (after 3 days), pointing to a 11-fold lower chance of stem cell apoptosis using green-synthesized SINAPs. The nontoxic nature was demonstrated when the cell viability of normal peripheral lymphocytes showed an astounding 117% and 109%, after a 6-hour treatment with 10 and 50 μg/mL (respectively) of SINAPs synthesized using the aqueous LE of *Albizia adianthifolia* [188]. When the epithelial cell line of humans, A549, was put to cell viability tests,

there was no change in the integrity of the cell membranes after treating them with the SINAPs made using the aqueous extract of garlic cloves, and hence proved nontoxic [189]. Similar results were obtained when the biocompatibility of SINAPs was tested with aneuploid keratinocyte cell line (HaCaT) derived from humans [190]. The nanoparticle synthesis was mediated by polyphenols present in tea.

12.4.8.2 Anticancer Applications

The advent of nanoparticles provides a safer alternative against cancer-causing cells. With a view to developing better antineoplastic medications, various researchers have tested the efficacy of SINAPs against different types of cancer cell lines using assays and microscopic techniques. The assays look for characteristic features of cells undergoing chemical and morphological changes if the green-synthesized SINAPs have an anti-proliferative effect. This cytotoxic effect is mainly attributed to the generation of ROS that include hydroxyl radical, superoxide radical and hydrogen peroxide, which have dire consequences against the cellular constituents like DNA, lipids and proteins [191].

The aqueous BE of *Butea monosperma* was used in the synthesis of SINAPs and then tested for anticancer activity against the human myeloid leukemia cell line, KG-1A [17]. As the nanoparticle dose ranged from 1 to 100 μg/mL, the cell viability was decreased from 13% to 98%, as depicted by the MTT assay. It was proven that the SINAPs portrayed rigorous cytotoxic influence on KG-1A with IC50 value of 11.47 μg/mL. The increasing fluorescence intensity of dichlorofluorescein implied a corresponding increase in formation of ROS. Blebbing of the cell membrane and appearance of apoptotic bodies further proved the strong anticancer effect of the SINAPs. The accelerated *in-vitro* growth of human breast adenocarcinoma cancer cell line (MCF-7) was inhibited by the SINAPs synthesized using the aqueous LE of *Andrographis echioides* [96]. The study showed that for the green-synthesized nanoparticles, an IC50 value of 31.5 μg/mL was achieved. *Ficus benghalensis* and *Azadirachta indica* barks served as the source of phytochemicals for the fabrication of SINAPs for anticancer testing against the osteosarcoma cell MG-63 [182]. The IC50 values, as determined by the MTT assay, were calculated to be 82 μg/mL and 76 μg/mL for the nanoparticles engineered using *A. indica* and *F. benghalensis*, respectively. When the samples were subjected to chromatin condensation assay using Hoechst staining technique, granulations were observed in the nuclei. *Spinacia oleracea* leaves were collected to obtain an aqueous broth in which SINAPs were produced and then evaluated for anticancer

activity against the myoblast cancer cell line C2C12 of mice [185]. When the cells were dosed with SINAPs in the range of 5 to 100 μg/mL over a 24-hour period, cell viability showed a decreasing trend, as observed from the MTT assay. Even at a low concentration of 20 μg/mL, complete cessation of growth was evidenced, which was unlike the case with the LE alone. When the treated cells were subjected to dual staining by acridine orange and ethidium bromide [192] and observed by confocal microscopy, the cell nuclei were condensed along with blebbed cell membranes, typical features of cells undergoing apoptosis. Even a much higher concentration of LE (100 μg/mL) failed to produce a similar effect on cells. Also, caspase (3 and 7) activity peaked up in the treated cells, which also suggested that apoptotic cell death was in progress. Similarly, MCF-7 cell line was also used to validate the anticancer effect of SINAPs synthesized using the aqueous extract of dried *Ficus carica* fruits [184]. MTT assay showed excellent cytotoxic effect by nanoparticles compared to the fruit extract alone. The finely powdered form of *Syzygium aromaticum* was boiled to an extract and the same served to synthesize SINAPs, whose cytotoxicity was evaluated by MTT assay [193]. The human-derived adenocarcinomic alveolar basal epithelial A549 cell line and MCF-7 cell line were treated with differing concentrations of SINAPs ranging from 50 to 100 μg/mL and the growth inhibition also showed a similar trend. The IC50 of the nanoparticles was registered as 50 μg/mL against A549 cell line and 60 μg/mL against MCF-7. The extract alone had an IC50 of 70 μg/mL, clearly indicating nanoparticles showed better promise. The petals of *Rosa damascena* served to prepare an aqueous extract with which SINAPs were synthesized and tested for their anti-proliferative activity against the A549 cell line [194]. With the aid of MTT assay, it was shown that cell viability decreased with an increase in nanoparticle concentration, yielding an IC50 of 80 μg/mL. The fruits of *Phyllanthus emblica* were used to obtain an aqueous extract with which SINAPs were biosynthesized [195]. A HeLa-derived Hep2 laryngeal carcinoma cell line was chosen to check if the nanoparticles had any cytotoxic effect. Maximum cell death occurred at a nanoparticle concentration of 50 μg/mL. Depolarization of mitochondria, DNA damage, generation of ROS and morphological changes related to apoptosis were observed in the cells treated with SINAPs. The cervical cancer HeLa cell line was chosen to study the cytotoxic effect of SINAPs synthesized using the LE of *Podophyllum hexandrum* [59]. At 50 μg/mL nanoparticle concentration, the mortality was 100% and the IC50 was fixed at 20 μg/mL. Intracellular concentration of ROS was significantly high in the cells treated with SINAPs. Owing to the cascade of caspases, the condensation of chromatin and shrinkage of cells was noted.

12.4.9 Larvicidal, Pupicidal, Pediculocidal and Acaricidal Applications

The diseases spread by mosquitoes are one of the grave public health concerns faced by developing countries. Malaria, dengue, chikungunya, filariasis, Zika fever and various forms of encephalitis are some examples of diseases for which mosquitoes are vectors. Multipronged techniques are ever-evolving to curb the mounting menace. Killing the mosquitoes while they are still in the larval phase of their life cycle is the best bet to free society from this pesky problem. Controlling the multiplication of the vectors through synthetic chemicals is largely failing due to the development of resistant strains of mosquitoes [196]. Most of the techniques attempt to target mosquito vectors like *Aedes aegypti*, *Anopheles stephensi* and *Culex quinquefasciatus*. Mosquito nets, chemical-based mosquito larvicides and repellents are methods that are losing effect over time. A sustainable action plan for effective control of vectors should be in place at the earliest to save precious lives. Design of plant-based formulations in the nano-sized format is fast emerging to be a key weapon in the control of larvae. Nanoparticles have effectively been proven to be a potent bio-control factor working against the spread of mosquitoes [197]. The mortality rate achieved by the use of SINAPs could be because of the extremely small size of the particles that permits an easy channel via the insect cuticle into the individual cells. Once inside, they are thought to affect physiological events [198].

The LE of *Tridax procumbens* was used as a reducing agent to synthesize SINAPs to be investigated for their larvicidal and pupicidal potential on *An. stephensi* [199]. The third instar, fourth instar and pupae were lab-grown and subjected to SINAPs at 1 to 5 ppm. Mortality was observed in all three stages, with 100% mortality being observed at 5 ppm. In a similar study, the LE of *Annona muricata* mediated the synthesis of SINAPs and its larvicidal efficacy was verified against the fourth instar larval phase of the vectors *Cx. quinquefasciatus*, *Ae. aegypti* and *An. stephensi* [200]. A dose-response was carried out with the LE and SINAPs, at which point it was found that the LC50 values against the vectors ranged from 516 to 618 ppm for the extract and 349 to 458 ppm for the silver moieties, thereby proving that the nanoagents were better. The same three vectors in their late third instar larval stage were picked up in a study with SINAPs prepared with a different plant source—the leaves of *Cassia roxburghii* [201]. The SINAPs were examined at concentrations between 12 and 60 µg/mL. The LC50 values of the nanoparticles were much better in this case, 26 to 31 µg/mL. This

only proved that the type and size of the nanoparticles produced played an important role in determining the larvicidal efficacy. Apart from testing the green-synthesized (with leaves of *Quisqualis indica*) nanoparticles against the same three vectors, an effort was made to check the effect of the SINAPs on non-target test organisms like *Deinococcus indicus* (bacterium), *Alpheus bouvieri* (snapping shrimp) and *Gambusia affinis* (freshwater fish) [202]. The study noted that the LE and SINAPs showed mid-level toxicity against all three organisms. However, the swimming activity and their overall survival were not influenced. The nanoparticles did show encouraging cytotoxic property against the mosquito larvae.

The leaf broth of *Rauvolfia serpentina* Benth. was chosen to mediate the synthesis of SINAPs, which were evaluated against the third instar larval phase of *Cx. quinquefasciatus* in the concentration range of 2.5 to 25 μg/mL [114]. After a 12-hour incubation, the LE exhibited nearly 18% mortality, whereas it was much higher at 62% (at 2.5 μg/mL) with the green-synthesized nanoparticles. The effect was maximum to the tune of 91% when the SINAP level went up to 25 μg/mL. The larvicidal action of SINAPs produced using the aqueous extract of cocoa beans was investigated [15]. A dose-dependent assay was carried out against the first instar anopheline larvae and the study gave an LC50 of 44 μg/mL after 1 hour. Within a duration of 3 hours, the larvicidal action was evident in the study. Using the aqueous LE of *Lippia citriodora*, SINAPs were prepared and tested for larvicidal action against the fourth instar period of *Cx. quinquefasciatus* [13]. The LC50 value after a 12-hour treatment period was 152 ppm and upon extending it by another 12 hours, the value came down to 138 ppm. Corresponding to a 24-hour treatment time, the mortality percentage was 93% for 250 ppm. The SINAPs fabricated by means of the leaf-based broth of *Euphorbia rothiana* showed significant larvicidal action against the third instar larval phase of *Ae. aegypti* [138]. Absolute mortality was achieved at 50 mg/L within two days and a LC50 value of 8 mg/L was obtained. Using stereomicroscopy, it was observed that *Ae. aegypti* displayed shrinkage of the cell along with lack of exterior hair (lateral and caudal). Histopathological analysis revealed the complete disintegration of caeca and mid-gut, signaling the ruin of the whole larval structure. The aqueous RE of *Parthenium hysterophorus* roots were employed to synthesize SINAPs, which were then tested against the late third instars of *Cx. quinquefasciatus* larvae [19]. The mortality rate was found to be both time- and dose-dependent. The study demonstrated that when compared to using the extract/metal salt solution in the 1:3 ratio, the mortality was approximately 21% and 26% higher when the ratio was 1:1 and 1:9, respectively.

The pediculocidal activity of SINAPs was evaluated using the LE of *Tinospora cordifolia* Miers. against *Pediculus humanus capitis* De Geer (head louse) [203]. The study also considered the larvicidal activity against the fourth instar larval stage of *Anopheles subpictus* Grassi and *Cx. quinquefasciatus*. Using the direct contact method, the LC50 value for the louse stood at 12 mg/L and for the mosquitoes it was between 6 and 7 mg/L. The SINAPs synthesized using the LE of *Manilkara zapota* showed acaricidal activity against a livestock tick, *Rhipicephalus microplus,* with an LC50 of 3.4 mg/L [204].

A lot of research homework needs to be carried out in order to fully understand the fate of nanoparticles in the environment. If SINAPs are commercially produced and exploited in insect repellents, their passage into other living systems and ultimately the food chain must be clearly comprehended. Their incorporation into water bodies must be seriously considered and long-term effect(s), if any, ought to be dealt with in the right spirit.

12.5 Environmental Applications

12.5.1 Catalytic Activity

12.5.1.1 Degradation of Dyes

The leaves of *Morinda tinctoria* were used in the synthesis of SINAPs, which were then tested for their catalytic ability in reducing the dye, methylene blue [205]. With the administration of nanoparticles under sunlight, the degradation was followed both visually and spectrophotometrically at 660 nm. Visually, the color progressed from deep blue to light blue to light green before turning colorless after 3 days. With time, the absorption bands at 660 nm took a dip and those for the SINAPs at 420 nm went up. The efficiency of photocatalytic degradation reached nearly 93% in 3 days. The characteristic bands vanished completely, signaling the absolute consumption of the dye. The degradation of the same dye was addressed using the SINAPs fabricated with the aqueous FE of *Saraca indica* [18]. Methylene blue was found to be completely reduced in under 20 min. The blue-colored dye turning colorless under oxidizing conditions points to the fact that it gets reduced to leucomethylene in the process [206]. The $n–\pi^*$ transition of the dye translates to the absorption band at 664 nm [207, 208]. The dye degradation process is aided by the SINAPs, which mediate the transfer of electrons from the dye to the reductant, sodium borohydride. These

nanoagents play redox catalysts in a process, which is dubbed as the "electron relay effect" [209, 210]. When the ability of SINAPs synthesized using *Lantana camara* LE was evaluated for methylene blue degradation, there was a significant reduction in the absorbance band at regular time intervals [211]. *Dimocarpus longan* seeds were the source of phytochemicals for the green synthesis of SINAPs used for verifying their photocatalytic efficiency against methylene blue [212]. When compared with the commercially available SINAPs, those that were green-synthesized degraded the dye up to 80% in just 30 min, while the former took the same amount of time to achieve 20%. The unique absorption band at 665 nm was found to decrease rapidly in the presence of SINAPs.

The reduction of the methyl orange, methylene blue and eosin yellow dyes was carried out in the presence of SINAPs and sodium borohydride synthesized using the aqueous extract of *Areca catechu* nut [213]. Their rates of degradation were monitored by observing the absorption bands at 664 nm [209], 516 nm [214] and 465 nm [215, 216], respectively, for methylene blue, eosin yellow and methyl orange. Here, the SINAPs were synthesized at two temperatures, 300K and 373K, wherein the nanoparticle formation was rapid in the latter condition. When the ratio of the extract-to-salt solution was fixed at 1:2, the rate constants of the dye degradation process catalyzed by SINAPs prepared at 373K and 300K were 0.34/min and 0.15/min, respectively, in the case of methylene blue. Under the same mixing ratio and temperature conditions, the constants were 0.36/min and 0.18/min for eosin yellow. For methyl orange, it turned out to be 0.37/min and 0.14/min. In a related study, SINAPs synthesized with the LE of *Mussaenda erythrophylla* helped in near complete degradation of methyl orange within a 45-min duration, unlike the nil progress exhibited when the reaction was devoid of nanoparticles [217].

Apart from methyl orange, the degradation of the secondary diazo anionic dye, Congo red, was carried out using SINAPs prepared using the kernel husk extract of *Anacardium occidentale* [218]. With an increase in treatment time, the absorption bands corresponding to Congo red and methyl orange at 490 nm and 466 nm, respectively, started declining. Complete degradation of methyl orange was attained in 20 min and it took another 10 min for Congo red to fully degrade. The near-instant degradation of the dyes upon the addition of SINAPs was evident from the color bleaching effect of the spectra. Degradation of the same dye was studied using SINAPs generated from a different source, the aqueous fruit extract of *Bridelia retusa* [148]. With a degradation rate constant of 0.056/min, the

pseudo-first-order reaction was completed in 24 min and the sample faded entirely from its initial intense red coloration. The dye degradation may be the outcome of surface electron excitation, subsequent reaction with oxygen and release of free hydroxyl radicals [219].

The FE of *Cassia auriculata* L. assisted in the synthesis of SINAPs, which were then used as the green catalyst for the degradation of the azo dye, methyl orange, in the presence of sodium borohydride [220]. The reaction that followed pseudo-first-order kinetics had a rate constant of 0.150/min. The characteristic absorption band of the dye at 464 nm decreased with time, with the reaction completed after 16 min. In a study aimed at the eco-friendly degradation of the azo dye, Direct Yellow 12, the aqueous BE of *Terminalia cuneata* was used to synthesize SINAPs [221]. The degradation of this dye, which shows maximum absorption at 404 nm, was monitored in the presence of the catalytic 25-nm nanoparticles. Within a duration of 40 min, the dye was completely degraded. In this approach, apart from being the electron donor, sodium borohydride also supplies hydrogen ions, altering the pH of the solution [222]. The net charge on the SINAPs, having turned positive, begins adsorbing the borohydride ion and the dye. It is at this point that the SINAPs initiate the catalysis by mediating electron flow from the borohydride ion to the dye [214]. The extract made with the double delight petals of *Rosa* 'ANDeli' was used to prepare zero-valent SINAPs [223]. The nanoparticles were employed to study the degradation of a Mexican dye, Putnam Sky Blue 39, in the presence of sunlight. Periodic spectrophotometric determination of residual dye concentration revealed that the percentage degradation reached 52% in the initial 15 min, which then went on to reach a maximum of 95% in 3 hours. Rhodamine Blue dye was subjected to catalytic degradation by SINAPs, synthesized with aqueous LE of *B. retusa* [224]. The reduction reaction, which took place in the presence of sodium tetrahydroborate, was monitored spectrophotometrically, focusing on the band at 555 nm arising from the $n \rightarrow \pi^*$ transition [225]. Modeled with pseudo-first-order kinetics, the reaction took a long 45 min to finish completely, with the degradation rate constant estimated at 0.07/min. However, in the presence of SINAPs, it took a mere 9 min for complete degradation, with the rate constant jumping to 0.13/min. The spectral study also noted the constant presence of the band at 420 nm corresponding to the SINAPs, establishing the part of the catalyst in the entire process.

All the dye degradation studies involving SINAPs show encouraging results as compared to the ones that do not include the particles. The particles show exceptional photocatalytic activity against the toxic dyes. This paves the way for their application in large-scale industrial effluent

treatment and water purification plants. The dyes are most encountered in industries concerned with textiles, paper, leather and food materials. With proper validation of the fate of SINAPs in the environment, they show utmost promise in arresting land and water pollution.

12.5.1.2 Degradation of other Pollutants

Assessment of the catalytic activity of the green-synthesized SINAPs is usually done with regard to the effectiveness with which toxic molecules are degraded. The nanoparticles take the role of heterogeneous nanocatalysts in degrading organic molecules like 4-nitrophenol (4-NP), which is reduced to 4-aminopheno (4-AP) using sodium borohydride as the reductant. In the absence of the nanoparticles, the reduction reaction is curtailed by thermodynamic barriers that these particles seek to break. Environmental pollution due to nitrophenol and its derivatives mostly occurs during the manufacture of dyes, herbicides, insecticides and pesticides [226, 227]. The harmful nature of 4-NP is minimized by converting it into the more industrially useful 4-AP. This conversion has been the catalytic reaction most used by researchers in testing the catalytic potential as well as the environmental viability of the nanoparticles. In this specific case, the approach is linked with the use of spectrophotometry, thus making it quantitative, by following the decrease of the absorption band (at 403 nm corresponding to 4-NP) and the corresponding increase of the absorption band (between 290–300 nm corresponding to 4-AP) [212, 226, 228]. The rate constant of the reaction is assumed to be independent of the reductant concentration, and hence the reaction is thought to follow pseudo-first-order kinetics.

The leaves of *Ziziphus spina-christi* were used to create zero-valent silver in the nano-range size, upon which, their catalytic activity was probed employing the conversion of 4-NP to 4-AP in the presence of sodium borohydride [229]. The size-based experimental strategy proved that the catalytic rate constant went up from 2.3×10^{-3} /s to 4.4×10^{-3} /s when the SINAP size was reduced from 19 mm to 15 mm. In general, when the size of the particle becomes smaller, it implies that the effective surface area on the catalyst available for electron relay will surge ahead, which in turn is evident in the increase of the degradation rate [228, 230]. The reaction was very fast, having completed within a duration of 14–20 min. In a similar work concerning 4-NP to 4-AP reduction, the seed extract of *Dimocarpus longan* mediated the green synthesis of SINAPs [212]. The evanescence of the yellow color of 4-NP materialized within 12 min, signaling its complete exhaustion. When the study attempted to compare biogenic nanoparticles against commercially available ones, the latter finished the reduction in

26 min. However, both forms of the nanoparticles followed a first-order reaction. The performance clearly underscored the suitability of the plant-derived nanoparticles for pollution abatement. The aqueous extract of green coffee bean was employed to synthesize SINAPs to mediate the catalysis of 4-NP to 4-AP, wherein an apparent rate constant of 0.0456/s was attained [231]. In another study, the reduction reaction to 4-NP occurred in nearly 10 min, when SINAPs were synthesized using the aqueous LE of *Cicer arietinum* [232]. The same reduction reaction had a rate constant of 0.159/min, when catalyzed by SINAPs derived from a reaction mediated by the phytochemicals in the aqueous FE of *C. auriculate* [220], wherein complete decolorization of 4-NP was wrapped up in 12 min. It was higher manifold when the same reaction was performed devoid of the nanoparticles.

An agro-industrial remnant, the peels of *Citrus aurantifolia,* was chosen to synthesize SINAPs and their catalytic activity was verified via the hydrogenation of 4-nitroaniline to 4-phenylenediamine [233]. In the spectrophotometric analysis, the transformation of absorption band involved the gradual flattening at 380 nm (pertaining to 4-nitroaniline and sodium borohydride) along with the prominence of bands at 240 nm and 310 nm (pertaining to 4-phenylenediamine). The reaction, which was shown to follow pseudo-first-order kinetics, exhibited a rate constant of 4.6×10^{-3} /s. When the concentration of the SINAPs was raised, the rate of hydrogenation also followed a similar trend.

The experimental studies and observations highly favor the use of SINAPs as an eco-friendly alternative to subvert the challenge posed by certain anthropogenic pollutants that threaten our ecosystem. Nearly all the results have clearly expounded the merit of biologically derived SINAPs as economically viable and biologically compatible agents for the diminution of certain forms of pollution.

12.5.2 Metal Ion Detection

Another significant application of SINAPs is in the detection of potentially hazardous heavy metal ions present in aqueous solutions. Long-term exposure to metal ions causes severe health hazards for humans and animals alike. Riding on the presence of organic functional groups in plant-based extracts, the concentration of metal ions is determined using simple colorimetric methods that are both economical and rapid. Examples of the application of green-synthesized SINAPs are discussed in this section.

The aqueous extracts of the stems and leaves of *Hibiscus sabdariffa* were employed to mediate the synthesis of SINAPs for the detection of mercury, lead and cadmium ions [234]. The presence of these hazardous metal

contaminants are colorimetrically sensed in aqueous solutions clearly down to the level of ppm. The significance of sunlight and pH conditions were also investigated and correlated with the stability of the SINAPs. The selectivity and sensitivity of detection varied with the plant source. Using the extract derived from *Azadirachta indica*, SINAPs were fabricated that showed exceptional specificity in the detection of copper from aqueous solutions [235]. Temperature and pH influenced the formation of the nanoparticles.

In a study using the juice of *Citrullus lanatus*, SINAPs were engineered to test their efficiency in detecting mercury and copper ions up to μM levels on a colorimetric basis [236]. With the addition of the nanoparticle solution, the color of various copper sample solutions was altered from yellow to blue, the intensity of which kept on increasing with an increase in copper ion levels. In the case of mercury, the transition was from yellow to black in a method where the nanoparticles were functionalized with the chelator, 3-mercapto-1,2-propanediol. The riboflavin found in the juice is deemed to be responsible for maintaining the stability of the SINAPs [237, 238], and the peptide bond could induce the formation of a coordination with copper ions [239, 240]. Latex obtained from the incisions on *Euphorbia heterophylla* leaves served as the source of capping/reducing agents for the synthesis of SINAPs [241]. Specifically, the divalent mercury ions attach with the nanoparticles on their surface, weaken their absorption band and aggregate the nanoparticle colloidal solution. The green approach depicted a high degree of specificity towards mercury and could detect the ions at levels as low as 100 ppb. The selectivity is largely because of the formation of complex consisting of mercury ions and –SH group of the latex on the surface of SINAPs [241]. The SINAPs synthesized using the fresh leaves of neem had the ability to sense mercury ions, while the dried version of the same leaves could sniff out both mercury and lead ions [242]. Apart from mercury, the bark of neem tree that gave rise to SINAPs could also detect zinc ions. Mercury and lead could be detected using SINAPs made with the extracts of mango leaves and green tea. Starting with the extract of pepper, detection of zinc, mercury and lead was possible. Above all, it is noteworthy that the approaches developed were fully viable in the broad pH spectrum between 2 and 11. Using gum kondagogu, SINAPs were synthesized to identify the presence of mercury in aqueous solutions [243]. Being highly selective, the technique was able to achieve mercury detection down to a minimum of 50 mM. The aqueous extract of commercially available *Camellia sinensis* was used in the preparation of SINAPs, which were then used for the detection of lead and copper ions [244]. The change of color was both visible and analyzed with fluorescence spectroscopy. In

the presence of heavy metal ions, catechol, epicatechin, gallic acid and other such polyphenolic molecules are previously recorded to manifest as coordination complexes. The two ions in this work, favorably bind to the –COOH moiety [235, 245, 246]. In a similar study using the aqueous extract of *Syzygium aqueum*, the SINAPs could selectively detect mercury at levels as low as 8.5×10^{-7} M in water samples obtained from domestic supply and lakes [247]. Similarly, the SINAPs made using *Rhaphidophora hongkongensis* LE showed outstanding selectivity in tracing the heavy metal ions Hg^{2+} and Fe^{3+} [248]. Accounts of such research investigations ratify the value of SINAPs for environmental applications.

12.6 Conclusions and Future Directions

Research involving the green synthesis of metal nanoparticles, especially that of silver, is currently on a roll. Rummaging through the piles of literature always yields meticulously researched data concerning many plants and parts thereof for the controlled engineering of SINAPs. Compared to other methods of nanoparticle fabrication, plant-mediated methods are advantageous in many ways. For instance, there is no need for plant sources to be maintained *in vitro* under controlled conditions in a laboratory. As and when required, a plant specimen could be harvested to tap the medically significant metabolites.

Apart from the allopathic system of medicine, various systems of medicine using plants are known the world over. When elucidating the mechanism of nanoparticles mediating a biomedical application, the role played by the nanoparticle itself is primarily the extremely specific surface area and its catalytic abilities on offer. The factor that maintains the stability of such a nanoparticle system lies squarely with the phytochemical composition of a plant part under question. The capping function provided by the phytochemicals has been outstanding. There are also a good number of reports concerning herbal plants yet to be considered concerning the storehouse of information that we possess on medicinal plants, and translating the huge scope of that data for exploitation in nanotechnology.

The biomedical applications of the SINAPs have been far-reaching due to the biocompatibility and efficacy in carrying out the desired reaction. The future might see the application of nanoparticles in a real-time mode during medical emergencies, considering the rapidity with which they interact in biological systems. Numerous researchers have explained the mechanisms behind each of the biomedical and environmental applications to which the nanoparticle has been put. In most of these cases, the

phytoextract has been employed straightaway for the synthetic protocol. Very few studies have dealt with purification of specific phytochemicals for nanoparticle synthesis. Research must be fast-tracked to investigate and comprehend the precise mechanism by which purified phytochemicals act as reducing as well as capping agents during SINAP synthesis. In order to reap the commercial benefits of the technology, the entire process, beginning from sourcing the plant material and nanoparticle synthesis up to the final application of the same, must experience a feasible scale-up strategy.

As illustrated and discussed at length, the applications of SINAPs are multifarious. Nevertheless, the fate of the nanoparticles, both *in vivo* and *in vitro*, must be comprehensively studied and validated. On the whole, the green synthesis of SINAPs holds great promise and furthering the technology, after duly considering safety aspects, would prove increasingly beneficial for humankind. So, there is an urgent need for induction of rigorous parameters for regulation of quality. Prior to human and animal consumption, strict guidelines must be in place, with certification obtained from competent regulatory authorities, formed specifically to look into nanotechnology-related developments. The pace of research concerning the optimization of nanoparticle synthesis and its application is bound to witness gargantuan growth in the coming years.

References

1. Iravani, S., Green synthesis of metal nanoparticles using plants. *Green Chem.*, 13, 2638–2650, 2011.
2. Thakkar, K.N., Mhatre, S.S., Parikh, R.Y., Biological synthesis of metallic nanoparticles. *Nanomed.-Nanotechnol.*, 6, 257–262, 2010.
3. Begum, N.A., Mondal, S., Basu, S., Laskar, R.A., Mandal, D., Biogenic synthesis of Au and Ag nanoparticles using aqueous solutions of Black Tea leaf extracts. *Colloids Surf. B,* 71, 113–118, 2009.
4. Li, X., Xu, H., Chen, Z.S., Chen, G., Biosynthesis of nanoparticles by microorganisms and their applications. *J. Nanomater.*, 2011, 1–6, 2011.
5. Roy, N., Biogenic synthesis of Au and Ag nanoparticles by Indian propolis and its constituents. *Colloids Surf. B,* 76, 317–325, 2010.
6. Das, V.L., Extracellular synthesis of silver nanoparticles by the Bacillus strain CS 11 isolated from industrialized area. *Biotech*, 4, 121–126, 2014.
7. El-Sonbaty, S.M., Fungus-mediated synthesis of silver nanoparticles and evaluation of antitumor activity. *Cancer Nanotechnol.*, 4, 73–79, 2013.
8. Kathiraven, T., Sundaramanickam, A., Shanmugam, N., Balasubramanian, T., Green synthesis of silver nanoparticles using marine algae *Caulerpa*

racemosa and their antibacterial activity against some human pathogens. *Appl. Nanosci.*, 5, 499–504, 2015.

9. Raja, S., Ramesh, V., Thivaharan, V., Green biosynthesis of silver nanoparticles using *Calliandra haematocephala* leaf extract, their antibacterial activity and hydrogen peroxide sensing capability. *Arab. J. Chem.*, 10, 253–261, 2017.
10. Kumar, V., Yadav, S.K., Plant-mediated synthesis of silver and gold nanoparticles and their applications. *J. Chem. Technol. Biotechnol.*, 84, 151–157, 2005.
11. Njagi, E.C., Biosynthesis of Iron and silver nanoparticles at room temperature using aqueous sorghum bran extracts. *Langmuir*, 27, 264–271, 2011.
12. Schröfel, A., Applications of biosynthesized metallic nanoparticles – A review. *Acta Biomater.*, 10, 4023–4042, 2014.
13. Elemike, E.E., Onwudiwe, D.C., Ekennia, A.C., Ehiri, R.C., Nnaji, N.J., Phytosynthesis of silver nanoparticles using aqueous leaf extracts of *Lippia citriodora*: Antimicrobial, larvicidal and photocatalytic evaluations. *Mater. Sci. Eng. C*, 75, 980–989, 2017.
14. Balashanmugam, P., Kalaichelvan, P.T., Biosynthesis characterization of silver nanoparticles using *Cassia roxburghii* DC. aqueous extract, and coated on cotton cloth for effective antibacterial activity. *Int. J. Nanomed.*, 10, 87–95, 2015.
15. Azeez, M.A., Lateef, A., Asafa, T.B., Yekeen, T.A., Akinboro, A., Oladipo, I.C., Gueguim-Kana, E.B., Beukes, L.S., Biomedical applications of cocoa bean extract-mediated silver nanoparticles as antimicrobial, larvicidal and anticoagulant agents. *J. Clust. Sci.*, 28, 149–164, 2017.
16. Mittal, A.K., Tripathy, D., Choudhary, A., Aili, P.K., Chatterjee, A., Singh, I.P., Banerjee, U.C., Bio-synthesis of silver nanoparticles using *Potentilla fulgens* Wall. ex Hook. and its therapeutic evaluation as anticancer and antimicrobial agent. *Mater. Sci. Eng. C*, 53, 120–127, 2015.
17. Pattanayak, S., Mollick, M.M.R., Maity, D., Chakraborty, S., Dash, S.K., Chattopadhyay, S., Roy, S., Chattopadhyay, D., Chakraborty, M., *Butea monosperma* bark extract mediated green synthesis of silver nanoparticles: Characterization and biomedical applications. *J. Saudi Chem. Soc.*, 21, 673–684, 2017.
18. Vidhu, V.K., Philip, D., Spectroscopic, microscopic and catalytic properties of silver nanoparticles synthesized using *Saraca indica* flower. *Spectrochim. Acta A*, 117, 102–108, 2014.
19. Mondal, N.K., Chowdhury, A., Dey, U., Mukhopadhya, P., Chatterjee, S., Das, K., Datta, J.K., Green synthesis of silver nanoparticles and its application for mosquito control. *Asian Pacific J. Trop. Dis.*, 4, 204–210, 2014.
20. Dutta, P.P., Bordoloi, M., Gogoi, K., Roy, S., Narzary, B., Bhattacharyya, D.R., Mohapatra, P.K., Mazumder, B., Antimalarial silver and gold nanoparticles: Green synthesis, characterization and *in vitro* study. *Biomed. Pharmacother.*, 91, 567–580, 2017.

21. Balalakshmi, C., Gopinath, K., Govindarajan, M., Lokesh, R., Arumugam, A., Alharbi, N.S., Kadaikunnan, S., Khaled, J.M., Benelli, G., Green synthesis of gold nanoparticles using a cheap *Sphaeranthus indicus* extract: Impact on plant cells and the aquatic crustacean *Artemia nauplii*. *J. Photochem. Photobiol. B Biol.*, 173, 598–605, 2017.
22. Paul, B., Bhuyan, B., Purkayastha, D.D., Vadivel, S., Dhar, S.S., One-pot green synthesis of gold nanoparticles and studies of their anticoagulative and photocatalytic activities. *Mater. Lett.*, 185, 143–147, 2016.
23. Yu, J., Xu, D., Guan, H.N., Wang, C., Huang, L.K., Facile one-step green synthesis of gold nanoparticles using *Citrus maxima* aqueous extracts and its catalytic activity. *Mater. Lett.*, 166, 110–112, 2016.
24. Khademi-Azandehi, P., Moghaddam, J., Green synthesis, characterization and physiological stability of gold nanoparticles from *Stachys lavandulifolia* Vahl extract. *Particuology*, 19, 22–26, 2015.
25. Philip, D., Green synthesis of gold and silver nanoparticles using *Hibiscus rosa sinensis*. *Physica E*, 42, 1417–1424, 2010.
26. Mishra, A., Kaushik, N.K., Sardar, M., Sahal, D., Evaluation of antiplasmodial activity of green synthesized silver nanoparticles. *Colloids Surf. B*, 111, 713–718, 2013.
27. Kanchana, A., Devarajan, S., Ayyappan, S.R., Green synthesis and characterization of palladium nanoparticles and its conjugates from *Solanum trilobatum* leaf extract. *Nano-Micro Lett.*, 2, 169–176, 2010.
28. Kalaiselvi, A., Roopan, S.M., Madhumitha, G., Ramalingam, C., Elango, G., Synthesis and characterization of palladium nanoparticles using *Catharanthus roseus* leaf extract and its application in the photo-catalytic degradation. *Spectrochim. Acta A*, 135, 116–119, 2015.
29. Nasrollahzadeh, M., Sajadi, S.M., Rostami-Vartooni, A., Khalaj, M., Green synthesis of Pd/Fe3O4 nanoparticles using *Euphorbia condylocarpa* M. bieb root extract and their catalytic applications as magnetically recoverable and stable recyclable catalysts for the phosphine-free Sonogashira and Suzuki coupling reactions. *J. Mol. Catal. A Chem.*, 396, 31–39, 2015.
30. Koupaei, M.H., Shareghi, B., Saboury, A.A., Davar, F., Semnani, A., Evini, M., Green synthesis of zinc oxide nanoparticles and their effect on the stability and activity of proteinase K. *RSC Adv.*, 6, 42313–42323, 2016.
31. Bala, N., Saha, S., Chakraborty, M., Maiti, M., Das, S., Basu, R., Nandy, P., Green synthesis of zinc oxide nanoparticles using *Hibiscus subdariffa* leaf extract: Effect of temperature on synthesis, anti-bacterial activity and anti-diabetic activity. *RSC Adv.*, 5, 4993–5003, 2015.
32. Jamdagni, P., Khatri, P., Rana, J.S., Green synthesis of zinc oxide nanoparticles using flower extract of *Nyctanthes arbor-tristis* and their antifungal activity. *J. King Saud Univ. - Sci.* 1–8, 2016.
33. Wei, Y., Fang, Z., Zheng, L., Tan, L., Tsang, E.P., Green synthesis of Fe nanoparticles using *Citrus maxima* peels aqueous extracts. *Mater. Lett.*, 185, 384–386, 2016.

34. Xiao, Z., Yuan, M., Yang, B., Liu, Z., Huang, J., Sun, D., Plant-mediated synthesis of highly active iron nanoparticles for Cr (VI) removal: Investigation of the leading biomolecules. *Chemosphere*, 150, 357–364, 2016.
35. Balamurughan, M.G., Mohanraj, S., Kodhaiyolii, S., Pugalenthi, V., *Ocimum sanctum* leaf extract mediated green synthesis of iron oxide nanoparticles: Spectroscopic and microscopic studies. *J. Chem. Pharm. Sci.*, 4, 201–206, 2014.
36. Makarov, V.V., Makarova, S.S., Love, A.J., Sinitsyna, O.V., Dudnik, A.O., Yaminsky, I.V., Taliansky, M.E., Kalinina, N.O., Biosynthesis of stable iron oxide nanoparticles in aqueous extracts of *Hordeum vulgare* and *Rumex acetosa* plants. *Langmuir*, 30, 5982–5988, 2014.
37. Shanker, U., Jassal, V., Rani, M., Green synthesis of iron hexacyanoferrate nanoparticles: Potential candidate for the degradation of toxic PAHs. *J. Environ. Chem. Eng.*, 5, 4108–4120, 2017.
38. Salem, N.M., Albanna, L.S., Awwad, A.M., Green synthesis of sulfur nanoparticles using *Punica granatum* peels and the effects on the growth of tomato by foliar spray applications. *Environ. Nanotechnol. Monit. Manag.* 6, 83–87, 2016.
39. Marimuthu, S., Rahuman, A.A., Jayaseelan, C., Kirthi, A.V., Santhoshkumar, T., Velayutham, K., Bagavan, A., Kamaraj, C., Elango, G., Iyappan, M., Siva, C., Acaricidal activity of synthesized titanium dioxide nanoparticles using *Calotropis gigantea* against *Rhipicephalus microplus* and *Haemaphysalis bispinosa*. *Asian Pac. J. Trop. Med.*, 6, 682–688, 2013.
40. Santhoshkumar, T., Rahuman, A.A., Jayaseelan, C., Rajakumar, G., Marimuthu, S., Kirthi, A.V., Velayutham, K., Thomas, J., Venkatesan, J., Kim, S.K., Green synthesis of titanium dioxide nanoparticles using *Psidium guajava* extract and its antibacterial and antioxidant properties. *Asian Pac. J. Trop. Med.*, 7, 968–976, 2014.
41. Sharma, J.K., Srivastava, P., Ameen, S., Akhtar, M.S., Sengupta, S.K., Singh, G., Phytoconstituents assisted green synthesis of cerium oxide nanoparticles for thermal decomposition and dye remediation. *Mater. Res. Bull.*, 91, 98–107, 2017.
42. Kannan, S.K., Sundrarajan, M., Green synthesis of ruthenium oxide nanoparticles: Characterization and its antibacterial activity. *Adv. Powder Technol.*, 26, 1505–1511, 2015.
43. Gopinath, K., Karthika, V., Gowri, S., Senthilkumar, V., Kumaresan, S., Arumugam, A., Antibacterial activity of ruthenium nanoparticles synthesized using *Gloriosa superba* L. leaf extract. *J. Nanostruct. Chem.*, 4, 83–89, 2014.
44. Keihan, A.H., Veisi, H., Veasi, H., Green synthesis and characterization of spherical copper nanoparticles as organometallic antibacterial agent. *Appl. Organomet. Chem.*, 31, 3642–3648, 2017.
45. Chung, I., Abdul Rahuman, A., Marimuthu, S., Vishnu Kirthi, A., Anbarasan, K., Padmini, P., Rajakumar, G., Green synthesis of copper nanoparticles using

Eclipta prostrata leaves extract and their antioxidant and cytotoxic activities. *Exp. Ther. Med.*, 14, 18–24, 2017.
46. Ghidan, A.Y., Al-Antary, T.M., Awwad, A.M., Green synthesis of copper oxide nanoparticles using *Punica granatum* peels extract: Effect on green peach Aphid. *Environ. Nanotechnol. Monit. Manag.* 6, 95–98, 2016.
47. Yugandhar, P., Vasavi, T., Uma Maheswari Devi, P., Savithramma, N., Bioinspired green synthesis of copper oxide nanoparticles from *Syzygium alternifolium* (Wt.) Walp: Characterization and evaluation of its synergistic antimicrobial and anticancer activity. *Appl. Nanosci.*, 7, 417–427, 2017.
48. Wei, Q., Kang, S.-Z., Mu, J., Green synthesis of starch capped CdS nanoparticles. *Colloids Surf. A*, 247, 125–127, 2004.
49. Goud, B.S., Suresh, Y., Annapurna, S., Singh, A.K., Bhikshamaiah, G., Green Synthesis and characterization of cadmium sulphide nanoparticles. *Mater. Today Proc.*, 3, 4003–4008, 2016.
50. Elango, G., Roopan, S.M., Green synthesis, spectroscopic investigation and photocatalytic activity of lead nanoparticles. *Spectrochim. Acta A*, 139, 367–373, 2015.
51. Elavazhagan, T., Arunachalam, K.D., *Memecylon edule* leaf extract mediated green synthesis of silver and gold nanoparticles. *Int. J. Nanomed.*, 6, 1265–1271, 2011.
52. Philip, D., *Mangifera indica* leaf-assisted biosynthesis of well-dispersed silver nanoparticles. *Spectrochim. Acta A*, 78, 327–331, 2011.
53. Raghunandan, D., Mahesh, B.D., Basavaraja, S., Balaji, S.D., Manjunath, S.Y., Venkataraman, A., Microwave-assisted rapid extracellular synthesis of stable bio-functionalized silver nanoparticles from guava (*Psidium guajava*) leaf extract. *J. Nanopart. Res.*, 13, 2021–2028, 2011.
54. Rao, Y.S., Kotakadi, V.S., Prasad, T.N.V.K.V., Reddy, A.V., Gopal, D.V.R.S., Green synthesis and spectral characterization of silver nanoparticles from Lakshmi tulasi (*Ocimum sanctum*) leaf extract. *Spectrochim. Acta A*, 103, 156–159, 2013.
55. Marimuthu, S., Rahuman, A.A., Rajakumar, G., Santhoshkumar, T., Kirthi, A.V., Jayaseelan, C., Bagavan, A., Zahir, A.A., Elango, G., Kamaraj, C., Evaluation of green synthesized silver nanoparticles against parasites. *Parasitol. Res.*, 108, 1541–1549, 2011.
56. Lukman, A.I., Gong, B., Marjo, C.E., Roessner, U., Harris, A.T., Facile synthesis, stabilization, and anti-bacterial performance of discrete Ag nanoparticles using *Medicago sativa* seed exudates. *J. Colloid Interface Sci.*, 353, 433–444, 2011.
57. Sathishkumar, G., Gobinath, C., Karpagam, K., Hemamalini, V., Premkumar, K., Sivaramakrishnan, S., Phyto-synthesis of silver nanoscale particles using Morinda citrifolia L. and its inhibitory activity against human pathogens. *Colloids Surf. B,* 95, 235–240, 2012.
58. Antony, J.J., Sivalingam, P., Siva, D., Kamalakkannan, S., Anbarasu, K., Sukirtha, R., Krishnan, M., Achiraman, S., Comparative evaluation of

antibacterial activity of silver nanoparticles synthesized using *Rhizophora apiculata* and glucose. *Colloids Surf. B,* 88, 134–140, 2011.

59. Jeyaraj, M., Rajesh, M., Arun, R., MubarakAli, D., Sathishkumar, G., Sivanandhan, G., Dev, G.K., Manickavasagam, M., Premkumar, K., Thajuddin, N., Ganapathi, A., An investigation on the cytotoxicity and caspase-mediated apoptotic effect of biologically synthesized silver nanoparticles using *Podophyllum hexandrum* on human cervical carcinoma cells. *Colloids Surf. B,* 102, 708–717, 2013.
60. Kumar, V., Yadav, S.C., Yadav, S.K., *Syzygium cumini* leaf and seed extract mediated biosynthesis of silver nanoparticles and their characterization. *J. Chem. Technol. Biotechnol.*, 85, 1301–1309, 2010.
61. Kumar, K.M., Sinha, M., Mandal, B.K., Ghosh, A.R., Kumar, K.S., Reddy, P.S., Green synthesis of silver nanoparticles using *Terminalia chebula* extract at room temperature and their antimicrobial studies. *Spectrochim. Acta A*, 91, 228–233, 2012.
62. Raghunandan, D., Borgaonkar, P., Bendegumble, B., Bedre, M., Bhagawanraju, M., Yalagatti, M., Huh, D., Abbaraju, V., Microwave-assisted rapid extracellular biosynthesis of silver nanoparticles using carom seed (*Trachyspermum copticum*) extract and *in vitro* studies. *Am. J. Anal. Chem.*, 2, 475–481, 2011.
63. Rodríguez-León, E., Iñiguez-Palomares, R., Navarro, R.E., Herrera-Urbina, R., Tánori, J., Iñiguez-Palomares, C., Maldonado, A., Synthesis of silver nanoparticles using reducing agents obtained from natural sources (*Rumex hymenosepalus* extracts). *Nanoscale Res. Lett.*, 8, 318–325, 2013.
64. Roni, M., Murugan, K., Panneerselvam, C., Subramaniam, J., Hwang, J.-S., Evaluation of leaf aqueous extract and synthesized silver nanoparticles using *Nerium oleander* against *Anopheles stephensi* (Diptera: Culicidae). *Parasitol. Res.*, 112, 981–990, 2013.
65. Sahu, N., Soni, D., Chandrashekhar, B., Sarangi, B.K., Satpute, D., Pandey, R.A., Synthesis and characterization of silver nanoparticles using *Cynodon dactylon* leaves and assessment of their antibacterial activity. *Bioprocess Biosyst. Eng.*, 36, 999–1004, 2013.
66. Suganya, A., Murugan, K., Kovendan, K., Mahesh Kumar, P., Hwang, J.-S., Green synthesis of silver nanoparticles using *Murraya koenigii* leaf extract against *Anopheles stephensi* and *Aedes aegypti*. *Parasitol. Res.*, 112, 1385–1397, 2013.
67. Vijayaraghavan, K., Nalini, S.P.K., Prakash, N.U., Madhankumar, D., One step green synthesis of silver nano/microparticles using extracts of *Trachyspermum ammi* and *Papaver somniferum*. *Colloids Surf. B*, 94, 114–117, 2012.
68. Geethalakshmi, R., Sarada, D.V., Gold and silver nanoparticles from *Trianthema decandra*: Synthesis, characterization, and antimicrobial properties. *Int. J. Nanomed.*, 7, 5375–5380, 2012.
69. Prasad, K.S., Pathak, D., Patel, A., Dalwadi, P., Prasad, R., Patel, P., Selvaraj, K. Biogenic synthesis of silver nanoparticles using *Nicotiana tobaccum* leaf

extract and study of their antibacterial effect. *Afr. J. Biotechnol.*, 10, 8122–8128, 2011.
70. Vigneshwaran, N., Nachane, R.P., Balasubramanya, R.H., Varadarajan, P.V., A novel one-pot 'green' synthesis of stable silver nanoparticles using soluble starch. *Carbohydr. Res.*, 341–348, 2006.
71. Patil, S.V, Borase, H.P., Patil, C.D., Salunke, B.K., Biosynthesis of Silver nanoparticles using latex from few *Euphorbian* plants and their antimicrobial potential. *Appl. Biochem. Biotechnol.*, 167, 776–790, 2012.
72. Arulkumar, S., Sabesan, M., Biosynthesis and characterization of gold nanoparticle using antiparkinsonian drug *Mucuna pruriens* plant extract. *Int. J. Res. Pharm. Sci.*, 1, 417–421, 2010.
73. Bankar, A., Joshi, B., Kumar, A.R., Zinjarde, S., Banana peel extract mediated novel route for the synthesis of silver nanoparticles. *Colloids Surf. A*, 368, 58–63, 2010.
74. Das, J., Das, M.P., Velusamy, P., *Sesbania grandiflora* leaf extract mediated green synthesis of antibacterial silver nanoparticles against selected human pathogens. *Spectrochim. Acta A*, 104, 265–270, 2013.
75. Gopinath, V., MubarakAli, D., Priyadarshini, S., Priyadharsshini, N.M., Thajuddin, N., Velusamy, P., Biosynthesis of silver nanoparticles from *Tribulus terrestris* and its antimicrobial activity: A novel biological approach. *Colloids Surf. B*, 96, 69–74, 2012.
76. Loo, Y.Y., Chieng, B.W., Nishibuchi, M., Radu, S., Synthesis of silver nanoparticles by using tea leaf extract from *Camellia sinensis*. *Int. J. Nanomed.*, 7, 4263–4267, 2012.
77. Marimuthu, S., Rahuman, A.A., Santhoshkumar, T., Jayaseelan, C., Kirthi, A.V., Bagavan, A., Kamaraj, C., Elango, G., Zahir, A.A., Rajakumar, G., Velayutham, K., Lousicidal activity of synthesized silver nanoparticles using *Lawsonia inermis* leaf aqueous extract against *Pediculus humanus capitis* and *Bovicola ovis*. *Parasitol. Res.*, 111, 2023–2033, 2012.
78. Pasupuleti, V.R., Prasad, T.N.V.K.V., Shiekh, R.A., Balam, S.K., Narasimhulu, G., Reddy, C.S., Rahman, I.A., Gan, S. H., Biogenic silver nanoparticles using *Rhinacanthus nasutus* leaf extract: Synthesis spectral analysis and antimicrobial studies. *Int. J. Nanomed.*, 8, 3355–3340, 2013.
79. Prabakar, K., Sivalingam, P., Rabeek, S.I.M., Muthuselvam, M., Devarajan, N., Arjunan, A., Karthick, R., Suresh, M.M., Wembonyama, J.P., Evaluation of antibacterial efficacy of phyto fabricated silver nanoparticles using *Mukia scabrella* (Musumusukkai) against drug resistance nosocomial gram negative bacterial pathogens. *Colloids Surf. B*, 104, 282–288, 2013.
80. Prakash, P., Gnanaprakasam, P., Emmanuel, R., Arokiyaraj, S., Saravanan, M., Green synthesis of silver nanoparticles from leaf extract of *Mimusops elengi,* Linn. for enhanced antibacterial activity against multi drug resistant clinical isolates. *Colloids Surf. B*, 108, 255–259, 2013.
81. Santhoshkumar, T., Rahuman, A.A., Rajakumar, G., Marimuthu, S., Bagavan, A., Jayaseelan, C., Zahir, A.A., Elango, G., Kamaraj, C., Synthesis of silver

nanoparticles using *Nelumbo nucifera* leaf extract and its larvicidal activity against malaria and filariasis vectors. *Parasitol. Res.*, 108, 693–702, 2011.
82. Kora, A.J., Beedu, S.R., Jayaraman, A., Size-controlled green synthesis of silver nanoparticles mediated by gum ghatti (*Anogeissus latifolia*) and its biological activity. *Org. Med. Chem. Lett.*, 2, 17–21, 2012.
83. Rajan, R., Chandran, K., Harper, S.L., Yun, S.-I., Kalaichelvan, P.T., Plant extract synthesized silver nanoparticles: An ongoing source of novel biocompatible materials. *Ind. Crops Prod.*, 70, 356–373, 2015.
84. Salunke, B.K., Sathiyamoorthi, E., Tran, T.K., Kim, B.S., Phyto-synthesized silver nanoparticles for biological applications. *Korean J. Chem. Eng.*, 34, 943–951, 2017.
85. Sathishkumar, M., Sneha, K., Won, S.W., Cho, C.W., Kim, S., Yun, Y.S., *Cinnamon zeylanicum* bark extract and powder mediated green synthesis of nano-crystalline silver particles and its bactericidal activity. *Colloids Surf. B*, 73, 332–338, 2009.
86. Alexander, J.W., History of the medical use of silver. *Surg Infect (Larchmt)*, 10, 289–295, 2009.
87. Shrivastava, S., Bera, T., Roy, A., Singh, G., Ramachandrarao, P., Dash, D., Characterization of enhanced antibacterial effects of novel silver nanoparticles. *Nanotechnology*, 18, 225103–225110, 2007.
88. Sondi, I., Salopek-Sondi, B., Silver nanoparticles as antimicrobial agent: A case study on *E-coli* as a model for Gram-negative bacteria. *J. Colloid Interface Sci.*, 275, 177–182, 2004.
89. Lok, C.N., Ho, C.M., Chen, R., He, Q.Y., Yu, W.Y., Sun, H., Tam, P.K.H., Chiu, J.F., Che, C.M., Proteomic analysis of the mode of antibacterial action of silver nanoparticles. *J. Proteome Res.*, 5, 916–924, 2006.
90. Danilczuk, M., Lund, A., Sadlo, J., Yamada, H., Michalik, J., Conduction electron spin resonance of small silver particles. *Spectrochim. Acta A*, 63, 189–191, 2006.
91. Kim, J.S., *et al.,* Antimicrobial effects of silver nanoparticles. *Nanomedicine: NBM*, 3, 95–101, 2007.
92. Bragg, P.D., Rainnie, D.J., The effect of silver ions on the respiratory chain of *Escherichia coli*. *Can. J. Microbiol.*, 20, 883–889, 1974.
93. McDonnell, G., Russell, A.D., Antiseptics and disinfectants: Activity, action, and resistance. *Clin. Microbiol. Rev.*, 12, 147–152, 1999.
94. Ahmed, S., Saifullah, Ahmad, M., Swami, B.L., Ikram, S., Green synthesis of silver nanoparticles using *Azadirachta indica* aqueous leaf extract. *J. Radiat. Res. Appl. Sci.*, 9, 1–7, 2016.
95. Ajitha, B., Reddy, Y.A.K., Reddy, P.S., Biogenic nano-scale silver particles by *Tephrosia purpurea* leaf extract and their inborn antimicrobial activity. *Spectrochim. Acta A*, 121, 164–172, 2014.
96. Elangovan, K., Elumalai, D., Anupriya, S., Shenbhagaraman, R., Kaleena, P.K., Murugesan, K., Phyto mediated biogenic synthesis of silver nanoparticles using leaf extract of *Andrographis echioides* and its bio-efficacy on

anticancer and antibacterial activities. *J. Photochem. Photobiol. B Biol.*, 151, 118–124, 2015.
97. Yuvarajan, R., Natarajan, D., Ragavendran, C., Jayavel, R., Photoscopic characterization of green synthesized silver nanoparticles from *Trichosanthes tricuspidata* and its antibacterial potential. *J. Photochem. Photobiol. B Biol.*, 149, 300–307, 2015.
98. Devadiga, A., Shetty, K.V., Saidutta, M.B., Timber industry waste-teak (*Tectona grandis* Linn.) leaf extract mediated synthesis of antibacterial silver nanoparticles. *Int. Nano Lett.*, 5, 205–214, 2015.
99. Vatandost, E., Chekin, F., Shahidi Yasaghi, S.A., Green synthesis of silver nanoparticles by pepper extracts reduction and its electocatalytic and antibacterial activity. *Russ. J. Electrochem.*, 52, 960–965, 2016.
100. Thatoi, P., Kerry, R.G., Gouda, S., Das, G., Pramanik, K., Thatoi, H., Patra, J.K., Photo-mediated green synthesis of silver and zinc oxide nanoparticles using aqueous extracts of two mangrove plant species, *Heritiera fomes* and *Sonneratia apetala* and investigation of their biomedical applications. *J. Photochem. Photobiol. B Biol.*, 163, 311–318, 2016.
101. Morales-Luckie, R.A., Lopezfuentes-Ruiz, A.A., Olea-Mejía, O.F., Liliana, A.F., Sanchez-Mendieta, V., Brostow, W., Hinestroza, J.P., Synthesis of silver nanoparticles using aqueous extracts of *Heterotheca inuloides* as reducing agent and natural fibers as templates: *Agave lechuguilla* and silk. *Mater. Sci. Eng. C*, 69, 429–436, 2016.
102. Ajitha, B., Reddy, Y.A.K., Rajesh, K.M., Reddy, P.S., *Sesbania grandiflora* leaf extract assisted green synthesis of silver nanoparticles: Antimicrobial activity. *Mater. Today Proc.*, 3, 1977–1984, 2016.
103. Kumar, V., Gundampati, R.K., Singh, D.K., Jagannadham, M.V., Sundar, S., Hasan, S.H., Photo-induced rapid biosynthesis of silver nanoparticle using aqueous extract of *Xanthium strumarium* and its antibacterial and antileishmanial activity. *J. Ind. Eng. Chem.*, 37, 224–236, 2016.
104. Sarkar, S., Jana, A.D., Samanta, S.K., Mostafa, G., Facile synthesis of silver nanoparticles with highly efficient anti-microbial property. *Polyhedron*, 26, 4419–4423, 2007.
105. Lee, J.H., Lim, J.M., Velmurugan, P., Park, Y.J., Park, Y.J., Bang, K.S., Oh, B.T., Photobiologic-mediated fabrication of silver nanoparticles with antibacterial activity. *J. Photochem. Photobiol. B Biol.*, 162, 93–99, 2016.
106. Rajeshkumar, S., Synthesis of silver nanoparticles using fresh bark of *Pongamia pinnata* and characterization of its antibacterial activity against gram positive and gram negative pathogens. *Resource-Efficient Technologies*, 2, 30–35, 2016.
107. Lockhart, S.R., Current epidemiology of *Candida* infection. *Clin. Microbiol. News.*, 36, 131–136, 2014.
108. Khan, Z.U., Chandy, R., Metwali, K.E., *Candida albicans* strain carriage in patients and nursing staff of an intensive care unit: a study of morphotypes and resistotypes. *Mycoses*, 46, 479–486, 2003.

109. Emmanuel, R., Palanisamy, S., Chen, S.M., Chelladurai, K., Padmavathy, S., Saravanan, M., Prakash, P., Ali, M.A., Al-Hemaid, F.M., Antimicrobial efficacy of green synthesized drug blended silver nanoparticles against dental caries and periodontal disease causing microorganisms. *Mater. Sci. Eng. C*, 56, 374–379, 2015.
110. Ghaedi, M., Yousefinejad, M., Safarpoor, M., Khafri, H.Z., Purkait, M.K., *Rosmarinus officinalis* leaf extract mediated green synthesis of silver nanoparticles and investigation of its antimicrobial properties. *J. Ind. Eng. Chem.*, 31, 167–172, 2015.
111. Velmurugan, P., Sivakumar, S., Young-Chae, S., Seong-Ho, J., Pyoung-In, Y., Sung-Chul, H., Synthesis and characterization comparison of peanut shell extract silver nanoparticles with commercial silver nanoparticles and their antifungal activity. *J. Ind. Eng. Chem.*, 31, 51–54, 2015.
112. Kuppusamy, P., Ichwan, S.J., Parine, N.R., Yusoff, M.M., Maniam, G.P., Govindan, N., Intracellular biosynthesis of Au and Ag nanoparticles using ethanolic extract of *Brassica oleracea* L. and studies on their physicochemical and biological properties. *J. Environ. Sci.*, 29, 151–157, 2015.
113. Yugandhar, P., Haribabu, R., Savithramma, N., Synthesis, characterization and antimicrobial properties of green-synthesised silver nanoparticles from stem bark extract of *Syzygium alternifolium* (Wt.) Walp. *Biotech*, 5, 1031–1039, 2015.
114. Panja, S., Chaudhuri, I., Khanra, K., Bhattacharyya, N., Biological application of green silver nanoparticle synthesized from leaf extract of *Rauvolfia serpentina* Benth. *Asian Pacific J. Trop. Dis.*, 6, 549–556, 2016.
115. Kumar, C.M., Yugandhar, P., Savithramma, N., Biological synthesis of silver nanoparticles from *Adansonia digitata* L. fruit pulp extract, characterization, and its antimicrobial properties. *J. Intercult. Ethnopharmacol.*, 5, 79–86, 2016.
116. Shivakumar, M., Nagashree, K.L., Yallappa, S., Manjappa, S., Manjunath, K.S., Dharmaprakash, M.S., Biosynthesis of silver nanoparticles using prehydrolysis liquor of *Eucalyptus* wood and its effective antimicrobial activity. *Enzyme Microb. Technol.*, 97, 55–62, 2017.
117. Taruna, Kaushal, J., Bhatti, J., Kumar, P., Green synthesis and physico-chemical study of silver nanoparticles extracted from a natural source *Luffa acutangula*. *J. Mol. Liq.*, 224, 991–998, 2016.
118. Ravichandran, V., Vasanthi, S., Shalini, S., Shah, S.A.A., Harish, R., Green synthesis of silver nanoparticles using *Atrocarpus altilis* leaf extract and the study of their antimicrobial and antioxidant activity. *Mater. Lett.*, 180, 264–267, 2016.
119. Bhuyan, B., Paul, A., Paul, B., Dhar, S.S., Dutta, P., *Paederia foetida* Linn. promoted biogenic gold and silver nanoparticles: Synthesis, characterization, photocatalytic and *in vitro* efficacy against clinically isolated pathogens. *J. Photochem. Photobiol. B Biol.*, 173, 210–215, 2017.
120. Ramkumar, V.S., Pugazhendhi, A., Gopalakrishnan, K., Sivagurunathan, P., Saratale, G.D., Dung, T.N.B., Kannapiran, E., Biofabrication and

characterization of silver nanoparticles using aqueous extract of seaweed *Enteromorpha compressa* and its biomedical properties. *Biotechnol. Rep.*, 14, 1–7, 2017.

121. Patra, J.K., Baek, K. H., Antibacterial activity and synergistic antibacterial potential of biosynthesized silver nanoparticles against foodborne pathogenic bacteria along with its anticandidal and antioxidant effects. *Front. Microbiol.*, 8, 167–172, 2017.
122. Jaidev, L.R., Narasimha, G., Fungal mediated biosynthesis of silver nanoparticles, characterization and antimicrobial activity. *Colloids Surf. B*, 81, 430–433, 2010.
123. Lodge, R., Descoteaux, A., Phagocytosis of *Leishmania donovani* amastigotes is Rac1 dependent and occurs in the absence of NADPH oxidase activation. *Eur. J. Immunol.*, 36, 2735–2744, 2006.
124. Mehta, A., Shaha, C., Mechanism of metalloid-induced death in *Leishmania* spp.: Role of iron, reactive oxygen species, Ca2+, and glutathione. *Free Radic. Biol. Med.*, 40, 1857–1868, 2006.
125. Zahir, A.A., Chauhan, I.S., Bagavan, A., Kamaraj, C., Elango, G., Shankar, J., Arjaria, N., Roopan, S.M., Rahuman, A.A., Singh, N., Green synthesis of silver and titanium dioxide nanoparticles using *Euphorbia prostrata* extract shows shift from apoptosis to G0/G1 Arrest followed by necrotic cell death in *Leishmania donovani*. *Antimicrob. Agents. Chemother.*, 59, 4782–4790, 2015.
126. Ahmad, A., Syed, F., Shah, A., Khan, Z., Tahir, K., Khan, A.U., Yuan, Q., Silver and gold nanoparticles from *Sargentodoxa cuneata*: Synthesis, characterization and antileishmanial activity. *RSC Adv.*, 5, 73793–73806, 2015.
127. Ahmad, A., Wei, Y., Syed, F., Khan, S., Khan, G.M., Tahir, K., Khan, A.U., Raza, M., Khan, F.U., Yuan, Q., *Isatis tinctoria* mediated synthesis of amphotericin B-bound silver nanoparticles with enhanced photoinduced antileishmanial activity: A novel green approach. *J. Photochem. Photobiol. B Biol.*, 161, 17–24, 2016.
128. Kalangi, S.K., Dayakar, A., Gangappa, D., Sathyavathi, R., Maurya, R.S., Rao, D.N., Biocompatible silver nanoparticles reduced from *Anethum graveolens* leaf extract augments the antileishmanial efficacy of miltefosine. *Exp. Parasitol.*, 170, 184–192, 2016.
129. Ghosh, S., Jagtap, S., More, P., Shete, U.J., Maheshwari, N.O., Rao, S.J., Kitture, R., Kale, S., Bellare, J., Patil, S., Pal, J.K., *Dioscorea bulbifera* mediated synthesis of novel Au core Ag shell nanoparticles with potent antibiofilm and antileishmanial activity. *J. Nanomater.*, 16(1), 161–166, 2015.
130. Pérez-Díaz, M., Alvarado-Gomez, E., Magaña-Aquino, M., Sánchez-Sánchez, R., Velasquillo, C., Gonzalez, C., Ganem-Rondero, A., Martínez-Castañon, G., Zavala-Alonso, N., Martinez-Gutierrez, F., Anti-biofilm activity of chitosan gels formulated with silver nanoparticles and their cytotoxic effect on human fibroblasts. *Mater. Sci. Eng. C*, 60, 317–323, 2016.

131. Du, J., Singh, H., Yi, T.-H., Antibacterial, anti-biofilm and anticancer potentials of green synthesized silver nanoparticles using benzoin gum (*Styrax benzoin*) extract. *Bioprocess Biosyst. Eng.*, 39, 1923–1931, 2016.
132. O'Toole, G.A., Kolter, R., Initiation of biofilm formation in *Pseudomonas fluorescens* WCS365 proceeds via multiple, convergent signalling pathways: A genetic analysis. *Mol. Microbiol.*, 28, 449–461, 1998.
133. Vijayakumar, S., Malaikozhundan, B., Ramasamy, P., Vaseeharan, B., Assessment of biopolymer stabilized silver nanoparticle for their ecotoxicity on *Ceriodaphnia cornuta* and antibiofilm activity. *J. Environ. Chem. Eng.*, 4, 2076–2083, 2016.
134. Jakubovics, N.S., Kolenbrander, P.E., The road to ruin: The formation of disease-associated oral biofilms. *Oral Dis.* 16, 729–739, 2010.
135. Goswami, S.R., Sahareen, T., Singh, M., Kumar, S., Role of biogenic silver nanoparticles in disruption of cell–cell adhesion in *Staphylococcus aureus* and *Escherichia coli* biofilm. *J. Ind. Eng. Chem.*, 26, 73–80, 2015.
136. Gurunathan, S., Han, J.W., Kwon, D.N., Kim, J. H., Enhanced antibacterial and anti-biofilm activities of silver nanoparticles against Gram-negative and Gram-positive bacteria. *Nanoscale Res. Lett.*, 9, 373–380, 2014.
137. Gupta, K., Barua, S., Hazarika, S.N., Manhar, A.K., Nath, D., Karak, N., Namsa, N.D., Mukhopadhyay, R., Kalia, V.C., Mandal, M., Green silver nanoparticles: Enhanced antimicrobial and antibiofilm activity with effects on DNA replication and cell cytotoxicity. *RSC Adv.*, 4, 52845–52855, 2014.
138. Banumathi, B., Vaseeharan, B., Chinnasamy, T., Vijayakumar, S., Govindarajan, M., Alharbi, N.S., Kadaikunnan, S., Khaled, J.M., Benelli, G., *Euphorbia rothiana*-fabricated Ag nanoparticles showed high toxicity on *Aedes aegypti* larvae and growth inhibition on microbial pathogens: A focus on morphological changes in mosquitoes and antibiofilm potential against bacteria. *J. Clust. Sci.*, 28, 2857–2872, 2017.
139. Saraswathi, V.S., Kamarudheen, N., BhaskaraRao, K.V., Santhakumar, K., Phytoremediation of dyes using *Lagerstroemia speciosa* mediated silver nanoparticles and its biofilm activity against clinical strains *Pseudomonas aeruginosa*. *J. Photochem. Photobiol. B Biol.*, 168, 107–116, 2017.
140. Mohanty, S., Mishra, S., Jena, P., Jacob, B., Sarkar, B., Sonawane, A., An investigation on the antibacterial, cytotoxic, and antibiofilm efficacy of starch-stabilized silver nanoparticles. *Nanomedicine*, 8, 916–920, 2012.
141. Namasivayam, S.K.R., Christo, B.B., Bharani, R.S.A., Arasu, S.M., Kumar, K.A.M., Deepak, K., Nanofabrication of catheter with biocompatible biogenic silver nanoparticles incorporated medicinal plant extracts for the antibiofilm activity against pyogenic bacteria. *Intl. J. Pharm. Pharm. Sci.*, 6, 376–382, 2014.
142. Hamedi, S., Shojaosadati, S.A., Mohammadi, A., Evaluation of the catalytic, antibacterial and anti-biofilm activities of the *Convolvulus arvensis* extract functionalized silver nanoparticles. *J. Photochem. Photobiol. B Biol.*, 167, 36–44, 2017.

143. Prandoni, P., Falanga, A., Piccioli, A., Cancer, thrombosis and heparin-induced thrombocytopenia. *Thromb. Res.*, 120, 137–141, 2007.
144. Davalos, D., Akassoglou, K., Fibrinogen as a key regulator of inflammation in disease. *Semin. Immunopathol.*, 34, 43–62, 2012.
145. Abbasi, Z., Feizi, S., Taghipour, E., Ghadam, P., Green synthesis of silver nanoparticles using aqueous extract of dried *Juglans regia* green husk and examination of its biological properties. *Green Process. Synth.*, 6, 477–485, 2017.
146. Singh, P., Kim, Y.J., Yang, D.C.A., A strategic approach for rapid synthesis of gold and silver nanoparticles by *Panax ginseng* leaves. *Artif. Cells, Nanomed. Biotechnol.*, 44, 1949–1957, 2016.
147. Raja, S., Ramesh, V., Thivaharan, V., Antibacterial and anticoagulant activity of silver nanoparticles synthesised from a novel source–pods of *Peltophorum pterocarpum*. *J. Ind. Eng. Chem.* 29, 257–264, 2015.
148. Vinayagam, R., Varadavenkatesan, T., Selvaraj, R., Evaluation of the Anticoagulant and Catalytic Activities of the *Bridelia retusa* Fruit Extract-Functionalized Silver Nanoparticles. *J. Clust. Sci.*, 28, 2919–2932, 2017.
149. Varadavenkatesan, T., Vinayagam, R., Selvaraj, R., Structural characterization of silver nanoparticles phyto-mediated by a plant waste, seed hull of *Vigna mungo* and their biological applications. *J. Mol. Struct.*, 1147, 629–635, 2017.
150. Banumathi, B., Vaseeharan, B., Chinnasamy, T., Vijayakumar, S., Govindarajan, M., Alharbi, N.S., Kadaikunnan, S., Khaled, J.M., Benelli, G., *Euphorbia rothiana*-fabricated Ag nanoparticles showed high toxicity on *Aedes aegypti* larvae and growth inhibition on microbial pathogens: A focus on morphological changes in mosquitoes and antibiofilm potential against bacteria. *Nanomed. Nanotech., Biol. Med.,* 8, 328–336, 2012.
151. Paul, B., Bhuyan, B., Purkayastha, D.D., Dhar, S.S., Green synthesis of silver nanoparticles using dried biomass of *Diplazium esculentum* (retz.) sw. and studies of their photocatalytic and anticoagulative activities. *J. Mol. Liq.*, 212, 813–817, 2015.
152. Lateef, A., Ojo, S.A., Elegbede, J.A., Azeez, M.A., Yekeen, T.A., Akinboro, A., Evaluation of some biosynthesized silver nanoparticles for biomedical applications: Hydrogen peroxide scavenging, anticoagulant and thrombolytic activities. *J. Clust. Sci.*, 28, 1379–1392, 2017.
153. Lateef, A., Akande, M., Azeez, M., Ojo, S., Folarin, B., Gueguim-Kana, E., Beukes, L., Phytosynthesis of silver nanoparticles (AgNPs) using miracle fruit plant (*Synsepalum dulcificum*) for antimicrobial, catalytic, anticoagulant, and thrombolytic applications. *Nanotechnol. Rev.*, 5, 507–511, 2016.
154. Guariguata, L., Whiting, D.R., Hambleton. I., Beagley, J., Linnenkamp, U., Shaw, J.E., Global estimates of diabetes prevalence for 2013 and projections for 2035. *Diabetes Res. Clin. Pract.*, 103, 137, 2014.
155. Etxeberria, U., de la Garza, A.L., Campión, J., Martínez, J.A., Milagro, F.I., Antidiabetic effects of natural plant extracts via inhibition of carbohydrate

hydrolysis enzymes with emphasis on pancreatic alpha amylase. *Expert Opin. Ther. Targets*, 16, 269–297, 2012.
156. Narkhede, M.B., Ajimire, P.V., Wagh, A.E., Mohan, M., Shivashanmugam, A.T., *In vitro* antidiabetic activity of *Caesalpina digyna* (R.) methanol root extract. *Asian J. Plant Sci. Res.* 1, 101–106, 2011.
157. Swarnalatha, L., Rachel, C., Ranjan, S., Baradwaj, P., Evaluation of *in vitro* antidiabetic activity of *Sphaeranthus amaranthoides* silver nanoparticles. *Int. J. Nanomater. Biostruct.*, 2, 25–32, 2012.
158. Saratale, G.D., Saratale, R.G., Benelli, G., Kumar, G., Pugazhendhi, A., Kim, D.S., Shin, H.S., Anti-diabetic potential of silver nanoparticles synthesized with *Argyreia nervosa* leaf extract high synergistic antibacterial activity with standard antibiotics against foodborne bacteria. *J. Clust. Sci.*, 28, 1709–1727, 2017.
159. Maddinedi, S.B., Mandal, B.K., Maddili, S.K., Biofabrication of size controllable silver nanoparticles – A green approach. *J. Photochem. Photobiol. B Biol.*, 167, 236–241, 2017.
160. Rajaram, K., Aiswarya, D.C., Sureshkumar, P., Green synthesis of silver nanoparticle using *Tephrosia tinctoria* and its antidiabetic activity. *Mater. Lett.*, 138, 251–254, 2015.
161. Prabhu, S., Vinodhini, S., Elanchezhiyan, C., Rajeswari, D., Evaluation of antidiabetic activity of biologically synthesized silver nanoparticles using *Pouteria sapota* in streptozotocin-induced diabetic rats. *J. Diabetes*, 10, 28–42, 2018.
162. Balan, K., Qing, W., Wang, Y., Liu, X., Palvannan, T., Wang, Y., Ma, F., Zhang, Y., Antidiabetic activity of silver nanoparticles from green synthesis using *Lonicera japonica* leaf extract. *RSC Adv.*, 6, 40162–40168, 2016.
163. Saratale, R.G., Shin, H.S., Kumar, G., Benelli, G., Kim, D.S., Saratale, G.D., Exploiting antidiabetic activity of silver nanoparticles synthesized using *Punica granatum* leaves and anticancer potential against human liver cancer cells (HepG2). *Artif. Cell. Nanomed. B.*, 46(1), 211–222, 2017.
164. S Sengottaiyan, A., Aravinthan, A., Sudhakar, C., Selvam, K., Srinivasan, P., Govarthanan, M., Manoharan, K., Selvankumar, T., Synthesis and characterization of *Solanum nigrum*-mediated silver nanoparticles and its protective effect on alloxan-induced diabetic rats. *J. Nanostruct. Chem.*, 6, 41–48, 2016.
165. Kavitha, S., Dhamodharan, M., Kannan, S., Synthesis, characterisation and antidiabetic, antibacterial activity of silver nanoparticle in terpenoid for *Andrographis paniculata*. *Int. J. Sci. Eng. Tech. Res.*, 3, 9467–9471, 2014.
166. Krishnaveni, S., Balasubramanian, T., Sadasivam, S., Sugar distribution in sweet stalk sorghum. *Food Chem.*, 15, 229–232, 1984.
167. Malik, C.P., Singh, M.B., *Plant Enzymology and Histoenzymology*, Kalyani Publishers, 1980.
168. Sreekanth, T.V.M., Ravikumar, S., Eom, I.-Y., Green synthesized silver nanoparticles using *Nelumbo nucifera* root extract for efficient protein

binding, antioxidant and cytotoxicity activities. *J. Photochem. Photobiol. B Biol.*, 141, 100–105, 2014.

169. Saratale, R.G., Shin, H.S., Kumar, G., Benelli, G., Ghodake, G.S., Jiang, Y.Y., Kim, D.S., Saratale, G.D., Exploiting fruit byproducts for eco-friendly nanosynthesis: *Citrus× clementina* peel extract mediated fabrication of silver nanoparticles with high efficacy against microbial pathogens and rat glial tumor C6 cells. *Environ. Sci. Pollut. Res.*, 25, 10250–10263, 2018.
170. Gurunathan, S., Han, J.W., Dayem, A.A., Eppakayala, V., Park, J.H., Cho, S.G., Lee, K.J., Kim, J.H., Green synthesis of anisotropic silver nanoparticles and its potential cytotoxicity in human breast cancer cells (MCF-7). *J. Ind. Eng. Chem.*, 19, 1600–1605, 2013.
171. Moldovan, B., David, L., Vulcu, A., Olenic, L., Perde-Schrepler, M., Fischer-Fodor, E., Baldea, I., Clichici, S., Filip, G.A., *In vitro* and *in vivo* anti-inflammatory properties of green synthesized silver nanoparticles using *Viburnum opulus* L. fruits extract. *Mater. Sci. Eng. C*, 79, 720–727, 2017.
172. Kumar, B., Smita, K., Debut, A., Cumbal, L., Extracellular green synthesis of silver nanoparticles using Amazonian fruit Araza (*Eugenia stipitata* McVaugh). *Trans. Nonferrous Met. Soc. China*, 26, 2363–2371, 2016.
173. Kumar, B., Smita, K., Cumbal, L., Angulo, Y., Fabrication of silver nanoplates using *Nephelium lappaceum* (Rambutan) peel: A sustainable approach. *J. Mol. Liq.*, 211, 476–480, 2015.
174. Kumar, B., Smita, K., Cumbal, L., Debut, A., Ultrasound agitated phytofabrication of palladium nanoparticles using Andean blackberry leaf and its photocatalytic activity. *J. Saudi Chem. Soc.*, 19, 574–580, 2015.
175. Niraimathi, K.L., Sudha, V., Lavanya, R., Brindha, P., Biosynthesis of silver nanoparticles using *Alternanthera sessilis* (Linn.) extract and their antimicrobial, antioxidant activities. *Colloids Surf. B*, 102, 288–291, 2013.
176. Kumar, B., Kumari, S., Cumbal, L., Debut, A., *Lantana camara* berry for the synthesis of silver nanoparticles. *Asian Pac. J. Trop. Biomed.*, 5, 192–195, 2015.
177. Cao, Z., Fu, H., Kang, L., Huang, L., Zhai, T., Ma, Y., Yao, J., Rapid room-temperature synthesis of silver nanoplates with tunable in-plane surface plasmon resonance from visible to near-IR. *J. Mater. Chem.*, 18, 2673–2678, 2008.
178. Kharat, S.N., Mendhulkar, V.D., Synthesis, characterization and studies on antioxidant activity of silver nanoparticles using *Elephantopus scaber* leaf extract. *Mater. Sci. Eng. C*, 62, 719–724, 2016.
179. Abdel-Aziz, M.S., Shaheen, M.S., El-Nekeety, A.A., Abdel-Wahhab, M.A., Antioxidant and antibacterial activity of silver nanoparticles biosynthesized using *Chenopodium murale* leaf extract. *J. Saudi Chem. Soc.*, 18, 356–363, 2014.
180. Inbathamizh, L., Ponnu, T.M., Mary, E.J., *In vitro* evaluation of antioxidant and anticancer potential of *Morinda pubescens* synthesized silver nanoparticles. *J. Pharm. Res.*, 6, 32–38, 2013.

181. Patra, S., Mukherjee, S., Barui, A.K., Ganguly, A., Sreedhar, B., Patra, C.R., Green synthesis, characterization of gold and silver nanoparticles and their potential application for cancer therapeutics. *Mater. Sci. Eng. C*, 53, 298–309, 2015.
182. Nayak, D., Ashe, S., Rauta, P.R., Kumari, M., Nayak, B., Bark extract mediated green synthesis of silver nanoparticles: Evaluation of antimicrobial activity and antiproliferative response against osteosarcoma. *Mater. Sci. Eng. C*, 58, 44–52, 2016.
183. Mohanta, Y.K., Panda, S.K., Bastia, A.K., Mohanta, T.K., Biosynthesis of silver nanoparticles from *Protium serratum* and investigation of their potential impacts on food safety and control. *Front. Microbiol.*, 8, 626–630, 2017.
184. Jacob, S.J.P., Prasad, V.L.S., Sivasankar, S., Muralidharan, P., Biosynthesis of silver nanoparticles using dried fruit extract of *Ficus carica* – Screening for its anticancer activity and toxicity in animal models. *Food Chem. Toxicol.*, 109, 951–956, 2017.
185. Ramachandran, R., Krishnaraj, C., Sivakumar, A.S., Prasannakumar, P., Kumar, V.A., Shim, K.S., Song, C.G., Yun, S.I., Anticancer activity of biologically synthesized silver and gold nanoparticles on mouse myoblast cancer cells and their toxicity against embryonic zebrafish. *Mater. Sci. Eng. C*, 73, 674–683, 2017.
186. Kummara, S., Patil, M.B., Uriah, T., Synthesis, characterization, biocompatible and anticancer activity of green and chemically synthesized silver nanoparticles – A comparative study. *Biomed. Pharmacother.*, 84, 10–21, 2016.
187. Amooaghaie, R., Saeri, M.R., Azizi, M., Synthesis, characterization and biocompatibility of silver nanoparticles synthesized from *Nigella sativa* leaf extract in comparison with chemical silver nanoparticles. *Ecotoxicol. Environ. Saf.*, 120, 400–408, 2015.
188. Gengan, R.M., Anand, K., Phulukdaree, A., Chuturgoon, A., A549 lung cell line activity of biosynthesized silver nanoparticles using *Albizia adianthifolia* leaf. *Colloids Surf. B*, 105, 87–91, 2013.
189. Ahamed, M., Khan, M.A.M., Siddiqui, M.K.J., AlSalhi, M.S., Alrokayan, S.A., Green synthesis, characterization and evaluation of biocompatibility of silver nanoparticles. *Physica E Low Dimens. Syst. Nanostruct.*, 43, 1266–1271, 2011.
190. Moulton, M.C., Braydich-Stolle, L.K., Nadagouda, M.N., Kunzelman, S., Hussain, S.M., Varma, R.S., Synthesis, characterization and biocompatibility of "green" synthesized silver nanoparticles using tea polyphenols. *Nanoscale*, 2, 763–770, 2010.
191. Xia, T., Kovochich, M., Brant, J., Hotze, M., Sempf, J., Oberley, T., Sioutas, C., Yeh, J.I., Wiesner, M.R., Nel, A.E., Comparison of the abilities of ambient and manufactured nanoparticles to induce cellular toxicity according to an oxidative stress paradigm. *Nano Lett.*, 6, 1794–1807, 2006.
192. Lakshmi, S., Dhanya, G.S., Joy, B., Padmaja, G., Remani, P., Inhibitory effect of an extract of *Curcuma zedoariae* on human cervical carcinoma cells. *Med. Chem. Res.*, 17, 335–344, 2008.

193. Venugopal, K., Rather, H.A., Rajagopal, K., Shanthi, M.P., Sheriff, K., Illiyas, M., Rather, R.A., Manikandan, E., Uvarajan, S., Bhaskar, M., Maaza, M., Synthesis of silver nanoparticles (Ag NPs) for anticancer activities (MCF 7 breast and A549 lung cell lines) of the crude extract of *Syzygium aromaticum*. *J. Photochem. Photobiol. B Biol.*, 167, 282–289, 2017.
194. Venkatesan, B., Subramanian, V., Tumala, A., Vellaichamy, E., Rapid synthesis of biocompatible silver nanoparticles using aqueous extract of *Rosa damascena* petals and evaluation of their anticancer activity. *Asian Pac. J. Trop. Med.* 7, 294–300, 2014.
195. Rosarin, F.S., Arulmozhi, V., Nagarajan, S., Mirunalini, S., Antiproliferative effect of silver nanoparticles synthesized using amla on Hep2 cell line. *Asian Pac. J. Trop. Med.*, 6, 1–10, 2013.
196. Wondji, C.S., Irving, H., Morgan, J., Lobo, N.F., Collins, F.H., Hunt, R.H., Coetzee, M., Hemingway, J., Ranson, H., Two duplicated P450 genes are associated with pyrethroid resistance in *Anopheles funestus,* a major malaria vector. *Genome Res.*, 19, 452–458, 2009.
197. Chan, Y.S., Don, M.M., Optimization of process variables for the synthesis of silver nanoparticles by *Pycnoporus sanguineus* using statistical experimental design. *J. Korean Soc. Appl. Biol. Chem.*, 56, 11–20, 2013.
198. Safaepour, M., Shahverdi, A.R., Shahverdi, H.R., Khorramizadeh, M.R., Gohari, A.R., Green synthesis of small silver nanoparticles using geraniol and its cytotoxicity against Fibrosarcoma-Wehi 164. *Avicenna J. Med. Biotechnol.*, 1, 111–116, 2009.
199. Nyakundi, E.O., Padmanabhan, M.N., Green chemistry focus on optimization of silver nanoparticles using response surface methodology (RSM) and mosquitocidal activity: *Anopheles stephensi* (Diptera: Culicidae). *Spectrochim. Acta A*, 149, 978–984, 2015.
200. Santhosh, S.B., Ragavendran, C., Natarajan, D., Spectral and HRTEM analyses of *Annona muricata* leaf extract mediated silver nanoparticles and its larvicidal efficacy against three mosquito vectors *Anopheles stephensi, Culex quinquefasciatus,* and *Aedes aegypti*. *J. Photochem. Photobiol. B Biol.*, 153, 184–190, 2015.
201. Muthukumaran, U., Govindarajan, M., Rajeswary, M., Green synthesis of silver nanoparticles from *Cassia roxburghii*—A most potent power for mosquito control. *Parasitol. Res.*, 114, 4385–4395, 2015.
202. Govindarajan, M., Vijayan, P., Kadaikunnan, S., Alharbi, N.S., Benelli, G., One-pot biogenic fabrication of silver nanocrystals using *Quisqualis indica*: Effectiveness on malaria and Zika virus mosquito vectors, and impact on non-target aquatic organisms. *J. Photochem. Photobiol. B Biol.*, 162, 646–655, 2016.
203. Jayaseelan, C., Rahuman, A.A., Rajakumar, G., Kirthi, A.V., Santhoshkumar, T., Marimuthu, S., Bagavan, A., Kamaraj, C., Zahir, A.A., Elango, G., Synthesis of pediculocidal and larvicidal silver nanoparticles by leaf extract from heartleaf moonseed plant, *Tinospora cordifolia* Miers. *Parasitol. Res.*, 109, 185–194, 2011.

204. Rajakumar, G., Rahuman, A.A., Acaricidal activity of aqueous extract and synthesized silver nanoparticles from *Manilkara zapota* against *Rhipicephalus* (*Boophilus*) *microplus*. *Res. Vet. Sci.*, 93, 303–309, 2012.
205. Vanaja, M., Paulkumar, K., Baburaja, M., Rajeshkumar, S., Gnanajobitha, G., Malarkodi, C., Sivakavinesan, M., Annadurai, G., Degradation of methylene blue using biologically synthesized silver nanoparticles. *Bioinorg. Chem. Appl.*, 2014, 1–10, 2014.
206. Galagan, Y., Su, W.-F., Reversible photoreduction of methylene blue in acrylate media containing benzyl dimethyl ketal. *J. Photochem. Photobiol. A Chem.*, 195, 378–383, 2008.
207. Rauf, M.A., Meetani, M.A., Khaleel, A., Ahmed, A., Photocatalytic degradation of methylene blue using a mixed catalyst and product analysis by LC/MS. *Chem. Eng. J.*, 157, 373–378, 2010.
208. Laoufi, I., Saint-Lager, M.C., Lazzari, R., Jupille, J., Robach, O., Garaudée, S., Cabailh, G., Dolle, P., Cruguel, H., Bailly, A., Size and catalytic activity of supported gold nanoparticles: An in operando study during CO oxidation. *J. Phys. Chem. C*, 115, 4673–4679, 2011.
209. Cheval, N., Gindy, N., Flowkes, C., Fahmi, A., Polyamide 66 microspheres metallised with *in situ* synthesised gold nanoparticles for a catalytic application. *Nanoscale Res. Lett.* 7, 182–188, 2012.
210. Gupta, N., Singh, H.P., Sharma, R.K., Metal nanoparticles with high catalytic activity in degradation of methyl orange: An electron relay effect. *J. Mol. Catal. A Chem.*, 335, 248–252, 2011.
211. Ajitha, B., Reddy, Y.A.K., Shameer, S., Rajesh, K.M., Suneetha, Y. and Reddy, P.S., Lantana camara leaf extract mediated silver nanoparticles: antibacterial, green catalyst. *J. Photochem. Photobiol. B Biol.* 149, 84–92, 2015.
212. Khan, F.U., Chen, Y., Khan, N.U., Khan, Z.U.H., Khan, A.U., Ahmad, A., Tahir, K., Wang, L., Khan, M.R., Wan, P., Antioxidant and catalytic applications of silver nanoparticles using *Dimocarpus longan* seed extract as a reducing and stabilizing agent. *J. Photochem. Photobiol. B Biol.*, 164, 344–351, 2016.
213. Rajan, A., Vilas, V., Philip, D., Catalytic and antioxidant properties of biogenic silver nanoparticles synthesized using *Areca catechu* nut. *J. Mol. Liq.*, 207, 231–236, 2015.
214. Vidhu, V. K., Philip, D., Catalytic degradation of organic dyes using biosynthesized silver nanoparticles. *Micron*, 56, 54–62, 2014.
215. Ghosh, S.K., Kundu, S., Mandal, M., Pal, T., Silver and gold nanocluster catalyzed reduction of methylene blue by arsine in a micellar medium. *Langmuir*, 18, 8756–8760, 2002.
216. Peral, J., Trillas, M., Domenech, X., Heterogeneous photochemistry: An easy experiment. *J. Chem. Educ.*, 72, 565–570, 1995.
217. Varadavenkatesan, T., Selvaraj, R., Vinayagam, R., Phyto-synthesis of silver nanoparticles from *Mussaenda erythrophylla* leaf extract and their application in catalytic degradation of methyl orange dye. *J. Mol. Liq.*, 221, 1063–1070, 2016.

218. Edison, T.N.J.I., Atchudan, R., Sethuraman, M.G., Lee, Y.R., Reductive-degradation of carcinogenic azo dyes using *Anacardium occidentale testa* derived silver nanoparticles. *J. Photochem. Photobiol. B Biol.*, 162, 604–610, 2016.
219. Kumari, R.M., Thapa, N., Gupta, N., Kumar, A., Nimesh, S., Antibacterial and photocatalytic degradation efficacy of silver nanoparticles biosynthesized using *Cordia dichotoma* leaf extract. *Adv. Nat. Sci. Nanosci. Nanotechnol.*, 7, 45009–45013, 2016.
220. Muthu, K., Priya, S., Green synthesis, characterization and catalytic activity of silver nanoparticles using *Cassia auriculata* flower extract separated fraction. *Spectrochim. Acta A*, 179, 66–72, 2017.
221. Edison, T.N.J.I., Lee, Y.R., Sethuraman, M.G., Green synthesis of silver nanoparticles using *Terminalia cuneata* and its catalytic action in reduction of direct yellow-12 dye. *Spectrochim. Acta A*, 161, 122–129, 2016.
222. Dong, Z., Le, X., Liu, Y., Dong, C., Ma, J., Metal organic framework derived magnetic porous carbon composite supported gold and palladium nanoparticles as highly efficient and recyclable catalysts for reduction of 4-nitrophenol and hydrodechlorination of 4-chlorophenol. *J. Mater. Chem. A*, 2, 18775–18785, 2014.
223. Suárez-Cerda, J., Alonso-Nuñez, G., Espinoza-Gómez, H., Flores-López, L.Z., Synthesis, kinetics and photocatalytic study of 'ultra-small' Ag-NPs obtained by a green chemistry method using an extract of *Rosa* 'Andeli' double delight petals. *J. Colloid Interface Sci.*, 458, 169–177, 2015.
224. Vinayagam, R., Varadavenkatesan, T., Selvaraj, R., Green synthesis, structural characterization, and catalytic activity of silver nanoparticles stabilized with *Bridelia retusa* leaf extract. *Green Process. Synth.*, 202–208, 2017.
225. Khorshidi, A., Mardazad, N., Flower-like silver nanoparticles: An effective and recyclable catalyst for degradation of Rhodamine B with H2O2. *Res. Chem. Intermed.*, 42, 7551–7558, 2016.
226. Gangula, A., Podila, R., Karanam, L., Janardhana, C., Rao, A.M., Catalytic reduction of 4-nitrophenol using biogenic gold and silver nanoparticles derived from *Breynia rhamnoides*. *Langmuir*, 27, 15268–15274, 2011.
227. Zosel, A., Rychter, K. Leikin, J., Dapsone-induced methemoglobinemia: Case report and literature review. *Am. J. Ther.*, 14, 585–590, 2007.
228. Zayed, M.F., Eisa, W.H., *Phoenix dactylifera* L. leaf extract phytosynthesized gold nanoparticles; controlled synthesis and catalytic activity. *Spectrochim. Acta A*, 121, 238–244, 2014.
229. Zayed, M.F., Eisa, W.H., Abdel-Moneam, Y.K., El-kousy, S.M., Atia, A., *Ziziphus spina-christi* based bio-synthesis of Ag nanoparticles. *J. Ind. Eng. Chem.*, 23, 50–56, 2015.
230. Zhang, W., Tan, F., Wang, W., Qiu, X., Qiao, X., Chen, J., Facile, template-free synthesis of silver nanodendrites with high catalytic activity for the reduction of p-nitrophenol. *J. Hazard. Mater.*, 217, 36–42, 2012.

231. Wang, M., Zhang, W., Zheng, X., Zhu, P., Antibacterial and catalytic activities of biosynthesized silver nanoparticles prepared by using an aqueous extract of green coffee bean as a reducing agent. *RSC Adv.*, 7, 12144–12149, 2017.
232. Arya, G., Sharma, N., Ahmed, J., Gupta, N., Kumar, A., Chandra, R., Nimesh, S., Degradation of anthropogenic pollutant and organic dyes by biosynthesized silver nano-catalyst from *Cicer arietinum* leaves. *J. Photochem. Photobiol. B Biol.*, 174, 90–96, 2017.
233. Dauthal, P., Mukhopadhyay, M., Agro-industrial waste-mediated synthesis and characterization of gold and silver nanoparticles and their catalytic activity for 4-nitroaniline hydrogenation. *Korean J. Chem. Eng.*, 32, 837–844, 2015.
234. Kumar, V.V., Anbarasan, S., Christena, L.R., SaiSubramanian, N., Anthony, S.P., Bio-functionalized silver nanoparticles for selective colorimetric sensing of toxic metal ions and antimicrobial studies. *Spectrochim. Acta A*, 129, 35–42, 2014.
235. Kirubaharan, C.J., Kalpana, D., Lee, Y.S., Kim, A.R., Yoo, D.J., Nahm, K.S., Kumar, G.G., Biomediated silver nanoparticles for the highly selective copper (II) ion sensor applications. *Ind. Eng. Chem. Res.*, 51, 7441–7446, 2012.
236. Maiti, S., Barman, G., Konar Laha, J., Detection of heavy metals (Cu+2, Hg+2) by biosynthesized silver nanoparticles. *Appl. Nanosci.*, 6, 529–538, 2016.
237. Huang, X., Wu, H., Liao, X., Shi, B., One-step{,} size-controlled synthesis of gold nanoparticles at room temperature using plant tannin. *Green Chem.*, 12, 395–399, 2010.
238. Prakash, C.V.S., Prakash, I., Bioactive chemical constituents from pomegranate (*Punica granatum*) juice, seed and peel—A review. *Int. J. Res. Chem. Environ.*, 1, 1–10, 2011.
239. Garland, W.T., Fritchif, C.J., Metalloflavoprotein models: The crystal structure of bis (riboflavin) bis (cupric perchlorate) dodecahydrate. *J. Biol. Chem.*, 249, 2228–2231, 1973.
240. Szilágyi, I., Labádi, I., Hernádi, K., Pálinkó, I., Nagy, N.V., Korecz, L., Rockenbauer, A., Kele, Z., Kiss, T., Speciation study of an imidazolate-bridged copper (II)–zinc (II) complex in aqueous solution. *J. Inorg. Biochem.*, 99, 1619–1629, 2005.
241. Borase, H.P., Patil, C.D., Salunkhe, R.B., Suryawanshi, R.K., Salunke, B.K., Patil, S.V., Mercury sensing and toxicity studies of novel latex fabricated silver nanoparticles. *Bioprocess Biosyst. Eng.*, 37, 2223–2233, 2014.
242. Karthiga, D., Anthony, S.P., Selective colorimetric sensing of toxic metal cations by green synthesized silver nanoparticles over a wide pH range. *RSC Adv.*, 3, 16765–16774, 2013.
243. Rastogi, L., Sashidhar, R.B., Karunasagar, D., Arunachalam, J., Gum kondagogu reduced/stabilized silver nanoparticles as direct colorimetric sensor for the sensitive detection of Hg2+ in aqueous system. *Talanta*, 118, 111–117, 2014.

244. Silva-De Hoyos, L.E., Mendieta, V.S., Nestor, A.R.V., López, M.A.C., Biogenic silver nanoparticles as sensors of Cu2+ and Pb2+ in aqueous solutions. *Univ. J. Mater. Sci.*, 5, 37–42, 2017.
245. Rababah, T.M., Hettiarachchy, N.S., Horax, R., Total phenolics and antioxidant activities of fenugreek, green tea, black tea, grape seed, ginger, rosemary, gotu kola, and ginkgo extracts, vitamin E, and tert-butylhydroquinone. *J. Agric. Food Chem.*, 52, 5183–5186, 2004.
246. Wang, C., Yu, C., Detection of chemical pollutants in water using gold nanoparticles as sensors: A review. *Rev. Anal. Chem.*, 32, 1–6, 2012.
247. Firdaus, M.L., Fitriani, I., Wyantuti, S., Hartati, Y.W., Khaydarov, R., McAlister, J.A., Obata H., Gamo, T., Colorimetric detection of mercury (II) ion in aqueous solution using silver nanoparticles. *Anal. Sci.*, 33, 831–836, 2017.
248. Phukan, A., Chetia, B., Biomediated synthesis of silver nanoparticles using *Rhaphidophora hongkongensis* leaf extract and its application for the selective Hg (II) and Fe (III) ions sensor. *Sens. Lett.*, 14, 319–323, 2016.

13

Green Synthesis of Silver, Copper and Iron Nanoparticles: Synthesis, Characterization and Their Applications in Wastewater Treatment

Th. Babita Devi and M. Ahmaruzzaman*

Department of Chemistry National Institute of Technology, Silchar, Assam, India

Abstract

In this chapter we discussed the green synthesis of metals nanoparticles such as silver, copper and iron nanoparticles using biological waste material. The metals nanoparticles were synthesized by using *Coccinia grandis* peel extract without using any external organic solvent. The flavonoid present in the peel extract acts as a reducing as well as stabilizing agent in the formation of metals nanoparticles. The morphology and size of the synthesized nanoparticles were characterized by using SEM (scanning electron microscope) and TEM (transmission electron microscope). The average particle sizes were calculated from the TEM images and it was found that silver nanoparticles were showed smallest particles size as compared with the copper and iron nanoparticles. The synthesized nanoparticles were successfully used as a catalyst in reduction of para-nitrophenol and photodegradation of Victoria Blue B dye. Due to smaller in size of silver nanoparticles, it showed better catalytic activities in the reduction as well as photodegradation process.

Keywords: Green, metal nanoparticles, reduction, photodegradation, catalyst

**Corresponding author*: mda2002@gmail.com

Suvardhan Kanchi and Shakeel Ahmed (eds.) Green Metal Nanoparticles, (441–466)
© 2018 Scrivener Publishing LLC

13.1 Introduction

Nanotechnology has emerged as a rapid growing field with multifaceted application for new materials at the nanoscale level. Nanoparticles are of great interest due to their unique physicochemical, magnetic, and optoelectronic properties that are governed by their size, shape, and size distribution [1–5] and it has small size and large surface area to volume ratio that leads to the significant differences in properties in their bulk form [6]. Due to unique physicochemical and optoelectronic properties, nanoparticles are interest for a number of applications like catalysts, chemical sensors, electronic components, medical diagnostic imaging, pharmaceutical products, and medical treatment protocols. Among various metal nanoparticles, silver nanoparticles have received great attention due to their distinctive surface plasmon resonance effects. It has been extensively used in cosmetic, waste water treatment [7–11], biomedical applications [12–14], separation sciences [15], disease diagnostics [16], and pharmaceuticals [17–18]. Silver metal nanoparticles have been found an excellent properties in anti-bacterial, anti-inflammatory and anticancer treatment, commercially available wound dressings, pharmaceutical preparations, and medical implant coatings [19–24].

Copper nanoparticles have prospective applications in optics, electronics, and medicine and in manufacturing of lubrications, nanofluids, conductive films, and antimicrobial agents [25–32]. The preference of copper nanoparticles compared to silver is due to the lower cost of copper than silver, the physical and chemical stability, and ease of mixing with polymers. Copper nanoparticles have been of great interests because of novel optical catalytic, tribological, electrical, and heat conduction properties [25–32]. In addition, the cost of Cu nanoparticles is much lower than that of the other comparable metallic materials such as gold and silver.

Similarly, magnetic nanoparticles, such as iron nanoparticles have emerged as a new class of important nanoparticles due to unique properties like super paramagnetic and high coercively [33–35].

Due to the advantages properties of silver, copper and iron metal nanoparticles, many researchers have been focused on the synthesis of metal nanoparticles using varieties of chemical and physical methods. However, these methods are accompanied by many problems including use of toxic solvents, generation of hazardous by-products, high energy consumption and quite expensive.

For the synthesis of metal nanoparticles, it was necessary metal ion into metallic form. Nowadays, $NaBH_4$ is used as a key reducing agent in synthesizing nanoparticles, which is very toxic to the ecosystem. In addition to

this, drawbacks of these methods include contamination of precursors and release of harmful by-products to the ecosystem.

Therefore, there is a need for the development of environmentally benign methods for the preparation of nanoparticles. The utilization of green and clean technology is expected to minimize the pollution in the environment. A very wide range of biological resources like microorganisms like bacteria, yeast, fungi, algae, and viruses [36–50] and plants extract can be used for synthesis of nanoparticles. Plant extracts (phytochemicals) reduce the metal ions into metallic form in a shorter time as compared to microbes. Depending upon plant type and concentration of phytochemicals, nanoparticles are synthesized within a few minutes or hours, whereas microorganism-based methods require a longer time and expensive technique also required some percussion. The major drawback of microbe-mediated nanoparticle is the obligatory constraint of aseptic conditions, which requires trained staff, and raises the scaling-up cost. Plants are easy availability in nature, inexpensive and environment friendly and renewable in nature. One of the major advantages in plants mediated synthesis of nanoparticles is the presence of phyto-compounds. These phyto-compounds act as reducing and stabilizing agents in the synthesis of metal nanoparticles and added advantages over routine chemical and physical methods and make them more preferred biological resources than microbes.

In the present chapter, the focus will be mainly plants mediated green synthesis of metal silver copper and iron nanoparticles, which was synthesized from biowaste extract and application in the wastewater treatment for removal of toxic dye and para-nitrophenol. In this chapter, we report the synthesis of silver, iron and copper nanoparticles using ivy gourd peel (biowaste) extract. The synthesized metals nanoparticles were used as a catalyst for the removal of toxic para-nitrophenol (PNP) and toxic dye like Victoria Blue B (VBB).

Toxic dye and phenol are also found in wastes of synthetic resin and plastics, rubber proofing, cutting-oil, dye manufacturing and many chemicals. During last few decades, due to high industrial growth, a large percentage of pollutants from industries, mainly textile, dyeing, food, printing and chemical, were discharged into water bodies without any treatment. Among various pollutants, dyes and toxic phenolic compounds are the principal source of water pollution, which were released from textile, dyeing and printing industries and most of dyes are carcinogenic, and mutagenic and less biodegradability. The discharge and disposal of these pollutants into water source renders the water toxic and poses a threat to aquatic and human life. It is very important to remove such pollutant from

the waste water. Many researchers have been reported the reduction and photodegradation process for the removal of nitro phenol and toxic dyes.

The synthesized metals, such as silver, copper, and iron nanoparticles were utilized for removal of such toxic pollutants from the waste water. Here, toxic para-nitrophenol (PNP) and toxic dye like Victoria Blue B (VBB) were selected as target pollutants for removal of toxic pollutants from wastewater.

13.2 Plants Mediated Green Synthesis of Metal Nanoparticles

In this chapter, we discussed about the biosynthesis of metal nanoparticles like silver, copper and iron nanoparticles using biowaste material like *Coccinia grandis* peel extract.

Coccinia grandis contain many bioactive compounds such as secondary metabolite like alkaloids, glycoside and saponin, bamyrine, lupeol, cucubbitacin, cephalandrol, cephalandrine and flavonoids. The leaves have many medicinal properties like anti-diabetic, anti-inflammatory, antipyretic, analgesic, antispasmodic, antimicrobial, and cathartic, expectorant activities and hypoglycemic, hypolipidemic and antioxidant activity. The main advantages of using *Coccinia grandis* was due to the less report in the literature for the synthesis of nanoparticles. In the literature it was found that many researchers have been synthesized metals nanoparticles using *Coccinia grandis* leaves and flower and fruit extract [51–52, 11]. But there was no report for the synthesis of nanoparticles using *Coccinia grandis* peel extract.

In this chapter, we report first time the synthesis of silver, copper and iron nanoaprticles using *Coccinia grandis* peel extract. The phytochemicals (flavonoids) were mainly responsible for the formation of the metals nanoparticles. The methods for the synthesis of metals nanoparticles were performed without using any reducing as well as stabilizing agents. Here, the phytochemicals act as a reducing as well as stabilizing agent.

13.3 Synthesis, Mechanism and Characterization of Synthesized Metals Nanoparticles

The starting materials silver nitrate ($AgNO_3$), copper sulphate ($CuSO_4{\cdot}5H_2O$) and iron (III) chloride hexahydrate ($FeCl_3{\cdot}6H_2O$) were of

AR grade. The target compounds para- nitrophenol (PNP), sodium borohydride ($NaBH_4$) and Victoria Blue B dye (VBB) obtained from Merck India Limited Chemicals and used without any further purification. All solutions were prepared in double-distilled water and all apparatus were rinsed with aqua regia (3:1 solution of HCl:HNO_3) and then washed with double-distilled water before use.

13.3.1 Synthesis of Silver, Copper and Iron Nanoparticles Using Bio-Waste (*Coccinia Grandis*) Peel Extract

Locally available *Coccinia grandis* peel were collected from Silchar Assam (India) and washed thoroughly with distilled water to remove dust particles. The peels were boiled and refluxed for 10 min in bottomed flask with a certain amount of distilled water to extract. The bio-waste extract were collected and filtered through a Whatmann filter paper no. 41 to remove the small fibers and unwanted dust particles from the extract.

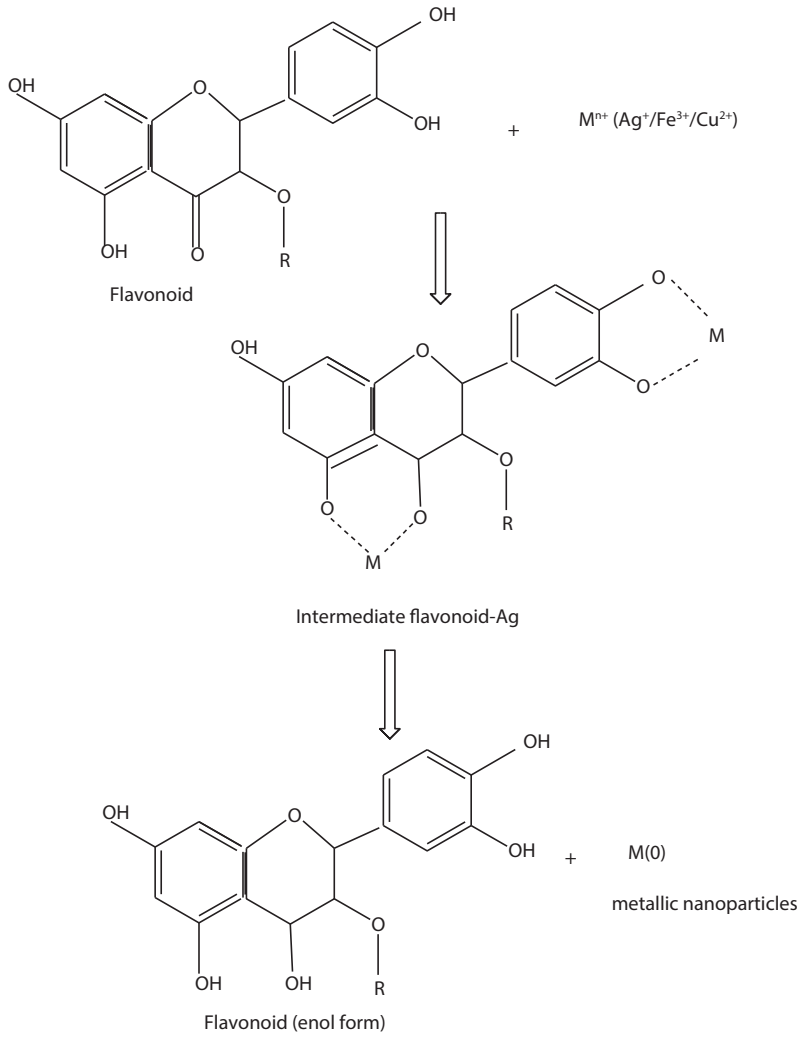
10 millilitre (mL) of 0.001 Molar (M) aqueous solutions of $AgNO_3$, $CuSO_4$, $FeCl_3$ were taken in different container and to that 10 mL of peel extract were added and stirred for 10 min at 40–45 °C and followed by slow cooling at room temperature. The solutions were then allowed to stabilize for one day. The solutions with brown sediments (silver and copper) and black colour precipitate (iron) were formed at the bottom of the containers after one day. It was clear indicated that the formation of silver, copper and iron nanoparticles.

Here, the phytochemicals mainly flavonoid were participated for the formation of the nanoparticles. The flavonoid acts as a reducing as well as stabilizing agent for the formation of the metal nanoparticles. When the flavonoids interact with the metals ions, it reduced the metals ion into metallic formed and as a result enol form of flavonoid complex was formed. The probable mechanism for the formation the metals nanoparticles were showed in the Scheme 13.1.

13.3.2 Characterization

13.3.2.1 Ultraviolet-Visible (UV-Vis) Spectroscopy

The synthesized nanoparticles were further confirmed by UV-Vis spectroscopy. Figure 13.1a,c represents the UV-Vis spectra of synthesized silver (Ag), copper (Cu) and iron (Fe) nanoparticles. Silver and copper have unique properties called surface plasmon resonance (SPR) which it



Scheme 13.1 Representation of the probable mechanism for the formation of metals nanoparticles.

gives absorption in the UV-Vis region at around (550–600) nm for copper and 400–450 nm for silver. In the Figure 13.1a,b the absorbance peaks was formed at around 450 nm (AgNPs) and 570 nm (CuNPs). From the UV-Vis spectra it was clearly indicates that the formation of silver and copper nanoparticles. The UV-Vis spectrum of iron nanoparticles was showed (Figure 13.1c) an absorbance peak at ~270 nm was due to the formation of iron nanoparticles.

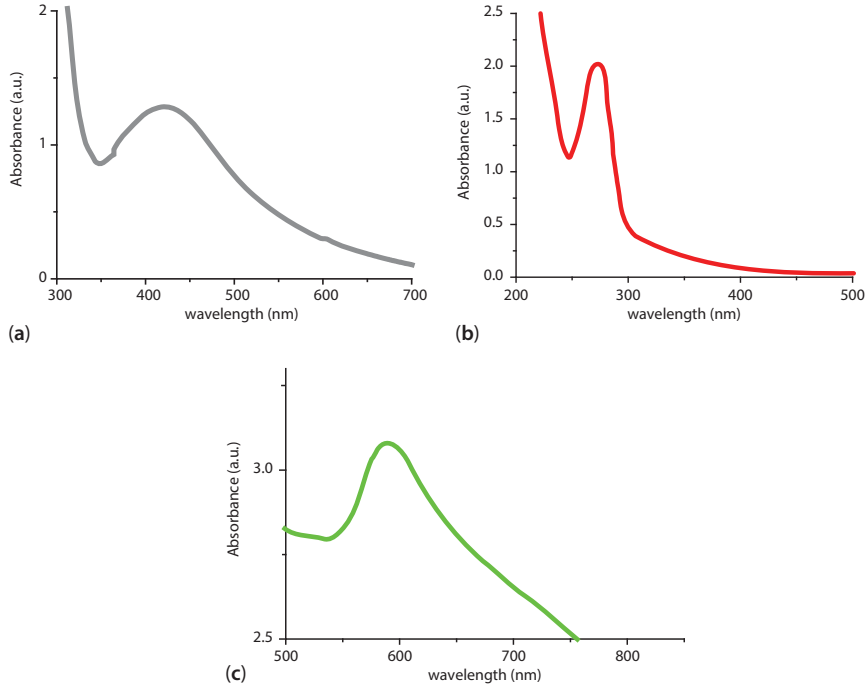


Figure 13.1 Representation of the UV-visible spectra of silver (a), copper (b) and iron (c) nanoparticles.

13.3.3 Morphology Studies (SEM and TEM)

13.3.3.1 Transmission Electron Microscopy (TEM) and Scanning Electron Microscopy (SEM) Analysis

The morphology, shape and sizes of the synthesized nanoparticles were confirmed by transmission electron microscope (TEM) and scanning electron microscope (SEM) techniques.

SEM images reveal the outside surface morphology of the synthesized nanoparticles and whereas, TEM images were gives the information about the inner surface morphology of the synthesized nanoparticles. Figure 13.2a–c presents the SEM images of AgNPs, CuNPs and FeNPs. The SEM images of the synthesized nanoparticles were observed as a rod (AgNPs), flower (CuNPs) and spherical (FeNPs) shapes. But in case of TEM images all the synthesized nanoparticles were observed as spherical shapes (Figure 13.2d–f). From the

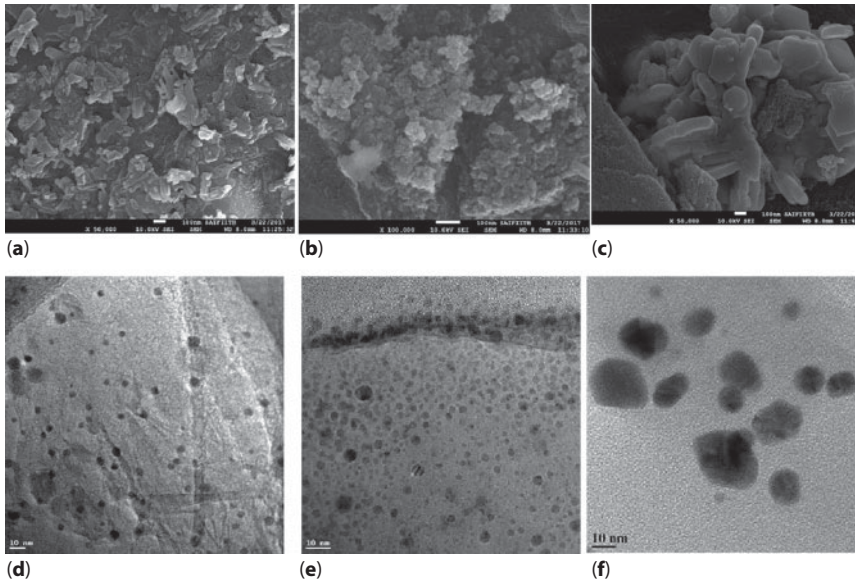


Figure 13.2 (a–f) SEM and TEM images of silver, copper and iron nanoparticles.

TEM images we can calculated the averages particles size of the nanoparticles and the calculated average particle sizes were found to be 4.5 nm, 8 nm and 25 nm for AgNPs, CuNPs and FeNPs respectively.

13.3.3.2 X-Ray Diffraction (XRD) Analysis

Figure 13.3a,b showed the characteristic XRD peaks of the synthesized Ag, Cu and Fe nanoparticles. In the XRD spectrum of AgNPs (Figure 13.3a), the peaks at 38.2°, 44.5°, 66.4°, 77.2° and 82° were corresponded to the lattice planes of (111), (200), (220), (311) and (222) reflected the face centered cubic (fcc) structure of Ag (JCPDS file: 65–2871). The XRD spectra of the synthesized Cu nanoparticles revealed the peaks at 2θ values of 43.4, 50.5 and 74.2°, respectively corresponding to (111), (200) and (220) lattice planes of fcc Cu (JCPDS-71-4610). From XRD spectrum of iron, we observed peaks at 44.5°, 65.01° and 82.41° corresponds to the lattice plane (110), (200) and (211) of the bcc structure of iron nanoparticles.

From the XRD spectra we can calculate the average crystallite particle sizes of the synthesized nanoparticles. It is calculated by Scherrer equation $d = K\lambda/\beta\cos\theta$, where d is the average crystalline particle size; K is a dimensionless shape factor, with a value close to unity (0.9); λ is the X-ray wavelength; β is the line broadening at half the maximum intensity (FWHM); θ is the Bragg angle of the crystal plane.

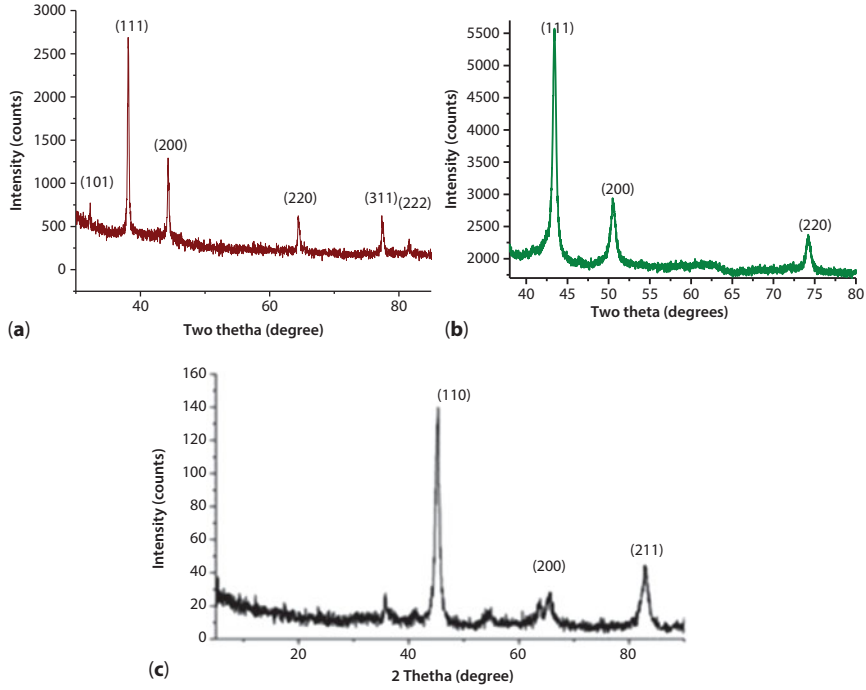


Figure 13.3 Represents the XRD spectra of silver (a), copper (b) and iron (c) nanoparticles.

The highly intense and narrow diffraction peaks revealed the highly crystalline nature of the synthesized nanoparticles. The calculated average crystallite particle sizes of Ag, Cu and Fe NPs were found to be 16 nm, 18 nm and 22.5 nm respectively.

13.3.3.3 Energy-Dispersive X-Ray Spectroscopy (EDX) Analysis

To determine the elemental composition of the synthesized nanoparticles we performed EDX analysis. In the EDX spectra of Ag, Cu and Fe NPs (Figure 13.4a–c), the most intense peaks around 3 keV, 1 keV and 6–7 keV correspond to the binding energies of Ag, Cu and iron. Hence it was confirmed the formation of AgNPs, CuNPs, and FeNPs. The remaining elements were due to the presence of phytochemicals in *Coccinia grandis* peel.

13.3.3.4 Fourier Transform Infrared (FTIR) Spectroscopy

From the FTIR spectra we can determine the functional groups which were responsible for the reduction process and formation of metals

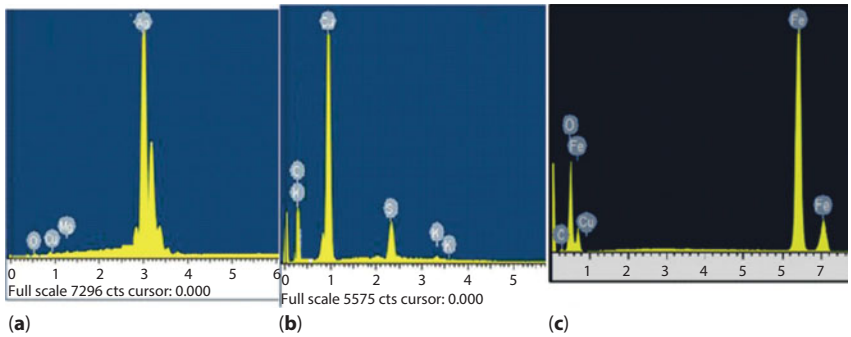


Figure 13.4 EDX spectra of silver (a), copper (b) and iron (c) nanoparticles.

nanoparticles. Figure 13.5a–c presents the FTIR spectra of the silver, copper and iron nanoparticles with *Coccinia grandia* peel extract. The FTIR spectrum of the peel extract showed absorption bands at 3450 cm^{-1}, 1636 cm^{-1} and 669 cm^{-1}. The peak at 3450 cm^{-1} corresponds to hydrogen bonded O-H stretching vibrations of alcohols. The remaining absorption peaks at 1636 cm^{-1} and peaks near 669 cm^{-1} were due to the -C=O asymmetric stretching vibration and -CH out of plane bending vibrations are substituted ethylene systems –CH=CH.

The peak at 3450 cm^{-1} of peel extract were shifted to 3455 cm^{-1} (AgNPs), 3446 cm^{-1} (CuNPs) and 3452 cm^{-1} (FeNPs) after the formation of metals nanoparticles. The shifting of peaks clearly indicated that the –OH groups were strongly involved in the formation of the nanoparticles.

The remaining peaks at 2923 cm^{-1}, 2075 cm^{-1}, 1628–1634 cm^{-1}, 1380 cm^{-1} and 1452 cm^{-1} were due to C–H and C–H (methoxy compounds) stretching vibration, C-O-H bending of carboxylic acids or in plane O-H bending vibrations, -C=O asymmetric stretching vibration and -C–O–O stretching band.

13.4 Catalytic Activities of Silver, Copper and Iron Nanoparticles for the Reduction and Photodegradation Process (Waste Water Treatment)

13.4.1 Reduction of Para-Nitrophenol (PNP) using AgNPs, CuNPs and FeNPs as Catalysts

The catalytic reduction of toxic aromatic nitrocompound was carried out by using sample of each AgNPs, CuNPs and FeNPs nanoparticles which

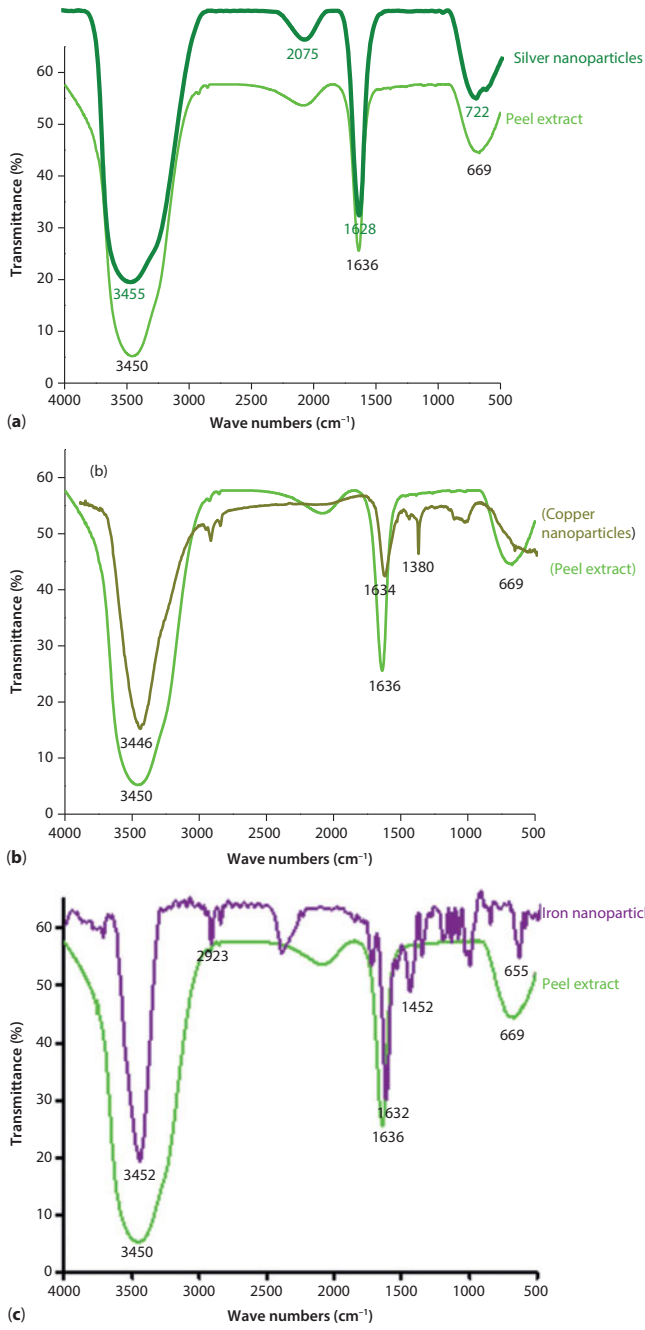


Figure 13.5 FTIR spectra of silver (a), copper (b) and iron (c) nanoparticles with peel extract.

were synthesized using biowaste material. The selection of the representative sample was done by performing the reduction experiments using all the synthesized metals nanoparticles and the better results shown by the corresponding AgNPs, CuNPs and FeNPs nanoparticles were illustrated in this chapter.

For the reduction of aromatic nitrocompounds, 2 mM solution of aromatic nitrocompound PNP and 0.1 M solution of $NaBH_4$ were prepared. Each metal AgNPs, CuNPs and FeNPs solution were prepared by dispersing 0.01 g of metal nanoparticles in 20 ml of water. The reduction of PNP was carried out separately using the three catalyst viz., Ag, Cu and Fe nanoparticles. Therefore, three sets of reduction reactions were carried out using metals (Ag, Cu and Fe) nanoparticles as catalyst in presence of $NaBH_4$ in aqueous medium.

All the reactions were carried out in a quartz cuvette and the absorbance was recorded in order to investigate the reduction process. In the cuvette, 2 ml of water was taken and to it 600μl of PNP and 350 μl of $NaBH_4$ solution were added and the absorption was recorded. To the above solution, 300 μl of each water dispersed metals nanoparticles were added to initiate the reduction process. The absorbance was recorded immediately and at regular interval of time in order to study the reduction of the aromatic nitrocompounds.

Figure 13.6a represented the UV-visible spectra of PNP which showed absorption maximum at 317 nm and it was evident that after the addition of $NaBH_4$ the absorption maximum was shifted to 403 nm due to the formation of p-nitrophenolate ions [53–54]. The color of the solution also changes to intense yellow after the addition of $NaBH_4$ due to the formation of p-nitrophenolate ions under alkaline condition. The peak at 403 nm remains unaltered after a couple of days in absence of any catalyst. This reaction is thermodynamically favorable however, kinetically restricted in the absence of any catalyst due to the large potential difference between PNP and BH_4^- [53–54]. Therefore, PNP reduction doesn't take place using only the reducing agent $NaBH_4$ in the absence of any catalyst. However, after the addition of metal nanoparticles (viz., Ag, Cu and Fe) the absorption maximum at 403 nm gradually decreases with time which indicated the reduction of PNP and the color of the solution also fades away. The metal nanoparticles act as an electron relay system to overcome this kinetic barrier. Figure 13.6b–d represented the absorption spectra of PNP with time using Ag, Cu and Fe respectively as heterogeneous catalyst in presence of $NaBH_4$ acting as reducing agent in aqueous medium. In each case, it was evident that a new peak centered at 300 nm started generating with an increase in reduction time. This peak arises due to the formation of

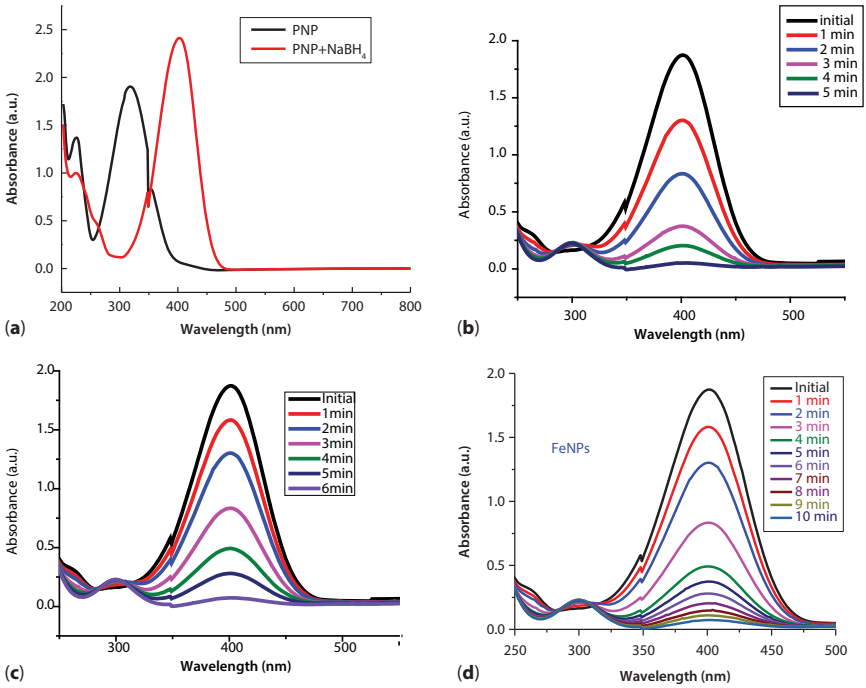


Figure 13.6 UV-Vis spectra of PNP and PNP with $NaBH_4$ (a), reduction of PNP using silver nanoparticles (b), copper nanoparticles (c) and iron nanoparticles (d).

p-aminophenol (PAP) which is the final reduced product [53–54]. The complete reduction of PNP takes place within 5, 6 and 10 min using Ag, Cu and Fe nanoparticles as catalysts, respectively.

It was also observed from the TEM images that the synthesized metals nanoparticles Ag, Cu and Fe having smaller size showed better results in the reduction of PNP. However, it is a well-known fact that with a decrease in particle size surface area increases. Moreover, from the literature it was also evident that with the increase in surface area, catalytic activity increases. Hence, due to this reason, AgNPs showed better catalytic properties as compared with the CuNPs and FeNPs.

About 97%, 96% and 95% of PNP was catalytically reduced within 5, 6 and 10 min using Ag, Cu and Fe nanoparticles, respectively. The rate constant (k) has been determined following first order kinetic from the linear plot of $\ln(C_0/C)$ versus time (t). The calculated rate constant of AgNPs, CuNPs and FeNPs were found to be $3.17 \times 10^{-2}\,min^{-1}$, $2.3 \times 10^{-2}\,min^{-1}$, and $1.7 \times 10^{-2}\,min^{-1}$ respectively (Figure 13.7a–c). In this protocol, based

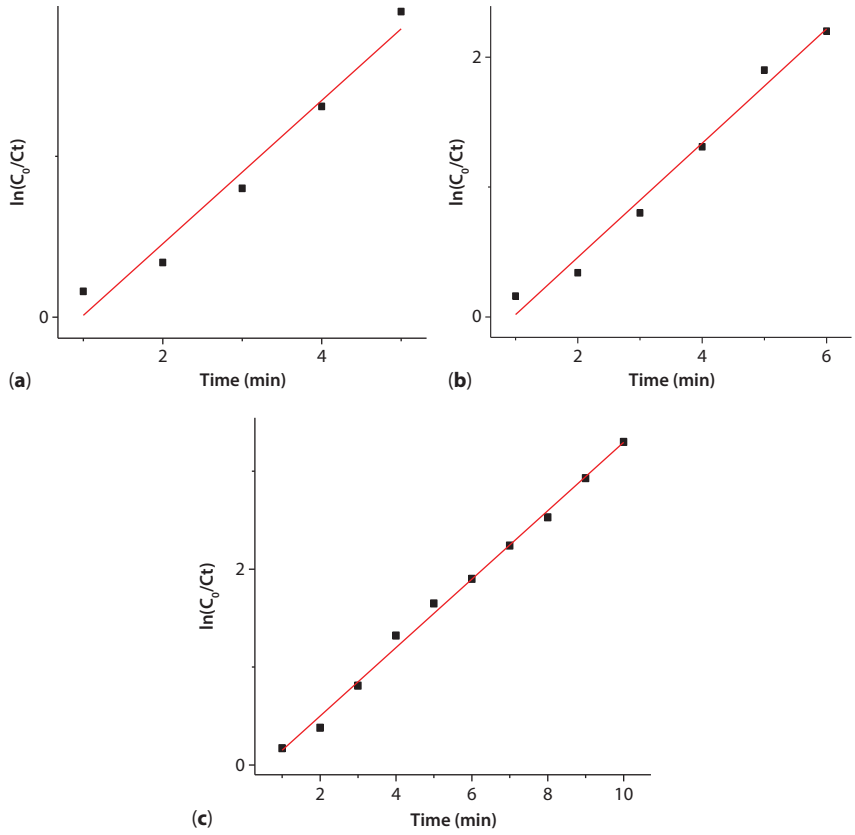


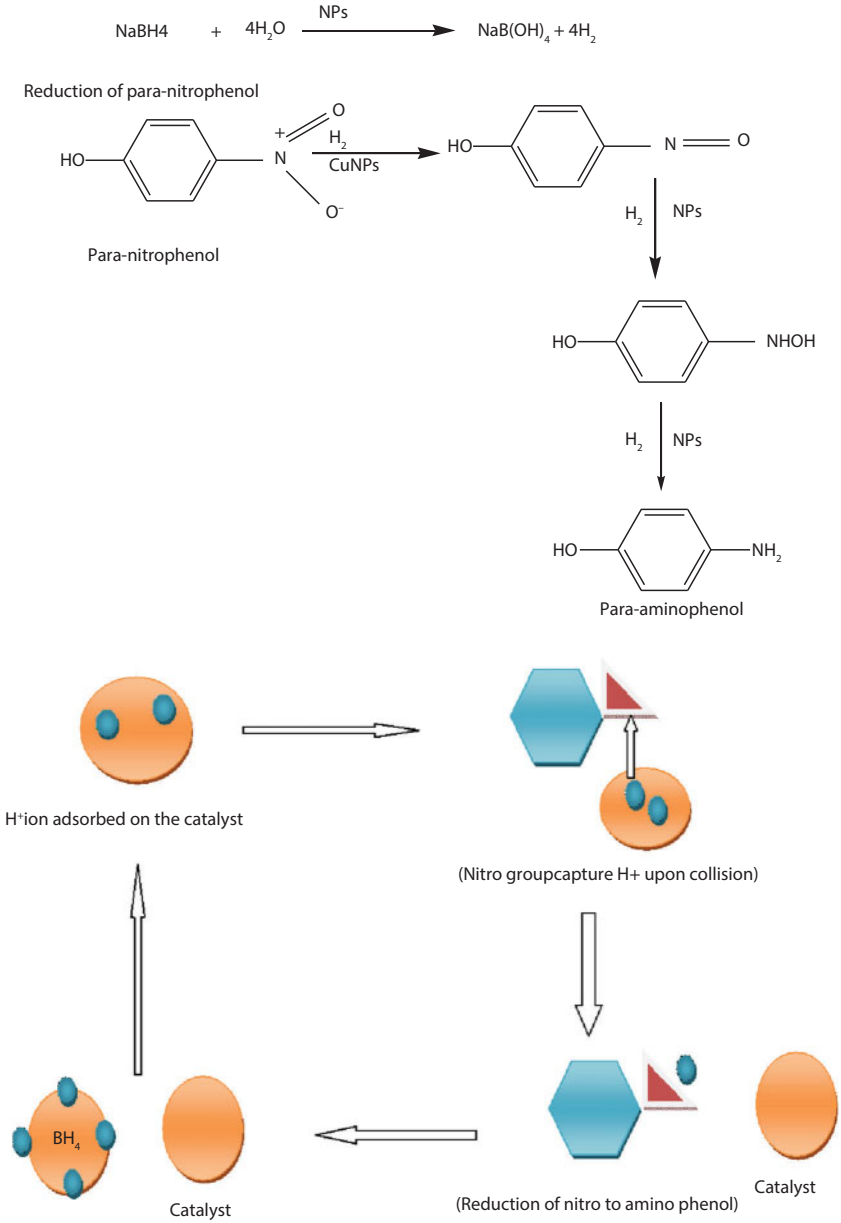
Figure 13.7 Kinetics plot of $\ln(C_0/C_t)$ verses reduction time using silver (a), copper (b) and iron nanoparticles (c).

on the Langmuir-Hinshel wood model we could discuss the mechanism of reduction of aromatic nitro-compounds to corresponding aromatic amino compounds by $NaBH_4$ in the presence of nanoparticles as nanocatalyst (Scheme 13.2) [55].

Mechanism of the reduction of nitrocompounds using AgNPs, CuNPs and FeNPs as a catalyst.

In this heterogeneous system, the mechanistic pathway for the hydrogenation of aromatic nitro compound involved the following steps:

In the first step, an adsorption process was occurred between reactants and surface of the nanoparticles. During this process on the surface of the NPs the borohydride ions (BH_4^-) get adsorbed and transfer surface hydrogen to the nanoparticles surface. In the second step desorption process was



Scheme 13.2 Schematic representation of reduction of para nitrophenol using nanoparticles as a catalyst.

occurred and form product on the surface of the nanoparticles. The metal surface is set free for catalytic cycle after the final product amino undergoes desorption.

13.4.2 Photocatalytic Activities of AgNPs, CuNPs and FeNPs for the Degradation of Toxic Dye Victoria Blue B under Solar Irradiation

Numerous efforts have been devoted for the removal of dye from industrial waste water. To reduce such toxic pollutant from waste water is a big challenge to many researchers. The conventional method such as adsorption of dye on activated carbon is inadequate for the treatment of dye waste water. Adsorption is a non-destructive method which transfers dye from one phase or substance to another and give rise to a new kind of pollution which requires a further treatment. In contrast, photo degradation process for treatment of dye using solar or UV irradiation in presence of a suitable photocatalyst is a green technique and proves to be an effective method for the degradation of dye. This method converts dye molecule into non-toxic compounds. In this chapter we have chosen Victoria Blue B dye as a target compound and metal nanoparticles were used as a catalyst for the photodegradation process.

The photocatalytic activity of the synthesized Ag, Cu and Fe nanoparticles were evaluated by the degradation of an organic dye, Victoria Blue B dye (VBB). A total of 10 mg of each photo catalyst AgNPs, CuNPs and FeNPs were dispersed in 250 ml of 10^{-4} M VBB aqueous solution. The solutions were then exposed to sunlight irradiation in presences of nanoparticles. At a regular interval of time, 3 ml of the suspensions were withdrawn and filtered immediately. The absorbance of the supernatants was then measured using the UV-Vis spectrophotometer. The absorbance was recorded till the peak due to the presence of VBB disappeared completely.

The photodegradation of the dye was carried out on a sunny day between 9 am and 3 pm when there were minimum fluctuations in solar intensity. The experiment was carried out in Silchar Assam city (India) on a sunny day.

The UV-Vis spectra of the dye (VBB) show a strong absorption band at 615 nm. It was observed that after the addition of metals nanoparticles, the intensity of the peaks gradually decreases with increase in irradiation time. Figure 13.8a–c represents the absorption spectra of photodegradation of Victoria Blue B using Ag, Cu and Fe nanoparticles under solar irradiation. After 140 min of irradiation time, it was observed that the color solutions of VBB dye becomes colorless which indicates complete destruction of the

chromophoric structure of VBB dye. The photodegradation of VBB dye is followed the pseudo-first order reaction and its kinetics may be expressed by the following reaction

$$\ln (C_0/Ct) = kt \tag{13.1}$$

where k is the rate constant, C_0 and Ct are the absorbance or concentration before and after degradation of VBB dye, respectively. The rate constant for the photo degradation of VBB dye was calculated using Equation 13.1. Figure 13.8d–f represents the plot of ln (C_0/Ct) versus irradiation time (t) of VBB dye using Ag, Cu and Fe photocatalyst. It indicates a linear relationship and the slope of the line represents the rate constant (k) for the photo degradation of VBB dye. The calculated values of k were found to be 4.1×10^{-2} min^{-1}, 3.3×10^{-2} min^{-1} and 1.1×10^{-2} min^{-1}.

The percentage efficiency of photo degradation of VBB dye was determined using the following equation:

$$X= [(C_0 - C)/C_0] \times 100 \tag{13.2}$$

where C_0 and C are the absorbance or concentration before and after degradation of VBB dye, respectively. Figure 13.9a–c shows the percentage efficiency curves of photodegradation of VBB dye using Ag, Cu and Fe nanoparticles, respectively. It was observed that 95%, 90% and 80% of the dye was degraded using Ag, Cu and Fe NPs within 140 min. Hence from the photo degradation process, AgNPs showed better photocatalytic properties as compared with the CuNPs and FeNPs.

Probable mechanism and formation of by-products during the photodegradation of Victoria Blue B dye using nanoparticles are shown in the Scheme 13.3.

13.5 Toxicity and Future Prospect

13.5.1 Toxicity of Silver Nanoparticles

Due to the toxic properties of silver nanoparticles, many researchers used silver nanoparticles as antimicrobial and anticancer properties. When bacterial cell membranes are exposed to silver metal nanoparticles, it penetrates them causing changes in their structural composition due to interaction with the bacteria's sulfate group, being the active site of enzymes. These blocks some of the bacterial enzymes meant for metabolism and

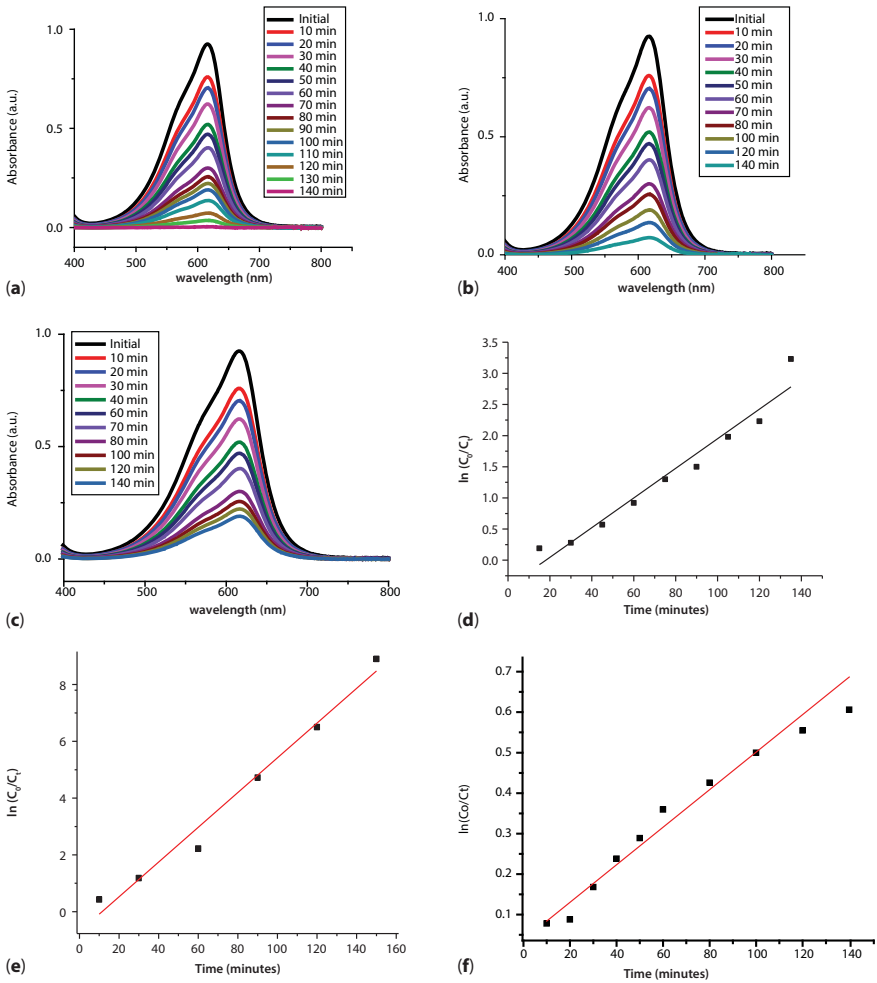


Figure 13.8 represents the photodegradation absorption spectra of Victoria Blue B dye using silver (a), copper (b) and iron nanoparticles (c). Kinetic plot ln (Co/Ct) versus time for the photodegradaton using silver (d), copper (e) and iron nanoparticles (f).

electrolyte transport thereby weakening bacterial survival and deteriorating its activity. Moreover, it also affects the DNA backbone of the bacteria hindering its replication process. The metal ions (Ag) further reduce its immunity by binding itself to the bacterial wall rendering structural imperfections within its cells. This leads to the collapse of bacteria. Hence, metal ions act as preventive tool in minimizing bacteria proliferation by inducting a defense system, deteriorating bacterial development and in due

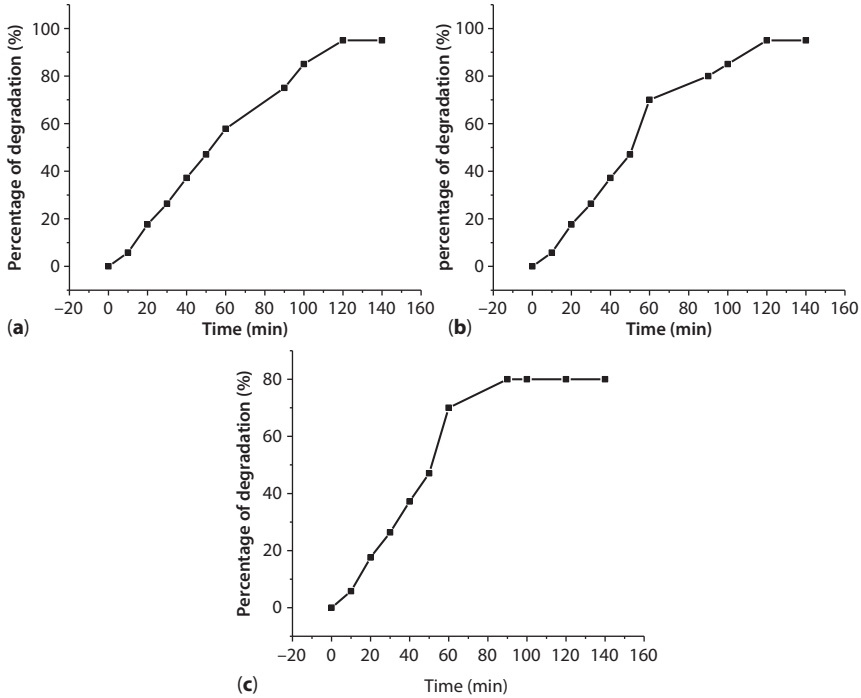


Figure 13.9 (a–c) The percentage efficiency curves of photodegradation of VBB dye using Ag, Cu and Fe nanoparticles respectively.

$$NPs + h\nu \rightarrow e^- + h^+$$

$$H_2O + h^+ \rightarrow OH^- + H^+$$

$$OH^- + h^+ \rightarrow \cdot OH$$

$$e^- + O_2 \rightarrow \cdot O^{2-}$$

$$\cdot O^{2-} + H^+ \rightarrow \cdot OOH$$

$$Dye + h\nu \rightarrow Dye^*$$

$$Dye^* + NPs \rightarrow Dye + NPs\,(e^-)$$

$$NPs\,(e^-) + O_2 \rightarrow NPs + O^{2-}$$

$$NPs\,(e^-) + \cdot O^{2-} + H^+ \rightarrow NPs + H_2O_2$$

$$NPs\,(e^-) + H_2O_2 \rightarrow NPs + \cdot OH + OH^-$$

$$h^+ + Dye \rightarrow \text{degradation products}$$

$$Dye^* + O_2 \text{ or } \cdot OH \text{ or } \cdot O^{2-} \rightarrow \text{degradation products}$$

Scheme 13.3 Schematic representation of mechanism action of nanoparticles and formation of by-products during photodegradation process.

course killing them. Similarly, silver metal ion damages human lung carcinoma epithelial-like cell line, primary testicular cells, human monocytic cell line and human intestinal cell line.

13.5.2 Toxicity of Iron Nanoparticles

Iron nanoparticles that are poised for use in large-scale pollution remediation can rapidly react with oxygen and cause lung cells to die.

The number of oxygen molecules associated with iron nanoparticles is an important factor in its toxicity to cells. Iron-based nanoparticles without attached oxygen molecules can react quickly when exposed to oxygen to form other reactive varieties that can damage lung cells. Zero-valent iron nanoparticles (nZVI) – has great potential for remediating pollutants such as chlorinated organic solvents, pesticides and metals found in contaminated groundwater. nZVI is already commercially available, and its use could introduce large amounts of the nanoparticles into the environment. However, the same qualities that make these particles potentially useful in environmental clean-up—namely their high reactivity—also make them potentially harmful to living things. Some of the reactions can release free radicals that can damage cell DNA in a process broadly called oxidative stress. nZVI nanoparticles might affect human lung cells if they were inhaled, researchers exposed lung cells to different levels of the nZVI nanoparticles and of another more volatile form called ferrous oxide (Fe(II)). This revealed that as the nZVI nanoparticles contact oxygen, their form rapidly changes and releases oxygen radicals that can damage lung cells. The Fe(II) form of iron was more reactive than the more stable ferric iron. It is the further reaction of Fe(II) with oxygen that leads to the oxidative stress that damages the cells. From the above discussion, it was concluded that oxidation state of the iron in nanoparticles is an important factor in its toxicity.

13.5.3 Toxicity of Copper Nanoparticles

Copper nanoparticles are now being widely manufactured because of the increasing demand due to their use in several applications. The toxicological effects of copper nanoparticles have been shown *in vivo* at organ levels in kidney, liver, and spleen of rats. It was reported in the literature that direct exposure of copper nanoparticles of sizes 40 nm, 60 nm, and 80 nm all had toxic effects on dorsal root ganglion (DRG) neurons of rats.

13.5.4 Future Prospect of Silver, Copper and Iron Nanoparticles

Based on the results presented in this chapter, the research work can be extended in order to explore the applicability of metal nanoparticles in various fields. Therefore, the future prospect of the research work can be summarized as follows:

- In future, metal nanoparticles may be fabricated by using more facile, greener and cost-effective method.
- The synthesized metal nanoparticles, such as Ag, Cu and Fe can be employed in the fabrication of sensors, solar cells, in biological applications such antibacterial, antifungal activities, anticancer and in the removal of emerging pollutants such as ibuprofen, clofibric acid, naproxen, etc.
- This chapter reported the photocatalytic activity of metal nanoparticles for the removal of toxic dyes from aqueous phase. These experiments were performed in a beaker in the laboratory. However, this work can be extended in near future by treating real waste water samples collected from different industries such as textile and paper industries with metal nanoparticles as photocatalyst. The removal of hazardous organic pollutants in large scale from such industrial waste water can be carried out in a well-equipped pilot plant.
- The toxicity of monometallic nanoparticles such as silver, copper, and iron nanoparticles can be reduced by combining with activated carbon, reduce graphene oxide, etc. The activated carbon, reduce graphene oxide can improve the activities or qualities of mono metallic nanoparticles.

13.6 Future of Green Route in Synthesis of Metal Nanoparticles

The "green" route for nanoparticles (NPs) synthesis is of great interest due to eco-friendliness, economic prospects, and feasibility and wide range of applications in nanomedicine, new category catalysis medicine, nano-optoelectronics, etc. It is a new and emerging area of research in the scientific world, where day-by-day developments is noted in warranting a bright future for this field. This green chemistry approach toward the synthesis of Ag, Cu, Fe and others have many advantages such as, ease with which

the process have economic viability, cheap, easily available and avoid using toxics chemicals etc. It was concluded that biological mediated synthesis of nanoparticles possesses potential antimicrobial, anticoagulant activity, and anticancer activities. The characterization analysis proved that the particle so produced in nano dimensions would be equally effective as that of antibiotics and other drugs in pharmaceutical applications. Many researchers are focused on evaluating the safety of nanomedicine and formulating the international regulatory guidelines for the same, which is critical for technology advancement. With vast technology push, there are many challenges head that need to be understood and solve in order to make the NP-based products commercially viable. Due to many disadvantages for the synthesis of nanoparticles, nowadays, researchers are looking into the development of cost-effective procedures for producing reproducible, stable and biocompatible metallic NPs from bio resources.

13.7 Concluding Summary

This chapter reported facile and green approach towards the development of different metal nanoparticles. The synthesis of AgNPs, CuNPs and FeNPs were successfully carried out by using biological method. The conclusive remarks comprising out of this chapter can be summarized as follows:

- The metals nanoparticles Ag, Cu and Fe were successfully synthesized by using *Coccinia grandis* peel extract (bio-waste).
- Flavonoids present in the peel extract acts as a reducing as well as stabilizing agents in the formation of AgNPs, CuNPs and FeNPs.
- The synthesized metals nanoparticles were characterized by using TEM, SEM, UV-Vis spectroscopy, FT-IR spectroscopy, EDX, XRD techniques.
- From the TEM images we calculated the average particles sizes of the metals nanoparticles. The calculated average particle sizes were found to be 4.5 nm, 8 nm, 25 nm for AgNPs, CuNPs and FeNPs respectively.
- The synthesized metals nanoparticles were successfully use as a catalyst and photocatalyst in the reduction of para nitrophenol and photodegradation of Victoria Blue B dye.
- It is a well-known fact that with a decrease in particle size surface area increases. Moreover, from the literature it was

also evident that with the increase in surface area, catalytic activity increases. Hence, due to this reason, AgNPs showed better catalytic properties in the reduction and photo degradation process as compared with the CuNPs and FeNPs.

- 95%, 90% and 80% of Victoria Blue B dye were degraded using photocatalyst AgNPs, CuNPs and FeNPs respectively in 140 irradiation time.
- The toxic para-nitrophenol were successfully reduced within 5, 6 and 10 min by using AgNPs, CuNPs and FeNPs catalyst, respectively.

References

1. Daniel, M.C., Astruc, D., Gold nanoparticles: Assembly, supramolecular chemistry, quantum-size-related properties, and applications toward biology, catalysis, and nanotechnology. *J. Chem. Rev.*, 104, 293–346, 2004.
2. Krolikowska, A., Kudelski, A., Michota, A., Bukowska, J., SERS studies on the structure of thioglycolic acid monolayers on silver and gold. *Surf. Sci.,* 532, 227–232, 2003.
3. Zharov, V.P., Kim, J.W., Curiel, D.T., Everts, M., Self-assembling nanoclusters in living systems: Application or integrated photothermal nanodiagnostics and nanotherapy. *Nanomedicine: NBM*, 1, 326–345, 2005.
4. Kumar, A., Mandal, S., Selvakannan, P.R., Parischa, R., Mandale, A.B., Sastry, M., Investigation into the interaction between surface-bound alkylamines and gold nanoparticles. *Langmuir*, 19, 6277–6282, 2003.
5. Bogunia-Kubik, K., Sugisaka, M., From molecular biology to nanotechnology and nanomedicine. *Biosystems*, 65, 123–138, 2002.
6. Awasthi, K.K., Awasthi, A., Kumar, N., Roy, P., Awasthi, K., John, P.J., Silver nanoparticle induced cytotoxicity, oxidative stress, and DNA damage in CHO cells, *J. Nanopart. Res.*, 15, 1898, 2013.
7. Devi, T.B., Ahmaruzzaman, M., Bio-inspired facile and green fabrication of Au@Ag@AgCl core–double shells nanoparticles and their potential applications for elimination of toxic emerging pollutants: A green and efficient approach for wastewater treatment. *Chem. Eng. J.*, 317, 726–741, 2017.
8. Devi, T.B., Begum, S., Ahmaruzzaman, M., Photo-catalytic activity of plasmonic Ag@AgCl nanoparticles (synthesized via a green route) for the effective degradation of Victoria Blue B from aqueous phase. *J. Photochem. Photobiol B*, 160, 260–270, 2016.
9. Devi, T.B., Ahmaruzzaman, M., Bio-inspired sustainable and green synthesis of plasmonic Ag/AgCl nanoparticles for enhanced degradation of organic compound from aqueous phase. *Environ. Sci. Pollut. Res. Int.*, 23, 17702–14, 2016.

10. Devi, T.B., Ahmaruzzaman, M., Begum, S., A rapid, facile and green synthesis of Ag@AgCl nanoparticles for the effective reduction of 2,4-dinitrophenyl hydrazine. *New J. Chem.*, 40, 1497–1506, 2016.
11. Devi, T.B., Ahamaruzzaman, M., Bioinspired green and facile fabrication of Au@Ag@AgCl hybrid nanoparticles and their catalytic and antimicrobial properties. *Chem. Selct.*, 2, 5950–5957, 2017.
12. Sperling, R.A., Gil, P.R., Zhang, F., Zanella, M., Parak, W.J., Biological applications of gold nanoparticles. *Chem. Soc. Rev.*, 37, 1896–1908, 2008.
13. Puvanakrishnan, P., Park, J., Chatterjee, D., Krishnan, S., Tunnel, J.W., *In vivo* tumor targeting of gold nanoparticles: Effect of particle type and dosing strategy. *Int. J. Nanomed*., 7, 1251–1258, 2012.
14. Bhattacharya, R., Murkherjee, P., Biological properties of "naked" metal nanoparticles. *Adv. Drug Deliv. Rev.*, 60, 1284–1306, 2008.
15. Sykora, D., Kasicka, V., Miksik, I., Rezanka, P., Zaruba, K., Matejka, P., Kral, V., Applications of gold nanoparticles in separation sciences. *J. Sep. Sci.*, 30, 372–387, 2010.
16. Torres-Chavolla, E., Ranasinghe, R.J., Alocilja, E.C., Characterization and functionalization of biogenic gold nanoparticles for biosensing enhancement. *IEEE Trans. Nanobiotechnol.*, 9, 533–538, 2010.
17. Cai, W., Gao, T., Hong, H., Sun, J., Applications of gold nanoparticles in cancer nanotechnology. *Nanotechnol. Sci. Appl.*, 1, 17–32, 2008.
18. Bhumkar, D.R., Joshi, H.M., Sastry, M., Pokharkar, V.B., Chitosan reduced gold nanoparticles as novel carriers for transmucosal delivery of insulin. *Pharm. Res.*, 24, 1415–1426, 2007.
19. Huang, Y., Li, X., Liao, Z., Zhang, G., Liu, Q., Tang, J., Peng, Y., Liu, X., Luo, Q., A randomized comparative trial between Acticoat and SD-Ag in the treatment of residual burn wounds including safety analysis. *Burns,* 33, 161–166, 2007.
20. Li, W.R., Xie, X.B., Shi, Q.S., Duan, S.S., Ouyang, Y.S., Chen, Y.B., Antibacterial effect of silver nanoparticles on *Staphylococcus aureus*. *Biometals*, 24, 135–141, 2011.
21. Cox, S.G., Cullingworth, L., Rode, H., Treatment of paediatric burns with a nanocrystalline silver dressing compared with standard wound care in a burns unit: A cost analysis. *S. Afr. Med. J.*, 101, 728–731, 2011.
22. Pollini, M., Paladini, F., Catalno, M., Taurino, A., Licciulli, A., Maffezzoli, A., Sannio, A., Antibacterial coatings on haemodialysis catheters by photochemical deposition of silver nanoparticles. *J. Mater. Sci. Mater. Med.*, 22, 2005–2012, 2011.
23. Cohen, M.S., Stern, J.M., Vanni, A.J., Kelley, R.S., Baumgart, E., Field, D., Libertino, J.A., Summerhayes, I.C., *In vitro* analysis of a nanocrystalline silver-coated surgical mesh. *Surg. Infect.*, 8, 397–403, 2007.
24. Asha-Rani, P.V., Mun, G.L.K., Hande, M.P., Valiyaveettil, S., Cytotoxicity and genotoxicity of silver nanoparticles in human cells. *ACS Nano*, 3, 279–290, 2003.

25. Lee, H.J., Lee, G., Jang, N.R., Yun, J.H., Song, J.Y., Kim, B.S., Biological synthesis of copper nanoparticles using plants extract. *Nanotechnology*, 1, 371–374, 2011.
26. Liu, X., Cai, W., Bi, H., Optical absorption of copper nanoparticles dispersed within pores of monolithic mesoporous silica, *J. Mater. Res.*, 17, 1125–1128, 2002.
27. Nasibulin, A.G., Ahonen, P.P., Richard, O., Kauppinen, E.I., Altman, I.S., Copper and copper oxide nanoparticle formation by chemical vapor nucleation from copper (II) acetylacetonate. *J. Nanopart. Res*., 3, 385–400, 2001.
28. Tarasov, S., Kolubaev, A., Belyaev, S., Lerner, M., Tepper, F., Study of friction reduction by nanocopper additives to motor oil. *Wear.,* 252, 63–69, 2002.
29. Choi, Y., Lee, C., Hwang, Y., Park, M., Lee, J., Choi, C., Jung, M., Tribological behavior of copper nanoparticles as additives in oil. *Curr. Appl. Phys.*, 9, 124–127, 2009.
30. Lee, Y.G., Choi, J.R., Lee, K.J., Stott, N.E., Kim, D.H., Large-scale synthesis of copper nanoparticles by chemically controlled reduction for applications of inkjet-printed electronics. *Nanotechnol.*, 19, 415604–415610, 2008.
31. Xuan, Y., Li, Q., Heat transfer enhancement of nanofluids, *Int. J. Heat Fluid Flow*, 21, 58–64, 2000.
32. Eastman, J.A., Choi, S.U.S., Li, S., Yu, W., Thompson, L.J., Anomalously increased effective thermal conductivities of ethylene glycol-based nanofluids containing copper nanoparticles. *Appl. Phys. Lett*., 78, 718–720, 2001.
33. Nadagouda, M.N., Castle, A.B., Murdock, R.C., Hussain, S.M., Varma, R.S., *In vitro* biocompatibility of nanoscale zerovalent iron particles (NZVI) synthesized using tea polyphenols. *Green Chem.*, 12, 114–122, 2010.
34. Shahwan, T., Abu Sirriah, S., Nairat, M., *et al.*, Green synthesis of iron nanoparticles and their application as a Fenton-like catalyst for the degradation of aqueous cationic and anionic dyes. *Chem. Eng. J.*, 172, 258–266, 2011.
35. Kuang, Y., Wang, Q., Chen, Z., Megharaj, M., Naidu, R., Heterogeneous Fenton-like oxidation of monochlorobenzene using green synthesis of iron nanoparticles. *J. Colloid Interface Sci.*, 410, 67–73, 2013.
36. Roh, Y., Lauf, R.J., McMillan, A.D., Zhang, C., Rawn, C.J., Bai, J., Phelps, T.J., Microbial synthesis and the characterization of metal-substituted magnetites. *Solid State Commun*., 118, 529–534, 2011.
37. Lengke, M., Southam, G., Bioaccumulation of gold by sulphate-reducing bacteria cultured in the presence of gold (I)-thiosulfate complex. *Geochim. Cosmochim. Acta.*, 70, 3646–3661, 2006.
38. Nair, B., Pradeep, T., Coalescence of nanoclusters and formation of submicron crystallites assisted by *Lactobacillus* strains. *Cryst. Growth Des.*, 2, 293–298, 2002.
39. Joerger, T.K., Joerger, R., Olsson, E., Granqvist, C.G., Bacteria as workers in the living factor: Metal accumulating bacteria and their potential for materials science. *Trends Biotechnol.*, 19, 15–20, 2001.
40. Husseiny, M.I., El-Aziz, M.A., Badr, Y., Mahmoud, M.A., Biosynthesis of gold nanoparticles using *Pseudomonas aeruginosa*. *Spectrochim. Acta A*, 67, 1003–1006, 2007.

41. Mukherjee, P., Ahmad, A., Mandal, D., Senapati, S., Sainkar, S.R., Khan, M.I., Parishcha, R., Aiayumar, P.V., Alam, M., Kumar, R., Sastry, M., Fungus-mediated synthesis of silver nanoparticles and their immobilization in the mycelia matrix: A novel biological approach to nanoparticles synthesis. *Nano Lett.*, 1, 515–519, 2001.
42. Ahmad, A., Senapati, S., Khan, M.I., Kumar, R., Ramani, R., Srinivas, V., Sastry, M., Intracellular synthesis of gold nanoparticles by a novel alkalotolerant actinomycete *Rhodococcus* species. *Nanotechnol.*, 14, 824–828, 2003.
43. Ahmad, A., Senapati, S., Khan, M.I., Kumar, R., Sastry, M., Extra-/intracellular, biosynthesis of gold nanoparticles by an alkalotolerant fungus, *Trichothecium* sp. *J. Biomed. Nanotechnol.*, 1, 47–53, 2005.
44. Kuber, C., Souza, S.F., Extracellular biosynthesis of silver nanoparticles using the fungus *Aspergillus fumigatus*. *Colloids Surf. B*, 47, 160–164, 2006.
45. Philip, D., Green synthesis of gold and silver nanoparticles using *Hibiscus rosa sinensis*. *Phys. E.*, 42, 1417–1424, 2010.
46. Kumar, P., Singh, P., Kumari, K., Mozumdar, S., Chandra, R., A green approach for the synthesis of gold nanotriangles using aqueous leaf extract of *Callistemon viminalis*. *Mater. Lett.*, 65, 595–597, 2011.
47. Lee, S.W., Mao, C., Flynn, C., Belcher, A.M., Ordering of quantum dots using genetically engineered viruses. *Science*, 296, 892–895, 2002.
48. Merzlyak, A., Lee, S.W., Phage as template for hybrid materials and mediators for nanomaterials synthesis. *Curr. Opin. Chem. Biol.*, 10, 246–252, 2006.
49. Dameron, C.T., Reeser, R.N., Mehra, R.K., Kortan, A.R., Carroll, P.J., Steigerwald, M.L., Brus, L.E., Winge, D.R., Biosynthesis of cadmium sulphide quantum semiconductor crystallites. *Nature*, 338, 596–597, 1989.
50. Kowshik, M., Arhtaputre, S., Kharrazi, S., Vogel, W., Urban, J., Kulkarni, S.K., Paknikar, K.M., Extracellular synthesis of silver nanoparticles by a silver-tolerant yeast strain MKY3. *Nanotechnol.*, 14, 95–100, 2003.
51. Arunachalam, R., Dhanasingh, S., Kalimuthu, B., Uthirappan, M., Rose, C., Mandal, A.B., Photosynthesis of silver nanoparticles using *Coccinia grandis* leaf extract and its application in the photocatalytic degradation. *Colloids Surf. B*, 94, 226–230, 2012.
52. Visvanathan, S., Janathul, F.S., Bharathi, V., Green synthesis of silver nanoparticles by *Coccinia grandis* flower extract. *WJPPS*, 3, 1777–1782, 2014.
53. Saha, S., Pal, A., Kundu, S., Basu, S., Pal, T., Photochemical green synthesis of calcium-alginate-stabilized Ag and Au Nanoparticles and Their Catalytic Application to 4-nitrophenol reduction. *Langmuir*, 26, 2885–2893, 2010.
54. Mondal, S., Rana, U., Bhattacharjee, R.R., Malik, S., One pot green synthesis of polyaniline coated gold nanorods and its applications. *RSC Adv.*, 4, 57282–57289, 2014.
55. Aditya, T., Pal, A., Pal, T., Nitroarene reduction: A trusted model reaction to test nanoparticle catalysts. *Chem. Commun.*, 51, 9410–9431, 2015.

Part III

BIOSYNTHESIS OF METAL OXIDE NANOPARTICLES

Suvardhan Kanchi and Shakeel Ahmed (eds.) Green Metal Nanoparticles, (467–512)
© 2018 Scrivener Publishing LLC

14

Current Scenario in Green Approaches for Metal/Metal Oxide Nanoparticles Synthesis

Selvaraj Mohana Roopan

Chemistry of Heterocycles & Natural Product Research Laboratory, Department of Chemistry, School of Advanced Sciences, Vellore Institute of Technology, Tamil Nadu, India

Abstract

Metal/metal oxide nanoparticles are considered to be the most important of several kinds of nanoparticles, having numerous applications in the biomedical field. There are many ways to synthesize metal/metal oxide nanoparticles, which include natural (Green), chemical and physical methods. But the main drawback to chemical or physical processes is their hazardous approach and elimination of toxic effluents, which cause a threat to the environment. To overcome this drawback, most researchers have been focusing on a biotechnological approach towards the synthesis of metal/metal oxide nanoparticles. In general, metal nanoparticles utilized in applications mingle with air and lead to some airborne diseases while metal oxide nanoparticles are very tiny in comparison. In this chapter, the most prominent research in the field of nanobiotechnology is discussed; moreover, an overview is given of metal/metal oxide nanoparticles and their applications.

Keywords: Metal/metal oxide nanoparticles, biotechnology, synthesis, applications

Corresponding author: mohanaroopan.s@vit.ac.in

Suvardhan Kanchi and Shakeel Ahmed (eds.) Green Metal Nanoparticles, (469–512)
© 2018 Scrivener Publishing LLC

14.1 Introduction

This review chapter brings to light the importance of nanotechnology, especially considering the current world scenario, as it impacts a large number of people across the world without their being very aware of it. A burgeoning branch of nanotechnology called green synthesis of metal nanoparticles is especially gaining momentum in the modern world. The rise of plant mediated synthesis is gaining a lot of attention because of its simplicity as well as the fact that there is a rapid increase in the growth rate of the metal nanoparticles in question [1]. The green synthesis process ensures that there is cell maintenance and management and it maintains a degree of environmental friendliness that is crucial for any technology to evolve in the modern world [2].

Manufactured materials are made from atoms. The properties of these materials depend on how these atoms are arranged. If one rearranges the atoms in coal, he gets diamonds, and if one arranges the atoms in sand, he gets computer chips [3]. One of the basic principles of matter is positional control. The control may be either macroscopic or microscopic level but the results could be much lighter, stronger and more precise. A new technology has created a new science called nanotechnology, which is about rearranging atoms whichever way we want. The term "umbrella" is most suitable for nanotechnology because it covers many areas of research which deal with materials/particles that are nanometer size [4]. The study of basic principles and concepts of particles in specific structures which possess one dimension in the 1–100 nm range is called nanoscience. Nanoscience is the study of the fundamental principles of atoms, molecules and structures with at least one dimension roughly between 1 and 100 nanometers. The fundamental goal of nanoscience or nanotechnology is to understand the evolution with decreasing crystal size of molecular properties of bulk properties [5].

Starting from the bulk, the first effect of reducing particle size is to create more surface sites. This changes the surface pressure and results in a change in the interparticle spacing. The change in the interparticle spacing and the larger surface to volume ratio in particles has a concomitant effect on the material properties [6]. Variations in surface free energy change the chemical potential. The variation in interparticle spacing and geometry also results in a variation in electronic properties with size [7]. The electronic states of small particles are not constant, but distinct, because of the confinement of the electron wave function. As the size decreases, the electronic bands become narrower and the delocalized electronic states are transformed to more localized molecular bonds. The electronic property

accessible for experimental measurements is the ionization potential. The ionization potentials at smaller sizes are higher than the bulk work function and show considerable fluctuations as a function of size. Photoelectronic spectroscopy is used to probe changes in electronic energy levels with size of free cluster. The anionic clusters are then crossed with a fixed frequency laser beam and the resulting photo-detached electrons are analyzed. Therefore, the spectra are fingerprints of the ground and excited states of the neutral cluster. They provide information on vertical and adiabatic electron affinities and the low-lying electronic states [8].

Furthermore, the large surface to volume ratio and the variations in geometry and electronic structures have a strong effect on catalytic properties [9]. The reactivity of small clusters is found to vary by order magnitude when the cluster size is changed by only a few atoms. A wide range of synthetic procedures are used in the preparation of nanomaterials such as gas phase evaporation method, reduction of metal ions, decomposition of organometallic compounds and cluster complexes, metal atom vapor synthesis, encapsulation in inert gas matrices, sol-gel processing; single-phase materials, multiphase materials, metal hybrids and vapor deposition polymerization [10].

14.1.1 Synthesis of Nanoparticles

Nanoparticles are synthesized by bringing together atoms or molecules which are initially a part to form a larger cluster of atoms. This is similar to how crystals grow in a solution. These manufacturing approaches fall under two categories: *bottom-up* and *top-down* (Figure 14.1a,b).

As in the case of nanoparticle synthesis, physical and chemical methods have been commonly used for all kinds of nanoparticles. These two methods are expensive and release toxic compounds; furthermore, they need a lab environment, which involves maintaining high pressure and high temperature, etc., which is not cost-effective. So, we usually adopt biological synthesis or green synthesis for producing nanoparticles. The ease of managing this process and its continuity, along with its extreme economic viability, has led to the fact that this process will continue to hold a lot of promise in the future [11]. Researchers are currently also trying to focus a lot on the future stability and compatibility of these so-called nanoparticles. In addition to all their technological advantages, like finding use in photo- and optoelectronic devices and catalysts in chemical reactions, to name just a few, they also have anticoagulant and cancer-inhibiting effects, which could be very fruitful in the medical and pharmaceutical industry and as a way of helping society in general. It should also be stressed that safety protocols should be followed while making them [12].

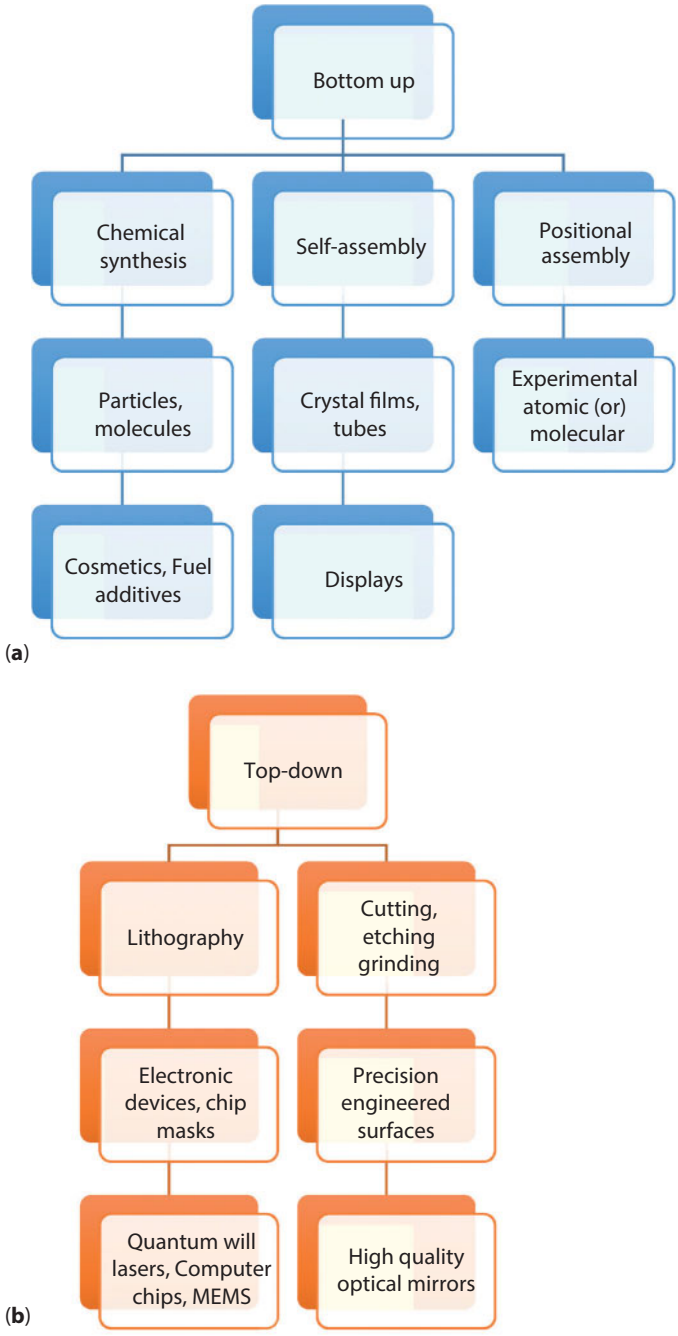


Figure 14.1 Different approaches of nanoparticle synthesis: (a) Top down and (b) Bottom up.

14.2 Overview of Biological Approach-Microbial Medium

Microbial mediated synthesis (Figure 14.2a) consists of several strains of bacteria, fungi, yeast, etc. [13]. These strains act as secondary metabolites which are responsible for the reduction of metal precursors to metal nanoparticles (Table 14.1) [14].

14.2.1 Silver Nanoparticles (AgNPs) Synthesis Using Different Microbial Sources

It is stated that the nanoparticles have a tremendous scope for growth and development in various technological and industrial fields, chief among

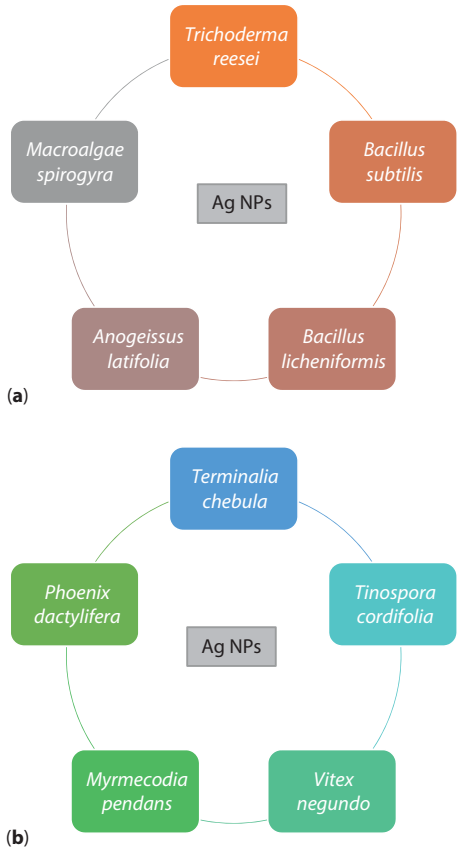


Figure 14.2 AgNPs synthesis using (a) microorganisms and (b) plants.

Table 14.1 Microorganisms mediated synthesis of metal NPs.

S. no	Microbial origin	NPs	Size (nm)	Morphology	Ref.
1	*Bacillus subtilis*	Ag	10–20	Crystalline	[17]
2	*Bacillus licheniformis*	Ag	18.69–63.42	Circular	[18]
3	*Aspergillus terreus*	Ag	1–20	Spherical	[22]
4	Macroalgae *Spirogyra varians*	Ag	17.6	Crystalline	[23]
5	*Bacillus marisflav*i	Au	~14	Crystalline	[26]
6	Filamentous cyanobacteria	Au	<10–25	Octahedral	[28]
7	*Aeromonas hydrophila*	Cu	5–30	Spherical	[36]

them being areas like therapeutics, antimicrobials and microelectronics, to name just a few of the wide-reaching areas and fields of interest in the subject. Also stated are the important advantages they hold in the long run, chief among them being low temperature dependence, a single-step concise growth method and, most importantly, requiring a much lesser amount of energy as compared to other methods. The important steps required for the synthesis of the overall process have also been described, chief among them being the environmentally friendly and cost-effective means of using leaf extracts (Figure 14.2b) of the plants *Ocimum sanctum, Azadirachta indica* and *Lawsonia inermis* (kadvi mehndi), etc.; and passing through an aqueous silver nitrate solution and aptly naming it green synthesis for the formation of silver nanoparticles (AgNPs). The samples were further confirmed and validated using UV spectrometry, particle size distribution (PSD) and morphological studies. The sizes of the various synthesized products were decidedly confirmed as 531, 540 and 543 nm. The PSD basis also led to further proof and verification using electron microscopy as well as scanning tunneling microscopy. It must be noted that sampling was done on the basis of aqueous content and absorption maxima of the given samples obtained. Also, D-50 analysis was further done to validate this proof, indicating the seriousness of the research. Further research is being undertaken in this particular field concerning the growth of synthesized nanoparticles and their continued use in the technological and industrial sectors [15].

14.2.1.1 Trichoderma Reesei

Detoxification of microclimates by fungi corresponds to the biosynthesis of nanoparticles, bioremediation of poisonous ions and biomining by human

beings. Among *Trichoderma* species, a well-known modern biotechnology agent, *Trichoderma reesei* is a decent decision for myco-synthesis of AgNPs. High stability, high carrier limit, probability of hydrophilic and hydrophobic substances fusing, adaptable detailing and controlled drug release in cancer treatment are just some of the benefits of metal nanoparticles-based medical applications. *Trichoderma*-delivered AgNPs have an antimicrobial and synergistic effect on antibacterial activity of ampicillin, kanamycin, erythromycin, and chloramphenicol against Gram-positive and Gram-negative microscopic organisms like bacteria. AgNPs have an antifungal effect through apoptosis and receptive oxygen species increments. Likewise, keeping the HIV-1 particles from attaching to host cells is another action of AgNPs [16].

14.2.1.2 Bacillus Subtilis

Bacillus subtilis EWP-46 cell-free extract was utilized for the reduction of nitrate ions to produce AgNPs. The generation of AgNPs was improved by a few factors, for example, hydrogen ion concentration, temperature, silver particle (Ag+ particle) and time. When conditions were maintained at pH 10.0, temperature 60 °C, 1.0 mM Ag^{+} particle and 720 min, more AgNPs synthesis was accomplished. UV-Vis spectroscopy demonstrated surface plasmon reverberation crest at 420 nm, and dispersive X-ray spectroscopy (SEM-EDX) spectra demonstrated the occurrence of pure silver structural components. Microscopy analysis revealed that synthesized nanoparticles are spherical with size of 10 to 20 nm, FTIR spectroscopy indicated the presence of functional group of silver ion, and XRD showed good crystallinity. SDS-PAGE (sodium dodecyl sulfate-polyacrylamide gel electrophoresis) was carried out to distinguish the proteins and their atomic mass in the decontaminated nitrate reductase from cell extract. What's more, the base inhibitory focus and least bactericidal convergence of AgNPs were examined against Gram-positive (*Staphylococcus aureus*) and Gram-negative (*Pseudomonas fluorescens*) bacteria [17].

14.2.1.3 Bacillus Licheniformis

Shanthi *et al.* synthesized probiotic *Bacillus licheniformis* cell-free extract (BLCFE) coated silver nanoparticles, denoted as BLCFE-AgNPs. The BLCFE-AgNPs were subjected to several analytical techniques. Morphological analysis results suggested an average particle size of 18–63 nm. The synthesized nanoparticles resulted in disintegrated biofilm formation of *Vibrio parahaemolyticus* DAV1 treated with BLCFE-AgNPs

compared to control. The above results confirmed that synthesized material has bioflim development capacity [18].

14.2.1.4 Anogeissus Latifolia

Gum ghatti (*Anogeissus latifolia*) is a protein-rich edible gum mostly found in Southeast Asia, which has been utilized in traditional Ayurvedic medicine and food ingredients for centuries in parts of the world. These gum extracts were utilized in a process to convert metal precursors to metal nanoparticles. Kora *et al.* synthesized size-controlled nanoparticles that will make them more compact and much easier to handle and control in several industrial applications. The monodispersed spherical size-controlled nanoparticles expected from this process were further verified by methods such as FTIR and Raman spectroscopy. They are also shown to have a much stronger antimicrobial impact on the Gram bacteria classes and have further applications for integration into various biological activities and applications, owing to the encapsulation of these AgNPs with functional group rich gum. Also, for a particular amount or concentration of the gum, the AgNPs efficiency does increase as the reaction time also increases for the nanoparticle. There are further investigations being conducted into the use of these so-called gum-based nanoparticles [19].

14.2.1.5 Aspergillus Flavus, Trichoderma Gamsii, Talaromyces Flavus and Aspergillus Oryzae

Anand *et al.* collected some marine sediment fungi (*Aspergillus flavus* SP-3, *Trichoderma gamsii* SP-4, *Talaromyces flavus* SP-5, and *Aspergillus oryzae* SP-6) from coastal regions in the southern peninsular region of India. All four filtrate fungal strains were treated with silver nitrate, which resulted in monodispersed AgNPs that were spherical in shape and had an average particle size of 20–60 nm. Further synthesized AgNPs were subjected to analysis for their antimicrobial properties; among the four strains, *T. gamsii* SP-4 resulted in high antimicrobial properties against both Gram-positive and Gram-negative bacterial strains. Furthermore, the fungal mediated synthesized AgNPs were subjected to cell line studies using HEp-2 cell lines, which resulted in LC_{50} estimation of 23 μg/mL [20].

14.2.1.6 Salmonella Typhirium

A study of a fast process of synthesizing AgNPs within 30 min was reported by Ghorbani using *Salmonella typhirium.* The synthesized AgNPs show

surface plasmon resonance at 415 nm, which confirms the formation of AgNPs. Further, the size of the synthesized AgNPs was measured using DLS and morphology was identified using TEM analysis [21].

14.2.1.7 Aspergillus Terreus

In their report, Li *et al.* synthesized AgNPs with the help of *Aspergillus terreus* filtrate. The synthesized AgNPs were subjected to various analytical techniques and the resultant particle size ranged from 1–20 nm. The authors reported that the fungal filtrate contains NADH, which acts as a secondary metabolite for the conversion of metal precursors to metal nanoparticles [22].

14.2.1.8 Spirogyra Varians

In a study by Salari *et al.*, AgNPs were orchestrated through bio-lessening of silver particles utilizing *Spirogyra varians*. The technique utilized is straightforward and manageable, making it appropriate for cost-efficient generation of AgNPs. The structure and morphology of AgNPs were described by various analytical techniques. These nanoparticles showed an assimilation crest at 430 nm in the UV-Vis range. The average crystallite size was evaluated at 17.6 nm and SEM images affirmed the union of generally uniform nanoparticles. The antibacterial impact of AgNPs was likewise tried on a few miniaturized scale life forms by measuring the hindrance zone, MIC and MBC. The outcomes affirmed that AgNPs can be used as an effective antibacterial agent against different pathogenic microbes [23].

14.2.1.9 Pestaloptiopsis Pauciseta

Nanoparticles can be synthesized by physical, compound and natural techniques. Various smaller scale life forms, such as microbes, parasites, yeasts and plants, either intra- or extracellular, which have higher generation yields at low cost have been observed. Fungi are perfect candidates in the preparation of metal nanoparticles, because of their capacity to emit a substantial amount of catalysts. This leads to the growth of *Pestaloptiopsis pauciseta*. In a study by Vardhana and Kathiravan, the combination of nanoparticles was observed to be between 123–195 nm. It has been shown that the endophytic fungus *P. pauciseta* is capable of delivering AgNPs extracellularly [24]. Further examinations in the field can prompt changes in the techniques used in medicine for the treatment of microbial contaminations.

14.2.2 Gold Nanoparticles (AuNPs) Synthesis by Microbial Medium

14.2.2.1 Actinobacter spp.

Improvement of synthesis techniques for anisotropic metal nanoparticles has been met with great enthusiasm due to their noteworthy optoelectronic properties. Different shapes ranging from bars to blocks to tetrapods and crystals might be obtained by combining techniques. Bharde *et al.* demonstrated that anisotropic AuNPs can be synthesized biologically by the bacterium *Actinobacter* spp. when tested with gold chloride in the presence of bovine serum albumin (BSA). It was also noted that synthesized AuNPs occur concurrently with the induction of the protease enzyme emitted by the bacterium in the presence of BSA. The presence of BSA increases the rate of AuNP biosynthesis and may also grant some shape control. Controlling basic test conditions, like incubation temperature and presence or absence of oxygen, have a strong effect on the reaction rate and morphology of the particles. Different test results demonstrate that the presence of chemical protease can act to decrease and also shape the coordinating agent [25].

14.2.2.2 Bacillus Marisflavi

The advancement of an eco-friendly method for the synthesis of nanomaterials is a vital part of nanotechnology exploration. A report by Nadaf and Kanase presents a greener methodology for the extracellular synthesis of AuNPs utilizing *Bacillus marisflavi* YCIS MN 5, in which addition of gold chloride solution into a cell-free extricate (CFE) of *B. marisflavi* brought about the their synthesis at room temperature inside 96 h. The combined nanoparticles were observed to be crystalline spheres with an average size in the range ~14 nm. The CFE acted as both reducing and stabilizing agent; subsequently, no additional capping and stabilizing agent were required. These AuNPs were evaluated for reduction of Congo red and methylene blue dyes. It was established that the reduction reaction follows pseudo-first-order kinetics with a reaction rate constant of 0.2192 and 0.2484 min^{-1} for Congo red and methylene blue, individually. In this manner, the synthesized AuNPs were found to have remarkable synergistic action in the degradation of Congo red and methylene blue. These outcomes suggest that *B. marisflavi* mediated synthesized gold nanoparticles as promising nanocatalysts for the degradation of Congo red and methylene blue dyes [26].

14.2.2.3 Pseudomonas Veronii AS41G

With the advent of nanotechnology, biogenic synthesis of nanoparticles has garnered much attention as an eco-friendly process. A study by Baker and Satish reported extracellular synthesis of AuNPs utilizing cell free supernatant of *Pseudomonas veronii* AS 41G, a novel endophyte isolated from *Annona squamosa* L. Formation of gold nanoparticles was confirmed with UV–visible spectrophotometry. FTIR analysis predicted different functional groups in charge of reduction of metal salts and stabilization of AuNPs. Nanoparticles were crystalline in nature, as shown in XRD pattern. TEM analysis uncovered morphological attributes of nanoparticles with various sizes. Baker and Satish subscribe to this easy process for the synthesis of AuNPs as an option to conventional methods, highlighting the new role of novel bacterium *Pseudomonas veronii* AS41G [27].

14.2.2.4 Plectonema Boryanum

In this report, Lengke *et al.* utilized a filamentous cyanobacterium, *Plectonema boryanum* UTEX 485, for synthesis of AuNPs. Results inferred that synthesized nanoparticles were cubic in shape with average size of 100 nm [28].

14.2.3 Zinc Oxide Nanoparticles (ZnO NPs) Synthesis Using Various Microbes

14.2.3.1 Aeromonas Hydrophila

Jayaseelan *et al.* synthesized ZnO NPs using reproducible bacteria *Aeromonas hydrophila* as an eco-friendly reducing and capping agent. The synthesized ZnO NPs were in spherical form with average particle size of 58 nm. The synthesized ZnO NPs were also subjected to antibacterial studies against various pathogens [29].

14.2.3.2 Alternaria Alternata

Alternaria alternata culture filtrate mediated synthesis of ZnO NPs was reported for the first time, which resulted in reduction of zinc sulfate to ZnO NPs. The obtained ZnO NPs had average particle size of 75 ± 5 nm. Also, the microorganisms mediated ZnO NPs were utilized to perform genotoxicity and cytotoxicity assays [30].

14.2.3.3 Aspergillus Fumigatus

In their study, Rai *et al.* reported that the syntheses of ZnO NPs were done using *Aspergillus fumigatus*. The synthesized ZnO NPs were said to be an average size of 7 nm with spherical shape. Moreover, the biosynthesized ZnO NPs utilized to increase plant biomass were successfully achieved [31].

14.2.3.4 Rhodococcus Pyridinivorans

Kundu *et al.* synthesized ZnO NPs at room temperature with the help of *Rhodococcus pyridinivorans* NT2. Furthermore, the synthesized ZnO NPs were subjected to various analytical techniques, which resulted in hexagonal phase, spherical shape nanoparticles with average particle size ranging from 100–200 nm. Then the microorganisms mediated ZnO NPs were tested against cancer cell lines to study antimicrobial activity [32].

14.2.3.5 Lactobacillus Plantarum

In their reported study, Selvarajan and Mohanasrinivasan synthesized ZnO NPs using probiotic bacteria *Lactobacillus plantarum* VITES07, which had hexagonal phase and average particle size of 7–19 nm with moderate stability [33].

14.2.3.6 Sargassum Muticum

In their reported study, Azizi *et al.* utilized a one-pot process for synthesis of ZnO NPs using *Sargassum muticum* aqueous extract. The synthesized ZnO NPs had hexagonal phase of wurtzite shape nanoparticles with average size of 30–57 nm [34].

14.2.3.7 Serratia Ureilytica

Dhandapani *et al.* synthesized ZnO NPs using ureolytic bacterial species *Serratia ureilytica*. The synthesized ZnO NPs were also subjected to various characterization techniques, which resulted in spherical- to nanoflower-shaped nanoparticles obtained with increasing time duration from 30 to 90 min. The synthesized ZnO NPs were further subjected to antimicrobial studies against toxic pathogens like *Escherichia coli* and *Staphylococcus aureus* [35].

14.2.4 Copper Nanoparticles (CuNPs) Synthesis Using Microorganisms

14.2.4.1 Kocuria Flava

Kaur *et al.* synthesized CuNPs using M-7 bacterial strain isolated from the Kanyakumari coast of India. Based on phylogenetic relationship, the strain was identified as *Kocuria flava*. Furthermore, with the help of *Kocuria flava*, CuNPs were synthesized and confirmed by using various analytical techniques which resulted in spherical-shaped nanoparticles with average particle size of 5–30 nm [36].

14.2.4.2 Pseudomonas Fluorescens

This report stated the biological synthesis of Cu NPs using non-pathogenic *Pseudomonas fluorescens*. Further the synthesized Cu NPs were subjected to various characterization techniques which resulted in average particle size around 49 nm with hexagonal and spherical shape were studied [37].

14.2.4.3 Morganella sp.

In a reported study, Shobha *et al.* utilized silver-resistant bacterium *Morganella* sp. for the synthesis of CuNPs, and also stated that the structural property of both Cu and Ag are very similar. Moreover, the synthesized CuNPs were subjected to analytical techniques, in which synthesized CuNPs in the range of 3–10 nm with irregular spherical shape were confirmed [38].

14.3 Biological Approach Using Plant Sources as Medium

14.3.1 Silver Nanoparticles (AgNPs) Synthesis by Plant Sources

14.3.1.1 Terminalia Chebula

Because of growing worldwide conflicts, there is a rising need to grow ecologically benign nanoparticles without the utilization of lethal chemicals. The bio-amalgamation of AgNPs utilizing *Terminalia chebula* (TC) leaf extract has become one of the areas of interest with the most potential. The bioreduction of metal particles is very fast and is readily performed at room temperature. Espenti *et al.* presented a quick and eco-friendly

amalgamation of TC-AgNPs utilizing TC leaf extract as part of a single-pot process, in which it was observed that the medium changes to a brown color with the addition of AgNPs. The obtained results were confirmed and the recorded UV spectra demonstrate the characteristic surface plasmon resonance band for TC-AgNPs in the range of 400–440 nm. The antibacterial activity of bio-orchestrated TC-AgNPs indicates effective inhibition against human pathogens, including *Bacillus subtilis* and *Escherichia coli*. The noteworthy results of this study will help formulate homegrown-based nanomaterials in biomedical and nanotechnology ventures [39].

14.3.1.2 Tinospora Cordifolia

A study by Selvam *et al.* reported an eco-friendly process for AgNPs synthesis utilizing *Tinospora cordifolia* as a reducing and capping agent. Diverse factors, such as silver nitrate ($AgNO_3$) concentration, fresh weight of *T. cordifolia* leaf (Table 14.2), incubation time, and pH influencing silver reduction were examined using response surface system-based Box-Behnken (BBD). The ideal conditions were $AgNO_3$ (1.25 mM), incubation time (15 h), temperature (45 °C) and pH (4.5). *T. cordifolia* leaf extract can reduce silver particles to AgNPs inside 30 min in the wake of heating the response blend (60 °C), as demonstrated by the created dark brownish color. The UV-Vis spectra of AgNPs recorded an increase in 430 nm centered strong resonance bands. AgNPs analyzed by X-ray diffraction (XRD) recorded their crystalline nature and an average nanoparticle size of 30 nm, as determined by Scherrer's equation. Fourier transform infrared (FTIR) spectroscopy affirmed the role of *T. cordifolia* leaf extract as a reducing and capping agent of silver particles. Application of scanning electron microscopy with energy-dispersive X-ray spectroscopy (SEM-EDS) showed spherical shape, confirming the presence of elemental silver. The synthesized AgNPs were discovered to have higher antioxidant activity than plant extract by dot plot assay. What's more, antibacterial action against *Staphylococcus* sp. (NCBI-Accession: KC688883.1) and *Klebsiella* sp. (NCBI-Accession: KF649832.1) demonstrated maximum zone of inhibition of 13 mm and 12.3 mm respectively, at 10 μg/mL of AgNPs. Based on the outcomes of the study, it was found that the synthesized AgNPs demonstrated higher antioxidant and antibacterial activity than the plant extract, and therefore could be used to produce biomedical items [40].

14.3.1.3 Tamarix Gallica

In an investigation by López-Miranda *et al.*, AgNPs with a size ranging from 5–40 nm have been quickly biosynthesized by *Tamarix gallica* plant

Table 14.2 Plant mediated synthesis of metal/metal oxide nanoparticles.

S. no	Plant origin	NPs	Size(nm)	Morphology	Ref.
1	*Tinospora cordifolia*	Ag	30	Crystalline	[46]
2	*Tamarix gallica*	Ag	5–40	Circular	[41]
3	*Tragia involucrata*	Ag	440–450	Cubic, Round, Hexagonal	[43]
4	*Geranium Leaf*	Ag	16–40	Spherical	[45]
5	*Cassia tora*	Ag	425	Circular, and hexagonal	[47]
6	Silk sericin	Ag	48–117	Spherical	[99]
7	*Macrococcus bovicus*	Ag	25–50	Circular	[50]
8	*Coleus aromaticus*	Ag	460	Spherical	[51]
9	*Heliotropium crispum*	Ag	428	Circular	[48]
10	*Jacaranda mimosifolia*	ZnO	2–4	Circular	[55]
11	*Plectranthus amboinicus*	ZnO	88	Rod	[56]
12	*Azadirachta indica*	ZnO	10–25	Circular	[57]
13	*Galaxaura elongata*	Au	3.85–77.13	Spherical, Rod, Triangular, Hexagonal	[64]
14	*Capsicum annuum*	Au	6–37	Triangle, Hexagonal,	[65]
15	*Magnolia kobus*	Au	5–300	Spherical	[70]
16	*Cassia Auriculata*	Au	20–30	Crystalline	[66]

extract. The biosynthesis process of spherical AgNPs showed a high rate of bioreduction. UV-Vis spectroscopy demonstrated a SPR band situated at 426.7 nm. The antibacterial activity against *Escherichia coli* of AgNPs synthesized with *Tamarix gallica* extract was affirmed [41].

14.3.1.4 Vitex Negundo

In a reported study by Zargar *et al.*, AgNPs were synthesized using water extract of *Vitex negundo* L., which simultaneously acted as reductant and stabilizer agents. The formations of Ag/*V. negundo* were determined by UV-Vis peak at 423 nm. The XRD analysis showed crystalline cubic structure. TEM images showed well-dispersed AgNPs with average particle size under 20 nm. The FTIR spectrum showed the presence of *V. negundo* in capping with AgNPs [42].

14.3.1.5 Tragia Involucrata, Cymbopogon Citronella, Solanum Verbascifolium and Tylophora Ovata

Development of an ecological and biogenic experimental procedure for synthesis of nanoparticles is becoming a critical branch of nanotechnology. As a critical metal, AgNPs have various applications in medical science. Since these AgNPs have been utilized for infection prevention in medical studies, it might be more significant to decrease their size by utilizing ancient homegrown herbal plants of India. A green, fast biogenic synthesis of silver nanoparticles utilizing *Tragia involucrata*, *Cymbopogon citronella*, *Solanum verbascifolium* and *Tylophora ovata* aqueous extracts was studied by Prabu and Johnson [43]. The nanoparticle pathway was developed via reduction of $AgNO_3$ by leaf extracts, which act as both reducing and capping agents. The formation of the AgNPs was seen within 15 min. The properties of the formed nanoparticles were described by visual examination (color change), UV absorption, FTIR spectroscopy and XRD. There was an intense surface plasmon resonance band at ~454 nm, ~452 nm, ~458 nm and ~447 nm in the UV-Vis spectrum. The FTIR spectrum affirms the presence of different functional groups of biomolecules capping the nanoparticles. XRD analysis revealed a high degree of crystallinity and monophasic Ag nanoparticles of face-centered cubic structure. The morphology of the formed particles consisted of different shapes, e.g., rod, flower-like, spherical and hexagonal. There is an ever-expanding demand for biosynthesis of nanoparticles due to increased interest in producing secure, cost-effective and eco-friendly technologies for the synthesis of nanomaterials [43].

14.3.1.6 Myrmecodia Pendans

Biosynthesis of AgNPs from silver nitrate solution utilizing water extract of *Myrmecodia pendans* (Sarang Semut plant) at room temperature was successfully performed. A visible change was seen in the reaction solution from colorless to dark brown after *M. pendans* water extract was added, demonstrating the development of the AgNPs. The obtained AgNPs were characterized by various analytical techniques. Typical surface plasmon resonance of the AgNPs was obtained, which was centered at around 448 nm. The structural phase of the AgNPs was found to be face-centered cubic (fcc) and the particle size was assessed to be in the range of 10–20 nm. At room temperature, biosynthesis of AgNPs utilizing water extract of *M. pendans* was successfully done through a straightforward, quick and eco-friendly process. The addition of the water extract changed the color of the reaction solution, demonstrating the successful formation of AgNPs. Water-soluble flavonoids in the water extract were responsible for the reduction of Ag^{+} to Ag^{0} nanoparticles. The structural phase of the AgNPs was assessed to be in the range of 10–20 nm [44].

14.3.1.7 Pelargonium Graveolens (Geranium)

In this reported study, Shankar *et al.* utilized Geranium (*Pelargonium graveolens*) leaf extract in the synthesis of AgNPs. The synthesized AgNPs had an average particle size of 16–40 nm and were spherical in shape [45].

14.3.1.8 Phoenix Dactylifera

In a reported study, Rashid *et al.* synthesized AgNPs from the extract of *Phoenix dactylifera* leaves and tested its potency against *E. coli* and *K. pneumoniae*. The morphological characteristics (size and shape) of their biogenic AgNPs were affirmed by scanning electron microscopy and X-ray diffraction analyses. Development active studies for *E. coli* and *K. pneumoniae* were performed in the presence of different concentrations of AgNPs (0, 8, 16, 32 and 64 μg mL^{-1}). Potency of 100% was achieved for *E. coli* (3.6×107 cfu mL^{-1}) and *K. pneumoniae* (3.2×107 cfu mL^{-1}) at the end of 3 h, whereas the minimum inhibitory concentration (MIC) against the former and latter bacteria was 8 and 16 μg mL^{-1} respectively. Surface morphological analysis of the dead bacteria demonstrated that AgNPs ruptured the cell membrane, which led to bacterial death. Subsequently, the discoveries of Rashid *et al.* affirm that AgNPs created from *P. dactylifera* leaves serve as a quick-acting, potent antibacterial agent. This practical and

cost-effective synthesis technique makes it a potential contender in pharmaceutical products and therapeutic devices [46].

14.3.1.9 Cassia Tora

Saravanakumar *et al.* utilized *Cassia tora* leaf extract for the synthesis of AgNPs at room temperature. The synthesized AgNPs had spherical, hexagonal and irregular shaped particles with 43 nm size. The antioxidant property of synthesized AgNPs was also tested in DPPH radical scavenging assay, and showed a higher percentage of inhibition in a concentration-dependent manner. Moreover, synthesized AgNPs were tested for their potential antibacterial activity against *Escherichia coli, Pseudomonas aeruginosa, Staphylococcus aureus* and *Bacillus subtilis*. The results showed that AuNPs exhibited higher antibacterial activity against *E. coli.* [47].

14.3.1.10 Allium Cepa (Onion)

An amazing strategy for one-pot biosynthesis of AgNPs utilizing onion extract as reductant and stabilizing agent. UV-Vis spectroscopy showed that the AgNPs absorption band was situated at a peak of 397 nm in aqueous solution. Both XRD and TEM affirm that the AgNPs were for the most part spherical with average diameters of of 6.0 nm by TEM and around 5.3–10.2 nm when calculated using XRD data. The ability of AgNPs to reduce charge transfer resistance was likewise examined utilizing electrochemical impedance spectroscopy. Lastly, the impact of synthesized NPs on ascorbic acid signal was investigated by square wave voltammetry. The peak current of square wave voltammograms of ascorbic acid increased linearly with concentration in the range of 0.4–450.0 μM; the detection limit for ascorbic acid was 0.1 μM [48].

14.3.1.11 Phyllanthus Amarus

Metal nanostructures have extraordinary physicochemical properties and organic activity in contrast to their mass bulk materials. Due to this, as of late, various physical, chemical and biological methods are being used for the advancement of metal nanoparticles (NPs). The Phyllanthus amarus plant has a place in the *Phyllanthaceae* family and the extracts of this herb have promising restorative properties for an extensive variety of human illnesses. Suspensions of Au and Ag nanoparticles resulted in the most extreme UV-Vis absorbance at 420 and 580 nm and XRD data showed characteristic diffraction examples of the essential stages.

Molecule size was resolved utilizing AFM (atomic force microscopy) and particle size analyzer, and was evaluated from the peak profiles. The FTIR spectra of the leaf extract before and after the synthesis of nanoparticles were resolved to permit identification of conceivable functional groups in charge of the bioconversion of metal particles to metal nanoparticles [49].

14.3.1.12 Terminalia Cuneata

Aqueous extract of *Terminalia cuneata* was utilized for the synthesis of AgNPs. Various parameters, like pH, time and effect of concentration, were studied using UV-Vis spectroscopy. Furthermore, the synthesized AgNPs were subjected to several analytical techniques to study their characteristics. The sizes of synthesized AgNPs were in the range of 25–50 nm. Also, the catalytic activity of AgNPs on the reduction of direct yellow-12 using NaBH4 was analyzed [50].

14.3.1.13 Coleus Aromaticus

In this report, Vanaja *et al.* synthesized AgNPs by using *Coleus aromaticus* leaf extract by bioreduction process. The synthesized AgNPs resulted in polydispersity of spherically shaped particles and leads to aggregation [51].

14.3.1.14 Argyreia Nervosa

A simple method for synthesis of biologically stable AgNPs was formulated using *Argyreia nervosa* seed extract. The nanoparticles formed using *A. nervosa* were distinguished by UV spectrophotometry, X-Ray diffraction, SEM-EDS, etc. The antibacterial and antifungal activity of AgNPs was analyzed against *Staphylococcus aureus, Bacillus subtilis, Aspergillus niger* and *Escherichia coli*. The synthesized AgNPs displayed strong antibacterial activity against Gram-negative bacteria and fungi, which has a lot of potential applications in medical and pharmaceutical fields [52].

14.3.1.15 Aloe Vera

There is burgeoning interest in AgNPs produced by various chemical reactions for use in applications due to their antibacterial effects, even though these processes exhibit a broad range of toxicity in both vertebrates and invertebrates alike. To avoid this, biosynthesis (green synthesis) of

metal nanoparticles is proposed as a cost-efficient and eco-friendly alternative. *Aloe vera* leaf extract is an effective agent with multiple medicinal properties such as the above-mentioned antibacterial effect. Moreover, the constituents of *A. vera* leaves include lignin, hemicellulose and pectins, which are used as reducing agents of silver ions to produce AgNPs with antibacterial activity [53].

14.3.1.16 Catuneregum Spinosa

Our research group synthesized AgNPs by using *Catuneregum spinosa* root bark as a green source. Here the synthesized AgNPs were in agglomerated spherical shaped particles which were 33 nm in size. Furthermore, the synthesized AgNPs were also studied by subjecting them to testing against toxic dye degradation [54].

14.3.2 Zinc Oxide Nanoparticles (ZnO NPs) Synthesis Using Green Sources

14.3.2.1 Jacaranda Mimosifolia

In a reported study, Sharma *et al.* synthesized ZnO NPs using waste material of fallen *Jacaranda mimosifolia* flowers. The resultant ZnO NPs were spherical in shape with average particle size of 2–4 nm. The synthesized ZnO NPs were subjected to antibacterial studies of both Gram-positive and Gram-negative bacteria. The results showed that the synthesized nanoparticles were more active against Gram-negative bacteria [55].

14.3.2.2 Plectranthus Amboinicus

A study by Fu and Fu shows the synthesis of ZnO NPs utilizing leaf concentrates of *Plectranthus amboinicus*. The incorporated ZnO NPs were described by UV-Vis spectroscopy, SEM, EDX, XRD, FTIR and photoluminescence spectroscopy. The SEM study revealed that the biosynthesized ZnO NPs have a rod-shaped structure with a normal size of 88 nm. UV-Vis diffuse reflectance spectroscopic study showed that the band hole of biosynthesized ZnO NPs is 3.07 eV. Photocatalytic property of the ZnO NPs was researched by photodegradation of methyl red (MR) under UV illumination. The photocatalytic performance of biosynthesized ZnO NPs was compared with hydrothermally synthesized ZnO NPs and P25. The results demonstrate that the biosynthesized ZnO NPs have superior photocatalytic activity towards degradation of MR [56].

14.3.2.3 Azadirachta Indica

ZnO NPs were synthesized using 25% (w/v) of *Azadirachta indica* leaf extract. The synthesized ZnO NPs were subjected to various characterization techniques to identify their nature and morphology. The resultant synthesized particles were 9.6–25.5 nm in size with spherical shape. The antibacterial activity of ZnO NPs was determined using shake flask technique, with the obtained results revealing that bacterial growth decreases with increase in concentration of biosynthesized ZnO NPs. The biosynthesized ZnO NPs also showed photocatalytic activity for enhancing the degradation of methylene blue [57].

14.3.2.4 Trifolium Pratense

Dobrucka and Długaszewska synthesized ZnO NPs using *Trifolium pratense* flower extract in an ecofriendly manner. The synthesized ZnO NPs size ranged from 100–190 nm with spherically shaped agglomerated particles. Further, it was tested against various pathogenic bacteria [58].

14.3.2.5 Pongamia Pinnata

In this study, Sundrarajan *et al.* synthesized ZnO NPs using *Pongamia pinnata* which were spherical shape with 26 nm size. Green synthesized ZnO NPs act as good bactericidal agents against several pathogens like Gram-positive and Gram-negative bacteria [59].

14.3.2.6 Laurus Nobilis

Vijayakumar *et al.* synthesized ZnO NPs using leaf extract of *Laurus nobilis* by green synthesis methods. The synthesized ZnO NPs were 47 nm in size with flower-like wurtzite structure. Then the green synthesized ZnO NPs were tested against various pathogens using an antimicrobial assay, which showed that the ZnO NPs can also act as antimicrobial agents [60].

14.3.2.7 Vitex Trifolia

In this report, Elumalai *et al.* synthesized eco-friendly ZnO NPs by secondary metabolites extracted from *Vitex trifolia* leaf. The authors identified the secondary metabolites present in the extract using gas chromatography and mass spectroscopy. They identified Vitrifolin A with higher area percentage of 22% compared to other secondary metabolites.

This Vitrifolin A will act as a reducing/stabilizing agent for the formation of ZnO NPs. The synthesized ZnO NPs were studied using various analytical techniques which resulted in particles that were 30 nm size of spherical shape [61].

14.3.2.8 Euphorbia Jatropa

The green synthesis method was used to achieve ZnO NPs using *Euphorbia jatropa* latex. The synthesized ZnO NPs were subjected to various characterization techniques, which led to average particle size of 15 nm with spherical shape.

14.3.2.9 Moringa Oleifera

Our research group synthesized ZnO NPs by using *Moringa oleifera* peel and utilized them in various applicational studies such as antifungal, hemolytic and antibacterial studies. The synthesized ZnO NPs were subjected to various analytical techniques, which inferred that the green synthesized ZnO NPs were spherical shape with average particle size of 40–45 nm [62].

14.3.2.10 Carrisa Edulis

Our research group also synthesized ZnO NPs using *Carissa edulis* methanol extract by microwave extraction method at 400 W and 70 °C. The synthesized ZnO NPs were utilized for degradation of toxic azo dye Congo red. The synthesized ZnO NPs were flower shape with average particle size of 40–45 nm with good stability were studied and reported [63].

14.3.3 Gold Nanoparticles (AuNPs) Synthesis Using Plant Sources

14.3.3.1 Galaxaura Elongata

The synthesis of gold nanoparticles (Au) using *Galaxaura elongata* (powder or extract) was demonstrated by Abdel-Raouf *et al.* Rapid formation of stable Au nanoparticles under normal atmospheric conditions has been achieved using *G. elongata* extract in aqueous medium. Transmission electron microscopy (TEM) determined the shapes of AuNPs, i.e., spherical in shape along with a few rod, triangular, truncated triangular and hexagonal shaped nanoparticles. The sizes of AuNPs were found to be in the

range of 3.85–77.13 nm, which were found by zeta potential measurements. FTIR spectroscopy revealed that the nanoparticle was embedded with algal compounds. The chemical constituents of the algal extract, viz., andrographolide, alloaromadendrene oxide, glutamic acid, hexadecanoic acid, oleic acid, 11-eicosenoic acid, stearic acid, gallic acid, epigallocatechin catechin and epicatechin gallate, were identified. These chemicals may act as reducing, stabilizing and capping agent. This study also evaluates the antimicrobial activities of Au nanoparticles. The nanoparticles synthesized from powder of *G. elongata* were found to be highly effective against *E. coli* and *K. pneumoniae* (13.5 and 13 mm), respectively; whereas the free ethanolic extract of *G. elongata* exhibits high activity only against MRSA (14 mm) [64].

14.3.3.2 Capsicum Annuum

The biological synthesis approach is viewed as a green, eco-friendly and cost-effective strategy for preparing nanoparticles without any lethal solvents and perilous by-products. Yuan *et al.* reported a simple and quick biosynthesis strategy for AuNPs from *Capsicum annuum* var. *grossum* pulp extract in a one-pot process. Aqueous pulp extract was utilized as biotic reducing agent for developing gold nanoparticles. Different shapes (triangular, hexagonal, and quasi-spherical shapes) were seen within the range of 6–37 nm. The UV-Vis spectra indicated surface plasmon resonance (SPR) peak for the formed AuNPs at 560 nm after 10 min incubation at room temperature. The conceivable impact of extract amounts, AuNPs concentration, incubation time, reaction temperature and solution pH was assessed to obtain the optimized conditions for synthesis. The impact of the test factors on the AuNPs synthesis process was likewise examined. The outcomes of their study showed that the AuNPs were well dispersed and stable with good catalytic activity; and also that biomolecules in the aqueous extract were responsible for the capping and stabilization of AuNPS [65].

14.3.3.3 Cassia Auriculata

In a study by Tharishini P *et al.,* AuNPs was prepared in an eco-friendly manner by means of aqueous *Cassia auriculata* leaf extract, which acted as stabilizing and reducing agent. Analysis of the AuNPs showed that a SPR peak was obtained at 530 nm; and HRTEM results showed spherical shaped nanoparticles in the size range of 20–30 nm. The elemental composition and purity of the AuNPs were analyzed by EDAX [66].

14.3.3.4 Euphorbia Hirta

Annamalai *et al.* synthesized eco-friendly, nontoxic AuNPs with the help of reducing agents from the leaf extract of *Euphorbia hirta*. The synthesized AuNPs ranged in size from 6–71 nm. The green synthesized AuNPs were subjected to various pathogens to study their antibacterial activity [49].

14.3.3.5 Olea Europaea (Olive)

In their study, Khalil *et al.* utilized olive leaf extract as a secondary metabolite for the preparation of AuNPs in an eco-friendly method. The AuNPs exhibited three different shapes, i.e., triangular, spherical and hexagonal, with an average crystallite size of 13 nm [67].

14.3.3.6 Solanum Tuberosum (Potato)

Castillo-López *et al.* utilized aqueous extract of the seed pod of *Solanum tuberosum* for synthesis of AuNPs. They reported agglomerated spherical particles with 18 nm size. Furthermore, the synthesized AuNPs were utilized for stability and various mechanisms of growth in plants [68].

14.3.3.7 Camellia Sinensis

Boruah *et al.* reported that eco-friendly processes of AuNPs were achieved with *Camellia sinensis* leaf. The formed AuNPs were found to be triangular and hexagonal in shape with 13 nm average particle size. Furthermore, the authors also tested various kinetic parameters to synthesize AuNPs [69].

14.3.3.8 Amomum Subulatum

In their study, Singh and Srivastava reported synthesized AuNPs by a one-step process using *Amomum subulatum* (black cardamom). Moreover, the AuNPs were studied by several characterization techniques which obtained average particle size of 30–35 nm with spherical shape cluster particles [70].

14.3.4 Copper Oxide Nanoparticles (CuO NPs) Synthesis Using Plant Sources

14.3.4.1 Punica Granatum

In a study by Ghidan *et al.,* CuO NPs were synthesized by a straightforward and green technique using *Punica granatum* peel extract at room

temperature. Biosynthesized CuO NPs were characterized by FTIR, SEM and XRD. The particles were crystalline in nature with average size 40 nm. The shape of the CuO NPs was controlled by the concentration of *P. granatum* peel aqueous solution and copper particles. This study also determined the mortality efficacy of the synthesized CuO NPs against green peach aphid [71].

14.3.4.2 Thymus Vulgaris

A reported study by Nasrollahzadeh *et al.* deals with the ecofriendly synthesis of CuO NPs using *Thymus vulgaris* aqueous extract. The synthesized CuO NPs were spherical shape and 30 nm in size. Moreover, the eco-friendly synthesized CuO NPs were studied for several catalytic activities [72].

14.3.4.3 Tecoma Castanifolia

A reported study by Govindasamy *et al.* deals with the eco-friendly synthesis of CuO NPs using *Tecoma castanifolia* leaf extract. The synthesized CuO NPs were characterized by various techniques, which showed spherical shape with size less than 100 nm. Furthermore, the green synthesized CuO NPs have effective optical and antibacterial properties [73].

14.3.4.4 Matricaria Chamomilla

Duman *et al.* utilized the medicinal plant *Matricaria chamomilla* as a reducing/capping material to synthesize CuO NPs. The synthesized CuO NPs were investigated by various analytical techniques, which resulted in monodispersed nanoparticles with 140 nm average particle size. Furthermore, the synthesized CuO NPs were tested for their antioxidant property [74].

14.3.5 Palladium Nanoparticles (PdNPs) Synthesis Using Plant Sources

14.3.5.1 Camellia Sinensis

In a study conducted by Lebaschi *et al.,* PdNPs were synthesized through an effortless and green process utilizing nontoxic renewable natural black tea leaves (*Camellia sinensis*) extract, as the reducing and stabilizing agent. The as-prepared Pd@B.tea catalyst was analyzed by UV-Vis spectroscopy,

FTIR, XRD, SEM, EDS and TEM. The Pd@B.tea catalyst was utilized for efficient and heterogeneous Suzuki coupling reactions between phenylboronic acid and a range of aryl halides (X=I, Br, Cl); and also for the reduction of 4-nitrophenol (4-NP) using sodium borohydride in an eco-friendly medium. Excellent yields of products were acquired with an wide range of substrates. The catalyst was reused seven times without any noteworthy loss of its catalytic activity [75].

14.3.5.2 Catharanthus Roseus

Kalaiselvi *et al.* utilized *Catharanthus roseus* leaf extract to prepare PdNPs. The PdNPs were spherical shape with 48 nm size. Moreover, the authors revealed that the phytochemical, 4-methylmyoinositol, is involved in the reduction of metal salt to metal nanoparticles. The synthesized PdNPs are suggested to have catalytic properties against phenol red, which reportedly results in better degradation [76].

14.3.5.3 Euphorbia Thymifolia

Nasrollahzadeh and Sajadi synthesized PdNPs using aqueous leaf extract of *Euphorbia thymifolia* at room temperature. The PdNPs have agglomerated spherical shape of 30 nm size, which can especially be used as a catalyst in several organic applications [77].

14.3.5.4 Salvia Hydrangea

Khodadadi *et al.* were the first to report on the use of *Salvia hydrangea* plant extract to synthesize PdNPs. The PdNPs, which were supported on Apricot kernel shell, showed excellent catalytic activity in the reduction of toxic dyes. In this study, the degradation efficiency of PdNPs/Apricot kernel shell catalyst against 4-nitrophenol, Rhodamine B, Congo red and methylene blue was assessed [78].

14.3.5.5 Cocos Nucifera

Our research group focused on the synthesis of PdNPs without any harmful effects to the environment. So, we chose the agricultural waste *Cocos nucifera* coir for synthesis of PdNPs using a one-step process. The PdNPs were utilized for many characterization methods and results inferred that they had spherical shape particles with average size 62 nm. We also studied the synthesized PdNPs for applications like larvicidal, ovicidal and toxicity testing [79].

14.3.5.6 Phyllanthus Emblica

A member of our research group utilized *Phyllanthus emblica* methanolic seed extract to prepare PdNPs. The obtained PdNPs were spherical shape with average particle size of 28 nm. The synthesized PdNPs were also subjected to various application studies to assess their antibacterial, hemolytic and cytotoxic activities, among others [80].

14.3.5.7 Annona Squamosa

Our research group initiated the synthesis of PdNPs using a plant source. We used aqueous extract of *Annona squamosa* peel to synthesize PdNPs which have average particle size of 85 nm and spherical shape. These eco-friendly synthesized PdNPs were utilized for various reported application studies [81].

14.3.6 Tin Oxide Nanoparticles (SnO_2 NPs) Synthesis Using Plant Sources

14.3.6.1 Cyphomandra Betacea

The eco-friendly preparation of SnO_2 NPs using the methanolic extract of *Cyphomandra betacea* was reported by Elango and Roopan. The authors synthesized SnO_2 NPs by a simple and effortless approach, which were further subjected to various characterization testing. The obtained results showed that the particles are rod shape with 21 nm size. The prepared SnO_2 NPs were also used to study the catalytic degradation of methylene blue, which resulted in 75% degradation within 70 min [82].

14.3.6.2 Persia Americana

Elango *et al.* synthesized SnO_2 NPs with the methanolic extract of *Persia americana* seed, an agricultural waste. The synthesized SnO_2 NPs were said to be agglomerated particles of 4 nm size, which is a smaller size compared to SnO_2 NPs synthesized by other methods. The synthesized materials were also subjected to various application studies like UV-radiation degradation, where phenol red dye was placed under UV radiation (325 nm), resulting in better degradation activity by SnO_2 NPs catalyst [83].

14.3.6.3 Catunaregum Spinosa

In this study, Haritha *et al.* synthesized SnO_2 NPs of spherical shape with 49 nm size, which they used for degradation of diazo dye Congo red

with catalyst SnO_2 NPs. The synthesized particles exhibited better catalyst activity with 89% degradation. They identified the possible secondary metabolites (7-hydroxy-6-methoxy-2H-1benzopyran-2-one) utilized for reduction of material precursors to metal nanoparticles [84].

14.3.6.4 Aspalathus Linearis

Diallo *et al.* were the first to synthesize SnO_2 NPs using *Aspalathus linearis,* which resulted in 2–20 nm size, spherical shape agglomerated particles. The synthesized SnO_2 NPs were subjected to testing for photocatalytic applications [85].

14.3.6.5 Piper Nigrum

Tammina *et al.* utilized *Piper nigrum* seed extract for synthesis of SnO_2 NPs by various calcination temperatures like 300, 500 and 900 °C. The synthesized SnO_2 NPs had an average particle size of 5–10 nm with spherical shape, which were further utilized to treat cancer cell lines [86].

14.3.7 Nickel and Nickel Oxide Nanoparticles (Ni and NiO NPs) Using Various Plant Sources

14.3.7.1 Cocos Nucifera

Elango *et al.* utilized *Cocos nucifera* coir methanolic extract for the synthesis of NiNPs by green process. The NiNPs were subjected to various characterization tests, resulting in cubical shape with an average particle size of 47 nm. Furthermore, the synthesized NiNPs were subjected to *Aedes aegypti* and *Callasobruchus maculates* for its larvicidal and pesticidal applications, in which the extract reportedly plays a bigger role compared to extract mediated NiNPs [87].

14.3.7.2 Ocimum Sanctum

Pandian *et al.* synthesized NiNPs using *Ocimum sanctum* leaf extract which are used to degrade pollutants in the environment. The NiNPs are spherical shape with 12–36 nm size. the authors of this report discuss the effect of various parameters used in the synthesis of NiNPs [88].

14.3.7.3 Agathosma Betulina

In this report, Thema *et al.* synthesized single-phase bunsenite NiO NPs using *Agathosma betulina* plant extract for the preparation of metal NPs.

The synthesized NiO NPs was spherical shape agglomerated particles with 25–30 nm size [89].

14.3.7.4 Moringa Oleifera

Moringa oleifera plant extract was used in the eco-friendly synthesis of NiO NPs. The synthesized NiO NPs were subjected to many characterization techniques and resulted in particles with spherical agglomeration and 10 nm size. Furthermore, the study reported that the synthesized NiO NPs have cytotoxic activity against various pathogenic cell lines [90].

14.4 Applications

Nanoparticles have a vast range of applications, which are clearly illustrated in Figure 14.3 and described below.

14.4.1 Biomedical Application

Nowadays nanoparticles play a major role in various application fields. Among other nanoparticles, AgNPs play several roles in biomedical applications. However, the focus has been on their potential applications in cancer diagnosis and treatment. In their article, Zhang *et al.* talk about

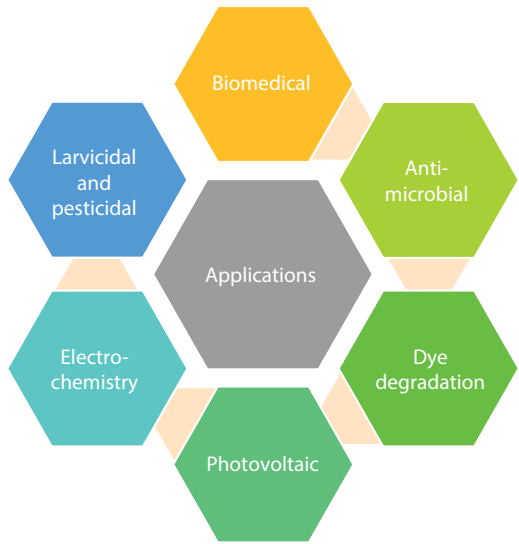


Figure 14.3 Various applications of nanoparticles.

the amalgamation of AgNPs utilizing physical, chemical and biological strategies. They also discuss the properties of AgNPs and techniques for their characterization. Along with having an important discussion of multifunctional bioapplications of AgNPs, they also talk about therapeutic approaches and the challenges associated with the use of AgNPs for cancer therapy. The article concludes with the future prospects of AgNPs [91].

Due to their fluorescence, AgNPs can be used for dose enhancement and detection purposes in X-ray irradiation applications. The characteristics of AgNPs can also be used in radiotherapy and radiodiagnostics. Nanoparticles from 5–20 nm in size were obtained using the method mentioned in the study by Mattea *et al.* [92], in which the fluorescence of aqueous suspensions of AgNPs was measured experimentally for different geometrical configurations and concentrations. The feasibility of using metal nanoparticles for the elaboration of Fricke gel dosimeters has been tested, obtaining a dose enhancement when compared with the same material irradiated below the silver K-edge [92].

Metallic nanoparticles are an emerging class of functional materials which have revolutionized the field of biomedical applications. Unlike metal NPs, AgNPs are one of the most comprehensively studied nanomaterials. The enhanced innovations of today and their implementation have ushered in a new period of technology called "the nano-revolution," in which parts of plant are used in the green synthesis of nanoparticles to synthesize stable and eco-friendly NPs. Utilizing plant extracts for synthesis of AgNPs has many advantages over other customary techniques such as the fact that they are easy to process, energy efficient, nonhazardous and environmentally benign; in addition to their having a wide range of biomolecules that can act as reducing and capping agents. There has been an upsurge in the use of biologically synthesized AgNPs in different areas of applications in various sectors such as electronics, clothing, food industry, paints, sunscreens, beauty products, biosensors, medications, drug delivery and medical devices. The expansive range of bioactivities of AgNPs shows their ability to solve numerous microbial resistance problems. The antibacterial, antifungal, antiviral, antiprotozoal, anti-inflammatory and anticancer activities of AgNPs have captured the imagination of researchers. In their review paper, Anjum *et al.* discuss plant mediated green synthesis of AgNPs and the mechanistic aspects involved in the reduction and stabilization of AgNPs. They present methods for the characterization of AgNPs, along with a wide range of the multifunctional activities of AgNPs and their potential biomedical applications. Their review also assesses the approaching human and environmental deathtraps connected with the

expanded use of AgNPs and safety issues concerning their biomedical applications [93, 94].

The last two decades have seen a dramatic increase in the number of studies which have led to the development of lab-on-a-chip (LOC) devices for nanomaterials. Thus, in their study, Krishna *et al.* have investigated these discoveries with a focus on the improvements that occurred later in this era. Also covered are the most recent developments of the decade. The authors have attempted to bring out the differences between chip-based as well as tubular continuous flow systems; and cover the various opportunities that tools from the field of computational fluid dynamics provide in designing LOC systems for synthesis of inorganic nanomaterials. Their study provides unique examples that demonstrate the need for a concerted effort to utilize LOC devices, not only for synthesis of inorganic nanomaterials, but also to carry out superior *in-vitro* studies, leading to faster clinical translation. Since LOC devices are likely to have a multi-step synthesis processes, it is amazing that such systems have not been used to carry out simultaneous synthesis of nanomaterials. The LOC devices are mainly based on microfluidic systems [95].

One of the most favored ways to ensure biocompatibility is fabrication of PEG coating on magnetite nanoparticles (MNPs). Illés *et al.* compared their own prepared comb-like PEG-polymer (PEGA-AA) with carboxy-PEG (PEG-C) and phosphate-PEG (PEG-P). The ATR FTIR data confirmed that all polymers formed complexes on the surface of MNPs. Dynamic light scattering (DLS) and electrophoresis experiments showed that the aggregation of coated nanomagnets was influenced by both the quantity and type of the polymers' anchoring groups. Magnetite particles became aggregated because PEG-C shell does not provide excess negative charges. PEGA-AA is more efficient for MNPs PEGylation because of uniform distribution of PEG chains and carboxylates along the carbon skeleton [96].

Cobalt ferrite was synthesized using oleic acid (OA) by hydrothermal technique. These nanoparticles are said to have superparamagnetic properties. The CFO nanoparticles coated with oleic acid are not well dispersible in water but are stable in nonpolar organic medium like hexane. The CFO nanoparticles were made more stable colloidal solution in water by modifying their surface using citric acid. The CFO nanoparticles which are coated with citric acid exhibit various properties like high zeta potential, moderate saturation magnetization, high dispersibility and very low coercivity. Munjal *et al.* used cytotoxicity testing in L929 cell line to demonstrate the biocompatibility of CFO nanoparticles [97, 98].

A one-step facile synthesis of glucose-derived polymers (GDP) coated magnetic nanoparticles (MNPs) through a hydrothermal

mechanochemical process has been reported. Magnetic nanoparticles (Fe_2O_3/Fe_3O_4) coated with polymer showed superparamagnetic behavior of AC magnetic field with sizes below 10 nm. Within 4–17 min, a temperature of 42 °C can be accomplished due to AC magnetic field intensity. Different functional groups are afforded by the surface polymerized layer, which makes the coated nanoparticles feasible for bioconjugation. It was pointed out with the help of *in-vitro* cytotoxicity evaluation that severe cell alteration is not caused by a relatively high concentration of magnetic nanoparticles coated with polymer, which suggests a good biocompatibility [96].

14.4.2 Antibacterial Properties

Because silver is considered one of the antimicrobial agents, silver nanoparticles (AgNPs) are used in silver-based wound dressings and for making silver-coated medical devices. The presence of silver also enhances the antibacterial activity of antibiotics. Silk can be affected by microorganisms due to its hygroscopic nature. Thus, impervious silk is utilized by antimicrobial specialists for treatments. AgNPs are a good antimicrobial agent compared to other metal nanoparticles. In their study, Rai *et al.* used BTCA as center material on silk sided with SHP sodium thio-phosphate. They used 3% SHP and 6% BTCA coated with AgNPs 250 ppm. The result indicates that the diversity of silk structure didn't change when it was impregnated with AgNPs. So, the authors reported that AgNPs can be utilized in antimicrobial wraps [99].

In a study by Aramwit *et al.*, a "green science" approach was used to synthesize silk sericin (SS)-capped AgNPs under alkaline conditions (pH 11), which used SS as a reducing and stabilizing agent rather than toxic chemicals. The SS-capped AgNPs were successfully synthesized at different concentrations of SS and $AgNO_3$. The SS-capped AgNPs showed a spherical shape with diameter at around 48–117 nm. Moreover, SS-capped AgNPs demonstrated strong antibacterial activity against different Gram-positive and Gram-negative microorganisms, with minimal inhibitory concentration (MIC) ranging from 0.001–0.004 mM. Consequently, the SS-capped AgNPs are considered safe candidates for antibacterial applications [100].

Macrococcus bovicus was locally isolated from soil and utilized to synthesize AgNPs. The antimicrobial activity of the AgNPs was applied against *Staphylococcus aureus, Escherichia coli* and *Candida albicans* using cup-plate and plate-count methods. The antimicrobial activity of the nano-scaling silver (NSAg)-modified clays was affirmed and ascribed to the caging of NSAg in montmorillonite (MMT) cavities. MMT3 was found

to increase microbial growth to as high as 65%, as observed from the plate count method [101].

A study by Lateef *et al.* reported the biogenic synthesis of AgNPs using pod extract of *Cola nitida*, an assessment of their antibacterial and cell reinforcement activity, and their application as antimicrobial additive in paint. UV-Vis spectroscopy, Fourier transform infrared (FTIR) spectroscopy, and transmission electron microscopy (TEM) were used to characterize the AgNPs. The AgNPs solution was dark brown with maximum absorbance occurring at 431.5 nm. The FTIR spectrum showed strong peaks at 3336.85, 2073.48 and 1639.49 cm^{-1}, indicating that proteins act as capping and stabilizing agents in the synthesis of AgNPs. The AgNPs were spherical, with sizes ranging from 12–80 nm. Energy dispersive X-ray (EDX) investigation showed that silver was the prominent metal present, while the selected area electron diffraction pattern conformed with the face-centered cubic phase and crystalline nature of AgNPs. At different concentrations between 50 and 150 μg/mL, the AgNPs had a strong inhibitory effect on the growth of multidrug-resistant strains of *Klebsiella granulomatis, Pseudomonas aeruginosa* and *Escherichia coli*. Also, at 5 μg/mL, the AgNPs completely inhibited the growth of *Staphylococcus aureus, E. coli, P. aeruginosa, Aspergillus niger, Aspergillus flavus* and *Aspergillus fumigatus* in a paint-AgNPs admixture. The AgNPs displayed potent antioxidant activity with an IC_{50} of 43.98 μg/ml against 2,2-diphenyl-1-picrylhydrazyl and a ferric ion reduction of 13.62–49.96% at concentrations of 20–100 μg/mL. The above study by Lateef and coworkers shows that biogenically synthesized AgNPs have potent antimicrobial and antioxidant activities for potential use in biomedical and industrial applications. To the best of our knowledge, their work was the first to utilize pod extract of *C. nitida* for the green synthesis of nanoparticles [102].

14.4.3 Dye Degradation

A majority of industries and research facilities directly affect the environment by releasing pollutants, such as some organic aromatics used to form dyes, pesticides and therapeutics, especially 4-nitro-phenol (4-NP), which is water-soluble and found in both soil and seawater, and hence could produce physio-chemical and biological changes in water quality that directly/indirectly affects human health. The textile industry in particular uses a large amount of methylene blue to color their products, which is a highly toxic dye that produces various diseases in man and animals. All of the techniques have several major drawbacks, such as insufficient dye elimination, expensive and high energy consumptions.

An effortless process for the green synthesis of AgNPs using aqueous bark extract of *Terminalia cuneata* was reported by Edison *et al.* [50]. UV-Vis spectroscopy showed appearance of yellow color with λmax around ~ 420 nm, which indicated the formation of AgNPs HRTEM analysis showed that the synthesized AgNPs were in the size range of 25–50 nm with an irregular spherical shape. The catalytic action of AgNPs on the reduction of direct yellow-12 using NaBH4 was analyzed using an UV-Vis spectrophotometer. This study demonstrated the efficiency of biogenic AgNPs in catalyzing the reduction of direct yellow-12 [103, 104].

14.4.4 Electrochemical Application

Microorganisms or microbes are tiny living things which are found all around us and include, for example, archaea, protozoa, fungi and algae. As of late, organisms have been investigated as novel precursors used to synthesize carbon-based nanomaterials and as substrates or frameworks to create carbon-containing nanocomposites. Being greener and more cost-efficient, metal-organic framework-derived carbons (MDCs) offer great potential for energy applications. MDCs have exceptionally favorable advantages. They can be used, for example, as anodes in supercapacitors and lithium-particle batteries, and as electrocatalysts for processes such as oxygen reduction, oxygen evolution, and hydrogen evolution reactions, which are crucial for power device and water electrolytic cells. Therefore, further exploration is needed that will potentially produce new types of MDCs [105, 106].

Electrostatically charging spherical and cylindrical conducting particles against an electrode with an applied electric field was investigated both theoretically and experimentally by Musinski *et al.* as a strategy to charge micro- and nano-NPs for use in high energy and high-speed applications, including NPs electrostatic space propulsion systems, materials processing and nanoprinting [107]. Increasing the NPs charge-to-mass ratios was critical for maximizing their velocities when accelerated with applied electric fields, which required minimizing the particles' sizes down to micro- and nano-meter ranges for some applications. An investigation by the authors revealed that the charge-to-mass ratio was maximized with low aspect ratio particles when the maximum electric field strength at the top of the particles was held constant. Experimental results of charging titanium and aluminum spherical and cylindrical particles were exhibited, which infers that under suitable conditions, the particles were charged as theoretically predicted. However, that electrical contact

resistance between the particles and electrode can impact the charging time. Finally, their investigation of the expected particle charging times showed a strong dependence on the conductivity and thickness of the oxide layer coating the particles [107].

Monometallic copper (Cu), palladium (Pd) and bimetallic $Pd_{98}Cu_2$, $Pd_{94}Cu_6$, $Pd_{86}Cu_{14}$ alloy nanoparticles (6–10 nm average diameter) were synthesized by a facile single-pot hydrothermal reduction with hydrazine solution at 75 °C in the absence of any special capping agent. Graphite supported bimetallic Pd/Cu alloy nanoparticles showed synergistic and enhanced electrocatalytic activity towards oxidation of methanol in alkali. In a study conducted by Chowdury *et al.*, maximum specific peak current of 987 mA mg^{-1} and equilibrium exchange current of 5×10^{-6} mA mg^{-1} of Pd was obtained for $Pd_{94}Cu_6$ alloy. Cyclic voltammograms of possible intermediates like formaldehyde and sodium formate and *ex-situ* FTIR spectroscopy and chromatographic studies of reaction products show Cu, rather than carbonate, is the plausible mechanism of the reactions [108].

14.5 Conclusion

Considering that nanoparticles are the new and emerging technology, we're likely to see them evolve in the future. In this chapter we have reviewed some of the most important articles pertaining to the synthesis of metal nanoparticles. Special emphasis has been given to plant mediated and microbe mediated synthesis of metal nanoparticles. In addition, we've covered some of the applications of metal nanoparticles. Through this article we would like to help anyone who is willing to delve deep into the synthesis of metal nanoparticles. This review will facilitate future researchers to focus their work on nano-synthesis.

Conflict of Interest

The authors declare that there is no conflict of interest.

Acknowledgment

The authors thank the management of Vellore Institute of Technology, Vellore, for providing all research facilities and their kind support.

Abbreviations

AFM	Atomic force microscope
BLCFE	*Bacillus licheniformis* cell-free concentrate
BSA	Bovine serum albumin
BTCA	Butane tetra carboxylic corrosive
CLSM	Confocal laser scanning microscope
DLS	Dynamic light scattering
EDX	Energy dispersive X-ray spectroscopy
FTIR	Fourier transform infrared spectroscopy
GCMS	Gas chromatography-mass spectroscopy
GDP	Glucose-derived polymers
HEp-2	Human epithelial type 2 cells
LOC	Lab on a chip
MBC	Minimum bactericidal concentration
MDR	Multidrug
MIC	Minimum inhibitory concentration
ODN	Oligodeoxynucleotide
PEG-PAA	Poly(ethylene glycol)-block-poly(aspartic acid)
SERS	Surface-enhanced Raman spectroscopy
SS	Silk sericin
TEM	Transmission electron microscope
XPS	X-ray photoelectron spectroscopy
XRD	X-ray diffraction

References

1. Jayandran, M., Haneefa, M.M., Balasubramanian, V., Green synthesis and characterization of manganese nanoparticles using natural plant extracts and its evaluation of antimicrobial activity. *J. Appl. Pharma. Sci.*, 5(12), 105–110, 2015.
2. Nethravathi, P.C., Shruthi, G.S., Suresh, D., Gowda, U.C., Bhushana, N., Sharma, S., *Garcinia xanthochymus* mediated green synthesis of ZnO nanoparticles: Photoluminescence, photocatalytic and antioxidant activity studies. *Ceram. Int.*, 41, 8680–8687, 2015.
3. Labulo, A.H., Adesuji, E.T., Dedeke, O.A., Bodede, O.S., Oseghale, C.O., Moodley, R., Nyamori, V.O., Dare, E.O., Adegoke, O.A., A dual-purpose silver nanoparticles biosynthesized using aqueous leaf extract of *Detarium microcarpum*: An under-utilized species. *Talanta*, 160, 735–744, 2016.
4. Mazumder, J.A., Ahmed, R., Sardar, M., Reusable magnetic nanobiocatalyst for synthesis of silver and gold nanoparticles. *Int. J. Biol. Macromol.*, 93, 66–74, 2016.

5. Dhamecha, D., Jalalpure, S., Jadhav, K., *Nepenthes khasiana* mediated synthesis of stabilized gold nanoparticles: Characterization and biocompatibility studies. *J. Photochem. Photobiol. B Biol.*, 154, 108–117, 2016.
6. Arul Dhas, N., Cohen, H., Gedanken, A., *In situ* preparation of amorphous carbon-activated palladium nanoparticles. *J. Phys. Chem. B.*, 101, 6834–6838, 1997.
7. Herea, D.D., Chiriac, H., Lupu, N., Grigoras, M., Stoian, G., Stoica, B.A., Petreus, T., Study on iron oxide nanoparticles coated with glucose-derived polymers for biomedical applications. *Appl. Surf. Sci.*, 352, 117–125, 2015.
8. Sathishkumar, G., Gobinath, C., Karpagam, K., Hemamalini, V., Premkumar, K., Sivaramakrishnan, S., Phyto-synthesis of silver nanoscale particles using *Morinda citrifolia* L. and its inhibitory activity against human pathogens. *Colloids Surf. B*, 95, 235–240, 2012.
9. Bindhu, M.R., Umadevi, M., Synthesis of monodispersed silver nanoparticles using *Hibiscus cannabinus* leaf extract and its antimicrobial activity. *Spectrochim. Acta A*, 101, 184–190, 2013.
10. Taranath, T.C., Patil, B.N., *Limonia acidissima* L. leaf mediated synthesis of zinc oxide nanoparticles: A potent tool against *Mycobacterium tuberculosis*. *Int. J. Mycobacteriol.*, 56(1), 197–204, 2016.
11. Ankamwar, B., Chaudhary, M., Sastry, M., Gold nanotriangles biologically synthesized using tamarind leaf extract and potential application in vapor sensing. *Inorg. Met. Nano-Metal Chem.*, 35, 19–26, 2005.
12. Amin, M., Anwar, F., Janjua, M.R.S.A., Iqbal, M.A., Rashid, U., Green synthesis of silver nanoparticles through reduction with *Solanum xanthocarpum* L. berry extract: Characterization, antimicrobial and urease inhibitory activities against *Helicobacter pylori*. *Int. J. Mol. Sci.*, 13, 9923–9941, 2012.
13. Wei, L., Lu, J., Xu, H., Patel, A., Chen, Z.S., Chen, G., Silver nanoparticles: Synthesis, properties, and therapeutic applications. *Drug. Discov. Today*, 17, 422–428, 2015.
14. Narayanan, K.B., Sakthivel, N., Biological synthesis of metal nanoparticles by microbes. *Adv. Colloid Interface Sci.*, 156, 1–3, 2010.
15. Kumar, V.G., Gokavarapu, S.D., Rajeswari, A., Dhas, T.S., Karthick, V., Kapadia, Z., Shrestha, T., Barathy, I.A., Roy, A., Sinha, S., Plant extract mediated synthesis of silver and gold nanoparticles and its antibacterial activity against clinically isolated pathogens. *Colloids Surf. B*, 87, 159–163, 2011.
16. Vahabi, K., Dorcheh, S.K., Biosynthesis of silver nano-particles by trichoderma and its medical applications. *Biotech. Biol. Trichod.*, 393–404, 2014.
17. Velmurugan, P., Iydroose, M., Mohideen, M.H.A.K., Mohan, T.S., Cho, M., Oh, B.T., Biosynthesis of silver nanoparticles using *Bacillus subtilis* EWP-46 cell-free extract and evaluation of its antibacterial activity. *Bioprocess Biosyst. Eng.*, 37, 1527–1534. 2014.
18. Shanthi, S., Jayaseelan, B.D., Velusamy, P., Vijayakumar, S., Chih, C.T., Vaseeharan, B., Biosynthesis of silver nanoparticles using a probiotic *Bacillus licheniformis* Dahb1 and their antibiofilm activity and toxicity effects in *Ceriodaphnia cornuta*. *Microb. Pathog.,* 93, 70–77, 2016.

19. Kora, A., Beedu, S., Jayaraman, A., Size-controlled green synthesis of silver nanoparticles mediated by gum ghatti (*Anogeissus latifolia*) and its biological activity. *Org. Med. Chem. Lett.*, 2, 17–21, 2012.
20. Anand, B.G., Thomas, C.K.N., Prakash, S., Kumar, C.S., Biosynthesis of silver nano-particles by marine sediment fungi for a dose dependent cytotoxicity against HEp2 cell lines. *Bio. Agric. Biotech.*, 4, 150–157, 2015.
21. Ghorbani, H.R., Biosynthesis of nanosilver particles using extract of *Salmonella typhirium*. *Arab. J. Chem.* 2013.
22. Li, G., He, D., Qian, Y., Guan, B., Gao, S., Cui, Y., Yokoyama, K., Wang, L., Fungus-mediated green synthesis of silver nanoparticles using *Aspergillus terreus*. *Int. J. Mol. Sci.*, 13, 466–476, 2012.
23. Salari, Z., Danafar, F., Dabaghi, S., Ataei, S.A., Sustainable synthesis of silver nanoparticles using macroalgae *Spirogyra varians* and analysis of their antibacterial activity. *J. Saudi Chem. Soc.*, 2014.
24. Vardhana, J., Kathiravan, G., Biosynthesis of silver nanoparticles by endophytic fungi *Pestaloptiopsis pauciseta* isolated from the leaves of *Psidium guajava* Linn. *Int. J. Pharm. Sci. Rev. Res.*, 31, 29–31, 2015.
25. Bharde, A., Kulkarni, A., Rao, M., Prabhune, A., Sastry, M., Bacterial enzyme mediated biosynthesis of gold nanoparticles. *J. Nanosci. Nanotech.*, 7, 4369–4377. 2007.
26. Nadaf, N.Y., Kanase, S.S., Biosynthesis of gold nanoparticles by *Bacillus marisflavi* and its potential in catalytic dye degradation. *Arab. J. Chem.* 2016.
27. Baker, S., Satish, S., Biosynthesis of gold nanoparticles by *Pseudomonas veronii* AS41G inhabiting *Annona squamosa* L. *Spectrochim. Acta A*, 150, 691–695, 2015.
28. Lengke, M.F., Fleet, M.E., Southam, G., Morphology of gold nanoparticles synthesized by filamentous cyanobacteria from gold(I)-thiosulfate and gold(III)-chloride complexes. *Langmuir*, 22, 2780–2787, 2006.
29. Jayaseelan, C., Rahuman, A.A., Krithi, A.V., Marimuthu, S., Santhoshkumar, T., Gaurav, K., Karthik, L., Rao, K.V., Novel microbial route to synthesize ZnO nanoparticles using *Aeromonas hydrophila* and their activity against pathogenic bacteria and fungi. *Spectrochim. Acta A*, 90, 78–86, 2012.
30. Sarkar, J., Ghosh, M., Mukherjee, A., Chattopadhyay, D., Acharya K., Biosynthesis and safety evaluation of ZnO nanoparticles. *Bioprocess Biosyst. Eng.* 37, 165–171, 2014.
31. Rai, M.K., Deshmukh, S.D., Ingle, A.P., Gade, A.K., Silver nanoparticles: The powerful nanoweapon against multidrug-resistant bacteria. *J. Appl. Microbiol.*, 112, 841–852, 2012.
32. Kundu, D., Hazra, C., Chatterjee, A., Chaudhari, A., Mishra, S., Extracellular biosynthesis of zinc oxide nanoparticles using *Rhodococcus pyridinivorans* NT2: Multifunctional textile finishing, biosafety evaluation and *in vitro* drug delivery in colon carcinoma. *J. Photochem. Photobiol. B*, 140, 194–204, 2014.
33. Selvarajan, E., Mohanasrinivasan, V., Biosynthesis and characterization of ZnO nanoparticles using *Lactobacillus plantarum* VITES07. *Mater. Lett.*, 112, 180–182, 2013.

34. Azizi, S., Ahmad, M.B., Namvar, F., Mohamad, R., Green biosynthesis and characterization of zinc oxide nanoparticles using brown marine macro alga *Sargassum muticum* aqueous extract. *Mat. Lett.*, 116, 275–277, 2014.
35. Dhandapani, P., Siddarth, A.S., Kamalasekaran, S., Maruthamuthu, S., Rajagopal, G., Bio-approach: Ureolytic bacteria mediated synthesis of ZnO nanocrystals on cotton fabric and evaluation of their antibacterial properties. *Carbohydr. Polym.*, 103, 448–455, 2014.
36. Kaur, H., Dolma, K., Kaur, N., Malhotra, A., Kumar, N., Dixit, P., Sharma, D., Mayilraj, S., Choudhury, A.R., Marine microbe as nano-factories for copper biomineralization. *Biotech. Bioprocess Eng.*, 20, 51–57, 2015.
37. Shantkriti, S., Rani P., Biological synthesis of copper nanoparticles using *Pseudomonas fluorescens*. *Int. J. Curr. Microbiol. App. Sci.*, 3, 374–383, 2014.
38. Shobha., G, Vinutha, M., Ananda, S., Biological synthesis of copper nanoparticles and its impact – A review. *Int. J. Pharm. Sci. Invent.*, 3, 28–38, 2014.
39. Espenti, C.S., Rao, K.S.V.K., Rao, K.M., Bio-synthesis and characterization of silver nanoparticles using *Terminalia chebula* leaf extract and evaluation of its antimicrobial potential. *Mater. Lett.*, 174, 129–133, 2016.
40. Selvam, K., Sudhakar, C., Govarthanan, M., Thiyagarajan, P., Sengottaiyan, A., Senthilkumar, B., Selvankumar, T., Eco-friendly biosynthesis and characterization of silver nanoparticles using *Tinospora cordifolia* (Thunb.) Miers and evaluate its antibacterial, antioxidant potential. *J. Radiat. Res. Appl. Sci.*, 10, 6–12, 2017.
41. López-Miranda, J.L., Vázquez, M., Fletes, N., Esparza, R., Rosas, G., Biosynthesis of silver nanoparticles using a *Tamarix gallica* leaf extract and their antibacterial activity. *Mater. Lett.*, 176, 285–289, 2016.
42. Zargar, M., Shameli, K., Najafi, G.R., Farahani, F., Plant mediated green biosynthesis of silver nanoparticles using *Vitex negundo* L. extract. *J. Ind. Eng. Chem.*, 20, 4169–4175, 2014.
43. Prabu, J.H., Johnson, I., Plant-mediated biosynthesis and characterization of silver nanoparticles by leaf extracts of *Tragia involucrata*, *Cymbopogon citronella*, *Solanum verbascifolium* and *Tylophora ovata. J. Mod. Sci.*, 1, 273–246, 2015.
44. Zuas, O., Hamim, N., Sampora, Y., Bio-synthesis of silver nanoparticles using water extract of *Myrmecodia pendan* (Sarang Semut plant). *Mater. Lett.*, 123, 156–159, 2014.
45. Shankar, S.S., Ahmad, A., Sastry, M., Geranium leaf assisted biosynthesis of silver nanoparticles. *Biotechnol. Prog.*, 19, 1627–1631, 2003.
46. Rashid, M.I., Mujawar, L.H., Rehan, Z.A., Qari, H., Zeb, J., Almeelbi, T. Ismail, I.M., One-step synthesis of silver nanoparticles using *Phoenix dactylifera* leaves extract and their enhanced bactericidal activity. *J. Mol. Liq.*, 223, 1114–1122, 2016.
47. Saravanakumar, A., Ganesh, M., Jayaprakash, J., Jang, H.T., Biosynthesis of silver nanoparticles using *Cassia tora* leaf extract and its antioxidant and antibacterial activities. *J. Ind. Eng. Chem.*, 28, 277–281, 2015.

48. Khalilzadeh, M.A., Borzoo, M., Green synthesis of silver nanoparticles using onion extract and their application for the preparation of a modified electrode for determination of ascorbic acid. *J. Food. Drug. Anal.*, 24, 796–803, 2016.
49. Khushboo, S., Manju, P., Sangeeta, K., Uma, C., Jaya, P.Y, Green silver nanoparticles of *Phyllanthus amarus*: As an antibacterial agent against multi drug resistant clinical isolates of *Pseudomonas aeruginosa*. *J. Nanobiotechnol.*, 12, 40–49, 2014.
50. Edison, T.N.J.I., Lee, Y.R., Sethuraman, M.G., Green synthesis of silver nanoparticles using *Terminalia cuneata* and its catalytic action in reduction of direct yellow-12 dye. *Spectrochim. Acta A*, 161, 122–129, 2016.
51. Vanaja, M., Rajeshkumar, S., Paulkumar, K., Gnanajobitha, G., Malarkodi, C., Annadurai, G., Kinetic study on green synthesis of silver nanoparticles using *Coleus aromaticus* leaf extract. *Adv. Appl. Sci. Res.*, 4, 50–55, 2013.
52. Thombre, R., Parekh, F., Patil, N., Green synthesis of silver nanoparticles using seed extract of *Argyreia nervosa*. *Int. J. Pharm. Biol. Sci.*, 15, 114–119, 2014.
53. Tippayawat, P., Phromviyo, N., Boueroy, P., Chompoosor, A., Green synthesis of silver nanoparticles in *Aloe vera* plant extract prepared by a hydrothermal method and their synergistic antibacterial activity. *Peer J. Preprints*, 4, 1912–1916, 2016.
54. Haritha, E., Roopan, S.M., Madhavi, G., Elango, G., Al-Dhabi, N.A., Arasu, M.V., Green chemical approach towards the synthesis of SnO_2 NPs in argument with photocatalytic degradation of diazo dye and its kinetic studies. *J. Photochem. Photobiol. B*, 162, 441–448, 2016.
55. Sharma, D., Sabela, M.I., Kanchi, S., Mdluli, P.S., Singh, G., Stenström, T.A., Bisetty, K., Biosynthesis of ZnO nanoparticles using *Jacaranda mimosifolia* flowers extract: Synergistic antibacterial activity and molecular simulated facet specific adsorption studies. *J. Photochem. Photobiol. B*, 162, 199–207, 2016.
56. Fu, L., Fu, Z., Plectranthus amboinicus leaf extract-assisted biosynthesis of ZnO nanoparticles and their photocatalytic activity. *Ceram. Int.*, 41, 2492–2496, 2015.
57. Bhuyan, T., Mishra, K., Khanuja, M., Prasad, R., Varma, A., Biosynthesis of zinc oxide nanoparticles from *Azadirachta indica* for antibacterial and photocatalytic applications. *Mater. Sci. Semicond. Process.*, 32, 55–61, 2015.
58. Dobrucka, R., Dugaszewska, J., Biosynthesis and antibacterial activity of ZnO nanoparticles using *Trifolium pratense* flower extract. *Saudi J. Bio. Sci.*, 23, 517–523, 2016.
59. Sundararajan, M., Ambika, S., Bharathi K., Plant-extract mediated synthesis of ZnO nanoparticles using *Pongamia pinnata* and their activity against pathogenic bacteria. *Adv. Powder Tech.*, 26, 1294–1299, 2015.
60. Vijayakumar, S., Vaseeharan, B., Malaikozhundan, B., Shobiya, M., *Laurus nobilis* leaf extract mediated green synthesis of ZnO nanoparticles:

Characterization and biomedical applications. *Biomed. Biother.*, 84, 1213–1222, 2016.
61. Elumalai, K., Velmurugan, S., Ravi, S., Kathiravan, V., Raj, G. A., Bio-approach: Plant mediated synthesis of ZnO nanoparticles and their catalytic reduction of methylene blue and antimicrobial activity. *Adv. Powder Technol.*, 26, 1639–1651, 2015.
62. Surendra, T.V., Roopan, S.M., Al-Dhabi, N.A., Arasu, M.V., Sarkar, G., Suthindhiran, K., Vegetable peel waste for the production of ZnO nanoparticles and its toxicological efficiency, antifungal, hemolytic, and antibacterial activities. *Nanoscale Res. Lett.*, 11, 546–551, 2016.
63. Fowsiya, J., Madhumitha, G., Al-Dhabi, N.A., Arasu, M.V., Photocatalytic degradation of Congo red using *Carissa edulis* extract. *J. Photochem. Photobiol. B*, 162, 395–401, 2016.
64. Abdel-Raouf, N., Al-Enazi, N.M., Ibraheem, I.B.M., Green biosynthesis of gold nanoparticles using *Galaxaura elongata* and characterization of their antibacterial activity. *Arab. J. Chem.,* 10, 3029–3039, 2013.
65. Yuan, C.-G., Huo, C., Yu, S., Gui, B., Biosynthesis of gold nanoparticles using *Capsicum annuum* var. *grossum* pulp extract and its catalytic activity. *Physica E*, 85, 19–26, 2017.
66. Priya Tharishini, P., Saraswathy, N.C., Smila, K.H., Yuvaraj, D., Chandran, M., Vivek, P., Green synthesis of gold nano particles from *Cassia auriculata* leaf aqueous extract and its cytotoxicity effect on *in vitro* cell line. *Int. J. ChemTech Res.*, 6, 4241–4250, 2014.
67. Khalil, M.M.H., Ismail, E.H., El-Magdoub, F., Biosynthesis of Au nanoparticles using olive leaf extract. *Arab. J. Chem.*, 5, 431–437, 2012.
68. Castillo-Lopez, D.N., Pal, U., Green synthesis of Au nanoparticles using potato extract: Stability and growth mechanism. *J. Nanopart. Res.*, 16, 2571–2576, 2014.
69. Boruah, S.K., Boruah, P.K., Sarma, P., Medhi, O.K., Green synthesis of gold nanoparticles using *Camellia sinensis* and kinetics of the reaction. *Adv. Mater. Lett.*, 3, 481–486, 2012.
70. Singh, A.K., Srivastava, O.N., One-step green synthesis of gold nanoparticles using black cardamom and effect of pH on its synthesis. *Nanoscale Res. Lett.*, 10, 353–355, 2015.
71. Ghidan, A.Y., Al-Antary, T.M., Awwad, A.M., Green synthesis of copper oxide nanoparticles using *Punica granatum* peels extract: Effect on green peach Aphid. *Environ. Nanotechnol.*, 6, 95–98, 2016.
72. Nasrollahzadeh, M., Sajadi, M.S., Rostami-Vartooni, A., Hussin, S.M., Green synthesis of CuO nanoparticles using aqueous extract of *Thymus vulgaris* L. leaves and their catalytic performance for N-arylation of indoles and amines. *J. Colloid. Inter. Sci.*, 466, 113–119, 2016.
73. Sharmila, G., Thirumaraimurugan. M., Sivakumar, M.V., Optical, catalytic and antibacterial properties of phytofabricated CuO nanoparticles using *Tecoma castanifolia* leaf extract. *Optik*, 127, 7822–7828, 2016.

74. Duman, F., Ocsoy, I., Kup, F.O., Chamomile flower extract-directed CuO nanoparticle formation for its antioxidant and DNA cleavage properties. *Mater. Sci. Eng. C*, 60, 333–338, 2016.
75. Lebaschi, S., Hekmati, M., Veisi, H., Green synthesis of palladium nanoparticles mediated by black tea leaves (*Camellia sinensis*) extract: Catalytic activity in the reduction of 4-nitrophenol and Suzuki-Miyaura coupling reaction under ligand-free conditions. *J. Colloid. Inter. Sci.*, 458, 223–231, 2017.
76. Kalaiselvi, A., Roopan, S.M., Madhumitha, G., Ramalingam, C., Elango, G., Synthesis and characterization of palladium nanoparticles using *Catharanthus roseus* leaf extract and its application in the photo-catalytic degradation. *Spectrochim. Acta A*, 135, 116–121, 2015.
77. Nasrollahzadeh, M., Sajadi, M.S., Green synthesis of Pd nanoparticles mediated by *Euphorbia thymifolia* L. leaf extract: Catalytic activity for cyanation of aryl iodides under ligand-free conditions. *J. Colloid. Inter. Sci.,* 469, 191–195, 2016.
78. Khodadadi, B., Bordbar, M., Nasrollahzadeh, M., Green synthesis of Pd nanoparticles at apricot kernel shell substrate using *Salvia hydrangea* extract: Catalytic activity for reduction of organic dyes. *J. Colloid. Inter. Sci.*, 490, 1–10, 2017.
79. Elango, G., Roopan, S.M., Al-dhabi, N.A., Arasu, M.V., Damodharan, K.I., Elumalai, K., *Cocos nucifera* coir-mediated green synthesis of Pd NPs and its investigation against larvae and agricultural pest. *Artif. Cells Nanomed. Biotechnol.*, 45, 158–157, 2016.
80. Dinesh, M., Roopan, S.M., Selvaraj, C.I., Arunachalam, P., *Phyllanthus emblica* seed extract mediated synthesis of PdNPs against antibacterial, heamolytic and cytotoxic studies. *J. Photochem. Photobiol. B*, 167, 64–71, 2017.
81. Roopan, S.M., Bharathi, A., Kumar, R., Khanna, V.G., Prabahkarn, A., Acaricidal, insecticidal, and larvicidal efficacy of aqueous extract of *Annona squamosa* L peel as biomaterial for the reduction of palladium salts into nanoparticles. *Colloids Surf. B*, 92, 209–212, 2012.
82. Elango, G., Roopan, S.M., Efficacy of SnO_2 nanoparticles toward photocatalytic degradation of methylene blue dye. *J. Photochem. Photobiol. B*, 155, 34–38, 2016.
83. Elango, G., Kumaran, S.M., Kumar, S.S., Muthuraja, S., Roopan, S.M., Green synthesis of SnO_2 nanoparticles and its photocatalytic activity of phenolsulfonphthalein dye. *Spectrochim. Acta A*, 145, 176–181, 2015.
84. Haritha, E., Roopan, S.M., Madhavi, G., Elango, G., Prabhakarn, A., *Catunaregum spinosa* capped Ag NPs and its photocatalytic application against amaranth toxic azo dye. *J. Mol. Liq.*, 225, 531–535, 2017.
85. Diallo, A., Manikandan, E., Rajendran, V., Maaza, M., Physical & enhanced photocatalytic properties of green synthesized SnO_2 nanoparticles via *Aspalathus linearis. J. Alloys Com.*, 681, 561–570, 2016.

86. Tammina, S.K., Mandal, B.K., Ranjan, S., Dasgupta, N., Cytotoxicity study of *Piper nigrum* seed mediated synthesized SnO_2 nanoparticles towards colorectal (HCT116) and lung cancer (A549) cell lines. *J. Photochem. Photobiol. B*, 166, 158–168, 2017.
87. Elango, G., Roopan, S.M., Damodharan, K.I., Elumalai, K., Al-dhabi, N.A., Arasu, M.V., Spectroscopic investigation of biosynthesized nickel nanoparticles and its larvicidal, pesticidal activities. *J. Photochem. Photobiol. B*, 162, 162–169, 2016.
88. Pandian, C.J., Palanivel, R., Dhanasekaran, S., Green synthesis of nickel nanoparticles using *Ocimum sanctum* and their application in dye and pollutant adsorption. *Chin. J. Chem. Eng.*, 23, 1307–1315, 2015.
89. Thema., F.T., Manikandan. E., Gurib-Fakim, A., Maaza, M., Single phase Bunsenite NiO nanoparticles green synthesis by *Agathosma betulina* natural extract. *J. Alloy. Com.*, 657, 655–661, 2016.
90. Ezhilarasi, A.A., Vijaya, J.J., Kaviyarasu. K., Maaza, M., Ayeshmariam, A., Kennedy, L.J., Green synthesis of NiO nanoparticles using *Moringa oleifera* extract and their biomedical applications: Cytotoxicity effect of nanoparticles against HT-29 cancer cells. *J. Photochem. Photobiol. B*, 164, 352–360, 2016.
91. Zhang, X.F., Liu, Z.G., Shen, W., Gurunathan, S., Silver nanoparticles: Synthesis, characterization, properties, applications, and therapeutic approaches. *Int. J. Mol.*, 17, 1534–1539, 2016.
92. Mattea, F., Vedelago, J., Malano, F., Gomez, C., Strumia, M.C., Valente, M., Silver nanoparticles in X-ray biomedical applications. *Rad. Phys. Chem.*, 130, 442–450, 2017.
93. Anjum, S., Abbasi, B.H., Shinwari, Z.K., Plant-mediated green synthesis of silver nanoparticles for biomedical applications: Challenges and opportunities. *Pak. J. Bot.*, 48, 1731–1760, 2016.
94. Farkhari, N., Abbasian, S., Moshaii, A., Nikkhah, M., Mechanism of adsorption of single and double stranded DNA on gold and silver nanoparticles: Investigating some important parameters in bio-sensing applications. *Colloids Surf. B*, 148, 657–664, 2016.
95. Krishna, K.S., Li, Y., Li, S., Kumar, C.S.S.R., Lab-on-a-chip synthesis of inorganic nanomaterials and quantum dots for biomedical applications. *Adv. Drug. Deliver. Rev.*, 65, 1470–1495, 2013.
96. Illés, E., Tombácz, E., Szekeres, M., Tóth, I.Y., Szabó, Á., Iván, B., Novel carboxylated PEG-coating on magnetite nanoparticles designed for biomedical applications. *J. Magn. Magn. Mater.*, 380, 132–139, 2015.
97. Munjal, S., Khare, N., Nehate, C., Koul, V., Water dispersible $CoFe_2O_4$ nanoparticles with improved colloidal stability for biomedical applications. *J. Magn. Magn. Mater.*, 404, 166–169, 2016.
98. Karimi, Z., Karimi, L., Shokrollahi, H., Nano-magnetic particles used in biomedicine: Core and coating materials. *Mater. Sci. Eng. C*, 33, 2465–2475, 2013.

99. Rai, M.K., Deshmukh, S.D., Ingle, A.P., Gade, A.K., Silver nanoparticles: The powerful nanoweapon against multidrug-resistant bacteria. *J. Appl. Microbiol.*, 112, 841–852, 2012.
100. Aramwit, P., Bang, N., Ratanavaraporn, J., Ekgasit, S., Green synthesis of silk sericin-capped silver nanoparticles and their potent anti-bacterial activity. *Nanoscale Res. Lett.*, 9, 79, 2014.
101. Abdel-Aziz, M.S., Abou-El-Sherbini, K.S., Hamzawy, E.M.A., Amr, M.H.A., El-Dafrawy, S., Green synthesis of silver nano-particles by *Macrococcus bovicus* and its immobilization onto montmorillonite clay for antimicrobial functionality. *Appl. Biochem. Biotechnol.*, 176, 2225–2241, 2015.
102. Lateef, A., Azeez, M.A., Asafa, T.B., Yekeen, T.A., Akinboro, A., Oladipo, I.C., Azeez, L., Ajibade, S.E., Oja, S.A., Gueguim-Kana, E.B., Beukes, L.S., Biogenic synthesis of silver nanoparticles using a pod extract of *Cola nitida*: Antibacterial and antioxidant activities and application as a paint additive. *J. Taibah Univ. Sci.*, 10, 551–562, 2016.
103. Zhao, P., Li, N., Astruc, D., State of the art in gold nanoparticle synthesis. *Coord. Chem. Rev.*, 257, 638–665, 2013.
104. Kim, S.P., Lee, D.U., Kim, E.K., Optical properties of metal-oxide nanoparticles embedded in the polyimide layer for photovoltaic applications. *Curr. Appl. Phys.*, 10, 478–480, 2010.
105. Li, J., Li, H., Hu, H., Zhao, Y., Wang, Q., Preparation and application of polymer nano-fiber doped with nano-particles. *Opt. Mater. (Amst)*, 40, 49–56, 2015.
106. Fedotov, A.A., Grigoriev, S.A., Millet, P., Fateev, V.N., Plasma-assisted Pt and Pt-Pd nano-particles deposition on carbon carriers for application in PEM electrochemical cells. *Int. J. Hydrogen Energy*, 8568–8574. 2013.
107. Musinski, L., Liu, T., Gilchrist, B., Gallimore, A., Electrostatic charging of micro- and nano-particles for use with highly energetic applications. *J. Electrostat.*, 67, 54–61, 2009.
108. Chowdhury, S.R., Mukherjee, P., Bhattachrya, S.K., Palladium and palladium–copper alloy nano particles as superior catalyst for electrochemical oxidation of methanol for fuel cell applications. *Int. J. Hydrogen. Energy*, 41(38), 17072–17083, 2016.

15

Advanced Tin-Oxide Nanostructures: Green Synthesis, Prospects and Challenges for Clean Energy and Environmental Sustainability

Dipyaman Mohanta and M. Ahmaruzzaman*

Department of Chemistry, National Institute of Technology, Silchar, Assam, India

Abstract

The endurance and affluence of the human race is being radically threatened by the increasing energy crisis and environmental pollution. In this regard, there has been an explosive development in nanotechnology, which has great potential to meet the future challenges that humankind is going to face. Nanotechnology continues to have promising prospects in solar photovoltaic cells, solar photocatalysis, efficient adsorption technology, etc., that can exploit clean renewable energies and efficiently deal with pollutants. In the past decade, tin oxide nanostructures and analogues have shown immense potential towards achieving this Holy Grail. The key is to design and fabricate cost-effective, green synthetic strategies to obtain advanced nanostructures that function as active electrodes or efficient catalyst and adsorbents towards energy and environmental applications. Also, it is of fundamental importance to deeply understand the relationship between structure and properties. This chapter summarizes the past developments, various challenges and future prospects of tin-based nanostructured materials towards clean energy generation, efficient energy storage and environmental remediation.

Keywords: Tin oxide nanomaterials, Green synthesis, pollutant detection and remediation, clean energy generation, advanced energy storage device

**Corresponding author*: mda2002@gmail.com

Suvardhan Kanchi and Shakeel Ahmed (eds.) Green Metal Nanoparticles, (513–552)
© 2018 Scrivener Publishing LLC

15.1 Introduction

The rapid pace of modernization of the human race has a profoundly adverse impact on the environment. Unscrupulous industrialization, atrocious waste management and the failure of people to use the environment sustainably has led to its deterioration [1]. The air has been the hardest hit element of the environment. Human activities like burning of fossil fuels, automobile exhausts and industrial emissions directly inject hazardous gases like NO_2, NO, N_2O, H_2S, CO, NH_3, CH_4, SO_2, CO_2, etc., into the atmosphere [2–3]. These toxic gases not only create environmental havoc like global warming, acid rain, photochemical smog, ozone layer depletion, etc., but are also noxious to public health [4–6]. Unlimited human interventions in the environment have also resulted in contamination of water bodies, thereby leading to ecological disarray and scarcity of clean water. Direct disposal of industrial wastes and utilization of chemical fertilizers and pesticides in agriculture contaminate water with various toxic chemicals, organic pollutants, heavy metals, pharmaceuticals, etc., which jeopardize both aquatic and humanoid biomes [7–9].

In parallel with this, the escalating energy demand and exhaustibility of fossil fuels have already begun to haunt the human race. The need for alternative energy sources and efficient energy storage systems is imperative to meet future energy demand [10–12]. Moreover, there is an interwoven connection of environmental pollution with nonrenewable energy sources; accordingly, in the search for clean and renewable sources of energy it is very significant to tackle future environmental concerns as well [13–15].

The rapid advancement in nanotechnology has gained a great deal of interest in its environmental applications. Detection and remediation of pollutants, clean energy generation, efficient energy storage, etc., themselves are massive challenges and, due to their exceptional physicochemical properties, nanomaterials have enormous potential to solve them [16–18]. Various natural and engineered nanostructured materials like TiO_2, ZnO, SnO_2, Fe_2O_3, CNTs and graphenes of different shapes/morphologies/forms have been reported to have significant environmental outcomes [19–25].

Tin oxide nanostructured materials have immense potential to be useful for environmental purposes due to their rational design structure and control over the band gap by suitable modifications [26]. Tin oxide nanomaterials form excellent chemiresistive gas sensor devices due to their low cost, high sensitivity and fast response and are capable of detecting large numbers of gases [27–28]. The tunable physical, chemical and electrical properties of tin-oxide nanostructures enable it as an efficient photocatalyst to degrade numerous textile dyes, pharmaceuticals

and other organic/inorganic contaminants [29–32]. The surface reactivity of SnO_2 nanoadsorbents, due to the accumulation of low coordinated atoms at surface, edge and vertex, can greatly improve the adsorption capacities of toxic sorbents and heavy metal ions from water [1]. In addition, high surface area to volume ratio and small particle size can impart high mobility in solution, thus the whole volume of water can be quickly scanned with small amounts of nanomaterials. The tunability of SnO_2 band structures with various modifications, like metal ion doping, noble metal-SnO_2, metal oxide-SnO_2, CNT/Gr-SnO_2 composites formation, and also with various morphologies, like hollow spheres, nanorods, nanowires, core-shells, etc., have led to SnO_2 being a potential candidate towards energy generation and storage applications [33–39]. This chapter focuses on the understanding of structure-property relationships of various tin-oxide nanostructures for pollutant sensing, decontamination of environment and for the development of solar energy conversion and storage devices.

15.2 Green Strategies for the Fabrication of Tin-Oxide Nanostructures

Fabrication of tin-oxide nanostructures of different morphologies, size, shape, composition and crystal structure is a key step towards nanotechnological applications. Among the most common synthetic strategies, solution processing methods, like sol-gel [40], hydrothermal synthesis [41] and microemulsion method [42], have widespread application. The basic principle involves the precipitation of $Sn(OH)_4$ which on subsequent heat treatment produces nanocrystalline SnO_2.

$$SnCl_4.5H_2O + 4NH_4OH + 4H_2O \longrightarrow Sn(OH)_4 + 4NH_4Cl + 6H_2O \quad (15.1)$$

$$Sn(OH)_4 \xrightarrow{\Delta} \text{Nano-}SnO_2 \quad (15.2)$$

The size and morphology depend upon the precursors, solvents, controlled feed rate of gel formation and partly on the mode of heat treatment [43]. In hydrothermal synthesis, the aqueous solutions of constituent reagents are medium heated above its boiling point under pressure. The temperature, pH and autogenic pressure play a vital role in the unique morphology evolution [44]. Microemulsion technique utilizes various

surfactants to form micelle structures to produce tailor-made products of unusual morphology and properties. The Ostwald ripening, coalescence and oriented attachments are also responsible for growth of tin oxide nanoparticles along facets to evolve as nanotubes, nanorods, mesoporous and hollow spheres [45–46].

The aforesaid methods of fabrication of tin-oxide nanostructures involve utilization of high temperature, toxic chemicals and surfactants and solvents, which make them environmentally impervious. Recently, researchers have been trying to develop green chemistry approaches to fabricate various tin-oxide nanostructures without compromising their utility. The green synthetic strategy involves substitution of conventional high and prolonged heat treatment techniques with microwave assistance due to its homogeneous and fast heating characteristics and utilization of various leaf extracts, plant juice, biomolecules, biowaste residues, bacteria, etc., to eliminate various conventional chemical stabilizers and complexing agents [47–51]. For instance, Srivastava and coworkers [52] reported a facile, green, biogenic method for the synthesis of SnO_2 nanoparticles using Gram-negative bacteria *Erwinia herbicola.* It was demonstrated that the bacterial protein and biomolecules act as the template for reduction and stabilization of SnO_2 and control the size and aggregation of nanoparticles (Figure 15.1a). Similarly, Gattu *et al.* [53] reported bio-green synthesis of Ni-doped tin oxide nanoparticles using remnant water (ideally kitchen waste) collected from soaked Bengal gram beans (*Cicer arietinum* L.). The as-synthesized particles were nearly spherical with average particle

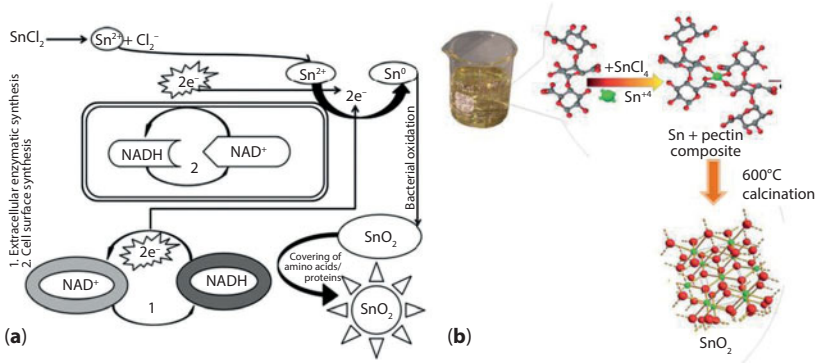


Figure 15.1 (a) Mechanism of biosynthesis of SnO_2 nanoparticles: 1, synthesis due to extracellular secretion of enzymes; 2, synthesis on the cell surface due to membrane-associated proteins. (b) Role of pectin in biosynthesis of tin oxide nanoparticles. (Reproduced from [52] and [53] with permission from ACS and RSC Publishing respectively)

size ranging from 30–60 nm. It was claimed that Pectin (complex polysaccharide present in plant extract) acts as a complexing and stabilizing agent which binds to the tin ions and inhibits the growth of the nanoparticles (Figure 15.1b).

Likewise, extracts from various plants such as *Daphne alpina* [54], *Plectranthus amboinicus* [55], *Ficus benghalensis, Baringtoria acutagularis, Cyclea peltata* [56], *Ficus carica* [57], dried peel of sugar apple (*Annona squamosa*) [58], *Aloe vera* [59], etc., have also been used for the bio-mediated green synthesis of SnO_2 nanoparticles.

Moreover, amino acids like glycine [60], Serine [61], tyrosine [62], lysine [63], etc., have also been extensively used for the synthesis of SnO_2 nanoparticles. Amino acids act as good complexing or capping agents, thereby eliminating toxic chemicals and solvents during the synthesis and also enabling modification of size, morphology and properties of as-synthesized nanocrystals. The most probable mechanistic pathway [60] for amino acid mediated synthesis of SnO_2 nanoparticles is as follows:

$$\mathrm{Sn\,(OOC\text{-}CH_2\text{-}NH_2)_n + xH_2O \longrightarrow Sn(OOC\text{-}CH_2\text{-}NH_2)_{n\text{-}x}(OH) + xNH_2\text{-}CH_2\text{-}COOH} \quad (15.3)$$

$$\mathrm{2\,Sn(OOC\text{-}CH_2\text{-}NH_2)_{n\text{-}x}(OH) \longrightarrow [(OH)_{x\text{-}1}(OOC\text{-}CH_2\text{-}NH_2)_{n\text{-}x}Sn]_2O + H_2O} \quad (15.4)$$

$$\mathrm{[(OH)_{x\text{-}1}(OOC\text{-}CH_2\text{-}NH_2)_{n\text{-}x}Sn]_2O \longrightarrow nano\text{-}SnO_2} \quad (15.5)$$

The development of new synthetic methodologies with clean, nontoxic, environmentally friendly green chemical approaches by utilizing biological entities, plants and microorganisms, etc., is still in the crawling stage and immense research is needed for better control over size and morphology of the nanoparticles.

15.3 Detection of Pollutants and Environmental Remediation

15.3.1 Advanced Tin-Oxide Nanostructured Materials as Sensors for Environmentally Hazardous Gases

The nastiest consequence of the global burden of human activity on the environment is probably the contamination of the atmosphere by toxic

gases. The most common sources of environmentally hazardous gases (H_2S, CO, NH_3, NO_2, CH_4, SO_2, etc.) include combustion in industries, chemical plants and automobiles [2]. The most hazardous gas is NO_x, which is a major component of photochemical smog, acid rain and ozone layer depletion. Carbon monoxide (CO) and hydrogen sulfide (H_2S) interact with hemoglobin in the blood and block oxygen from being carried to vital organs and tissues. Various health effects caused by excessive SO_2 and CO_2 include respiratory illness, asthma, cardiovascular diseases and many more [64–65]. Due to the increasing concerns about atmospheric pollution on public safety and health, the development of efficient and economical systems for detection and quantification of environmentally hazardous gases in real time have become increasingly significant.

Metal-oxide semiconductor-based gas sensors attract the broadest interest to monitor all aspects of the environment due to their low cost, high sensitivity, speedy response/recovery time, direct electronic interface and the ability to detect a large number of gases [66]. Tin-oxide-based nanostructured materials show great potential towards sensing of various environmentally hazardous gases due to their remarkable change in resistance under oxidizing or reducing gas environment [67]. The change in resistance of metal oxides on exposure to analyte gases occurs due to the interaction of the gas with the dominant charge carriers on the surface of the semiconductor. Tin-oxide, being n-type semiconductor, shows a decrease in resistance in the presence of reducing gases (like H_2S, NH_3, etc.), while increased resistance in oxidizing gas environment (NO_2, CO_2, etc.) [68].

15.3.1.1 Mechanism of Gas Sensing

Under ambient condition, a space charge layer is generated over the surface of tin oxide semiconductor due to the adsorption of oxygen over the metal oxide surface. The chemisorbed oxygen molecules accept electrons from the conduction band of the material to form ionic oxygen species (O_2^-, O^- & O^{2-}), thereby altering the surface charge of the semiconductor (Eqs. 15.6–15.9) [2].

$$O_2\,(\text{gas}) \longrightarrow O_2\,(\text{absorbed}) \tag{15.6}$$

$$O_2\,(\text{absorbed}) + e^- \longrightarrow O_2^- \tag{15.7}$$

$$O_2^- + e^- \longrightarrow 2\,O^- \tag{15.8}$$

$$O^- + e^- \longrightarrow O^{2-} \tag{15.9}$$

The adsorbed ionic oxygen species assist various oxidizing gases to accept electrons from the conduction band and get adsorbed over the surface of the metal oxide. This result further decreases the electron density on the metal oxide surface, which in turn increases the resistance of the material considerably (Eqs. 15.10–15.17) [2]. However, in reducing gas environment, the chemisorbed oxygen species interact with the gas thereby releasing electrons back to the conduction band and as a result the resistance of the tin-oxide material decreases (Eq. 15.18–15.27) [2]. Thus, the measurement of resistance under various gaseous analyte forms the basis of tin-oxide gas sensors. A schematic representation of the gas-sensing mechanism of n-type semiconductor sensor is shown in Figure 15.2.

$$NO_2\,(gas) + e^- \longrightarrow NO^{2-}\,(ads) \tag{15.10}$$

$$NO^{2-}\,(ads) + O^-\,(ads) + 2\,e^- \longrightarrow NO\,(gas) + 2O^{2-}\,(ads) \tag{15.11}$$

$$NO\,(gas) + e^- \longrightarrow NO^-\,(ads) \tag{15.12}$$

$$2NO^-\,(ads) \longrightarrow N_2\,(gas) + 2O^-\,(ads) \tag{15.13}$$

$$N_2O\,(gas) + e^- \longrightarrow N_2O^-\,(ads) \tag{15.14}$$

$$N_2O^-\,(ads) \longrightarrow N_2\,(gas) + O^-\,(ads) \tag{15.15}$$

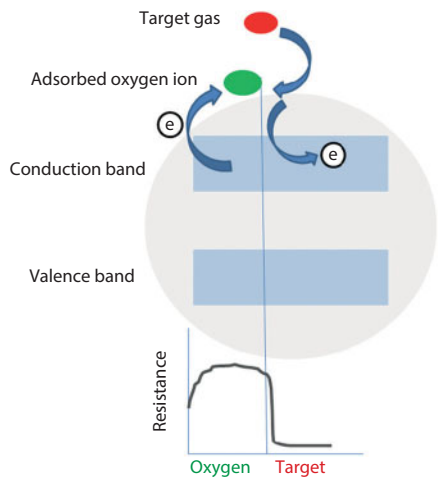


Figure 15.2 Schematic representation of gas-sensing mechanism by n-type semiconductor.

$$CO_2\,(gas) + e^- \longrightarrow CO^{2-}\,(ads) \quad (15.16)$$

$$CO^{2-}\,(ads) + O^-\,(ads) + 2\,e^- \longrightarrow CO\,(gas) + 2O^{2-}\,(ads) \quad (15.17)$$

$$2NH_3 + 3O^-\,(ads) \longrightarrow N_2 + 3H_2O + 3\,e^- \quad (15.18)$$

$$2NH_3 + 3O^{2-}\,(ads) \longrightarrow N_2 + 3H_2O + 6\,e^- \quad (15.19)$$

$$H_2S + 3O^-\,(ads) \longrightarrow H_2O + SO_2 + 3\,e^- \quad (15.20)$$

$$H_2S + 3O^{2-}\,(ads) \longrightarrow H_2O + SO_2 + 6\,e^- \quad (15.21)$$

$$CO + O^-\,(ads) \longrightarrow CO_2 + e^- \quad (15.22)$$

$$CO + O^{2-}\,(ads) \longrightarrow CO_2 + 2\,e^- \quad (15.23)$$

$$SO_2 + O^-\,(ads) \longrightarrow SO_3 + e^- \quad (15.24)$$

$$SO_2 + O^{2-}\,(ads) \longrightarrow SO_3 + 2\,e^- \quad (15.25)$$

$$CH_4 + 4O^-\,(ads) \longrightarrow 2H_2O + CO_2 + 4\,e^- \quad (15.26)$$

$$CH_4 + 4O^{2-}\,(ads) \longrightarrow 2H_2O + CO_2 + 8\,e^- \quad (15.27)$$

15.3.1.2 Effect of Morphology on Gas-Sensing Properties of SnO_2

The properties of nanomaterials are a direct function of shape, surface area and porosity of the material and gas sensing is no exception to this. The tin oxide grain size largely affects the response and selectivity to a specific gas because grain boundaries act as electron scattering centers. For instance, Xu *et al.* [69] reported that when the grain size is smaller than twice the depth of space charge layer, the depletion layer extends over the entire grain and the gas sensitivity increases steeply. Thus, the smaller the grain size, the higher the gas sensitivity. Likewise, Sedghi *et al.* [70] reported low temperature sensing of CO and CH_4 using SnO_2 quantum dots (d = 2.2 nm) with nearly three times increased sensitivity. The dramatic increase in sensitivity was attributed to the dimension effects. It has been demonstrated that when grain size becomes comparable to quantum dimensions, they are completely depleted by charge carriers (Figure 15.3). As a result, a flat band case arises where the neck

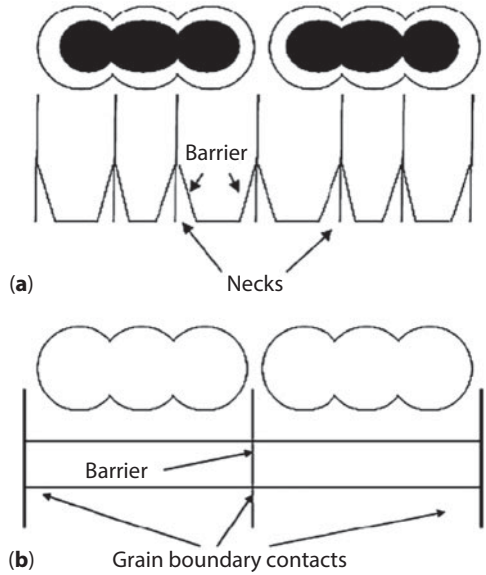


Figure 15.3 Resistance distribution in (a) Grain boundary and (b) Flat band condition. (Reproduced from [70] with permission from Elsevier)

height is very small or negligible; electrons face an exceedingly high resistance to hop to the surface, which allows maximum response of the sensor.

Furthermore, different morphologies of tin oxide nanostructures, viz., thin films, nanowires, hollow nanotubes, quantum wires, nanobelts, porous nanofilm, etc. [71–75], were utilized for enhanced detection of various toxic gases. Ingole and coworkers [72] showed improved sensitivity of tin oxide thin films towards NO_2 gas @ 200 °C with a maximum response of 403% (100 ppm NO_2) and as low as 1 ppm NO_2 with 23% response value (Figure 15.4a). Kolmakov *et al.* [74] demonstrated higher activity of tin oxide nanowires towards CO detection. The radius of the nanowire being of the order of Debye length, the flat band condition applies, which results in the superior sensing application (Figure 15.4b). Recently, Ma and colleagues [76] utilized dodecahedron like SnO_2 nanomaterials towards low temperature sensing of SO_2 and established the close relationship of high surface energy (221) facets with gas sensitivity (Figure 15.4c). Due to the presence of dangling bond-rich (221) facets, SnO_2 dodecahedron can provide more active sites and a larger resistance change compared to the usual (110) facets, and hence the improved sensitivity towards SO_2.

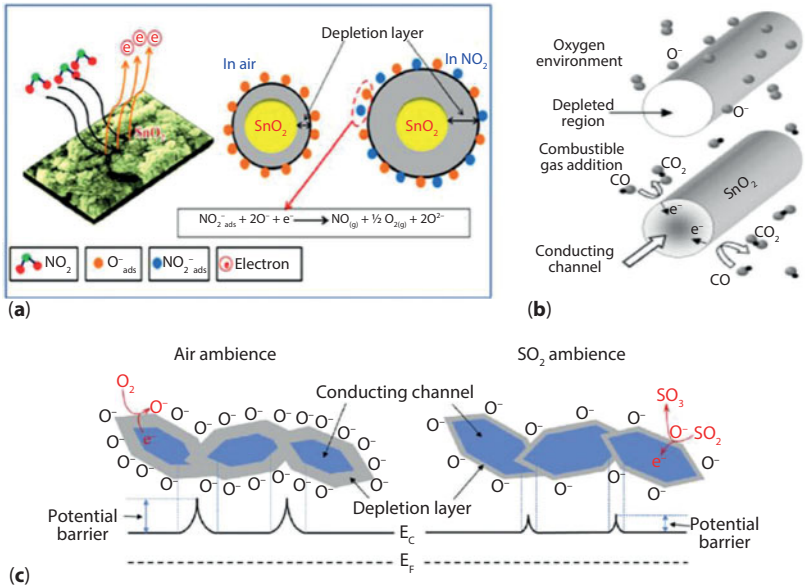


Figure 15.4 Schematic representation of sensing mechanism of (a) SnO_2 films with NO_2 gas, (b) SnO_2 nanowires with CO gas, (c) SnO_2 dodecahedron with SO_2 gas. (Reproduced from [72], [74] and [75] with permission from Elsevier and Wiley)

15.3.1.3 Effect of Heterojunction on Gas-Sensing Properties of SnO_2

Heterojunction is the interface that occurs between two regions of dissimilar crystalline solids. When there is a difference in Fermi energies between two connected solids, diffusion of charge carriers occurs until the Fermi energy is equilibrated, resulting in a depletion layer at the interface. The flow of charge carriers alters the resistance of the material and makes it sensitive towards oxidizing and reducing gases [77].

Noble metal nanoparticles, such as Pt, Pd, Ag, and Au, decorated on SnO_2 nanoparticles constitute Schottky junction [78–81]. It has been reported that surface fictionalization of SnO_2 nanoparticles with noble metals alters the Schottky barriers at the metal-semiconductor interface. The Femi level of metal being much lower than that of semiconductor, electrons tend to flow from SnO_2 to metal to achieve equilibrium, thereby creating large depletion layer on SnO_2. This results in significant decrease in conductivity [82]. In most cases, this facilitates a large increase in sensing response, dynamic characteristics and decrease in optimal operating temperature. Choudhary *et al.* [81] demonstrated enhanced H_2, CH_4 and CO sensing performances by incorporating Pd nanoparticles on SnO_2

thick films. Li *et al.* [80] showed that the electron migration from SnO_2 to Pd facilitates the addition and dissociation of oxygen over the nanomaterials surface thereby resulting in dramatic improvement in gas response (Figure 15.5).

Replacement of noble metals with trace amounts of metal ion additives also found to improve the selectivity and sensitivity of SnO_2 gas sensors. Ghosh *et al.* [83] reported improved CO sensing using Ca-doped SnO_2 nanocrystals, Li *et al.* [84] utilized Ni-doped SnO_2 for NO_2 sensing; Wang *et al.* [85] demonstrated that Cu doping enhances the sensing response of pristine SnO_2 towards H_2S many fold; and Wang *et al.* [27] investigated the effect of Sn doping in SnO_2 gas-sensing behavior. Metal ion doping influences the structure and electric conductivity of SnO_2 surface, thereby enhancing the response.

The role of oxide/oxide interface in the gas-sensing properties of semiconductor nanocomposites is also very significant. Tin oxide, being n-type semiconductor, when decorated with p-type semiconductor like NiO electron depletion layer and hole accumulation layer is generated over SnO_2 and NiO surface respectively. Due to concentration gradient of charge carriers at the p-n junction, the transfer of electrons from SnO_2 to NiO and holes from NiO to SnO_2 occurs until the equalization

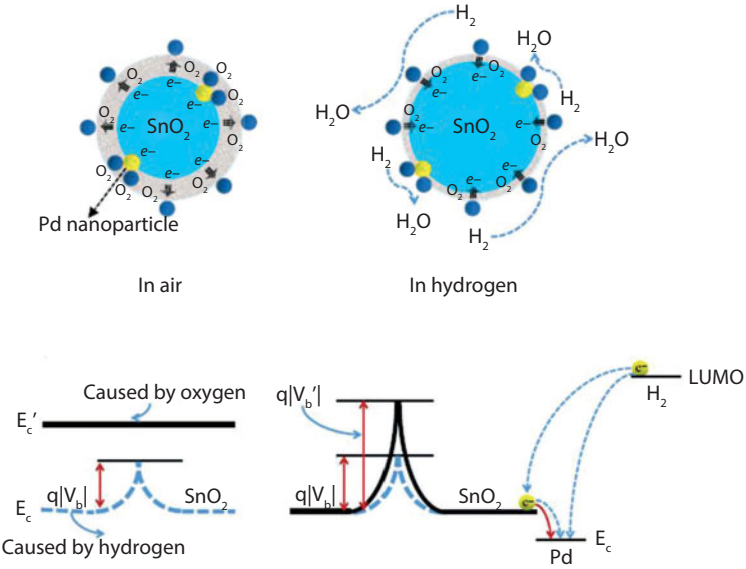


Figure 15.5 Schematic representation of hydrogen sensing mechanism of Pd-SnO_2 composite nanospheres. (Reproduced from [80] with permission from Elsevier)

of the Fermi level [86]. The Fermi level of a n-type is usually higher than that of a p-type, which results in the formation of thick space charge layers around the p-n junction, which significantly narrow the electrical transport channels and the sensor resistance is increased accordingly (Figure 15.6). This allowed the researchers to enhance the sensing performance of gas sensors towards both oxidizing and reducing gases by tuning the charge conduction channel with appropriate selection of p-type oxide. Tyagi *et al.* [87] demonstrated improved SO_2 sensing by NiO-SnO_2 system. Similarly, n-SnO_2/p-Co_3O_4 [88], n-SnO_2/p-Sb_2O_5 [89] and n-SnO_2/p-Fe_2O_3 [90] systems have been reported for drastically improved gas-sensing response at very low concentration compared to pristine SnO_2.

Moreover, Park *et al.* [91] achieved remarkable NO_2 sensing performance via n-n heterojunction prepared using SnO_2Core/ZnO-Shell nanowires. Similarly, n-n junctions, like SnO_2/SnS_2 [92], SnO_2/WO_3 [93], etc., were also utilized for improved sensing of toxic gases. Unlike p-n junction where electron-hole recombination may lower the free charge

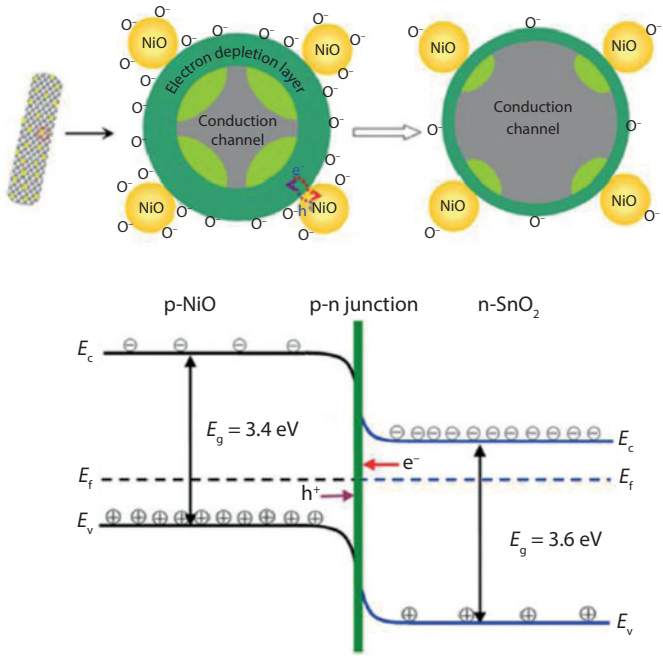


Figure 15.6 Schematic representation of sensing mechanism of heterostructured NiO/SnO_2 porous nanorods and energy band structure diagram of p-NiO/n-SnO_2 heterojunction. (Reproduced from [86] with permission from Elsevier)

carriers, the interface at n-n junction simply transfers electrons from the materials with a high Fermi level to the one with a low Fermi level, thus forming depletion layer, narrowing the conduction channel and enhancing the response. Recently, Nguyet *et al.* [94] developed advanced n-p-n heterojunction using carbon nanotube SnO_2 nanowires for superior enhancement of NO_2 and H_2S gas response.

As various SnO_2 heterojunctions allow modulation of depletion area by proper choice of second phase, these materials are probably the most promising candidates towards selective sensing of hazardous gases.

15.3.1.4 Effect of Carbon Composites on Gas-Sensing Properties of SnO_2

The surface attachment of carbon nanomaterials (CNTs, graphenes, rGO, etc.) with SnO_2 nanoparticles has excellent advantage in gas-sensing applications due to their enormously high electronic mobility at room temperature, unprecedented structure and excellent physical/mechanical properties. Properties of rGO, like high surface area, rich active sites, strong adsorption ability to gases, etc., make rGO–SnO_2 hybrid materials very attractive towards sensing of various toxic gases at room temperature. Chen *et al.* [95] coupled SnO_2 nanorods with rGO for highly sensitive low temperature detection of NH_3 in humid conditions. The synergic effect of the couple was found to be superior to the individual constituents. Also, SnO_2 nanorods provided large surface area with pore volume for gas adsorption while rGO provided effective electron transfer and high response sensitivity at room temperature. It was claimed that due to the formation of ohmic junctions between rGO and semiconductor interface in SnO_2-rGO structure, the resistance of the interface was much lower than that of the semiconductor itself, which results in the efficient transfer of electrons from SnO_2 surface to the rGO substrate, thereby facilitating the improved detection capacity at very low temperature compared to pristine SnO_2 (Figure 15.7) [96].

Similarly, Zhang *et al.* [97] developed SnO_2-graphene-based sensors for quantitative detection of HCHO and NH_3 at room temperature of 20 °C; Song *et al.* [98] showed enhanced activity of SnO_2 quantum wire-rGO nanocomposites for selective room temperature detection of H_2S. Furthermore, Xiao *et al.* [99] and Zhang and coworkers [100] found SnO_2-rGO very effective towards low temperature NO_2 sensing. Moreover, Tyagi *et al.* [101] and Liu *et al.* [102] constructed MWCNT-SnO_2 and MWCNT-SnO_2-rGO nanohybrids for enhanced sensing performance of SO_2 and NO_2 respectively.

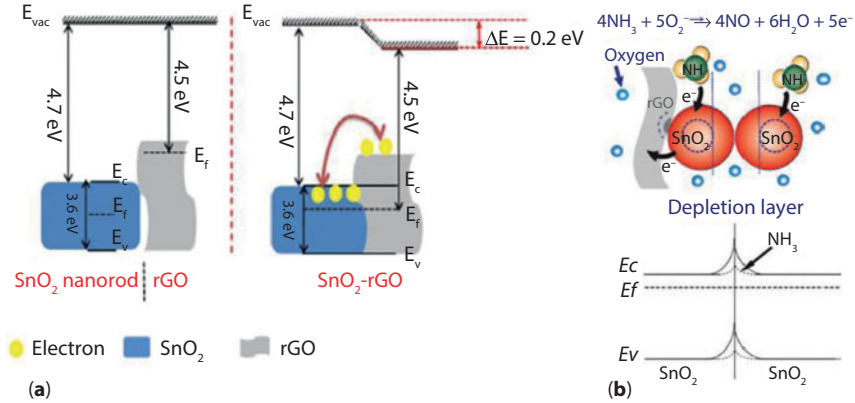


Figure 15.7 (a) Band diagram of SnO_2/rGO before and after combination; (b) Schematic representation of NH_3 sensing mechanism of SnO_2/rGO. (Reproduced from [95] and [96] with permission from Elsevier)

Although the tin oxide nanostructures and various modifications show immense potential towards detection of various hazardous gases with superior sensitivity and low operating temperature; however, there are some shortcomings like cost-effectiveness, durability, complicated synthetic strategies, complex nanostructures for high sensitivity, etc., which limit their practical applications.

15.3.2 Advanced Tin-Oxide Nanostructures as Efficient Photocatalysts and Adsorbents for Decontamination of Wastewater

Rapid urbanization, industrialization and modifications in agricultural techniques have enhanced human interaction with the environment, thereby leading to the disruption of ecological and environmental equilibrium. The dissolution of various toxic chemicals, heavy metals, hazardous textile dyes, pesticides, pharmaceutical compounds, nitrophenols, etc., in water can deteriorate the eminence of water, thereby affecting human health and the environment [103]. Moreover, the existence of this redundant contamination may create havoc in aquatic life as well. Thus, monitoring and disarticulation of these pollutants from water is very crucial for environmental security purpose [104–105].

Tin oxide nanocrystals, being wide band gap semiconductor, have enormous potential as an efficient photocatalyst for degradation of various organic dyes, pharmaceuticals and other organic contaminants to

mineralized products. Bhattacharjee and coworkers [60–61, 106–109] reported degradation of common textile dyes, like eosin Y, methylene blue, rose bengal, methyl violet 6B, etc., using direct sunlight which is a very cost-effective method and scalable to a large extent compared to common UV-assisted photodegradation technique. Elango *et al.* [110] used SnO_2 nanoparticles for complete degradation of phenolsulfonphthalein dye. Srivastava *et al.* [52] showed activity of SnO_2 towards degradation of methylene blue, eriochrome black T, and methyl orange dyes. Likewise, Prakash *et al.* [111] reported superior photocatalytic activity of SnO_2 hollow nanospheres towards methylene blue and Begum *et al.* [112] reported complete degradation of humic acid from aqueous solution using SnO_2 quantum dots. The mechanism of degradation of organic contaminants could be understood from the Figure 15.8.

The photocatalytic activity is greatly hindered by the recombination of photogenerated electrons and holes. Various methods, like doping, oxide combinations, metal deposition, composite formation, etc., have been employed for anti-recombination of carriers. Pan *et al.* [113] reported that the indium tin oxide nanoparticles show higher photodegradation efficiency of rhodamine B than the commercial P25 TiO_2 within the given concentration range. Furthermore, Sinha and coworkers [114–115] investigated the light-assisted degradation of MB, methyl violet 6B, malachite green, rhodamine B, methyl green, and rose bengal using Sn-SnO_2 NPs

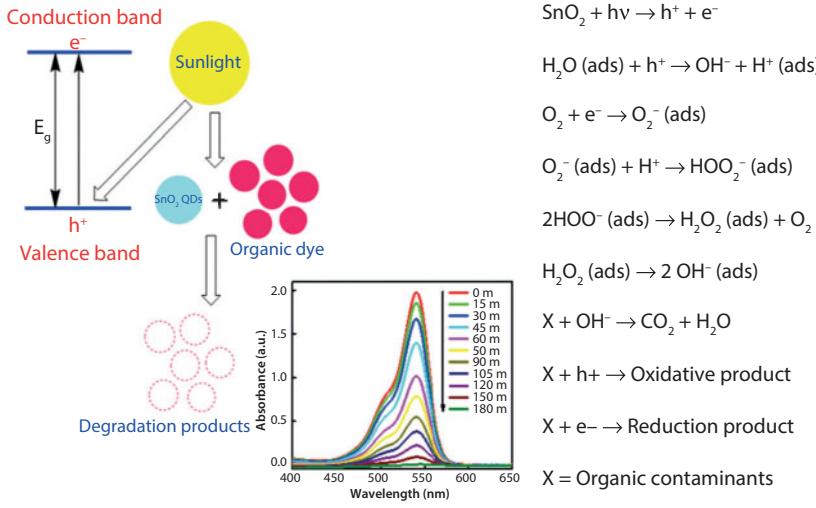


Figure 15.8 Schematic representation of mechanism of degradation of dyes by SnO_2 nanophotocatalyst. (Reproduced from [108] with permission from Elsevier)

and Ag-SnO_2 NPs respectively, and claimed that the presence of metal nanoparticles, like Ag(0), Sn(0), etc., over spherical SnO_2 nanoparticles improves the charge (electrons and holes) separation efficiency, thereby enhancing the rate of degradation.

Kumar *et al.* [116] designed binary SnO_2-CuO nanocomposite for drastically enhanced photocatalytic activity towards degradation of malachite green dye. The p-n interfaces between SnO_2 nanoparticles and CuO nanoparticles can supply an optimal environment and the force to drive the transfer of the electrons/holes to the surfaces of the catalysts, thereby improving rate of degradation (Figure 15.9). Furthermore, Dutta and coworkers [117] decorated SnO_2 quantum dots onto silica nanoparticles and achieved 100% removal of cationic dyes within 5 minutes over a considerable concentration range.

Other than SnO_2 photocatalysts, efficient SnO_2-based nanoadsorbents were also utilized to tackle wastewater contaminants. For example, Dutta *et al.* [118] designed SnO_2-rGO composites for efficient removal of different organic dyes (methylene blue (MB), methyl orange (MO)

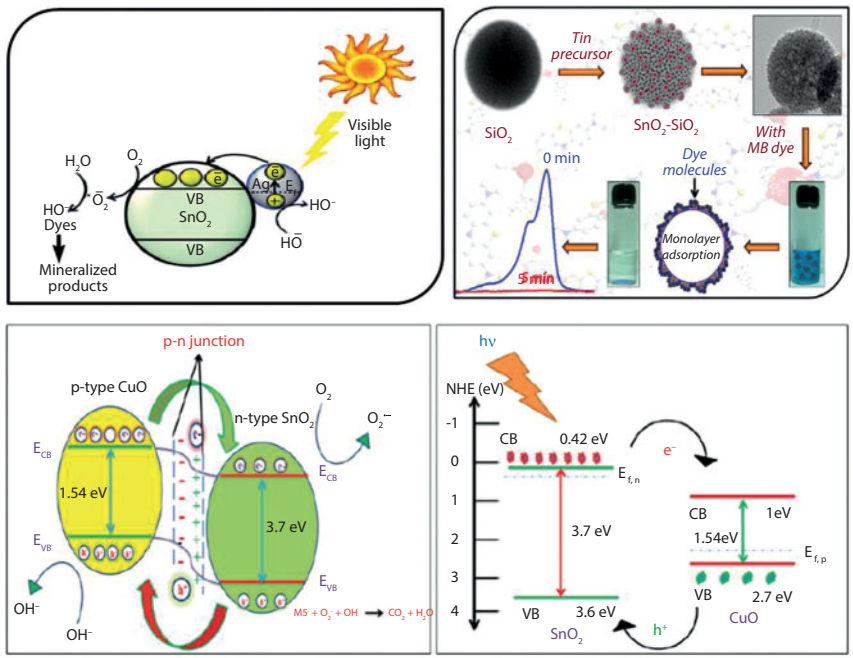


Figure 15.9 Schematic representation of mechanism of degradation by (a) Ag-SnO_2 nanocomposite, (b) SnO_2-SiO_2 nanocomposite, and (c) CuO-SnO_2 nanocomposite. (Reproduced with permission from [115], [117] and [116] respectively).

and rhodamine B (RhB)), toxic metal ions (Co^{2+}, Ni^{2+}, Cu^{2+}, Cd^{2+}, Cr^{3+}, Pb^{2+}, Hg^{2+} and As^{3+}), and pathogenic bacteria (*E. coli*) from wastewater. The adsorption efficiency can be attributed to the electrostatic attraction between the negative surface of QDs-RGO and cationic dyes and heavy metals, and the π-π interactions between the dye molecules and the aromatic rings of graphene. Similarly, Shamsizadeh *et al.* [119] used tin oxide nanoparticle loaded on activated carbon for efficient removal of malachite green-oxalate; Shanmugam *et al.* [120] utilized graphene-SnO_2-PMMA nanohybrid for removal of methylene blue; Vidal *et al.* [121] showed tin oxide pillared montmorillonite (Figure 15.10) as an efficient adsorbent for removal of common pharmaceuticals like trimethoprim and sulfamethoxazole present in wastewater and many more.

Efforts have also been made to construct tin oxide nanostructure-based efficient adsorbents for decontamination of water from toxic ions and heavy metals. Nilchi *et al.* [122] demonstrated the superior adsorption capacity of nanocrystalline tin oxide towards removal of uranium and thorium ions adsorption from aqueous solutions, whereas Parashar *et al.* [123] showed rapid and efficient removal of fluoride ions using a polypyrrole coated hydrous tin oxide nanocomposite. Thus, it is evident that tin-oxide-based materials have immense potential to be used as an efficient photocatalyst as well as a superior nanoadsorbent for the disarticulation of various contaminants from water. However, there is a wide range of improvements regarding efficiency, easy synthetic strategy and convenient mode of operation to robustly take on water pollution.

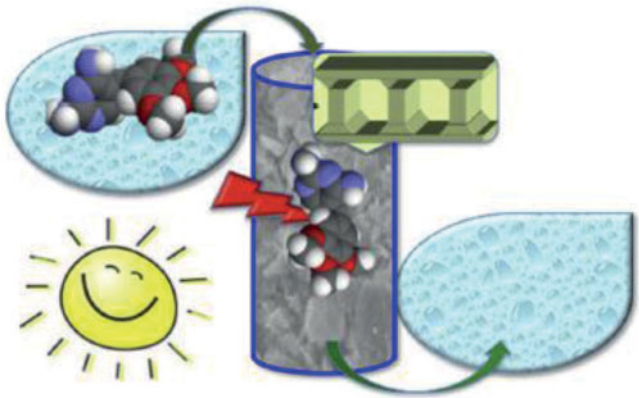


Figure 15.10 Schematic representation of water decontamination using SnO_2 nanoadsorbents. (Reproduced from [121] with permission from Elsevier)

15.4 Clean Energy Generation and Efficient Energy Storage

Sustainable clean energy production and development of next generation energy storage devices are almost certainly the global need of the 21st century due to rapid annihilation of fossil fuels and alarming environmental concerns. Tin oxide nanostructured materials have attracted much attention due to their tremendous potential to address the emerging global challenge of energy generation and storage and find extensive applications in hydrogen production, dye-sensitized solar cells, advanced Li-ion batteries and supercapacitors.

15.4.1 Clean Energy Generation

15.4.1.1 Advanced Tin-Oxide-Based Photo-Electro-Catalyst for Water Splitting

Clean energy generation in the form of hydrogen by water splitting is probably the most promising supplement of fossil fuel as water is plentiful on earth and the process produces oxygen as by-product. However, oxidation of water ($2H_2O \rightarrow O_2 + 4H^+ + 4e^-$) is a high energy process and requires efficient catalyst to occur. Mohanta *et al.* [124] demonstrated the effect of MnO doping on SnO_2 quantum dots towards visible light-induced photoelectrocatalytic water oxidation. It has been reported that the trace amount of MnO impurity activated wide band gap SnO_2 towards water oxidation. The catalyst showed good stability over a considerable amount of time and enhanced photoelectrocatalytic activity for the oxidation of water under alkaline conditions with low overpotential of ~370 mV at 1.0 mA cm^{-2}. Furthermore, Zhao *et al.* [125] reported carbon quantum dots/SnO_2-Co_3O_4 composite for highly efficient electrochemical water oxidation and long-term stability, which was better than either pristine Co_3O_4 or SnO_2-Co_3O_4 composite (Figure 15.11).

Moreover, tin-oxide nanostructures have been extensively employed as support material to enhance activity of many water oxidation catalysts. For instance, Yin and his team [126] used metal-oxide-based tree-like heterostructures grown on fluorine-doped tin oxide as an efficient light-harvesting photoanode to generate H_2 through the water-splitting process. Likewise, ATO nanorod scaffolds supported over FTO have been used to improve hematite's photoelectrochemical water oxidation performance [127]. Recently, mesoporous indium tin oxide electrodes and cobalt modified fluorine doped tin oxide electrodes were also utilized for enhanced photoelectrochemical water oxidation performance [128–129].

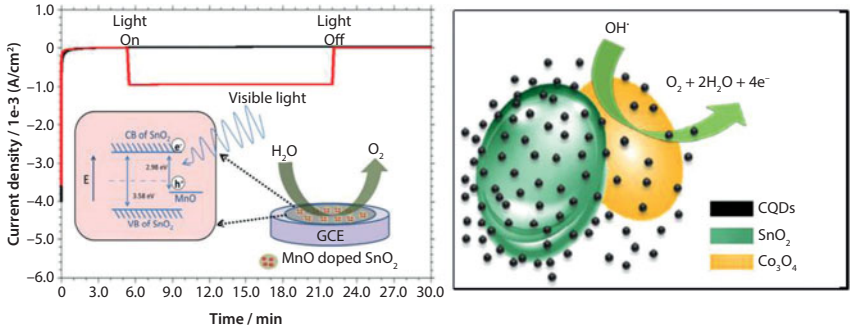


Figure 15.11 Schematic representation of mechanism of water oxidation by (a) MnO-SnO_2 quantum dots, (b) CQDs/SnO_2-Co_3O_4 (Sn:Co = 1:3) nanocomposites. (Reproduced from [124] and [125] respectively with permission from Elsevier)

15.4.1.2 Advanced Tin-Oxide Nanostructures as Anode Materials for Dye-Sensitized Solar Cells

Dye-sensitized solar cells (DSSCs) are green energy devices that directly convert sunlight into electricity and consist of metal oxide semiconductor photoanodes, redox electrolytes, and dye molecules incorporated into photoanode and electrolyte. The dye molecules (S) collect photons and produce the excited electrons (S*) from the HOMO in the ground state to the LUMO in the excited state. The excited dye molecules rapidly inject electrons into the conduction band of the metal oxide semiconductors (SnO_2), which travel through the external circuit and finally reach the counter electrode (Pt), thereby producing photocurrent (Figure 15.12). The oxidized dye receives electron from I^- ion redox to replace the lost electron and the iodide molecules are then oxidized into tri-iodide ions (I_3^-) which then release the electron to the cathode, thereby completing the circuit [130–131].

The performance of DSSCs using SnO_2 nanostructured materials as photoanode is due to their high electron mobility, high redox cycles without undergoing decomposition, ability to attach dye molecules effectively and capability of absorbing radiation of considerable wavelength [132]. Various morphologies of SnO_2 nanostructures, like hierarchical SnO_2 octahedra [133], nanowires [134], quintuple-shelled SnO_2 hollow microspheres [135] and macroporous SnO_2 nanospheres [136], have been employed to achieve superior activity. For example, ordered mesoporous SnO_2 [137] has been reported to have improved efficiency, greater dye-loading capability and enhanced light scattering for DSSC applications. Ga-doped SnO_2 photoanodes [138] were found to have increased performance compared to

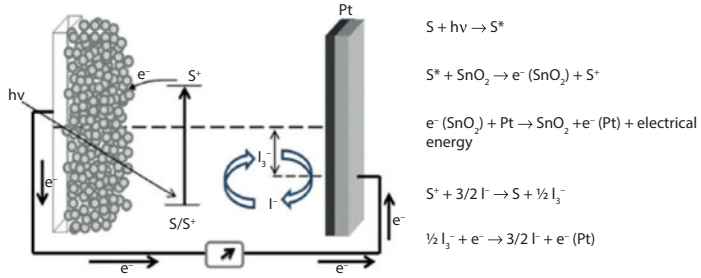


Figure 15.12 Schematic representation and principle of operation of SnO_2-based DSSCs. (Reproduced from [131] with permission from Elsevier)

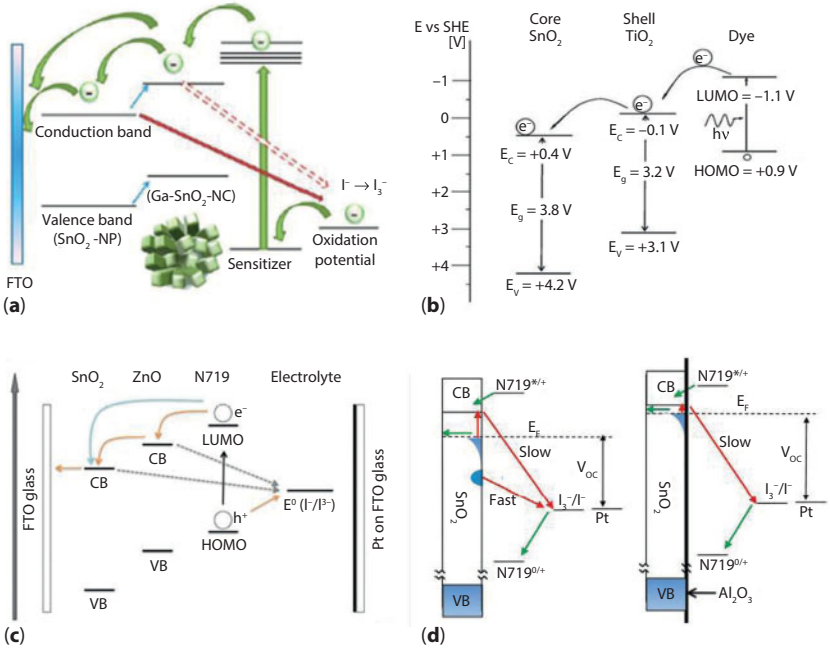


Figure 15.13 Schematic representation of band structure and electron transfer of (a) Ga-SnO_2 photoanode, (b) SnO_2-core/TiO_2-shell photoanode, (c) ZnO-SnO_2 bilayer and (d) SnO_2-Al_2O_3 passivation layer. (Reproduced with permission from [138], [142], [144] and [147] respectively)

pristine SnO_2 due to moderate up-shifting of the band edge, which facilitated electron injection from the sensitizer to the electrode, and hindered electron recombination with the electrolyte (Figure 15.13a). Moreover, to enhance the efficiency of the photoanode, various heterojunctions, like TiO_2-SnO_2, ZnO-SnO_2, SnO_2-Al_2O_3, etc. [139–147], have also been utilized.

For instance, branched and interconnected tin oxide nanowires hybridized with TiO_2 nanoparticles [142] were reported to have superior efficiency and performance due to fast transport of electrons which allows lowering the recombination rate (Figure 15.13b). Similarly, Milan *et al.* [144] demonstrated that ZnO@SnO_2 layered architecture can increase the electron diffusion rate and the charge recombination rate can be lowered for the bilayer structure compared to that of the pristine SnO_2 (Figure 15.13c). Furthermore, Prasittichai and Hupp [147] proposed that a thin layer of Al_2O_3 over SnO_2 photoelectrode is sufficient to extend the electron survival time within the electrode by 2 to 3 orders of magnitude. This modification resulted in a 5-fold increase in energy conversion efficiency and made it possible to use those dyes which were otherwise incapable of injecting electrons into SnO_2.

15.4.2 High-Performance Energy Storage Devices

15.4.2.1 Tin-Oxide-Based Nanomaterials for High-Energy Lithium Ion Batteries

Rechargeable lithium ion batteries, due to their high capacity, high cyclability and flexible design, have been utilized as the most favored power sources for portable electronic devices. SnO_2-based materials have attracted much interest as anode material owing to their high theoretical lithium storage capacity (781 mAh/g), which is more than twice that of conventional graphite anodes (372 mAh/g) [148]. However, there are some limitations, like poor capacity retention over large cycles, large volume change and agglomeration charge/discharge processes, etc., which hinder their practical applicability to a great extant [149]. The limitation of SnO_2-based anode can be related to the following two-step process:

$$SnO_2 + 4Li^+ + 4e^- \longleftrightarrow Sn + 2Li_2O \qquad \text{(Reaction 1)}$$

$$Sn + xLi^+ + xe^- \longleftrightarrow Li_xSn\ (0 \le x \le 4.4) \qquad \text{(Reaction 2)}$$

The first reaction gives the high theoretical capacity; however, being usually irreversible in nature, the capacitance may be lost after the first cycle itself. The second reaction is completely reversible and provides high capacity, but it involves huge volume change, thereby resulting in decrease in capacitance after a few cycles owing to the mechanical damage. Thus, the efficiency of SnO_2-based anodes for Li-ion batteries depends on the reversibility of Reaction 1 and mechanical vulnerability of Reaction 2 [150–151].

Tin-oxide nanostructured materials of different morphologies have been employed to overcome the irreversibility of Reaction 15.1. For example, Ko *et al.* [152] and Meduri *et al.* [148] reported hybrid tin oxide nanowires; and Ning *et al.* [153] reported tin oxide nanoflowers for better reversibility of Reaction 15.1. Likewise, Etacheri *et al.* [154] *constructed* ordered network of interconnected SnO_2 nanoparticles, which showed outstanding discharge capacity of 778 mAh g^{-1} at a current density of 0.1 C. It was claimed that the interconnected mesoporous microstructure of SnO_2 nanoparticles prevents particle agglomeration, accommodates volume changes during the lithiation-delithiation process, and improves solid-state Li-ion diffusion and electrode/electrolyte contact. In this respect, Hu *et al.* [155] recently achieved a dramatic reversibility of the Reaction 15.1 by SnO_2 thin-film electrode, which showed a stable capacitance of 800 mAh g^{-1} over 200 cycles.

To account for the mechanical vulnerability of the tin-oxide anode, hybridization of SnO_2 with carbonaceous materials has been utilized. The carbon-matrix cushions the mechanical strain during volume change, thereby overcoming the effect of volume change, and also provides nanostructured electron collector to homogenize lithiation/delithiation. For example, Wu *et al.* [156] reported that CNTs@SnO_2@C coaxial nanocables can maintain 462.5 mAh g^{-1} after 65 cycles, and Wang *et al.* [157] developed porous SnO_2 nanotubes with coaxially grown carbon nanotube overlayers that can provide 542 mAh g^{-1} after 200 cycles. Similarly, Hu *et al.* [158] showed SnO_2/CNT nanocomposite can provide a capacity of 430 mAh g^{-1} after 300 cycles. Likewise, graphene-SnO_2 nanohybrids were reported to be very promising due to their high surface area, excellent electronic mobility, mechanical support and enhanced stability. Wang *et al.* [159] reported the charge capacities of SnO_2/graphene composites as 590 mAh g^{-1} and 270 mAh g^{-1}, up to 50 cycles; Zhong *et al.* [160] reported 590 mAh g^{-1} after 200 cycles; and Prabakar *et al.* [161] found an excellent capacity of 872 mAh g^{-1} after 100 cycles.

Recently, various new materials with diverse combinations of carbon and tin oxide with different morphologies have been utilized to enhance performance. For instance, SnO_2/polypyrrole hollow spheres [162], hierarchical SnO-SnO_2 composite [163], conductive framework of SnO_2 hollow nanofibers [164], graphene-encapsulated CNT@SnO_2 composite [165], multiwalled carbon nanotubes@C@SnO_2 quantum dots [166], SnO_2 NPs dispersed on graphene wrapped carbon nanotubes [167], binary SnO_2/NiO/C and Sn/C composite nanofibers [168], SnO_2 quantum dots/graphene aerogel composite [169] and many other nanohybrids have been extensively explored for high lithium storage capacity and enhanced durability.

Another approach is to incorporate dopants in carbon-SnO_2 materials to enhance the performance of the anode. Chemical functionalization of carbonaceous materials could potentially produce localized highly reactive regions and thus exhibit unexpected properties. For example, Pham-Cong *et al.* demonstrated exceptional performance and superior cycle stability of nitrogen-doped carbon-coated tin oxide hollow nanofibers [170]. A high specific capacity (1776 mAh g^{-1} at 120 cycles at a current density of 0.2 A g^{-1}) and a good capability (391 mAh g^{-1} at a current density of 3 A g^{-1}) has been reported for the SnO_2/NC hNFs. It was claimed that the exceptional results are due to the trapping phenomenon of Li^+ in N-doped carbon-coated layers and the high efficiency carrier transport effect of the carbon-coated hNFs (Figure 15.14).

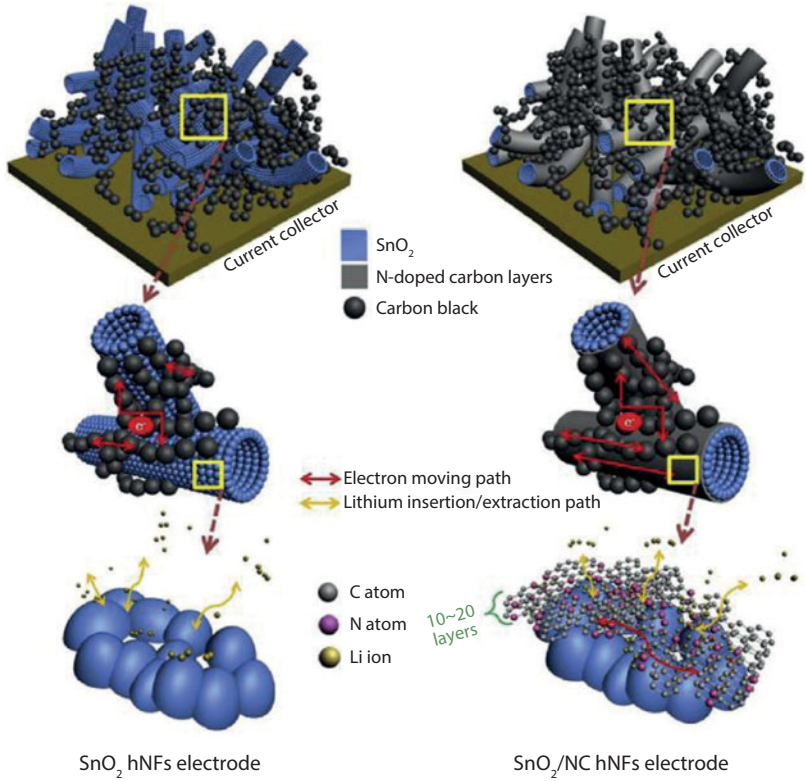


Figure 15.14 Schematic of the lithiation/delithiation processes in both SnO_2 hNF and SnO_2/NC hNF electrodes. In the case of the SnO_2/NC hNFs, several carbon layers contain the N-doping, defects, and vacancies form on the surface of the SnO_2 hNFs, leading to enhanced performance. (Reproduced from [170] with permission from Elsevier)

Likewise, tungsten-doped SnO_2 and graphene nanocomposites [171], fluorine-doped SnO_2 nanoparticles anchored on reduced graphene oxide [172], Sb-doped SnO_2 nanoparticles coated $LiNi_{0.8}Co_{0.15}Al_{0.05}O_2$ [173], SnO_2 quantum dots on nitrogen-doped reduced graphene oxide composite [174] and many more were reported to have high flexibility, superior rate capacity and long life cycle as anode materials in lithium ion batteries.

15.4.2.2 Tin-Oxide Nanomaterials-Based Supercapacitors

High energy storage systems are very essential when dealing with the intermittent nature of renewable energy sources. Although advanced batteries have been successfully employed on a low-power scale, the need for new methodologies to store large amounts of power efficiently is an urgent necessity. Supercapacitors as ideal energy storage devices have attracted intense interest, due to their exceptional electrochemical performance such as high-power capability, fast charging-discharging rate and excellent cycle stability [175]. Unfortunately, SnO_2-based electrodes have some drawbacks, like low electrical conductivity and large volume expansion/shrinkage during the charge-discharge process, which limit their practical usage in supercapacitors. However, various methodologies have been adopted to eliminate the limitations and to enhance the performance [176]. Bonu *et al.* [177] studied the electrochemical supercapacitor behavior of aqua stable pure SnO_2 QDs and reported that small-sized nanocrystals have better stability, low ion diffusion time, higher-ion flux and low pulverization. The capacitance loss for the SnO_2 QDs was reported to be less than 2% after 1000 cycles of charging/discharging. Hao *et al.* [178] demonstrated superior rate capability of 541.0 F g^{-1} at 10.0 A g^{-1} and good cycle stability with capacitance retention of 98.1% after 1000 cycles by three-dimensional Ni foam-supported porous SnO_2 films. It has been claimed that the porous structure of SnO_2 materials resulted in the reduction of resistance and enhancement of active surface area, thereby enhancing the supercapacitance behavior. Likewise, Yan *et al.* [179] utilized MnO_2 coated on SnO_2 nanowires to achieve high specific capacitance of 637 F g^{-1} at a scan rate of 2 mVs^{-1} and excellent long-term cyclic stability with less than1.2% decrease of the specific capacitance after 2000 CV cycles.

The carbon-SnO_2 nanohybrids have also been thoroughly investigated for superior capacitance behavior, as they have excellent cyclic stability and long service lifetime since the electrode does not undergo any chemical change during the charge/discharge processes. For instance, specific capacitance of 294 F g^{-1} was obtained by 2D tin dioxide nanoplatelets decorated graphene [180] and SnO_2/G composite showed specific capacitance of

818.6 F/g at 5 mV/s scan rate [181]. Likewise, SnO_2-decorated multiwalled carbon nanotubes exhibited a specific capacitance of 133.33 F g^{-1} measured at 0.5 mA cm^{-2} and, recently, improved specific capacitance (0.148 F/g), energy density (15.06 mWh/kg), and power density (1.16 W/kg) were obtained by tin oxide nanorod-embedded woven carbon fiber composite supercapacitor [182].

It is evident that SnO_2 nanostructures with various modifications have the potential to address the issues of clean energy generation and efficient high energy storage. However, further technological advancement regarding diversity in morphology, maximization of surface area, meso- and microporous structures, advanced nanocomposites and hybrid nanostructures, etc., is always indispensable to explore the full potential of SnO_2 materials and to optimize their performance towards energy generation and storage.

15.5 Discussion and Future Prospects

The above discussion clearly demonstrates that tin-oxide nanomaterials have enormous potential and innumerable possibilities to address environmental concerns. SnO_2 nanostructures with various morphological/compositional modifications have been successfully utilized for efficient detection of toxic gases with improved sensitivity, decontamination of water from various toxic dyes, pharmaceuticals, organic pollutants, heavy metals, etc., and also as electrode materials in advanced energy generation/storage devices like DSSCs, Li-ion batteries and supercapacitors.

SnO_2-based gas sensors have great advantages, like high sensitivity and selectivity, low operation temperature, fast response/recovery, low power consumption, cost efficiency and easy operation, and thus could be ideal candidates for the next generation gas sensors. In this respect, engineered CNT/graphene-SnO_2 nanostructures, noble metal-SnO_2/metal oxoide-SnO_2 heterojunctions, etc., showed great promise in the enhancement of sensor performance. Similarly, band gap engineering of SnO_2 semiconductors with cation/anion doping and composite formation have improved the visible light-induced photocatalytic behavior of SnO_2 nanostructures towards effective degradation of various toxic dyes, organic contaminants, pharmaceuticals, etc. Furthermore, carbon composites, like activated carbon-SnO_2, CNT-SnO_2, Gr-SnO_2, etc., have also imparted great adsorption capacity to SnO_2 nanostructures towards toxic heavy metals and organic/inorganic adsorbates. Likewise, doped tin oxides, n-n/n-p heterojunction, etc., have been successfully utilized as efficient water oxidation

catalyst as well as improved anode materials for efficient dye-sensitized solar cells. Moreover, various advanced nanostructures of tin oxide with morphological and compositional diversity have eliminated most of the limitations of Li-ion batteries and supercapacitors, thereby enabling them as next generation energy storage devices.

However, before envisaging the widespread practical applications and commercialization of tin oxide nanostructured materials towards environmental applications, some practical challenges need to be weathered. The degradation in performance and quality is expected during large-scale fabrication of the complex nanostructures and hybridized materials. Therefore, more adoptable low-cost fabrication methods for large-scale production are urgently needed. Moreover, utilization of bio-derivatives, like leaves, seeds, seed coats, waste of natural products, etc., as a source of carbon for developing CNTs, graphenes and activated carbons and various biomolecules and leaf extracts as stabilizers during the formation of tin-oxide nanocomposites, can cut down on the cost and also eliminate the use of toxic chemicals and solvents during the synthesis. Thus, breakthrough research is needed to develop environment friendly synthetic strategies and utilization of bio-precursors for advanced tin-oxide nanohybrids and heterostructures with scalability and retention of essential properties. Furthermore, the toxicological assessment and environmental benignity of the synthesized nanomaterials have created a dilemma as nanomaterials, due to the fact that their minute size, which is even smaller than various cellular organelles, can penetrate the basic biological structures, thereby disrupting their normal function and becoming life threatening. It is unethical to find a solution to a big problem which may, by chance, lead to a greater concern. So, it is compulsory to eradicate every possibility of nanotoxicity before commercialization and widespread application of nanostructured materials.

15.6 Conclusion

Increasing concerns about pollution of air/water and rapid annihilation of fossil fuels have exaggerated the need to develop effective materials for toxic gas sensing, water decontamination, clean energy generation and effective energy storage. Tin oxide nanostructured materials have immense potential to address these smoldering environmental issues. This chapter presented a comprehensive outline of green synthetic procedures for the development of tin-oxide nanostructures, various physical/chemical and morphological modifications and detailed mechanisms

which impart enhanced sensing, photocatalytic, photovoltaic, electrochemical and photoelectrochemical properties, thereby enabling them to deal with various environmental problems. However, the fabrication cost, assembly of nanomaterials for precisely controlled structures, high performance and nanotoxicity are still a challenge. Nevertheless, the development of green synthetic strategies, utilization of bio-precursors and exploitation of other possible modifications to enhance properties are believed to have great potential to switch the curiosity-driven discoveries to practical utility of tin oxide nanostructures in resolving environmental concerns.

References

1. Khin, M.M., Nair, A.S., Babu, V.J., Murugan, R., Ramakrishna, S., A review on nanomaterials for environmental remediation. *Ener. Environ. Sci.*, 5(8), 8075–8109, 2012.
2. Wetchakun, K., Samerjai, T., Tamaekong, N., Liewhiran, C., Siriwong, C., Kruefu, V., Wisitsoraat, A., Tuantranont, A., Phanichphant, S., Semiconducting metal oxides as sensors for environmentally hazardous gases. *Sens. Actuators. B*, 160(1), 580–591, 2011.
3. Khreis, H., Kelly, C., Tate, J., Parslow, R., Lucas, K., Nieuwenhuijsen, M., Exposure to traffic-related air pollution and risk of development of childhood asthma: A systematic review and meta-analysis. *Environ. Int.*, 100, 1–31, 2017.
4. Dincer, I., Renewable energy and sustainable development: A crucial review. *Renew. Sust. Energ. Rev.*, 4(2), 157–175, 2000.
5. Khafaie, M.A., Yajnik, C.S., Salvi, S.S., Ojha, A., Critical review of air pollution health effects with special concern on respiratory health. *J. Air Pollut. Health*, 1(2), 123–136, 2016.
6. Lipfert, F.W., A critical review of the ESCAPE project for estimating long-term health effects of air pollution. *Environ. Int.*, 99, 87–96, 2017.
7. Duan, W., Meng, F., Wang, F., Liu, Q., Environmental behavior and ecotoxicity of xylene in aquatic environments: A review. *Ecotoxicol. Environ. Saf.*, 145, 324–332, 2017.
8. Wang, Q., Yang, Z., Industrial water pollution, water environment treatment, and health risks in China. *Environ. Pollut.*, 218, 358–365, 2016.
9. Wan, L., Cai, W., Jiang, Y., Wang, C., Impacts on quality-induced water scarcity: Drivers of nitrogen-related water pollution transfer under globalization from 1995 to 2009. *Environ. Res. Lett.*, 11(7), 074017–074021, 2016.
10. Hosseini, S.E., Wahid, M.A., Hydrogen production from renewable and sustainable energy resources: Promising green energy carrier for clean development. *Renew. Sust. Energ. Rev.*, 57, 850–866, 2016.

11. Apak, S., Atay, E., Tuncer, G., Renewable hydrogen energy and energy efficiency in Turkey in the 21st century. *Int. J. Hyd. Ener.*, 42(4), 2446–2452, 2017.
12. Shmelev, S.E., van den Bergh, J.C., Optimal diversity of renewable energy alternatives under multiple criteria: An application to the UK. *Renew. Sust. Energ. Rev.*, 60, 679–691, 2016.
13. Perera, F.P., Multiple threats to child health from fossil fuel combustion: Impacts of air pollution and climate change. *Environ. Health Perspect.*, 125(2), 141–148, 2017.
14. Zaman, K., Abdullah, I., Ali, M., Decomposing the linkages between energy consumption, air pollution, climate change, and natural resource depletion in Pakistan. *Environ. Prog. Sust.*, 36(2), 638–648, 2017.
15. Khan, S.A.R., Zaman, K., Zhang, Y., The relationship between energy-resource depletion, climate change, health resources and the environmental Kuznets curve: Evidence from the panel of selected developed countries. *Renew. Sust. Energ. Rev.*, 62, 468–477, 2016.
16. Hyeon, T., Manna, L., Wong, S.S., Sustainable nanotechnology. *Chem. Soc. Rev.*, 44(16), 5755–5757, 2015.
17. Ibrahim, R.K., Hayyan, M., AlSaadi, M.A., Hayyan, A., Ibrahim, S., Environmental application of nanotechnology: Air, soil, and water. *Environ. Sci. Pollut. Res.*, 23(14), 13754–13788, 2016.
18. Hussein, A.K., Applications of nanotechnology in renewable energies—A comprehensive overview and understanding. *Renew. Sust. Energ. Rev.*, 42, 460–476, 2015.
19. Ong, W.J., Tan, L.L., Chai, S.P., Yong, S.T., Mohamed, A.R., Facet-dependent photocatalytic properties of TiO_2-based composites for energy conversion and environmental remediation. *ChemSusChem*, 7(3), 690–719, 2014.
20. Sharma, P., Umar, A., Rana, D.S., Kumar, R., Chauhan, S., Chauhan, M.S., Growth and characterization of α-Fe2O3 nanoparticles for environmental remediation and chemical sensor applications. *Sci. Adv. Mater.*, 7(12), 2747–2754. 2015.
21. Lamba, R., Umar, A., Mehta, S.K., Kansal, S.K., ZnO doped SnO_2 nanoparticles heterojunction photo-catalyst for environmental remediation. *J. Alloys Compd.*, 653, 327–333, 2015.
22. Zou, Y., Wang, X., Khan, A., Wang, P., Liu, Y., Alsaedi, A., Wang, X., Environmental remediation and application of nanoscale zero-valent iron and its composites for the removal of heavy metal ions: A review. *Environ. Sci. Technol.*, 50(14), 7290–7304, 2016.
23. Ravi, S., Vadukumpully, S., Sustainable carbon nanomaterials: Recent advances and its applications in energy and environmental remediation. *J. Environ. Chem. Eng.*, 4(1), 835–856, 2016.
24. Wong, K.V., Bachelier, B., Carbon nanotubes used for renewable energy applications and environmental protection/remediation: A review. *J. Energy Resour. Technol.*, 136(2), 021601, 2014.

25. Shi, K., Ren, M., Zhitomirsky, I., Activated carbon-coated carbon nanotubes for energy storage in supercapacitors and capacitive water purification. *ACS Sus. Chem. Eng.*, 2(5), 1289–1298, 2014.
26. Liu, Y., Jiao, Y., Zhang, Z., Qu, F., Umar, A., Wu, X., Hierarchical SnO_2 nanostructures made of intermingled ultrathin nanosheets for environmental remediation, smart gas sensor, and supercapacitor applications. *ACS Appl. Mater. Interfaces*, 6(3), 2174–2184. 2014.
27. Wang, H., Dou, K., Teoh, W.Y., Zhan, Y., Hung, T.F., Zhang, F., Rogach, A.L., Engineering of facets, band structure, and gas-sensing properties of hierarchical Sn^{2+}-Doped SnO_2 nanostructures. *Adv. Funct. Mater.*, 23(38), 4847–4853, 2013.
28. Wang, H., Rogach, A.L., Hierarchical SnO_2 nanostructures: Recent advances in design, synthesis, and applications. *Chem. Mater.*, 26(1), 123–133, 2013.
29. Holkar, C.R., Jadhav, A.J., Pinjari, D.V., Mahamuni, N.M., Pandit, A.B., A critical review on textile wastewater treatments: Possible approaches. *J. Environ. Manage.*, 182, 351–366, 2016.
30. Holkar, C.R., Jadhav, A.J., Pinjari, D.V., Mahamuni, N.M., Pandit, A.B., A critical review on textile wastewater treatments: Possible approaches. *J. Environ. Manage.*, 182, 351–366, 2016.
31. Farhadi, A., Mohammadi, M.R., Ghorbani, M., On the assessment of photocatalytic activity and charge carrier mechanism of TiO_2@SnO_2 core-shell nanoparticles for water decontamination. *J. Photochem. Photobiol. A*, 338, 171–177, 2017.
32. Jia, B., Jia, W., Qu, F., Wu, X., General strategy for self assembly of mesoporous SnO_2 nanospheres and their applications in water purification. *RSC Adv.*, 3(30), 12140–12148, 2013.
33. Duan, T., Chen, Y., Wen, Q., Yin, J., Wang, Y., Three-dimensional macroporous CNT–SnO_2 composite monolith for electricity generation and energy storage in microbial fuel cells. *RSC Adv.*, 6(64), 59610–59618, 2016.
34. Zhang, S., Zhang, P., Wang, Y., Ma, Y., Zhong, J., Sun, X., Facile fabrication of a well-ordered porous Cu-doped SnO_2 thin film for H_2S sensing. *ACS Appl. Mater. Interfaces*, 6(17), 14975–14980, 2014.
35. Chen, W.G., Li, Q.Z., Gan, H.L., Zeng, W., Study of CuO–SnO_2 heterojunction nanostructures for enhanced CO gas sensing properties. *Adv. Appl. Ceram.*, 113(3), 139–146, 2014.
36. Jiang, Y., Wang, W.N., Biswas, P., Fortner, J.D., Facile aerosol synthesis and characterization of ternary crumpled graphene–TiO_2–magnetite nanocomposites for advanced water treatment. *ACS Appl. Mater. Interfaces*, 6(14), 11766–11774, 2014.
37. Pei, L., Jin, Q., Zhu, Z., Zhao, Q., Liang, J., Chen, J., Ice-templated preparation and sodium storage of ultrasmall SnO_2 nanoparticles embedded in three-dimensional graphene. *Nano Res.*, 8(1), 184–192, 2015.
38. Jeong, H.M., Kim, J.H., Jeong, S.Y., Kwak, C.H., Lee, J.H., Co_3O_4–SnO_2 Hollow heteronanostructures: Facile control of gas selectivity by compositional

tuning of sensing materials via galvanic replacement. *ACS Appl. Mater. Interfaces*, 8(12), 7877–7883, 2016.
39. Ju, D.X., Xu, H.Y., Qiu, Z.W., Zhang, Z.C., Xu, Q., Zhang, J., Cao, B.Q., Near room temperature, fast-response, and highly sensitive triethylamine sensor assembled with Au-loaded ZnO/SnO_2 core–shell nanorods on flat alumina substrates. *ACS Appl. Mater. Interfaces*, *7*(34), 19163–19171, 2015.
40. Gu, F., Wang, S.F., Lü, M.K., Zhou, G.J., Xu, D., Uan, D.R., Photoluminescence properties of SnO_2 nanoparticles synthesized by sol–gel method. *J. Phys. Chem. B*, 108(24), 8119–8123, 2004.
41. Lin, Q., Li, Y., Yang, M., Tin oxide/graphene composite fabricated via a hydrothermal method for gas sensors working at room temperature. *Sens. Actuators B*, 173, 139–147. 2012.
42. Wang, Y., Lee, J.Y., Chen, B.H., Microemulsion synthesis of tin oxide-graphite nanocomposites as negative electrode materials for lithium-ion batteries. *Electrochem. Solid-State Lett.*, 6(1), A19-A22, 2003.
43. Mohanta, D., Ahmaruzzaman, M., Tin oxide nanostructured materials: An overview of recent developments in synthesis, modifications and potential applications. *RSC Adv.*, 6(112), 110996–111015, 2016.
44. Zhang, H., Yang, D., Ma, X., Ji, Y., Xu, J., Que, D., Synthesis of flower-like ZnO nanostructures by an organic-free hydrothermal process. *Nanotechnol.*, 15(5), 622–626, 2004.
45. Yec, C.C., Zeng, H.C., Synthesis of complex nanomaterials via Ostwald ripening. *J. Mat. Chem. A*, 2(14), 4843–4851, 2014.
46. Illa, S., Boppella, R., Manorama, S.V., Basak, P., Mesoporous assembly of cuboid anatase nanocrystals into hollow spheres: Realizing enhanced photoactivity of high energy {001} facets. *J. Phys. Chem. C.*, 120(32), 18028–18038, 2016.
47. Kou, J., Bennett-Stamper, C., Varma, R.S., Green synthesis of noble nanometals (Au, Pt, Pd) using glycerol under microwave irradiation conditions. *ACS Sustain. Chem. Eng.*, 1(7), 810–816. 2013.
48. Duan, H., Wang, D., Li, Y., Green chemistry for nanoparticle synthesis. *Chem. Soc. Rev.*, 44(16), 5778–5792, 2015.
49. Iravani, S., Green synthesis of metal nanoparticles using plants. *Green Chem.*, 13(10), 2638–2650, 2011.
50. Fayaz, A.M., Balaji, K., Girilal, M., Yadav, R., Kalaichelvan, P.T., Venketesan, R., Biogenic synthesis of silver nanoparticles and their synergistic effect with antibiotics: A study against gram-positive and gram-negative bacteria. *Nanomed. Nanotech. Biol. Med.*, 6(1), 103–109, 2010.
51. Raveendran, P., Fu, J., Wallen, S.L., Completely "green" synthesis and stabilization of metal nanoparticles. *J. Am. Chem. Soc.*, 125(46), 13940–13941, 2003.
52. Srivastava, N., Mukhopadhyay, M., Biosynthesis of SnO_2 nanoparticles using bacterium *Erwinia herbicola* and their photocatalytic activity for degradation of dyes. *Ind. Eng. Chem. Res.*, 53(36), 13971–13979, 2014.

53. Gattu, K.P., Ghule, K., Kashale, A.A., Patil, V.B., Phase, D.M., Mane, R.S., Han, S.H., Sharma, R., Ghule, A.V., Bio-green synthesis of Ni-doped tin oxide nanoparticles and its influence on gas sensing properties. *RSC Adv.*, 5(89), 72849–72856, 2015.
54. Haq, S., Rehman, W., Waseem, M., Shahid, M., Shah, K.H., Nawaz, M., Adsorption of Cd^{2+} ions on plant mediated SnO_2 nanoparticles. *Mater. Res. Express*, 3(10), 105019–105023, 2016.
55. Fu, L., Zheng, Y., Ren, Q., Wang, A., Deng, B., Green biosynthesis of SnO_2 nanoparticles by *Plectranthus amboinicus* leaf extract their photocatalytic activity toward rhodamine B degradation. *J. Ovonic Res.*, 11(1), 21–26, 2015.
56. Sudhaparimala, S., Green synthesis of tin based nano medicine: Assessment of microstructure and surface property. *Am. J. Nanosci. Nanotechnol.*, 2(4), 75–80, 2014.
57. Hu, J., Science, J.A., Biosynthesis of SnO_2 nanoparticles by fig (*Ficus carica*) leaf extract for electrochemically determining Hg(II) in water samples. *Int. J. Electrochem. Sci.*, 10, 10668–10676, 2015.
58. Roopan, S.M., Kumar, S.H.S., Madhumitha, G., Suthindhiran, K., Biogenic-production of SnO_2 nanoparticles and its cytotoxic effect against hepatocellular carcinoma cell line (HepG2). *Appl. Biochem. Biotechnol.*, 175(3), 1567–1575, 2014.
59. Gowri, S., Gandhi, R.R., Sundrarajan, M., Green synthesis of tin oxide nanoparticles by *Aloe vera*: Structural, optical and antibacterial properties. *J. Nanoelectron. Optoe.*, 8(3), 240–249, 2013.
60. Bhattacharjee, A., Ahmaruzzaman, M., Sil, A.K., Sinha, T., Amino acid mediated synthesis of luminescent SnO_2 nanoparticles. *J. Ind. Eng. Chem.*, 22, 138–146, 2015.
61. Bhattacharjee, A., Ahmaruzzaman, M., Facile synthesis of SnO_2 quantum dots and its photocatalytic activity in the degradation of eosin Y dye: A green approach. *Mater. Lett.*, 139, 418–421, 2015.
62. Tammina, S.K., Mandal, B.K., Tyrosine mediated synthesis of SnO_2 nanoparticles and their photocatalytic activity towards Violet 4 BSN dye. *J. Mol. Liq.*, 221, 415–421, 2016.
63. Begum, S., Devi, T.B., Ahmaruzzaman, M., l-Lysine monohydrate mediated facile and environment friendly synthesis of SnO_2 nanoparticles and their prospective applications as a catalyst for the reduction and photodegradation of aromatic compounds. *J. Environ. Chem. Eng.*, 4(3), 2976–2989, 2016.
64. Kampa, M., Castanas, E., Human health effects of air pollution. *Environ. Pollut.*, 151(2), 362–367, 2008.
65. Curtis, L., Rea, W., Smith-Willis, P., Fenyves, E., Pan, Y., Adverse health effects of outdoor air pollutants. *Environ. Int.*, 32(6), 815–830, 2006.
66. Wang, C., Yin, L., Zhang, L., Xiang, D., Gao, R., Metal oxide gas sensors: Sensitivity and influencing factors. *Sensors*, 10(3), 2088–2106, 2010.

67. Barsan, N., Weimar, U., Understanding the fundamental principles of metal oxide based gas sensors; The example of CO sensing with SnO_2 sensors in the presence of humidity. *J. Phys. Condens. Matter*, 15(20), R813–818, 2003.
68. Eranna, G., Joshi, B.C., Runthala, D.P., Gupta, R.P., Oxide materials for development of integrated gas sensors—A comprehensive review. *Crit. Rev. Solid State*, 29(3–4), 111–188, 2004.
69. Xu, C., Tamaki, J., Miura, N., Yamazoe, N., Grain size effects on gas sensitivity of porous SnO_2-based. *Sens. Actuators B*, 3, 147–155, 1991.
70. Mosadegh Sedghi, S., Mortazavi, Y., Khodadadi, A., Low temperature CO and CH_4 dual selective gas sensor using SnO_2 quantum dots prepared by sonochemical method. *Sens. Actuators B*, 145(1), 7–12, 2010.
71. Comini, E., Faglia, G., Sberveglieri, G., Pan, Z., Wang, Z.L., Stable and highly sensitive gas sensors based on semiconducting oxide nanobelts. *Appl. Phys. Lett.*, 81(10), 1869–1871, 2002.
72. Ingole, S.M., Navale, S.T., Navale, Y.H., Bandgar, D.K., Stadler, F.J., Mane, R.S., Ramgir, N.S., Gupta, S.K., Aswal, D.K., Patil, V.B., Nanostructured tin oxide films: Physical synthesis, characterization, and gas sensing properties. *J. Colloid Interface Sci.*, 493(2), 162–170, 2017.
73. Zhang, W., Cheng, X., Zhang, X., Xu, Y., Gao, S., Zhao, H., Huo, L., High selectivity to ppb-level HCHO sensor based on mesoporous tubular SnO_2 at low temperature. *Sens. Actuators B*, 247, 664–672, 2017.
74. Kolmakov, A., Zhang, Y., Cheng, G., Moskovits, M., Detection of CO and O_2 using tin oxide nanowire sensors. *Adv. Mater.*, 15(12), 997–1000, 2003.
75. Long, H., Harley-Trochimczyk, A., He, T., Pham, T., Tang, Z., Shi, T., Zettl, A., Mickelson, W., Carraro, C., Maboudian, R., *In situ* localized growth of porous tin oxide films on low power microheater platform for low temperature CO detection. *ACS Sensors*, 1(4), 339–343, 2016.
76. Ma, X., Qin, Q., Zhang, N., Chen, C., Liu, X., Chen, Y., Li, C., Ruan, S., Synthesis of SnO_2 nano-dodecahedrons with high-energy facets and their sensing properties to SO_2 at low temperature. *J. Alloys Compd.*, 723, 595–601, 2017.
77. Miller, D.R., Akbar, S.A., Morris, P.A., Nanoscale metal oxide-based heterojunctions for gas sensing: A review. *Sens. Actuators B*, 204, 250–272, 2014.
78. Abideen, Z.U., Kim, J., Kim, S.S., Optimization of metal nanoparticle amount on SnO_2 nanowires to achieve superior gas sensing properties. *Sens. Actuators B*, 238, 374–380, 2017.
79. Wang, Y., Zhao, Z., Sun, Y., Li, P., Ji, J., Chen, Y., Zhang, W., Hu, J., Fabrication and gas sensing properties of Au-loaded SnO_2 composite nanoparticles for highly sensitive hydrogen detection. *Sens. Actuators B*, 240, 664–673, 2017.
80. Li, Y., Deng, D., Chen, N., Xing, X., Liu, X., Xiao, X., Wang, Y., Pd nanoparticles composited SnO_2 microspheres as sensing materials for gas sensors with enhanced hydrogen response performances. *J. Alloys Compd.*, 710, 216–224, 2017.

81. Choudhary, M., Mishra, V.N., Dwivedi, R., Pd-doped tin-oxide-based thick-film sensor array for detection of H_2, CH_4, and CO. *J. Electron. Mater.*, 42(9), 2793–2797, 2013.
82. Li, T., Zeng, W., Wang, Z., Quasi-one-dimensional metal-oxide-based heterostructural gas-sensing materials: A review. *Sens. Actuators B*, 221, 1570–1585, 2015.
83. Ghosh, S., Narjinary, M., Sen, A., Fast detection of low concentration carbon monoxide using calcium-loaded tin oxide sensors. *Sens. Actuators B*, 203, 490–496, 2014.
84. Lin, Z., Li, N., Chen, Z., Fu, P., The effect of Ni doping concentration on the gas sensing properties of Ni doped SnO_2. *Sens. Actuators. B.*, 239, 501–510, 2017.
85. Wang, C., Zeng, W., Luo, L., Zhang, P., Wang, Z., Gas-sensing properties and mechanisms of Cu-doped SnO_2 spheres towards H_2S. *Ceram. Int.*, 42(8), 10006–10013, 2016.
86. Sun, G., Chen, H., Li, Y., Chen, Z., Zhang, S., Ma, G., Jia, T., Cao, J., Bala, H., Wang, X., Zhang, Z., Synthesis and improved gas sensing properties of NiO-decorated SnO_2 microflowers assembled with porous nanorods. *Sens. Actuators B*, 233, 180–192, 2016.
87. Tyagi, P., Sharma, A., Tomar, M., Gupta, V., SnO_2 thin film sensor having NiO catalyst for detection of SO_2 gas with improved response characteristics. *Sens. Actuators B*, 248, 998–1005, 2017.
88. Kwon, Y.J., Na, H.G., Kang, S.Y., Choi, M.S., Bang, J.H., Kim, T.W., Mirzaei, A., Kim, H.W., Attachment of Co_3O_4 layer to SnO_2 nanowires for enhanced gas sensing properties. *Sens. Actuators B*, 239, 180–192, 2017.
89. Ni, Y., Le, K., Du, W., Fang, W., Chen, X., Liu, W., Wang, Y., Liu, J., High response to nitrogen dioxide derived from antimony peroxide modified tin oxide porous nanocomposites serving as gas sensing material. *Sens. Actuators B*, 247, 216–223, 2017.
90. Choi, K.S., Park, S., Chang, S.P., Enhanced ethanol sensing properties based on SnO_2 nanowires coated with Fe_2O_3 nanoparticles. *Sens. Actuators B*, 238, 871–879, 2017.
91. Park, S., An, S., Mun, Y., Lee, C., UV-enhanced NO_2 gas sensing properties of SnO_2-core/ZnO-shell nanowires at room temperature. *ACS Appl. Mater. Interfaces,* 5(10), 4285–4292, 2013.
92. Xu, K., Li, N., Zeng, D., Tian, S., Zhang, S., Hu, D., Xie, C., Interface bonds determined gas-sensing of SnO_2–SnS_2 hybrids to ammonia at room temperature. *ACS Appl. Mater. Interfaces*, 7(21), 11359–11368, 2015.
93. Ling, Z., Leach, C., Freer, R., NO_2 sensitivity of a heterojunction sensor based on WO_3 and doped SnO_2. *J. Eur. Ceram. Soc.*, 23(11), 1881–1891, 2003.
94. Nguyet, Q.T.M., Van Duy, N., Phuong, N.T., Trung, N.N., Hung, C.M., Hoa, N.D., Van Hieu, N., Superior enhancement of NO*2* gas response using n-p-n transition of carbon nanotubes/SnO_2 nanowires heterojunctions. *Sens. Actuators B*, 238, 1120–1127, 2017.

95. Chen, Y., Zhang, W., Wu, Q., A highly sensitive room-temperature sensing material for NH_3: SnO_2-nanorods coupled by rGO. *Sens. Actuators B*, 242, 1216–1226, 2017.
96. Feng, Q., Li, X., Wang, J., Percolation effect of reduced graphene oxide (rGO) on ammonia sensing of rGO-SnO_2 composite based sensor. *Sens. Actuators B*, 243, 1115–1126, 2017.
97. Zhang, D., Liu, J., Jiang, C., Liu, A., Xia, B., Quantitative detection of formaldehyde and ammonia gas via metal oxide-modified graphene-based sensor array combining with neural network model. *Sens. Actuators B*, 240, 55–65, 2017.
98. Song, Z., Wei, Z., Wang, B., Luo, Z., Xu, S., Zhang, W., Yu, H., Li, M., Haung, Z., Zang, J., Yi, F., Liu, H., Sensitive room-temperature H_2S gas sensors employing SnO_2 quantum wire/reduced graphene oxide nanocomposites. *Chem. Mater.*, 28(4), 1205–1212, 2016.
99. Xiao, Y., Yang, Q., Wang, Z., Zhang, R., Gao, Y., Sun, P., Sun, Y., Lu, G., Improvement of NO_2 gas sensing performance based on discoid tin oxide modified by reduced graphene oxide. *Sens. Actuators B*, 227, 419–426, 2016.
100. Zhang, H., Feng, J., Fei, T., Liu, S., Zhang, T., SnO_2 nanoparticles-reduced graphene oxide nanocomposites for NO_2 sensing at low operating temperature. *Sens. Actuators B*, 190, 472–478, 2014.
101. Tyagi, P., Sharma, A., Tomar, M., Gupta, V., A comparative study of RGO-SnO_2 and MWCNT-SnO_2 nanocomposites based SO_2 gas sensors. *Sens. Actuators B*, 248, 980–986, 2017.
102. Liu, S., Wang, Z., Zhang, Y., Zhang, C., Zhang, T., High performance room temperature NO_2 sensors based on reduced graphene oxide-multiwalled carbon nanotubes-tin oxide nanoparticles hybrids. *Sens. Actuators B*, 211, 318–324, 2015.
103. Misra, V., Pandey, S.D., Hazardous waste, impact on health and environment for development of better waste management strategies in future in India. *Environ. Int.*, 31(3), 417–431, 2005.
104. Schwarzenbach, R.P., Escher, B.I., Fenner, K., Hofstetter, T.B., Johnson, C.A., Von Gunten, U., Wehrli, B., The challenge of micropollutants in aquatic systems. *Science*, 313(5790), 1072–1077, 2006.
105. Pal, A., He, Y., Jekel, M., Reinhard, M., Gin, K.Y.H., Emerging contaminants of public health significance as water quality indicator compounds in the urban water cycle. *Environ. Int.*, 71, 46–62, 2014.
106. Bhattacharjee, A., Ahmaruzzaman, M., A green and novel approach for the synthesis of SnO_2 nanoparticles and its exploitation as a catalyst in the degradation of methylene blue under solar radiation. *Mater. Lett.*, 145, 74–78, 2015.
107. Bhattacharjee, A., Ahmaruzzaman, M., Sinha, T., A novel approach for the synthesis of SnO_2 nanoparticles and its application as a catalyst in the reduction and photodegradation of organic compounds. *Spectrochim. Acta A,* 136, 751–760, 2015.

108. Bhattacharjee, A., Ahmaruzzaman, M., A novel and green process for the production of tin oxide quantum dots and its application as a photocatalyst for the degradation of dyes from aqueous phase. *J. Colloid Interface Sci.*, 448, 130–139, 2015.
109. Bhattacharjee, A., Ahmaruzzaman, M., Devi, T.B., Nath, J., Photodegradation of methyl violet 6B and methylene blue using tin-oxide nanoparticles (synthesized via a green route). *J. Photochem. Photobiol. A*, 325, 116–124, 2016.
110. Elango, G., Kumaran, S.M., Kumar, S.S., Muthuraja, S., Roopan, S.M., Green synthesis of SnO_2 nanoparticles and its photocatalytic activity of phenolsulfonphthalein dye. *Spectrochim. Acta A,* 145, 176–180, 2015.
111. Prakash, K., Senthil Kumar, P., Pandiaraj, S., Saravanakumar, K., Karuthapandian, S., Controllable synthesis of SnO_2 photocatalyst with superior photocatalytic activity for the degradation of methylene blue dye solution. *J. Exp. Nanosci.*, 11(14), 1138–1155, 2016.
112. Begum, S., Devi, T.B., Ahmaruzzaman, M., Surfactant mediated facile fabrication of SnO_2 quantum dots and their degradation behavior of humic acid. *Mater. Lett.*, 185, 123–126, 2016.
113. Pan, R., Pan, S., Zhou, J., Wu, Y., Surface-modification of indium tin oxide nanoparticles with titanium dioxide by a nonaqueous process and its photocatalytic properties. *Appl. Surf. Sci.*, 255(6), 3642–3647, 2009.
114. Sinha, A.K., Pradhan, M., Sarkar, S., Pal, T., Large-scale solid-state synthesis of Sn–SnO_2 nanoparticles from layered SnO by sunlight: A material for dye degradation in water by photocatalytic reaction. *Environ. Sci. Technol.*, 47(5), 2339–2345, 2013.
115. Sinha, T., Ahmaruzzaman, M., Adhikari, P.P., Bora, R., Green and environmentally sustainable fabrication of Ag-SnO_2 nanocomposite and its multifunctional efficacy as photocatalyst and antibacterial and antioxidant agent. *ACS Sustainable Chem. Eng.,* 5(6), 4645–4655, 2017.
116. Kumar, A., Rout, L., Achary, L.S.K., Mohanty, A., Marpally, J., Chand, P.K., Dash, P., Design of binary SnO_2-CuO nanocomposite for efficient photocatalytic degradation of malachite green dye, in: *AIP Conference Proceedings*, vol. 1724, no. 1, 020027, AIP Publishing, 2016.
117. Dutta, D., Thakur, D., Bahadur, D., SnO_2 quantum dots decorated silica nanoparticles for fast removal of cationic dye (methylene blue) from wastewater. *Chem. Eng. J.*, 281, 482–490, 2015.
118. Dutta, D., Thiyagarajan, S., Bahadur, D., SnO_2 quantum dots decorated reduced graphene oxide nanocomposites for efficient water remediation. *Chem. Eng. J.*, 297, 55–65, 2016.
119. Shamsizadeh, A., Ghaedi, M., Ansari, A., Azizian, S., Purkait, M.K., Tin oxide nanoparticle loaded on activated carbon as new adsorbent for efficient removal of malachite green-oxalate: Non-linear kinetics and isotherm study. *J. Mol. Liq.*, 195, 212–218, 2014.
120. Shanmugam, M., Alsalme, A., Alghamdi, A., Jayavel, R., Photocatalytic properties of Graphene-SnO2-PMMA nanocomposite in the degradation of

methylene blue dye under direct sunlight irradiation. *Mater. Express*, 5(4), 319–326, 2015.
121. Vidal, C.B., dos Santos, A.B., do Nascimento, R.F., Bandosz, T.J., Reactive adsorption of pharmaceuticals on tin oxide pillared montmorillonite: Effect of visible light exposure. *Chem. Eng. J.*, 259, 865–875, 2015.
122. Nilchi, A., Dehaghan, T.S., Garmarodi, S.R., Kinetics, isotherm and thermodynamics for uranium and thorium ions adsorption from aqueous solutions by crystalline tin oxide nanoparticles. *Desalination*, 321, 67–71, 2013.
123. Parashar, K., Ballav, N., Debnath, S., Pillay, K., Maity, A., Rapid and efficient removal of fluoride ions from aqueous solution using a polypyrrole coated hydrous tin oxide nanocomposite. *J. Colloid Interface Sci.*, 476, 103–118, 2016.
124. Mohanta, D., Barman, K., Jasimuddin, S., Ahmaruzzaman, M., MnO doped SnO_2 nanocatalysts: Activation of wide band gap semiconducting nanomaterials towards visible light induced photoelectrocatalytic water oxidation. *J. Colloid Interface Sci.*, 505, 756–762, 2017.
125. Zhao, S., Li, C., Liu, J., Liu, N., Qiao, S., Han, Y., Kang, Z., Carbon quantum dots/SnO_2–Co_3O_4 composite for highly efficient electrochemical water oxidation. *Carbon*, 92, 64–73, 2015.
126. Yin, Z., Wang, Z., Du, Y., Qi, X., Huang, Y., Xue, C., Zhang, H., Full solution-processed synthesis of all metal oxide-based tree-like heterostructures on fluorine-doped tin oxide for water splitting. *Adv. Mater.*, 24(39), 5374–5378, 2012.
127. Sun, Y., Chemelewski, W.D., Berglund, S.P., Li, C., He, H., Shi, G., Mullins, C.B., Antimony-doped tin oxide nanorods as a transparent conducting electrode for enhancing photoelectrochemical oxidation of water by hematite. *ACS Appl. Mater. Interfaces*, 6(8), 5494–5499, 2014.
128. Kato, M., Cardona, T., Rutherford, A.W., Reisner, E., Photoelectrochemical water oxidation with photosystem II integrated in a mesoporous indium–tin oxide electrode. *J. Am. Chem. Soc.*, 134(20), 8332–8335, 2012.
129. Kent, C.A., Concepcion, J.J., Dares, C.J., Torelli, D.A., Rieth, A.J., Miller, A.S., Meyer, T.J., Water oxidation and oxygen monitoring by cobalt-modified fluorine-doped tin oxide electrodes. *J. Am. Chem. Soc.*, 135(23), 8432–8435, 2013.
130. Shalini, S., Prasanna, S., Mallick, T.K., Senthilarasu, S., Review on natural dye sensitized solar cells: Operation, materials and methods. *Renew. Sustain. Energ. Rev.*, 51, 1306–1325, 2015.
131. Ludin, N.A., Mahmoud, A.A.A., Mohamad, A.B., Kadhum, A.A.H., Sopian, K., Karim, N.S.A., Review on the development of natural dye photosensitizer for dye-sensitized solar cells. *Renew. Sustain. Energ. Rev.*, 31, 386–396, 2014.
132. Gong, J., Sumathy, K., Qiao, Q., Zhou, Z., Review on dye-sensitized solar cells (DSSCs): Advanced techniques and research trends. *Renew. Sustain. Energ. Rev.*, 68, 234–246, 2017.
133. Wang, Y.F., Li, J.W., Hou, Y.F., Yu, X.Y., Su, C.Y., Kuang, D.B., Hierarchical tin oxide octahedra for highly efficient dye-sensitized solar cells. *Chem. Eur. J.*, 16(29), 8620–8625, 2010.

134. Gubbala, S., Russell, H.B., Shah, H., Deb, B., Jasinski, J., Rypkema, H., Sunkara, M.K., Surface properties of SnO_2 nanowires for enhanced performance with dye-sensitized solar cells. *Energy Environ. Sci.*, 2(12), 1302–1309, 2009.
135. Dong, Z., Ren, H., Hessel, C.M., Wang, J., Yu, R., Jin, Q., Zhao, H., Quintuple-shelled SnO_2 hollow microspheres with superior light scattering for high-performance dye-sensitized solar cells. *Adv. Mater.*, 26(6), 905–909, 2014.
136. Li, K.N., Wang, Y.F., Xu, Y.F., Chen, H.Y., Su, C.Y., Kuang, D.B., Macroporous SnO_2 synthesized via a template-assisted reflux process for efficient dye-sensitized solar cells. *ACS Appl. Mater. Interfaces*, 5(11), 5105–5111, 2013.
137. Ramasamy, E., Lee, J., Ordered mesoporous SnO_2–based photoanodes for high-performance dye-sensitized solar cells. *J. Phys. Chem. C*, 114(50), 22032–22037, 2010.
138. Teh, J.J., Ting, S.L., Leong, K.C., Li, J., Chen, P., Gallium-doped tin oxide nano-cuboids for improved dye sensitized solar cell. *ACS Appl. Mater. Interfaces*, 5(21), 11377–11382, 2013.
139. Ahn, S.H., Kim, D.J., Chi, W.S., Kim, J.H., One-dimensional hierarchical nanostructures of TiO_2 nanosheets on SnO_2 nanotubes for high efficiency solid-state dye-sensitized solar cells. *Adv. Mater.*, 25(35), 4893–4897, 2013.
140. Desai, U.V., Xu, C., Wu, J., Gao, D., Hybrid TiO_2–SnO_2 nanotube arrays for dye-sensitized solar cells. *J. Phys. Chem. C*, 117(7), 3232–3239, 2013.
141. Ahn, S.H., Kim, D.J., Chi, W.S., Kim, J.H., Hierarchical double-shell nanostructures of TiO_2 nanosheets on SnO_2 hollow spheres for high-efficiency, solid-state, dye-sensitized solar cells. *Adv. Funct. Mater.*, 24(32), 5037–5044, 2014.
142. Gubbala, S., Chakrapani, V., Kumar, V., Sunkara, M.K., Band-edge engineered hybrid structures for dye-sensitized solar cells based on SnO_2 nanowires. *Adv. Funct. Mater.*, 18(16), 2411–2418, 2008.
143. Huu, N.K., Son, D.Y., Jang, I.H., Lee, C.R., Park, N.G., Hierarchical SnO_2 nanoparticle-ZnO nanorod photoanode for improving transport and life time of photoinjected electrons in dye-sensitized solar cell. *ACS Appl. Mater. Interfaces*, 5(3), 1038–1043. 2013.
144. Milan, R., Selopal, G.S., Epifani, M., Natile, M.M., Sberveglieri, G., Vomiero, A., Concina, I., ZnO@ SnO2 engineered composite photoanodes for dye sensitized solar cells. *Sci. Rep.*, 5, 1–12, 2015.
145. Qian, J., Liu, P., Xiao, Y., Jiang, Y., Cao, Y., Ai, X., Yang, H., TiO_2-coated multilayered SnO_2 hollow microspheres for dye-sensitized solar cells. *Adv. Mater.*, 21(36), 3663–3667, 2009.
146. Thapa, A., Zai, J., Elbohy, H., Poudel, P., Adhikari, N., Qian, X., Qiao, Q., TiO_2 coated urchin-like SnO_2 microspheres for efficient dye-sensitized solar cells. *Nano Res.*, 7(8), 1154–1163, 2014.
147. Prasittichai, C., Hupp, J.T., Surface modification of SnO_2 photoelectrodes in dye-sensitized solar cells: significant improvements in photovoltage via Al_2O_3 atomic layer deposition. *J. Phys. Chem. Lett.*, 1(10), 1611–1615, 2010.

148. Meduri, P., Pendyala, C., Kumar, V., Sumanasekera, G.U., Sunkara, M.K., Hybrid tin oxide nanowires as stable and high capacity anodes for Li-ion batteries. *Nano Lett.*, 9(2), 612–616, 2009.
149. Du, G., Zhong, C., Zhang, P., Guo, Z., Chen, Z., Liu, H., Tin dioxide/carbon nanotube composites with high uniform SnO_2 loading as anode materials for lithium ion batteries. *Electrochim. Acta*, 55(7), 2582–2586, 2010.
150. Dong, W., Xu, J., Wang, C., Lu, Y., Liu, X., Wang, X., Yuan, X., Wang, Z., Lin, T., Sui, M., Chen, I., Huang, F., A robust and conductive black tin oxide nanostructure makes efficient lithium-ion batteries possible. *Adv. Mater.,* 29, 1700136, 2017.
151. Lu, L., Han, X., Li, J., Hua, J., Ouyang, M., A review on the key issues for lithium-ion battery management in electric vehicles. *J. Power Sources*, 226, 272–288, 2013.
152. Ko, Y.D., Kang, J.G., Park, J.G., Lee, S., Kim, D.W., Self-supported SnO_2 nanowire electrodes for high-power lithium-ion batteries. *Nanotechnol.*, 20(45), 455701–455706 2009.
153. Ning, J., Dai, Q., Jiang, T., Men, K., Liu, D., Xiao, N., Zou, G., Facile synthesis of tin oxide nanoflowers: A potential high-capacity lithium-ion-storage material. *Langmuir*, 25(3), 1818–1821, 2008.
154. Etacheri, V., Seisenbaeva, G.A., Caruthers, J., Daniel, G., Nedelec, J.M., Kessler, V.G., Pol, V.G., Ordered network of interconnected SnO_2 nanoparticles for excellent lithium-ion storage. *Adv. Energy Mater.*, 5(5), 140289–140294, 2015.
155. Hu, R., Chen, D., Waller, G., Ouyang, Y., Chen, Y., Zhao, B., Liu, M., Dramatically enhanced reversibility of Li_2O in SnO_2-based electrodes: The effect of nanostructure on high initial reversible capacity. *Energy Environ. Sci.*, 9(2), 595–603, 2016.
156. Wu, P., Du, N., Zhang, H., Yu, J., Yang, D., CNTs@SnO_2@C coaxial nanocables with highly reversible lithium storage. *J. Phys. Chem. C*, 114(51), 22535–22538, 2010.
157. Wang, Y., Zeng, H.C., Lee, J.Y., Highly reversible lithium storage in porous SnO_2 nanotubes with coaxially grown carbon nanotube overlayers. *Adv. Mater.*, 18(5), 645–649, 2006.
158. Hu, R., Sun, W., Liu, H., Zeng, M., Zhu, M., The fast filling of nano-SnO_2 in CNTs by vacuum absorption: A new approach to realize cyclic durable anodes for lithium ion batteries. *Nanoscale*, 5(23), 11971–11979, 2013.
159. Xin, X., Zhou, X., Wang, F., Yao, X., Xu, X., Zhu, Y., Liu, Z., A 3D porous architecture of Si/graphene nanocomposite as high-performance anode materials for Li-ion batteries. *J. Mater. Chem.*, 22(16), 7724–7730, 2012.
160. Zhong, C., Wang, J., Chen, Z., Liu, H., SnO_2–graphene composite synthesized via an ultrafast and environmentally friendly microwave autoclave method and its use as a superior anode for lithium-ion batteries. *J. Phys. Chem. C*, 115(50), 25115–25120, 2011.

161. Prabakar, S.J., Hwang, Y.H., Bae, E.G., Shim, S., Kim, D., Lah, M.S., Pyo, M., SnO_2/graphene composites with self-assembled alternating oxide and amine layers for high li-storage and excellent stability. *Adv. Mater.*, 25(24), 3307–3312, 2013.
162. Yuan, J., Chen, C., Hao, Y., Zhang, X., Zou, B., Agrawal, R., Xiong, Z., SnO 2/ polypyrrole hollow spheres with improved cycle stability as lithium-ion battery anodes. *J. Alloys Compd.*, 691, 34–39, 2017.
163. Kim, J. H., Jeon, K. M., Park, J. S., Kang, Y. C., Excellent Li-ion storage performances of hierarchical SnO-SnO 2 composite powders and SnO nanoplates prepared by one-pot spray pyrolysis. *J. Power Sources*, 359, 363–370, 2017.
164. Pham-Cong, D., Kim, J.Y., Park, J.S., Kim, J.H., Kim, J.P., Jeong, E.D., Cho, C.R., Conductive framework supported high rate performance of SnO_2 hollow nanofibers for lithium battery anodes. *Electrochim. Acta*, 161, 1–9, 2015.
165. Zhou, D., Li, X., Fan, L.Z., Deng, Y., Three-dimensional porous graphene-encapsulated CNT@SnO_2 composite for high-performance lithium and sodium storage. *Electrochim. Acta*, 230, 212–221, 2017.
166. Jin, R., Meng, Y., Li, G., Multiwalled carbon nanotubes@C@SnO_2 quantum dots and SnO_2 quantum dots@C as high rate anode materials for lithium-ion batteries. *Appl. Surf. Sci.*, 423, 476–483, 2017.
167. Sahoo, M., Ramaprabhu, S., Solar synthesized tin oxide nanoparticles dispersed on graphene wrapped carbon nanotubes as a Li ion battery anode material with improved stability. *RSC Adv.*, 7(23), 13789–13797, 2017.
168. Agubra, V.A., Zuniga, L., Flores, D., Campos, H., Villarreal, J., Alcoutlabi, M., A comparative study on the performance of binary SnO_2/NiO/C and Sn/C composite nanofibers as alternative anode materials for lithium ion batteries. *Electrochim, Acta*, 224, 608–621, 2017.
169. Wang, Y., Jin, Y., Zhao, C., Duan, Y., He, X., Jia, M., SnO_2 quantum dots/ graphene aerogel composite as high-performance anode material for sodium ion batteries. *Mater. Lett.*, 191, 169–172 2017.
170. Pham-Cong, D., Park, J.S., Kim, J.H., Kim, J., Braun, P.V., Choi, J.H., Cho, C.R., Enhanced cycle stability of polypyrrole-derived nitrogen-doped carbon-coated tin oxide hollow nanofibers for lithium battery anodes. *Carbon*, 111, 28–37, 2017.
171. Wang, S., Shi, L., Chen, G., Ba, C., Wang, Z., Zhu, J., Yuan, S., *In situ* synthesis of tungsten-doped SnO_2 and graphene nanocomposites for high-performance anode materials of lithium-ion batteries. *ACS Appl. Mater. Interfaces*, 9(20), 17163–17171, 2017.
172. Cui, D., Zheng, Z., Peng, X., Li, T., Sun, T., Yuan, L., Fluorine-doped SnO_2 nanoparticles anchored on reduced graphene oxide as a high-performance lithium ion battery anode. *J. Power Sources*, 362, 20–26. 2017.
173. He, X., Du, C., Shen, B., Chen, C., Xu, X., Wang, Y., Yin, G., Electronically conductive Sb-doped SnO_2 nanoparticles coated LiNi 0.8 Co 0.15 Al 0.05

O 2 cathode material with enhanced electrochemical properties for Li-ion batteries. *Electrochim. Acta*, 236, 273–279, 2017.
174. Zhang, W., Li, M., Xiao, X., Huang, X., Jiang, Y., Fan, X., Chen, L., *In situ* synthesis of ultrasmall SnO_2 quantum dots on nitrogen-doped reduced graphene oxide composite as high performance anode material for lithium-ion batteries. *J. Alloys Compd.,* 2, 258–264, 2017.
175. González, A., Goikolea, E., Barrena, J.A., Mysyk, R., Review on supercapacitors: technologies and materials. *Ren. Sust. Energy Rev.*, 58, 1189–1206, 2016.
176. Wang, G., Zhang, L., Zhang, J., A review of electrode materials for electrochemical supercapacitors. *Chem. Soc. Rev.*, 41(2), 797–828. 2012.
177. Bonu, V., Gupta, B., Chandra, S., Das, A., Dhara, S., Tyagi, A.K., Electrochemical supercapacitor performance of SnO_2 quantum dots. *Electrochim. Acta*, 203, 230–237, 2016.
178. Hao, S., Sun, Y., Liu, Y., Zhang, Y., Hu, G., Facile synthesis of porous SnO_2 film grown on Ni foam applied for high-performance supercapacitors. *J. Alloys Compd.*, 689, 587–592, 2016.
179. Yan, J., Khoo, E., Sumboja, A., Lee, P.S., Facile coating of manganese oxide on tin oxide nanowires with high-performance capacitive behavior. *ACS Nano*, 4(7), 4247–4255, 2010.
180. Li, Z., Chang, T., Yun, G., Guo, J., Yang, B., 2D tin dioxide nanoplatelets decorated graphene with enhanced performance supercapacitor. *J. Alloys Compd.*, 586, 353–359, 2014.
181. Velmurugan, V., Srinivasarao, U., Ramachandran, R., Saranya, M., Grace, A.N., Synthesis of tin oxide/graphene (SnO_2/G) nanocomposite and its electrochemical properties for supercapacitor applications. *Mater. Res. Bull.*, 84, 145–151. 2016.
182. Vinoth, V., Wu, J.J., Asiri, A.M., Lana-Villarreal, T., Bonete, P., Anandan, S., SnO_2-decorated multiwalled carbon nanotubes and Vulcan carbon through a sonochemical approach for supercapacitor applications. *Ultra. Sonochem.*, 29, 205–212. 2016.

Part IV

BIOSYNTHESIS OF NOBLE METAL NANOPARTICLES

Suvardhan Kanchi and Shakeel Ahmed (eds.) Green Metal Nanoparticles, (553–602)
© 2018 Scrivener Publishing LLC

16

Green Synthesis of Noble Metal Nanoparticles: A Step Forward to Economical and Sustainable Development

Santanu Patra, Rashmi Madhuri*

Department of Applied Chemistry, Indian Institute of Technology (Indian School of Mines), Dhanbad, Jharkhand, India

Abstract

Mankind has been fascinated by gold and silver since prehistoric times, due to their wide variety of biological and medical use. Following the entry of nanotechnology into our day-to-day lives, the place of noble metals has been taken by their nanostructural analogues, i.e., noble metal nanoparticles. The noble metal nanoparticles have attracted a huge amount of interest in the scientific community owing to their fabulous properties and diverse applications. Numerous studies have been reported on their various synthesis strategies or applications. In recent times, after our activities have caused so much environmental harm, our concern towards the environment have awaken us to the use of chemicals in research. Therefore, a class of green chemistry has come to light, which may be treated as a gift to the environment from scientists. The green chemistry approach for nanoparticle synthesis has been presented as a cost-effective and environmentally friendly alternative to the toxic and costly chemical and physical approaches. As the two most common ways to synthesize nanoparticles in a greener way, plant-mediated and microbe-mediated synthesis approaches have opened up a new possibility of eco-friendly synthesis of nanostructures. In this chapter we have summarized the different synthesis approaches used so far for the designing of noble metal—i.e., gold (Au), silver (Ag) and platinum (Pt) nanoparticles—in a green way. The green-synthesis approach for metal nanoparticles synthesis is mostly confined towards

**Corresponding author*: patra.santanu82@gmail.com

Suvardhan Kanchi and Shakeel Ahmed (eds.) Green Metal Nanoparticles, (555–602)
© 2018 Scrivener Publishing LLC

development of spherical-shaped nanoparticles. However, recently synthesis of non-spherical or different shaped metal nanoparticles has also been reported through green synthesis approach, and therefore considered in this chapter. This chapter is an effort to compile reported green synthesis approaches for noble metal nanoparticles with a special emphasis on the fabrication of different shaped nanomaterials. A critical discussion regarding the future, advantages and disadvantages of these green noble metal nanoparticles synthesis are also incorporated in this chapter.

Keywords: Green synthesis, green chemistry, nanoparticles, noble metals, plant mediated synthesis, microbes mediated synthesis, algae and fungi mediated synthesis

16.1 Overview of Nanoparticles

The transformation of matter at the nanoscale, i.e., synthesis of nanomaterials, is the most promising discovery of this century. The word "Nano" originated from the Greek word "Dwarf," and stands for "a billionth" of a meter, which can be calculated as 25,400,000 nanometers in one inch [1]. The diameter of a sole gold atom is around one third of a nanometer, whereas, one nanometer can be compared to one second of growth of a fingernail. It is true that modern nanoscience and nanotechnology are quite new; however, it is a misconception that nanoparticles are a discovery of this century or era. Actually, nanoparticles have a very long history and were used by artisans in the ninth century to create color and luster in the stained glass windows of medieval churches by just altering the size of gold and silver particles [2]. The only difference we have achieved nowadays is that artists back then were using the process just to create beautiful works of art without knowing the theory or concept behind it. The scientists and engineers of recent days have started to make materials within a nano-size to take advantage of their improved magnetic, optoelectronic and physicochemical properties, directed by the shape and size of nanoparticles [3]. Having an extremely small size, i.e., in the nanometer range, the surface area to volume ratio gets enhanced, which leads to the development of some extraordinary properties in the nanomaterials, which cannot be observed in the same material in bulk or larger form [4]. Owing to their unique optoelectronic and physicochemical properties, nanoparticles have entered almost every aspect of our daily lives, from food/drink, household items, medical services (drugs or diagnosis), electronic gadgets, books to everything else [5]. By the simple concept of business, the things

used more often will be in demand, so more are required to be developed or made.

As the demand for nanoparticle applications is increasing, a number of strategies have been discovered for the large-scale synthesis of nanoparticles. Primarily, the synthesis of nanoparticles is based on two broad categories, i.e., bottom-up and top-down approaches [6]. As the name suggests, the classification was done on the basis of selection of precursors used to synthesize nanoparticles. We can either make a big thing to a small one or many small things can gather together to make a big thing. The transformation could be done either through chemical process or physical process. For example, in the top-down approach the bigger material could be altered to nanometer size either by using some externally controlled tools, like cutting, milling, etching, etc., or the nanoparticles could be synthesized through the reduction of a suitable bulk material into nanoparticles having a desired size using chemicals, i.e., chemical etching [7]. Some very popular physical methods for the top-down approach are laser ablation [8], lithography [9], pyrolysis [10], thermolysis [11], radiation-induced methods [12] and electrospinning [13]. Although these methods are very popular and used by several researchers/scientist in the literature, they suffer from certain limitations like high instrumentation cost, are tedious to do and high skill is needed to perform the synthesis [7, 14]. In addition, they lead to the construction of defects on the surface structures of nanoparticle and consequently the property of nanoparticles might change [7, 14]. A vast amount of energy consumption takes place to maintain the high pressure and high temperature conditions used during the synthesis processes, which is the other considerable limitation of the top-down approaches [7, 14].

In contrast to the "bottom-up approaches," also called self-assembly approaches, nano-sized materials are primarily fabricated through the association of the molecules, clusters or atoms. In bottom-up approaches, one can get a more homogeneous chemical composition at low cost. The popularly reported bottom-up method includes chemical [15], electrochemical [16], sonochemical [17] and polyol reduction [18] procedures. Among these, the wet chemical procedures prove to be the most effective way to synthesize nanoparticles in a cost-effective way [19]. However, they also suffer from some negatives, like utilization of nonpolar organic solvents, toxic chemicals, capping agents and stabilizing agents, which restrict their applications in the biomedical and/or clinical field.

So, in the initial development stage of nanotechnology, everyone is just oriented towards the pros and no one counts or thinks about the cons.

Initially, we all are so hypnotized by the fascinating face of this technology, that we fail to see its evil face. For the development of nanoparticles, we searched for and researched so many synthesis processes and used enormous amounts of chemicals, but we forgot to think about our environment. Therefore, a hike in the demand for nanoparticles, rapid industrialization, and an upsurge in the field of research has resulted in the weakening of earth's atmosphere and an enormous amount of unwanted and hazardous substances being freed into it. Now, it is high time for us to save the environment and stop its deformation and destruction.

16.1.1 What is Green Chemistry and Why Is It Gaining Importance Nowadays?

Based on the problems discussed above, the term "green synthesis" is a solution and is regarded by scientists and researchers as a gift from the gods to the environment. Green synthesis or green chemistry is actually a way to use the secrets of nature and its natural products and implement them in the synthesis of nanoparticles [20]. As a replacement for toxic and costly chemical and physical approaches, the green-synthesis approach is a very reliable, nontoxic, clean, biocompatible and most importantly environment friendly method. Green chemistry, which is currently in the beginning phase, has two priorities:

1. Inventing new synthesis procedures for nanoparticles without using harmful chemical or toxic reagents, which does not harm the environment further.
2. Developing new technologies using nanoparticles as a solution to the existing problems related to the environment and human health.

In order to fulfill these two goals, the foremost step will be synthesis of nano-sized materials in a green way with less energy consumption, atom economy, full use of natural/renewable sources and less toxic or water like reagents or solvents. The green synthesis of nanoparticles is a kind of bottom-up synthesis approach, having much similarity to the chemical reduction method. But in the case of green synthesis, a costly chemical reducing agent is interchanged with natural products like plant extract, fruit juice, leaf extract, etc. However, the physical methods using less toxic chemicals and minimum energy consumption, like laser ablation, microwave/ultrasonication mediated reaction or radiolysis, are also considered green-synthesis methods.

In the year 1988, Anastas and Warner proposed twelve rules or principles of green chemistry, which is now being used as a typical guideline for chemical technologists and chemists working in the field of green synthesis [21].

I. Prevention
According to the principle, it is best to avoid (prevent) waste formation during the synthesis than to clear the waste after its formation in bulk.

II. Atom Economy
We should pay serious attention to design research methods, which will convert all the materials of the process into the final product.

III. Less Hazardous Chemical Syntheses
The synthetic methods should be designed in such a way that that material to be used or to be formed should have little or no toxicity to the environment and human health.

IV. Designing Safer Chemicals
Chemical products should be designed in such a fashion, which will minimize their toxicity.

V. Safer Solvents and Auxiliaries
The use of separation agents, solvents, etc., should only be limited in necessary conditions and should be harmless when used.

VI. Design for Energy Efficiency
The requirements for energy in any chemical processes should be minimized and can only be used after knowing their economic and environmental impacts. Preferably, synthetic procedures should be carried out at ambient pressure and temperature.

VII. Use of Renewable Feedstocks
Renewable nature of the raw material or feedstock will be economically and technically feasible.

VIII. Reduce Derivatives
In a chemical reaction, the temporary modification of physical/chemical processes, use of blocking groups, and protection/deprotection must be avoided or minimized, as these steps involve additional reagents and can also generate waste.

IX. Catalysis
Catalytic reagents are preferable to the stoichiometric reagents.

X. Design for Degradation
One should design the chemical products in such a way that at the end of their function, they will degrade to innocuous products and do not persist in the environment.

XI. Real-Time Analysis for Pollution Prevention
The development of analytical procedures should be done to allow control, real-time and in-process monitoring of the formation of hazardous substances.

XII. Inherently Safer Chemistry for Accident Prevention
Any chosen substances in the chemical process should have the potential to minimize chemical accidents, including explosions, fire and releases.

In this chapter, we have tried our best to include all the possibilities explored for noble metal nanoparticles synthesis using a biological entity mediated green-synthesis approach. We have confined our discussion towards the role of biological or natural species like plant, microorganism, etc., towards the synthesis of noble metal nanoparticles only.

16.1.2 Literature Survey on the Green Synthesis of Nanoparticles

By applying any one of the twelve rules mentioned in the previous section, nanoparticle synthesis could be done in a greener way. As there is no complete rule to rate a method's "greenness," stating that one specific synthesis process is always more "green" in comparison to another is an arguable statement. In Figure 16.1, we have compiled the different aspects or processes popularly used for green methods for the synthesis of nanoparticles using biological entities. Among various types of nanoparticles, more interest and attention has been given to synthesis of metallic nanoparticles. A good number of review articles and research papers have been reported in the literature describing the synthesis protocol for silver, gold, platinum, gold-silver alloy, tellurium, selenium, palladium, titania, silica, magnetite, zirconia, uraninite nanoparticles and quantum dots using the green-synthesis approach. For example, Nath and Banerjee have summarized the reported synthesis approaches for the noble metal nanoparticles and discussed the application of those nanoparticles in the biomedical field [22]. Shankar *et al.* have focused their review article on the synthesis of

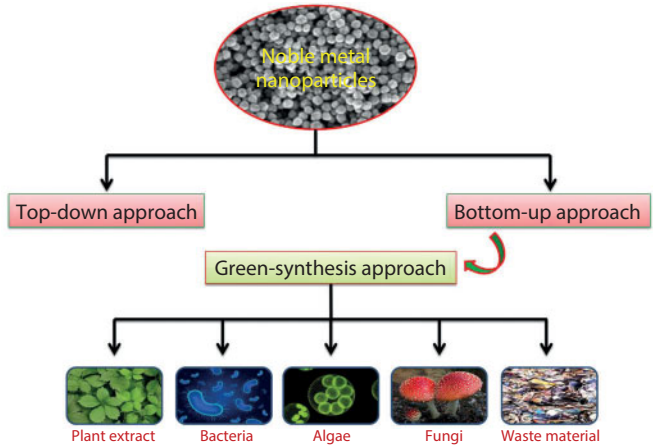


Figure 16.1 Biosynthesis of noble metal nanoparticles using various biological agents. Reproduced with permission from [23].

metallic nanoparticles like silver and gold using microalgae [23]. Roy *et al.* have published a mini-review on the similar topic [24]. In another review article by Teimuri-Mofrad *et al.*, recent developments in the plant extracts mediated green-synthesis of gold nanoparticles have been discussed [25]. Makarov *et al.* have also discussed the similar topic with an emphasis on the role of plants in the metal nanoparticles synthesis [20]. In addition to these review articles, a number of studies are presented in the literature where different aspects of the green-synthesis approach are discussed. In this chapter, we have made an effort to summarize all the possible green-synthesis approaches taken so far for the synthesis of noble metal nanoparticles. Additionally, we have also discussed the role of green synthesis in the designing or tailoring of various shaped or anisotropic noble metal nanoparticles. Lastly, there is a critical discussion of the advantages and disadvantages of the green-synthesis approaches compiled in this chapter.

16.2 Green Synthesis of Noble Metal Nanoparticles

In chemistry, the metals which are oxidation as well as corrosion resistant in the presence of moist air are categorized as noble metals. In the list of chemically noble metals, silver (Ag), gold (Au), platinum (Pt), palladium (Pd), ruthenium (Ru), iridium (Ir), osmium (Os), and hodium (Rh) are mainly included. While according to the literature, mercury (Hg), rhenium (Re) and copper (Cu) can also be included in the list. Among the different noble metals, the nanoparticles of Au, Ag, and Pt are more popular

than the others. Silver and gold are considered as belonging to the group of "metals of antiquity," which have been used since 4000 BC and 6000 BC, respectively [26].

In recent time, synthesis of noble metal nanoparticles via green-chemistry approach using microorganisms and biological systems have especially gained in popularity and are of interest to researchers. The reason behind the popularity of biological system-based green chemistry is its fast speed and easy formation of nanoparticle without using expensive, toxic and harsh reagents. For example, AgNPs production using chemical reduction needs sodium borohydride, hydrazine, ethylene glycol, etc., which may be adsorbed onto the surface of synthesized nanoparticles as capping agents and results in high toxicity of nanoparticles [24]. In comparison to this, the biological entities used for the synthesis of nanoparticle vary from eukaryotic plant cells to prokaryotic bacterial cells. Actually, if you think about it, the secret of nature, i.e., synthesis of nanoparticle using biological things, has opened a new and very exciting way to develop new tiny things in a simpler way. In one review article, the author has discussed three important aspects which should be considered prior to synthesis of nanoparticle using biological materials:

1. The first and foremost step towards green synthesis is selection of the best organisms. In other words, researchers must focus on the organisms' fundamental properties before selecting them as reducing agents. For example, plants having potential towards metal accumulation or adsorption could be the best candidates for synthesis.
2. During the synthesis, an optimal condition should be chosen where the cell growth will not be hampered or enzyme activity will not degrade.
3. When going towards industrial-scale or large-scale synthesis, the yield and the production rate should also be kept in mind.

In this chapter, we have broadly classified biological entity-based green synthesis of noble metal nanoparticles into four categories and discussed them one by one:

1. Plant mediated synthesis
2. Microbe mediated synthesis
3. Algae mediated synthesis
4. Other miscellaneous approaches

16.2.1 Plant Mediated Synthesis

The noble metal nanoparticles synthesis using plant extract has received more attention than any other method owing to their low cost and large-scale production ability [20, 25]. Using plant extracts provides an additional elastic control on the shape and size of the nanoparticles and enables easy purification. Meaningfully, this process occurs much faster, reaction proceeds very quickly and one can use various parts of the plant, like fruits, chili peppers [27], seeds [28], leaves [29] and barks [30], to make the extract or juice. It has also been revealed that various plant metabolites, like alkaloids, polyphenols, phenolic acids, terpenoids, proteins and sugars, play a significant role in the bio-reduction of metal ions to get nanoparticles [20]. The structures of the compounds present in the plants which are capable of reducing metal ions are shown in Figure 16.2a. Among the different metabolites, terpenoids are often found associated with nanoparticles [31]. It has been verified that the terpenoids class of organic polymers display strong antioxidant activity and are produced from isoprene units in plants. Another compound having a high efficiency in the bioreduction is flavonoids. They are a member of polyphenolic groups and include several subclasses like anthocyanins, flavonols, isoflavonoids, flavanones, flavones and chalcones. These compounds have the ability to chelate and reduce the metal ions to nano-sized materials. From a mechanistic point of view, the reactive hydrogen atom is released due to the flavonoids tautomeric transformations from the enol-form to the keto-form, which can be considered the main material behind the reduction of metal ions for the formation of nanoparticles [32]. From extensive research it has also been understood that the presence of sugars in plant extracts can also encourage the formation of nanoparticles. It is already assumed that aldehyde group of monosaccharides, like glucose, have the ability to reduce the metal ions. During their performance as reducing agent, oxidation of aldehyde group through the nucleophilic addition of hydroxyl ion occurs to get a carboxyl group. This leads to the synthesis of nanoparticles via the reduction of metal ions. Studies have also revealed the association of proteins and amino acids during the nanoparticle synthesis.

Overall, the synthesis approach of metal nanoparticle using plants/plant extracts consists of three main phases [20, 33]. The first phase is the activation phase (in this phase, first the reduction of metal ions takes place followed by nucleation steps of the already reduced metal atoms). The second phase is the growth phase, where the small-sized nanoparticles extemporaneously combine with each other to form larger size particle. This method is denoted as Ostwald ripening, in which thermodynamic

stability of nanoparticles also gets increased. The third phase of the process is termination phase, which determines the nanoparticle's final shape. An overall schematic diagram for the nanoparticles formation can be seen in Figure 16.2b.

Apart from the nature of a plant extract, some other factors, like concentration, pH of reaction mixture, reaction time, electrochemical potential of metal ion and incubation temperature, can also affect the formation of nanoparticle [20, 34, 35]. The pH value of the plant extract has the maximum influence, as the change in pH value will also change the charge on the phytochemicals of the plant extract [36]. This affects their binding as well as the ability to reduce metal cations and anions during the synthesis of nanoparticle. It may also affect the size, yield and shape of the prepared nanoparticles. The formation of nanoparticles can also be affected by the incubation temperature [37]. As a whole, the efficiency over the synthesis of nanoparticles and reaction rate will increase with the increase in temperature. The other important factor affecting the nanoparticle formation

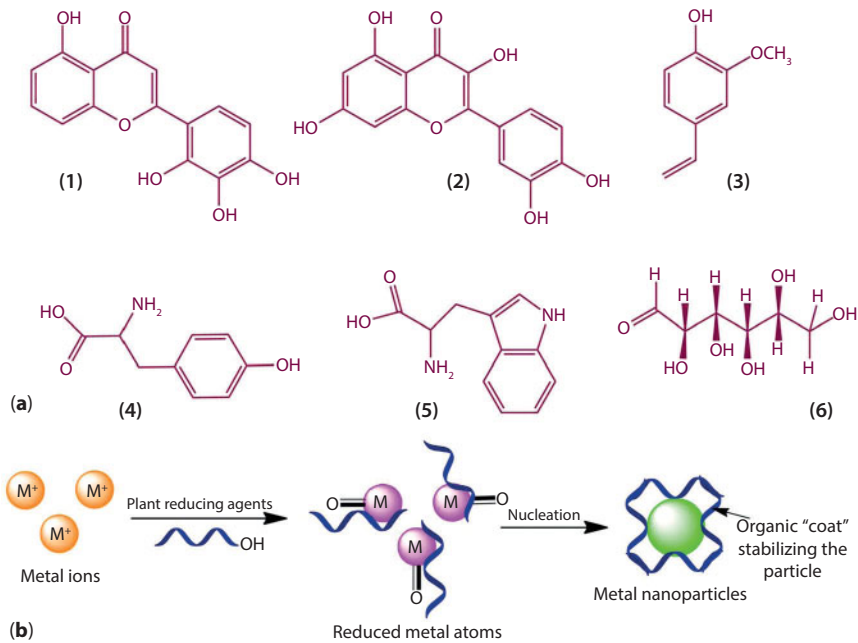


Figure 16.2 (a) Plant metabolites involved in the green synthesis of nanoparticles: 1) flavonoids (luteolin), 2) a reducing hexose with the open chain form, 3) tryptophan, 4) tyrosine, 5) terpenoids (eugenol), 6) flavonoids (quertcetin); (b) A schematic representation of metal nanoparticle synthesis in a plant extract. (Reproduced with permission from [20])

is the electrochemical potential of the metal ion [34]. It has been observed that large positive electrochemical potential containing metal ions can be reduced earlier than low electrochemical potential containing ions by the plant extract.

Initially, the plant extract is only used as capping and reducing agents in synthesis of nanoparticles. But, now, the scenario has been changed and different aspects of plants are also used for nanoparticle synthesis. Plants having a very strong metal ion accumulation property may be applied for extracting the precious metals from land, also known as phytomining [20]. The metals accumulated by the plants are recovered by using smelting and sintering methods. Similar techniques are gaining popularity nowadays for nanoparticle synthesis also. According to a reported study, *Medicago sativa* (alfalfa) and *Brassica juncea* (mustard greens), when grown on $AgNO_3$ as a substrate, have the ability to accumulate 50 nm size AgNPs at a level which is ~13.6% of their own weight [38]. Additionally, 4-nm-size gold icosahedra can be detected using *M. sativa* [39], and 2-nm-size semi-spherical Cu particles can be detected using *Iris pseudacorus* (yellow iris) [40] after growing on substrates composed of salts of the respective metals. But, for real-time nanoparticles fabrication, this technique is not found to be very suitable.

Above, we have discussed the reaction mechanism and factors that may affect plant mediated nanoparticle synthesis. Now, the next section will be dedicated to discussing the different synthesis methods used so far for noble metal nanoparticles.

16.2.1.1 Synthesis of AuNPs

Gold has been used in India for medical purposes as *Swarna bhasma* (gold ash) ever since 1000–600 BC. The gold nanoparticles (AuNPs) have found their own significance due to their excellent electrical conductivity, high electrocatalytic activity and high specific surface area. Owing to their biomedical significance, AuNPs are very popular in the field of medical science. In the literature, a number of articles have been published related to different synthesis processes for AuNPs, while those focusing on the green-synthesis approach are much less. In this section, we only discuss the synthesis of AuNPs using plant extracts (Table 16.1).

In this context, Anuradha *et al.* have used the aqueous extracts of neem (*Azadirachta indica*) for the synthesis of AuNPs [41]. It has been reported that the nanoparticle formation began as soon as the neem extract and the Au(III) solution were mixed with each other. For completion of the synthesis procedure, 24 hours' time is required and during this period the

Table 16.1 Green-synthesis approaches for the preparation of AuNPs and their applications.

S. No.	Green material	Reducing agent	Particle characteristics		Application	Ref.
			Shape	Size (nm)		
1.	Plant (leaf)	*Carica papaya* and *Catharanthus roseus*	Spherical	6–18	Antitumor and antibacterial study	[42]
2.	Plant (flower)	Crocin extracted from Iranian saffron stigma	Spherical	4–10	Anticancer activity	[43]
3.	Plant (peel)	*Vitis vinifera* L	Spherical	20–40	Cytotoxicity and apoptotic cell death	[45]
4.	Plant (leaf)	*Salix alba*	Spherical	50–80	Antibacterial, antifungal, antinociceptive, muscle relaxant and sedative activities	[46]
5.	Plant (seed)	*Elettaria cardamomum*	Spherical	15.2	Antioxidant, antibacterial and anticancer activity	[47]
6.	Plant (peel)	Onion peel extract	Spherical and triangular	45.42	Antioxidant and antibacterial activity	[48]
7.	Plant (leaf)	*Momordica co-chinchinensis* Spreng.	Spherical, triangular and oval	10–80	Anticoagulative and photocatalytic activity	[49]
8.	Plant (fruit)	*Citrus maxima*	Spherical and rod	25.7±10	Catalytic activity	[50]
9.	Plant (leaf)	*Stevia rebaudiana*	Spherical	5–20	–	[110]
10.	Plant (fruit)	*Sterculia acuminata*	Spherical	9.37–38.12	Catalytic activity	[111]

11.	Plant (bark)	*Eucommia ulmoides*	Spherical	–	Catalytic activity	[112]
12.	Microbe	*Streptomyces* sp.	Spherical	20–80	–	[113]
13.	Others	Gelatin	Spherical and triangular	57 and 52	Biological effects on osteoblast cells	[114]
14.	Bacteria	*Deinococcus radiodurans*	Spherical and triangular	43.75	Antibacterial activity	[68]
15.	Microbe	*Klebsiella pneumoniae*	Spherical	10–15	Antibacterial activity	[69]
16.	Algae	*Cystoseira baccata*	Spherical	8.4	Activity in colon cancer cells	[76]
17.	Algae	*Sargassum swartzii*	Spherical	35	Cytotoxic effect in HeLa cells	[78]
18.	Algae	*Spirulina platensis*	Spherical	2–8	Antibacterial activity	[79]
19.	Algae	*Stoechospermum marginatum*	Spherical, hexagonal, trigonal	18.7–93.7	Antibacterial activity	[80]
20.	Other	Honey	Spherical	~ 15	–	[89]
21.	Waste	Banana peel	Nanoplate	–	Antimicrobial activity	[37]
22.	Waste	Eggshell membrane	Spherical and triangular	< 20	–	[92]

characteristic plasmon vibration peak of AuNPs was stabilized at 557±1 nm. The synthesis process and the associated studies were described using the scanning electron microscopy (SEM) and energy dispersive X-ray spectroscopy (EDX) techniques [41]. Recently, Muthukumar *et al.* have used a one-pot green synthesis approach for AuNPs using the *Catharanthus roseus* and *Carica papaya* leaf extracts individually and in combination [42]. The size, morphology and crystallinity of the as-synthesized AuNPs were well characterized. The synthesized AuNPs were tested on cancer and bacterial cell lines. The morphological study revealed that most of the prepared AuNPs were spherical in nature and were observed to have hexagonal and triangular shape. The microscopies and infrared spectroscopic studies confirmed the presence of proteins, flavonoids and alkaloids on the surface of AuNPs. It is expected that their presence was pretty much advantageous for the non-agglomeration, biological activity and stabilization. The anticancer and antibacterial activity of the nanoparticles was also investigated. Due to the synergistic effects of both plant extracts, the AuNPs prepared using both leaf extracts showed an enhanced activity compared to the others [42].

In another study, an interesting synthesis approach has been reported by a group of researchers from Iran [43], in which they used crocin for the synthesis of AuNPs. For the separation of crocin, first ethanolic extract of saffron was prepared and placed in a glass column packed with neutral aluminum oxide. As elution solvents, 50% ethanol and 50% mixture of ethanol and acetic acid were used. Afterwards, the collection of crocin fractions and the absorbency value at 440 nm was checked to confirm their presence. Using crocin, they obtained spherical, stable and uniform AuNPs, which were characterized by transmission electron microscopy (TEM), X-ray diffraction (XRD) and UV-Vis techniques. The particle size of the AuNPs was calculated to be around 4–10 nm. Both 3-(4,-5-dimethylthiazol-2-yl)-2-5-diphenyltetrazolium bromide (MTT) and lactate dehydrogenase (LDH) tests were performed to check the anticancer activities of the synthesized AuNPs. The whole study concluded that AuNPs can be synthesized simply and quickly by this method, which have important pharmaceutical and clinical activities for potential future application in human breast cancer [43].

Gonnelli *et al.* have reported *Cucurbita pepo* plant extract for the synthesis of AuNPs [44]. The study reveals the ability of different plant parts towards the formation of AuNPs is different, as the amount of reducing agent is different in different parts. In their study, the number of spherical-shaped AuNPs obtained from the shoot extract was larger than the root extract of plant. The authors have reported a reaction time of 30 min and

temperature of 40 °C using $HAuCl_4$ as gold precursor with shoot extract of plant. The synthesized AuNPs exhibited an absorption peak at about 570 nm. The dynamic light scattering (DLS) study revealed that about 93% AuNPs have a particle size of approximately 627 nm [44].

Recently, a group of researchers have reported the use of *Vitis vinifera* L (grapes) peel containing polyphenols as both stabilizing and reducing agents for the green synthesis of AuNPs [45]. UV-visible spectroscopy, TEM, XRD, particle size distribution, zeta potential analysis and Fourier transform infrared spectroscopy (FTIR) were used to characterize the as-synthesized AuNPs. The spherical shape of the nanoparticles with a size of 20–40 nm was obtained from the TEM analysis. The presence of polyphenols capped onto the peel-derived AuNPs was confirmed by the FTIR spectroscopy. The synthesized AuNPs were studied for their antiproliferative activities and show induction of apoptosis at the inhibitory concentration of 23.6 μM. From the whole study, it was confirmed that the synthesized AuNPs render powerful antioxidant characteristics and might serve as anticancer agents in killing cancer cells. The synergistic action of the phenolic moieties as well as the AuNPs is the main reason behind the cytotoxic and apoptotic effect of *V. vinifera* peel-derived AuNPs [45].

Another study has reported the use of *Salix alba* leaf extract for the synthesis of AuNPs [46]. The stability of AuNPs was evaluated in contrast to varying volumes of pH and sodium chloride, as well as at elevated temperature. They have also studied the effect of enzymes inhibition, antibacterial, antifungal, antinociceptive, muscle relaxant and sedative activities on the synthesized AuNPs. A 540 nm surface plasmon resonance (SPR) band was observed from the UV-Vis spectra of the AuNPs, which proves the formation of AuNPs. The morphological study by atomic force microscopy (AFM) and SEM analyses concluded the particle size of 63 nm and 50–80 nm, respectively. From the FTIR spectra, the involvement of amines, amide and aromatic groups in capping and reduction of AuNPs was confirmed. This study also concluded that the leaf extract of *S. alba* is a very good bioreductant for the synthesis of AuNPs and the prepared nanoparticles have the possibility to be used in various biomedical and pharmaceutical fields [46]. Rajan *et al.* have recently reported the *Elettaria cardamomum* seed mediated rapid synthesis of AuNPs with a size of 15.2 nm [47]. The synthesis method was very simple, where only the simple addition of seed extract to the boiling $HAuCl_4$ was carried out. They have characterized the AuNPs by means of XRD, TEM and UV-Vis study. The antioxidant, antibacterial and anticancer activities of the nanoparticles were also studied [47].

In another study, onion peel extract was used for the preparation of AuNPs (Figure 16.3) [48]. The formation of AuNPs was monitored by a

visual color change at different time intervals after the addition of peel extract (Figure 16.3b). As-synthesized nanoparticles possess an average particle size of 45.42 nm and the AuNPs were first characterized by XRD, FTIR, UV-Vis spectroscopy, EDX, field emission scanning electron microscopy (FESEM) and differential thermogravimetric analysis (DT-TGA). An SPR spectrum was obtained at 535 nm, which confirmed the synthesis of AuNPs (Figure 16.3c). The involvement of phenolic compounds and cysteine derivatives was observed from the FTIR spectra of synthesized nanoparticles. The synthesized nanoparticles displayed a strong synergistic antibacterial and anticandidal activity along with antioxidant and strong proteasome inhibitory potential. The results obtained in the whole study suggested food waste materials mediated easy green synthesis of AuNPs and their possibility to be used in biomedical fields such as antibacterial, cancer treatments, proteasome inhibitors, cosmetic industries as sunscreen lotion and anti-aging creams [48].

Paul *et al.* have reported the use of dried biomass of *Momordica cochinchinensis* (Lour.) Spreng. leaf for the green synthesis of AuNPs [49]. The characterization techniques were the same as that of the synthesis approach discussed earlier and the authors have found SPR band at 552 nm. The obtained synthesized nanoparticles were mostly spherical, along with some oval and triangular shapes, with size 10–80 nm. Contrary to the

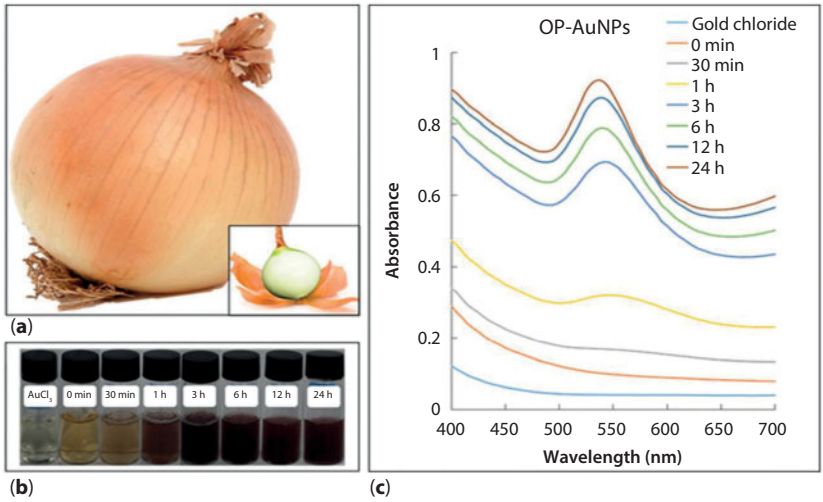


Figure 16.3 (a) Bulb of *Allium cepa* with dried outer peels; (b) Change in color of the reaction mixture with respect to time; (c) UV-Vis spectroscopy of the reaction mixture at different time intervals of the synthesized OP-AuNPs. (Reproduced with permission from [48])

other reported techniques; they have applied the as-synthesized AuNPs for the photocatalytic dye degradation under sunlight. The ability of AuNPs to inhibit coagulation of human blood plasma was also investigated in their study [49].

Recently, Yu *et al.* have reported a low-cost environmental friendly method for the synthesis of AuNPs using *Citrus maxima* fruit extracts [50]. The obtained peak at 535 nm in the UV-Vis spectrum of the synthesized AuNPs, proves their successful formation. The nanomaterials were reported to have a particle size of 25.7±10 nm. *C. maxima* acts as both stabilizing and reducing agent during the synthesis of AuNPs. The prepared AuNPs were applied as a catalyst for the reduction of 4-nitrophenol to 4-amino phenol. The study further supports the usefulness of green-synthesized AuNPs in the field of catalysis [50].

16.2.1.2 Synthesis of AgNPs

Silver is considered as one of the important noble metals and has been widely applied in several biomedical fields since prehistoric times. There is a growing importance in silver nanoparticles (AgNPs) synthesis due to their antiproliferative effects, excellent plasmonic activity, optical, electromagnetic, bacteriostatic, bactericidal effects and catalytic properties. Since their discovery, they have been applied in many industries like catalysis, clothing, dentistry, electronics, photography, mirrors, food packaging and optics [51]. This has led to a sharp hike in their market value. Due to rising demand, large-scale synthesis has begun, which needs lots of chemicals and money. So, over the last few years, the green-synthesis approach has been explored for large-scale synthesis of less-toxic AgNPs at low cost.

Plant extracts are the most economically and environmentally friendly materials for the synthesis of AgNPs. All parts of a plant, including roots, leaves, seeds, stems and fruits, contain antioxidants or sugars and can be used in the synthesis process [52]. Hazardous chemicals like sodium borohydride ($NaBH_4$) will surely be replaced by this method. Plant extracts for the synthesis of nanoparticles have become very popular, as they have been reported to act as both capping and reducing agents.

Tea is one of the most popular beverages consumed by human beings. Besides its use as a beverage, it has also been employed for the green synthesis of AgNPs. Moulton *et al.* have used tea (*Camellia sinensis*) as a capping as well as reducing agent for the synthesis of AgNPs using $AgNO_3$ as the precursor [53]. Some other groups have also used tea extract for the synthesis of AgNPs [54, 55]. The obtained AgNPs were characterized by TEM, XRD, FTIR, TGA, and zeta potential analyzer to understand the

morphology and capping of AgNPs. To evaluate the stability of AgNPs, the time-dependent release of silver ions from the tea extract was also measured. The as-synthesized AgNPs were found to have a spherical geometry having a size of 20–90 nm. Certain reaction conditions, like the dosage of the tea extract and temperature, were also optimized by means of production efficiency and the formation rate of AgNPs. The high stability of the nanoparticles can be defined by the capping of functional groups from the tea extract on the AgNPs. The biosynthesized AgNPs were reported to show slight antibacterial activity against *E. coli* [55].

Beside tea leaves, other plant extracts have also been used for the preparation of AgNPs in an eco-friendly manner. Recently, Dong *et al.* have reported a simple and low-cost method for the synthesis of small size, well dispersed and crystalline, spherical-shaped AgNPs with a size distribution from 3–15 nm by using wolfberry fruit (*Lycium barbarum*) extract [56]. Like other reported techniques, they have also characterized the AgNPs using XRD, TEM and UV-Vis spectroscopy. They have also optimized certain factors, like the concentrations of silver nitrate, reaction times, and amount of fruit extract, during the synthesis of AgNPs.

A group of researchers have used extract of *Skimmia laureola leaves* for the room temperature synthesis of AgNPs [57]. A color change to dark brown from pale yellow in the reaction mixture was witnessed during the synthesis. The synthesized AgNPs exhibited SPR at around 460 nm. The *S. laureola* leaf extract was reported to have chemical constituents tritepenoids, skimmidiol and coumarins, which are mainly responsible for the formation of AgNPs. Additionally, they also investigated the antibacterial potential of biosynthesized AgNPs and concluded that it can be used as a suitable nanomaterial for biomedical application [57]. Ghaedi *et al.* reported the use of simple *Rosmarinus officinalis* leaf extract for the synthesis of AgNPs [58]. The TEM image of the nanoparticles suggests the spherical morphology of AgNPs with the size range of 10–33 nm. The FTIR data confirmed the reduction of $AgNO_3$ by phenolic agents of *R. officinalis* extract. The antimicrobial activity of the AgNPs was also tested against Gram-positive bacteria *S. aureus* and *B. subtilis* and Gram-negative bacteria, i.e., *E. coli* and *P. aeruginosa* [58].

The leaf extract of *Ginkgo biloba*, a highly abundant medicinal plant in China, was used for the first time by Ren *et al.* for biosynthesis [59]. The initial concentration of Ag^+ and the pH of the reaction mixture were also optimized during the synthesis. TEM images revealed the spherical shape of AgNPs with a size range between 10–16 nm with lattice fringes of 0.23 nm (Figure 16.4). From the FTIR spectra, bands of -NH_2, -OH, and others were obtained, which confirmed that groups from biological

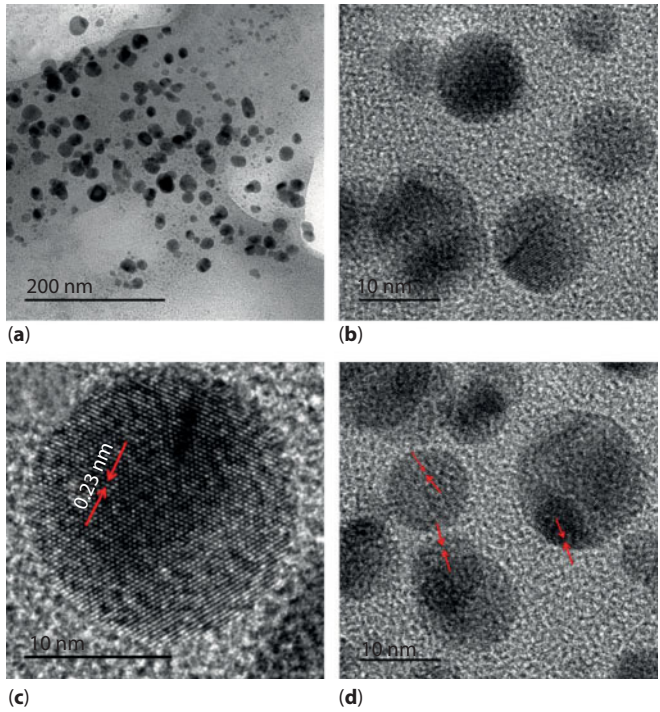


Figure 16.4 TEM images of AgNPs (a) and (b) under different magnification; (c,d) high-resolution image of single nanocrystal showing lattice fringes with spacing of 0.23 nm (Reproduced with permission from [59]).

macromolecules were present on the surface of the nanoparticles. The as-prepared AgNPs were tested for their antibacterial activity towards Gram-positive and Gram-negative bacteria [59].

Besides these, some other efficient syntheses have also been reported in recent times. For example, Velusamy *et al.* have used a simple synthesis approach for AgNPs using autoclave-assisted gum extract of neem (*Azadirachta indica*) [60]. The synthesized AgNPs revealed a high antibacterial activity against *Bacillus cereus* and *Salmonella enteritidis*. They confirmed the antibacterial activity of the AgNPs by degradation of test bacterial DNA [60].

Scientists have also used the bark of plants to synthesize the nanoparticles. As can be seen in the literature, Nayak *et al.* have used the bark extracts of *Azadirachta indica* and *Ficus benghalensis* for the green synthesis of AgNPs [61]. From the FTIR spectra, the presence of -OH and -NH functional groups can be clearly observed. The functional groups arise due

to the flavonoids, terpenoids and phenols. The AgNPs show potential antibacterial activity against human pathogenic Gram-negative bacteria like *V. cholera, E. coli* and *P. aeruginosa* and Gram-positive bacteria like *B. subtilis*. It was also demonstrated that the AgNPs synthesized by using bark extract of *A. indica* displayed better antimicrobial activity based on activity and yield than the synthesized AgNPs from leaf extract of the same plant [61]. Another group of researchers have used *Butea monosperma* bark extract for the green synthesis of AgNPs [62]. The SAED pattern of the nanoparticles confirms the crystalline nature of AgNPs and from high resolution transmission electron microscopic (HRTEM) images the average size of the nanoparticles obtained was ~ 35 nm. The synthesized AgNPs demonstrated high antibacterial activity against both Gram-positive and Gram-negative bacteria [62].

Another research group used Amazonian Araza fruit (*Eugenia stipitata*) for the biosynthesis of AgNPs [63]. The FTIR study of the nanoparticles depicted that malic acid, citric acid, and carotenoids of Araza fruit were involved in the synthesis of AgNPs (Figure 16.5). Furthermore, in the antioxidant study, it was observed that the surface modified AgNPs demonstrated nearly double the antioxidant efficiency than Araza fruit extract against 1,1-diphenyl-2-picrylhydrazyl [63]. Khalilzadeh and Borzoo used onion extract as reductant and stabilizer for one-pot biosynthesis of AgNPs [64]. They have also studied the ability of AgNPs to reduce charge transfer

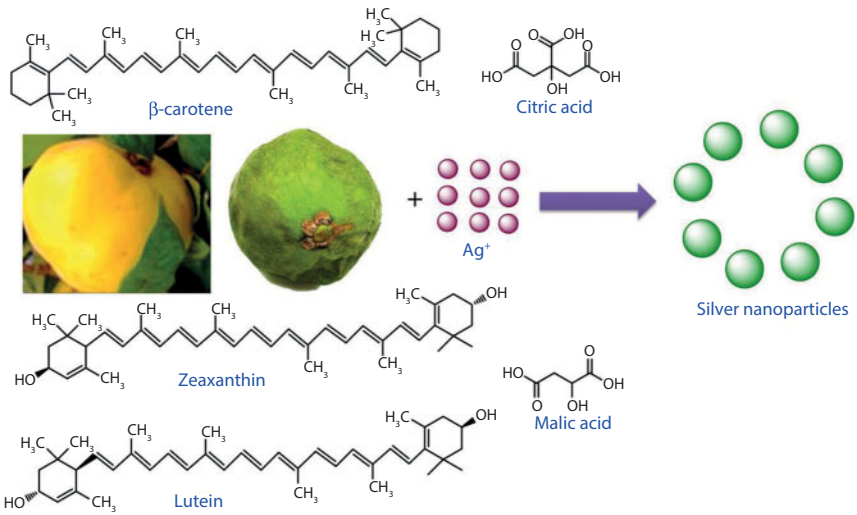


Figure 16.5 Schematic diagram for biosynthesis of AgNPs using fruit extract of Araza along with digital photographs of the fruits. (Reproduced with permission from [63]).

resistance using electrochemical impedance spectroscopy. Finally, they have also investigated the sensing ability of the prepared AgNPs on ascorbic acid signal by square-wave voltammetry. They have obtained a linear concentration range of 0.4–450.0 μM peak with a detection limit of 0.1 μM for ascorbic acid [64]. Additionally, a list has been compiled summarizing recent synthesis approaches, nanoparticle sizes, etc., related to plant mediated synthesis of AgNPs, which is presented in Table 16.2.

16.2.2 Microbes Mediated Synthesis of Nanoparticles

Microorganisms are mainly known for their harmful effects on mankind and animals. But, they have also been used as probable "nano-factories" for advancement of environmental friendly green synthesis of the nanoparticles. During the synthesis procedure, whenever the microorganisms receive the target ions from their environment, enzymes (as generated via the cell activities) of the microorganism used for the biosynthesis of nanoparticles get started, where the metal ions are converted into the elemental metal atoms. According to location of nanoparticles formation, the synthesis approach can be divided into two types: intracellular and extracellular synthesis. In the case of extracellular synthesis approach, the metal ion gets trapped on the cell surface and after that, in the presence of enzymes, the reduction process gets started [23]. On the other hand, in the case of intracellular synthesis approach, the metal ions are conveyed into the microbial cell to produce nanoparticles in the presence of enzyme. Among the microorganism, bacterial cells are more popular to form inorganic nanomaterials through extracellular and intracellular approach and have been deemed efficient biofactories for the production of Ag/AuNPs.

16.2.2.1 AuNPs by Microbe Mediated Synthesis

Prokaryotic bacteria have become highly popular for the synthesis of AuNPs. In the literature, bacteria like *Pseudomonas stutzeri, Escherichia coli, Pseudomonas aeruginosa, Salmonella typlus, Plectonema boryanum, Vibrio cholerae, Staphylococcus currens,* etc., are commonly used for the synthesis of extracellular and intracellular AuNPs. In the case of bacteria mediated synthesis of AuNPs, the formation of AuNPs can be visually predicted by the color change of the reaction mixture. Husseiny *et al.* have used bacterial isolates of *P. aeruginosa* for the synthesis of AuNPs and adopted a similar procedure [65]. The formation of biofilm of *Cupriavidus metallidurans* on Au grains is very popular. Reith *et al.* first isolated *C. metallidurans* from soils of tropical and temperate Australian sites which was

Table 16.2 Green-synthesis approaches for the preparation of AgNPs and their applications.

S. No.	Green material	Reducing agent	Particle characteristics		Application	Ref.
			Shape	Size (nm)		
1.	Plant (leaf)	Tea	Spherical	20–90	Antibacterial activity	[55]
2.	Plant (Fruit)	Wolfberry fruit	Spherical	3–15	–	[56]
3.	Plant (leaf)	*Skimmia laureola*	Spherical and hexagonal	–	Antibacterial activity	[57]
4.	Plant (leaf)	*Rosmarinus officinalis*	Spherical	10–33	Antimicrobial activity	[58]
5.	Plant (leaf)	*Ginkgo biloba*	Spherical	10–16	Antimicrobial activity	[59]
6.	Plant (gum)	Neem	Spherical	< 20	Antibacterial activity	[60]
7.	Plant (Bark)	*Ficus benghalensis* and *Azadirachta indica*	Spherical	60	Antimicrobial activity and antiproliferative response against osteosarcoma	[61]
8.	Plant (Bark)	*Butea monosperma*	Spherical	18–50	Antibacterial and cytotoxic activity	[62]
9.	Plant (Fruit)	*Eugenia stipitata*	Spherical	15–45	Antioxidant ability	[63]
10.	Plant (leaf)	*Ziziphora tenuior*	Spherical	8–40	–	[115]
11.	Plant (leaf)	*Alternanthera dentata*	Spherical	50–100	Antimicrobial activity	[116]
12.	Plant (seed)	*Pistacia atlantica*	Spherical	10–50	Antibacterial activity	[117]
13.	Plant (root)	Onion	Spherical	5.3–10.2	Detection of ascorbic acid	[64]
14.	Bacteria	*Lactobacillus*	Spherical	6	Antibacterial and anti-biofouling activity	[118]
15.	Bacteria	URAK enzyme	Spherical	50–80	–	[119]

16.	Algae	*Enteromorpha flexuosa*	Spherical	2–32	Antimicrobial activity	[81]
17.	Algae	*Chlorella vulgaris*	Spherical	1.6–34.4	Antimicrobial activity	[82]
18.	Algae	*Gracilaria birdiae*	Spherical	–	Antimicrobial activity	[83]
19.	Algae	*Streptomyces rochei* MHM13	Spherical	22–85	Antibacterial and anticancer activity	[84]
20.	Algae	*Sargassum boveanum*	Spherical	–	Detection of hydrogen peroxide	[85]
21.	Waste	Saffron (*Crocus sativus* L.) wastage	Spherical	15	Antibacterial activity	[95]
22.	Other	Sunlight	Rod	5–10	–	[97]
23.	Plant (Fruit)	*Sesbania grandiflora*	Spherical	~ 20	Antimicrobial activity	[120]
24.	Plant (Crude)	*Bergenia ciliata*	Spherical	~ 35	Antioxidant, cytotoxic and antimicrobial activities	[121]
25.	Fungus	*Trichoderma harzianum*	Irregular	50.10	Antibacterial activity	[122]
26.	Plant (seed)	Pomegranate	Spherical, oval, rod and flower	~ 50 nm, 100 nm and 550	Antibacterial activity	[104]
27.	Others	Starch from rice	Spherical, rod, hexagonal and flower	–	Sensing of phenformin	[105]
28.	Plant (Fruit)	Lemon juice	Spherical, cube and hexagonal	~10	Sensing of Tramadol	[106]

used for the biosynthesis of AuNPs [66]. Here, the isolated bacteria interacted with Au(III) ions to produce homogeneous AuNPs within the cell walls. *Rhodopseudomonas capsulata* was also used to synthesize AuNPs on their surface using $HAuCl_4$ as precursor [67]. The synthesis process takes 48 hours of incubation for the transformation of aqueous chloroaurate ions to AuNPs by reduction. Li *et al.* have recently described the biosynthesis of AuNPs using *Deinococcus radiodurans* [68]. The synthesized AuNPs possess a diameter of 43.75 with spherical geometry. From the FTIR and X-ray photoelectron spectroscopy (XPS) study, it was concluded that the Au(III) state of gold has been reduced to Au(I), and further Au(0) via the interactions with phospho, amine, hydroxyl and carboxyl groups of proteins. They have also optimized certain parameters during the biosynthesis of AuNPs, like the solution pH, initial concentration of precursor salt, temperature and bacterial growth period. AuNPs have also been applied to study their antibacterial activity against both Gram-negative and Gram-positive bacteria [68].

In another recent published report, Prema *et al.* have employed an easy synthesis method using *Klebsiella pneumoniae* (MTCC-4030) for the synthesis of AuNPs [69]. To synthesize the colloidal AuNPs, the gold ions were exposed to *K. pneumoniae* and incubated at 37 °C for 24 h. The SEM image of the nanoparticles suggests a spherical morphology and from the AFM image, they have calculated the nanoparticles size of 10–15 nm. The reductive group's involvement on the nanoparticles surface was confirmed by the FTIR spectra. The prepared nanoparticles were tested for their antibacterial activity towards the bacteria and show a highest inhibitory zone of 25.60 mm against *Escherichia coli* [69]. In Table 16.1, some of the microbe mediated synthesis approaches for AuNPs have also been summarized.

16.2.2.2 Microbe Mediated Synthesis of AgNPs

Like AuNPs, some microbe mediated AgNPs synthesis has also been reported in the literature. For example, a bacterial strain of *Proteus mirabilis* PTCC 1710 was used to synthesize AgNPs [70]. Samadi *et al.* have employed TEM, UV-Vis spectroscopy, atomic absorption spectrometry (AAS) and EDX for the characterization of synthesized nanoparticles. The TEM images suggested that 10–20 nm diameters of AgNPs were synthesized with spherical geometry. They demonstrated that extracellular synthesis of the AgNPs can be obtained in the case of cell incubation in Muller-Hinton broth medium and for intracellular method, the incubation of cell was carried out in tryptic soy broth.

In another work, Ramanathan *et al.* have investigated the use of *Morganella psychrotolerans,* a silver-resistant psychrophilic bacterium, for the synthesis of AgNPs [71]. During biological synthesis, the shape of nanoparticle was controlled by the growth kinetics. They have conducted some electrochemistry experiments after the interaction between bacterial cells and the silver ions. The method can provide a better understanding of the mechanistic characteristics of bacteria mediated silver reduction [71]. In another study, Sadhasivam *et al.* have reported the use of *Streptomyces hygroscopicus* for the biosynthesis of AgNPs and studied their activity against Gram-negative bacteria (*Salmonella typhimurium* and *Escherichia coli*), Gram-positive bacteria (*Enterococcus faecalis* and *Bacillus subtilis*) and yeast (*Candida albicans*) [72]. The results of the study indicate the usefulness of nanoparticles as potential nanomedicine for the elimination of pathogenic microorganisms. In Table 16.2, some of the microbe mediated synthesis approaches for AgNPs have also been summarized.

16.2.3 Algae Mediated Synthesis

Like microbes, algae are also considered a "biofactory" for metallic nanoparticles synthesis. Among the different kinds of bioreductants, seaweeds have gotten special attention owing to their macroscopic structure, low cost and high metal uptake capacity [73]. It has been found that the marine-derived biological entities comprise characteristic nanostructures like sponges and diatoms, fabricated with nanostructured silica and coral reefs. In the literature, we can find the use of several marine-derived species for the synthesis of different nanoparticles like lead, gold, cadmium, silver, etc. (Figure 16.6). Marine algae are rich with certain vitamins, minerals, lipids, and other substances such as polyphones, polysaccharides and proteins. They have also found their medicinal applications in cancer, inflammation, allergy, thrombosis, oxidative stress and hypertensive diseases [74, 75]. The phytochemicals in the algae have been reported to contain carboxyl, amino and hydroxyl functional groups, which can function both as effective capping agents as well as reducing agents during the single-step synthesis of nanoparticles. As we discussed earlier, the algae mediated bioreduction mechanism involves three main phases, i.e., activation, growth and termination, which are discussed in detail in Section 16.2.1 (Plant Mediated Synthesis). The graphical representation describing the full process of the algae mediated nanoparticles synthesis is shown in Figure 16.7. Here also, the intracellular synthesis approach can be affected by change in the

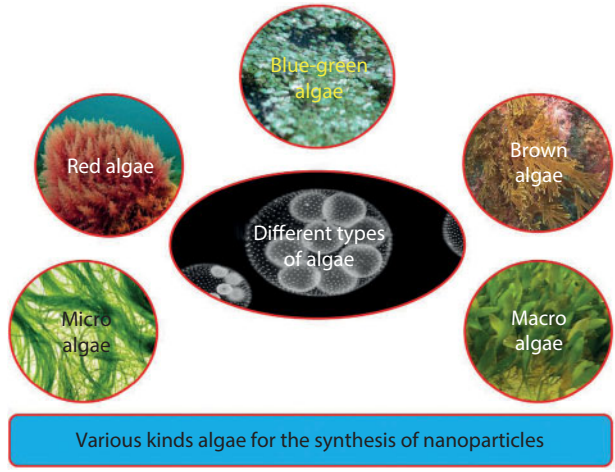


Figure 16.6 Different sources of algae for the synthesis of nanoparticles. (Reproduced with permission from [23])

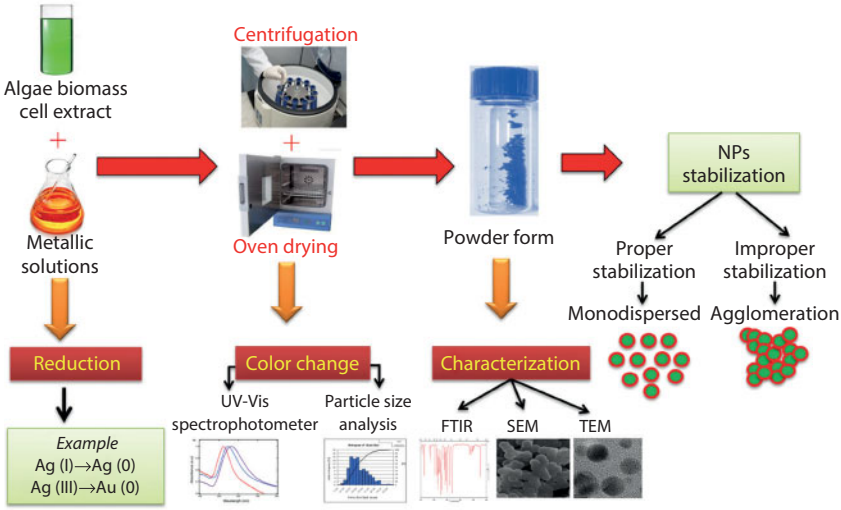


Figure 16.7 Overview of synthesis, characterization and stabilization of NP using algae. (Reproduced with permission from [23])

physicochemical parameters like pH, temperature, and concentration of the substrate. The mechanism of extracellular and intracellular synthesis approaches is shown in Figure 16.8. In Tables 16.1 and 16.2, some of the algae mediated synthesis approaches for both AuNPs and AgNPs, respectively, have been summarized.

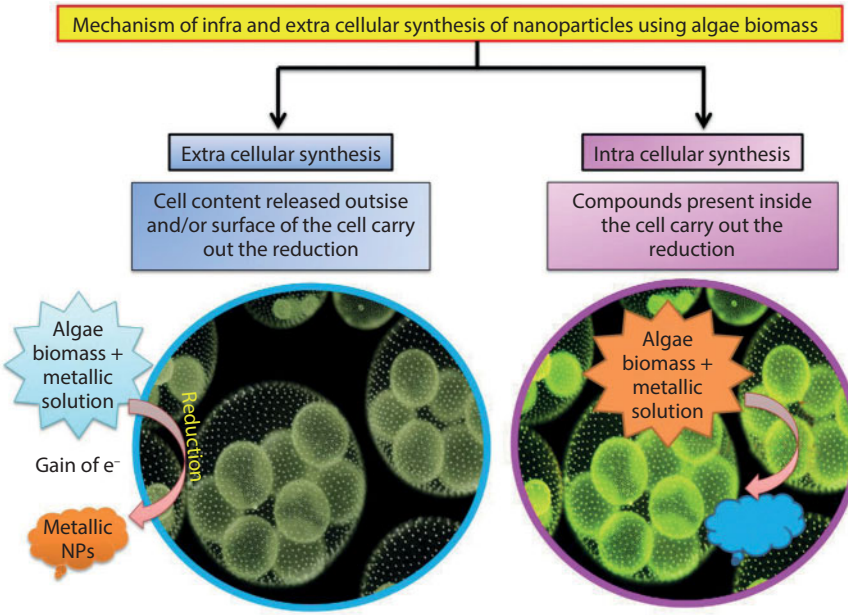

Mechanism of infra and extra cellular synthesis of nanoparticles using algae biomass
Extra cellular synthesis
Intra cellular synthesis
Cell content released outsise and/or surface of the cell carry out the reduction
Compounds present inside the cell carry out the reduction
Algae biomass + metallic solution
Reduction
Gain of e⁻
Metallic NPs
Algae biomass + metallic solution

Figure 16.8 Proposed mechanism of intracellular and extracellular synthesis of NP. (Reproduced with permission from [23])

16.2.3.1 AuNPs Synthesis

The extracellular and intracellular syntheses of AuNPs have been reported by many researchers using brown marine algae such as *Sargassum muticum* and *Tetraselmis kochinensis* [23]. González-Ballesteros *et al.* have used the aqueous extract of *Cystoseira baccata* to synthesize AuNPs through an eco-friendly, fast, one-pot synthetic route [76]. The development of the nanoparticle was further characterized by TEM, UV-Vis spectroscopy, HRTEM and zeta potential measurements, which confirmed the preparation of stable, polycrystalline nanoparticles with spherical geometry having a diameter of 8.4 ± 2.2 nm. The algae extract also acted as a protective agent by keeping them separated, eluding the aggregation and coalescence of nanoparticles. The elemental composition and the functional group of biomolecules present in the extract and nanoparticles were characterized by EDS and FTIR study. From an application point of view, the nanoparticles were tested *in vitro* on the colon cancer cell lines Caco-2 and HT-29. The apoptotic activity of the nanoparticles was also determined. The whole study proposed that the synthesized AuNPs have significant potential to be used for the treatment of colorectal cancer [76].

In another reported study, the biosynthesis of AuNPs was carried out using *Sargassum wightii* for a short duration [77]. The TEM images of the synthesized nanoparticles suggest the formation of spherical shape AgNPs with a size of around 11 nm [77]. *Sargassum swartzii* was also used for the AuNPs synthesis [78]. In the synthesis procedure, chloroauric acid was used for the formation of AuNPs within 5 min at water bath temperature of 60 °C. The formation of the AuNPs was monitored by using a UV-Vis spectrophotometer. The prepared nanoparticles were spherical in geometry with a size of 35 nm. The nanoparticles showed a zeta potential of –27.6 mV, suggesting the high stability of nanoparticles. A dose-dependent cytotoxicity was demonstrated by the synthesized nanoparticles against human cervical carcinoma (HeLa) cells [78].

In another synthesis approach, Uma Suganya *et al.* have synthesized AuNPs used blue green alga *Spirulina platensis* and explored their antibacterial activity against *Staphylococcus aureus* and *Bacillus subtilis*. The prepared AuNPs had an average size of ~ 5 nm with uniform shape [79]. Researchers have also used *Stoechospermum marginatum* biomasses for the synthesis of AuNPs [80]. The preparation of the AuNPs was witnessed within 10 min and the properties of the as-prepared nanoparticles were studied by FTIR, SEM, TEM, XRD, photoluminescence (PL) spectra, X-ray fluorescence spectrophotometry and particle size analysis. The synthesized gold nanoparticles were found to have good PL property and showed absorption spectra at 550 nm. The TEM images of the nanoparticles reveal a spherical structure of 18.7–93.7 nm size. The as-synthesized AuNPs were found to be very effective against bacterial pathogens [80].

16.2.3.2 Algae and Fungi Mediated Synthesis of AgNPs

Over the past three decades, during the search for effective new medicines of natural origin, marine algae entered the limelight to become very popular for this purpose. Several compounds are being synthesized by seaweeds, like carbohydrates, flavonoids, steroids, alkaloids, phenols and saponins, which are very promising for application in both biotechnological and industrial fields. Marine algae have also been applied in a significant way for the synthesis of AgNPs. The green alga *Enteromorpha flexuosa* (Wulfen) J. Agardh has been used by Yousefzadi *et al.* for the ecofriendly biosynthesis of silver nanoparticles [81]. For the synthesis, they simply mixed the seaweed *E. flexuosa* extract and silver nitrate and the resultant nanoparticles were characterized by XRD, UV-Vis spectra, EDS and TEM analysis. The TEM study indicated nanoparticles of nearly spherical structure having a size range within 2–32 nm and mean diameter of

15 ± 1.5 nm. The synthesized nanoparticles were employed to study their antimicrobial activity [81].

Da Silva Ferreira *et al.* have reported a green approach for the preparation of microalgae-based silver chloride nanoparticle [82]. *Chlorella vulgaris* was used as the microalgae for the synthesis. In a typical synthesis procedure, first, the *C. vulgaris* culture was made and then the cell-free culture supernatant was used for the synthesis of AgCl NPs by incubating with silver nitrate for 5 days at 25 °C under dark conditions. UV-Vis spectroscopy and visual color change was used for monitoring the reduction reaction. For purification of the nanoparticles from the conditioned medium, it was centrifuged and stabilized by using 1% sodium citrate solution in water. The TEM images of the nanoparticles revealed a spherical morphology, and from the FTIR spectra it was concluded that the molecular species involved in AgCl nanoparticles formation are the cell proteins. Finally, their antimicrobial activity was also tested against pathogenic bacteria [82].

A group of researchers from Brazil have reported the use of red algae, *Gracilaria birdiae,* found along the coast of Piauí, Brazil, for the biosynthesis of AgNPs [83]. For the synthesis, they first extracted the polysaccharide from the red algae and used altered concentrations of 0.05, 0.03 and 0.02% v/v at two different pH values, i.e., 10 and 11. The mixture was stirred for 30 min at 90 °C. The hydrodynamic diameter of the synthesized AgNPs was calculated and found to be between 20.2 nm and 94.9 nm. Additionally, the synthesized nanoparticles have a spherical shape, small size and negative zeta potential value. They also studied the stability of the nanoparticles and after 4 months, no agglomeration in the nanomaterials was observed. Finally, the AgNPs were tested for antimicrobial activity using *Staphylococcus aureus* and *Escherichia coli* [83].

Abd-Elnaby *et al.* have extracellularly synthesized AgNPs using an actinomycete isolated from sediment from the Gulf of Suez (Red Sea) in Egypt [84]. They have tested about 41 actinomycetes and found that only two of them have the ability to synthesize AgNPs with antibacterial activity. Among the two, *Streptomyces rochei* MHM13 (accession number KR108310) is best suited for the synthesis, having a better morphological and physiological properties, together with 16S r-RNA sequence. The synthesized AgNPs can significantly inhibit the growth of pathogenic bacteria, which is of medical importance [84].

The synthesis of AgCl nanoparticles have been reported using brown algae (*Sargassum boveanum*) collected from the Persian Gulf [85]. The synthesized silver chloride nanoparticles were applied for the visual detection of H_2O_2. The interaction mechanism for the AgCl with H_2O_2 in both gas

and solvent phase was studied using density functional theory. For a potential sensing application, the selectivity of the sensor was also studied in the presence of high concentrations of organic substances, anions and some heavy metal ions. The sensor exhibited a linear range of 1–120 μM with a detection limit 8.6 nM for H_2O_2 [85].

Other scientists have used fungal species for the biosynthesis of AgNPs [86, 87]. Li *et al.* have used *Aspergillus terreus*, a very well-known fungi, for the preparation of organic acids. By this method, they have obtained stable and spherical-shaped AgNPs having size in the range of 1–20 nm [86]. Nicotinamide adenine dinucleotide hydrate (NADH) was considered the key reducing agent and this coenzyme is found in all living organisms. In this regard, it was concluded that the preparation of AgNPs may be an extracellular process, mediated by enzyme [86]. *Trichoderma asperellum*, a popular culturable fungus from soil, was also examined for their efficiency in AgNPs synthesis [87]. The kinetics of the reaction was studied by UV-Vis spectroscopy, which revealed a SPR band corresponding to the AgNPs at 410 nm was observed. The XRD and TEM analyses revealed that the size of the nanoparticle was in the range of 13–18 nm. From the stability study, it was concluded that the silver nanoparticles can maintain a constant size and shape after storage of 6 months [87].

16.2.4 Other Environmental Friendly Synthesis Approaches for Ag/AuNPs

Besides plant extract, microbe and algae mediated synthesis procedures, certain other environmental friendly synthesis approaches were also reported for synthesis of noble metal nanoparticles. In this section, we will discuss other popular green-synthesis methods based on biological specimens.

The first biological product we have included in this discussion is "honey," which is widely applied for metal nanoparticles synthesis. The special chemical composition of honey is the main reason for its wide use in the field of nanoparticle synthesis. The major ingredients of honey are carbohydrate (80–85%, generally fructose and glucose), water (15–17%), protein (0.1–0.4%), ash (0.2%) and a very small percent of vitamins, enzymes and amino acids, along with phenolic antioxidants [88]. In addition, the honey mediated synthesis approach also has several advantages over microorganism mediated methods. Moreover, this process is faster than the microbial method and does not require a difficult culturing process of microorganisms, which needs extreme care and time lag for the conversion of nanoparticles by microorganisms. In addition, the

separation of synthesized nanoparticles from microorganisms is a difficult task.

Daizy Philip from Mar Ivanios College, India, was the first to report honey mediated synthesis of AuNPs [89]. The reduction of $HAuCl_4$ was carried out using different volumes of diluted honey and it was observed that with an increase in volume, the reduction speed of gold particles increases. The synthesized nanoparticles were of spherical shape with a size ~15 nm and possess a high crystallinity demonstrated by SAED pattern, in which bright circular spots were observed. In the HRTEM image, clear lattice fringes can be observed. FTIR study suggests the presence of amide I and II bands and carboxylic acid group bands, demonstrating the protein binds to the Au surface through the amine group instead of the carboxyl group. According to the literature, fructose may have acted as the prime reducing agent in tandem with vitamin C (a mild reducing agent). Additionally, they also postulated that H_2O_2 and gluconic acid may be produced while honey was diluted with distilled water, and this may facilitate the reduction process [89]. In another reported study by Sreelakshmi *et al.*, a similar synthesis approach for the AuNPs has been reported [90]. The antimicrobial activity of synthesized nanoparticles was studied against *Candida albicans* and pathogenic bacteria for the first time.

In our daily life, after extracting useful materials, we always throw away the waste. Banana is considered a favorite food worldwide, and according to statistics reported in the literature, more than 100 million tons of bananas are consumed worldwide every year and their peels are dumped as garbage [91]. However, it is reported that the banana peel is compose of biopolymers, such as cellulose, hemicelluloses, pectin, lignin and proteins, which suggest their applicability towards nanoparticles synthesis. Bankar *et al.* have used banana peel extract for a nontoxic, eco-friendly and simple synthesis method for AuNPs [37]. For this, first they boiled the banana peel, and then it was crushed, precipitated in acetone and lastly air-dried to get powder form. The obtained powder was used for the reduction of chloroauric acid. They have also studied the effect of various conditions, like pH, peel content, concentration of precursors and temperature, on the nanoparticles formation. The synthesized nanoparticles exhibited high antimicrobial activity towards most of the bacterial and fungal cultures [37].

Chicken eggshell membrane (ESM) is also a huge waste source and has no value in our daily life. ESM is known as a double-layered membrane composed of amino acids, like alanine uronic acid and glycine and glycoproteins with collagen types I, V and X. Devi *et al.* have prepared highly fluorescent AuNPs using ESM (reported as one of nature's gifts by

the authors), having size below 20 nm [92]. The unique properties of this membrane is considered to be the main novelty of this technique, i.e., safe handling, resistance towards pH, and their obtainability in nature. The easy abundance of the source material also indicates the cost-effective preparation of AuNPs by this method [92].

He *et al.* have reported the use of rice husks for the AgNPs synthesis [93]. According to the Food and Agriculture Organization (FAO), 582 million tons of rice are produced worldwide in a year, among which, 145 million tons or 25 mass % is in the form of rice husks. The husks have very less commercial use and also cause serious pollution to the environment. The use of these husks in various fields has been already tried by many research groups. The main ingredient of these husks is silica, which is around 34.4% in the ash samples. A mixture of silver salt, ammonia, glucose and the rice husks was used for the synthesis of AgNPs [93]. It was reported that the C=C groups on rice husks might increase the reduction to Ag(0) from Ag(I). These types of ash-derived materials have been marketed by the Tata Corporation in India, known by the name Swach water filter. In the Tata Swach water filter, the ratio of Ag(0) to Ag(I) in the final prepared sample was 95/5 and the authors have found a slightly lower proportion of Ag(0) than the Tata Swach (in their case the ratio was 93/7), possibly resulting from the use of sodium borohydride (a strong reductant) in producing the Tata Swach. The AgNP-impregnated rice husks also exhibited a very strong bactericidal behavior against *S. aureus* and *E. coli*. The results associated with the study indicate the applicability of these types of green materials in environmental applications in the near future [93].

In another study, local waste vegetable fibers of *Murraya koenigii* (curry leaves), *Moringa oleifera* (drumstick tree) and *Luffa acutangula* (ridged gourd) were applied as reducing and stabilizing agents for the AgNPs synthesis [94]. For the sample preparation, the collected vegetables were dried, ground to powder and refluxed with distilled water. The extract was then cooled, centrifuged and kept in a freezer until use. In the synthesis procedure, silver nitrate solution was poured into the extract with constant stirring at room temperature and the yellow colored solution of the extract slowly turned to brown, indicating the bioreduction of Ag(I) ions to Ag(0) within 20 min. The prepared nanoparticles were used to study their antibacterial activity against *S. aureus* [94].

In another study, Bagherzade *et al.* have reported the use of extract of saffron (*Crocus sativus* L.) wastage for the biosynthesis of AgNPs [95]. The XRD data suggests the size of the nanoparticles was ~ 12–20 nm, and from TEM images it was concluded that spherical-shaped nanoparticles were formed with a size of 15 nm. The nanoparticles were applied to test their

antibacterial activity. From the results of antibacterial activities, it was concluded that the nanoparticles have inhibiting activity against *Klebsiella pneumoniae, Pseudomonas aeruginosa, Escherichia coli, Shigella flexneri* and *Bacillus subtilis* [95].

Chiu *et al.* have reported a mica clay mediated synthesis approach for AgNPs [96]. They first exfoliated the synthetic mica to get delaminated nano-sized mica platelets (Mica) by means of poly-oxypropylene-amine salt (POP-salt) (Figure 16.9). It has been reported that POP-amine can serve as an instant reducing agent and is the main material behind the reduction of $AgNO_3$ during the mica clay mediated synthesis of AgNPs. The reaction mechanism can be given as [96]:

$$\mathbf{Ag^+ + NO_3^- + \textit{POP-amine} \rightarrow (Ag^+ + \textit{POP-amine}) + NO_3^-} \quad (16.1)$$

$$\mathbf{(Ag^+ + \textit{POP-amine}) + NO_3^- \rightarrow Ag^0 + Oxidative\textit{POP-amine}NO_3^-} \quad (16.2)$$

The POP-amines composed of hydroxyl and amine functional groups have a dual function in the reaction, i.e., as a stabilizer and organic reducing agent for AgNPs. To obtain highly efficient AgNPs from this method, the effects of $AgNO_3$/Mica plate weight ratio were also studied. The TEM images revealed the spherical geometry of the AgNPs having a diameter of 8 nm.

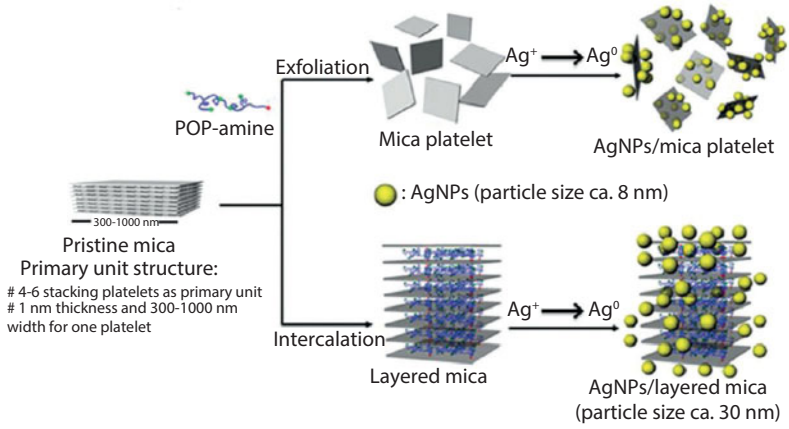


Figure 16.9 Conceptual illustration of AgNP-supported mica platelet. (Reproduced with permission from [96])

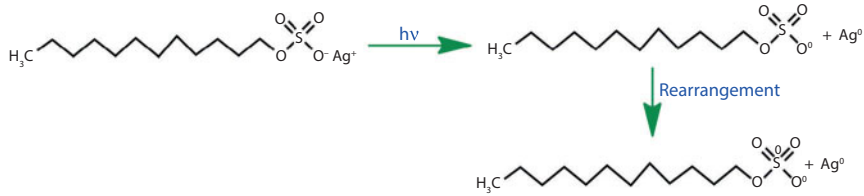


Figure 16.10 Schematic representation of the formation of AgNPs by SDS and natural sunlight.

Sunlight has also been used for silver nitrate reduction and the synthesis of AgNPs. Bhaduri *et al.* have used an anionic surfactant, sodium dodecyl sulphate (SDS), without using any additional reducing agents at room temperature under sunlight for the synthesis of AgNPs [97]. It has been reported that both SDS and natural sunlight were simultaneously responsible for the AgNPs formation, as shown in Figure 16.10.

The morphology and size of the prepared nanoparticles were studied using TEM images, and it was observed that the majority of nanoparticles possess a diameter below 30 nm. The nanoparticles were crystalline in nature with a face-centered cubic (fcc) lattice [97].

Some other efficient environmental friendly methods have also been used for the synthesis of AgNPs, like microwave heating method. By microwave heating, we can obtain smaller sizes of nanomaterials with a higher degree of crystallization and narrow size distribution. Microwave technique has certain advantageous effects like less energy consumption, better product yields and very low reaction times. By this way, it can also prevent the agglomeration of the prepared nanomaterials [98]. Nadagouda *et al.* have discussed and summarized the production of AgNPs by a microwave-assisted synthetic method [98]. Under microwave heating conditions, spherical-shaped nanoparticles can be obtained within a few minutes; but sometimes rods, polygonal plates, sheets, wires, dendrites and tubes are also formed. Microwave heating not only has the advantages reported above but can also significantly reduce chemical waste formation and lower reaction times.

16.2.5 Green Synthesis of Platinum Nanoparticles

Like gold and silver, platinum-based nanomaterials have also been applied in biomedical fields and can be used as excellent therapeutic agents [99]. Platinum compounds like cisplatin, carboplatin and oxaliplatin are often used in chemotherapy, particularly in the treatment of ovarian and

testicular tumors. In comparison to gold and silver, the application of green synthesis approach for synthesis of platinum nanoparticles (PtNPs) is less explored. Herein, we have added the recent green-synthesis techniques used for PtNPs preparation.

Neem (*Azadirachta indica*) is known for its medicinal characteristics and has been applied in the green synthesis of PtNPs by some research groups [100]. The formation of the nanoparticles was characterized by FTIR spectroscopy, TEM and UV-Vis study. The TEM images of the synthesized nanoparticles suggest the synthesis of nearly spherical shape nanostructure with a size of 5–50 nm. From the FTIR study, it was revealed that the protein molecules present in the neem extract is the probable biomolecule accountable for the reduction of chloroplatinic ion to PtNPs [100].

Nadaroglu *et al.* have used quail egg yolk for the biosynthesis of PtNPs [101]. Quail egg yolk has a high vitamin and protein content, which suggests its usefulness in biosynthesis of nanoparticles. During the course of their study, various reaction conditions, like pH, temperature, time and concentration of metal salt, were also optimized. From the optimization study, it was concluded that the highest platinum nanoparticles were synthesized at a temperature of 20 °C, pH = 6.0, reaction time of 4 h; and the optimal concentration of metal ions was 0.5 mM [101].

As we discussed earlier, tea has great potential in the biosynthesis of nanoparticles. In this case, tea has also been applied for the synthesis of PtNPs, where it acts in both reduction and surface modification of the nanoparticles [102]. The flower shape morphology (size: 30–60 nm) and the crystalline nature of the prepared tea polyphenol-functionalized platinum nanoparticles (TPP@Pt) was observed from their TEM images. Alshatwi *et al.* have treated the cervical cancer cells with different concentrations of TPP@Pt and the effects of TPP@Pt on cell cycle distribution, nuclear morphology and cell viability were also studied. The obtained results highlight the potential use of TPP@Pt in cervical cancer treatment [102].

The extract of *Punica granatum* peel, an agro-industrial waste, was also applied for the synthesis of PtNPs by Dauthal and Mukhopadhyay [103]. Polyphenolic compounds like gallic acid, quercetin and ellagic acid are the main constituents of the *P. granatum* peel. The probable mechanism based on ellagic acid reduction is shown in Figure 16.11. The TEM images of the nanoparticles have revealed the spherical shape of the nanoparticles with size of 16–23 nm. The FTIR study confirms the utilization of phenolic hydroxyls group in this bioreduction reaction. Lastly, the fabricated nanoparticles were applied to study their catalytic activity towards the reduction of anthropogenic pollutant, i.e., 3-nitrophenol, in the presence of $NaBH_4$ as reducing agent [103].

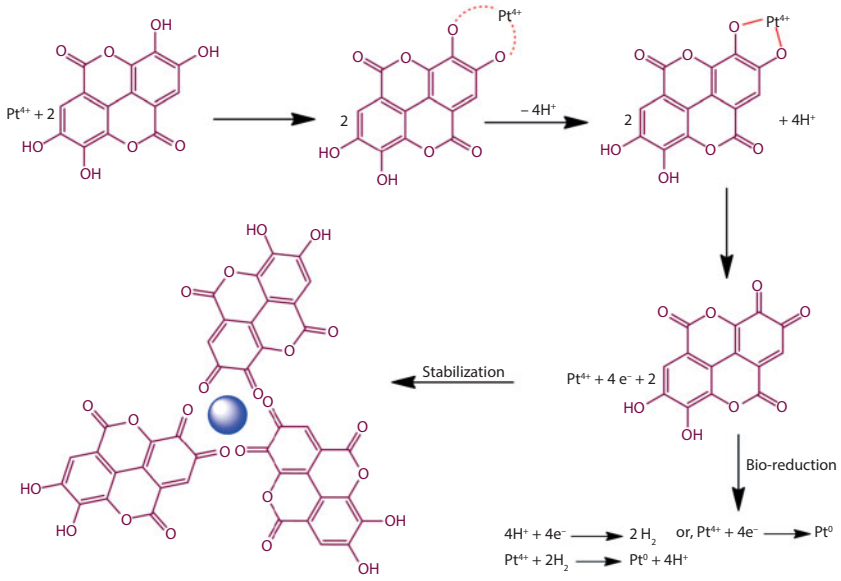


Figure 16.11 Proposed mechanism for biofabrication and stabilization of Pt-NPs by ellagic acid. (Reproduced with permission from [103])

16.3 Synthesis of Different Shaped Noble Metal Nanoparticles by Green Synthesis Approach

Recently, major emphasis has been given to the design and manipulation of well-defined nanostructures with a specific facet exposure. This will deliver a different way to improve the physicochemical properties of the nanomaterials. Previously, the reported method for obtaining different shapes was mainly based on the use of harsh and toxic chemicals, but nowadays significant attention has also been given to their green-synthesis approach.

Kou *et al*., have reported a green synthesis approach for the preparation of different shaped noble metals nanoparticles like Au, Pt, Pd using glycerol as the reducing agent [104]. The synthesis procedure was performed under microwave irradiation conditions and the shape of the nanoparticles was varied by adding different surfactant. Additionally, they have also studied the effect of reaction time, temperature, magnetic stirring and the change in surfactant on the shape of the nanoparticles. They have found that Au nanosheets can be prepared within 2 min and the size of Au nanosheets can be controlled by the glycerol content and microwave irradiation time. Scanning Electron Microscopic (SEM) technique was used to confirm the morphology of the prepared nanoparticles. As can be seen in Figure 16.12,

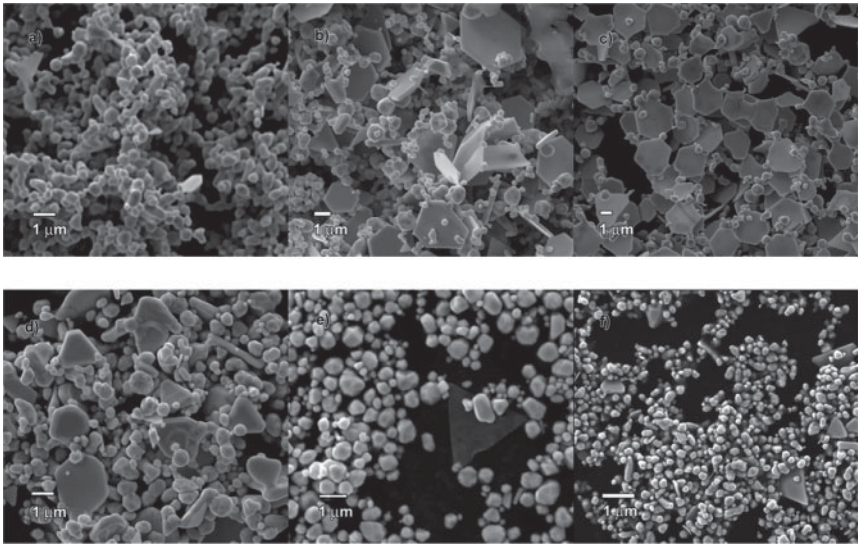


Figure 16.12 SEM images of the as-prepared Au samples with or without surfactant (other chemical: 2 mL Au aqueous solution (10 g/L), 4 mL glycerol, and 2 mL water). (a) no surfactant; (b) 0.05 mmol CTAB; (c) 0.1 mmol CTAB; (d) 0.2 mmol CTAB; (e) 0.4 mmol CTAB; (f) 2 mL ethanol was used to replace 2 mL water, 0.1 mmol CTAB (Reproduced after permission from [104]).

when the reaction was performed in the absence of surfactant, particles with the diameter ~500 nm were formed. When the amount of CTAB was 0.05 mmol, they have obtained some hexagonal nanosheets along with nanoparticles. Further enhancing the amount of CTAB (using 0.1 mmol), the formation of nanosheets was increased and the ratio between nanosheet to nanoparticles was reached >90%. Further enhancing the CTAB content, the formation of Au nanosheets was get hindered, as can be depicted in Figure 16.12 (d) and (e). The study provides a beautiful and step-by-step approach for the fabrication of different shaped nanoparticles.

In another work, Rout et al., have reported the synthesis of different shaped (i.e., Spherical, Triangular and Rod) silver nanoparticles using Mulberry (Morus rubra L.) leaves extract as the green reducing agent. The shape dependent bacterial activity of silver nanoparticles was studied against Escherichia coli in both agar plates and liquid systems. They have found a high reactivity in case of truncated triangular nanoplates that the other shaped (spherical and rod) silver nanoparticles. The study provides an understanding of how the surface areas of a nanomaterial can influence the killing activity [105].

Other literatures can also be found based on different shaped noble metal nanoparticles synthesis but maximum of them does not study the shape effects. For example, Aljabali *et al.*, have reported a simple and quick method for the synthesis of AuNPs using aqueous extract of the Ennab leaves (Ziziphus zizyphus) [106]. The prepared AuNPs were characterized by different characterization techniques: scanning electron microscopy, transmission electron microscopy, atomic force microscopy, energy dispersive X-ray spectroscopy and UV-vis spectroscopy. They have also studied the antifungal and antibacterial properties of the prepared monodisperse AuNPs, with various geometries against yeast (Candida albicans) and Gram-negative bacteria (E. coli).

Shankar *et al.* have used an extracellular synthesis approach for AuNPs applying geranium leaves (*Pelargonium graveolens*) and an endophytic fungus (*Colletotrichum* sp.) growing in the leaves [107]. In the case of AuNPs synthesized using geranium leaves, terpenoids are the major capping as well as reducing agents, while in the case of *Colletotrichum* sp., polypeptides/enzymes play the same role. The fungus mediated synthesized AuNPs possess a spherical shape while leaves mediated synthesized AuNPs possess a variety of shapes, including triangles, flat sheets and rods. Although they have not provided the exact reasons for variation in shape variability, the results suggest the possibility of achieving shape control nanoparticles using a host leaf-fungus system as reducing agent [107].

Besides the synthesis of spherical-shaped PtNPs, there are certain other published studies which also have reported the fabrication of anisotropic PtNPs. Dobrucka has reported *Fumariae herba* extract for the synthesis of hexagonal- and pentagonal-shaped PtNPs [108]. The catalytic activity of the synthesized PtNPs was explored towards the reduction of two organic dyes, i.e., methylene blue and crystal violet [108]. Dried leaf powder of *Anacardium occidentale* has also been used for the synthesis of rod-shaped, crystalline PtNPs [109]. From the FTIR spectra, it was found that proteins are bound to PtNPs and quantity of leaf powder is the main factor towards the size of particles. To study the catalytic activity of the nanoparticles, the as-synthesized nanoparticles were applied for the reduction of aromatic nitro compound [109].

16.4 Conclusion and Future Scope

In this chapter, we have discussed the biological mediated green synthesis procedures reported for synthesis of noble metal nanoparticles. In addition, the mechanisms involved in the synthesis and the potential use of synthesized nanoparticles were also discussed. Taking into account the

considerations outlined in this chapter, it appears that the green synthesis approach exemplifies a promising route for nanoparticles production. Indeed, green synthesis reduces energy consumption, in comparison to the general chemical synthesis methods. Furthermore, by changing the amount of the precursor material, the shape and size of the nanoparticles can be controlled, which points to their bright future in nanotechnology. The green synthesis approach possesses benefits for the initiation of a safe and sustainable nanotechnology. In most cases, the published works dealt with microorganism-based green-synthesis, where the identification of the exact nature of the agents responsible for the process is very difficult. Therefore, more research is needed using biological fractions and cell-free extracts, by which a thorough understanding and identification of regulatory processes can be carried out.

When discussing the cost of nanoparticle synthesis compared to a chemical-based synthesis procedure, the primary cost of the prepared nanoparticles is mostly calculated by the cost of both reducing agents and metal salts. But, whenever we use "green" synthesis, the only costs will be the metal salts, which obviously reduce the entire cost of synthesis to a great extent. Additionally, popularity in the use of waste materials towards nanoparticle synthesis has provided another direction for companies who are interested in recycling waste.

Although numerous research papers have been reported in the last four to five years with different possibilities and novelties in the field of nanoparticle synthesis via green-chemistry approach, not a single one has been commercialized. Most of the works are at the proof-of-concept stage or lab-scale stage only. In fact, they can operate only under the highly specific conditions and settings of research laboratories, whereas their translation into clinical trials still seems very remote. A detailed study towards their commercialization is highly required at this stage to make them applicable and useful in real terms also.

Acknowledgment

Mr. Patra has given the major contribution in writing this book chapter along with drawing the Figures and Tables, taking the copy right permission etc.

References

1. Boholm, B., The use and meaning of nano in American English: Towards a systematic description. *Ampersand*, 3, 163–173, 2016.

2. Sciau, P., Nanoparticles in ancient materials: The metallic lustre decorations of medieval ceramics, in: *The Delivery of Nanoparticles*, Hashim, A.A. (Ed.), pp. 525–550, InTech, 2012.
3. Uskoković, V., Entering the era of nanoscience: Time to be so small. *J. Biomed. Nanotechnol.*, 9, 1441–1470, 2013.
4. Gatoo, M.A., Naseem, S., Arfat, M.Y., Dar, A.M., Qasim, K., Zubair, S., Physicochemical properties of nanomaterials: Implication in associated toxic manifestations. *BioMed Res. Int.*, 2014, 1–9, 2014.
5. Nikalje, A.P., Nanotechnology and its applications in medicine. *Med. Chem.*, 5, 81–89, 2015.
6. Wang, Y., Xia, Y., Bottom-up and top-down approaches to the synthesis of monodispersed spherical colloids of low melting-point metals. *Nano Lett.*, 4, 2047–2050, 2004.
7. Khan, I., Saeed, K., Khan, I., Nanoparticles: Properties, applications and toxicities. *Arab. J. Chem.*, 1–70, 2017.
8. Ganjali, M., Ganjali, M., Vahdatkhah, P., Marashi, S.M.B., Synthesis of Ni nanoparticles by pulsed laser ablation method in liquid phase. *Procedia Mater. Sci.*, 11, 359–363, 2015.
9. Colson, P., Henrist, C., Cloots, R., Nanosphere lithography: A powerful method for the controlled manufacturing of nanomaterials. *J. Nanomater.*, 2013, 1–10, 2013.
10. Mueller, R., Mädler, L., Pratsinis, S.E., Nanoparticle synthesis at high production rates by flame spray pyrolysis. *Chem. Eng. Sci.*, 58, 1969–1976, 2003.
11. Subramania, A., Vijaya Kumar, G., Sathiya Priya, A.R., Vasudevan, T., Polyol-mediated thermolysis process for the synthesis of MgO nanoparticles and nanowires. *Nanotechnology*, 18(22), 225601–225612, 2007.
12. Al-Resheedi, A., Alhokbany, N.S., Mahfouz, R.M., Radiation induced synthesis of In_2O_3 nanoparticles - part 1: Synthesis of In_2O_3 nanoparticles by sol-gel method using un-irradiated and γ-irradiated indium acetate. *Mater. Res.*, 17, 346–351, 2014.
13. Bai, J., Lia, Y., Li, M., Wang, S., Zhang, C., Yang, Q., Electrospinning method for the preparation of silver chloride nanoparticles in PVP nanofiber. *Appl. Surf. Sci.*, 254, 4520–4523, 2008.
14. Biswas, A., Bayer, I.S., Biris, A.S., Wang, T., Dervishi, E., Faupel, F., Advances in top–down and bottom–up surface nanofabrication: Techniques, applications & future prospects. *Adv. Colloid Interface Sci.*, 170, 2–27, 2012.
15. Yu, C.-H., Tam, K., Tsang, E.S.C., Chemical methods for preparation of nanoparticles in solution, in: *Handbook of Metal Physics*, chap. 5, pp. 113–141, 2008.
16. Anandgaonker, P., Kulkarni, G., Gaikwad, S., Rajbhoj, A., Synthesis of TiO_2 nanoparticles by electrochemical method and their antibacterial application. *Arab. J. Chem.*, 1–8, 2014.

17. Zhu, J., Koltypin, Y., Gedanken, A., General sonochemical method for the preparation of nanophasic selenides: Synthesis of ZnSe nanoparticles. *Chem. Mater.*, 12, 73–78, 2000.
18. Donati, I., Travan, A., Pelillo, C., Scarpa, T., Coslovi, A., Bonifacio, A., Sergo, V., Paoletti, S., Polyol synthesis of silver nanoparticles: Mechanism of reduction by alditol bearing polysaccharides. *Biomacromolecules*, 10, 210–213, 2009.
19. Betke, A., Kickelbick, G., Bottom-up, wet chemical technique for the continuous synthesis of inorganic nanoparticles. *Inorganics*, 2, 1–15, 2014.
20. Makarov, V.V., Love, A.J., Sinitsyna, O.V., Makarova, S.S., Yaminsky, I.V., Taliansky, M.E., Kalinina, N.O., "Green" nanotechnologies: Synthesis of metal nanoparticles using plants. *Acta Naturae*, 6, 35–44, 2014.
21. Anastas, P.T., Warner, J.C., *Green Chemistry: Theory and Practice*, Oxford University Press: New York, 1998.
22. Nath, D., Banerjee, P., Green nanotechnology—A new hope for medical biology. *Environ. Toxicol. Pharmacol.*, 36, 997–1014, 2013.
23. Shankar, P.D., Shobana, S., Karuppusamy, I., Pugazhendhid, A., Ramkumare, V.S., Arvindnarayan, S., Kumar, G., A review on the biosynthesis of metallic nanoparticles (gold and silver) using bio-components of microalgae: Formation mechanism and applications. *Enzyme Microb. Technol.*, 95, 28–44, 2016.
24. Roy, N., Gaur, A., Jain, A., Bhattacharya, S., Rani, V., Green synthesis of silver nanoparticles: An approach to overcome toxicity. *Environ. Toxicol. Pharmacol.*, 36, 807–812, 2013.
25. Teimuri-Mofrad, R., Hadi, R., Tahmasebi, B., Farhoudian, S., Mehravar, M., Nasiri, R., Green synthesis of gold nanoparticles using plant extract: Mini-review. *Nanochem. Res.*, 2, 1–12, 2017.
26. Patra, S., Roy, E., Tiwari, A., Madhuri, R., Sharma, P.K., 2-Dimensional graphene as a route for emergence of additional dimension nanomaterials. *Biosens. Bioelectron.*, 89, 8–27, 2017.
27. Li, S., Shen, Y., Xie, A., Yu, X., Qiu, L., Green synthesis of silver nanoparticles using *Capsicum annuum* L. extract. *Green. Chem.* 9, 852–858, 2007.
28. Bar, H., Bhui, D.K., Sahoo, G.P., Sarkar, P., Pyne, S., Green synthesis of silver nanoparticles using seed extract of *Jatropha curcas*. *Colloids Surf. A*, 348, 212–216, 2009.
29. Song, J.Y., Kim, B.S., Rapid biological synthesis of silver nanoparticles using plant leaf extracts. *Bioprocess Biosyst. Eng.*, 32, 79–84, 2009.
30. Sathishkumar, M., Sneha, K., Won, S.W., Cho, C.W., Kim, S., *Cinnamon zeylanicum* bark extract and powder mediated green synthesis of nano-crystalline silver particles and its bactericidal activity, *Colloids Surf. B*, 73, 332–338, 2009.
31. Shankar, S.S., Ahmad, A., Pasrichaa, R., Sastry, M., Bioreduction of chloroaurate ions by geranium leaves and its endophytic fungus yields gold nanoparticles of different shapes. *J. Mater. Chem.*, 13, 1822–1826, 2003.

32. Ahmad, N., Sharma, S., Alam, M.K., Singh, V.N., Shamsi, S.F., Mehta, B.R., Fatma, A., Rapid synthesis of silver nanoparticles using dried medicinal plant of basil. *Colloids Surf. B*, 81, 81–86, 2010.
33. Si, S., Mandal, T.K., Tryptophan-based peptides to synthesize gold and silver nanoparticles: A mechanistic and kinetic study. *Chemistry*, 13, 3160–3168, 2007.
34. Haverkamp, R., Marshall, A.T., The mechanism of metal nanoparticle formation in plants: Limits on accumulation. *J. Nanopart. Res.*, 11, 1453–1463, 2009.
35. Selvakannan, P., Mandal, S., Phadtare, S., Gole, A., Pasricha, R., Adyanthaya, S.D., Sastry, M., Water-dispersible tryptophan-protected gold nanoparticles prepared by the spontaneous reduction of aqueous chloroaurate ions by the amino acid. *J. Colloid Interface Sci.*, 269, 97–102, 2004.
36. Ghodake, G.S., Deshpande, N.G., Lee, Y.P., Jin, E.S., Pear fruit extract-assisted room-temperature biosynthesis of gold nanoplates. *Colloids Surf. B*, 75, 584–589, 2010.
37. Bankar, A., Joshi, B., Ravi Kumar, A., Zinjarde, S., Banana peel extract mediated synthesis of gold nanoparticles. *Colloids Surf. B*, 80, 45–50, 2010.
38. Harris, A., Bali, R., On the formation and extent of uptake of silver nanoparticles by live plants. *J. Nanopart. Res.*, 10, 691–695, 2008.
39. Gardea-Torresdey, J.L., Parsons, J., Gomez, E., Peralta-Videa, J., Troiani, H., Santiago, P., Yacaman, M., Formation and growth of Au nanoparticles inside live alfalfa plants. *Nano Lett.*, 2, 397–401, 2002.
40. Manceau, A., Nagy, K.L., Marcus, M.A., Lanson, M., Geoffroy, N., Jacquet, T., Kirpichtchikova, T., Formation of metallic copper nanoparticles at the soil-root interface. *Environ. Sci. Technol.*, 42, 1766–1772, 2008.
41. Anuradha, J., Abbasi, T., Abbasi, S., Green synthesis of gold nanoparticles with aqueous extracts of neem (*Azadirachta indica*). *Res. J. Biotechnol.*, 5, 75–79, 2010.
42. Muthukumara, T., Sudhakumari, R., Sambandam, B., Aravinthand, A., Sastrya, T.P., Kim, J.H., Green synthesis of gold nanoparticles and their enhanced synergistic antitumor activity using HepG2 and MCF7 cells and its antibacterial effects. *Process Biochem.*, 51, 384–391, 2016.
43. Hoshyar, R., Khayati, G.R., Poorgholami, M., Kaykhaii, M., A novel green one-step synthesis of gold nanoparticles using crocin and their anti-cancer activities. *J. Photochem. Photobiol., B*, 159, 237–242, 2016.
44. Gonnelli, C., Cacioppo, F., Cristiana, G., Capozzoli, L., Salvatici, C., Salvatici, M.C., Colzi, I., Bubba, M.D., Ancillotti, C., Ristori, S., *Cucurbita pepo* L. extracts as a versatile hydrotropic source for the synthesis of gold nanoparticles with different shapes. *Green Chem. Lett. Rev.*, 8, 39–47, 2015.
45. Nirmala, J.G., Akila, S., Narendhirakannan, R.T., Chatterjee, S., *Vitis vinifera* peel polyphenols stabilized gold nanoparticles induce cytotoxicity and apoptotic cell death in A431 skin cancer cell lines. *Adv. Powder Technol.*, 28, 1170–1184, 2017.

46. Islam, N.U., Jalil, K., Shahid, M., Rauf, A., Muhammad, N., Khan, A., Shah, M.R., Khan, M.A., Green synthesis and biological activities of gold nanoparticles functionalized with *Salix alba*. *Arab. J. Chem.,* 1–42, 2015.
47. Rajan, A., Rajan, A.R., Philip, D., *Elettaria cardamomum* seed mediated rapid synthesis of gold nanoparticles and its biological activities. *OpenNano*, 2, 1–8, 2017.
48. Patra, J.K., Kwon, Y., Baek, K.-H., Green biosynthesis of gold nanoparticles by onion peel extract: Synthesis, characterization and biological activities. *Adv. Powder Technol.*, 27, 2204–2213, 2016.
49. Paul, B., Bhuyan, B., Purkayastha, D.D., Vadivel, S., Dhar, S.S., One-pot green synthesis of gold nanoparticles and studies of their anticoagulative and photocatalytic activities. *Mater. Lett.*, 185, 143–147, 2016.
50. Yu, X., Xu, D., Guan, H.N., Wang, C., Huang, L.K., Chi, D.F., Facile one-step green synthesis of gold nanoparticles using *Citrus maxima* aqueous extracts and its catalytic activity. *Mater. Lett.*, 166, 110–112, 2016.
51. Abdel-Hafez, S.I.I., Nafady, N.A., Abdel-Rahim, I.R., Shaltout, A.M., Mohamed, M.A., Biogenesis and optimisation of silver nanoparticles by the endophytic fungus *Cladosporium sphaerospermum*. *Int. J. Nano. Chem.*, 2, 11–19, 2016.
52. Kuppusamy, P., Yusoff, M.M., Maniam, G.P., Govindan, N.G., Biosynthesis of metallic nanoparticles using plant derivatives and their new avenues in pharmacological applications—An updated report. *Saudi Pharm. J.*, 24, 473–484, 2016.
53. Moulton, M.C., Braydich-Stolle, L.K., Nadagouda, M.N., Kunzelman, S., Hussain, S.M., Varma, R.S., Synthesis, characterization and biocompatibility of "green" synthesized silver nanoparticles using tea polyphenols. *Nanoscale*, 2, 763–770, 2010.
54. Vilchis-Nestor, A.R., Sánchez-Mendieta, V., Camacho-López, M.A., Gómez-Espinosa, R.M., Camacho-López, M.A., Arenas-Alatorre, J.A., Solventless synthesis and optical properties of Au and Ag nanoparticles using *Camellia sinensis* extract. *Mater. Lett.* 62, 3103–3105, 2008.
55. Sun, Q., Cai, X., Li, J., Zheng, M., Chen, Z., Yu, C.P., Green synthesis of silver nanoparticles using tea leaf extract and evaluation of their stability and antibacterial activity. *Colloids Surf. A*, 444, 226–231, 2014.
56. Dong, C., Cao, C., Zhang, X., Zhan, Y., Wang, X., Yang, X., Zhou, K., Xiao, X., Yuan, B., Wolfberry fruit (*Lycium barbarum*) extract mediated novel route for the green synthesis of silver nanoparticles. *Optik*, 130, 162–170, 2017.
57. Ahmed, M.J., Murtaza, G., Mehmood, A., Bhatti, T.M., Green synthesis of silver nanoparticles using leaves extract of *Skimmia laureola*: Characterization and antibacterial activity. *Mater. Lett.*, 153, 10–13, 2015.
58. Ghaedi, M., Yousefinejad, M., Safarpoor, M., Zare Khafri, H., Purkait, M.K., *Rosmarinus officinalis* leaf extract mediated green synthesis of silver nanoparticles and investigation of its antimicrobial properties. *J. Ind. Eng. Chem.*, 31, 167–172, 2015.

59. Ren, Y.-Y., Yang, H., Wang, T., Wang, C., Green synthesis and antimicrobial activity of monodisperse silver nanoparticles synthesized using *Ginkgo biloba* leaf extract. *Phys. Lett. A*, 380, 3773–3777, 2016.
60. Velusamya, P., Das, J., Pachaiappan, R., Vaseeharan, R., Pandian, K., Greener approach for synthesis of antibacterial silver nanoparticles using aqueous solution of neem gum (*Azadirachta indica* L.). *Ind. Crops Prod.*, 66, 103–109, 2015.
61. Nayak, D., Ashe, S., Rauta, P.R., Kumari, M., Nayak, B., Bark extract mediated green synthesis of silver nanoparticles: Evaluation of antimicrobial activity and antiproliferative response against osteosarcoma. *Mater. Sci. Eng. C*, 58, 44–52, 2016.
62. Pattanayak, S., Mollick, M.M.R., Maity, D., Chakraborty, S., Dash, S.K., Chattopadhyay, S., Roy, S., Chattopadhyay, D., Chakraborty, M., *Butea monosperma* bark extract mediated green synthesis of silver nanoparticles: Characterization and biomedical applications. *J. Saudi Chem. Soc.*, 21, 673–684, 2017.
63. Kumar, B., Smita, K., Debut, A., Cumbal, L., Extracellular green synthesis of silver nanoparticles using Amazonian fruit Araza (*Eugenia stipitata* McVaugh). Trans. Nonferrous Met. Soc. China, 26, 2363–2371, 2016.
64. Khalilzadeh, M.A., Borzoo, M., Green synthesis of silver nanoparticles using onion extract and their application for the preparation of a modified electrode for determination of ascorbic acid. *J. Food Drug Anal.*, 24, 796–803, 2016.
65. Husseiny, I.M., El-Aziz, A.M., Badr, Y., Mahmoud, A.M., Biosynthesis of gold nanoparticles using *Pseudomonas aeruginosa*. *Spectrochim. Acta A*, 67, 1003–1006, 2007.
66. Reith, F., Etschmann, B., Grosse, C., Moors, H., Benotmane, M.A., Monsieurs, P., Grass, G., Doonan, C., Vogt, S., Lai, B., Martinez-Criado, G., George, G.N., Nies, D.H., Mergeay, M., Pring, A., Southam, G., Brugger, J., Mechanisms of gold biomineralization in the bacterium *Cupriavidus metallidurans*. *Proc. Natl. Acad. Sci. USA*, 106, 17757–17762, 2009.
67. He, S., Zhang, Y., Guo, Z., Gu, N., Biological synthesis of gold nanowires using extract of *Rhodopseudomonas capsulata*. *Biotechnol. Prog.*, 24, 476–480, 2008.
68. Li, J., Li, Q., Ma, X., Tian, B., Li, T., Yu, J., Dai, S., Weng, W., Hua, Y., Biosynthesis of gold nanoparticles by the extreme bacterium *Deinococcus radiodurans* and an evaluation of their antibacterial properties. *Int. J. Nanomed.*, 11, 5931–5944, 2016.
69. Prema, P., Iniya, A., Immanuel, G., Microbial mediated synthesis, characterization, antibacterial and synergistic effect of gold nanoparticles using *Klebsiella pneumoniae* (MTCC- 4030). *RSC Adv.*, 6, 4601–4607, 2016.
70. Samadi, N., Golkaran, D., Eslamifar, A., Jamalifar, H., Fazeli, M.R., Mohseni, F.A., Intra/extracellular biosynthesis of silver nanoparticles by an autochthonous strain of *Proteus mirabilis* isolated from photographic waste. *J. Biomed. Nanotech.*, 5, 247–253, 2009.

71. Ramanathan, R., O'Mullane, A.P., Parikh, R.Y., Smooker, P.M., Bhargava, S.K., Bansal, V., Bacterial kinetics-controlled shape-directed biosynthesis of silver nanoplates using *Morganella psychrotolerans*. *Langmuir*, 27, 714–719, 2011.
72. Sadhasivam, S., Shanmugam, P., Yun, K., Biosynthesis of silver nanoparticles by *Streptomyces hygroscopicus* and antimicrobial activity against medically important pathogenic microorganisms. *Colloids Surf. B*, 81, 358–362, 2010.
73. Davis, T.A., Volesky, B., Mucci, A., A review of the biochemistry of heavy metal biosorption by brown algae. *Water Res.*, 37, 4311–4330, 2010.
74. Zuercher, A.W., Fritsche, R., Corthesy, B., Mercenier, A., Food products and allergy development: Prevention and treatment. *Curr. Opin. Biotechnol.*, 17, 198–203, 2006.
75. Mohamed, S., Hashim, S.N., Rahman, H.A., Seaweeds: A sustainable functional food for complementary and alternative therapy. *Trends Food Sci. Technol.*, 23, 83–96, 2012.
76. González-Ballesteros, N., Prado-López, S., Rodríguez-González, J.B., Lastra, M., Rodríguez-Argüelles, M.C., Green synthesis of gold nanoparticles using brown algae *Cystoseira baccata*: Its activity in colon cancer cells. *Colloids Surf. B*, 153, 190–198, 2017.
77. Singaravelu, G., Arockiamary, J.S., Ganesh Kumar, V., Govindaraju, K., A novel extracellular synthesis of monodisperse gold nanoparticles using marine alga, *Sargassum wightii* Greville. *Colloids Surf. B*, 57, 97–101, 2007.
78. Dhas, T.S., Ganesh Kumar, V., Karthick, V., Govindaraju, K., Narayana, T.S., Biosynthesis of gold nanoparticles using *Sargassum swartzii* and its cytotoxicity effect on HeLa cells. *Spectrochim. Acta A*, 133, 102–106, 2014.
79. Uma Suganya, K.S., Govindaraju, K., Ganesh Kumar, V., Dhas, T.S., Karthick, V., Singaravelu, G., Elanchezhiyan, M., Blue green alga mediated synthesis of gold nanoparticles and its antibacterial efficacy against Gram positive organisms. *Mater. Sci. Eng. C*, 47, 351–356, 2015.
80. Rajathi, F.A.A., Parthiban, C., Ganesh Kumar, V., Anantharaman, P., Biosynthesis of antibacterial gold nanoparticles using brown alga, *Stoechospermum marginatum* (kützing). *Spectrochim. Acta A*, 99, 166–173, 2012.
81. Yousefzadi, M., Rahimi, Z., Ghafori, V., The green synthesis, characterization and antimicrobial activities of silver nanoparticles synthesized from green alga *Enteromorpha flexuosa* (Wulfen) J.Agardh. *Mater. Lett.*, 137, 1–4, 2014.
82. da Silva Ferreira, V., ConzFerreira, M.E., Lima, L.M., Frasés, S., de Souza, W., Sant'Anna, C., Green production of microalgae-based silver chloride nanoparticles with antimicrobial activity against pathogenic bacteria. *Enzyme Microb. Technol.*, 97, 114–121, 2017.
83. De Aragão, A., de Oliveira, T.M., Quelemes, P.V., Perfeito, M.L.G., Araújo, M.C., Santiago, J.A.S., Cardoso, V.S., Quaresma, P., Leite, J.R.S.A, da Silva, D.A., Green synthesis of silver nanoparticles using the seaweed *Gracilaria birdiae* and their antibacterial activity. *Arab. J. Chem.*, 1–17, 2016.

84. Abd-Elnaby, H.M., Abo-Elala, G.M., Abdel-Raouf, U.M., Hamed, M.M., Antibacterial and anticancer activity of extracellular synthesized silver nanoparticles from marine *Streptomyces rochei* MHM13. *Egypt. J. Aquat. Res.*, 42, 301–312, 2016.
85. Farrokhnia, M., Karimi, S., Momeni, S., Khalililaghab, S., Colorimetric sensor assay for detection of hydrogen peroxide using green synthesis of silver chloride nanoparticles: Experimental and theoretical evidence. *Sens. Actuators B*, 246, 979–987, 2017.
86. Li, G., He, D., Qian, Y., Guan, B., Gao, S., Cui, Y., Yokoyama, K., Wang, L., Fungus-mediated green synthesis of silver nanoparticles using *Aspergillus terreus*. *Int. J. Mol. Sci.*, 13, 466–476, 2011.
87. Mukherjee, P., Roy, M., Mandal, B.P., Dey, G.K., Mukherjee, P.K., Ghatak, J., Tyagi, A.K., Kale, S.P., Green synthesis of highly stabilized nanocrystalline silver particles by a non-pathogenic and agriculturally important fungus *T. asperellum*. *Nanotechnology,* 19, 1–7, 2008.
88. Balasooriya, E.R., Jayasinghe, C.D., Jayawardena, U.A., Ruwanthika, R.W.D, de Silva, R.M., Udagama, P.V., Honey mediated green synthesis of nanoparticles: New era of safe nanotechnology. *J. Nanomater.*, 2017, 1–11, 2017.
89. Philip, D., Honey mediated green synthesis of gold nanoparticles. *Spectrochim. Acta A*, 73, 650–653, 2009.
90. Sreelakshmi, C., Datta, K.K.R., Yadav, J.S., Subba Reddy, B.V., Honey derivatized Au and Ag nanoparticles and evaluation of its antimicrobial activity. J. Nanosci. Nanotech., 11, 6995–7000, 2011.
91. Sharma, D., Kanchi, S., Bisetty, K., Biogenic synthesis of nanoparticles: A review. *Arab. J. Chem.,* 1–67, 2015.
92. Devi, P.S., Banerjee, S., Chowdhury, S.R., Kumar, G.S., Eggshell membrane: A natural biotemplate to synthesize fluorescent gold nanoparticles. *RSC Adv.*, 2, 11578–11585, 2012.
93. He, D., Ikeda-Ohno, A., Boland, D.D., Waite, T.D., Synthesis and characterization of antibacterial silver nanoparticle-impregnated rice husks and rice husk ash. *Environ. Sci. Technol.*, 47, 5276–5284, 2013.
94. Jaybhaye, S.V., Antimicrobial activity of silver nanoparticles synthesized from waste vegetable fibers. *Materials Today: Proceedings*, 2, 4323–4327, 2015.
95. Bagherzade, G., Tavakoli, M.M., Namaei, M.H., Green synthesis of silver nanoparticles using aqueous extract of saffron (*Crocus sativus* L.) wastages and its antibacterial activity against six bacteria. *Asian Pac. J. Trop. Biomed.*, 7, 227–233, 2017.
96. Chiu, C.-W., Hong, P.-D., Lin, J.-J., Clay-mediated synthesis of silver nanoparticles exhibiting low-temperature melting. *Langmuir*, 27, 11690–11696, 2011.
97. Bhaduria, G.A., Little, R., Khomane, R.B., Lokhande, S.U., Kulkarni, B.D., Mendis, B.G., Siller, L., Green synthesis of silver nanoparticles using sunlight. *J. Photochem. Photobiol. A*, 258, 1–9, 2013.
98. Nadagouda, M.A., Speth, T.F., Varma, R.S., Microwave-assisted green synthesis of silver nanostructures. *Acc. Chem. Res.*, 44, 469–478, 2011.

99. Siddiqi, K.S., Husen, A., Green synthesis, characterization and uses of palladium/platinum nanoparticles. *Nanoscale Res. Lett.*, 11, 482, 2016.
100. Thirumurugan, A., Aswitha, P., Kiruthika, C., Nagarajan, S., Christy, A.N., Green synthesis of platinum nanoparticles using *Azadirachta indica*—An eco-friendly approach. *Mater. Lett.*, 170, 175–178, 2016.
101. Nadaroglu, H., Gungor, A.A., Ince, S., Babagil, A., Green synthesis and characterisation of platinum nanoparticles using quail egg yolk. *Spectrochim. Acta A*, 172, 43–47, 2017.
102. Alshatwi, A.A., Athinarayanan, J., Subbarayan, P.V., Green synthesis of platinum nanoparticles that induce cell death and G2/M-phase cell cycle arrest in human cervical cancer cells. *J. Mater. Sci. Mater. Med.*, 26(7), 1–9, 2015.
103. Dauthal, P., Mukhopadhyay, M., Biofabrication, characterization, and possible bio-reduction mechanism of platinum nanoparticles mediated by agro-industrial waste and their catalytic activity. *J. Ind. Eng. Chem.*, 22, 185–191, 2015.
104. Kou, J., Bennett-Stamper, C., Varma, R. S., Green Synthesis of Noble Nanometals (Au, Pt, Pd) Using Glycerol under Microwave Irradiation Conditions. *ACS Sustainable Chem. Eng.* 1, 810–816, 2013.
105. Rout, A., Jena, P.K., Sahoo, D., Bindhani, B.K., Green Synthesis of Silver Nanoparticles of different Shapes and its Antibacterial Activity against *Escherichia coli. Int. J. Curr. Microbiol. App. Sci*. 3, 374–383, 2014.
106. Aljabali, A.A.A., Akkam, Y., Al Zoubi, M.S., Al-Batayneh, K.M., Al-Trad, B., Alrob, O.A., Alkilany, A.M., Benamara, B., Evans, D.J., Synthesis of Gold Nanoparticles Using Leaf Extract of *Ziziphus zizyphus* and their Antimicrobial Activity. *Nanomaterials*, 8, 174, 2018.
107. Shankar, S.S., Ahmad, A., Pasricha, R., Sastry, M., Bioreduction of chloroaurate ions by geranium leaves and its endophytic fungus yields gold nanoparticles of different shapes. *J. Mater. Chem.*, 13, 1822–1826, 2003.
108. Dobrucka, R., Biofabrication of platinum nanoparticles using *Fumariae herba* extract and their catalytic properties. *Saudi J. Biol. Sci.*, 1–18, 2016.
109. Sheny D.S., Philip, D., Mathew, J., Synthesis of platinum nanoparticles using dried *Anacardium occidentale* leaf and its catalytic and thermal applications. *Spectrochim. Acta A*, 114, 267–271, 2013.
110. Sadeghi, B., Mohammadzadeh, M., Babakhani, B., Green synthesis of gold nanoparticles using *Stevia rebaudiana* leaf extracts: Characterization and their stability. *J. Photochem. Photobiol. B*, 148, 101–106, 2015.
111. Bogireddy, N.K.R., Anand, K.K.H., Mandal, B.K., Gold nanoparticles—Synthesis by *Sterculia acuminata* extract and its catalytic efficiency in alleviating different organic dyes. *J. Mol. Liq.*, 211, 868–875, 2015.
112. Guo, M., Li, W., Yang, F., Liu, H., Controllable biosynthesis of gold nanoparticles from a *Eucommia ulmoides* bark aqueous extract. *Spectrochim. Acta A*, 142, 73–79, 2015.
113. Manivasagan, P., Venkatesan, J., Kang, K.H., Sivakumar, K., Park, S.-J., Kim, S.-K., Production of α-amylase for the biosynthesis of gold nanoparticles using *Streptomyces* sp. MBRC-82. *Int. J. Biol. Macromol.,* 72, 71–78, 2015.

114. Suarasan, S., Focsan, M., Soritau, O., Maniu, M., Astilean, S., One-pot, green synthesis of gold nanoparticles by gelatin and investigation of their biological effects on Osteoblast cells. *Colloid Surf. B*, 132, 122–131, 2015.
115. Sadeghi, B., Gholamhoseinpoor, F., A study on the stability and green synthesis of silver nanoparticles using *Ziziphora tenuior* (Zt) extract at room temperature. *Spectrochim. Acta A*, 134, 310–315, 2015.
116. Kumar, D.A., Palanichamy, V., Roopan, S.M., Green synthesis of silver nanoparticles using *Alternanthera dentata* leaf extract at room temperature and their antimicrobial activity. *Spectrochim. Acta A*, 127, 168–171, 2014.
117. Sadeghi, B., Rostami, A., Momeni, S.S., Facile green synthesis of silver nanoparticles using seed aqueous extract of *Pistacia atlantica* and its antibacterial activity. *Spectrochim. Acta A*, 134, 326–332, 2015.
118. Zhang, M., Zhang, K., De Gusseme, B., Verstraete, W., Field, R., The antibacterial and anti-biofouling performance of biogenic silver nanoparticles by *Lactobacillus fermentum*. *Biofouling*, 30, 347–357, 2014.
119. Deepak, V., Umamaheshwaran, P.S., Guhan, K., Nanthini, R.A., Krithiga, B., Jaithoon, N.M.H., Gurunathan, S., Synthesis of gold and silver nanoparticles using purified URAK. *Colloids Surf. B*, 86, 353–358, 2011.
120. Ajitha, B., Reddy, Y.A.K., Rajesh, K.M., Reddy, P.S., *Sesbania grandiflora* leaf extract assisted green synthesis of silver nanoparticles: Antimicrobial activity. *Materials Today: Proceedings*, 3, 1977–1984, 2016.
121. Phull, A.-R., Abbas, Q., Ali, A., Raza, H., Kim, S.J., Zia, M., Haq, I.-U., Antioxidant, cytotoxic and antimicrobial activities of green synthesized silver nanoparticles from crude extract of *Bergenia ciliate*. *Future J. Pharm. Sci.*, 2, 31–36, 2016.
122. Ahluwalia, V., Kumar, J., Sisodia, R., Shakil, N.A., Walia, S., Green synthesis of silver nanoparticles by *Trichoderma harzianum* and their bio-efficacy evaluation against *Staphylococcus aureus* and *Klebsiella pneumonia*. *Ind. Crops Prod.*, 55, 202–206, 2014.

17

Green Synthesis of Platinum Nanoparticles and Their Biomedical Applications

Niranjan Thondavada, Rajasekar Chokkareddy and Gan G. Redhi*

Electroanalytical Laboratories, Department of Chemistry, Durban University of Technology, Durban, South Africa

Abstract

Nanotechnology is a fundamental, enabling technology, allowing innovation in almost every conceivable technological discipline. Even though nano means small (10^{-9} m), it has high potency in a wide range of emerging applications, breaking through all disciplines of knowledge and leading to industrial and technological growth.Therefore, nanoparticle synthesis plays a major part in the progress of current worldwide research. Among the various metallic nanoparticles, platinum nanoparticles (PtNPs) have more advantages and applications, especially in the biomedical fields. This chapter mainly describes the different methods of PtNPs synthesis such as chemical, physical and biological approaches. In addition, the biomedical applications are elaborately discussed. The content described herein will be extremely useful for researchers in clinical fields and industrial researchers in biologics, enabling them to find new insights into their respective fields.

Keywords: Green synthesis, platinum nanoparticles, nanotechnology, biomedical applications, nanomedicine, nanodiagnostics

17.1 Introduction

Platinum nanoparticles have strong applications in chemical, medical, electronics and biological fields among others [1–4]. The applications of nanoparticles mainly depend upon their size, shape, morphology

**Corresponding author*: redhigg@dut.ac.za

Suvardhan Kanchi and Shakeel Ahmed (eds.) Green Metal Nanoparticles, (603–627)
© 2018 Scrivener Publishing LLC

and dispersions [4–7]. The demand for this material in technological applications and the luxury sector is increasing, whilst the presence of Platinum(Pt) in the Earth's crust(around 0.01 ppm) is being threatened. In terms of the current Pt outputs, the highest amount of Pt (up to 35–40%) is used in automobile catalytic converters, followed by jewellery [8]; such extensive use and the expected demand for its future applications have had a significant effect on its increasing value and price.

Platinum is a praised noble metal and its nanoparticles have a wide range of applications in various fields. The metallic platinum compound, i.e., cis-diammine-dichloro-platinum, is currently applied as a cancer drug [9]. PtNPs has been used in fuel cells and hydrogen storage materials [10, 11]. Theywere found to have substantially more catalytic applications than bulk materials [12]. Moreover, PtNPs were also proven to be the most valuable catalyst in the proton exchange membrane fuel cells [13]. PtNPs are also extensively used in most of the hydrogenation reactions; for example, hydrogenation of o-chloronitrobenzene and cinnamaldehyde [14, 15]. In addition, PtNPs have recently been used for the synthesis of organic dyes [16]. Moreover, several complexes of platinum have been used against different Gram-positive and Gram-negative bacterial species.

A series of conventional protocols have been used in preparation of noble metal nanoparticles, i.e., UV irradiation reduction [17], laser ablation [18], electrolysis methods [19], thermal decomposition [20], microwave processing [21], ion implantation [22], chemical reduction [23, 24], etc. All these methods have some major drawbacks; for example, the use of expensive and precarious chemicals, and this has motivated researchers to introduce environmentally friendly alternative procedures using biological systems in preparation of nanoparticles. It is well recognized that biological systems have a strong efficiency for production of spherical, small size and highly stable nanoparticles. With this in mind, researchers have introduced medicinal plants as an alternative for the preparation of nanoparticles instead of precarious chemicals, because they are nontoxic, cheap and easily available [25]. In the synthesis of nanoparticles, phytochemicals of the plants play an important role. The water-soluble organic moiety of the medicinal plants is not only used for the reduction of the nanoparticles but also stabilizes the prepared nanoparticles. The current literature reports reveal that plant extracts are more beneficial for the preparation of metal nanoparticles over other conservative methods because they contain high concentrations of biomolecules, i.e., terpenoids, phenols, alkaloids, flavonoids, quinines, tannins, etc., which are responsible for the reduction and stabilization of metal nanoparticles. Noble metal nanoparticles (NMNPs) are potential antibacterial agents possessing strong antibacterial efficiency

with negligible bacterial resistance against them [26]. It has been previously reported that the ions of noble metals damage the bacterial DNA, cell membrane, critical enzymes and destroy bacteria by a process called respiratory burst mechanism [27, 28]. Moreover, the nanoparticles of noble metals have the ability of producing reactive oxygen species, which are responsible for inhibition of pathogenic microbes.

17.2 Synthesis of Platinum Nanoparticles

Industrial and biomedical applications of PtNPs are strongly affected by their size, shape, elemental composition, electronic surface structure and capping agent, pushing researchers to develop new synthetic techniques to optimize such features [2, 8, 28–33] (see Figure 17.1). The engineering of PtNPs for biomedical applications is also guided by recent data revealing that their physicochemical properties, as well as their dispersion state and stability in a biological environment, play a major role in defining their safety or toxicity. Considering the possible use of PtNPs as drug carriers and antioxidant materials, a critical challenge is the production of biocompatible PtNPs, with precisely defined properties and the absence of contaminants (e.g., endotoxin, Pt precursors, toxic unreacted reagents, organic solvents, etc.) during their production [34]. In this chapter, several classes of synthetic methods, namely chemical, physical, and biologically assisted procedures, are discussed.

17.2.1 Chemical Processes

Among chemical processes, wet chemical reduction (WCR) [33], electrochemical reduction [36–38], galvanic displacement [39, 40] and chemical vapor deposition [41] have recently added interest in an attempt to exactly control NP physicochemical properties. In particular, WCR is often applied in laboratory research, as it assures better control of NP characteristics. WCR, which involves the use of a reducing agent to produce PtNPs from Pt precursors in solution [33], permits a stern control of shape and size, by varying the Pt compound concentration, the temperature of the reaction [8], and the use of organic or inorganic ligands [42, 43]. Solid research has also been devoted to the expansion of WCR methods to obtain shaped PtNPs with improved catalytic performances. Several shape-directing agents have been employed to favor the unequal growth of the PtNPs. On the other hand; several polymers, surfactants and capping agents have been exploited. Multiphase synthetic setups have

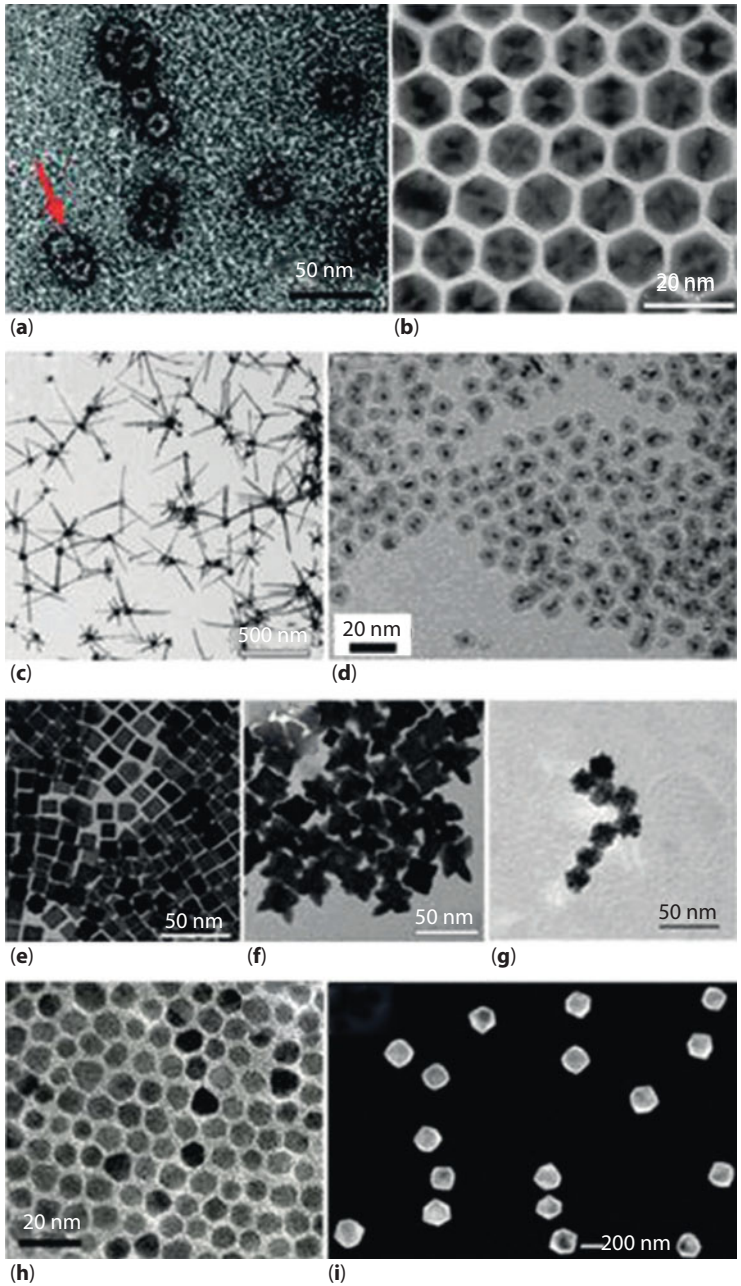


Figure 17.1 TEM images of PtNPs with controlled shape. (a)Apoferritin encapsulated, (b) Icosahedral PtNPs, (c)Pt branched rods, (d)FePt@Fe_2O_3 yolk–shell NPs, (e)Pt cubes, (f)Pt octapods, (g)Pt nanoflowers, (h)FePt bimetallic NPs, (i)Pt tetrahexahedrons. (Reproduced from [35])

also been designed [44, 45], such as the use of reducing agents in the gas phase to achieve better control of the reaction parameters [46]. The limit of this approach to produce PtNPs for nanomedicine is the use of large amounts of capping agents, surfactants, and organic solvents that could affect the toxicological profile of NPs. Moreover, their large-scale production can pose environmental risks. To allow for industrial scale-up and lower the environmental impact, microwave heating and glycerol, both as a reducing agent and solvent, have been proposed [47, 48]. To synthesize PtNPs the usage of thiol-chemistry is also often exploited with increased stability in an aqueous environment or in organic media. Pt clusters with controlled size and shape were achieved and stabilized by thiol ligands, such as alkane thiols [49, 50] or thiol-bearing polar groups [51, 52]. On the other hand, these chemicals show potential adverse effects, as aliphatic, aromatic, and amino-terminated thiols could be toxic *in vitro* and *in vivo* [53]. To attain biocompatible PtNPs, the more encouraging strategy is to use "green reagents," such as ascorbic acid and sodium citrate, with strong control of reagent purity and solvent [54, 55]. These synthetic procedures can also guarantee accurate control of size, shape, and catalytic properties, together with reasonable production yield [53]. For example, it has been recently shown that citrate-capped PtNPs show good cytocompatibility together with high antioxidant abilities [54]. Furthermore, these synthetic strategies permit easy functionalization of the NP surface. This is crucial to design PtNPs for biomedical applications, as the biological identity of nanomaterials strongly depends on their exposed surface area.

17.2.2 Physical Methods

Among the physical methods, the aerosol-assisted deposition [56], laser ablation techniques [57], flame synthesis [58], electron-beam-induced reduction [59], have all recently gained interest in an effort to overcome some of the boundaries of the chemical procedures (e.g., organic solvents, toxic reagents, etc.). The laser ablation method utilizes a high power laser beam to volatilize PtNPs from a solid source [60]. The laser beam can be applied in continuous or pulsed mode. This adjustable approach is based on the control of temperature, pulses, and ambient gas pressure to attain definite PtNP properties [60]. The main advantage of this technique is the lack of unwanted stabilizers, coatings, and solvent contaminations that might represent an issue in nanomedicine [60]. On the other hand, the mechanism of PtNP production is not totally understood, and the high dilution and the difficulties in tuning the PtNPs shape, size, and production yield restrict their use [61]. Also, the stability of these PtNPs in a biological

environment could raise some issues. The NPs obtained by laser ablation are stable in aqueous solution in the absence of stabilizers, due to electrical repulsion effects resulting from charges present on the surface of the NPs [62]. However, this could represent an issue in biological experiments, as precipitation and aggregation might occur when PtNPs are incubated in complex environments, such as cell culture media and high ionic strength solutions. Another simple physical method to produce PtNPs for several applications involves the use of cathodic corrosion, converting a bulk alloy electrode in a suspension of NPs with the same composition [63]. The latter approach, however, has similar constraints, i.e., limited production yield and size tunability.

17.2.3 Biological Processes

Bio-assisted syntheses, based on biological processes by unicellular and multicellular organisms, have been recommended as alternatives to chemical and physical methods. Benefits of biomedical applications include the absence of undesired reaction solvents. Biological syntheses have been reported mainly for noble metal nanomaterials, as they can be easily reduced by weak reducing agents [64, 65]. Only limited reports in the literature describe the synthesis of PtNPs [66, 67]. Successful protocols have been developed to produce monodispersed and stable PtNPs through biosynthesis within bacteria [68, 69], cyanobacteria [70], seaweeds [71], fungi [72], plants [73–75], as well as by means of bio-derived products, such as aqueous honey solutions [76]. Several reports have stated that reduction of Pt(IV) into PtNPs in sulphate-reducing bacteria exploit the activity of specific hydrogenase enzymes [77]. Similar to WCR, in biogenic synthesis, Pt salts and protein concentrations play an important role in controlling the NP shape and size [78]. PtNP synthesis using fungi, such as *Neurospora crassa* [79] and *Fusarium oxysporum* [80], have been similarly reported for use as a valuable "scale-up" approach. Biological synthesis of metal NPs was also performed using plant extracts and wood [73], exploiting their phytochemical constituents as capping agents. The Pt biosynthesis in plants was described for the first time in 2009 by Song *et al.*, who obtained 2–12 nm PtNPs using leaf extracts with ca. 90% yield, by using very low concentration of leaf biomass [81]. Currently, the literature describes various sets of vegetable-derived products to synthesize PtNPs, such as *Diopyros kaki* [81], *Ocimum sanctum* [82], *Medicago sativa* and *Brassica juncea* [83]. Raut *et al.* reported a rapid protocol to produce monodispersed spherical 1–6 nm PtNPs in an aqueous medium at room temperature, using the root extract of *Asparagus racemosus* Linn [84]. The number

of reports describing a variety of organism-mediated PtNP syntheses is rapidly increasing. All these protocols demonstrated several ecological, low-toxic and cost-effective routes to produce NPs, often avoiding complex laboratory setups. However, their large-scale use for nanomedicine applications could be limited by the presence of undesired contaminants, such as endotoxins and fragments of biological materials with unwanted biological activity, which require difficult, expensive, and time-consuming purification procedures. Moreover, even if bio-assisted procedures are promising, up to now they typically have failed to achieve fine control over the NP properties. In conclusion, the richness of the available methods for PtNP synthesis together with the complexity of the biological environment makes it difficult to select a"universal" strategy to achieve biocompatibility, stability, and productivity, since each technique presents some advantages and drawbacks. However, synthetic methods based on "green reagents," such as ascorbic acid and sodium citrate, seem to be particularly promising, as they offer an accurate control of some important properties for biomedical applications, i.e., size, shape, stability, catalytic properties, and production efficiency, coupled withthe possibility of post-synthesis surface functionalization [53].

17.3 Toxicology of PtNPs

Currently, the applications of nano-Pts in biomedicine is still ongoing, due to its unclear toxicological characterization. The toxic effect of other types of NPs is repeatedly characterized by the induction of DNA damage, oxidative stress, and cell cycle arrest [85, 86], leading to specific organ failure [87]. However, several data obtained proves that the important role in cell function damage is frequently played by the different toxins present, like endotoxins, harmful coatings, or NP synthesis reaction by-products [88, 89]. Although it has been verified that diverse metallic NPs release ions once inside the cell, there are no conclusive data proving that cell destruction detected after PtNP control might be similarly due to the release of Pt ions [90, 91]. Investigations concentrating on the role of PtNP size in cytotoxicity [92, 93] indicate that it could represent an important parameter affecting molecular mechanisms inside the cell, although with contradictory results. While 8 nm NPs did not show harmful effects, administration of 1 nm PtNPs to renal cells in culture induced cytotoxicity in a dose-dependent way in the same range of concentrations [94]. After testing NP sizes ranging from 1 to 21 nm on a Neuro 2 cell line, it was observed that PtNPs of 5–6 nm were fully cytocompatible, whereas PtNPs of other sizes

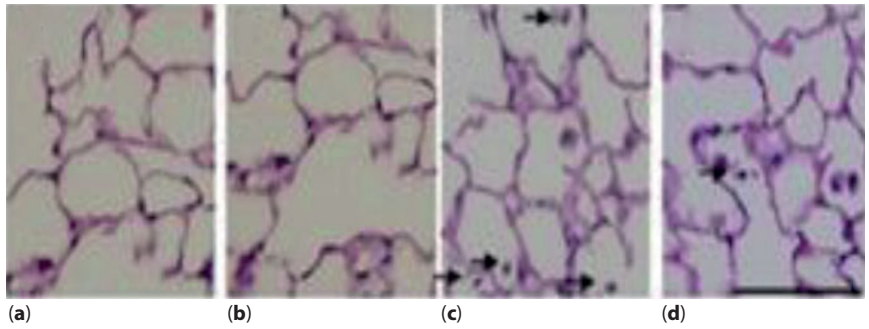


Figure 17.2 Lung tissue sections stained with hematoxylin and eosin obtained from mice that received (a) saline and (b) PAA-Pt and were exposed to controlled air, (c) saline and (d) PAA-Pt and were exposed to cigarette smoke.

induced cellular damage [92]. On the other hand, polyvinylpyrrolidone PVP-PtNPs of 6 nm induced a decrease of metabolic activity and genotoxic effects, and even though they did not alter the morphology, viability and migration capability of primary keratinocytes [95], 57 nm PtNPs are less harmful for keratinocytes than the smaller ones. Smaller PtNPs presented stronger ability than 57 nm ones to produce DNA instability and metabolic dysfunction at a concentration of 25 mg mL^{-1} [95]. In a meticulous study, Hamasaki and colleagues [96] did not observe cytotoxicity in a wide set of other types of adherent cells (i.e., TIG-1, HeLa, HepG2, WI-38 and MRC-5) after exposure to 1–5 nm PtNPs at concentrations as high as 50 mg mL^{-1}. In the same paper, the authors expanded their investigation *in vivo* without reporting negative effects in mice after intraperitoneal administration [96] (see Figure 17.2).

17.4 Biomedical Applications of PtNPs

17.4.1 PtNPs in Cancer Therapy

Pt-based compounds with a defined geometrical distribution of the ligands around the Pt atom are among the most important drugs currently available to treat several types of cancers. The agent worth mentioning in this area is cisplatin, which uses its cytotoxic effect by selectively bonding with N^7 atom of purine bases in DNA [97] with the genesis of a DNA–platinum adduct that twists the structure of the DNA duplex, damaging its replication and transcription. Such a toxicity mechanism was shown to be exactly controlled by ligand geometry (i.e., the cis conformation), and solid

attempts have been dedicated to finding agents similar to cisplatin with fewer side effects and better efficacy [98, 99]. In this rivulet of research, some reports reveal that Pt nanomaterials are related tocisplatin and studied as possible alternatives for anticancer treatment [100, 101].

To improve the toxic performance of PtNPs, some researchers have introduced a second material, persuading critical changes in the physicochemical properties of NPs to raise their cessation within cells. In the case of bimetallic NPs, the release of Pt ions might become relevant, as the strength of the Pt–Pt bond may be weakened by the presence of another metallic ion, favoring the acidic conditions of the material [102, 103]. The FePt@CoS_2 yolk-shell nanocrystals are reported to release Pt ions in a cellular environment as a consequence of FePt core dissolution and generate time-dependent apoptosis in HeLa cells [90]. However, the part played by Fe ions was not investigated in these studies. Likewise, López *et al.* suggested a new nanostructure based on TiO_2 and SiO_2 containing 3–4% of Pt in the form of NPs for local cancer therapy. They observed a decrease in tumor size, weight and aggressiveness in the experimental model of C6 brain tumors, which was correlated with the delivery of toxic ions [102, 104]. The usage of PtNPs implant in an *in-situ* crosslinkable hyaluronic acid gel was examined for applications in intraperitoneal chemotherapy [105]. The release of PtNPs in the tumor site was attenuated by the presence of hyaluronic acid carboxyl groups complexed with Pt. After 3 days, the authors suggested that all Pt ions were released from the PtNP hybrid system, showing cytotoxic effects, probably due to the combined degradation of hyaluronic acid and Pt ion release [105]. Despite some *in-vitro* and *in-vivo* reports on the anticancer ability of PtNPs, further studies are required to assess the role of pristine NPs and the contribution of the ions and coatings to the chemotherapeutic effect, as well as the purity and polydispersity of the NP preparation and other elements included in the NP complex. Extensive purification procedures are crucial to minimizing the presence of pathogenic spores or bioactive molecules, like bacterial toxins, that can easily overcome the beneficial effects of the pure material and the green coatings.

17.4.2 PtNPs in Photothermal Therapy and Radiotherapy

Due to the toxic side effects of anticancer chemotherapies, medical researchers are developing more effective and site-specific treatments against malignant tumors. Among them, photothermal therapy (PTT) is a non-invasive treatment based on the use of the NP plasmonic effect to locally increase the cellular temperature upon irradiation, causing DNA and RNA damage,

membrane rupture, and protein denaturation, and finally leading to cancer cell death [106]. In this context, research attempts are mostly attentive tocarbon nanotubes, copper sulphide, graphene NPs, and noble metal NPs (i.e., gold nanoshells, nanocages and nanorods) capable of absorbing NIR laser light and evaporating it into heat. In principle, cytocompatibility and catalytic characteristics of PtNPs might be combined to improve novel tools for PTT. However, the plasmon resonance of this substance declines in the UV region [107, 108], so that its efficiency is anticipated to be significantly lower than that of the other metal nanostructures mentioned above. The optimal PtNP dimensions to be used in PTT demonstrated that PVP-PtNP phototoxicity was related to the particle and found that 5–6 nm PtNPs have minor or nontoxic effects themselves, but they are able to cause cell death once irradiated by near-IR laser. The optical properties of bimetallic FePtNPs have also been exploited to perform PTT of solid tumors. It was reported that the 12 nm folate-functionalized 3-mercaptopropionic acid FePtNPs with a cubic shape, when excited by a NIR laser, elicited intracellular damage proportional to the NP number, causing necrosis of cancer cells similar to Au nanorods [109] (see Figure 17.3). These results were observed even though the absorption intensity at 800 nm of FePtNPs was five-fold lower than that of AuNPs. Recently, the use of biocompatible 13 nm trifolium-like PtNPs (TPNs) has been investigated as a possible new photothermal agent. Overall, PtNPs have shown to be good candidates for PTT and radiotherapy, as they are able to induce cellular damage in selective area following laser irradiation or radiation exposure.

17.4.3 Antibacterial Applications of PtNPs

The development of new bactericidal agents is currently one of the greatest challenges, due to rising concerns about bacterial resistance to antibiotics. Metallic NPs could play a role in this field. Some NPs, like Ag, Pd, Au, Cu, ZnO and TiO_2, have shown promising results [110], but their therapeutic use is incomplete because of undesired side effects in *vivo*. The antimicrobial

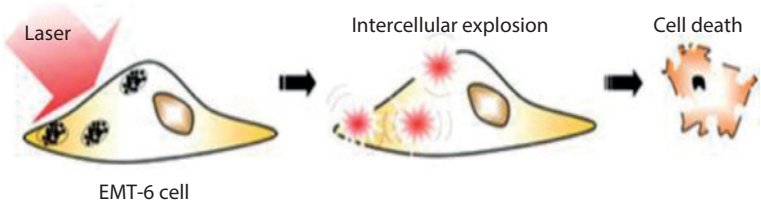


Figure 17.3 Lung tissue sections stained with hematoxylin and eosin.

activities of Pt ions on *Escherichia coli* have been described ever since 1965 [111, 112], but the antibacterial activity of PtNPs has been poorly explored. But, their enzyme mimetic activity might be utilized to induce intracellular hyper production of ATP, causing bacteriotoxic effects, growth inhibition and DNA damage [113]. Indeed, the antibacterial effect of PtNPs is due to their capability to increase ATP levels, causing the overexpression of a kinase responsible for the bacterial growth arrest. Until now, few publications have shown PtNP antibacterial properties [114, 115], which are reported to depend on size and surface chemistry. Gopal *et al.* studied the antibacterial properties of different shapes of PVP-PtNPs with sizes varying from 1 to 20 nm on *P. aeruginosa*. They found significant bacteriotoxic properties with smaller PtNPs (1–3 nm) independent of their shape, even at low concentrations (8.5 mg mL^{-1}). The TEM analysis of NP confirms that size plays an important part, as larger PtNPs (45 nm) only interact with cell membranes, while smaller ones are reported to enter bacteria [116]. Size-dependent toxicity of PtNPs was additionally verified by using PVP-PtNPs of 6 and 57 nm against Gram-negative (*E. coli*) and Gram-positive (*S. aureus*) bacteria [95]. A systematic study of pectin-capped PtNPs (2 to 5 nm) showed toxicity against Gram-positive (*B. subtilis, S. aureus*) and Gram-negative (*P. aeruginosa, E. coli*) bacteria, indicating clear toxic effects in both *in-vitro* and *in-vivo* studies. The mechanism of PtNP exploitingt he *in-vitro* case was coordinated with reactive oxygen species (ROS) overproduction and bacterial membrane disruption. Despite this, the antibacterial properties and mechanism of action of PtNPs are still matters of discussion. Exploiting the wide variety of possible surface functionalization, the construction of PtNP-bacterial vehicles was proposed as a promising system able to transport drugs to specific targets in the body.

17.5 Enzymatic Properties of PtNPs and Their Applications

17.5.1 PtNPs in Nanomedicine

PtNPs are good candidates as nanozymes for the treatment of oxidative stress-related diseases, due to their ability to act as artificial CAT, HRP and SOD enzymes (see Figure 17.4).

The PtNPs display safe applications for some human pathologies, as demonstrated recently [117]. The PtNPs are different from other metal nanoparticles, and they show great stability in acidic cellular vesicle environments, cytocompatibility, forecasting and tolerance *in vivo*. The PtNPs

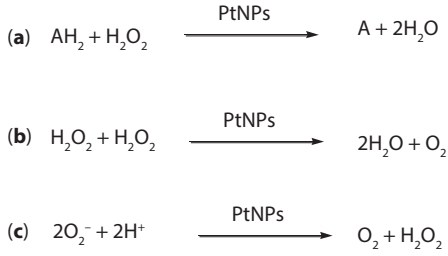


Figure 7.4 Schemes of the main antioxidant chemical reactions catalyzed by PtNPs as peroxidase: Catalase (b) and superoxide dismutase (c) mimics.

in-vitro enzyme-like properties have a wide range of applications in nanomedicine, and it is even hypothesized that PtNPs can be used as a preventive therapy for some types of cancer and cardiovascular diseases [118]. The scavenging abilities of PtNPs are maintained in a cellular environment [119, 120], as PtNPs are able to shield the cells from reactive oxygen species ROS-induced death after exposure to UVA, X-rays [121] or ultrasound [122]. Recently, PtNPs embedded in dendrimers were defined as horseradish peroxidase (HRP) and catalase (CAT)-mimetic enzymes [123], but PtNPs encapsulated within the cavity of apoferritin were stated to show peroxide-quenching and superoxide-quenching activities, both in cell-free solution and within cells, reducing H_2O_2-induced apoptotic cell death in a concentration-dependent way. The combined action of apoferritin encapsulating PtNPs improved their antioxidant properties. When cerium oxide NPs were compared with PtNPs, the antioxidant activity of PtNPs was indicated to be more effective by assessing apoptosis prevention in HT-1080 human breast fibrosarcoma cells exposed to 200 mM H_2O_2. These results are likely due to PtNPs chemical stability and resistance to aggregation, despite their lower superoxide dismutase (SOD) activity *in vitro.* Also, *in vivo,* 1–2 nm polyvinyl pyrrolidone (PVP)-PtNPs are capable of extending the lifetime of the short-lived mutant nematode *Caenorhabditis elegans,* which is affected by high levels of oxidative stress. The effect of the nanomaterial was more pronounced than that obtained with EUK-8, a well-known SOD/CAT mimetic used in the same range of concentrations (see Figure 17.5).

17.5.2 PtNPs in Nanodiagnostics

In recent years, PtNPs have attained interest in biomedical applications. For example, fluorescent Pt nanoclusters havebeen successfully synthesized

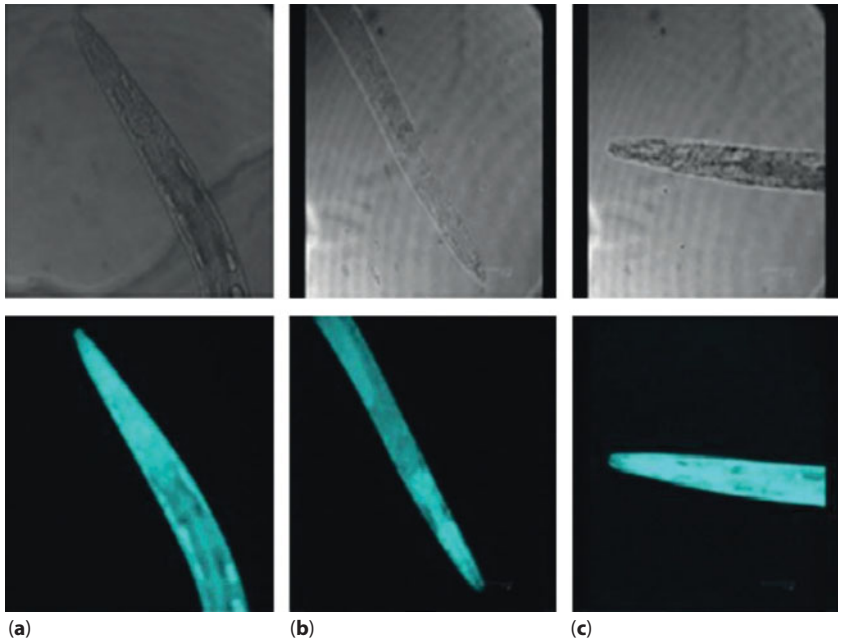


Figure 17.5 Reactive oxygen species scavenging properties of PtNPs. (a–c) Nomarski images and DCF staining of untreatedPtNPs; (a) 0.5 mM PtNP treated; (b) 0.5 mM EUK-8 treated;(c)*Caenorhabditis elegans.* (Reproduced from [124])

as novel biocompatible bioimaging probes for diagnostic purposes [125]. Likewise, an interesting approach counts on the usage of Pt nanomaterials as a part of catalytic nanomotors to build-up molecular devices and motion-based detection methods. For example, the motion of chemically powered nanomotors built on bisegment Au-Pt nanowires has lately been utilized to identify silver ions, DNA and ribosomal RNA, a starting gateway for new concepts in diagnostics [126, 127]. The PtNPs have emerged as perfect candidates as enzyme alternatives in diagnostic analyses [128]. The PtNPs have several advantages, including easy and cost-effective production and stability, purification, resistance to proteases, high catalytic activity even at high pH and temperature, and affinity for HRP substrates. The affinity of DNA-stabilized PtNPs for tetramethylbenzidine (TMB) is eighttimes greater when compared to natural HRP enzyme. Protein detection uses the chemiluminescent reaction of luminol with H_2O_2 catalyzedby aptamer-PtNP complexes [129] and an amperometric biosensor for the detection of thrombin [130]. PtNP-based colorimetric assays have been developed [131], including the detection of DNA [132], cancer cells [133], tumor markers [134], metal ions [135], penicillin antibiotics [136], drugs

[127], hydrogen peroxide [137], glucose [138], cholesterol [139], L-cysteine [140], choline and acetylcholine [141], proteins [142], viruses [143], bacteria [144] and antibodies [145]. Overall, the engineering of PtNPs and the detailed study of their mechanism of interactions with biological systems may have an enormous effect on the growth of novel and simple point-of-care systems for the detection of environmental pollutants or biomarkers.

17.6 Conclusion

The Pt-based nanomaterials are key players in many realms of science and technology. In particular, as discussed in the previous sections, they are promising candidates in biomedical applications, integrating the functions of nanocarriers and nanozymes. In point-of-care diagnostic technology, PtNPs can be used as artificial enzymes to replace expensive and sensitive HRP and CAT in new colorimetric and fluorometric biosensors, and to develop novel naked-eye diagnostic approaches. This is a particularly interesting field, since the very high catalytic efficiency of nano Pt combined with their stability in a wide range of conditions (including pH and temperature) can lead to the development of ultrasensitive, low-cost and portable tests, which can be stored for months at room temperature and performed outside specialized laboratories, with no temperature control or instrumental requirements. In nanomedicine, PtNPs can be useful for combination therapy in the treatment of complex diseases caused by the accumulation of intracellular reactive oxygen species (ROS). By exploiting NP versatile surface functionalization with their intrinsic antioxidant properties, PtNPs can be used to produce multifunctional nanoformulations with ROS scavenging properties. Moreover, it may be envisioned that PtNPs could be further engineered to replace damaged proteins in defective molecular pathways leading to diseases. Interestingly, several reports have shown the higher potential of PtNPs compared to other nanozymes, such as ceria and fullerenes, for the therapy of several human pathologies. To completely disclose the potential of PtNPs in biomedicine, however, a detailed picture of their diverse properties is still required, including a precise investigation of the underlying antioxidant mechanisms and their toxicological aspects.

References

1. Ozin, G.A., Nanochemistry: Synthesis in diminishing dimensions. *Adv. Mater.*, 4, 612–649, 1992.

2. Daniel, M.-C., Astruc, D., Gold nanoparticles: Assembly, supramolecular chemistry, quantum-size-related properties, and applications toward biology, catalysis, and nanotechnology. *Chem. Rev.*, 104, 293–346, 2004.
3. El-Nour, K.M.A., Eftaiha, A.A., Al-Warthan, A., Ammar, R.A., Synthesis and applications of silver nanoparticles. *Arab. J. Chem.*, 3, 135–140, 2010.
4. Alivisatos, A.P., Semiconductor clusters, nanocrystals, and quantum dots. *Science*, 271, 933–937, 1996.
5. Coe, S., Woo, W.-K., Bawendi, M., Bulović, V., Electroluminescence from single monolayers of nanocrystals in molecular organic devices. *Nature*, 420, 800, 2002.
6. Kelly, K.L., Coronado, E., Zhao, L.L., Schatz, G.C., The optical properties of metal nanoparticles: The influence of size, shape, and dielectric environment, *J. Phys. Chem. B*, 107, 668–677, 2003.
7. Gangula, A., Podila, R., Karanam, L., Janardhana, C., Rao, A.M., Catalytic reduction of 4-nitrophenol using biogenic gold and silver nanoparticles derived from *Breynia rhamnoides*. *Langmuir*, 27, 15268–15274, 2011.
8. Leong, G.J., Schulze, M.C., Strand, M.B., Maloney, D., Frisco, S.L., Dinh, H.N., Pivovar, B., Richards, R.M., Shape-directed platinum nanoparticle synthesis: Nanoscale design of novel catalysts. *Appl. Organomet. Chem.*, 28, 1–17, 2014.
9. Hall, M.D., Mellor, H.R., Callaghan, R., Hambley, T.W., Basis for design and development of platinum (IV) anticancer complexes. *J. Med. Chem.*, 50, 3403–3411, 2007.
10. Wen, Z., Liu, J., Li, J., Core/shell Pt/C nanoparticles embedded in mesoporous carbon as a methanol-tolerant cathode catalyst in direct methanol fuel cells. *Adv. Mater.*, 20, 743–747, 2008.
11. Li, Y., Yang, R.T., Liu, C.-j., Wang, Z., Hydrogen storage on carbon doped with platinum nanoparticles using plasma reduction. *Ind. Eng. Chem. Res.*, 46, 8277–8281, 2007.
12. Narayanan, R., El-Sayed, M.A., Catalysis with transition metal nanoparticles in colloidal solution: Nanoparticle shape dependence and stability.*J. Phys. Chem. B*, 109, 12663–12676, 2005.
13. Schmidt, T., Gasteiger, H., Behm, R., Rotating disk electrode measurements on the CO tolerance of a high-surface area Pt/vulcan carbon fuel cell catalyst. *J. Electrochem. Soc.*, 146, 1296–1304, 1999.
14. Cheng, H., Xi, C., Meng, X., Hao, Y., Yu, Y., Zhao, F., Polyethylene glycol-stabilized platinum nanoparticles: The efficient and recyclable catalysts for selective hydrogenation of o-chloronitrobenzene to o-chloroaniline. *J. Colloid Interface Sci.*, 336, 675–678, 2009.
15. Manikandan, D., Divakar, D., Rupa, A.V., Revathi, S., Preethi, M.E.L., Sivakumar, T., Synthesis of platinum nanoparticles in montmorillonite and their catalytic behaviour. *Appl. Clay Sci.*, 37, 193–200, 2007.
16. Santhanalakshmi, J., Kasthuri, J., Rajendiran, N., Studies on the platinum and ruthenium nanoparticles catalysed reaction of aniline with

4-aminoantipyrine in aqueous and microheterogeneous media. *J. Mol. Catal. A: Chem.*, 265, 283–291, 2007.
17. Liu, Y., Chen, S., Zhong, L., Wu, G., Preparation of high-stable silver nanoparticle dispersion by using sodium alginate as a stabilizer under gamma radiation. *Radiat. Phys. Chem.*, 78, 251–255, 2009.
18. Darroudi, M., Ahmad, M.B., Zamiri, R., Abdullah, A.H., Ibrahim, N.A., Shameli, K., Husin, M.S., Preparation and characterization of gelatin mediated silver nanoparticles by laser ablation. *J. Alloys Compd.*, 509, 1301–1304, 2011.
19. Dong, C., Zhang, X., Cai, H., Green synthesis of monodisperse silver nanoparticles using hydroxy propyl methyl cellulose. *J. Alloys Compd.*, 583, 267–271, 2014.
20. Shim, I.-K., Lee, Y.I., Lee, K.J., Joung, J., An organometallic route to highly monodispersed silver nanoparticles and their application to ink-jet printing. *Mater. Chem. Phys.*, 110, 316–321, 2008.
21. Wani, I.A., Ganguly, A., Ahmed, J., Ahmad, T., Silver nanoparticles: Ultrasonic wave assisted synthesis, optical characterization and surface area studies. *Mater. Lett.*, 65, 520–522, 2011.
22. Popok, V., Stepanov, A., Odzhaev, V., Synthesis of silver nanoparticles by the ion implantation method and investigation of their optical properties. *J. Appl. Spectrosc.*, 72, 229–234, 2005.
23. Khan, Z., Hussain, J.I., Kumar, S., Hashmi, A.A., Silver nanoplates and nanowires by a simple chemical reduction method. *Colloids Surf. B*, 86, 87–92, 2011.
24. Vitulli, G., Bernini, M., Bertozzi, S., Pitzalis, E., Salvadori, P., Coluccia, S., Martra, G., Nanoscale copper particles derived from solvated Cu atoms in the activation of molecular oxygen. *Chem. Mater.*, 14, 1183–1186, 2002.
25. Tahir, K., Nazir, S., Li, B., Khan, A.U., Khan, Z.U.H., Ahmad, A., Khan, F.U., An efficient photo catalytic activity of green synthesized silver nanoparticles using *Salvadora persica* stem extract. *Sep. Purif. Technol.*, 150, 316–324, 2015.
26. Ahmad, A., Syed, F., Shah, A., Khan, Z., Tahir, K., Khan, A.U., Yuan, Q., Silver and gold nanoparticles from *Sargentodoxa cuneata*: Synthesis, characterization and antileishmanial activity. *RSC Adv.*, 5, 73793–73806, 2015.
27. Chamakura, K., Perez-Ballestero, R., Luo, Z., Bashir, S., Liu, J., Comparison of bactericidal activities of silver nanoparticles with common chemical disinfectants. *ColloidsSurf. B*, 84, 88–96, 2011.
28. Morones, J.R., Elechiguerra, J.L., Camacho, A., Holt, K., Kouri, J.B., Ramírez, J.T., Yacaman, M.J., The bactericidal effect of silver nanoparticles. *Nanotechnology*, 16, 2346, 2005.
29. Chen, A., Holt-Hindle, P., Platinum-based nanostructured materials: Synthesis, properties, and applications. *Chem. Rev.*, 110, 3767–3804, 2010.
30. Cheong, S., Watt, J.D., Tilley, R.D., Shape control of platinum and palladium nanoparticles for catalysis. *Nanoscale*, 2, 2045–2053, 2010.
31. Le Guével, X., Trouillet, V., Spies, C., Jung, G., Schneider, M., Synthesis of yellow-emitting platinum nanoclusters by ligand etching. *J. Phys. Chem. C*, 116, 6047–6051, 2012.

32. Xiong, Y., Wiley, B.J., Xia, Y., Nanocrystals with unconventional shapes—A class of promising catalysts. *Angew. Chem. Int. Ed.*, 46, 7157–7159, 2007.
33. Bönnemann, H., Richards, R.M., Nanoscopic metal particles–Synthetic methods and potential applications. *Eur. J. Inorg. Chem.*, 2001, 2455–2480, 2001.
34. Crist, R., Grossman, J., Patri, A., Stern, S., Dobrovolskaia, M., Adiseshaiah, P., Clogston, J., McNeil, S., Common pitfalls in nanotechnology: Lessons learned from NCI's nanotechnology characterization laboratory. *Integr. Biol. (Camb.)*, 5(1), 66–73, 2013.
35. Zhang, L., Laug, L., Munchgesang, W., Pippel, E., Gösele, U., Brandsch, M., Knez, M., Reducing stress on cells with apoferritin-encapsulated platinum nanoparticles. *Nano Lett.*, 10, 219–223, 2009.
36. Mahima, S., Kannan, R., Komath, I., Aslam, M., Pillai, V.K., Synthesis of platinum Y-junction nanostructures using hierarchically designed alumina templates and their enhanced electrocatalytic activity for fuel-cell applications. *Chem. Mater.*, 20, 601–603, 2007.
37. Li, Y., Jiang, Y., Chen, M., Liao, H., Huang, R., Zhou, Z., Tian, N., Chen, S., Sun, S., Electrochemically shape-controlled synthesis of trapezohedral platinum nanocrystals with high electrocatalytic activity. *Chem. Commun.*, 48, 9531–9533, 2012.
38. Zhao, W., Zhou, X., Xue, Z., Wu, B., Liu, X., Lu, X., Electrodeposition of platinum nanoparticles on polypyrrole-functionalized graphene. *J. Mater. Sci.*, 48, 2566–2573, 2013.
39. Mahmoud, M., El-Sayed, M., Time dependence and signs of the shift of the surface plasmon resonance frequency in nanocages elucidate the nanocatalysis mechanism in hollow nanoparticles. *Nano Lett.*, 11, 946–953, 2011.
40. Mahmoud, M., Saira, F., El-Sayed, M., Experimental evidence for the nanocage effect in catalysis with hollow nanoparticles. *Nano Lett.*, 10, 3764–3769, 2010.
41. Saminathan, K., Kamavaram, V., Veedu, V., Kannan, A., Preparation and evaluation of electrodeposited platinum nanoparticles on *in situ* carbon nanotubes grown carbon paper for proton exchange membrane fuel cells. *Int. J. Hydrogen Energy*, 34, 3838–3844, 2009.
42. Lim, S.I., Ojea-Jiménez, I., Varon, M., Casals, E., Arbiol, J., Puntes, V., Synthesis of platinum cubes, polypods, cuboctahedrons, and raspberries assisted by cobalt nanocrystals. *Nano Lett.*, 10, 964–973, 2010.
43. Miyabayashi, K., Nakamura, S., Miyake, M., Synthesis of small platinum cube with less than 3 nm by the control of growth kinetics. *Cryst. Growth Des.*, 11, 4292–4295, 2011.
44. Shahbazali, E., Hessel, V., Noël, T., Wang, Q., Metallic nanoparticles made in flow and their catalytic applications in organic synthesis. *Nanotechnol. Rev.*, 3, 65–86, 2014.
45. Kang, Y., Ye, X., Murray, C.B., Size-and shape-selective synthesis of metal nanocrystals and nanowires using CO as a reducing agent. *Angew. Chem. Int. Ed.*, 49, 6156–6159, 2010.

46. Zhou, W., Wu, J., Yang, H., Highly uniform platinum icosahedra made by hot injection-assisted GRAILS method. *Nano letters*.13, 2870–2874, 2013.
47. Grace, A.N., Pandian, K., One pot synthesis of polymer protected Pt, Pd, Ag and Ru nanoparticles and nanoprisms under reflux and microwave mode of heating in glycerol—A comparative study. *Mater. Chem. Phys.*, 104, 191–198, 2007.
48. Kou, J., Bennett-Stamper, C., Varma, R.S., Green synthesis of noble nanometals (Au, Pt, Pd) using glycerol under microwave irradiation conditions. *ACS Sustain. Chem. Eng.*, 1, 810–816, 2013.
49. Sarathy, K.V., Raina, G., Yadav, R., Kulkarni, G., Rao, C., Thiol-derivatized nanocrystalline arrays of gold, silver, and platinum. *J. Phys. Chem. B*, 101, 9876–9880, 1997.
50. Yang, J., Lee, J.Y., Deivaraj, T., Too, H.-P., An improved procedure for preparing smaller and nearly monodispersed thiol-stabilized platinum nanoparticles. *Langmuir*, 19, 10361–10365, 2003.
51. Perez, H., Pradeau, J.-P., Albouy, P.-A., Perez-Omil, J., Synthesis and characterization of functionalized platinum nanoparticles. *Chem. Mater.*, 11, 3460–3463, 1999.
52. Eklund, S.E., Cliffel, D.E., Synthesis and catalytic properties of soluble platinum nanoparticles protected by a thiol monolayer. *Langmuir*, 20, 6012–6018, 2004.
53. Adil, S.F., Assal, M.E., Khan, M., Al-Warthan, A., Siddiqui, M.R.H., Liz-Marzán, L.M., Biogenic synthesis of metallic nanoparticles and prospects toward green chemistry. *Dalton Trans.*, 44, 9709–9717, 2015.
54. Moglianetti, M., De Luca, E., Pedone, D., Marotta, R., Catelani, T., Sartori, B., Amenitsch, H., Retta, S.F., Pompa, P.P., Platinum nanozymes recover cellular ROS homeostasis in an oxidative stress-mediated disease model. *Nanoscale*, 8, 3739–3752, 2016.
55. Bommersbach, P., Chaker, M., Mohamedi, M., Guay, D., Physico-chemical and electrochemical properties of platinum–Tin Nanoparticles Synthesized by Pulsed Laser Ablation for Ethanol Oxidation. *J. Phys. Chem. C*, 112, 14672–14681, 2008.
56. Paschos, O., Choi, P., Efstathiadis, H., Haldar, P., Synthesis of platinum nanoparticles by aerosol assisted deposition method. *Thin Solid Films*, 516, 3796–3801, 2008.
57. Rakshit, R., Bose, S., Sharma, R., Budhani, R., Vijaykumar, T., Neena, S., Kulkarni, G., Correlations between morphology, crystal structure, and magnetization of epitaxial cobalt-platinum films grown with pulsed laser ablation. *J. Appl. Phys.*, 103, 023915, 2008.
58. Choi, I.D., Lee, H., Shim, Y.-B., Lee, D., A one-step continuous synthesis of carbon-supported Pt catalysts using a flame for the preparation of the fuel electrode. *Langmuir*, 26, 11212–11216, 2010.
59. Ke, X., Bittencourt, C., Bals, S., Van Tendeloo, G., Low-dose patterning of platinum nanoclusters on carbon nanotubes by focused-electron-beam-induced deposition as studied by TEM. *Beilstein J. Nanotechnol.*, 4, 77, 2013.

60. Dhand, C., Dwivedi, N., Loh, X.J., Ying, A.N.J., Verma, N.K., Beuerman, R.W., Lakshminarayanan, R., Ramakrishna, S., Methods and strategies for the synthesis of diverse nanoparticles and their applications: A comprehensive overview. *RSC Adv.*, 5, 105003–105037, 2015.
61. Scaramuzza, S., Zerbetto, M., Amendola, V., Synthesis of gold nanoparticles in liquid environment by laser ablation with geometrically confined configurations: Insights to improve size control and productivity.*J. Phys. Chem. C*, 120, 9453–9463, 2016.
62. Correard, F., Maximova, K., Esteve, M.-A., Villard, C., Roy, M., Al-Kattan, A., Sentis, M., Gingras, M., Kabashin, A.V., Braguer, D., Gold nanoparticles prepared by laser ablation in aqueous biocompatible solutions: Assessment of safety and biological identity for nanomedicine applications. *Int. J. Nanomed.*, 9, 5415, 2014.
63. Yanson, A.I., Rodriguez, P., Garcia-Araez, N., Mom, R.V., Tichelaar, F.D., Koper, M., Cathodic corrosion: A quick, clean, and versatile method for the synthesis of metallic nanoparticles. *Angew. Chem. Int. Ed.*, 50, 6346–6350, 2011.
64. Torres-Chavolla, E., Ranasinghe, R.J., Alocilja, E.C., Characterization and functionalization of biogenic gold nanoparticles for biosensing enhancement. *IEEE Trans. Nanotechnol.*, 9, 533–538, 2010.
65. Shah, M., Fawcett, D., Sharma, S., Tripathy, S.K., Poinern, G.E.J., Green synthesis of metallic nanoparticles via biological entities. *Materials*, 8, 7278–7308, 2015.
66. Isaac, R., Gobalakrishnan, S., Rajan, G., Wu, R.-J., Pamanji, S.R., Khagga, M., Baskaralingam, V., Chavali, M., An overview of facile green biogenic synthetic routes and applications of platinum nanoparticles. *Adv. Sci. Eng. Med.*, 5, 763–770, 2013.
67. Siddiqi, K.S., Husen, A., Green synthesis, characterization and uses of palladium/platinum nanoparticles. *Nanoscale Res. Lett.*, 11, 482, 2016.
68. Rashamuse, K., Mutambanengwe, C., Whiteley, C., Enzymatic recovery of platinum (IV) from industrial wastewater using a biosulphidogenic hydrogenase. *Afr. J. Biotechnol.*, 7, 1087–1095, 2008.
69. Baskaran, B., Muthukumarasamy, A., Chidambaram, S., Sugumaran, A., Ramachandran, K., Manimuthu, T.R., Cytotoxic potentials of biologically fabricated platinum nanoparticles from *Streptomyces* sp. on MCF-7 breast cancer cells. *IET Nanobiotechnol.*, 11, 241–246, 2016.
70. Brayner, R., Barberousse, H., Hemadi, M., Djedjat, C., Yéprémian, C., Coradin, T., Livage, J., Fiévet, F., Couté, A., Cyanobacteria as bioreactors for the synthesis of Au, Ag, Pd, and Pt nanoparticles via an enzyme-mediated route. *J. Nanosci. Nanotechnol.*, 7, 2696–2708, 2007.
71. Shiny, P., Mukherjee, A., Chandrasekaran, N., DNA damage and mitochondria-mediated apoptosis of A549 lung carcinoma cells induced by biosynthesised silver and platinum nanoparticles. *RSC Adv.*, 6, 27775–27787, 2016.
72. Govender, Y., Riddin, T., Gericke, M., Whiteley, C.G., Bioreduction of platinum salts into nanoparticles: A mechanistic perspective. *Biotechnol. Lett.*, 31, 95–100, 2009.

73. Nellore, J., Pauline, C., Amarnath, K., *Bacopa monnieri* phytochemicals mediated synthesis of platinum nanoparticles and its neurorescue effect on 1-methyl 4-phenyl 1,2,3,6 tetrahydropyridine-induced experimental parkinsonism in zebrafish. *Neurodegener. Dis.*, 2013, 972391, 2013.
74. Velmurugan, P., Shim, J., Kim, K., Oh, B.-T., *Prunus×yedoensis* tree gum mediated synthesis of platinum nanoparticles with antifungal activity against phytopathogens. *Mater. Lett.*, 174, 61–65, 2016.
75. Karthik, R., Sasikumar, R., Chen, S.-M., Govindasamy, M., Kumar, J.V., Muthuraj, V., Green synthesis of platinum nanoparticles using *Quercus glauca* extract and its electrochemical oxidation of Hydrazine in water samples. *Int. J. Electrochem. Sci.*, 11, 8245–8255, 2016.
76. Leo, A.J., Oluwafemi, O.S., Plant-mediated synthesis of platinum nanoparticles using water hyacinth as an efficient biomatrix source–An eco-friendly development. *Mater. Lett.*, 196, 141–144, 2017.
77. Riddin, T., Govender, Y., Gericke, M., Whiteley, C., Two different hydrogenase enzymes from sulphate-reducing bacteria are responsible for the bioreductive mechanism of platinum into nanoparticles. *Enzyme Microb. Technol.*, 45, 267–273, 2009.
78. Riddin, T., Gericke, M., Whiteley, C., Biological synthesis of platinum nanoparticles: effect of initial metal concentration. *Enzyme Microb. Technol.*, 46, 501–505, 2010.
79. Longoria, E.C., Nestor, A.V., Borja, M.A., Production of platinum nanoparticles and nanoaggregates using *Neurospora crassa*. *J. Microbiol. Biotechnol.*22, 1000–1004, 2012.
80. Syed, A., Ahmad, A., Extracellular biosynthesis of platinum nanoparticles using the fungus *Fusarium oxysporum*. *Colloids Surf. B*, 97, 27–31, 2012.
81. Song, J.Y., Kwon, E.-Y., Kim, B.S., Biological synthesis of platinum nanoparticles using *Diopyros kaki* leaf extract. *Bioprocess. Biosyst. Eng.*, 11, 159, 2009.
82. Soundarrajan, C., Sankari, A., Dhandapani, P., Maruthamuthu, S., Ravichandran, S., Sozhan, G., Palaniswamy, N., Rapid biological synthesis of platinum nanoparticles using *Ocimum sanctum* for water electrolysis applications. *Bioprocess. Biosyst. Eng.*, 35, 827–833, 2012.
83. Bali, R., Siegele, R., Harris, A.T., Biogenic Pt uptake and nanoparticle formation in *Medicago sativa* and *Brassica juncea*. *J. Nanopart. Res.*, 12, 3087–3095, 2010.
84. Raut, R.W., Haroon, A.S.M., Malghe, Y.S., Nikam, B.T., Kashid, S.B., Rapid biosynthesis of platinum and palladium metal nanoparticles using root extract of *Asparagus racemosus* Linn. *Adv. Mater. Lett.*, 4, 650–654, 2013.
85. Oberdörster, G., Oberdörster, E., Oberdörster, J., Nanotoxicology: An emerging discipline evolving from studies of ultrafine particles. *Environ. Health Perspect.*, 113, 823, 2005.
86. Teow, Y., Asharani, P., Hande, M.P., Valiyaveettil, S., Health impact and safety of engineered nanomaterials. *Chem. Commun.*, 47, 7025–7038, 2011.

87. Sharifi, S., Behzadi, S., Laurent, S., Forrest, M.L., Stroeve, P., Mahmoudi, M., Toxicity of nanomaterials. *Chem. Soc. Rev.*, 41, 2323–2343, 2012.
88. Oostingh, G.J., Casals, E., Italiani, P., Colognato, R., Stritzinger, R., Ponti, J., Pfaller, T., Kohl, Y., Ooms, D., Favilli, F., Problems and challenges in the development and validation of human cell-based assays to determine nanoparticle-induced immunomodulatory effects. *Part. Fibre Toxicol.*, 8, 8, 2011.
89. Dobrovolskaia, M.A., Neun, B.W., Clogston, J.D., Grossman, J.H., McNeil, S.E., Choice of method for endotoxin detection depends on nanoformulation. *Nanomedicine*, 9, 1847–1856, 2014.
90. Gao, J., Liang, G., Zhang, B., Kuang, Y., Zhang, X., Xu, B., FePt@CoS2 yolk–shell nanocrystals as a potent agent to kill HeLa cells. *J. Am. Chem. Soc.*, 129, 1428–1433, 2007.
91. Pelka, J., Gehrke, H., Esselen, M., Türk, M., Crone, M., Bräse, S., Muller, T., Blank, H., Send, W., Zibat, V., Cellular uptake of platinum nanoparticles in human colon carcinoma cells and their impact on cellular redox systems and DNA integrity. *Chem. Res. Toxicol.* 22, 649–659, 2009.
92. Manikandan, M., Hasan, N., Wu, H.-F., Platinum nanoparticles for the photothermal treatment of Neuro 2A cancer cells. *Biomater.*, 34, 5833–5842, 2013.
93. Buchtelova, H., Dostalova, S., Michalek, P., Krizkova, S., Strmiska, V., Kopel, P., Hynek, D., Richtera, L., Ridoskova, A., Adam, P., Size-related cytotoxicological aspects of polyvinylpyrrolidone-capped platinum nanoparticles. *Food Chem. Toxicol.*, 105, 337–346, 2017.
94. Yamagishi, Y., Watari, A., Hayata, Y., Li, X., Kondoh, M., Tsutsumi, Y., Yagi, K., Hepatotoxicity of sub-nanosized platinum particles in mice. *Die. Pharmazie.*, 68, 178–182, 2013.
95. Konieczny, P., Goralczyk, A.G., Szmyd, R., Skalniak, L., Koziel, J., Filon, F.L., Crosera, M., Cierniak, A., Zuba-Surma, E.K., Borowczyk, J., Effects triggered by platinum nanoparticles on primary keratinocytes. *Int. J. Nanomed.*, 8, 3963, 2013.
96. Hamasaki, T., Kashiwagi, T., Imada, T., Nakamichi, N., Aramaki, S., Toh, K., Morisawa, S., Shimakoshi, H., Hisaeda, Y., Shirahata, S., Kinetic analysis of superoxide anion radical-scavenging and hydroxyl radical-scavenging activities of platinum nanoparticles. *Langmuir*, 24, 7354–7364, 2008.
97. Comenge, J., Sotelo, C., Romero, F., Gallego, O., Barnadas, A., Parada, T.G.-C., Domínguez, F., Puntes, V.F., Detoxifying antitumoral drugs via nanoconjugation: The case of gold nanoparticles and cisplatin. *PloS One*, 7, e47562, 2012.
98. Johnstone, T.C., Suntharalingam, K., Lippard, S.J., The next generation of platinum drugs: targeted Pt (II) agents, nanoparticle delivery, and Pt (IV) prodrugs. *Chem. Rev.*, 116, 3436–3486, 2016.
99. Teng, B., Yu, C., Zhang, X., Feng, Q., Wen, L., Li, C., Cheng, Z., Jin, D., Lin, J., Upconversion nanoparticles loaded with eIF4E siRNA and platinum (IV)

prodrug to sensitize platinum based chemotherapy for laryngeal cancer and bioimaging. *J. Mater. Chem. B*, 5, 307–317, 2017.
100. Estrela-Llopis, V., Chevichalova, A., Trigubova, N., Ryzhuk, E., Heterocoagulation of polysaccharide-coated platinum nanoparticles with ovarian-cancer cells. *Colloid J.*, 76, 609–621, 2014.
101. Yin, T., Wang, Z., Li, X., Li, Y., Bian, K., Cao, W., He, Y., Liu, H., Niu, K., Gao, D., Biologically inspired self-assembly of bacitracin-based platinum nanoparticles with anti-tumor effects. *New J. Chem.*, 41, 2941–2948, 2017.
102. López, T., Alvarez, M., González, R., Uddin, M., Bustos, J., Arroyo, S., Sánchez, A., Synthesis, characterization and *in vitro* cytotoxicity of Pt-TiO_2 nanoparticles. *Adsorption*, 17, 573–581, 2011.
103. Morozkin, E., Zaporozhchenko, I., Kharkova, M., Cherepanova, A., Laktionov, P., Vlasov, V., Sukhov, B., Prozorova, G., Trofimov, B., Khvostov, M., Cytotoxic and immunomodulating properties of silver and platinum nanocomposites.*Chem. Sustain. Develop.*, 21, 147, 2013.
104. López, T., Figueras, F., Manjarrez, J., Bustos, J., Alvarez, M., Silvestre-Albero, J., Rodriguez-Reinoso, F., Martínez-Ferre, A., Martínez, E., Catalytic nanomedicine: a new field in antitumor treatment using supported platinum nanoparticles. *In vitro* DNA degradation and *in vivo* tests with C6 animal model on Wistar rats. *Eur. J. Med. Chem.*, 45, 1982–1990, 2010.
105. Cho, E.J., Sun, B., Doh, K.-O., Wilson, E.M., Torregrosa-Allen, S., Elzey, B.D., Yeo, Y., Intraperitoneal delivery of platinum with *in-situ* crosslinkable hyaluronic acid gel for local therapy of ovarian cancer. *Biomater.*, 37, 312–319, 2015.
106. Au, L., Zheng, D., Zhou, F., Li, Z.-Y., Li, X., Xia, Y., A quantitative study on the photothermal effect of immuno gold nanocages targeted to breast cancer cells. *ACS Nano*, 2, 1645–1652, 2008.
107. Bigall, N.C., Härtling, T., Klose, M., Simon, P., Eng, L.M., Eychmüller, A., Monodisperse platinum nanospheres with adjustable diameters from 10 to 100 nm: synthesis and distinct optical properties. *Nano Lett.*, 8, 4588–4592, 2008.
108. Gharibshahi, E., Saion, E., Influence of dose on particle size and optical properties of colloidal platinum nanoparticles. *Int. J. Mol. Sci.*, 13, 14723–14741, 2012.
109. Chen, C.-L., Kuo, L.-R., Lee, S.-Y., Hwu, Y.-K., Chou, S.-W., Chen, C.-C., Chang, F.-H., Lin, K.-H., Tsai, D.-H., Chen, Y.-Y., Photothermal cancer therapy via femtosecond-laser-excited FePt nanoparticles. *Biomater.*, 34, 1128–1134, 2013.
110. Beyth, N., Houri-Haddad, Y., Domb, A., Khan, W., Hazan, R., Alternative antimicrobial approach: nano-antimicrobial materials. *Evid. Based Complement. Alternat. Med.*, 2015, 246012, 2015.
111. Rosenberg, B., Van Camp, L., Grimley, E.B., Thomson, A.J., The inhibition of growth or cell division in *Escherichia coli* by different ionic species of platinum (IV) complexes. *J. Biol. Chem.*, 242, 1347–1352, 1967.

112. Rosenberg, B., Vancamp, L., Trosko, J.E., Mansour, V.H., Platinum compounds: A new class of potent antitumour agents. *Nature*, 222, 385, 1969.
113. Zhao, Y., Ye, C., Liu, W., Chen, R., Jiang, X., Tuning the composition of AuPt bimetallic nanoparticles for antibacterial application. *Angew. Chem. Int. Ed.*, 53, 8127–8131, 2014.
114. Chwalibog, A., Sawosz, E., Hotowy, A., Szeliga, J., Mitura, S., Mitura, K., Grodzik, M., Orlowski, P., Sokolowska, A., Visualization of interaction between inorganic nanoparticles and bacteria or fungi. *Int. J. Nanomed.*, 5, 1085, 2010.
115. Kebede, M.A., Imae, T., Wu, C.-M., Cheng, K.-B., Cellulose fibers functionalized by metal nanoparticles stabilized in dendrimer for formaldehyde decomposition and antimicrobial activity. *Chem. Eng. J.*, 311, 340–347, 2017.
116. Gopal, J., Hasan, N., Manikandan, M., Wu, H.-F., Bacterial toxicity/compatibility of platinum nanospheres, nanocuboids and nanoflowers. *Sci. Rep.*, 3, 1260, 2013.
117. Kim, Y.-J., Kim, D.-B., Lee, Y.-H., Choi, S.-Y., Park, J.-S., Lee, S.-Y., Park, J.-W., Kwon, H.-J., Effects of nanoparticulate saponin-platinum conjugates on 2, 4-dinitrofluorobenzene-induced macrophage inflammatory protein-2 gene expression via reactive oxygen species production in RAW 264.7 cells. *BMB Rep.*, 42, 304–309, 2009.
118. Hosaka, H., Haruki, R., Yamada, K., Böttcher, C., Komatsu, T., Hemoglobin–albumin cluster incorporating a Pt nanoparticle: Artificial O_2carrier with antioxidant activities. *PLoS One*9, e110541, 2014.
119. Tsuji, G., Hashimoto-Hachiya, A., Takemura, M., Kanemaru, T., Ichihashi, M., Furue, M., Palladium and Platinum Nanoparticles Activate AHR and NRF_2 in Human Keratinocytes-Implications in Vitiligo Therapy. *J. Investig. Dermatol.*, 137, 1582, 2017.
120. Lee, J.-W., Son, J., Yoo, K.-M., Lo, Y.M., Moon, B., Characterization of the antioxidant activity of gold@platinum nanoparticles. *RSC Adv.*, 4, 19824–19830, 2014.
121. Jawaid, P., Rehman, M.U., Yoshihisa, Y., Li, P., li Zhao, Q., Hassan, M.A., Miyamoto, Y., Shimizu, T., Kondo, T., Effects of SOD/catalase mimetic platinum nanoparticles on radiation-induced apoptosis in human lymphoma U937 cells. *Apoptosis*, 19, 1006–1016, 2014.
122. Jawaid, P., Rehman, M.U., Hassan, M.A., Zhao, Q.L., Li, P., Miyamoto, Y., Misawa, M., Ogawa, R., Shimizu, T., Kondo, T., Effect of platinum nanoparticles on cell death induced by ultrasound in human lymphoma U937 cells. *Ultrason. Sonochem.*, 31, 206–215, 2016.
123. Ju, Y., Kim, J., Dendrimer-encapsulated Pt nanoparticles with peroxidase-mimetic activity as biocatalytic labels for sensitive colorimetric analyses. *Chem. Commun.*, 51, 13752–13755, 2015.
124. Kim, J., Takahashi, M., Shimizu, T., Shirasawa, T., Kajita, M., Kanayama, A., Miyamoto, Y., Effects of a potent antioxidant, platinum nanoparticle, on the lifespan of *Caenorhabditis elegans*. *Mech. Ageing Dev.*, 129, 322–331, 2008.

125. Kawasaki, H., Yamamoto, H., Fujimori, H., Arakawa, R., Inada, M., Iwasaki, Y., Surfactant-free solution synthesis of fluorescent platinum subnanoclusters. *Chem. Commun.*, 46, 3759–3761, 2010.
126. Wu, J., Balasubramanian, S., Kagan, D., Manesh, K.M., Campuzano, S., Wang, J., Motion-based DNA detection using catalytic nanomotors. *Nat. Commun.*, 1, 36, 2010.
127. Pedone, D., Moglianetti, M., De Luca, E., Bardi, G., Pompa, P.P., Platinum nanoparticles in nanobiomedicine. *Chem. Soc. Rev.*, 46, 4951–4975, 2017.
128. Sun, Y., Wang, J., Li, W., Zhang, J., Zhang, Y., Fu, Y., DNA-stabilized bimetallic nanozyme and its application on colorimetric assay of biothiols. *Biosens. Bioelectron.*, 74, 1038–1046, 2015.
129. Gill, R., Polsky, R., Willner, I., Pt nanoparticles functionalized with nucleic acid act as catalytic labels for the chemiluminescent detection of DNA and proteins. *Small*, 2, 1037–1041, 2006.
130. Polsky, R., Gill, R., Kaganovsky, L., Willner, I., Nucleic acid-functionalized Pt nanoparticles: Catalytic labels for the amplified electrochemical detection of biomolecules. *Anal. Chem.*, 78, 2268–2271, 2006.
131. Hu, X., Saran, A., Hou, S., Wen, T., Ji, Y., Liu, W., Zhang, H., Wu, X., Rod-shaped Au@PtCu nanostructures with enhanced peroxidase-like activity and their ELISA application. *Chin. Sci. Bull.*, 59, 2588–2596, 2014.
132. Chen, W., Fang, X., Li, H., Cao, H., Kong, J., DNA-mediated inhibition of peroxidase-like activities on platinum nanoparticles for simple and rapid colorimetric detection of nucleic acids. *Biosens. Bioelectron.*, 94, 169–175, 2017.
133. Zhang, L.-N., Deng, H.-H., Lin, F.-L., Xu, X.-W., Weng, S.-H., Liu, A.-L., Lin, X.-H., Xia, X.-H., Chen, W., *In situ* growth of porous platinum nanoparticles on graphene oxide for colorimetric detection of cancer cells. *Anal. Chem.*, 86, 2711–2718, 2014.
134. Choi, G., Kim, E., Park, E., Lee, J.H., A cost-effective chemiluminescent biosensor capable of early diagnosing cancer using a combination of magnetic beads and platinum nanoparticles. *Talanta*, 162, 38–45, 2017.
135. Chau, L.Y., He, Q., Qin, A., Yip, S.P., Lee, T.M., Platinum nanoparticles on reduced graphene oxide as peroxidase mimetics for the colorimetric detection of specific DNA sequence. *J. Mater. Chem. B*, 4, 4076–4083, 2016.
136. Kwon, D., Lee, W., Kim, W., Yoo, H., Shin, H.-C., Jeon, S., Colorimetric detection of penicillin antibiotic residues in pork using hybrid magnetic nanoparticles and penicillin class-selective, antibody-functionalized platinum nanoparticles. *Anal. Methods*, 7, 7639–7645, 2015.
137. Hu, X., Saran, A., Hou, S., Wen, T., Ji, Y., Liu, W., Zhang, H., He, W., Yin, J.-J., Wu, X., Au@ PtAg core/shell nanorods: tailoring enzyme-like activities via alloying. *RSC Adv.*, 3, 6095–6105, 2013.
138. Ji, X., Lau, H.Y., Ren, X., Peng, B., Zhai, P., Feng, S.P., Chan, P.K., Highly sensitive metabolite biosensor based on organic electrochemical transistor

integrated with microfluidic channel and poly (N-vinyl-2-pyrrolidone)-capped platinum nanoparticles. *Adv. Mater. Technol.*, 1, 2016.
139. Shi, W., Fan, H., Ai, S., Zhu, L., Honeycomb-like nitrogen-doped porous carbon supporting Pt nanoparticles as enzyme mimic for colorimetric detection of cholesterol. *Sens. Actuators B Chem.*, 221, 1515–1522, 2015.
140. Wu, L.-L., Wang, L.-Y., Xie, Z.-J., Pan, N., Peng, C.-F., Colorimetric assay of l-cysteine based on peroxidase-mimicking DNA-Ag/Pt nanoclusters. *Sens. Actuator B-Chem.*, 235, 110–116, 2016.
141. He, S.-B., Wu, G.-W., Deng, H.-H., Liu, A.-L., Lin, X.-H., Xia, X.-H., Chen, W., Choline and acetylcholine detection based on peroxidase-like activity and protein antifouling property of platinum nanoparticles in bovine serum albumin scaffold. *Biosens. Bioelectron.*, 62, 331–336, 2014.
142. Gao, F., Du, L., Zhang, Y., Zhou, F., Tang, D., A sensitive sandwich-type electrochemical aptasensor for thrombin detection based on platinum nanoparticles decorated carbon nanocages as signal labels. *Biosens. Bioelectron.*, 86, 185–193, 2016.
143. Yang, Z.-H., Zhuo, Y., Yuan, R., Chai, Y.-Q., A nanohybrid of platinum nanoparticles-porous ZnO–hemin with electrocatalytic activity to construct an amplified immunosensor for detection of influenza. *Biosens. Bioelectron.*, 78, 321–327, 2016.
144. Dutta, G., Nagarajan, S., Lapidus, L.J., Lillehoj, P.B., Enzyme-free electrochemical immunosensor based on methylene blue and the electro-oxidation of hydrazine on Pt nanoparticles. *Biosens. Bioelectron.*, 92, 372–377, 2017.
145. Gao, Z., Xu, M., Hou, L., Chen, G., Tang, D., Irregular-shaped platinum nanoparticles as peroxidase mimics for highly efficient colorimetric immunoassay. *Anal. Chim. Acta*, 776, 79–86, 2013.

18

Eco-Friendly Noble Metal Nanoparticles for Therapeutic Applications: Present and Future Scenario

Raksha Choudhary[1] and Rashmi Madhuri[2,*]

[1]Department of Applied Chemistry, Indian Institute of Technology (Indian School of Mines), Jharkhand, Dhanbad, India
[2]Functional Nanomaterials Research Laboratory, Department of Applied Physics, Indian Institute of Technology (Indian School of Mines), Dhanbad, Jharkhand, India

Abstract

Noble metals have been used since ancient times; only their shape, size or nature has been modified based on our daily needs. Over the past decade, considerable progress has been made in the synthesis and application of noble metal nanoparticles. With their development, the synthesis routes have been modified towards a greener one, leading to the development of eco-friendly, stable and cost-effective nanoparticles. With the use of the green synthesis approach for noble metal nanoparticle preparation, a pathway has been opened to a wide range of biomedical applications. Therefore, this chapter mainly focuses on biomedical applications of green noble metal nanoparticles and their potential applications, which both inspire and challenge us. First, we provide an overview of noble metal nanoparticles synthesized via the green synthesis route. Next, we cover the key applications of these nanoparticles in sensor fabrication for biologically important compounds, medicine, treatment and imaging. Finally, we present the current challenges and opportunities related to their development and commercial applications.

Keywords: Green synthesis, noble metals, anticancer agent, acaricidal agent, anti-biofouling agent, anti-inflammatory agent and anti-cholinesterase

**Corresponding author*: rakshachoudhary121@gmail.com

Suvardhan Kanchi and Shakeel Ahmed (eds.) Green Metal Nanoparticles, (629–665)
© 2018 Scrivener Publishing LLC

18.1 Introduction

Nanotechnology is the new superhero of this generation. This technology has allowed us to work with materials ranging between 1–100 nm [1–3]. At the nanoscale, synthesized materials have several novel properties in comparison to their corresponding bulk materials. Nanomaterials are a multitalented material, which can be used in various disciplines, i.e., engineering science, natural science, biomedical field, etc. [2]. They can be used to design different kinds of sensors/biosensors or can be used as an excellent catalyst, owing to their specific surface area and high reactivity. Due to their increased applicability in various fields, the demands have also increased significantly. Therefore, a large number of synthesis processes (chemical, physical or biological) are currently employed in designing different types of nanoparticles (NPs)/nanomaterials with desired properties. The commonly used synthesis process for nanoparticles is portrayed in Figure 18.1.

Nanoparticles are commonly synthesized by bottom-up or top-down approach. In the top-down approach, various chemical and physical methodologies are used to reduce the suitable precursor material in nano-size particles [4] such as radiation-induced methods [5], thermolysis [6], pyrolysis [7], lithography [8], etc. The major drawback associated with this approach is formation of irregularity on the surface of synthesized nanostructures, which results in a noticeable change in their surface and physical properties [5]. In addition, the approach requires a very high

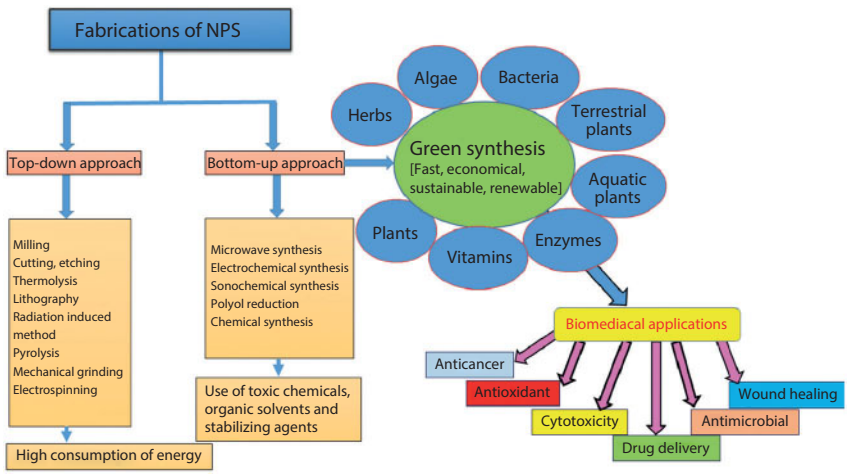


Figure 18.1 General and popular synthesis process used for nanoparticle preparation.

temperature and pressure for the synthesis of NPs, which consumes a tremendous amount of energy. In contrast to this, in the bottom-up approach, which is also known as self-assembly approach, NPs synthesis was done through assembly of the cluster, molecules or atoms [9]. The bottom-up approach presents a better opportunity to design NPs with more homogeneous chemical composition and less surface imperfection at a low cost. The most common process used in NPs synthesis is through wet synthesis method, which includes, polyol reduction [10], sonochemical [11, 12], electrochemical [13] and chemical [14] based synthesis. Having several advantages over the top-down approach, bottom-up approaches also suffer from some of the drawbacks, like use of capping/stabilizing agents, nonpolar organic solvents and hazardous chemicals, which restrict their use in biomedical and clinical applications.

To overcome these problems, researchers have moved towards an alternative, nontoxic, reliable, and eco-friendly synthesis technology for production of nanoparticles, called green-synthesis approach. Green synthesis or green chemistry results in economic, less-toxic, high yield generation of nanoparticles without harming the environment or living organisms. The discovery of "Green chemistry" has been a gift to researchers, which allows large-scale preparation of nanoparticles using less chemicals, thereby eliminating the amount of toxic residues affecting nature and human health [15]. Among the various types of nanoparticles (metallic, non-metallic, polymeric, etc.), noble metal-based nanoparticles are very popular in the field of biomedical science. This may be the reason that the green chemistry approach for synthesis of noble metal nanoparticles is very popular and a number of new findings have been developed in this area. Synthesis of metallic nanoparticles via green synthesis approach has many merits over conventional methods such as:

1. This is a nature-friendly and cost-effective approach which depends on natural resources like algae, fungi, microorganisms or plants that act as reducing agent, capping agent and stabilizing agent;
2. Synthesis requires minimum energy;
3. Very simple, self-efficient and clean method;
4. Requires much less use of toxic chemicals and no capping agent on the surface of nanoparticles, resulting in nontoxic products;
5. Needs medium temperature and pressure;
6. Does not require any external ligand or stabilizing or capping agent during nanoparticles synthesis.

Based on the advantages, synthesis of noble metal nanoparticles is becoming more popular every day and is found suitable for various applications, mainly biomedical, diagnosis, drug delivery, etc. [16]. In this chapter, we have compiled the applications of various noble metal nanoparticles in the field of biomedical science only

18.2 Why Noble Metal Nanoparticles are Gaining in Popularity in the Biomedical Field

About 5000 years ago, many Romans, Persians, Egyptians and Greeks routinely used silver for food storage [17]. Even though they probably were not aware of the antimicrobial activity of silver, silver utensils were used for eating, drinking and storage of various eatable and drinkable products [18]. Therapeutic application of silver is present in records as early as 300 BC. In the Hindu religion, silver utensils were also used for the "panchamrit" preparation using curd, *Ocimum sanctum* (tulsi), honey and other ingredients. In ancient Indian, a book on Ayurvedic medicine entitled *Charaka Samhitā* mentioned the therapeutic ability of many metals [19]. Silver was commonly used as an antimicrobial agent prior to the discovery of antibiotics by Alexander Fleming. In the past few years, the nanoparticles of noble metals—i.e., gold nanoparticles (AuNPs) and silver nanoparticles (AgNPs)—have attracted the attention of researchers due to their extraordinary defense mechanism against a broad range of microorganisms, which enhances the effect of most commonly used antibiotics against drug-resistant bacteria, in comparison to their bulk form [20]. The outstanding features of Au/AgNPs have allowed them to be used in broad fields such as agricultural [21], water treatment [22], drug delivery [23], biological medicine [24], etc. Also, AgNPs have high electrical conductivity; therefore, they are used in electronic paste, inks and adhesives in device making [25]. Noble metal NPs are also widely used as a medicinal agent for therapeutic and diagnostic applications of various severe diseases such as cardiovascular disease, cancer, tuberculosis, spinal cord injury, cirrhosis, hepatitis, arthritis, HIV/AIDS, Parkinson's, Alzheimer's, diabetes, etc.

18.3 Biomedical Applications of Noble Metal Nanoparticles

Noble metal nanoparticles related research is a multitasking, continuously expanding field, tending towards use in real world and biomedical

applications. But, to design NPs which can be used in the biomedical field, it is necessary to engineer them with the desired effect, i.e., with minimal severe environmental effect and toxicity. Metallic NPs play a very interesting role in the biomedical field, which, owing to their supposed safety effect on human beings, are greatly used as an antibacterial [26], insecticidal [27] and antifungal [28]. Due to their having several interesting properties, metallic NPs are used in ultrasound gels [29, 30], medical devices, bone cements, wound dressings, creams, topical ointments, food processing, therapeutics, cell imaging, targeted drug delivery [31] and surgical implants because of their medically relevant surface plasmon absorption [32], cytotoxic [33] and optical [34] properties.

18.3.1 As Anticancer Agent

In the modern world, cancer is one of the leading causes of mortality, with 10 million new cases reported every year [35]. Cancer is a well-established multifactorial disease, which occurs due to a combination of complex environmental and genetic factors [36–38]. Nanoparticles (NPs) of varying architecture, shape, composition and size have been discovered for the treatment of cancer in various forms, like photothermal agent or nanomedicine. Green synthesized NPs have potential against many cancer cell lines through cytotoxicity [39], antimetastatic [40], antiproliferative [41] and apoptosis [42]. Nanotechnology has proved to be a miracle in life science as a therapeutic or diagnostic agent. They are present in every step of our medical treatments, starting from diagnosis to final surgery. They are involved in magnetic resonance imaging, fluorescent imaging, computed tomography, radiothermal and photothermal therapy, magnetic hyperthermia treatment as well as a drug vehicle (Figure 18.2) [43].

Once the tumor is directly connected to the main blood circulation system, NPs can exploit several characteristics of the newly formed vasculature to efficiently target it. Tumor cells are supplied by blood capillaries that perfuse the cells of the tissue where NPs can (i) passively accumulate or (ii) anchor through targeting moieties to biomarkers overexpressed in tumor cells. NPs can act simultaneously as therapeutic agents, inducing hyperthermia, enhancing radiotherapy, silencing genes and/or delivering drugs to induce tumor cell death; and as imaging enhancers or contrast agents to help track the therapeutic effects in real time.

The formation of free radicals and antiproliferative activity of many cancer cell lines have been reported through AgNPs synthesized using aqueous extract of *Alternanthera sessilis* [41]. All around the cancer tissue, free electrons are generated by the free radicals, which leads to damage and

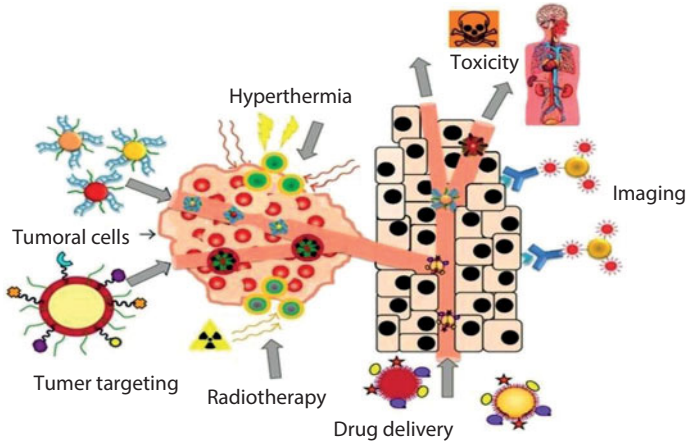


Figure 18.2 Role of noble metal nanoparticles in cancer treatment. (Reproduced with permission from [43]).

shrinking of the cell surface, followed by restricted signal and irregular nutrient supply, finally resulting in cell death. Similarly, antimetastatic activity of AuNPs has been reported by Karuppaiya *et al.*, where extract of *Dysosma pleiantha* rhizome has been used as a green precursor for the synthesis of AgNPs. The biosynthesized AgNPs were found to be nonhazardous to cell proliferation and can stop the chemoattraction of cell migration in fibrosarcoma cancer cell line in humans by disturbing the actin polymerization pathway interference [40]. Thus, the synthesized AuNPs from *D. pleiantha* rhizome can act as a strong candidate in the gene and drug delivery to metastatic cancer. Muthukumar *et al.* have prepared AuNPs via leaf extract of *Carica papaya* (CP) and *Catharanthus roseus* (CR) and blended the extract of both plant leaves to see its symbiotic effect on the *in-vitro* anticancer and antibacterial activity against cancer cell lines. The effect of AuNPs on the cell viability of two cancer cell lines was done via MTT assay 3-(4,5-dimethylthiazol-2-yl)-2,5-diphenyltetrazolium bromide (MTT) technique, which is used for determining cell metabolic activity by colorimetric assay. It was found that with increase in concentration of AuNPs, a sharp increase in cell death was also observed [44]. The demand for noble metal nanoparticle as an anticancer agent is increasing day by day.

Nowadays, photothermal treatment of cancer is gaining a lot of importance owing to their relatively non-destructive and less-harmful effects on human beings. In photothermal therapy, NPs are sent to the cancerous cells and cells are exposed to near infrared (NIR) radiation. The AuNPs have properties to absorb the NIR radiation and convert them to heat.

The localized increase in the temperature of cancer cells results in their death. Various forms of NPs, like gold nanorod, gold-gold sulfide, gold-iron oxide, gold-silica nanoshell, etc., have been reported for photothermal activity. The main problem with photothermal therapy is the requirement of NPs, which show intense NIR stability and absorptivity. In addition, the NPs used for the therapy should not be toxic to the system, which may cause problems if a few of them remain in the body.

For the synthesis of nontoxic or less-harmful noble metal nanoparticles, various phytochemical reagents, such as grape seed extract [45], garlic extract [46], soybeans [47], tea extract [48], lemongrass extract [49], etc., have been used. The NPs of varying shapes and sizes could be synthesized by these green materials and the resultant NPs show good biocompatibility and stability. In addition, these NPs have also exhibited maximum absorbance in the wavelength range of 800–1000 nm, at which absorption by the tissue is very high. In this regard, several works have been reported in the literature where AuNPs were synthesized from the green-synthesis approach, resulting in NPs used in cancer treatment. For example, Fazal *et al.* have reported AuNPs via *Theobromo cacao* (cocoa) extract without use of any capping agent. The particle displayed good biocompatibility with cells. During the study with cells present in epidermoid carcinoma, the cell death is induced when irradiated with a laser for a femtosecond at 800 nm. It proves the suitability of eco-friendly synthesized NIR absorbing anisotropic gold nanoparticles for photothermal degradation of cancer cells. The synthesized NPs also showed good X-ray contrast when tested via computed tomography (CT), which makes it feasible to use them as contrasting agent also [50].

Patra *et al.* demonstrated the green approach for the preparation of Ag and AuNPs using *Butea monosperma* (BM) leaf extract, where BM leaves act as stabilizing, capping as well as reducing agent. The synthesized AgNPs and AuNPs are found biocompatible towards cancer cell lines as well as normal endothelial cells and stable in biological buffer. In comparison to pristine drug, the synthesized NPs in combination with doxorubicin (DOX) showed better inhibition of cancer cell growth [16].

Hoshyar *et al.* have proposed a novel method for the production of AuNPs using crocin as an antioxidant compound. Crocin ($C_{44}H_{64}O_{24}$) is a main carotenoid obtained from the stigma of saffron, which is also water soluble. After AuNPs-crocin entered the cancer cell, the proliferation of breast cancer cells was significantly suppressed after 24 and 48 h of incubation [51].

González-Ballesteros *et al.* reported the use of brown macroalgae *Cystoseira baccata* (CB) extracts for the synthesis of gold nanoparticles

(Au@CB) as a fast, eco-friendly, one-pot synthetic route. Au@CB was tested against two colorectal cancer cell lines and the fibroblast cell line, showing strong cytotoxic activity. Remarkably, Au@CB exhibits an excellent biocompatibility on the healthy cell line. Au@CB has shown potential in the treatment of colorectal cancer [52].

Leukemia is basically a type of cancer which arises in bone marrow and leads to abnormality of white blood cells. The most common form of leukemia is B-chronic lymphocytic leukemia (B-CLL). It is a cancer that normally affects males, in which the B-lymphocytes are affected by the disease, leading to immune suppression as well as malignant cell infiltration into organs. Rapid increase in marrow vasculature causes abnormal angiogenesis, which can be detected in the marrow of B-CLL patient [53]. As reported in the literature, *in-vitro* cytotoxicity of PdNPs derived from extract of *Pelargonium graveolens* was performed by using human leukemia cell lines by an MTT cell viability assay, and the results showed that the cytotoxicity depended on the dose. The as-synthesized green PdNPs were found to be cost-effective, nature friendly and nontoxic in nature. Green synthesized NPs are suitable replacements for the chemically and physically synthesized NPs due to the above-mentioned properties of the green synthesized NPs [54].

18.3.2 Acaricidal Agent

Ticks are obligate haematophagous external parasites of wild as well as domestic animals. It has been estimated that 80% of the cattle population in the world is suffering from tick infestation. At present, use of synthetic chemical acaricides is the major preventive measure against tick infestation in animals. But, due to overdosing and continuous use, ticks have now developed resistance to most of the drugs or chemical acaricides. Besides this, they are also involved in environmental pollution, remain as residue in the food and show side effects/toxicity in workers. *Rhipicephalus (Boophilus) microplus* cattle tick is the most common ectoparasite of cattle found in subtropical and tropical regions, including India. These ticks are not only affecting the health of cattle but they are also becoming a problem in terms of economic loss. The *Rhipicephalus* affects the milk production rate because of cattle's blood loss, weight gain, tick worry, injection of toxins, etc. An estimated cost of US $ 498.7 million per annum is consumed in the control of ticks and tick-borne diseases in the dairy sector [55].

Therefore, there is an urgent need to develop an alternative safe method to control ticks. Phytoacaricides have many advantages over synthetic acaricides since they are eco-friendly, biodegradable, cheaper and have

minimal toxicity. Moreover, these botanicals can delay the resistance development process in the ticks because these herbal products are not a single compound but a mixture of active substances. Many plant extracts were discovered to have acaricidal effects, like *Azadirachta indica*, commonly known as neem, which is a renowned plant in India used for acaricidal treatment. Currently, green nanoparticles derived from these phytoacaricides are preferred against tick control due to their many advantages such as fast synthesis, less cost, safe for therapeutic use and eco-friendly nature. For example, Rajakumar *et al.* have synthesized AgNPs from *Manilkara zapota* leaf extract and studied its acaricidal activity. The killing rate of ticks depends upon the dose of AgNPs. Synthesized AgNPs show higher killing rate in comparison to *M. zapota* leaf extract and $AgNO_3$ solution. In the concurrent assay the distilled water (control) showed no killing effect. The complete killing of *R. microplus* was observed with synthesized AgNPs only [56].

Avinash *et al.* have reported the acardial activity of neem-coated silver nanoparticles (N-AgNPs) against *Rhipicephalus (Boophilus) microplus*. *In-vito* super-acaricidal activity was observed for both adult and larval *Rhipicephalus (Boophilus) microplus* [57]. Currently, green synthesized NPs are being used to control ticks due to its great importance and is deemed to be safe for therapeutic applications, environmentally friendly, nontoxic and cost-effective.

18.3.3 Anti-Biofouling Agent

Biofouling is the undesirable accumulation or colonization of plants, animals and microorganisms on artificial and natural surfaces immersed in aquatic environment. Macrofouling is when larva of higher organisms, like mussels, barnacles, etc., attach on marine biofilms. Microfouling is when bacteria and other microorganisms attach on the immersed surface and form a marine biofilm. The establishment of a fouling community takes place in several stages. Initially, any surface which is submerged in an aquatic environment gets coated by a conditioning film made of inorganic and organic molecules. The subsequent onset of macrofouling may be preceded by the formation of bacterial biofilms (bacterial fouling) on the surface and such a biofilm may have a deleterious effect on the ability of the surface to remain free from larger fouling organisms. The development of unwanted biofilms on the membrane surface leads to lifetime damage of the membrane and also reduces its water flux [58].

Use of chemical antifouling agents is one of the easy and common approaches to control fouling caused by macro- and microfoulers. But it

was found that many antimicrobial materials are less effective on microorganisms in biofilms compared to their planktonic counterparts. Therefore, higher concentrations of chemicals are required for the effective control of fouling, which results in harmful effects [59]. In order to control the biofouling in membrane systems various processes are present such as reverse osmosis, chemical cleaning of the membranes and pretreatment of feed solution. However, complete reduction of biofouling cannot be accomplished by the above methods because of the self-replicating nature of the survived bacteria. To stop the formation of biofilm, the surface of the membrane is modified with antibacterial additives, which is studied to be an effective approach. Therefore, researchers have been focusing on the surface immobilization of polyamide thin film composite (TFC) membrane with AgNPs to empower them with direct, effective, and long-lasting antibacterial activities [60]. Initially, for fabrication of AgNPs embedded or decorated membrane formation, toxic reducing agents such as sodium borohydride ($NaBH_4$) were used, but the use of toxic chemicals affects the environment. Therefore, it has become important to find an environment friendly, facile and cheap process for *in-situ* AgNPs immobilization onto the reverse osmosis membrane surface for carrying out anti-biofouling property without affecting the permselectivity of the membrane.

Krupa and Raghavan have reported the use of *Aegle marmelos* extract for the biosynthesis of AgNPs. The ability of the as-synthesized nanoparticles to prevent/control the biofilm-forming bacterial communities was determined by conducting anti-biofouling studies. For the study they have selected the microtiter plate method, where direct quantification of the attached bacteria can be done. In this study, for the detection of biofilm it was stained with crystal violet and the optical density was measured at 570 nm. It was found that the optical density value for the AgNPs loaded wells were somewhat lower than the control wells, i.e., in the absence of NPs. According to the literature, the AgNPs cause cell death by damaging the bacterial cell via changing the permeability of the cell membrane. The as-synthesized AgNPs were found to be an effective source of anti-biofouling, which leads to a decrease in the growth of marine biofilm-forming bacteria [59].

Another group of researchers have reported the green synthesis of AgNPs aqueous extract of *Turbinaria conoides* seaweed and studied their activity against anti-biofouling. In this work, *A. hydrophila, S. liquefaciens, E. coli* and *Salmonella* sp. bacterial strains were collected from different immersed and substratum from Thondi coastal waters of Palk Bay and the southeast coast of India. For 24 hours, all four bacterial strains were incubated with the green synthesized NPs. Confocal laser scanning microscopic (CLSM) analysis was used for imaging and observing the changes. CLSM analysis

confirmed that a considerable amount of synthesized AgNPs were efficient against formation and adherence of biofilm (Figure 18.3). The disintegrated and weak adherence of the biofilm was observed. Among the studied bacterial strains, *E. coli* has shown maximum zone of inhibition, followed by *Salmonella* sp. then *S. liquefaciens,* and minimum value was found for *A. hydrophila*. The green synthesized AgNPs are efficient in inhibiting the formation of biofilm formed by bacteria and can be applied over the surface of aquaculture installations and other marine systems to stop the growth and settlement of fouling. The synthesized AgNPs are eco-friendly in nature, cost-effective and nontoxic to aquatic system and are a good alternative to chemically synthesized NPs for antifouling applications [61].

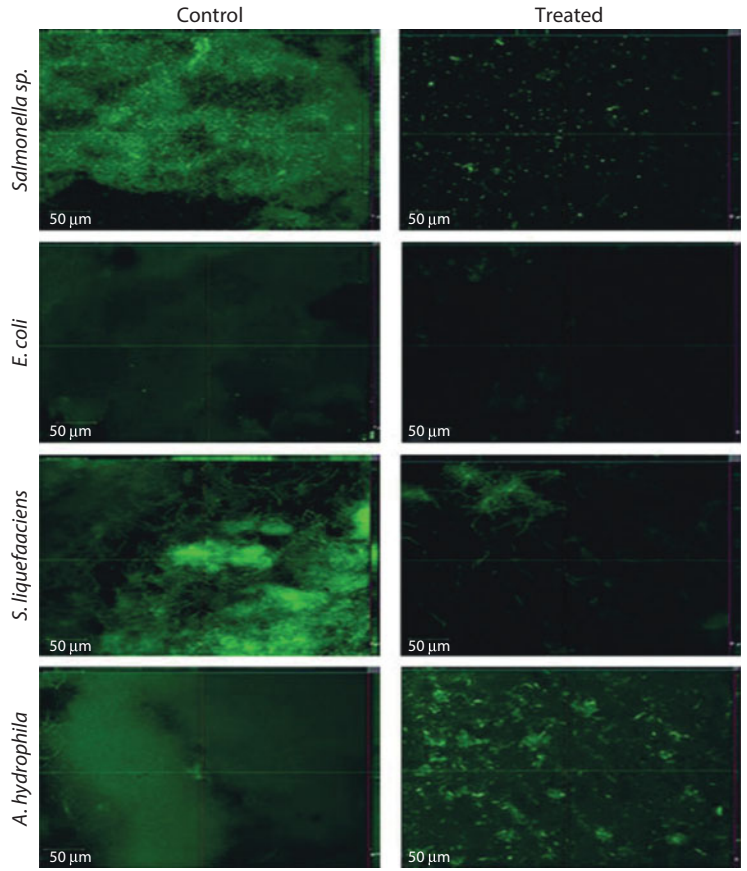


Figure 18.3 CLSM images representing the antibiofilm activity of AgNPs against marine biofilm-forming isolates of *Salmonella* sp., *E. coli*, *S. liquefaciens* and *A. hydrophila.* (Reproduced with permission from [61])

18.3.4 As an Anti-Inflammatory Agent and Anti-Cholinesterase

Inflammation is the immune system's response to injury and infection which leads to the removal of offending factors and restoration of tissue structure and physiological function. The acute phase of inflammation is characterized by a complex response which causes swelling, redness, pain and heat. Chronic or acute are the two major class of inflammation based on the time duration of the inflammatory action by the immune system. Various inflammatory disorders (such as rheumatoid arthritis) can be caused by loss of regulation of this process. Steroidal anti-inflammatory drugs and non-steroidal anti-inflammatory agents are the two most important groups of drugs that are used at present for pharmacological management of inflammation. They work very well but have various side effects, like acute renal failure, cardiovascular harm, excessive hair growth, joint destruction, fat redistribution, etc., which has forced researchers to discover new alternative materials which can solve the problem of inflammation in a modulatory, well-tolerated, homeostatic way [62].

Phytomedicine is an alternative treatment for these inflammatory disorders. Discovery of new anti-inflammatory drugs obtained from purified natural compounds from plants has led to the formation of less toxic and high therapeutic values. However, lack of quality in the production, quality, trade and prescription of phytomedicinal products are the major disadvantages of drugs made from plants. Aparna *et al.* have reported the synthesis of AgNPs from fruit extract of *Piper nigrum*, in which Piperine alkaloid also acts as capping agent [63]. The *in-vitro* assays were performed using reported NPs towards interleukins-6 (IL-6), tumor necrosis factor α (TNFα) and interleukins-1β (IL-1β). Using reverse transcription polymerase chain reaction (RT PCR), inhibition of TNFα was measured and the potential inhibition was showed by synthesized AgNPs at lower concentration, but decreased inhibition was seen at higher concentration. As a consequence, the derived AgNPs showed good anti-inflammatory effect. According to the authors, the as-synthesized NPs have potential to inhibit even at low concentration in comparison to commercial AgNPs and the plant extract alone, and also the IL-6 and IL-1β. This can be due to the various phytochemicals present in *Piper nigrum* extract and the synergistic anti-inflammatory activity of silver. The expression of IL-6 is inhibited by Piperine and the naturally synthesized AuNPs have shown excellent wound repair process and tissue regeneration in inflammatory function [63].

Esterase is an enzyme that breaks choline-based esters or neurotransmitters and known as cholinesterase or choline esterase. These

are basically two enzymes responsible for catalysing the hydrolysis of cholinergic neurotransmitters. Rajakumar and Abdul Rahuman have reported the anti-cholinesterase property of AgNPs, which was prepared from *Millettia pinnata* flower extract. The as-synthesized AgNPs showed increased efficiency towards ChF value of inhibitor concentration in comparison to flower extract and has an excellent inhibitory efficacy against butyrylcholinesterase and acetylcholinesterase. The plant leaf extract has a weaker inhibitory effect then AgNPs on both butyrylcholinesterase (BChE) and acetylcholinesterase (AChE). The IC_{50} values of NPs and extracts were compared, and the inhibition potency of these materials in AChE was nearly 2- and 8-fold higher than the BChE inhibition. So far, there is no clear explanation as to how the nanoparticles interact with ChE proteins. Moreover, so far there has been no clear explanation for the binding mechanism of the NPs with ChEs because of the hydrophobicity of the enzyme environment and the lipophilicity of NPs in ICE molecule [64].

18.3.5 Antileishmanial Agent

Leishmania has emerged as a new uncontrollable disease worldwide, which is known to be a major health problem causing the remarkable rate of mortality and morbidity in the America, Africa and Asia. It is caused by the protozoa of the genus *Leishmania* and could be classified as visceral, cutaneous and mucocutaneous type. More than 80 countries and approximately 12 million people around the world are affected by the disease. Around 0.5 and 1.5 million annual incidences of cutaneous and visceral leishmaniasis have been detected and around 3 million people are at risk worldwide. In recent times, the anti-leishmanial drugs have had various side effects and are also very expensive. In addition, the available anti-leishmanial therapies are now becoming resistant to the several *Leishmania* species. Therefore, it has become important to discover new therapeutic procedures, which are more effective, eco-friendly and cost-effective, so that they can be easily prescribed to the poor communities also, because they are mostly affected by this disease.

In this regard, Ahmed *et al.* have reported AgNPs synthesis from aqueous extract of *Isatis tinctoria* (herb) and tested it on the parasite [65]. It was found that synthesized AgNPs showed good anti-leishmanial activity. Furthermore, 96% inhibitory potential was display by NPs against the tested parasite in visible light irradiated samples. This discovery was found to be an economic and effective way to treat cutaneous leishmaniasis.

Ullah *et al.* studied the role of AgNPs prepared from leaf extract of *Fagonia indica* towards anti-leishmanial activities [66]. It was found that the growth of parasites is affected by the concentration of AgNPs. The growth rate decreases as the NPs concentration increases. Only 15% of the cells were able to survive in the leaf extract medium and 9% of cells survived in the AgNPs treatment at 200 μg/ml concentration in an MTT viability test. It was also found that cells exposed to AgNPs and leaf extracts have shown retardation in the percentage rate of 51.13% and 44.65% respectively. Ahmad *et al.* have synthesized Au and AgNPs via green synthesis approach using *Maytenus* extract and studied their anti-leishmanial activity. Au and Ag NPs coated with *Maytenus royleanus* extract show symbiotic antimicrobial effects and low concentration of NPs is useful to inhibit *Leishmania* very easily and effectively [67].

18.3.6 Antimicrobial and Antifungal

Microorganisms always try to develop resistance towards different antibiotics by acquiring new genes from other microbial strains or by mutating their existing genes. According to the report, "Antimicrobial Resistance: Global Report on Surveillance," published by the World Health Organization (WHO) in April 2014, worldwide, more than half a million people die each year from antibiotic-resistant bacterial infections. Therefore, there is a need to move towards a post-antibiotic era and fulfill the demand of naturally derived materials having antimicrobial properties or search for alternatives to antibiotics and chemical compounds. Various phytochemicals, which are present in herbal extracts, have an antimicrobial effect on the destruction of RNA, DNA, protein translocation and cell wall [68]. Nanoparticles are the new and promising invention of this century, which have antimicrobial activity. But, green NPs with lower toxicity are still underdeveloped at this stage. It has been known since ancient times that silver-based materials have high toxicity towards more than 16 species of microorganisms, including *Syphilis typhus*, *Staphylococcus aureus, Vibrio cholerae, Pseudomonas aeruginosa, Bacillus subtilis*, *Escherichia coli,* herpes simplex virus and hepatitis B virus. Silver ion (Ag^+) stops the growth of bacteria by supressing the respiratory enzymes and electron transporting unit by blocking the functioning of DNA [69]. By attaching silver ions to the cell surface of microorganism, the respiratory and permeability functions of the cell membrane becomes hampered. Silver closely interacts with the surface of the membrane and penetrates deep inside the bacterial cell; as a consequence, DNA loses its replicability and finally dies. Many

of the researchers' discoveries have shown that silver has lower antimicrobial activity against Gram-positive bacteria than Gram-negative bacteria, which mostly occurs due to the presence of beta-barrel proteins, called porins, and the thin peptidoglycan layer in their cell wall structure [70]. In addition, it is also known that AgNPs with high specific surface to volume ratio release Ag^{+}, which increases their interaction with microorganisms, improves the dissolution of silver ions and improves the biocidal effect. The antimicrobial activity of AgNPs mainly depends on temperature, pH, $AgNO_3$ concentration and microorganism type. The smaller size nanoparticles have larger surface area, which results in large bactericidal effects in comparison to larger particles. The nanoparticles antibacterial action is a little complicated, so the mechanism cannot be explained clearly. NPs can be categorized by two types of antimicrobial action: bactericidal action and inhibitory action. In bactericidal action, the bacterial cells die due to NPs activity, while bacterial cells division is only prevented without killing any cell is done in inhibitory action (Figure 18.4).

Based on these two kinds of actions, there are commonly three popular methods used to study the antibacterial properties of any material:

a. Disc diffusion method;
b. Minimum inhibitory concentration determination (MIC);
c. Minimum bactericidal concentration determination (MBC).

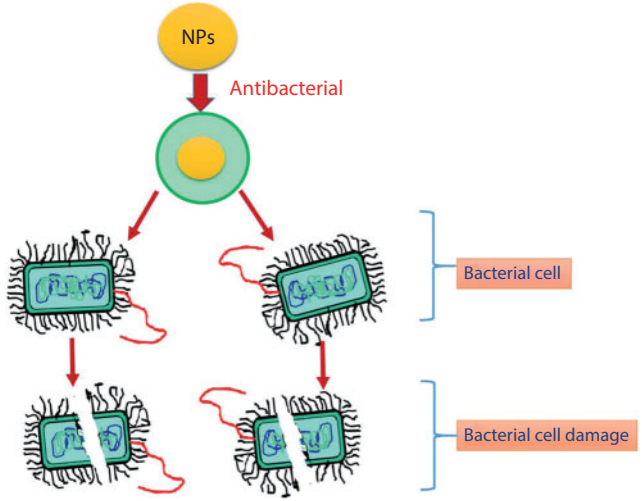


Figure 18.4 Schematic representation showing the killing of bacterial cell by nanoparticles.

18.3.6.1 Disc or Well Diffusion Method

Generally, the disc diffusion method is used to prove the antimicrobial action of the AgNPs. In this method, the nanoparticles are coated on the surface of suitable absorbent materials having uniform size and disc shape. During the study, the disc is placed over the surface of the targeted microbe and the antimicrobial action of AgNPs is reflected by the formation of an inhibition zone around the disc (Figure 18.5). In the well diffusion method, small disc-shaped pits are present instead of disc and the pits are formed on the surface of the agar plate for filling the test solution. In both processes, the plates are inoculated with microbes and are incubated under clean condition to obtain clear inhibition zone. The effect of AgNPs on the selected microbes can be easily visualized by the diameter of the inhibition zone around the well or disc. Gomathi *et al.* have reported the green synthesis of AgNPs using *Datura stramonium* leaf extract and determined

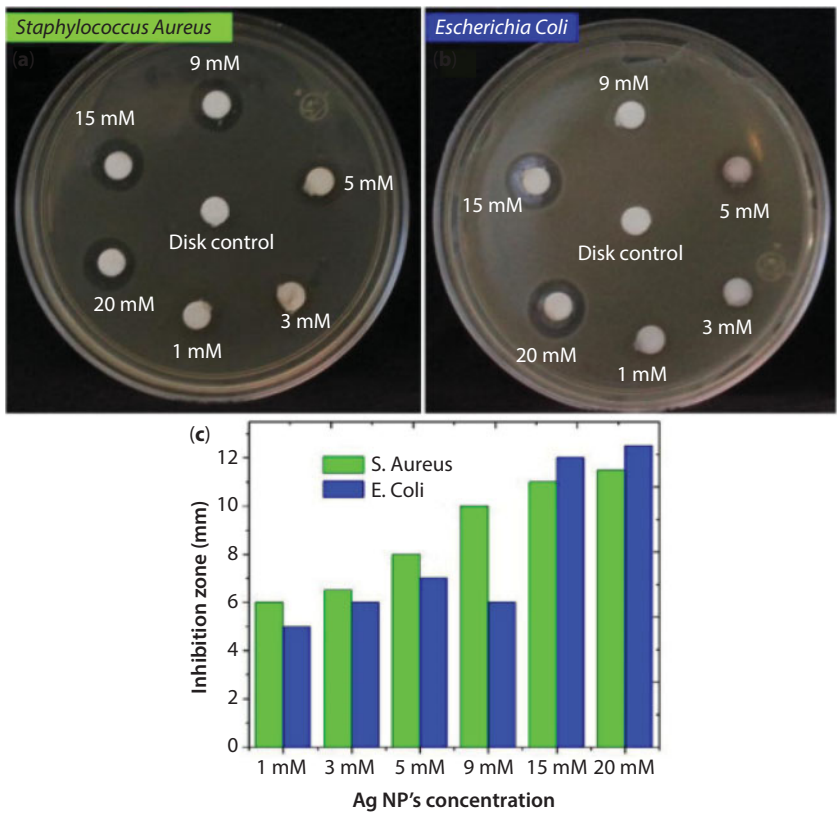


Figure 18.5 Antimicrobial activity of the AgNP's against (a) Staphylococcus aureus, (b) Escherichia coli and (c) Inhibition zone graph. (Reproduce with permission from [73]).

its antibacterial activity by well diffusion method against Gram-negative (*Escherichia coli*) and Gram-positive (*Staphylococcus aureus*) bacteria. As the dose of stack solution increases the antibacterial activity of the AgNPs also increases and better antibacterial activity of AgNPs was displayed against *E. coli* [71].

18.3.6.2 Minimum Inhibitory Concentration (MIC) or Minimum Bactericidal Concentration (MBC)

Minimum inhibitory concentration (MIC) is defined as the 100% visible growth of the targeted microbe after 24 hours incubation with minimum concentration of nanoparticle. MIC is determined by observing the growth of the bacteria in the culture tubes having equal amount of the bacterial culture with different concentrations of AgNPs. The minimum amount of AgNPs required to inhibit the growth of the bacteria is known as the MIC. The determination of MBC was done by using a fixed amount of AgNPs, which is usually higher than the MIC value. In the nutrient medium containing developing bacterial inoculum, AgNPs are added and the growth of bacteria is monitored using UV-Vis spectroscopy or plate analyzer in terms of change in the optical density of the samples. For MIC and MBC analysis, broth dilution tests are also used, in which the results are compared with the standard data after completion of the experiment. Khamhaengpol and Siri have reported the green synthesis of AgNPs by tissue extract of weaver ant larvae (*Oecophylla smaragdina*). The green synthesized AgNPs showed potential antibacterial activity against both *Staphylococcus aureus* and *Escherichia coli*. The MBC and MIC against both bacteria were found lowest in comparison to the other reported literature [72].

Ruíz-Baltazar *et al*. have synthesized AgNPs using a Melissa officinalis leaf and studied their antimicrobial properties against S. aureus and E. coli. The antibacterial activity was studied by disc diffusion method and MBC/MIC test. The corresponding results were shown in Figure 18.5 (a) and (b), respectively. It was found that all the AgNPs solutions of different concentrations (starting from 1 mM to 20mM) showed inhibitory effect. In addition, the Figure 18.5 (c) showed the comparative antibacterial activity of AgNPs towards S. aureus and E. coli. In both cases, these results obtained for inhibition zone confirmed the antibacterial properties of prepared AgNPs synthesized through green synthesis approach. El-Sherbiny *et al.* have reported the photoinduced green synthesis and antimicrobial assessment of poly(ε-caprolactone)/curcumin/grape leaf extract-Ag hybrid nanoparticles (PCL/Cur/GLE-AgNPs). High bactericidal effect was observed in bacterial strains incubated with high concentration of PCL/

Cur/GLE-Ag hybrid NPs in comparison to GLE, GLE/AgNPs and PCL/Cur/GLE plain NPs. The high surface area of PCL/Cur/GLE-Ag hybrid NPs allow them to make direct contact with bacterial cells and free radicals generated from AgNPs which are responsible for damaging bacterial cell membrane [74].

Pethakamsetty *et al.* have reported the green synthesis of AgNPs from silver acetate using methanolic root extracts of *Diospyros sylvatica* (member of the Ebenaceae family) as reducing agent. The as-synthesized AgNPs showed mild activity against *Proteus vulgaris* and *Streptococcus pyogenes,* while moderate activity towards *Escherichia coli, Staphylococcus aureus* and *Klebsiella pneumoniae*. However, maximum activity was observed against *Bacillus subtilis*, *Bacillus pumilis* and *Pseudomonas aeuriginosa* [75]. It was reported by the authors that synthesized AgNPs provide better contact with the microorganism because of their extremely large surface area. Manikandan *et al.* have reported eco-friendly synthesis of palladium NPs from *Prunus x yedoensis* tree leaf extract. The effect of control penicillin and PdNPs was studied on Gram-negative and Gram-positive bacteria and found remarkable activity towards both bacterial strains [76].

18.3.7 As Antioxidant

In general terms, a molecule that obstructs the oxidation of other molecules is known as an antioxidant,. Free radicals are responsible for many pathological conditions, varying from cancer to aging, diabetes, atherosclerosis, Alzheimer's and cardiovascular disease. Therefore, the discovery of green synthesized NPs for the treatment of many free-radical-associated medical conditions, along with further investigation of their properties, can be used in medical applications. In the past few years, various researchers have been engaged in searching for the *in-vitro* free radical scavenging potential of green NPs and their role in the treatment of many pathophysiological states. The intake of antioxidant provides protection from damage caused by free radicals [77]. Markus *et al.* have reported the use probiotic *Lactobacillus kimchicus* (DCY51T) isolated from Korean kimchi for the synthesis of AuNPs through an intracellular membrane-bound mechanism. The NPs was used against DPPH (2,2-diphenyl-1-picrylhydrazyl), which is rarely reduced by accepting electron or hydrogen from NPs, because it is composed of very stable free radical. Researchers observed that the scavenging activity of AuNPs is dose dependent and was found to be a little higher than that observed with corresponding precursor salts. The scavenging capability was increased with increase in concentration [78].

Kumar *et al.* have reported the use of Lavender (*Lavandula angustifolia*) as a reducing and stabilizing agent for the synthesis of AuNPs and showed its antioxidant property. The antioxidant activity was determined by comparing the % inhibition of DPPH using AuNPs and Lavender leaf extract (LLE). Better DPPH quenching activity at lower concentration was observed for AuNPs in comparison to LLE. The DPPH scavenging activity of AuNPs decrease with increase in concentration, whereas an opposite trend was shown by LLE, owing to AuNPs being less soluble [79]. Patra and Baek used watermelon rind as a fruit waste for the synthesis of AuNPs, which showed high synergistic activity in combination with the standard antibiotics, i.e., rifampicin and kanamycin. The antioxidant potential of synthesized AuNPs may be attributed to the presence of citrulline, lycopene, vitamins and a variety of phenolic compounds, which are the major constituents of watermelon rind [80]. Gomaa reported the green synthesis of AgNPs via onion (*Allium cepa*) extract and found that the synthesized NPs have antioxidant potential. The author used three methods to study the antioxidant activity of as-synthesized NPs because the excellent antioxidant property cannot be determined by a single method. These methods are:

a. Potassium ferricyanide reduction method: which acts as indicator of potential antioxidant activity;
b. Phosphomolybdenum method: which determines the total antioxidant capacity based on the reduction of Mo(VI) to Mo(V) by the antioxidant compound and formation of a green phosphate/Mo(V) complex;
c. DPPH scavenging capacity test: a very popular method to test antioxidant activity, owing to its speed, simplicity and stable radical formation strategy.

Based on the above tests, the results show that NPs have high antioxidant activity, which increases with an increase in the concentration [81].

18.3.8 Wound Healing

Wound healing is a natural response to tissue injury and is accomplished by a complex cascade of cellular events and biochemicals that generate restoration, resurfacing and reformation of the injured skin. The whole process includes four phases: inflammation, proliferation, maturation and hemostasis, which finally results in scar. For wound healing fibrin production is very important and is also the primary component of the wound matrix

into which plasma proteins and cells migrate. During the first 2–4 days of healing (inflammatory phase), macrophages and neutrophils (inflammatory cells) remove injured tissue and protect the skin from infection and release mitogenic and chemotactic factors [82]. During the proliferative phase, for the production of collagen the fibroblasts from the surrounding tissue begin to proliferate onto the fibrin matrix, which is a deciding event during skin reformation along with epithelialization, angiogenesis and proliferative phase. The newly formed collagen molecules crosslink with already present collagen and protein molecules in the final step of the maturation phase, which increases the tensile strength of the scar. By the end of the second week, the maturation phase begins the healing process, which may continue for an unknown period of time [83]. For centuries, silver has been known as a cure for a variety of diseases and has been used for procedures such as cauterization of skin wounds, pleurodesis, etc.

Naraginti *et al.* have reported green synthesized Au and Ag NPs from *Coleus forskohlii* and tried it for ameliorating full thickness excision wounds in albino Wistar male rats. After incorporation of NPs, the macroscopic changes appeared in the wound, which was monitored by varying the size of cutaneous excision. Through a wound scoring system, the changes were visually determined, which help in scoring the degree of inflammation and wound closure rate (WCR). No adverse effect on bodyweight, behavior or general health of rats was observed by topical treatment of these NPs. After three days of post-wounding, the least healing was observed in the control group. Figure 18.6 photographically represents wound healing with different treatments; G1 (Control), G2 (Standard drug), G3 (Silver nanoparticles) and G4 (Gold nanoparticles) after 0, 3, 6, 9 and 14 days post-wounding. The WCR was observed to be 5% for control (G1), 19% for SD (G2), 28% for AgNPs (G3), and 36% for AuNPs (G4) treated groups, 3 days after wounding. The closest apposition of the wound edges was evaluated as the best healing that can be seen clearly in the AuNPs treated group. After 14 days of post-wounding, G1 showed partial healing with 51% WCR, followed by G3 with 96%, G2 with 88% WCR and G4 with 100%. In this experiment, the wounds treated with formulated Au and Ag NPs healed faster than G2 and those of the control group, which reveals that the topical application of formulated Ag and Au NPs exhibited accelerated rate of wound healing [84].

18.3.9 Drug Delivery and Hemolytic Activity

Many of the clinically used drugs for the treatment of cancer are compounds with low molecular weight which diffuse very fast into healthy tissues, as

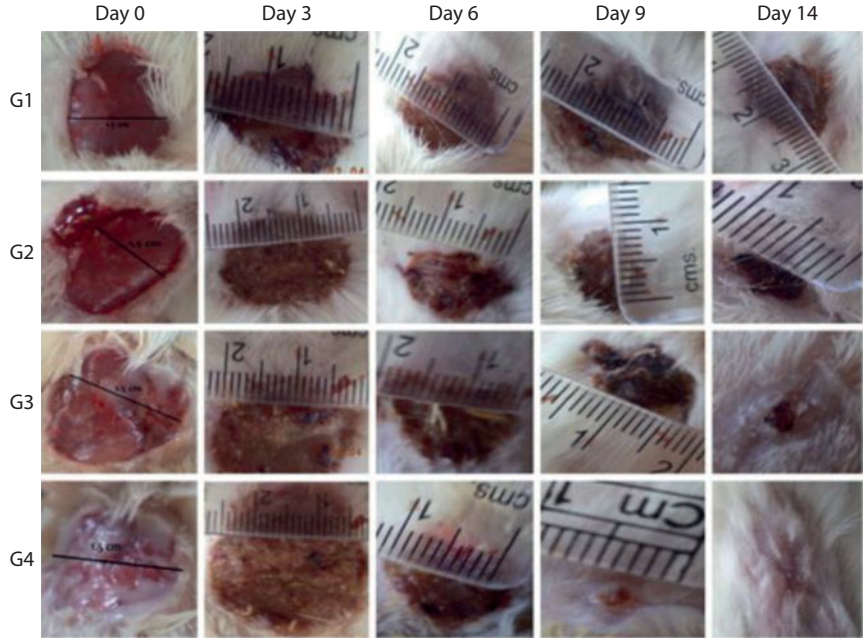


Figure 18.6 Image representation of the wound healing process in control (G1), standard drug (G2), Silver nanoparticle (G3) and Gold nanoparticle (G4) treated groups at 0, 3, 6, 9 and 14 days post wounding. (Reproduced with permission from [84]).

the tissues are evenly distributed in the body, and display a small life span in the bloodstream. As a result, a very small amount of drug reaches the targeted site, and its distribution causes side effects in healthy tissue. To solve this problem, researchers have used NPs for targeting cancer cell/tissue to improve the drugs biodistribution.

Kumar *et al.* have reported the green synthesis of AuNPs by using *Zingiber officinale* extract and reported its application as a biosensor and in gene and drug delivery. The basic need of biogenically synthesized nanomaterials must be biocompatibility and it should not produce any toxic effect. The biocompatibility is mainly related with the surface of the particle size and can be resolute based on the adversative host reaction concentration [85]. From the results, it is clear that AuNPs have no hemolytic properties against red blood cells at different concentrations. Furthermore, it is known that AuNPs are nontoxic in nature, stable, inert and have high binding capability, which is why gold nanoparticles are used for anticancer drug carrier.

Surendra *et al.* have reported the synthesis of *Moringa oleifera* capped palladium NPs by using *M. oleifera* peel extract. The green synthesized

M. oleifera capped PdNPs have been used by the authors for testing the toxicity on RBC. The result showed that *M. oleifera* capped PdNPs are not toxic to RBC because they do not participate in the RBC cell cutting in the cell permeability [86].

18.3.10 Antidiabetic and Cytotoxic

Nowadays, diabetes is the most common metabolic disease worldwide. It mostly occurs due to a loss of glucose homeostasis with instability in fat metabolism, carbohydrate and protein resulting in disturbance in the action and secretion of insulin. Adipose tissue, skeletal muscle and the liver are not able to use and take up glucose from blood circulation when improper secretion of insulin takes place inside the body, resulting in increased glucose level in the body, which is known as hyperglycemia [87]. Daisy and Saipriya have reported the synthesis of AuNPs from *Cassia fistula* stem bark. They studied the effect of as-synthesized NPs on streptozotocin-induced diabetes and found that continuous administration of aqueous extract of AuNPs for four weeks results in remarkable reduction in the blood glucose level. According to the literature, for the treatment of diabetes mellitus and their other associated complications, the green synthesized AuNPs can act as a better hypoglycemic agent [88]. Another group has reported the *in-vitro* antidiabetic activity of AgNPs derived from *Halymenia poryphyroides,* a marine red alga. It was found in the study that the activity of α-glucosidase and α-amylase enzymes can be inhibited by the synthesized green AgNPs [89].

Kumar *et al.* have reported the green synthesis of AuNPs from *Cassia auriculata* aqueous leaf extract. The authors successfully investigated the antidiabetic activity of synthesized AuNPs derived from medicinal plants [90]. The effect of AuNPs concentration was studied against cancer cells. The cancer cells incubated with the green synthesized AuNPs from aqueous extract of the red alga *Corallina officinalis* for two days had rounded and clumped dead cells. The plasma membrane had an inflated balloon-like appearance on its rupture site, which could be caused by necrosis. By the implementation of green synthesized AuNPs around 50% of the cells died [91]. The cytotoxicity has a direct relationship to the concentrations of synthesized AuNPs, which indicated that the activity and the cell growth have been stopped while using the lower concentration of AuNPs. The nanomaterials also showed anti-leishmanial activity. Different scientists used different plant extracts and found them to be active. Even at a very low amount of concentrations, they showed significant activity. The reactive oxygen species (ROS) were created by noble metal NPs to kill

microorganisms by a very simple method called respiratory burst mechanism. Macrophages are the distinctive resistant cells of human existence that can produce high concentrations of ROS to extinguish pathogens that enter cells. The leishmanial organisms are capable of preventing some enzymes of ROS from creating a path in macrophages and can live in the resistant cells. The uses of AuNPs as leishmanicidal mediator will act as a great reservoir of Au ions that will afford a nano enzymatic foundation of ROS and extinguish the entered organisms. The reactions between electrons generated by AuNPs and O_2 at the surface of nanoparticles-generated ROS (O_2, eOH), the radicals generated during the reaction are responsible for destroying DNA and other cellular parts of the species and finally lead to death.

Jeyaraj *et al.* reported the green synthesis of AgNPs by leaf extract of *Podophyllum hexandrum* and determined its caspase-mediated apoptotic effect and cytotoxicity on human cervical carcinoma cells via MTT assay, analysis of western blotting technique, reverse transcription polymerase chain reaction (RT-PCR) and reactive oxygen species (ROS) methods. In the inner apoptotic pathway, ROS create imbalance in mitochondria by moderating the expression. The authors also reported high antibacterial activity of the proposed AgNPs in comparison to anticancer drug (cisplatin). The report emphasizes eco-friendly, low-cost and single-step AgNPs synthesis and its application in cancer diagnosis, drug delivery and cancer treatment [92]. In addition to the above-mentioned biomedical applications of noble metal nanoparticles, some recent work has also been included in this chapter and displayed in Table 18.1.

18.4 Conclusions and Future Directions

Nanotechnology is one of the new fields in science and its best invention is the nanoparticles, which are used for multifunctional applications such as drug delivery, detection of heavy metal, sensing, degradation of water-soluble organic pollutant, wound healing, cosmetics, etc. Plant extracts help in the synthesis of nanoparticles and phenolic compounds act as reducing agent to stabilize the zero-valent metal. The reduced form of metals is highly reactive and used in various fields such as biology, electrochemistry and photochemistry. The activities of NPs mainly depend on the surface area and particles size. The small sized and highly dispersed NPs have various biomedical applications, especially for use in cancer treatment. The NPs synthesized by green method show good activity against Gram-positive and Gram-negative bacteria. Noble metal nanoparticles are used against several types of parasitic

Table 18.1 Biomedical properties of noble metal nanoparticles synthesized via green synthesis.

S. No.	NPs	Reducing agents	Biological activity	Ref.
1.	Ag	Aloe vera	Antibacterial	[93]
2.	Ag	*Abutilon indicum*	Antibacterial	[94]
3.	Ag	*Pistacia atlantica*	Antibacterial	[95]
4.	Ag	*Garcinia mangostana* leaves	Antibacterial, Antioxidant	[96]
5.	Ag	*Tinospora cordifolia* stem	Antibacterial, Antioxidant	[97]
6.	Ag	*Viburnum lantana* leaves	Antibacterial, Antifungal	[98]
7.	Ag	*Ziziphora tenuior* leaf	Antimicrobial	[99]
8.	Ag	*Coleus aromaticus* leaf	Bactericidal, Wound healing	[100]
9.	Ag	*Lantana camara*	Antibacterial	[101]
10.	Ag	*Elettaria cardamom*	Antibacterial	[102]
11.	Ag	*Hibiscus rosa-sinensis* petals	Antimicrobial	[103]
12.	Ag	*Solanum indicum* L.	Antibacterial, Cytotoxicity	[104]
13.	Ag	*Pongamia pinnata*	Antibacterial	[105]
14.	Ag	*Cinnamomum zeylanicum* bark	Antioxidant	[106]
15.	Ag	*Azadirachta indica*	Antimicrobial	[107]
16.	Ag	*Urtica dioica* Linn.	Antibiotic	[108]
17.	Ag	*Emblica officinalis* fruit	Antibacterial	[109]
18.	Ag	*Gnetum bucholzianum*	Antimicrobial	[110]
19.	Au	*Couroupita guianensis*	Anticancer	[111]
20.	Ag	*Morinda citrifolia* root	Cytotoxicity	[39]
21.	Au	*L. montevidensis*	Anticancer	[42]
22.	Au	*P. hexandrum*	Anticancer	[112]
23.	Ag	*Cleistanthus collinus*	Antioxidant, Cytotoxicity	[113]
24.	Ag	*Ficus religiosa*	Antitumer	[114]
25.	Ag	*Melia azedarach*	Cytotoxicity	[115]
26.	Ag	*Albizia adianthifolia* leaf	Cytotoxicity	[116]

(*Continued*)

Table 18.1 Cont.

S. No.	NPs	Reducing agents	Biological activity	Ref.
27.	Ag	*Erythrina indica* Lam.	Antibacterial, Cytotoxicity	[117]
28.	Au	*Vites vinefera*	Cytotoxicity	[118]
29.	Ag	*Trachyspermum ammi*	Biological applications	[119]
30.	Au	*Mangifera indica*	Biological applications	[120]
31.	Ag	*Plectranthus amboinicus*	Antimicrobial	[121]
32.	Ag	*Phyllanthus emblica*	Antiproliferative effect	[122]
33.	Ag	*Sacha inchi* leaf	Medical applications	[123]
34.	Ag	*Hibiscus subdariffa*	Antidiabetic, Antibacterial	[124]
35.	Au, Ag	*Prunus armeniaca*	Antioxidant	[125]
36.	Au	*Curcuma pseudomontana*	Cytotoxicity	[126]
37.	Au	*Geranium*	Biological applications	[127]
38.	Au	*Solanum nigrum*	Antioxidant, Antibacterial	[128]
39.	Au, Ag	Krishna Tulsi	Biological applications	[129]
40.	Au, Ag	*S. torvum*	Antioxidant, Antibacterial	[130]
41.	Ag	*Citrus sinensis*	Antioxidant, Antimicrobial	[131]
42.	Ag	*S. cumini*	Anticancer, Antioxidant	[132]
43.	Pd	*Terminalia chebula*	Biological applications	[133]
44.	Au	*Piper longum*	Antioxidant, Cytotoxicity, Antibacterial	[134]
45.	Au	*Stachys lavanduli Folia Vahl*	Medical applications	[135]
46.	Au, Ag	*Murraya koenigii*	Biological applications	[136]
47.	Au	Maple leaf and pine needle	Tumor therapy	[137]
48.	Au	*Magnolia kobus*, *Diopyros kaki*	Biological applications	[138]
49.	Au	*Hovenia dulcis*	Biological activities	[139]
50.	Au	*Ocimum basilicum*	Antidiabetic, Antimicrobial	[140]

infections like leishmaniasis. Green synthesis is one of the best environment friendly methods for the synthesis of noble metal nanoparticles.

In the present chapter, we studied the green synthesis of nanoparticles and their applications in medicine. We found that the synthesized noble metal nanoparticles are one of the cheapest and easiest methods to synthesize the required nanoparticles. Based on the above compilation and studies we strongly recommend the green chemistry approach for the synthesis of nanoparticles. The eco-friendly synthesis of metallic NPs using green precursors will help researchers in developing nontoxic nanomaterials and also provide a better understanding of the safety and health issues regarding NPs. In addition to the existing green approaches, researchers are also pursuing various other eco-friendly capping agents derived from plant waste, which can be used for the dual purpose of reducing/chelating agent as well as capping agent in the green synthesis of NPs. Using the combination of such natural and multifunctional agents, the resulting NPs will be free from aggregation and further reactions, due to which their longevity and stability could be increased to a large extent. In addition, some new techniques must also be developed which can take the green synthesis approach from laboratory- to industrial-scale synthesis of NPs.

Acknowledgment

Ms. Karfa has given the major contribution in writing this book chapter along with drawing the Figures and Tables, taking the copy right permission etc.

References

1. Donaldson, K., Stone, V., Nanoscience fact versus fiction. *Commun. ACM*, 47, 113–115, 2004.
2. Masciangioli, T., Zhang, W., Environmental nanotechnology: Potential and pitfalls. *Environ. Sci. Technol.*, 37, 102–108, 2003.
3. Future Technologies, Today's Choices, Greenpeace, UK, 2003. http://www.greenpeace.ork.uk/contentlookup.cfm?ucidparam=2003072113521&menupoint=%5CA-L.
4. Mittal, A.K., Chisti, Y., Banerjee, U.C., Synthesis of metallic nanoparticles using plant extracts. *Biotechnol. Adv*., 31, 346–356, 2013.
5. Treguer, M., de Cointet, C., Remita, H., Khatouri, J., Mostafavi, M., Amblard, J., Belloni, J., de Keyzer, R., Dose rate effects on radiolytic synthesis of gold-silver bimetallic clusters in solution. *J. Phys. Chem. B*, 102, 4310–4321, 1998.

6. Shubin, Y., Plyusnin, P., Sharafutdinov, M., *In situ* synchrotron study of Au-Pd nanoporous alloy formation by single-source precursor thermolysis. *Nanotechnology*, 23, 405302–405307, 2012.
7. Tsai, S.C., Song, Y.L., Tsai, C.S., Yang, C.C., Chiu, W.Y., Lin, H.M., Ultrasonic spray pyrolysis for nanoparticles synthesis. *J. Mater. Sci.*, 39, 3647–3657, 2004.
8. Li, Y., Duan, X., Qian, Y., Yang, L., Liao, H., Nanocrystalline silver particles: Synthesis, agglomeration, and sputtering induced by electron beam. *J. Colloid Interface Sci.*, 209, 347–349, 1999.
9. Thakkar, K.N., Mhatre, S.S., Parikh, R.Y., Biological synthesis of metallic nanoparticles. *Nanomedicine*, 6, 257–262, 2010.
10. Xiong, Y., Chen, J., Wiley, B., Xia, Y., Aloni, S., Yin, Y., Understanding the role of oxidative etching in the polyol synthesis of Pd nanoparticles with uniform shape and size. *J. Am. Chem. Soc.*, 127, 7332–7333, 2005.
11. Mizukoshi, Y., Sato, K., Konno, T.J., Masahashi, N., Dependence of photocatalytic activities upon the structures of Au/Pd bimetallic nanoparticles immobilized on TiO_2 surface. *Appl. Catal. B*, 94, 248–253, 2010.
12. Nemamcha, A., Rehspringer, J.L., Khatmi, D., Synthesis of palladium nanoparticles by sonochemical reduction of palladium(II) nitrate in aqueous solution. *J. Phys. Chem. B*, 110, 383–387, 2006.
13. Yang, F., Cheng, K., Wu, T., Zhang, Y., Yin, J., Wang, G., Cao, D., Au-Pd nanoparticles supported on carbon fiber cloth as the electrocatalyst for H_2O_2 electroreduction in acid medium. *J. Power Sources*, 233, 252–258, 2013.
14. Pritchard, J., Kesavan, L., Piccinini, M., He, Q., Tiruvalam, R., Dimitratos, N., Lopez-Sanchez, J.A., Carley, A.F., Edwards, J.K., Kiely, C.J., Hutchings, G.J., Direct synthesis of hydrogen peroxide and benzyl alcohol oxidation using Au-Pd catalysts prepared by sol immobilization. *Langmuir*, 26, 16568–16577, 2010.
15. Melchert, W.R., Reis, B.F., Rocha, F.R., Green chemistry and the evolution of flow analysis. A review. *Anal. Chim. Acta*, 714, 8–19, 2012.
16. Patra, S., Mukherjee, S., Barui, A.K., Ganguly, A., Sreedhar, B., Patra, C.R., Green synthesis, characterization of gold and silver nanoparticles and their potential application for cancer therapeutics. *Mater. Sci. Eng. C*, 53, 298–309, 2015.
17. Grier, N., Silver and its compounds, in: *Disinfection, Sterilization and Preservation*, Block, S.S. (Ed.), pp. 375–398, Lee and Febiger: Philadelphia, 1968.
18. Hill, W.R., Pillsbury, D.M., Argyria—The Pharmacology of Silver, Williams and Williams: Baltimore, 1939.
19. Galib, B.M., Mashru, M., Jagtap, C., Patgiri, B.J., Prajapati, P.K., Therapeutic potentials of metals in ancient India: A review through Charaka Samhita. *J Ayurveda Integr. Med.*, 2, 55–63, 2011.
20. Sharma. V.K., Yngard, R.A., Lin, Y., Silver nanoparticles: Green synthesis and their antimicrobial activities. *Adv. Colloid Interface Sci.*, 145, 83–96, 2009.

21. Nair, R., Varghese, S.H., Nair. B.G., Maekawa. T., Yoshida, Y., Sakthi Kumar, D., Nanoparticulate material delivery to plants. *Plant Science*, 179, 154–163, 2010.
22. Dankovich, T.A., Gray, D.G., Bactericidal paper impregnated with silver nanoparticles for point-of-use water treatment. *Environ. Sci. Technol.*, 45, 1992–1998, 2011.
23. Prow, T.W., Grice, J.E., Lin, L.L., Faye, R., Butler, M., Becker, W., Wurm, E.M.T., Yoong, C., Robertson, T.A., Soyer, H.P., Roberts, M.S., Nanoparticles and microparticles for skin drug delivery. *Adv. Drug Delivery Rev.*, 63, 470–491, 2011.
24. Chaloupka, K., Malam, Y., Seifalian, A.M., Nanosilver as a new generation of nanoproduct in biomedical applications. *Trends Bioethanol*, 28, 580–588, 2010.
25. Park, K., Seo, D., Lee, J., Conductivity of silver paste prepared from nanoparticles. *Colloids Surf. A*, 313, 351, 2008.
26. Seralathan, J., Stevenson, P., Subramaniam, S., Raghavan, R., Pemaiah, B., Sivasubramanian, A., Veerappan, A., Spectroscopy investigation on chemocatalytic, free radical scavenging and bactericidal properties of biogenic silver nanoparticles synthesized using *Salicornia brachiata* aqueous extract. *Spectrochim. Acta A*, 118, 349–355, 2014.
27. Netala, V.R., Kotakadi, V.S., Nagam, V., Bobbu, P., Ghosh, S.B., Tartte, V., First report of biomimetic synthesis of silver nanoparticles using aqueous callus extract of *Centella asiatica* and their antimicriobial activity. *Appl. Nanosci.*, 5, 801–807, 2015.
28. Mallikarjuna, K., Sushma, N.J., Subba Reddy, B.V., Narasimha, G., Deva Prasad Raju, B., Palladium nanoparticles: Single-step plant mediated green chemical procedure using *Piper betle* leaves broth and their anti-fungal studies. *Int. J. Chem. Anal. Sci.*, 4, 14–18, 2013.
29. Marambio-Jones, C., Hoek, E.M.V., A review of the antibacterial effects of silver nanomaterials and potential implications for human health and the environment. *J. Nanopart. Res.*, 12, 1531–1551, 2010.
30. He, Y., Du, Z.Y., Lv, H.B., Jia, Q.F., Tang, Z.K., Zheng, X., Zhang, K., Zhao, F.H., Green synthesis of silver nanoparticles by *Chrysanthemum morifolium* Ramat. extract and their application in clinical ultrasound gel. *Int. J. Nanomed.*, 8, 1809–1815, 2013.
31. Venkatpurwar, V., Shiras, A., Pokharkar, V., Porphyran capped gold nanoparticles as a novel carrier for delivery of anticancer drug: *In vitro* cytotoxicity study. *Int. J. Pharm.*, 409, 314–320, 2011.
32. Patra, C.R., Bhattacharya, R., Mukhopadhyay, D., Mukherjee, P., Fabrication of gold nanoparticles for targeted therapy in pancreatic cancer. *Adv. Drug Delivery Rev.*, 62, 346–361, 2010.
33. Alanazi, F.K., Radwan, A.A., Alsarra, I.A., Biopharmaceutical applications of nanogold. *Saudi Pharm. J.*, 18, 179–193, 2010.
34. Pankhurst, Q.A., Thanh, N.T.K., Jones, S.K., Dobson, J., Progress in applications of magnetic nanoparticles in biomedicine. *J. Phys. D: Appl. Phys.*, 42, 224001–224007, 2009.

35. Jemal, A., Siegel, R., Xu, J., Ward, E., Cancer statistics, 2010, *CA Cancer J. Clin.*, 60, 277–300, 2010.
36. Ponder, B.A.J., Cancer genetics. *Nature*, 411, 336–341, 2001.
37. Hanahan, D., Weinberg, R.A., The hallmarks of cancer. *Cell*, 100, 57–70, 2000.
38. Balmain, A., Gray, J., Ponder, B., The genetics and genomics of cancer. *Nature Genetics*, 33, 238–244, 2003.
39. Suman, T.Y., Radhika Rajasree, S.R., Kanchana, A., Elizabeth, S.B. Biosynthesis, characterization and cytotoxic effect of plant mediated silver nanoparticles using *Morinda citrifolia* root extract. *Colloids Surf. B*, 106, 74–78, 2013.
40. Karuppaiya, P., Satheeshkumar, E., Chao, W.T., Kao, L.Y., Chen, E.F., Tsay, H.S., Anti-metastatic activity of biologically synthesized gold nanoparticles on human fibrosarcoma cell line HT-1080. *Colloids Surf. B*, 110, 163–170, 2013.
41. Firdhouse, M.J., Lalitha, P., Biosynthesis of silver nanoparticles using the extract of *Alternanthera sessilis* antiproliferative effect against prostate cancer cells. *Cancer Nanotechnol.*, 4, 137–143, 2013.
42. Mukherjee, S., Dasari, M., Priyamvada, S., Kotcherlakota, R., Bollu, V.S., Patra, C.R., A green chemistry approach for the synthesis of gold nanoconjugates that induce the inhibition of cancer cell proliferation through induction of oxidative stress and their *in vivo* toxicity study. *J. Mater. Chem. B*, 3, 3820–3830, 2015.
43. Conde, J., Doria, G., Baptista, P., Noble Metal Nanoparticles Applications in Cancer. *J. Drug Delivery*, Article ID 751075, 12 pages, 2012.
44. Muthukumar, T., Sudhakumari, Sambandam, B., Aravinthan, A., Sastry, T.P., Kim, J.-H., Green synthesis of gold nanoparticles and their enhanced synergistic antitumor activity using HepG2 and MCF7 cells and its antibacterial effects. *Process Biochem.*, 51, 384–391, 2016.
45. Narayanan, S., Sathy, B.N., Mony, U., Koyakutty, M., Nair, S.V., Menon, D. Biocompatible magnetite/gold nanohybrid contrast agents via green chemistry for MRI and CT bioimaging. *ACS Appl. Mater. Interfaces*, 4, 251–60, 2012.
46. Menon, D., Basanth, A., Retnakumari, A., Manzoor, K., Nair, S.V. Green synthesis of biocompatible gold nanocrystals with tunable surface plasmon resonance using garlic phytochemicals. *J. Biomed. Nanotechnol.*, 8, 901–911, 2012.
47. Shukla, R., Nune, S.K., Chanda, N., Katti, K., Mekapothula, S., Kulkarni, R.R., Welshons, W.V., Kannan, R., Katti, K.V. Soybeans as a phytochemical reservoir for the production and stabilization of biocompatible gold nanoparticles. *Small*, 4, 1425–36, 2008.
48. Nune, S.K., Chanda, N., Shukla, R., Katti, K., Kulkarni, R.R., Thilakavathi, S., Mekapothula, S., Kannan, R., Katti, K.V. Green nanotechnology from tea: Phytochemicals in tea as building blocks for production of biocompatible gold nanoparticles. *J. Mater. Chem.*, 19, 2912–2920, 2009.

49. Shankar, S.S., Rai, A., Ankamwar, B., Singh, A., Ahmad, A., Sastry, M., Biological synthesis of triangular gold nanoprisms. *Nat. Mater.*, 3, 482–488, 2004.
50. Fazal, S., Jayasree, A., Sasidharan, S., Koyakutty, M., Nair, S.V., Menon, D., Green synthesis of anisotropic gold nanoparticles for photothermal therapy of cancer. *ACS Appl. Mater. Interfaces*, 6, 8080–8089, 2014.
51. Hoshyar, R., Khayati, G.R., Poorgholami, M., Kaykhaii, M., A novel green one-step synthesis of gold nanoparticles using crocin and their anti-cancer activities. *J. Photochem. Photobiol. B*, 159, 237–242, 2016.
52. González-Ballesteros, N., Prado-López S., Rodríguez-González, J.B., Lastra, M., Rodríguez-Argüelles, M.C., Green synthesis of gold nanoparticles using brown algae *Cystoseira baccata*: Its activity in colon cancer cells. *Colloids Surf. B*, 153, 190–198, 2017.
53. Mukherjee. P., Bhattacharya, R., Bone, N., Lee, Y.K., Patra, C.R., Wang. S., Lu, L., Secreto, C., Banerjee, P.C., Yaszemski, M.J., Kay, N.E., Mukhopadhyay, D., Potential therapeutic application of gold nanoparticles in B-chronic lymphocytic leukemia (BCLL): Enhancing apoptosis. *J. Nanobiotechnol.*, 5, 4, 2007.
54. Li, Y., Wang, H., Zhang, R., Zhang, G., Yang, Y., Liu, Z., Biofabrication of polyphenols coated Nano palladium and its *in-vitro* cytotoxicity against human leukemia cell lines (K562). *J. Photochem. Photobiol. B,* 175, 173–177, 2017.
55. Mondal, D.B., Sarma, K., Saravanan, M., Upcoming of the integrated tick control program of ruminants with special emphasis on livestock farming system in India. *Ticks Tick Borne Dis.,* 4, 1–10, 2013.
56. Rajakumar, G., Abdul Rahuman, A., Acaricidal activity of aqueous extract and synthesized silver nanoparticles from *Manilkara zapota* against *Rhipicephalus (Boophilus) microplus*. *Res. Vet. Sci.,* 93, 303–309, 2012.
57. Avinash, B., Venu**,** R., Raj, M.A., Rao, K.S., Srilatha, C., Prasad, T.N., *In vitro* evaluation of acaricidal activity of novel green silver nanoparticles against deltamethrin resistance *Rhipicephalus* (*Boophilus*) *microplus*. *Vet. Parasitol.*, 237, 130–136, 2017.
58. Mansouri, J., Harrisson, S., Chen, V., Strategies for controlling biofouling in membrane filtration systems: Challenges and opportunities. *J. Mater. Chem.*, 20, 4567–4586, 2010.
59. Krupa, A.N.D., Raghavan, V., Biosynthesis of silver nanoparticles using *Aegle marmelos* (Bael) fruit extract and its application to prevent adhesion of bacteria: A strategy to control microfouling. *Bioinorg. Chem. Appl.*, 949538, 8, 2014.
60. Soroush, A., Ma, W., Silvino, Y., Rahaman, M.S., Surface modification of thin film composite forward osmosis membrane by silver-decorated graphene-oxide nanosheets. *Environ. Sci. Nano*, 2, 395–405, 2015.
61. Vijayan, S.R., Santhiyagu, P., Singamuthu, M., Ahila, N.K., Jayaraman, R., Ethiraj, K., Synthesis and characterization of silver and gold nanoparticles

using aqueous extract of seaweed, *Turbinaria conoides*, and their antimicrofouling activity. *Sci. World J.*, 1–11, 2014.
62. Recio, M.C., Andujar, I, Rios, J.L., Anti-inflammatory agents from plants: Progress and potential. *Curr. Med. Chem.*, 19, 2088–2103, 2012.
63. Aparna Mani, K.M., Seethalakshmi, S., Gopal, V., Evaluation of *in-vitro* anti-inflammatory activity of silver nanoparticles synthesised using *Piper nigrum* extract. *J. Nanomed. Nanotechnol.*, 6, 268–275, 2015.
64. Rajakumar, G., Gomathi, T., Thiruvengadam, M., Rajeswari, V.D., Kalpana, V.N., Chung, I.-M., Evaluation of anti-cholinesterase, antibacterial and cytotoxic activities of green synthesized silver nanoparticles using from *Millettia pinnata* flower extract. *Microb. Pathog.*, 103,123–128, 2017.
65. Ahmad, A., Wei, Y., Syed, F., Khan, S., Khan, G. M., Tahir, K., Khan, A.U., Raza, M., Khan, F.U., Yuan, Q., *Isatis tinctoria* mediated synthesis of amphotericin B-bound silver nanoparticles with enhanced photoinduced antileishmanial activity: A novel green approach. *J. Photochem. Photobiol. B*, 161, 17–24, 2016.
66. Ullah, I., Shinwari, Z.K., Khalil A.T., Investigation of the cytotoxic and antileishmanial effects of *Fagonia indica* l. extract and extract mediated silver nanoparticles (AgNPs). *Pak. J. Bot.,* 49, 1561–1568, 2017.
67. Ahmad, A., Syed, F., Shah, A., Khan, Z., Tahir, K., Khan, A.U., Yuan, Q., Silver and gold nanoparticles from *Sargentodoxa cuneata*: Synthesis, characterization and antileishmanial activities. *RSC Adv.*, 5, 73793–73806, 2015.
68. Lambert, R., Skandamis, P.N., Coote, P.J., Nychas, G.J., A study of the minimum inhibitory concentration and mode of action of oregano essential oil, thymol and carvacrol, *J. Appl. Microbiol.*, 91, 453–462, 2001.
69. Galdiero, S., Falanga, A., Vitiello, M., Cantisani, M., Marra, V., Galdiero, M., Silver nanoparticles as potential antiviral agents. *Molecules* 16, 8894–8918, 2011.
70. Geoprincy, G., Srri, B.V., Poonguzhali, U., Gandhi, N.N., Renganathan, S., A review on green synthesis of silver nano particles. *Asian J. Pharm. Clin. Res.*, 6, 8–12, 2013.
71. Gomathi, M., Rajkumar, P.V., Prakasam, A., Ravichandran, K., Green synthesis of silver nanoparticles using *Datura stramonium* leaf extract and assessment of their antibacterial activity. *Resource-Efficient Technologies,* 3, 280–284, 2017.
72. Khamhaengpol, A., Siri, S., Green synthesis of silver nanoparticles using tissue extract of weaver ant larvae. *Mater. Lett.*, 192, 72–75, 2017.
73. Ruíz-Baltazar, Á. de J., Reyes-López, S. Y., Larrañaga, D., Estévez, M., Pérez, R., Green synthesis of silver nanoparticles using a Melissa officinalis leaf extract with antibacterial properties. *Results in Physics*, 7, 2639–2643, 2017.
74. El-Sherbiny, I.M., El-Shibiny, A., Salih, E., Photo-induced green synthesis and antimicrobial efficacy of poly(ε-caprolactone)/curcumin/grape leaf extract-silver hybrid nanoparticles. *J. Photochem. Photobiol. B*, 160, 355–363, 2016.

75. Pethakamsetty, L., Kothapenta, K., Nammi, H.R., Ruddaraju, L.K., Kollu, P., Yoon, S.G., Pammi, S.V.N., Green synthesis, characterization and antimicrobial activity of silver nanoparticles using methanolic root extracts of *Diospyros sylvatica*. *J. Environ. Sci.*, 55, 157–162, 2017.
76. Manikandan, V., Velmurugan, P., Park, J.H., Lovanh, N., Seo, S.K., Jayanthi, P., Park, Y.J., Cho, M., Oh, B.T., Synthesis and antimicrobial activity of palladium nanoparticles from *Prunus x yedoensis* leaf extract. *Mater. Lett.*, 185, 335–338, 2016.
77. Dauthal, P., Mukhopadhyay M., Noble metal nanoparticles: Plant-mediated synthesis, mechanistic aspects of synthesis, and applications. *Ind. Eng. Chem. Res.*, 55, 9557–9577, 2016.
78. Markus, J., Mathiyalagan, R., Kim, Y.-J., Abbai, R., Singh, P., Ahn, S., Perez, Z.E.J., Hurh, J., Yang, D.C., Intracellular synthesis of gold nanoparticles with antioxidant activity by probiotic *Lactobacillus kimchicus* DCY51T isolated from Korean kimchi. *Enzyme Microb. Technol.*, 95, 85–93, 2016.
79. Kumar, B., Smita, K., Vizuete, K.S., Cumbal, L., Aqueous phase Lavender leaf mediated green synthesis of gold nanoparticles and evaluation of its antioxidant activity. *Biol Med (Aligarh)*, 8(3), 1–4, 2016.
80. Patra, J.K., Baek, K.-H., Novel green synthesis of gold nanoparticles using *Citrullus lanatus* rind and investigation of proteasome inhibitory activity, antibacterial, and antioxidant potential. *Int. J. Nanomed.*, 10, 7253–7264, 2015.
81. Gomaa, E.Z., Antimicrobial, antioxidant and antitumor activities of silver nanoparticles synthesized by *Allium cepa* extract: A green approach. *J. Genet. Eng. Biotechnol.*, 15, 49–57, 2017.
82. Midwood, K.S., Williams, L.V., Schwarzbauer, J.E., Tissue repair and the dynamics of the extracellular matrix. *Int. J. Biochem. Cell Biol.*, 36, 1031–1037, 2004.
83. Ziv-Polata, O., Topaz, M., Brosh, T., Margel, S., Enhancement of incisional wound healing by thrombin conjugated iron oxide nanoparticles. *Biomaterials*, 31, 741–747, 2010.
84. Naraginti, S., Kumari, P.L., Das, R.K., Sivakumar, A., Patil, S.H., Andhalkar V.V., Amelioration of excision wounds by topical application of green synthesized, formulated silver and gold nanoparticles in albino Wistar rats. *Mater. Sci. Eng. C*, 62, 293–300, 2016.
85. Kumar, K.P., Paul, W., Sharma, C.P., Green synthesis of gold nanoparticles with *Zingiber officinale* extract: Characterization and blood compatibility. *Process Biochem.*, 46, 2007–2013, 2011.
86. Surendra, T.V., Roopan, S.M., Arasu, M.V., Al-Dhabi, N.A., Rayalu, G.M., RSM optimized *Moringa oleifera* peel extract for green synthesis of *M. oleifera* capped palladium nanoparticles with antibacterial and hemolytic property. *J. Photochem. Photobiol. B*, 162, 550–557, 2016.
87. Edwin, J., Balakrishnan, J.S., Chandra, J.D., Diabetes vs herbal medicines. *Iran. J. Pharmacol. Ther.*, 7, 97–106, 2008.

88. Daisy, P., Saipriya, K., Biochemical analysis of *Cassia fistula* aqueous extract and phytochemically synthesized gold nanoparticles as hypoglycemic treatment for diabetes mellitus. *Int. J. Nanomed.*, 7, 1189–1202, 2012.
89. Kiran, M.V., Murugesan, S., Biogenic silver nanoparticles by *Halymenia poryphyroides* and its *in vitro* anti-diabetic efficacy. *J. Chem. Pharm. Res.*, 5, 1001–1008, 2013.
90. Kumar, V.G., Gokavarapu, S.D., Rajeswari, A., Dhas, T.S., Karthick, V., Kapadia, Z., Shrestha, T., Barathy, I.A., Roy, A., Sinha, S., Facile green synthesis of gold nanoparticles using leaf extract of antidiabetic potent *Cassia auriculata*. *Colloids Surf. B*, 87, 159–163, 2011.
91. El-Kassas, H.Y., El-Sheekh, M.M., Cytotoxic activity of biosynthesized gold nanoparticles with an extract of the red seaweed *Corallina officinalis* on the MCF-7 human breast cancer cell line. *Asian Pac. J. Cancer Prev.* 15, 4311–4317, 2014.
92. Jeyaraj, M., Rajesh, M., Arun, R., MubarakAli, D., Sathishkumar, G., Sivanandhan, G., Dev, G.K., Manickavasagam, M., Premkumar, K., Thajuddin, N., Ganapathi, A., An investigation on the cytotoxicity and caspase-mediated apoptotic effect of biologically synthesized silver nanoparticles using *Podophyllum hexandrum* on human cervical carcinoma cells. *Colloids Surf. B*, 102, 708–717, 2013.
93. Tippayawat, P., Phromviyo, N., Boueroy, P., Chompoosor, A., Green synthesis of silver nanoparticles in aloe vera plant extract prepared by a hydrothermal method and their synergistic antibacterial activity. *Peer J.*, 4, 1–2, 2016.
94. Mata, R., Nakkala, J.R., Sadras, S.R., Biogenic silver nanoparticles from *Abutilon indicum*: Their antioxidant, antibacterial and cytotoxic effects *in vitro*, *Colloids Surf. B*, 128, 276–286, 2015.
95. Sadeghi, B., Rostami, A., Momeni, S.S., Facile green synthesis of silver nanoparticles using seed aqueous extract of *Pistacia atlantica* and its antibacterial activity. *Spectrochim. Acta A*, 134, 326–332, 2015.
96. Rajakannu, S., Shankar, S., Perumal, S., Subramanian, S., Original research article biosynthesis of silver nanoparticles using *Garcinia mangostana* fruit extract and their antibacterial, antioxidant activity. *Int. J. Curr. Microbiol. Appl. Sci.*, 4(1), 944–952, 2015.
97. Selvam, K., Sudhakar, C., Govarthanan, M., Thiyagarajan, P., Sengottaiyan, A., Senthilkumar, B., Selvankumar, T., Eco-friendly biosynthesis and characterization of silver nanoparticles using *Tinospora cordifolia* (Thunb.) Miers and evaluate its antibacterial, antioxidant potential. *J. Radiat. Res. Appl. Sci.*, 10, 6–12, 2017.
98. Shafaghat, A., Synthesis and characterization of silver nanoparticles by phytosynthesis method and their biological activity. *Synth. React. Inorg. Met. Nano-Metal Chem.*, 45, 381–387, 2015.
99. Sadeghi, B., Gholamhoseinpoor, F., A study on the stability and green synthesis of silver nanoparticles using *Ziziphora tenuior* (Zt) extract at room temperature. *Spectrochim. Acta A*, 134, 310–315, 2015.

100. Vanaja, M., Annadurai, G., *Coleus aromaticus* leaf extract mediated synthesis of silver nanoparticles and its bactericidal activity. *Appl. Nanosci.*, 3, 217–223, 2013.
101. Ajitha, B., Reddy, Y.A.K., Shameer, S., Rajesh, K.M., Suneetha, Y., Reddy, P.S., *Lantana camara* leaf extract mediated silver nanoparticles: Antibacterial, green catalyst. *J. Photochem. Photobiol. B Biol.*, 149, 84–92, 2015.
102. Omprakash, V., Sharada, S., Green synthesis and characterization of silver nanoparticles and evaluation of their antibacterial activity using *Elettaria cardamom* seeds. *J. Nanomed. Nanotechnol.*, 6, 266–271, 2015.
103. Nayak, B., Rauta, P.R., Ashe, S., Nayak, D., Biosynthesis, characterisation and antimicrobial activity of silver nanoparticles using *Hibiscus rosa-sinensis* petals extracts. *IET Nanobiotechnol.*, 9, 288–293, 2015.
104. Sengottaiyan, A., Mythili, R., Selvankumar, T., Aravinthan, A., Kamala-Kannan, S., Manoharan, K., Thiyagarajan, P., Govarthanan, M., Kim, J.-H., Green synthesis of silver nanoparticles using *Solanum indicum* L. and their antibacterial, splenocyte cytotoxic potentials. *Res. Chem. Intermed.*, 42, 3095–3103, 2016.
105. Rajeshkumar, S., Synthesis of silver nanoparticles using fresh bark of *Pongamia pinnata* and characterization of its antibacterial activity against gram positive and gram negative pathogens. *Resour. Technol.*, 2, 30–35, 2016.
106. Gauthami, M., Srinivasan, N., Goud, N.M., Boopalan, K., Thirumurugan, K., Synthesis of silver nanoparticles using *Cinnamomum zeylanicum* bark extract and its antioxidant activity. *Nanosci. Nanotechnol. Asia*, 5, 2–7, 2015.
107. Ahmed, S., Saifullah, Ahmad, M., Swami, B.L., Ikram, S., Green synthesis of silver nanoparticles using *Azadirachta indica* aqueous leaf extract. *J. Radiat. Res. Appl. Sci.*, 9, 1–7, 2016.
108. Jyoti, K., Baunthiyal, M., Singh, A., Characterization of silver nanoparticles synthesized using *Urtica dioica* Linn. leaves and their synergistic effects with antibiotics. *J. Radiat. Res. Appl. Sci.*, 9, 217–227, 2016.
109. Ramesh, P.S., Kokil, T., Geetha, D., Plant mediated green synthesis and antibacterial activity of silver nanoparticles using *Emblica officinalis* fruit extract. *Spectrochim. Acta A*, 142, 339–343, 2015.
110. Meva, F.E., Ebongue, C.O., Fannang, S.V., Segnou, M.L., Ntoumba, A.A., Kedi, P.B.E., Loudang, R.-E.N., Wanlao, A.Y., Mang, E.R., Mpondo1, E.A.M., Natural substances for the synthesis of silver nanoparticles against *Escherichia coli*: The case of *Megaphrynium macrostachyum* (Marantaceae), *Corchorus olitorus* (Tiliaceae), *Ricinodendron heudelotii* (Euphorbiaceae), *Gnetum bucholzianum* (Gnetaceae), and *Ipomoea batatas* (Convolvulaceae). *J. Nanomater.*, 2017, 6834726, 2017.
111. Geetha, R., Ashokkumar, T., Tamilselvan, S., Govindaraju, K., Sadiq, M., Singaravelu, G., Green synthesis of gold nanoparticles and their anticancer activity. *Cancer Nanotechnol.*, 4, 91–98, 2013.

112. Raliya, R., Biswas, P., Environmentally benign bio-inspired synthesis of Au nanoparticles, their self-assembly and agglomeration. *RSC Adv.*, 5, 42081–42087, 2015.
113. Kanipandian, N., Kannan, S., Ramesh, R., Subramanian, P., Thirumurugan, R. Characterization, antioxidant and cytotoxicity evaluation of green synthesized silver nanoparticles using *Cleistanthus collinus* extract as surface modifier. *Mater. Res. Bull.*, 49, 494–502, 2014.
114. Antony, J.J., Sithika, M.A.A., Joseph, T.A., Suriyakalaa, U., Sankarganesh, A., Siva, D., Kalaiselvi, S., Achiraman, S., *In vivo* antitumor activity of biosynthesized silver nanoparticles using *Ficus religiosa* as a nanofactory in DAL induced mice model. *Colloids Surf. B*, 108, 185–190, 2013.
115. Sukirtha, R., Priyanka, K.M., Antony, J.J., Kamalakkannan, S., Thangam, R., Gunasekaran, P., Krishnan, M., Achiraman, S., Cytotoxic effect of green synthesized silver nanoparticles using *Melia azedarach* against *in vitro* HeLa cell lines and lymphoma mice model. *Process Biochem.*, 47, 273–279, 2012.
116. Gengan, R.M., Anand, K., Phulukdaree, A., Chuturgoon, A. A 549 lung cell line activity of biosynthesized silver nanoparticles using *Albizia adianthifolia* leaf. *Colloids Surf. B*, 105, 87–91, 2013.
117. Rathi Sre, P.R., Reka, M., Poovazhagi, R., Arul Kumar, M., Murugesan, K., Antibacterial and cytotoxic effect of biologically synthesized silver nanoparticles using aqueous root extract of *Erythrina indica* Lam. *Spectrochim. Acta A*, 135, 1137–1144, 2015.
118. Amarnath, K., Mathew, N.L., Nellore, J., Siddarth, C.R.V., Kumar, J. Facile synthesis of biocompatible gold nanoparticles from *Vites vinefera* and its cellular internalization against HBL-100 cells. *Cancer Nanotechnol.*, 2, 121–132, 2011.
119. Vijayaraghavan, K., Nalini, S.P.K., Prakash, N.U., Madhankumar, D., One step green synthesis of silver nano/microparticles using extracts of *Trachyspermum ammi* and *Papaver somniferum*. *Colloids Surf. B*, 94, 114–117, 2012.
120. Philip, D., Rapid green synthesis of spherical gold nanoparticles using *Mangifera indica* leaf. *Spectrochim. Acta A*, 77, 807–810, 2010.
121. Ajitha, B., Reddy, Y.A.K., Reddy, P.S., Biosynthesis of silver nanoparticles using *Plectranthus amboinicus* leaf extract and its antimicrobial activity. *Spectrochim. Acta A*, 128, 257–262, 2014.
122. Rosarin, F.S., Arulmozhi, V., Nagarajan, S., Mirunalini, S., Antiproliferative effect of silver nanoparticles synthesized using amla on Hep2 cell line. *Asian Pac. J. Trop. Med.*, 6, 1–10, 2013.
123. Kumar, B., Smita, K., Cumbal, L., Debut, A., Synthesis of silver nanoparticles using *Sacha inchi* (*Plukenetia volubilis* L.) leaf extracts. *Saudi J. Biol. Sci.*, 21, 605–609, 2014.
124. Bala, N., Saha, S., Chakraborty, M., Maiti, M., Das, S., Basu, R., Nandy, P., Green synthesis of zinc oxide nanoparticles using *Hibiscus subdariffa* leaf extract: Effect of temperature on synthesis, anti-bacterial activity and anti-diabetic activity. *RSC Adv.*, 5, 4993–5003, 2015.

125. Dauthal, P., Mukhopadhyay, M., *In-vitro* free radical scavenging activity of biosynthesized gold and silver nanoparticles using *Prunus armeniaca* (apricot) fruit extract. *J. Nanopart. Res.*, 15, 1366–1376, 2013.
126. Muniyappan, N., Nagarajan, N.S., Green synthesis of gold nanoparticles using *Curcuma pseudomontana* essential oil, its biological activity and cytotoxicity against human ductal breast carcinoma cells T47D. *J. Environ. Chem. Eng.*, 2, 2037–2044, 2014.
127. Romano, M.F., Gil, M.L.A., Santander, J.M.P., Jaén, J.J.D., Rodríguez, I.N., Cisneros, J.L.H.d., Aguilera, L.M.C., Sonosynthesis of gold nanoparticles from a *Geranium* leaf extract. *Ultrason. Sonochem.*, 21, 1570–1577, 2014.
128. Muthuvel, A., Adavallan, K., Balamurugan, K., Krishnakumar, N., Biosynthesis of gold nanoparticles using *Solanum nigrum* leaf extract and screening their free radical scavenging and antibacterial properties. *Biomed. Prev. Nutr.*, 4, 325–332, 2014.
129. Philip, D., Unni, C., Extracellular biosynthesis of gold and silver nanoparticles using Krishna tulsi (*Ocimum sanctum*) leaf. *Phys. E*, 43, 1318–1322, 2011.
130. Ramamurthy, C.H., Padma, M., Samadanam, I.D.M., Mareeswaran, R., Suyavaran, A., Kumar, A.S., Premkumar, K., Thirunavukkarasu, C., The extra cellular synthesis of gold and silver nanoparticles and their free radical scavenging and antibacterial properties. *Colloids Surf. B*, 102, 808–815, 2013.
131. Konwarh, R., Gogoi, B., Philip, R., Laskar, M.A., Karak, N., Biomimetic preparation of polymer-supported free radical scavenging, cytocompatible and antimicrobial "green" silver nanoparticles using aqueous extract of *Citrus sinensis peel. Colloids Surf. B*, 84, 338–345, 2011.
132. Mittal, A.K., Bhaumik, J., Kumar, S., Banerjee, U.C., Biosynthesis of silver nanoparticles: Elucidation of prospective mechanism and therapeutic potential. *J. Colloid Interface Sci.*, 415, 39–47, 2014.
133. Kumar, K.M., Mandal, B.K., Kumar, K.S., Reddy, P.S., Sreedhar, B., Biobased green method to synthesise palladium and iron nanoparticles using *Terminalia chebula* aqueous extract. *Spectrochim. Acta A*, 102, 128–133, 2013.
134. Reddy, J., Nagoor Vali, D., Rani, M., Rani, S.S., Evaluation of antioxidant, antibacterial and cytotoxic effects of green synthesized silver nanoparticles by *Piper longum* fruit. *Mater. Sci. Eng. C*, 34, 115–122, 2014.
135. Azandehi, P.K., Moghaddam, J., Green synthesis, characterization and physiological stability of gold nanoparticles from *Stachys lavandulifolia* Vahl extract. *Particuology*, 19, 22–26, 2015.
136. Philip, D., Unni, C., Aromal, S.A., Vidhu, V.K., *Murraya koenigii* leaf-assisted rapid green synthesis of silver and gold nanoparticles. *Spectrochim. Acta A*, 78, 899–904, 2011.
137. Krishnaswamy, K., Orsat, V., Insight into the nanodielectric properties of gold nanoparticles synthesized from maple leaf and pine needle extracts. *Ind. Crops Prod.*, 66, 131–136, 2015.

138. Song, J.Y., Jang, H.K., Kim, B.S., Biological synthesis of gold nanoparticles using *Magnolia kobus* and *Diopyros kaki* leaf extracts. *Process Biochem.*, 44, 1133–1138, 2009.
139. Basavegowda, N., Idhayadhulla, A., Lee, Y.R., Phyto-synthesis of gold nanoparticles using fruit extract of *Hovenia dulcis* and their biological activities. *Ind. Crops Prod.*, 52, 745–751, 2014.
140. Veshara, M., Mbatha, J.N., Gengan, R.M., Anand, K., Biosynthesis of bimetallic Au-Ag nanoparticles using *Ocimum basilicum* (L.) with antidiabetic and antimicrobial properties. *Adv. Mater. Lett.*, 6 (12), 1050–1057, 2015.

Part V

SYNTHESIS OF BIOPOLYMER NANOPARTICLES AND QUANTUM DOTS

Suvardhan Kanchi and Shakeel Ahmed (eds.) Green Metal Nanoparticles, (667–688)
© 2018 Scrivener Publishing LLC

19

Role of Bioconjugated Quantum Dots in Detection and Reduction of Pathogenic Microbes

Angappan Rameshkumar[1,2], Devanesan Arul Ananth[1,3], Sivagurunathan Periyasamy[4], Deviram Garlapati[5], Thilagar Sivasudha[1,*]

[1]Department of Environmental Biotechnology, Bharathidasan University, Tamil Nadu, India
[2]TÜV SÜD South Asian Company, Bangalore, India
[3]Department of Food Quality and Safety, Gilat Research Center, Agricultural Research Organization, Negev, Israel
[4]Center for Materials Cycles and Waste Management Research, National Institute for Environmental Studies, Tsukuba, Japan
[5]National Facility for Marine Cyanobacteria, Bharathidasan University, Tamil Nadu, India

Abstract

Quantum dots are very tiny particles composed of hundreds to thousands of atoms. These tiny particles can differ in color and fluorescence emission depending on their size. QDs play a major role in nanomedicine, biomedical and analytical applications. One of the main applications of QDs is that they can act as a fluorescent probe for cell labelling and antimicrobial agent. Due to their excellent optical properties, QDs have the potential to be formulated as novel antimicrobial materials. The antibacterial potential of QDs is through degradation of cell wall of the target organism, free radicals (singlet oxygen) induced bacterial cell death, and QDs can also inhibit the antioxidative genes which are responsible for the increase of reactive oxygen species in cells, leading to cell death. Furthermore, the fluorescence nature of QDs can be used to visualize bacterial species. QDs

**Corresponding author*: sudacoli@yahoo.com; sudha@bdu.ac.in

Suvardhan Kanchi and Shakeel Ahmed (eds.) Green Metal Nanoparticles, (669–688)
© 2018 Scrivener Publishing LLC

inert fluorescent tags are for suitable for labeling of microbial species. This chapter will discuss the importance of QDs for antimicrobial activity and microbial photolabeling.

Keywords: Quantum dots, antimicrobial activity, photolabeling, bioimaging, fluorescent probes and antimicrobial activity

19.1 Introduction

The present chapter demonstrates the application of Quantum dots (QDs) in microbial detection and reduction mechanisms. The changing trends in modern lifestyle are increasing our exposure to various environmental challenges, including pathogenic bacterial species, thereby instigating various infectious diseases. As a result, the need for the production of antibiotics is very high, and therefore pharmaceutical companies and researchers are searching for new antimicrobial agents. Nanoscale materials have emerged as novel antimicrobial agents owing to their large surface area to volume ratio and unique chemical and physical properties [1, 2]. Nanotechnology is a fast-growing technology that deals with the production and utilization of nano-sized particles in the range of tens or hundreds of nanometers [3]. Nowadays, we are using nano products in various applications in medical, research and pharmaceutical fields, which are proved to have a remarkable impact on health care. Nanoparticle application is gaining momentum in the present century due to their explicit chemical, optical and mechanical properties. To turn down the microbial resistance against metal ions and antibiotics the metallic nanoparticles are found to be most promising candidates with their antibacterial properties [4].

Nanotechnology is already being used in commercial applications for bulk products, such as sunscreens and anti-aging creams with nanoparticles with the ability to target deeper into the skin of the body. Titanium dioxide (TiO_2) is one of the commercially used nanoparticles in sunscreens and anti-aging creams [5]. It acts as both sunscreen and antimicrobial agent. TiO_2 helps in killing microbes and also assists in decomposing the cells of fungi, algae and viruses. The dead cells are decomposed by photocatalytic action of the nanocarriers used, meanwhile the toxins are formed at the end. Different types of antimicrobial agents, such as zinc, titanium, copper [6], magnesium, gold [7], alginate [8] and silver, are used as nanoparticles. Silver has been proved to be effective because it has good antimicrobial activity against bacteria, viruses and other eukaryotic microorganisms. The usage of silver nanoparticles as drug carriers has resulted in side effects like agyrosis and argyria, which are toxic to mammalian cells [9]. Recently,

QDs have been gaining in importance due to their fluorescence spectrum, which renders them as optimal fluorophores for biomedical imaging [10,11]. QDs can be conjugated with bioactive moieties (e.g., antibodies, receptor ligands) to target specific biologic events and cellular structures, such as labeling neoplastic cells [12, 13], deoxyribonucleic acid (DNA) [14], and cell membrane receptors [15, 16] (Figure 19.1). Many pharmacological reports have confirmed the antimicrobial property of quantum dots besides acting as a nanocarrier. Addition of quantum dots enhances the antimicrobial effect of different compounds. Lu *et al.* [17] reported that Cadmium telluride (CdTe) QDs effectively kill the bacteria (*Escherichia coli*) in a concentration-dependent manner. Kloepfer *et al.* [18] proposed that the free radicals formed in the microbial cells by QDs help in regulating the antimicrobial property. Our previous study shows the enhancement of the antimicrobial effect of *Merremia emarginata* and *Pergularia daemia* plant extracts with the use of thioglycolic acid (TGA)-CdTeQDs as a carrier. Also, we suggested the possible mechanism of cell damage in antimicrobial activity [19, 20]. But, so far, the mechanism behind QDs exhibiting antimicrobial activity is still unclear. This chapter tries to give the possible mode of action and properties of QDs having the antimicrobial potential which has been studied and reported in the literatures so far.

19.2 About QDs

At the beginning of the 1980s, QDs were discovered by Alexei Ekimov in a glass matrix and by Louis E. Brus (Professor of Chemistry at Columbia University) in colloidal solutions. The term "quantum dot" was coined by Mark Reed and researchers have studied the use of quantum dots in transistors, solar cells, light-emitting diode (LEDs) and diode lasers. They

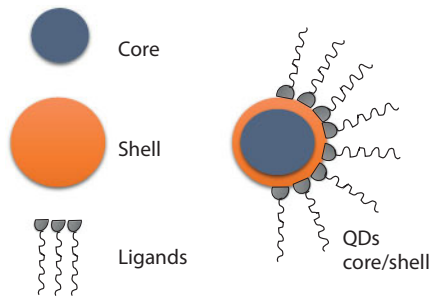


Figure 19.1 Basic architecture of core/shell/ligands in QDs.

have also investigated them as agents for medical imaging. QDs are semiconductors, made from an element like silicon or germanium, or from a compound such as cadmium sulfide or cadmium selenide (CdS or CdSe). These tiny particles can differ in color depending on their size. QDs have gained lots of interest in research due to their existing size- and shape-dependent properties such as photobleaching threshold, stability, relatively narrow and symmetric luminescence bands, good spectral property, etc. [21]. The most common quantum dots are CdTe, CdSe, CdS, etc. QDs like ZnSe (Zinc selenide) and ZnTe (Zinc telluride) have less quantum efficiency and require higher time for preparation [22]. The fluorescence particles, CdTe QDs are used as luminescence probes and sensors. These are widely preferred due to their large excitation and fluorescence time [23, 24]. The high absorbance coefficient over a wide region in the visible spectra and a high fluorescence quantum yield at 546 nm and 578 nm is the result of a combination of CdTe QDs [25]. Furthermore, electron-hole pair recombination of QDs is attributed to their fluorescence nature [26]; because of their high fluorescence nature, they are applicable in biological research and medical fields.

19.3 General Applications of QDs

Applications of QDs have increased tremendously in the last decades. QDs have enormous optical properties (exhibiting emission wavelength up to 900 nm), including high brightness, resistance to photobleaching and tunable wavelength. Modern developments in surface alteration of QDs enable their potential application in cancer imaging. Sentinel lymph-node mapping that aids in biopsy and surgery can be possible with near-infrared emission of QDs. *In-vivo* targeting of tumors, recognizing metastatic tumor cells, quantifying the level of specific target molecules and targeted therapy of cancer can be achieved through QDs. Byrne *et al.* [27] have reported CdTe QDs which are employed for enhanced live cell imaging and extensively studied them in biolabeling of cells, imaging, drug delivery, separation, protein detection, optical sensing, etc. [28, 29]. QDs are used in the diagnosis of cancer and targeted therapy of cancer cells.

19.3.1 Applications of QDs as Analytical Fluorescent Probes

QDs are dominant fluorescent probes exclusively for long-standing, multiplexed and quantitative imaging and detection. Recently, quantum dots have been engineered not only to generate strong signals for *in-vivo* cellular

imaging, but also to have a modified surface with multiple active functional groups in order to facilitate conjugation with targeting moieties and therapeutic agents. It has become an excellent material with which to study drug delivery in cells and small animals. The fluorescent property of QDs will provide important information in the rational design of biocompatible drug carriers and will serve as a greater substitute for magnetic and radioactive imaging contrast agents in preclinical drug screening, validation and delivery research. The applications of QDs in this field provide a perspective for future research [30]. Li *et al.* [31] have reported QDs as a fluorescent probe for exploring the mechanism of competence development in *E. coli.* A high resolution, three-dimensional image can be achieved with reconstructed consecutive focal-plane images, which is due to the superior photostability of QDs [32]. The unusual photostability of QDs probes the real-time tracking of molecules and cells over extended periods of time [33]. Antibodies, peptides [34], streptavidin [35] and nucleic acid aptamers [36] are used to target a specific protein on the cells.

19.3.2 Application of QDs in Bioimaging

In-vitro and *in-vivo* labeling of cells through static fluorescent tags can be achieved with QDs. QDs labeling has no visible toxicity to the labeled cells or the host animal. The application of QDs in combination with multi-photon and emission-scanning microscopy provides the opportunity to concurrently identify and study the interactions of numerous different populations of tumor cells and tissue cells within the same animal. With the support of QDs spectral imaging, five different populations of cells can be identified instantaneously using multi-photon laser excitation [29]. It shows that QDs are inert fluorescent tags which are suitable for labeling the cells for *in-vivo* studies. Metastases are an obstacle to the development of effective cancer therapies. In respect to this, semiconductor nanocrystals and QDs offer considerable reward over organic fluorophores for this purpose; QDs capped with (mecaptopropionic) MPA, CdSe/ZnS QDs or avidin conjugated QDs were used for labeling the cells for *in-vitro* imaging study [37, 38].

Active and passive targeting are the two types of schemes observed in QDs where active targeting selectively functionalizes tumor cells and their respective tumor-specific binding sites. Passive targeting utilizes the improved permeation and preservation of tumor cells for the delivery of quantum dot probes. Rapidly growing tumor cells have more permeable cell membranes than normal healthy cells, and tumor cell allows the leakage of small nanoparticles into the cell body. In addition, tumor cells

require an effective lymphatic drainage system, which leads to consequent nanoparticle accretion of collagen imaging in normal and cancer tissue, which can be achieved through second harmonic generation (SHG) and QDs imaging [39–41]. Tissue penetrability can be measured with different sizes and wavelengths of QDs microbeads. QDs have also been used to examine tumor cell extravasations and seeding [29] by labeling five distinct populations of cells with differently colored QDs and tracking them. QDs might find a more immediate application in the assaying of cell motility, which is widely accepted to correlate strongly with metastatic potential of the cells [42]. This can be used to provide therapeutic options in cancer treatment.

19.4 Mechanism of Action of QDs in Cell Lines

The enormous appeal of QDs is owing to their manipulated surfaces, yielding multifunctional QDs applicable in different biological models. The surface of QDs was modified with N-acetylcysteine (NAC) and altered by QD physical and biological properties. The cytotoxicity of the cells is correlated with upregulation of Fas enzymes on the surface of treated cells. The increased expression of Fas, membrane lipid peroxidation of QD treated cells had increased, and it was measured by the fluorescent BODIPY-C11 dye. Using MTT reduction assay, peroxide lipids were detected at mitochondrial level and were imaged through a confocal microscope with fluorescent JC-1 dye [43, 44]. CdTe QDs-induced toxicity is involved in the upregulation of the Fas receptor and lipid peroxidation, this toxicity induction leads to impairment of neuroblastoma cell functions. The core size of QDs, biological media stability and surface chemistry are the factors which define the cytotoxicity induced by CdTe QDs to level the cellular internalization [45]. CdTe QDs-induced mechanisms of toxicity include damage in multiple organelles and involved increased Fas receptor expression and cell membrane lipid peroxidation in SH-SY5Y neuroblastoma cells [43]. These damages bring death of cell both by apoptosis and necrosis [46].

19.5 QDs as Antimicrobial Agents

Recently, with their extensive applications, study on antimicrobial activity of QDs has also been reasonably fueled up. It has been noted that regulated concentrations of CdTe QDs can kill bacteria in an effective manner [17]. An improved effect of killing may be due to free radical or oxidative damage

to the bacterial cell wall and membranes of bacteria caused by bringing the QDs in close proximity to the surface of bacteria via antibody binding [18]. The antimicrobial activity of QDs can be due to the production of singlet oxygen, a source of free radicals, under irradiation. Recently, Luo *et al.* [47] have reported that a QDs-Rocephin (antibiotic) complex exhibits antibacterial activity through ROS mediated oxidative damage to bacteria and through a stable electrostatic interaction of the QDs-Rocephin complex on the cell surface of *E. coli*. Rocephin can be categorized as one of the most predominantly used antibiotics. It was reassembled to attain considerably higher antimicrobial effect than that of pure CdTe QDs or Rocephin complex alone. In addition, fluorescent properties of CdTe QDs were adopted to synchronously observe the concentration changes in *E. coli* and to determine the optimum dosage of antimicrobial agents.

19.6 Mechanism of QDs Exhibiting Antimicrobial Activity

19.6.1 Mechanism of Action of QDs Alone

The mechanism of antimicrobial activity of CdTe QDs was analyzed by comparing the capability of colony forming in non-treated and QD-treated bacteria. Regulating the concentration of CdTe QDs can lyse the bacteria in a very effective way. It is quite similar to the reported antibacterial effect of CdSe core QDs; when their concentration was increased, the number of colony forming units (CFUs) was reduced [18]. CdTe QDs effect on *E. coli* surface morphology can be evaluated with the help of atomic force microscopy (AFM). The rod shape, surface structure and flagella of individual *E. coli* cells can be clearly seen under AFM. CdTe QDs treatment significantly changes the morphology of the bacterium (Figure 19.2). CdTe-core QDs can also act as an antibacterial nanomaterial. QDs can bind on the bacterial surface and negatively affect the function of cellular antioxidative systems, including down regulations of antioxidative genes and decrease of antioxidative enzyme activities. The concentration exposure of QDs elects the survivability of bacteria. The proposed mechanism of the antimicrobial activity of MSA-capped CdTe QDs is formation of the QDs-bacteria complex and a QD-related ROS-mediated pathway [17]. It has been reported that QDs could induce cytotoxicity to animal cells. QDs can be formulated as novel antimicrobial materials coupled with excellent optical properties [48]. Very recently, Courtney *et al.* [49] reported that multidrug-resistant clinical bacterial isolates, such as methicillin-resistant *Staphylococcus aureus,*

carbapenem-resistant *E. coli*, extended-spectrum β-lactamase-producing *Klebsiella pneumoniae* and *Salmonella typhimurium,* were killed by photoinduced CdTe QDs. The cellular effect of oxidation and reduction prospective of QDs, also separating the outcome from material and the band gap, were confirmed by the experiment. These results might be used in semiconductor QDs phototherapy under clinical conditions.

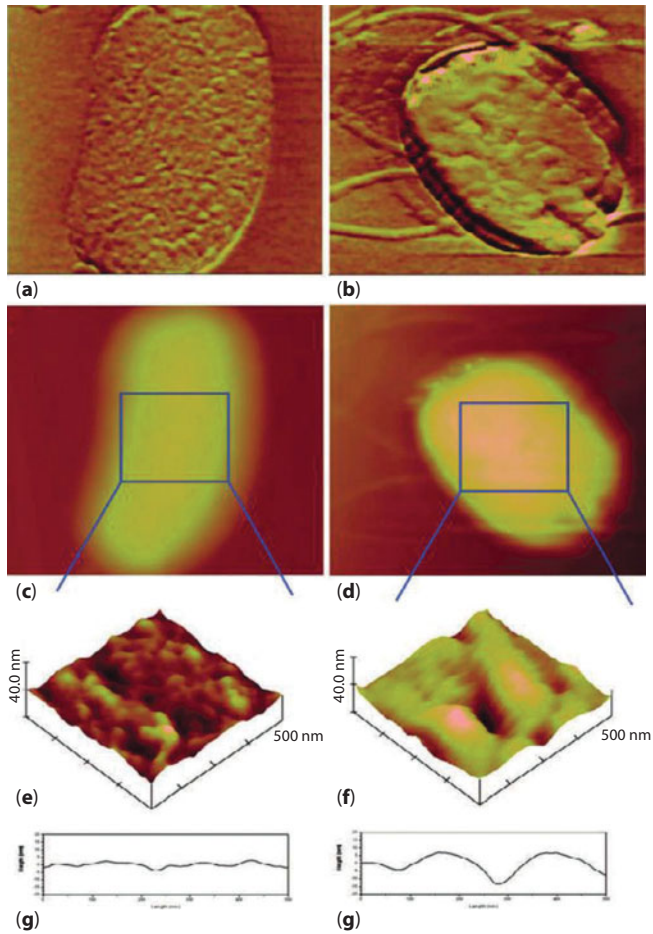


Figure 19.2 CdTe QD-induced surface morphological change of *E. coli.* (a) Friction image of nontreated *E. coli.* (b) Friction image of QD-treated *E. coli.* (c) Height image of nontreated *E. coli.* (d) Height image of QD-treated *E. coli.* The image size in panels A–D is 4 μm. (e) 3-D height magnified image of nontreated *E. coli* surface. (f) 3-D height magnified image of QD-treated *E. coli* surface. The image size of panels E and F is 500 nm. (g) Section curve for image E. (h) Section curve for image F. (Reproduced from [17]; Copyright © 2008 American Chemical Society)

19.6.2 Mechanism of Action of QDs with Complex Molecules

The fluorescence nature of QDs helps in antimicrobial effects and pathogen detection. Recently, Fang *et al.* [50] have reported that CdTe QDs-Rocephin complex inhibited *E. coli* growth. Rocephin (ceftriaxone) is a third-generation cephalosporin antibiotic marketed by Hoffman-La Roche. It is used to treat many kinds of infections which are caused by bacteria, and includes severe or life-threatening forms. Rocephin is arranged on the outer surface of CdTe QDs due to electrostatic attraction and forms a steady antimicrobial collection. The antibacterial activity of nanomaterial depends on its contact surface. The increased interactions with organic and inorganic molecules are the result of large surface area provided by the nanoparticles, and the enlargement of specific area extends antimicrobial activity. A combination of Rocephin and CdTe QDs causes high oxidative damage to the bacteria when compared to their individual activity. Rocephin inactivates bacterium's transpeptidase enzymes channeling inhibition in peptidoglycan synthesis and condenses the cell membrane permeability. The lifespan of ROS induced by QDs is short (about 10^{-6} to 10^{-5} s) and can react with only molecules surrounding it. The ROS concentrations per QDs are higher inside the cell than that of cell membrane [51]. However, CdTe QD might not go into the bacteria inertly through membrane transportation. Due to the absence of receptor-specific QD bioconjugates, CdTe QDs are too huge to disperse into cells. Rocephin can damage some of the cells and only those damaged cells can facilitate CdTe QDs entering into the intracellular environment. Under normal suitable conditions, cells are able to protect themselves against ROS damage with the help of enzymes such as superoxide dismutases (SOD), catalases, lactoperoxidases, glutathione peroxidases and peroxiredoxins. CdTe QDs can also confine the antioxidative gene expressions inside the cell, which results in low level of antioxidative enzyme translations, thereby halting their ability to remove ROS [52]. Thus, the CdTe QDs have the effect of both breaking the balance of oxidant/antioxidant and producing the accumulation of ROS in bacteria. Bacteria tolerate the antibiotics through the multidrug efflux pump, this efflux pump helps to pump out unwanted toxic substances through specific efflux pumps. Amphiphilic molecule antibiotics acquire both hydrophilic and hydrophobic characteristics and can be easily documented by many efflux pumps. However, QDs may be deprived of efflux substrates for efflux pumps because the known substrates pumped out all small molecules [53]. Thus, the QDs-Rocephin complex may persuade more enhanced synergistic antibacterial behavior than pure CdTe QDs and Rocephin. The likely overall mechanism of synchronous monitoring

of *E. coli* contents is the water-soluble CdTe QDs coated with thioglycolic acid (TGA) by thiol group-Cd coordination, and the functional carboxylic acids of TGA can easily bond with amine groups on the surface of skin cells such as peptides, proteins and amino acids. And the connection with bacterial cell may help to prevent the agglomeration of CdTe QDs and provide better stability and larger surface area to CdTe QDs [28]. Thus, the higher activity of CdTe QDs is directly related to the increased intensity of CdTe QDs. Based on this mechanism, reduction of *E. coli* concentration in the antibacterial process could be realized (Figure 19.3). Rameshkumar *et al.* [19] and Ananth *et al.* [20] reported that QDs exhibit maximum antimicrobial activity against *E. coli* compared with their individual effects. The cooperative antimicrobial activity of CdTe QDs with plant extract might be due to membrane binding, oxidative stress-induced microbial cell death and free radicals (singlet O_2) produced by QDs (Figure 19.4). Similarly, Wansapura *et al.* [54] studied Chitin–CdTe QDs film which exhibited an excellent antibacterial activity against both *S. aureus* and *Pseudomonas aeruginosa* bacterial isolates. Also, Chitin–CdTe QDs might be used in several biomedical applications in the near feature. Recently, Galdiero *et al.* [55] observed the ecotoxic properties of antimicrobial peptide indolicidin

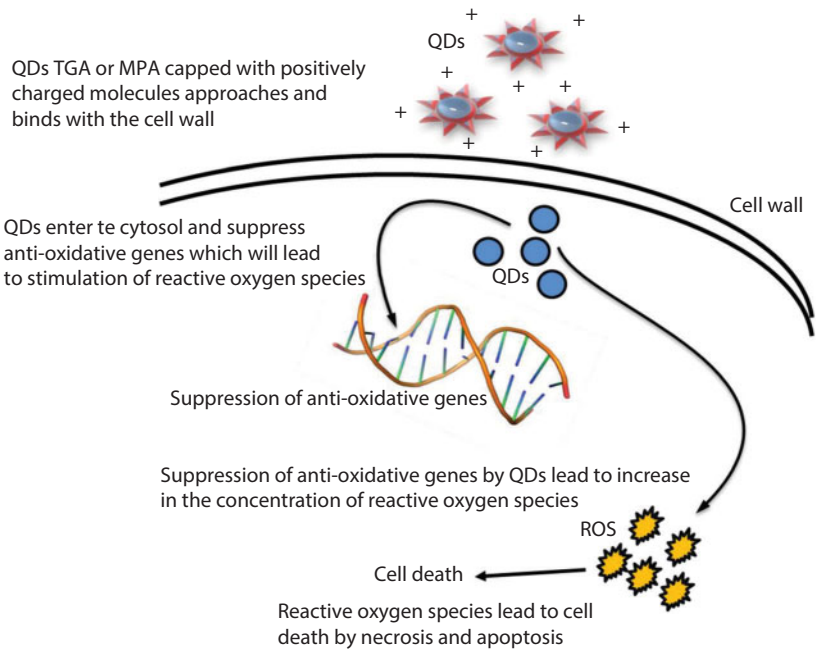

QDs
QDs TGA or MPA capped with positively charged molecules approaches and binds with the cell wall
Cell wall
QDs enter te cytosol and suppress anti-oxidative genes which will lead to stimulation of reactive oxygen species
QDs
Suppression of anti-oxidative genes
Suppression of anti-oxidative genes by QDs lead to increase in the concentration of reactive oxygen species
ROS
Cell death
Reactive oxygen species lead to cell death by necrosis and apoptosis

Figure 19.3 Schematic diagram of TGA- or MPA-capped QDs cell death mechanism.

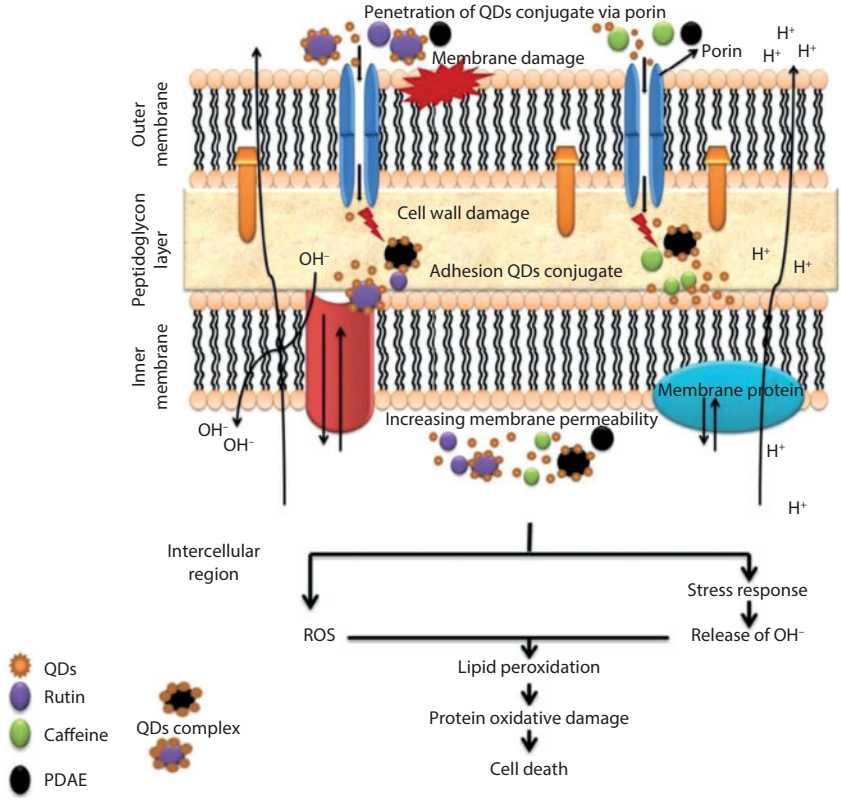


Figure 19.4 Schematic diagram of the antibacterial mechanism of the QDs conjugate. (Reproduced from [20])

coated and uncoated QDs. In this study, they examined antibacterial activity against *S. aureus, E. coli, Pseudomonas aeruginosa* and *Klebsiella sp.* The antimicrobial mechanism of bioconjugated QDs were similar to previous reports. They suggested QDs were highly toxic to *Daphnia magna*; on the other hand, the QDs-indolicidin complex has less toxicity, but both led to oxidative stress and DNA damage that finally lead to cell death.

19.6.3 Mechanism of Action of QDs in Fluorescence Image Detection on Bacteria

Lu *et al.* [17] reported that high fluorescent mercaptosuccinic acid (MSA)-capped CdTe QDs was used for detection of *E. coli*. The authors showed confocal micrographs which demonstrate the connection of QDs with bacteria (Figure 19.5). The majority of the *E. coli* cells exposed to QDs

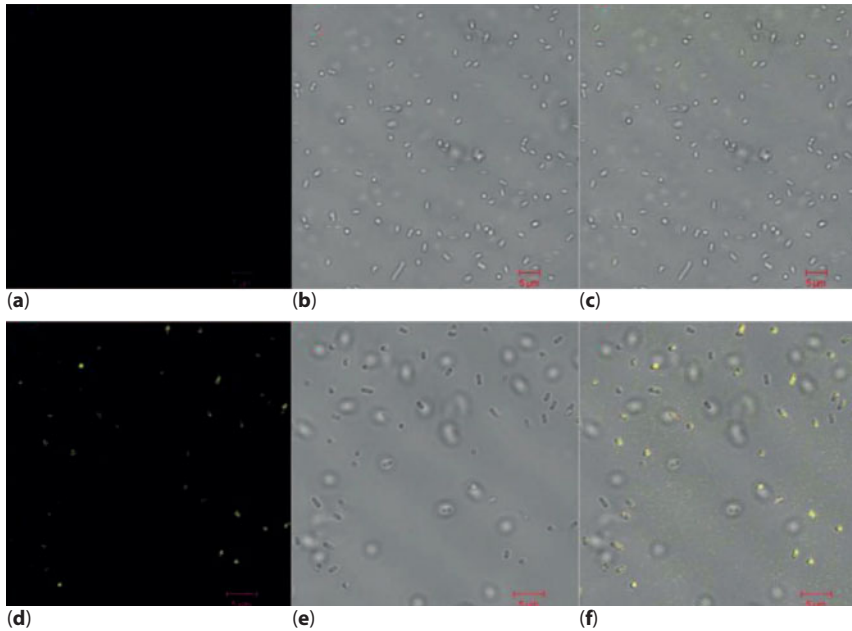


Figure 19.5 Confocal micrographs of nontreated and QD-treated *E. coli.* (a) Fluorescent micrograph of nontreated *E. coli.* (b) Bright field micrograph of nontreated *E. coli.* (c) Merged micrograph of A and B. (d) Fluorescent micrograph of nontreated *E. coli.* (e) Bright field micrograph of nontreated *E. coli.* (f) Merged micrograph of D and E. (Reproduced from [17]; Copyright © 2008 American Chemical Society)

exhibited fluorescence under irradiation. As reported earlier, surface conjugation plays an important role here, and QDs without surface conjugations cannot be transported into the bacterial cell due to lack of endocytosis mechanism. QDs have to be adsorbed on the surface and the flagella of *E. coli.* The QDs can bind on the flagella and cell wall of *E. coli* cells. It can be concluded from this study that MSA-capped CdTe QDs can bind on the bacterial surface and provide a direct contact for the easy diffusion of free radicals into the bacterium, which in turn plays a vital role in the antibacterial activity of QDs. Kuo *et al.* [56] reported on CdTe QDs conjugated with antibody for *E. coli* detection (Figure 19.6). Bovine serum albumin (BSA) is denatured chemically and coated with water-soluble CdTe QDs, then productively conjugated to an anti-*E. coli* antibody by means of a crosslinking reaction. *E. coli* and *Listeria monocytogenes* were detected with anti-*E. coli* antibody-conjugated CdTe QDs using fluorescence microscopy. Succinylated dBSA-coated CdTe QDs were also prepared to conjugate with the anti-*E. coli* antibody. The applications of bioconjugated CdTe QDs in

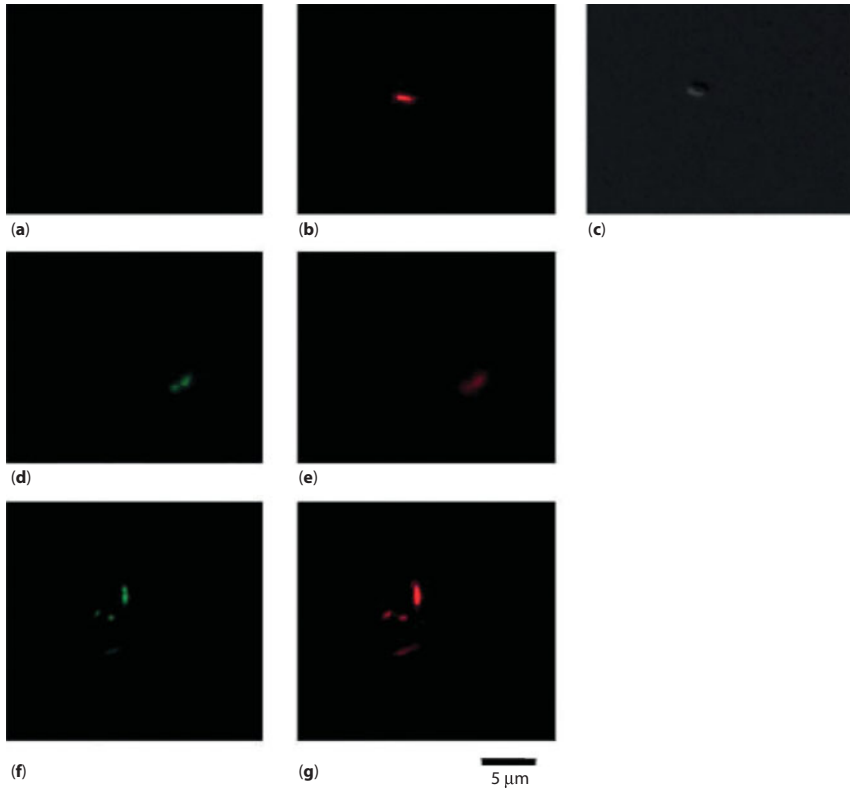


Figure 19.6 Fluorescence images of *E. coli* O157:H7 detection using: (a and b) denatured bovine serum albumin (dBSA)-coated CdTe QDs; (d and e) anti-*E. coli* antibody-conjugated CdTe QDs; and (f and g) anti-*E. coli* antibody conjugated succinylated dBSA-coated CdTe QDs. Panels a, d, and f were obtained with band-pass filters for green fluorescence (excitation: 488 [10 nm] and emission: 520 [30 nm]), while panels b, e, and g were obtained with band-pass filters for red fluorescence (excitation: 550 [10 nm] and emission: 630 [30 nm]). For comparison, the DIC image of *E. coli* O157:H7 is shown in panel c. (Reproduced from [56]; Copyright © 2008 American Chemical Society)

antibody-specific fluorescence-based pathogen detection by both *in-vitro* and *in-vivo* imaging are highlights of the present study. Kloepfer *et al.* [18] have briefly reported that the fluorescent QDs with adenine conjugates were taken up by *Bacillus subtilis*. When QDs were added in early log phase, the *Bacillus* sp. often died or sporulated, and when QDs were added during stationary phase or declining phase, it rarely led to fluorescence labeling. Figure 19.7 shows the effect of QDs on *Bacillus* sp. and demonstrates QDs used for multi-complex formation such as pathogen targeting antibody and

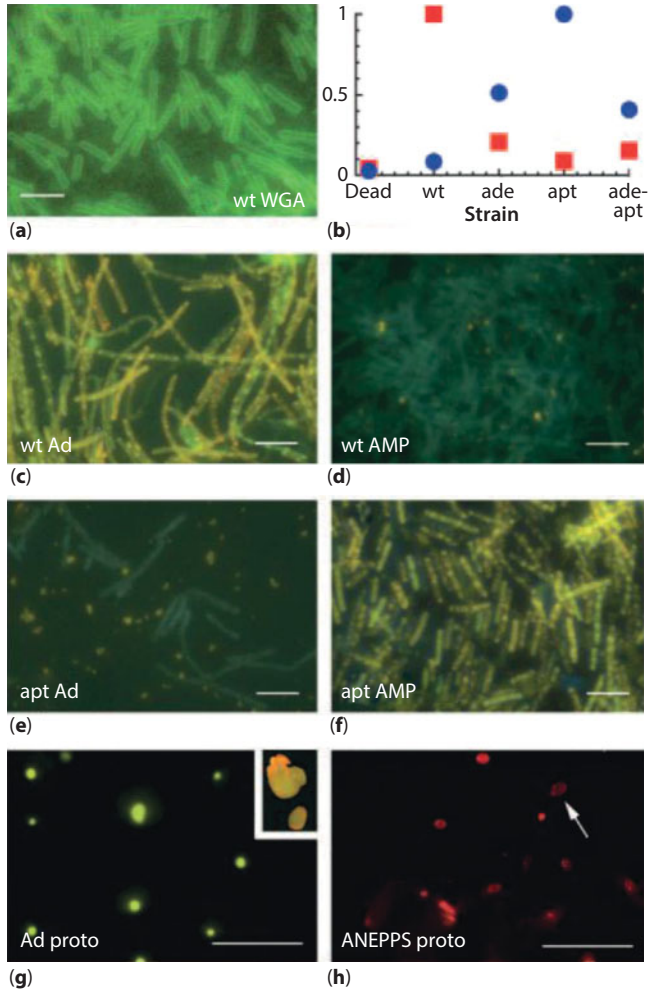


Figure 19.7 Metabolism-specific fluorescent labeling of *B. subtilis* with QD-adenine and QD-AMP. QDs are yellow emitting, corresponding to the second column in 1. All points are averages of n 3 (error bars smaller than symbols); scale bars, 5 m. (a) *B. subtilis* incubated with QD-WGA conjugates shows a typical pattern of external labeling for contrast with appearance of internal labeling. wt, wild type. (b) Relative fluorescence peaks of various strains exposed to QD-adenine (red squares) and QD-AMP (blue circles). Peaks were normalized to the brightest strain, which controlled for differences in quantum yield between QD-adenine and QD-AMP. (c) Wild type with QD-adenine. (d) Wild type with QD-AMP. (e) The apt mutant with QD-adenine (Ad). (f) The apt mutant with QD-AMP. The ade mutant and ade-apt double mutant are similar but not quite as bright (not shown). (g) Protoplasts (proto) of the wild type after incubation with QD-adenine. Insert, upper right: QD-adenine protoplasts after staining with the membrane dye di-4-ANEPPS. (h) Control protoplasts cannot be visualized unstained but staining with d-4-ANEPPS shows the appearance of membrane labeling in the absence of cell wall (arrow). (Reproduced from [18]; Copyright © 2005 American Society for Microbiology)

antibiotics drugs. It exhibits multifunctional applications such as pathogen reduction, detection and targetable drug delivery.

19.7 Advantage and Disadvantages of QDs as Antimicrobial Agent

Foodborne disease outbreaks have alerted the public to food safety issues. The Centers for Disease Control and Prevention (CDC) estimates that approximately 76 million cases of foodborne disease occur each year in the U.S. [57]. The most commonly recognized foodborne infections are caused by bacteria, including *Salmonella sp., E. coli, L. monocytogenes,* etc. Therefore, food safety should be ensured by developing new antimicrobial agents. Currently, the most common antimicrobial inorganic materials are TiO_2 and immobilized antimicrobial metals such as copper and silver. The confinement phenomenon of quantum dots was also observed in the 7 nm sized nanoparticles of zinc oxide (ZnO) QDs. ZnO QDs show antimicrobial activity against *E. coli* in apple cider and orange juice.

QDs possess antimicrobial effects against the growth of bacteria. The inhibitory effect of QDs is concentration-dependent and synergistic in nature when combined with Nisin, a bacteriocin produced by certain strains of *Lactococcus lactis*. It is used as a biopreservative in 57 countries around the world. Nisin is nontoxic, heat stable and does not interfere with flavors. It is used in commercially available food to inhibit the growth of foodborne pathogens. The growth of microorganisms *E. coli* and *Salmonella* sp. can be inhibited with a combination of nisin and QDs. This shows the antimicrobial activity of QDs nanoparticle in food safety. QDs have emerged as a talented antimicrobial agent in several applications because nanoparticles can damage the cells of bacteria by destroying the enzymes of bacteria that transport the nutrient of cells and abating the cell membrane or cell wall and cytoplasm of the prokaryotic cell [58]. The mechanisms for QDs nanoparticles-induced toxicity include the effects of this particle on cell membranes, mitochondria and genetic material. Pulmonary infections triggered by the nanoparticles leads to changes in the permeability of membranes, making the particles move away from the lung [59]. Nanoparticles have the additional ability of affecting cardiovascular disease and could also cause new types of effects not already seen with larger particles, like uptakes via olfactory epithelium, mitochondrial damage and other cardiovascular effects [60].

19.8 Conclusion and Future Prospects

The present chapter highlighted QDs antimicrobial activity with photolabeling capability. It could be concluded that among the different antimicrobial agents, QDs could be the one most extensively studied and used to fight infections and prevent spoilage. QDs are also found to be nontoxic to humans in limited concentrations. The unique physical and chemical properties of QDs serve in the development of new antibacterial agents. QDs can bind on the bacterial surface and negatively affect the function of cellular antioxidative system, which increases the reactive oxygen species through singlet oxygen production. Inflammatory cells produce ROS where their accumulation is mostly observed in allergic and non-allergic inflammations. ROS have destructive actions on both DNA and proteins. Under strong inflammatory conditions, ROS is triggered as part of a defense mechanism may also destroy tissues coupled with specific antimicrobial activity. However, antioxidants (reduced glutathione, catalase, superoxide dismutase) usually prevent tissue damage under normal conditions. The generation of ROS in antimicrobial defense mechanisms mainly occurs in phagocytes due to the activation of the Nicotinamide adenine dinucleotide phosphate (NADPH) oxidase and is called respiratory burst. QDs can penetrate the cell wall and suppress the cellular antioxidative genes. The bacterial cell lysis takes place after the destruction of DNA and protein by the induced ROS. Thus, strong evidence is provided of the antimicrobial activity of QDs.

References

1. Morones, J.R., Elechiguerra, J.L., Camacho, A., Holt, K., Kouri, J.B., Ramírez, J.T., Yacaman, M.J., The bactericidal effect of silver nanoparticles. *Nanotech.,* 16, 2346–2353, 2005.
2. Kim, J.S., Kuk, E., Yu, K.N., Kim, J.H., Park, S.J., Lee, H.J., Kim, S.H., Park, Y.K., Park, Y.H., Hwang, C.Y., Kim, Y.K., Lee, Y.S., Jeong, D.H., Cho, M.H., Antimicrobial effects of silver nanoparticles. *Nanomed.,* 3, 95–101, 2007.
3. Panyala, N.R., Pena-Mendez, E.M., Havel, J., Silver or silver nanoparticles: A hazardous threat to the environment and human health. *J. Appl. Biomed.,* 6, 117–129, 2008.
4. Rai, M., Yadav, A., Gade, A., Silver nanoparticles as a new generation of antimicrobials. *Biotech. Adv.,* 27, 76–83, 2009.
5. Labille, J., Feng, J., Botta, C., Borschneck, D., Sammut, M., Cabie, M., Auffan, M., Rose, J., Bottero, J.Y., Aging of TiO_2 nanocomposites used in sunscreen.

Dispersion and fate of the degradation products in aqueous environment. *Environ. Pollut.,* 158, 3482–3489, 2010.
6. Retchkiman-Schabes, P.S., Canizal, G., Becerra-Herrera, R., Zorrilla, C., Liu, H.B., Ascencio, J.A., Biosynthesis and characterization of Ti/Ni bimetallic nanoparticles. *Opt. Mat.,* 29, 95–99, 2006.
7. Gu, H., Ho, P.L., Tong, E., Wang, L., Xu, B., Presenting vancomycin on nanoparticles to enhance antimicrobial activities. *Nano. Lett.,* 9, 1261–1263, 2003.
8. Ahmad, Z., Pandey, R., Sharma, S., Khuller, G.K., Alginate nanoparticles as antituberculosis drug carriers: Formulation development, pharmacokinetics and therapeutic potential. *Ind. J. Chest. Dis. Allied Sci.,* 48, 171–176, 2006.
9. Gong, P., Li, H., He, X., Wang, K., Hu, J., Zhang, S., Yang, X., Preparation and antibacterial activity of Fe_3O_4 and Ag nanoparticles. *Nanotech*., 18, 604–611, 2007.
10. Alivisatos, A.P., The use of nanocrystals in biological detection. *Nat. Biotech*., 22, 47–52, 2004.
11. Chan, W.C.W., Maxwell, D.J., Gao, X., Bailey, R.E., Han, M., Nie, S., Luminescent quantum dots for multiplexed biological detection and imaging. Curr. Opin. Biotech., 13, 40–46, 2002.
12. Gao, X., Cui, Y., Levenson, R.M., Chung, L.W., Nie, S., *In vivo* cancer targeting and imaging with semiconductor quantum dots. *Nat. Biotech.,* 22, 969–976, 2004.
13. Wu, X., Liu, H., Liu, J., Haley, K.N., Treadway, J.A., Larson, J.P., Ge, N., Peale, F., Bruchez, M.P., Immunofluorescent labeling of cancer marker Her2 and other cellular targets with semiconductor quantum dots. *Nat. Biotech.,* 21, 41–46, 2003.
14. Dubertret, B., Skourides, P., Norris, D.J., Noireaux, V., Brivanlou, A.H., Libchaber, A., *In vivo* imaging of quantum dots encapsulated in phospholipid micelles. *Science.,* 298, 1759–1762, 2002.
15. Beaurepaire, E., Buissette, V., Sauviat, M.P., Giaume, D., Lahlil, K., Mercuri, A., Casanova, D., Huignard, A., Martin, J.L., Gacoin, T., Boilot, J.P., Alexandrou, A., Functionalized fluorescent oxide nanoparticles: Artificial toxins for sodium channel targeting and imaging at the single molecule level. *Nano. Lett.,* 4, 2079–2083, 2004.
16. Lidke, D.S., Nagy, P., Heintzmann, R., Arndt-Jovin, D.J., Post, J.N., Grecco, H.E., Jares-Erijman, E.A., Jovin, T.M., Quantum dot ligands provide new insights into erbB/HER receptor mediated signal transduction. *Nat. Biotech.,* 22, 198–203, 2004.
17. Lu, Z., Li, C.M., Bao, H., Qiao, Y., Toh, Y., Yang, X., Mechanism of antimicrobial activity of CdTe quantum dots. *Langmuir,* 2, 5445–5452, 2008.
18. Kloepfer, J.A., Mielke, R.E., Nadeau, J.L., Uptake of CdSe and CdSe/ZnS quantum dots into bacteria via purine dependent mechanisms. *Appl. Environ. Microbiol.,* 71, 2548–2557, 2005.

19. Rameshkumar, A., Sivasudha, T., Jeyadevi, R., Sangeetha, B., Ananth, D.A., Aseervatham, G.S.B., Nagarajan, N., Renganathan, R., Kathiravan, A., *In vitro* antioxidant and antimicrobial activities of *Merremia emarginata* using thio glycolic acid-capped cadmium telluride quantum dots. *Colloids Surf. B,* 101,74–82, 2013.
20. Ananth, D.A., Rameshkumar, A., Jeyadevi, R., Jagadeeswari, S., Nagarajan, N., Renganathan, R., Sivasudha, T., Antibacterial potential of rutin conjugated with thio glycolic acid capped cadmium telluride quantum dots (TGA-CdTe QDs). *Spectrochim. Acta A,* 138, 684–692, 2015.
21. Marcel, B.J., Mario, M., Peter, G., Shimon, W., Alivisatos, A.P., Semiconductor nanocrystal as fluorescent biological labels. *Science,* 281, 2013–2016, 1998.
22. Xu, Y., Al-Salim, N., Bumby, C.W., Tilley, R.D., Synthesis of SnS quantum dots. *J. Am. Chem. Soc.,* 131. 15990–15991, 2009.
23. Susha, A.S., Javier, A.M., Parak, W.J., Rogach, A.L., Luminescent CdTe nanocrystals as ion probes and pH sensors in aqueous solutions. *Colloids Surf. A,* 281, 40–43, 2006.
24. Yuan, J., Guo, W., Wang, E., Utilizing a CdTe quantum dots enzyme hybrid system for the determination of both phenolic compounds and hydrogen peroxide. *Anal. Chem.,* 80, 1141–1145, 2008.
25. Idowu, M., Chena, J.Y., Nyokong, T., Photoinduced energy transfer between water soluble CdTe quantum dots and aluminium tetrasulfonated phthalocyanine. *New J. Chem.,* 32, 290–296, 2008.
26. Bae, P.K., Kim, K.N., Lee, S.J., Chang, H.J., Lee, C.K., Park, J.K., The modification of quantum dot probes used for the targeted imaging of his-tagged fusion proteins. *Biomaterials,* 30, 836–842, 2009.
27. Byrne, S.J., Corr, S.A., Rakovich, T.Y., Gun'ko, T.K., Rakovich, Y.P., Donegan, J.F., Mitchell, S., Volkov, Y., Optimisation of the synthesis and modification of CdTe quantum dots for enhanced live cell imaging. *J. Mater. Chem.,* 16, 2896–2902, 2006.
28. Chan, W.C.W., Nie, S., Quantum dot bioconjugates for ultrasensitive nonisotopic detection. *Science,* 281, 2016–2018, 1998.
29. Voura, E.B., Jaiswal, J.K., Mattoussi, H., Simon, S.M., Tracking metastatic tumor cell extravasation with quantum dot nanocrystals and fluorescence emission-scanning microscopy. *Nat. Med.,* 10, 993–998, 2004.
30. Qi, L., Gao, X., Emerging application of quantum dots for drug delivery and therapy. *Expert. Drug Deliv.,* 5, 263–267, 2008.
31. Li, W., Xie, H., Xie, Z., Lu, Z., Ou, J., Chen, X., Shen, P., Exploring the mechanism of competence development in *Escherichia coli* using quantum dots as fluorescent probes. *J. Biochem. Biophys. Meth.,* 58, 59–66, 2004.
32. Tokumasu, F., Fairhurst, R.M., Ostera, G.R., Brittain, N.J., Hwang, J., Wellems, T.E., Dvorak, J.A., Band 3 modifications in *Plasmodium falciparum* infected AA and CC erythrocytes assayed by autocorrelation analysis using quantum dots. *J. Cell. Sci.,* 118, 1091–1098, 2005.

33. Dahan, M., Lévi, S., Luccardini, C., Rostaing, P., Riveau, B., Triller, A., Diffusion dynamics of glycine receptors revealed by single quantum dot tracking. *Science,* 302, 442–445, 2003.
34. Akerman, M.E., Chan, W.C., Laakkonen, P., Bhatia, S.N., Ruoslahti, E., Nanocrystal targeting *in vivo*. *Proc. Natl. Acad Sci. USA*, 99, 12617–12621, 2002.
35. Howarth, M., Liu, W., Puthenveetil, S., Zheng, Y., Marshall, L.F., Schmidt, M.M., Wittrup, K.D., Bawendi, M.G., Ting, A.Y., Monovalent, reduced size quantum dots for imaging receptors on living cells. *Nat. Methods,* 5, 397–399, 2008.
36. Dwarakanath, S., Bruno, J.G., Shastry, A., Phillips, T., John, A.A., Kumar, A., Stephenson, L.D., Quantum dot antibody and aptamer conjugates shift fluorescence upon binding bacteria. *Biochem. Biophy. Res. Com.,* 325, 739–743, 2004.
37. Li, H., Shih, W.Y., Shih, W.H., Synthesis and characterization of aqueous carboxyl capped CdS quantum dots for bioapplications. *Ind. Eng. Chem. Res.,* 46, 2013–2019, 2007.
38. Jaiswal, J.K., Mattoussi, H., Mauro, J.M., Simon, S.M., Long term multiple color imaging of live cells using quantum dot bioconjugates. *Nat. Biotech.,* 21, 47–51, 2003.
39. Williams, R.M., Zipfel, W.R., Webb, W.W., Multiphoton microscopy in biological research. *Cur. Opin. Chem. Biol.,* 5, 603–608, 2001.
40. Zoumi, A., Yeh, A., Tromberg, B.J., Imaging cells and extracellular matrix *in vivo* by using second-harmonic generation and two-photon excited fluorescence. *Proc. Natl. Acad. Sci USA.*, 99, 11014–11019, 2002.
41. Brown, E., Mckee, T., di Tomaso, E., Pluen, A., Seed, B., Boucher, Y., Jain, R.K., Dynamic imaging of collagen and its modulation in tumors *in vivo* using second harmonic generation. *Nat. Med.,* 9, 796–800, 2003.
42. Partin, A.W., Schoeniger, J.S., Mohler, J.L., Coffey, D.S., Fourier analysis of cell motility: Correlation of motility with metastatic potential. *Proc. Natl. Acad. Sci. USA,* 86, 1254–1258, 1989.
43. Choi, A.O., Cho, S.J., Desbarats, J., Lovrić, J., Maysinger, D., Quantum dot-induced cell death involves Fas upregulation and lipid peroxidation in human neuroblastoma cells. *J. Nanobiotech.,* 5, 1–13, 2007.
44. Leary, S.P., Liu, C.Y., Apuzzo, M.L., Toward the emergence of nanoneurosurgery: Part II–Nanomedicine: Diagnostics and imaging at the nanoscale level. *Neurosurgery,* 58, 805–23, 2006.
45. Clarke, S.J., Hollmann, C.A., Zhang, Z., Suffer, D., Bradforth, S.E., Dimitrijevic, N.M., Minarik, W.G., Nadeau, J.L., Photophysics of dopamine modified quantum dots and effects on biological systems. *Nat. Mater.,* 5, 409–417, 2006.
46. Lovric, J., Bazzi, H.S., Cuie, Y., Fortin, G.R.A., Winnik, F.M., Maysinger, D., Differences in subcellular distribution and toxicity of green and red emitting CdTe quantum dots. *J. Mol. Med (Berl),* 83, 377–385, 2005.

47. Luo, Z., Wu, Q., Zhang, M., Li, P., Ding, Y., Cooperative antimicrobial activity of CdTe quantum dots with Rocephin and fluorescence monitoring for *Escherichia coli*. J. *Colloid Interface Sci.,* 362, 100–106, 2011.
48. Hardman, R., A toxicologic review of quantum dots: Toxicity depends on physicochemical and environmental factors. *Environ. Health Perspect.*, 114, 165–172, 2006.
49. Courtney, C.M., Goodman, S.M., McDaniel, J.A., Madinger, N.E., Chatterjee, A., Nagpal, N., Photoexcited quantum dots for killing multidrug-resistant bacteria. *Nat. Mater.,*15, 529–534, 2016
50. Fang, T.T., Li, X., Wang, Q.S., Zhang, Z.J., Liu, P., Zhang, C.C., Toxicity evaluation of CdTe quantum dots with different size on *Escherichia coli*. *Toxicol. In Vitro*, 26, 1233–1239, 2012.
51. Zhang, J., Campbell, R.E., Ting, A.Y., Tsien, R.Y., Creating new fluorescent probes for cell biology. *Nat. Rev. Mol. Cell. Biol.,* 3, 906–918. 2002.
52. Perni, S., Piccirillo, C., Pratten, J., Prokopovich, P., Chrzanowski, W., Parkin, I.P., Wilson, M., The antimicrobial properties of light-activated polymers containing methylene blue and gold nanoparticles. *Biomaterials,* 30, 89–93, 2009.
53. Medintz, I.L., Uyeda, H.T., Goldman, E.R., Mattoussi, H., Quantum dot bioconjugates for imaging, labelling and sensing. *Nat. Mater.,* 4, 435–446, 2005.
54. Wansapura, P.T., Dassanayake, R.S., Hamood, A., Tran, P., Moussa, H., Abidi, N., Preparation of chitin-CdTe quantum dots films and antibacterial effect on *Staphylococcus aureus* and *Pseudomonas aeruginosa*. *J. Appl. Pol. Sci.,* 134, 1–10, 2017.
55. Galdiero, E., Siciliano, A., Maselli, V., Gesuele, R., Guida, M., Fulgione, D., Stefania Galdiero, S., Lombardi, L., Falanga, A., An integrated study on antimicrobial activity and ecotoxicity of quantum dots and quantum dots coated with the antimicrobial peptide indolicidin. *Int. J. Nanomed.*, 11, 4199–4211, 2016.
56. Kuo, Y.C., Wang, Q., Ruengruglikit, C., Yu, H., Huang, Q., Antibody conjugated CdTe quantum dots for *Escherichia coli* detection. *J. Phys. Chem C,* 112, 4818–4824, 2008.
57. Mead, P.S., Slutsker, L., Dietz, V., McCaig, L.F., Bresee, J.S., Shapiro, C., Griffin, P.M., Tauxe, R.V., Food-related illness and death in the United States emerging. *Infect. Dis.,* 5, 607–625, 1999.
58. Rana, S., Kalaichelvan, P.T., Antibacterial activities of metal nanoparticles. *Adv. Bio. Tech.,* 11, 21–23, 2011.
59. Oberdörster, G., Maynard, A., Donaldson, K., Castranova, V., Fitzpatrick, J., Ausman, K., Carter, J., Karn, B., Kreyling, W., Lai, D., Olin, S., Monteiro-Riviere, N., Warheit, D., Yang, H., Principles for characterizing the potential human health effects from exposure to nanomaterials: Elements of a screening strategy. *Part. Fibre. Toxicol.,* 2, 1–35, 2005.
60. DeJong, W.H., Borm, P.J.A., Drug delivery and nanoparticles: Application and hazards. *Int. J. Nanomed.,* 3, 133–149, 2008.

Index

Acaricidal agent, 636
Adenocarcinoma alveolar basal epithelium, 153
Ag nanoparticles, 208
AgNPs, 30–38, 49, 446–448, 450, 452–454, 456–457, 462
Algae mediated synthesis, 579
Algae, bacteria, fungi, diatoms, 114
Alkane thiols, 607
Amalgamation, 481, 482, 498
Anabaena oryzae, 176
Antibacterial, 222, 230, 442, 670, 675, 677–680, 684–686, 688
Antibacterial efficiency, 604
Anti-biofouling agent, 637
Anticancer treatment, 442
Anticanceragent, 633
Anti-cholinesterase, 640
Antifungal agent, 38
Anti-inflammatory, 442
Anti-inflammatory agent, 640
Antileishmania agent, 641
Antimicrobial, 218, 219, 220, 224, 231, 669–671, 674–675, 677–679, 683–688,
Antimicrobial activity, 115
  gastroenterology, 115
  respiratory medicine, 115
Antimicrobial agents, 168
Antimicrobial and antifungal, 642
Antioxidant, 36, 233, 234, 646, 677, 684, 686,
Antioxidant materials, 605
Apoferritin, 606, 614
Applications of Nanoparticles,
  acaricidal, 412
  antibacterial, 391–394
  antibiofilm, 398–400
  anticancer, 408–409
  anticoagulant, 400–401
  antidiabetic, 402–403
  antifungal, 394–396
  antileishmanial, 396–398
  antioxidant, 404–406
  biocompatibilty, 406–408
  larvicidal, 410–411
  pediculocidal, 412
  pupicidal, 410
Aqua chemical synthesis, 24
Aqua regia (3:1 solution of $HCl:HNO_3$), 445
AR grade, 444
Aromatic nitrocompunds, 452, 454
Ascorbic acid, 609
Aspergillus fumigatus, 147
Aspergillus Terreus, 477
AuNPs, 38, 51

Bacillus sp, 681
Bacillus subtilis, 126
Bacterial DNA, 605
Bacterial species, 604
Bactericidal activity, 40
Bacteriotoxic effects, 613
BCC structure, 448
Bifurcaria bifurcata, 148
Binding energies, 449
Bioactive polyphenols, 118

Suvardhan Kanchi and Shakeel Ahmed (eds.) Green Metal Nanoparticles, (689–694)

© 2018 Scrivener Publishing LLC

alkaloids, 118
proteins, 118
sugars, 118
Biocompatibility, 230, 499, 500
Biocomposite, 205, 207
Biogenic, 80, 82, 97, 101
Bioimaging, 670, 673
Biological fields, 603
Biological oxygen demand, 263
Bioreduction mechanism, 201–202
Biosynthesis of nanoparticles, 200
Boreduction mechanism of metal ions, 328–329
Bovine serum albumin, 150
Bulk form, 442

Cadmium selenide (CdSe), 672–673, 675, 685
Cadmium telluride (CdTe), 671
Caenorhabditis, 614
Caenorhabditis elegans, 158
Cancer cells, 615
Cancers, 610
Candida albicans, 174
Capping agents, 25, 27, 36, 49, 607
Cardiovascular, 614
Carrisa edulis, 490
Catalysts, 441–443, 450, 452–453.
Catharanthus roseus, 494
CdTe QDs, 671–672, 674–681, 686
CeNPs, 40
Chemical sensors, copper sulphate ($CuSO_4.5H_2O$), 444
Chemogenic, 82, 97
Chemotherapy, 228
Chicken eggshell membrane mediated synthesis, 585
Chlamydomonas reinhardtii, 151, 176
Chloroaurate ions, 220
Cholesterol, 616
Chrysopelea paradisi, 122
CIS-diammine-dichloro-platinum, 604
Cisplatin, 615
Citrus maxima, 222, 223
Clinical fields, 603
Clusters, 471
Coccinia grandis peel extract, 441, 444–445, 462
Colorimetric, 616
Congo red, 478, 490, 493, 495, 496
Conjugated, 669, 671, 673, 679–681, 686, 688
Conventional synthetic methods, 26
Copper, 441–448, 451–452, 453–454, 458, 460–461
Cu and/or CuxOx nanoparticles, 212
CuNPs, 446–448, 450, 452–457, 462–463
CuO NPs, 40
Cyanobacteria, 608
Cytoplasm, 180
Cytotoxicity, 129, 609

Degradation of,
4-nitroaniline, 416
4-nitrophenol, 415–416
Deoxyribonucleic acid (DNA), 671, 679, 684
Deposition, 143
Dermatology, 115
Detection of,
cadmium, 416, 417
copper, 417
iron, 418
lead, 416, 417
mercury, 416, 417, 418
zinc, 417
Detoxification, 30, 47
Diamagnetic, 248, 252
Different shaped noble metal nanoparticles, 590
Diopyros kaki, 608
Disc or well diffusion nethod, 644
Double-distilled water, 445
Drug delivery, 648
Dulbecco's modified Eagle medium, 152
Dye, 456–459, 461

Dye degradation, 257, 263, 412–415
congo red, 413
direct yellow, 414
eosin yellow, 413
methyl orange, 413, 414
methylene blue, 412–413
putnam sky blue, 414
rhodamine blue, 414
Dye sensitised solar cells, 531

E. coli, 671, 673, 675–681, 683
Earth's crust, 604
Elemental composition, 449
Elettaria cardamomum, 233
Endotoxins, 609
Energy-dispersive x-ray spectroscopy (EDX), 449
Epithelial microvilli, 150
Escherichia coli, 173, 185, 613
Eugenol, 225
Exudate, 80–81, 90–91, 93–95

Face centered cubic (fcc), 448
Fe_3O_4 NPs, 47, 54
Feedstocks, 79–81, 101
FeNPs, 447, 448–450, 451–452, 454, 456, 462–463
Fenton's reagent, 262, 264
FeOx nanoparticles, 202
Ferromagnetic, 248, 251–252
Flavonoids, 36, 38, 445
Fluorescence, 669, 671–672, 677, 679–682, 686–688
Fluorometric, 616
Free radical, 669, 671, 674–675, 678, 680
FT-IR, 449–451
Fuel cells, 604
Fungi mediated synthesis, 583
Fusarium oxysporum, 608

Galvanic displacement, 605
Gas sensing properties of SnO_2 nanostructures,
effect of carbon composite, 525
effect of heterojunction, 522
effect of morphology, 520
mechanism, 518
Green synthesis, 474, 487, 489, 490, 498, 499, 502
Glutathione, 230
Glycerol, 607
Green, 3, 22, 441, 443–444, 456, 461–462
Green chemistry, 79, 81–82, 101
Green synthesis, 25, 47
Green synthesis mechanism, 29
Green synthesis of metallic nanoparticles using food and agro wastes,
gold nanoparticles (AuNPs), 355–357
iron oxide nanoparticles (IONPs), 360–362
nickel nanoparticles (NiNPs), 358
palladium nanoparticles (PdNPs), 358–359
platinum nanoparticles (PtNPs), 359
silver nanoparticles (AgNps), 352–355
titanium dioxide nanoparticles (TiO_2NPs), 360
zinc oxide nanoparticles (ZnO NPs), 357–358
Green Synthesis of MNPs,
green synthesis of MNPs uing herbal plant extracts, 304–305
green Synthesis of MNPs using biopolymers, 300–301
Green synthesis of nanoparticles, 201
Green synthesis of SnO_2 nanostructures,
using bacteria, 516
using biomolecules, 517
using plant extract, 517

Half the maximum intensity (FWHM), 448

HeLa cells, 615
Hemolytic activity, 648
Hexagons, 119
  cubes, 119
  ellipsoids, 119
  nanorods, 119
  nanowires, 119
  pentagons, 119
  spheres, 119
  triangles, 119
Honey mediated synthesis, 584
Horseradish, 614
Hyaluronic acid, 615

Industrial researchers, 603
Ion implantation, 604
Iron (III) chloride hexahydrate ($FeCl_3 \cdot 6H_2O$), 444

Jewellery, 604

Keratinocytes, 610
KeV, 449
Kocuria flava, 481

Langmuir-Hinshel wood model, 454
Lithium ion batteries, 533
LN(C_0/C), 453
Local waste vegetable fibers mediated synthesis, 586

Malachite green, 259, 264, 265, 266
Mechanical milling, lithography, laser ablation, and sputtering, 169
Medicinal plants, 604
Metabolites, 26, 28
Metal ions, 29, 47
Metal Nanoparticles, , 203, 208–213
  bottom-up approaches, 298–300
  top-down approaches, 298
Metal oxides, 143, 159
Metallic form, 442
Metallic nanoparticle synthesis, 323–324
MgO NPs, 40, 54
Mica clay mediated synthesis, 587
Microbe-mediated nanoparticle, 443
Microbes mediated synthesis, 575
Microbial extract, 48
Micro-wave processing, 604
Minimum inhibitory concentration, 645
Morganella sp, 481
Morphology, 447, 603

NaBH4, 442, 445, 452–453.
Nanoadsorbents, 295, 528
Nanomaterials, 142, 143, 146, 149, 159, 200
  carbon-based, 295
  metal-based Nanomaterials, 296
  polymer-based, 295
Nanoparticles, 141–164, 200, 441–450, 452–463
Nanoscale, 442
Nanotechnology, 3, 22, 24, 442, 469, 470, 478, 479, 482, 484
Nanotechnology in environmental applications,
  wastewater treatment, 362–363
Nanotoxicity, 142, 162
Nepenthes khasiana, 131
Nicotinamide adenine dinucleotide phosphate (NADPH, 684
NK-cell, 150
NM, 446, 448–449, 452–453, 456, 458, 460, 462
Nostoc muscorum, 176
NZVI, 460

O-chloronitrobenzene, 604
Orange peel pith, 199, 203, 206, 213
Organic solvents, 605
Oxidative damage, 674–675, 677, 679
Oxidative stress, 678–679

P. aeruginosa, 678–679
P-aminophenol-, 453

Paramagnetic, 250, 251
Para-nitrophenol (PNP), 441, 443–445, 450, 455, 462–463
Pathogen, 669–670, 677, 681, 683
Pathogenic microbes, 605
Phenolic acids, 118
  terpenoids, 118
Photocatalyst, 456–457, 461–463
Photodegradation, 36, 40, 441, 444, 450, 456–457, 459, 462
Photodegradation of organic pollutants, 526–527
Photolabeling, 670, 684
Photothermal therapy, 615
Phototoxicity, 612
Physicochemical, 442
Physicochemical properties, 605
Phytochemicals, 27, 28, 38
Phytomining, 117
Phytosynthesis, 79–80, 82
Plant extract, 28
Plant mediated synthesis, 563
Plants used to produce metallic NPs, 330–332
  biosynthesis of metallic nanoparticles, 348–349
  copper oxide nanoparticles (CuO NPs), 337–339
  gold nanoparticles (AuNPs), 344–347
  iron oxide nanoparticles (FeO NPs), 341–342
  nickel nanoparticles (NiNPs), 347–348
  palladium nanoparticles (PdNPs), 334–336
  platinum nanoparticles (PtNPs), 336–337
  secondary metabolites effect in the bioreduction reaction, 330
  silver nanoparticles (AgNPs), 342–344
  titanium dioxide nanoparticles (TiO_2 NPs), 339–340
  zinc oxide nanoparticles (ZnO NPs), 332–334
P-nitrophenolate ions, 452
Polycyclic aromatic hydrocarbon, 261, 277
Polymers, 605
Polyphenols, 225, 234
Polyvinylpyrrolidone, 610
Process, 3–6, 9,
Proteins, 26, 37, 38, 50
Pseudo-first order reaction-, 457
Pseudokirchneriella subcapitata, 153
Pseudomonas aeruginosa, 173
Pseudomonas stutzeri AG259, 173
Pt NPs, 53

Quantum dots (QDs), 669–688

Radiotherapy, 612
Rate constant (k), 453, 457
Reactive oxigen Species (ROS), 669, 675, 677–679, 684
Reducing agent, 445
Reduction, 449–450, 452–455, 462–463
Remediation by nanoparticles, 202
Renewable, 79, 81, 101
Rhizoclonium fontinale, 147
Ribosomal, 615
Rice husks mediated synthesis, 586
Rocephin, 675, 677, 688

S. aureus, 675, 678–679
Sargassum muticum, 148
Scanning electron microscope (SEM), 447
Scherrer equation $d = K\lambda/\beta\cos\theta$, 448
Scrobicularia plana, 156
Seaweeds, 608
Silica NPs, 53
Silver nitrate ($AgNO_3$), 444
Sodium citrate, 607
Sodium dodecyl sulfate, 182
Sodium thio-phosphate, 500

Stabilizing agent, 445
Staphylococcus aureus, 181
Supercapacitors, 536
Superparamagnetic, 252, 266
Surface area to volume ratio, 443
Surface plasmon resonance, 443, 445
Sustainability, 4–6, 8, 9, 14, 15, 18, 21
Synthesis, 3–5, 10–13, 21
Synthesis of nanoparticles, examples, 389
  mechanism, 389–390
Synthetic procedures, 24

Tephrosia tinctoria, 184
Terminalia chebula, 481
Terpenoids, 604
Tetrahymena thermophila, 153
Tetramethylbenzidine, 615
Thermal methods, 143
Thiol ligands, 607
Titania NPs, 53
Top-down, 253
Top-down approaches, 557

UV-Vis spectroscopy, 445

VBB, 443–445, 456–457, 459
Vibrio fischeri, 154
Victoria Blue B (VBB)., 441, 443–445, 456–458, 462–463

Water oxidation, 530
Wet chemical reduction, 605
Wound healing, 647

Xenopus laevis, 154
X-ray diffraction (XRD), 448–449, 462

Yeast, and human cells, 114
Yolk-shell nanocrystals, 615

Zero-valent iron, 249, 255, 256, 258, 261, 262, 264, 269, 273, 274
Zingiber officinale, 130
ZnO Nanoparticles, 204

β-d-glucose, polyoxometalates, polysaccharides, amino acids, 171